

The Guadalupian Symposium

*Bruce R. Wardlaw, Richard E. Grant,
and David M. Rohr*

EDITORS

ISSUED

AUG 21 2000

SMITHSONIAN INSTITUTION



SMITHSONIAN INSTITUTION PRESS

Washington, D.C.

2000

ABSTRACT

Wardlaw, Bruce R., Richard E. Grant, and David M. Rohr, editors. The Guadalupian Symposium. *Smithsonian Contributions to the Earth Sciences*, number 32, 415 pages, frontispiece, 191 figures, 43 plates, 45 tables, 2000.—The internal stratigraphy of the Cutoff Formation in the Guadalupe Mountains is clarified, and the unit is divided into three members: the Shumard Canyon, the El Centro, and the Williams Ranch members. The Shumard Canyon Member of the Cutoff Formation in the Guadalupe Mountains correlates to the upper part of the Cathedral Mountain Formation in the Glass Mountains. The El Centro and Williams Ranch members of the Cutoff Formation and the lower part of the Brushy Canyon Formation, including the Pipeline Shale in the Guadalupe Mountains, correlate to the Road Canyon Formation. The changeover in conodonts from transitional forms to *Mesogondolella nankingensis* (= *M. serrata*) provides a basal definition for the Guadalupian and occurs within correlation unit 3 in the El Centro Member of the Cutoff Formation and cycle 2 of the Road Canyon Formation.

The geology, stratigraphy, and depositional setting of the Permian in the Del Norte Mountains and of the Word Formation in the Glass Mountains are discussed in detail, and this data suggest deposition in a foreland basin or backbay between the Marathon Fold Belt and the Delaware basin. The internal stratigraphy of the Road Canyon, Word, Vidrio, Altuda, Capitan, and Tessey formations reveal the following: (1) the Road Canyon was deposited in four cycles and the Word in six cycles; (2) the Altuda can be divided into five informal members and the Tessey into three members; (3) the Vidrio is an unconformity-bounded unit; and (4) the Capitan displays characteristic platform margin to slope foresets.

Biozonation of the Guadalupian is discussed, and details are provided on the fusulinid and conodont zonations. Changes in conodont fauna, based on the succession of *Mesogondolella* species from *M. nankingensis* to *M. altudaensis*, divide the Guadalupian into five zones.

Five new species of conodonts (*Sweetina crofti* Wardlaw, *Mesogondolella shannoni* Wardlaw, *Hindeodus wordensis* Wardlaw, *Iranognathus punctatus* Wardlaw, and *Sweetognathus bicarinum* Wardlaw) and two new species of fusulinids (*Codonofusiella (Lantschichites) altudaensis* Wilde and Rudine and *Rauserella bengeensis* Wilde and Rudine) are described.

OFFICIAL PUBLICATION DATE is handstamped in a limited number of initial copies and is recorded in the Institution's annual report, *Annals of the Smithsonian Institution*. SERIES COVER DESIGN: Volcanic eruption at the island of Krakatau in 1883.

Library of Congress Cataloging-in-Publication Data

The Guadalupian symposium / Bruce R. Wardlaw, Richard E. Grant, and David M. Rohr, editors.

p. cm. — (Smithsonian contributions to the earth sciences ; no. 32)

Includes bibliographic references.

1. Geology—Guadalupe Mountains (N.M. and Tex.)—Congresses. 2. Geology, Stratigraphic—Congresses. 3. Paleontology—Guadalupe Mountains (N.M. and Tex.)—Congresses. 4. Guadalupe Mountains (N.M. and Tex.)—Congresses. I. Wardlaw, Bruce R. II. Grant, Richard E., 1927-1994. III. Rohr, David Malcolm, 1947- . IV. Series.

QE1.S227 no. 32 [QE79] 550 s-dc21 [557.64'9] 99-12440

© The paper used in this publication meets the minimum requirements of the American National Standard for Permanence of Paper for Printed Library Materials Z39.48—1984.

Contents

	<i>Page</i>
Preface	v
Memorial to Richard Evans Grant	vii
1. GUADALUPIAN STUDIES IN WEST TEXAS, by Richard E. Grant, Bruce R. Wardlaw, and David M. Rohr	1
2. GUIDEBOOK TO THE GUADALUPIAN SYMPOSIUM, by David M. Rohr, Bruce R. Wardlaw, Shannon F. Rudine, Mohammad Haneef, A. John Hall, and Richard E. Grant	5
3. GUADALUPIAN CONODONT BIOSTRATIGRAPHY OF THE GLASS AND DEL NORTE MOUNTAINS, by Bruce R. Wardlaw	37
4. FORMAL MIDDLE PERMIAN (GUADALUPIAN) SERIES: A FUSULINACEAN PERSPECTIVE, by Garner L. Wilde	89
5. MEMBERS FOR THE CUTOFF FORMATION, WESTERN ESCARPMENT OF THE GUADALUPE MOUNTAINS, WEST TEXAS, by Mark T. Harris	101
6. CYCLIC DEPOSITION OF THE PERMIAN ROAD CANYON FORMATION, GLASS MOUNTAINS, WEST TEXAS, by Bruce R. Wardlaw, Charles A. Ross, and Richard E. Grant	121
7. COMPARISON OF THE DEPOSITIONAL ENVIRONMENTS AND PHYSICAL STRATIGRAPHY OF THE CUTOFF FORMATION (GUADALUPE MOUNTAINS) AND THE ROAD CANYON FORMATION (GLASS MOUNTAINS): LOWERMOST GUADALUPIAN (PERMIAN) OF WEST TEXAS, by Mark T. Harris, Daniel J. Lehrmann, and Lance L. Lambert	127
8. CORRELATION OF THE ROAD CANYON AND CUTOFF FORMATIONS, WEST TEXAS, AND ITS RELEVANCE TO ESTABLISHING AN INTERNATIONAL MIDDLE PERMIAN (GUADALUPIAN) SERIES, by Lance L. Lambert, Daniel J. Lehrmann, and Mark T. Harris	153
9. FUSULINID BIOSTRATIGRAPHY AND PALEONTOLOGY OF THE MIDDLE PERMIAN (GUADALUPIAN) STRATA OF THE GLASS MOUNTAINS AND DEL NORTE MOUNTAINS, WEST TEXAS, by Zhendong Yang and Thomas E. Yancey	185
10. CARBONATE DEPOSITION OF THE PERMIAN WORD FORMATION, GLASS MOUNTAINS, WEST TEXAS, by James D. Rathjen, Bruce R. Wardlaw, David M. Rohr, and Richard E. Grant	261
11. GEOLOGY AND DEPOSITIONAL ENVIRONMENTS OF THE GUADALUPIAN ROCKS OF THE NORTHERN DEL NORTE MOUNTAINS, WEST TEXAS, by Shannon F. Rudine, Bruce R. Wardlaw, David M. Rohr, and Richard E. Grant	291
12. THE ALTUDA FORMATION OF THE GLASS AND DEL NORTE MOUNTAINS, by Bruce R. Wardlaw and Shannon F. Rudine	313
13. A DEEP WATER TURBIDITY ORIGIN FOR THE ALTUDA FORMATION (CAPITANIAN, PERMIAN), NORTHWESTERN GLASS MOUNTAINS, TEXAS, by Mohammad Haneef, David M. Rohr, and Bruce R. Wardlaw	319
14. ANATOMY AND ORIGIN OF CAPITAN LIMESTONE FORESET BEDS IN THE GLASS MOUNTAINS, WEST TEXAS, by Mohammad Haneef	333
15. LATE GUADALUPIAN BIOSTRATIGRAPHY AND FUSULINID FAUNAS, ALTUDA FORMATION, BREWSTER COUNTY, TEXAS, by Garner L. Wilde and Shannon F. Rudine	343

16. LITHOFACIES AND DEPOSITIONAL HISTORY OF THE TESSEY FORMATION, FRENCHMAN HILLS, WEST TEXAS, by Mohammad Haneef and Bruce R. Wardlaw 373
17. CONODONT BIOSTRATIGRAPHY OF THE PERMIAN BEDS AT LAS DELICIAS, COAHUILA, MEXICO, by Bruce R. Wardlaw, Shannon F. Rudine, and Merlynd K. Nestell 381
18. ANCESTRAL ARAXOCERATINAE (UPPER PERMIAN AMMONOIDEA) FROM MEXICO AND IRAN, by Claude Spinoso and Brian F. Glenister 397
19. DEPOSITIONAL CONTROLS ON SELECTIVE SILICIFICATION OF PERMIAN FOSSILS, SOUTHWESTERN UNITED STATES, by Douglas H. Erwin and David L. Kidder 407

Preface

The Guadalupian Symposium was held from 13 to 15 March 1991. It consisted of a one day meeting of oral presentations, which were given at the campus of Sul Ross State University, Alpine, Texas, and a two day field trip to outcrops in the Glass and Del Norte mountains. The meeting at Sul Ross was highlighted by anecdotal presentations by Norman D. Newell and Lloyd Pray. Most of the presentations are represented as papers herein. The field trip was highlighted by Heinz Kozur finding several rattlesnakes, Dick Grant being attacked by a dog, and stirring discussions on the breccia outcrops that form the base of the type section of the Road Canyon Formation.

The term Guadalupian was first proposed as a subdivision of the Permian by Girty in 1902. Glenister and Furnish (1961) concluded that the Permian could be divided into five world-wide stages, including the Guadalupian, which was further divided into the Wordian and Capitanian substages. One of the three primary objectives resulting from the 1989 meeting of the International Subcommittee on Permian Stratigraphy was the designation of the Guadalupian in the United States. Guadalupian strata in the Guadalupe Mountains are well known. They have served as the primary example for the development of sequence stratigraphy. The original concepts of the divisions for the regional stratotype for the Guadalupian, however, included both the Guadalupe Mountains and the Glass Mountains. In order to better document the Guadalupian rocks and faunas for worldwide correlation, the Guadalupian Symposium was organized by the editors. The presentations highlighted new and significant work in the Glass and Del Norte mountains and the correlation between these strata and the Guadalupe Mountains.

The symposium provided the impetus for Glenister et al. (1992) to formally propose the Guadalupian as the international standard reference for the Middle Permian Series. Four Titular Members and three Corresponding Members of the Subcommittee on Permian Stratigraphy attended the symposium and were unanimous in their support of the Guadalupian as the international standard. This volume, along with the previous monographs by Girty (1909), P.B. King (1931, 1948), R.E. King (1931), Miller and Furnish (1940), and Cooper and Grant (1972, 1974, 1975, 1976a,b, 1977), serve as the primary documentation for the Middle Permian Guadalupian Series.

It should be noted that the Guadalupian Symposium and the articles that comprise this volume predate the use of the conodont genus "*Jinogondolella*" and the abandonment of stage names, such as "Leonardian" or "Dzhulfian." The use, or lack of use, of some of these antiquated terms does not indicate acceptance or disapproval.

Literature Cited

- Cooper, G.A., and R.E. Grant
1972. Permian Brachiopods of West Texas, I. *Smithsonian Contributions to Paleobiology*, 14:1-231, plates 1-23.
1974. Permian Brachiopods of West Texas, II. *Smithsonian Contributions to Paleobiology*, 15:233-793, plates 24-191.
1975. Permian Brachiopods of West Texas, III. *Smithsonian Contributions to Paleobiology*, 19:795-1921, plates 192-502.
1976a. Permian Brachiopods of West Texas, IV. *Smithsonian Contributions to Paleobiology*, 21:1923-2607, plates 503-662.
1976b. Permian Brachiopods of West Texas, V. *Smithsonian Contributions to Paleobiology*, 24:2609-3159, plates 663-780.
1977. Permian Brachiopods of West Texas, VI. *Smithsonian Contributions to Paleobiology*, 32:3161-3370.

- Girty, G.H.
1902. The Upper Permian in Western Texas. *American Journal of Science*, fourth series, 14:363–368.
1909 (“1908”). The Guadalupian Fauna. *United States Geological Survey Professional Paper*, 58: 651 pages, 31 plates. [Date on title page is 1908; actually published in 1909.]
- Glenister, B.F., and W.M. Furnish
1961. The Permian Ammonoids of Australia. *Journal of Paleontology*, 35:673–736.
- Glenister, B.F., D.W. Boyd, W.M. Furnish, R.E. Grant, M.T. Harris, H. Kozur, L.L. Lambert, W.W. Nassichuk, N.D. Newell, L.C. Pray, C. Spinosa, B.R. Wardlaw, G.L. Wilde, and T.E. Yancey
1992. The Guadalupian: Proposed International Standard for a Middle Permian Series. *International Geology Review*, 34(9):857–888.
- King, P.B.
1931 (“1930”). The Geology of the Glass Mountains, Texas, Part 1: Descriptive Geology. *University of Texas Bulletin*, 3038: 167 pages, 15 plates. [Date on title page is 1930; actually published in 1931.]
1948. Geology of the Southern Guadalupe Mountains, Texas. *United States Geological Survey Professional Paper*, 215: 183 pages, 23 plates.
- King, R.E.
1931 (“1930”). The Geology of the Glass Mountains, Texas, Part 2: Faunal Summary and Correlation of the Permian Formations with Description of Brachiopoda. *University of Texas Bulletin*, 3042: 245 pages, 44 plates. [Date on title page is 1930; actually published in 1931.]
- Miller, A.K., and W.M. Furnish
1940. Permian Ammonoids of the Guadalupe Mountain Region and Adjacent Areas. *Geological Society of America, Special Paper*, 26: 242 pages, 44 plates.

Memorial to Richard Evans Grant

J. Thomas Dutro, Jr., and Bruce R. Wardlaw
Washington, D.C., and Reston, Virginia

Our esteemed colleague Dick Grant passed away while assembling this collection of manuscripts for the sound establishment of the Guadalupian as a Middle Permian standard. His loss delayed the final editing of this volume and severely threatened our ability to accomplish it. We dedicate "The Guadalupian Symposium" to the memory of Dick and his undying love of the Permian.

Richard Evans Grant, curator of invertebrate paleontology at the National Museum of Natural History, Smithsonian Institution, for more than 35 years, died of a heart attack on December 7, 1994. He was 67 years old. Grant was a world-renowned brachiopod specialist who was best known for his work on Permian brachiopod systematics and biostratigraphy. For more than 20 years he worked with G. Arthur Cooper on the Permian of West Texas; their collaboration resulted in a magnificent series of monographs published by the Smithsonian Institution Press between 1972 and 1977. Dick was particularly interested in the functional morphology and paleoecology of brachiopods, and he contributed many basic ideas about the living habits and evolution of two major groups: the productids and the rhynchonellids.

Born on June 18, 1927, in St. Paul, Minnesota, Dick was the son of Dr. Charles L. Grant, a Lutheran minister, and Gladys N.E. Grant. He spent his first 20 years in Minnesota, except for two years in the U.S. Navy (1945–1946). His choice to serve in the Navy was a reflection of his passion for boats, which he built as a child. Dick majored in philosophy and received his B.A. degree from the University of Minnesota in 1949. He switched to geology for his M.S., which he received from the same university in 1953. A student of W. Charles Bell, he moved with Charlie to the University of Texas, in Austin, Texas, where he was awarded a Ph.D. in 1957 for his study of the Cambrian of southwestern Montana. His thesis was published as *Geological Society of America Memoir* 96 in 1965. While in Austin working on his thesis, Dick spent two years as an instructor in the geology department as Bell's assistant.

Dick came to the Smithsonian in 1957 as an assistant to G.A. Cooper, whereupon he permanently switched paleontologic allegiances from trilobites to brachiopods. The appointment, which was on Cooper's NSF grant, was for four years. He next worked as a paleontologist for the U.S. Geological Survey (U.S.G.S.) from 1961 to 1972, expanding his experiences and knowledge of the Permian from West Texas to the entire world. During his U.S.G.S. career, he performed field work in such far off places as Tunisia, Sicily, Greece, Yugoslavia, Iran, Pakistan, Thailand, Alaska, and the northern Rocky Mountains. Much of his work on productoid living habits, functional morphology, and general ecology was completed during this period.

Dick returned to the National Museum of Natural History in 1972 to replace Cooper as brachiopod curator after Cooper's retirement. He spent the rest of his career working in the Department of Paleobiology, and he served as its chairman from 1972 to 1977. It was during that time that he and Cooper published their impressive six-volume monograph on the Permian brachiopods of West Texas.

Grant received many honors, including the Director's Award for Outstanding Achievement in 1977 and the National Academy of Science's Daniel Giraud Elliot Medal in 1979. He was president of the Paleontological Society from 1978 to 1979 and treasurer of the International Palaeontological Association from 1980 to 1989. He was a Fellow of the Geological Society of America and the American Association for the Advancement of Sciences and was a member of the Society of Economic Paleontologists and Mineralogists,

the American Association of Petroleum Geologists, the Geological Society of Washington, and the Paleontological Society of Washington.

For the past 20 years, Dick had been active in the affairs of the Subcommittee on Permian Stratigraphy, in particular the Permian–Triassic boundary working group. He had nearly completed editing this volume (with Wardlaw and Rohr), which records the proceedings of the Guadalupian Symposium in Alpine, Texas, in 1991; this work establishes a Middle Permian Series for the Permian System. Dick also was concluding his major contributions to the revision of the Brachiopod volumes of the *Treatise on Invertebrate Paleontology*; these included revision of the superfamilies Productoidea (with C.H.C. Brunton and S. Lazerev), Stenoscismatoidea, Oldhaminoidea, and Richthofenioidea, and the family Gemmellaroidae.

During the 1980s, Dick published a wide variety of important contributions, including monographs on the stenocismids, the cardiarinids, and the gemmellaroids. He also described the faunas of several of the regions with which he had been involved as far back as the 1960s: Hydra, Greece; Axel Heiberg Island, Arctic Canada; Guatemala; and elsewhere.

Dick worked with a wide variety of specialists and foreign visitors during his career. In particular, he helped several Chinese paleontologists, including Jin Yugan, Xu Guirong, and Shi Xiaoying, with getting their brachiopod systematic papers published. In addition to Cooper, Brunton, and Lazerev, Dick collaborated with E.E. Brabb, B.F. Glenister, P.M. Kier, M.K. Nestell, D.M. Rohr, A.J. Rowell, F.G. Stehli, C.K. Stropoli, and B.R. Wardlaw.

He is survived by his wife, Lucy Grant of Alexandria, Virginia, sons Charles Lewis Grant and Evan Richard Grant of Richmond, Virginia, and Lauren Philip Grant of Morgantown, North Carolina, and sister Ruth Grant-Rugh of Cornwall-on-Hudson, New York.

Dick Grant was a vibrant and forceful presence in the world of brachiopod and Permian studies for more than three decades, and he was an energetic, imaginative, and resourceful member of the paleontological community in the National Museum for most of his long and productive career.

Selected Bibliography

1962. Trilobite Distribution, Upper Franconia Formation (Upper Cambrian), Southeastern Minnesota. *Journal of Paleontology*, 36:965–998.
1962. [with G.A. Cooper] *Torynechus*, New Name for Permian Brachiopod *Uncinuloides* King. *Journal of Paleontology*, 36:1128–1129.
1963. Unusual Attachment of a Permian Linoproductid Brachiopod. *Journal of Paleontology*, 37:134–140.
1964. [with G.A. Cooper] New Permian Stratigraphic Units in Glass Mountains, West Texas. *Bulletin of the American Association of Petroleum Geologists*, 48:1581–1588.
- 1965a. The Brachiopod Superfamily Stenoscismatacea. *Smithsonian Miscellaneous Collections*, 148(2):1–192.
- 1965b. Faunas and Stratigraphy of the Snowy Range Formation (Upper Cambrian) in Southwestern Montana and Northwestern Wyoming. *Geological Society of America, Memoir*, 96:1–171.
1965. [with D.V. Ager, D.J. McLaren, and H. Schmidt] Rhynchonellida. In Raymond C. Moore, editor, *Treatise on Invertebrate Paleontology*, Part H, Brachiopoda: 552–632. Lawrence, Kansas: University of Kansas Press for the Geological Society of America.
1965. [with P.M. Kier] Echinoid Distribution and Habits, Key Largo Coral Preserve, Florida. *Smithsonian Miscellaneous Collections*, 149(6):1–68.
- 1966a. Late Permian Trilobites from the Salt Range, West Pakistan. *Palaeontology*, 9:64–73.
- 1966b. A Permian Productoid Brachiopod, Life History. *Science*, 152:660–662.
- 1966c. Spine Arrangement and Life Habits of the Productoid Brachiopod *Waacenoconcha*. *Journal of Paleontology*, 40:1063–1069.
1966. [with G.A. Cooper] Permian Rock Units in the Glass Mountains, West Texas. *United States Geological Survey Bulletin*, 1244-E:EI–E9.
1968. Structural Adaptation in Two Permian Brachiopod Genera, Salt Range, West Pakistan. *Journal of Paleontology*, 42:1–32.
1969. [with G.A. Cooper] New Permian Brachiopods from West Texas. *Smithsonian Contributions to Paleobiology*, 1: 20 pages.

- 1970a. Brachiopods from Permian–Triassic Boundary Beds and Age of Chhidru Formation, West Pakistan. In B. Kummel and C. Teichert, editors, *Stratigraphic Boundary Problems: Permian and Triassic of West Pakistan. University of Kansas, Department of Geology Special Publication*, 4:117–151.
- 1970b. Brachiopods in the Permian Reef Environment of West Texas. *Proceedings of the First North American Paleontological Convention, Sept. 5–7, 1969, Part J*:1444–1481.
1970. [with F.G. Stehli] Permian Brachiopods from Huehuetenango, Guatemala. *Journal of Paleontology*, 44:23–36.
1971. Taxonomy and Autecology of Two Arctic Permian Rhynchonellid Brachiopods. In J. Thomas Dutro, Jr., editor, *Paleozoic Perspectives: A Paleontological Tribute to G. Arthur Cooper. Smithsonian Contributions to Paleobiology*, 3:313–335.
1971. [with E.E. Brabb] Stratigraphy and Paleontology of the Revised Type Section for the Tahkandit Limestone (Permian) in East-Central Alaska. *United States Geological Survey Professional Paper*, 703:1–26.
1971. [with F.G. Stehli] Permian Brachiopods from Axel Heiberg Island, Canada, and an Index of Sampling Efficiency. *Journal of Paleontology*, 45:502–521.
1972. The Lophophore and Feeding Mechanism of the Productidina (Brachiopoda). *Journal of Paleontology*, 46:213–248.
1972. [with G.A. Cooper] Permian Brachiopods of West Texas, I. *Smithsonian Contributions to Paleobiology*, 14:1–231.
1973. [with G.A. Cooper] Dating and Correlating the Permian of the Glass Mountains in Texas. In A. Logan and L.V. Hills, editors, *The Permian and Triassic Systems and Their Mutual Boundary. Canadian Society of Petroleum Geologists, Memoir*, 2:363–377.
1973. [and G.A. Cooper] Brachiopods and Permian Correlations. In A. Logan and L.V. Hills, editors, *The Permian and Triassic Systems and Their Mutual Boundary. Canadian Society of Petroleum Geologists, Memoir*, 2:572–595.
1974. [with G.A. Cooper] Permian Brachiopods of West Texas, II. *Smithsonian Contributions to Paleobiology*, 15:233–793.
1975. [with G.A. Cooper] Permian Brachiopods of West Texas, III. *Smithsonian Contributions to Paleobiology*, 19:795–1921.
1976. Permian Brachiopods from Southern Thailand. *Journal of Paleontology*, 50(3)supplement: 269 pages. [*Paleontological Society Memoir*, 9.]
- 1976a. [with G.A. Cooper] Permian Brachiopods of West Texas, IV. *Smithsonian Contributions to Paleobiology*, 21:1923–2607.
- 1976b. [with G.A. Cooper] Permian Brachiopods of West Texas, V. *Smithsonian Contributions to Paleontology*, 24:2609–3159.
1977. [with G.A. Cooper] Permian Brachiopods of West Texas, VI. *Smithsonian Contributions to Paleontology*, 32:3161–3370.
- 1980a. The Human Face of the Brachiopod. *Journal of Paleontology*, 54:499–507.
- 1980b. Koskinoid Perforations in Brachiopod Shells: Function and Mode of Formation. *Lethaia*, 13:313–319.
1981. Living Habits of Ancient Articulate Brachiopods. In J.T. Dutro, Jr., and R.S. Boardman, organizers, *Lophophorates, Notes for a Short Course. University of Tennessee, Department of Geological Sciences, Studies in Geology*, 5:127–140.
1987. Brachiopods of Enewetak Atoll. In D.M. Delaney and others, editors, *The Natural History of Enewetak Atoll, Volume 2, Biogeography and Systematics*, pages 77–84. U.S. Department of Energy.
1987. [with A.J. Rowell] Phylum Brachiopoda. In R.S. Boardman, A.H. Cheetham, and A.J. Rowell, editors, *Fossil Invertebrates*, pages 445–496. Palo Alto, California: Blackwell Scientific Publications.
1988. The Family Cardiarinidae (Late Paleozoic Rhynchonellid Brachiopoda). *Senckenbergiana Lethaea*, 69:121–135.
1990. [with B.R. Wardlaw] Conodont Biostratigraphy of the Permian Road Canyon Formation, Glass Mountains, Texas. *United States Geological Survey Bulletin*, 1895-A:A1–A18.
1990. [with B.R. Wardlaw, R.A. Davis, and D.M. Rohr] Leonardian–Wordian (Permian) Deposition in the Northern Del Norte Mountains, West Texas. *United States Geological Survey Bulletin*, 1881-A:A1–A14.
1991. [with C.K. Stropoli and B.R. Wardlaw] Wordian (Permian) Brachiopod Assemblages, Western USA. In D.I. MacKinnon, D.E. Lee, and J.D. Campbell, editors, *Brachiopods Through Time. Proceedings of the Second International Brachiopod Congress, University of Otago, Dunedin, New Zealand, 5–9 February, 1990*, pages 227–232. Rotterdam: A.A. Balkema.
1991. [with M.K. Nestell, A. Baud, and C. Jenny] Permian Stratigraphy of Hydra Island, Greece. *Palaios*, 6:479–497.
1992. [with B.F. Glenister and others] The Guadalupian: Proposed International Standard for a Middle Permian Series. *International Geology Review*, 34:857–888.
1992. [with Xu Guirong] Permo-Triassic Brachiopod Successions and Events in South China. In W.C. Sweet, Yang Zunyi, and Yin Hongfu, editors, *Permo-Triassic Events in the Eastern Tethys*, pages 98–108. Cambridge: Cambridge University Press.
- 1993a. The Brachiopod Family Gemmellaroidea. *Journal of Paleontology*, 67:53–60.

- 1993b. Permian Brachiopods from Khios Island, Greece. *Journal of Paleontology*, 67(4)supplement: 21 pages. [*Paleontological Society Memoir*, 33.]
1993. [with Shi Xiaoying] Jurassic Rhynchonellids: Internal Structures and Taxonomic Revisions. *Smithsonian Contributions to Paleobiology*, 73: 190 pages.
1994. [with Xu Guirong] Brachiopods Near the Permian-Triassic Boundary in South China. *Smithsonian Contributions to Paleobiology*, 76: 68 pages.



FRONTISPIECE.—Dick Grant, Bruce Wardlaw, Xu Guirong, and Shannon Rudine in the Sierra Del Norte, Texas.

1. Guadalupian Studies in West Texas

*Richard E. Grant, Bruce R. Wardlaw,
and David M. Rohr*

Murchison established the Permian System in the Ural Mountains of Russia in 1841. The first North American Permian fossils were discovered by Hall (1856) about 15 years later. The fossils, which were collected in New York State, were initially described as Carboniferous (Hall, 1856) but were subsequently recognized as Permian by Girty (1902). Benjamin F. Shumard (1858), however, was the first to place an unequivocal Permian designation on some North American fossils, which had been collected by his brother George G. Shumard from the Guadalupe Mountains in Texas. A half century passed before Girty (1908) made known an extensive Guadalupian fauna, although his field work in Texas and his study of this fauna already had led him to propose a Guadalupian “period” (Girty, 1902). Girty’s suggestion was accepted only when it was formalized as the Guadalupe Series by Adams et al. (1939). The “Guadalupian fauna” was based upon fossils that Girty collected in 1901 on an expedition headed by Robert T. Hill, a revered figure in Texas geology.

Hill (1901) was the first to recognize that the strata making up most of the south-facing scarp of the Glass Mountains (Sierra del Vidrio) are Paleozoic in age. Johan A. Udden visited the Glass Mountains and the nearby Del Norte Mountains in 1904 and published a description of the section near Altuda (Udden, 1907) in which he classified the rocks as Upper Carboniferous. Udden, Baker, and Böse (1916) named the Leonard, Word, Vidrio, and Gilliam formations in the Glass Mountains, and the next year Udden (1917) added the Wolfcamp, Hess, and Tessey formations, correlating the section there with units in the Delaware and Guadalupe mountains.

Philip B. and Robert E. King (brothers) mapped the Glass and Del Norte mountains for their doctoral dissertations at Yale University, under the direction of Carl O. Dunbar and Charles

Schuchert who were, at the same time, the graduate advisors of G. Arthur Cooper. Robert E. King (1931) described the Permian brachiopods and gave a faunal summary with worldwide correlations. Philip B. King (1931) described the geology and named the Altuda Member of the Capitan Formation (P.B. King, 1927), the Bissett Formation (then deemed entirely Triassic), and numbered the carbonate members of the Leonard and Word formations. Cooper and Grant (1964) gave names to the numbered members of the Word, calling “Limestone Number 1” the Road Canyon Member, “Number 2” the China Tank Member, “Number 3” the Willis Ranch Member, and “Number 4” the Appel Ranch Member. They followed P.B. King (1931) in considering the Vidrio a member of the Word. As studies continued, the Road Canyon took on increasing importance and a more “Leonardian” aspect, so Cooper and Grant (1966) elevated it to the rank of formation and removed it to the Leonard Series. The formation was accepted immediately, but the age assignment proved controversial. Fusulinid specialists insisted that because it contained *Parafusulina rothi* it was Guadalupian; ammonoid specialists saw *Perrinites* and agreed with the assignment to the Leonardian. Furnish (1966, 1973) sought to cleave the Gordian knot by creating a Roadian Stage, which he assigned to the Leonard Series. Attempts to stifle the new stage name (Grant and Wardlaw, 1984; Wardlaw and Grant, 1987, 1990) proved futile, and participants at the Guadalupian Symposium seemed to accept it wholeheartedly. Consensus did, however, support the age assignment by Wardlaw and Grant (1990) that placed the Leonardian–Guadalupian boundary at the change in conodont species from *Mesogondolella idahoensis* to *M. serrata* (now considered a synonym of *M. nankingensis*), within the lower part of the Road Canyon Formation. This placed the larger part of the formation, and the Roadian Stage, back into the Guadalupian where P.B. King (1931) had placed it originally.

The purpose of the Guadalupian Symposium was to determine if the Permian Period should be divided into three worldwide stages, instead of the currently recognized two. The participants had differing opinions on where reference sections

Richard E. Grant (deceased), Department of Paleobiology, National Museum of Natural History, Smithsonian Institution, Washington, D.C. 20560-0121. Bruce R. Wardlaw, U.S. Geological Survey, 926A National Center, Reston, Virginia 20192. David M. Rohr, Department of Geology, Sul Ross State University, Alpine, Texas 79832.

for the Lower Permian and the Upper Permian might be located; these are stated below in the individual contributions. We agreed by vote, however, that the Middle Permian should be the Guadalupian Stage, and that the reference section should be in the Guadalupe Mountains National Park, where the rocks are well exposed and access is assured. A formal statement that proposed such a move was submitted for publication in the proceedings of the International Congress on the Permian System of the World that was held at Perm, Russia, 1991, commemorating the 150th anniversary of the Permian System (Glenister et al., 1992). The papers presented herein provide detailed data that support the general area of West Texas as an appropriate region for study of the middle part of the Permian.

The most abundantly fossiliferous Permian rocks in the world are in the Glass Mountains. Thus, the first paper included herein presents a guide to localities there and in the Del Norte and Guadalupe mountains by the organizers of the symposium. The Glass Mountains cannot be designated an international reference section, however, because all of the land there is privately owned, and access cannot be guaranteed. The Guadalupe Mountains, on the other hand, are in a national park where they are accessible to all who obtain the proper permits from the U.S. Department of the Interior, National Park Service, Southwest Region, Santa Fe, NM 87501.

Wardlaw and Grant (1987, 1990) described the conodont zones in the Cathedral Mountain and Road Canyon formations of the Glass and Del Norte mountains. Wardlaw's paper herein continues that work for the Guadalupian of that region. Wilde then presses formal recognition of the Guadalupian Series as the standard for the Middle Permian of the world time scale, based to some extent on his zonation of the fusulinids. Fusulinid zones can be traced worldwide, except in the Arctic. The top of the Guadalupian can be correlated with the Dzhulfian of Iran via ammonoids of the section at Las Delicias, Mexico.

Wardlaw's field and museum work in China, in 1992, under the guidance of Jin Yu-gan revealed that *M. serrata* is a junior synonym of *M. nankingensis*, and more importantly, that the species is indeed worldwide in distribution. In addition, it marks a biostratigraphic level within the Permian that can be recognized wherever it occurs. This is the base of the Guadalupian. In China it occurs at the base of the Kuhfeng Formation, which may therefore be correlated to the lower part of the Road Canyon Formation in Texas. The change from *M. idahoensis* to *M. nankingensis* thus proves to be a recognizable horizon that can be taken as the base of the Guadalupian everywhere that Permian rocks occur, making the Middle Permian a viable worldwide stage. The top of the Guadalupian, of course, is defined by the base of the succeeding stage, which will probably be defined in China by a zone succeeding that of *M. altudaensis*. In Texas, the highest Guadalupian unit is the Altuda Formation in the Glass and Del Norte mountains and the Lamar Limestone Member of the Bell Canyon Formation in the Guadalupe and Delaware mountains. The youngest Permian conodont fauna within the Guadalupian units is found in the

uppermost part of the Altuda Formation and is highlighted by *M. altudaensis* (Kozur, 1992).

Harris emphasizes the lower part of the Guadalupian in an analysis of the Cutoff Formation of the Guadalupe Mountains. He presents three new members of that formation, which can be traced along the western escarpment. The Cutoff proves to be more complex than hitherto recognized, and it contains the Leonardian-Guadalupian boundary. Harris discusses correlations to the San Andres Formation farther north in the Guadalupe, and to the Road Canyon Formation to the south in the Glass Mountains. Harris, Lehrmann, and Lambert extend the discussion of the Cutoff, interpreting the environments in which the members were deposited. They make a detailed comparison with the Road Canyon Formation and offer an interpretation of that formation's relationship to the Permian basin and shelf.

The discussion is continued by Lambert, Lehrmann, and Harris, with emphasis on the place of the Cutoff in a proposed world stratotype for the Middle Permian. They accept the idea of a Roadian Stage based on conodont zones in the Road Canyon Formation, with the base of the Guadalupian defined on the transition from *Mesogondolella idahoensis* to *M. nankingensis*.

Wardlaw, Ross, and Grant build on earlier work by Wardlaw and Grant (1990) regarding the Road Canyon Formation by recognizing cyclic sedimentary packages that have the "fining upward" character that is seen so widely throughout the geologic column. The environmental setting for these packages was set forth by Stropoli, Grant, and Wardlaw (1991).

Yang and Yancey outline the fusulinid biostratigraphy of the Guadalupian region that makes it possible to serve as a world standard for the Middle Permian. They describe some new taxa based upon excellently preserved material that was newly collected by Yang from the Glass and Del Norte mountains.

The paper by Rathjen, Wardlaw, Rohr, and Grant presents a fresh view of the deposition of the Word Formation in its type area. The passage from shelf to slope to basin is marked by distinct facies within the carbonate members that lie within the generally siltstone matrix of the formation. The authorship reflects a thesis by Rathjen that was revised for publication by the supervising committee.

Rudine, Wardlaw, Rohr, and Grant offer an in-depth study of the Guadalupian rocks of the Del Norte Mountains. They clarify the status of the lower massive and upper massive members of the Capitan Limestone, and they describe carbonate mounds (buildups) in the upper part of the Word Formation that, heretofore, were thought to terminate in the Road Canyon. The discussion is continued by Wilde and Rudine, who focus upon fusulinid zones in the Altuda Formation of the western part of the Glass Mountains. They demonstrate the correlation of the Altuda to units in the Guadalupe Mountains, specifically to the Tansill Formation (a shelf unit) and the Lamar Limestone Member of the Bell Canyon Formation (a basinal unit). Wardlaw and Rudine divide the Altuda Formation into five informal units and demonstrate that the Altuda was deposited in shelf as well as basinal settings.

Haneef documents the shelf edge to basinal facies associated with the upper part of the Capitan Limestone. The collapse breccias that have been confused with the Capitan are assigned to the Tessey Formation, and an example of the unit is documented and interpreted by Haneef and Wardlaw.

Wardlaw, Rudine, and Nestell use conodont zones to correlate the Texas Guadalupian with rocks of the same age at Las Delicias, Coahuila, Mexico. The Permian section at Las Delicias is important to world correlations because it contains ammonoids, conodonts, and fusulinids that link the Texas sections to those of Armenia, Iran, and China. It contains Permian rocks with diagnostic fossils that are younger than any in Texas, so it is useful in defining the limits to the Guadalupian. Spinosa and Glenister emphasize these links from Texas to the world at large through northern Mexico, with prime focus upon the zonation of ammonoids. The Dzhulfian is demonstrably younger than the Guadalupian, and its base could define the top of the Guadalupian. The section at Las Delicias contains fossils that define this boundary.

The final paper, by Erwin and Kidder, addresses the phenomenon of silicification of fossils, a condition that is widespread in Permian strata. Certain fossils, such as brachiopods and echinoderms, are silicified more commonly and more completely than some others, such as bivalves and fusulinids. Erwin and Kidder explain these biases by reference to depositional conditions that favor silicification.

The Guadalupian Symposium was the culmination of a decade of cooperative Permian studies by the Smithsonian Institution, the U.S. Geological Survey, and Sul Ross State University. What began as an attack on the "Road Canyon problem" by Grant and Wardlaw burgeoned into a full scale survey of biostratigraphy and depositional environments of the entire section above the Wolfcampian in the Glass and Del Norte mountains and of the Guadalupian of the Guadalupe Mountains. The present volume testifies to the continuing and widespread interest in this important segment of the history of the Earth, the period that marked the end of the Paleozoic Era.

In the course of compiling this volume, it became obvious that the formational names needed to be standardized. Several new names are also introduced. Table 1-1 lists the names accepted for use in this volume.

TABLE 1-1.—Recognized Permian formation names and units in the West Texas area. (* not in GNULEX (1992).)

Altuda Formation
Bell Canyon Formation
Hegler Limestone Member*
Lamar Limestone Member*
McCombs Limestone Member*
Pinery Limestone Member*
Rader Limestone Member*
Bissett Conglomerate
Bone Spring Limestone
Brushy Canyon Formation*
Pipeline Shale Member*
Capitan Limestone
Castile Formation (Gypsum)
Cathedral Mountain Formation
Cherry Canyon Formation*
Getaway Limestone Member*
Manzanita Limestone Member*
South Wells Limestone Member*
Cutoff Formation* (redescribed by Harris, 1988a,b)
El Centro Member*, established this volume
Shumard Member*, established this volume (confusion from Glenister et al., 1992, where Shumard and Shumard Canyon Member are used interchangeably and Shumard Canyon is herein repressed)
Williams Ranch Member*, established this volume
Delaware Mountain Group
Gilliam Limestone
Goat Seep Limestone (Dolomite)
Grayburg Formation
Hess Formation
Lenox Hills Formation
Neal Ranch Formation
Queen Formation
Road Canyon Formation
Salado Formation
San Andres Formation (Limestone)
Seven Rivers Formation
Skinner Ranch Formation
Tansill Formation
Tessey Formation*, revised this symposium
Victorio Peak Limestone
Vidrio Formation*, revised this symposium
Word Formation
Appel Ranch Member
China Tank Member
Willis Ranch Member
Yates Formation
Yeso Formation

Literature Cited

- Adams, J.E., M.F. Cheney, R.K. Deford, R.I. Dickey, C.O. Dunbar, J.M. Hills, R.E. King, R.E. Lloyd, A.K. Miller, and C.E. Needham
1939. Standard Permian Section of North America. *Bulletin of the American Association of Petroleum Geologists*, 23(11):1673-1681.
- Cooper, G.A., and R.E. Grant
1964. New Permian Stratigraphic Units in Glass Mountains, West Texas. *Bulletin of the American Association of Petroleum Geologists*, 48(9):1581-1588.
1966. Permian Rock Units in the Glass Mountains, West Texas. *United States Geological Survey Bulletin*, 1244-E:E1-E9, plates 1, 2.
- Furnish, W.M.
1966. Ammonoids of the Upper Permian *Cyclolobus*-Zone. *Neues Jahrbuch für Geologie und Paläontologie, Abhandlungen*, 125: 265-296, plates 23-26.
1973. Permian Stage Names. In A. Logan and L.V. Hills, editors, *The Permian and Triassic Systems and Their Mutual Boundary. Canadian Society of Petroleum Geologists, Memoir*, 2:522-548.
- Girty, G.H.
1902. The Upper Permian in Western Texas. *American Journal of Science*, series 4, 14:363-368.

- 1909 ("1908"). The Guadalupian Fauna. *United States Geological Survey Professional Paper*, 58: 651 pages, 31 plates. [Date on title page is 1908; actually published in 1909.]
- Glenister, B.F., D.W. Boyd, W.M. Furnish, R.E. Grant, M.T. Harris, H. Kozur, L.L. Lambert, W.W. Nassichuk, N.D. Newell, L.C. Pray, C. Spinosa, B.R. Wardlaw, G.L. Wilde, and T.E. Yancey
1992. The Guadalupian: Proposed International Standard for a Middle Permian Series. *International Geology Review*, 34(9):857–888.
- GNULEX
1992. Geologic Names Unit Lexicon (GNULEX). In Stratigraphic Nomenclature Databases for the United States, Its Possessions and Territories, Compiled by M.E. MacLachlan, W.A. Bryant, T.W. Judkins, E.D. Koozmin, R.C. Orndorff, M.L. Hubert, C.R. Murdock, S.W. Starratt, J.R. LeCompte. *United States Geological Survey, Digital Data Series, DDS-6*. [Computer CD.]
- Grant, R.E., and B.R. Wardlaw
1984. Redefinition of Leonardian–Guadalupian Boundary in Regional Stratotype for the Permian of North America. [Abstract.] *27th International Geological Congress, Moscow, USSR, Abstracts*, 1:58.
- Hall, James
1856. Descriptions and Notices of the Fossils Collected upon the Route. In Whipple's Reconnaissance near the 35th Parallel. *United States Thirty-third Congress, Second Session, Senate Executive Document 78 and House Executive Document 91*, 4:99–105.
- Harris, M.T.
- 1988a. Sedimentology of the Cutoff Formation (Permian), Western Guadalupe Mountains, West Texas. In S.T. Reid, R.O. Bass, and P. Welch, editors, *Guadalupe Mountains Revisited, Texas and New Mexico. West Texas Geological Society, Publication*, 88-84:133–140.
- 1988b. Postscript on the Cutoff Formation: The Regional Perspective and Some Suggestions for Nomenclature. In S.T. Reid, R.O. Bass, and P. Welch, editors, *Guadalupe Mountains Revisited, Texas and New Mexico. West Texas Geological Society, Publication*, 88-84:141–142.
- Hill, R.T.
1901. Physical Geography of the Texas Region. *United States Geological Survey, Topographic Atlas of the United States*, folio 3:4.
- King, P.B.
1927. The Bissett Formation, a New Stratigraphic Unit in the Permian of West Texas. *American Journal of Science*, series 5, 14:212–221.
- 1931 ("1930"). The Geology of the Glass Mountains, Texas, Part I: Descriptive Geology. *University of Texas Bulletin*, 3038: 167 pages, 15 plates. [Date on title page is 1930; actually published in 1931.]
- King, R.E.
- 1931 ("1930"). The Geology of the Glass Mountains, Texas, Part II: Faunal Summary and Correlation of the Permian Formations with Description of Brachiopoda. *University of Texas Bulletin*, 3042: 245 pages, 44 plates. [Date on title page is 1930; actually published in 1931.]
- Kozur, Heinz
1992. Dzhulfian and Early Changxingian (Late Permian) Tethyan Conodonts from the Glass Mountains, West Texas. *Neues Jahrbuch für Geologie und Paläontologie, Abhandlungen*, 187(1):99–114, figures 1–21.
- Murchison, R.I.
1841. First Sketch of Some of the Principal Results of the Second Geological Survey of Russia. *Philosophical Magazine*, 19:417–422.
- Shumard, B.F.
1858. Notice of New Fossils from the Permian Strata of New Mexico and Texas, Collected by Dr. George G. Shumard of the United States Government Expedition for Obtaining Water by Means of Artesian Wells along the 32d Parallel, under the Direction of Capt. John Pope, U.S. Corps of Top. Eng. *Transactions of the Academy of Science of St. Louis*, 1(2):108, 113, 290–297.
- Stropoli, C.K., R.E. Grant, and B.R. Wardlaw
1991. Wordian (Permian) Brachiopod Assemblages, Western USA. In D.I. MacKinnon, D.E. Lee, and J.D. Campbell, editors, *Brachiopods through Time. Proceedings of the Second International Brachiopod Congress, University of Otago, Dunedin, New Zealand, 5–9 February 1990*, pages 227–232. Rotterdam: A.A. Balkema.
- Udden, J.A.
1907. Sketch of the Geology of the Chisos Country. *University of Texas Bulletin*, 93:18–27.
1917. Notes on the Geology of the Glass Mountains. *University of Texas Bulletin*, 1753: 59 pages.
- Udden, J.A., C.L. Baker, and E. Böse
1916. Review of the Geology of Texas. *University of Texas Bulletin*, 44: 164 pages.
- Wardlaw, B.R., and R.E. Grant
1987. Conodont Biostratigraphy of the Cathedral Mountain and Road Canyon Formations, Glass Mountains, West Texas. In D. Cromwell and L.J. Mazzullo, editors, *The Leonardian Facies in W. Texas and S.E. New Mexico and Guidebook to the Glass Mountains, West Texas. Society of Economic Paleontologists and Mineralogists, Permian Basin Section, Publication*, 87-27:63–66.
1990. Conodont Biostratigraphy of the Permian Road Canyon Formation, Glass Mountains, Texas. *United States Geological Survey Bulletin*, 1895-A:A1–A18, plates 1–4.

2. Guidebook to the Guadalupian Symposium

*David M. Rohr, Bruce R. Wardlaw, Shannon F. Rudine,
Mohammad Haneef, A. John Hall, and Richard E. Grant*

Introduction

Compared to the Guadalupe Mountains of Texas and New Mexico the depositional environments of the Permian strata of the Glass Mountains (and adjacent Del Norte Mountains) are less well known. In general, the Guadalupian facies in the Glass and Del Norte mountains changes from predominantly carbonate facies in the northeast to thicker clastic facies in the southwest. Philip B. King (1931) originally considered this trend to reflect an uplifted clastic source to the southwest, with carbonate facies developing away from the source area. Ross (1986) interpreted the eastern portion of the Road Canyon and Word formations to consist of shelf, shelf-edge bioherm, and reef facies, and the southwest area to consist of deeper water siliceous shale, clastic limestone, and basinal sandstone facies.

Probably the best known controversy in the Glass Mountains Permian involves the depositional environment of the Skinner Ranch Formation (Leonardian according to Ross, 1986; Wolfcampian according to Cooper and Grant, 1972) at its type section on Leonard Mountain. Cooper and Grant (1964) identified in situ patch reefs at the base of the section, which were subsequently interpreted as displaced limestone blocks deposited in a slope environment (Rogers, 1972; Cys and Mazzullo, 1978; Ross, 1986). Later Flores, McMillan, and Watters (1977) interpreted the same units as subtidal and intertidal deposits. The Skinner Ranch Formation illustrates the complexities involved in interpreting the paleogeography of the Glass Mountains. If the Skinner Ranch contains displaced blocks, some eroded from older units, it explains the occurrence of Wolfcampian fossils in the Skinner Ranch (Ross, 1986). The slope facies interpretation also is used to place the shelf edge at that time between the Skinner Ranch outcrops at Leonard Mountain and the lagoonal, backreef deposits of the Hess Formation to the east, although most of the actual shelf edge is not preserved (Ross, 1987:30).

David M. Rohr, Shannon F. Rudine, Mohammad Haneef, and A. John Hall, Geology Department, Sul Ross State University, Alpine, Texas 79832. Bruce R. Wardlaw, U.S. Geological Survey, 926A National Center, Reston, Virginia 20192. Richard E. Grant (deceased), Department of Paleobiology, National Museum of Natural History, Smithsonian Institution, Washington, DC 20560-0121.

Similar conflicting interpretations exist in younger rocks in the western facies of the Leonardian Guadalupian to the southwest in the Del Norte Mountains. Ross (1986, 1987) considered the western facies of the Road Canyon and Word formations to be basinal shales and turbidites. Wardlaw et al. (1990) and Rohr et al. (1987) have interpreted this area to be shallow intertidal to lagoonal environments adjacent to an uplifted area to the south.

The type section of the Road Canyon Formation is also a subject of disagreement and will be discussed in more detail later.

Conclusions from Recent Work in the Glass Mountains

Philip B. King (1931) superbly documented the geology of the Glass and Del Norte mountains. Most of his map units and his interpretations stand today. Over the last decade, collaboration between the Smithsonian Institution, the U.S. Geological Survey, Sul Ross State University, and Chevron Oil Co. has provided some critical observations that refine the depositional setting and the geology first described by King (1931). These key observations are as follows:

1. The lower massive member of the Capitan Limestone and the Vidrio Member of the Word Formation (the Vidrio is raised to formation status in this volume) are the same unit.
2. The Vidrio is unconformably bounded.
3. The supposed relationship of the Vidrio interfingering with the Altuda Formation does not exist. The Vidrio is everywhere unconformably overlain by the Altuda Formation or Gilliam Limestone, implying that the Altuda and Gilliam interfinger.
4. Permian rocks mapped as Capitan Limestone in, and along, the margin of the Hovey-Sheffield channel are actually post-Guadalupian. These rocks are collapse breccias, and they indicate an evaporitic basin and basin margin infill similar to the Castile Formation in the Delaware basin. This unit is herein referred to as a basinal or a breccia facies of the Tessey Formation.
5. The Word Formation generally shows a progression of lithofacies from bioturbated lime mudstone/wackestone with

crinoid-fusulinid packstone/grainstone channels to skeletal wackestone/packstone to peloidal packstone to siltstone. The bioturbated lime mudstone/wackestone with crinoid-fusulinid packstone/grainstone facies is commonly recrystallized or dolomitized and represents a shoal facies that was repeatedly exposed. The remaining lithofacies commonly appear in succession in section and are repeated in several cycles (shown as numbers in Figure 2-1).

6. Conodont distribution provides an important correlating tool. The changeover from a transitional morphotype of *Mesogondolella idahoensis* to *M. nankingensis* (= *M. serrata*)

is remarkably sharp in most sections and occurs within the basal few meters of cycle 2 of the Road Canyon Formation.

7. The Altuda Formation shows a wide variety of lithofacies, from shallow lagoon sediments to basinal turbidites.

8. Lithologically and paleontologically, the Road Canyon Formation is more allied with the Word Formation, which is where King (1931) originally placed it.

9. The top of the Skinner Ranch and Hess formations is marked by a karstic surface. The base of the overlying Cathedral Mountain Formation is generally conglomeratic,

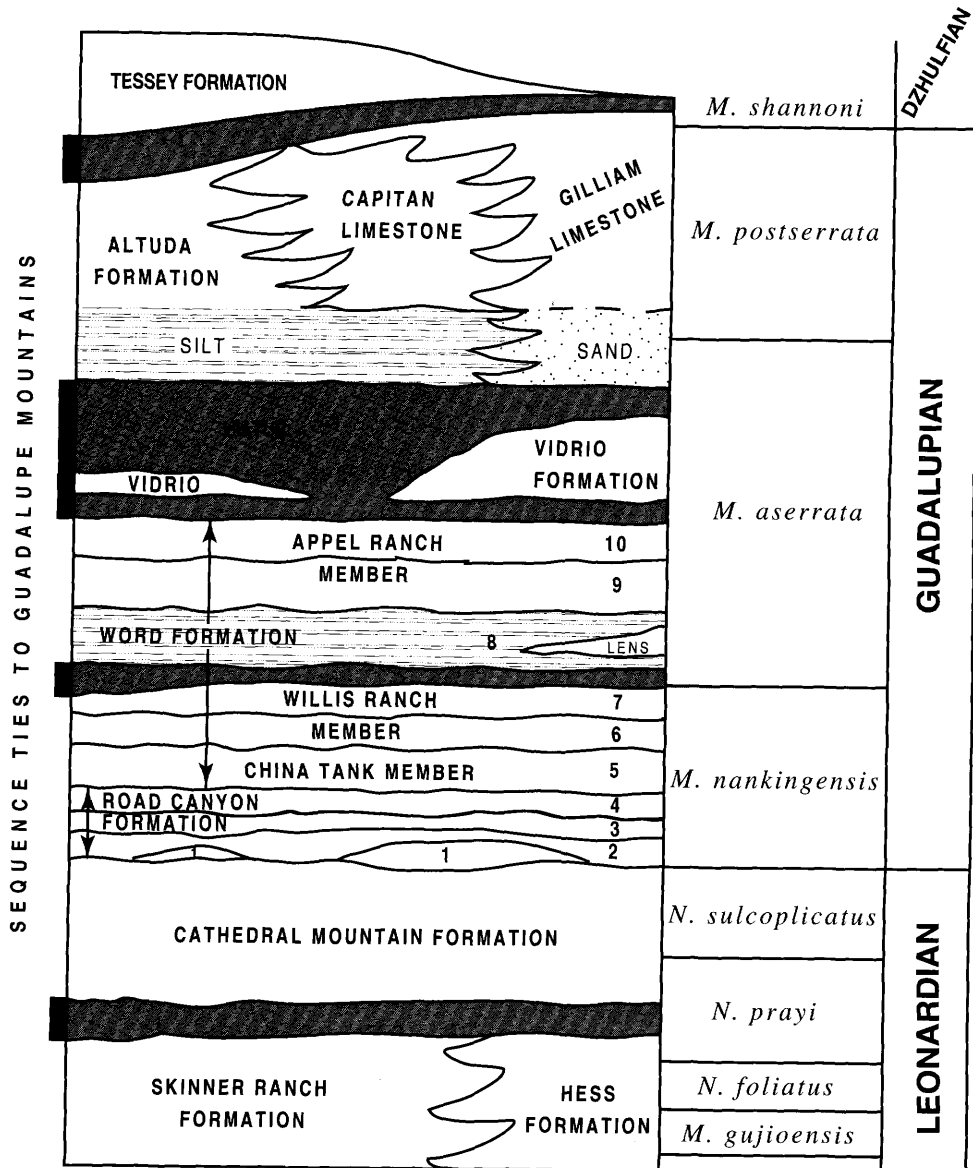


FIGURE 2-1.—General stratigraphic relations of Leonardian to Dzhulfian age rocks in the Glass and Del Norte mountains. Major sequence ties to the Guadalupe Mountains are shown at left. Cycles in the Road Canyon and Word formations are represented by numbers. The conodont zonation is shown at right. (*M.* = *Mesogondolella*; *N.* = *Neostreptognathodus*.)

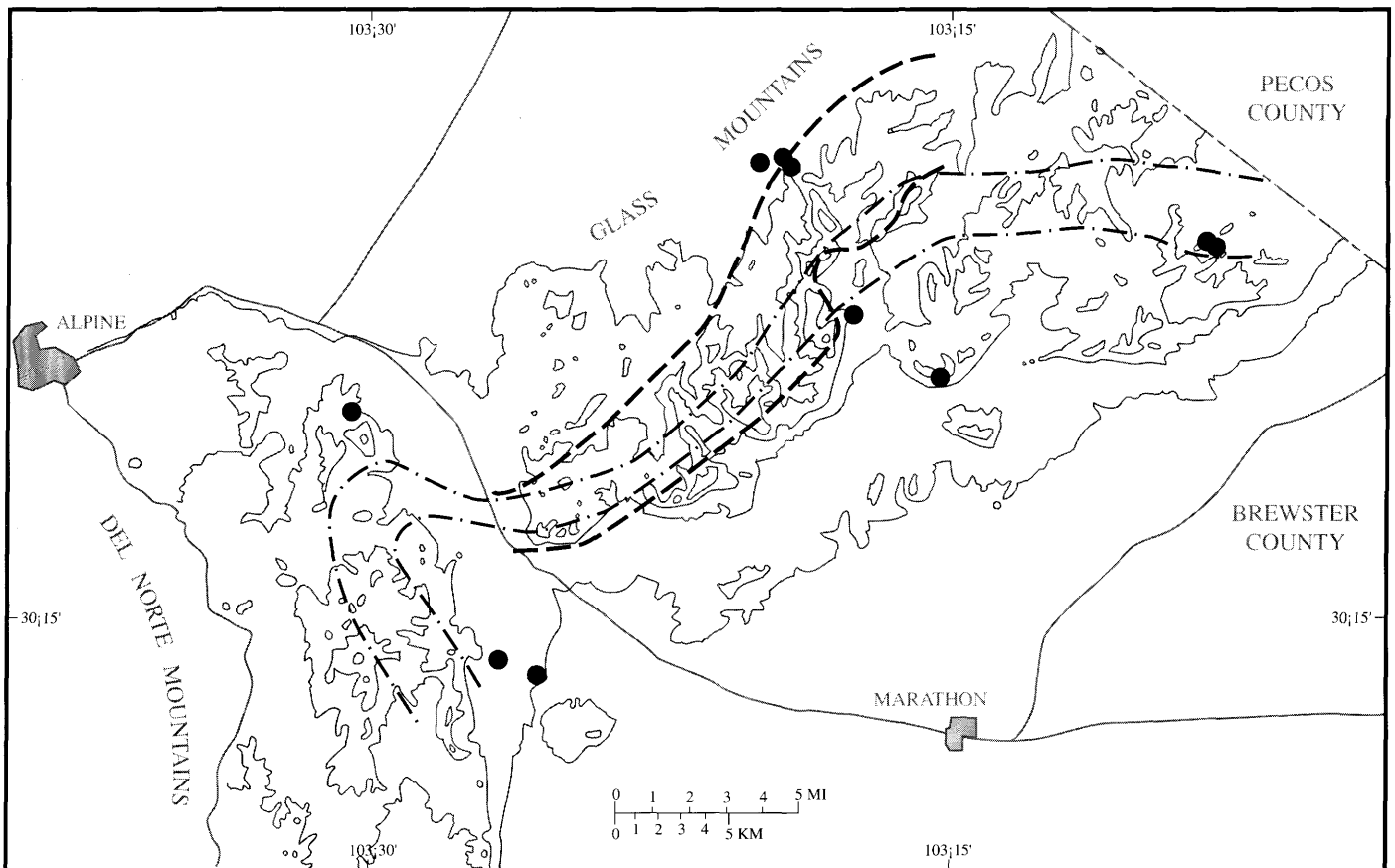


FIGURE 2-2.—Areal distribution of Capitan Limestone foreset beds (dashed lines), shelf margin crest to toe margin in general northwest direction, general distribution of shoal facies in Word Formation (dot-dashed lines), and relationship of proposed field trip stops (large black dots) to shelf margin facies.

indicating a major unconformity that ties exactly to the sequence boundary between the Yeso and lower San Andres formations in the Algerita Escarpment, northern Guadalupe Mountains.

10. The top of the Willis Ranch Member of the Word Formation is commonly recrystallized and dolomitized and indicates subaerial exposure. The unconformity represented by this surface ties with the Grayburg/Queen unconformity in the Guadalupe Mountains.

11. The Vidrio appears to correspond to the Manzanita Limestone Member of the Cherry Canyon Formation in the Guadalupe Mountains.

12. The Tessey breccia is equivalent to the Castile and Salado formations of the Delaware basin and unconformably overlies the Capitan Limestone.

The deposition of the Capitan Limestone and its equivalents is fairly straightforward and is summarized by Haneef et al. (1990:46):

Capitanian stratigraphy of the Glass Mountains is not as well documented as the type section in the Guadalupe Mountains. The Capitanian sequence is represented by the Altuda, Capitan, and Gilliam formations. The Altuda

Formation and Gilliam Limestone have disconformable lower contacts with the Vidrio Member of the Word Formation. The Altuda is siliciclastic, bioclastic, dolomitic wackestone to packstone interbedded with thin-bedded sandstone. The Gilliam Limestone is dolomitic fusulinid grainstone and stromatolitic dolostone interbedded with fine sandstone and possible evaporites and contains pisolite and tepee structures. The Capitan Limestone has an undulatory erosional lower contact with the Altuda Formation and is massive, dolomitic, heavily recrystallized mudstone to algal-sponge wackestone. The Capitan also grades into the Altuda in large foresets where the Altuda displays thin planar to graded bedding, slump structures, flow structures, and wavy channel bedding with channel lag. Conodonts and fusulinids demonstrate that the Altuda, where it underlies the Capitan, is equivalent to the lower Bell Canyon Formation, and, where it is laterally equivalent to the Capitan, it is equivalent to the upper Bell Canyon Formation. Lower Capitanian deposition is represented by dolomites and clastics of the Gilliam and Altuda formations in a shelf to slope transition on a ramp. Upper Capitanian deposition is represented by dolomites of the Gilliam, Capitan, and Altuda formations in a shelf, margin, and slope-basin transition on a platform.

The distribution of foresets of the Capitan Limestone can be mapped (Figure 2-2), and they represent a clear demarcation of the transition from a shelf margin to a basin. Recrystallized limestone and dolostone of the bioturbated lime mudstone/wackestone with crinoid-fusulinid packstone/grainstone chan-

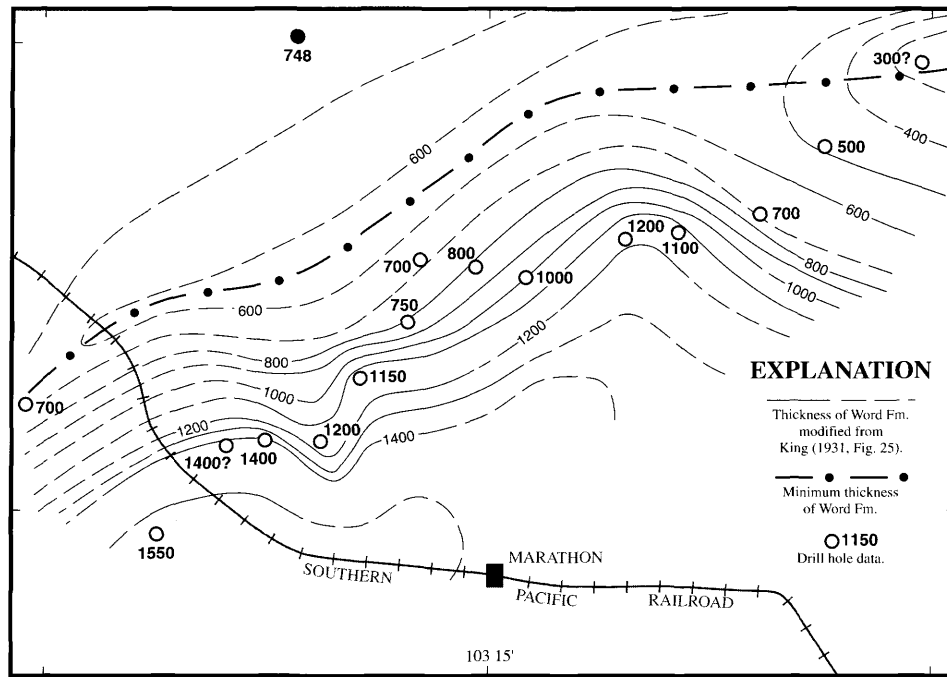


FIGURE 2-3.—Isopachous map of the Word Formation from King (1931, fig. 25) but modified by drill-hole data, showing area of minimum thickness as dot-dashed line.

nel facies (shoal facies) within the Word Formation show a similar trend to the foreset distribution (Figure 2-2), but they are slightly more shoreward. A modified isopach map of the Word (from King, 1931, with the addition of drill hole data) displays an area of minimum thickness that almost exactly follows the front of the shoal facies (Figure 2-3). The location of the Symposium's field trip stops are also shown on Figure 2-2, displaying their relationship to the proposed shoal-shelf margin.

Recently, Sarg et al. (1988) developed a sea-level curve based on the well-established sequence stratigraphy of the Guadalupe Mountains. This sea-level curve can be taken and compared to the sequence stratigraphy, conodont biostratigraphy, and depositional setting that has been developed for the Glass Mountains (Figure 2-4). In order to compare the Glass Mountains sequence to this curve, modeling has to be done without scale because the sea-level curve developed for the Guadalupe Mountains is based on the true thickness of the sequence. In subsequent publications modeling will incorporate true thickness and distance. The Glass Mountain sequence appears to show a relatively "deep" backbay of a foreland basin that was largely infilled during Cathedral Mountain deposition. This backbay, or lagoon, explains the relative shallow slope deposition that is observed in many of the Permian units.

The Del Norte Mountains contain an abundance of sand and silt sediments related to the encroachment of a delta complex from the uplifted Marathon Thrust Belt (Rudine et al., 1987).

Day 1: Alpine to Marathon, Dugout Mountain, Iron Mountain Ranch, Bruce Ranch

MILEAGE

Interval Cumulative

0.0	0.0	Head eastward on U.S. 90 from entrance #2 of Sul Ross State University, Alpine. Most of the rocks in the immediate Alpine area are Tertiary volcanics. To the west is Twin Peaks (elev. 6084), a syenite intrusion. In the distance to the north are the Davis Mountains, containing Tertiary volcanics of Oligocene to Eocene age and minor exposures of Cretaceous rocks. The highest peak in the Davis Mountains is Mt. Livermore at 8381 ft. Sul Ross State University is located on Hancock Hill, which is composed of the Eocene Crossen Trachyte with minor interbeds of fresh-water limestone (Collinsworth and Rohr, 1986).
7.4	7.4	Junction with U.S. 67 (to Ft. Stockton); continue straight on U.S. 90, now heading south-eastward. Ahead are the Glass Mountains on the left side of the road and the Del Norte Mountains to the right. The highest portions of the Glass Mountains now visible are the Capitan Limestone. Cretaceous limestone is

present south of the road and on the lower slopes to the northwest.

2.8 10.2 The quarry on the left side of the road is in Cretaceous limestone. The roadcut immediately beyond the quarry exposes Cretaceous limestone lying unconformably over Upper Permian (Tessey) limestone (Figure 2-5). Altuda (or Bird) Mountain to the right (Figure 2-21) consists of 73 m of Cretaceous limestone overlying cliff-forming Upper Permian limestone breccias. Below the cliffs are interbedded siltstones and limestones of the Word and Altuda formations. To the right of the peak is Bird Mine and a resistant breccia pipe.

In many previous guidebooks, the cliff-forming unit has been identified as Capitan reef facies prograding over basinal Altuda. A recent study (Wardlaw et al., 1990) has shown this

interpretation to be incorrect. In this area, the Word Formation and the underlying Cathedral Mountain Formation (Leonardian) are shallow, intertidal deposits of siltstone, sandstone, and limestone. The Road Canyon equivalent is a deltaic sequence containing fossil leaves (Mamay et al., 1985, 1988) and silicified wood. The overlying Altuda to the south of Bird Mountain contains tidal channels and tidal flats; deeper shelf-slope facies are found in the Bird Mine area. The post-Guadalupian (Dzhulfian) collapse breccia was formed by the solutioning of evaporite (sabkha?) deposits.

0.6 10.8 Bissett Mountain is in the background at 9 o'clock. It is capped by Lower Cretaceous limestones, and the main slopes are composed of limestone conglomerates and red beds of the Bissett Formation. Bissett conglomerate, sand-

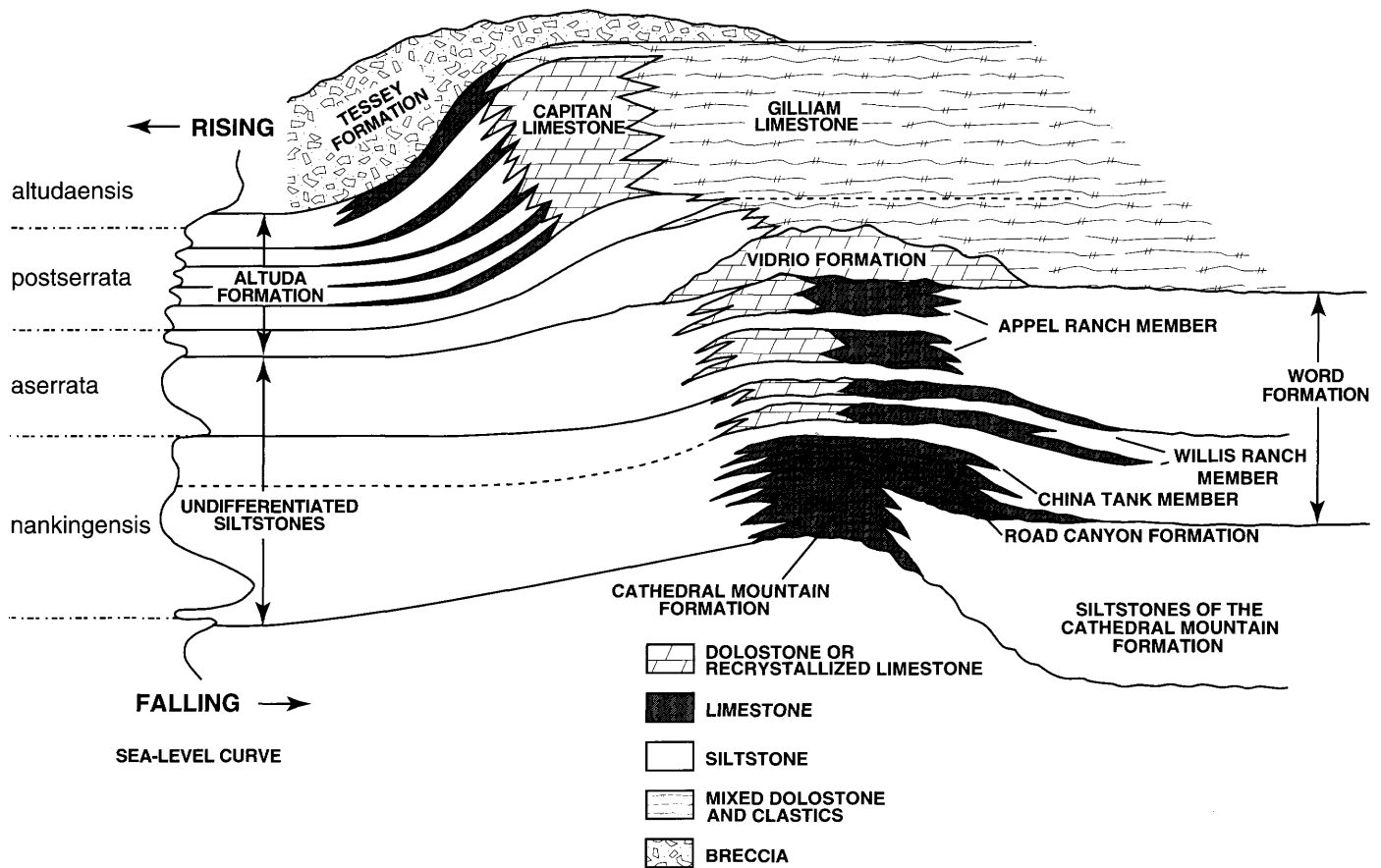


FIGURE 2-4.—Model of depositional setting and sequence stratigraphy of the Glass Mountains in relation to the sea-level curve of Sarg et al. (1988) for the sequence in the Guadalupe Mountains. The sequence ties to the Guadalupe Mountains are shown as solid lines (dashed where inferred or unknown). Conodont datums (zone boundaries) are shown as dot-dashed lines. The curve fits well the depositional sequence in the upper part, implying that both are responding to the same eustatic signal. The lower depositional sequence does not, implying that it is driven by local tectonics.

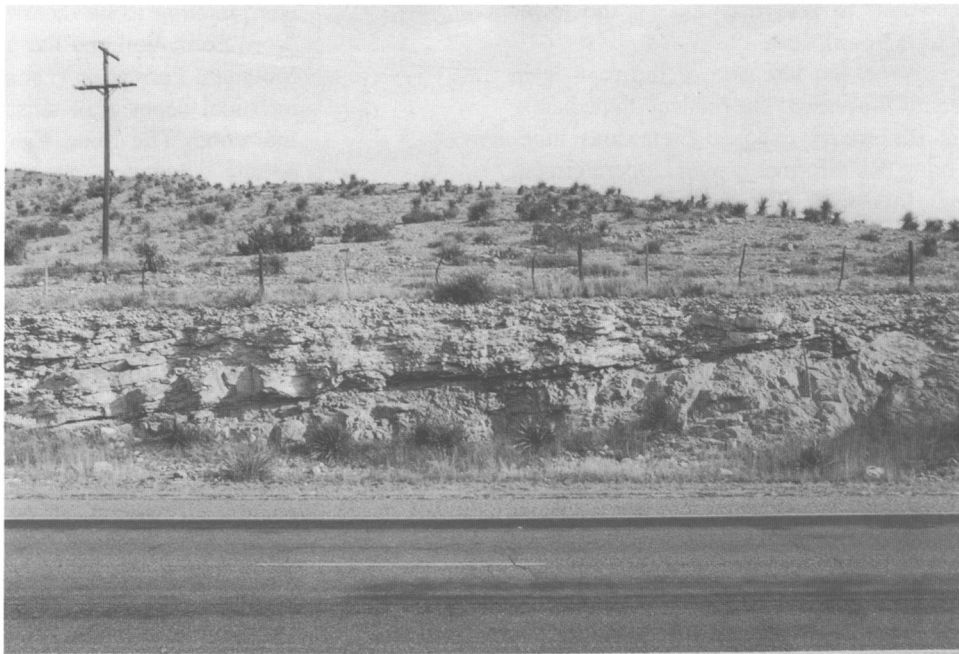


FIGURE 2-5.—Section along U.S. 90 showing Cretaceous limestone unconformably overlying Upper Permian (Tessey) limestone.

stone, and shale unconformably overlie the Permian Tessey Limestone here. An angular unconformity separates the Bissett Formation from the overlying Fort Terrett Formation (Cretaceous). The Bissett Formation has been shown by Wilcox et al. (1986, 1987) to be Cretaceous and not Triassic as previously thought.

- 2.3 13.1 Altuda siding.
- 1.9 15.0 Approximate top of Altuda Pass. To the south, the low hills nearest the road are the Vidrio and Altuda formations, which make up the nose of a north-trending anticline. To the north, the lower slopes are Word siltstones, the limestone bed about mid-slope is Appel Ranch-equivalent limestone, the upper ledge of the hill is Vidrio, and the cap is Altuda. The upper surface of the Vidrio is irregular along the unconformable contact.
- 1.4 16.4 Road bends to the left. To the left is the Vidrio Formation. King (1931) recognized three members in the Capitan Limestone: the lower massive, the Altuda, and the upper massive. Later, King (1937) combined the lower massive and Altuda members into an undivided Capitan on his geologic map, but in the text he considered the lower massive to be equivalent to the lower tongue of the Vidrio Member. Conodont biostratigraphy suggests that the

Vidrio (lower massive of King, 1931) is age-equivalent to the upper part of the Word Formation in the Glass Mountains; therefore, it is Wordian, not Capitanian in age (Rudine et al., 1987). Capitanian and Wordian strata are separated by an unconformity (Rudine et al., 1988). The unconformity is expressed in the Del Norte Mountains by the irregular preservation and thickness of the Vidrio Formation. In the Glass Mountains it is expressed by an undulatory surface on top of the Vidrio Formation. The Altuda Formation overlies the Vidrio in the Del Norte Mountains and western Glass Mountains, and the Gilliam Formation overlies the Vidrio in the eastern Glass Mountains. The Vidrio is generally recrystallized to dolostone and displays a karstic upper surface in the Del Norte Mountains. The unconformity appears to mark the change in fusulinid faunas from those dominated by *Parafusulina* below, to those dominated by *Polydiexodina* above. The conodont zone of *Mesogondolella aserrata* spans the unconformity, occurring in units above and below. These relationships compare directly to the well known unconformity above the Goatseep/Manzanita in the Guadalupe Mountains and imply that the Word-Capitan formational boundary is marked by an unconformity that may be correlated throughout the world.



FIGURE 2-6.—View of Cathedral Mountain representing the front of the Glass Mountains on the way to Marathon. The Road Canyon Formation caps the low cuesta on the right. Word Formation clastics form the highly dissected slopes below the massive dolomite cliffs of the Vidrio Formation. The Vidrio Formation unconformably overlies the Word Formation in this portion of the Glass Mountains. Here, the Vidrio Formation can be subdivided into three members, each of which is unconformably bound. The Altuda Formation unconformably overlies the Vidrio Formation. Shelf margin carbonates of the Capitan Limestone form the hill behind Cathedral Mountain.

Straight ahead and to the left of the road are the Lenox Hills. A broad valley to the left of the road gives a view of the scarp face of Cathedral Mountain, with the high knob of Sullivan Peak in the distance to the northeast (Figure 2-6). The long, low dipping slope just below Sullivan Peak, extending out into the valley and nearly closing its upper end, contains the upper part of the Cathedral Mountain Formation. The Cathedral Mountain Formation is capped by the Road Canyon Formation, which forms the northwest dipping upper surface.

- 3.5 21.0 Turn off to right to Catto-Gage Ranch. Dugout Mountain is the large cuesta to the east of the north-south trending Del Norte Mountains (Figure 2-7). The Del Norte Mountains are the upthrown side of a linear fault that exposes the Cathedral Mountain through Road Canyon and basal Word formations in its lower part. The major part of the scarp, particularly to the south, is Cretaceous limestone. Dugout Mountain consists of the Pennsylvanian Gaptank Formation on the eastern slopes and the Permian Lenox Hills through Skinner Ranch formations on the upper slopes. Coombs (1990) completed

a detailed study of Dugout Mountain, and his results are summarized below.

At Dugout Mountain the Lenox Hills and Skinner Ranch formations represent deposition in fluvial and shallow marine environments along the southern shelf of the Delaware basin. Intense deformation to the south created an uplifted source area along the toe of the Dugout and Marathon allochthons from which terrigenous sediments were derived. During Skinner Ranch deposition, coarse pebble-cobble-boulder conglomerate with shallow-marine bioclasts, and coarse sandy skeletal packstones developed as sheetflood- and debris-flow deposits on the distal fan-delta. Conglomerates of the Decie Ranch Member of the Skinner Ranch were deposited in response to renewed tectonic activity along the Marathon foldbelt through earliest Leonardian time, producing local avalanche/landslide deposits with a maximum clast size of 40 m. The remainder of the Skinner Ranch deposition was marked by a prolonged period of relative tectonic quiescence. Fan deltas prograded into the Delaware



FIGURE 2-7.—View of Dugout Mountain. STOP 1.2 is just outside frame of photograph NE of Dugout Mountain.

basin, forming a complex delta plain composed of intertidal siltstones with meandering tidal channel deposits of sand and pebble conglomerates. Trace fossils of the *Scoyenia* ichnofacies suggests at least intermittent exposure of the delta plain.

- 0.2 21.7 Railroad crossing.
- 0.1 22.0 Road forks, take middle fork (private ranch road).
- 4.1 26.1 Proceed on main ranch road to Payne Ranch site of the Catto-Gage Ranch until junction. Continue straight.
- 1.3 27.4 Follow dirt track past substation to STOP 1.1 (Figure 2-8), which is the Road Canyon Formation (Figure 2-9) and USNM loc. 732z. This abundant ammonoid locality was mapped as a limestone channel in the basal unit of the Word Formation (Rudine, 1988). Furnish and Glenister (in Cooper and Grant, 1977:3308) noted that "this locality, discovered by Cooper and Grant about 1965, has been the source of the largest collection of Permian ammonoids in West Texas. It is also a critical locality in that it combines faunal elements from the basin with those normally found on the shelf and is believed to provide a basis for detailed correlation from the Glass Mountains to the Guadalupe." Furnish and Glenister also provided the following faunal list:

Agathiceras uralicum (Karpinsky)
Epithalassoceras n. sp.
Eumedlicottia whitneyi (Böse)?
Glassoceras normani (Miller and Furnish)
Paraceltites elegans Girty
Peritrochia erebus Girty
 ?*Propinacoceras* sp.
Pseudogastrioceras cooperi Miller?
Texoceras texanum (Girty)

Wilde (in Cooper and Grant, 1977:3316) identified the following fusulinids from USNM loc. 732z:

Parafusulina attenuata Dunbar and Skinner [abundant]
P. boesi Dunbar and Skinner [abundant]
P. splendens Dunbar and Skinner [not common]

A silty fusulinid skeletal packstone is overlain by an irregular channelform of massive cherty, silty (sponge) skeletal packstone at the base of the outcrop in the Road Canyon Formation (Figure 2-10). Fusulinids are common in the silty skeletal packstone channels above and below USNM loc. 732z.

- 0.6 28.0 Return on dirt track, but turn left on track heading to substation.
- 0.5 28.5 Continue to knob to the south, which is the dip slope of the Road Canyon Formation, STOP 1.2

(Figure 2-8). Studies by Rudine et al. (1987) of the sedimentary structures, petrology, and paleontology of the carbonates and clastics of the Cathedral Mountain, Road Canyon, Word, Vidrio, and Altuda formations in the Del Norte Mountains indicate deposition in a delta-fan complex on a shallow shelf, and in a tidal lagoon for various units of these formations. Channel conglomerates, overbank deposits, stromatolitic limestones, and abundant sedimentary features indicate shallow shelf/delta deposition of these units. Paleontological evidence includes shallow-shelf conodont biofacies and abundant, excellently preserved leaves and logs that occur in parts of the section (Figure 2-10). The outcrop here displays several sedimentation cycles dominated by the peloidal packstone facies. Note the weathering, jointing, and chertification pattern at the top of the outcrop. This rectangular pattern is common

to the top of peloidal packstones throughout the Road Canyon and Word formations.

0.3	28.8	Return to main road to Payne Ranch site. Turn left.
0.4	29.2	Return to junction of main road and road to Payne Ranch site and backtrack to U.S. 90.
4.4	33.6	Turn right on U.S. 90 and head east to Marathon. To the left of the road are the Decie Hills, which are composed of the Skinner Ranch Formation. Massive white <i>Scacchinella</i> beds are visible near the end of the hills. The deposition of these beds, as with many others in the Glass Mountains, are controversial as it is unknown whether they are displaced reef blocks or in-place bioherms.
4.2	37.8	Roadcut on the right side of the road is USNM loc. 708b. The upper ledge of limestone is Wolfcampian (Neal Ranch Formation?) unconformably overlying the Pennsylvanian Gaptank Formation.

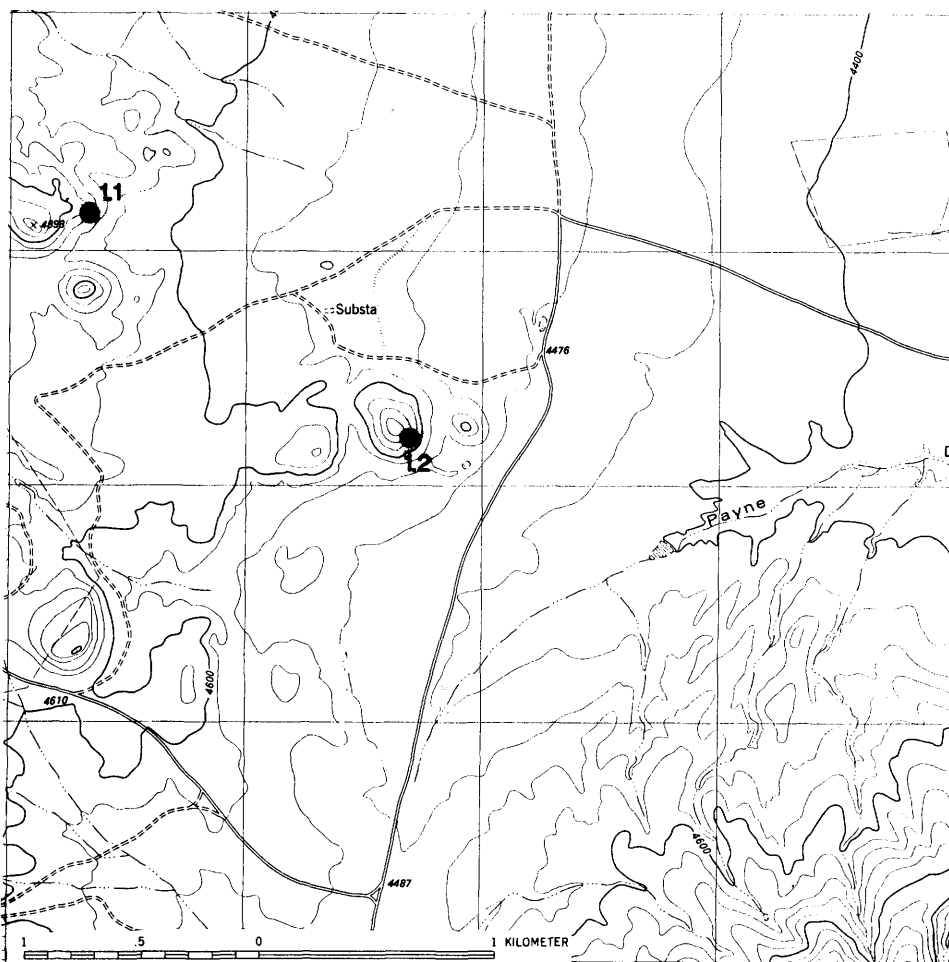
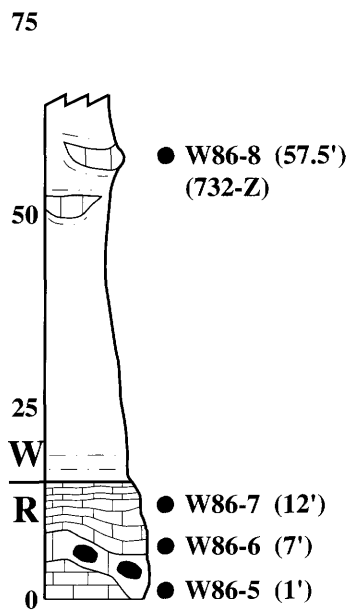


FIGURE 2-8.—Location of STOPS 1.1 and 1.2; Dugout Mountain 7.5 min. quadrangle.



FIGURE 2-9.—View of STOP 1.1. Ledge is Road Canyon Formation. Section goes through ledge to barely perceptible lens on hill above, which laterally yields abundant ammonoids.

STOP 1.1



STOP 1.2

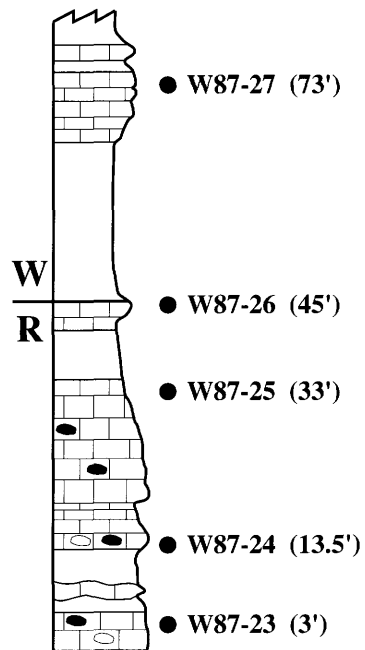


FIGURE 2-10.—Columnar sections of STOPS 1.1 and 1.2. (R = Road Canyon Formation; W = Word Formation.)

- 7.2 40.8 Proceed on U.S. 90 through Marathon. Turn left just before Exxon station at east end of town.
- 0.3 41.1 Turn right at end of street.
- 1.5 42.6 Go one block east and turn north onto dirt road. Proceed to Iron Mountain Ranch entrance and continue through gate (private road).
- 4.9 47.8 Road enters from right; turn right over cattle guard. Iron Mountain Ranch headquarters is on the left. Leonard Mountain, on the right, exposes the Haymond, Gaptank, Lenox Hills, and Skinner Ranch formations. The western slope of Leonard Mountain and the hill to the north contain the type sections of the Skinner Ranch, Cathedral Mountain, and Road Canyon formations of Cooper and Grant (1964).
- 0.3 47.8 Road crossing, continue straight.
- 0.2 48.0 Road forks, stay left. Right fork goes to skeet range.
- 0.3 48.3 Road forks, turn right.
- 1.6 49.9 Continue on dirt track bearing right at fork in track at 0.7 miles. Stop at water trough. To the north is STOP 1.3 (Figure 2-11), the cliffy outcrop of the Road Canyon Formation type section. The lower slopes are the Cathedral Mountain Formation. The climb to the Road Canyon stratotype is very strenuous. In the gully immediately north of the water trough, conglomeratic ammonoid and sparse brachiopod-bearing beds of the middle part of the Cathedral Mountain Formation are exposed and may prove of interest to those not making the climb.

Mesogondolella idahoensis is common to the top bed exposed in the gully. *Xaniognathus abstractus*, *Neostreptognathodus sulcopicatus*, *Sweetina festiva*, and sponge spicules are rare. In the middle of the exposed beds scattered ammonoids can be found and only sparse *Sweetina festiva* is recoverable.

Cooper and Grant (1964) proposed replacing King's (1931) First Limestone Member with the Road Canyon as a member of the Word Formation. Later, Cooper and Grant (1972) moved the Road Canyon to the Leonardian. The type section was designated by Cooper and Grant (1964, 1972) along King's (1931) section 17, which is the same as Cys' (1981) proposed lectostratotype (Figures 2-12-2-15). The Road Canyon Formation has worldwide significance as a candidate for a Permian stratotype to define the base of the Guadalupian and the Lower/Middle Permian boundary. The boundary is defined by a marked changeover in conodont faunas from a transitional morphotype of

Mesogondolella idahoensis to *M. nankingensis* and by a nearly simultaneous change in fusulinid faunas from the *Parafusulina boesi* zone to the *P. rothi* zone.

Interpretations of the depositional setting of the Road Canyon type section are varied. Cooper and Grant (1972:65) described the lower part of the Road Canyon type section as "bioherms with *Coscinophora* at the base, followed by bioherms abounding in *Hercostria*." In their "concluding remarks" section, Cooper and Grant (1977:3330) stated,

We had no problems with the Road Canyon fauna until we started work in the hills northwest of the Hess Ranch. On the east side of hill 5801 exposures are excellent, the sequence fairly well provided with bioherms at the base and near the top. Here we noted some brachiopods with Word affinities such as *Echinosteges*, *Costispinifera*, *Spiriferella*, and *Paucispinifera*. We suspected a possibility of having collected float blocks from the Word (Willis Ranch Member) higher on the hill, but a close search of the slopes revealed no blocks.

Lehrmann (1988:123-124) interpreted the lower portion of the type section to represent a thick megabreccia interval, which he said

represents at least two amalgamated deposits. This interpretation is made on the basis of hints of internal bedding and the transition from *Mesogondolella idahoensis* to *M. serrata* [= *M. nankingensis*] occurring near the middle of this interval. A debris flow deposit generally contains no internal bedding. Possible internal bedding near the middle of the interval might represent the interface between two amalgamated debris flow units. A single debris flow deposit is deposited essentially instantaneously. Clasts and fossils within a debris flow deposit are generally randomly distributed. If the thick megabreccia interval represented a single debris flow deposit, it should not contain the transition from *M. idahoensis* to *M. serrata* (ie. the conodonts should be randomly distributed). Therefore, the thick megabreccia interval probably represents at least two amalgamated debris flow deposits with the conodont transition occurring between deposits.

Yancey (1989, in litt.) also favored a megabreccia origin for the lower Road Canyon with lenticular conglomerate channel fills that have exposed, through erosion, as much as 9 m of the underlying units.

Measures and Wardlaw (1990:309) pointed out that a heavy diagenetic overprint obscures many primary features of the breccia in the lower part of the type section and referred to this portion of the section as a paleokarst. They overstated their case, probably to stay in keeping with previous workers.

The paleokarst is formed of a chaotic mixture of poorly sorted boulders in a matrix of quartz silt, iron-rich clay, and whole-body fossils. The boulders are composed of carbon-

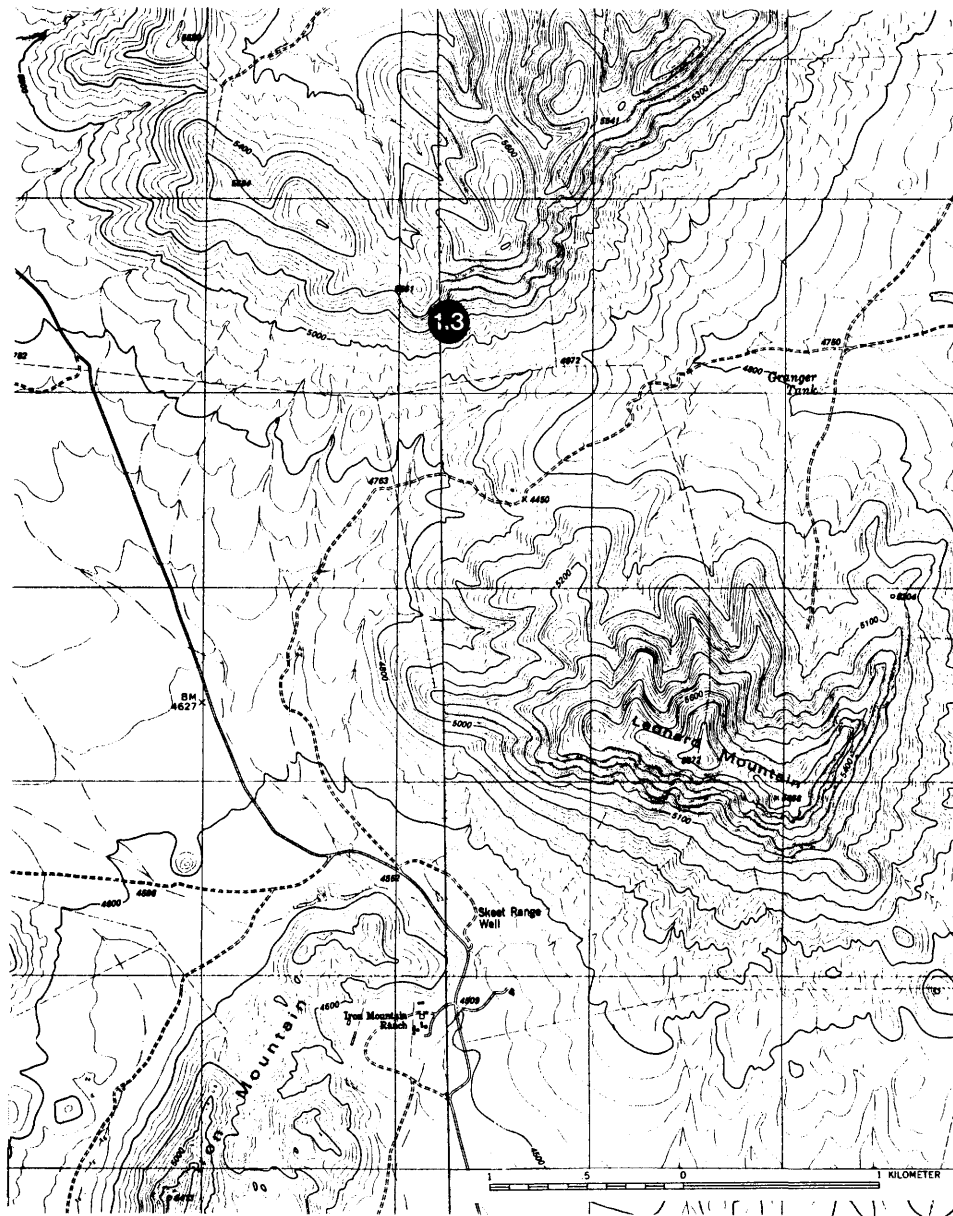


FIGURE 2-11.—Location of STOP 1.3, the type section of the Road Canyon Formation; Iron Mountain Ranch, Leonard Mountain, and Gilliland Peak 7.5 min. quadrangles.

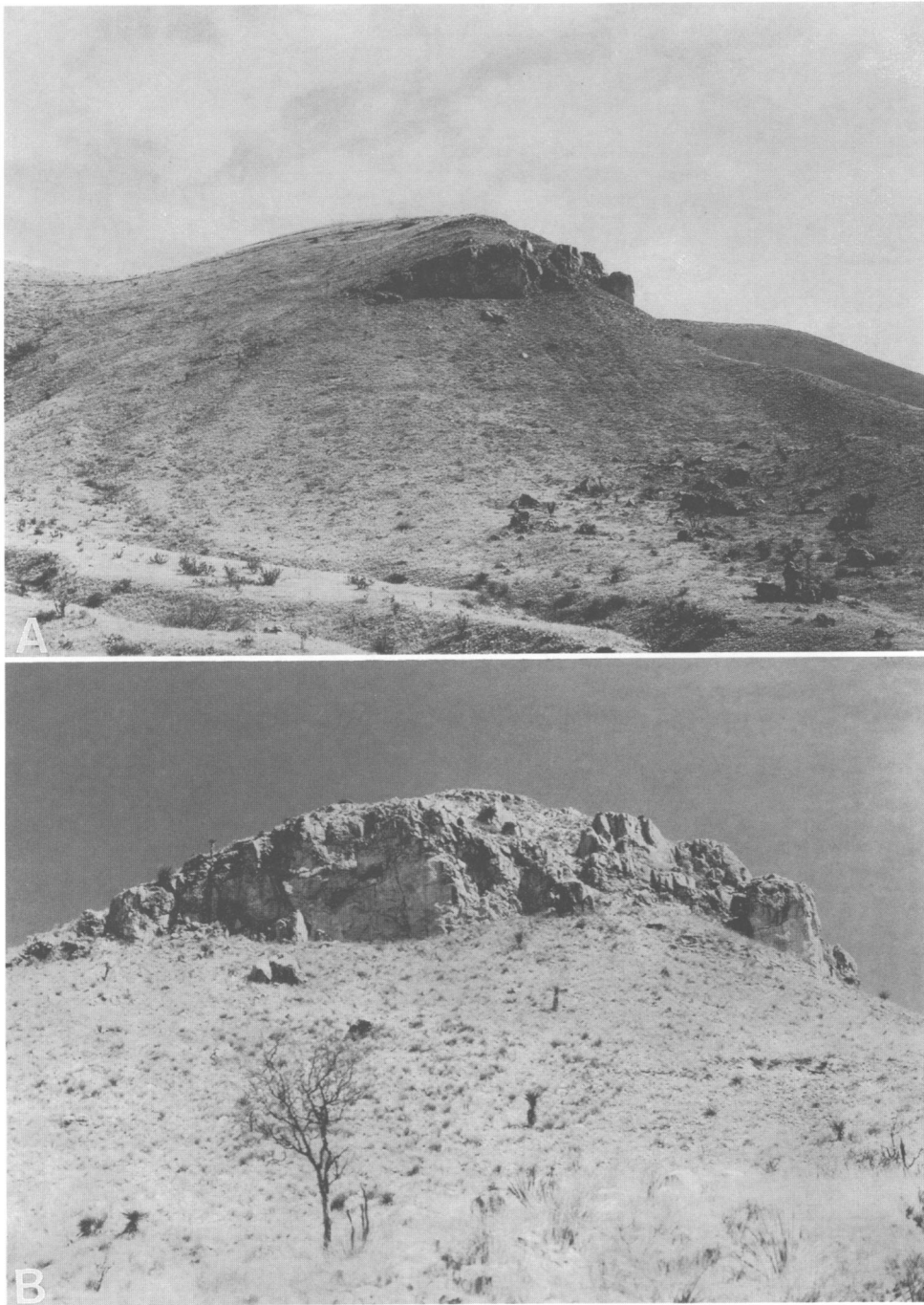


FIGURE 2-12.—Views of the Road Canyon Formation type section at STOP 1.3: A, from the west; B, from the south, immediately below outcrop.

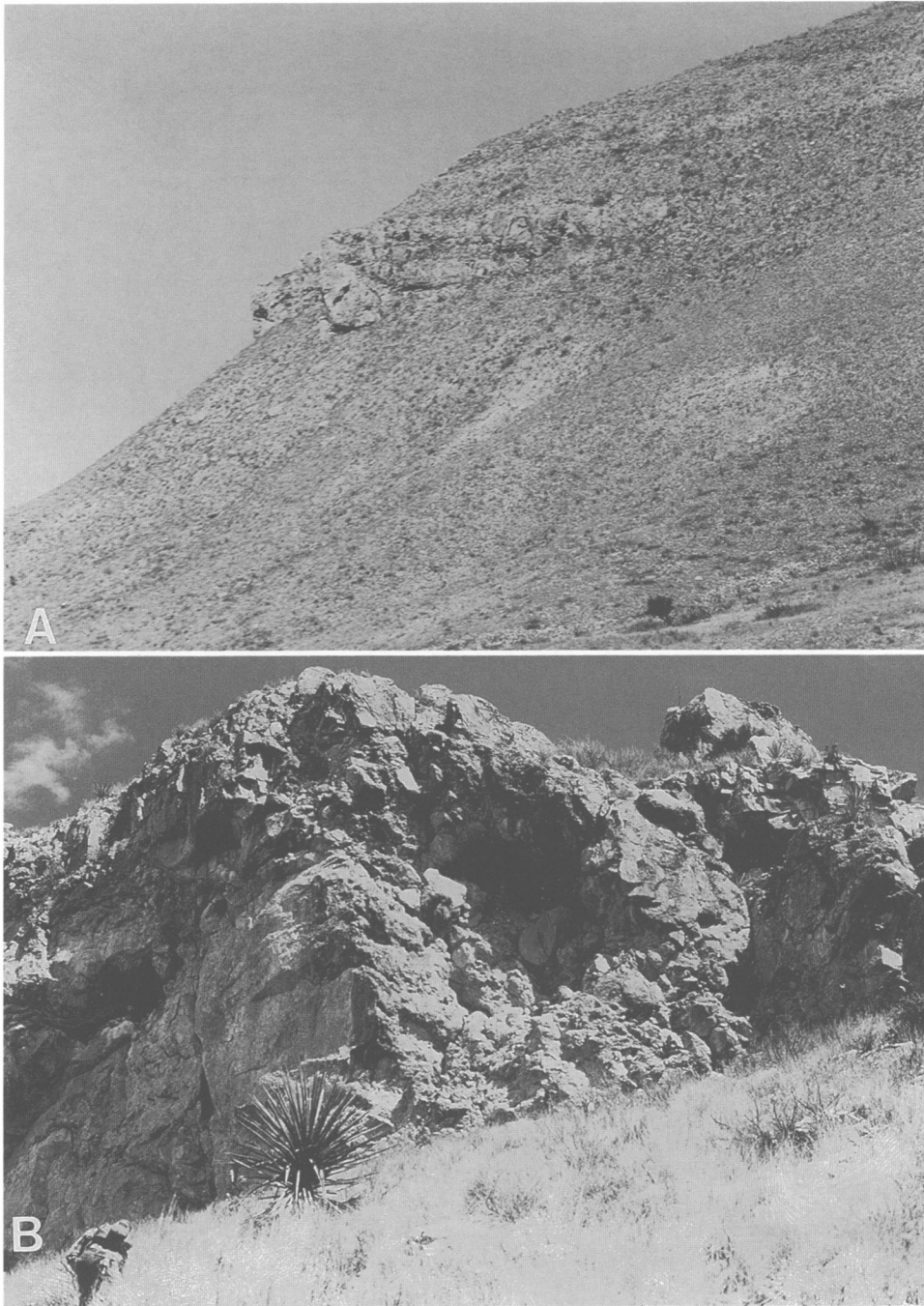


FIGURE 2-13.—Views of the Road Canyon Formation type section at STOP 1.3: A, from the east; B, close-up showing breccia.



FIGURE 2-14.—Breccia in the lower part of Road Canyon Formation type section at STOP 1.3.

ates of normal marine, shallow-shelf deposition found as normally bedded deposits adjacent to the paleokarst. The matrix shows extensive dissolution of grains, contains no large spar-filled voids, and is cemented by fine crystalline carbonate. The matrix is non-luminescent to rarely dully luminescent indicating a large freshwater component. Extensive dissolution and lack of blocky spar cement and flow stone deposits indicate presence of waters undersaturated with calcium carbonate and possibly an arid environment at the time of cave collapse. The conodonts are corroded, fractured, and broken throughout the paleokarst interval and show mixing only in this section compared to 17 other measured sections.

Lehrmann (1989, in litt.) noted that “the Road Canyon Formation is best exposed at its type section; however, the type section exposes some of the most complex stratigraphy in the Road Canyon Formation. Understanding of the sedimentologic and stratigraphic relationships here is crucial to erecting correct biostratigraphy.”

- 1.6 51.5 Return to main dirt road and turn right.
- 3.7 55.2 Proceed on main road up Gilliland Canyon to fork in road; take sharp left to paved road that leads to the Blakemore Hacienda. While traveling up Gilliland Canyon, note the small clay slide on the cuesta that contains the Road Canyon stratotype just visited. Immediately above the small clay slide, which is in the upper part of the Cathedral Mountain Formation, is section RC II of Wardlaw and Grant (1990) through the Road Canyon Formation. Here the Road Canyon is not very conglomeratic and shows only floating clasts, generally siltstone, near the base of skeletal wackestones/packstones.
- 1.3 56.5 Proceed up to Blakemore Hacienda and turn around.
- 0.4 56.9 Drive back down road to outcrop of Willis Ranch Member of the Word Formation (STOP 1.4, Alternate Stop, Figures 2-16, 2-17). Here the Willis Ranch Member is dominantly peloidal packstone with locally common ammonoids. After examining the Willis Ranch, note that the hill above the Blakemore Hacienda displays in succession, the upper part of the Word Formation, the Vidrio Formation, the Altuda Formation, and the Capitan Limestone. All contacts are undulatory and appear unconformable.
- 12.1 69.0 Backtrack to U.S. 90 in Marathon.
- 1.1 70.1 Turn left on U.S. 90 and proceed to intersection of U.S. 385 and U.S. 90.
- 6.3 76.4 Take U.S. 385 North (turn left). Proceed to Hess Ranch entrance.
- 6.0 82.4 Proceed on Hess Ranch private road to fork, turn right to bypass ranch.
- 1.0 83.4 A road enters from left. Across Hess Canyon is the eastern end of the cuesta containing the Road Canyon stratotype. Section RC VII of Wardlaw and Grant (1990) and *Perrinites* and *Waagenoceras* faunas are found at this end of the cuesta.
- 2.5 85.9 Proceed on main road. Just before Hess Tank, at a small turnout on the right, is the path to the knoll containing USNM loc. 702c. This was the most prolific brachiopod locality of Cooper and Grant (1972), which is in the Road Canyon Formation.
- 1.4 87.3 Old Word Ranch site. Here the Road Canyon Formation is a very thin ledge, exposed just north of the road past the old ranch site and tank.
- 0.7 88.0 Proceed to Bruce Ranch (previously the Appel

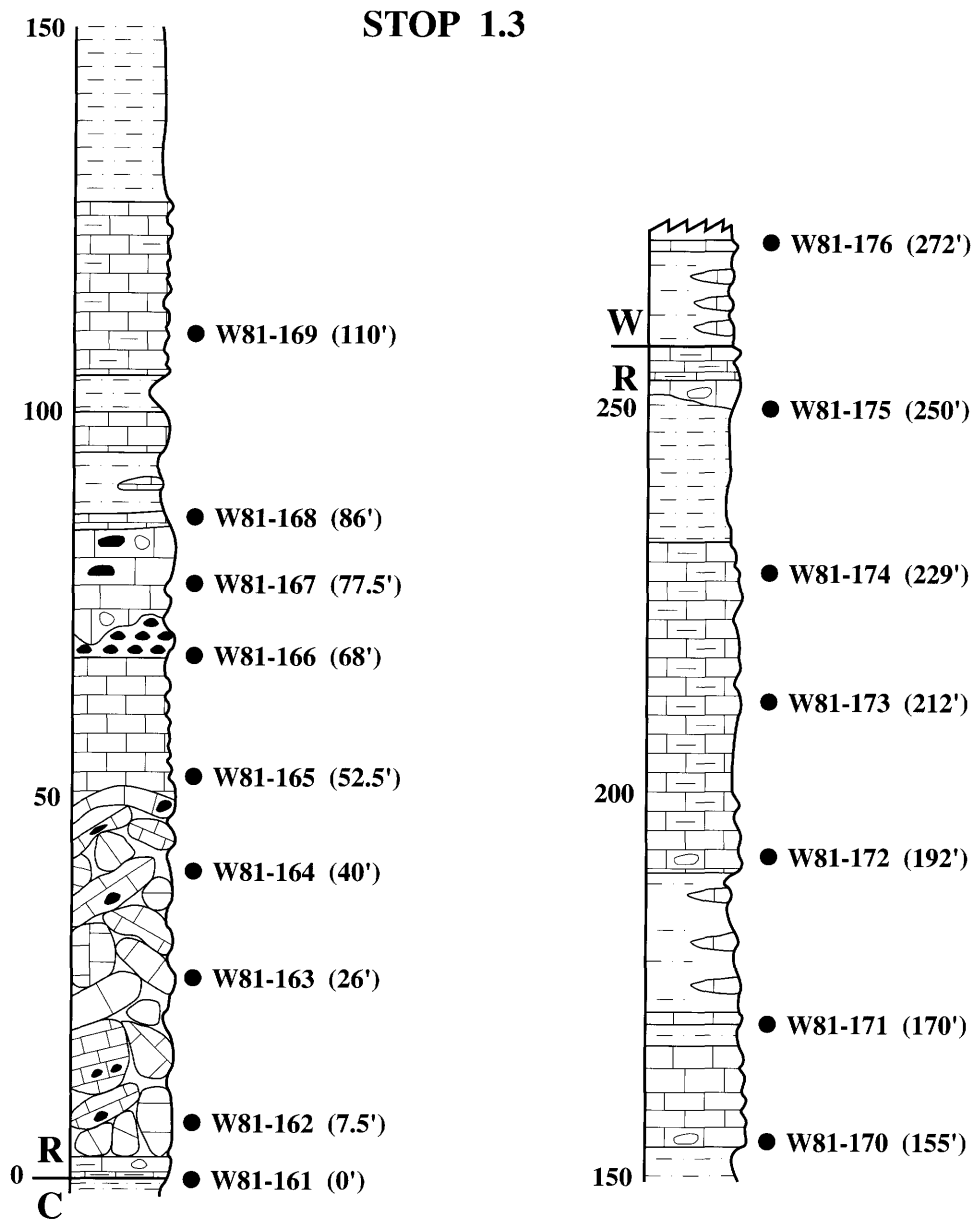


FIGURE 2-15.—Columnar section of the Road Canyon Formation type section. (C = Cathedral Formation; R = Road Canyon Formation; W = Word Formation.)

Ranch) to check-in. Backtrack 150 yards to road heading east.

1.4 89.4 Proceed past Split Tank to saddle. STOP 1.5 is in the gully to the right (Figures 2-18, 2-19). This is the same section as displayed in Cooper and Grant (1972, fig. 22), and it represents one of the most carbonate-rich sections of the Cathedral Mountain Formation (Figure 2-20). Wardlaw and Chevron Oil Co. have worked on a detailed chemostratigraphy of this section and the overlying Word, which is exposed back at

Split Tank. Go down the section and examine the karstified surface of the top of the Hess Formation and the overlying basal conglomerate of the Cathedral Mountain Formation (Figure 2-19A).

0.3 89.7 Backtrack to Split Tank, which is on a small hill to the north of the road. STOP 1.6 is the remainder of Wardlaw's reference section of the Cathedral Mountain through the lower Word formations, as shown in Figure 2-20.

20.1 109.8 Backtrack to Marathon.

30.1 139.8 Return to Alpine.

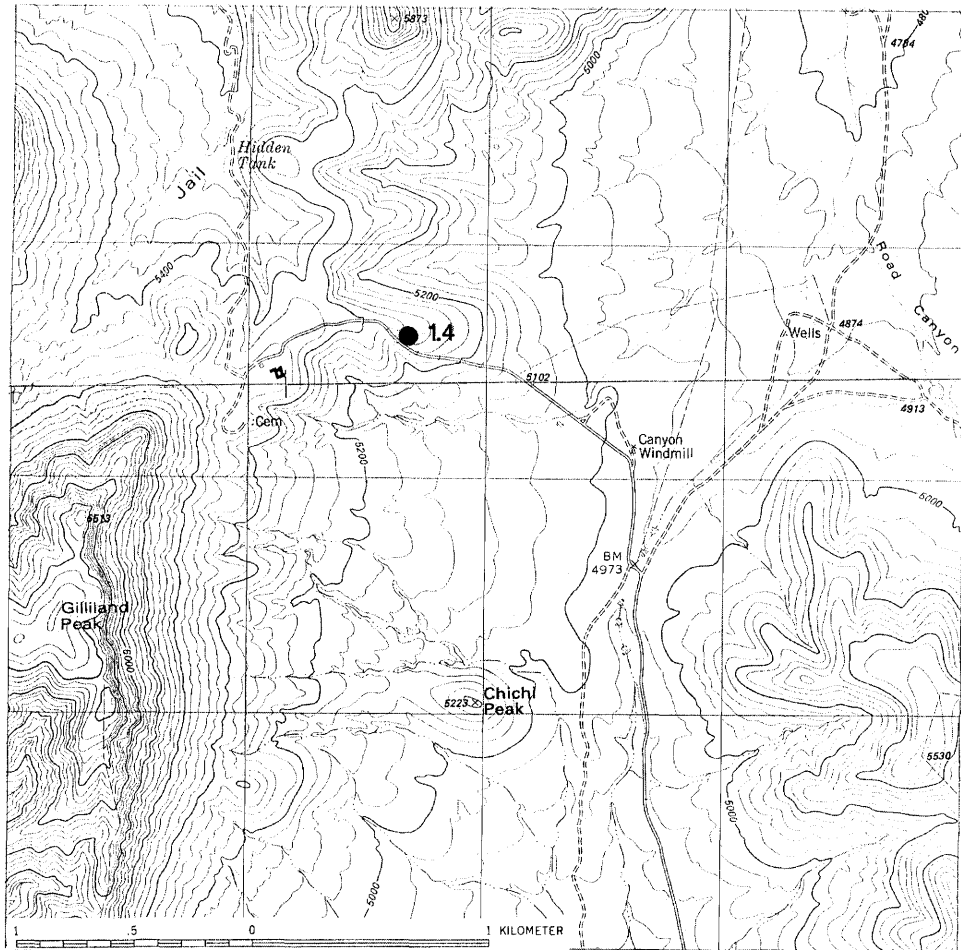


FIGURE 2-16.—Location of alternate STOP 1.4; Gilliland Peak and Old Blue Mountain 7.5 min. quadrangles.

STOP 1.4 (Alternate)

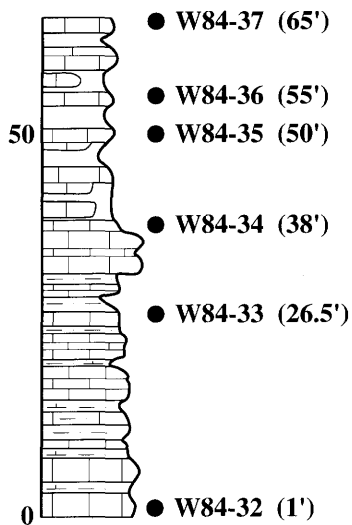


FIGURE 2-17.—Columnar section of the Willis Ranch Member of the Word Formation at alternate STOP 1.4.

Day 2: Alpine to Bird Mine, Benge Ranch, and Old Blue Mountain

Bird Mine, on the north side of Bird (or Altuda) Mountain, is near an intrusion of syenite porphyry into the Permian Altuda and Tessey formations. This area and the Benge Ranch contain the youngest Guadalupian rocks yet found in the Glass and Del Norte mountains.

The thick section of the Capitan Limestone at Old Blue Mountain differs markedly from the typical Capitan in the Guadalupe Mountains. The large foresets on Old Blue Mountain consist of dolomitic mudstone-wackestone, but no boundstone has been observed on the south side of the mountain (Faliskie, 1989). The shelf edge in the Glass Mountains may have been more like a steepened bank-ramp complex. Pray (1988) noted that a bank-ramp complex has “bank-type” loose carbonate sediment and lacks depositional boundstone. The 10° depositional dips on Old Blue Mountain are steeper than the few degrees stated by Pray (1988), but they are considerably less than the 30° dips in the Guadalupe Mountains. In the field mapping performed in preparation for this symposium, and just subsequent to it, a few slightly

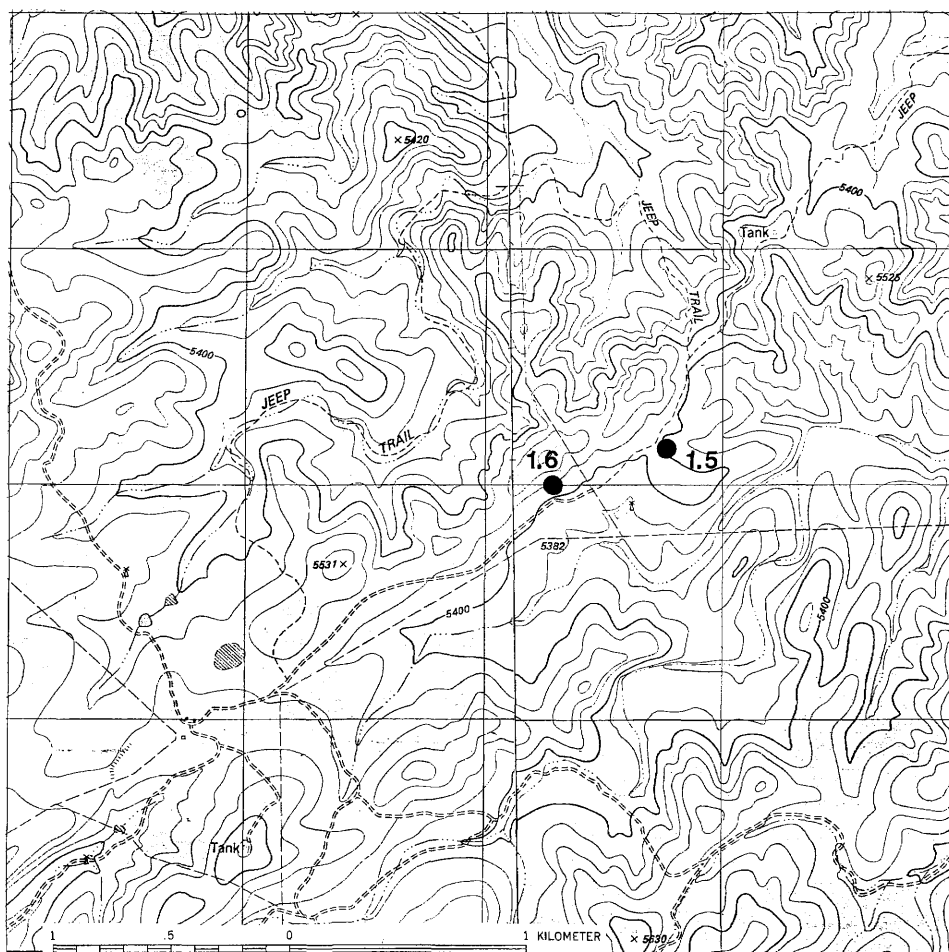


FIGURE 2-18.—Location of STOPS 1.5 and 1.6; Glass Mountain Ranch and Hess Canyon 7.5 min. quadrangles.

recrystallized windows in the bank deposits have been found just above the proximal foreset beds on the north side of Old Blue Mountain. These deposits contain abundant boundstone fabrics of sponges and *Tubiphytes*, suggesting a similar depositional setting to the Capitan Limestone in the Guadalupe Mountains.

MILEAGE

Interval Cumulative

- 0.0 0.0 Head eastward on U.S. 90 from entrance #2 of Sul Ross State University, Alpine.
- 7.4 7.4 Junction with U.S. 67 (to Ft. Stockton), continue straight on U.S. 90 toward Marathon.
- 4.5 12.3 Turn right onto small dirt track heading for Bird Mine (private road). Continue up valley toward intrusion (Figure 2-21).
- 2.4 14.7 Take right branch of road and proceed to stream crossing near mine (Figure 2-22), STOP 2.1. Walk up low slope WSW of road. The

limestone cropping out in this area is the upper Altuda Formation and is about 30 m stratigraphically below the contact with the overlying Tessey Formation (Figure 2-23). The cliff-forming outcrops above the mine area to the south are the Tessey Formation (Dzhulfian), formerly mapped as the upper massive member of the Capitan Limestone. The collapse breccias of the Tessey are well exposed around the mine opening just to the north. The ammonoid-bearing beds contain abundant *Mesogondolella postserrata* and the fusulinid *Reichelina* (Yang, pers. comm., 1990).

- 2.4 17.1 Backtrack to U.S. 90; turn left to go toward Alpine.
- 4.5 21.6 Junction with U.S. 67 (to Ft. Stockton), turn right and continue northward. Tertiary volcanics of the Davis Mountains are on the left (west), and the Glass Mountains are on the right. The highest portions of the Glass Moun-



FIGURE 2-19.—STOP 1.5. A, View of the base of section showing conglomerate at the base of the Cathedral Mountain Formation. B, Typical exposure of the Cathedral Mountain Formation in section.

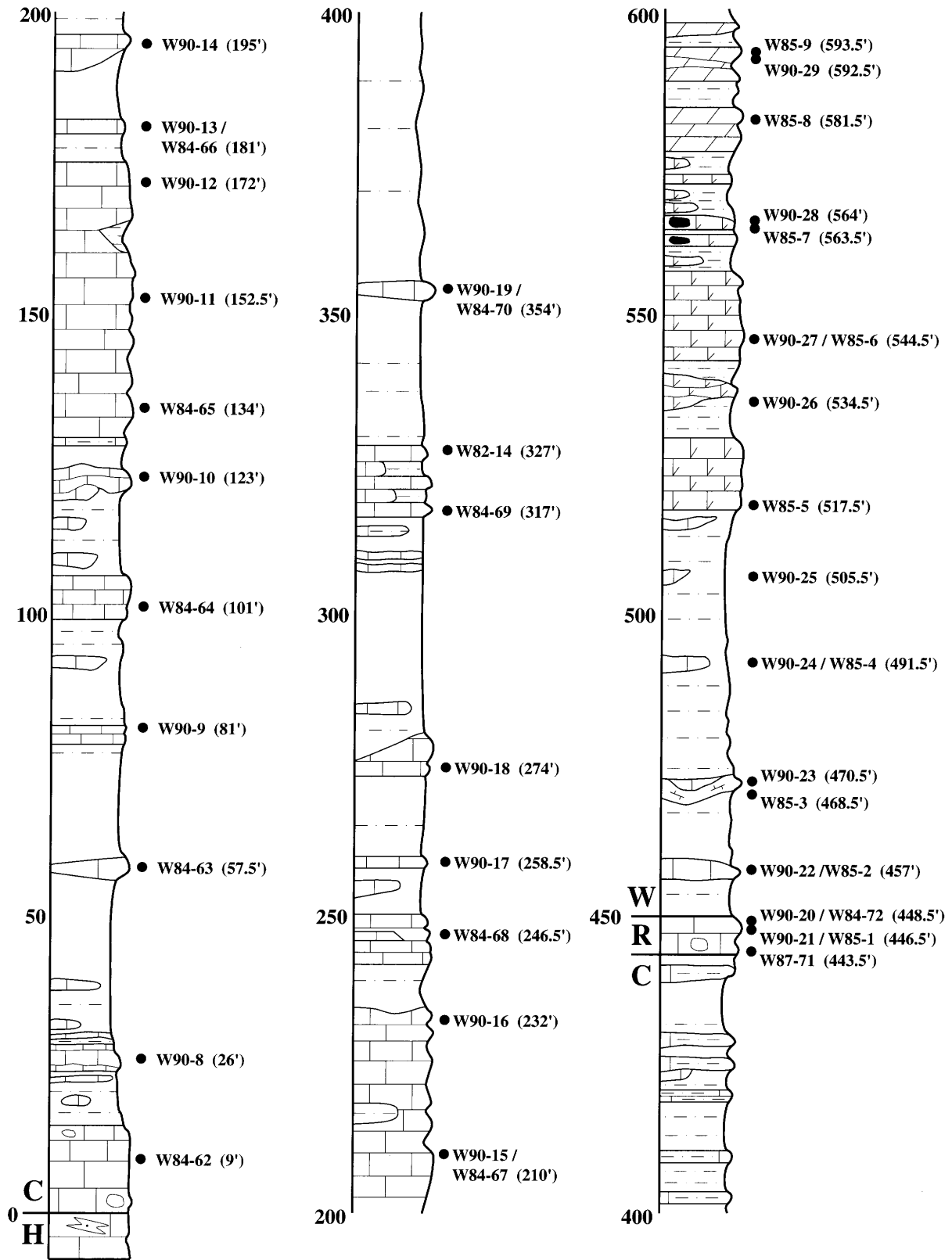


FIGURE 2-20.—Composite columnar section of STOPS 1.5 and 1.6. (C = Cathedral Mountain Formation; H = Hess Formation; R = Road Canyon Formation; W = Word Formation.)



FIGURE 2-21.—View of Bird (Altuda) Mountain. Massive cliffs are the Tessey Formation. Ammonoid locality (STOP 2.1) lies in arroyo north (right) of Bird Mountain.

- tains now visible are the Capitan Limestone; the hills in the foreground are Cretaceous.
- 4.5 26.1 Turn right onto gravel county road. Old Blue Mountain is directly ahead on the horizon.
- 1.6 27.7 Cross first cattle guard.
- 1.9 29.6 Cross second cattle guard.
- 1.3 30.9 Cross third cattle guard. The low hills on the right and left are Cretaceous carbonates. Bisset Mountain is the high, flat-topped mountain on the right.
- 1.4 32.3 Cross fourth cattle guard.
- 1.0 33.3 Cross fifth cattle guard. The Frenchman Hills ahead are the Tessey Formation.
- 1.7 35.0 Road branches, bear left, go through next cattle guard, and turn right to Bengé Ranch headquarters (private road).
- 0.3 35.8 At Bengé Ranch headquarters, continue straight through gate by barn and go up hill to saddle.
- 0.2 36.0 STOP 2.2 is at crest of saddle in the lower Tessey Formation (Figures 2-24–2-26). The Frenchman Hills were mapped by King (1931) as the upper massive member of the Capitan Limestone, but this member has since been reinterpreted as a member of the post-Guadalupean Tessey Formation. The Tessey Formation is the youngest Permian formation (Dzhulfian) in the Glass Mountains. The Dzhulfian age is based on a correlation between the

Tessey and the Rustler Formation of the Guadalupe Mountains. This age was determined by Vacuum Oil Company's Elsinore well No. 1 in Pecos County, Texas, and the Rustler's stratigraphic position is above the documented Lamar–post-Lamar (highest Bell Canyon/Guadalupean) equivalent fusulinid horizons. The Tessey Formation was named for the old Tessey Post Office, which marked the northern extent of the Tessey outcrop. Udden (1917) originally considered it to be a separate formation, but it was reduced in rank to a member of the Capitan Limestone by King (1931). He considered the Capitan to consist of three members: the Vidrio, Gilliam, and Tessey. The Tessey was returned to formation rank in 1937 by P.B. King.

The Tessey Formation in the Frenchman Hills (Figure 2-27) can be subdivided into three lithologically distinct units. The lowermost unit is a finely laminated lime mudstone ("papery limestone" of King, 1931), which overlies the Altuda Formation. This unit is characterized by planar, millimeter-scale laminations formed by alternating dark organic lime mudstone and light lime mudstone/spar lamina. The spar layers are a few millimeters to a few centimeters thick and exhibit depositional fabrics

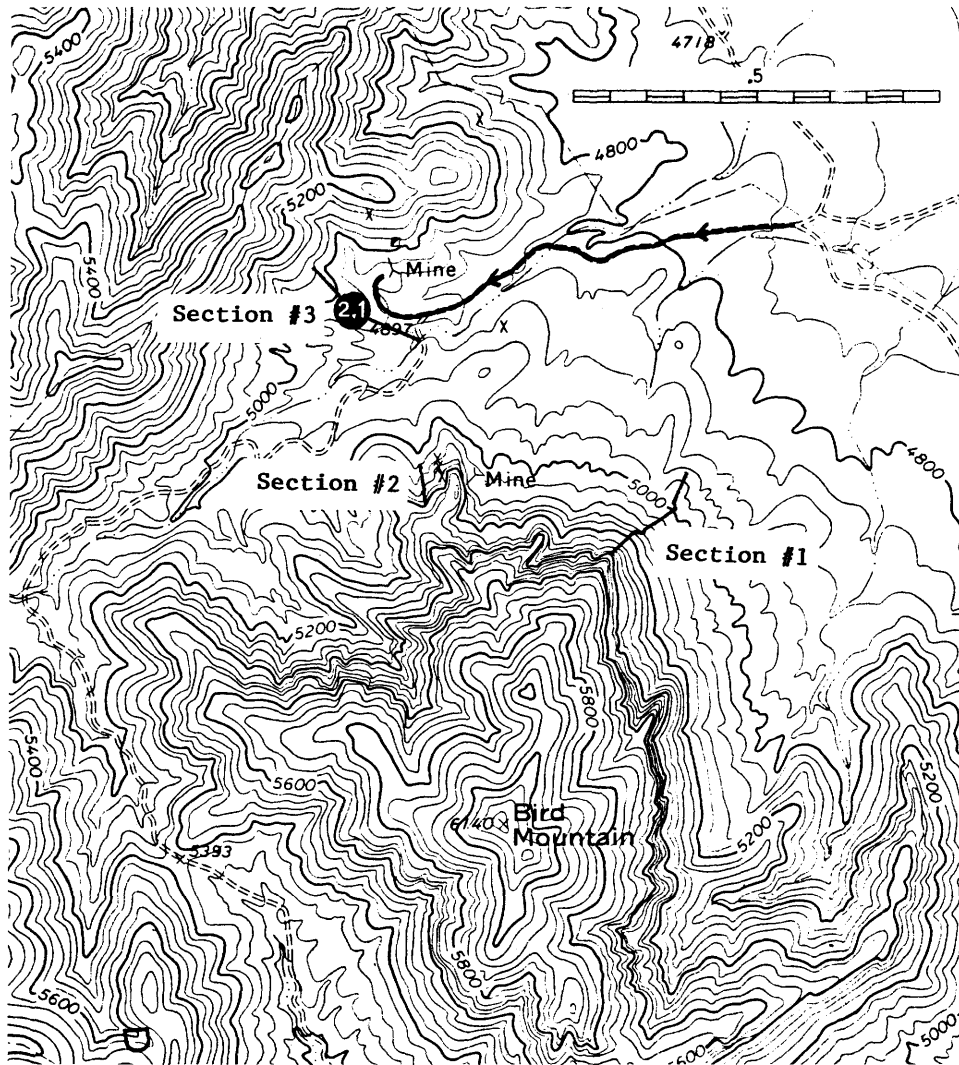


FIGURE 2-22.—Location of STOP 2.1 and sections nearby; Bird Mountain 7.5 min. quadrangle.

analogous to nodular mosaic and chicken wire fabric of anhydrite. The unit is devoid of any fossils and shows localized brecciation, fracturing, and folding of the beds with subsequent spar filling.

Overlying the "papery limestone" is spar-cemented, clast supported lime mudstone breccia. It is a massive, ledge and slope-forming, angular to subangular, non-fossiliferous breccia composed of laminated lime mudstone. Solution and karst features are present with lenticular pods of lime mudstone and spar-cemented limestone conglomerates. The breccias are interpreted to have been deposited as alternating beds of lime mudstone and anhydrite in an euxinic salina setting. Climatically controlled cyclic exposure of these

beds resulted in the solution of evaporites and the collapse of the overlying beds. The presence of anhydrite fabric, distinct karst features, and localized brecciation support this interpretation.

The uppermost unit of the Tessey Formation in the Frenchman Hills consists of matrix-supported dolomudstone breccias. The clasts are exclusively dolomudstone in a dolostone matrix. The clasts vary in size from a few millimeters to 4 cm. Algal laminations, fenestral fabric, and a lack of fossils suggest a supratidal depositional setting.

To the east, the Tessey Formation disconformably overlies the Gilliam Limestone. East of Hess Canyon the formations are separated by a persistent sandstone at the top of the Gilliam. West of Hess Canyon the sandstone dies out,

STOP 2.1 BIRD MINE

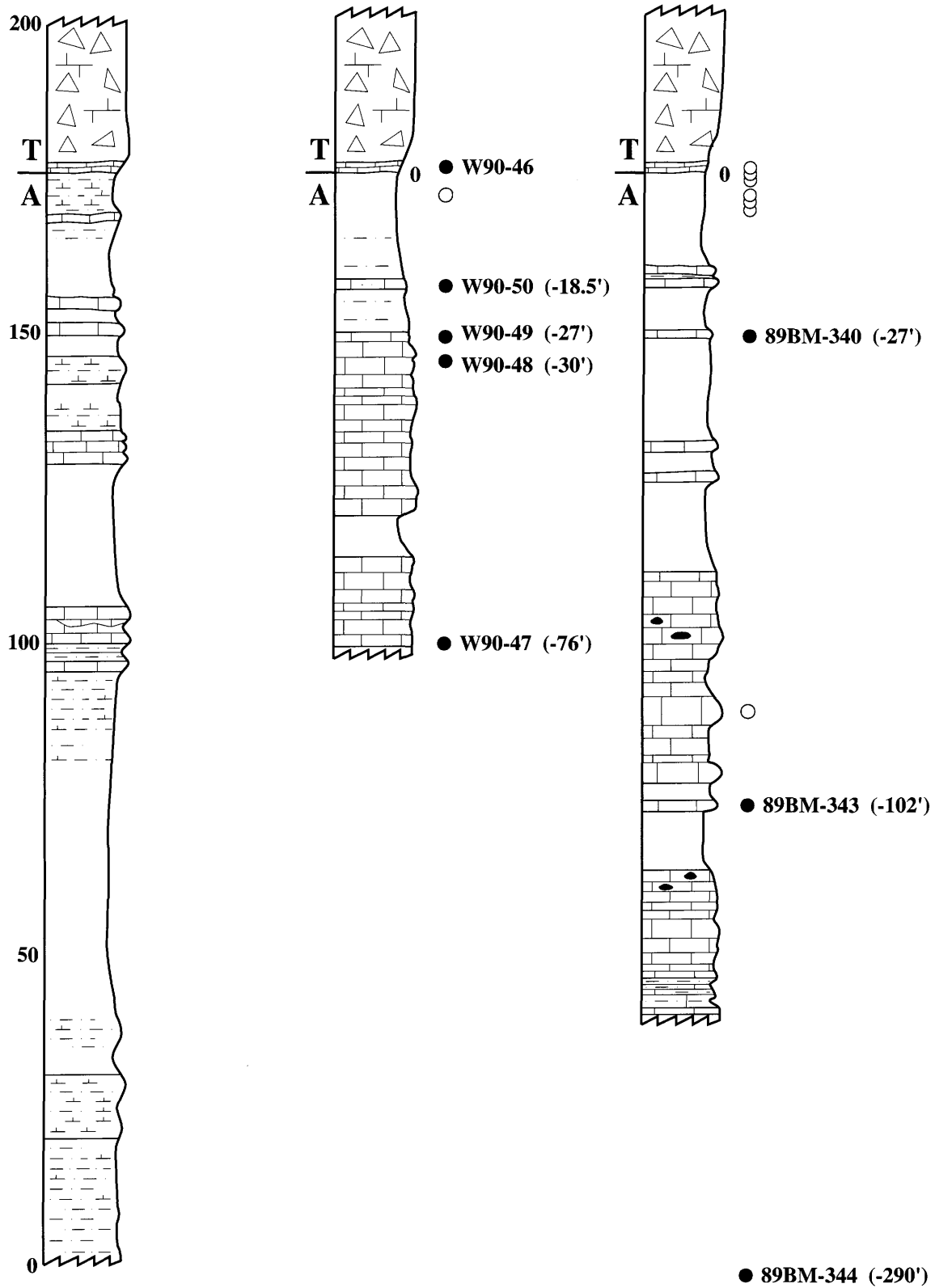


FIGURE 2-23.—Columnar sections in the Bird Mine area. (A = Altuda Formation; T = Tessey Formation; open circles represent subsequent collections.)

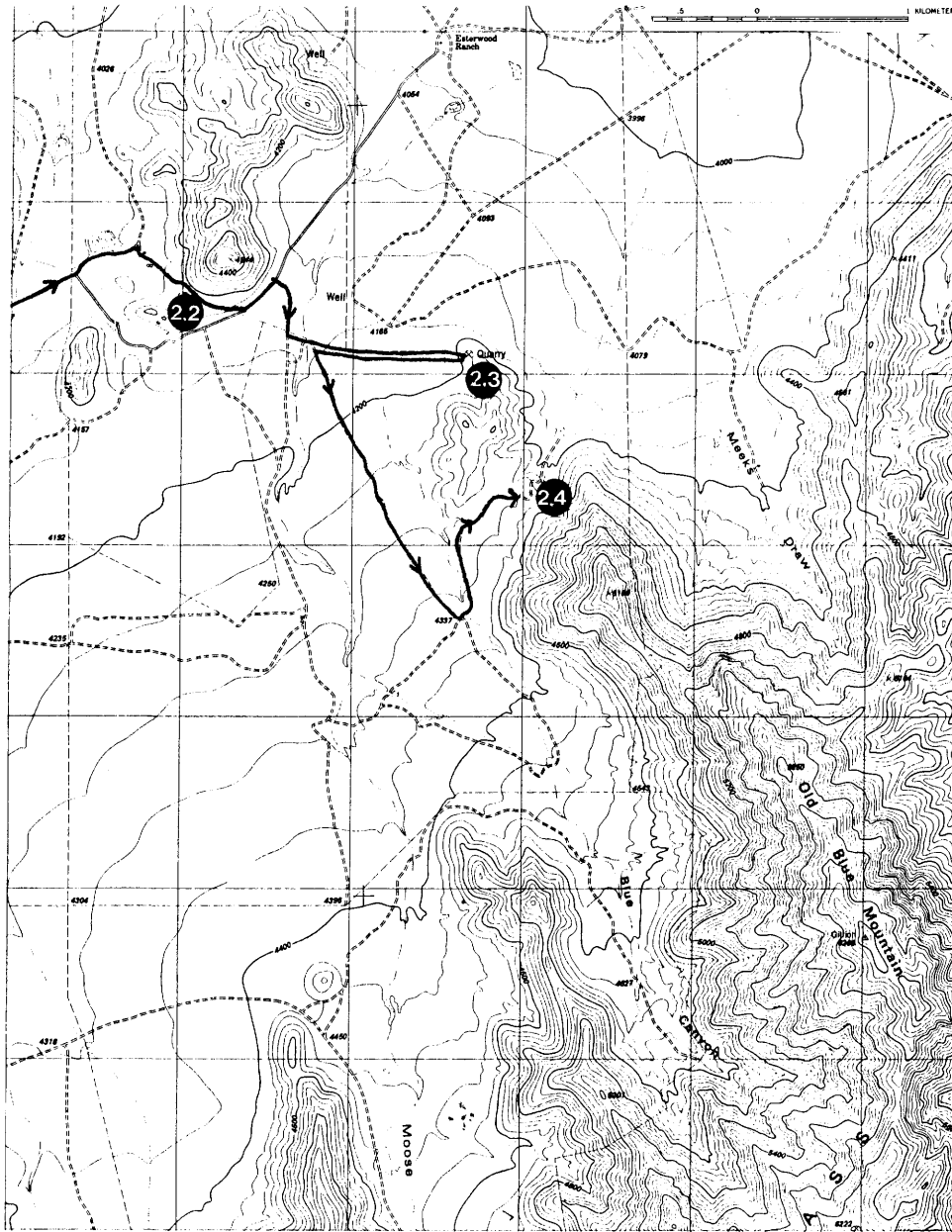


FIGURE 2-24.—Location of STOPS 2.2, 2.3, and 2.4; Old Blue Mountain 7.5 min. quadrangle.

and the two formations are difficult to differentiate. Southwestern (Hovey channel) exposures are delineated by a very thinly laminated limestone that occurs at the base of the Tessey. The Gilliam also contains a more varied lithology with abundant fossils in some places. The Tessey tends to be petroliferous, and the first occurrence of a breccia horizon marks the transition between the Tessey and the Gilliam. Fossils in the Tessey are sparse and consist of poorly preserved gastropods and brachiopods.

Udden (1917) reported oolitic textures and foraminifera; however, this description appears to be of the Gilliam instead. Robert E. King (1931) collected *Permophorus*, a pelecypod, from the Tessey in its northern extent.

0.2	36.2	At road junction, go left.
0.1	36.3	Take dirt road to right.
0.2	36.5	Go through gate and immediately turn left, go across creek, and continue straight along fence line to rock quarry.



FIGURE 2-25.—STOP 2.2. A, View of the Tessey Formation east of Benge Ranch. Lower slope of the hill is the Altuda Formation with “paper limestone” just below the break in the slope. B, Collapse breccia typical of the Tessey Formation. Note the laminated clasts.

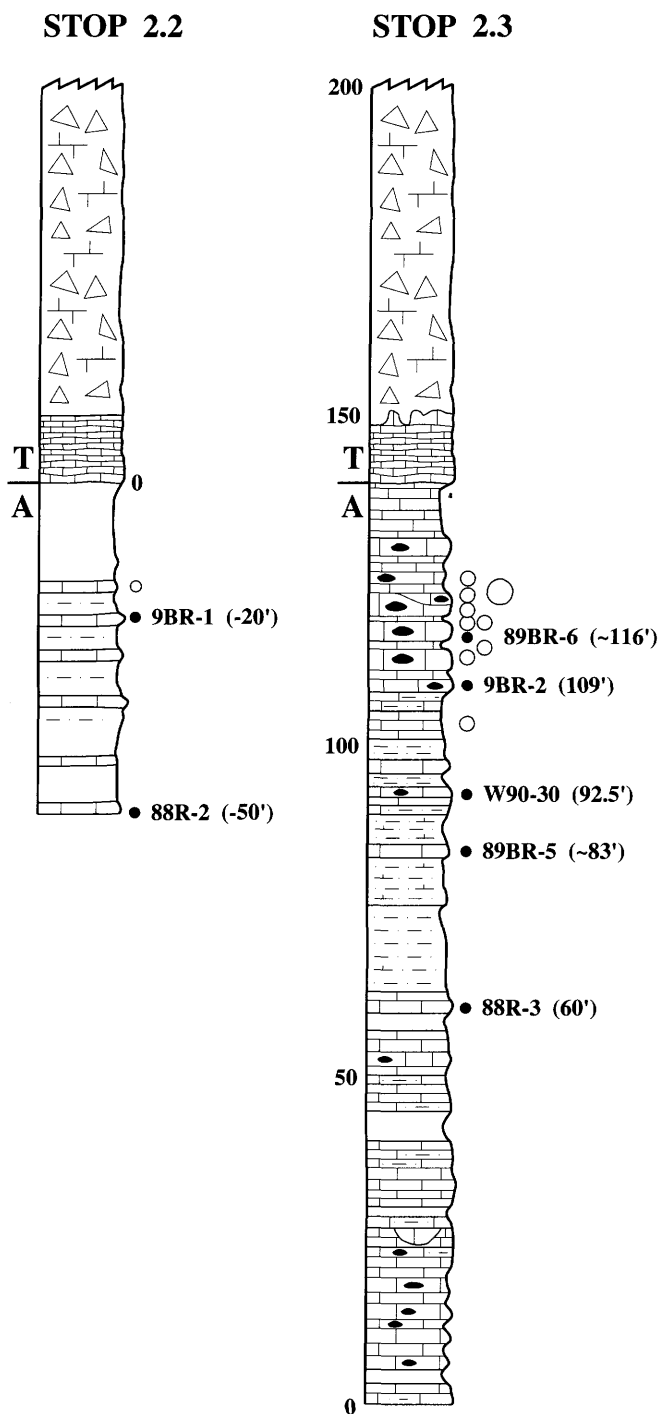


FIGURE 2-26.—Columnar sections of STOPS 2.2 and 2.3. (A = Altuda Formation; T = Tessey Formation; open circles represent subsequent collections.)

0.7 37.2 Park in quarry and continue by foot up jeep trail on ridge for about 300 m, STOP 2.3. This section (Figure 2-26) exposes some of the youngest Guadalupian beds in the Glass Mountains and probably represents a lower slope

facies equivalent of parts of the Altuda Formation and the Capitan Limestone. The Altuda Formation here is thin- to medium-bedded siltstone, fine quartz sandstone, and dolomudstone to lime wacke-packstone. It exhibits vertical as well as lateral variations in lithology, texture, and sedimentary structures. These variations can be attributed to two lithologically different, but time equivalent, slope and basin facies.

The basinal facies is planar, thin-bedded siltstone, fine sandstone, and dolomudstone, with interbeds showing distinct gradation from coarse, shallow water, normal marine bioclastic lags to fine, hemipelagic lime-mud with calcispheres, siliceous sponge spicules, and radiolaria. The beds display convolute bedding, flame structures (Figure 2-28), dish structures, chert-replaced anhydrite rosettes, rippled contourites, chert nodules, and horizontal branching burrows.

The slope facies includes interfingering Altuda Formation with the large foreset beds of the Capitan Limestone. The slope facies of the Altuda Formation contains features typical of subaqueous gravity flows, such as slump structures, ball and pillow structures, and recumbent folds outlined by chert. In Old Blue Mountain, several Capitan foresets are mappable (Figure 2-29). The individual foresets are composed of brecciated dolomudstone with spar-filled vugs and fractures and rare skeletal debris. The base of each foreset is wavy with sandstone and siltstone clasts of millimeter to centimeter size. Their lower and upper contacts with the Altuda Formation pinch and swell, implying that these foresets were deposited as prograding tongues of debris flows off of the shelf. The foresets generally taper towards the basin and die out. Locally, the slope facies contain large, slightly rotated slump blocks displaying similar lithologic characteristics to that of the Capitan foresets. On the southwestern slope of Old Blue Mountain, a 15 m wide bioclastic wacke-packstone slide block is surrounded by siltstone and fine sandstone of the Altuda Formation. The basal part of the block contains rounded to subrounded lithoclasts of yellowish sandstone varying in diameter from 5 to 10 cm. The geopetal fabric does not indicate any overturning or rotation.

Present in the limestone beds exposed on the jeep trail above the quarry are the small

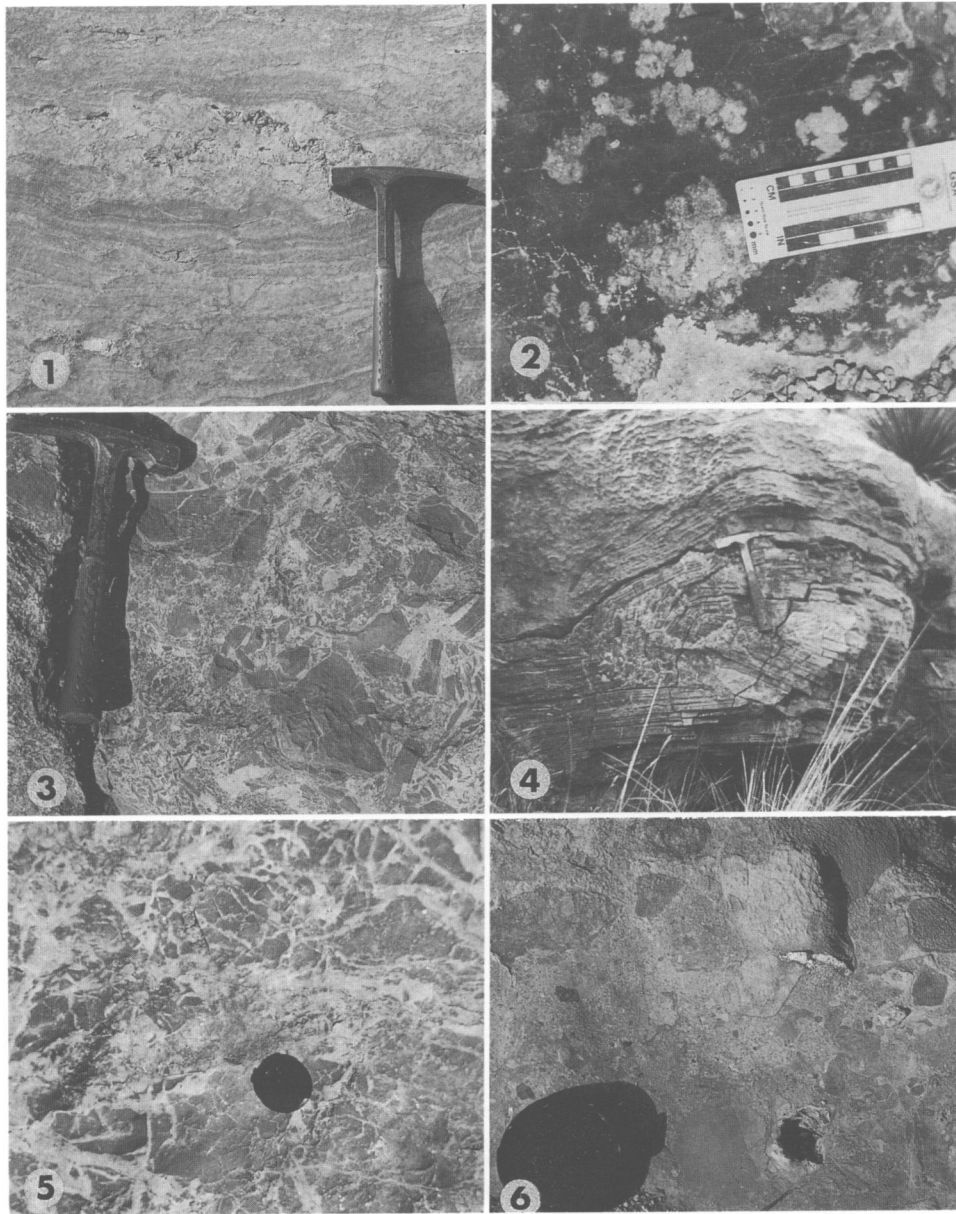


FIGURE 2-27.—Features associated with the Tessey Formation. 1, Planar laminated mudstone facies in the Frenchman Hills. Note the alternating dark organic-rich mudstone and light spar layers. Hammer head is on nodular mosaic fabric after anhydrite. 2, Calcite nodular fabric after precursor anhydrite within the middle facies. 3, Clast-supported breccia. Note the localized brecciation of laminated clasts. 4, Folding within the planar laminated mudstone facies. 5, Clast-supported, spar-cemented breccia. Note the spar-filled fractures. 6, Clast-supported conglomerate pod composed of limestone and chert clasts. These conglomerates are laterally discontinuous and are interpreted as indicators of subaerial exposure.

fusulinids *Paraboultonia* (Wilde, pers. comm., 1990), and *Lantschichites* (= *Paraboultonia*) (Yang, pers. comm., 1990), brachiopods, and poorly preserved ammonoids. See Wilde and Rudine (this volume) and Yang and Yancey (this volume) for more detailed descriptions of the fusulinids. Wardlaw (this volume) identified the conodonts *Mesogondolella postser-*

rata, *M. shannoni*, and *M. altudaensis* from these beds.

The fossils listed above indicate a correlation with the Lamar Member of the Bell Canyon or post-Lamar Guadalupian according to Wilde (1990). At the top of the hill is the Tessey Formation. Separating the Altuda from the Tessey breccias is a distinctive, dark gray,

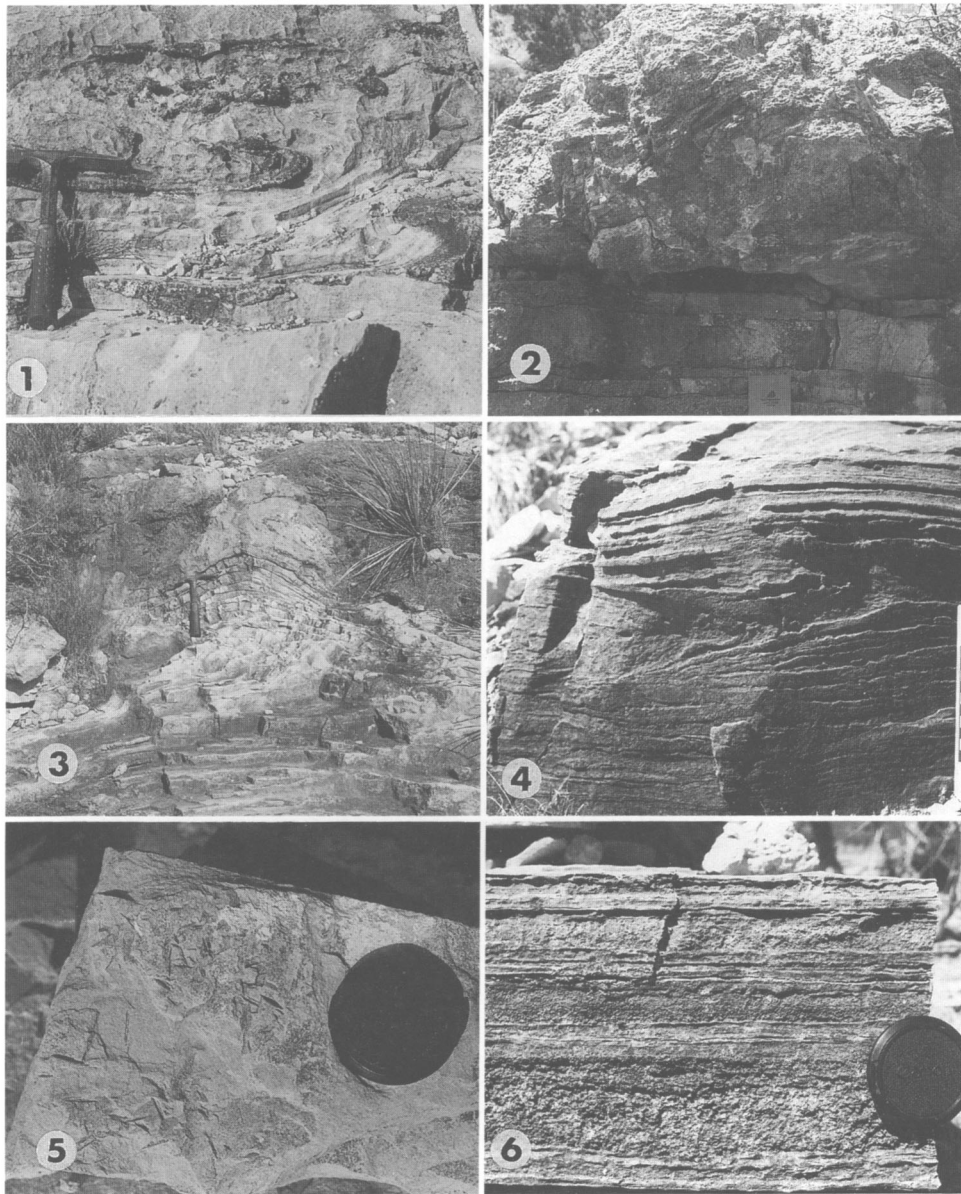


FIGURE 2-28.—Bedforms displayed by slope facies. 1, Recumbent folding outlined by chert layers within Capitan foreset beds. Hammer head is parallel to the subaqueous gravity flow direction. Note lower wavy contact with dolomudstones of the Altuda Formation. 2, Allochthonous slump block of Capitan Limestone within the Altuda Formation in the slope facies. The block contains sandstone lithoclasts. 3, Drag folding in thin-bedded siliciclastic dolomudstones of the Altuda Formation caused by an overriding debris flow of Capitan foreset. 4, Soft sediment deformation outlined by chert layers in the sandstone beds of the Altuda Formation (scale on the right in centimeters). 5, Gypsum crystal casts in the planar, thin-bedded siltstone basal facies of the Altuda Formation (lens cap is 6 cm). 6, Thin planar bed of the Altuda Formation displaying several turbidite units. The base of each turbidite unit is wavy, followed by a coarse bioclastic lag composed of shelf derived-fauna, and grades upward into laminated silty mudstone with abundant sponge spicules, calcispheres, and radiolaria.

finely laminated lime mudstone, which King (1931) called his “papery limestone.” This unit is generally only a few feet thick, but it was reported by King (1931) to occur extensively in the western Glass Mountains.

The Tessey Formation capping this hill (and the Frenchman Hills to the west) consists of

massive carbonate breccias and conglomerate. The Tessey in this area is interpreted to be collapse breccias of late basin-filling stage, probably equivalent to the Castile or Rustler in the Delaware basin. The difference in lithology is thought to be due to the proximity to the southern entrance of the Delaware basin



FIGURE 2-29.—View of the northeast side of Old Blue Mountain that displays a series of foresets prograding to the northwest. Benge Ranch is off of photo to the right.

(Hovey channel), which was becoming increasingly restricted during late Guadalupian and Dzhulfian time. This is supported by the presence of more limestone-rich conglomerates to the south at Bird Mountain (Rudine, pers. comm., 1990) and the transition to more evaporitic facies to the north in the subsurface.

- 0.5 37.7 Backtrack to stream crossing, and turn left just before stream.
- 1.2 38.9 Make sharp left turn onto road heading for saddle.
- 0.7 39.6 Drive into saddle and park near deer feeder and deer-hunting tower, STOP 2.4. The taller hill to the east is an extension of Old Blue Mountain. The lower hill to the west of the saddle is Tessey breccia. Walk up the gully to the east, which exposes Altuda siltstones and foresets of Capitan carbonate, to the first large resistant carbonate ledge (Figures 2-30, 2-31).

The cliffy ledge of carbonate to the left of the gully is part of the Capitan foreset, which is exposed across the hillside. The foreset is dipping westward. The outcrop illustrates several features of foresets, including massively bedded dolomicrites, channeling, and disturbed

thin bedding (Figure 2-31). Some evaporite casts are present, as well as rare bioclastic beds with brachiopods. These beds are interpreted to be lower foresets of the Capitan interbedded with siltstones that are also being shed off of the shelf edge, which has at least 200 m of relief. Penecontemporaneous slumping and folding of carbonate beds is relatively common. The basin margin at this location is oriented north-south.

Acknowledgments

We are grateful to those land owners who allowed us access to their ranches to study the Permian rocks over the last 10 years. We are also grateful to those ranchers who allowed us on their land for this field conference, including Mr. and Mrs. Mac Benge, Mr. William Blakemore, and the Woodward family.

Research by those associated with Sul Ross State University was supported by the Petroleum Research Fund of the American Chemical Society and by the Sul Ross Research Enhancement Fund. The Smithsonian Institution provided collaborative research funds to Grant and Wardlaw for the last decade, and the U.S. Geological Survey supported the collaboration of Wardlaw with Rohr and many Sul Ross State students.

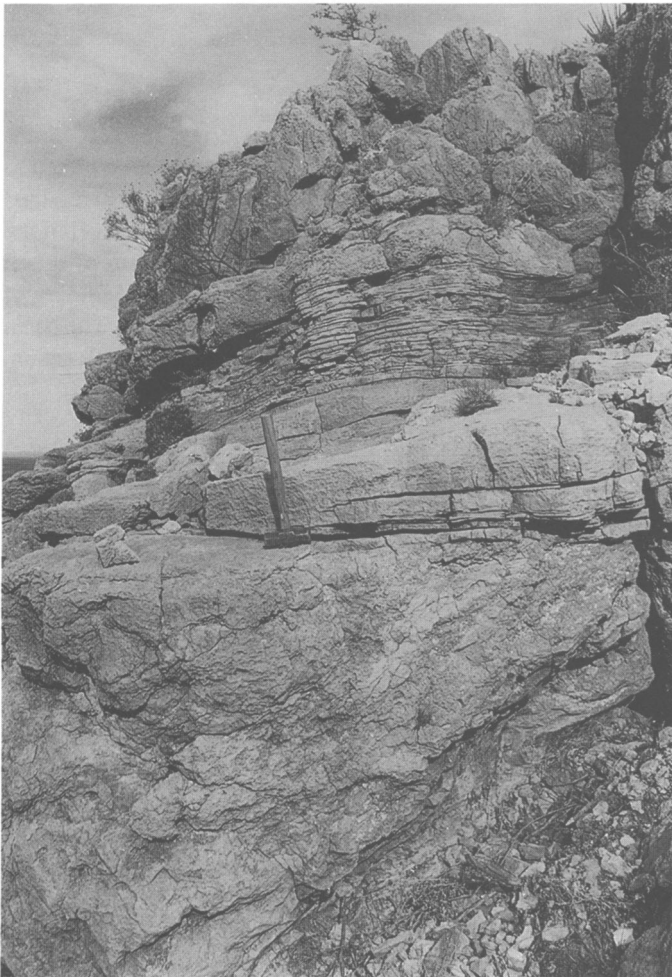
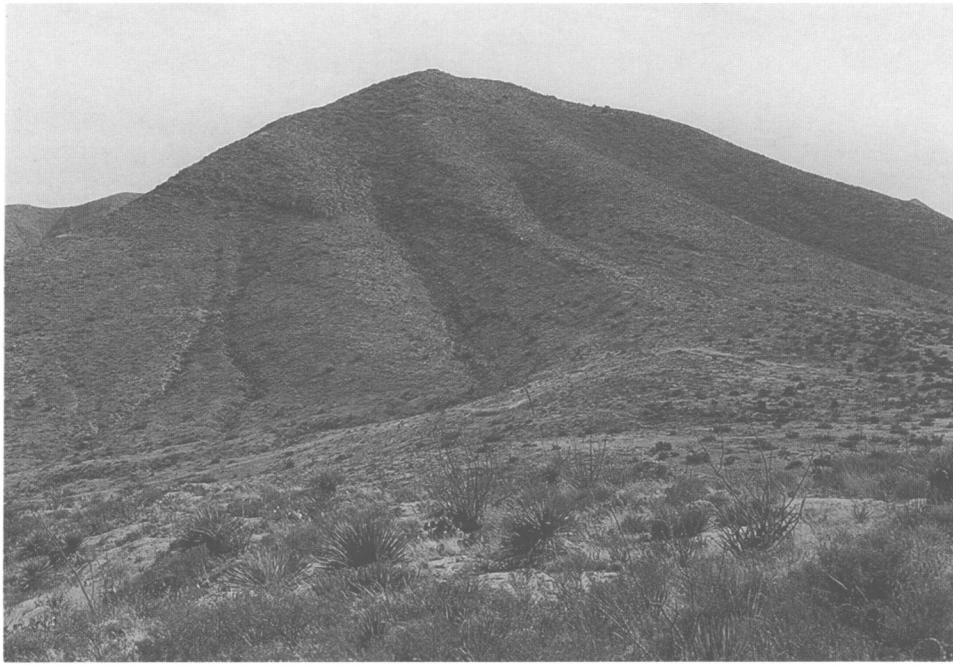


FIGURE 2-30 (above).—View of hill north of Old Blue Mountain displaying foreset. STOP 2.4 is located just left of major arroyo cutting foreset (ledge).

FIGURE 2-31 (left).—STOP 2.4. Close-up of foreset exposure. The lower half of the photograph shows a foreset tongue, or channel, of recrystallized calcitic dolomudstone bearing clasts of skeletal dolomudstone, which overlies thin, load-deformed beds of dolomudstone. The upper surface is truncated by thin, foreset beds of dolomudstone.

References

- Collinsworth, B.C., and D.M. Rohr
1986. An Eocene Carbonate Lacustrine Deposit, Brewster County, West Texas. In P.H. Pausé and R.G. Spears, editors, *Geology of the Big Bend Area and Solitario Dome, Texas*. *West Texas Geological Society, Publication*, 86-82:117-124.
- Coombs, L.M.
1990. Depositional Environments of Permian Strata on Dugout Mountain, Brewster County, Texas. 115 pages. Unpublished master's thesis, Sul Ross State University, Alpine, Texas.
- Cooper, G.A., and R.E. Grant
1964. New Permian Stratigraphic Units in Glass Mountains, West Texas. *Bulletin of the American Association of Petroleum Geologists*, 48(9):1581-1588.
1972. Permian Brachiopods of West Texas, I. *Smithsonian Contributions to Paleobiology*, 14:1-231, plates 1-23.
1974. Permian Brachiopods of West Texas, II. *Smithsonian Contributions to Paleobiology*, 15:233-793, plates 24-191.
1975. Permian Brachiopods of West Texas, III. *Smithsonian Contributions to Paleobiology*, 19:795-1921, plates 192-502.
1976a. Permian Brachiopods of West Texas, IV. *Smithsonian Contributions to Paleobiology*, 21:1923-2607, plates 503-662.
1976b. Permian Brachiopods of West Texas, V. *Smithsonian Contributions to Paleobiology*, 24:2609-3159, plates 663-780.
1977. Permian Brachiopods of West Texas, VI. *Smithsonian Contributions to Paleobiology*, 32:3161-3370.
- Cys, J.M.
1981. Preliminary Report on Proposed Leonardian Lectostratotype Section, Glass Mountains, West Texas. In Marathon-Marfa Region of West Texas Symposium and Guidebook. *Society of Economic Paleontologist and Mineralogists, Permian Basin Section, Publication*, 81-10:183-205.
- Cys, J.M., and S.J. Mazzullo
1978. Lithofacies and Sedimentation of Lower Permian Carbonate of the Leonard Mountain Area, Glass Mountains, Western Texas: A Discussion. *Journal of Sedimentary Petrology*, 48(4):1363-1368.
- Davis, R.A.
1984. Depositional Environments of the Western Cathedral Mountain, Road Canyon, Word and Capitan Formations (Permian), Glass Mountains Area, West Texas. 104 pages. Unpublished master's thesis, Sul Ross State University, Alpine, Texas.
- Davis, R.A., D.M. Rohr, and J.M. Miller
1983. Depositional Environments of the Western Word Formation (Permian), Glass Mountains Area, West Texas. [Abstract.] *Geological Society of America, Abstracts with Programs*, 16:6.
- Faliskie, R.A.
1989. Vidrio Member of the Word, Altuda, and Capitan Formations (Upper Permian) in the Northwestern Glass Mountains, West Texas. 100 pages. Unpublished master's thesis, Sul Ross State University, Alpine, Texas.
- Finks, R.M.
1969. Late Paleozoic Sponge Faunas of the Texas Region. *Bulletin of the American Museum of Natural History*, 120: 160 pages.
- Flores, R.M., T.L. McMillan, and G.E. Watters
1977. Lithofacies and Sedimentation of Lower Permian Carbonate of the Leonard Mountain Area, Glass Mountains, Western Texas. *Journal of Sedimentary Petrology*, 47(4):1610-1622.
- Girty, G.H.
1909 ("1908"). The Guadalupian Fauna. *United States Geological Survey Professional Paper*, 58: 651 pages, 31 plates. [Date on title page is 1908; actually published in 1909.]
- Glenister, B.F., and W.M. Furnish
1961. The Permian Ammonoids of Australia. *Journal of Paleontology*, 35(4):673-736, plates 78-86.
- Haneef, Mohammad, S.F. Rudine, and B.R. Wardlaw
1990. Shelf to Basin Transition in the Capitanian (Permian) Deposition in the Glass Mountains, West Texas. [Abstract.] *Geological Society of America, Abstracts with Programs*, 22:A46.
- King, P.B.
1931 ("1930"). The Geology of the Glass Mountains, Texas, Part I: Descriptive Geology. *University of Texas Bulletin*, 3038: 167 pages, 15 plates. [Date on title page is 1930; actually published in 1931.]
1937. Geology of the Marathon Region, Texas. *United States Geological Survey Professional Paper*, 187: 148 pages, 24 plates.
- King, R.E.
1931 ("1930"). The Geology of the Glass Mountains, Texas, Part II: Faunal Summary and Correlation of the Permian Formations with Description of Brachiopoda. *University of Texas Bulletin*, 3042: 245 pages, 44 plates. [Date on title page is 1930; actually published in 1931.]
- Lehrmann, D.L.
1988. Sedimentology and Conodont Biostratigraphy of the Road Canyon Formation (Permian), Glass Mountains, Southwest Texas. 170 pages. Unpublished master's thesis, University of Wisconsin, Madison, Wisconsin.
- Mamay, S.H., J.M. Miller, and D.M. Rohr
1984. Late Leonardian Plants from West Texas: The Youngest Paleozoic Plant Megafossils in North America. *Science*, 223:279-281.
- Mamay, S.H., J.M. Miller, D.M. Rohr, and W.E. Stein
1988. Foliar Morphology and Anatomy of the Gigantopterid Plant *Delnortea abbotti*, from the Lower Permian of West Texas. *American Journal of Botany*, 75:1409-1433.
- Measures, E.A., and B.R. Wardlaw
1990. Recognition of Paleokarst in the Road Canyon Formation, Permian Regional Stratotype, West Texas. [Abstract.] *Geological Society of America, Abstracts with Programs*, 22(7):309.
- Newell, N.D., and D.W. Boyd
1970. Oyster-like Permian Bivalvia. *Bulletin of the American Museum of Natural History*, 143(4):217-283.
- Peterson, J.A.
1980. Permian Paleogeography and Sedimentary Provinces, West-Central United States. In T.D. Fouch and E.R. Magathan, editors, *Paleozoic Paleogeography of the West-Central United States: Rocky Mountain Paleogeography Symposium 1*, pages 271-293. Denver, Colorado: Society of Economic Paleontologists and Mineralogists, Rocky Mountain Section.
- Pray, L.C.
1988. The Western Escarpment of the Guadalupe Mountains, Texas. In: S.T. Reid, R.O. Bass, and P. Welch, editors, *Guadalupe Mountains Revisited, Texas and New Mexico*. *West Texas Geological Society, Publication*, 88-84:23-31.
- Rathjen, J.D.
1985. Microfacies and Depositional Environment of the Word Formation (Permian), Glass Mountains, Texas. 138 pages. Unpublished master's thesis, Sul Ross State University, Alpine, Texas.
- Rogers, W.B.
1972. Depositional Environments of the Skinner Ranch and Hess Formation (Lower Permian), Glass Mountains, West Texas. 392 pages. Unpublished doctoral dissertation, University of Texas, Austin, Texas.
- Rohr, D.M., R.A. Davis, S.H. Mamay, and J.M. Miller
1987. Leonardian Plant-Bearing Beds from the Del Norte Mountains, West Texas. In D. Cromwell and L.J. Mazzullo, editors, *The Leonardian*

- Facies in W. Texas and S.E. New Mexico and Guidebook to the Glass Mountains, West Texas. *Society of Economic Paleontologists and Mineralogists, Permian Basin Section, Publication*, 87-27:67-68.
- Ross, C.A.
 1963. Fusulinids from the Word Formation (Permian), Glass Mountains, Texas. *Contributions from the Cushman Foundation for Foraminiferal Research*, 14(1):17-31, plates 3-5.
 1986. Paleozoic Evolution of Southern Margin of Permian Basin. *Bulletin of the Geological Society of America*, 97(5):536-554.
 1987. Leonardian Series (Permian), Glass Mountains, West Texas. In D. Cromwell and L.J. Mazzullo, editors, *The Leonardian Facies in W. Texas and S.E. New Mexico and Guidebook to the Glass Mountains, West Texas. Society of Economic Paleontologists and Mineralogists, Permian Basin Section, Publication*, 87-27:25-33.
- Ross, C.A., and J.P. Ross
 1987. Late Paleozoic Sea Levels and Depositional Sequences. In C.A. Ross and D. Haman, editors, *Timing and Depositional History of Eustatic Sequences: Constraints on Seismic Stratigraphy. Cushman Foundation for Foraminiferal Research, Special Publication*, 24:137-150.
- Rudine, S.F.
 1988. Geology and Depositional Environments of the Permian Rocks, Northern Del Norte Mountains, Brewster County, Texas. 186 pages. Unpublished master's thesis, Sul Ross State University, Alpine, Texas.
- Rudine, S.F., R.A. Faliskie, D.M. Rohr, B.R. Wardlaw, and R.E. Grant
 1988. Major Unconformity Defines Wordian-Capitanian Boundary (Upper Permian) in Glass and Del Norte Mountains, Texas. [Abstract.] *Geological Society of America, Abstracts with Programs*, 20:122-123.
- Rudine, S.F., B.R. Wardlaw, D.M. Rohr, R.A. Davis, and R.E. Grant
 1987. Depositional Setting of Late Leonardian-Wordian (Permian) Rocks, Southern Margin, Permian Basin: Basin or Lagoon? [Abstract.] *Geological Society of America, Abstracts with Programs*, 19:826.
- Sarg, J.F., C. Rossen, D.J. Lehrmann, and L.C. Pray, editors
 1988. Geologic Guide to the Western Escarpment, Guadalupe Mountains, Texas. *Society of Economic Paleontologists and Mineralogists, Permian Basin Section, Publication*, 88-30: 60 pages.
- Udden, J.A.
 1917. Notes on the Geology of the Glass Mountains. *University of Texas Bulletin*, 1753: 59 pages.
- Wardlaw, B.R., R.A. Davis, D.M. Rohr, and R.E. Grant
 1990. Leonardian-Wordian (Permian) Deposition in the Northern Del Norte Mountains, West Texas. *United States Geological Survey Bulletin*, 1881-A:A1-A14.
- Wardlaw, B.R., and R.E. Grant
 1990. Conodont Biostratigraphy of the Permian Road Canyon Formation, Glass Mountains, Texas. *United States Geological Survey Bulletin*, 1895-A:A1-A18, plates 1-4.
- Wilcox, R.E., W. Langston, Jr., and S.C. Good
 1986. The Non-Marine Bissett Formation of the Western Glass Mountains, Trans-Pecos Texas: Evidence for an Early Cretaceous (Neocomian?-Albian) Age. [Abstract.] *Geological Society of America, Abstracts with Programs*, 17:272.
- Wilcox, R.E., and D.M. Rohr
 1987. The Stratigraphy and Depositional Systems of the Bissett Formation; an Early Cretaceous Alluvial Fan-Lacustrine Complex, Glass Mountains, Trans-Pecos, Texas. [Abstract.] *Geological Society of America, Abstracts with Programs*, 18:788.
- Wilde, G.L.
 1990. Practical Fusulinid Zonation: The Species Concept; with Permian Basin Emphasis. *West Texas Geological Society, Bulletin*, 29(7): 5-34.
- Yochelson, E.L.
 1956. Permian Gastropoda of the Southwestern United States, 1: Euomphalacea, Trochonematacea, Pseudophoracea, Anomphalacea, Craspedostomatacea, and Platyceratacea. *Bulletin of the American Museum of Natural History*, 110:177-275.
 1960. Permian Gastropoda of the Southwestern United States, 3: Bellerophonacea and Patellacea. *Bulletin of the American Museum of Natural History*, 119:209-293.

3. Guadalupian Conodont Biostratigraphy of the Glass and Del Norte Mountains

Bruce R. Wardlaw

ABSTRACT

The Guadalupian Series in the Glass and Del Norte mountains is divided into five conodont zones. One zone, *Mesogondolella nankingensis*, is divided into two subzones; the subzone boundary nearly coincides with the Roadian–Wordian stage boundary as perceived by Glenister et. al. (1992). The base of the Guadalupian is easily defined by the evolutionary transition from *Mesogondolella idahoensis* to *M. nankingensis* (Grant and Wardlaw, 1986; Lambert and Wardlaw, 1992; Lambert et al., this volume).

The depositional setting of the majority of the rocks found in the Glass and Del Norte mountains is that of a foreland basin, with the clastic sediments derived from the Marathon Fold Belt and the carbonate and carbonate debris derived from a shoal formed on the geanticline between the foreland basin and the “deep” Delaware basin depositional complex.

The taxonomy of the many serrated *Mesogondolella* species is clarified, and several species are synonymized. New species described are *Sweetina crofti*, *Hindeodus wordensis*, *Iranognathus punctatus*, and *Sweetognathus bicarinum*.

Rohr had just become a professor at the small, nearby university (Sul Ross State), and much of this work and that of this volume evolved from the special relationship developed with the Sul Ross State University Geology Department and, specifically, with David Rohr and his students. I have suggested many topics and have worked alongside many students, and our thoughts and work have intermingled so that it is now difficult to identify where individual ideas began. This spirit of cooperation has expanded to most other workers in the field, including those that still do not agree with our interpretations of the biostratigraphy of this region. This volume, and in particular this article, is dedicated to that spirit of cooperation in our quest to unravel the complex history of the Permian of West Texas.

Brief descriptions of the general depositional setting (based on my interpretations) and of conodont biostratigraphic distribution are presented first. This is followed by a revision of conodont systematics, which comprises the bulk of this paper.

All figured conodont specimens are repositated at the National Museum of Natural History, formerly the United States National Museum (USNM). Unfigured specimens are retained in the conodont collections at the U.S. Geological Survey in Reston, Virginia.

Introduction

Shortly after Cooper and Grant (1972, 1974, 1975, 1976a,b, 1977) finished publishing their monographs on the Permian brachiopods of West Texas, Richard E. Grant and I started a project to describe in detail the conodont biostratigraphy, with special reference to the incredibly diverse brachiopod localities in the Glass Mountains. Our first year in the field was 1981, and one or both of us has not missed a field season since. David M.

Bruce R. Wardlaw, U.S. Geological Survey, 926A National Center, Reston, Virginia 20192.

GENERAL DEPOSITIONAL SETTING

The outcrop belt of the Permian rocks in the Glass and Del Norte mountains does not intersect depositional strike as clearly as it does in the Guadalupe Mountains. Instead, it parallels depositional strike, for the most part. The general Permian deposition can be summarized in two north–south schematics: one for the Glass Mountains (Figure 3-1) and one for the Del Norte Mountains (Figure 3-2). Deposition for each schematic transect can be generalized into three broad depositional regimes (trending from south to north): foreland basin, shoal, and Delaware basin (Hovey and Sheffield channels). Deposition in the Delaware basin is dominated by

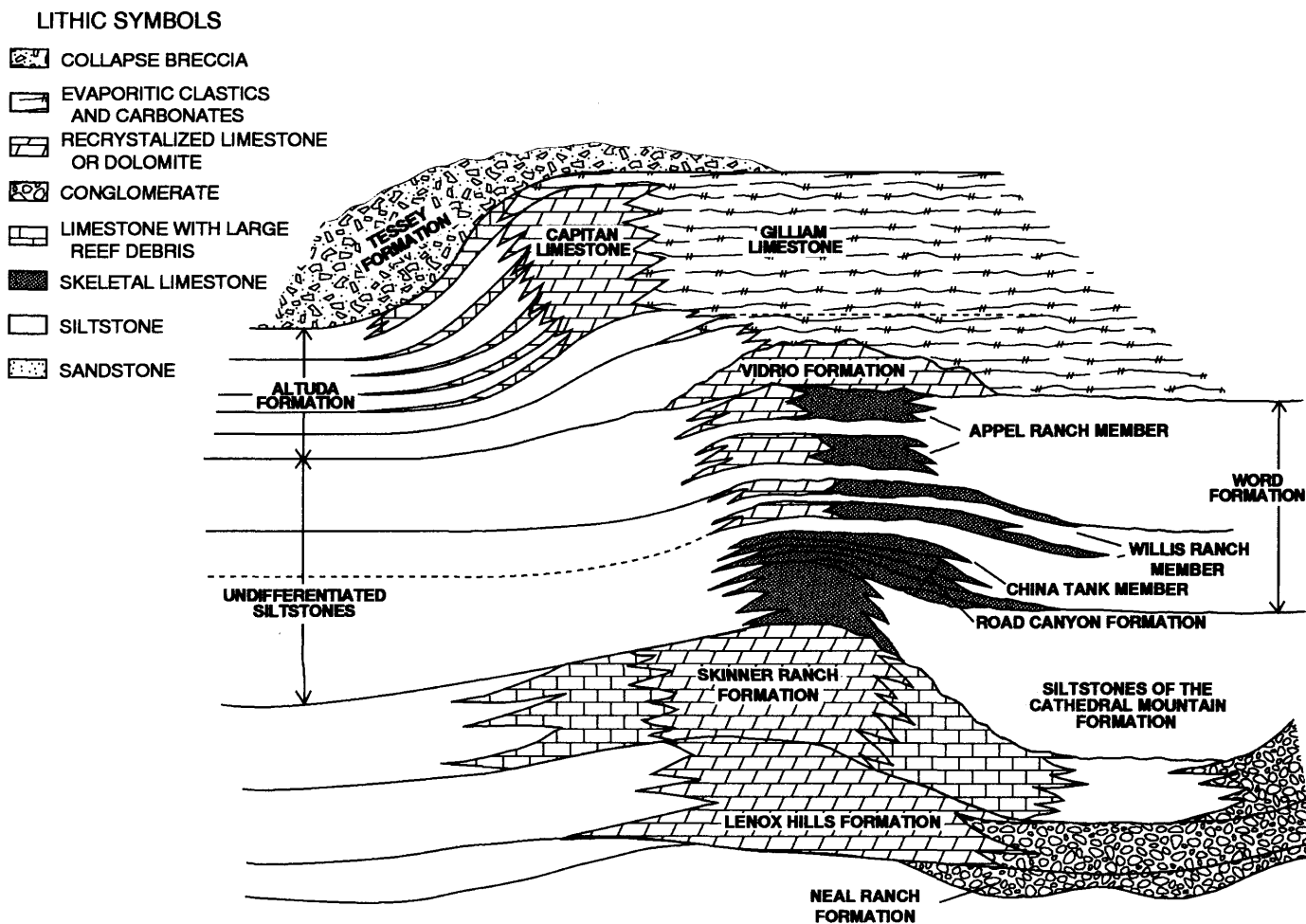


FIGURE 3-1.—Schematic north-south transect through the central Glass Mountains, West Texas, showing the stratigraphic relationships of Permian formations.

siltstone turbidites with rare limestone (skeletal lime mudstone) throughout the Permian. Carbonate appears more common in the basin during deposition of the Hess Formation (Leonardian) and the Capitan Limestone (Capitanian) on the shoal, implying more carbonate shedding. Deposition in the foreland basin is dominated by coarse conglomerate in the Lower Permian and siltstone and mudstone in the middle Permian. During the Wolfcampian and Leonardian, conglomerate represents shoreward deposition of fan- and braid-deltas (Rudine, 1988; Coombs, 1990; Wardlaw et al., 1990). Conglomeratic deposition commonly swamped the whole foreland basin and infringed on the shoal. Carbonate, conglomeratic carbonate, conglomerate, and siltstone were deposited on the shoal in both schematic transects during the Wolfcampian, and this process continued into the Leonardian in the Del Norte Mountains. In the Glass Mountains during the early Leonardian, shoal deposition is represented by dolomitic and silty lime mudstone of the Hess Formation. Skeletal and conglomeratic wackest-

ones, packstones, and rudstones shed from the shoal and/or deposited on the shoal flanks into the foreland basin represent the Skinner Ranch Formation. Conglomerate deposition was still widespread through the Cathedral Mountain deposition in the foreland basin along the Del Norte schematic transect. Sandstone, containing some conglomerate and generally capped by conglomerate, dominated deposition of the Cathedral Mountain Formation in the Del Norte Mountains. Common channeliform limestones, laterally discontinuous, also occur. In the Glass Mountain schematic transect, the Cathedral Mountain Formation is dominantly represented by siltstone. Carbonate, richly skeletal, is limited to a narrow part of the shoal and is commonly interbedded with siltstone. The foreland basin appears to have been largely filled in with siltstone during this time.

The Guadalupian was deposited on top of this accumulation of the Permian, thus continuing the general depositional setting. The Road Canyon Formation is represented by

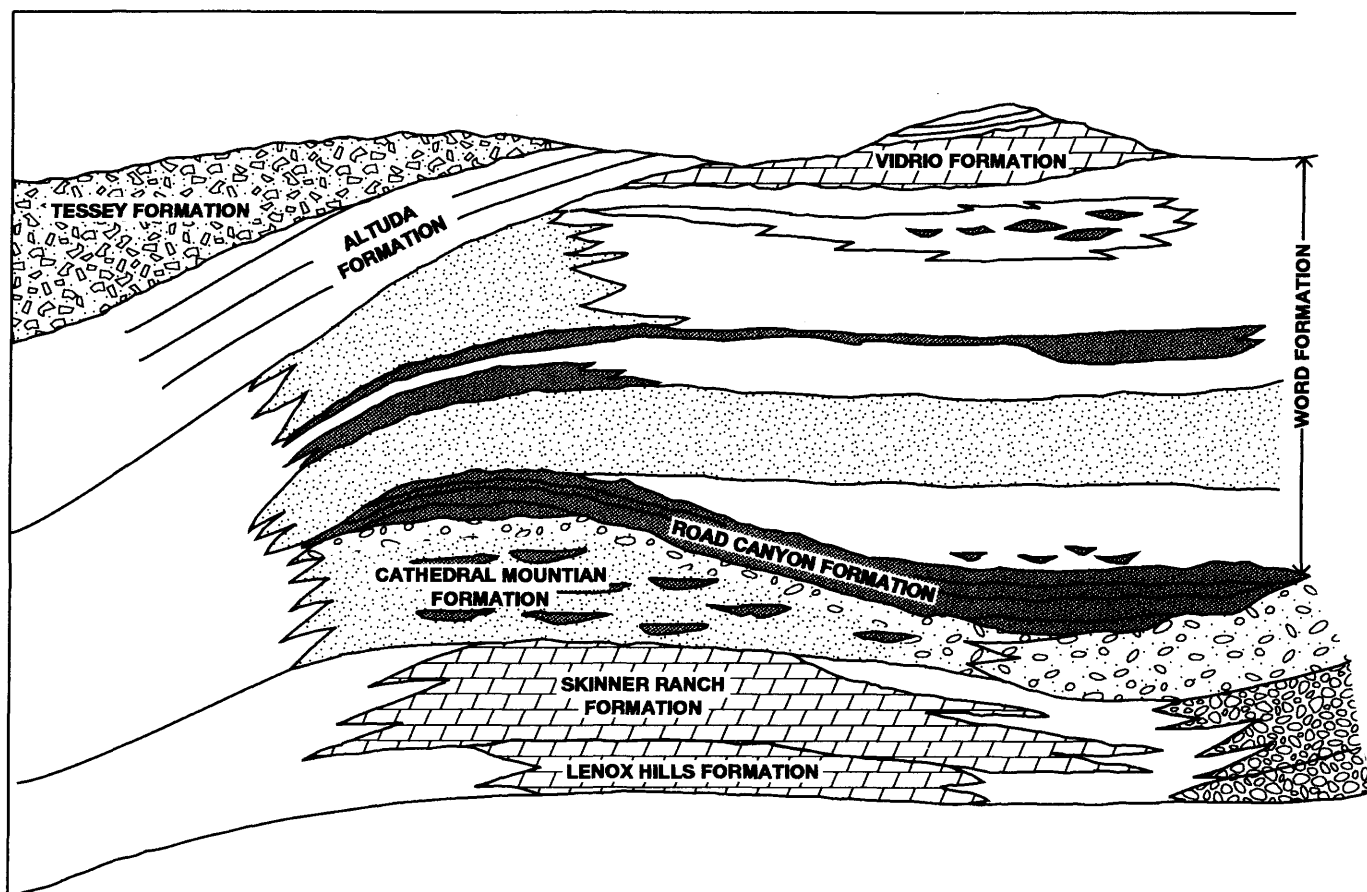


FIGURE 3-2.—Schematic north-south transect through the northern part of the Del Norte Mountains, West Texas, showing the stratigraphic relationships of Permian formations.

extensive channeliform, skeletal, sparsely conglomeratic limestones separated by sandstone and siltstone in the Del Norte Mountains in both the shoal area and the foreland basin, perhaps indicating a cessation of significant differentiation of the two sedimentary regimes. In the Glass Mountains, the Road Canyon is represented by a series of conglomeratic to skeletal limestones separated by siltstones deposited on the flank of the shoal. Foreland basin deposition is characterized by peloidal packstone (marginal to the shoal) and siltstone. The shoal facies is rarely discernible, but it is characterized by bioturbated lime mudstone to wackestone cut by several skeletal packstone to grainstone channels. This depositional sequence continues upward through the entire Word Formation where the shoal facies becomes more common, more recrystallized and dolomitized, and the siltstone becomes finer, changing to mudstone. In contrast, in the Del Norte Mountains, following Road Canyon deposition, the foreland basin is filled with siltstone with scattered channeliform skeletal limestones, rarely conglomeratic, followed by the shoal and foreland basin being covered by a blanket delta/delta front sand. The foreland basin is dominated by siltstone deposition following the blanket sand

deposition. The upper limestone of the Willis Ranch Member extends across most of the basin as channeliform carbonates and thin skeletal beds interbedded with siltstone and sandstone, and this interrupts the siltstone deposition in the foreland basin. The upper part of the Word Formation is represented by sand deposition on the shoal and silt deposition in the foreland basin. Within the basin, the Appel Ranch Member is represented by siltstone and numerous carbonate masses that appear to have been shed from a carbonate shoal that is now eroded away.

The Vidrio Formation is found only along the shoal and flanks to the foreland basin in both the Del Norte Mountains and Glass Mountains transects and is represented by extensive carbonate buildup that has been heavily recrystallized and dolomitized. This strongly suggests repeated subaerial exposure and shallow deposition. A limey siltstone divides the Vidrio in the middle of the Glass Mountains (Figure 3-3), suggesting deposition similar to the upper part of the Appel Ranch Member of the Word Formation, but on a much more extensive carbonate shoal. The Vidrio is also everywhere unconformably bounded.

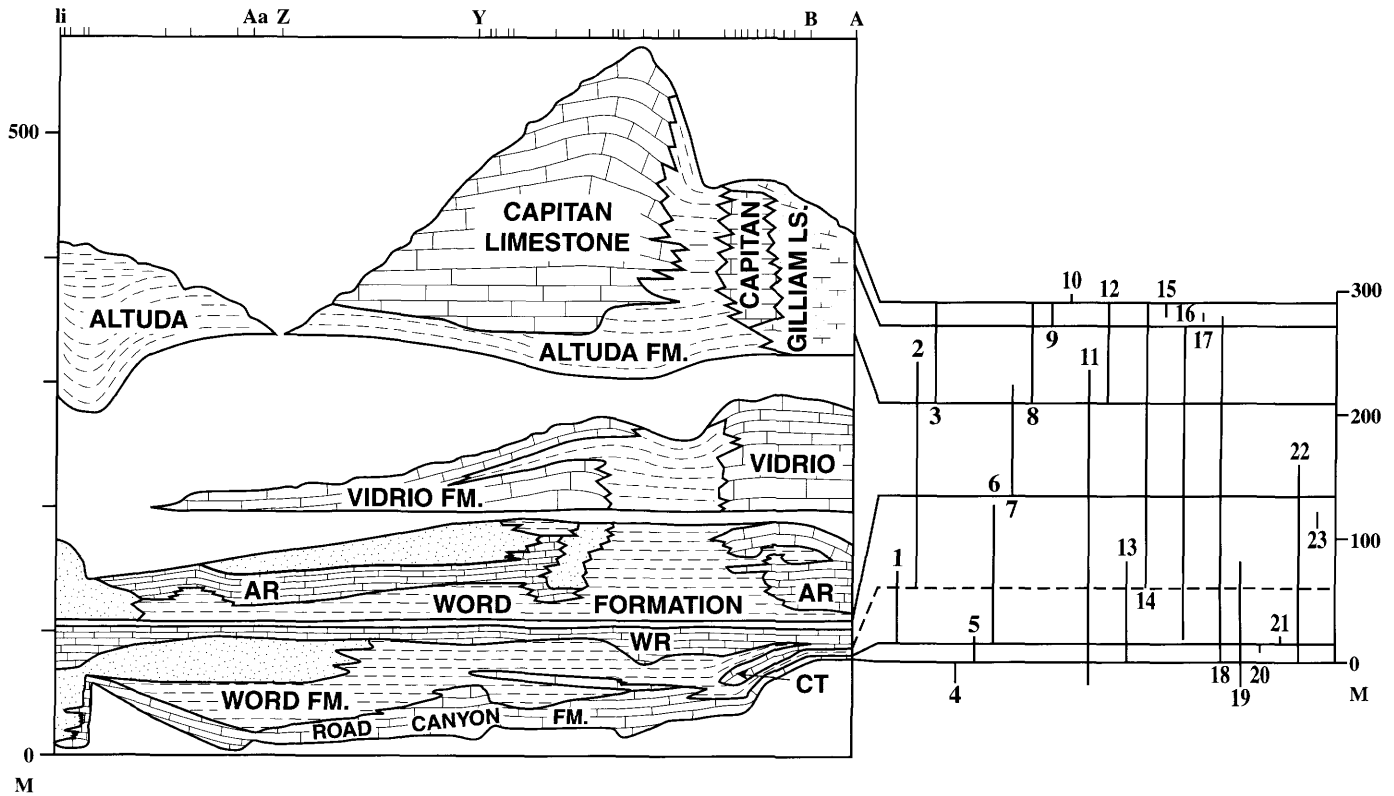


FIGURE 3-3.—Interpretative diagram of formations in a general east-west transect in sedimentary packages, true thickness, and true distance from the first stratigraphic section (A) 12PW, displaying conodont ranges and zonation. Letters represent stratigraphic sections from A to li (listed below). Numbers represent all recognized conodont species (same as Table 3-1).

A = 12PW	S = 7 (Wardlaw and Rudine)
B = Word I	T = Word II
C = 9AR	U = RC V
D = Upper Hess Canyon	V = RC VI
E = AR I (Middle Hess Canyon)	W = RC III
F = Lower Hess Canyon	X = RC IV
G = AR III	Y = RC IX
H = RC X	Z = RC XIV
I = Little Blue Mountain	Aa = RC XV
J = 10AR	Bb = RC XVI
K = AR II	Cc = SEC III
L = BR II	Dd = SEC VI
M = RC VII	Ee = DAV III
N = 10 (Wardlaw and Rudine)	Ff = DAV IV
O = 9 (Wardlaw and Rudine) & WR III	Gg = AL 1
P = RC I	Hh = AL 2
Q = RC II	li = AL 3
R = 8 (Wardlaw and Rudine) & WR IV	

In the Del Norte Mountains transect, the Vidrio Formation is overlain by the Altuda Formation. The Altuda thickens and develops more flow features and soft-sediment deformation northward, suggesting a change from shelf to slope deposition in a northern direction. In the Glass Mountain transect, the Gilliam Limestone, dominated by limey sandstones in its lower

part, was deposited in the foreland basin and on the shoreward side of the shoal. The Altuda Formation, dominated by carbonates and limey siltstones, was deposited on the basinward side of the shoal and into the Delaware basin. Either the Altuda or Gilliam overlies the Vidrio Formation in the Glass Mountains, indicating that the lower parts of both formations

are laterally equivalent. In the Glass Mountains, the Capitan Limestone developed on the shoal after deposition of unit 1 of the Altuda Formation (of Wardlaw and Rudine, this volume), which everywhere underlies the Capitan. The upper part of the Gilliam Limestone, represented by pisolitic limestones, evaporitic siltstones, and sandstone replete with tepee structures, is deposited in the foreland basin. Foresets of the Capitan Limestone interfinger with the upper part of the Altuda Formation on the basinward side of the shoal, and deposits from the upper part of the Altuda are on the slope and in the Delaware basin. A thin finger of the Gilliam appears to overlie the Capitan in a few sections. No Capitan Limestone (as currently defined) has been found in the Del Norte Mountains, as was suspected to be the case. Three informal units of the Altuda Formation (Wardlaw and Rudine, this volume) are found over its entire extent in the Del Norte Mountains, which indicates that Altuda deposition continued on the shoal/foreland basin, whereas it had ended on the shoal in the Glass Mountains and was restricted to just the foreslope and basin. It is unknown what, if anything, was deposited above the third unit of the Altuda in the southern part of the Del Nortes as erosion has destroyed any evidence of deposition. Additional units of the Altuda are found in the northern part (slope deposition) of the Del Norte Mountains.

BIOSTRATIGRAPHY

Because the nature of outcrops in the Glass and Del Norte mountains is one of cuestas commonly capped by carbonate and because the intervening valleys are dominated by poorly exposed siltstone and mudstone, complete long sections are difficult to find and measure. The measured sections are pieced together from several good, but relatively short, exposures. To understand the stratigraphic zonation of conodont species, each section was graphically correlated to standardize their relative distributions. The methodology used is that of Shaw (1964) and Edwards (1984). The data used is the presence-absence data in the distribution table (Appendix 3-1). Table 3-1 lists the composite ranges for each species recognized for this study. Five conodont zones, based on the range zones of *Mesogondolella* species, are recognized in the Guadalupian. These are the Transition Zone (transitional morphotype between *M. idahoensis* and *M. nankingensis*), the *M. nankingensis* Zone, the *M. aserrata* Zone, the *M. postserrata* Zone, and the *M. shannoni* Zone. An overlying, post-Guadalupian zone is suggested by the occurrence of *M. altudaensis* Kozur. In addition, an underlying zone, the *M. idahoensis*-*N. sulcopicatus* Zone (Wardlaw and Grant, 1987), is represented at a few places in the very base of the Road Canyon Formation. The *M. nankingensis* zone can be subdivided into two subzones based on the "synchronous" first occurrences of *Sweetina triticum* Wardlaw and Collinson and *Hindeodus wordensis*, new species, within the upper part of the range of *Mesogondolella nankingensis* (Ching). *Sweetina festiva* (Bender and Stoppel), and *Hindeodus excavatus*

TABLE 3-1.—Composite ranges of conodont species (in meters).

Species	Range
1. <i>Sweetina festiva</i>	0.15–74.75
2. <i>Sweetina triticum</i>	55.84–236.14
3. <i>Sweetina crofti</i>	210.00–290.18
4. <i>Mesogondolella idahoensis</i>	–29.20–2.29
5. <i>Mesogondolella idahoensis</i> – <i>nankingensis</i> transition	0.15–22.10
6. <i>Mesogondolella nankingensis</i>	13.47–128.03
7. <i>Mesogondolella aserrata</i>	136.07–223.79
8. <i>Mesogondolella postserrata</i>	210.00–288.08
9. <i>Mesogondolella shannoni</i>	272.96–290.18
10. <i>Mesogondolella altudaensis</i>	290.18–292.09
11. <i>Xaniognathus abstractus</i>	–29.20–236.14
12. <i>Xaniognathus hydraensis</i>	210.00–290.18
13. <i>Hindeodus excavatus</i>	0.00–82.45
14. <i>Hindeodus wordensis</i>	55.84–290.18
15. <i>Diplognathodus?</i>	280.07–290.18
16. <i>Diplognathodus</i> sp.	22.10–272.96
17. <i>Iranognathus</i> aff. <i>I. punctatus</i>	279.92
18. <i>Pseudohindeodus ramovsi</i>	0.15–280.07
19. <i>Neostreptognathodus clinei</i>	–27.22–153.60
20. <i>Neostreptognathodus sulcopicatus</i>	11.94–13.47
21. <i>Neostreptognathodus newelli</i>	13.47–14.66
22. <i>Sweetognathus bicarinum</i>	0.15–162.46
23. Reworked Ordovician–Permian Conodonts	113.24–123.40

(Behnken) are common within the lower part of the range of *M. nankingensis*. These subzones are referred to as A (lower) and B (upper).

The base of the Transition Zone occurs at or near the base of the Road Canyon Formation. The base of the *M. nankingensis* A Zone occurs within the lower third of the Road Canyon Formation, near the base of cycle 2 (Wardlaw, Ross, and Grant, this volume). The base of the *M. nankingensis* B Zone occurs at the base of the China Tank Member of the Word Formation and its equivalents (base of cycle 5 of Wardlaw, Ross, and Grant, this volume). The base of the *M. aserrata* Zone occurs just above the top of the Willis Ranch Member of the Word Formation. The base of the *M. postserrata* Zone occurs within the lower part of the Altuda Formation (within unit 2 of Wardlaw and Rudine, this volume) and the lower part of the Gilliam Limestone. The base of the *M. shannoni* Zone occurs in the upper part of the Altuda Formation (within unit 5 of Wardlaw and Rudine, this volume) and the upper part of the Capitan Limestone. The *M. altudaensis* Zone occurs at the uppermost beds of the Altuda Formation. It appears that *M. shannoni* Wardlaw may represent a short-lived transitional morphotype and zone between *M. postserrata* (Behnken) and *M. altudaensis*.

Reworked conodonts are common in a few samples from the upper part of the Willis Ranch Member of the Word Formation (upper part of the *M. nankingensis* B Zone) and may indicate the last significant tectonic signal from the Marathon Orogenic belt in the Permian in the Glass and Del Norte mountains.

Systematics

Phylum CONODONTA Pander, 1856

Class CONODONTI Branson, 1938

Order PRIONIODINIDA Sweet, 1988

Family ELLISONIIDAE Clark, 1972

Sweetina Wardlaw and Collinson, 1986

Sweetina was established for common ellisoniid ramiform elements that occur in the Lower and middle Permian. The apparatus is very similar to *Merrillina* and *Stepanovites*. Kozur (1975) named the type species of *Stepanovites*, *S. meyeri*, based on a partial apparatus. The apparatuses for *Sweetina* and *Merrillina* have been described by Wardlaw and Collinson (1986). In large collections, *Stepanovites* does not display the diagnostic Pa element of either *Sweetina* or *Merrillina* (Kozur, pers. comm., 1993) but appears to be like *Ellisonia* with two digyrate elements in its apparatus.

Sweetina crofti, new species

PLATE 3-4: FIGURES 14-23

DIAGNOSIS.—Characterized by a Pa element with a short, posteriorly directed lateral process bearing 0-1 denticle.

DESCRIPTION.—The Pa element is pastinate and arched. A posteriorly directed lateral process emerges from the outside of the cusp. The cusp is fairly large and recurved. The denticles on the anterior process of the cusp are evenly spaced; of nearly equal size, about half the size of the cusp, but decrease slightly anteriorly; and generally number just two or three. The denticles on the posterior process alternate in size, either minuscule or large, and generally there are at least two of each size. The lateral process bears either no denticle or one poorly developed denticle. The lower side has a groove under each process that merges with a triangular basal cavity under the cusp.

The Pb element is similar to the Pa element, except it lacks the lateral process and is oriented in the opposite direction (i.e., the anterior process of the Pb is more like the posterior process of the Pa). The cusp is slightly longer than the closest large denticles. The anterior process is downturned with a slight distal inflection or upturning. It bears three to six denticles, alternating thin and thick anterior to the first denticle next to the cusp, which is thick and nearly as large as the cusp. The denticles generally decline in height distally. The posterior process bears four to six denticles. The first denticle is definitely thinner and shorter than the cusp. The next two denticles are thick and relatively long; additional denticles decline in size distally. The lower side has a prominent groove and a small zone of recessive attachment surface.

The Sa element is alate and bears a large cusp, short lateral processes, and a long posterior process. Each lateral process

bears two to four denticles, depending on the size of the element, that decrease in size distally. The cusp is long and strongly recurved. Thin costae are directed to the top of each denticle, which are generally worn and not apparent. The denticles on the posterior process alternate in size, either minuscule or large, and are widely spaced immediately behind the cusp, becoming regularly spaced, but not compressed, after the second or third large denticle. Minuscule denticles on the posterior half of process commonly are overgrown and barely noticeable on larger specimens. The lower side is characterized by a large groove under each process and a zone of recessive attachment surface along the lateral sides of each process.

The Sb element has a large recurved cusp, an inward directed anterior-lateral process, and a long somewhat curved posterior process. The anterior-lateral process bears two to four denticles, decreasing in size distally. The posterior process bears many slightly compressed denticles; small thin denticles are sporadically preserved between the larger denticles. The lower surface is similar to the Sa element.

The Sc element has a large recurved cusp and a short anterior process that is directed slightly laterally; the process is straight to upturned. Sc elements are common but usually only as fragments. The denticulation of the Sc element is very similar to that of the Sa, with the anterior processes of the Sc comparing to the lateral processes of the Sa and with the posterior processes of both elements virtually the same. The lower surface of the Sc element is also similar to that of the Sa element.

The M element is digyrate and has a large reclined cusp, two short lateral processes, and a large flared basal cavity. The processes are denticulate, bearing one to three small to medium-sized denticles. The lower surface has a pronounced groove under each process.

TYPE SPECIMEN.—USNM 482636, Plate 3-4: Figure 20.

OCCURRENCE.—*Sweetina crofti* is common to the Capitanian rocks of the Permian basin (West Texas and New Mexico) and Wuchiapinian rocks of South China.

REMARKS.—*Sweetina crofti* differs from *S. festiva* by having a much less developed lateral process on the Pa element and having more small denticles between large denticles on the anterior and posterior processes. It is like *S. triticum* in having a reduced lateral process, but *S. triticum* has many more small denticles between large denticles on each process. The anterior process of both *S. triticum* and *S. festiva* are much longer than *S. crofti*.

Sweetina festiva (Bender and Stoppel)

PLATE 3-12: FIGURES 6-8

Lonchodina festiva Bender and Stoppel, 1965:345-346, pl. 15: figs. 9, 10.
Stepanovites festiva (Bender and Stoppel).—Kozur, 1975:23; 1978, pl. 5: fig. 29.—Kozur and Movschovitsch in Movschovitsch et al., 1979:119, pl. 4: figs. 1, 2.
Sweetina festiva (Bender and Stoppel).—Wardlaw and Collinson, 1986:138.

DIAGNOSIS.—Characterized by a Pa element with a large lateral process bearing 2–5 large denticles.

REMARKS.—Typically, *S. festiva* has only one small denticle anterior to the cusp.

Sweetina triticum Wardlaw and Collinson

PLATE 3-12: FIGURE 9

Sweetina triticum Wardlaw and Collinson, 1986:135, fig. 20.

DIAGNOSIS.—Characterized by a Pa element with a short lateral process generally bearing 1 or 2 denticles of variable size.

REMARKS.—When broken, the Pa element looks similar to that of *S. crofti* (see Plate 3-4: Figure 19), but the lateral process is more laterally directed and the break shows a much larger process than is typical for *S. crofti*.

Family GONDOLELLIDAE Linström, 1970

Mesogondolella Kozur, 1989

Kozur (1989) established the genus *Mesogondolella*, although he (Kozur, 1989) referred to an abstract (Kozur, 1988) as the citation. Clearly, Permian gondolellids are different from Triassic ones, and this has been common knowledge since Clark and Mosher (1966) demonstrated the distinctive bottom features of Permian and Triassic gondolellids. There is also a hiatus between the last of the Permian forms and the first of the Triassic forms (true *Neogondolella*), suggesting a new name is needed. The differentiation of the two genera of Permian gondolellids recognized by Kozur (1989), *Mesogondolella* and *Clarkina*, is less clear but is provisionally accepted herein pending more detailed work and better definition. The suspicion is that cool-water faunas, exemplified by *Clarkina? bitteri* Wardlaw and Collinson, gave rise to most Late Permian gondolellids, and they can be differentiated from *Mesogondolella* on the basis of bottom features, including a more complex basal pit and loop along with the presence of a free blade (the difference cited by Kozur, 1989). Nevertheless, all the forms recognized herein from the Permian of West Texas belong to the genus *Mesogondolella*.

The succession of *Mesogondolella* species generally show transitional forms for a short interval between species. The transitional form between *M. idahoensis* and *M. nankingensis* was described by Lambert and Wardlaw (1992) and persists for a significant, though short, stratigraphic interval. The transitional forms from *M. aserrata* to *M. postserrata* and *M. postserrata* to *M. shannoni* appear to be much shorter lived. They are illustrated and described herein, but they are not given specific recognition. *Mesogondolellas* of the “*serrata*” complex (Clark and Behnken, 1979) appear to have evolved from species to species through transitional forms that combined the features diagnostic for predecessor and successor. Lambert and Wardlaw (1992) described the evolution of the transitional

form from *M. idahoensis* to *M. nankingensis* (= *M. serrata*) as a heterochronic process of neoteny that produced progressive juvenilization.

Clark and Behnken (1979) described several species that are not recognized. These species were established on visual determination of symmetry (*aserrata*, *postserrata*, *babcocki*, *wilcoxi*), or preservation (*denticulata*), or on the presence of a split carina (*rosenkrantzi*). Split carinae occur in all examined samples of abundant *Mesogondolella*, *Clarkina*, and *Neogondolella* from the Early Pennsylvanian to the Late Triassic at a frequency of about 2%–5% in each sample. It is not a useful species determiner, and the topotypes of *M. rosenkrantzi* (= *M. phosphoriensis*) commonly do not display this feature at a different frequency (for examples of types and topotypes see Bender and Stoppel, 1965; Sweet, 1976; Wardlaw and Collinson, 1979). The pristine preservation of the denticles of the carina, a rare occurrence as they are commonly abraded or worn in most specimens, is also a poor species determiner of no stratigraphic utility or biologic basis.

Clark and Behnken (1979:265, fig. 2) devised a visual determination of symmetry that at best is tenuous. The platform of species of the “*serrata*” complex is variable. The platform normally has different widths on each side of the carina, rarely forms a brim around the posterior cusp, and commonly terminates at unequal positions on each side of the cusp. The cusp is commonly directed laterally. A nonquantified or unsystematic measure for symmetry could be very misleading. For instance, 1,000 whole specimens of *M. postserrata* were tallied from one sample of the Rader Limestone Member of the Bell Canyon Formation using the symmetry diagram of Clark and Behnken (1979, fig. 2). Four categories were counted: symmetric elements, asymmetric elements with symmetrically placed cusp, sinistral elements, and dextral elements, which yielded 8, 6, 494, and 492 for each category, respectively. That is, at best, 1.4% symmetrical for a unit that Clark and Behnken reported 22% (1979, table 1) symmetrical elements. The methodology, which is questionable, is unreproducible, and therefore invalid. What is interesting is the 50 : 50 division of sinistral and dextral elements that was obtained from both Clark and Behnken’s data (1979) and the above tallies. If all asymmetric aspects are considered, the percentage of symmetric elements (those not placed in sinistral or dextral categories) ranges from 0.8% to 6.7%. In the case of the 1,000 elements counted from the Rader, 49.7% are sinistral and 49.5% are dextral. It appears *Mesogondolella postserrata* occurs as a pair of sinistral and dextral Pa elements. Croft (1978, pl. 3: figs. 1, 2) recovered one such pair fused together in his material from the Bell Canyon Formation. The species *Mesogondolella aserrata* (see below) and *M. wilcoxi* (= serrated morphotype of *Clarkina bitteri*, Wardlaw and Collinson, 1979) can be differentiated on other criteria, so they are retained and redefined.

Mesogondolella, *Clarkina*, *Gondolella*, and *Xaniognathus* all have similar apparatuses. *Mesogondolella* and *Clarkina*

generally lose their apparatuses through growth and can be treated as a paired Pa element in species determinations. *Xaniognathus*, the successor of "nude" *Gondolella* species, has an apparatus that is the same as *Gondolella* and does not occur in studied collections below the late Wolfcampian. *Mesogondolella* probably derived from *Idioproniodus* in the late Morrowan, although no direct predecessor is clear. It occasionally occurs with an apparatus that can be differentiated from that of *Gondolella* or *Xaniognathus*, although it is similar. *Xaniognathus* is included as the apparatus of *Mesogondolella* and *Clarkina* by many workers, and this may be due to the lack of detailed work or descriptions.

Finally, the examination of the two extant topotypes of *M. nankingensis*, which were part of the paradigm for the species concept, leads one to conclude that *M. serrata* and *M. nankingensis* are one in the same and coincident in time; therefore, *M. nankingensis* has priority, and the commonly used *M. serrata* is a junior synonym. Lambert and Wardlaw (in prep.) attempt to demonstrate this with their morphometrics to distinguish species.

***Mesogondolella idahoensis* (Youngquist, Hawley, and Miller), new combination**

PLATE 3-10: FIGURES 1-3

Gondolella idahoensis Youngquist, Hawley, and Miller, 1951:361, pl. 54: figs. 1-3, 14, 15.—Clark and Ethington, 1962:108, figs. 15, 16.—Clark and Mosher, 1966:388, pl. 47: figs. 9-12.—Clark and Behnken, 1971:431, pl. 1: fig. 9.

Neogondolella idahoensis (Youngquist, Hawley, and Miller).—Behnken, 1975:306-307, pl. 1: figs. 28-30.—Wang, 1978:220-221, pl. 2: figs. 23-26.—Igo, 1981:38, pl. 1: figs. 11-13, 15, 16.

Gondolella phosphoriensis Youngquist, Hawley, and Miller, 1951:362, pl. 54: figs. 27, 28 [in part].—Clark and Ethington, 1962:108, pl. 2: figs. 17, 18.

DIAGNOSIS.—Platform (Pa element) of moderate width, gradually narrowing in the anterior two-thirds of length, and with a blunt, squared posterior platform margin. Cusp moderately large, prominent, circular in cross section; denticles generally increase in size anteriorly, except for anterior one or two; furrows well-developed. Lower side with a simple loop around posterior of slit-like basal pit, loop terminal on posterior of lower attachment surface; lower attachment surface a moderate-sized V-shaped impression posteriorly, becoming either a narrow V-shaped impression anteriorly (Plate 3-10: Figure 1), an inverted elevated scar anteriorly (Plate 3-10: Figure 2), or a slightly elevated keel in anterior one-fourth of element (Plate 3-10: Figure 3).

REMARKS.—*Mesogondolella idahoensis* can be distinguished from *M. zsuksannae* (Kozur) by its more blunt posterior platform termination, larger, more robust cusp, more parallel-sided margins, different denticulation pattern (*M. zsuksannae* has at least one smaller denticle in the middle of the posterior carina, whereas denticles on *M. idahoensis* increase in

size anteriorly), more fused carina, and generally lacks a distinct buttress. *Mesogondolella idahoensis* differs from the transitional form to *M. nankingensis* by not having serrations in small forms or showing the faint overgrown serrations along the furrow in large specimens as does the transitional form.

Morphological Transition from *Mesogondolella idahoensis* to *Mesogondolella nankingensis*

PLATE 3-2: FIGURES 38, 39; PLATE 3-10: FIGURES 4-7

Morphological transition from *Mesogondolella idahoensis* to *Mesogondolella nankingensis*, Lambert and Wardlaw, 1992:879-880.

DIAGNOSIS.—Platform (Pa element) displaying characters transitional between *M. idahoensis* and *M. nankingensis*, the most striking being appearance of serrations in small specimens. In large specimens, serrations initially masked at margins, leaving faint relict serrations adjacent to furrows; serrations eventually fully masked beneath successive growth laminae. In stratigraphically higher samples, moderate-sized specimens displaying faint serrations; on small specimens serrations better defined. Incrementally increasing pattern of serration carried progressively later through ontogeny with increasingly younger faunas, until pronounced serrations distinctly visible in side view as notches cut into anterior platform margins. Notches not discernible from this perspective on earlier transitional forms. In lower view, broad, flat, and commonly recessed basal attachment surface of large specimens of *Mesogondolella idahoensis* becoming narrower and developing a consistently elevated keel through transition. In large specimens of *M. idahoensis*, fused anteriormost denticles of carina separate, becoming discrete during the transition, a character of both *M. nankingensis* and small specimens of *M. idahoensis*. Cusp subtly migrates posterolaterally, becoming less pronounced.

All these characters can be seen to have evolved through a mosaic heterochronic pedomorphocline.

REMARKS.—Lambert and Wardlaw (1992, and in prep.) detailed the transitional morphotype, especially in the later paper where they used morphometrics on tightly constrained stratigraphic samples to illustrate this morphocline transition.

***Mesogondolella nankingensis* (Ching [Jin]), new combination**

PLATE 3-10: FIGURES 8-10

Gondolella nankingensis Ching [Jin], 1960:246, pl. 2: figs. 5-8.

Gondolella serrata Clark and Ethington, 1962:108-109, pl. 1: figs. 10, 11, 15, 19, pl. 2: figs. 1, 5, 8, 9, 11-14.—Clark and Mosher, 1966:389, pl. 47: figs. 13-15.—Clark and Behnken, 1971:431, pl. 1: fig. 10.

Neogondolella serrata (Clark and Ethington).—Clark and Behnken, 1979: 268-271, pl. 1: fig. 12.—Wang, 1978:222, pl. 2: figs. 6-8, 14, 15, 20-22.—Wardlaw and Collinson, 1984:270, pl. 2: figs. 13-15.

Neogondolella serrata serrata (Clark and Ethington).—Behnken, 1975:308, pl. 2: figs. 21-24, 37.

DIAGNOSIS.—Platform of moderate width, generally short and arched, narrowing anterior to middle, and with round to blunt posterior margin; lateral platform margin variably serrated, usually with at least 3 or more paired serrations on the anterior tapering part, rarely serrated for almost entire margin. Cusp moderate, circular in cross section; denticles generally increasing in size anteriorly, except commonly 1 or 2 smaller denticles along middle of carina and 1 or 2 denticles at anterior end; furrows moderately developed, smooth. Lower side with well-developed single loop around posterior of slit-like basal pit; loop subterminal on posterior of lower attachment surface; lower attachment surface a relatively narrow V-shaped impression with slightly elevated margins, becoming a keel in anterior one-fourth of element.

REMARKS.—*Mesogondolella nankingensis* is clearly different from *M. idahoensis* by its retention of lateral serrations in all growth stages, its more rounded (less blunt) posterior platform margin termination, and its more sharply narrowing anterior platform.

***Mesogondolella aserrata* (Clark and Behnken),
new combination**

PLATE 3-3: FIGURES 1-16; PLATE 3-5: FIGURES 1-7;
PLATE 3-10: FIGURES 11-17

Neogondolella aserrata Clark and Behnken, 1979:271-272, pl. 1: figs. 1-11.

DIAGNOSIS.—Platform of moderate width and length, slightly arched and bowed, widest posterior to middle, narrowing gradually to anterior from widest point; platform with a bluntly rounded posterior end with a brim in most large specimens. Nearly 50% of specimens with slight to marked inflection along inner lateral margin in posterior one-third of specimen; lateral platform margin serrated to slightly serrated (1 or 2 poorly developed pairs) on anterior one-third of platform. Cusp small to moderate, circular to elongate in cross section; denticles generally of varying size and height on posterior one-third to one-half of platform before increasing steadily in size anteriorly, except distalmost, which decrease in size; generally denticles in middle section of carina the lowest and most fused; furrows shallow and not well demarcated (micro-ornamentation infringing on furrows), and margins only slightly upturned (reflecting the shallower furrows). Lower side with poorly to well-developed double loop posterior to slit-like basal pit; loop posteriorly terminal on lower attachment surface; lower attachment surface appears as a shallow V-shaped impression with slightly elevated margins forming a keel anteriorly and a narrow, slightly elevated groove as an inner keel in anterior one-third of element.

REMARKS.—The poorly defined and shallow furrows that are not completely smooth distinguish this species from its predecessor (*M. nankingensis*) and successor species (*M. postserrata*), both of which have nicely incised, smooth furrows. Most specimens of *M. aserrata* are less arched and

have a less upturned margin than either *M. nankingensis* and *M. postserrata*. In addition, the anterior platform shows less dramatic narrowing toward the anterior than it does in the other two species.

***Mesogondolella postserrata* (Behnken),
new combination**

PLATE 3-4: FIGURE 28; PLATE 3-5: FIGURES 13-20; PLATE 3-6: FIGURES 1-7;
PLATE 3-7: FIGURES 1-11; PLATE 3-10: FIGURES 18, 19;
PLATE 3-11: FIGURES 1-4

Neogondolella serrata postserrata Behnken, 1975:307-308, pl. 2: figs. 31, 32, 35.

Neogondolella postserrata Behnken.—Clark and Behnken, 1979:272, pl. 1: figs. 13-17, 21.

Neogondolella babcocki Clark and Behnken, 1979:272-274, pl. 2: figs. 5, 6, 11-15, 17, 18.

Neogondolella denticulata Clark and Behnken, 1979:272, pl. 1: figs. 18-20, 22, 23.

Neogondolella rosenkrantzi (Bender and Stoppel).—Clark and Behnken, 1979:272-273, pl. 2: figs. 1-4, 7-9.

Mesogondolella "babcocki" (Clark and Behnken).—Kozur, 1992:103, fig. 4 [in part].

DIAGNOSIS.—Platform of narrow width but moderate length, arched and bowed, widest usually posterior to middle, but rarely widest near posterior end; platform narrowing gradually or platform margins subparallel from anterior of widest point to anterior one-fourth at position of both a slight increase to anterior narrowing and a sharp downward turn to platform; platform with asymmetric and blunt posterior end, subrounded to rounded, if rounded, generally very narrow, with a very narrow brim in most large specimens; many specimens with slight inflection along inner lateral margin in posterior one-third of specimen; lateral platform margin serrated on anterior one-third. Cusp moderate size, circular to elongate in cross section; denticles generally decreasing in size to middle of platform, except first and third or fourth denticles anterior to cusp may be larger; denticles anterior to middle of platform increasing steadily in size anteriorly except distalmost decreasing in size; denticles in mid-section of carina generally the lowest and most fused; platform margin in many specimens upturned and nearly equal to height of carina in its mid-section; furrows well developed, narrow, generally deeply incised, and smooth. Lower side with well-developed double loop around posterior of slit-like basal pit; loop terminally located on posterior of lower attachment surface; lower attachment surface shallow V-shaped impression with slightly elevated margins forming a keel anteriorly and forming a narrow, slightly elevated groove as an inner keel in anterior one-half of element.

REMARKS.—*Mesogondolella postserrata* displays transitional morphologies during its short overlap with its predecessor, *M. aserrata* (e.g., Plate 3-5: Figures 13-20; Plate 3-10: Figures 18, 19), and its successor, *M. shannoni* (e.g., Plate 3-6: Figures 1-7; Plate 3-7: Figures 1-11; Plate 3-11: Figures 1-4). Commonly, *M. postserrata* can be easily distinguished by its

subparallel posterior platform margins, slight inflection on the inner posterior margin, and smooth well-incised furrows. In many respects *M. postserrata* more closely resembles *M. nankingensis*, but it can be differentiated by its narrower platform, rounded posterior platform termination, common presence of a brim, serrations restricted to the anterior one-third, and double loop around the basal pit.

The figure caption for the specimens illustrated by Clark and Behnken (1979, pl. 1) as *M. denticulata* is confusing. Their figs. 18, 19, and 22 are listed as upper, lateral, and lower views, respectively, implying that they are the views of the same specimen when, in fact, they are views of different specimens from the same locality. The holotype, fig. 19, with its highly upturned margin, is different from most *M. postserrata* and may be a pathological morphotype. Similar specimens were not found in the moderately extensive Guadalupe Mountains material from the same or nearby beds. The specimens illustrated in figs. 18, 20, 22, and 23 (Clark and Behnken, 1979, pl. 1) do not possess this highly upturned margin and are not different from *M. postserrata*.

***Mesogondolella shannoni* Wardlaw in Mei, Jin,
and Wardlaw**

PLATE 3-4: FIGURES 26, 27, 29, 30; PLATE 3-6: FIGURES 8-15; PLATE 3-7:
FIGURES 12-25; PLATE 3-8: FIGURES 1-22; PLATE 3-9: FIGURES 1-27;
PLATE 3-11: FIGURES 5-14

Mesogondolella shannoni Wardlaw in Mei, Jin, and Wardlaw, 1994:228, pl. 1:
fig. 21.

Clarkina? wilcoxi (Clark and Behnken).—Kozur, 1992, figs. 7, 8.

? *Clarkina* cf. *subcarinata* (Sweet).—Kozur, 1992, fig. 21.

DIAGNOSIS.—Platform broad, arched and slightly bowed, widest in posterior one-third, narrowing gradually from widest point with a slight increase in narrowing or a “pinch” near beginning of anterior one-fourth of platform; platform with broadly rounded posterior end, and with well-developed brim in large specimens; lateral platform margin with a few to many serrations on anterior (narrower or narrowing) one-fourth. Cusp generally high conical, occasionally merging with small posterior denticle or first denticle anterior to cusp to form a large elongate denticle in some large specimens; denticles crudely decreasing in size anteriorly to midpoint and then increasing in size until distalmost, with distalmost being smaller; posterior denticles with general pattern of crudely decreasing size, but denticles alternate between relatively larger and smaller size, especially in width; furrows generally narrow and well incised, but variable, ranging from those like *M. postserrata* to those like *M. altudaensis*; commonly, boundary between reticulate and smooth ornament near furrow edge indistinct. Lower side with well-developed double loop around posterior of basal pit; loop subterminally located on posterior of lower attachment surface; lower attachment surface a shallow V-shaped impression with slightly elevated margins forming a keel anteriorly and forming a narrow, slightly elevated groove as an inner keel in anterior one-third to one-half of element.

TYPE SPECIMEN.—USNM 482680, Plate 6: Figure 14.

OCCURRENCE.—*Mesogondolella shannoni* is found in the uppermost part of the Altuda Formation in the Glass and Del Norte mountains and is common in the upper part of the Wuchiaping Formation in South China.

REMARKS.—*Mesogondolella shannoni* and *M. altudaensis* are very similar, and *M. shannoni* is the morphologically transitional form from *M. postserrata* to *M. altudaensis*. *Mesogondolella shannoni* has a short but significant range, so it is separated herein. *Mesogondolella shannoni* differs from *M. postserrata* by having a broader platform that has a well-rounded posterior termination, a generally well-developed brim, and a less-upturned inner lateral margin. Its denticulation pattern is similar to that of *M. postserrata*, but it lacks the variability of *M. postserrata* in the posterior carina. *Mesogondolella postserrata* has denticles of different sizes (height and width) that occur in an overall pattern of decreasing size, whereas the denticles of *M. shannoni* just display a general decrease in height but vary in width. *Mesogondolella shannoni* has a much better developed double loop around the posterior of the basal pit that is generally raised much higher than that of *M. postserrata*.

Large samples of this species have shown many large “pathologically” unusual and bizarre morphotypes (e.g., Plate 3-7: Figure 25). The form illustrated by Kozur (1992, fig. 21) appears to be a corroded pathological morphotype of this species. Transverse ridges are common to a small percentage of large specimens in most large populations (Plate 3-7: Figures 20, 24; Plate 3-8: Figure 20).

***Mesogondolella altudaensis* (Kozur),
new combination**

PLATE 3-5: FIGURES 8-12; PLATE 3-11: FIGURES 15-17

Clarkina altudaensis Kozur, 1992:103-106, figs. 9-12, 14-17.

Mesogondolella “babcocki” (Clark and Behnken).—Kozur, 1992:103, figs. 5, 6 [in part].

Clarkina n. sp. Kozur, 1992, fig. 13.

DIAGNOSIS.—Platform broad, widest near midline or posterior to midline, narrowing smoothly, but sharply, posteriorly and narrowing gradually anteriorly, commonly with a small “pinching” of platform at or about where the anterior denticles become high, platform then turns slightly downward at this point to the anterior; most specimens slightly to subtly serrated at, and anterior to, platform pinching, only rare specimens appearing smooth; platform forming small brim around the posterior end; specimens with a narrow posterior platform develop primitive buttress. Cusp of small to moderate size, elongate-oval in cross section; generally at least one of the first posterior denticles clearly larger than cusp, first 4-6 denticles posterior to the cusp initially increase then decrease in size, then denticles generally increase in size anteriorly, except for distalmost one or two; furrows generally broad and shallow, with vague boundary between smooth and reticulate micro-ornamentation. Lower surface with well-developed double loop around posterior of basal pit; posterior of inner loop very

elevated; loop subterminally located on posterior of lower attachment surface; lower attachment surface a shallow V-shaped impression with slightly elevated margins forming a keel anteriorly and forming a narrow slightly elevated groove as an inner keel in anterior one-half or more of element.

REMARKS.—Kozur (1992:105) implied in his remarks (but not in his diagnosis!) that all specimens have smooth anterior margins, although his illustrations, with the exception of the holotype, all display distinct to indistinct serrations. An examination of the abundant material from large samples from studied sections (including that used by Kozur) indicates that the apparently smooth morphotypes are rare.

Mesogondolella altudaensis can be distinguished from *M. shannoni* by its much smaller, very reduced cusp, less distinct furrows, and slightly less upturned platform margin. Also, the platform of *M. altudaensis* is widest near the midline, whereas that of *M. shannoni* is widest nearer the posterior end, and this is expressed as narrower posterior shoulders in *M. altudaensis*, less distinct serrations, more pronounced anterior pinching or narrowing of the platform, and more fused denticles, especially in the middle part of the carina.

Xaniognathus Sweet, 1970

Xaniognathus abstractus (Clark and Ethington)

- Subbryantodus abstractus* Clark and Ethington, 1962:112–113, pl. 1: figs. 16, 20, 21, pl. 2: fig. 2.
Lonchodina mulleri Tatge.—Clark and Ethington, 1962:110–111, pl. 1: fig. 4.
Apatognathus tribulosus Clark and Ethington, 1962:107, pl. 1: figs. 3, 7, 13, 17.—Wardlaw and Collinson, 1984:271 [placed in synonymy].
Ozarkodina tortilis Tatge.—Clark and Behnken, 1971:433, pl. 2: fig. 8.
Xaniognathus abstractus (Clark and Ethington).—Behnken, 1975:313, pl. 1: fig. 15.—Wardlaw and Collinson, 1984:271, pl. 2: figs. 1–12; 1986:135, figs. 18, 17–23.—Behnken, Wardlaw, and Stout, 1986:185, figs. 5.4–7, 6.7–20.—Wardlaw and Grant, 1990:A8, pl. 4: figs. 1–22.
Xaniognathus tortilis (Tatge).—Behnken, 1975:313, pl. 2: fig. 13.
Xaniognathus sp. Maikowski and Szaniawski, 1976:83, pl. 1: fig. 2.
Sweetocristatus arcticus Szaniawski, 1979:254, pl. 9: figs. 1–7.—Wardlaw and Collinson, 1984:271 [placed in synonymy].

DIAGNOSIS.—Sb (*Apatognathus tribulosus*) element delicate, greatly recurved, with large cusp and low denticles on one process; large variable Pb element with a twisted posterior process commonly bearing 5–8 denticles, rare specimens with more denticles; anterior process variable, robust to relatively thin and delicate, commonly bearing 7–11 or more denticles, with midlateral rib extending most of process length.

REMARKS.—The apparatus of *X. abstractus* from West Texas material is well illustrated in Wardlaw and Grant (1990).

Xaniognathus hydraensis Nestell and Wardlaw

PLATE 3-4: FIGURES 1–13; PLATE 3-12: FIGURES 3–5

- Xaniognathus hydraensis* Nestell and Wardlaw, 1987:770–771, figs. 7.1–7.13.
Gondolella orientalis Barskov and Koroleva.—Kozur, 1975:18–19, pl. 2: figs. 11–15 [in part]; 1978, pl. 8: figs. 9–11, 13.

Gondolella leveni Kozur, Mostler, and Pjatakova.—Kozur, 1975:16–17, pl. 3: figs. 6, 7 [in part, not fig. 8a,b (= *Merrillina?* sp.)]; 1978, pl. 7: figs. 8, 9 [in part, not fig. 11a,b (= *Merrillina?* sp.)].

DIAGNOSIS.—Pb element with long large cusp, nearly straight anterior process, and short twisted posterior process generally with 4 or 5 denticles.

REMARKS.—Nestell and Wardlaw (1987) first illustrated the apparatus of this species from scrappy material from Hydra Island, Greece. The material figured herein better illustrate all the elements of the apparatus. *Xaniognathus hydraensis* is distinguished from *X. abstractus* by a Pb element that has a shorter, less twisted posterior process, a larger cusp, slightly more discrete denticles, and a thinner anterior process.

Order OZARKODINIDA Dzik, 1976

Family ANCHIGNATHODONTIDAE Clark, 1972

Hindeodus Rexroad and Furnish, 1964

Hindeodus excavatus (Behnken)

PLATE 3-2: FIGURES 1–21

- Ellisonia excavata* Behnken, 1975:302–303, pl. 1: figs. 9–14.
Anchignathodus minutus (Ellison).—Behnken, 1975:297, pl. 1: figs. 16–18.—Kozur, 1975:5–7, pl. 1: fig. 16 [in part].
Anchignathodus minutus permicus Igo, 1981:26–27, pl. 10: figs. 1–4. [New synonymy].
Hindeodus? excavatus (Behnken).—Sweet, 1977:215–217, pl. 1: figs. 7–11.

DIAGNOSIS.—Pa element with narrow, pointed cusp and with denticles of nearly equal width except for the posterior-most few, these being narrower and decreasing in height posteriorly; 3–4 denticles immediately posterior to cusp less fused than more posterior denticles. Small specimens (the most common) triangular in lateral profile. Sa element with downward-directed processes at about a 40° angle from horizontal; processes nearly straight and bearing thin, fine denticles of variable height, with 2–3 large lateral denticles at or near distal end, and with a small distal denticle only sometimes developed; denticles on processes straight to slightly recurved.

Hindeodus wordensis, new species

PLATE 3-4: FIGURES 24, 25; PLATE 3-12: FIGURES 1, 2

- Hindeodus excavatus* (Behnken).—Wardlaw and Collinson, 1984:268–269, pl. 5: figs. 1, 2, 4–9; 1986:133, fig. 17.13–20.—Wardlaw and Grant, 1990: A6, pl. 2: figs. 1–15, pl. 3: figs. 4, 5, 9–11 [in part, not figs. 3, 6–8].—Gullo and Kozur, 1992:218, fig. 5E.

DIAGNOSIS.—Pa element with large cusp; denticles increasing in width posteriorly, except for posteriormost, and generally decreasing in height posteriorly, except for posteriormost three, which may be of subequal height; cusp much higher than denticles; Sa element with short lateral processes;

processes slightly upturned laterally and bearing, for at least part of their length, denticles of alternating (smaller versus larger) sizes.

TYPE SPECIMEN.—USNM 404252 (Wardlaw and Collinson, 1986, fig. 17.20).

OCCURRENCE.—*Hindeodus wordensis* is common in the Word, Altuda, and Bell Canyon formations of West Texas and in the Gerster Limestone and the upper part of the Phosphoria and related rocks in the Great Basin and northern Rocky Mountains.

REMARKS.—Gullo and Kozur (1992) correctly pointed out that two different types of Pa elements have been included in *H. excavatus* and that one is illustrated by Igo (1981) as *H. permicus* and the other is illustrated by Wardlaw and Collinson (1984, 1986) as *H. excavatus*. The ramiform elements of *Hindeodus* are diagnostic (Wardlaw and Stamm, 1992), and those originally described by Behnken (1975) as *Ellisonia excavata* belong to the Pa described as *H. permicus*, thus leaving Wardlaw and Collinson's illustrated material in open nomenclature. It is proposed here that the specimen illustrated in Wardlaw and Collinson (1986, fig. 17.20) serves as the holotype of *Hindeodus wordensis* and that the apparatus illustrated from sample 3LM1628 in fig. 17.13–20 represents the entire apparatus of the species. The description of Wardlaw and Collinson (1984:268–269) will serve as the diagnosis of the species. Wardlaw and Stamm have a much more detailed description of all recognized *Hindeodus* species in preparation (Wardlaw and Stamm, 1992). Wardlaw and Grant (1990) illustrated many well-preserved specimens (all but the Sa element) from material at the top of the Road Canyon Formation stratotype taken from a bed that is considered equivalent to the China Tank Member of the Word Formation.

Family SWEETOGNATHIDAE Ritter, 1986

Diplognathodus Kozur and Merrill, 1975

Diplognathodus sp.

PLATE 3-1: FIGURES 1–4

REMARKS.—Two corroded Pa elements were recovered from sample USGS 31535-PC. Both are illustrated herein. No specific determination was attempted based on such poor material. Another very poorly preserved specimen is from sample USGS 31600-PC, and it is questionably assigned to *Diplognathodus*.

Iranognathus Kozur, Mostler, and Rahimi-Yazd, 1975

Iranognathus punctatus, new species

PLATE 3-12: FIGURES 12–25

DIAGNOSIS.—Pa element bearing several lateral nodes or "punctae" on upper surface of flaring basal cavity; single carina

covered with nodes posteriorly and forming a ridge anteriorly; lateral and carinal nodes and carinal ridge with pustulose micro-ornamentation; some lateral nodes merging in larger specimens.

DESCRIPTION.—The Pa element is carminiscaphate with a wide, flaring basal cavity. The free blade is commonly one-third of the element, and it becomes a carinal ridge posteriorly, extending to the posteriormost of the element. The free blade/carinal ridge is slightly bowed laterally and may become very bowed laterally at its posteriormost end in large specimens. The ridge is ornamented by pustulose nodes posteriorly and is only pustulose anteriorly. The upper surface of the flaring basal cavity is ornamented by numerous lateral nodes, or punctae, which are more common on the inner side and generally become larger with some merging with the nearest nodes during growth. The anteriormost inner nodes are arranged in a diverging pattern from the carinal ridge, with the anteriormost nodes most likely to merge to form one or two short diverging "adcarinal" ridges, whereas the outer nodes are arranged in a roughly subparallel pattern, with the anteriormost nodes most likely to merge to form one adcarinal ridge.

The remainder of the apparatus is poorly represented. The Pb element is angulate and has a large reclined cusp, a relatively broad anterior process, and a distally narrowing posterior process. Both processes bear short, laterally compressed but thick denticles. The denticles on the posterior processes appear to alternate in size (small versus moderate) but are generally overgrown with apatite. The Sa element is alate, with short lateral processes that are downward directed and emerge at a nearly 90° angle from the posterior process, and bears a very large slightly reclined cusp. The M element is dolabrate and has small denticles on the anticusp, a proclined cusp of moderate size, and a posterior? process bearing subequal-sized and subevenly spaced moderate denticles that slightly increase in size and spacing distally.

TYPE SPECIMEN.—USNM 482789, Plate 3-12: Figure 23.

OCCURRENCE.—*Iranognathus punctatus* is common to the middle part of the Wargal Formation, Salt Range, Pakistan.

REMARKS.—The described species of *Iranognathus*, *I. unicosatus* and *I. tarazi*, are very unlike other specimens studied from the Wargal Formation of the Salt Range, Pakistan, and the Del Norte Mountains, West Texas, in that they lack nodose ornamentation of the upper surface of the flaring basal cavity. This species shows a lot of variability (plasticity), which is common for very shallow, nearshore forms. The forms from Pakistan and West Texas (Plate 3-2: Figures 36, 37) are dissimilar in node pattern, but the mutual presence of nodes make them more similar to each other than to the other described species. Until more material is illustrated (especially from China), the one recovered specimen from West Texas is illustrated herein and is placed as *I. aff. punctatus*. The apparatus of *Iranognathus*, although poorly represented, appears to be a fairly typically sweetognathid apparatus.

***Iranognathus* aff. *I. punctatus* Wardlaw**

PLATE 3-2: FIGURES 36, 37

REMARKS.—A single, poorly preserved specimen from the Del Norte Mountains has nodose ornamentation on the upper surface of the flaring basal cavity. The nodes roughly form two lines that merge on the inner side of the basal cavity to form an adcarinal ridge. This specimen is like *I. punctatus* in that it has nodose ornamentation, but it differs in that it does not have additional nodes between the two lines of nodes or adcarinal ridges. In addition, the line of nodes on each side curve outward distally, whereas the lines on *I. punctatus* curve inward distally.

***Neostreptognathodus* Clark, 1972**

Species of *Neostreptognathodus*, which are common in the late Artinskian and Leonardian, are rare in the Guadalupian. *Neostreptognathodus sulcopicatus*, which occurs in a few samples at the base of the Road Canyon Formation and is diagnostic of the uppermost Leonardian, is listed in the distribution table and is used for biostratigraphy, but it is not described herein. *Neostreptognathodus newelli* is characteristic of the basal Guadalupian zone in the Great Basin (Wardlaw and Collinson, 1986) and is only rarely found in the West Texas section. The best specimen was illustrated in Wardlaw and Grant (1990) where the species was discussed. *Neostreptognathodus clinei* also was illustrated and discussed in Wardlaw and Grant (1990), but it is only sporadically found through the Road Canyon Formation and the lower part of the Word Formation. Small specimens are easily confused with *Sweetognathus bicarinum*, so it is illustrated and discussed herein.

***Neostreptognathodus clinei* Behnken**

PLATE 3-12: FIGURE 10

Neostreptognathodus clinei Behnken, 1975:309–310, pl. 2: figs. 15, 16.—Sweet, 1977:237, pl. 1: fig. 4.—Wardlaw and Collinson, 1984:270, pl. 5: fig. 13.—Behnken, Wardlaw, and Stout, 1986:183, fig. 4.6, 7.

DIAGNOSIS.—Platform element (Pa) with 2 carinae; carinae either smooth or only faintly ornamented posteriorly by poorly developed nodes; carinae separated by a distinct groove; blade joins platform at center.

REMARKS.—Small specimens of *N. clinei* are difficult to distinguish from small specimens of *Sweetognathus bicarinum*, and the two species may be closely related. They have similar Gnathodid apparatuses, and pustulose micro-ornamentation occurs on the denticles or nodes of many specimens of *Neostreptognathodus*, attesting to their close relationship. It appears that *N. clinei* consistently has a groove dividing the carinae, even in very small specimens, which appears to be the distinguishing feature. It also has less pustulose micro-ornamentation than similar-sized specimens of *Sweetognathus bicarinum*.

***Pseudohindeodus* Gullo and Kozur, 1992**

This genus is based on small platform elements that are common in the middle Permian. These elements look like those of *Hindeodus*, but they can be identified as belonging to sweetognathid apparatuses by the moderate length of the posterior process on the Sa element. Sweetognathid apparatuses follow the typical Gnathodid apparatus layout, but sweetognathoid apparatuses have ramiforms of moderate length and more robust elements (especially the M), and they commonly display a recessive zone of basal attachment. These characters are indicative of the preferred habitat of sweetognathids of nearshore, high energy environments.

The species that clearly belong to *Pseudohindeodus*, namely *P. ramovsi*, *P. augustus* (Igo), and *P. oertlii* (Kozur, especially as illustrated by Igo, 1981), all have a diagnostic crimp around the fringe of the extremely flared basal cavity, which may be diagnostic of the genus.

***Pseudohindeodus ramovsi* Gullo and Kozur**

PLATE 3-1: FIGURES 5–24

Pseudohindeodus ramovsi Gullo and Kozur, 1992:223–224, fig. 4A–H.
Anchignathodus minutus (Ellison).—Ramovš, 1982:425, fig. 4/7 [in part].
Anchignathodus typicalis Sweet.—Behnken, 1975:297–298, pl. 2: fig. 12.
Hindeodus excavatus (Behnken).—Wardlaw and Grant, 1990:A6, pl. 3: figs. 3, 6, 7, 8 [in part].

DIAGNOSIS.—Pa element completely denticulate; denticles compressed and laterally expanded, but posteriormost 3 or 4 less compressed and decreasing in size distally; in upper view, surface above fringing crimp spade-shaped.

DESCRIPTION.—The Pa element is segminate, and an anterior “blade” or cusp is formed by the fusion of two high and postero-anteriorly wide, but laterally thin, denticles. The first denticle posterior to the cusp is commonly one-half the height of the cusp and one-half again the height of the next posterior denticle. The denticles give the general impression of decreasing in height from the cusp; however, the laterally widest three denticles, which are also the posteriormost compressed denticles (3 or 4 from the posterior end), are commonly slightly higher than surrounding denticles, forming a slight hump. The denticles following the first posterior denticle are very compressed and fused and are of near equal height or slightly decreasing or increasing in height, but they consistently increase in lateral width posteriorly. The posteriormost three or four denticles are much less compressed and fused, become free posteriorly, and sharply decrease in size distally (in all aspects). The posteriormost denticle is small and is located just above the fringing crimp. The fringing crimp extends nearly completely around the element; in large specimens it may be absent on the anteriormost part of the cusp, or it may form a slight notch in lateral profile at the anterior end. The lower surface is made up of an extremely flared and wide basal cavity that is deep, widest near the midline, and narrows to a deep groove beneath the cusp.

The Pb element is angulate and laterally twisted posteriorly. The anterior process bears several relatively high denticles that decrease in size distally. The posterior process bears several small denticles that are partly fused and appear to decrease in size slightly to the posterior. The first posterior denticle is considerably higher than the others and is mostly fused to the cusp. The lower surface has a small pit below the cusp, a well-developed groove, and a zone of recessive attachment laterally.

The M element is digyrate. The cusp is high and sinuous. The antero-lateral process is more like an anticusp and bears one to three small, highly fused denticles. The posterolateral process bears seven or eight well-developed denticles that decrease in size anteriorly; the denticle closest to the cusp is approximately one-half the size of the cusp. The lower surface has a pit beneath the cusp, grooves under each process, and a well-developed zone of recessive attachment surface that tapers away distally on the anterolateral process before the anterior end and abruptly curves away near the end of the posterolateral process.

The Sa element is alate and of moderate length and has two short lateral processes that bear two to four slightly compressed denticles. The cusp is large and reclined and bears costae directed toward each process. The posterior process bears four or five moderately high, compressed and partly fused denticles behind the cusp. Posteriorly, the denticles become less fused and compressed and more reclined. The lower surface is represented by a groove under all the processes.

The Sb element is bipennate, with a sharply downturned and slightly incurved anterior process bearing several compressed denticles. The first denticle anterior to the cusp is noticeably smaller than all but the most distal denticle. The remainder of the denticles appear to decrease in size distally. The cusp is moderately high (broken in all examined specimens) and recurved. The posterior process is moderately long and bears many denticles. The first five to seven denticles behind the cusp appear to alternate in size between small and moderate, and they are more compressed and fused than the remainder. The remainder are of subequal height, becoming more reclined and longer posteriorly. A few smaller denticles occur on the process, but they do not form a recognizable pattern. The lower surface is represented by a groove under each process.

The Sc element is bipennate, with a slightly downturned and incurved anterior process that generally bears four denticles that alternate in size. The denticle closest to the cusp is small, whereas the anteriormost is the largest. The cusp is of moderate height and is reclined. The posterior process is of moderate length and shows either the same or a similar denticulation pattern as the Sb element. The lower surface is represented by a groove under each process.

OCCURRENCE.—*Pseudohindeodus ramovsi* is a rare form that occasionally occurs abundantly. It sporadically occurs throughout the Road Canyon, Word, and Altuda formations. It also has been recovered abundantly from a sample of the South Wells Limestone Member of the Cherry Canyon Formation.

Gullo and Kozur (1992) reported it from Wordian strata in Sicily.

REMARKS.—The abraded and poorly preserved large specimens referred to as *Diplognathodus* sp. (Plate 3-1: Figures 1-4), which are from the same sample that was used to illustrate *Pseudohindeodus*, are clearly different in that they have a well-developed top notch posterior to the cusp and a marked posterior side notch observed in lateral profile, and, although abraded, they do not show signs of pronounced denticulation. The fringing crimp is absent.

Sweetognathus Clark, 1972

A species of *Sweetognathus* is common in the collected samples. It is difficult to see any differentiation in the specimens through the stratigraphic column examined in this study. They do, though, have a marked ontogenetic change, developing a second carinae through growth (see Wardlaw and Grant, 1990), and this appears to be a diagnostic characteristic. A complete apparatus has been recovered, and it is illustrated herein.

Sweetognathus bicarinum, new species

PLATE 3-2: FIGURES 22-35; PLATE 3-3: FIGURES 17-20;
PLATE 3-12: FIGURE 11

Sweetognathus iranicus Kozur, Mostler, and Rahimi-Yazd.—Wardlaw and Grant, 1990:A8, pl. 3: figs. 12-17.

DIAGNOSIS.—Pa element with carina of rounded denticles or nodes having pustulose micro-ornamentation; primary row of nodes connected by thin, pustulose, laterally (not centrally) placed longitudinal ridge; secondary row of nodes variably developed but with growth becoming larger than, and merging with, primary row to form transverse ridges; mature specimens with shallow depression (or furrow) separating two rows of nodes (now carina) and depressing transverse ridges (see Wardlaw and Grant, 1990, pl. 3: fig. 16).

DESCRIPTION.—The upper surface of the Pa element is described in the diagnosis. The lower surface has a moderately flared basal cavity (generally broken) that becomes a groove anteriorly.

The Pb element is angulate, thick, and arched. The anterior process is downturned and very thick and bears five to nine, highly fused, short denticles that become more reclined posteriorly. The cusp is moderately high, thick, and very reclined. The posterior process is downturned but has a slight inflection or upturning at the distal end. The four or five denticles next to the cusp are fused but become less fused distally. The lower surface has an oval basal cavity below the cusp and grooves beneath the processes.

The M element is dolabrate, with a short anticusp and long denticulate process. The cusp reclines over the anticusp so that it is posterior and the long process is anterior (this is the opposite from *Hindeodus*). The anterior process bears nine or more well-developed, moderately high denticles that are

strongly reclined distally, becoming less so near the cusp. Either the first (usually) or the second (occasionally) denticle is the smallest. The third denticle is usually the largest, and thereafter the denticles decrease in size distally. The lower surface has a small pit below the cusp and a groove under the anterior process.

The Sa element is alate, with short lateral processes that are anteriorly directed and bear about three denticles. The posterior process is broken and has not been observed, but it should be like that of the Sb and Sc elements, namely, moderately long with denticles of alternating size close to the cusp and becoming more equal-sized, longer, and more reclined distally except for probably the distalmost. The lower surface has a groove under each process.

The Sb element is bipennate, with a low cusp and a short downward and inward curving anterior process and a moderately long posterior process. The anterior process bears four to six denticles that increase in size anteriorly except when a small distalmost denticle is developed; then the largest is the next to last denticle. At the position of the largest denticle, the anterior process turns strongly inward. The posterior process bears many denticles. Generally two short denticles are followed by a low cusp (several of the posteriormost denticles are larger than the cusp). Posterior to the cusp, the denticles alternate in size from long and wide to short and narrow. These alternating pairs become progressively longer and wider distally, except for the distalmost, which is smaller. The lower surface has a groove under each process.

The Sc element is bipennate, with a moderately high cusp, a slightly downward and inward turned anterior process, and a moderately long posterior process. The anterior process bears about six denticle pairs that alternate in size, the pairs become progressively larger distally, with the distalmost denticle the largest. The posterior process bears many denticles similar in pattern to the Sb element, except the smaller denticles following the cusp may be more numerous (2–4) before the alternating pairs develop. The lower surface has a groove under each process.

TYPE SPECIMEN.—USNM 406952 (Wardlaw and Grant, 1990, pl. 3: figs. 12, 16).

OCCURRENCE.—*Sweetognathus bicarinum* is common to the Guadalupian of West Texas, appearing at the base of the Road Canyon Formation and ranging nearly to the top of the Altuda Formation.

REMARKS.—Middle and Late Permian *Sweetognathus* species are not well documented, so they are difficult to compare or identify. The species at hand differs from *S. guzhouensis* Bando et al. (1980) and most Early Permian forms by lacking a well-defined carinal “midline” ridge, rib, or train of pustules. The nodes on the anterior carina of *S. hanzhongensis* (Wang, 1978) become completely fused and form a flat ridge in lateral profile. Both *S. iranicus* and *S. hanzhongensis* have a single carina and do not display the development of two carina in larger forms that is diagnostic for *S. bicarinum*. The similarity of small specimens of *N. clinei* and *S. bicarinum* is discussed under *N. clinei*.

APPENDIX 3-1.—Continued.

USGS PC #	Field #	Height (m)	<i>Sweetina festiva</i>	<i>Sweetina triticum</i>	<i>Sweetina crofti</i> , new species	<i>Mesogondolella idahoensis</i>	<i>Mesogondolella idahoensis-nankingensis</i> transition	<i>Mesogondolella nankingensis</i>	<i>Mesogondolella aserrata</i>	<i>Mesogondolella postserrata</i>	<i>Mesogondolella shannoni</i>	<i>Mesogondolella altudaensis</i>	<i>Xantognathus abstractus</i>	<i>Xantognathus hydraensis</i>	<i>Hindeodus excavatus</i>	<i>Hindeodus wordensis</i> , new species	<i>Diplognathodus?</i>	<i>Diplognathodus</i> sp.	<i>Iranognathus</i> aff. <i>I. punctatus</i>	<i>Pseudohindeodus ramovsi</i>	<i>Neostreptognathodus clinei</i>	<i>Neostreptognathodus sulcopicatus</i>	<i>Neostreptognathodus newelli</i>	<i>Sweetognathus bicarinum</i> , new species	Reworked Ordovician-Pennsylvanian conodonts	
RC IX, bases at 30°18.00'N, 103°20.26'W and 30°18.39'N, 103°20.12'W																										
31463	(W81244)	0.00	-	-	-	+	-	-	-	-	-	-	-	-	-	-	-	-	-	-	-	-	-	-	-	
31464	(W81243)	1.52	-	-	-	+	-	-	-	-	-	-	-	-	-	-	-	-	-	-	-	-	-	-	-	
31465	(W81241)	22.56	-	-	-	+	-	-	-	-	-	-	-	-	-	-	-	-	-	-	-	-	-	-	-	
-	(W8242)	28.96	-	-	-	-	-	-	-	-	-	-	-	-	-	-	-	-	-	-	-	-	-	-	-	
-	(W8244)	34.76	-	-	-	-	-	-	-	-	-	-	-	-	-	-	-	-	-	-	-	-	-	-	-	
-	(W8243)	42.53	-	-	-	-	-	-	-	-	-	-	-	-	-	-	-	-	-	-	-	-	-	-	-	
-	(W81242)	43.90	-	-	-	-	-	-	-	-	-	-	-	-	-	-	-	-	-	-	-	-	-	-	-	
-	(W8245)	48.78	-	-	-	-	-	-	-	-	-	-	-	-	-	-	-	-	-	-	-	-	-	-	-	
-	(W8246)	59.45	-	-	-	-	-	-	-	-	-	-	-	-	-	-	-	-	-	-	-	-	-	-	-	
31466	(W81236)	75.00	-	-	-	-	+	-	-	-	-	-	-	+	-	+	-	-	-	-	-	-	-	-	-	
31467	(W81237)	76.68	-	-	-	-	+	-	-	-	-	-	-	-	-	+	-	-	-	-	-	-	-	-	-	
31468	(W81238)	83.08	-	-	-	-	+	-	-	-	-	-	-	-	-	-	-	-	-	-	-	-	-	-	-	
31469	(W81239)	85.82	-	-	-	-	+	-	-	-	-	-	-	+	-	+	-	-	-	-	-	-	-	-	-	
31470	(W81240)	88.72	-	-	-	-	+	-	-	-	-	-	-	+	-	-	-	-	-	-	-	-	-	-	-	
31471	(W8734)	103.96	-	+	-	-	+	-	-	-	-	-	-	+	-	+	-	-	-	-	-	-	-	-	-	
31628	(W8735)	263.87	-	+	-	-	-	+	-	-	-	-	-	+	-	+	-	-	-	-	-	-	-	-	-	
RC X (14WR), base at 30°23.26'N, 103°10.42'W																										
31472	(W877)	0.30	+	-	-	-	+	-	-	-	-	-	+	-	+	-	-	-	-	-	-	-	-	-	-	
31473	(W878)	8.84	-	-	-	-	+	-	-	-	-	-	-	-	+	-	-	-	-	-	-	-	-	-	-	
31474	(W879)	15.85	-	-	-	-	+	-	-	-	-	-	+	-	+	-	-	-	-	-	-	-	-	-	-	
31475	(W8710)	45.43	-	+	-	-	+	-	-	-	-	-	+	-	+	-	-	-	-	-	-	-	-	-	-	
31476	(14WR5)	46.04	-	-	-	-	+	-	-	-	-	-	+	-	+	-	-	-	-	-	-	-	-	-	-	
31477	(W8711)	52.59	-	+	-	-	+	-	-	-	-	-	+	-	+	-	-	-	-	-	-	-	-	-	-	
31478	(14WR72)	60.98	-	-	-	-	+	-	-	-	-	-	-	-	+	-	-	-	-	-	-	-	-	-	-	
31479	(W8712)	63.72	-	+	-	-	+	-	-	-	-	-	+	-	+	-	-	-	-	-	-	-	-	-	-	
31480	(W8713)	80.18	-	+	-	-	+	-	-	-	-	-	-	-	+	-	-	-	-	-	-	-	-	-	-	
31481	(14WR172)	81.01	-	-	-	-	-	-	-	-	-	-	-	+	-	+	-	-	-	-	-	-	-	-	-	
31482	(W8714)	100.30	-	+	-	-	+	-	-	-	-	-	+	-	+	-	-	-	-	-	-	-	-	-	-	
-	(14WR285)	110.98	-	-	-	-	-	-	-	-	-	-	-	-	-	-	-	-	-	-	-	-	-	-	-	
-	(W8715)	113.72	-	-	-	-	-	-	-	-	-	-	-	-	-	-	-	-	-	-	-	-	-	-	-	
31483	(14WR345)	121.95	-	+	-	-	+	-	-	-	-	-	-	-	+	-	-	-	-	-	-	-	-	-	-	
31484	(W8716)	127.74	-	+	-	-	+	-	-	-	-	-	+	-	+	-	-	-	-	-	-	-	-	-	-	
RC XI (USNM loc. 702c), base at 30°22.99'N, 103°09.57'W																										
31485	(W81225)	0.15	+	-	-	-	+	+	-	-	-	-	+	-	+	-	-	-	-	-	-	-	+	+	-	
31486	(W876)	1.07	+	-	-	-	+	+	-	-	-	-	+	-	+	-	-	-	-	-	-	-	-	+	-	
31487	(702c)	1.68	-	-	-	-	+	-	-	-	-	-	+	-	+	-	-	-	-	-	-	-	-	-	-	
RC XII, base at 30°24.47'N, 103°07.01'W																										
31488	(W8471)	0.15	+	-	-	-	+	-	-	-	-	-	+	-	+	-	-	-	-	-	-	-	+	-	+	
31489	(W8472)	1.68	+	-	-	-	+	-	-	-	-	-	+	-	+	-	-	-	-	-	-	-	-	+	-	
31490	(W9020)	1.68	-	-	-	-	-	-	-	-	-	-	-	-	+	-	-	-	-	-	-	-	?	-	-	

Literature Cited

- Bando, Y., D.K. Bhatt, V.J. Gupta, S.H. Hayashi, H. Kozur, K. Nakazawa, and Z.H. Wang
1980. Some Remarks on the Conodont Zonation and Stratigraphy of the Permian. *Recent Research in Geology*, 8:1-53.
- Behnken, F.H.
1975. Leonardian and Guadalupian (Permian) Conodont Biostratigraphy in Western and Southwestern United States. *Journal of Paleontology*, 49(2):284-315, plates 1, 2.
- Behnken, F.H., B.R. Wardlaw, and L.N. Stout
1986. Conodont Biostratigraphy of the Permian Meade Peak Phosphatic Shale Member, Phosphoria Formation, Southeastern Idaho. *University of Wyoming, Contributions to Geology*, 24:169-190, 6 figures.
- Bender, H., and D. Stoppel
1965. Perm-Conodonten. *Geologisches Jahrbuch*, 82:331-364.
- Branson, C.C., and M.G. Mehl
1938. The Conodont Genus *Icriodus* and Its Stratigraphic Distribution. *Journal of Paleontology*, 12(2):156-166, plate 26.
- Ching, Yu-Kan [Jin Yugan]
1960. Conodonts from the Kufeng Suite of Lungtan, Nanking. *Acta Paleontologica Sinica*, 8:242-248, plates 1, 2.
- Clark, D.L.
1972. Early Permian Crisis and Its Bearing on Permo-Triassic Conodont Taxonomy. *Geologica et Paleontologica*, 1:147-158.
- Clark, D.L., and F.H. Behnken
1971. Conodonts and Biostratigraphy of the Permian. In W.R. Sweet and S.M. Bergstrom, editors, *Symposium on Conodont Biostratigraphy*. *Geological Society of America, Memoir*, 127:415-439, plates 1, 2.
1979. Evolution and Taxonomy of the North American Upper Permian *Neogondolella serrata* Complex. *Journal of Paleontology*, 53(2):263-275, plates 1, 2, figures 1-4, table 1.
- Clark, D.L., and R.L. Ethington
1962. Survey of Permian Conodonts in Western North America. *Brigham Young University Geology Studies*, 9:102-114, plates 1, 2.
- Clark, D.L., and L.C. Mosher
1966. Stratigraphic, Geographic, and Evolutionary Development of the Conodont Genus *Gondolella*. *Journal of Paleontology*, 40(2):376-394, plates 45-47.
- Coombs, L.M.
1990. Depositional Environments of Permian Strata on Dugout Mountain, Brewster County, Texas. 115 pages. Unpublished master's thesis, Sul Ross State University, Alpine, Texas.
- Cooper, G.A., and R.E. Grant
1972. Permian Brachiopods of West Texas, I. *Smithsonian Contributions to Paleobiology*, 14:1-231, plates 1-23.
1974. Permian Brachiopods of West Texas, II. *Smithsonian Contributions to Paleobiology*, 15:233-793, plates 24-191.
1975. Permian Brachiopods of West Texas, III. *Smithsonian Contributions to Paleobiology*, 19:795-1921, plates 192-502.
1976a. Permian Brachiopods of West Texas, IV. *Smithsonian Contributions to Paleobiology*, 21:1923-2607, plates 503-662.
1976b. Permian Brachiopods of West Texas, V. *Smithsonian Contributions to Paleobiology*, 24:2609-3159, plates 663-780.
1977. Permian Brachiopods of West Texas, VI. *Smithsonian Contributions to Paleobiology*, 32:3161-3370.
- Croft, J.S.
1978. Upper Permian Conodonts and Other Microfossils from the Pinery and Lamar Limestone Members of the Bell Canyon Formation and from the Rustler Formation, West Texas. 176 pages, 8 plates. Unpublished master's thesis, Ohio State University, Columbus, Ohio.
- Dzik, Jerzy
1976. Remarks on the Evolution of Ordovician Conodonts. *Acta Palaeontologica Polonica*, 21:395-455.
- Edwards, L.E.
1984. Insights on Why Graphic Correlation (Shaw's Method) Works. *Journal of Geology*, 92:583-597.
- Glenister, B.F., D.W. Boyd, W.M. Furnish, R.E. Grant, M.T. Harris, H. Kozur, L.L. Lambert, W.W. Nassichuk, N.D. Newell, L.C. Pray, C. Spinosa, B.R. Wardlaw, G.L. Wilde, and T.E. Yancey
1992. The Guadalupian: Proposed International Standard for a Middle Permian Series. *International Geology Review*, 34(9):857-888.
- Grant, R.E., and B.R. Wardlaw
1984. Redefinition of Leonardian-Guadalupian Boundary in Regional Stratotype for the Permian of North America. [Abstract.] *27th International Geological Congress, Moscow, USSR, Abstracts*, 1:58.
- Gullo, Maria, and Heinz Kozur
1992. Conodonts from the Pelagic Deep-Water Permian of Central Western Sicily (Italy). *Neues Jahrbuch für Geologie und Paläontologie, Abhandlungen*, 184(2):203-234, figures 1-8.
- Igo, Hisaharu
1981. Permian Conodont Biostratigraphy of Japan. *Paleontological Society of Japan, Special Paper*, 24:1-50, 12 plates.
- Kozur, Heinz
1975. Beiträge zur Conodontenfauna des Perm. *Geologisch-Paläontologische Mitteilungen Innsbruck*, 5(4):1-44, 4 plates.
1978. Beiträge zur Stratigraphie des Perm, Teil II: Die Conodonten-Chronologie des Perms. *Freiberger Forschungshefte*, 334:85-161, 8 plates.
1988. Division of the Gondolellid Platform Conodonts. [Abstract.] First Part 2, Abstracts of Meeting. *Courier Forschungsinstitut Senckenberg*, 102:244-245.
1989 ("1990"). The Taxonomy of the Gondolellid Conodonts in the Permian and Triassic. In W. Ziegler, editor, First International Senckenberg Conference and Fifth European Conodont Symposium (ECOS V), Contributions III. *Courier Forschungsinstitut Senckenberg*, 117:409-469. [Date on title page is 1990; actually published in 1989.]
1992. Dzhulfian and Early Changxingian (Late Permian) Tethyan Conodonts from the Glass Mountains, West Texas. *Neues Jahrbuch für Geologie und Paläontologie, Abhandlungen*, 187(1):99-114, figures 1-21.
- Kozur, Heinz, and G.K. Merrill
1975. *Diplognathodus* new genus. In Heinz Kozur, Beiträge zur Conodontenfauna des Perm. *Geologisch-Paläontologische Mitteilungen Innsbruck*, 5(4):9.
- Kozur, Heinz, Helfried Mostler, and Ali Rahimi-Yazd
1975. Beiträge zur Mikrofauna Permtriadischer Schichtfolgen, Teil II: Neue conodonten aus dem Ober Perm und der basalen Trias von Nord- und Zentraliran. *Geologische-Paläontologische Mitteilungen Innsbruck*, 5(3):1-23.
- Lambert, L.L., D.J. Lehrmann, and M.T. Harris
2000. Correlation of the Road Canyon and Cutoff Formations, West Texas, and Its Relevance to Establishing an International Middle Permian (Guadalupian) Series. In B.R. Wardlaw, R.E. Grant, and D.M. Rohr, editors, *The Guadalupian Symposium. Smithsonian Contributions to the Earth Sciences*, 32:153-183, 11 figures, 4 plates, 3 tables.
- Lambert, L.L., and B.R. Wardlaw
1992. Appendix II: Morphological Transition from *Mesogondolella idahoensis* to *M. serrata*: Basal Guadalupian Definition. In Glenister et al., *The Guadalupian: Proposed International Standard for a Middle Permian Series. International Geology Review*, 34(9):876-880.

- In prep. Morphological Analysis of the Transition from *Mesogondolella idahoensis* to *M. serrata* (Conodonts) and the Significance for Worldwide Permian Correlation. *Journal of Paleontology*.
- Linström, Maurits
1970. A Suprageneric Taxonomy of the Conodonts. *Lethaia*, 3:427–445.
- Małkowski, Krzysztof, and Hubert Szaniawski
1976. Permian Conodonts from Spitsbergen and Their Stratigraphic Significance: A Preliminary Note. *Norsk Polarinstitut, Arbok*, 1975:79–87, 1 plate.
- Movschovitsch, E.V., Heinz Kozur, A.M. Pavlov, V.P. Pnev, A.N. Polosova, B.N. Chuvashov, and M.O. Bogoslovskaya
1979. Complexes of Conodonts from the Lower Permian of the Pre-Urals and Problems of Correlation of Lower Permian Deposits. In G.N. Papulov and V.N. Puchkov, editors, Conodonts from the Urals and Their Stratigraphic Significance. *Trudy Institute of Geology and Geochemistry, Urals Science Center, Akademia Nauk SSSR, Sverdlovsk*, 145:94–131, 4 plates.
- Nestell, M.K., and B.R. Wardlaw
1987. Upper Permian Conodonts from Hydra, Greece. *Journal of Paleontology*, 61(4):758–772, figures 1–7.
- Pander, C.H.
1856. *Monographie der fossilen Fische des Silurischen Systems der Russisch-Baltischen Gouvernements*. 91 pages, 9 plates. St. Petersburg: Akademia Wiss.
- Ramovš, Anton
1982. Unterperm-Conodonten aus den Karawanken (Slovenian, NW Jugoslawein) [Lower Permian Conodonts from the Karavanke Mountains (Slovenia NW Jugoslavia)]. *Neues Jahrbuch für Geologie und Paläontologie, Abhandlungen*, 164(3):414–427, 4 figures. [In German.]
- Rexroad, C.B., and W.M. Furnish
1964. Conodonts from the Pella Formation (Mississippian), South-Central Iowa. *Journal of Paleontology*, 38(4):667–676, plate 111.
- Ritter, S.M.
1986. Taxonomic Revision and Phylogeny of Post-Early Permian Crisis *bisselli-whitei* Zone Conodonts with Comments on Late Paleozoic Diversity. *Geologica et Palaeontologica*, 20:139–165.
- Rudine, S.F.
1988. Geology and Depositional Environments of the Permian Rocks, Northern Del Norte Mountains, Brewster County, Texas. 186 pages. Unpublished master's thesis, Sul Ross State University, Alpine, Texas.
- Shaw, A.B.
1964. *Time in Stratigraphy*. 365 pages. New York: McGraw-Hill.
- Sweet, W.C.
1970. Uppermost Permian and Lower Triassic Conodonts of the Salt Range and Trans-Indus Ranges, West Pakistan. In B. Kummel and C. Teichert, editors, Stratigraphic Boundary Problems: Permian and Triassic of West Pakistan. *University of Kansas, Department of Geology, Special Publication*, 4:207–275.
1976. Conodonts from the Permian-Triassic Boundary Beds of Kap Stosch Area, East Greenland. *Meddelelser om Grønland*, 197:51–54.
1977. *Hindeodus*. In W. Ziegler, editor, *Catalogue of Conodonts*, volume 3: pages 203–224, 2 plates. Stuttgart: E. Schweizerbart'sche Verlagsbuchhandlung.
1988. The Conodonta: Morphology, Taxonomy, Paleoecology, and Evolutionary History of a Long-Extinct Animal Phylum. *Oxford Monographs on Geology and Geophysics*, 10: 212 pages.
- Szaniawski, Hubert
1979. *Sweetocristatus articus* sp. n. In Hubert Szaniawski and Krzysztof Małkowski, Conodonts from the Kapp Starostin Formation (Permian) of Spitsbergen. *Acta Palaeontologica Polonica*, 24:254, plate 9.
- Wang, Zhi-hao
1978. Permian-Lower Triassic Conodonts of the Liangshan Area, Southern Shaanxi. *Acta Palaeontologica Sinica*, 17:213–227, 2 plates.
- Wardlaw, B.R.
1994. *Mesogondolella shannoni* new species. In Mei Shilong, Jin Yugan, and B.R. Wardlaw, Zonation of Conodonts from the Maokouan-Wuchiapingian Boundary Strata, South China. *Palaeoworld*, 4: 228–229, plate 1.
- Wardlaw, B.R., and J.W. Collinson
1979. Youngest Permian Conodont Faunas from the Great Basin and Rocky Mountain Regions. In C.A. Sandberg and D.L. Clark, editors, Conodont Biostratigraphy of the Great Basin and Rocky Mountains. *Brigham Young University Geology Studies*, 26:151–163.
1984. Conodont Paleoecology of the Permian Phosphoria Formation and Related Rocks of Wyoming and Adjacent Areas. In D.L. Clark, editor, Conodont Biofacies and Provincialism. *Geological Society of America, Special Paper*, 196:263–281, plates 1–5.
1986. Paleontology and Deposition of the Phosphoria Formation. *University of Wyoming, Contributions to Geology*, 24:107–142, 20 figures.
- Wardlaw, B.R., R.A. Davis, D.M. Rohr, and R.E. Grant
1990. Leonardian-Wordian (Permian) Deposition in the Northern Del Norte Mountains, West Texas. *United States Geological Survey Bulletin*, 1881-A:A1–A14, plates 1–4.
- Wardlaw, B.R., and R.E. Grant
1987. Conodont Biostratigraphy of the Cathedral Mountain and Road Canyon Formations, Glass Mountains, West Texas. In D. Cromwell and L.J. Mazzullo, editors, The Leonardian Facies in W. Texas and S.E. New Mexico and Guidebook to the Glass Mountains, West Texas. *Society of Economic Paleontologists and Mineralogists, Permian Basin Section, Publication*, 87-27:63–66.
1990. Conodont Biostratigraphy of the Permian Road Canyon Formation, Glass Mountains, Texas. *United States Geological Survey Bulletin*, 1895-A:A1–A18, plates 1–4.
- Wardlaw, B.R., C.A. Ross, and R.E. Grant
2000. Cyclic Deposition of the Permian Road Canyon Formation, Glass Mountains, West Texas. In B.R. Wardlaw, R.E. Grant, and D.M. Rohr, editors, The Guadalupian Symposium. *Smithsonian Contributions to the Earth Sciences*, 32:121–126, 3 figures.
- Wardlaw, B.R., and S.F. Rudine
2000. The Altuda Formation of the Glass and Del Norte Mountains. In B.R. Wardlaw, R.E. Grant, and D.M. Rohr, editors, The Guadalupian Symposium. *Smithsonian Contributions to the Earth Sciences*, 32:313–318, 4 figures.
- Wardlaw, B.R., and R.L. Stamm
1992. *Hindeodus*. [Abstract.] *Geological Society of America, Abstracts with Programs*, 24:70.
- Youngquist, W.L., R.W. Hawley, and A.K. Miller
1951. Phosphoria Conodonts from Southeastern Idaho. *Journal of Paleontology*, 25(3):356–364, plate 54.

Plates 3-1-3-12

PLATE 3-1*Diplognathodus* and *Pseudohindeodus*

FIGURES 1–4.—*Diplognathodus* sp.: 1, 2, lateral view ($\times 156$) and upper view ($\times 158$), Pa element, USNM 482540; 3, 4, lateral view ($\times 80.6$) and upper view ($\times 79.4$), Pa element, USNM 482541. All specimens from USGS 31535-PC (89BM-343). (Reduced to 72% of original for publication.)

FIGURES 5–24.—*Pseudohindeodus ramovsi* Gullo and Kozur: 5, lateral view, Sa element ($\times 81.5$), USNM 482542; 6, inner view, Sb element ($\times 82.9$), USNM 482543; 7, inner view, Sb element ($\times 82.9$), USNM 482544; 8, inner view, Sb element ($\times 81.5$), USNM 482545; 9, inner view, Sc element ($\times 82.9$), USNM 482546; 10, oblique upper view, Pa element ($\times 82.9$), USNM 482547; 11, upper view, Pa element ($\times 80.9$), USNM 482548; 12, upper view, Pa element ($\times 80.8$), USNM 482549; 13, upper view, Pa element ($\times 80.8$), USNM 482550; 14, lateral view, Pa element ($\times 160$), USNM 482551; 15, lateral view, Pa element ($\times 161$), USNM 482552; 16, lateral view, Pb element ($\times 80.8$), USNM 482553; 17, posterolateral view, M element ($\times 80.8$), USNM 482554; 18, posterolateral view, M element ($\times 80.8$), USNM 482555; 19, 20, lateral view ($\times 160$) and upper view ($\times 162$), Pa element, USNM 482556; 21, 22, lateral view ($\times 160$) and upper view ($\times 162$), Pa element, USNM 482557; 23, 24, lateral view ($\times 162$) and upper view ($\times 159$), Pa element, USNM 482558. Figures 5–13 from USGS 29813-PC (W85-15); Figures 14–24 from USGS 31535-PC (89BM-343). (Reduced to 72% of original for publication.)

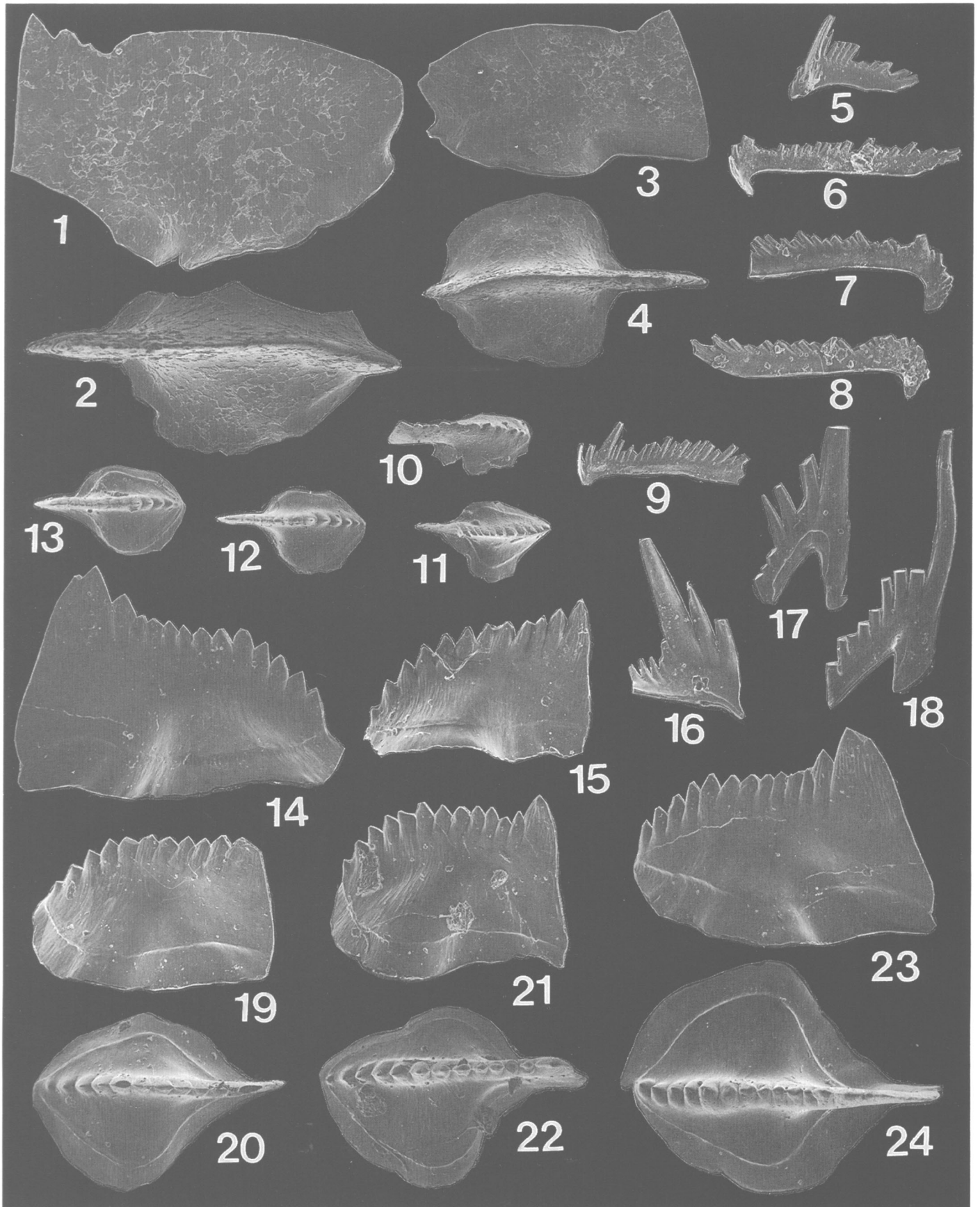


PLATE 3-2

Hindeodus, *Sweetognathus*, *Iranognathus*, and *Mesogondolella*

FIGURES 1–21.—*Hindeodus excavatus* (Behnken): 1, posterior view, Sa element ($\times 79.4$), USNM 482559; 2, posterior view, Sa element ($\times 79.4$), USNM 482560; 3, posterior view, Sa element ($\times 79.4$), USNM 482561; 4, posterolateral view, Sb element ($\times 79.4$), USNM 482562; 5, posterolateral view, Sb element ($\times 79.4$), USNM 482563; 6, posterolateral view, Sb element ($\times 79.4$), USNM 482564; 7, inner view, Pb element ($\times 79.4$), USNM 482565; 8, inner view, Pb element ($\times 79.4$), USNM 482566; 9, posterolateral view, M element ($\times 79.4$), USNM 482567; 10, posterolateral view, M element ($\times 79.4$), USNM 482568; 11, inner view, Sc element ($\times 79.4$), USNM 482569; 12, inner view, Sc element ($\times 79.4$), USNM 482570; 13, inner view, Sc element ($\times 79.4$), USNM 482571; 14, inner view, Sc element ($\times 79.4$), USNM 482572; 15, inner view, Sc element ($\times 81.6$), USNM 482573; 16, lateral view, Pa element ($\times 79.1$), USNM 482574; 17, lateral view, Pa element ($\times 79.1$), USNM 482575; 18, lateral view, Pa element ($\times 80.8$), USNM 482576; 19, lateral view, Pa element ($\times 80.8$), USNM 482577; 20, lateral view, Pa element ($\times 81.5$), USNM 482578; 21, lateral view, Pa element ($\times 79.1$), USNM 482579. All specimens from USGS 31500-PC (W90-1s). (Reduced to 72% of original for publication.)

FIGURES 22–35.—*Sweetognathus bicarinum*, new species: 22, posterolateral view, M element ($\times 79.4$), USNM 482580; 23, posterolateral view, M element ($\times 79.4$), USNM 482581; 24, lateral view, Pb element ($\times 79.4$), USNM 482582; 25, lateral view, Pb element ($\times 79.4$), USNM 482583; 26, lateral view, Pb element ($\times 79.4$), USNM 482584; 27, anterolateral view, Sa element ($\times 79.4$), USNM 482585; 28, inner view, Sb element ($\times 79.4$), USNM 482586; 29, inner view, Sc element ($\times 79.4$), USNM 482587; 30, inner view, Sc element ($\times 79.4$), USNM 482588; 31, inner view, Sc element ($\times 79.4$), USNM 482589; 32, inner view, Sb element ($\times 79.4$), USNM 482590; 33, upper view, Pa element ($\times 159$), USNM 482591; 34, upper view, Pa element ($\times 159$), USNM 482592; 35, upper view, Pa element ($\times 159$), USNM 482593 (Figures 33–35 illustrate growth sequence from young adult to juvenile). All specimens from USGS 31500-PC (W90-1s). (Reduced to 72% of original for publication.)

FIGURES 36, 37.—*Iranognathus* aff. *I. punctatus* Wardlaw: 36, upper view, Pa element ($\times 161.6$), showing pustulose ornament; 37, upper view, Pa element ($\times 80.8$), showing whole specimen, USNM 482594. Specimen from USGS 31531-PC (W90-50). (Reduced to 72% of original for publication.)

FIGURES 38, 39.—*Mesogondolella idahoensis* transitional to *M. nankingensis*, juvenile specimens showing faint serration along anterior margin, which is lost in adult: 38, upper view, Pa element ($\times 79.4$), USNM 482595; 39, upper view, Pa element ($\times 159$), USNM 482596. All specimens from USGS 31500-PC (W90-1s). (Reduced to 72% of original for publication.)

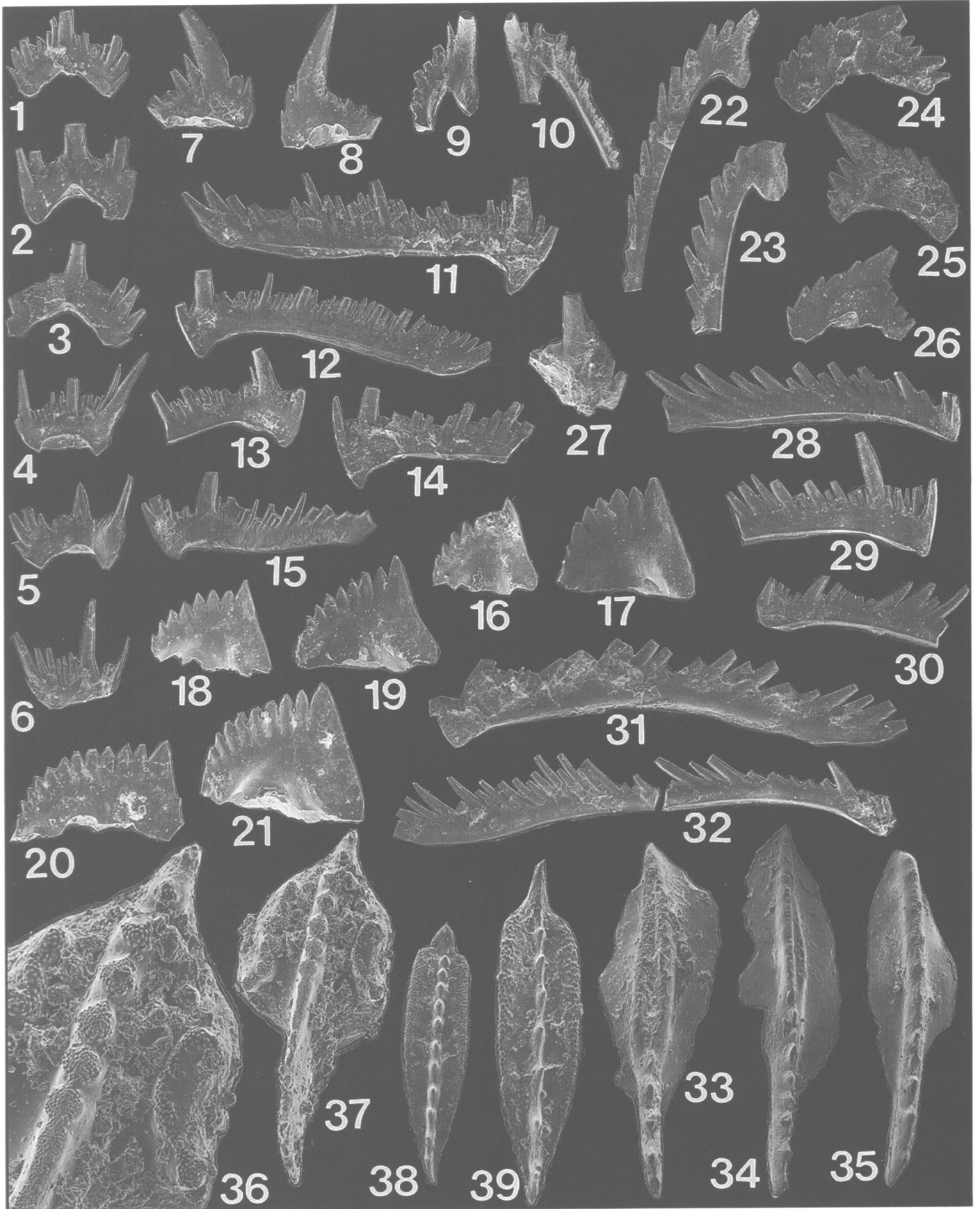


PLATE 3-3*Mesogondolella and Sweetognathus*

FIGURES 1-16.—*Mesogondolella aserrata* (Clark and Behnken): 1, upper view, Pa element ($\times 79.5$), USNM 482597; 2, upper view, Pa element ($\times 80.8$), USNM 482598; 3, upper view, Pa element ($\times 80.8$), USNM 482599; 4, upper view, Pa element ($\times 80.8$), USNM 482600; 5, upper view, Pa element ($\times 80.8$), USNM 482601; 6, upper view, Pa element ($\times 80.8$), USNM 482602; 7, upper view, Pa element ($\times 80.8$), USNM 482603; 8, upper view, Pa element ($\times 80.8$), USNM 482604; 9, upper view, Pa element ($\times 80.8$), USNM 482605; 10, upper view, Pa element ($\times 80.8$), USNM 482606; 11, upper view, Pa element ($\times 80.8$), USNM 482607; 12, upper view, Pa element ($\times 80.8$), USNM 482608; 13, upper view, Pa element ($\times 80.8$), USNM 482609; 14, upper view, Pa element ($\times 80.8$), USNM 482610; 15, upper view, Pa element ($\times 80.8$), USNM 482611; 16, upper view, Pa element ($\times 80.8$), USNM 482612. All specimens from USGS 29814-PC (W85-16). (Reduced to 72% of original for publication.)

FIGURES 17-20.—*Sweetognathus bicarinum*, new species: 17, inner view, Sb element ($\times 100$), USNM 482613; 18, lateral view, Pb element ($\times 100$), USNM 482614; 19, inner view, Sc element ($\times 100$), USNM 482615; 20, upper view, Pa element ($\times 130$), USNM 482616. All specimens from USGS 31583-PC (W85-1). (Reduced to 72% of original for publication.)

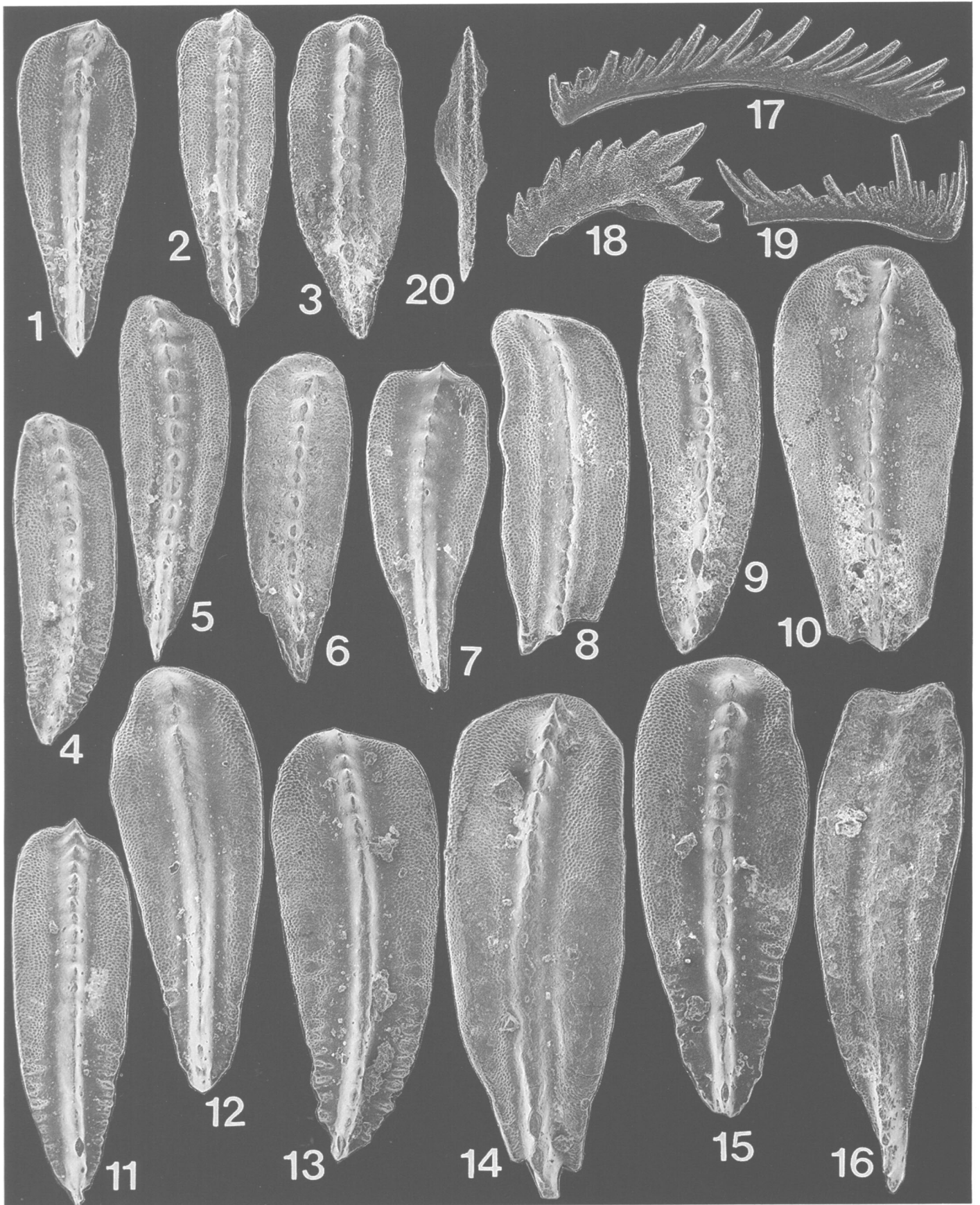


PLATE 3-4*Xaniognathus*, *Sweetina*, *Hindeodus*, and *Mesogondolella*

FIGURES 1–13.—*Xaniognathus hydraensis* Nestell and Wardlaw: 1, posterolateral view, Sb element ($\times 79.4$), USNM 482617; 2, posterolateral view, Sb element ($\times 79.4$), USNM 482618; 3, posterior view, Sa element ($\times 80.8$), USNM 482619; 4, posterior view, Sa element ($\times 79.4$), USNM 482620; 5, posterior view, M element ($\times 79.4$), USNM 482621; 6, posterior view, M element ($\times 79.4$), USNM 482622; 7, lateral view, Pa element ($\times 79.4$), USNM 482623; 8, lateral view, Pa element ($\times 79.4$), USNM 482624; 9, inner view, Pb element ($\times 79.4$), USNM 482625; 10, inner view, Pb element ($\times 79.4$), USNM 482626; 11, lateral view, Sc element ($\times 79.4$), USNM 482627; 12, lateral view, Sc element ($\times 80.8$), USNM 482628; 13, lateral view, Sc element ($\times 80.8$), USNM 482629. All specimens from USGS 31535-PC (89BM-343). (Reduced to 72% of original for publication.)

FIGURES 14–23.—*Sweetina croftii*, new species: 14, lateral view, Sc element ($\times 79.4$), USNM 482630; 15, lateral view, Sc element ($\times 79.4$), USNM 482631; 16, posterolateral view, M element ($\times 79.4$), USNM 482632; 17, lateral view, Sa element ($\times 79.4$), USNM 482633; 18, inner view, Sb element ($\times 79.4$), USNM 482634; 19, lateral view, Pa element ($\times 81.5$), USNM 482635; 20, lateral view, Pa element ($\times 81.5$), USNM 482636, holotype; 21, lateral view, Pb element ($\times 79.4$), USNM 482637; 22, lateral view, Pb element ($\times 79.4$), USNM 482638; 23, lateral view, Pb element ($\times 79.4$), USNM 482639. All specimens from USGS 31528-PC (W90-47). (Reduced to 72% of original for publication.)

FIGURES 24, 25.—*Hindeodus wordensis*, new species: 24, lateral view, Pa element ($\times 80.8$), USNM 482640, specimen abraded and broken so that it appears like *H. julfensis*; 25, lateral view, Pa element ($\times 80.8$), USNM 482641. Both specimens from USGS 31625-PC (9BR-5). (Reduced to 72% of original for publication.)

FIGURES 26, 27, 29, 30.—*Mesogondolella shannoni* Wardlaw: 26, upper view, anterior fragment of Pa element ($\times 80.8$), USNM 482642; 27, upper view, Pa element ($\times 80.8$), USNM 482643; 29, upper view, Pa element ($\times 80.8$), USNM 482644; 30, upper view, Pa element ($\times 80.8$), USNM 482645. Figures 26, 27 from USGS 31618-PC (W90-33); Figures 29, 30 from USGS 31625-PC (9BR-5). (Reduced to 72% of original for publication.)

FIGURE 28.—*Mesogondolella postserrata* (Behnken): upper view, Pa element ($\times 80.8$), USNM 482646. Specimen from USGS 31620-PC (89PR-1). (Reduced to 72% of original for publication.)

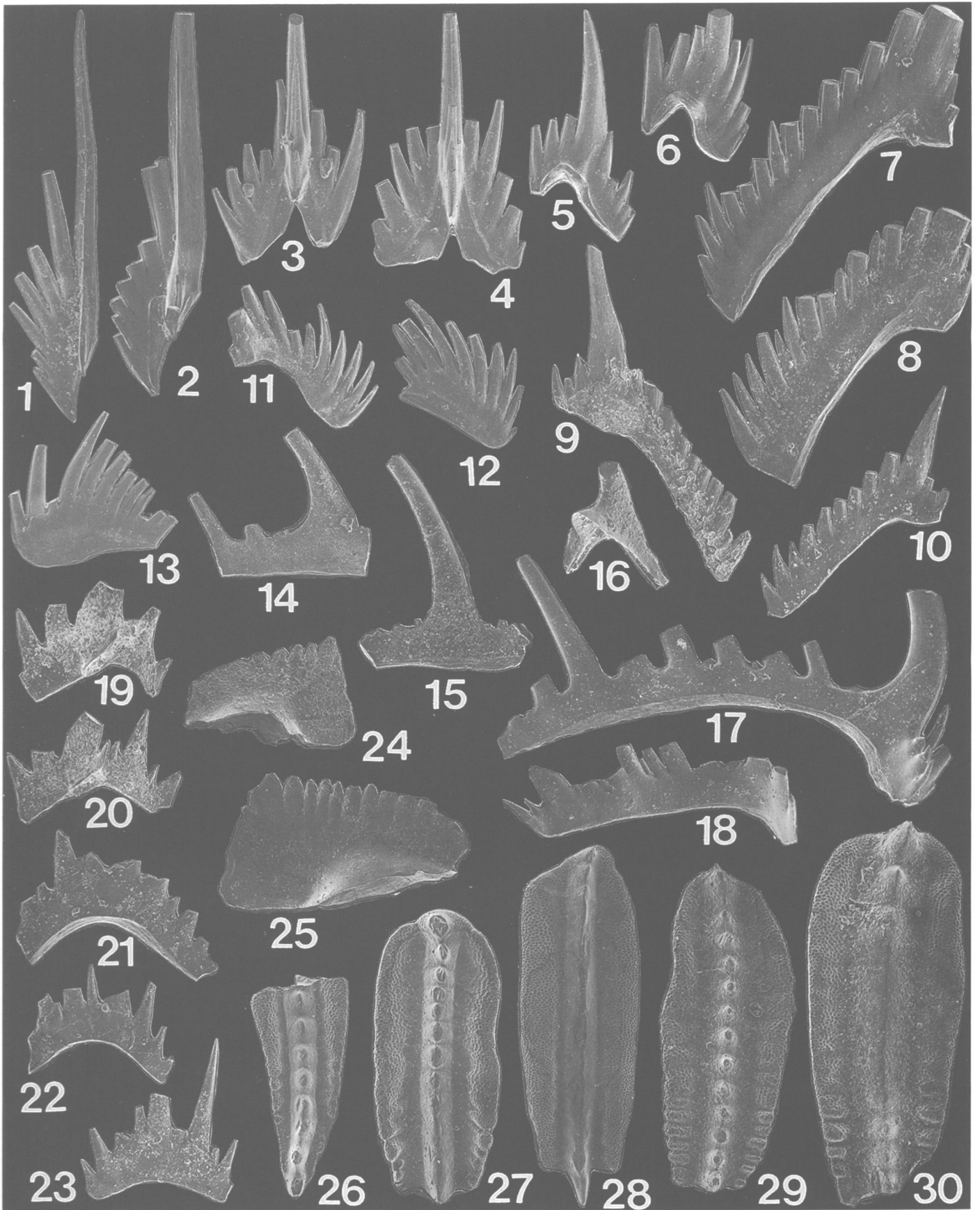


PLATE 3-5*Mesogondolella*

FIGURES 1–7.—*Mesogondolella aserrata* (Clark and Behnken): 1, upper view, Pa element ($\times 80.8$), USNM 482647; 2, upper view, Pa element ($\times 80.8$), USNM 482648; 3, upper view, Pa element ($\times 80.8$), USNM 482649; 4, upper view, Pa element ($\times 80.8$), USNM 482650; 5, upper view, Pa element ($\times 80.8$), USNM 482651; 6, upper view, Pa element ($\times 80.8$), USNM 482652; 7, upper view, Pa element ($\times 80.8$), USNM 482653. All specimens from USGS 29818-PC (W85-20). (Reduced to 72% of original for publication.)

FIGURES 8–12.—*Mesogondolella altudaensis* (Kozur): 8, upper view, Pa element ($\times 80.8$), USNM 482654; 9, upper view, Pa element ($\times 80.8$), USNM 482655; 10, upper view, Pa element ($\times 80.8$), USNM 482656; 11, upper view, Pa element ($\times 80.8$), USNM 482657; 12, upper view, Pa element ($\times 80.8$), USNM 482658. All specimens from USGS 31627-PC (W91-3). (Reduced to 72% of original for publication.)

FIGURES 13–20.—*Meosogondolella postserrata* (Behnken): 13, upper view, Pa element ($\times 80.8$), USNM 482659; 14, upper view, Pa element ($\times 80.8$), USNM 482660; 15, upper view, Pa element ($\times 80.8$), USNM 482661; 16, upper view, Pa element ($\times 80.8$), USNM 482662; 17, upper view, Pa element ($\times 80.8$), USNM 482663; 18, upper view, Pa element ($\times 80.8$), USNM 482664; 19, upper view, Pa element ($\times 80.8$), USNM 482665; 20, upper view, Pa element ($\times 80.8$), USNM 482666. All specimens from USGS 29818-PC (W85-20). (Reduced to 72% of original for publication.)

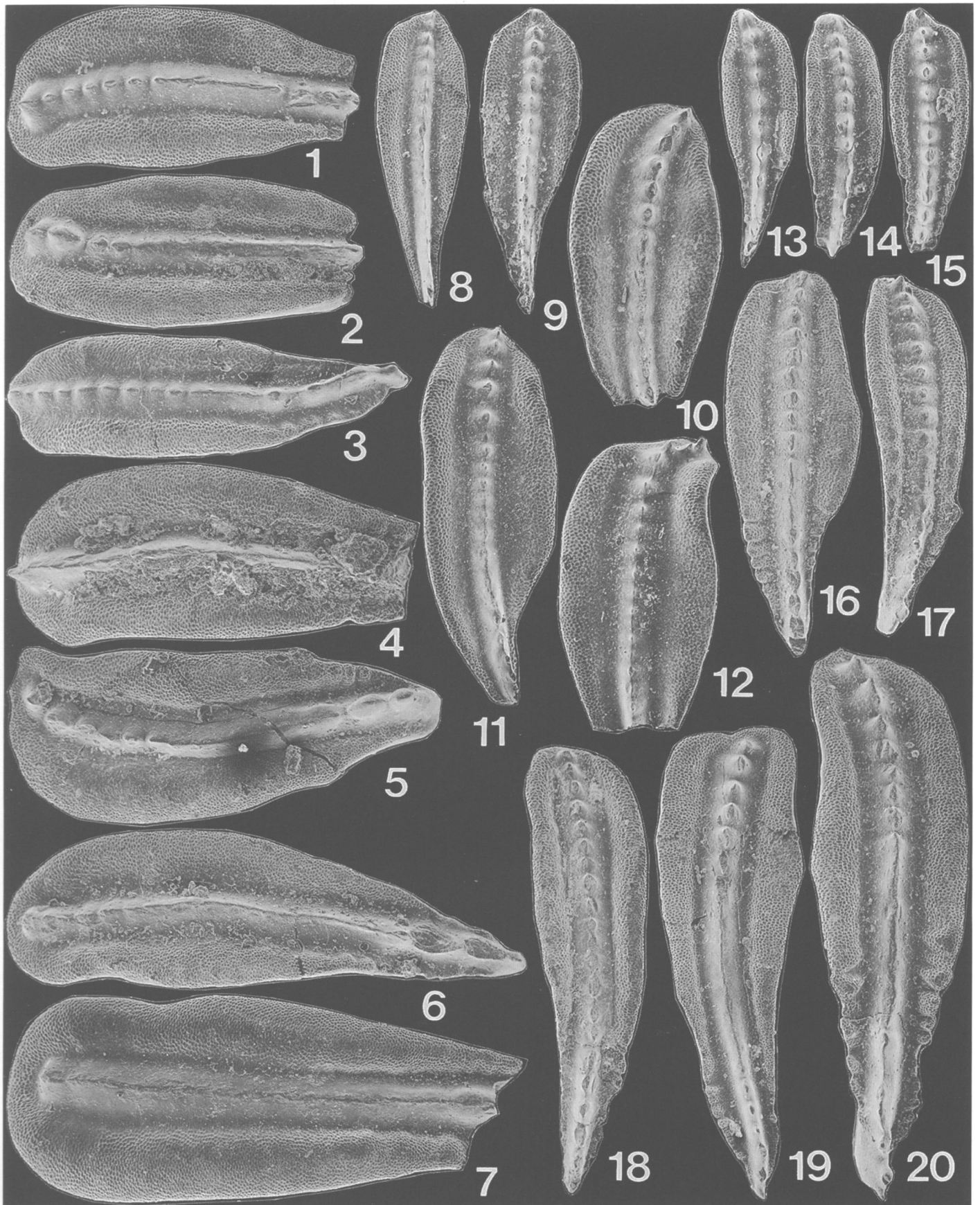


PLATE 3-6*Mesogondolella*

FIGURES 1–7.—*Mesogondolella postserrata* (Behnken): 1, upper view, Pa element ($\times 80.8$), USNM 482667; 2, upper view, Pa element ($\times 80.8$), USNM 482668; 3, upper view, Pa element ($\times 80.8$), USNM 482669; 4, upper view, Pa element ($\times 80.8$), USNM 482670; 5, upper view, Pa element ($\times 80.8$), USNM 482671; 6, upper view, Pa element ($\times 80.8$), USNM 482672; 7, upper view, Pa element ($\times 80.8$), USNM 482673. All specimens from USGS 31536-PC (W91-1). (Reduced to 72% of original for publication.)

FIGURES 8–15.—*Mesogondolella shannoni* Wardlaw: 8, upper view, Pa element ($\times 80.8$), USNM 482674; 9, upper view, Pa element ($\times 80.8$), USNM 482675; 10, upper view, Pa element ($\times 80.8$), USNM 482676; 11, upper view, Pa element ($\times 80.8$), USNM 482677; 12, upper view, Pa element ($\times 80.8$), USNM 482678; 13, upper view, Pa element ($\times 80.8$), USNM 482679; 14, upper view, Pa element ($\times 80.8$), USNM 482680, holotype; 15, upper view, Pa element ($\times 80.8$), USNM 482681. All specimens from USGS 31536-PC (W91-1), same as above, showing transitional morphotypes between each species. (Reduced to 72% of original for publication.)

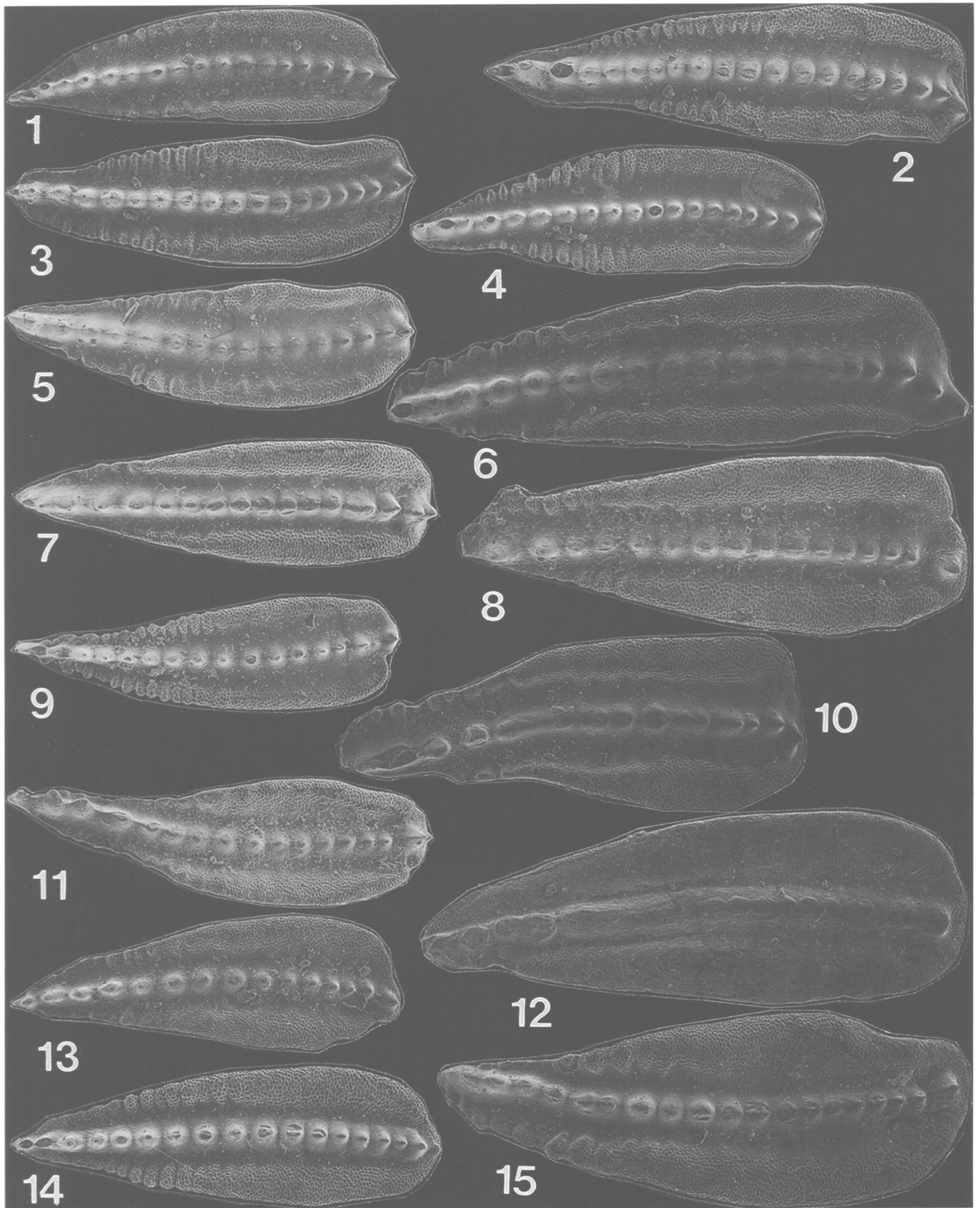


PLATE 3-7*Mesogondolella*

FIGURES 1–11.—*Mesogondolella postserrata* (Behnken): 1, upper view, Pa element ($\times 80.8$), USNM 482682; 2, upper view, Pa element ($\times 80.8$), USNM 482683; 3, upper view, Pa element ($\times 80.8$), USNM 482684; 4, upper view, Pa element ($\times 80.8$), USNM 482685; 5, upper view, Pa element ($\times 80.8$), USNM 482686; 6, upper view, Pa element ($\times 80.3$), USNM 482687; 7, upper view, Pa element ($\times 81.3$), USNM 482688; 8, upper view, Pa element, ($\times 80.3$), USNM 482689; 9, upper view, Pa element ($\times 81.3$), USNM 482690; 10, upper view, Pa element ($\times 80.8$), USNM 482691; 11, upper view, Pa element ($\times 80.8$), USNM 482692. All specimens from USGS 31621-PC (9BR-1). (Reduced to 72% of original for publication.)

FIGURES 12–25.—*Mesogondolella shannoni* Wardlaw: 12, upper view, Pa element ($\times 79.4$), USNM 482693; 13, 14, upper view ($\times 79.4$) and oblique lateral view ($\times 80.3$), Pa element, USNM 482694; 15, 16, upper view ($\times 79.4$) and oblique lateral view ($\times 82.3$), Pa element, USNM 482695; 17, upper view, Pa element ($\times 81.3$), USNM 482696; 18, 19, upper view ($\times 80.8$) and oblique lateral view ($\times 82.3$), Pa element, USNM 482697; 20, 21, upper view ($\times 80.8$) and lateral view ($\times 80.3$), Pa element, USNM 482698, showing large transverse ridge; 22, 23, lateral view ($\times 80.3$) and upper view ($\times 81.3$), Pa element, USNM 482699; 24, upper view, Pa element ($\times 80.8$), USNM 482700, showing large (pathologic?) development of transverse ridge; 25, upper view, Pa element ($\times 80.8$), USNM 482701, showing large pathologic specimen. All specimens from USGS 31621-PC (9BR-1), same as above, showing transitional morphotypes between each species. (Reduced to 72% of original for publication.)

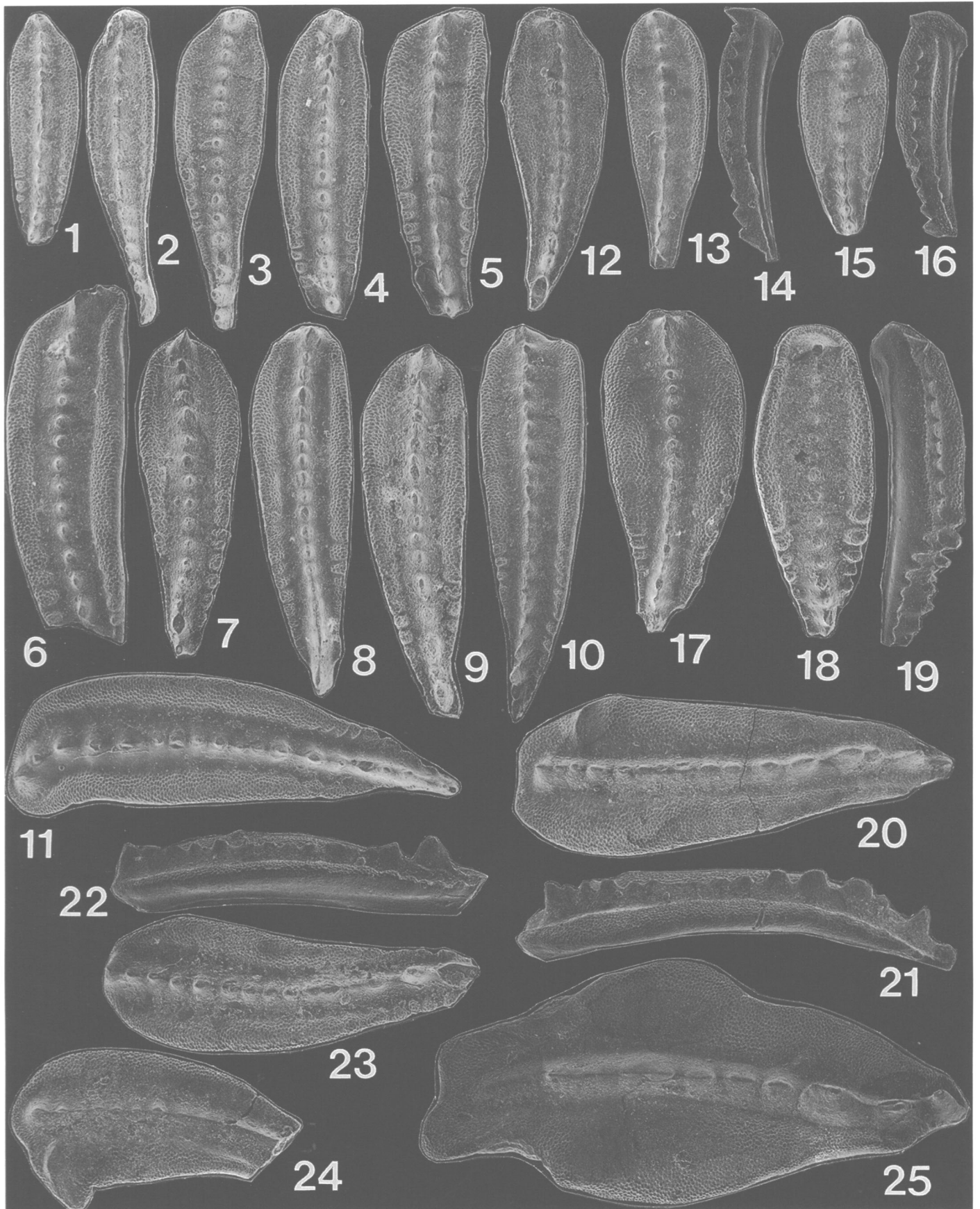


PLATE 3-8*Mesogondolella*

FIGURES 1-16, 20.—*Mesogondolella shannoni* Wardlaw: 1, 2, lateral view ($\times 81.6$) and upper view ($\times 83.3$), Pa element, USNM 482702; 3, 4, lateral view ($\times 81.4$) and upper view ($\times 81.6$), Pa element, USNM 482703; 5, upper view, Pa element ($\times 81.4$), USNM 482704, transitional form to *M. altudaensis*; 6, 7, upper view ($\times 79.3$) and lateral view ($\times 80.0$), Pa element, USNM 482705; 8, 9, upper view ($\times 78.2$) and lateral view ($\times 79.8$), Pa element, USNM 482706; 10, 11, lateral view ($\times 81.6$) and upper view ($\times 81.4$), Pa element, USNM 482707, transitional form to *M. altudaensis*; 12, lateral view, Pa element ($\times 79.9$), USNM 482708; 13, upper view, Pa element ($\times 79.3$), USNM 482709; 14, 15, lateral view ($\times 79.5$) and upper view ($\times 78.2$), Pa element, USNM 482710; 16, oblique lateral view, Pa element ($\times 79.4$), USNM 482711; 20, upper view, Pa element ($\times 81.4$), USNM 482712, showing development of transverse ridges. All specimens from USGS 31531-PC (W90-50). (Reduced to 72% of original for publication.)

FIGURES 17-19, 21, 22.—*Mesogondolella shannoni* transitional to *Mesogondolella altudaensis*: 17, 18, upper view ($\times 81.6$) and lateral view ($\times 81.6$), Pa element, USNM 482713; 19, oblique upper view, Pa element, ($\times 80.8$), USNM 482714; 21, 22, upper view ($\times 82.3$) and lateral view ($\times 81.4$), Pa element, USNM 482715. All specimens from USGS 31531-PC (W90-50). (Reduced to 72% of original for publication.)

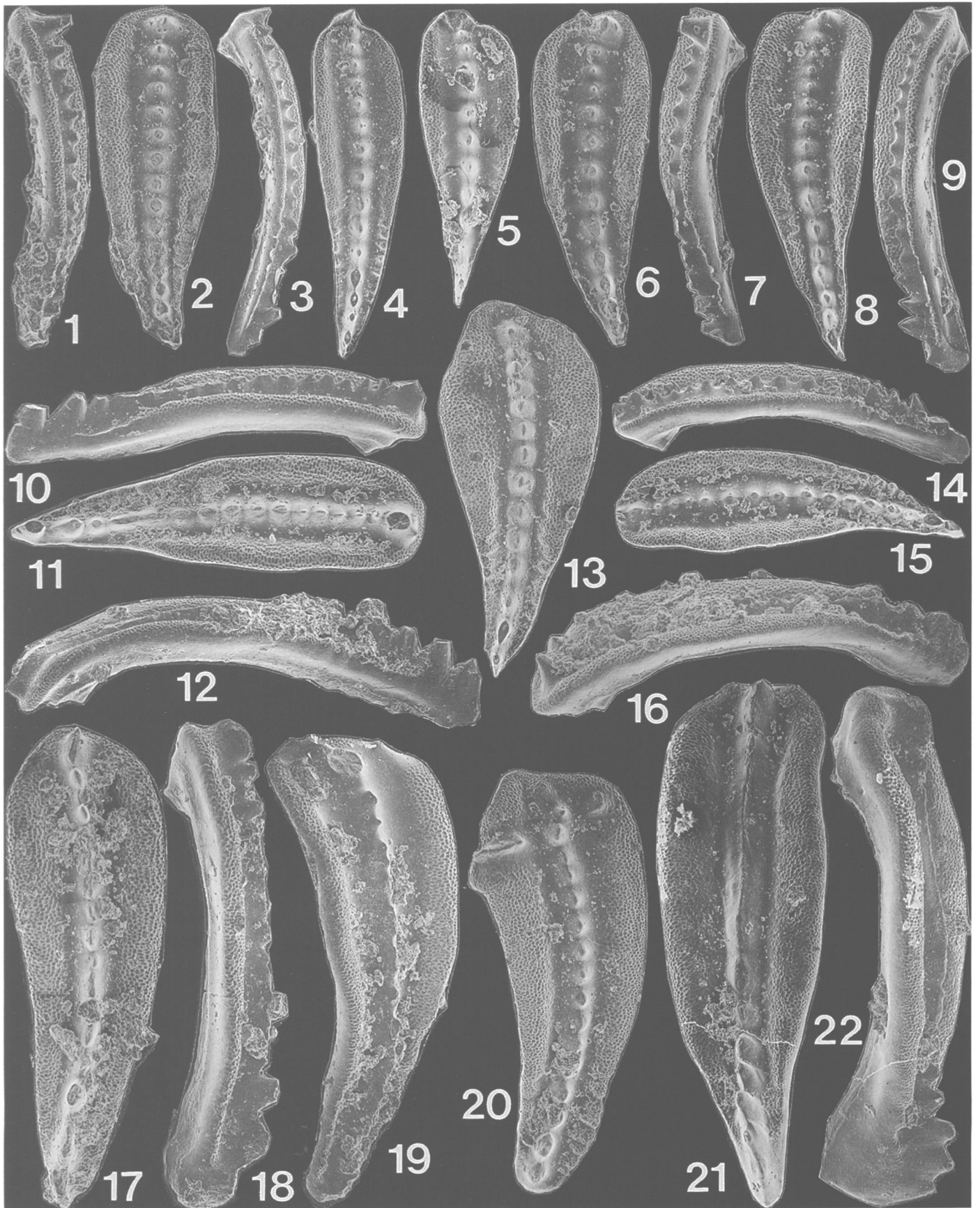


PLATE 3-9*Mesogondolella*

FIGURES 1–27.—*Mesogondolella shannoni* Wardlaw: 1, 2, upper view (×81.8) and lateral view (×81.4), Pa element, USNM 482716; 3, 4, upper view (×79.6) and lateral view (×79.5), Pa element, USNM 482717; 5, 6, upper view (×79.9) and lateral view (×81.5), Pa element, USNM 482718; 7, lateral view, Pa element (×81.6), USNM 482719; 8, upper view, Pa element (×82.0), USNM 482720; 9, 10, upper view (×81.8) and lateral view (×81.4), Pa element, USNM 482721; 11, 12, lateral view (×81.8) and upper view (×79.9), Pa element, USNM 482722; 13, 14, lateral view (×79.9) and upper view (×79.6), Pa element, USNM 482723; 15, 16, lateral view (×77.8) and upper view (×77.7), Pa element, USNM 482724; 17, 18, lateral view (×79.5) and upper view (×79.6), Pa element, USNM 482725; 19, upper view, Pa element (×79.6), USNM 482726; 20, 21, upper view (×79.6) and lateral view (×80.0), Pa element, USNM 482727; 22, 23, upper view (×82.0) and lateral view (×82.0), Pa element, USNM 482728; 24, 25, lateral view (×79.9) and upper view (×79.6), Pa element, USNM 482729; 26, 27, upper view (×81.6) and lateral view (×81.6), Pa element, USNM 482730. All specimens from USGS 31533-PC (W91-2). (Reduced to 72% of original for publication.)

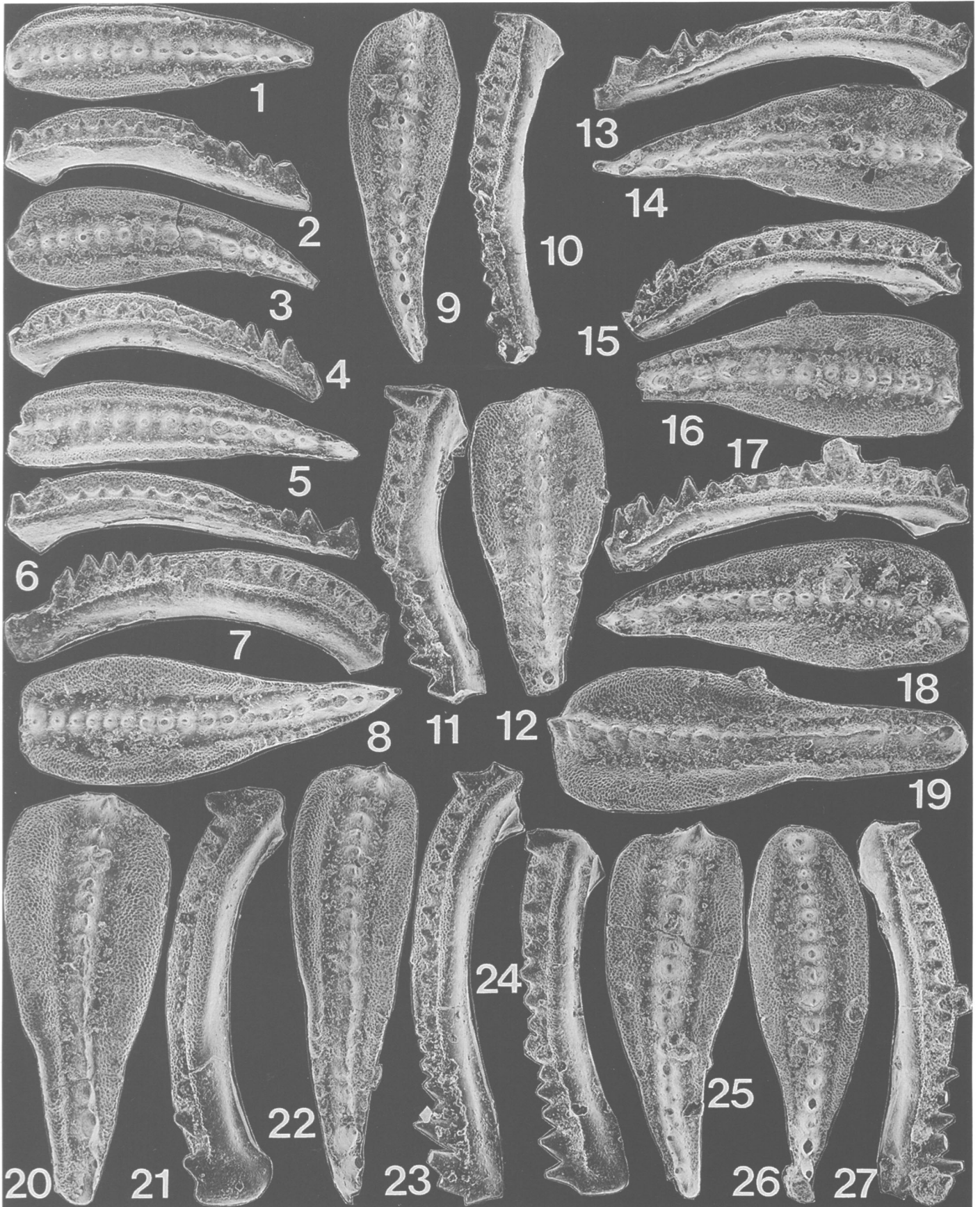


PLATE 3-10

Mesogondolella

FIGURES 1-3.—*Mesogondolella idahoensis* (Youngquist, Hawley, and Miller): 1, lower view, Pa element ($\times 82.9$), USNM 482731; 2, lower view, Pa element ($\times 80.8$), USNM 482732; 3, lower view, Pa element ($\times 81.5$), USNM 482733. All specimens from USGS 31639-PC (W90-8), Cathedral Mountain Formation, Split Tank section. (Reduced to 72% of original for publication.)

FIGURES 4-7.—*Mesogondolella idahoensis* transitional to *M. nankingensis*: 4, lower view, Pa element ($\times 80.8$), USNM 482734; 5, lower view, Pa element ($\times 81.5$), USNM 482735; 6, lower view, Pa element ($\times 80.8$), USNM 482736; 7, lower view, Pa element ($\times 80.8$), USNM 482737. Figures 4, 5 from USGS 29403-PC (W83-47) and Figures 6, 7 from USGS 29404-PC (W83-48). (Reduced to 72% of original for publication.)

FIGURES 8-10.—*Mesogondolella nankingensis* (Ching [Jin]): 8, lower view, Pa element ($\times 81.5$), USNM 482738; 9, lower view, Pa element ($\times 80.8$), USNM 482739; 10, lower view, Pa element ($\times 81.5$), USNM 482740. All specimens from USGS 31421-PC (W81-176). (Reduced to 72% of original for publication.)

FIGURES 11-17.—*Mesogondolella aserrata* (Clark and Behnken): 11, lower view, Pa element ($\times 79.3$), USNM 482741; 12, lower view, Pa element ($\times 80.8$), USNM 482742; 13, lower view, Pa element ($\times 82.9$), USNM 482743; 14, lower view, Pa element ($\times 82.9$), USNM 482744; 15, lower view, Pa element ($\times 80.8$), USNM 482745; 16, lower view, Pa element ($\times 81.5$), USNM 482746, transitional form to *M. postserrata*; 17, lower view, Pa element ($\times 80.8$), USNM 482747, transitional form to *M. postserrata*. Figures 11-15 from USGS 29814-PC (W85-16) and Figures 16, 17 from USGS 29818-PC (W85-20). (Reduced to 72% of original for publication.)

FIGURES 18, 19.—*Mesogondolella postserrata* (Behnken): 18, lower view, Pa element ($\times 81.5$), USNM 482748; 19, lower view, Pa element ($\times 81.5$), USNM 482749. Both specimens from USGS 29818-PC (W85-20). (Reduced to 72% of original for publication.)

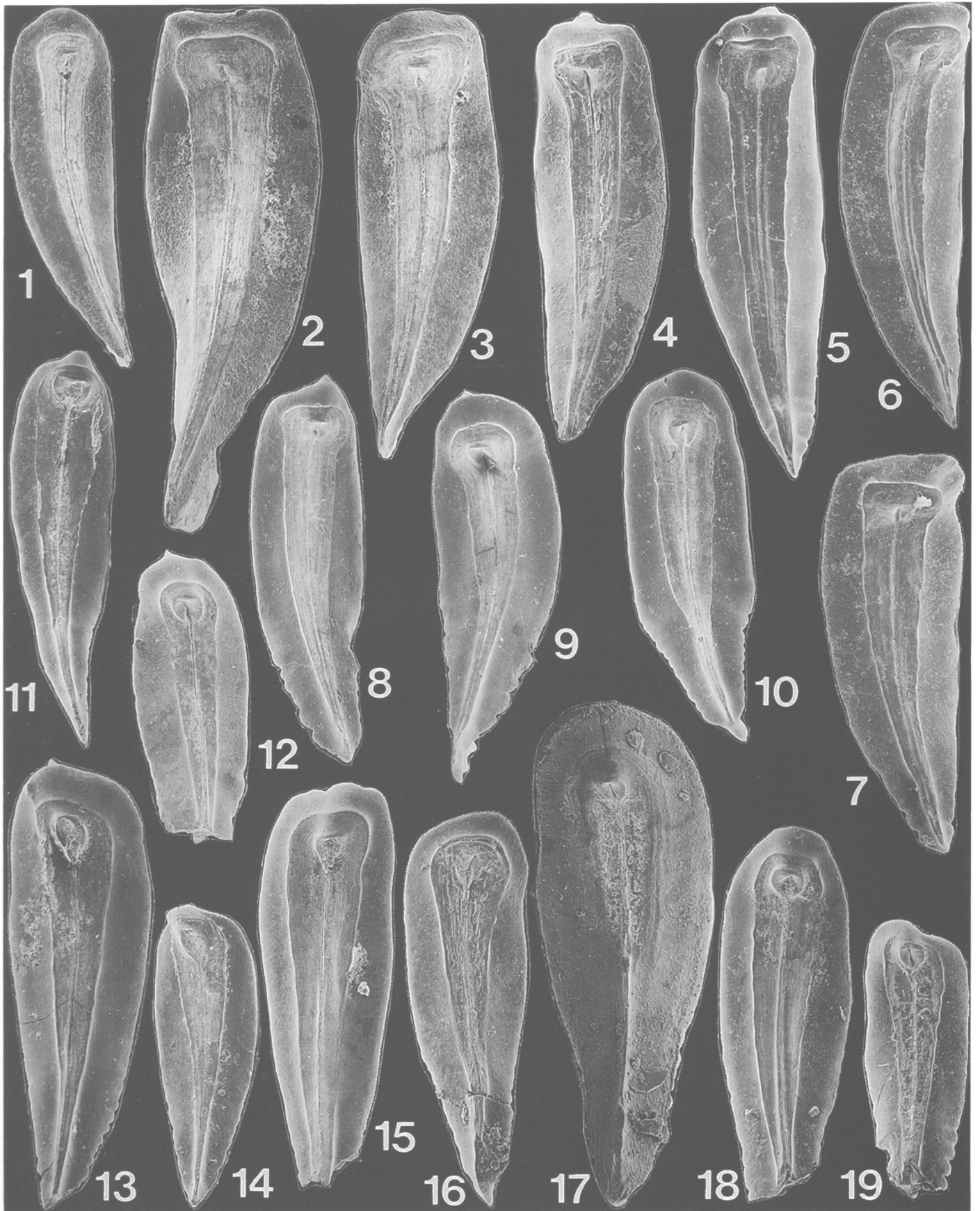


PLATE 3-11*Mesogondolella*

FIGURES 1-4.—*Mesogondolella postserrata* transitional to *M. shannoni*: 1, lower view, Pa element ($\times 80.8$), USNM 482750; 2, lower view, Pa element ($\times 81.5$), USNM 482751; 3, lower view, Pa element ($\times 80.8$), USNM 482752, showing attached basal plate; 4, lower view, Pa element ($\times 80.8$), USNM 482753. All specimens from USGS 31536-PC (W91-1). (Reduced to 72% of original for publication.)

FIGURES 5-14.—*Mesogondolella shannoni* Wardlaw: 5, lower view, Pa element ($\times 79.8$), USNM 482754; 6, lower view, Pa element ($\times 80.8$), USNM 482755; 7, lower view, Pa element ($\times 82.2$), USNM 482756, showing attached basal plate; 8, lower view, Pa element ($\times 80.8$), USNM 482757; 9, lower view, Pa element ($\times 82.9$), USNM 482758; 10, lower view, Pa element ($\times 80.8$), USNM 482759; 11, lower view, Pa element ($\times 80.8$), USNM 482760; 12, lower view, Pa element ($\times 80.8$), USNM 482761; 13, lower view, Pa element ($\times 80.8$), USNM 482762; 14, lower view, Pa element ($\times 81.3$), USNM 482763. Figures 5-8 from USGS 31536-PC (W91-1), Figures 9-12 from USGS 31531-PC (W90-50), and Figures 13, 14 from USGS 31533-PC (W91-2). (Reduced to 72% of original for publication.)

FIGURES 15-17.—*Mesogondolella altudaensis* (Kozur): 15, lower view, Pa element ($\times 80.8$), USNM 482764; 16, lower view, Pa element ($\times 82.9$), USNM 482765; 17, lower view, Pa element ($\times 80.8$), USNM 482766. All specimens from USGS 31533-PC (W91-2). (Reduced to 72% of original for publication.)

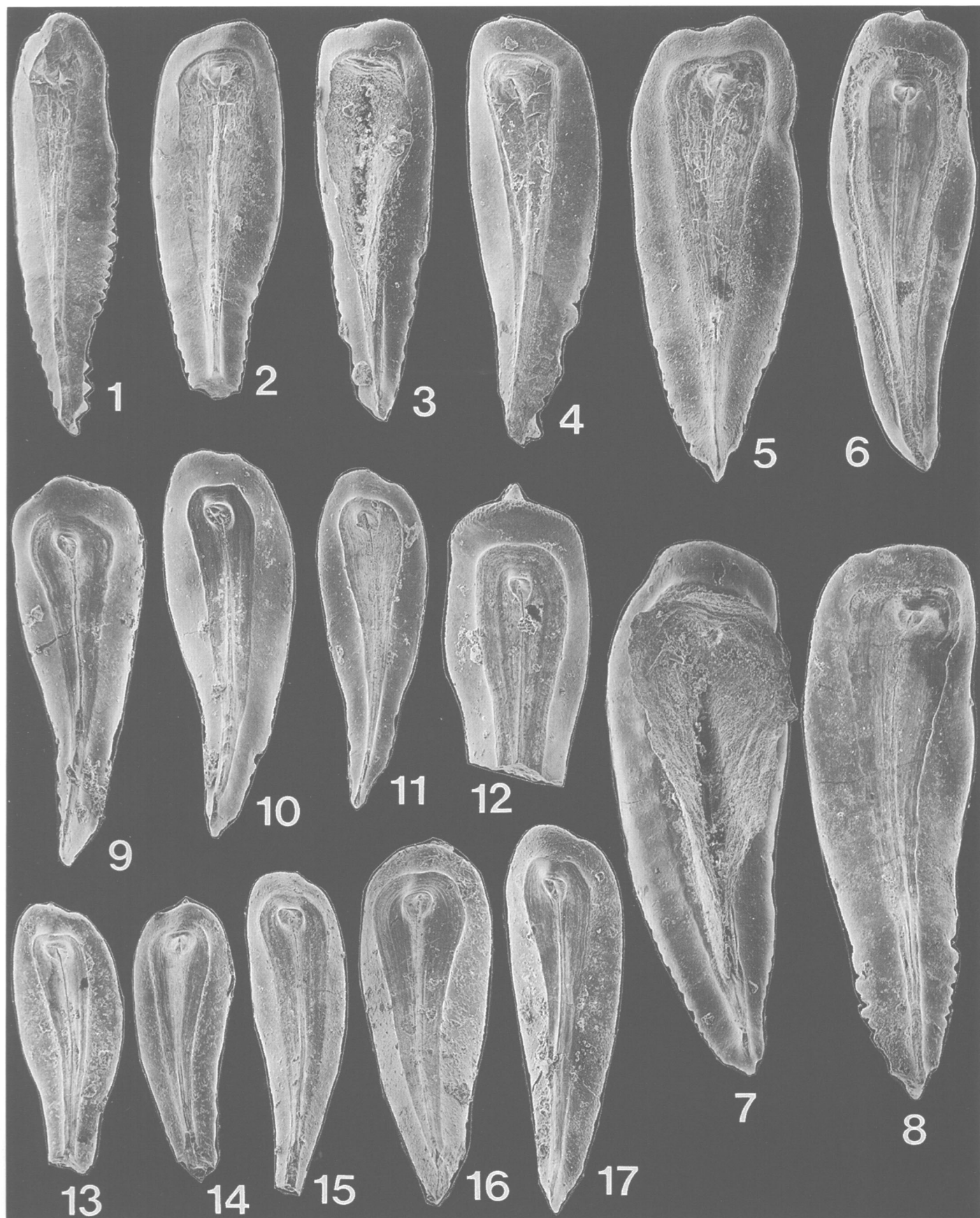


PLATE 3-12

Iranognathus, *Hindeodus*, *Neostreptognathodus*, *Sweetognathus*, *Sweetina*, and *Xaniognathus*

FIGURES 1, 2.—*Hindeodus wordensis*, new species: 1, lateral view, Pa element ($\times 76.0$), USNM 482767; 2, lateral view, Pa element ($\times 76.0$), USNM 482768. Both specimens from USGS 31570-PC (W847). (Reduced to 72% of original for publication.)

FIGURES 3–5.—*Xaniognathus hydraensis* Nestell and Wardlaw: 3, inner view, Pb element ($\times 76.0$), USNM 482769; 4, outer view, Pa element ($\times 76.0$), USNM 482773; 5, inner view, Pa element ($\times 76.0$), USNM 482771. All specimens from USGS 31535-PC (89BM-343). (Reduced to 72% of original for publication.)

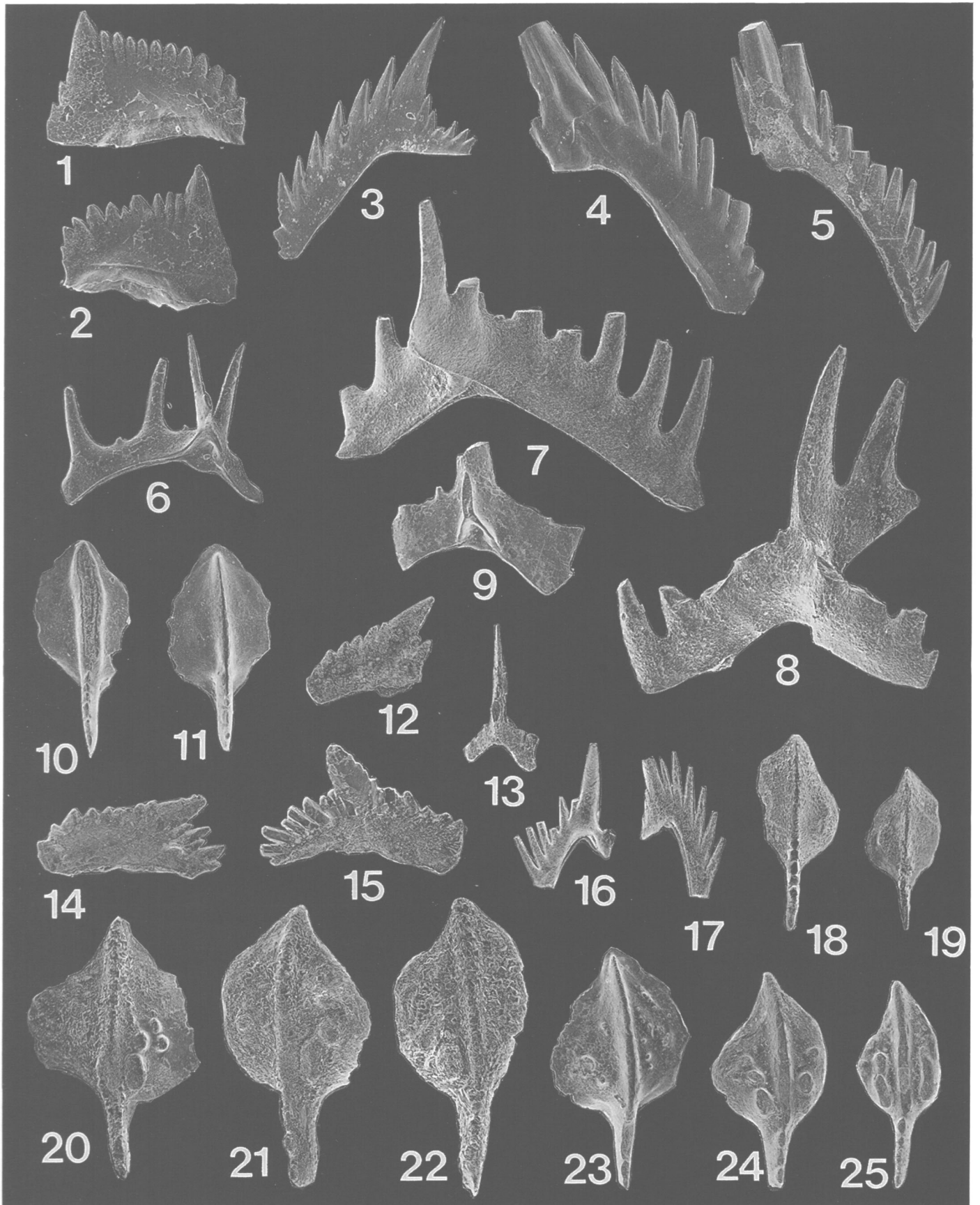
FIGURES 6–8.—*Sweetina festiva* (Bender and Stoppel): 6, lower lateral view, Pa element ($\times 76.0$), USNM 482772; 7, lateral view, Pa element ($\times 76.0$), USNM 482773; 8, upper lateral view, Pa element ($\times 76.0$), USNM 482774. Figure 6 from USGS 31472-PC (W877); Figures 7, 8 from USGS 31640-PC (W9016), Cathedral Mountain Formation, Split Tank section. (Reduced to 72% of original for publication.)

FIGURE 9.—*Sweetina triticum* Wardlaw and Collinson: lateral view, Pa element ($\times 76.0$), USNM 482775. Specimen from USGS 31569-PC (W846). (Reduced to 72% of original for publication.)

FIGURE 10.—*Neostreptognathodus clinei* Behnken: 10, upper view, Pa element ($\times 76.0$), USNM 482776. Specimen from USGS 31575-PC (W8435). (Reduced to 72% of original for publication.)

FIGURE 11.—*Sweetognathus bicarinum*, new species: upper view, Pa element ($\times 76.0$), USNM 482777. Specimen from USGS 31575-PC (W8435). (Reduced to 72% of original for publication.)

FIGURES 12–25.—*Iranognathus punctatus*, new species: 12, lateral view, Pb element ($\times 76.0$), USNM 482778, from USGS 31641-PC (WP8635); 13, upper oblique view, Sa element ($\times 76.0$), USNM 482779, from USGS 31642-PC (WP8634); 14, lateral view, Pb element ($\times 76.0$), USNM 482780, from USGS 31643-PC (WP8611); 15, lateral view, Pb element ($\times 76.0$), USNM 482781, from USGS 31644-PC (WP8617); 16, lateral view, M element, ($\times 76.0$), USNM 482782, from USGS 31645-PC (WP8632); 17, lateral view, M element ($\times 76.0$), USNM 482783, from USGS 31646-PC (WP8634); 18, upper view, Pa element ($\times 76.0$), USNM 482784, from USGS 31641-PC (WP8635); 19, upper view, Pa element ($\times 76.0$), USNM 482785, from USGS 31641-PC (WP8635); 20, upper view, Pa element ($\times 76.0$), USNM 482786, from USGS 31642-PC (WP8634); 21, upper view, Pa element ($\times 76.0$), USNM 482787, from USGS 31647-PC (WP8613); 22, upper view, Pa element ($\times 76.0$), USNM 482788, from USGS 31645-PC (WP8632); 23, upper view, Pa element ($\times 76.0$), holotype, USNM 482789, from USGS 31645-PC (WP8632); 24, upper view, Pa element ($\times 76.0$), USNM 482790, from USGS 31643-PC (WP8611); 25, upper view, Pa element ($\times 76.0$), USNM 482791, from USGS 31643-PC (WP8611). (Reduced to 72% of original for publication.)



4. Formal Middle Permian (Guadalupian) Series: A Fusulinacean Perspective

Garner L. Wilde

ABSTRACT

The Guadalupian Symposium brought into focus the remarkable agreement that exists between workers from a number of disciplines as to the importance of proposing the Guadalupian Series as an International Standard for the Middle Permian. Glenister (1991) and Glenister et al. (1992) have outlined both the criteria required and the desirable attributes of the Guadalupian Series (Girty, 1902, 1908) for fulfilling the necessary requirements. The present paper seeks to elucidate the importance of fusulinaceans in helping to fulfill these requirements. Fusulinaceans occur, often in abundance, throughout the Carboniferous and Permian, and species of this large group of microfossils form an ideal evolutionary continuum. Along with conodonts and ammonoids, in particular, fusulinaceans offer an excellent means by which the well-established sedimentological history of the West Texas Permian can be zoned and applied on a worldwide basis.

Introduction

Since the early establishment of the Guadalupian Series by Girty (1902), there has been an abundance of research on the fauna and flora, as well as the sedimentology, of this diverse group of rocks, particularly in the Guadalupe and Glass mountains. Indeed, the way was paved for later research by the publication of the Guadalupian Fauna (Girty, 1908) and the mapping by P.B. King (1931) in the Glass Mountains and the Guadalupe Mountains (1948).

Early work on the fusulinids by Dunbar and Skinner (1937), on the brachiopods by R.E. King (1931), and on the ammonoids by Miller and Furnish (1940) established the

importance of these faunas for local as well as worldwide correlation. The more recent work on the fusulinids by Ross (1963), Skinner and Wilde (1954, 1955), Wilde (1955, 1986a,b, 1988, 1990), and Wilde and Rudine (this volume), on the brachiopods by Cooper and Grant (1964, 1966, 1972, 1974, 1975, 1976a,b, 1977), and on the ammonoids by Furnish et al. (1991), Glenister (1991), and Glenister et al. (1991) has served to emphasize the importance of these fossil groups in zoning the Permian rocks of North America. Very recently the conodonts have achieved an important place in zonation, particularly in the middle Permian (Guadalupian) rocks (Behnken, 1975; Grant and Wardlaw, 1984; Wardlaw, 1991; Wardlaw and Grant, 1987, 1990; and Lambert et al., this volume).

The continuing work on all of these fossil groups has been augmented tremendously by modern sedimentological methods (Newell et al., 1953; Boyd, 1958; Pray and Esteban, 1977; Harris, 1982, 1988a,b; Sarg, 1986; Sarg and Lehman, 1986a,b). Lloyd Pray has made enormous contributions to the overall knowledge of the stratigraphy and sedimentology of the region through his students and colleagues, who are too numerous to list here. As a consequence, a well-understood Guadalupian concept has emerged that should fulfill the necessary requirements for the establishment of the Guadalupian Series as the international standard for the Middle Permian. Notwithstanding the closeness of understanding among the various workers, much detailed effort still remains to be done before the task is accomplished. Thus, suggestions put forth in the present paper, based largely upon an understanding of fusulinaceans, are offered to inspire a further effort in finalizing this important work.

The Guadalupian study group (Glenister et al., 1992) proposed that the Guadalupian Series comprises three stages; in ascending order these are the Radian Stage, the Wordian Stage, and the Capitanian Stage. For convenience, these are commonly referred to as early, middle, and late Guadalupian (King, 1948; Wilde and Todd, 1968). Complete agreement has not been reached as to the manner in which certain rock units fit into these categories, but the basic understandings are in place.

Guadalupe Series

EARLY GUADALUPIAN

Roadian Stage

The Roadian Stage was originally proposed by Furnish (1966, 1973), although at the time he included the Roadian as the youngest stage of the Leonardian (Artinskian) Series, based largely upon the supposed index *Perrinites* ammonoid fauna. Recent field work (Lambert et al., 1991, this volume) provided a basis for a better understanding of the lateral relationships of Roadian rocks from basin to shelf, thus helping to clarify earlier stratigraphic concepts regarding ammonoid occurrences. Indeed, Furnish et al. (1991) currently recognizes both Leonardian and Guadalupian elements in the Roadian.

Wilde has reported in numerous publications (Wilde and Todd, 1968; Wilde, 1986a,b, 1988, 1990) the typical fusulinid faunas of the Roadian, particularly those that occur in the Road Canyon Formation of the Glass Mountains and those of the Cutoff Formation and its lateral equivalents (lower and middle San Andres Formation) of the Guadalupe Mountains. In the Guadalupe and Apache mountains, some stratigraphic detail has been offered; however, in the Glass and northern Del Norte mountains, stratigraphic data has been reported in only a general way. Such generalized reporting could result in criticism as to occurrences reported, even though the author is unaware of queries of such nature. On the other hand, the literature ought to reflect the close stratigraphic control that is available.

Notwithstanding many years of data gathering at the surface and in the subsurface, which produced data that are basically unavailable for general publication, there are abundant data recorded in Cooper and Grant (1977) of fusulinid identifications from many localities in the Glass and Del Norte mountains. The majority of these identifications were made by Wilde, including practically all that were made from the Road Canyon Formation.

As is often the case in the early stages of stratigraphic work, fusulinid identifications by various workers were preliminary determinations, having been made from broken rock surfaces; however, numerous sets of thin sections of a portion of the Cooper and Grant material fortunately have been retained. At the time they were sent, Cooper (pers. comm., 1991) also supplied some basic stratigraphic data. From this data eight measured sections were able to be reconstructed (Figures 4-1, 4-2) in the northern Del Norte and western Glass mountains to demonstrate some of the fusulinid control of the Road Canyon Formation. Keeping in mind that these collections represent a very small percentage of the total that was available, one is struck by the amazing consistency from section to section. The measured sections shown herein have not been rechecked in the field, and of necessity they are generalized. Recent field work, conducted by numerous workers, particularly of the type Road Canyon Formation, will be more definitive in terms of thickness and bed description.

Wilde's zonation paper (1990) listed the assemblage zone of *Parafusulina boesei*-*Skinerina* (PG-1) as the main zone of the Roadian. At present, two main subzones of the Roadian are recognizable in the Road Canyon Formation on the basis of fusulinid species occurrences (PG-1-A, PG-1-B), and these subzones appear to coincide with two basic lithofacies in the eight measured sections herein being considered. The lowest lithofacies is dominated by gray to bluish gray shale intervals, with shale thickness of up to 50 feet (15.2 m). These are interbedded with clastic carbonates (calcirudites), conglomerates, and occasional biohermal beds. This lower unit contains *Parafusulina boesei* Dunbar and Skinner, *P. splendens* Dunbar and Skinner, *P. attenuata* Dunbar and Skinner, and undescribed *Rausserella* (PG-1-A). Individual shells of *P. boesei* are commonly small for the species but appear to fall well within the range of size variation.

The upper of the two lithofacies is dominated by yellowish shales interbedded with cherty, platy limestones, and thick biohermal beds. A greater diversity of fusulinid species is found in this unit, including *Parafusulina boesei*, *P. splendens*, *P. rothi* Dunbar and Skinner, *P. attenuata*, *P. bakeri?* Dunbar and Skinner, *P. sullivanensis* Ross, *P. ironensis* Ross, *Skinerina rotundata* (Dunbar and Skinner), and *Rausserella* sp. (PG-1-B). *Skinerina* has not been identified with any certainty in the collections, but the approximate stratigraphic position for two collections of Ross (1964) have been located in the present sections. Ross collected his material from sections very near the two reported herein.

In the Apache and Guadalupe mountains, similar fusulinid faunas are present, and a guarded possibility occurs for the correlation of the two lithofacies of the Glass Mountains-Del Norte Mountains area with the described members of the Cutoff Formation, especially in the Guadalupe Mountains area.

Harris (1982, 1988a) originally separated the Cutoff Formation of King (1948) into five correlation units, to which he simply applied numbers. The lowest, unit 1, appears to rest unconformably upon Leonardian (Bone Spring, Victorio Peak) rocks, and it is overlain unconformably by the next three successive units, units 2-4. These, in turn, are overlain unconformably by unit 5. In the Guadalupe Mountains, Wilde (1986a,b, 1988) reported the occurrence of the following fusulinid species from the Cutoff Formation and/or its lateral shelf equivalent, the lower and middle San Andres Formation: *Parafusulina boesei*, *P. splendens*, *P. maleyi* Dunbar and Skinner, *Rausserella* sp., and *Skinerina fusiformis* Skinner (originally reported as *S. rotundata* (Dunbar and Skinner)).

In the Cutoff Formation of the Apache Mountains, Wilde identified the following (in Wilde and Todd, 1968): *Parafusulina* cf. *P. boesei*, *P. cf. P. splendens*, *P. attenuata*, *P. maleyi*, *P. sp.*, *Skinerina rotundata*, *Rausserella* sp., and *Boultonia* sp.

In the Guadalupe Mountains type section of the Cutoff Formation at Cutoff Mountain, *Skinerina fusiformis* was collected from the lower part of Harris' unit 5, whereas in the Apache Mountains, *S. fusiformis* and *S. rotundata* were

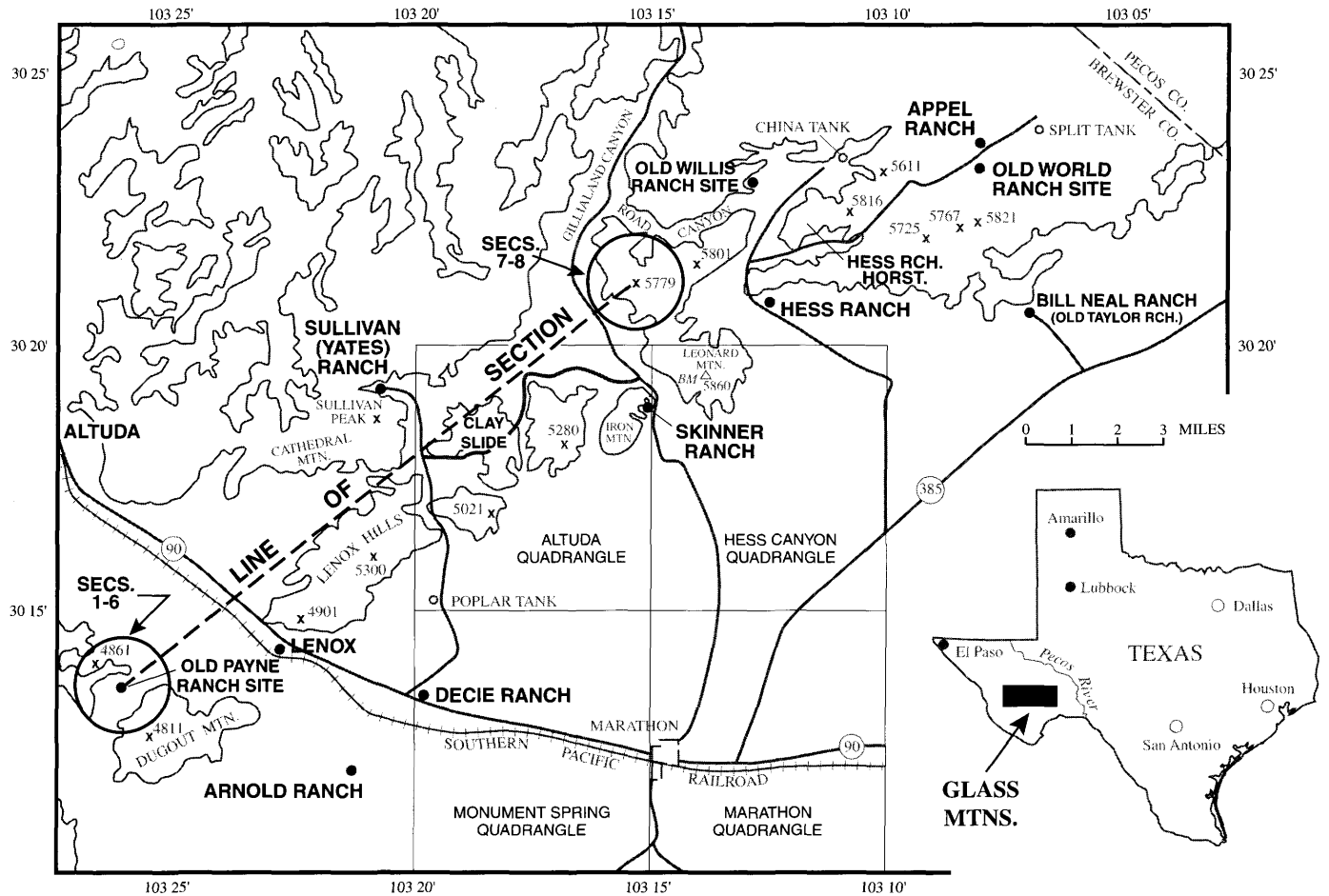


FIGURE 4-1.—Map of the Glass and Del Norte mountains, Brewster County, Texas, showing the location of the sections illustrated in Figure 4-2 (modified after Cooper and Grant, 1977).

collected from the lower part of the Cutoff section, not far above the Leonardian Victorio Peak. The specimens of *S. fusiformis* from Cutoff Mountain were badly abraded, but they appeared to belong to an allodapic sequence. It is possible that two entirely different zones of *Skinnerina* are represented by these occurrences.

Harris (this volume) has now given member names to his (1982, 1988a) original correlation units of the Cutoff Formation, as follows:

- Unit 5 = Williams Ranch Member
- Units 2-4 = El Centro Member
- Unit 1 = Shumard Member

Closer stratigraphic control than that, which the fusulinids can provide, might possibly be provided by the conodonts. It is conceivable, however, that the El Centro Member of the Cutoff Formation in the Guadalupe Mountains is coeval with the lower, gray shale-dominated lithofacies of the Glass and Del Norte mountains, and the Williams Ranch Member may be coeval with the yellow shale-dominated lithofacies of the same areas. A serious question still exists as to the presence or

absence of a Shumard Member equivalent unit in the Glass Mountains, one which is also poorly represented in the Guadalupe Mountains because of severe erosion on the unconformity at its top. If the *Skinnerina* zone of the basal Cutoff in the Apache Mountains is an older zone than that of the Road Canyon occurrences in the Glass and Del Norte mountains, it is also conceivable that this section and the section of the Cutoff Formation at South Mesa, Sierra Diablo (western Texas), also represent lithofacies equivalents of the El Centro and Williams Ranch members (Wilde in Wilde and Todd, 1968, fig. 3).

Lambert et al. (this volume) suggests that because the transition between the Leonardian conodont elements known as *Mesogondolella idahoensis* (= *Neogondolella*) and the Roadian conodont elements *M. serrata* [= *nankingensis*] begins at the base of the El Centro Member of the Cutoff Formation, the lower boundary of the Guadalupian should fall somewhere within the El Centro Member. The logical boundary point would seem to occur at about the contact of Harris' original units 2 and 3. This could possibly represent the actual base of the Road Canyon Formation of the Glass Mountains. The break

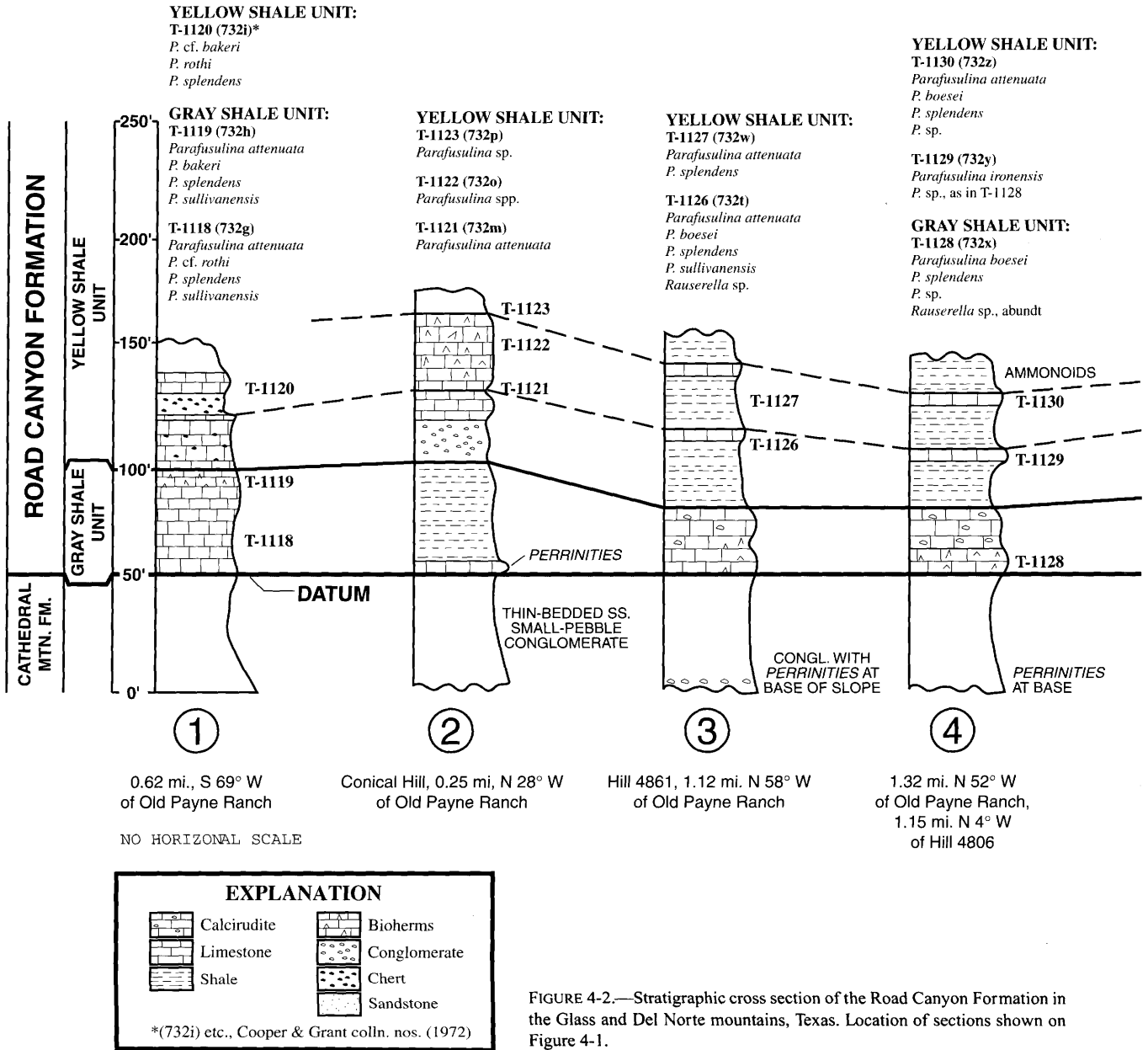


FIGURE 4-2.—Stratigraphic cross section of the Road Canyon Formation in the Glass and Del Norte mountains, Texas. Location of sections shown on Figure 4-1.

YELLOW SHALE UNIT:

T-1134 (733e)
Parafusulina splendens

T-1133 (733d)
Parafusulina splendens

① Ross (1964)

T-1132 (733c)
Parafusulina aff. rothi
P. spp.

GRAY SHALE UNIT:

T-1131 (733b)
Parafusulina boesei

YELLOW SHALE UNIT:

T-1066 (724d)
Parafusulina rothi
P. sullivanensis

T-1068 (724h)
Parafusulina boesei
P. sullivanensis

T-1067 (724e)
Parafusulina sullivanensis
② Ross (1964)

T-1046 (721qc)
Parafusulina cf. splendens
P. sp.

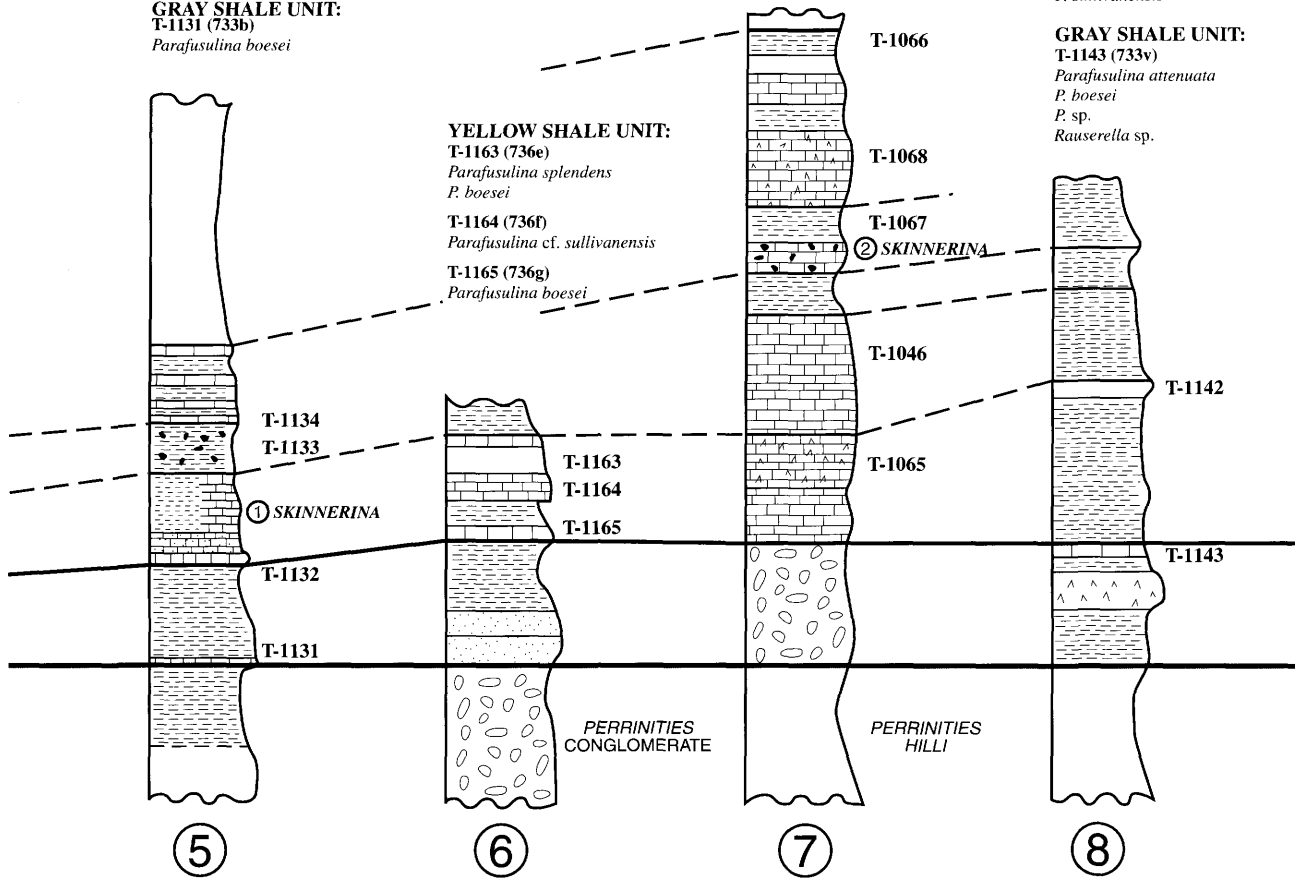
T-1065 (724c)
Parafusulina splendens?
P. rothi
P. sp.

YELLOW SHALE UNIT:

T-1142 (733u)
Parafusulina boesei
P. sullivanensis

GRAY SHALE UNIT:

T-1143 (733v)
Parafusulina attenuata
P. boesei
P. sp.
Rausserella sp.



⑤
1.55 mi. N 64° W
of Old Payne Ranch

⑥
Hill 0.55 mi. N 75° W
of Hill 4861, 1.6 mi. N 72° W
of Old Payne Ranch

⑦
Road Canyon Fm. Type Section
SE face of spur, 0.5 mi. due
north of Skinner Ranch

⑧
1.82 mi. N 84° W,
Hess Ranch House
0.27 mi. S 28°E of Hill 5674,
Hess Canyon quadrangle

does not contradict the presently known fusulinid occurrences at the outcrop; however, this horizon ought to correlate stratigraphically to within the lower San Andres Formation of the Algerita Escarpment, northern Guadalupe Mountains (Sarg, 1986; Sarg and Lehmann, 1986a,b; Wilde, 1986a). Such a position seems somewhat high inasmuch as lower San Andres fusulinid faunas have been found throughout the Permian Basin in thousands of well bores, and they are always of Guadalupian aspect rather than Leonardian. Dolomitization of the San Andres shelf on the Algerita Escarpment has left much to be desired for recovery of identifiable fusulinid faunas in the critical intervals.

At present, it is little more than speculation to suggest that the Pipeline Shale Member (King's southern Cutoff) at the mouth of Brushy Canyon could be equivalent to any part of the type Cutoff Formation as suggested by Wilde (Wilde and Todd, 1968), and this problem is still being explored. Although there seems to be little support for this correlation at present, it is believed that a genetic relationship does exist based upon certain fusulinid occurrences. Glenister (oral comm., 1991) suggested that indeed the ammonoid faunas are not as yet sufficiently studied, but that the Pipeline Shale Member can definitely be shown to lie above the highest Cutoff; however, its lithic aspect seems closer to the Cutoff than to the Brushy Canyon.

A rather sticky problem exists also regarding various "reworked" occurrences of *Boultonia guadalupensis* Skinner and Wilde. The types came from the large allocthonous blocks in the Cutoff Formation of the Bone Canyon area on the western side of the Guadalupe Mountains. There they are well preserved, occur in large clasts, and are accompanied by other clasts containing species of *Parafusulina*. Skinner and Wilde collected similar material from King's southern Cutoff (Pipeline Shale) at the mouth of Brushy Canyon, except that the individual specimens of *B. guadalupensis* were abraded. The same was true in collections made by Lehmann, Sarg, Rossen, and Wilde at Chinaman's Hat, about 2.5 miles (4.0 km) south of Brushy Canyon, and in recent collections made by Lloyd Pray and Mark Harris (pers. comm., 1991) of grainstones from a debris flow at the well-known black cut near the highway, which is a little more than a mile north of the Brushy Canyon locality. This last material, which has been examined by the author, appears to belong to the Williams Ranch Member of the Cutoff, according to Pray and Harris. Occurring with the abraded *Boultonia guadalupensis* were also abraded *Parafusulina*, one of which appeared to be close to *P. attenuata* Dunbar and Skinner.

Harris (per. comm., 1991) believed that the allocthonous blocks in the south wall of Bone Canyon ("patch reefs" of Newell et al., 1953) possibly fall somewhere near the base of the El Centro Member of the Cutoff Formation, but he suggested that the solution to this problem of stratigraphic placement is further complicated because of the presence of erosion surfaces, channelizing, and intertonguing of strata in strategic areas.

It is possible that all of the above-cited occurrences of *B. guadalupensis* represent a single genetic package, beginning with the large, and possibly older, megabreccias at Bone Canyon, and proceeding basinward to the finer grainstones and microbreccias farther out into the basin. It makes little difference whether or not the original material was reworked from the Leonardian (Victorio Peak) or from an unrecognized Roadian shelf margin, not seen on the west face of the Guadalupe Mountains. The essential question to be answered is whether these disparate occurrences represent a package of similar events during a short period of geologic time comprising the Roadian Stage.

MIDDLE GUADALUPIAN

Wordian Stage

"Brushyan"

There is little doubt that a close relationship exists between the fusulinid faunas of the Cutoff Formation and the overlying Brushy Canyon Formation (Wilde and Todd, 1968; Wilde, 1990). For this reason, the "Brushyan" has been retained in the early Guadalupian (Figure 4-3) as a younger fusulinid zone than the Roadian. There could be many problems associated, on the other hand, with making the Brushy Canyon part of the middle Guadalupian (Wordian). Because of the difficulty in establishing an unequivocal shelf equivalent for the Brushy Canyon, most workers have avoided dealing with this important rock sequence. Until the upper boundary of the Roadian is sufficiently understood, most workers will continue to carry the "Brushyan" as the basal Wordian, notwithstanding a history (similar faunas, eroded shelf margin, etc.) analogous to the Cutoff Formation.

Suffice it to say that the main zone of *Parafusulina rothi-P. maleyi* (PG-2, Wilde, 1990) embraces the Brushy Canyon Formation of the Delaware basin. The type locality for each species is the Brushy Canyon of the Guadalupe and northern Delaware mountains (Dunbar and Skinner, 1937). In fact, the *P. maleyi* types came from only 250 feet (76 m) below the top of the Brushy Canyon. It is likely that the Brushy Canyon was deposited rapidly (perhaps 1 M.Y.), which could easily explain the seemingly long range of its main zonal species. If the Roadian Stage covered 2 M.Y., this would give an absolute maximum of about 3 M.Y. for these forms, which is not unreasonable for most fusulinid species, whose span varies from 1 to 3 M.Y. and averages perhaps 1.5 M.Y.

Parafusulina sullivanensis Ross is another species that occurs commonly in the Roadian and has been seen in lower Brushy Canyon beds (Wilde, 1990). As to whether the upper Road Canyon Formation represents, in part, a Brushy Canyon equivalent, is at present unknown; however, if such correlation were to be fusulinid-dependent, the answer would be one of affirmation. Numerous undescribed *Parafusulina* that have been found in the Brushy Canyon should serve to strengthen this correlation once they are authenticated in the literature.

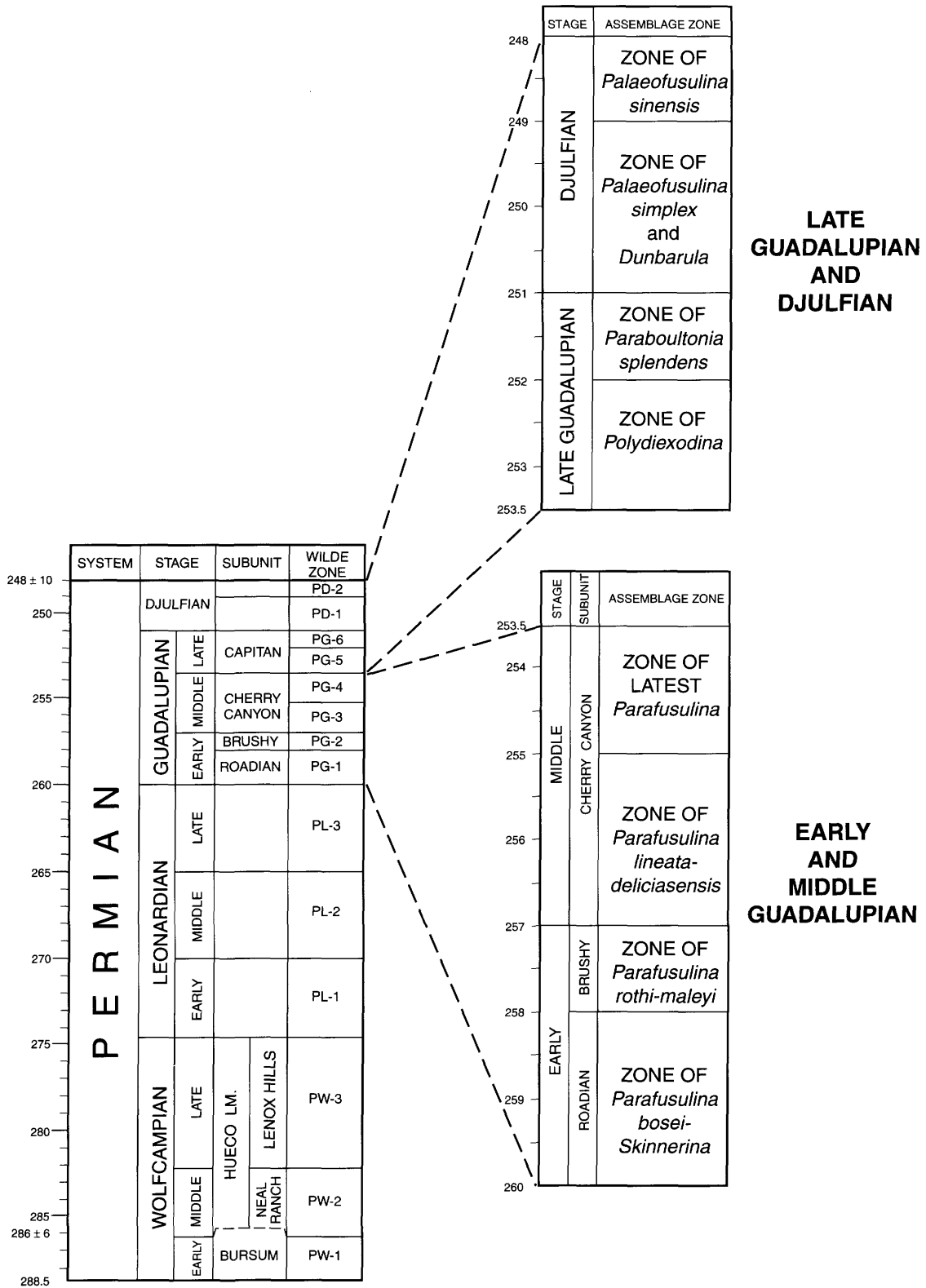


FIGURE 4-3.—The fusulinid zonation of the Permian, with emphasis on the Guadalupian (modified after Wilde, 1990).

"Cherryan"

LATE GUADALUPIAN

Capitanian Stage

Two important zones of *Parafusulina* comprise the main part of the middle (Wordian) Guadalupian Series, which is represented lithically by the Cherry Canyon Formation of the Delaware basin and its shelf equivalents, namely, the upper San Andres, Grayburg, and Queen formations. The Goat Seep reef separates the Queen from the basinal Cherry Canyon. In the Glass Mountains, the lithic equivalents are portions of the Word and Vidrio formations.

The lowest zone is *Parafusulina lineata*-*P. deliciosensis* (PG-3, Wilde, 1990). The marker species are accompanied by the tiny fusulinid *Leella fragilis* Dunbar and Skinner, progenitor to the larger *L. bellula* Dunbar and Skinner of the Capitanian. *Parafusulina sellardsi* Dunbar and Skinner is an outstanding and readily recognizable species of this zone, which occurs, often in abundance, in the Word Formation of the Glass Mountains and elsewhere.

Parafusulina sellardsi Dunbar and Skinner is indeed a large, strongly fluted species, but the zone of latest *Parafusulina* (PG-4, Wilde, 1990) contains species of extremely large size. These include *P. kingorum* Dunbar and Skinner, *P. wordensis* Dunbar and Skinner, and *P. antimonioensis* Dunbar, as well as numerous undescribed species. *Leella fragilis* Dunbar and Skinner also occurs in this zone. The author does not accept the reported occurrence of *Rauserella erratica* in the Word Formation as reported by Ross (1964). It is believed that Ross' species is not the same and that *R. erratica* is restricted to the late Guadalupian (Capitanian).

Eopolydiexodina Wilde (1975) is a rather unique representative of zone PG-4 in the Asian world, but it has not been identified with certainty in North America. *Eopolydiexodina* is a transitional genus between *Skinnerina* and *Polydiexodina*; its sporadic supplementary tunnels and lack of a well-defined central tunnel is characteristic of the former genus, whereas its elongation with heavy axial filling and squared septal folds is characteristic of the latter genus.

At the outcrop in the Guadalupe Mountains, the prominent unconformity that separates the Grayburg of the shelf from the Goat Seep reef (Fekete et al., 1986) and overlying Queen Formation may also separate zones PG-3 and PG-4. The only evidence of this, however, is provided by the presence of *Parafusulina deliciosensis* Dunbar and Skinner and *P. lineata* Dunbar and Skinner at a single locality on the outcrop (Wilde, 1986a) where dolomitization is pervasive and in the subsurface Grayburg of the McElroy Field, Upton County, Texas. Fusulinid faunas of the Queen Formation are very poorly known, but they appear to be a continuation of the *P. lineata*-*P. deliciosensis* types of the Grayburg, judging from poor collections that Wilde examined of those reported on by Newell et al. (1953). The Goat Seep reef is strongly dolomitized, and the youngest Cherry Canyon (Manzanita Limestone Member) is poor in fusulinaceans; however, presumed equivalents in Sonora, Mexico, contain some of the largest and most advanced parafusulinid shells known (Dunbar, 1953).

The two main zones of the Capitanian from oldest to youngest are *Polydiexodina* (PG-5) and *Paraboultonia splendens* (PG-6) (Figure 4-3), although a number of subzones should be recognizable within this framework. The Capitan Limestone is actually the reef portion of the shelf margin of the late Guadalupian in the Guadalupe Mountains. On the shelf, but behind the reef tract are, from oldest to youngest, the Seven Rivers, Yates, and Tansill formations. These are represented in the Delaware basin by the Bell Canyon Formation, which is largely a basinal sand, as are the underlying Cherry Canyon and Brushy Canyon formations. Interspersed throughout the Bell Canyon are limestone members that were deposited during highstand periods when sand deposition was either choked off completely or severely constrained. The uppermost limestone member of the Capitan is the Lamar Limestone, which is coeval with the Tansill Formation on the shelf. We may speak of the pre-Lamar Capitan and the Lamar-post Lamar Capitan when we consider the two main zones, for although the post-Lamar beds were not included by King (1948) in the Guadalupe Series, they are clearly late Guadalupian rather than Ochoan in lithologic as well as faunal aspect. Representative species of zone PG-5 are *Polydiexodina capitanensis* Dunbar and Skinner, *P. shumardi* Dunbar and Skinner, *Codonofusiella paradoxica* Dunbar and Skinner, *Rauserella erratica* Dunbar and Skinner, and *Leella bellula* Dunbar and Skinner. An evolutionary continuum appears to be represented in *Polydiexodina*, but at present there are no published studies to corroborate this observation.

Polydiexodina ranges upward in the Capitan to the McCombs Limestone Member (pre-Lamar), where it vanishes. This level is represented within the Yates Formation on the shelf. In the McCombs occurs *Codonofusiella extensa* Skinner and Wilde, which developed from *C. paradoxica* Dunbar and Skinner. These changes represent important steps in the evolution of a group of genera that are extremely important for zonation purposes. Evidence of the abrupt demise of *Polydiexodina*, with an attendant proliferation of the codonofusiellid line, has recently been documented in the basinal Altuda Formation (Bell Canyon equivalent) of the Glass Mountains (Wilde and Rudine, this volume) and constitutes an extremely important change in late Guadalupian fusulinacean evolution.

The zone of *Paraboultonia splendens* Skinner and Wilde comprises the remainder of the late Guadalupian (PG-6, Wilde, 1990). This zone encompasses the Lamar and post-Lamar units of King (1948). Within this framework, from oldest to youngest, are the following subzones: *Yabeina texana* Skinner and Wilde (PG-6-A), *Paradoxiella pratti* Skinner and Wilde (PG-6-B), *Reichelina lamarensis* Skinner and Wilde (PG-6-C), and *Paraboultonia splendens* Skinner and Wilde (PG-6-D). This identical zonation has been observed both in the Lamar-post Lamar of the basin side and in the Tansill Formation on the shelf side (see especially Tyrrell et al., 1978).

Wilde and Rudine (this volume) have discovered an almost identical sequence in the Altuda Formation of the Glass Mountains. *Yabeina* has not been located, but *Paradoxiella*, *Reichelina*, and *Paraboultonia* have been observed in that order, with some overlap, from oldest to youngest. Occurring with *Paraboultonia* is the Asian form *Lantschichites*, with which *Paraboultonia* has been consistently confused. *Lantschichites* always uncoils and is really an elongated codonofusiellid, whereas *Paraboultonia* never uncoils (Wilde, 1975:80). Strangely, *Lantschichites* has not been seen in the Guadalupe Mountains or Delaware Mountains sequence, but in time it will probably be discovered, as will *Yabeina*, in the Glass Mountains.

Returning to the *Codonofusiella* evolutionary line, the following scenario is suggested. *Codonofusiella* probably developed out of *Boultonia*, a common genus in Wolfcampian, Leonardian, and early Guadalupian equivalents. Uncoiling, which is not uncommon, has been observed in numerous fusulinacean groups throughout the Carboniferous and Permian. Well-known examples are *Millerella*, a simple, discoidal profusulinellid, and *Nipponitella*, a schwagerinid.

The simple *Codonofusiella paradoxica* gave rise to new species, such as *C. extensa*, by elongation of the axis of coiling. Ultimately, more and more elongation of shells gave rise to forms such as *Lantschichites*. In fact, *C. extensa* and *Lantschichites* are very close in their development, the main difference being in the size and shape of the coiled portion. But because uncoiling was proceeding at the same time, the shells developed an irregular axis in the polar extremities. Next, this extension and uncoiling gave rise to the implantation of succeeding septa on the back side of the coiled portions of the shell. This process continued until the septa from opposing ends of the shell actually met, causing a bridging over of the septa. Finally, the whorls became completely annular, giving rise to *Paradoxiella* (Skinner and Wilde, 1955).

Somewhere along the way, the paraboultonids developed, possibly directly from the boultonids, with a mere inflation of the final whorl. The essential difference, then, between the paraboultonids and the codonofusiellids is that the antetheca of the former never lifted off of the coiled portion of the shell, whereas septa of the latter group always lifted off and then succeeding septa implanted themselves on the previously uncoiled septation. That is precisely what happened in *Lantschichites* and is precisely why no generic synonymy exists with *Paraboultonia*.

Termination of the Guadalupian

Recently, largely in oral presentations and discussions, consideration has been offered as to which taxa should be utilized for stabilization of the top of the Guadalupian Series and coincident Capitanian Stage. The top must also, by definition, determine, or be determined by, the base of the highest Permian, the Dzhulfian Series.

Glenister et al. (1992) discussed the range of the cyclolobin ammonoid genus *Timorites* and its possibilities, inasmuch as its species start early in the Capitanian Stage and range into the Dzhulfian. Here, as is often a common problem for the ammonoids, rarity of specimens from critical zones can cause difficulties. The ammonoids, however, still offer some of the best tools for long-range correlation due to their pelagic nature.

The conodonts offer, as they have for the base of the Guadalupian, excellent potential for helping to establish a Guadalupian–Dzhulfian boundary, particularly within the *Mesogondolella postserrata* continuum and its related genus *Clarkina*.

Fusulinaceans offer an excellent resource for determining the Guadalupian–Dzhulfian boundary. Unless conodont elements or ammonoids can be recovered from evaporitic sequences, which overly the Capitanian, the fusulinids may be the most useful group. A brief consideration of just how and why this may be true deserves some attention.

The highest zone of the Capitanian, *Paraboultonia splendens* (PG-6, Wilde, 1990), includes the Lamar and post-Lamar beds of the Bell Canyon Formation. These, in turn, are overlain by the Castile Formation, a thick, thinly laminated, evaporitic unit, which appears at first glance to be an extremely shallow water deposit. At its contact with the underlying Bell Canyon, best seen at Seven Heart Gap, in the southern Delaware Mountains, the two formations are gradational (Wilde, 1975; Cys, 1975, 1978). In fact, one has some difficulty in deciding the proper lithologic boundary. The Bell Canyon, on the other hand, appears to have been deposited in deep water; indeed, Newell et al. (1953) have shown that water depths at the close of Bell Canyon deposition must have been in excess of 1700 feet (518 m). Whatever the cause, the Delaware basin must have become a sealed, or partly sealed, basin at the time. This insured deep water evaporite deposition at least until the basin had become sufficiently filled with sediment to allow for a rapid change to shallow-water evaporitic conditions, including thick salt deposits (Salado Formation).

Thus, conditions at the close of the Capitanian (Bell Canyon) became totally unfavorable for life in the Delaware basin. But, just prior to these events some of the most uniquely important fusulinaceans ever seen in the geologic column had lived, assuring the establishment of a worldwide correlation of the top of the Guadalupian Series.

The tiny *Yabeina texana* at the base of the Lamar Limestone Member (Subzone PG-6-A) was considered an enigma when first reported (Skinner and Wilde, 1955). It was thought to be too small, possibly another genus. But the advanced development of septula in the species placed it within the *Yabeina* zone. A few feet above was the strange *Paradoxiella pratti* (Subzone PG-6-B), a *Codonofusiella* gone awry. Later Ishii and Takahashi (1960) described *Paradoxiella japonica* from conglomerates of the Kwanto Massif in Japan, but its stratigraphic position was undetermined until Sada and Skinner (1977) discovered *Paradoxiella* in the Akasaka Limestone, Gifu Prefecture, Japan. Its associated fauna included

Codonofusiella sp., *Kahlerina* sp., and *Yabeina globosa* (Yabe), this last being the main zone fossil of the Japanese *Yabeina* zone.

At the top of the Bell Canyon Formation the occurrence of *Paraboultonia splendens* (Subzone PG-6-D) is definitive. For a number of years some workers have assumed that *Paraboultonia* is a junior subjective synonym of *Lantschichites* Toumanskaya (1953). Indeed, Toumanskaya described one species as *L. splendens* (Skinner and Wilde). Now, however, Wilde and Rudine (this volume) have shown that the two genera are different, as discussed above, but that they commonly occur together. Toumanskaya's forms came from late Guadalupian equivalents of the Ussuri Region of Russia. Sheng (1963), Sosnina (1968), and Wang et al. (1981) also have described material from Kwangsi Province of South China, from Russia, and from the Qinghai-Xizang Plateau of China, respectively, all of which they identify as *Lantschichites*. Some of their material represents that genus, with its characteristic uncoiling, but some of the material also appears to represent true *Paraboultonia*.

Reichelina lamarensis (Subzone PG-6-C) is mentioned last for a reason. In the Guadalupe and Glass mountains, the subzone is clearly older than the *Paraboultonia splendens* subzone (Skinner and Wilde, 1954, 1955; Wilde, 1955; Tyrrell, 1962, 1969; Tyrrell et al., 1978; Wilde and Rudine, this volume). But the genus is long ranging, overlapping with numerous zones below and occurring commonly in the higher Dzhulfian Series in other parts of the world. Nestell (pers. comm.), who has been studying all occurrences of the genus, believes that *R. lamarensis* might not belong to the genus *Reichelina*. Be this as it may, *R. lamarensis* is one of the subzonal markers with which the late Guadalupian is partly defined. In fact, Tyrrell et al. (1978:85) stated that "*Reichelina* (referring to *R. lamarensis*) slightly overlaps the lower part of

the *Paraboultonia* zone, but otherwise is restricted to the middle Tansill and to all except the lower Lamar."

As regards overlapping ranges of zonal and subzonal markers, this represents the real world of fossil ranges. Furthermore, this also represents a continuum that helps to insure the absence of major breaks in a given sequence, which, in turn, strengthens the definition of series such as the Guadalupian.

Dzhulfian equivalent rocks younger than the Guadalupian, being evaporitic and unfossiliferous in the Delaware basin, must be defined in fossiliferous sequences in such areas as the Dzhulfa region of northern Iran and southern China. There, two main zones of fusulinids are fairly well known. The lower zone of *Palaeofusulina simplex* and *Dunbarula* (PD-1) and the upper zone of *Palaeofusulina sinensis* (PD-2) are not presently known anywhere in North America (Wilde, 1990). Continuity is assured, however, in the upper La Colorada beds at La Difunta, Mexico, where the ammonoids *Eoaraxoceras*, *Kingoceras*, and *Timorites* occur in the youngest Permian beds, precisely as they do in Iran in basal Dzhulfian beds (Glenister et al., 1991).

The close of the Permian was marked by major extinctions of many faunal and floral groups. The fusulinaceans appear to have succumbed to these extinctions also, for no survivors are known to have extended into the Triassic.

Acknowledgments

The author thanks Brian Glenister for recommending this paper for inclusion in the present volume, and for critically reading the manuscript. Thanks also are extended to Bruce Wardlaw, David Rohr, and Richard Grant for their critical reading of the manuscript. Rex Doescher converted the typescript to diskette.

Literature Cited

- Behnken, F.A.
1975. Leonardian and Guadalupian (Permian) Conodont Biostratigraphy in Western and Southwestern United States. *Journal of Paleontology*, 49(2):284-315, plates 1, 2.
- Boyd, D.W.
1958. Permian Sedimentary Facies, Central Guadalupe Mountains, New Mexico. *Bulletin of the New Mexico Bureau of Mines and Mineral Resources*, 49: 100 pages, 5 plates.
- Cooper, G.A., and R.E. Grant
1964. New Permian Stratigraphic Units in Glass Mountains, West Texas. *Bulletin of the American Association of Petroleum Geologists*, 48(9):1581-1588.
1966. Permian Rock Units in the Glass Mountains, West Texas. *United States Geological Survey Bulletin*, 1244-E:E1-E9, plates 1, 2.
1972. Permian Brachiopods of West Texas, I. *Smithsonian Contributions to Paleobiology*, 14:1-231, plates 1-23.
1974. Permian Brachiopods of West Texas, II. *Smithsonian Contributions to Paleobiology*, 15:233-793, plates 24-191.
1975. Permian Brachiopods of West Texas, III. *Smithsonian Contributions to Paleobiology*, 19:795-1921, plates 192-502.
1976a. Permian Brachiopods of West Texas, IV. *Smithsonian Contributions to Paleobiology*, 21:1923-2607, plates 503-662.
1976b. Permian Brachiopods of West Texas, V. *Smithsonian Contributions to Paleobiology*, 24:2609-3159, plates 663-788.
1977. Permian Brachiopods of West Texas, VI. *Smithsonian Contributions to Paleobiology*, 32:3161-3370.
- Cys, J.M.
1975. New Observations on the Stratigraphy of Key Permian Sections of West Texas. In Permian Exploration Boundaries, and Stratigraphy. *West Texas Geological Society and Permian Basin Section, Society of Economic Paleontologists and Mineralogists, Publication*, 75-65:22-42.

1978. Transitional Nature and Significance of the Castile-Bell Canyon Contact. *New Mexico Bureau of Mines and Mineral Resources, Circular*, 159:53-56.
- Dunbar, C.O.
1953. A Giant Permian Fusuline from Sonora. In G.A. Cooper, C.O. Dunbar, H. Duncan, A.K. Miller, and J.B. Knight, Permian Fauna at El Antimonio, Western Sonora, Mexico. *Smithsonian Miscellaneous Collections*, 119(2):14-19, plates 2, 3.
- Dunbar, C.O., and J.W. Skinner
1937. Permian Fusulinidae of Texas: The Geology of Texas, Part 2. *University of Texas Bulletin*, 3701:519-825, plates 42-81.
- Fekete, T.E., E.K. Franseen, and L.C. Pray
1986. Deposition and Erosion of the Grayburg Formation (Guadalupian, Permian) at the Shelf-to-Basin Margin, Western Escarpment, Guadalupe Mountains, Texas. In G.E. Moore and G.L. Wilde, editors, Lower and Middle Guadalupian Facies, Stratigraphy, and Reservoir Geometries, San Andres/Grayburg Formations, Guadalupe Mountains, New Mexico and Texas. *Society of Economic Paleontologists and Mineralogists, Permian Basin Section, Publication*, 86-25:69-81.
- Furnish, W.M.
1966. Ammonoids of the Upper Permian *Cyclolobus*-Zone. *Neues Jahrbuch für Geologie und Paläontologie, Abhandlungen*, 125: 265-296, plates 23-26.
1973. Permian Stage Names. In A. Logan and A.V. Hills, editors, The Permian and Triassic Systems and Their Mutual Boundary. *Canadian Society of Petroleum Geologists, Memoir*, 2:522-548.
- Furnish, W.M., B.F. Glenister, and L.L. Lambert
1991. Ammonoid Biostratigraphy of the Road Canyon Formation and Correlatives. [Abstract.] In B.R. Wardlaw, R.E. Grant, and D.M. Rohr, editors, *Proceedings of the Guadalupian Symposium, March 13-15, 1991, Sul Ross State University, Alpine, Texas*, page 11.
- Girty, G.H.
1902. The Upper Permian in Western Texas. *American Journal of Science*, series 4, 14:363-368.
1909 ("1908"). The Guadalupian Fauna. *United States Geological Survey Professional Paper*, 58: 651 pages, 31 plates. [Date on title page is 1908; actually published in 1909.]
- Glenister, B.F.
1991. The Guadalupian: A Proposed International Standard for Middle Permian Series. [Abstract.] *International Congress on the Permian System of the World, Program and Abstracts*, Perm, USSR-1991, pages A9-A10. Urals Branch, USSR Academy of Sciences; and Earth Sciences and Resources Institute, University of South Carolina.
- Glenister, B.F., D.W. Boyd, W.M. Furnish, R.E. Grant, M.T. Harris, H. Kozur, L.L. Lambert, W.W. Nassichuk, N.D. Newell, L.C. Pray, C. Spinoso, B.R. Wardlaw, G.L. Wilde, and T.E. Yancey
1992. The Guadalupian: Proposed International Standard for a Middle Permian Series. *International Geology Review*, 34(9):857-888.
- Glenister, B.F., C. Spinoso, W.M. Furnish, and Zhou Zuren
1991. Ammonoid Correlation of the Guadalupian/Dzhulfian Boundary. [Abstract.] In B.R. Wardlaw, R.E. Grant, and D.M. Rohr, editors, *Proceedings of the Guadalupian Symposium, March 13-15, 1991, Sul Ross State University, Alpine, Texas*, page 14.
- Grant, R.E., and B.R. Wardlaw
1984. Redefinition of Leonardian-Guadalupian Boundary in Regional Stratotype for the Permian of North America. *27th International Geological Congress, Moscow, USSR, Abstracts*, 1:58.
- Harris, M.T.
1982. Sedimentology of the Cutoff Formation (Permian), Western Guadalupe Mountains, West Texas and New Mexico. 186 pages. Unpublished master's thesis, University of Wisconsin, Madison, Wisconsin.
- 1988a. Sedimentology of the Cutoff Formation (Permian), Western Guadalupe Mountains, West Texas. In S.T. Reid, R.O. Bass, and P. Welch, editors, *Guadalupe Mountains Revisited, Texas and New Mexico. West Texas Geological Society, Publication*, 88-84:133-140.
- 1988b. Postscript on the Cutoff Formation: The Regional Perspective and Some Suggestions for Nomenclature. In S.T. Reid, R.O. Bass, and P. Welch, editors, *Guadalupe Mountains Revisited, Texas and New Mexico. West Texas Geological Society, Publication*, 88-84:141-142.
2000. Members for the Cutoff Formation, Western Escarpment of the Guadalupe Mountains, West Texas. In B.R. Wardlaw, R.E. Grant, and D.M. Rohr, editors, *The Guadalupian Symposium. Smithsonian Contributions to the Earth Sciences*, 32:101-120, 8 figures.
- Ishii, A., and T. Takahashi
1960. Fusulinids from the Upper Permian Ogamata Formation, Central Part of the Kwanto Massif, Japan. *Science Reports, Tokyo Kyoiku Daigaku*, section C, 66:205-216.
- King, P.B.
1931 ("1930"). The Geology of the Glass Mountains, Texas, Part I: Descriptive Geology. *University of Texas Bulletin*, 3038: 167 pages, 15 plates. [Date on title page is 1930; actually published in 1931.]
1948. Geology of the Southern Guadalupe Mountains, Texas. *United States Geological Survey Professional Paper*, 215: 183 pages, 23 plates.
- King, R.E.
1931 ("1930"). The Geology of the Glass Mountains, Texas, Part 2: Faunal Summary and Correlation of the Permian Formations with Description of Brachiopoda. *University of Texas Bulletin*, 3042: 245 pages, 44 plates. [Date on title page is 1930; actually published in 1931.]
- Lambert, L.L., D.J. Lehrman, and M.T. Harris
1991. Faunal Correlation of the Road Canyon and Cutoff Formations, West Texas, and Its Bearing on the Leonardian/Guadalupian Boundary. [Abstract.] In B.R. Wardlaw, R.E. Grant, and D.M. Rohr, editors, *Proceedings of the Guadalupian Symposium, March 13-15, 1991, Sul Ross State University, Alpine, Texas*, page 7.
2000. Correlation of the Road Canyon and Cutoff Formations, West Texas, and Its Relevance to Establishing an International Middle Permian (Guadalupian) Series. In B.R. Wardlaw, R.E. Grant, and D.M. Rohr, editors, *The Guadalupian Symposium. Smithsonian Contributions to the Earth Sciences*, 32:153-183, 11 figures, 4 plates, 3 tables.
- Miller, A.K., and W.M. Furnish
1940. Permian Ammonoids of the Guadalupe Mountain Region and Adjacent Areas. *Geological Society of America, Special Paper*, 26: 242 pages, 44 plates.
- Newell, N.D., J.K. Rigby, A.G. Fischer, A.J. Whiteman, J.E. Hickox, and J.S. Bradley
1953. *The Permian Reef Complex of the Guadalupe Mountains Region, Texas and New Mexico: A Study in Paleogeology*. 236 pages. San Francisco: W.H. Freeman and Company.
- Pray, L.C., and M. Esteban, editors
1977. Upper Guadalupian Facies, Permian Reef Complex, Guadalupe Mountains, New Mexico and West Texas: 1977 Field Conference Guidebook, volume 2. *Society of Economic Paleontologists and Mineralogists, Permian Basin Section, Publication*, 77-16: 194 pages.
- Ross, C.A.
1963. Fusulinids from the Word Formation (Permian), Glass Mountains, Texas. *Contributions from the Cushman Foundation for Foraminiferal Research*, 14(1):17-31, plates 3-5.
1964. Two Significant Fusulinid Genera from the Word Formation (Permian), Texas. *Journal of Paleontology*, 38(2):311-315, plate 50.

- Sada, K., and J.W. Skinner
1977. *Paradoxiella* from Japan. *Journal of Paleontology*, 51(2):421.
- Sarg, J.F.
1986. Facies and Stratigraphy of Upper San Andres Basin Margin and Lower Grayburg Inner Shelf. In G.E. Moore and G.L. Wilde, editors, Lower and Middle Guadalupian Facies, Stratigraphy, and Reservoir Geometries, San Andres/Grayburg Formations, Guadalupe Mountains, New Mexico and Texas. *Society of Economic Paleontologists and Mineralogists, Permian Basin Section, Publication*, 86-25:83-93.
- Sarg, J.F., and P.J. Lehmann
1986a. Lower-Middle Guadalupian Facies and Stratigraphy, San Andres/Grayburg Formations, Permian Basin, Guadalupe Mountains, New Mexico. In G.E. Moore and G.L. Wilde, editors, Lower and Middle Guadalupian Facies, Stratigraphy and Reservoir Geometries, San Andres/Grayburg Formations, Guadalupe Mountains, New Mexico and Texas. *Society of Economic Paleontologists and Mineralogists, Permian Basin Section, Publication*, 86-25:1-8.
1986b. Facies and Stratigraphy of Lower-Upper San Andres Shelf Crest and Outer Shelf and Lower Grayburg Inner Shelf. In G.E. Moore and G.L. Wilde, editors, Lower and Middle Guadalupian Facies, Stratigraphy, and Reservoir Geometries, San Andres/Grayburg Formations, Guadalupe Mountains, New Mexico and Texas. *Society of Economic Paleontologists and Mineralogists, Permian Basin Section, Publication*, 86-25:9-35.
- Sheng, J.C.
1963. Permian Fusulinids of Kwangsi, Kueichow, and Szechuan. *Palaeontologia Sinica*, 149, new series B(10): 247 pages, 35 plates. [In Chinese and English.]
- Skinner, J.W.
1971. The Fusulinid Genera *Polydiexodina* and *Skinnerina*. *University of Kansas Paleontological Contributions, Paper*, 57: 10 pages, 8 plates.
- Skinner, J.W., and G.L. Wilde
1954. The Fusulinid Subfamily *Boultoniinae*. *Journal of Paleontology*, 28(4):434-444, plates 42-45.
1955. New Fusulinids from the Permian of West Texas. *Journal of Paleontology*, 29(6):927-940, plates 89-95.
- Sosnina, M.L.
1968. New Species of Fossil Plants and Invertebrates of the USSR. *Ministry of Geology of the USSR, Nedra Press*, 2 (part 1):124-128, plate 31. [In Russian.]
- Toumanskaya, O.G.
1953. *O verhnepermiskikh fuzulinidakh yuzhno-Ussuriyskogo kraja* [Concerning Upper Permian Fusulinids in the Southern Ussuri Territory]. Pages 19-21, plates 10-12. Moscow: Trudy, Vsesoyuznogo Nauchno-Issledovatel'skogo Geologicheskogo Instituta (VSEGEI). [In Russian.]
- Tyrrell, W.W., Jr.
1962. Petrology and Stratigraphy of Near-Reef Tansill-Lamar Strata, Guadalupe Mountains, Texas and New Mexico. In Permian of the Central Guadalupe Mountains, Eddy County, New Mexico. *West Texas Geological Society, Roswell and Hobbs Geological Society Guidebook, Publication*, 62-48:59-69.
1969. Criteria Useful in Interpreting Environments of Unlike but Time-Equivalent Carbonate Units (Tansill-Capitan-Lamar), Capitan Reef Complex, West Texas and New Mexico. In G.M. Friedman, editor, *Depositional Environments in Carbonate Rocks: A Symposium. Society of Economic Paleontologists and Mineralogists, Special Publication*, 14:80-97.
- Tyrrell, W.W., Jr., D.H. Lokke, G.A. Sanderson, and G.J. Verville
1978. Late Guadalupian Correlations, Permian Reef Complex, West Texas and New Mexico. *New Mexico Bureau of Mines and Mineral Resources, Circular*, 159:84-85.
- Wang, Y., J.C. Sheng, and L. Zhang
1981. Fusulinids from Xizang, China. In *The Comprehensive Scientific Expedition of the Qinghai-Xizang Plateau*. 80 pages, 21 plates. Beijing: Palaeontology of Xizang, Science Press, Book 111.
- Wardlaw, B.R.
1991. Conodont Biostratigraphy and Depositional Setting of the Guadalupian Rocks of the Glass and Del Norte Mountains. [Abstract.] In B.R. Wardlaw, R.E. Grant, and D.M. Rohr, editors, *Proceedings of the Guadalupian Symposium, March 13-15, 1991, Sul Ross State University, Alpine, Texas*, page 17.
- Wardlaw, B.R., and R.E. Grant
1987. Conodont Biostratigraphy of the Cathedral Mountain and Road Canyon Formations, Glass Mountains, West Texas. In D. Cromwell and L.J. Mazzullo, editors, *The Leonardian Facies in W. Texas and S.E. New Mexico and Guidebook to the Glass Mountains, West Texas. Society of Economic Paleontologists and Mineralogists, Permian Basin Section, Publication*, 87-27:63-66.
1990. Conodont Biostratigraphy of the Permian Road Canyon Formation, Glass Mountains, Texas. *United States Geological Survey Bulletin*, 1895-A:A1-A18, plates 1-4.
- Wilde, G.L.
1955. Permian Fusulinids of the Guadalupe Mountains. In Permian Field Conference, October 1955. *Society of Economic Paleontologists and Mineralogists, Permian Basin Section, Publication*, 55-1:59-62.
1975. Fusulinid-Defined Permian Stages. In J.M. Cys and D.F. Toomey, editors, *Permian Exploration, Boundaries, and Stratigraphy. Society of Economic Paleontologists and Mineralogists, West Texas Geological Society and Permian Basin Section, Publication*, 75-65:67-83.
1986a. Stratigraphic Relationship of the San Andres and Cutoff Formations, Northern Guadalupe Mountains, New Mexico and Texas. In G.E. Moore and G.L. Wilde, editors, Lower and Middle Guadalupian Facies, Stratigraphy, and Reservoir Geometries, San Andres/Grayburg Formations, Guadalupe Mountains, New Mexico and Texas. *Society of Economic Paleontologists and Mineralogists, Permian Basin Section, Publication*, 86-25:49-63, plates 1-5.
1986b. An Important Occurrence of Early Guadalupian (Roadian) Fusulinids from the Cutoff Formation, Western Guadalupe Mountains, Texas. In G.E. Moore and G.L. Wilde, editors, Lower and Middle Guadalupian Facies, Stratigraphy and Reservoir Geometries, San Andres/Grayburg Formations, Guadalupe Mountains, New Mexico and Texas. *Society of Economic Paleontologists and Mineralogists, Permian Basin Section, Publication*, 86-25:65-68, plate 1.
1988. Fusulinids of the Roadian Stage. In S.T. Reid, R.O. Bass, and P. Welch, editors, *Guadalupe Mountains Revisited, Texas and New Mexico. West Texas Geological Society, Publication*, 88-84:143-147, plates 1, 2 [no text].
1990. Practical Fusulinid Zonation: The Species Concept; with Permian Basin Emphasis. *West Texas Geological Society, Bulletin*, 29(7):5-34.
- Wilde, G.L., and S.F. Rudine
2000. Late Guadalupian Biostratigraphy and Fusulinid Faunas, Altuda Formation, Brewster County, Texas. In B.R. Wardlaw, R.E. Grant, and D.M. Rohr, editors, *The Guadalupian Symposium. Smithsonian Contributions to the Earth Sciences*, 32:343-371, 3 figures, 9 plates.
- Wilde, G.L., and R.G. Todd
1968. Guadalupian Biostratigraphic Relationships and Sedimentation in the Apache Mountain Region, West Texas. In B.A. Silver, editor, *Guadalupian Facies, Apache Mountains Area, West Texas. Society of Economic Paleontologists and Mineralogists, Permian Basin Section, Publication*, 68-11:10-31.

5. Members for the Cutoff Formation, Western Escarpment of the Guadalupe Mountains, West Texas

Mark T. Harris

ABSTRACT

The boundary between the Leonardian and Guadalupian Stages (North American usage) occurs within the Cutoff Formation, which crops out along the western escarpment of the Guadalupe Mountains, West Texas. The internal stratigraphy within the Cutoff Formation is complex, and to date only informal schemes have been proposed. Three members are defined, which in ascending order are the Shumard Member, the El Centro Member, and the Williams Ranch Member. Type sections for these members are all located in the southern part of the western escarpment within the Guadalupe Mountains National Park.

These members are proposed to reinforce the revisions in the stratigraphic framework for these beds since the pioneering work of King (1942, 1948) and Newell et al. (1953). These members can be traced throughout the western escarpment region and are stratigraphically distinct units separated by unconformities or lithologic changes. The proposed members probably represent the extent to which previous faunal collections can be located. These collections are important because these strata are a candidate for an international boundary stratotype (Glenister et al., 1991; Glenister, 1991). Three measured sections of basinal Cutoff Formation are included as a framework for future paleontological collections.

Introduction

The strata within the Cutoff Formation comprise the boundary beds between the Leonardian and Guadalupian stages (North American usage). The stratigraphic position of Cutoff faunas relates directly to the definition of this boundary. Recent

proposals to designate this section as a candidate for an international boundary stratotype were presented to the Subcommittee on Permian Stratigraphy of the International Commission on Stratigraphy (Glenister, 1991). This paper proposes formal lithostratigraphic members for these strata, which will replace the earlier, informal subdivisions.

General Nomenclature Review

The Cutoff Formation crops out in various ranges located around the edges of the Permian Delaware basin in West Texas. The type section is located at Cutoff Mountain in the Guadalupe Mountains (King, 1942, 1948), and equivalent strata occur in the northern Guadalupe Mountains (Boyd, 1958; Hayes, 1959), Sierra Diablo (King, 1965), Wylie Mountains (Hay-Roe, 1957), and Apache Mountains (Wood, 1968) (Figure 5-1).

King (1942, 1948) established the basic stratigraphic nomenclature for the type area in the Guadalupe Mountains, designating the Cutoff Shale as a member of the Bone Spring Limestone (Figure 5-2). At the Cutoff type section (Cutoff Mountain) and southward to Shumard Canyon, the dark gray color and shale content of the basal Cutoff strata contrast with the underlying light gray dolomites of the Victorio Peak. However, to the south the Victorio Peak changes facies into the black limestone beds of the Bone Spring Limestone, and King (1942, 1948) did not separate out the Cutoff Shale Member.

Newell et al. (1953) recognized the basinal shaly equivalent to the shale at the base of the Cutoff and adjusted the terminology accordingly. They also realized that the overlying basinal limestones ("Upper Bone Spring Limestone") equate to the limestone in the upper part of the Cutoff Shale shelf section. King (1965) raised the Cutoff to formational status as the Cutoff Shale, which Harris (1988a) suggested be redefined as the Cutoff Formation (without change of formation rank, type section, or boundaries) based upon the lithological predominance of limestone (60%–70%) over shale (30%–40%).

Mark T. Harris, Department of Geosciences, University of Wisconsin-Milwaukee, Milwaukee, Wisconsin 53201.

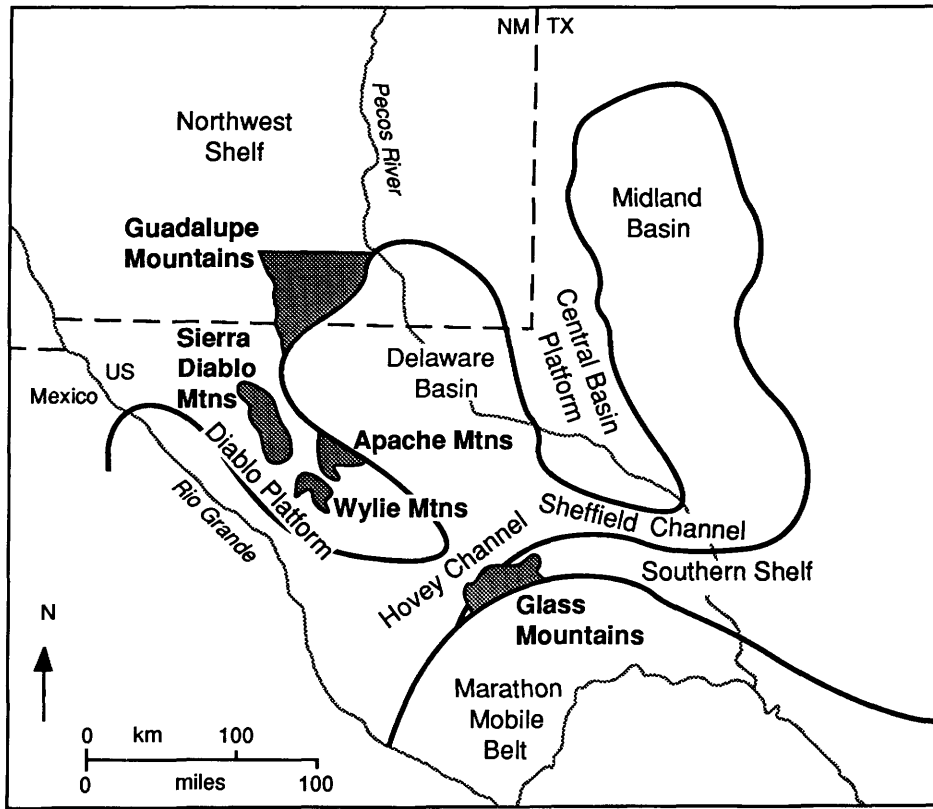


FIGURE 5-1.—Location of the Guadalupe Mountains and other ranges mentioned in the text relative to Permian paleogeography. Modified from King (1948).

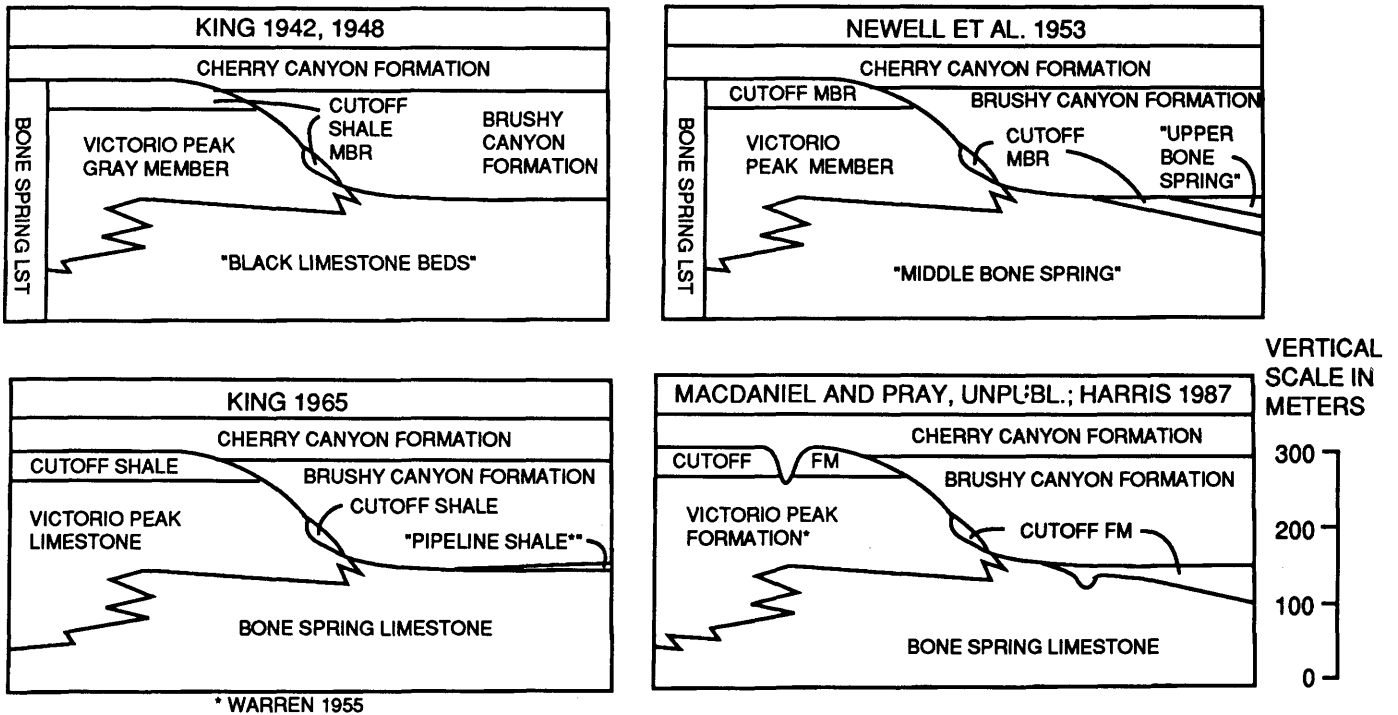


FIGURE 5-2.—Nomenclature changes in the Leonardian-Guadalupean boundary strata in the Guadalupe Mountains.

King (1948) recognized informal "upper" and "lower" Cutoff units in the slope exposures (Shumard Canyon). Harris (1982, 1988a) extended these to the shelf and basin areas and introduced a succession of five informal "correlation units," which clarified the shelf-to-basin physical correlation of the Cutoff strata (Figure 5-3). In the basin, the lowermost correlation unit (#1) is separated from the lithologically similar underlying Bone Spring Limestone by an unconformity; therefore, Harris (1988b) suggested that the basin part of correlation unit 1 be included within the Bone Spring Limestone. That suggestion is not being used in this proposal. Instead, the unconformity is used to define the base of the Cutoff Formation in all areas.

The transition of Cutoff strata into the shallow-water shelf facies of the San Andres Formation in the northern Guadalupe Mountains was mapped by Boyd (1958) and was subsequently interpreted by Sarg and Lehmann (1986a) in terms of sequence stratigraphy.

Due to Permian erosion and syndepositional slope processes, the Cutoff Formation is discontinuous along the outcrop belt. It overlies the Leonardian carbonate bank and basin deposits of the Victorio Peak-Bone Spring Limestone (Figures 5-4, 5-5). Prior to Cutoff deposition, erosion steepened the Leonardian bank shelf-to-basin profile to approximately 20° and formed a paleoslope with a relief of 300 m (McDaniel and Pray, 1968; Pray, 1971; Harms and Pray, 1974; Pray et al., 1980; Harris, 1982, 1988a; Kirkby, 1988). Post-Cutoff erosion locally removed the Cutoff strata along the paleoslope, making correlation of the Cutoff from shelf to basin problematical (King, 1948; Wilde and Todd, 1968) until recent work (Harris, 1982, 1988a). Preserved strata occur in three distinct areas, as defined by the pre-Cutoff shelf profile (Figure 5-5): (1) a flat shelf (0°-1° dip), (2) a steeply dipping slope (5°-20°), and (3) a low relief basin that flattens out to a low angle (1°-5°).

Proposed Members

The three members formally proposed below subdivide the Cutoff Formation into units that are unambiguously recognizable in slope and basinal areas. Figure 5-4 is a geological map of the Cutoff Formation and adjacent formations in the slope and basin margin areas. The locations of the type sections of each member are indicated in Figure 5-6. Lithotype designations follows the Embry and Klován (1971) modification of Dunham (1963). Bedding terminology follows Ingram (1954). The rock color follows the GSA Rock-Color Chart (Goddard et al., 1970).

SHUMARD MEMBER

SELECTION AND DERIVATION OF NAME.—The geographic name derives from Shumard Canyon, where the characteristic features of the member are apparent. This canyon is the area where the member was first recognized by King (1948) as an informal unit.

STRATOTYPE.—The type section for the Shumard Member is located on the north side of the south fork of Shumard Canyon (western escarpment of the Guadalupe Mountains) (Figures 5-6, 5-7; Appendix 5-1, section A).

DESCRIPTION.—The total thickness of the Shumard Member measured at the type section is 49 m. The predominant lithology is black to dark gray (N1 to N3), medium-bedded, cherty lime mudstone. Black chert is abundant (5%-15%), occurring as thin (2 cm) seams and nodules in nearly every bed. Thin laminations are common. In the type section, three additional lithologies occur below the lime mudstone. From the base upward, these are (1) 1-2 m of thinly-laminated, very fine-grained, quartz sandstone, (2) intraclastic rudstone lenses up to 2 m thick, and (3) 1 m of shale.

BOUNDARIES.—The Shumard Member is bounded above

King 1942, 1948	Newell et al. 1953	Harris 1987, 1988	Harris in press		
Brushy Canyon Fm.	Brushy Canyon Fm.	Brushy Canyon Fm.	Brushy Canyon Fm.		
Bone Spring Limestone	Bone Spring Lst.	Cutoff Formation	Cutoff Formation		
	"Upper Bone Spring"			"upper unit" correlation unit 5	Williams Ranch Member
	Cutoff Member			corr. units 4 3 2	El Centro Member
	"Middle Bone Spring"	"lower unit" corr. unit 1	Shumard Member		
		Bone Spring Limestone	Bone Spring Limestone		

FIGURE 5-3.—History of nomenclature for basin Cutoff strata in the Guadalupe Mountains from Bone Canyon to the south. Beds assigned to the Cutoff were first identified by Newell et al., 1953. (NOTES: 1. King (1942, 1948) recognized informal upper and lower units for his Cutoff member for slope outcrops (Shumard Canyon). He suggested that the basal beds of the Brushy Canyon may be Cutoff basinal equivalents. 2. The Pipeline Shale of Warren (1955) is a basinward shale at the base of the Brushy Canyon Formation that pinches out south of Bone Canyon. 3. All correlation units of Harris (1988a,b) are informal stratigraphic units.)

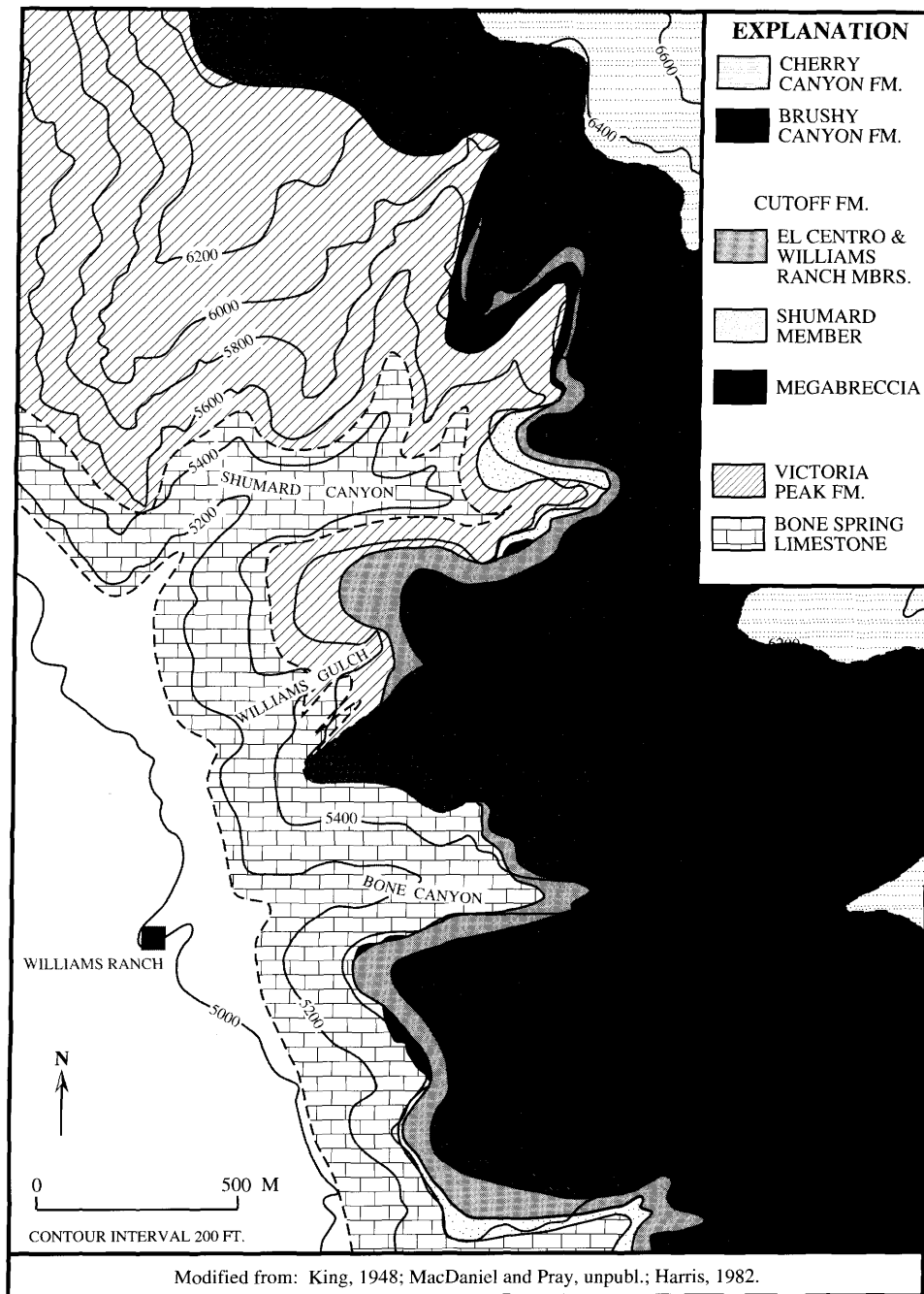


FIGURE 5-4.—Geologic map of the Bone Canyon-Shumard Canyon area in the western Guadalupe Mountains. This area is the lower slope environment during Cutoff Formation deposition (compare with Figure 5-5).

and below by unconformities. The lower boundary is the pre-Cutoff unconformity, which truncated the Victoria Peak and Bone Spring strata. The Shumard Member stratotype occurs within a 40 m deep channel cut into the Victoria Peak Limestone. The upper boundary occurs at an intra-Cutoff unconformity, which truncated the Shumard Member strata. The contact with the overlying El Centro Member is marked by

an abrupt lithological change. These unconformities bound the Shumard Member throughout the western escarpment outcrops.

HISTORICAL BACKGROUND.—These strata were recognized by King (1948) as a distinct unit within the Cutoff based upon their lithology and bounding unconformities (see King, 1948, pl. 12B). He gave them the informal designation of the Cutoff

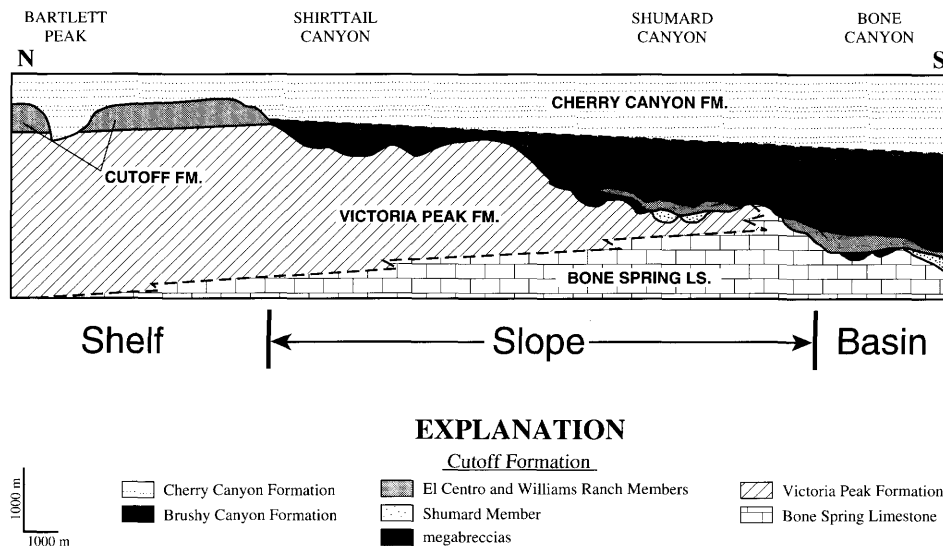


FIGURE 5-5.—North-south cross section of the Cutoff Formation as seen along the western escarpment of the Guadalupe Mountains. Note that the vertical exaggeration is $\times 2$.

“lower unit.” Subsequently, Harris (1982, 1988a) informally termed them “correlation unit 1” while retaining the informal “lower Cutoff” nomenclature.

DISTRIBUTION AND THICKNESS.—In Shumard Canyon, the Shumard Member is limited to the channel fill that is bisected by the south fork of the canyon. The type section records the thickest expression of the unit in this area. The similar section, which occurs on the opposite canyon wall, includes a megabreccia lens at the top of the member. These strata fill the extension of the channel occupied by the stratotype.

The member occurs in the Cutoff Formation type section at Cutoff Mountain where it varies between 1.6 and 5 m in thickness. South of Cutoff Mountain, this member is not present in the western escarpment between Bartlett Peak and Shirrtail Canyon. This distribution is interpreted to be the result of truncation along the unconformity at the top of the member. Laminations are faint or not present in this shelf setting. A low-angle truncation surface separates the Shumard Member from the underlying Victoria Peak Limestone. Where the Shumard Member is absent, the pre-Cutoff unconformity and the intra-Cutoff unconformity are merged.

To the south of Bone Canyon, a black cherty limestone below the El Centro Member is interpreted as the Shumard Member (Figure 5-8). The unconformity at the base of the Shumard Member, which separates it from the underlying Bone Spring Limestone, can be traced and mapped in the field to the limit of the outcrop (Figure 5-4). The Shumard Member (as interpreted by tracing this unconformity) is approximately 33.5 m thick below the El Centro Member type section. This section of the Shumard Member contains thin skeletal and intraclastic rudstone lenses, chert bands, and small (2 m) folds. Thin laminations mark the lower 17 m. Three different lamination

styles occur in the overlying beds: well-laminated textures, laminations disrupted by horizontal burrows, and nonlaminated textures. The upper boundary of the Shumard Member is placed at an obvious truncation surface that is interpreted as the intra-Cutoff unconformity. A reference section for the Shumard Member in the basin area is located in the first canyon south of Bone Canyon (0.85 km south of Bone Canyon) along the western escarpment of the Guadalupe Mountains (Appendix 5-1, section B).

GEOLOGICAL AGE.—The Shumard Member is probably latest Leonardian (Artinskian), based upon paleontological studies in progress (Lambert, pers. comm., 1991; Lambert et al., this volume).

LATERAL EXTENT AND CORRELATIONS.—The Shumard Member is recognizable along the western escarpment of the Guadalupe Mountains at Cutoff Mountain (shelf area), Shumard Canyon (slope area, including the type section), and south of Bone Canyon to its disappearance into the subsurface (basin area). Correlation of this member beyond the western escarpment is uncertain because of the lack of faunal studies of this strata.

EL CENTRO MEMBER

SELECTION AND DERIVATION OF NAME.—The geographic name derives from El Centro Draw, an arroyo south of Bone Canyon. The northeastern part of the drainage includes lithologies characteristic of the member.

STRATOTYPE.—The type section of the El Centro Member is located in the first canyon south of Bone Canyon (0.85 km south of Bone Canyon) along the western escarpment of the Guadalupe Mountains (Figure 5-6; Appendix 5-1, section B).

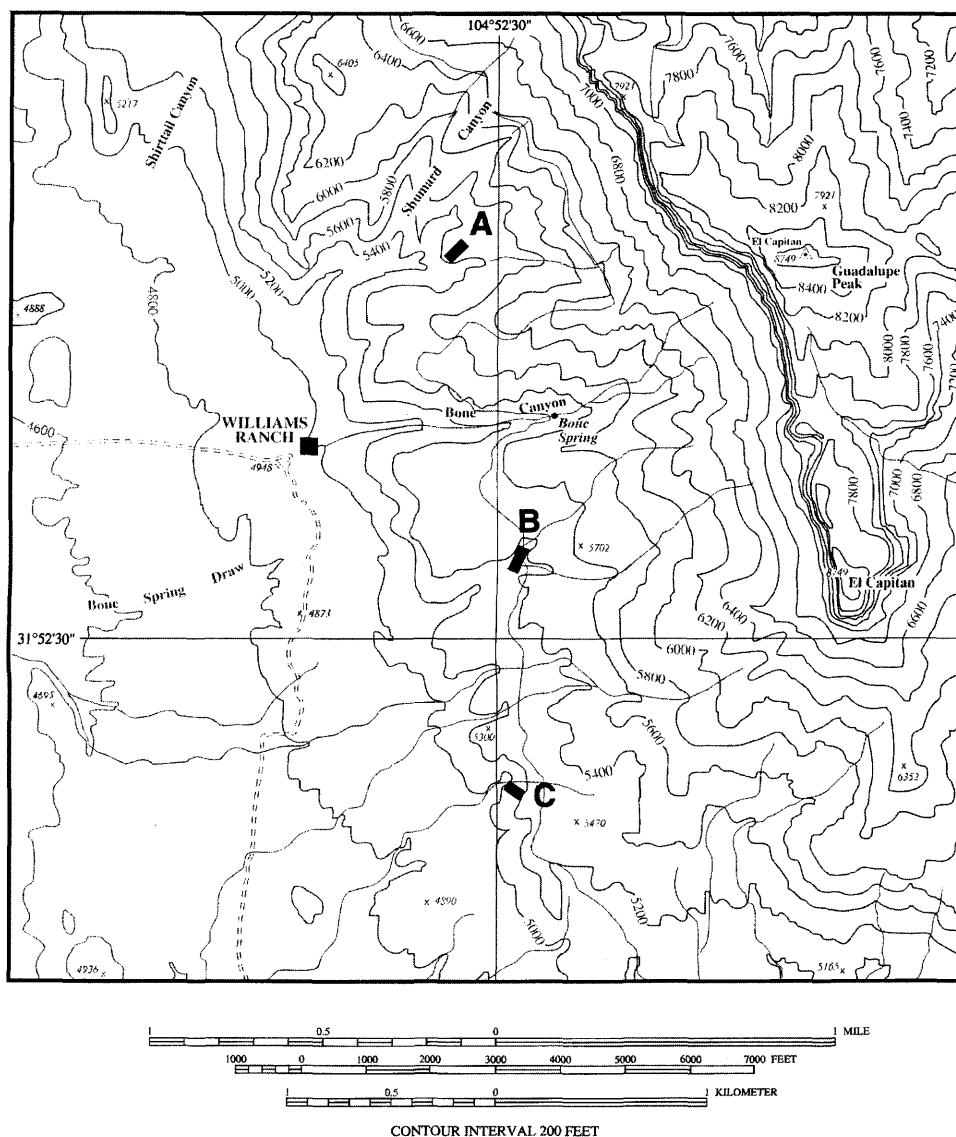


FIGURE 5-6.—Location of the type sections for the proposed members of the Cutoff Formation. Section A is the stratotype for the Shumard Member. Section B is the stratotype for the El Centro Member and the Williams Ranch Member. Section B is also a reference section for the Shumard Member, and Section C is a reference section for the El Centro Member and the Williams Ranch Member. The dark lines delineate longitude 104°52'30" and latitude 31°52'30", which are the borders of the four 7½' quadrangle topographic maps that make up this composite, namely, PX Flat (northwest), Patterson Hills (southwest), Guadalupe Peak (northeast), and Guadalupe Pass (southeast).

DESCRIPTION.—The total thickness of the El Centro Member measured at the type section is 20.5 m. It consists of two lithologies: interbedded lime mudstone–shale and medium-bedded lime mudstone.

Interbedded thinly-laminated lime mudstone, shale, and siltstone are characteristic of the El Centro Member. The lime mudstone and shale are both dark gray (N3) to black (N1) to dark brown (10YR 4/3). They locally alternate in centimeter-thick intervals, but typically one lithology occurs vertically for several meters. The lithologies intergrade, as the lime mudstone

is argillaceous and the shale may be calcareous. They are virtually identical in field appearance and can only be distinguished by testing with dilute hydrochloric acid. The shale contains carbonate concretions (up to 0.3 m across) that formed prior to the bulk of shale compaction. Scattered thin to very thin beds of dark brown to tan, thinly laminated siltstone occur within the interbedded lime mudstone–shale lithology.

A pronounced interval of dark gray (N2 to N4), medium-bedded, lime mudstone occurs within the interbedded lime mudstone–shale in most locations. The lime mudstone lacks

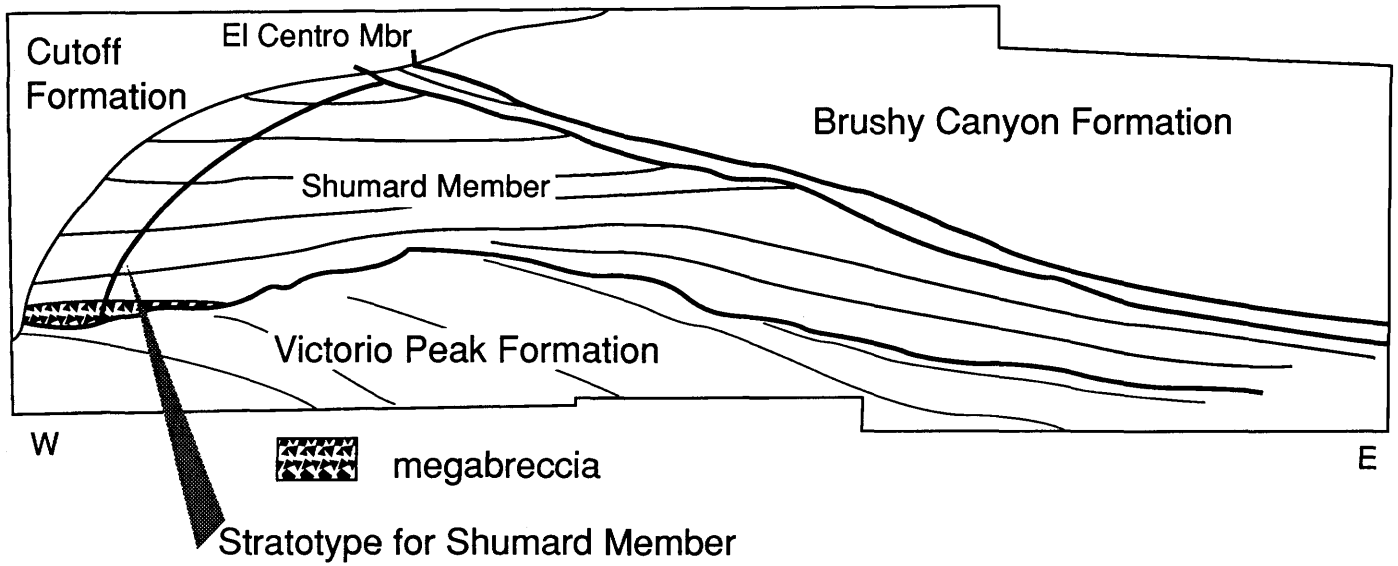


FIGURE 5-7.—Location of the Shumard Member stratotype in the north wall of south Shumard Canyon.

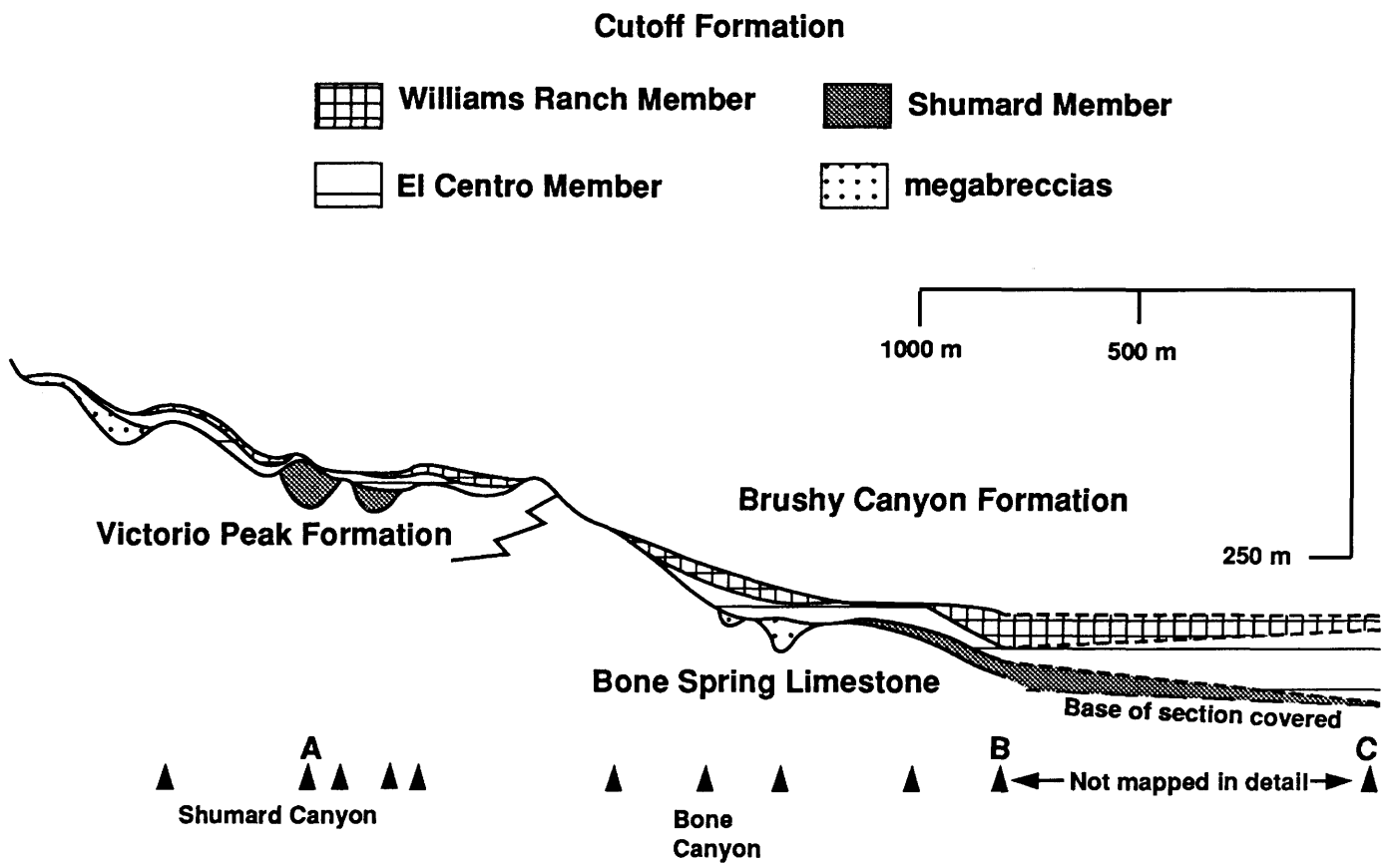


FIGURE 5-8.—Cross section of the Cutoff Formation (western Guadalupe Mountains) in the slope and basin areas (right side of Figure 5-5), illustrating the thickness variations in the proposed members. Measured section locations are indicated by arrows along the base of the diagram. Thickness and paleotopography are properly scaled. Vertical exaggeration is $\times 2.5$.

chert, in contrast to the Shumard Member, and is similar to the limestones that make up the overlying Williams Ranch Member. This lime mudstone interval comprises about one-half of the member (11 m of the 20.5 m total) in the El Centro type section. This interval serves as a useful marker horizon within the member (see the section below on regional aspects).

BOUNDARIES.—The lower boundary of the El Centro Member is placed along an intra-Cutoff unconformity that truncates the underlying Shumard Member. An abrupt shift from cherty lime mudstone to interbedded lime mudstone–shale marks this boundary in the El Centro type section. The El Centro Member unconformably overlies the cherty limestones of the Bone Spring Limestone where the Shumard Member is absent.

The upper boundary with the overlying Williams Ranch Member is conformable except where minor channel scours are present, as in the type section. Locally within Shumard Canyon the Williams Ranch Member is missing and the El Centro Member is unconformably overlain by the sandstones, siltstones, and conglomerates of the Brushy Canyon Formation.

HISTORICAL BACKGROUND.—The interbedded lime mudstone–shale of the El Centro Member are the strata that resulted in the establishment of the Cutoff Shaly Member of the Bone Spring Limestone by King (1942, 1948). He did not recognize the basin equivalent of these shaly beds and included the strata of the type section in the Bone Spring Limestone. Newell et al. (1953) recognized the basin equivalents, which they termed the Cutoff Member of the Bone Spring Limestone. King's (1965) elevation of the Cutoff to formational rank, as the Cutoff Shale, reflected his focus on these shaly beds. Harris (1982, 1988a) informally named the vertical succession of interbedded lime mudstone–shale, lime mudstone, interbedded lime mudstone–shale as “correlation units 2, 3 and 4,” respectively.

DISTRIBUTION AND THICKNESS.—The El Centro Member is thin to absent in the slope sections but is present in all shelf and basin sections. It is always the last part of the Cutoff strata truncated by the post-Cutoff unconformity.

The vertical lutite triplet of interbedded lime mudstone–shale with middle lime mudstone beds is recognizable across the depositional profile. All three units thicken basinward from the El Centro type section. The member is 78 m thick in a section 0.85 km to the south, and the middle limestone unit is 34 m thick. In contrast, the lime mudstone unit thins rapidly to the north; 0.5 km north (just south of the mouth of Bone Canyon) it thins to 5.5 m thick, with a total El Centro Member thickness of 19 m. The lime mudstone unit pinches out in the south wall of Bone Canyon where the entire member is about 20 m thick. The entire member disappears in the north wall of Bone Canyon due to onlap of the pre-Cutoff surface and truncation along the post-Cutoff surface. The channel-filling megabreccias, which occur at the base of the El Centro Member in the south wall of Bone Canyon (Pray and Stehli, 1963), are tentatively assigned to the El Centro Member.

In the slope area (Shumard Canyon) the Williams Ranch Member is thinned or absent due to truncation along the post-Cutoff unconformity (Figure 5-8). However, the El Centro lutite triplet can be traced across these exposures. It is 13–18 m thick where complete, but it is irregularly thinned from the top. The large megabreccia sheet, which occurs below the interbedded lime mudstone–shale in northern Shumard Canyon (Figures 5-4, 5-5, 5-8), is assigned to the El Centro Member.

A section measured southwest of Bartlett Peak contains a shelf section (north of Shirttail Canyon) of the El Centro Member that is about 43.5 m thick. The lime mudstone interval expands to 26 m, a similar proportion as in the basal outcrops. In the Cutoff Formation's type section, the member is 34.5 m thick, but its unique middle lime mudstone cannot be recognized because the approximate interval of the lime mudstone unit is more argillaceous than the Bartlett Peak section.

GEOLOGICAL AGE.—The El Centro Member is probably latest Leonardian (Artinskian) to earliest Guadalupian, based upon paleontological studies in progress (Lambert, pers. comm., 1991; Lambert et al., this volume).

LATERAL EXTENT AND CORRELATIONS.—The El Centro Member is the most widespread of the Cutoff members along the western escarpment of the Guadalupe Mountains. It is roughly equivalent to the lower part of the Road Canyon Formation of the Glass Mountains, based upon paleontological studies (Lambert et al., this volume). Sarg and Lehmann (1986a) interpreted these strata as the equivalent of the lower San Andres Formation of the northern Guadalupe Mountains.

WILLIAMS RANCH MEMBER

SELECTION AND DERIVATION OF NAME.—The geographic name derives from the Williams Ranch House located at the mouth of Bone Canyon. The lime mudstone outcrops that form the low hills, which extend from Bone Canyon south to U.S. 62/180, contain typical exposures of this member.

STRATOTYPE.—The type section of the Williams Ranch Member is located in the north fork of the first canyon south of Bone Canyon (0.85 km south of Bone Canyon) along the western escarpment of the Guadalupe Mountains (Figure 5-6; Appendix 5-1, section B).

DESCRIPTION.—The total thickness of the Williams Ranch Member measured at the type section is 13 m. Dark gray (N2 to N4), medium-bedded lime mudstone predominates in the type section. The beds are defined by thin shaly partings, and individual bed thickness varies due to minor (cm scale) scours at the top of beds. A well-laminated texture predominates in the type section and other basinal areas, although burrows disrupt laminations in some beds. Faint laminations and nonlaminated textures are more common in a shelfward direction (to the north). Small (< 1 m thick) intraclastic and skeletal rudstone lenses occur in the Williams Ranch Member, and these

typically occur as small channel fills. An intraclastic rudstone marks the base of the member in the type section.

BOUNDARIES.—The lower boundary is conformable with the El Centro Member except where small channel scours occur along the contact. In the type section, the boundary is abrupt. Generally, the lower boundary is placed at the top of the uppermost bed of the interbedded lime mudstone–shale that is characteristic of the El Centro Member.

The upper boundary is placed at the post-Cutoff unconformity. The overlying Brushy Canyon Formation is marked by sandstone, siltstone, conglomerates containing sandstone within the matrix or as clasts (as in the type section), or shale (basinward sections).

HISTORICAL BACKGROUND.—King (1948) included these strata within his Bone Spring Limestone in the area from Bone Canyon to the south. Newell et al. (1953) termed these strata the “Upper Bone Spring Limestone.” Harris (1982, 1987) informally termed them “correlation unit 5” within an upper Cutoff unit.

DISTRIBUTION AND THICKNESS.—The Williams Ranch Member varies in thickness due to truncation along the post-Cutoff unconformity (Figure 5-8). The maximum preserved thickness occurs to the south in the basinmost sections (13 m in the Williams Ranch type section expands to 16 m in a section 0.85 km to the south) and to the north in shelf sections (approximately 43 m in the Cutoff type section). In the slope area, the Williams Ranch Member is thinned or entirely absent due to truncation along the post-Cutoff unconformity. A ammonoid-rich zone at the top of the member occurs in the Williams Ranch type section (Lambert, pers. comm., 1991) and in the U.S. 62/180 highway cuts to the south (Spinosa et al., 1975; Lambert, pers. comm., 1991). The persistence of this faunal occurrence may indicate that erosion of the Williams Ranch Member was minor southward from its type section.

The lithology and definition of the lower boundary of the member varies along the depositional profile. The dark gray color predominates in basin and slope areas (from Shumard Canyon south). Laminated texture increases basinward. The lower contact is relatively sharp and unambiguous; however, the lithologies within the Williams Ranch Member change in the shelf section (Cutoff Mountain to the pinchout north of Shirttail Canyon). Here, the dark gray lime mudstone passes upwards into medium gray (N5 to N6), medium-bedded lime mudstone. Southwest of Bartlett Peak the Williams Ranch Member is 17–18 m thick; the upper 4 m consist of the medium gray lime mudstone. At Cutoff Mountain, the member is approximately 43 m thick. Only the lower 4.5 meters are dark gray lime mudstone; the remainder is medium gray lime mudstone with interbedded beds of graded lime packstone to wackestone (interpreted as storm deposits). In these shelf sections, white chert nodules locally occur in the uppermost beds of the Williams Ranch Member.

GEOLOGICAL AGE.—The Williams Ranch Member is proba-

bly earliest Guadalupian, based upon paleontological studies in progress (Lambert, pers. comm., 1991; Lambert et al., this volume) and the fusulinid identification of Wilde (1986b).

LATERAL EXTENT AND CORRELATIONS.—The Williams Ranch Member occurs widely in the western escarpment of the Guadalupe Mountains, although in the slope areas it is thinned and locally truncated by the post-Cutoff unconformity. The Williams Ranch Member is equivalent, at least in part, to the upper Road Canyon Formation in the Glass Mountains (Lambert et al., this volume) and the upper San Andres Formation of the northern Guadalupe Mountains (Sarg and Lehmann, 1986a; Wilde, 1986a,b).

Discussion

The revised Cutoff stratigraphy for the western escarpment of the Guadalupe Mountains is illustrated by Figure 5-8. The interrelations of the members and the positions of the unconformities are shown.

Formal members for the Cutoff Formation are proposed for three principle reasons. First, use of this nomenclature will help reinforce the revisions made in the stratigraphic framework for these beds since the pioneering work of King (1942, 1948) and Newell et al. (1953). Clarifying the stratigraphic succession will allow better understanding of the overall geologic history.

Second, these members can be traced throughout the western escarpment region and are stratigraphically distinct units separated by unconformities or lithologic changes. Subsurface differentiation of the Shumard Member in well-log sections will rely upon recognition of the pre-Cutoff unconformity. The overlying El Centro and Williams Ranch members are sufficiently thick and lithologically distinct for subsurface recognition.

Third, this level of stratigraphic detail probably represents the extent to which previous faunal collections can be located. The black limestone hills south of El Capitan are largely formed by the Williams Ranch Member to which the “Upper Bone Spring” collections of Newell et al. (1953) should be related. Many of King’s (1948) Bone Spring Limestone faunal collections are from the member as well. Similarly, faunal collections from shaly Cutoff strata are probably from the El Centro Member. The proper placement of the prior faunal collections will be important if these strata become an international boundary stratotype (Glenister, 1991).

A reference section for the El Centro Member and Williams Ranch Member is located near the southern limit of complete exposures of the El Centro Member (Appendix 5-1, section C). To the south, the base of the El Centro is covered. The hills of black lime mudstone, which extend to U.S. 62/180, predominantly consist of the overlying Williams Ranch Member. This reference section is included as a framework for future paleontological collections at the thickest and most basinward outcrop of the complete El Centro–Williams Ranch section.

Acknowledgments

The author wishes to thank Lloyd C. Pray, Lance L. Lambert, and Nancy J. Harris for their advice and patience. Richard A. Paull considerably improved this manuscript. The author also

wants to thank the attendees at the 1991 Guadalupian Symposium, particularly Bruce R. Wardlaw and Garner L. Wilde, for their encouragement to finally name these units. Reviews by Richard E. Grant and Bruce R. Wardlaw helped clarify some points.

Appendix 5-1: Stratigraphic Sections

Format

The stratigraphic nomenclature uses the members proposed herein. The informal "correlation units" of Harris (1982, 1988a) are provided for convenience and reference to earlier work.

The scale of the graphic log is presented in both feet and meters. The profile represents the weathering profile noted in the field.

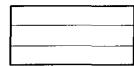
The lithology presentation involves three columns. The predominant lithology is either carbonate (limestone for all Cutoff sections shown) or noncarbonate (siliceous shales and sandstones). Both carbonate and siliciclastic lithologies are described using Dunham (1962) depositional texture terminology; therefore, in this column, grain-supported sandstones (arenites) are graphed as packstones or grainstones (dependent upon mud content), shales are graphed as mudstones, and megabreccias with mud-filled intraclastic spaces are graphed as packstone. The maximum grain size completes the description by illustrating the maximum obvious grain size. This log depicts the size of the coarsest common grains; a single large grain is ignored. For example, a single large fossil in several feet of lime mudstone would not be shown, but silt distributed throughout would appear. Used together, these three columns describe the basic lithology.

The final columns indicate the color and darkness of the rock (increasing to the right).

KEY FOR GRAPHIC COLUMN OF STRATIGRAPHIC SECTIONS



Interbedded lime mudstone-shale



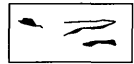
Medium-bedded limestone



Intraclastic rudstone or megabreccia



Sandstone

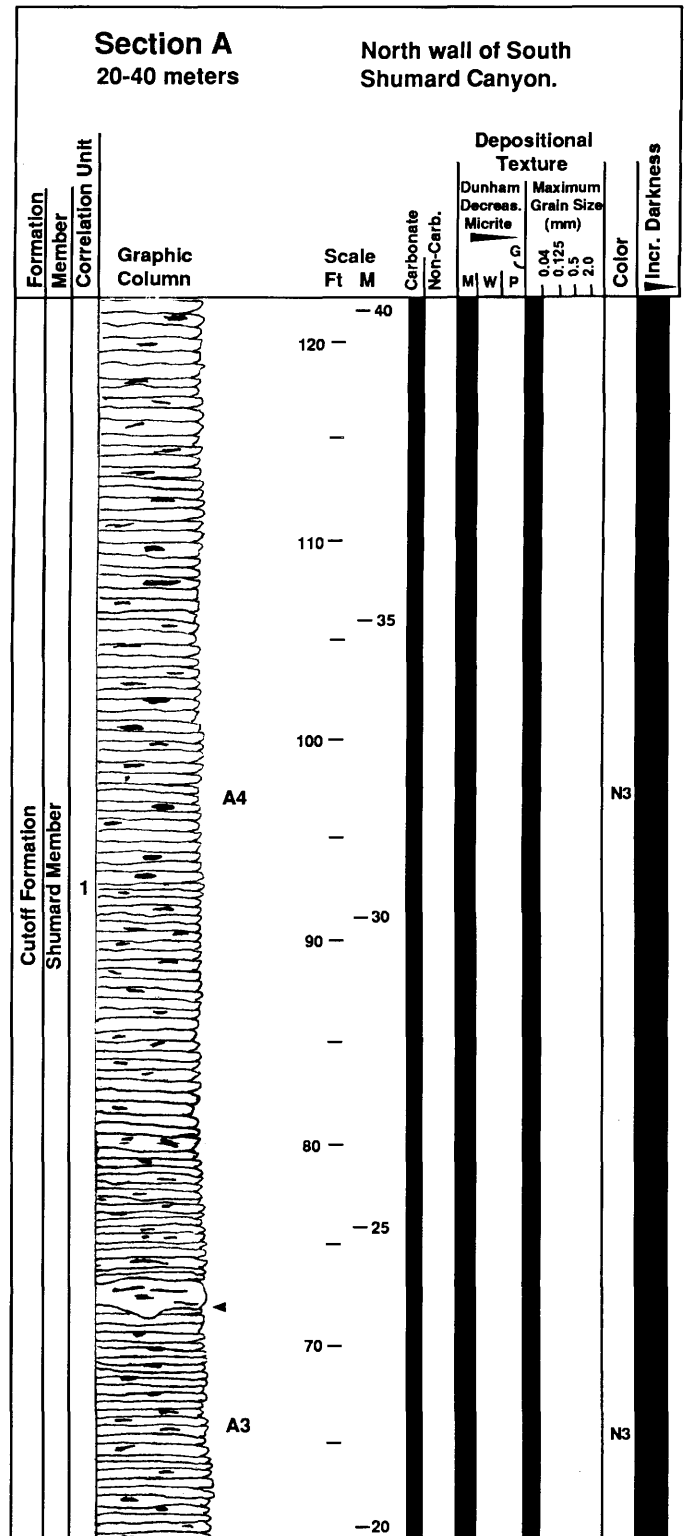
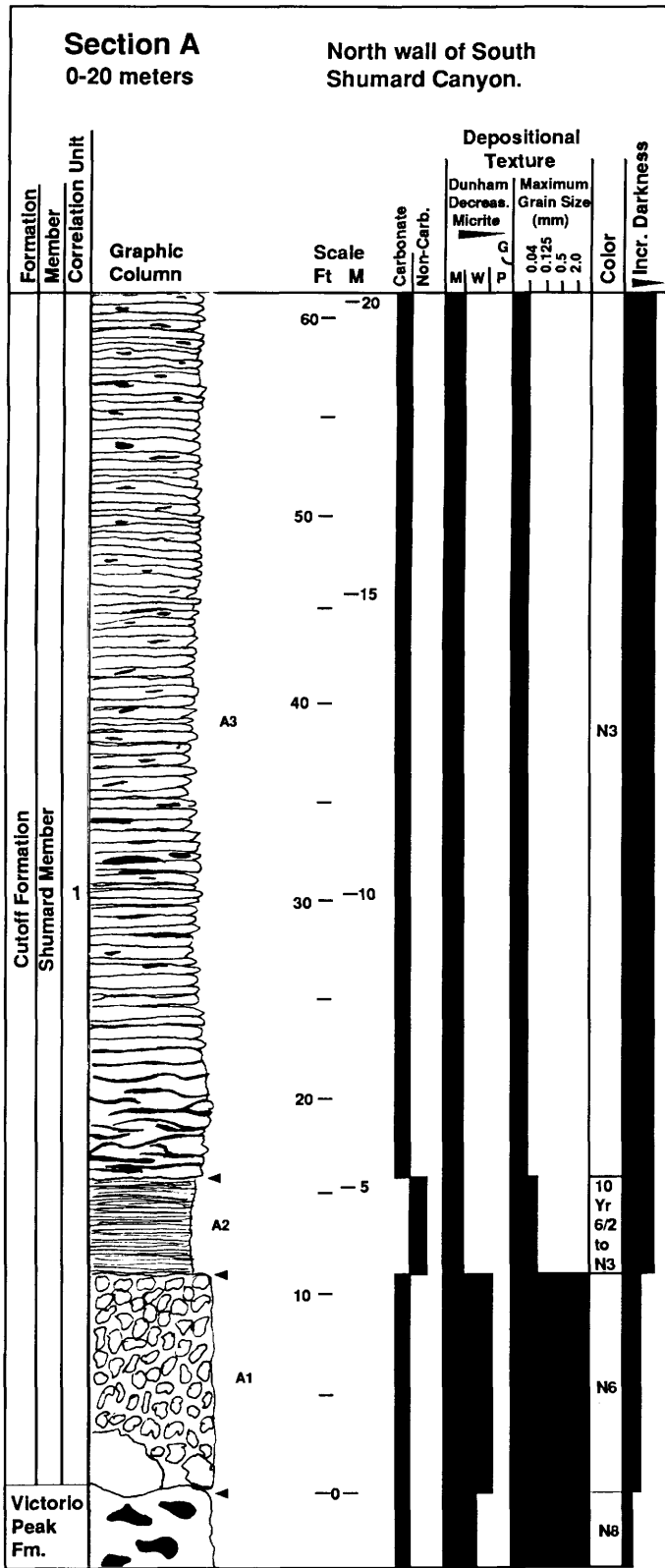


Chert seams and nodules

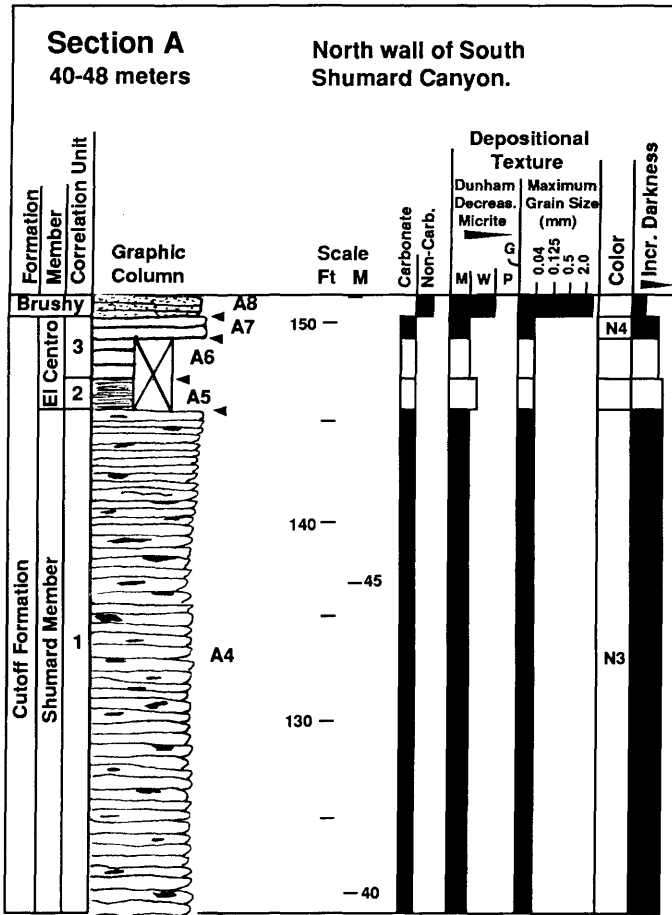


Carbonate concretions

APPENDIX 5-1.—Continued.

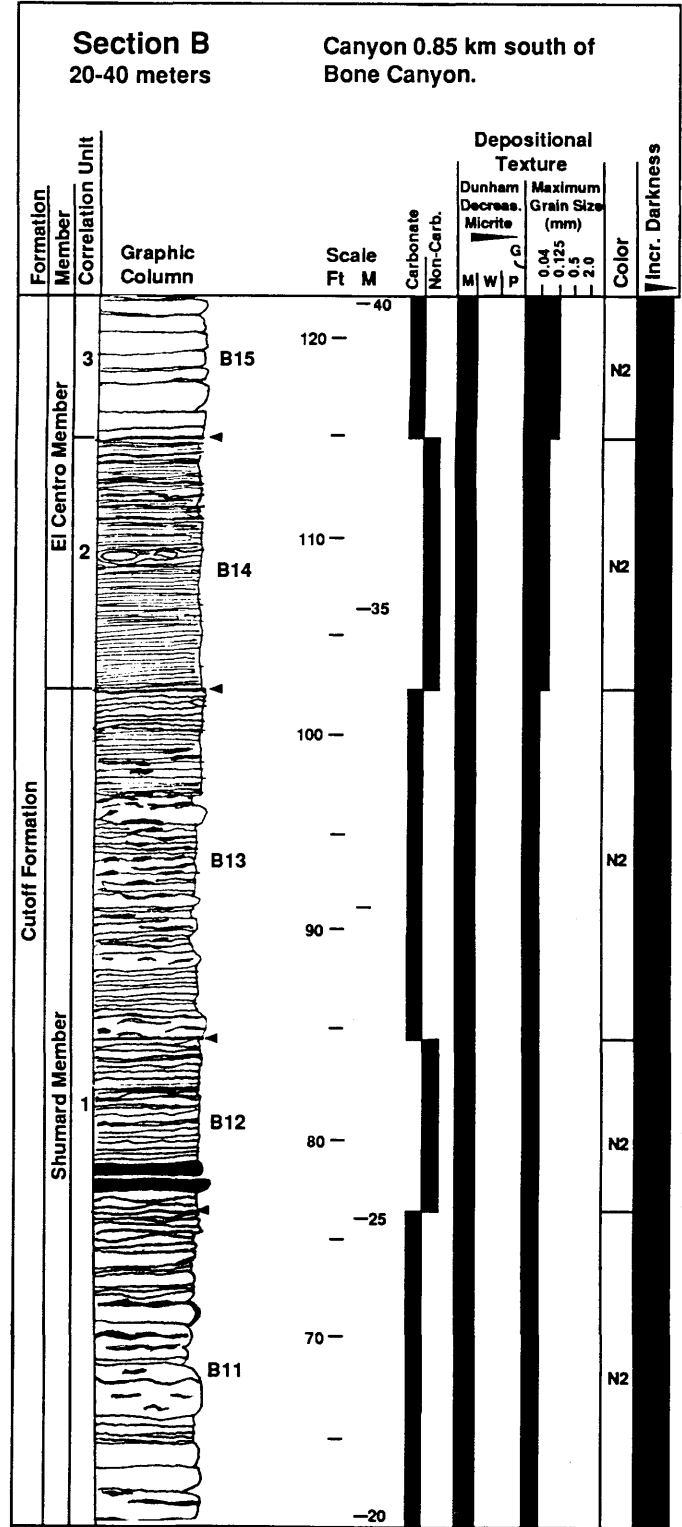
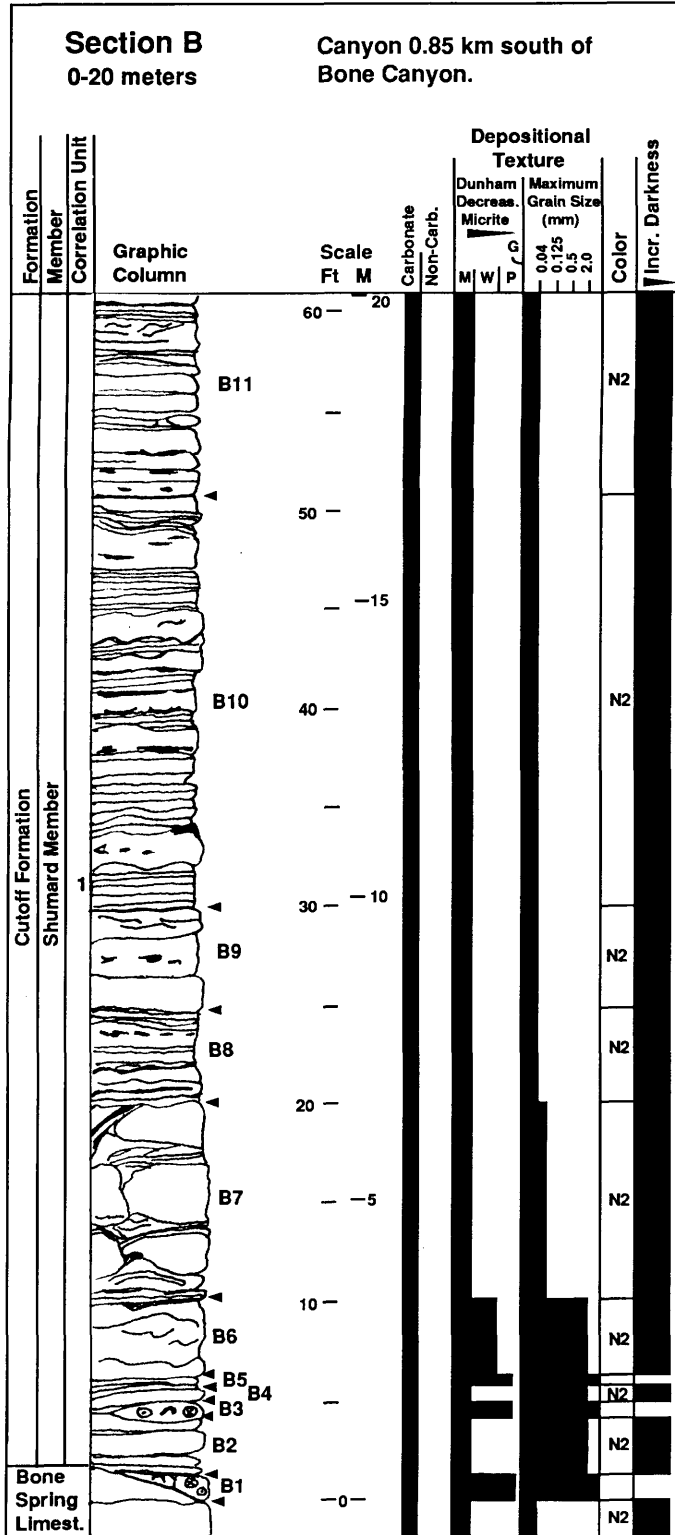


SECTION A.—Graphic representation of Section A, the type section for the Shumard Member. Letters and numbers to the right of the graphic column indicate the described units.



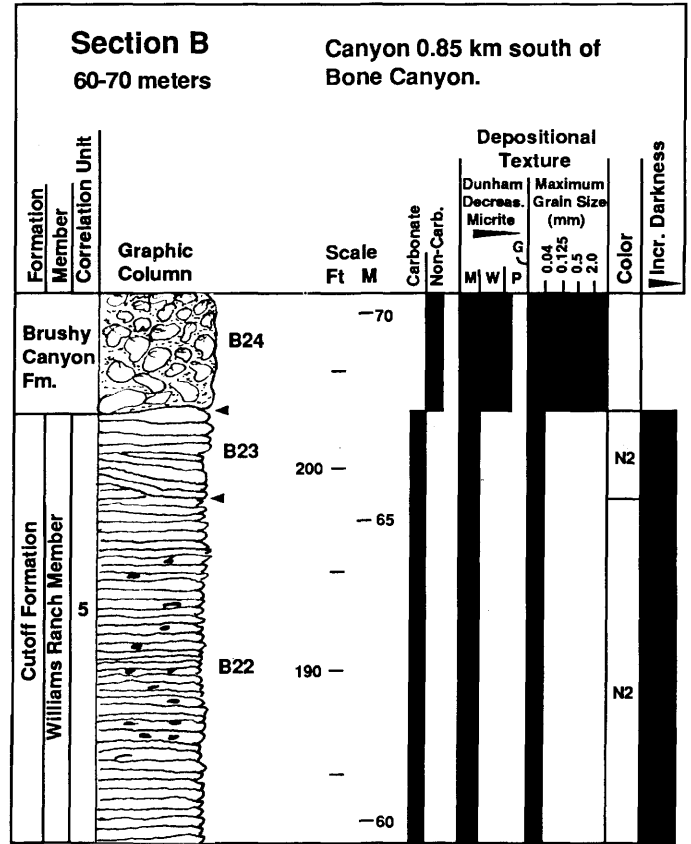
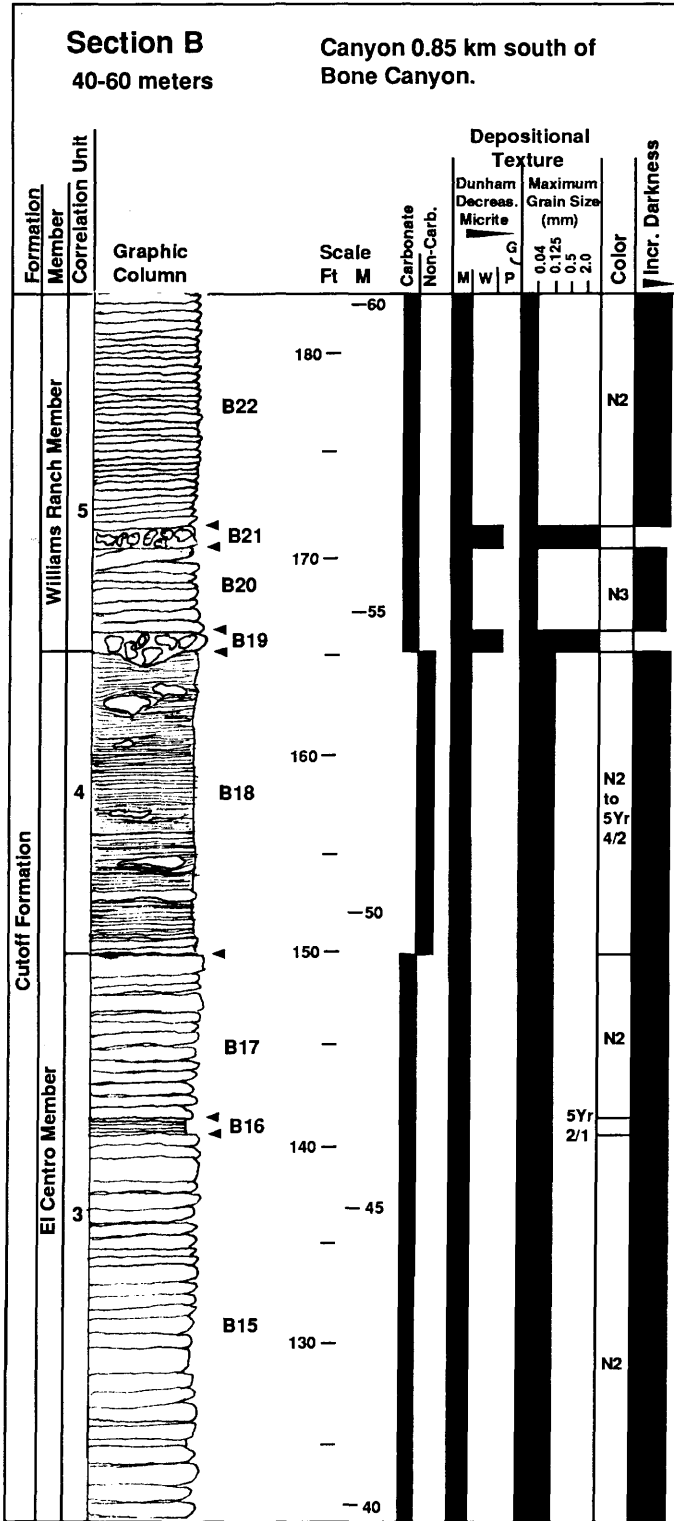
SECTION A.—Continued.

APPENDIX 5-1.—Continued.



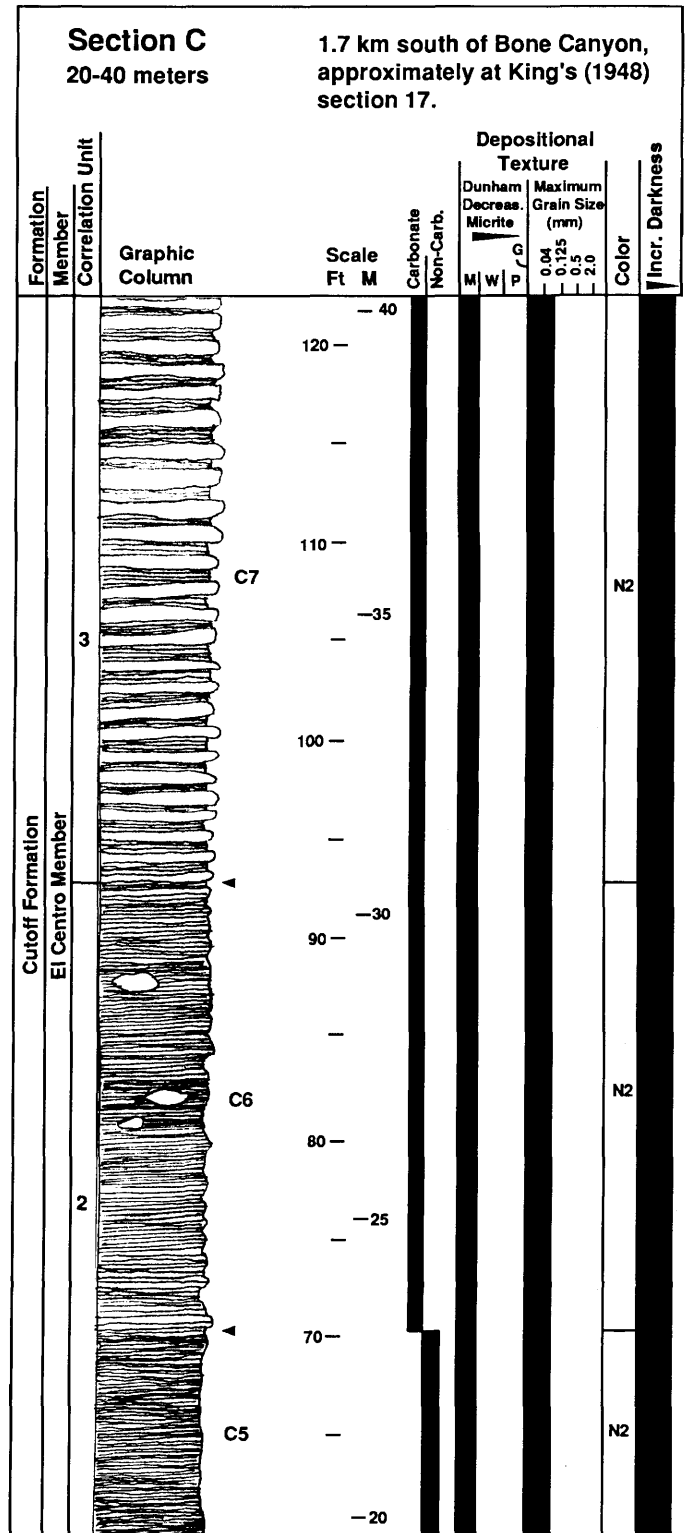
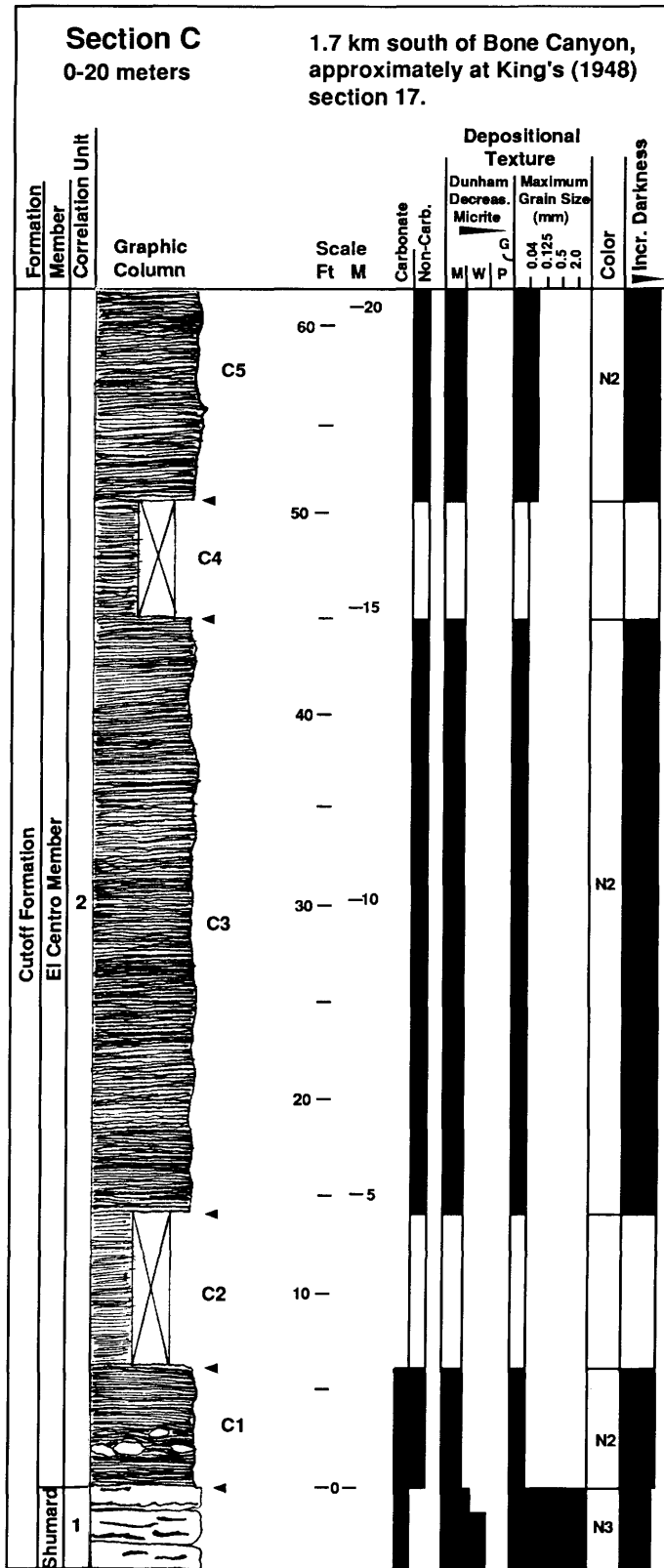
SECTION B.—Graphic representation of Section B, a reference section for the Shumard Member and the type section for the El Centro Member and the Williams Ranch Member. Letters and numbers to the right of the graphic column indicate the described units.

APPENDIX 5-1.—Continued.



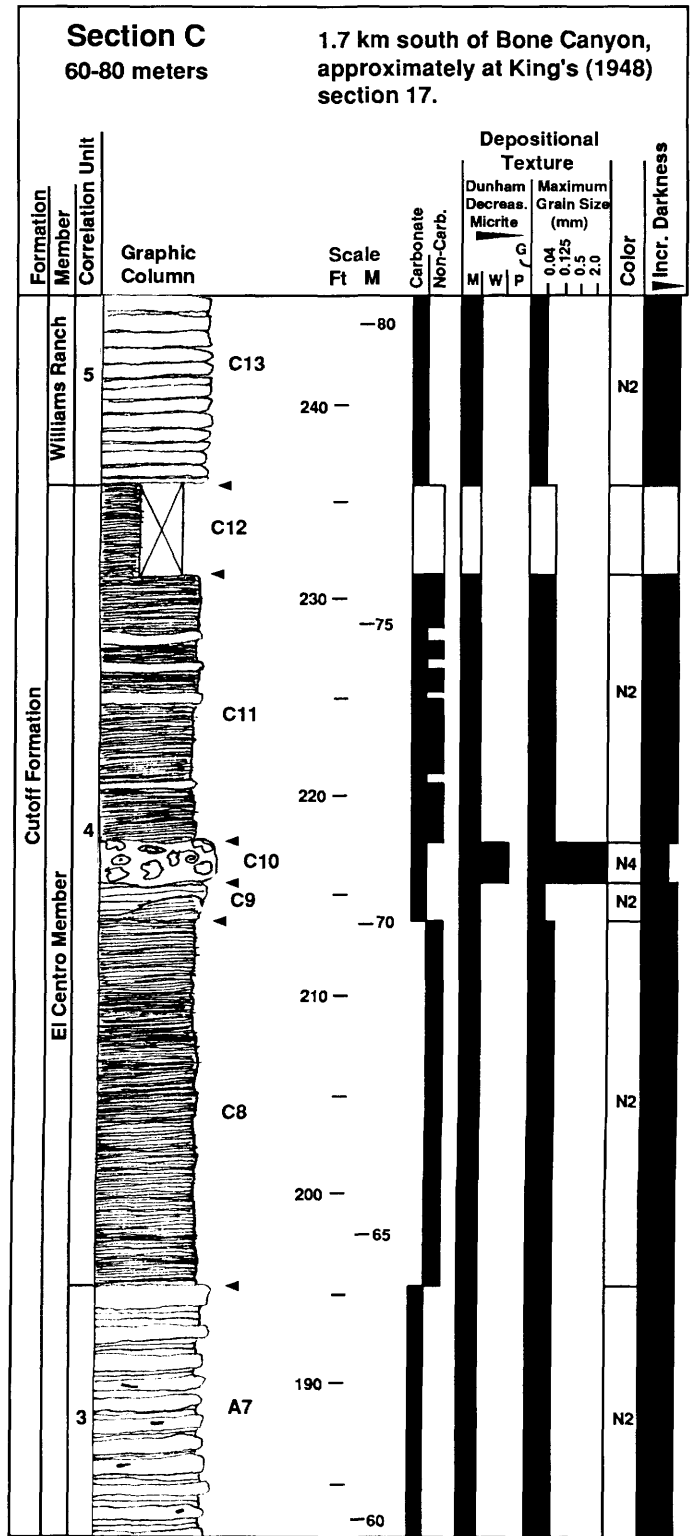
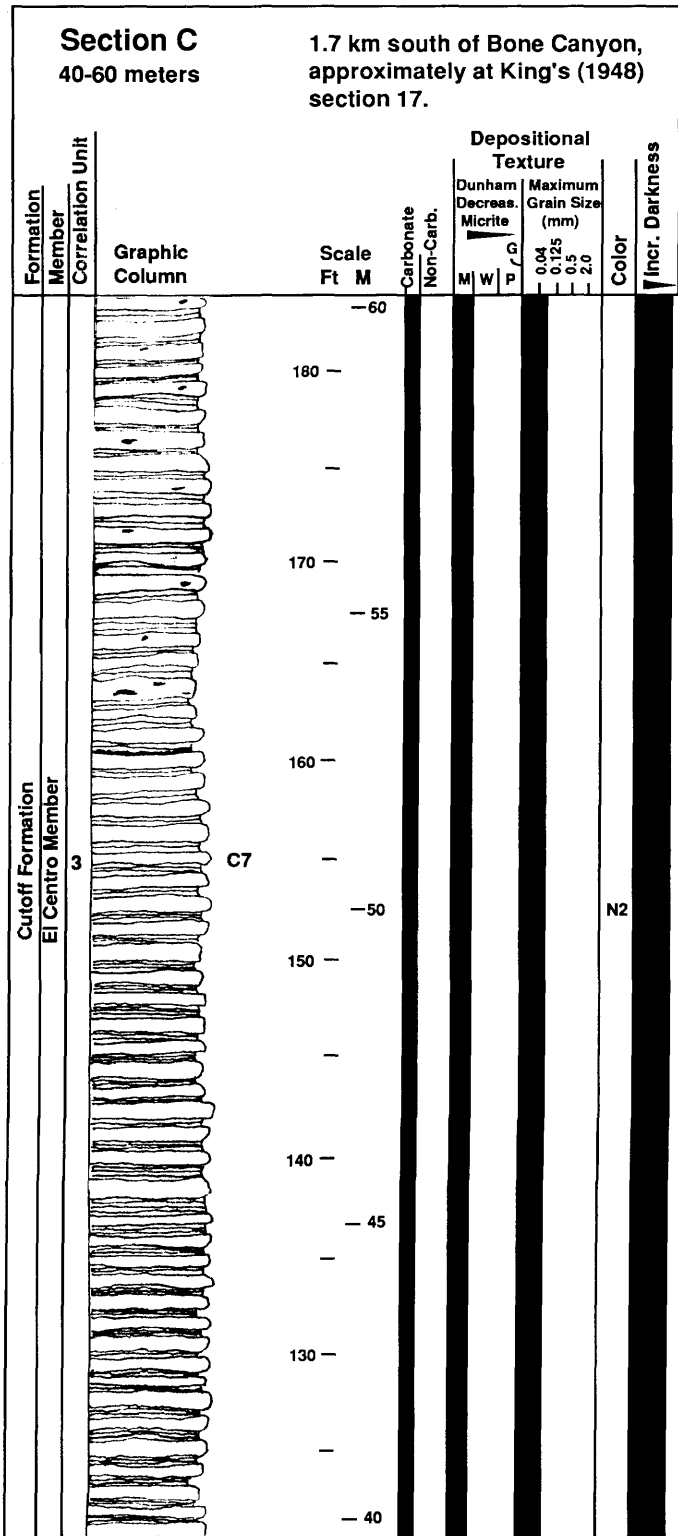
SECTION B.—Continued.

APPENDIX 5-1.—Continued.

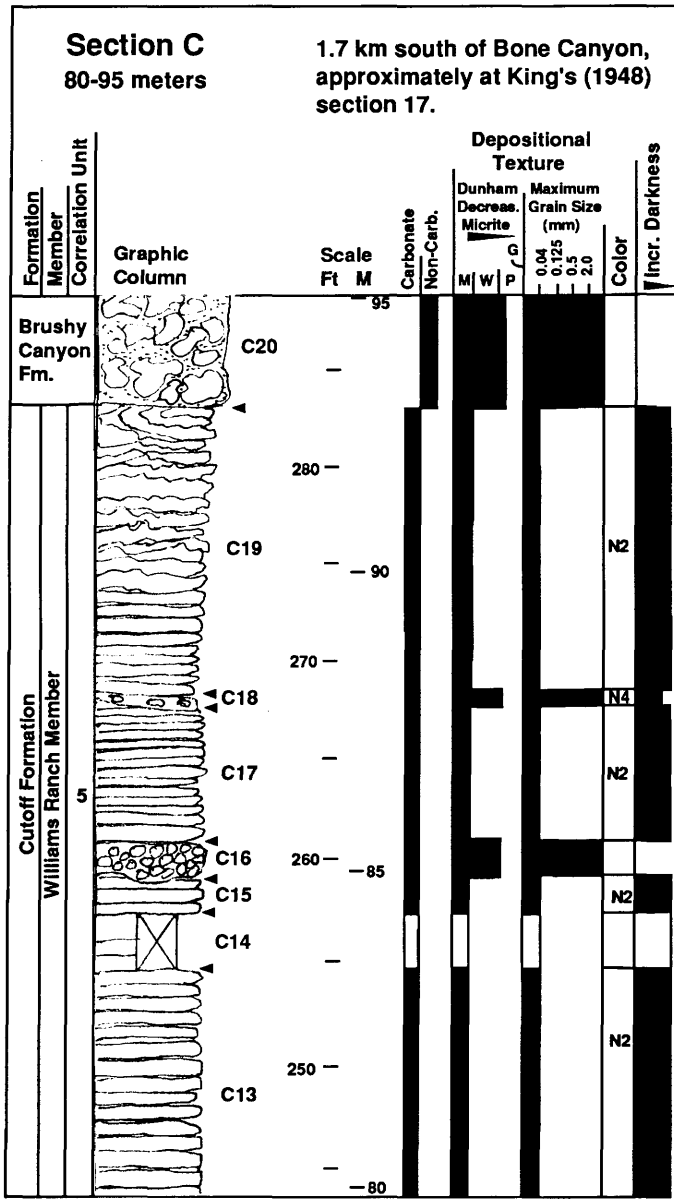


SECTION C.—Graphic representation of Section C, a reference section for the El Centro Member and the Williams Ranch Member. This section is located near the southern limit of complete exposures of the El Centro Member. To the south, the base of the unit is covered. Letters and numbers to the right of the graphic column indicate the described units.

APPENDIX 5-1.—Continued.



APPENDIX 5-1.—Continued.



SECTION C.—Continued.

Literature Cited

- Boyd, D.W.
1958. Permian Sedimentary Facies, Central Guadalupe Mountains, New Mexico. *Bulletin of the New Mexico Bureau of Mines and Mineral Resources*, 49: 100 pages, 5 plates.
- Dunham, R.J.
1962. Classification of Carbonate Rocks According to Depositional Texture. In W.E. Ham, editor, *Classification of Carbonate Rocks: A Symposium. American Association of Petroleum Geologists, Memoir*, 1:108-121, plates 1-7.
- Embry, A.V., and J.E. Klovan
1971. A Late Devonian Reef Tract on Northeast Banks Island, Northwest Territories. *Bulletin of Canadian Petroleum Geology*, 19:730-781.
- Glenister, B.F.
1991. The Guadalupian: A Proposed International Standard for Middle Permian Series. [Abstract.] *International Congress on the Permian System of the World, Program and Abstracts*, Perm, USSR—1991, pages A9-A10. Urals Branch, USSR Academy of Sciences; and Earth Sciences and Resources Institute, University of South Carolina.
- Glenister, B.F., C. Spinosa, W.M. Furnish, and Zhou Zuren
1991. Ammonoid Correlation of the Guadalupian/Dzhulfian Boundary. [Abstract.] In B.R. Wardlaw, R.E. Grant, and D.M. Rohr, editors, *Proceedings of the Guadalupian Symposium, March 13-15, 1991, Sul Ross State University, Alpine, Texas*, page 14.
- Goddard, E.N., P.D. Trask, O.N. Rove, J.T. Singewald, Jr., and R.M. Overbeck
1970. *Rock Color Chart*. Geological Society of America (reprinting).
- Harms, J.C., and L.C. Pray
1974. Erosion and Deposition along the Mid-Permian Intracratonic Basin Margin, Guadalupe Mountains, Texas. [Abstract.] In R.H. Dott, Jr., and R.H. Shaver, editors, *Modern and Ancient Geosynclinal Sedimentation. Society of Economic Paleontologists and Mineralogists, Special Publication*, 19:37.
- Harris, M.T.
1982. Sedimentology of the Cutoff Formation (Permian), Western Guadalupe Mountains, West Texas and New Mexico. 186 pages. Unpublished master's thesis, University of Wisconsin, Madison, Wisconsin.
1988a. Sedimentology of the Cutoff Formation (Permian), Western Guadalupe Mountains, West Texas. In S.T. Reid, R.O. Bass, and P. Welch, editors, *Guadalupe Mountains Revisited, Texas and New Mexico. West Texas Geological Society, Publication*, 88-84:133-140.
1988b. Postscript on the Cutoff Formation: The Regional Perspective and Some Suggestions for Nomenclature. In S.T. Reid, R.O. Bass, and P. Welch, editors, *Guadalupe Mountains Revisited, Texas and New Mexico. West Texas Geological Society, Publication*, 88-84:141-142.
- Hayes, P.T.
1959. San Andres Limestone and Related Permian Rocks in Last Chance Canyon and Vicinity, Southeastern New Mexico. *Bulletin of the American Association of Petroleum Geologists*, 43(9):2197-2213.
- Hay-Roe, H.
1957. Geology of Wylie Mountains and Vicinity, Culberson and Jeff Davis Counties, Texas. *Bureau of Economic Geology, University of Texas, Austin, Geologic Quadrangle Map*, 21.
- Ingram, R.L.
1954. Terminology for the Thickness of Stratification and Parting Units in Sedimentary Rocks. *Bulletin of the Geological Society of America*, 65(9):937-938.
- King, P.B.
1942. Permian of West Texas and Southeastern New Mexico. *Bulletin of the American Association of Petroleum Geologists*, 26(4):535-763.
1948. Geology of the Southern Guadalupe Mountains, Texas. *United States Geological Survey Professional Paper*, 215: 183 pages, 23 plates.
1965. Geology of the Sierra Diablo Region, Texas. *United States Geological Survey Professional Paper*, 480: 185 pages, 16 plates.
- Kirkby, K.C.
1988. Deposition and Permian Erosion of the Upper Victorio Peak Formation (Leonardian), Western Escarpment, Guadalupe Mountains, West Texas. In S.T. Reid, R.O. Bass, and P. Welch, editors, *Guadalupe Mountains Revisited, Texas and New Mexico. West Texas Geological Society, Publication*, 88-84:149-154.
- Lambert, L.L., D.J. Lehrmann, and M.T. Harris
2000. Correlation of the Road Canyon and Cutoff Formations, West Texas, and Its Relevance to Establishing an International Middle Permian (Guadalupian) Series. In B.R. Wardlaw, R.E. Grant, and D.M. Rohr, editors, *The Guadalupian Symposium. Smithsonian Contributions to the Earth Sciences*, 32:153-183, 11 figures, 4 plates, 3 tables.
- McDaniel, P.N., and L.C. Pray
1968. Bank to Basin Transition in Permian (Leonardian) Carbonates, Guadalupe Mountains, Texas. *Bulletin of the American Association of Petroleum Geologists*, 51(3):474.
- Newell, N.D., J.K. Rigby, A.G. Fisher, A.J. Whiteman, J.R. Hickox, and J.S. Bradley
1953. *The Permian Reef Complex of the Guadalupe Mountains Region, Texas and New Mexico: A Study in Paleocology*. 236 pages. San Francisco: W.H. Freeman and Company.
- Pray, L.C.
1971. Submarine Slope Erosion along Permian Bank Margin, West Texas. *Bulletin of the American Association of Petroleum Geologists*, 55(2):358.
- Pray, L.C., G.A. Crawford, M.T. Harris, and K.C. Kirkby
1980. Early Guadalupian (Permian) Bank Margin Erosion Surfaces, Guadalupe Mountains, Texas. *Bulletin of the American Association of Petroleum Geologists*, 64(5):768.
- Pray, L.C., and F.G. Stehli
1963. Allochthonous Origin, Bone Spring "Patch Reefs," West Texas. [Abstract.] *Geological Society of America, Special Paper*, 73:218-219.
- Sarg, J.F., and P.J. Lehmann
1986a. Lower-Middle Guadalupian Facies and Stratigraphy, San Andres/Grayburg Formations, Permian Basin, Guadalupe Mountains, New Mexico. In G.E. Moore and G.L. Wilde, editors, *Lower and Middle Guadalupian Facies, Stratigraphy, and Reservoir Geometries, San Andres/Grayburg Formations, Guadalupe Mountains, New Mexico and Texas. Society of Economic Paleontologists and Mineralogists, Permian Basin Section, Publication*, 86-25:1-8.
- Spinosa, C., W.M. Furnish, and B.F. Glenister
1975. The Xenodiscidae, Permian Ceratitoid Ammonoids. *Journal of Paleontology*, 49(2):239-283, plates 1-8.
- Wilde, G.L.
1986a. Stratigraphic Relationship of the San Andres and Cutoff Formations, Northern Guadalupe Mountains, New Mexico and Texas. In G.E. Moore, and G.L. Wilde, editors, *Lower and Middle Guadalupian Facies, Stratigraphy, and Reservoir Geometries, San Andres/Grayburg Formations, Guadalupe Mountains, New Mexico and Texas. Society of Economic Paleontologists and Mineralogists, Permian Basin Section, Publication*, 86-25:49-63, plates 1-5.
1986b. An Important Occurrence of Early Guadalupian (Roadian) Fusulinids from the Cutoff Formation, Western Guadalupe Mountains, Texas. In G.E. Moore, and G.L. Wilde, editors, *Lower and Middle Guadalupian Facies, Stratigraphy, and Reservoir Geometries, San Andres/Grayburg Formations, Guadalupe Mountains, New Mexico*

and Texas. *Society of Economic Paleontologists and Mineralogists, Permian Basin Section, Publication*, 86-25:65-68, plate 1.

Wilde, G.L., and R.G. Todd

1968. Guadalupian Biostratigraphic Relationships and Sedimentation in the Apache Mountain Region, West Texas. In B.A. Silver, editor, *Guadalupian Facies, Apache Mountains Area, West Texas. Society*

of Economic Paleontologists and Mineralogists, Permian Basin Section, Publication, 68-11:10-31.

Wood, J.W.

1968. Geology of the Apache Mountains, Trans-Pecos Texas. *Bureau of Economic Geology, University of Texas, Austin, Geologic Quadrangle Map*, 33: 32 pages.

6. Cyclic Deposition of the Permian Road Canyon Formation, Glass Mountains, West Texas

*Bruce R. Wardlaw, Charles A. Ross,
and Richard E. Grant*

ABSTRACT

The Road Canyon Formation represents a maximum of four apparent transgressive (progradational) depositional cycles of conglomeratic skeletal wackestone over a minor exposure surface, followed in succession by peloidal packstone and siltstone. These cycles actually represent carbonate shedding from a shoal on the geanticline developed between the Delaware basin and the Marathon foreland basin. The Road Canyon was deposited in the foreland basin as (1) a skeletal wackestone deposited behind a shoal (geanticline), (2) a peloidal packstone deposited on the slope, and (3) a siltstone deposited in the basin. The cycles represent shoalward progradation of the basinal deposits. Rudstone was deposited in channels immediately behind the shoal. Back shoal facies are represented by bioturbated lime mudstone with common channels of conglomeratic wackestone.

Introduction

The depositional setting of the Permian rocks of the Glass Mountains on the southern shelf of the Permian basin (see Rohr et al., this volume) is controversial. Unlike the rather straightforward setting for rocks in the Guadalupe Mountains on the north side of the Delaware basin where shelf, shelf margin, abrupt slope, and basin are clearly discernible, the

Bruce R. Wardlaw, U.S. Geological Survey, 926A National Center, Reston, Virginia 20192. Charles A. Ross, GeoBioStrat, 600 Highland Drive, Bellingham, Washington 98225-6410. Richard E. Grant (deceased), Department of Paleobiology, National Museum of Natural History, Smithsonian Institution, Washington, D.C. 20560-0121.

basinal aspects of the southern shelf of the Permian basin have long been debated (see Cys and Mazzullo, 1978; Flores et al., 1978). The Glass Mountains contain most of the North American Permian regional stratotype.

The Road Canyon Formation is a fossiliferous unit that has been variously placed in the Guadalupian or Leonardian Series. Brachiopods show a strong Leonardian affinity, whereas fusulinids show a strong Wordian (lower Guadalupian) affinity, and various ammonoids show a strong affinity to either series. The Road Canyon was originally mapped as the base of the Word Formation, but it was later separated from the Word because of its faunal affinities. The mixture of faunal affinities led Furnish (1973) to propose a separate stage between the Leonardian and Wordian based on the Road Canyon. The Guadalupian has been recognized worldwide, but it is best represented in West Texas, and the definition of its lower boundary is important for international correlation. Grant and Wardlaw (1984) proposed that a significant conodont fauna changeover within the Road Canyon provides an excellent marker for the definition of the base of the Guadalupian. It is very important to understand the depositional setting of the Road Canyon Formation in order to properly establish the base of the Guadalupian.

Stratigraphy

The Road Canyon Formation was measured at 18 sections in the Glass Mountains and northern Del Norte Mountains (Figures 6-1, 6-2). Sections that appear incomplete in Figure 6-2 were measured only to the top of the exposure (commonly a hill) and were not continued over dip slopes and covered valleys. The sections were measured and collected and remeasured and recollected over annual spring field trips from 1981 to the present. Section RC I (Figure 6-2) represents the stratotype of the Road Canyon Formation.

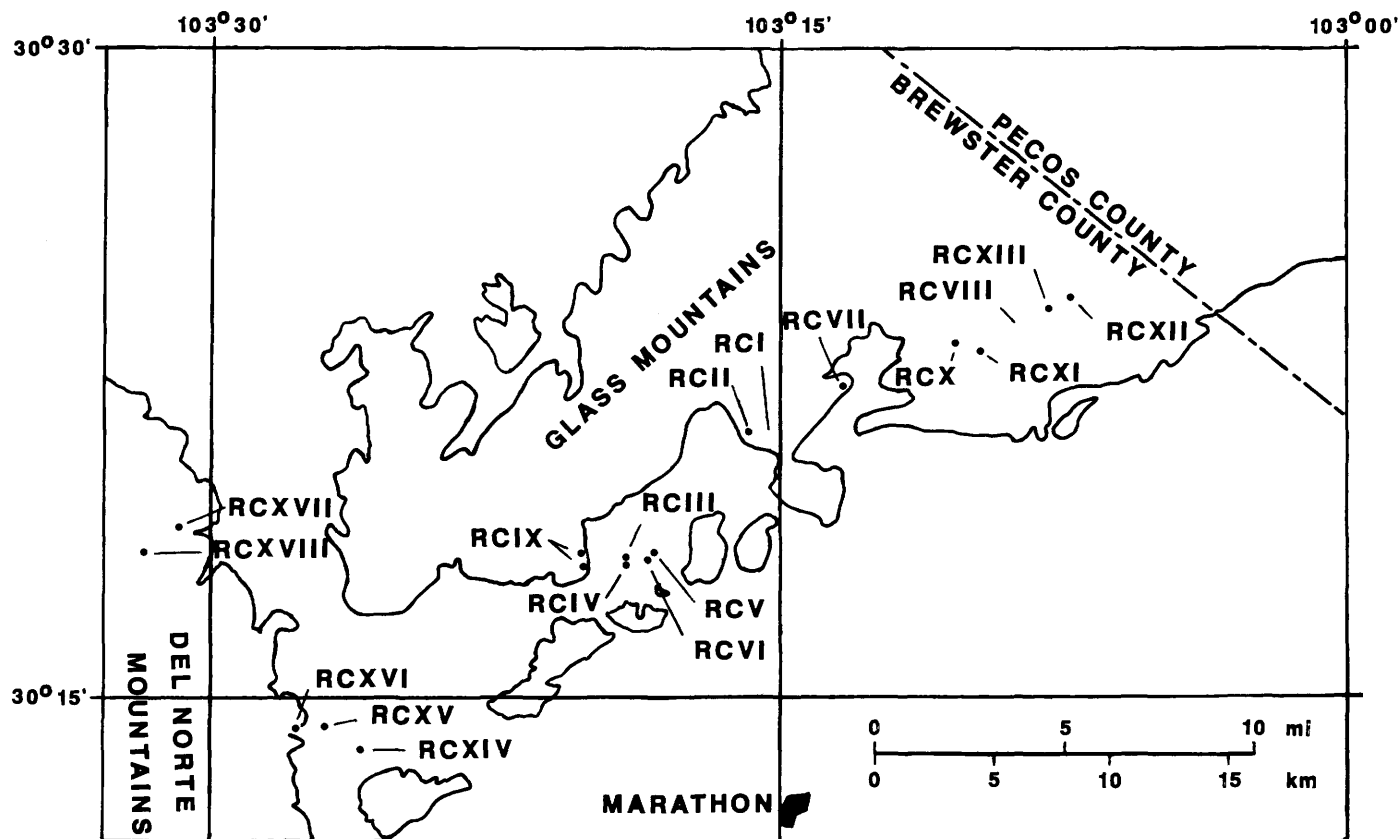


FIGURE 6-1.—Location of sections of the Road Canyon Formation in the Glass Mountains and northern Del Norte Mountains.

Originally, the Road Canyon Formation was described as the first limestone member of the Word Formation (King, 1931). Cooper and Grant (1964) named the informal members proposed by King and designated the first limestone member of the Word Formation as the Road Canyon Member. Later, for largely faunal reasons, Cooper and Grant (1966) elevated the Road Canyon to formation status to separate it from the Word.

The Road Canyon Formation is the predominantly limestone unit situated between the shales (actually siltstones and mudstones) of the Cathedral Mountain Formation below and the Word Formation above. Thus, it is both easily visible and easily mappable. The Word Formation continues the cyclic deposition of the Road Canyon, but it does not display much conglomeratic deposition within the basal skeletal wackestones and it also contains more siltstone in each cycle. As a consequence of the transitional nature of the upper contact and the inability of finding a mappable boundary atop a predominantly limestone unit, the top of the Road Canyon Formation is drawn through various cycles of deposition from section to section (Figure 6-2).

A major faunal changeover of conodonts from *Mesogondolella idahoensis* (Youngquist, Hawley, and Miller) to *M. nankingensis* (Ching) (see Wardlaw, this volume; Lambert et

al., this volume) occurs at the base of, or within the lower part of, cycle 2 deposition of the Road Canyon Formation (Figure 6-2). This faunal changeover is sharp and is found in many sections throughout the world, so it represents a significant correlatable horizon. Lambert and Wardlaw (1992) documented the transition from *M. idahoensis* to *M. nankingensis* through a short-lived transitional form. The major faunal changeover is marked as the first occurrence of *M. nankingensis* (sensu strictu; = *M. serrata*) above the transitional form in sequential samples.

General Lithofacies

Throughout the outcrop area, the majority of the rocks of the Road Canyon Formation can be placed into seven general lithofacies: rudstone, conglomeratic skeletal wackestone, skeletal wackestone/packstone, peloidal packstone/grainstone, siltstone, sandstone, and bioturbated skeletal lime mudstone.

RUDSTONE.—This facies is rare and is commonly found only in sections RC I and RC IX. It is composed of a variety of cobble- to boulder-size clasts of carbonate, which range from skeletal wackestone to boundstone, and scattered clasts of siltstone. The clasts are irregular in shape and size. The matrix

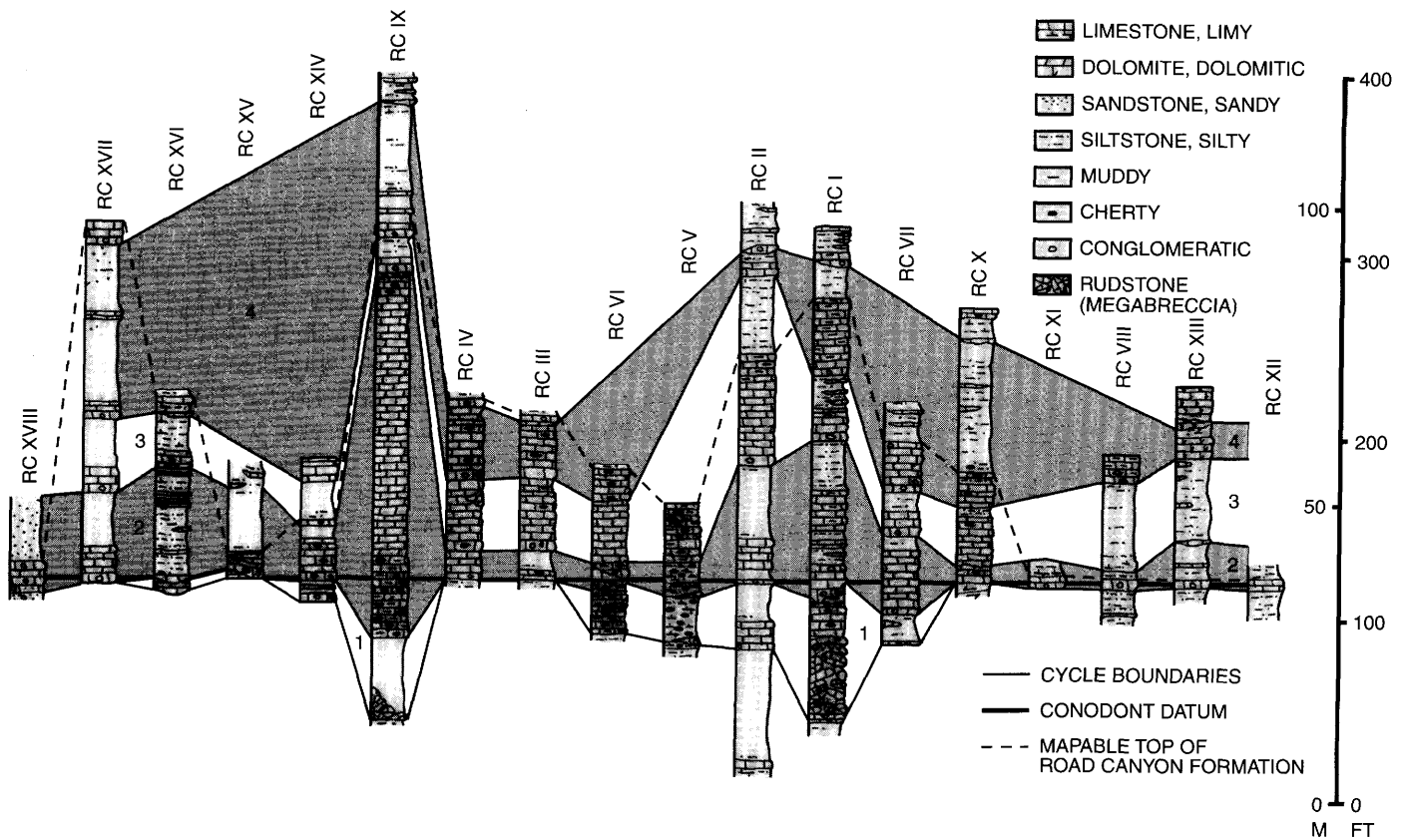


FIGURE 6-2.—Columnar sections of the Road Canyon Formation and some underlying and overlying beds that display four cycles of sedimentation and the beginning of a fifth cycle.

is generally lime-mud and silt when present, and there is abundant evidence for postdepositional corrosion and meteoric diagenesis (Measures and Wardlaw, 1990) in the matrix. The rudstone can be classified as a megabreccia. It forms massive beds that are confined laterally in channelform lenses.

CONGLOMERATIC SKELETAL WACKESTONE.—This facies is similar to the skeletal wackestones, but it contains scattered pebble- to small boulder-size clasts of carbonate and siltstone. The carbonate clasts are generally skeletal wackestones and peloid packstones. The siltstone clasts are flat or irregular in shape. It forms beds that are generally massive.

SKELETAL WACKESTONE/PACKSTONE.—Wackestones are common and consist of very coarse grains of broken to whole skeletal elements, peloids, lime and terrigenous mud, and minor quartz silt. It forms beds that are generally thick to massive.

PELOIDAL PACKSTONE/GRAINSTONE.—Peloidal packstones are very common. They are sparsely fossiliferous and primarily consist of fecal pellets, algal peloids, and lime-mud (when packstones). The algal peloids are coated and micritized rounded grains representing a variety of allochems that include unrecognizable debris, skeletal grains, and quartz sand. Commonly, these rocks are poorly sorted. Peloidal packstones are generally medium bedded.

SILTSTONE.—Siltstones are common and consist of quartz silt and sand, silicified calcispheres, radiolarians?, sponge spicules, and clay. They vary from moderately sorted to poorly sorted and generally form thin, platy to medium-thick beds. The siltstones are largely unfossiliferous, with only scattered traces and burrows and sparse brachiopods and fusulinids.

SANDSTONE.—Sandstones are rare and occur only in the westernmost exposures in the northern Del Norte Mountains, where they are poorly exposed. They appear to be similar to the sandstones that were described by Wardlaw et al. (1990) as overlying the lower part of the Word Formation in the same area as lower delta plain deposits. They consist of generally fine, immature to submature quartz sand that contains siliceous and calcareous cement.

BIOTURBATED SKELETAL LIME MUDSTONE.—Lime mudstones are rare and occur in only three sections, RC V, RC VI, and RC IX. The skeletal grains are broken, abraded, and scattered and commonly are derived from brachiopods. This facies is similar to the bioturbated wackestone found commonly in the Appel Ranch Member of the Word Formation where Rathjen (1985) interpreted the facies to represent a shelf flat. In the Appel Ranch Member, the carbonate is generally recrystallized and dolomitized. In the Road Canyon it is only recrystallized.

Depositional Cycles in the Road Canyon

Each cycle begins over a minor exposure surface, which is represented by reworked siltstones from the underlying unit or cycle. The overlying basal carbonate commonly has an undulating base, and it rarely cuts out, or channels, through the underlying beds. Rarely, an overlying cycle erodes through a significant part of the underlying cycle. Generally, when erosion reaches to a carbonate in an underlying cycle, the carbonate shows chertification and minor recrystallization near its upper surface. The idealized cycle (Figure 6-3) begins with a conglomeratic skeletal wackestone at its base and grades upward to skeletal wackestone and then to peloidal packstone. Peloidal packstone grades to siltstone by becoming more silty and displays alternating beds of peloidal packstone and siltstone, which gradually gives way to entirely siltstone. This idealized sequence is represented throughout the area in most of the cycles, but each lithology is represented by vastly varying thicknesses of rock. Cycle 1 (Figure 6-2) is the only cycle that is commonly cut out, thus indicating a more significant erosional surface between cycles 1 and 2. Cycle 2 is the most widespread cycle represented in the Road Canyon. Cycles 3 and 4 are lost in the deltaic sandstones in the western part of the Del Norte Mountains (section RC XVIII) and become obscure in the dolostones of the eastern Glass Mountains (the section above RC XII and eastward, Figure 6-1).

Sequences that truly vary from the model appear to be those that contain bioturbated lime mudstone, which only occur at section RC IX in cycle 2, section RC V in cycles 1-3, and section RC VI in cycle 1. In each, a conglomeratic base is followed by generally cherty lime mudstone, with the chert replacing burrows. The basal unit is commonly a lens or channel of skeletal, conglomeratic carbonate. Peloidal packstones and siltstones are rare or absent. Channels of skeletal wackestone occur within some cycles. These deposits appear to be related to the encroachment of the shoal facies, which is represented by a recrystallized, channelized mud flat similar to that described for the Word Formation (Rathjen, 1985; Rathjen et al., this volume), but this facies is rarely preserved in the Road Canyon Formation.

In addition, in apparent variation from the model, cycle 1 at sections RC I and RC IX is obscured by a tremendous amount of conglomerate.

FAUNAS FROM THE CYCLES.—Conodonts show a major faunal changeover from a transitional form of *Mesogondolella idahoensis* to *M. nankingensis* at or near the base of cycle 2. Fusulinids appear to show clear Cathedral Mountain affinities in cycle 1 and change to Word affinities in cycle 2. Ammonoids show a less clear distribution, with most indicating Leonardian affinities, but the one definite occurrence of *Waagenoceras* (Wordian affinities) within the Road Canyon appears to be in cycle 4. Brachiopods show general Lower Permian (Leonar-

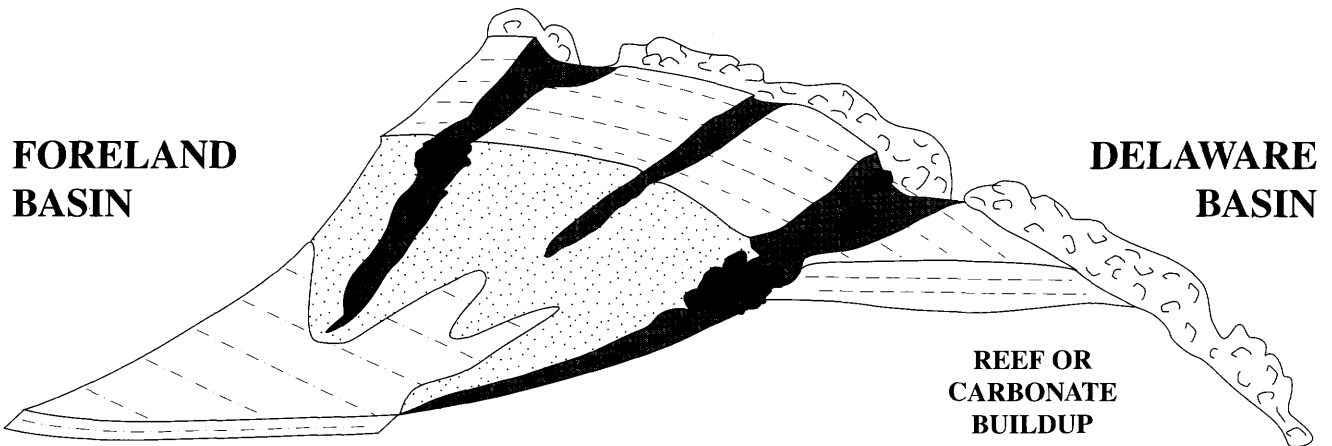
dian) affinities throughout the Road Canyon, and cycles 1-4 all contain abundant *Coscinophora*, which is absent in cycle 5. It appears that the most marked faunal changeover is at or near the base of cycle 2, which involves both conodonts and fusulinids.

CORRELATION OF THE CYCLES.—The boundary between cycle 1 and cycle 2 is the most extensive exposure surface within the Road Canyon. This surface occurs just below the first appearance of *Mesogondolella nankingensis*. In the Guadalupe Mountains, the downlap surface of Sarg and Lehmann (1986a), which is within the Cutoff Formation and divides the lower San Andres Formation from the middle San Andres Formation, occurs just below the first appearance of *M. nankingensis*. These surfaces appear to strongly correlate. A downlap surface separates a transgressive system from a highstand depositional system. To have an exposure surface in the Glass Mountains at the same time as a highstand in the Guadalupe Mountains suggests that there is a local relative uplift in the Glass Mountains area that outstripped sea level at stillstand (highstand) and caused exposure. During sea level rise (transgressive deposition), the relative sea level rise exceeded any local uplift depositing the first cycle in the Road Canyon Formation at the same time the upper part of the lower San Andres Formation in the Guadalupe Mountains was being deposited. The sequence boundary below the lower San Andres Formation (an exposure surface) correlates well with the exposure surface below the Cathedral Mountain Formation in the Glass Mountains (within the same conodont zone, *Neostreptognathodus prayi*-*Mesogondolella idahoensis* Zone). The upper sequence boundary at the top of the middle San Andres Formation (a rather major unconformity) is less well constrained by conodonts (falling within the relatively long-ranging *Mesogondolella nankingensis* Zone) but may correlate to cycle 5, the base of the China Tank Member of the Word Formation in the Glass Mountains. The exposure surfaces at the base of cycles 1, 3, and 4 do not have easily correlated counterparts in the Guadalupe Mountains. This suggests that although part of the cyclicity is due to response to regional sea level changes, most of it appears to be due to local uplift and subsidence.

Depositional Setting

The Road Canyon Formation was deposited on the narrow southern shelf of the Permian basin of West Texas adjacent to the Marathon folded belt (see Rohr et al., this volume). The Marathon folded belt was an active thrust belt (accretionary wedges overriding the North American plate) in the Pennsylvanian and Early Permian (Ross, 1986). The sequence of lithofacies, lack of any significant flow features, and the peloidal packstones with well-coated, poorly-sorted grains indicate reasonably shallow shelf deposition of the Road Canyon Formation. The abundance of silt- and clay-sized material in all the lithofacies indicates a relatively low energy

MODEL FOR DEPOSITION



IDEALIZED SEQUENCE OBSERVED IN ROAD CANYON FM. CYCLES 1-3

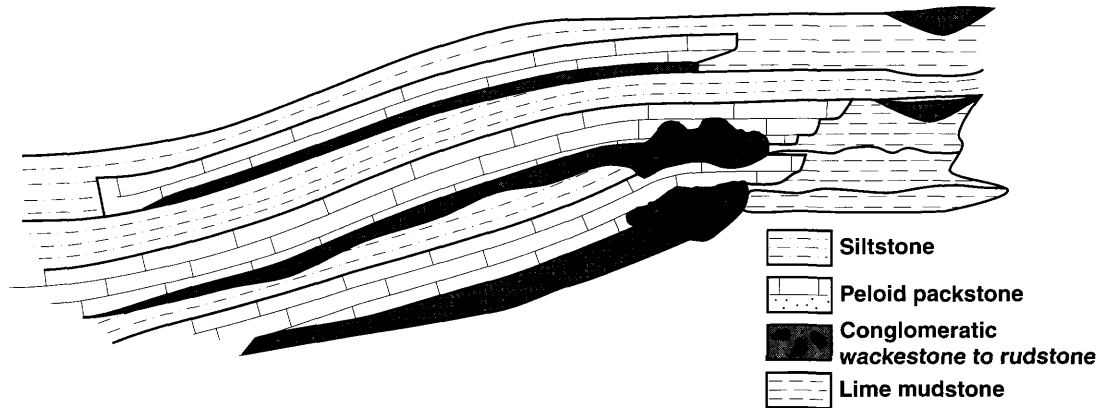


FIGURE 6-3.—Idealized cycle of sedimentation and its relation to change in relative sea level and the generalized depositional setting of the lithofacies.

depositional regime. Models for similar lithofacies in the Word Formation (Rathjen, 1985) suggest a shoal and back-bay setting, with peloidal packstones representing the deepest bay depositional environment. Conodonts are abundant in the skeletal wackestones, but they are sparse in the peloidal packstones, and, when found in such packstones, they are generally in shallow, nearshore biofacies (Wardlaw and Grant, 1990). This distribution is very unlike that of the basinal deposits of the Guadalupe Mountains and Delaware basin and suggests that the peloidal packstones do not represent normal marine basinal deposition. Brachiopods and other normal marine fossils are also sparse in the peloidal packstones, suggesting they represent elevated salinities, which would be expected in a shoaled bay.

The generalized depositional setting (Figure 6-3) appears to be one of skeletal wackestones deposited behind a shoal, which is represented by recrystallized bioturbated lime-mudstone containing skeletal channels. Peloidal packstones represent shallow back-bay deposition, and siltstones represent nearshore and back-bay deposition shed from the still active Marathon folded belt. The cycles are transgressive depositional cycles over exposure surfaces that represent relative deepening (to peloidal packstone deposition) and then shallowing (to siltstones and then exposure). In this depositional setting, the cycles also represent the progradation of shore facies over a shelf margin shoal. The cycles appear to be largely in response to local uplift and subsidence rather than to changes in regional sea level.

Literature Cited

- Cooper, G.A., and R.E. Grant
 1964. New Permian Stratigraphic Units in Glass Mountains, West Texas. *Bulletin of the American Association of Petroleum Geologists*, 48(9):1581-1588.
1966. Permian Rock Units in the Glass Mountains, West Texas. *United States Geological Survey Bulletin*, 1244-E:E1-E9, plates 1, 2.
- Cys, J.M., and S.J. Mazzullo
 1978. Lithofacies and Sedimentation of Lower Permian Carbonate of the Leonard Mountain Area, Glass Mountains, Western Texas: A Discussion. *Journal of Sedimentary Petrology*, 48(4):1363-1368.
- Flores, R.M., T.L. McMillan, and G.E. Watters
 1978. Lithofacies and Sedimentation of Lower Permian Carbonate of the Leonard Mountain Area, Glass Mountains, Western Texas: A Reply. *Journal of Sedimentary Petrology*, 48(4):1368-1377.
- Furnish, W.M.
 1973. Permian Stage Names. In A. Logan and L.V. Hills, editors, *The Permian and Triassic Systems and Their Mutual Boundary*. *Canadian Society of Petroleum Geologists, Memoir*, 2:522-548.
- Grant, R.E., and B.R. Wardlaw
 1984. Redefinition of Leonardian-Guadalupian Boundary in Regional Stratotype for the Permian of North America. *27th International Geological Congress, Moscow, USSR, Abstracts*, 1:58.
- King, P.B.
 1931 ("1930"). The Geology of the Glass Mountains, Texas, Part I: Descriptive Geology. *University of Texas Bulletin*, 3038: 167 pages, 15 plates. [Date on title page is 1930; actually published in 1931.]
- Lambert, L.L., D.J. Lehrmann, and M.T. Harris
 2000. Correlation of the Road Canyon and Cutoff Formations, West Texas, and Its Relevance to Establishing an International Middle Permian (Guadalupian) Series. In B.R. Wardlaw, R.E. Grant, and D.M. Rohr, editors, *The Guadalupian Symposium. Smithsonian Contributions to the Earth Sciences*, 32:153-183, 11 figures, 4 plates, 3 tables.
- Lambert, L.L., and B.R. Wardlaw
 1992. Appendix II: Morphological Transition from *Mesogondolella idahoensis* to *M. serrata*: Basal Guadalupian Definition. In Glenister et al., *The Guadalupian: Proposed International Standard for a Middle Permian Series. International Geology Review*, 34(9):876-880.
- Measures, E.A., and B.R. Wardlaw
 1990. Recognition of Paleokarst in the Road Canyon Formation, Permian Regional Stratotype, West Texas. [Abstract.] *Geological Society of America, Abstracts with Programs*, 22(7):A309.
- Rathjen, J.D.
 1985. Microfacies and Depositional Environment of the Word Formation (Permian) Glass Mountains, Texas. 139 pages. Unpublished master's thesis, Sul Ross State University, Alpine, Texas.
- Rathjen, J.D., B.R. Wardlaw, D.M. Rohr, and R.E. Grant
 2000. Carbonate Deposition of the Permian Word Formation, Glass Mountains, West Texas. In B.R. Wardlaw, R.E. Grant, and D.M. Rohr, editors, *The Guadalupian Symposium. Smithsonian Contributions to the Earth Sciences*, 32:261-289, 22 figures.
- Rohr, D.M., B.R. Wardlaw, S.F. Rudine, M. Haneef, J.A. Hall, and R.E. Grant
 2000. Guidebook to the Guadalupian Symposium. In B.R. Wardlaw, R.E. Grant, and D.M. Rohr, editors, *The Guadalupian Symposium. Smithsonian Contributions to the Earth Sciences*, 32:5-36, 31 figures.
- Ross, C.A.
 1986. Paleozoic Evolution of Southern Margin of Permian Basin. *Bulletin of the Geological Society of America*, 97(5):536-554.
- Sarg, J.F., and P.J. Lehmann
 1986a. Lower-Middle Guadalupian Facies and Stratigraphy, San Andres/Grayburg Formations, Permian Basin, Guadalupe Mountains, New Mexico. In G.E. Moore and G.L. Wilde, editors, *Lower and Middle Guadalupian Facies, Stratigraphy, and Reservoir Geometries, San Andres/Grayburg Formations, Guadalupe Mountains, New Mexico and Texas. Society of Economic Paleontologists and Mineralogists, Permian Basin Section, Publication*, 86-25:1-8.
- Wardlaw, B.R.
 2000. Guadalupian Conodont Biostratigraphy of the Glass and Del Norte Mountains. In B.R. Wardlaw, R.E. Grant, and D.M. Rohr, editors, *The Guadalupian Symposium. Smithsonian Contributions to the Earth Sciences*, 32:37-87, 3 figures, 12 plates, 1 table.
- Wardlaw, B.R., R.A. Davis, D.M. Rohr, and R.E. Grant
 1990. Leonardian-Wordian (Permian) Deposition in the Northern Del Norte Mountains, West Texas. *United States Geological Survey Bulletin*, 1881-A:A1-A14.
- Wardlaw, B.R., and R.E. Grant
 1990. Conodont Biostratigraphy of the Permian Road Canyon Formation, Glass Mountains, Texas. *United States Geological Survey Bulletin*, 1895-A:A1-A18, plates 1-4.

7. Comparison of the Depositional Environments and Physical Stratigraphy of the Cutoff Formation (Guadalupe Mountains) and the Road Canyon Formation (Glass Mountains): Lowermost Guadalupian (Permian) of West Texas

*Mark T. Harris, Daniel J. Lehrmann,
and Lance L. Lambert*

ABSTRACT

Major paleoenvironmental changes near the Leonardian–Guadalupian boundary are recorded in both the Cutoff Formation (Guadalupe Mountains) and the Road Canyon Formation (Glass Mountains). The Cutoff Formation is composed of a basal facies dominated by carbonate and siliciclastic lutites that were deposited over an eroded Leonardian (Victorio Peak–Bone Spring) bank margin. These lithologies resulted from an abrupt eustatic deepening (40–50 m), which brought anoxic (dysaerobic) conditions onto the outer shelf and caused the shallow-water shelf to retreat 19–23 km to the northwest. Coarse rudstone and megabreccia deposits consisting of allochthonous clasts occur in slope channels. Prominent submarine unconformities at the base, as well as within and at the top of the Cutoff strata, extend from the shelf to the basin. Pre-Cutoff erosion steepened the underlying bank margin to a 5°–20° slope. Post-Cutoff erosion locally removed Cutoff strata, resulting in a discontinuous outcrop along the slope. The recognition of five intra-Cutoff correlation units, based upon lutite composition, provides a detailed stratigraphic framework that helps resolve shelf-to-basin correlations. A complete shelf-to-basin profile, exposed at a high angle to the shelf margin, provides unambiguous evidence that the unconformities are regional surfaces, and that the coarse deposits are down-slope debris.

Mark T. Harris, Department of Geosciences, University of Wisconsin-Milwaukee, Milwaukee, Wisconsin 53201. Daniel J. Lehrmann, Department of Geology, University of Kansas, Lawrence, Kansas 66045. Lance L. Lambert, Physics Department, Southwest Texas State University, San Marcos, Texas 78666-4616.

The Road Canyon Formation consists largely of organic-rich lutites bearing spiculites and radiolarians. Like the Cutoff Formation, it contains allochthonous megabreccias, conglomerates, and sand sheets. Megabreccias and conglomerates occur as channelized deposits, whereas coarse carbonate sands occur in sheet geometries. Lamination textures in the lutites indicate that the allochthonous material was deposited in an anoxic (dysaerobic to anaerobic) slope or deep shelf setting. The recognition of a succession of seven depositional units allows correlation across the central Glass Mountains. No regionally extensive unconformity surfaces were noted.

The comparison of the two formations indicates a similar depositional environment: an anoxic slope-to-basin setting with both fine-grained autochthonous sediments and coarse-grained allochthonous debris. The Road Canyon outcrop belt, however, nearly parallels depositional strike, making its interpretation more difficult (and comparison to Cutoff strata more useful). The recognition of the depositional environments, detailed internal successions, and relative stratigraphic completeness provides the necessary framework for better interpreting the biostratigraphic data relevant to defining the Leonardian–Guadalupian boundary as discussed in an accompanying contribution (Lambert, Lehrmann, and Harris, this volume).

Introduction

Leonardian–Guadalupian boundary sections are exposed in various mountains around the rim of the Permian basin. In addition to the Leonardian and Guadalupian type areas, respectively located in the Glass Mountains (King, 1931) and

the southern Guadalupe and Delaware mountains (King, 1942, 1948; Newell et al., 1953), these rocks occur in the northern Guadalupe Mountains (Boyd, 1958; Hayes, 1959), Sierra Diablo (King, 1965), Wylie Mountains (Hay-Roe, 1957), and Apache Mountains (Wood, 1968) (Figure 7-1).

This report focuses on the physical stratigraphy and depositional environment of two important areas in this region: the western Guadalupe Mountains (Cutoff Formation) and the Glass Mountains (Road Canyon Formation). The Guadalupe Mountains expose a complete shelf-to-basin transect, which provides a useful comparison to the Glass Mountains. Detailed stratigraphic studies are essential for evaluating the Roadian stage and defining the Leonardian-Guadalupian series boundary. Identification of depositional settings, internal stratigraphies, and relative stratigraphic completeness provides a stratigraphic framework for interpreting paleontological data. Lambert, Lehrman, and Harris (this volume) present new biostratigraphic data and stratigraphic revision of past collections.

The Cutoff Formation of the Guadalupe Mountains

The Cutoff Formation is a drape of basin-style facies that overlies Leonardian carbonate bank deposits of the Victoria

Peak-Bone Spring limestones (Figure 7-2). Prior to Cutoff deposition, erosion steepened the Leonardian shelf-to-basin profile to approximately 20° and formed a paleoslope with a relief of 300 m (McDaniel and Pray, 1967; Pray, 1971; Harms and Pray, 1974; Harris, 1982, 1988a; Kirkby, 1988). Post-Cutoff erosion locally removed Cutoff strata along the paleoslope making correlation of the Cutoff from shelf to basin problematical (King, 1948; Wilde and Todd, 1968). Strata are preserved in three distinct areas as defined by the pre-Cutoff shelf profile (Figures 7-2, 7-3): (1) flat shelf (0° - 1° dip), (2) steeply-dipping slope (5° - 20° dip), and (3) low-relief basin edge (dip less than 5°) that flattened basinward. Herein, "slope" is used to describe a depositional setting with a perceptible dip and water depths greater than about 50 m.

Stratigraphic nomenclature used in this paper follows Harris (this volume) (Figure 7-4). The Cutoff Formation consists of three members in most of the study area. In ascending order these are the Shumard Member, the El Centro Member, and the Williams Ranch Member. The Shumard Member is equivalent to King's (1948) informal lower Cutoff unit; the two overlying members are equivalent to his upper Cutoff unit. The Cutoff is Roadian (early Guadalupian) age (Lambert et al., this volume) (Figure 7-5); for a review of the nomenclature history see Harris (this volume).

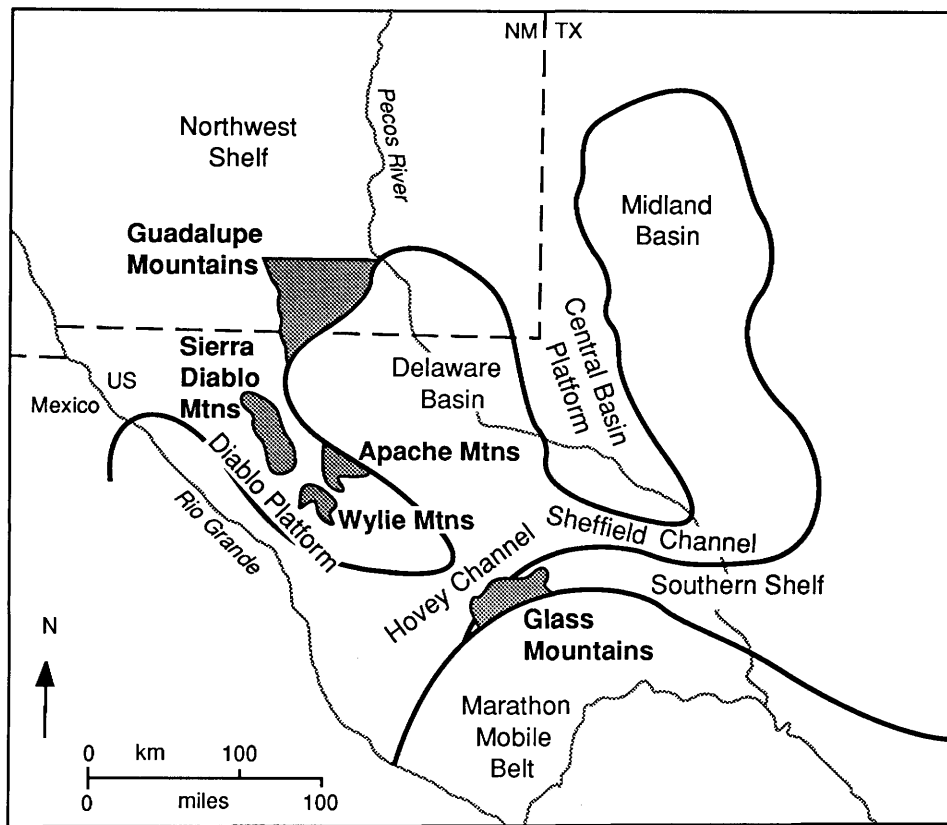


FIGURE 7-1.—Location of the mountain ranges mentioned in the text relative to Permian paleogeography. Modified from King (1948).

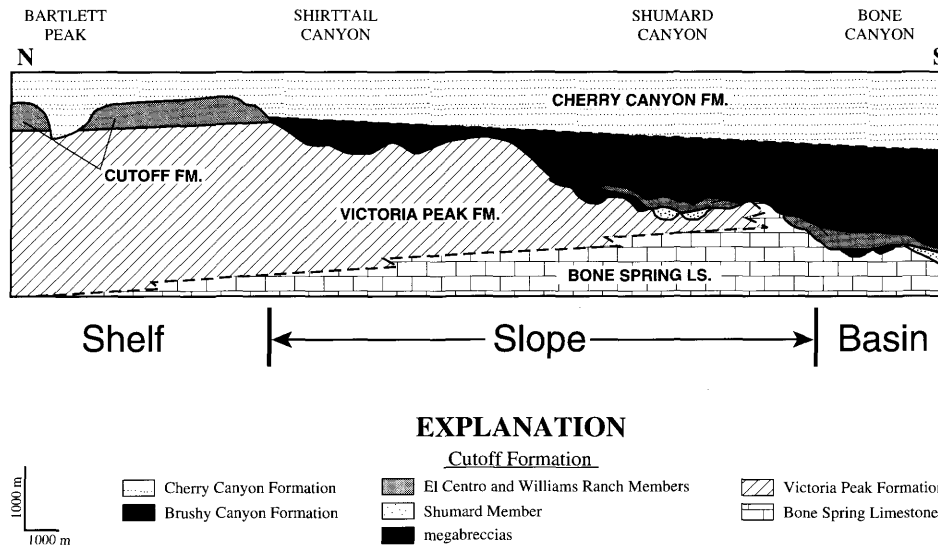


FIGURE 7-2.—North-south cross section of the Cutoff Formation along the western escarpment of the Guadalupe Mountains. Note that the vertical exaggeration is $\times 2$.

The most significant observations concerning the Cutoff Formation in the context of this paper are as follows: (1) the strata were deposited over a paleoslope with a relief of 300 m; (2) draping lutites are the dominant lithology; (3) these lutites occur in correlatable units that help resolve the shelf margin-to-basin correlation; (4) eroded channels and coarser-grained lithologies occur along the slope and basin edge; and (5) three erosional unconformities bracket and subdivide the formation.

LUTITE LITHOLOGIES

The Cutoff Formation consists of lime mudstone and shale (95%+ of the strata), with coarser-grained lithologies that locally occur along the slope and basin edge (for details, see Harris, 1982, 1988a). (Herein we use the carbonate rock classification of Embry and Klovan's (1971) modification of Dunham (1962).) In slope and basin areas, three types of lutites occur: (1) medium-bedded, black, cherty lime mudstone with abundant black chert seams (5%–15%) and variable laminations; (2) medium-bedded, dark gray lime mudstone with shaly partings, variable laminations, a very sparse brachiopod fauna, and minor quartz silt; and (3) interbedded argillaceous lime mudstone and calcareous shale, which are both dark brown to dark gray to black, unfossiliferous, thinly laminated, and fissile. In places, thin to very thin beds of finely laminated siltstone occur. In outer (more basinward) shelf areas (Shirttail Canyon to Cutoff Mountain), medium-bedded medium gray lime mudstone comprises the top of the section. Several thin skeletal-rich wackestone layers occur within the medium gray lime mudstone at the type section.

The lutites are suspension deposits that drape pre-existing topography. Slight bedding thickness variations indicate only minor current activity during deposition. The distribution of skeletal fauna, bioturbation, and lamination styles within the lime mudstones indicate deposition in an anoxic basin (Byers, 1971; Harris, 1988a). Dysaerobic (oxygen-poor) waters extended northward onto the outer shelf where the initial water depth during Cutoff deposition was approximately 40–50 m. Anaerobic (oxygen-depleted) conditions in the lower slope and basin areas existed at paleodepths of over 250 m. Shelf sections thicken northward, and carbonate textures indicate upward and landward shallowing that was probably related to the progradation of the shallow-water skeletal facies of the San Andres Formation (Boyd, 1958; Sarg and Lehmann, 1986a).

SHELF-TO-BASIN CORRELATION

A vertical succession of five correlation units is recognized within the Cutoff strata from the shelf edge to the basin. This succession provides a stratigraphic framework that helps resolve shelf-to-basin correlation (Figure 7-6). The five-fold succession is as follows:

Williams Ranch Member	Unit 5: Medium-bedded lime mudstone
El Centro Member	Unit 4: Interbedded lime mudstone and shale Unit 3: Medium-bedded lime mudstone Unit 2: Interbedded lime mudstone and shale
Shumard Member	Unit 1: Black, cherty lime mudstone

The Shumard Member has the most restricted distribution in the shelf and slope areas due to erosion along an intraforma-

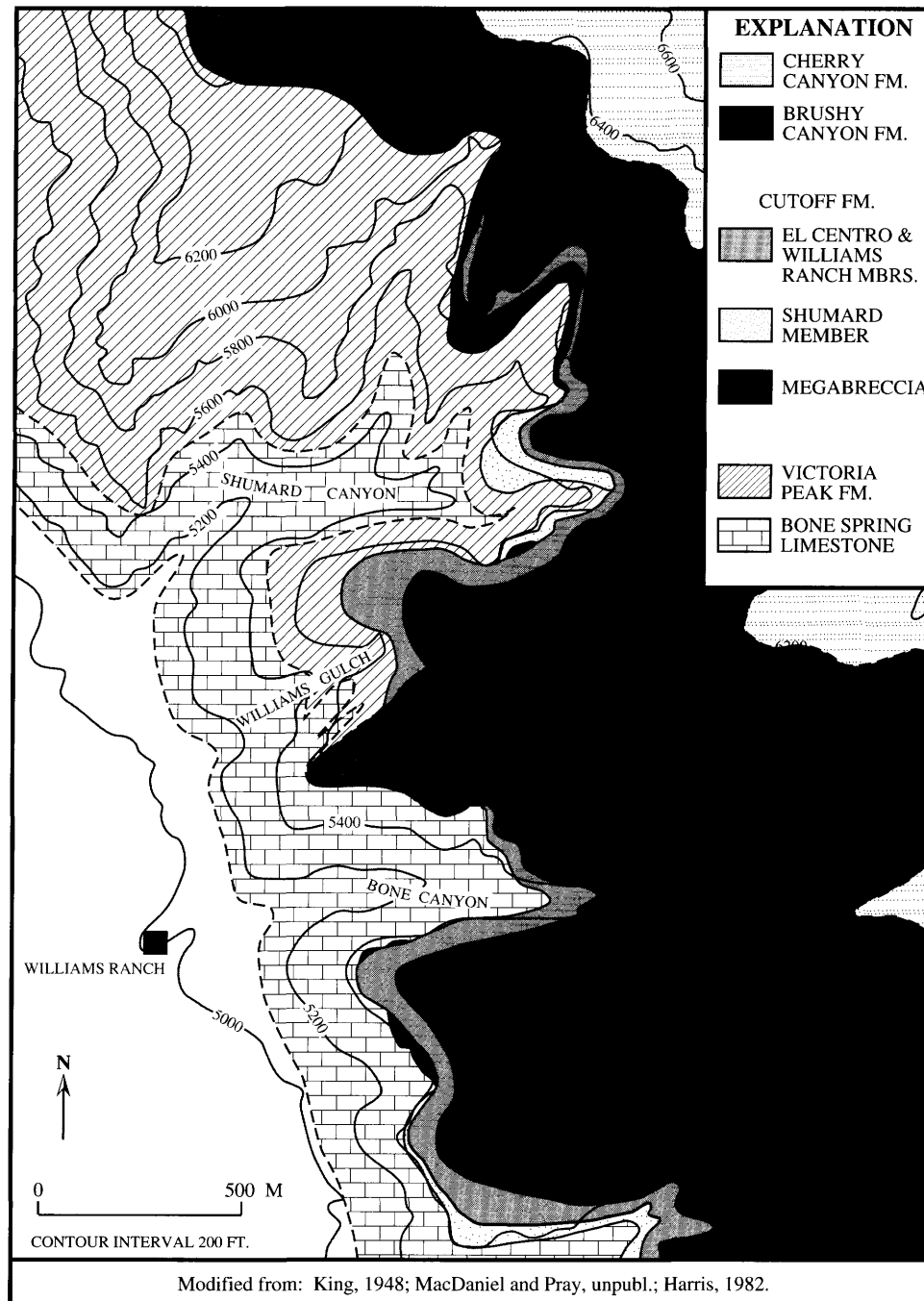


FIGURE 7-3.—Geologic map of the Bone Canyon–Shumard Canyon area in the western Guadalupe Mountains. This area is the lower slope environment during Cutoff Formation deposition (compare with Figure 7-2).

tional unconformity that separates the Shumard and El Centro members. The El Centro Member (units 2, 3, and 4) consists of a distinct “triplet” of two shale packages separated by a thin limestone bench. The Williams Ranch Member locally thins beneath the unconformity at the top of the Cutoff Formation. It thickens basinward to comprise about one-half of the upper Cutoff strata south of Bone Canyon.

The textures and faunal content within the lime mudstone units support the anoxic basin model; but within the interbedded lime mudstone and shale (units 2 and 4), diagenesis of these clay-rich rocks has obliterated any variation in depositional laminations. The cause of the alternation of limestone and shale units is unclear. It may relate to variations in carbonate shelf position related to backstepping and prograde-

Formations	Members
Brushy Canyon Formation	undifferentiated
Cutoff Formation	Williams Ranch Member El Centro Member Shumard Canyon Member
Bone Spring Limestone	undifferentiated

FIGURE 7-4.—Stratigraphic nomenclature for the Cutoff Formation of the western Guadalupe Mountains (modified from Harris, this volume).

tion (Sarg and Lehmann, 1986a). Because the correlation units consist of suspension deposits, they are interpreted to be the result of synchronous changes in shelf-derived lutite material. Faunal correlations support synchroniety (Lambert et al., this volume).

COARSER ROCK TYPES

Coarser-grained lithologies (sandstone, rudstone, and mega-

breccia) occur as lens-shaped channel fills or as sheet-like bodies in slope and basin areas. They are distributed vertically throughout the Cutoff strata, and most overlie truncation surfaces. These grain-supported rocks are ungraded and may be divided into two groups: poorly-sorted textures with mud-filled intergranular spaces, and well-sorted textures with mud-free intergranular spaces. The first group includes megabreccias and most intraclastic rudstones. Skeletal rudstones, quartz sandstones, and some intraclastic rudstones comprise the second group. For both groups, grain-supported textures, erosive bases, and channel morphologies all suggest that these rocks are turbulent flow deposits. The poorly sorted lithologies may be modified debris flows. The well-sorted lithologies are probably normal traction deposits.

Megabreccia and rudstone clasts produce most of the megafauna attributed to the Cutoff strata in the western escarpment area. Megabreccia clasts in channel lenses at the base of the Cutoff section are derived from the underlying Victorio Peak Limestone and Bone Spring Limestone. Higher in the section, the principal clast source shifts to the lutites of the Cutoff Formation, indicating erosion of the shelf edge and/or upper slope.

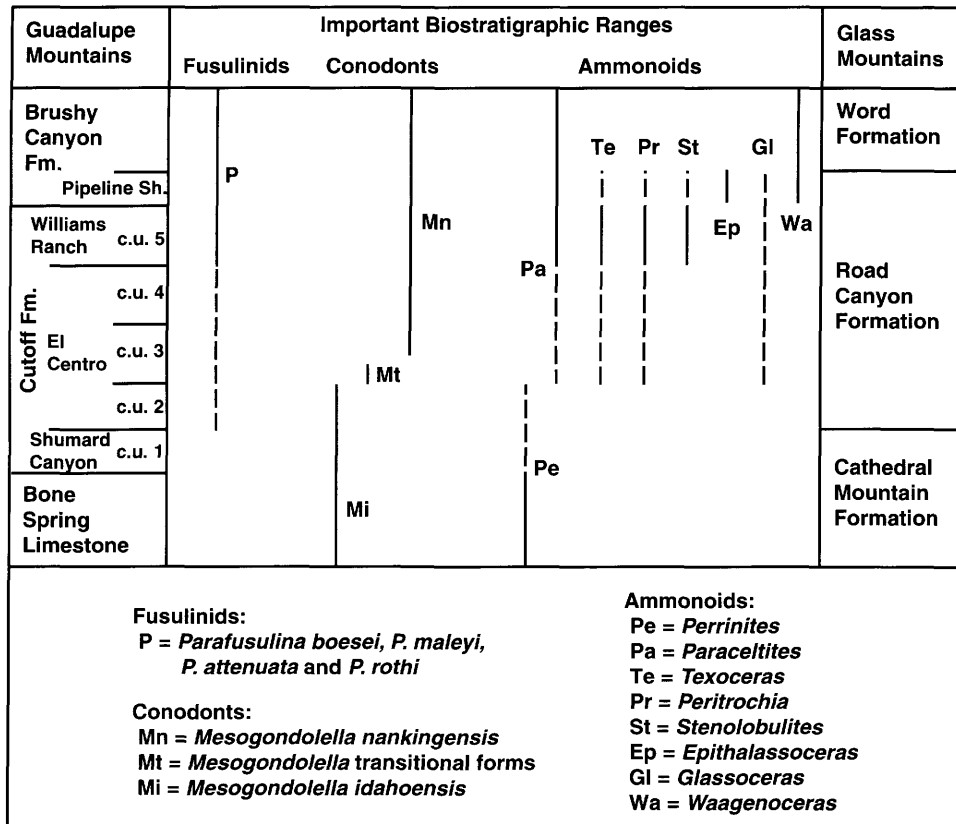


FIGURE 7-5.—Correlation of the Cutoff Formation (Guadalupe Mountains) to the Road Canyon Formation (Glass Mountains). Dashed ranges only occur in the Glass Mountains. *Glassoceras* may include specimens now assignable to *Demarezites*. Fusulinid data from Wilde, 1990. (For more information, see Lambert et al., this volume.)

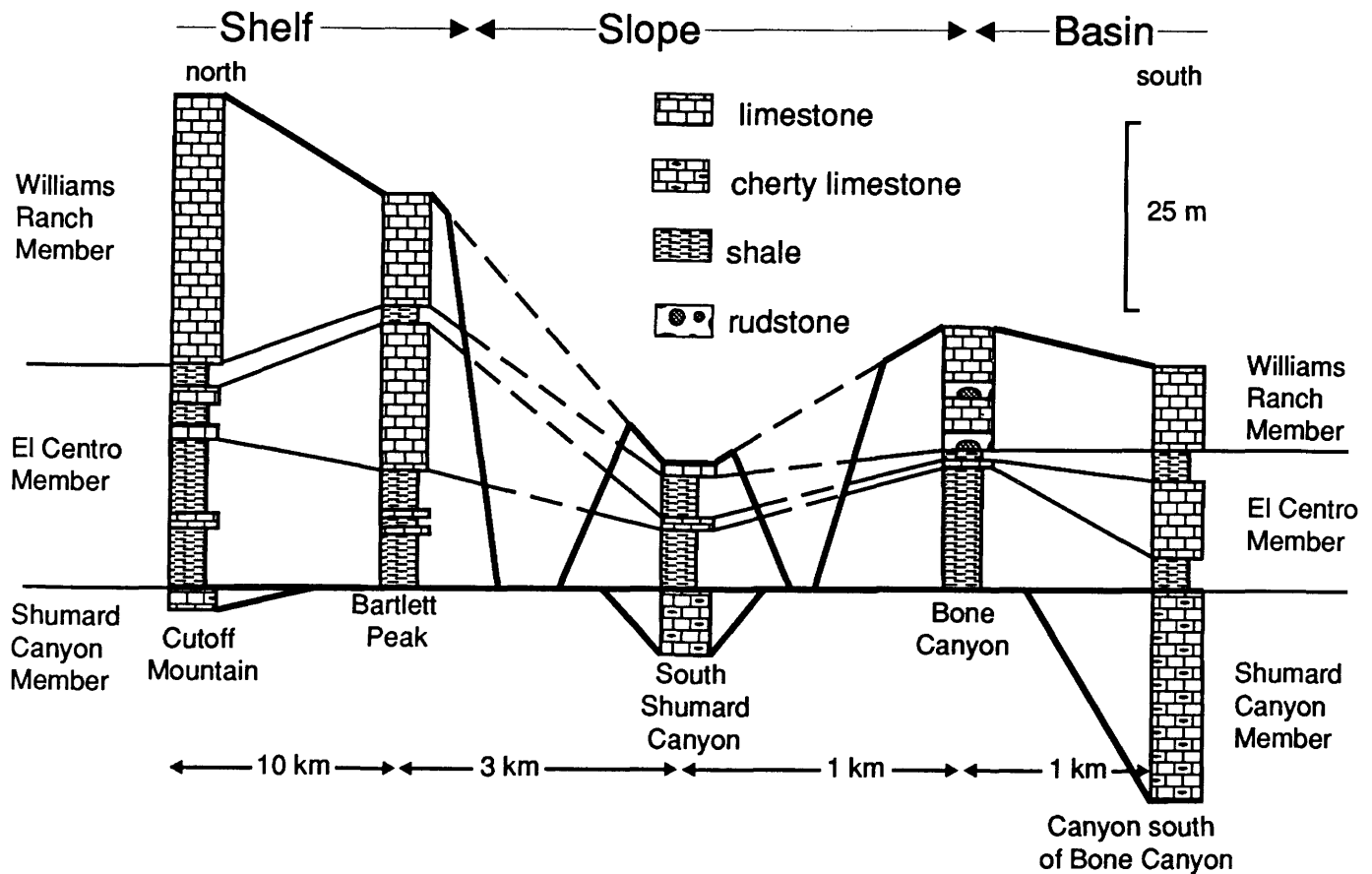


FIGURE 7-6.—Correlation of representative sections of the members of the Cutoff Formation (western Guadalupe Mountains), illustrating the informal correlation units. (Thin lines = correlation lines; thick lines = the three major unconformities of the Cutoff Formation.)

TRUNCATION SURFACES

Submarine truncation surfaces occur vertically throughout the Cutoff Formation and are concentrated at the slope and basin edge. They occur in three forms: (1) channel cross-sections with a relief ranging from a few centimeters to 50 m, (2) spoon-shaped "half-channels" that truncate more than 100 m of strata at the shelf edge (Pray et al., 1980; Franseen et al., 1988), and (3) low-angle (1° – 5°) truncation of beds in shelf and basin areas over a distance of several kilometers.

Several points should be noted about these truncation surfaces (for a fuller discussion see Harris, 1987). First, three widespread shelf-to-basin unconformities occur at the base and top of the Cutoff strata (Pray, 1971) and between the Shumard and El Centro members throughout the western escarpment outcrops (Harris, 1982, 1988a) (Figure 7-6). Second, truncation surfaces cause the discontinuous distribution of Cutoff strata along the shelf-to-basin transect. This is due to both truncation along the unconformities and intraformational surfaces. Third, both coarse, channel-filling lithologies and lutites overlie these truncation surfaces. The coarse channel fills occur in a lower

slope to basin-edge position along the profile (Figure 7-6). The megabreccia-filled channels (Pray and Stehli, 1963; "patch reefs" of Newell et al., 1953) only occur along unconformity surfaces. Fourth, the sandstone at the base of the Shumard Member in Shumard Canyon sits immediately above the lower unconformity. It may be correlative to a more basinward, thicker sandstone unit in a similar stratigraphic position in Brushy Canyon (Delaware Mountains, Christine Rossen, pers. comm., 1991). Finally, the basinal sections (south of Bone Canyon) appear to be the most complete, based upon the thickness of the different correlation units.

The Cutoff truncation surfaces are interpreted as subaqueous because of (1) a lack of features typical of vadose, subaerial, or shallow marine environments, (2) the basinal nature of Cutoff strata, and (3) the similarity of these surfaces to features in the overlying deep-water deposits of the Delaware Mountain Group (Harms and Pray, 1974; Harris, 1988a). The occurrence of channel forms along truncation surfaces and the coarse redeposited clasts in the channel fills imply the surfaces are, at least in part, erosional in origin.

FIELD RELATIONS

This section describes the field relations along a north-to-south transect from the top of the steep paleoslope north of Shumard Canyon to the edge of the basin south of Bone Canyon. The preserved depositional dip profile allows truncation surfaces, lutites, and coarser lithologies to be located in their appropriate depositional setting.

SHELF (Cutoff Mountain to north of Shirttail Canyon).—The Cutoff shelf strata overlies a low angle unconformity surface that truncates beds of the Victorio Peak Limestone (Harris, 1987; Kirkby, 1988). The Cutoff Formation is 60–75 m thick from the type section southward to the outer shelf edge (Figures 7-2, 7-6). The Shumard Member is absent from the outer shelf area, but 2–4 m occur at the Cutoff type section; this distribution is due to truncation along the undulatory intraformational unconformity between the Shumard and the overlying El Centro. The upper Cutoff strata consists of a lower shale-dominated section (El Centro Member) and an upper carbonate section (Williams Ranch Member). Near Bartlett Peak, 2.5 km north of the shelf edge, a large channel filled with Cherry Canyon sandstone and two carbonate megabreccia sheets cuts through 75 m of Cutoff strata and 30 m into the Victorio Peak Limestone (Harms, 1974; Harris, 1988a; Kirkby, 1988). The southernmost Cutoff shelf section is delineated by an erosional surface, which truncates the entire Cutoff Formation and the uppermost Victorio Peak Limestone north of Shirttail Canyon (Harris, 1988a; Kirkby, 1988; Rossen and Sarg, 1988) (Figure 7-7).

SLOPE (north of Shirttail Canyon to Bone Canyon).—The Cutoff Formation is discontinuous in the slope area because of erosion along the intraformational and post-Cutoff unconformities (Figures 7-2, 7-3, 7-6). A broad lens of Cutoff strata occurs

in the Shumard Canyon area (Figure 7-8), separated from the shelf equivalents by a distance of 1.5 km. A less extensive gap (350 m wide) separates these exposures from the Bone Canyon outcrops.

The recognition of Cutoff correlation units 2–5 facilitates correlation of the outcrops in southern Shumard Canyon and the draw to the south (informally termed Williams Gulch) with those in Bone Canyon. The distinctive El Centro shale-carbonate–shale triplet, overlain by the thick Williams Ranch carbonate, is recognizable in both areas despite truncation along the post-Cutoff unconformity (Figures 7-6, 7-9, 7-10). In southern Shumard Canyon, cherty lime mudstones of the Shumard Member occur within a single channel fill along with minor basal beds of intraclastic rudstone and quartz sandstone (Figures 7-8, 7-9). This channel is oriented south to southwest and cuts 47 m into the underlying Victorio Peak.

Numerous channels locally truncate strata in the upper Cutoff Formation. Channel forms are best exposed at the base of the slope in Bone Canyon (Figures 7-11, 7-12). Two channel types occur: broad (100–160 m) forms with flattened ($< 10^\circ$) sides predominantly filled with lutites and minor intraclastic rudstone lenses, and narrow (< 30 m), steep-sided ($> 10^\circ$) forms with megabreccia channel fillings (Pray and Stehli, 1963; the “patch reefs” of Newell et al., 1953). Megabreccias at the base of the Cutoff Formation contain Victorio Peak and Bone Spring clasts, reflecting erosion of the pre-existing Leonardian bank. Victorio Peak and Cutoff clasts within upper Cutoff intraclastic rudstones record the continued shelfward retreat of the shelf edge.

BASIN (south of Bone Canyon).—The Cutoff thickens basinward by the stratigraphic thickening of individual units and by the decreasing truncation along unconformity surfaces. The Shumard Member appears about 450 m south of Bone

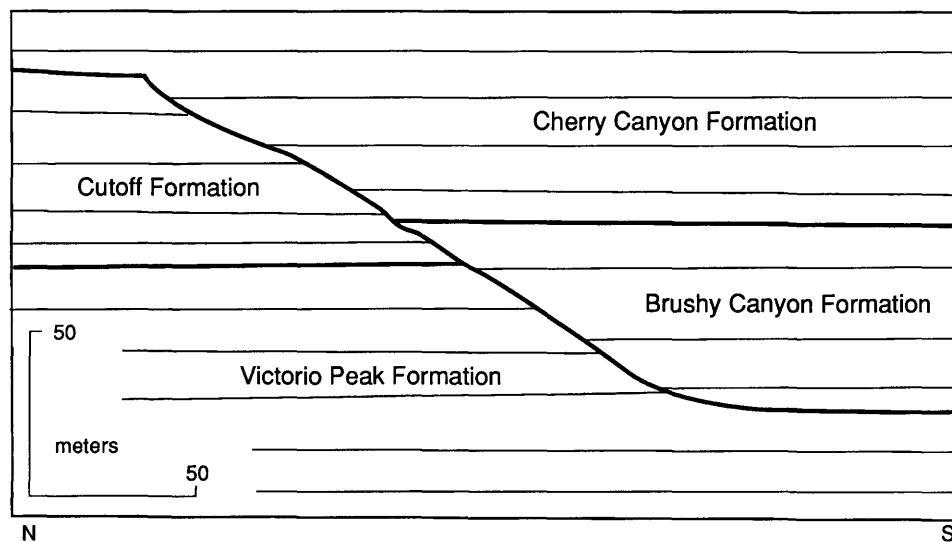


FIGURE 7-7.—Pinchout of the Cutoff Formation at the shelf edge. (Adapted from an original by Kirkby for Pray et al., 1980.)

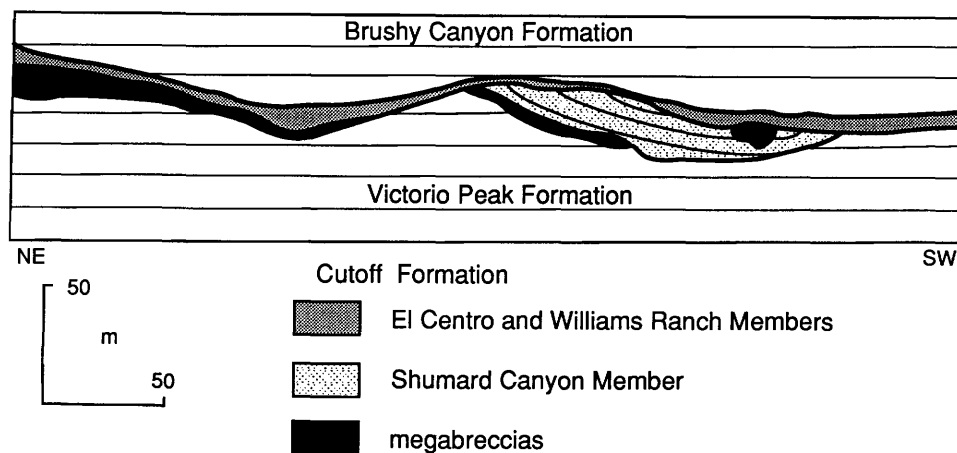


FIGURE 7-8.—Overview of Shumard Canyon from the north. Note the channel-filling geometry of the lower Cutoff strata. (Adapted from an original by Kirkby for Pray et al., 1980.)

Canyon and overlies an unconformity that separates it from the Bone Spring Limestone. Its contact with the El Centro Member is also an unconformity, similar to that in the slope settings. Stratal truncation along this unconformity decreases to the south, so that the Shumard Member increases in thickness from its truncated feather edge to 34 m over a distance of 0.5 km. Further south it disappears into the subsurface.

The El Centro and Williams Ranch members thicken basinward from 40 m, in the south wall of Bone Canyon, to 93 m over a distance of 1.7 km to the south. Truncation along the upper Cutoff surface decreases basinward to essentially zero within a kilometer of Bone Canyon. This expanded upper Cutoff section has been traced into the low black hills south and southwest of El Capitan. King (1948) and Newell et al. (1953) considered these hills to be composed of the Bone Spring Limestone. Conodonts confirm the correlation of these strata with the upper Cutoff to the north (Lambert et al., this volume). In the most basinward sections, the Shumard Member constitutes approximately one-fourth of the entire Cutoff section, although it is absent over most of the steeply dipping paleoslope.

Small, poorly exposed channels, with relief of up to 1 m, and rare slump features occur within the basinal Cutoff strata. These are inferred to be similar in their geometry to the well-exposed channels in the slope area. The Bone Spring fauna reported by King (1948) from this area was collected from these channel deposits.

CUTOFF FORMATION DEPOSITIONAL SETTING

The Cutoff Formation records an abrupt deepening of the outer Northwest Shelf of the Delaware basin. Shallow-water shelf deposition retreated to southern New Mexico (Boyd, 1958; Sarg and Lehmann, 1986a) and fine-grained shales and lime-muds mantled the underlying shallow-water lithologies of

the Victorio Peak Limestone. Anoxic waters transgressed over the outer shelf, estimated at 40–50 m in depth (Harris, 1988a). These anoxic conditions, recorded in the lime mudstone units, indicate that a stable, stratified water column existed throughout Cutoff deposition. Submarine truncation and erosion disrupted stratigraphic continuity. Coarse megabreccia and rudstone deposits containing shallow-water lithoclasts are readily identifiable as downslope allochthonous debris because of the preserved depositional profile.

The depositional style and associated erosion surfaces of the Cutoff strata are consistent with the density current model proposed by Harms (1974) and Harms and Pray (1974) for the overlying Brushy Canyon Formation, but modified for an anoxic carbonate basin setting. The Cutoff suspension-deposited lutites are punctuated by erosional features and traction deposits from denser, bottom-hugging currents. The predominance of lutites is probably due to the general lack of sand-sized particles. Bottom currents are recorded largely by erosion surfaces. The abundance of megabreccias and intraclastic rudstones was probably due to the availability of clasts from erosion of updip lithified Victorio Peak and Cutoff carbonates. Alternations of erosion and deposition along the slope produced a complex pattern of truncation and bedding surfaces.

The Road Canyon Formation of the Glass Mountains

The Road Canyon Formation consists of organic-rich spiculitic lutites and coarse allochthonous limestones. It is sandwiched between silicious shales, siltstones, and spiculitic lutites of the Cathedral Mountain Formation (Leonardian) and similar lithologies of the lower Word Formation (Guadalupian) (Figure 7-13). In the eastern Glass Mountains the Road Canyon Formation occurs above the Hess Formation shelf facies, whereas in the western Glass Mountains it occurs above the

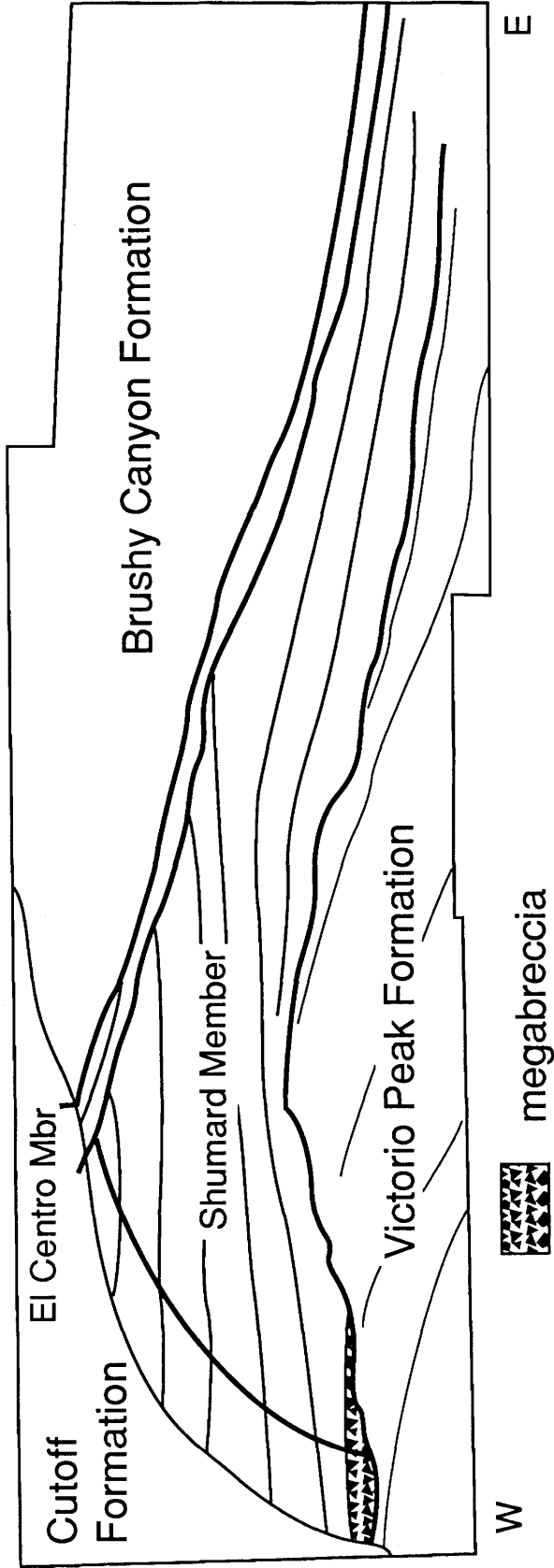


FIGURE 7-9.—North wall of south Shumard Canyon. Note the channel-filling geometry of the lower Cutoff strata and unconformities.

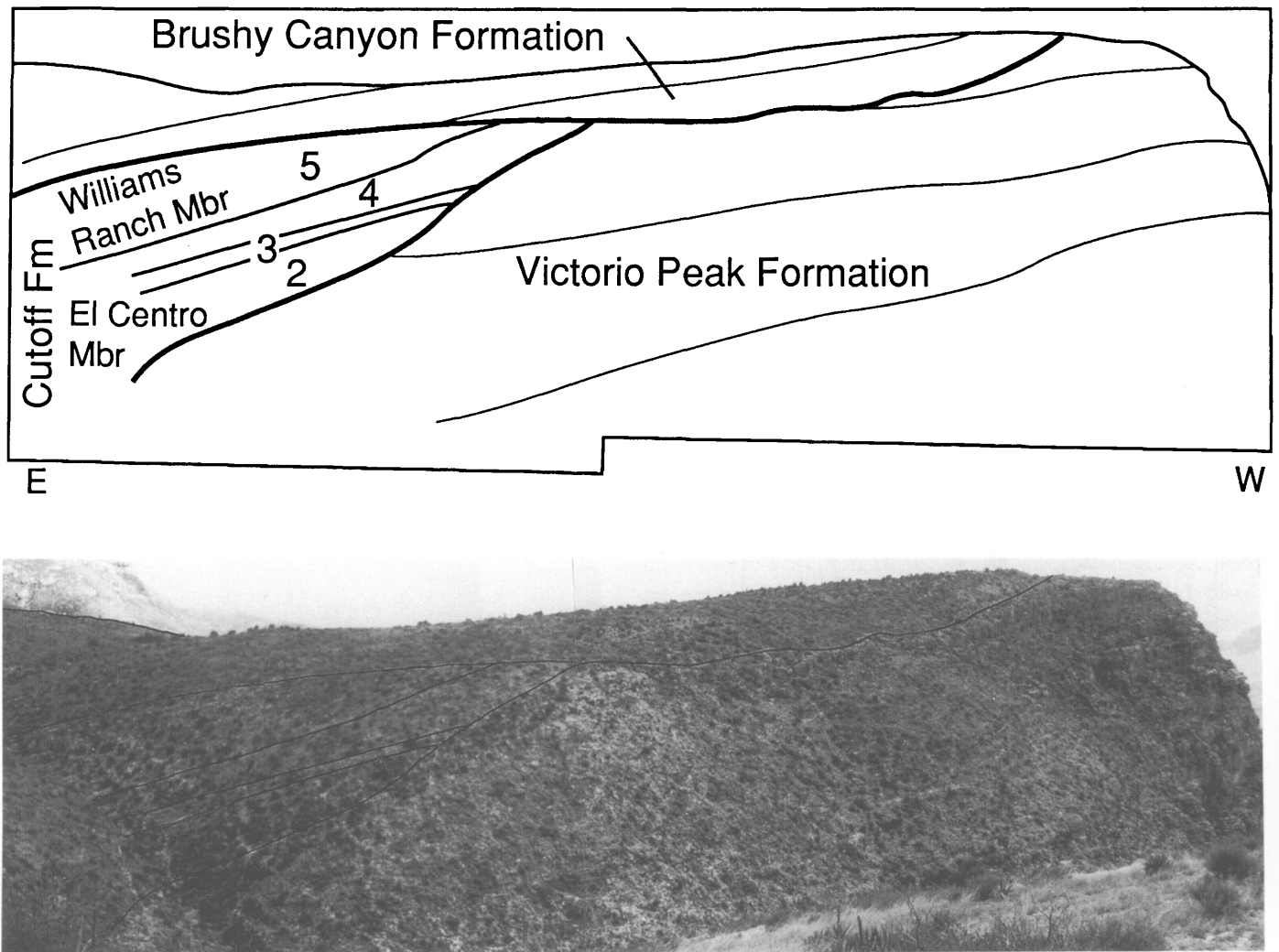


FIGURE 7-10.—South wall of Williams Gulch, illustrating the basinward pinchout of the Cutoff strata in the lower slope position. Note the channel-like morphology of the stratal onlap (C. Rossen, pers. comm., 1991).

slope and basal facies (King, 1942; Rogers, 1972, 1978; Cys and Mazzullo, 1978; Cys, 1981; Ross, 1986, 1987) of the Skinner Ranch and Cathedral Mountain Formations. Philip B. King (1931) interpreted the Glass Mountains as exposing a highly oblique cross section through a northeast-southwest trending shelf-to-basin margin with reef and backreef environments to the southeast and the basin to the northwest. Thus, in the Glass Mountains, shelf facies in the east contrast with more basinward facies in the west.

The stratigraphic nomenclature used herein follows Cooper and Grant's (1966) modification of King (1931) (Figures 7-13, 7-14, 7-16); see Ross (1987) and Lehrmann (1988) for further nomenclature history. The Road Canyon Formation is the basis of the Roadian Stage (Furnish, 1966, 1973), and its type section lies in the central Glass Mountains (Cooper and Grant, 1964). Its contact with the overlying Word Formation is gradational

and is generally selected on the relative proportion of carbonate to siliceous shale. In this study, the bed selected for the contact is the uppermost persistent (50–100 m laterally) limestone greater than 60 cm thick. This definition includes a variable proportion of lutites but agrees with King's (1931) original definition. To the east (Old Word Ranch area), the Road Canyon Formation merges with the next higher carbonate unit (China Tank Member of Cooper and Grant, 1966) in the Word Formation by pinch out of the intervening shale. Strata equivalent to the Road Canyon are included within undifferentiated Word Formation in this area (Figure 7-15; section 1 of Figure 7-16).

The most significant observations and interpretations concerning the Road Canyon Formation for this paper are (1) the outcrop trend is highly oblique to depositional dip, (2) the strata consists of fine-grained spiculitic lutites (which indicate a deep

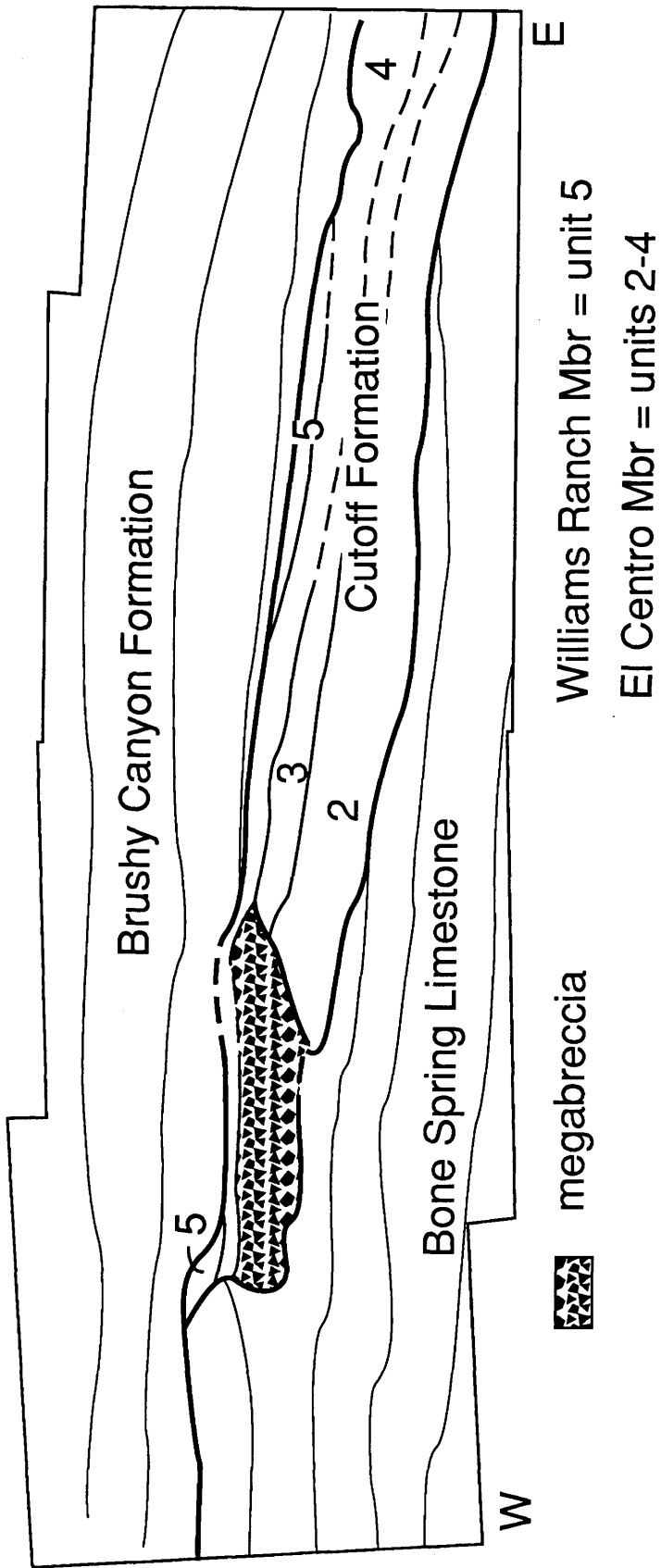


FIGURE 7-11.—North wall of Bone Canyon, illustrating the updip pinchout of the basal Cutoff strata due to the merging of two unconformities.

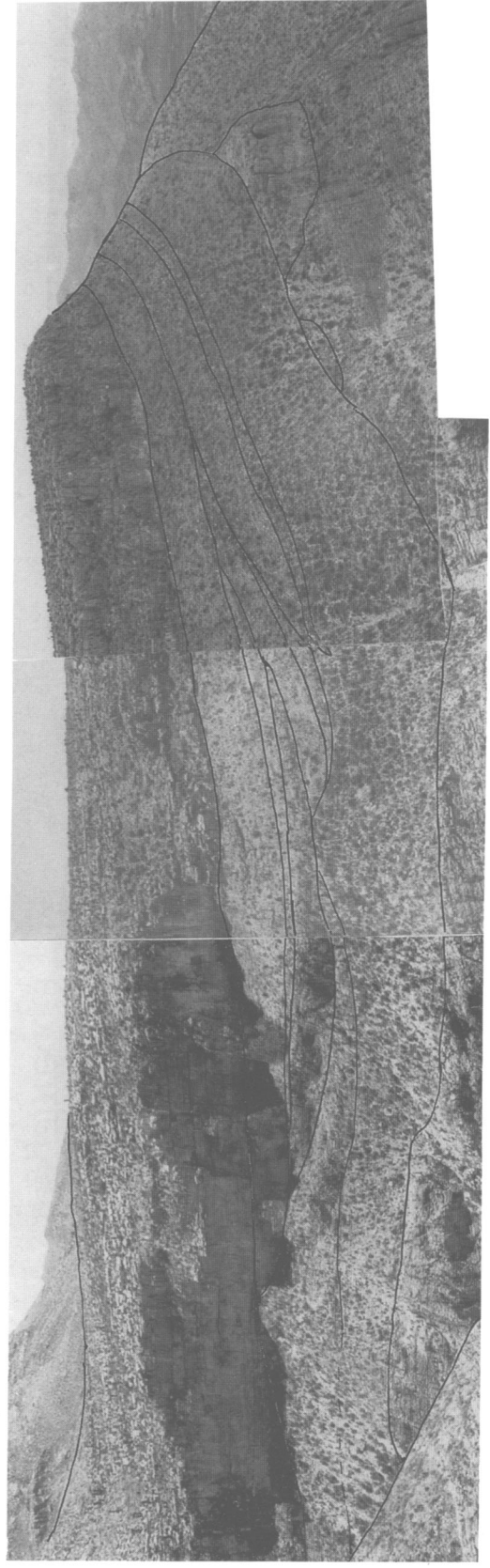
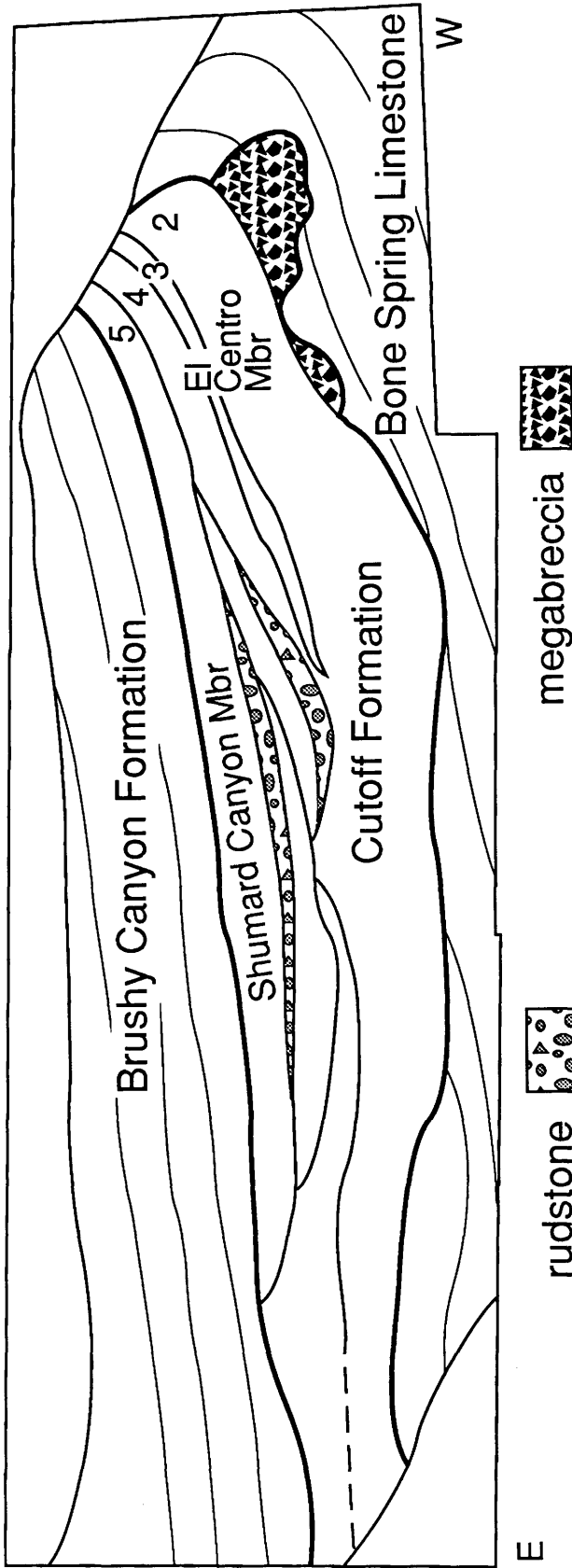


FIGURE 7-12.—Exposures in the south wall of Bone Canyon illustrate the occurrence of broad, low-angle channels predominantly filled with lutites, although some have early intraclastic rudstone fills. The megabreccias fill narrow, steep-sided channels at the base of the formation.

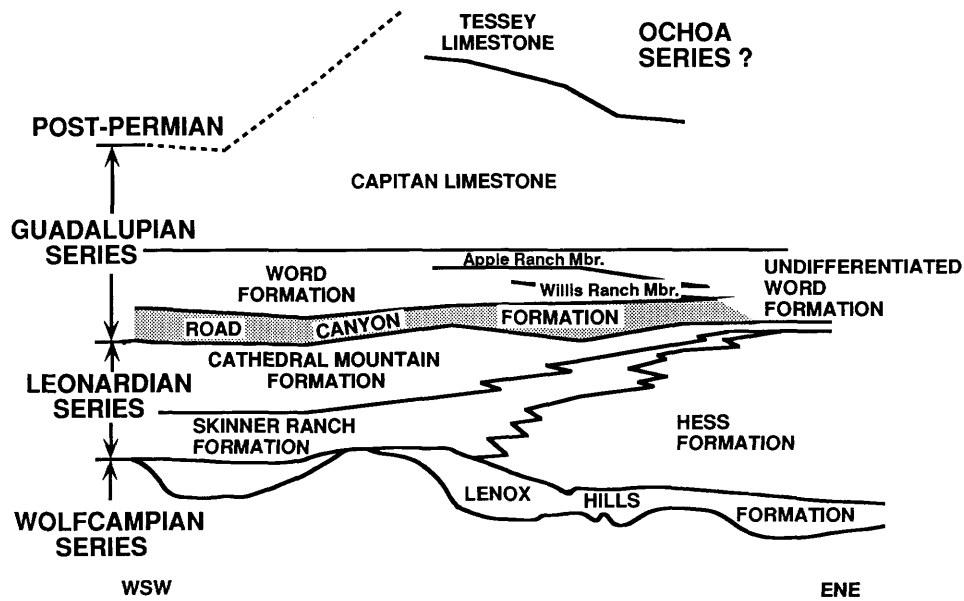


FIGURE 7-13.—Stratigraphic cross section of the Glass Mountains. (Modified from Ross, 1986.)

King 1930	Cooper and Grant 1964	Cooper and Grant 1966
Third Lst.	Apple Ranch Mbr	Apple Ranch Mbr
Word Formation	Word Formation	Word Formation
Second Lst.	Willis Ranch Mbr.	Willis Ranch Mbr.
First Lst.	Road Canyon Mbr.	Road Canyon Formation
Leonard Formation (top)	Cathedral Mountain Formation	Cathedral Mountain Formation

FIGURE 7-14.—Changes in Road Canyon nomenclature.

shelf or slope setting into which allochthonous deposits were introduced) with allochthonous channelized breccia and sand-sheet deposits, (3) two major intervals of megabreccia (with locally truncational bases) and a graded carbonate sand sheet (higher in the section) can be traced across the central Glass Mountains, and (4) channelized deposits and sparse current indicators support King's (1948) interpretation of basin direction.

LUTITE LITHOLOGIES

Lutites in the Road Canyon Formation are composed of lime-mud and fine-grained siliciclastics, with variable amounts of sponge spicules, radiolarians, and silicification. The lutites

can be subdivided into dark organic-rich lutite and orange lutite. Dark organic-rich lutite occurs in recessive fissile-laminated beds (Figure 7-17A) as well as resistant beds ranging from 3 to 12 cm thick with discontinuous wavy laminations (Figure 7-17B). This lithology locally contains syndimentary faults, which displace laminae up to 2.5 cm (Figure 7-17B), and folds adjacent to conglomeratic lens deposits. Orange lutite commonly weathers into thin, recessive, highly fissile beds or into more resistant silicified beds up to 13 cm thick. Spiculite/radiolarian-rich laminae and muddy layers alternate with coarser skeletal concentrations and organic-lean lenses and form fine parallel (Figure 7-17D) to thicker (1–2 mm) wavy, discontinuous (Figure 7-17B) laminations. Flattened

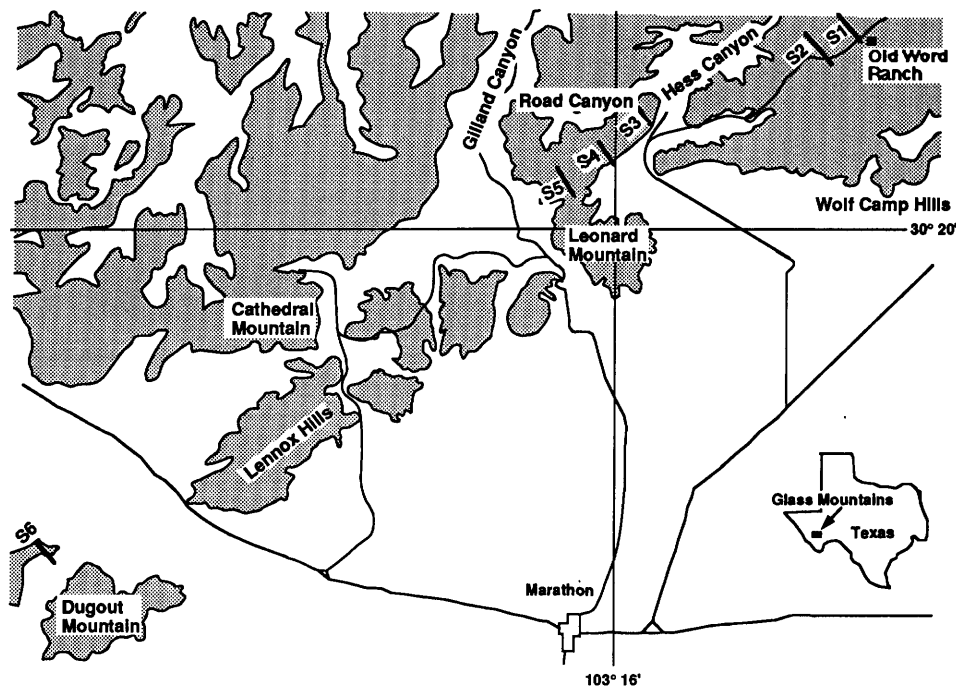


FIGURE 7-15.—Glass Mountains location map. S1 through S6 are the locations of the stratigraphic sections of Figure 7-16. (Modified from Cooper and Grant, 1966.)

organic-lean lenses are interpreted as horizontal feeding traces. In thin section, the high organic content causes the matrix to be dark-colored to opaque (Figure 7-17C). The major difference between orange and dark organic-rich lutite lithologies is the organic content. Orange weathering lutite has a lighter matrix, indicating lower organic content and more common silicification. Both lithologies contain silt-size sponge spicules and radiolarians, which have a patchy distribution (Figures 7-17C, 7-18). The internal lattice structures of radiolarians are preserved in some samples (Figure 7-18).

The lamination style and fossil content of the dark lutites indicate dysaerobic conditions that are similar to the Cutoff slope strata. Fine lamination, laminae-parallel bioturbation structures, lack of shelly fauna, and the high organic content suggest suspension deposition in the dysaerobic zone. Bottom currents that interrupted pelagic deposition formed the skeletal concentrations within the wavy laminations. The orange weathering lutite differs from the dark lutite in having a lower organic content and more common silicification. Dark lutite predominates in the eastern and western Glass Mountains, but it occurs only locally in the central Glass Mountains, where it grades laterally into the orange lutite (Figure 7-16). Orange lutite occurs predominantly in the upper half of the Road Canyon Formation in the central Glass Mountains. The transition from dark to orange lutite represents an environmental change to a more oxygenated depositional setting or a diagenetic effect (silicification?).

SKELETAL PACKSTONES AND GRAINSTONES

Fossiliferous packstones and grainstones occur as both bedded and lenticular deposits. These allodapic carbonates contain abundant peloids and skeletal grains and are locally oolitic (Figure 7-19A; P.B. King, 1931). Common skeletal grains include fine sand to granule-size bryozoans, brachiopods, crinoids, and fusulinids, all of which are commonly abraded and micritized.

Medium-bedded (15–30 cm thick beds) packstone to grainstone deposits occur in the central Glass Mountains within the lower half of the Road Canyon Formation, and they overly both the lower and upper megabreccia units (Figure 7-16). They are thicker over the edges of the underlying megabreccias, and they onlap over the central portions of the megabreccias. In the type section (section 5 of Figure 7-16), the medium-bedded grainstone unit overlying the lower megabreccia contains tabular cobble-size intraclasts near its base. Scour and drag marks at the base of this unit probably formed via dragging of the cobble-size intraclasts during transport. Skeletal packstone lenses (1–60 cm thick and 1–6 m wide) with flat upper surfaces (Figure 7-19C) truncate the underlying spiculite laminations (Figure 7-19B). Thicker, normally graded skeletal packstone lenses (> 30 cm) occur in the upper portion of the Road Canyon Formation in the central Glass Mountains (Figure 7-19D), whereas thinner lenses tend to occur in the eastern and western Glass Mountains.

These packstones and grainstones are interpreted to be

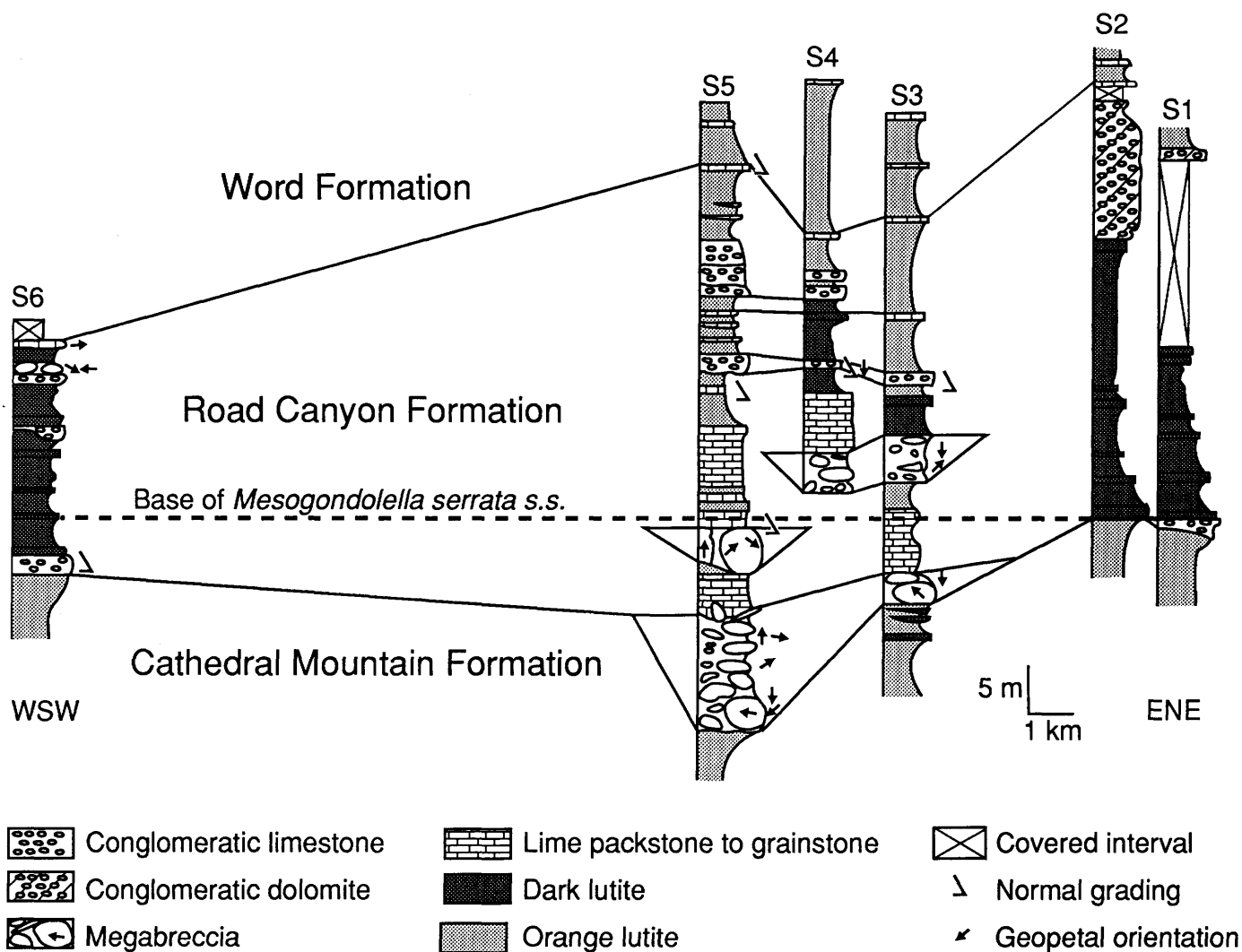


FIGURE 7-16.—Road Canyon Formation stratigraphic cross section. Section locations are shown in Figure 7-15. Section datum is the lowest occurrence of *Mesogondolella serrata* s.s. (now = *M. nankingensis* s.s.). Note widespread channeling at Road Canyon–Cathedral Mountain Formation contact. Distribution of conodonts detailed in Lambert et al. (this volume).

allodapic deposits transported downslope from shallow-water carbonate environments by bottom currents. The basal cobble-size clasts, scour and drag marks, and onlap against adjacent strata observed in the bedded units correspond to Harms (1974) model for deep-water clastic deposition. Skeletal packstone lenses are interpreted as carbonate turbidites based upon their erosive bases, planer upper surfaces, well-developed grading, and laminations in the upper portion.

COARSE INTRACLASTIC CONGLOMERATE AND MEGABRECCIA

Two size categories of coarse lithologies occur in the Road Canyon Formation: conglomeratic limestone and dolomite, and megabreccia. The conglomeratic limestone occurs as resistant,

partially silicified lenses and sheets that weather to a light gray to brown color. The clast-supported texture contains prominent pebble- to cobble-size clasts (up to 1 m across; Figure 7-20A) in a fossiliferous rudstone to packstone matrix. Clasts are angular to subrounded and include skeletal wackestone, packstone and grainstone, *Tubiphytes* boundstone, dark lutite, and orange lutite lithologies (Figure 7-20B). The matrix contains fragments of brachiopods, bryozoans, crinoids, fusulinids, rugose corals, *Tubiphytes*, and quartz silt. Conglomeratic limestones commonly truncate underlying beds and exhibit normal or inverse grading with parallel-bedded upper parts. In the Old Word Ranch area, conglomeratic limestones occur as conspicuous channel fills that truncate the underlying black spiculitic lutite at different levels (Figure 7-20C) up to 12 m above the base of

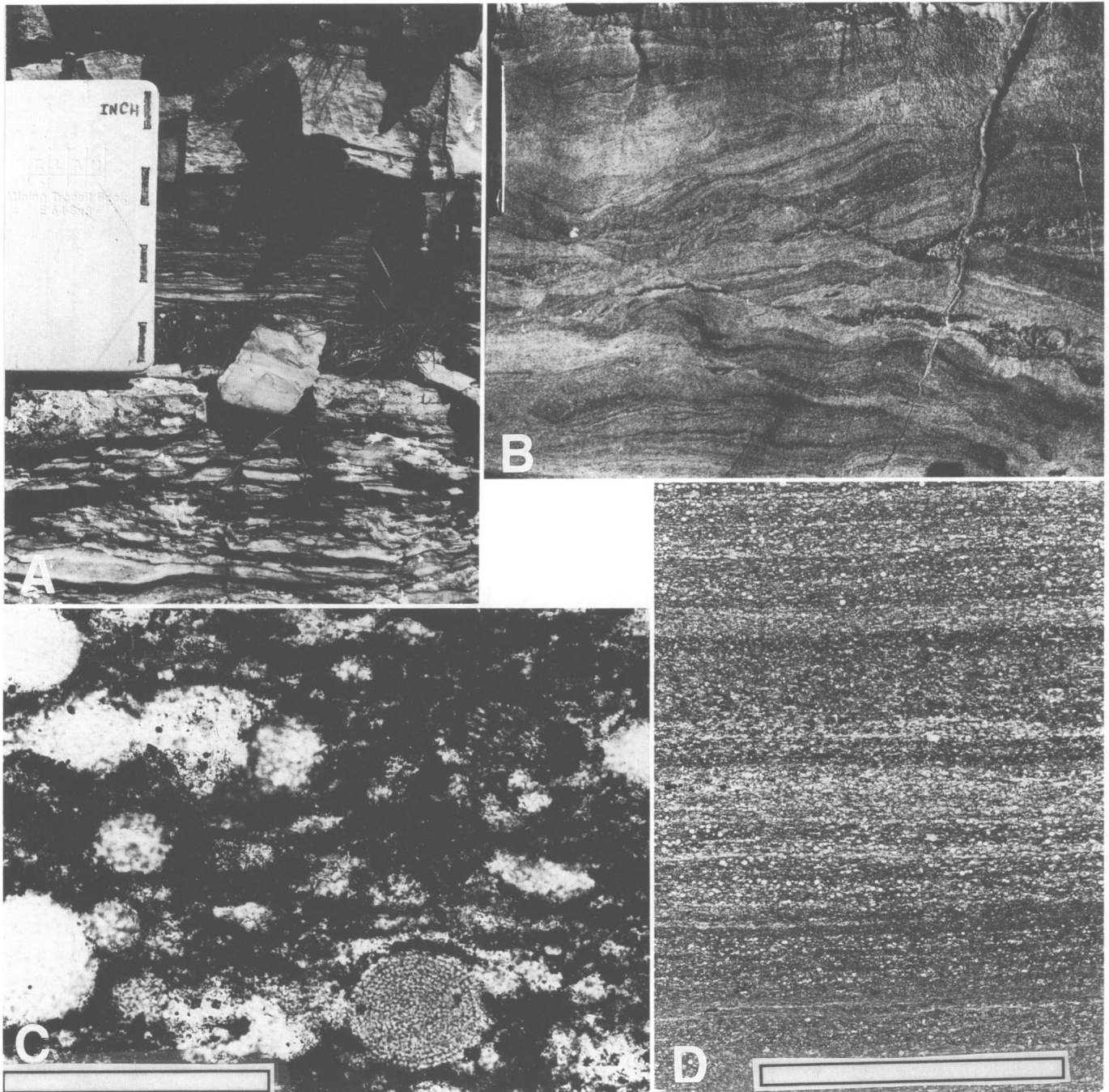


FIGURE 7-17.—Spiculitic lutite lithologies of the Road Canyon Formation. A, finely laminated black spiculitic lutite, eastern Glass Mountains, section 2. B, wavy, discontinuously laminated black spiculitic lutite with syndimentary faults, eastern Glass Mountains, section 2. C, radiolarians in spiculitic lutite. Spherical grains are silica. Internal radiolarian lattice structure is preserved in darker grains, possibly due to organic films, central Glass Mountains, section 5 (scale = 1 mm). D, fine parallel laminations in orange spiculitic lutite, central Glass Mountains, section 5 (scale = 1 cm).

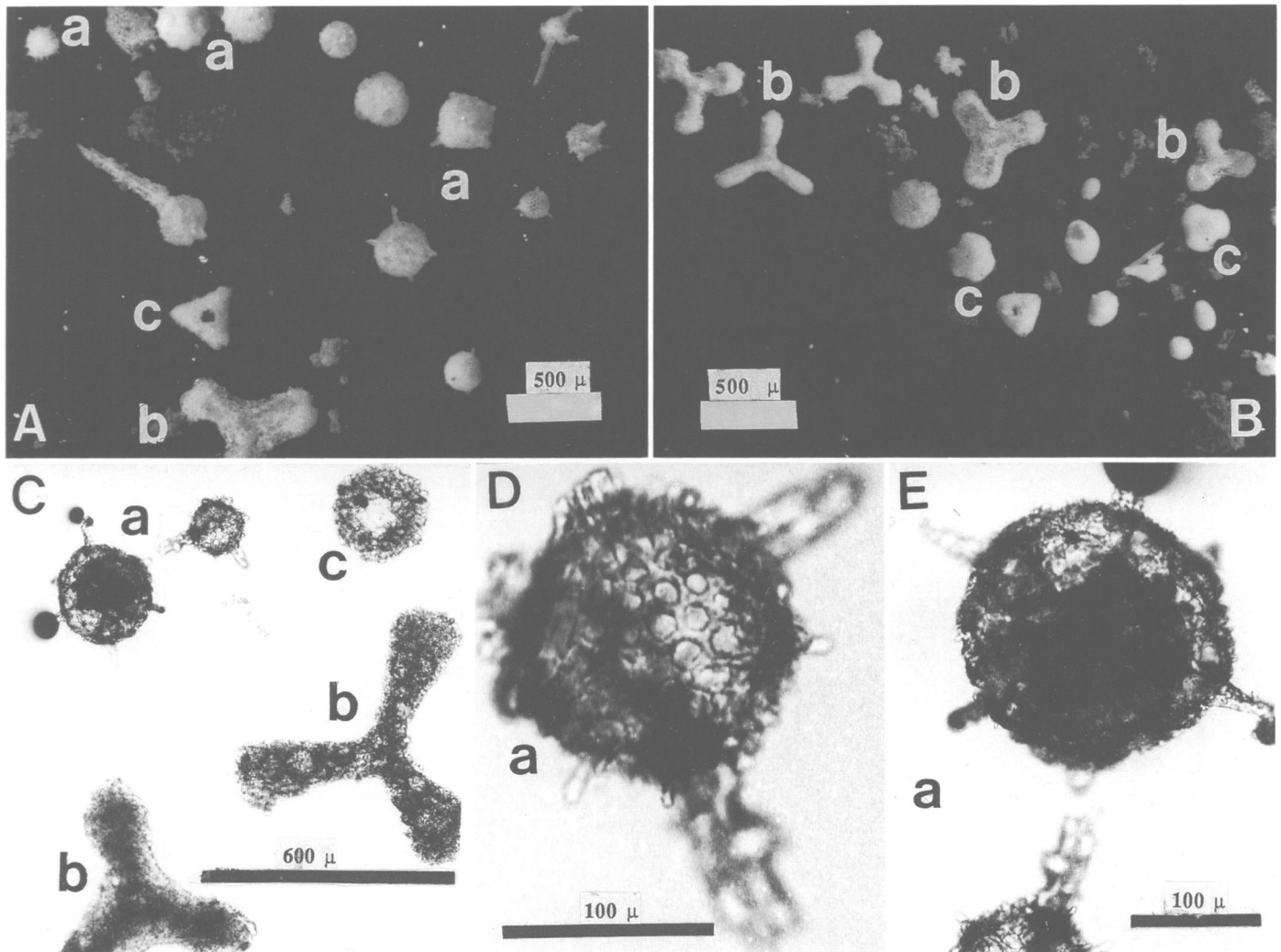


FIGURE 7-18.—Radiolarians from insoluble residues of black spiculitic lutites of the Road Canyon Formation in the central and eastern Glass Mountains in reflected light (A and B) and transmitted light (C, D, E). Spherical Spumellarians with lattice wall structure and with radial symmetry as indicated by preserved radial spines (a). Spongodiscid and/or Hagiastrid Spumellarians with spongy wall structure and discoidal-triradiate morphology (b). Discoidal radiolarians with spongy wall structure and triangular to circular discoidal shape with poorly developed radial arms (c).

the Road Canyon Formation. Overlying conglomerates in the upper Road Canyon are dolomitized and form the crests and dip slopes of hills in the area.

Megabreccia lenses are restricted to the central and western Glass Mountains (Figure 7-16), where they generally occur within the lower half of the Road Canyon Formation. This resistant lithology weathers gray or tan and forms ledges and cliffs. It is composed of pebble- to boulder-size limestone clasts (including blocks greater than 1 m across) in a skeletal rudstone to packstone matrix. Clast support is more common than matrix support. Within the matrix, pebble-size limestone clasts are commonly clast supported. Finer matrix material consists of fossil fragments, lime-mud, and minor quartz silt (Figure 7-20D). In some areas, a normally graded lithology (conglomeratic rudstone to mudstone) caps the megabreccia deposits.

Geopetals show these clasts to be randomly oriented. Geopetal data is summarized in Figure 7-16; arrows indicate the original top for measured geopetals.

Megabreccia clast lithologies include skeletal lime wackestones, packstones and grainstones (Figure 7-20E, F), boundstones (*Tubiphytes* boundstone, branching bryozoan framestone, and "reefal" brachiopod packstone), and dark lutite (Figure 7-20G). Rounded lutite clasts contain deformed internal laminations and margins sheared into the matrix (Figure 7-20G). *Tubiphytes* boundstone megaclasts contain geopetals with irregular cavities that are similar to those described from the Skinner Ranch Formation (Rogers, 1978). Further details of the megabreccia geometries and clast orientations in the Road Canyon type area (central Glass Mountains) are presented in Appendix 7-1.

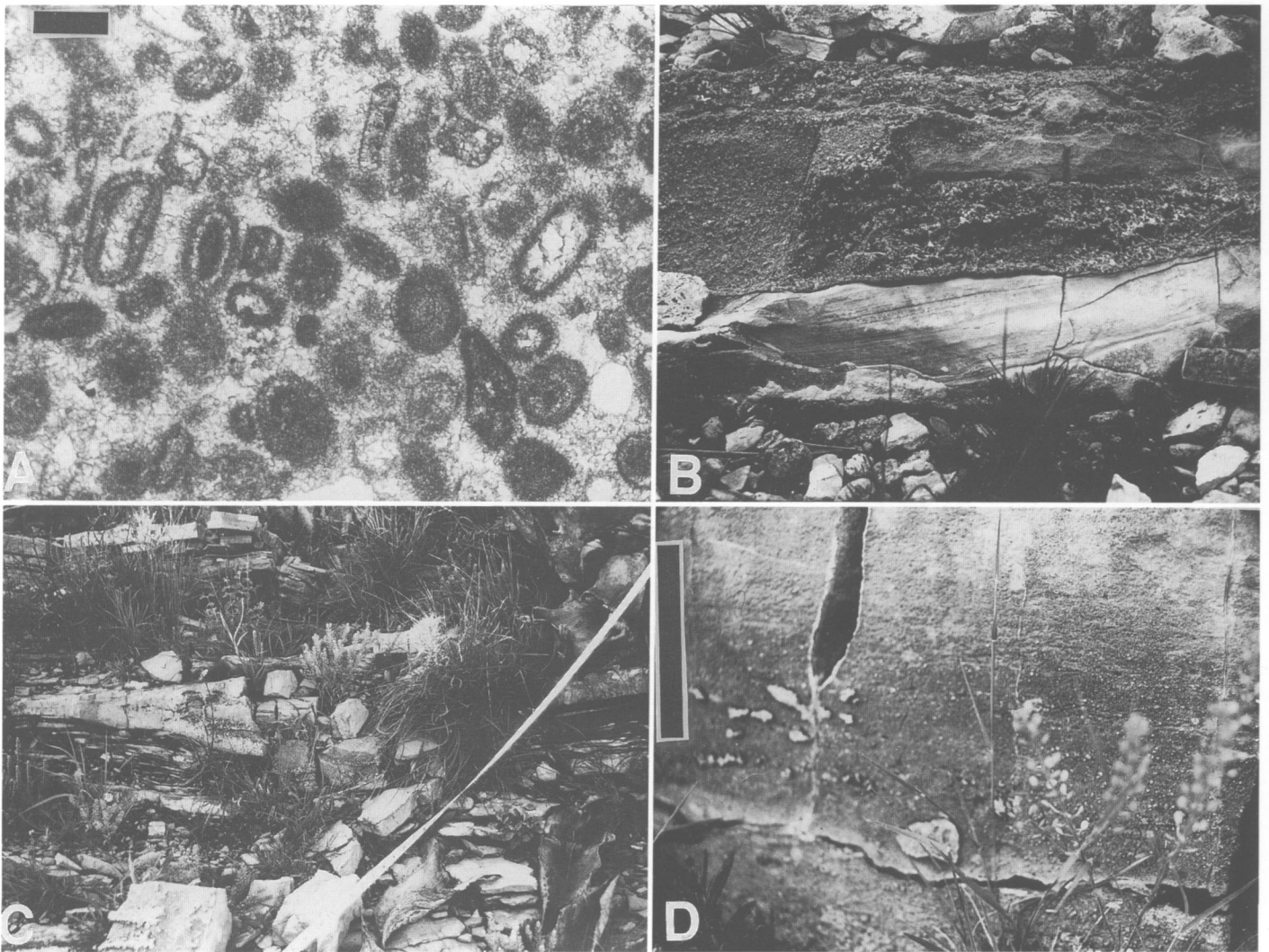


FIGURE 7-19.—Packstone and grainstone lithologies of the Road Canyon Formation. A, coated grains in medium-bedded packstone to grainstone lithofacies. Most grains contain one to a few coatings (“superficial oolites”) (scale = 1 mm). B, skeletal lime packstone lens truncating laminations of underlying black spiculitic lutite, eastern Glass Mountains, section 2. C, skeletal lime packstone lens interbedded with fissile orange spiculitic lutite, central Glass Mountains, section 5. Note the concave base and flat top. Maximum lens thickness is approximately 20 cm. D, normally graded packstone lens, central Glass Mountains, section 5 (scale = 10 cm).

The determination that the conglomeratic carbonates and megabreccias are allochthonous deposits that were transported as turbulent gravity flows is based upon (1) the fabric contrast with surrounding lutites, (2) the channelized geometry with erosive bases, (3) sedimentary structures, such as normal grading and cap facies, and (4) the shearing of the lutite clast boundaries into the matrix. The numerous clast types represent mixed sources from both the shelf and slope environments.

INTERNAL STRATIGRAPHY

The following internal stratigraphy of the Road Canyon Formation can be traced over 4 km in the central Glass Mountains (Figure 7-21):

Road Canyon Formation	spiculitic lutite graded limestone sheet spiculitic lutite medium-bedded packstone/grainstone upper megabreccia spiculitic lutite medium-bedded packstone/grainstone lower megabreccia
Cathedral Mountain Formation	spiculitic lutite

Recognition of a detailed internal stratigraphy provides a framework that facilitates biostratigraphic studies. The lower and upper megabreccia units contain more than one amalgamated gravity flow deposit. These megabreccia units are

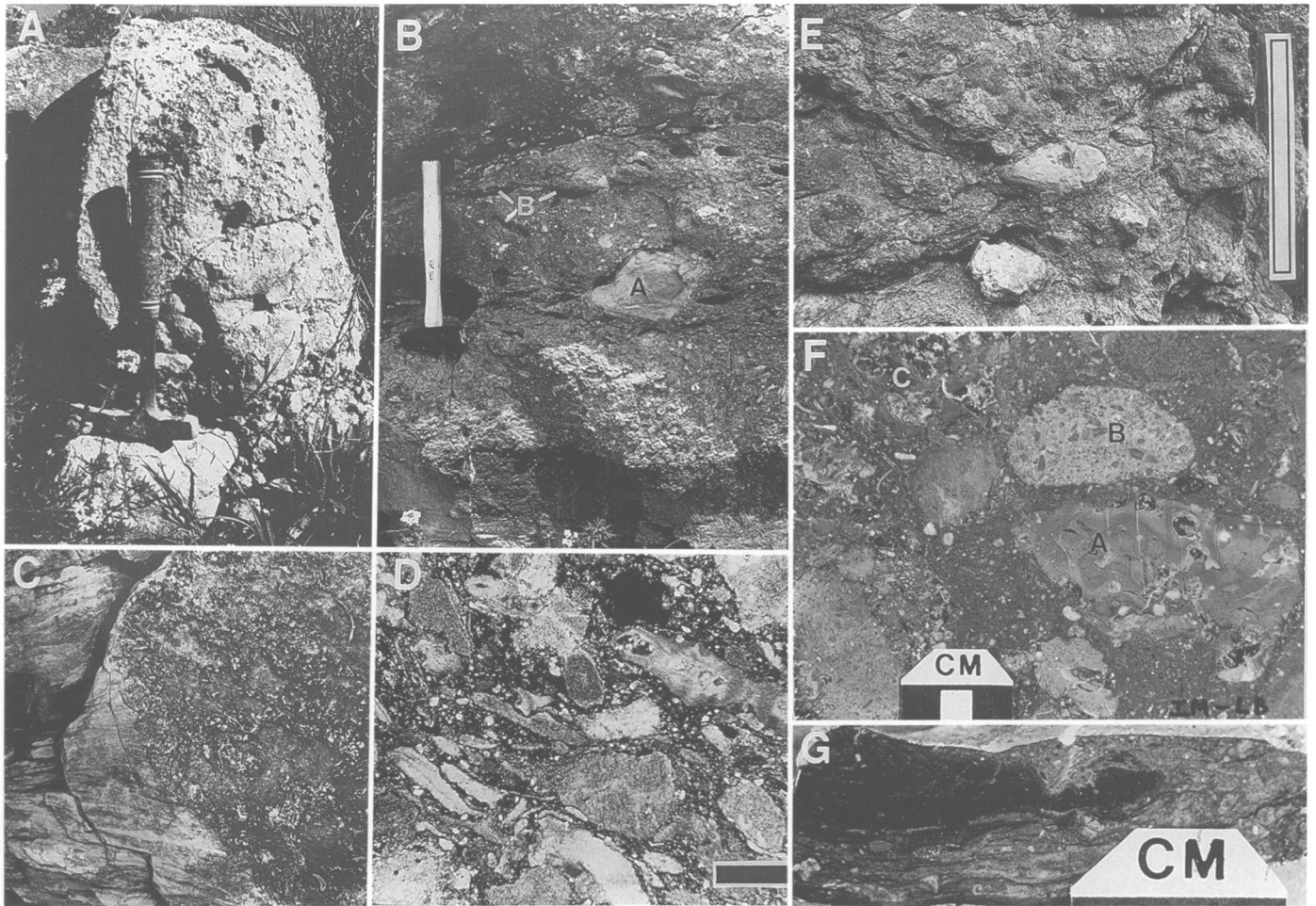


FIGURE 7-20.—Conglomerates and megabreccias of the Road Canyon Formation. A, cobble to boulder conglomerate channel-filling lens from the base of the Road Canyon Formation, eastern Glass Mountains, section 1. Note that this lens was interpreted as a bioherm by Cooper and Grant (1972). B, conglomeratic limestone with recessively weathering clasts of grey spiculite (*a*) and orange spiculite (*b*). Upper part of the Road Canyon Formation, central Glass Mountains, section 5. C, conglomeratic limestone channel fill with truncation of spiculitic lutite lamination at the channel margin. Lower part of the Road Canyon Formation, eastern Glass Mountains, section 1. D, packstone matrix of megabreccia with bryozoan and crinoid fragments, lime-mud, and quartz silt, central Glass Mountains, section 5. E, conglomeratic texture within megabreccia, central Glass Mountains, section 5. The different clasts lithologies are obviously due to weathering differences. Matrix texture is packstone to rudstone. F, conglomerate from megabreccia containing brachiopod wackestone (*a*), fusulinid packstone (*b*), and boundstone (*c*) clasts within a packstone matrix. G, dark orange spiculite clast from megabreccia illustrating deformed internal lamination and shearing of laminations into the matrix, central Glass Mountains, section 5.

discontinuous but widespread across the outcrop and are interpreted to represent two major episodes of downslope transport.

ROAD CANYON FORMATION DEPOSITIONAL SETTING

The Road Canyon Formation represents a deep shelf or slope setting. Organic-rich spiculite- and radiolarian-bearing lutites were deposited from suspension in quiet anaerobic to dysaerobic waters. Lutite deposition was interrupted episodically by scour and by the deposition of coarse allochthonous carbonate

that was transported downslope from shallower aerobic environments.

The direction of the shelf-to-basin transition in the Glass Mountains has remained problematical. Basin directions toward the Hovey channel to the west (Ross, 1987), toward the Delaware basin to the northwest (King, 1931, 1942), and toward the east (Ross, 1962) have been suggested. The major difficulty for reconstructing the Road Canyon shelf-to-basin transition in the Glass Mountains is its highly oblique cross section. Sole marks in the Road Canyon Formation have a mean southeast–northwest orientation, but the downslope

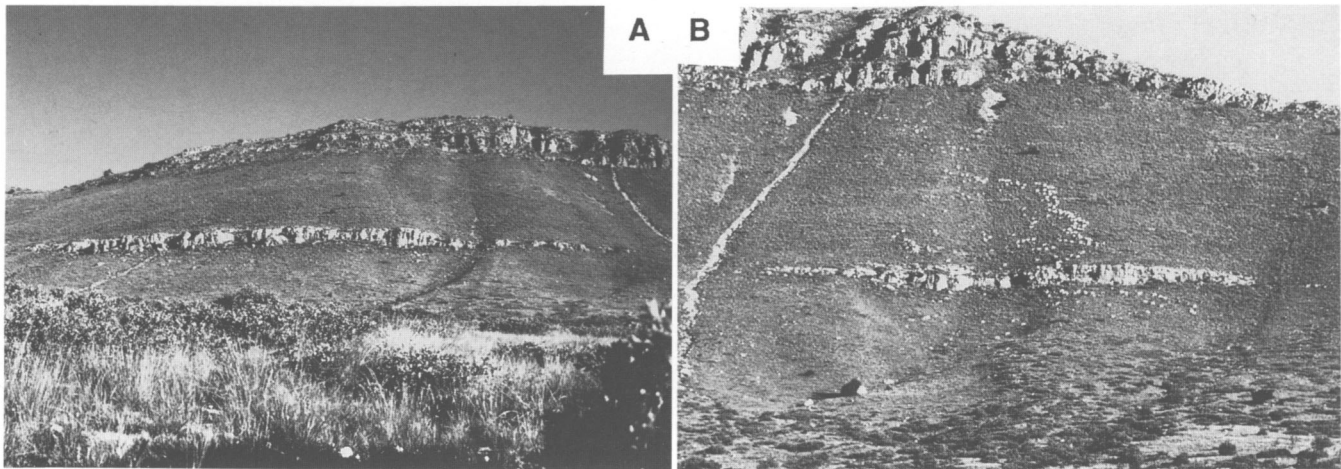
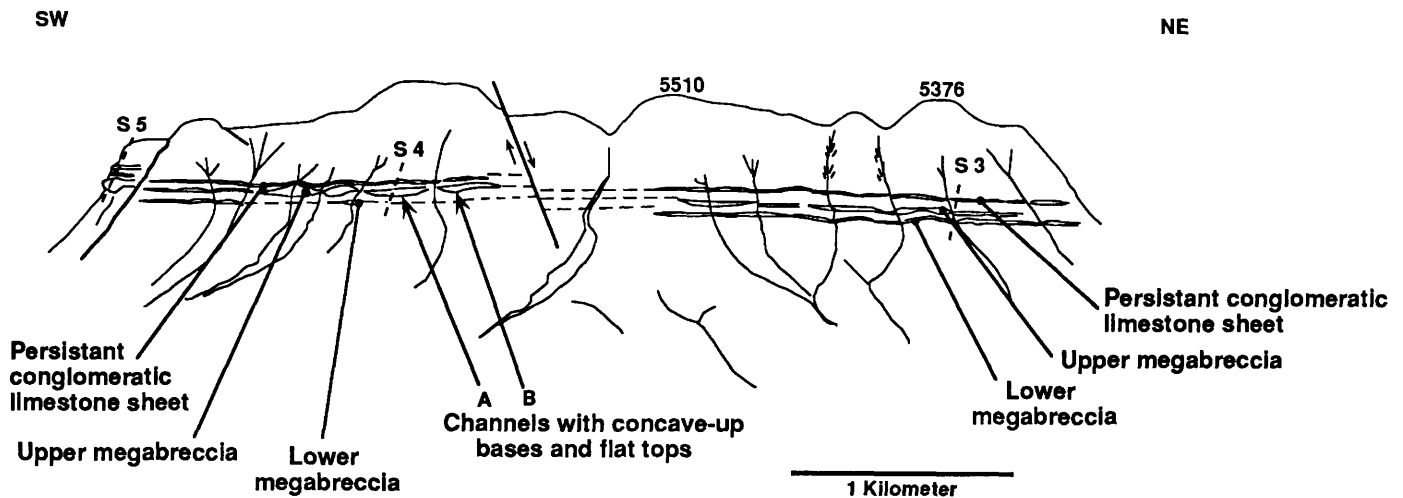


FIGURE 7-21.—Road Canyon Formation in the central Glass Mountains (southeast facing flank of triangular group of hills north of Leonard Mountain). Inserts A and B illustrate channels within the formation.

transport direction is indeterminate (Figure 7-22). This orientation is perpendicular to King's interpreted northeast-trending shelf margin. King's interpretation of the paleoslope is herein agreed with based on the northeast-southwest trending facies belts, the northwest primary dips overlain by nearly flat-lying Cretaceous strata, and the abrupt stratal thinning to the northwest (King, 1931, 1948). Supporting this model, the Road Canyon Formation occurs over the Hess Formation shelf facies in the east and the slope facies to the west (Ross, 1986, 1987). Ross (1986) interpreted the Skinner Ranch and Cathedral Mountain formations to step progressively shelfward over the Hess Formation, representing drowning of the outer shelf. This probably represents the major flooding event that caused the shelfward transgression of the Cutoff facies in the Guadalupe Mountains.

Comparison of the Cutoff and Road Canyon Formations

The Cutoff Formation and the Road Canyon Formation provide two stratigraphic sections that straddle the Leonardian-Guadalupian boundary at opposite ends of the Delaware basin. The Cutoff exposures along the western escarpment of the Guadalupe Mountains are oriented nearly perpendicular to the shelf margin, whereas the Road Canyon outcrops in the Glass Mountains lie nearly parallel to the shelf margin. Because of these contrasting orientations, the Cutoff strata more clearly express large-scale depositional relations and provides a model that helps to interpret the Road Canyon Formation.

Key elements in the Cutoff depositional model are the abrupt sea-level rise that resulted in the drowning of the eroded Leonardian bank by fine-grained carbonates and siliciclastics, the facies variations in the lutites that relate to anoxic basin

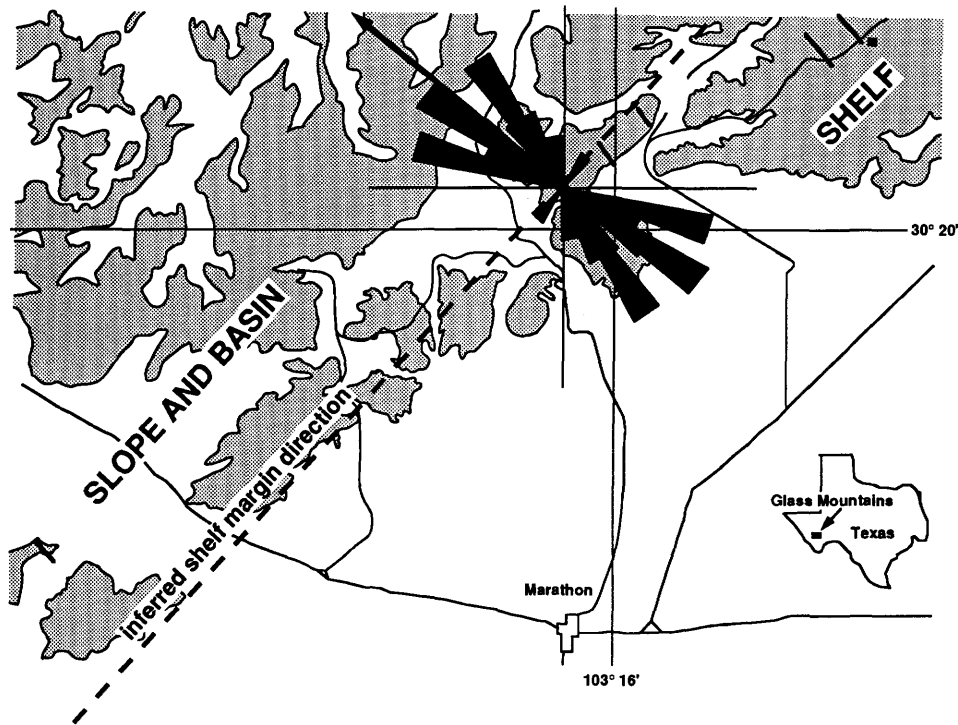


FIGURE 7-22.—Current indicators and inferred basin direction during Roadian time. Sole markings were measured near the base of the medium-bedded packstone and grainstone units in section 5 (25 measurements).

conditions, the occurrence of numerous channels and erosion surfaces with associated allochthonous fauna and coarse lithoclasts in the slope and basin areas, and the three major unconformities extending from the shelf to the basin that control the distribution of Cutoff strata.

Most of these key points also apply to the Road Canyon Formation. The Road Canyon extends above both the shelf (Hess Formation) and the slope-to-basinal facies (Skinner Ranch and Cathedral Mountains formations), which indicates drowning of a shallow-water Leonardian carbonate bank. The fine-grained lutites that dominate the Road Canyon section record the deepening to dysaerobic depths (estimated minimum water depth of 40–50 m for the Cutoff strata), and perhaps to the edge of the anaerobic zone (estimated as 250 m depth in Cutoff rocks). The lithoclastic and fossiliferous conglomerate and megabreccia lenses and sheets found in both formations are virtually identical in clast type, range of grain size, and erosive bases. Intraformational clasts are mixed with shallow-water carbonates irrespective of their source area. Any regional unconformities bracketing Road Canyon strata are not presently recognized, although this may be a function of available outcrop.

The implication of this comparison is that the Road Canyon records an intrusion of deeper-water facies over the Leonardian bank-top. Biostratigraphic correlation studies of the sections

suggests that the two deepening events may have been synchronous (Figure 7-5). The coincidence of two orders (second-order and third-order) of eustatic sea-level rise may have produced a large, rapid flooding event (Sarg and Lehmann, 1986a). One result was that the shelf margin retreated 19–23 km in the Guadalupe Mountains, and its progradation did not extend that far basinward again until late Capitan time. Such a eustatic change would have had a major effect on middle Permian stratigraphy; therefore, it is suggested that this event be considered when examining the strata of this age for recognition of time-rock units.

Recommendations for Future Work Related to the Series/Stage Boundary

A significant implication of comparing the Cutoff and Road Canyon strata is the importance of integrating sedimentological and paleontological data. Downslope megabreccia lenses in the Cutoff Formation (Newell et al., 1953) and discontinuous limestone bodies in the Road Canyon Formation (Cooper and Grant, 1972) have been interpreted as in-place bioherms. Pray and Stehli (1963) recognized the Cutoff examples as allochthonous mixtures of carbonate debris from different environments; similarly we interpret the Road Canyon lenses as allochthonous channel fills. A majority of the reported macrofauna from these formations was derived from alloch-

thonous deposits, stressing the importance of considering the lithologic setting for interpreting paleontologic collections.

Regional correlation of the mid-Permian shelf-drowning events in the Guadalupe Mountains (Victorio Peak Limestone overlain by the Cutoff Formation) and the Glass Mountains (Hess Formation overlain by the Cathedral Mountain and Road Canyon formations) will require biostratigraphic confirmation. The important implications of a regional or global sea-level control (Sarg and Lehmann, 1986a) should be tested in other mid-Permian sections.

The detailed stratigraphic framework developed herein also allows paleontologic sampling to be tied into finer lithologic units. Lambert et al. (this volume) use this approach to better define the biostratigraphic ranges in these units. Recognition of this fine-scale physical stratigraphy is vital for identifying an appropriate datum for this important time-rock unit boundary (Glenister et al., 1992).

Conclusions

The Cutoff Formation (Guadalupe Mountains) provides a model of slope depositional processes that is applicable to the Road Canyon Formation (Glass Mountains). The Cutoff basal facies are dominated by fine-grained lime mudstones and shales that were deposited across an eroded Leonardian bank margin. These facies record an abrupt deepening (40–50 m) that brought anoxic (dysaerobic) conditions onto the outer shelf. Coarse rudstone and megabreccia deposits consisting of allochthonous clasts fill downslope channels. Prominent submarine unconformities bracket Cutoff strata and extend from shelf to basin. Five intra-Cutoff correlation units provide a detailed internal stratigraphy that resolves shelf-to-basin correlations and increases biostratigraphic resolution.

The Road Canyon Formation consists largely of fine-grained organic-rich spiculite- and radiolarian-bearing lutites with

channelized megabreccia and conglomerate and sand sheets. Lutite lamination textures indicate an anoxic slope or deep shelf setting. The coarser deposits are interpreted as downslope, allochthonous deposits. A succession of seven depositional units within the Road Canyon Formation allows correlation across the central Glass Mountains. No extensive unconformity surfaces were noted. Interpretation of the Road Canyon depositional setting is difficult because the outcrop belt is oriented nearly parallel to depositional strike; however, sedimentological features indicate a slope position similar to the Cutoff Formation.

Biostratigraphic studies of the Leonardian–Guadalupian boundary are significantly improved by the increased resolution offered by the fine-scale internal stratigraphies within the Cutoff and Road Canyon formations (Lambert et al., this volume). This greater biostratigraphic resolution provides opportunities to test the global eustatic sea-level rise postulated to have occurred at the beginning of the Roadian. If confirmed, such an event would assist world-wide correlation of this important chronostratigraphic boundary.

Acknowledgments

The authors would like to thank many people for sharing their insights on Permian stratigraphy with them, particularly Lloyd C. Pray, David L. Clark, Rick Sarg, Patrick Lehmann, Christine Rossen, Evan Franseen, Brian F. Glenister, William M. Furnish, and Fred Behnken. They also wish to thank the past and present staff of the Guadalupe Mountains National Park, in particular Roger Reisch, Donald Dayton, and Vidal Davila, for their assistance with these studies. They also acknowledge Windy Lewis, Ed Hammond, Mary Hess, William Blackemore II, Vernon Williams, Joseph Courand, Jr., and Lloyd Stuessey for kindly allowing access to their ranchlands.

Appendix 7-1: Features at the Road Canyon Type Section (Central Glass Mountains)

This appendix presents pertinent field data regarding the Road Canyon type area (type section = S5, Figure 7-15). It was prepared by Lehrmann and was based on his thesis research (Lehrmann, 1988).

Detailed depositional geometries of megabreccia units and associated strata are well exposed in the Road Canyon Formation type section area. The lower one-third of the Road Canyon Formation, including the lower and upper megabreccia units, fills a northwest-trending channel. Viewed from the southeast (Figure 7-23), the lower Road Canyon strata pinch out to the northeast by onlap against a channel margin cut into

recessive (slope forming) Cathedral Mountain Formation. Although this level is covered northeast of the breccias (Figure 7-23), the absence of outcrop suggests the underlying lithology is recessive Cathedral Mountain Formation. Viewed from the southwest, the lower Road Canyon Formation appears to pinch out to the northwest (Figure 7-24), with the lower and upper megabreccias represented by thin exposures northwest of the type area (Figure 7-24). In three dimensions, however, the megabreccia units thin and pinch out toward the southwest. Thus, the lower Road Canyon Formation fills a broad northwest-oriented channel and pinches out to the northeast

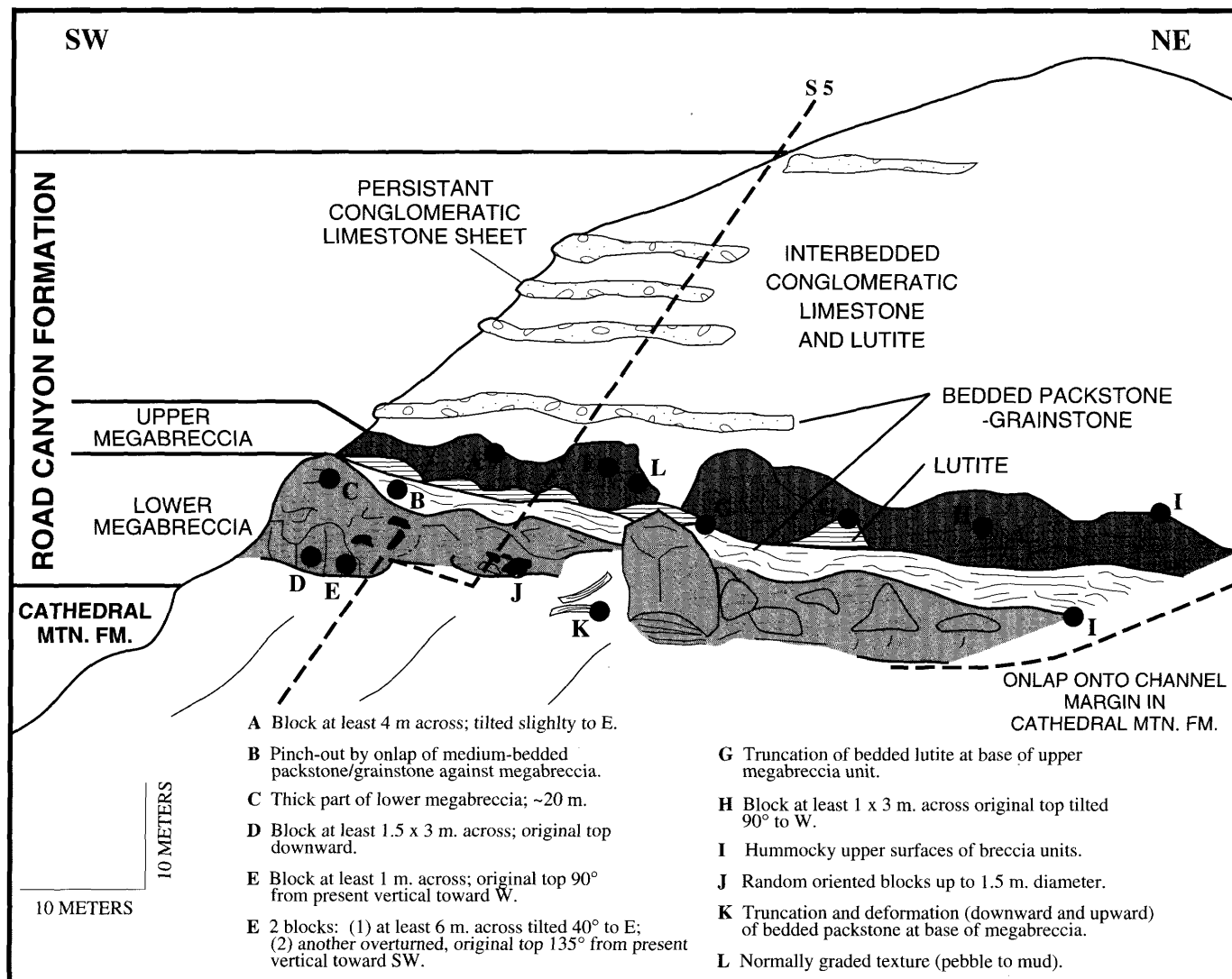


FIGURE 7-23.—Road Canyon Formation type section area (section 5) viewed from the southeast.

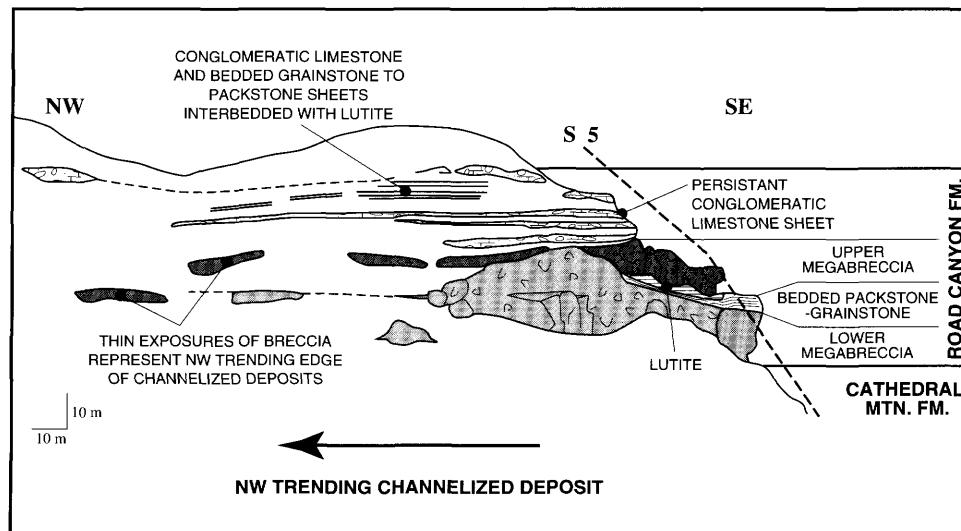


FIGURE 7-24.—Road Canyon Formation type section area (section 5) viewed from the southwest.

and southwest. Thin exposures of megabreccia northwest of the type area (Figure 7-24) represent the northwest-trending edge of the southwest side of the channel.

The lower and upper megabreccia units vary in thickness across the outcrop because of their truncational bases and hummocky upper surfaces (Figure 7-23). The lower megabreccia unit thickens from 9 m east of the section line to 20 m west of it (Figure 7-23C). The upper megabreccia varies from 4.5 to 10 m in thickness. Near the base of the Road Canyon Formation, the lower megabreccia truncates approximately 3 m of medium-bedded skeletal packstone (Figure 7-23K). These beds are deformed upward and downward by the adjacent megabreccia. The upper megabreccia truncates up to 2 m of underlying lutite beds (Figure 7-23G).

Weathering accentuates the margins between clasts and matrix east of the section line (Figures 7-20E, 7-23J). In contrast, to the west (Figure 7-23D,E), the lower megabreccia weathers massively, obscuring clast margins. Aligned geopetals define two megaclasts (Figure 7-25): one is at least 1.5×3 m in size and is overturned (15 aligned geopetals; Figure 7-23D); the other is at least 1 m across and is tilted on its side (8 aligned geopetals, original top toward west; Figure 7-23E). Above this massively weathered area, approximately 6 m from the cliff base (Figure 7-25), the lower megabreccia contains a 4.5 m long horizontal, tabular block composed of laminated lime packstone with its margins sheared into the breccia matrix. Farther west at the cliff base, a tabular megaclast composed of laminated grainstone is tilted on end (Figure 7-25).

Massively weathered limestone cliffs of the upper megabreccia (Figure 7-23A,F) were interpreted to be composed of in-place biohermal limestone by Cooper and Grant (1972). East of the section line (Figure 7-23F), a block composed of branching bryozoan and *Tubiphytes* boundstone is at least 6 m

across and contains 12 aligned geopetals tilted toward the east; the original top is 40° from present vertical. Farther east (Figure 7-23F), a brachiopod skeletal packstone block, at least 2.5 m across and defined by 5 geopetals, is overturned with the original top 135° from present vertical. The boundary between these two blocks is obscured by weathering. Immediately west of the section line (Figure 7-23A) a brachiopod packstone block, at least 4.5 m across, is tilted slightly to the east.

Medium-bedded packstone and grainstone overlies the lower megabreccia unit and onlaps a thickened part west of the section line (Figure 7-23B). Scouring, sole markings, and intraclasts indicate an allodapic origin. The upper megabreccia unit is overlain by a graded (pebble to laminated mud) cap (Figure 7-23L).

On the southeast-facing flank of the hills northeast of the type section, megabreccia units have hummocky to flat upper surfaces and channelized to flat bases (Figure 7-22). The channel fills that are roughly symmetrical in cross section (Figure 7-22) indicate the mountain front is a strike section cut perpendicular to the channel axes.

Measures and Wardlaw (1990) interpreted the megabreccia at the base of the Road Canyon type section (section 5 of Figure 7-15) as a Permian karst collapse feature. Similar megabreccias, however, occur across the central and western Glass Mountains (sections 3, 4, 5, and 6 of Figure 7-15), and similar but less coarse channel-filling conglomerates occur in the eastern Glass Mountains. A karst collapse origin is unlikely for the Road Canyon Formation megabreccia for several reasons. First, lutite lithologies surround the megabreccia, and there is no obvious source for coarse carbonate debris. Second, medium-bedded packstone and grainstone deposits thin and onlap over thicker portions of the megabreccia, indicating the topography over the megabreccias predates the deposition of

the packstone and grainstone beds. Third, collapse breccias typically contain intergranular cement, whereas the intergranular spaces in the Road Canyon megabreccias are completely

filled with packstone and rudstone matrix. Fourth, the channeled bases and deformed clasts with their sheared margins appear more consistent with a depositional origin.

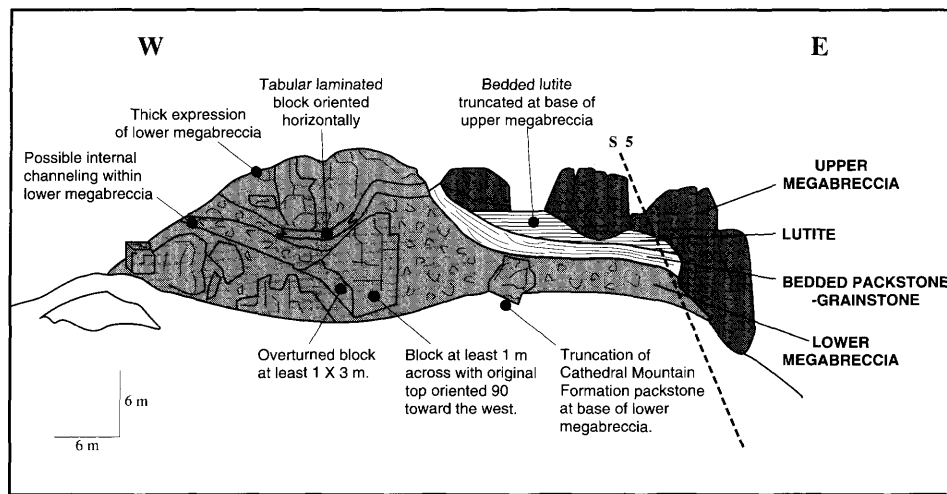


FIGURE 7-25.—Road Canyon Formation type section area (section 5) viewed from the south.

Literature Cited

- Boyd, D.W.
1958. Permian Sedimentary Facies, Central Guadalupe Mountains, New Mexico. *Bulletin of the New Mexico Bureau of Mines and Mineral Resources*, 49: 100 pages, 5 plates.
- Byers, C.W.
1977. Biofacies Patterns in Euxinic Basins: A General Model. In H.E. Cook and P. Enos, editors, Deep-Water Carbonate Environments. *Society of Economic Paleontologists and Mineralogists, Special Publication*, 25:5-17.
- Cooper, G.A., and R.E. Grant
1964. New Permian Stratigraphic Units in Glass Mountains, West Texas. *Bulletin of the American Association of Petroleum Geologists*, 48(9):1581-1588.
1966. Permian Rock Units in the Glass Mountains, West Texas. *United States Geological Survey Bulletin*, 1244-E:E1-E9, plates 1, 2.
1972. Permian Brachiopods of West Texas, I. *Smithsonian Contributions to Paleobiology*, 14:1-231, plates 1-23.
- Cys, J.M.
1981. Preliminary Report on Proposed Leonardian Lectostratotype Section, Glass Mountains, West Texas. In Marathon-Marfa Region of West Texas Symposium and Guidebook. *Society of Economic Paleontologists and Mineralogists, Permian Basin Section, Publication*, 81-10:183-203.
- Cys, J.M., and S.J. Mazzullo
1978. Lithofacies and Sedimentation of Lower Permian Carbonate of the Leonard Mountain Area, Glass Mountains, Western Texas: A Discussion. *Journal of Sedimentary Petrology*, 48(4):1363-1368.
- Dunham, R.J.
1962. Classification of Carbonate Rocks According to Depositional Texture. In W.E. Ham, editor, *Classification of Carbonate Rocks: A Symposium. American Association of Petroleum Geologists, Memoir*, 1:108-121, plates 1-7.
- Embry, A.V., and J.E. Klovan
1971. A Late Devonian Reef Tract on Northeast Banks Island, Northwest Territories. *Bulletin of Canadian Petroleum Geology*, 19:730-781.
- Franseen, E.K., T.E. Fekete, and L.C. Pray
1988. Evolution and Destruction of a Carbonate Bank at the Shelf Margin: Grayburg Formation (Permian), Western Escarpment, Guadalupe Mountains, Texas. In P.D. Crevello, J.L. Wilson, J.F. Sarg, and J.F. Read, editors, *Controls on Carbonate Platform and Basin Development. Society of Economic Paleontologists and Mineralogists, Special Publication*, 44:289-304.
- Furnish, W.M.
1966. Ammonoids of the Upper Permian *Cyclolobus*-Zone. *Neues Jahrbuch für Geologie und Paläontologie, Abhandlungen*, 125: 265-296, plates 23-26.
1973. Permian Stage Names. In A. Logan and L.V. Hills, editors, *The Permian and Triassic Systems and Their Mutual Boundary. Canadian Society of Petroleum Geologists, Memoir*, 2:522-548.
- Glenister, B.F., D.W. Boyd, W.M. Furnish, R.E. Grant, M.T. Harris, H. Kozur, L.L. Lambert, W.W. Nassichuk, N.D. Newell, L.C. Pray, C. Spinosa, B.R. Wardlaw, G.L. Wilde, and T.E. Yancey
1992. The Guadalupian: Proposed International Standard for a Middle Permian Series. *International Geology Review*, 34(9):857-888.
- Harms, J.C.
1974. Brushy Canyon Formation, Texas: A Deep Water Density Current Deposit. *Bulletin of the Geological Society of America*, 85(11): 1763-1784.
- Harms, J.C., and L.C. Pray
1974. Erosion and Deposition along the Mid-Permian Intracratonic Basin

- Margin, Guadalupe Mountains, Texas. [Abstract.] *In* R.H. Dott, Jr., and R.H. Shaver, editors, *Modern and Ancient Geosynclinal Sedimentation. Society of Economic Paleontologists and Mineralogists, Special Publication*, 19:37.
- Harris, M.T.
1982. Sedimentology of the Cutoff Formation (Permian), Western Guadalupe Mountains, West Texas and New Mexico. 186 pages. Unpublished master's thesis, University of Wisconsin, Madison, Wisconsin.
- 1988a. Sedimentology of the Cutoff Formation (Permian), Western Guadalupe Mountains, West Texas. *In* S.T. Reid, R.O. Bass, and P. Welch, editors, *Guadalupe Mountains Revisited, Texas and New Mexico. West Texas Geological Society, Publication*, 88-84:133-140.
- 1988b. Postscript on the Cutoff Formation: The Regional Perspective and Some Suggestions for Nomenclature. *In* S.T. Reid, R.O. Bass, and P. Welch, editors, *Guadalupe Mountains Revisited, Texas and New Mexico. West Texas Geological Society, Publication*, 88-84:141-142.
2000. Members for the Cutoff Formation, Western Escarpment of the Guadalupe Mountains, West Texas. *In* B.R. Wardlaw, R.E. Grant, and D.M. Rohr, editors, *The Guadalupian Symposium. Smithsonian Contributions to the Earth Sciences*, 32:101-120, 8 figures.
- Hayes, P.T.
1959. San Andres Limestone and Related Permian Rocks in Last Chance Canyon and Vicinity, Southeastern New Mexico. *Bulletin of the American Association of Petroleum Geologists*, 43(9):2197-2213.
- Hay-Roc, H.
1957. Geology of Wylie Mountains and Vicinity, Culberson and Jeff Davis Counties, Texas. *Bureau of Economic Geology, University of Texas, Austin, Geologic Quadrangle Map*, 21.
- King, P.B.
- 1931 ("1930"). The Geology of the Glass Mountains, Texas, Part I: Descriptive Geology. *University of Texas Bulletin*, 3038: 167 pages, 15 plates. [Date on title page is 1930; actually published in 1931.]
1942. Permian of West Texas and Southeastern New Mexico. *Bulletin of the American Association of Petroleum Geologists*, 26(4):535-763.
1948. Geology of the Southern Guadalupe Mountains, Texas. *United States Geological Survey Professional Paper*, 215: 183 pages, 23 plates.
1965. Geology of the Sierra Diablo Region, Texas. *United States Geological Survey Professional Paper*, 480: 185 pages, 16 plates.
- Kirkby, K.C.
1988. Deposition and Permian Erosion of the Upper Victorio Peak Formation (Leonardian), Western Escarpment, Guadalupe Mountains, West Texas. *In* S.T. Reid, R.O. Bass, and P. Welch, editors, *Guadalupe Mountains Revisited, Texas and New Mexico. West Texas Geological Society, Publication*, 88-84:149-154.
- Lambert, L.L., D.J. Lehrman, and M.T. Harris
2000. Correlation of the Road Canyon and Cutoff Formations, West Texas, and Its Relevance to Establishing an International Middle Permian (Guadalupian) Series. *In* B.R. Wardlaw, R.E. Grant, and D.M. Rohr, editors, *The Guadalupian Symposium. Smithsonian Contributions to the Earth Sciences*, 32:153-183, 11 figures, 4 plates, 3 tables.
- Lehrmann, D.J.
1988. Sedimentology and Conodont Biostratigraphy of the Road Canyon Formation (Permian), Glass Mountains, Southwest Texas. 170 pages. Unpublished master's thesis, University of Wisconsin, Madison, Wisconsin.
- McDaniel, P.N., and L.C. Pray
1968. Bank to Basin Transition in Permian (Leonardian) Carbonates, Guadalupe Mountains, Texas. *Bulletin of the American Association of Petroleum Geologists*, 51(3):474.
- Measures, E.A., and B.R. Wardlaw
1990. Recognition of Paleokarst in the Road Canyon Formation, Permian Regional Stratotype, West Texas. [Abstract.] *Geological Society of America, Abstracts with Programs*, 22(7):309.
- Newell, N.D., J.K. Rigby, A.G. Fisher, A.J. Whiteman, J.R. Hickox, and J.S. Bradley
1953. *The Permian Reef Complex of the Guadalupe Mountains Region, Texas and New Mexico: A Study in Paleocology*. 236 pages. San Francisco: W.H. Freeman and Company.
- Pray, L.C.
1971. Submarine Slope Erosion along Permian Bank Margin, West Texas. *Bulletin of the American Association of Petroleum Geologists*, 55(2):358.
- Pray, L.C., G.A. Crawford, M.T. Harris, and K.C. Kirkby
1980. Early Guadalupian (Permian) Bank Margin Erosion Surfaces, Guadalupe Mountains, Texas. *Bulletin of the American Association of Petroleum Geologists*, 64(5):768.
- Pray, L.C., and F.G. Stehli
1963. Allochthonous Origin, Bone Spring "Patch Reefs," West Texas. [Abstract.] *Geological Society of America, Special Paper*, 73:218-219.
- Rogers, W.B.
1972. Depositional Environments of the Skinner Ranch and Hess Formations (Lower Permian), Glass Mountains, West Texas. 392 pages. Unpublished doctoral dissertation, University of Texas, Austin, Texas.
1978. Megaclast-Bearing Conglomerate Beds in the Skinner Ranch Formation, Glass Mountains, West Texas. *In* S.J. Mazzullo, editor, *Tectonics and Paleozoic Facies of the Marathon Geosyncline, West Texas. Society of Economic Paleontologists and Mineralogists, Permian Basin Section, Publication*, 78-17:191-214.
- Ross, C.A.
1962. Permian Tectonic History in Glass Mountains, Texas. *Bulletin of the American Association of Petroleum Geologists*, 46(9):1728-1746.
1986. Paleozoic Evolution of Southern Margin of Permian Basin. *Bulletin of the Geological Society of America*, 97(5):536-554.
1987. Leonardian Series (Permian), Glass Mountains, West Texas. *In* D. Cromwell and L.J. Mazzullo, editors, *The Leonardian Facies in W. Texas and S.E. New Mexico and Guidebook to the Glass Mountains, West Texas. Society of Economic Paleontologists and Mineralogists, Permian Basin Section, Publication*, 87-27:25-33.
- Rossen, C., and J.F. Sarg
1988. Sedimentology and Regional Correlation of a Basinally Restricted Deep-Water Siliciclastic Wedge: Brushy Canyon Formation Cherry Canyon Tongue (Lower Guadalupian), Delaware Basin. *In* S.T. Reid, R.O. Bass, and P. Welch, editors, *Guadalupe Mountains Revisited, Texas and New Mexico. West Texas Geological Society, Publication*, 88-84:127-132.
- Sarg, J.F., and P.J. Lehmann
- 1986a. Lower-Middle Guadalupian Facies and Stratigraphy San Andres/Grayburg Formations, Permian Basin, Guadalupe Mountains, New Mexico. *In* G.E. Moore and G.L. Wilde, editors, *Lower and Middle Guadalupian Facies, Stratigraphy, and Reservoir Geometries, San Andres/Grayburg Formations, Guadalupe Mountains, New Mexico and Texas. Society of Economic Paleontologists and Mineralogists, Permian Basin Section, Publication*, 86-25:1-8.
- Wilde, G.L.
1990. Practical Fusulinid Zonation: The Species Concept; with Permian Basin Emphasis. *West Texas Geological Society, Bulletin*, 29(7):5-34.
- Wilde, G.L., and R.G. Todd
1968. Guadalupian Biostratigraphic Relationships and Sedimentation in the Apache Mountain Region, West Texas. *In* B.A. Silver, editor, *Guadalupian Facies, Apache Mountains Area, West Texas. Society of Economic Paleontologists and Mineralogists, Permian Basin Section, Publication*, 68-11:10-31.
- Wood, J.W.
1968. Geology of the Apache Mountains, Trans-Pecos Texas. *Bureau of Economic Geology, University of Texas, Austin, Geologic Quadrangle Map*, 33: 32 pages.

8. Correlation of the Road Canyon and Cutoff Formations, West Texas, and Its Relevance to Establishing an International Middle Permian (Guadalupian) Series

*Lance L. Lambert, Daniel J. Lehrmann,
and Mark T. Harris*

ABSTRACT

Recent detailed field mapping and a new understanding of the internal stratigraphy of the Road Canyon and Cutoff formations have provided the necessary framework to improve the biostratigraphic resolution of the Roadian Stage (early Guadalupian Series). Shumard's (1860) basal "black limestone" at the bottom of Guadalupe Pass was explicitly included as the lowermost unit when Girty (1902) proposed the Guadalupian Series. Adams et al. (1939) considered the black limestone to represent the Bone Spring Limestone, and its fossils to be Leonardian. Accurate correlation demonstrates that the black limestone is the upper unit of the basinal Cutoff Formation. The reassignment of previously described fossil localities to their correct stratigraphic position clarifies temporal faunal relationships, and the Road Canyon and Cutoff formations are proven to be largely correlative. Roadian ammonoid, conodont, and fusulinid faunas are distinctive, and the biostratigraphy records when each of these important groups is first represented by characteristic Guadalupian forms. Predicated on both the improved database and consideration of priority and stability, a return to Girty's original Guadalupian Series concept is recommended. This supports retaining the Roadian as the basal stage of the Guadalupian Series. It is also proposed that the mutual basal boundary of the Guadalupian and Roadian be established within the morphological continuum through which the conodont species *Mesogondolella idahoensis* evolved into *M. nankingensis*. Thus defined, the Guadalupian Series is a leading candidate as the

international standard for establishing a formal Middle Permian Series.

Introduction

One of the most outstanding records of Permian marine sedimentation is present in the mountain ranges of Trans-Pecos Texas (Figure 8-1). These strata have been intensively studied for both their scientific merit and economic value in the nearby Permian basin petroleum province. As a result, they have been used as a regional standard for many years. A large proportion of these rocks accumulated during the middle part of the Permian Period, and they rank among the world's most diversely fossiliferous and well exposed. Several excellent sections exist for selecting the primary reference types (body stratotypes and boundary stratotypes) necessary to establish a formal Middle Permian Series. That series would be equivalent to the Guadalupian of North America.

Definition of the basal Guadalupian (the Leonardian-Guadalupian boundary) has remained unsettled, in part because of evolving stratigraphic nomenclature and previous misunderstanding of important faunal ranges. This reflects historical contingency: the Guadalupian Series was defined in the Guadalupe Mountains, whereas the preceding Leonardian Series was based on strata exposed 150 miles (240 km) to the southeast in the Glass Mountains (Figure 8-2). Precise correlation between the two mountain ranges has long remained elusive. Different expressions of corresponding paleoenvironments and complex facies relationships have contributed to equivocal correlations.

Lance L. Lambert, Physics Department, Southwest Texas State University, San Marcos, Texas 78666-4616. Daniel J. Lehrmann, Department of Geology, University of Kansas, Lawrence, Kansas 66045. Mark T. Harris, Department of Geosciences, University of Wisconsin-Milwaukee, Milwaukee, Wisconsin 53201.

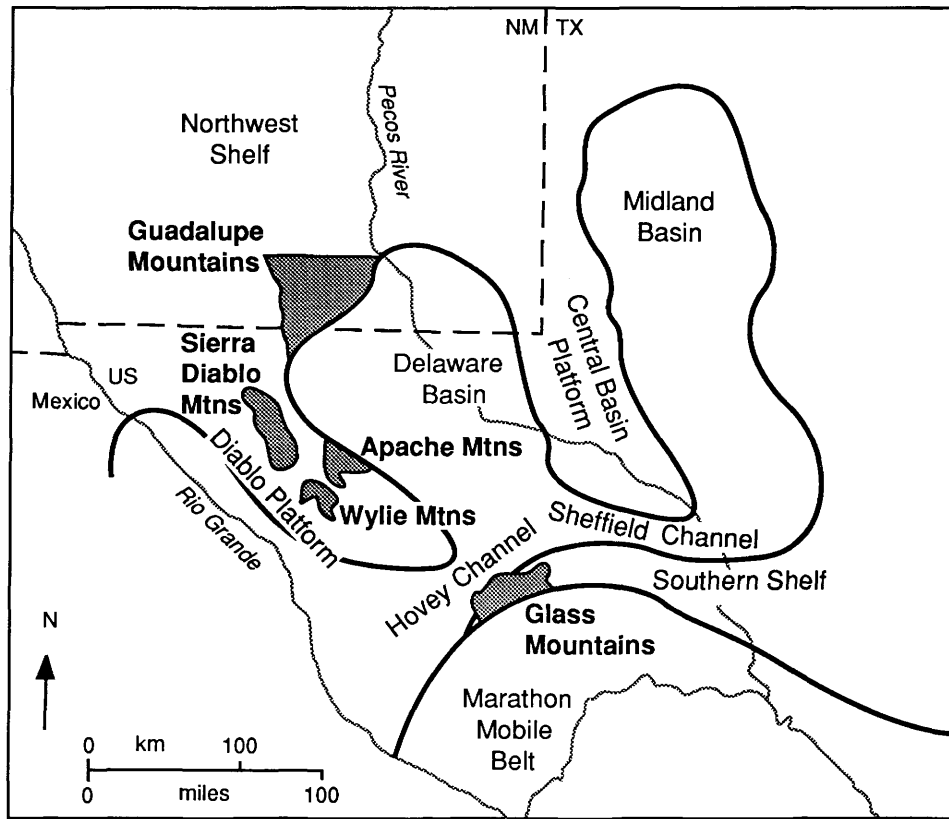


FIGURE 8-1.—Location of the Guadalupe Mountains, Glass Mountains, and other ranges mentioned in the text relative to Permian structural elements. (Modified from King, 1948.)

Resolution of the Leonardian–Guadalupian boundary is ultimately tied to the disposition of the Roadian Stage. Numerous workers have recognized the Roadian worldwide since its proposal (Furnish, 1966, 1973; Furnish and Glenister, 1970); however, some have misapplied the concept, which has led others to advocate its abandonment by incorporating the Roadian into overlying and/or underlying stages. The distinctive nature of Roadian faunas has been repeatedly demonstrated in comparison to both Leonardian and Guadalupian taxa. Yet a more thorough assessment of faunal ranges through the Roadian needs to be documented within carefully measured and sampled sections, especially in the Leonardian and Guadalupian type areas. Only then can a more meaningful biostratigraphic analysis firmly establish the Roadian Stage boundaries.

Subdivision of the Road Canyon and Cutoff formations into recognizable lithostratigraphic components provides a consistent internal stratigraphy amenable to field mapping (Harris et al., this volume). This finer stratigraphic resolution results in unambiguous recognition of the basal Cutoff Formation and improved correlation of the Road Canyon Formation from the eastern to the western Glass Mountains. The lateral integrity of these units establishes a lithostratigraphic framework for increasing biostratigraphic precision and for interpreting faunal

data relevant to defining boundaries of the Roadian Stage. The greater biostratigraphic resolution distinguishes taxa previously blurred by stratigraphic uncertainties, clarifies the stratigraphic assignment of previously described ammonoid faunas, and upholds previous fusulinid correlations between the Glass and Guadalupe mountains. A better understanding of facies relationships strengthens established correlations between shelf and basin faunas, and these correlations are confirmed by conodonts collected along shelf to basin transects.

This paper summarizes the increased biostratigraphic resolution by (1) correcting errors introduced through changes in stratigraphic nomenclature that resulted in misassignment of previous faunal collections, and (2) incorporating significant new data. The results support the formal recognition of the Roadian as the basal stage of the Guadalupian Series. Discovery of a morphological continuum in the evolution of the conodont *Mesogondolella idahoensis* (Youngquist, Hawley, and Miller) into *M. nankingensis* (Ching) near the base of classic Roadian strata provides an opportunity to select a boundary definition meeting all criteria for establishing a Global Stratotype Section and Point. This lower boundary definition closely matches Girty's (1902) original concept for the Guadalupian Series. It is therefore recommended that the

SERIES	GENERAL LOCATION OF REFERENCE	BASIS OF CONCEPT
OCHOAN	Subsurface: T24S, R34E, Lea County, New Mexico	Superposition (unfossiliferous)
GUADALUPIAN	Guadalupe Mountains	UPPER = CAPITANIAN <u>Ammonoids</u> Waagenoceras + Timorites <u>Fusulinids</u> Polydiexodina
		LOWER = WORDIAN <u>Ammonoids</u> Waagenoceras <u>Fusulinids</u> Advanced Parafusulina
LEONARDIAN	Glass Mountains	<u>Ammonoids</u> Perrinites <u>Fusulinids</u> Primitive Parafusulina <u>Brachiopods</u> Prorichthofenia Scacchinella Dictyoclostus bassi
WOLFCAMPIAN	Glass Mountains	<u>Ammonoids</u> Properrinites <u>Fusulinids</u> Schwagerina Pseudoschwagerina Paraschwagerina <u>Brachiopods</u> Parakeyserlingina

FIGURE 8-2.—North American Permian series nomenclature established by Adams et al. (1939), with the general location of the reference and the stated conceptual basis for each series.

Guadalupian be endorsed as the international standard reference for a formal Middle Permian Series, based on improved lithostratigraphic and biostratigraphic resolution, stability, and priority (see Glenister, 1991; Glenister et al., 1992).

Chronostratigraphic Concepts and Nomenclatural History

Girty proposed the Guadalupian Series in a statement directed primarily toward announcing the unique aspect of fossils collected from the southern Guadalupe Mountains (Girty, 1902). The faunas represented an overview of the entire stratigraphic column (Plate 8-1), ranging from the base of Guadalupe Pass (the “black limestone” of Shumard, 1860) to the summit of the range (the “white limestone”). Disparate collections from across the region were included in his analysis, along with several fossils from the Guadalupe Mountains collected by previous workers. Girty’s Permian studies culminated with the publication of his landmark monograph “The Guadalupian Fauna” (1908). He explicitly included the black limestone and its faunal components in the Guadalupian

(e.g., Girty, 1908:23). In terms of diversity, more than one-half of the ammonoid genera that Girty studied were from these black limestone localities.

Girty’s (1908) research material included a small fauna from the Glass Mountains collected by R.T. Hill. Udden (1917) published the first broad geologic reconnaissance of that range, which, along with Böse’s (1919) ammonoid studies, established a useful stratigraphic framework. King (1931) conducted a comprehensive stratigraphic survey based on detailed field mapping that continues to form the basis of modern research. Stratigraphic resolution developed further with the extensive studies of Cooper and Grant (1964, 1966, 1972, 1974, 1975, 1976a,b, 1977). They renamed King’s first limestone member of the Word Formation the Road Canyon Member (Cooper and Grant, 1964) and later elevated it to a formation (Cooper and Grant, 1966; Figure 8-3). Cooper and Grant (1966) transferred the Road Canyon Formation from the basal Guadalupian Series to the uppermost Leonardian Series to accommodate the interpreted Leonardian attributes of the Road Canyon brachiopod and ammonoid faunas. Their designated type section for

King 1931	Cooper and Grant 1964		Cooper and Grant 1966	
Third Lst.	Guadalupian Series	Apple Ranch Mbr.	Guadalupian Series	Apple Ranch Mbr.
Word Fm.		Word Fm.		Word Fm.
Second Lst.		Willis Ranch Mbr.		Willis Ranch Mbr.
First Lst.		Road Canyon Mbr.		Road Canyon Formation
Leonard Formation (top)	Leonardian Series	Cathedral Mountain Formation	Leonardian Series	Cathedral Mountain Formation

FIGURE 8-3.—History of nomenclature and series assignment for the Road Canyon Formation.

the Road Canyon Formation was included by Cys (1981) in the Leonardian lectostratotype.

Blanchard and Davis (1929) had previously named the Bone Spring Limestone for an extensive section of thin-bedded black limestone exposed along the western escarpment of the Guadalupe Mountains. They correlated the Bone Spring Limestone with Shumard's (1860) basal black limestone at the bottom of Guadalupe Pass. They also equated the Bone Spring Limestone with the Leonard Formation of the Glass Mountains, based largely on fossils collected from the black limestone. King (1934) subsequently adopted their correlations, citing Girty's (1908:23) remark that, although the black limestone fauna is "unmistakably related to the overlying faunas, [it] has an individual facies." These widely accepted correlations became firmly established following the publication of King's (1948) monumental Guadalupe Mountains monograph.

Preliminary results from King's Guadalupe Mountains work decisively influenced the Permian subdivisions of Adams et al. (1939; Figure 8-2), who placed the Leonardian-Guadalupian boundary at the Bone Spring-Brushy Canyon contact in the Guadalupe Mountains. This lithostratigraphic distinction between Leonardian and Guadalupian strata became accepted dogma; however, correlation between the western escarpment and more basinward deposits continued to confound stratigraphers. Because the basinal black limestone was considered to be Bone Spring a priori, the faunas recovered from it had to be Leonardian, and several contrasting lithostratigraphic correlations were proposed (Figure 8-4). The most often cited are those of King (1942, 1948) and Newell et al. (1953).

King tentatively correlated the Cutoff Shaly Member (uppermost Bone Spring Limestone at that time) of the western escarpment shelf and slope areas with a generally covered interval south of Bone Canyon that is informally referred to as

the "southern Cutoff" (King, 1948). The southern Cutoff overlies the black limestone, which King correlated with the Bone Spring. The nonresistant southern Cutoff interval included what is now called the Pipeline Shale Member (Warren, 1955), presently considered to be the basal unit of the Brushy Canyon Formation. In contrast to King, Newell et al. (1953) traced the Cutoff Shaly Member into the basin below an overlying thin-bedded black limestone they informally termed the "upper Bone Spring," which in turn underlies the Pipeline Shale (= *Waagenoceras* Shale of Newell et al., 1953). As a consequence, they projected the Cutoff shaly strata into the subsurface below the upper Bone Spring beds.

King differentiated the Cutoff Member as a distinct formation in a later study on the geology of the Sierra Diablo, located just southwest of the Guadalupe Mountains (King, 1965). He retained the shelf deposits at Cutoff Mountain in the northern Guadalupe Mountains as the formation's type section. King continued to treat the basinal black limestone in Guadalupe Pass and further south in the Delaware Mountains as equivalent to the Bone Spring Limestone along the western escarpment. He may have considered it probable that the pre-Brushy Canyon erosional event had entirely removed Cutoff strata from the basin, although no such interpretation was advanced. King (1965) simply stated that his previous correlation was untenable, and he left the basinal Cutoff correlation unresolved.

The correct temporal position of the basinal black limestone is critical to understanding the proper shelf-to-basin correlations (lithostratigraphic units) and to clarifying the Leonardian-Guadalupian boundary (chronostratigraphic units). Newell et al. (1953) mapped the rocks accurately but felt compelled to remain within the established stratigraphic nomenclature. They had traced the El Centro Member, a diagnostic shale-

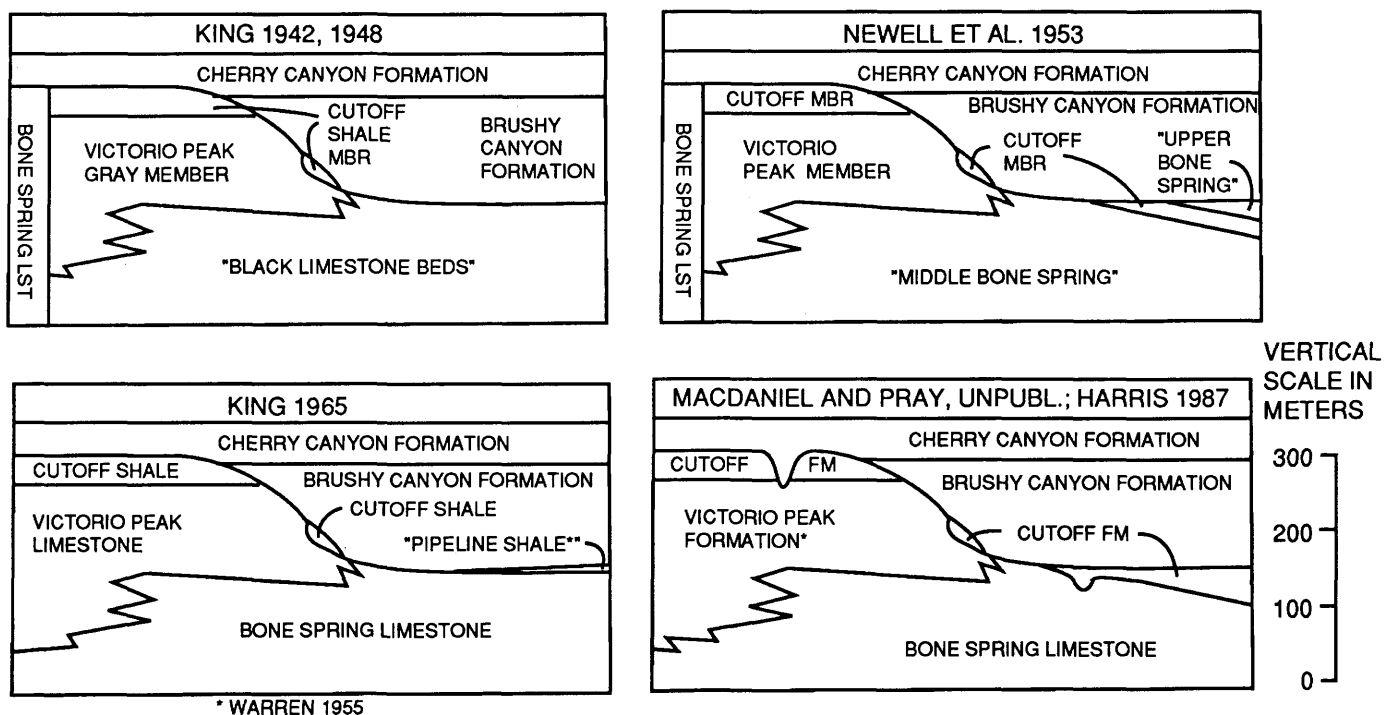


FIGURE 8-4.—History of nomenclature and correlation for the Cutoff Formation.

Girty 1902		King 1942, 1948		Newell et al., 1953		Harris 1987		This paper; Harris, this volume	
Guadalupian Series	Yellow Quartzose Sandstone	Guad. Series	Brushy Canyon Fm.	Guad. Series	Brushy Canyon Fm.	Guadalupian Series	Brushy Canyon Fm.	Guadalupian Series	Brushy Canyon Fm.
	Basal Black Limestone	Leonardian Series	Bone Spring Limestone	Leonardian Series	"Upper Bone Spring"	Cutoff Fm. ("upper unit")	correlation unit 5	Cutoff Formation	Williams Ranch Mbr.
					Cutoff Member		correlation units 4		El Centro Member
					"Middle Bone Spring"		correlation unit 3		Shumard Member
					?	("lower unit")	correlation unit 2		
				Leon. Series	Bone Spring Limestone	correlation unit 1	Leon. Series	Bone Spring Limestone	

FIGURE 8-5.—Nomenclature, series assignment, and history of subdivision for the strata originally referred to Shumard's (1860) "black limestone," including members of the Cutoff Formation used in this paper (formally proposed in Harris, this volume).

limestone–shale triplet, in the Cutoff Formation (Figures 8-4, 8-5; see Harris, this volume) basinwards as the Cutoff Shale in toto. The thin-bedded black limestone overlying the El Centro triplet (the Williams Ranch Member) was not recognized as

Cutoff but was correctly interpreted as equivalent to the basal black limestone. The basal Williams Ranch Member–black limestone thus came to be the upper Bone Spring of Newell et al. (1953; Figure 8-5).

Harris (1988a) recognized three consistent lithostratigraphic subdivisions within the Cutoff Formation. He traced the Williams Ranch Member (correlation unit 5) to the edge of the basin just south of Bone Canyon, and he suggested that the low hills of black limestone south and west of El Capitan are comprised of that member of the Cutoff. Subsequent field work (Lambert, unpub.) corroborated this hypothesis by tracing the black limestone–Brushy Canyon contact through those low hills and into the slope area, working towards the shelf from the basinal black limestone outcrops. The Pipeline Shale Member was noted to be discontinuous along this transect, cut out in many places by later Brushy Canyon sandstones and shales (Lambert, unpub.). The Pipeline Shale Member pinches out at the basin edge one-half mile (0.8 km) south of Bone Canyon. Our collections of ammonoids and conodonts made along this basin to slope transect confirm that the black limestone is the basinal Williams Ranch Member of the Cutoff Formation.

The Leonardian–Guadalupian series boundary was delineated by Adams et al. (1939) between the Leonard and Word formations in the Glass Mountains, and between the Bone Spring Limestone and Brushy Canyon Formation in the Guadalupe Mountains (Figure 8-2). This stratigraphic designation was promoted prior to the differentiation of the Cutoff as a separate formation, and it incorporated the miscorrelation of the basinal black limestone. These lithostratigraphically derived boundary definitions were based, in part, on the contemporary interpretations of ammonoid zonal differences. Indeed, the fauna always cited in the literature as “Bone Spring” of the southern Guadalupe Mountains is that of the Cutoff Formation (black limestone). The Leonard and Word formations and their ammonoid zones (see below) were largely the basis for the Adams et al. (1939) series concepts.

Wilde has pointed out that fusulinid data strongly suggest the Road Canyon and Cutoff formations are at least partially correlative (e.g., Wilde and Todd, 1968; Wilde, 1990). Furthermore, these fusulinid faunas bear greater similarity to their Guadalupian descendants than their Leonardian predecessors. Several species range through these formations and into the overlying strata, but no holdover species from the underlying strata are known to occur in either the Road Canyon or Cutoff formations. Because current stratigraphic practice predicts greater precision by correlating first occurrences, Wilde has assigned all rocks containing these forms to the basal Guadalupian. Wilde’s age assignments have been adopted by many Permian basin workers.

The Cutoff Formation, originally a member of the Bone Spring Limestone, was initially retained in the Leonardian Series; nevertheless, it has become treated as Guadalupian by an increasing number of workers. Similarly, the Road Canyon was once a member of the Word Formation (Guadalupian Series), but, when elevated to formation status, it was reassigned to the Leonardian Series (Figures 8-3, 8-4). These juggled stratigraphic assignments were justifiable at the time because both the Cutoff (black limestone / Bone Spring) and

Road Canyon formations contain fossil communities comprising elements transitional between typical Leonardian and Guadalupian forms (Grant and Cooper, 1973:578). Furnish (1966, 1973) recognized the broad utility of erecting a separate stage to represent these transitional faunas, and he proposed the Roadian as the youngest stage of the Leonardian (Artinskian) Series. The Roadian Stage was readily adopted by many Permian stratigraphers.

Stratigraphic Framework

The Cutoff Formation forms a drape deposit overlying eroded Victorio Peak bank sediments and the basinal Bone Spring Limestone. Shoreward, the Cutoff passes laterally into shelf deposits of the lower and middle San Andres Formation (Boyd, 1958; Hayes, 1959; Sarg and Lehmann, 1986a). Well-exposed outcrops along the western escarpment of the Guadalupe Mountains expose a dip section cutting across an essentially complete shelf-to-basin profile (Figures 8-6, 8-7). The Cutoff is composed predominantly of very fine-grained basinal carbonate and clastic facies that accumulated under generally anoxic conditions during a pronounced marine transgression. Coarse rudstones and megabreccias occur primarily as channel fill in slope and proximal basin positions.

A vertical succession of five internal depositional units used for field correlation provides a consistent stratigraphic framework for mapping the Cutoff Formation. They are critical for understanding the formation because of discontinuous exposure along its paleo-slope. These units provide correlation within the stratigraphically complex slope area, as well as with more distant exposures both shelfward and basinward. The discontinuous character of the slope strata and the depositional topography on which the Cutoff Formation was deposited resulted from erosional episodes prior, during, and after Cutoff deposition (Harris, 1988a; Harris et al., this volume).

The Road Canyon Formation overlies slope and basinal facies of the Cathedral Mountain Formation (Figure 8-8). Where exposed, the contact of these formations commonly appears to represent a significant surface of channelling and scour (Figures 8-9, 8-10). The upper Road Canyon Formation is gradational with basinal facies of the Word Formation, and the contact is poorly defined. Most Road Canyon strata can be grouped into three primary sediment types: (1) fossiliferous packstones and grainstones, (2) fine-grained radiolarian and spicule-rich lutites, and (3) coarse sheet or lensoidal conglomerates and channelized megabreccias. Both the conglomerates and megabreccias are comprised of allochthonous clasts. Similarly, packstone and grainstone lithologies of the Road Canyon contain variable amounts of transported material. The Road Canyon Formation is interpreted to have accumulated in a distal shelf-to-slope setting (Harris et al., this volume).

The pattern of lithofacies succession and their relative proportions in the Road Canyon Formation is highly variable,

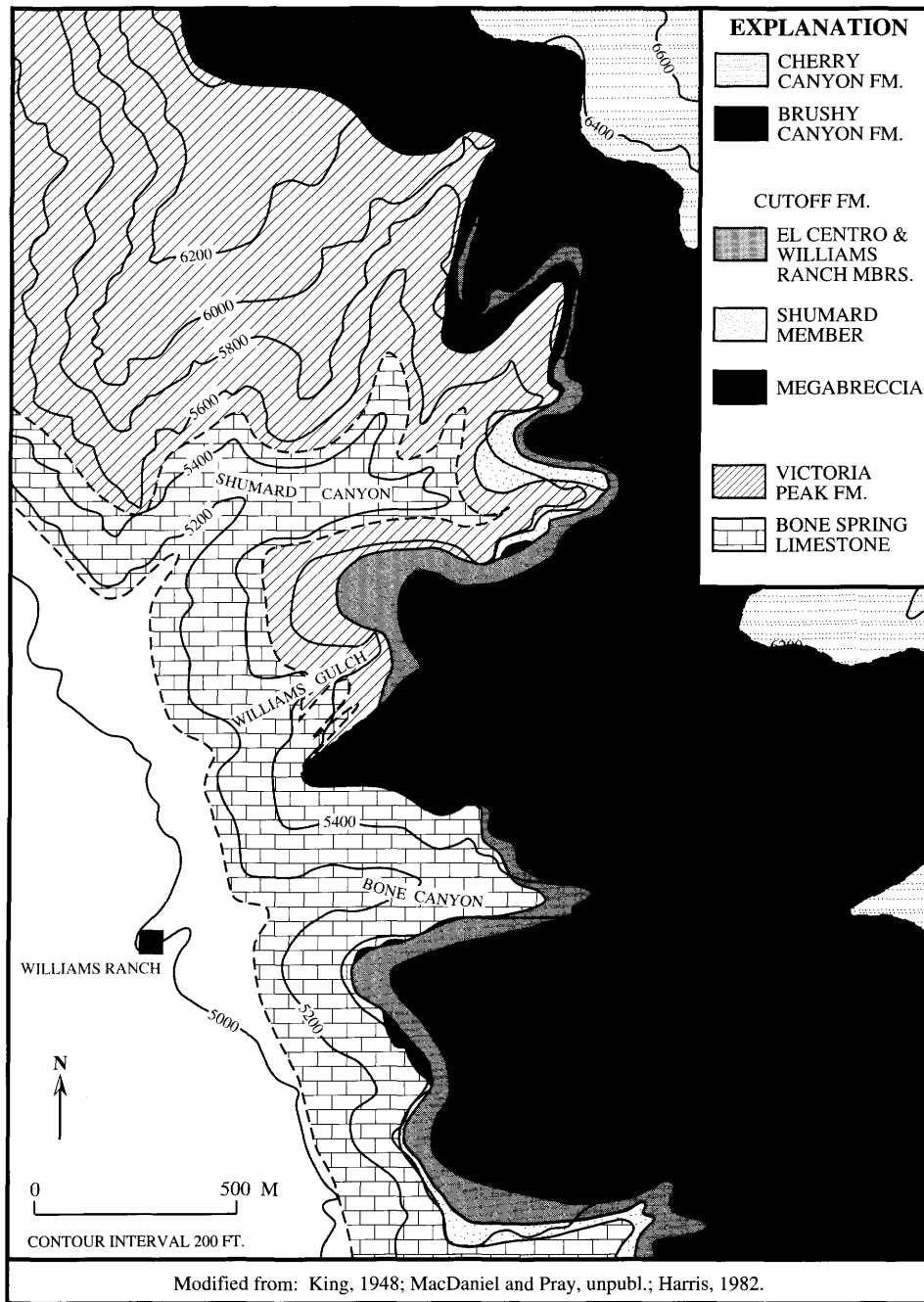


FIGURE 8-6.—General paleoenvironmental setting and distribution of the Cutoff Formation along the western escarpment of the Guadalupe Mountains. This area represents the paleoslope during Cutoff Formation deposition (compare with Figure 8-7).

particularly in comparisons between the easternmost and the westernmost Road Canyon (or Road Canyon equivalent) exposures. The formation outcrop parallels depositional strike, rendering the recognition of possible regional discontinuities corresponding to those of the Cutoff Formation, as well as other distinctive marker horizons, difficult to recognize. Despite

these complexities, an internal stratigraphic framework can be established by recognizing a stratigraphic pattern that records two successive episodes of major down-slope transport, which are overlain by deposits of a lesser magnitude transport episode. In the central Glass Mountains, the major transport episodes are recorded most commonly by megabreccia units.

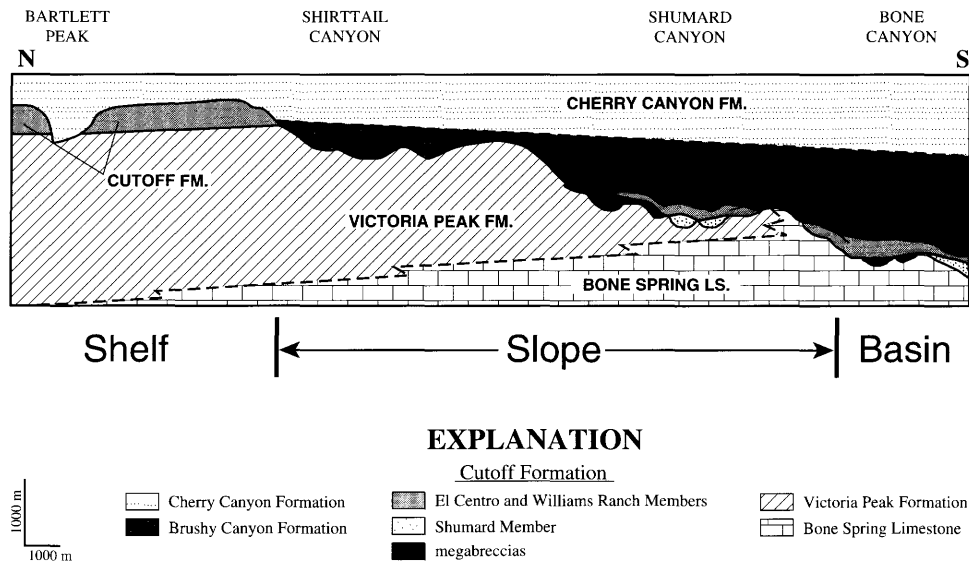


FIGURE 8-7.—North-south cross section of the Cutoff Formation as seen along the western escarpment of the Guadalupe Mountains. Note that the vertical exaggeration is $\times 2$.

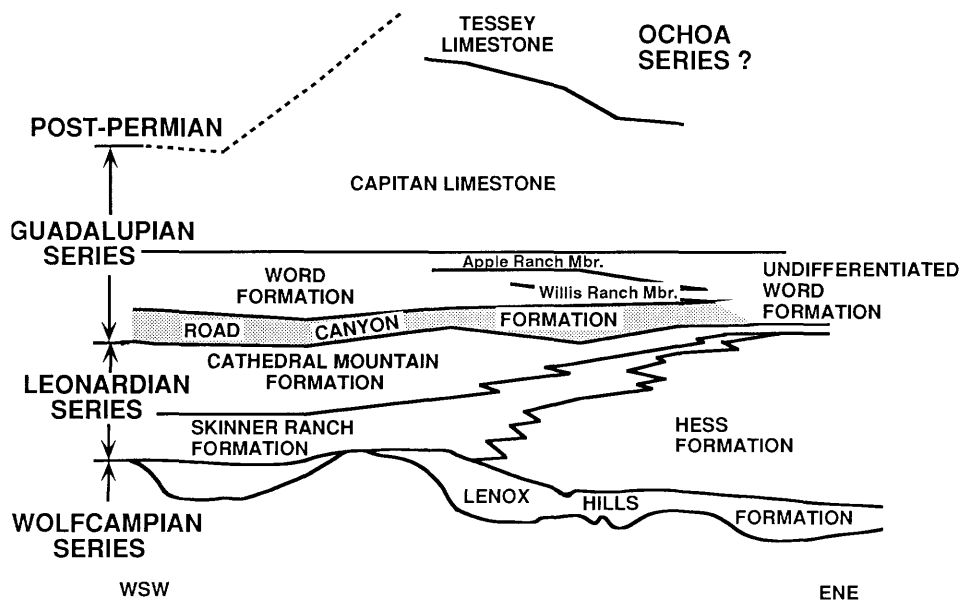


FIGURE 8-8.—Schematic cross section of the stratigraphy exposed along the Glass Mountains Front. (Modified from Ross, 1986.)

The other primary evidence of transport is distribution of the conglomeratic facies. Deposits of each transport episode are capped by a lower-energy facies (Harris et al., this volume).

The Road Canyon and Cutoff formations record a major, relatively rapid increase in sea level. Subdivision of both formations into smaller lithostratigraphic packages that represent contemporaneous depositional episodes provides the consistent internal stratigraphy necessary for precise biostratigraphy. A detailed review of the physical stratigraphy and

depositional environment of the Road Canyon and Cutoff formations is covered in a companion paper (Harris et al., this volume). Stratigraphic subdivision of the Cutoff Formation helps resolve the black limestone problem that confounded previous workers, which in turn clarifies the stratigraphic assignment of both old and new fossil collections. Recognition of the temporal sequence of Road Canyon transport episodes similarly provides for an improved assessment of new and previously collected faunas.

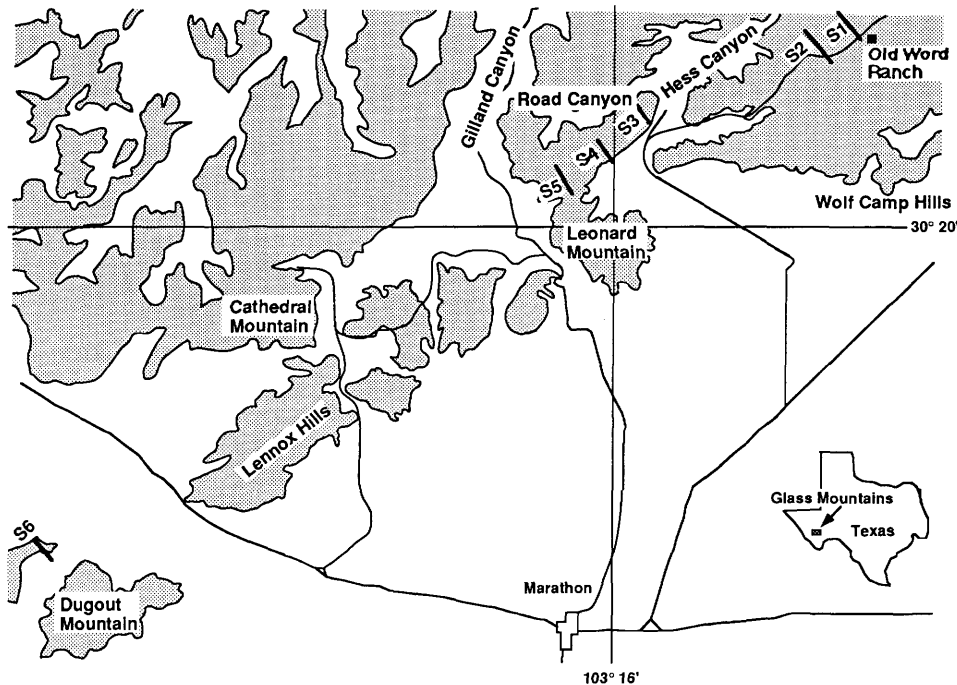


FIGURE 8-9.—Index map of Road Canyon Formation sections measured along the Glass Mountains Front, which were used to construct Figure 8-10. (Modified from Cooper and Grant, 1966.)

Distribution of Faunal Elements

AMMONOIDS

Böse (1919) established the *Perrinites* Zone for the Leonard Formation and the *Waagenoceras* Zone for the Word Formation (Figure 8-2). He correlated these zones with other previously described Permian ammonoid assemblages. Böse's pioneering ammonoid studies formed much of the basis for the series standardized by Adams et al. (1939). Later a conceptual problem arose when both *Perrinites* and *Waagenoceras* were reported from the first limestone member of the Word Formation (e.g., Clifton, 1945). Miller (e.g., 1938, 1945; Miller and Furnish, 1940) had insisted that these genera could not occur together. He argued that the first limestone member must be at least partially Leonardian in age because *Perrinites* is one of the most abundant taxa recovered from the base of that member. King (1947) pointed out that both taxa were present in the basal Word at the limits of their ranges; thus, he concluded that no real problem existed. However, when Cooper and Grant (1966) considered *Perrinites* and *Waagenoceras* along with brachiopods bearing a Leonardian aspect, they decided to erect the Road Canyon Formation for the first limestone member of the Word, and they reassigned it to the Leonardian Series (Figure 8-3).

Glassoceras, a rare ammonoid considered at the time of its discovery to be the stem cyclolobid (and thus the direct ancestor of *Waagenoceras* as *Stacheoceras normani* Miller and

Furnish, 1957), subsequently became an ammonoid index for the Road Canyon Formation. Although morphologically similar to the Cyclolobidae (Plate 8-2), *Glassoceras* is now classified as representing a distinct subfamily of the Vidrioceratidae (Ruzhentsev, 1960; Glenister and Furnish, 1987). The taxonomic concept of *Demarezites* was stabilized by Glenister and Furnish (1987) to represent ancestral cyclolobins. Its morphological characters intergrade with those of its descendant, *Waagenoceras*. Reports of *Waagenoceras* low in the Road Canyon Formation most likely represent occurrences of *Demarezites*, which is now also regarded as a Roadian ammonoid index. This possibility is presently being investigated. Transitional forms currently considered to be earliest *Waagenoceras* have been recovered from the topmost bed of the Road Canyon type section. Interestingly, *Perrinites* and *Demarezites* (*Waagenoceras* of older literature) have yet to be collected in direct association; however, museum records indicate that *Glassoceras* may occur with *Perrinites* in the Old Word Ranch area (AMNH loc. 503; see Appendix 8-1). It should be noted that *Perrinites* largely represents a shelf biotope, whereas *Demarezites* and most other cyclolobins represent basinal water masses. An old report of possible *Perrinites* from the black limestone (King, 1934, citing a footnote on page 160 in Böse, 1919) has not been substantiated.

Scattered ammonoids are present throughout the Road Canyon Formation. Most have been documented from beds in which they are especially abundant, but sampling has been uniquely extensive due in part to the comprehensive acid

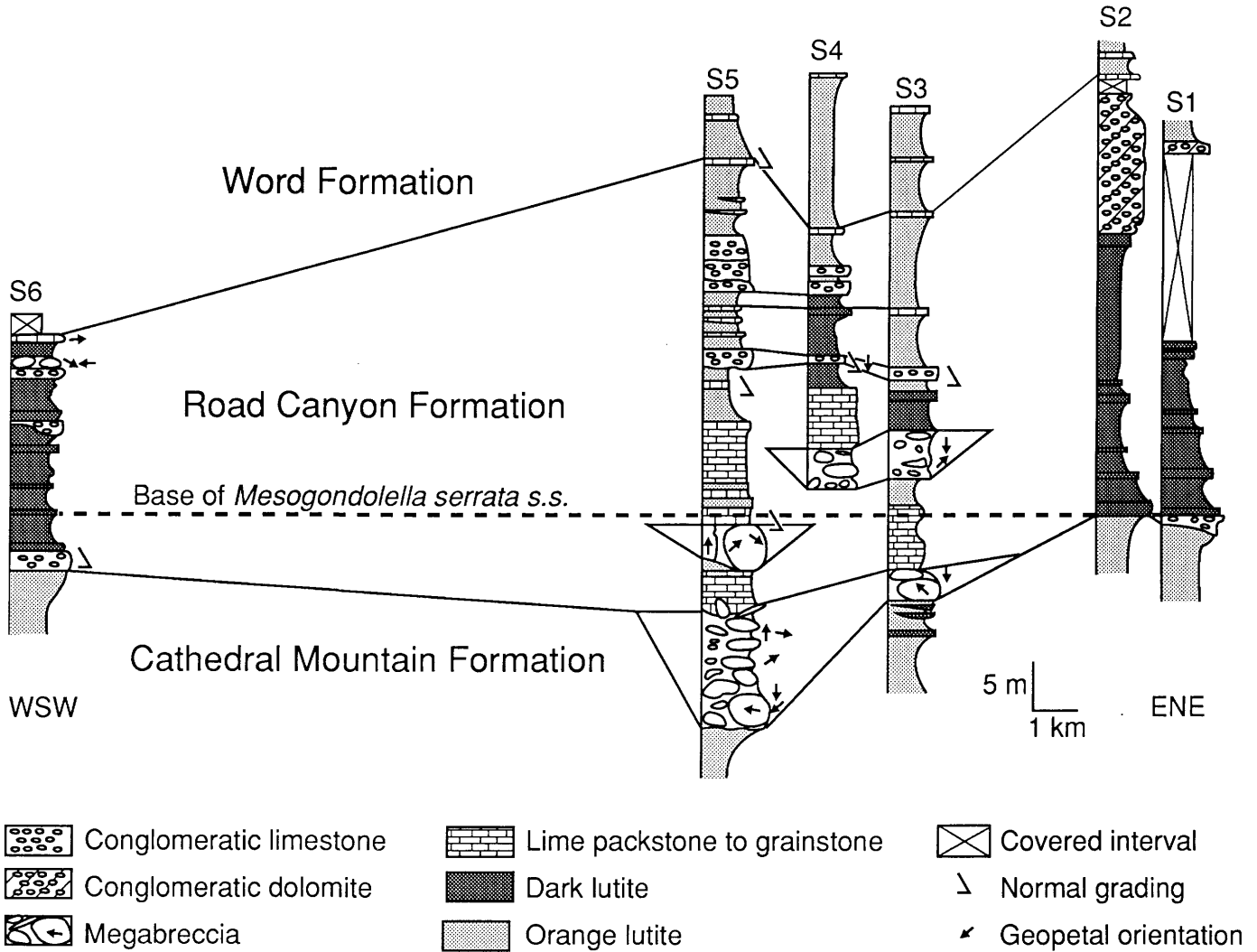


FIGURE 8-10.—Schematic of Road Canyon Formation measured sections. Datum is the lowest recovered *Mesogondolella nankingensis* s.s (senior synonym of *M. serrata*). Note widespread channelling at Road Canyon–Cathedral Mountain Formation contact.

etching program of Cooper and Grant (1972, 1974, 1975, 1976a,b, 1977). Ammonoid diversity is remarkably high in the Road Canyon, and the spatial distribution of forms is complex. Both result from the fact that the formation contains a mixture of taxa representing shelf and basinal paleoenvironments. The mixing may result primarily from physical depositional processes, or it may represent overlapping communities at their intergradational boundary. Table 8-1 lists the ammonoids that are well-documented from the Road Canyon. This diverse assemblage comprises much of the Roadian ammonoid fauna of North America (Plates 8-2, 8-3).

A particularly important Road Canyon ammonoid locality is USNM loc. 732z. It represents a microcosm of the entire Road Canyon ammonoid fauna, which contains an admixture of shelf and basin faunal elements. It is the source of the largest

collection of Permian ammonoids from West Texas, and it provides the primary data for detailed correlation between the Glass and Guadalupe mountains (Furnish and Glenister, 1977). Most of the ammonoids are exquisitely preserved as ferric molds, showing fine details of ornamentation and sutural configuration. *Paraceltites elegans* (Girty), *Peritrochia erebus* (Girty), and *Texoceras texanum* (Girty) are extremely abundant in both the basinal Cutoff Formation and at loc. 732z but are uncommon elsewhere. Noteworthy rare ammonoids recovered from this locality also have their counterparts in the Cutoff Formation (black limestone) of the Guadalupe Mountains. For example, *Peritrochia* n. sp. is represented in the Cutoff Formation by a single specimen, and the only other known specimen is from Road Canyon Formation locality USNM loc. 732z. *Epithalassoceras* (?) n. sp. has only been recovered from

TABLE 8-1.—Ammonoids documented from the Road Canyon Formation.

<i>Agathiceras girtyi</i>
<i>Agathiceras uralicum</i>
<i>Daubichites cooperi</i>
<i>Epithalassoceras(?)</i> n. sp.
<i>Eumedlicottia burckhardti</i>
<i>Glassoceras normani</i>
<i>Neocrimites</i> spp.
<i>Paraceltites elegans</i>
<i>Peritrochia erebus</i>
<i>Peritrochia</i> n. sp.
<i>Perrinites vidriensis</i>
<i>Propinacoceras</i> spp.
<i>Roadoceras roadense</i>
<i>Stachaeoceras</i> spp.
<i>Stenolobulites stenolobulus</i>
<i>Texoceras texanum</i>
<i>Waagenoceras</i> n. sp.

the Glass Mountains (USNM locs. 732z and 739d) and the Guadalupe Mountains (Pipeline Shale Member type section). Similarly, *Stenolobulites stenolobulus* Mikesch, Glenister, and Furnish is present in the basinal Cutoff Formation, and most Road Canyon specimens are from USNM loc. 732z.

The majority of ammonoids collected from the Cutoff Formation have been recovered from the Williams Ranch Member. Scattered specimens are present throughout that member, but preservation is best and diversity is highest in the ammonoid-rich horizons near the top. Newell et al. (1953) noted the presence of ammonoids all along the top of the Cutoff as they traced the upper Bone Spring basinward from Bone Canyon. That is still the case, confirmed recently by tracing the black limestone northward from the basin to Bone Canyon (Lambert, unpub.). This extensive concentration of ammonoids may represent a single widespread sedimentological event in the Delaware basin (*sensu* Spinosa et al., 1975), or it could have resulted from accumulation during a brief period of sediment starvation.

The components of the Cutoff ammonoid fauna form a diagnostic assemblage that should be immediately recognizable as the Bone Spring (black limestone) fauna of past studies (Table 8-2). The basinal Cutoff Formation of the southern Guadalupe Mountains is the type stratum of *Texoceras texanum*, *Peritrochia erebus*, and *Paraceltites elegans* (Girty, 1908). These taxa are by far the most common ammonoids in the basinal Cutoff. The first two of these are not known outside of correlative strata in West Texas. *Paraceltites elegans* more typically comprises a widespread but rare component of Guadalupian ammonoid faunas. Most of the other taxa present are also comparatively rare. *Stenolobulites stenolobulus* has a restricted distribution similar to that of *T. texanum* and *P. erebus*. The single thalassoceratid fragment so far recovered from the Cutoff represents an advanced form, but it is at such an early stage of ontogeny that generic assignment is unwarranted. A few forms (e.g., *Agathiceras*) represent widespread ammonoid taxa with little biostratigraphic utility.

Ammonoids recovered from other members of the Cutoff Formation are poorly documented. A possible example is an incomplete pseudogastrioceratin mold from the base of the Cutoff (El Centro Member ?) preserved in a fault block west of Bartlett Peak (Warren, 1955). During the present study, fossils that may represent poorly preserved ammonoids were occasionally noted in the middle limestone of the El Centro Member along the western escarpment of the Guadalupe Mountains. Unfortunately, these specimens are unusually fragile and are tightly held within the matrix. As a consequence, they typically break across the fossils rather than crack out of the rock, and they are not preserved by differential weathering. A specimen of *Perrinites* described by Miller and Furnish (1940) from USGS loc. 7701-PC along the western escarpment south of Bone Canyon could be either from the Shumard Member of the Cutoff Formation or from the upper Bone Spring Limestone. Indeterminate ammonoids were recently noted in the upper Bone Spring Limestone near that locality.

The San Andres Formation of the northern Guadalupe Mountains is the updip equivalent of the Cutoff Formation and is comprised of middle to distal shelf deposits (Boyd, 1958; Hayes, 1959; Sarg and Lehmann, 1986a). The San Andres produces rare ammonoids from scattered localities. *Perrinites vidriensis* Böse, *Paraceltites elegans*, and *Stenolobulites stenolobulus* have been recorded from the northern Guadalupe, confirming correlation with the Cutoff and Road Canyon formations (see Wilkerson et al., 1991). Strata assigned to the Cutoff Formation in the Apache Mountains located to the southeast (Wood, 1968) are slightly different lithologically from the Cutoff elsewhere, but they have produced *P. elegans*, *Stenolobulites* aff. *S. stenolobulus*, and a weathered specimen of *Texoceras texanum*. These ammonoid taxa again strongly support previous fusulinid correlations (Wilde and Todd, 1968). Several poorly preserved specimens from localities assigned to the Bone Spring Limestone in the Delaware Mountains to the south and the Sierra Diablo to the south-southwest (the latter cited in King, 1964) may, in part, be from the Cutoff Formation or an equivalent, but field verification is needed for confident stratigraphic assignment.

Immediately overlying the basinal Cutoff Formation (and its abundant Williams Ranch ammonoid fauna) is the Brushy Canyon Formation. The lowermost unit of the Brushy Canyon

TABLE 8-2.—Ammonoids documented from the Williams Ranch Member of the Cutoff Formation.

<i>Agathiceras girtyi</i>
<i>Eumedlicottia burckhardti</i>
<i>Paraceltites elegans</i>
<i>Peritrochia erebus</i>
<i>Peritrochia</i> n. sp.
<i>Stenolobulites stenolobulus</i>
<i>Texoceras texanum</i>
<i>Thalassoceras(?)</i> spp.

is the discontinuous Pipeline Shale Member (Warren, 1955). In at least its type locality in the basin, the Pipeline Shale Member produces another diagnostic and important ammonoid fauna consisting of the taxa listed in Table 8-3. King (1948) stated that the Pipeline Shale is continuous in the Delaware Mountains, but his interpretation appears to have been based on mapping covered slopes, where typical Brushy Canyon sandstones and siltstones are indistinguishable from the nonresistant Pipeline Shale. We could not confirm these relations because of restricted access to the land. The Cutoff-Brushy Canyon contact has been traced into Guadalupe Mountains National Park, where the Pipeline Shale Member pinches out against the basin edge just south of Bone Canyon.

Referring to Table 8-3, note that the Pipeline Shale Member duplicates only *Eumedlicottia burckhardtii* Böse (and possibly the thalassoceratid) from the immediately underlying Cutoff ammonoid fauna. A cursory examination of the ammonoid taxa listed on these tables might suggest that the faunal differences are pronounced; however, cyclolobins have yet to be collected from strata older than the Pipeline Shale Member in the Guadalupe Mountains. The *Waagenoceras* present in the Pipeline Shale appears to be conspecific with the transitional *Demarezites-Waagenoceras* recovered from the uppermost type Road Canyon. Moreover, all but two ammonoid species collected from the Cutoff Formation and the Pipeline Shale Member occur together in the Road Canyon Formation. As discussed previously, *Demarezites* is probably present but misidentified as *Waagenoceras* and/or *Glassoceras*. *Altudoceras*, *Daubichites*, and *Roadoceras* are closely related pseudogastrioceratin genera with overlapping ranges and similar paleoenvironmental distributions. Consequently, a faunal comparison with the Road Canyon Formation strongly suggests that the disconformity separating the Brushy Canyon (Pipeline Shale Member) and Cutoff formations represents only a minor hiatus in the Delaware basin.

The ammonoid assemblages recovered from the Pipeline Shale Member (Brushy Canyon) and the Road Canyon and Cutoff formations reflect affinities with both Leonardian and Guadalupian faunas. *Perrinites* is the most abundant genus recovered from the Glass Mountains front, on which the type Road Canyon was established. It represents the last of a family that characterizes the entire Lower Permian, and it is the index taxon for the classic Leonardian ammonoid zone. Conversely, *Paraceltites* first appears in these strata, and it is the oldest genus in the suborder Ceratitina. The Ceratitina flourished in the Upper Permian and eventually gave rise to most Mesozoic ammonoids (Spinosa et al., 1975). *Stenolobulites* represents the earliest Pseudogastrioceratinae, a group that similarly flourished in the Upper Permian. The Pseudogastrioceratinae is the only subfamily of the Goniatitina that may have extended into the Triassic, although only briefly. Ammonoid biostratigraphy and correlations in the middle through Upper Permian are largely based on evolutionary lineages within the Cyclolobidae (Furnish and Glenister, 1970; Glenister, 1981). This important

TABLE 8-3.—Ammonoids documented from the Pipeline Shale Member, basal Brushy Canyon Formation.

<i>Altudoceras altudense</i>
<i>Demarezites</i> n. sp.
<i>Epithalassoceras</i> (?) n. sp.
<i>Eumedlicottia burckhardtii</i>
<i>Waagenoceras</i> n. sp.

family evolved during Roadian time and is first represented in West Texas by *Demarezites*. A strong case can thus be made that Roadian ammonoids reflect stronger Guadalupian attributes rather than Leonardian.

A recently discovered locality at the Road Canyon type section is important because it produces ammonoids in direct association with a conodont morphotype transitional between the species *Mesogondolella idahoensis* and its descendant, *M. nankingensis* (see below). The small silicified ammonoids are poorly preserved with few external sutures, but conch form and internal sutures are sufficiently diagnostic to assign many specimens to the genus level with confidence. Preliminary study records representatives of *Eumedlicottia*, *Paraceltites*, *Peritrochia*, and *Stenolobulites*. Other specimens include very poorly preserved propinacoceratids, thalassoceratids, and intriguing globular forms that may represent cyclolobids. Comparison with other specimens recovered from the Road Canyon Formation suggests some specific assignments (e.g., the *Peritrochia* are probably *P. erebus*); however, insufficient data is presently available to determine whether the globular forms represent *Glassoceras* or *Demarezites*. This locality is significant in that (1) it produces an abundant and diverse fauna comprised of characteristically Guadalupian ammonoids considered typical of the Roadian, with no representatives of *Perrinites*, (2) this Guadalupian ammonoid fauna coincides with the upper range of a transitional form between the conodonts *M. idahoensis* and *M. nankingensis*, and (3) the locality is part of the Road Canyon type section. This fauna further strengthens Road Canyon ammonoid ties with the Guadalupian rather than the Leonardian Series.

CONODONTS

Conodont faunas from both the Road Canyon and Cutoff formations are dominated by the genus *Mesogondolella*. Other faunal components include *Diplognathodus*, *Hindeodus*, *Neostreptognathodus*, *Sweetina*, *Sweetognathus*, and *Xaniognathus*. Only the *Mesogondolella* lineage will be considered in the present discussion because it provides the primary database for conodont biostratigraphy and correlation in the middle Permian (Clark and Behnken, 1979; Clark et al., 1979). The predominance of *Mesogondolella* along the western escarpment and in Guadalupe Pass suggests that exclusively basin-type conditions prevailed for the Cutoff Formation, following the biofacies distribution model of Wardlaw and

Collinson (1984). The relative proportions of genera present (Wardlaw and Grant, 1990), along with a relatively sparse ramiform element representation (reflecting the degree of apparatus completeness), support interpreting an offshore milieu with elevated hydrodynamic energy for the mixed shelf and basinal components of the Road Canyon Formation.

Geochemical conditions related to the paleoenvironment resulted in lithologies that are difficult and time-consuming to process for microfossils. Facies in both formations are dominated by organic-rich lutites that accumulated under dysaerobic to anoxic conditions, and samples often require complex methods of disaggregation. The pervasive organics, particularly characteristic of the Cutoff Formation, typically release petroliferous lixivium into solution during acid digestion of carbonate lithologies. This interferes with further carbonate dissolution. Abundant disseminated argillaceous material also commonly insulates carbonate samples from complete acid digestion. A significant portion of insoluble residues is composed of sponge spicules, radiolarians, and other siliceous microdetritus. Fissile lithologies are commonly enriched in silica cements from these sources, and they are similarly resistant to acid digestion. As a result, multiple processing methods over a series of runs are needed to completely break down the rock. Nevertheless, persistence is rewarded with pristinely preserved specimens. The relative abundance of conodonts in the Cutoff Formation varies significantly between samples, but the average is roughly five elements per kilogram of rock. Samples from the Road Canyon Formation almost always produce conodonts, but in variable amounts related to the sample's lithology (Lehrmann, 1988; Wardlaw and Grant, 1990).

The conodont biostratigraphy of the Road Canyon Formation has been examined recently by Lehrmann (1988) and Wardlaw and Grant (1987, 1990). Lehrmann (1988) found the evolutionary succession from *Mesogondolella idahoensis* (which largely characterizes the Leonard Formation) to *M. nankingensis* to occur low in the Road Canyon, commonly within the basal beds of the formation. Wardlaw and Grant (1990) reported the changeover to occur slightly higher, at various horizons in the lower one-third of the Road Canyon Formation. They described the changeover to be rapid, often represented by the co-occurrence of both species within a single sample. The apparent synchronicity of this evolutionary succession across the North American continent (possibly worldwide) led them to recommend the first occurrence of *M. nankingensis* to mark the base of the Guadalupian. They recognized that such a boundary definition would closely match the original Leonardian-Guadalupian boundary in the Glass Mountains. The rapid conodont changeover within the Road Canyon Formation, however, also led them to recommend abandoning the Roadian Stage (Grant and Wardlaw, 1984; Wardlaw and Grant, 1990).

The confusion over precisely where the changeover occurs stems from the way that *Mesogondolella idahoensis* evolved

into *M. nankingensis*. The anterior platform margins of *M. nankingensis* have conspicuous serrations that variably extend toward the posterior of the element. This striking character serves to distinguish *M. nankingensis* from *M. idahoensis*, its direct ancestor, which has unornamented platform margins. Basinal deposits of the Cutoff Formation along the western escarpment of the Guadalupe Mountains preserve a complete record of the morphological transition from *M. idahoensis* to *M. nankingensis*. Faunal suites representing juvenile through adult stages of development provide a detailed chronicle of the clinal pattern by which this transition proceeded. Several important characters, in addition to platform serration, evolved at different rates relative to each other, resulting in a mosaic pattern of transition from one species into the next (Plate 8-4). The clinal record preserved in the Cutoff Formation can be used to interpret the complex distribution of morphotypes characteristic of the lower Road Canyon Formation.

Mesogondolella idahoensis has a Pa element with parallel to slightly tapering sides through the posterior three-fourths of the platform. It tapers more markedly, yet evenly, through the remaining one-fourth to its anterior termination. The platform is usually widest at its posterior end, but very large individuals can be slightly wider at mid-platform. The posterior termination is blunt, commonly with squared lateral margins. The entire element may be gently bowed, arched, or both.

Carina denticles are moderately high in the anterior portion of *M. idahoensis*, but they decrease in size toward the posterior cusp. These denticles are compressed and fused anteriorly, round and variably discrete posteriorly, and transitional along the mid-platform. Denticles typically become more fused and less pronounced in larger elements. Adcarinal furrows are wide, shallow, and typically well defined. The posterior platform margins are often thickened around the posterior end of the adcarinal furrows, which results in a characteristically steep cul-de-sac posterior termination of the furrows.

The rounded cusp of *M. idahoensis* is erect and conspicuously large, usually more than twice the size of the adjacent carinal denticle. It is often fused with this posterior-most carinal denticle, producing an ellipsoidal cusp cross section. In large specimens, the cusp is commonly fused to the posterior lateral margins as well, resulting in a distinctive triangular cross section. A blade-like secondary carina can be developed by the incorporation of a small accessory denticle posterior of the cusp, which is fused to the cusp complex and sometimes to the adjacent carina denticle. This entire denticle amalgamation is compressed and is usually oriented toward the inner lateral terminus.

Viewed from the bottom, the lower attachment surface of *M. idahoensis* forms a broad, open V-shaped groove that is elevated anteriorly to form a short open keel. Posteriorly, this groove is recessed for three-fourths to four-fifths of the platform length. It is flat in subadults. The posterior loop surrounding the basal pit is poorly developed and often asymmetrical.

Mesogondolella nankingensis is characterized by a Pa element that tapers through its anterior one-half to one-third, with distinctively pronounced serrations along the tapering anterior margins. These serrations cut the lateral margins in the anterior one-third to one-half of the platform, are subdued to subtle in the mid-platform, and are absent to subtle in the posterior one-third of the platform. *Mesogondolella serrata* (Clark and Ethington, 1962) is a junior synonym of *M. nankingensis* (Ching, 1960).

The anterior platform of *M. nankingensis* terminates at or, more characteristically, just short of the anteriormost carina denticle. Elements may be quadrate or possess a modified tear-drop shape posteriorly. The former have a blunt posterior termination and are marginally widest in the posteriormost one-fourth of the element. Forms with a tear-drop shape are significantly more common and tend to be widest near the platform midpoint. Bowing is relatively rare in *M. nankingensis*. Elements are typically arched gently through the posterior part of the element. The tapered serration-bearing anterior tends to be straight, producing a prominent tangential profile in contrast to the arched posterior platform.

Carina denticles of *M. nankingensis* are moderately high in the anterior portion but low in the middle and posterior platform. Denticles are discrete, round, and pointed. They are compressed in the anterior and become decreasingly compressed toward the posterior. The denticles become subdued and sometimes partially fused posteriorly with increasing specimen size. Adcarinal furrows are commonly well defined but tend to be moderately thin and shallow. The relative width and degree of their development is often inversely proportional to that of the enclosing serrations.

The cusp of *M. nankingensis* is relatively subdued, often no larger than the posterior carina denticles. It becomes increasingly distinct in larger specimens. The cusp is most commonly circular to elliptical in cross section, and it often comprises the posteriormost part of the platform. Accessory denticles and secondary carinae are rare; however, in submature specimens the cusp may comprise a pair of denticles that are offset by a gap, but which otherwise are identical with the adjacent posterior carina denticles. These twinned cusp denticles coalesce with full maturity and produce a distinctly elliptical cusp that is, nevertheless, only slightly larger than the adjacent carina denticles. Although usually erect, the cusp can be proclined in a small percentage of specimens.

In lower view, the attachment surface of *M. nankingensis* is generally narrow, with a very well-defined keel. The keel usually extends one-fourth (maximum of one-third) of the length of the lower surface, opposite the tapering portion of the platform. The keel is characteristically elevated above the rest of the lower surface, although in very large specimens the posterior portion may be comparatively flat. The posterior loop surrounding the basal pit is well defined and conspicuous.

The most striking and consistent character through the transition from *M. idahoensis* to *M. nankingensis* is platform

ornamentation. Serrations first occur in specimens above the basal shale of the El Centro Member, where they are restricted to juvenile specimens. Subadult and adult forms mask the serrations beneath successive laminae. The smoothed serrations are initially masked at the margins, leaving subdued relict serrations adjacent to the adcarinal furrows. Slightly higher in the El Centro Member, subadult specimens display the subdued serrations, whereas those on juveniles become better defined. This incrementally expanding pattern of serration is carried progressively later through ontogeny with increasingly younger faunas. Adult specimens from the middle El Centro Member attain the pronounced serrations characteristic of *M. nankingensis* sensu stricto, which are distinctly visible in side view as notches in the anterior platform margins. Notches are not discernible from this perspective on earlier transitional forms. This type of progressive juvenilization through character development results from the heterochronic process of neoteny (Alberch et al., 1979; McNamara, 1986).

In lower view, the broad, flat, and often recessed basal attachment surface of adult *M. idahoensis* narrows and develops a consistently elevated keel through the transition. Correspondingly, the posterior loop becomes increasingly well developed at all stages of ontogeny. This reflects a reverse pattern of the ontogenetic development of *M. idahoensis*. The fused anteriormost denticles of the carina in adult *M. idahoensis* also progressively separate and tend to become discrete during the transition, a character of both *M. nankingensis* and juvenile *M. idahoensis*. The cusp and posterior carina denticles become less pronounced and less fused. The adcarinal furrows also become less prominent by continued thinning and shallowing. The amalgamated cusp complex of *M. idahoensis* becomes increasingly rare, and the cusp attains a simplified circular to elliptical cross section. All of these characters can be seen to have passed through different stages of ontogeny during the transition, and together they represent a mosaic heterochronic paedomorphocline (McNamara, 1990).

The temporal pattern of increasingly developed serration accounts for the discrepancy between where Lehrmann (1988) and Wardlaw and Grant (1987, 1990) recognized the basal *Mesogondolella nankingensis* Zone. Lehrmann placed the boundary at the first serrated conodont recovered from each section, whereas Wardlaw and Grant selected the first occurrence of populations in which serrations were exhibited by adult specimens. The latter authors referred early transitional forms to *M. idahoensis* because of the unserrated adult morphologies. The level within the transition where some subadults first became serrated accounts for the Road Canyon samples described by Wardlaw and Grant (1990) as containing both *M. idahoensis* and *M. nankingensis*.

It should be noted that in certain places Lehrmann (1988) and Wardlaw and Grant (1990) selected the same boundary horizon, in part because the record of transition in the Road Canyon Formation is confounded by stratigraphic admixture and, in most localities, is less complete than in the Cutoff

Formation. This results from sedimentological complications related to the predominance of allochthonous carbonate lithologies in the lower Road Canyon Formation of the eastern and central Glass Mountains (Figure 8-10). A better record of the transition is preserved in the western Glass Mountains, where transportation events were less pervasive and scouring was less intensive in the subdued energy of a more basinward setting. Although the species transition preserved in the Glass Mountains is significantly less straightforward than it is in the Guadalupe Mountains, enough of the record is present that, particularly if an early point in the transitional continuum is selected to define the basal Guadalupian boundary, the majority of the Road Canyon Formation will be included in the Guadalupian.

Mesogondolella idahoensis characterizes the Bone Spring Limestone of the Guadalupe Mountains western escarpment (Behnken, 1975). It is also present in the Shumard Member of the Cutoff Formation in the basal rudstone of the type section, and it has been recovered near the top of the member from several samples in paleo-slope and basin localities. The transition from *M. idahoensis* to *M. nankingensis* takes place entirely within the middle El Centro Member. Bruce Wardlaw has kindly made his conodont collections available for study, and they include an abundant occurrence of the transitional form from flank beds associated with the large megabreccia just south of Bone Canyon. The remainder of the Cutoff Formation and the lower Brushy Canyon Formation are characterized by *M. nankingensis*. Relatively abundant *M. nankingensis* from several black limestone localities in the basin confirm that it is correlative with the upper Cutoff Formation.

Mesogondolella nankingensis was the first in a sequence of variably serrated species that characterize the Guadalupian (Clark and Behnken, 1979). This gives the Roadian a distinctly Guadalupian aspect with respect to conodonts. The authors concur with Grant and Wardlaw (1984) and Wardlaw and Grant (1990) that the Leonardian–Guadalupian boundary should be recognized at the first occurrence of *M. nankingensis* (i.e., somewhere within the morphological continuum between *M. idahoensis* and *M. nankingensis*). With the additional information summarized herein, that level is demonstrated to closely match the base of the original Guadalupian Series in the Guadalupe Mountains and the original Leonardian–Guadalupian boundary in the Glass Mountains. It would accordingly settle the continuing confusion that results from previous miscorrelations. Additionally, the various interrelated changes in morphology provide a complex pattern on which a precise definition of the basal Guadalupian boundary can be established.

FUSULINIDS

Fusulinids are abundant and diverse through most of the Road Canyon Formation. Ross (1963) was the first specialist to study the Road Canyon fauna in detail. During the extensive

work of Cooper and Grant (1964, 1966, 1972, 1974, 1975, 1976a,b, 1977), fusulinid specimens were referred to C.A. Ross, J.W. Skinner, and G.L. Wilde for identification and biostratigraphic interpretation (Cooper and Grant, 1977). Since then Wilde has dealt extensively with Road Canyon correlations based on fusulinid data (Wilde and Todd, 1968; Wilde 1975, 1986a,b, 1990, this volume). Other recent fusulinid studies include those of Yang and Yancey (this volume).

Wilde (1990) assigned the Road Canyon to the *Parafusulina boesei*–*Skinnerina* Zone. *Parafusulina boesei* Dunbar and Skinner, *P. attenuata* Dunbar and Skinner, and *P. splendens* Dunbar and Skinner are particularly abundant. Other species of *Parafusulina* and *Skinnerina* are important faunal associates (notably *P. rothi* Dunbar and Skinner). Fusulinid workers have long agreed that this fauna bears a much closer affinity to the overlying Guadalupian faunas than to the preceding Leonardian ones. Indeed, neither Ross nor Wilde found a single Road Canyon species in common with those of the Leonardian Formation, although several are shared by the Road Canyon and younger Guadalupian faunas (Ross, 1963; Wilde, 1975, 1990). An unpublished report by Skinner (mentioned in Wilde, 1975) is sometimes referred to during discussions in support of a Leonardian affinity for Road Canyon fusulinids. The discrepancy is probably because of the old dogma: the upper Bone Spring fusulinids studied by Skinner were probably collected from basinal flow deposits located in the upper black limestone—and were considered to be from the Bone Spring Limestone a priori, rather than the truly correlative Cutoff Formation.

Fusulinids are relatively rare in the Cutoff Formation along the western escarpment and in basinal exposures of the Guadalupe Mountains. Warren (1955) reported fusulinids from the type Cutoff at Cutoff Mountain, but specific identifications were not mentioned, nor were the collections successfully duplicated until recently. Wilde (1988) illustrated two fusulinid genera and species from approximately the middle of the type section: *Parafusulina splendens* Dunbar and Skinner and *Skinnerina rotundata* (Dunbar and Skinner). The only other published fusulinids from the Cutoff Formation proper were those collected by Harris from the Williams Ranch Member just west of El Capitan. These specimens were recovered from two intraclastic rudstone flows near the base of the member. Wilde (1986b) identified these specimens as *P. boesei* and *P. maleyi* Dunbar and Skinner. All of these taxa consistently support the correlation and age assignment of the Road Canyon and Cutoff formations to a Roadian fusulinid Zone of *Parafusulina boesei*–*Skinnerina* (Wilde, 1990), which bears a distinctly Guadalupian aspect.

Implications and Recommendation for Permian Chronostratigraphy

Ammonoid, conodont, and fusulinid faunas are accorded premier importance for Upper Paleozoic biostratigraphy and correlation. The foregoing discussion illustrates the unique

character of each of these major taxa in the Road Canyon and Cutoff formations and demonstrates the excellent correlation between the Road Canyon and the combined Cutoff–Pipeline faunas. All three faunal groups are first represented in Roadian strata by forms considered characteristic of the Guadalupian. The temporal distribution of biostratigraphically important taxa and our correlation of Roadian sections in the Guadalupe and Glass mountains are summarized in Figure 8-11.

The faunal correlations are corroborated by physical depositional evidence that these widely separated sections accumulated during a major marine transgression (Harris et al., this volume). The magnitude of this event was such that its correlation potential was recognized before sequence stratigraphy was developed and used in a similar manner (e.g., Wilde in Wilde and Todd, 1968). If this sea-level rise can be demonstrated to be eustatic, it will provide an additional criterion on which correlations outside the Trans-Pecos region can be based.

The Road Canyon and Cutoff formations have long been part of the standard reference for the Permian of North America. This regional reference gained increasing international status as it became widely recognized that the middle Permian deposits of the Ural Mountains (type Permian) are comprised largely of evaporitic and continental strata. When Girty (1902) erected the Guadalupian it became the first series-level chronostratigraphic unit for rocks of middle Permian age. The Guadalupian Series, therefore, has priority as the type for a formal Middle Permian Series.

Stabilization of the lower Guadalupian Series boundary is the only remaining step. Recent field studies have clarified lithostratigraphic relationships in both the Guadalupe and Glass mountains (Harris et al., this volume). In turn, biostratigraphic resolution has been greatly increased, and previous miscorrelations have been corrected. Both priority and stability are best served by restoring Girty's original (1902) Guadalupian Series concept. The lower portion of the Guadalupian, excluded by

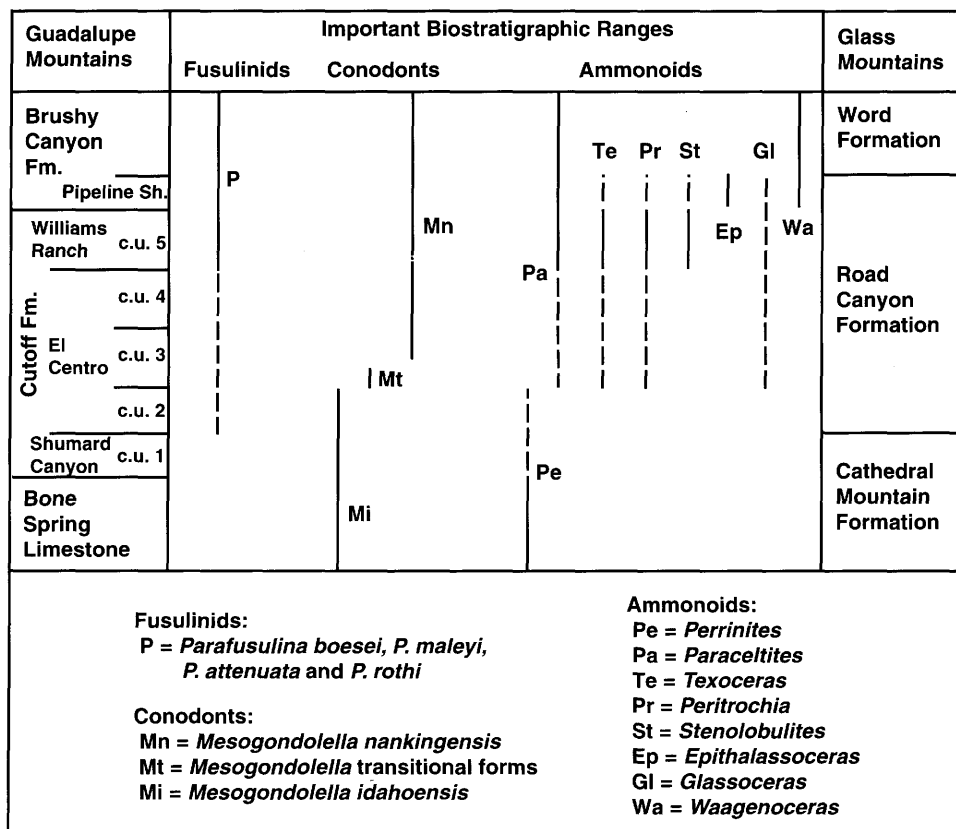


FIGURE 8-11.—Correlation and faunal range summary for the Cutoff (Guadalupe Mountains) and Road Canyon (Glass Mountains) Formations. Dashed ranges are those documented only in the Glass Mountains. Note that “P” includes other species of *Parafusulina*, and *Skinnerina* as well (see Wilde, 1990, this volume). “Gl” may include early species of *Demarezzites* in the Road Canyon; “Wa” includes *Demarezzites* n. sp. in the Pipeline Shale. Distribution of the *Mesogondolella idahoensis*–*M. nankingensis* transitional form strongly suggests that the discontinuity between the Shumard and El Centro members of the Cutoff Formation corresponds with the basal Road Canyon channelling event. The uninterrupted faunal record of the upper Road Canyon and its similarity to the record in the Guadalupe Mountains suggests that the Cutoff–Pipeline discontinuity represents a condensed section or a minor hiatus, rather than a major unconformity.

Adams et al. (1939), is retained as the Roadian Stage. The section in the type Guadalupian that correlates directly to the Road Canyon Formation is the upper Cutoff Formation (El Centro and Williams Ranch members) through the Pipeline Shale Member. Grant and Wardlaw (1984) and Wardlaw and Grant (1987, 1990) proposed that the Leonardian–Guadalupian boundary be based on the conodont changeover from *Mesogondolella idahoensis* to *M. nankingensis*, which is recognizable worldwide (e.g., Clark and Wang, 1988). The middle limestone in the El Centro Member of the Cutoff Formation contains a complete record of the evolutionary continuum through which this transition occurred. The transition and the beds from which it has been recorded meet all criteria for establishing a Global Stratotype Section and Point.

The authors therefore recommend the following: (1) recognition of the Guadalupian Series as originally proposed (Girty, 1902), with a complete body stratotype to be established along the western escarpment within Guadalupe Mountains National Park; (2) the Roadian constitute the basal stage of the Guadalupian Series; and (3) precise definition of the concurrent basal Guadalupian Series and Roadian Stage boundary within the clinal transition from *Mesogondolella idahoensis* to *M. nankingensis*. These results strongly support the Guadalupian Series as the candidate for the international standard reference of a formal Middle Permian Series, as proposed by Glenister et al. (1992).

Acknowledgments

Financial support for field and related expenses were provided to Lambert by a grant from the Atlantic Richfield Company (ARCO), the National Geographic Society, and the Max and Lorraine Littlefield Fund (Department of Geology, University of Iowa). Additional funding was secured from the National Science Foundation, U.S.–China Cooperative Research Program administered to Brian F. Glenister. Financial support for Harris was provided by a grant from the New Mexico Bureau of Mines and Mineral Resources. A special thanks is extended to the National Park Service. In addition to the individuals acknowledged in Harris et al. (this volume), Roy Mapes provided the septate specimen of *E. burckhardtii* from the basinal Cutoff Formation, and Bruce Wardlaw provided access to his extensive Road Canyon and Cutoff conodont collections. Scott Ritter provided conodont collections from the type Cutoff Formation and supplemental faunas from the San Andres Formation as part of a previous collaborative project. Shannon Rudine provided assistance with land access in the Glass Mountains, and Paul Brenckle (AMOCO) provided conodont sample bags. Julia Golden arranged for loans of critical type specimens. This paper was reviewed by Bruce Wardlaw and Garner Wilde.

All figured specimens are deposited at the University of Iowa.

Appendix 8-1: Locality Register for Figured Specimens

1. Pipeline Shale Member type section, Brushy Canyon Formation (31°50'5"N, 104°50'5"W). 3.5 mi (5.8 km) SSW of El Capitan, 0.4 mi (0.7 km) along El Paso Gas Company right-of-way pipeline road, west of junction with U.S. 62/180, Culberson County, Texas. Samples from basal phosphatic interval with carbonate concretions containing abundant ammonoids. Private ranch, permission to collect required.
 2. Williams Ranch Member, Cutoff Formation (31°50'2"N, 104°50'6"W). Top beds of Cutoff Formation, containing abundant large allochthonous clasts; exposed primarily by road grading and pipeline construction (see Locality 1). Private ranch, permission to collect required.
 3. Williams Ranch Member, Cutoff Formation (31°50'3"N, 104°50'3"W). East wall of ravine S of Pipeline Shale Member type section (see Locality 1). Sample from uppermost resistant bed without allochthonous clasts. Private ranch, permission to collect required.
 4. Williams Ranch Member, Cutoff Formation (31°49'7"N, 104°49'42"W). Quarry along right-of-way on NW side of U.S. 62/180, 1.8 mi (3 km) NE of junction with Hwy 54, Culberson County, Texas.
 5. El Centro Member, Cutoff Formation (31°52'58"N, 104°52'48"W). Along westward facing scarp, south wall of Bone Canyon. Sample from upper-middle of carbonate unit as exposed. Guadalupe Mountains National Park, permission to collect required.
 6. El Centro Member, Cutoff Formation (31°53'25"N, 104°52'33"W). South wall of southern branch of Shumard Canyon, directly over channel filled with Shumard Member. Sample from basal bed of middle carbonate unit. Guadalupe Mountains National Park, permission to collect required.
 7. Road Canyon Formation type section (30°20'53"N, 103°15'2"W). SE face of spur 0.5 mi (0.8 km) SE of Peak 5779, 2.4 mi (4 km) due N of Skinner Ranch, Altuda quadrangle, Brewster County, Texas. (Description from Cooper and Grant, 1964.) Samples from 10 ft (3 m) above top of drape beds overlying uppermost megabreccia (within unit 8 of Cys, 1981). Private ranch, permission to collect required.
 8. Leonardian Lectostratotype, Cathedral Mountain Formation (30°20'52"N, 103°15'2"W). Sample from uppermost bed underlying large Road Canyon megabreccia block that is sunk into the top of the Cathedral Mountain Formation, just E of Cys (1981) section (see Locality 7). Private ranch, permission to collect required.
 9. Victorio Peak Limestone (31°11'42"N, 104°36'1"W). Hills W of Old Jones Ranch house and Ranch Road 2185, western Apache Mountains, Culberson County, Texas. Sample from uppermost bed of Victorio Peak Limestone, in gully just S of Wood's (1968) Measured Section I. Private ranch, permission to collect required.
- USNM Loc. 732z. Road Canyon Formation (30°14'24"N, 103°27'0"W). 1.36 mi (2.3 km) N50°W of Old Payne Ranch site, 1.2 mi (2 km) N2°W of hill 4806, Monument Spring quadrangle. (Description from Cooper and Grant, 1977.) Private ranch, permission to collect required.
- AMNH Loc. 503. Road Canyon Formation (30°23'28"N, 103°8'47"W). Near top of slope 3.5 mi (5.8 km) S75°W of Old Word Ranch, 1.15 mi (1.9 km) S37°E of hill 5507, and 0.65 mi (1.1 km) SW of road fork to Appel Ranch house, Hess Canyon quadrangle. (Description from Cooper and Grant, 1972.) Private ranch, permission to collect required.

Literature Cited

- Adams, J.E., M.F. Cheney, R.K. DeFord, R.I. Dickey, C.O. Dunbar, J.M. Hills, R.E. King, R.E. Lloyd, A.K. Miller, and C.E. Needham
1939. Standard Permian Section of North America. *Bulletin of the American Association of Petroleum Geologists*, 23(11):1673-1681.
- Alberch, P., S.J. Gould, G.F. Oster, and D.B. Wake
1979. Size and Shape in Ontogeny and Phylogeny. *Paleobiology*, 5:296-317.
- Behnken, F.H.
1975. Leonardian and Guadalupian (Permian) Conodont Biostratigraphy in Western and Southwestern United States. *Journal of Paleontology*, 49(2):284-315, plates 1, 2.
- Blanchard, W.G., and M.J. Davis
1929. Permian Stratigraphy and Structure of Parts of Southeastern New Mexico and Southwestern Texas. *Bulletin of the American Association of Petroleum Geologists*, 13(8):957-995.
- Böse, E.
1919 ("1917"). The Permo-Carboniferous Ammonoids of the Glass Mountains, West Texas, and Their Stratigraphic Significance. *University of Texas Bulletin*, 1762: 241 pages, 11 plates.
- Boyd, D.W.
1958. Permian Sedimentary Facies, Central Guadalupe Mountains, New Mexico. *Bulletin of the New Mexico Bureau of Mines and Mineral Resources*, 49: 100 pages, 5 plates.
- Ching, Yu-Kan [Jin, Yu-Gan]
1960. Conodonts from the Kufeng Suite (Formation) of Lungtan, Nanjing. *Acta Palaeontologica Sinica*, 3:242-248. [In Chinese and English.]
- Clark, D.L., and F.H. Behnken
1979. Evolution and Taxonomy of the North American Upper Permian *Neogondolella serrata* Complex. *Journal of Paleontology*, 53(2):263-275, plates 1, 2, figures 1-4, table 1.
- Clark, D.L., T.R. Carr, F.H. Behnken, B.R. Wardlaw, and J.W. Collinson
1979. Permian Conodont Biostratigraphy in the Great Basin. In C.A. Sandberg and D.L. Clark, editors, *Conodont Biostratigraphy of the Great Basin and Rocky Mountains*. *Brigham Young University Geology Studies*, 26:143-147.
- Clark, D.L., and Wang Cheng-Yuan
1988. Permian Neogondolellids from South China: Significance for Evolution of the *serrata* and *carinata* Groups in North America. *Journal of Paleontology*, 62(1):132-138.
- Clark, D.L., and R.L. Ethington
1962. Survey of Permian Conodonts in Western North America. *Brigham Young University Geology Studies*, 9:102-114.
- Clifton, R.L.
1945. Permian Word Formation: Its Faunal and Stratigraphic Correlatives, Texas. *Bulletin of the American Association of Petroleum Geologists*, 29(12):1766-1776.
- Cooper, G.A., and R.E. Grant
1964. New Permian Stratigraphic Units in Glass Mountains, West Texas. *Bulletin of the American Association of Petroleum Geologists*, 48(9):1581-1588.
1966. Permian Rock Units in the Glass Mountains, West Texas. *United States Geological Survey Bulletin*, 1244-E:E1-E9, plates 1, 2.
1972. Permian Brachiopods of West Texas, I. *Smithsonian Contributions to Paleobiology*, 14:1-231, plates 1-23.
1974. Permian Brachiopods of West Texas, II. *Smithsonian Contributions to Paleobiology*, 15:233-793, plates 24-191.
1975. Permian Brachiopods of West Texas, III. *Smithsonian Contributions to Paleobiology*, 19:795-1921, plates 192-502.
1976a. Permian Brachiopods of West Texas, IV. *Smithsonian Contributions to Paleobiology*, 21:1923-2607, plates 503-662.
1976b. Permian Brachiopods of West Texas, V. *Smithsonian Contributions to Paleobiology*, 24:2609-3159, plates 663-780.
1977. Permian Brachiopods of West Texas, VI. *Smithsonian Contributions to Paleobiology*, 32:3161-3370.
- Cys, J.M.
1981. Preliminary Report on Proposed Leonardian Lectostratotype Section, Glass Mountains, West Texas. In Marathon-Marfa Region of West Texas, Symposium and Guidebook. *Society of Economic Paleontologists and Mineralogists, Permian Basin Section, Publication*, 81-20:183-203.
- Furnish, W.M.
1966. Ammonoids of the Upper Permian *Cyclolobus*-Zone. *Neues Jahrbuch für Geologie und Paläontologie, Abhandlungen*, 125: 265-296, plates 23-26.
1973. Permian Stage Names. In A. Logan and L.V. Hills, editors, *The Permian and Triassic Systems and Their Mutual Boundary*. *Canadian Society of Petroleum Geologists, Memoir*, 2:522-548.
- Furnish, W.M., and B.F. Glenister
1970. Permian Ammonoid *Cyclolobus* from the Salt Range. In B. Kummel and C. Teichert, editors, *Stratigraphic Boundary Problems: Permian and Triassic of West Pakistan*. *University of Kansas, Department of Geology, Special Publication*, 4:153-175.
1977. Ammonites. In G.A. Cooper and R.E. Grant, *Permian Brachiopods of West Texas, VI*. *Smithsonian Contributions to Paleobiology*, 32:3304-3309.
- Girty, G.H.
1902. The Upper Permian in Western Texas. *American Journal of Science*, series 4, 14:363-368.
1909 ("1908"). The Guadalupian Fauna. *United States Geological Survey Professional Paper*, 58: 651 pages, 31 plates. [Date on title page is 1908; actually published in 1909.]
- Glenister, B.F.
1981. Permian Ammonoid "Zones." In M.R. House and J.R. Senior, editors, *The Ammonoidea: The Evolution, Classification, Mode of Life and Geological Usefulness of a Major Fossil Group*. *The Systematics Association*, special volume, 18:389-396. Academic Press.
1991. The Guadalupian: A Proposed International Standard for Middle Permian Series. [Abstract.] *International Congress on the Permian System of the World, Program and Abstracts*, Perm, USSR-1991, pages A9-A10. Urals Branch, USSR Academy of Sciences and Earth Sciences and Resources Institute, University of South Carolina.
- Glenister, B.F., D.W. Boyd, W.M. Furnish, R.E. Grant, M.T. Harris, H. Kozur, L.L. Lambert, W.W. Nassichuk, N.D. Newell, L.C. Pray, C. Spinosa, B.R. Wardlaw, G.L. Wilde, and T.E. Yancey
1992. The Guadalupian: Proposed International Standard for a Middle Permian Series. *International Geology Review*, 34(9):857-888.
- Glenister, B.F., and W.M. Furnish
1987. New Permian Representatives of Ammonoid Superfamilies Marathonitaceae and Cyclolobaceae. *Journal of Paleontology*, 61(5):982-998.
- Grant, R.E., and G.A. Cooper
1973. Brachiopods and Permian Correlations. In A. Logan and L.V. Hills, editors, *The Permian and Triassic Systems and Their Mutual Boundary*. *Canadian Society of Petroleum Geologists, Memoir*, 2:572-595.
- Grant, R.E., and B.R. Wardlaw
1984. Redefinition of Leonardian-Guadalupian Boundary in Regional Stratotype for the Permian of North America. *27th International Geological Congress, Moscow, USSR, Abstracts*, 1:58.
- Harris, M.T.
1982. Sedimentology of the Cutoff Formation (Permian), Western Guadalupe Mountains, West Texas and New Mexico. 186 pages.

- Unpublished master's thesis, University of Wisconsin, Madison, Wisconsin.
- 1988a. Sedimentology of the Cutoff Formation (Permian), Western Guadalupe Mountains, West Texas. In S.T. Reid, R.O. Bass, and P. Welch, editors, *Guadalupe Mountains Revisited, Texas and New Mexico. West Texas Geological Society, Publication*, 88-84:133-140.
- 1988b. Postscript on the Cutoff Formation: The Regional Perspective and Some Suggestions for Nomenclature. In S.T. Reid, R.O. Bass, and P. Welch, editors, *Guadalupe Mountains Revisited, Texas and New Mexico. West Texas Geological Society, Publication*, 88-84:141-142.
2000. Members for the Cutoff Formation, Western Escarpment of the Guadalupe Mountains, West Texas. In B.R. Wardlaw, R.E. Grant, and D.M. Rohr, editors, *The Guadalupian Symposium. Smithsonian Contributions to the Earth Sciences*, 32:101-120, 8 figures.
- Harris, M.T., D.J. Lehrmann, and L.L. Lambert
2000. Comparison of the Depositional Environments and Physical Stratigraphy of the Cutoff Formation (Guadalupe Mountains) and the Road Canyon Formation (Glass Mountains): Lowermost Guadalupian (Permian) of West Texas. In B.R. Wardlaw, R.E. Grant, and D.M. Rohr, editors, *The Guadalupian Symposium. Smithsonian Contributions to the Earth Sciences*, 32:127-152, 25 figures.
- Hayes, P.T.
1959. San Andres Limestone and Related Permian Rocks in Last Chance Canyon and Vicinity, Southeastern New Mexico. *Bulletin of the American Association of Petroleum Geologists*, 43(9):2197-2213.
- King, P.B.
- 1931 ("1930"). The Geology of the Glass Mountains, Texas, Part I: Descriptive Geology. *University of Texas Bulletin*, 3038: 167 pages, 15 plates. [Date on title page is 1930; actually published in 1931.]
1934. Permian Stratigraphy of Trans-Pecos Texas. *Bulletin of the Geological Society of America*, 45(4):697-797, plates 103-107.
1942. Permian of West Texas and Southeastern New Mexico. *Bulletin of the American Association of Petroleum Geologists*, 26(4):535-763.
1947. Permian Correlations. *Bulletin of the American Association of Petroleum Geologists*, 31(4):774-777.
1948. Geology of the Southern Guadalupe Mountains, Texas. *United States Geological Survey Professional Paper*, 215: 183 pages, 23 plates.
1965. Geology of the Sierra Diablo Region, Texas. *United States Geological Survey Professional Paper*, 480: 185 pages.
- Kozur, H.
- 1989 ("1990"). The Taxonomy of the Gondolellid Conodonts in the Permian and Triassic. In W. Ziegler, editor, *First International Senckenberg Conference and Fifth European Conodont Symposium (ECOS V), Contributions III. Courier Forschungsinstitut Senckenberg*, 117:409-469. [Date on title page is 1990; actually published in 1989.]
- Lambert, L.L., and B.R. Wardlaw
1992. Appendix II: Morphological Transition from *Mesogondolella idahoensis* to *M. serrata*: Basal Guadalupian Definition. In B.F. Glenister et al., *The Guadalupian: Proposed International Standard for a Middle Permian Series. International Geology Review*, 34(9):876-880.
- Lehrmann, D.J.
1988. Sedimentology and Conodont Biostratigraphy of the Road Canyon Formation (Permian), Glass Mountains, Southwest Texas. 170 pages. Unpublished master's thesis, University of Wisconsin, Madison, Wisconsin.
- McNamara, K.J.
1986. A Guide to the Nomenclature of Heterochrony. *Journal of Paleontology*, 60(1):4-13.
1990. The Role of Heterochrony in Evolutionary Trends. In K.J. McNamara, editor, *Evolutionary Trends*. Pages 59-74. London: Belhaven Press.
- Mikesh, D.L., B.F. Glenister, and W.M. Furnish
1988. *Stenolobulites* n. gen., Early Permian Ancestor of Predominantly Late Permian Paragastrioceratid Subfamily Pseudogastrioceratinae. *University of Kansas Paleontological Contributions, Paper*, 123: 19 pages.
- Miller, A.K.
1938. Comparison of Permian Ammonoid Zones of Soviet Russia with Those of North America. *Bulletin of the American Association of Petroleum Geologists*, 22(8):1014-1019.
1945. Some Exceptional Permian Ammonoids from West Texas. *Journal of Paleontology*, 19(1):14-21, plates 6-8.
- Miller, A.K., and W.M. Furnish
1940. Permian Ammonoids of the Guadalupe Mountain Region and Adjacent Areas. *Geological Society of America, Special Paper*, 26: 242 pages, 44 plates.
1957. Ammonoids of the Basal Word Formation, Glass Mountains, West Texas. *Journal of Paleontology*, 31(6):1052-1056.
- Newell, N.D., J.K. Rigby, A.G. Fischer, A.J. Whiteman, J.E. Hickox, and J.S. Bradley
1953. *The Permian Reef Complex of the Guadalupe Mountains Region, Texas and New Mexico: A Study in Paleocology*. 236 pages. San Francisco: W.H. Freeman and Company.
- Ross, C.A.
1963. Fusulinids from the Word Formation (Permian), Glass Mountains, Texas. *Contributions from the Cushman Foundation for Foraminiferal Research*, 14(1):17-31, plates 3-5.
1986. Paleozoic Evolution of Southern Margin of Permian Basin. *Bulletin of the Geological Society of America*, 97(5):536-554.
- Ruzhentssev, V.E.
1960. Printsipy sistematiki, sistema i filogeniya Paleozoiskikh ammonoidov [Principle Systematics, System and Phylogeny of Paleozoic Ammonoidea]. *Trudy, Paleontologicheskogo Instituta, Akademiia Nauk SSSR*, 83: 331 pages.
- Sarg, J.F., and P.J. Lehmann
- 1986a. Lower-Middle Guadalupian Facies and Stratigraphy, San Andres/Grayburg Formations, Permian Basin, Guadalupe Mountains, New Mexico. In G.E. Moore and G.L. Wilde, editors, *Lower and Middle Guadalupian Facies, Stratigraphy, and Reservoir Geometries, San Andres/Grayburg Formations, Guadalupe Mountains, New Mexico and Texas. Society of Economic Paleontologists and Mineralogists, Permian Basin Section, Publication*, 86-25:1-8.
- Shumard, G.G.
- 1860 ("1858"). Observations on the Geological Formations of the Country between the Rio Pecos and the Rio Grande, in New Mexico, Near the Line of the 32d Parallel, Being an Abstract of a Portion of the Geological Report of the Expedition under Capt. John Pope, Corps of Topographical Engineers, U.S. Army, in the Year 1855. *St. Louis Academy of Science Transactions*, 1(2):273-289.
- Spinosa, C., W.M. Furnish, and B.F. Glenister
1975. The Xenodiscidae, Permian Ceratitoid Ammonoids. *Journal of Paleontology*, 49(2):239-283, plates 1-8.
- Udden, J.A.
1917. Notes on the Geology of the Glass Mountains. *University of Texas Bulletin*, 1753: 59 pages.
- Wardlaw, B.R., and J.W. Collinson
1984. Conodont Paleocology of the Permian Phosphoria Formation and Related Rocks of Wyoming and Adjacent Areas. In D.L. Clark, editor, *Conodont Biofacies and Provincialism. Geological Society of America, Special Paper*, 196:263-281, plates 1-5.
- Wardlaw, B.R., and R.E. Grant
1987. Conodont Biostratigraphy of the Cathedral Mountain and Road Canyon Formations, Glass Mountains, West Texas. In D. Cromwell

- and L.J. Mazzullo, editors, The Leonardian Facies in W. Texas and S.E. New Mexico and Guidebook to the Glass Mountains, West Texas. *Society of Economic Paleontologists and Mineralogists, Permian Basin Section, Publication*, 87-27:63-66.
1990. Conodont Biostratigraphy of the Permian Road Canyon Formation, Glass Mountains, Texas. *United States Geological Survey Bulletin*, 1895-A:A1-A18, plates 1-4.
- Warren, W.C.
1955. Introduction to Field Trip. In J.M. Cys and D.F. Toomey, editors, Permian Exploration, Boundaries, and Stratigraphy. *Society of Economic Paleontologists and Mineralogists, Permian Basin Section, Permian Field Conference Guidebook*, pages 11-14.
- Wilde, G.L.
1975. Fusulinid-Defined Permian Stages. In J.M. Cys and D.F. Toomey, editors, Permian Exploration, Boundaries, and Stratigraphy. *Society of Economic Paleontologists and Mineralogists, West Texas Geological Society and Permian Basin Section, Publication*, 75-65:67-83.
- 1986a. Stratigraphic Relationship of the San Andres and Cutoff Formations, Northern Guadalupe Mountains, New Mexico and Texas. In G.E. Moore and G.L. Wilde, editors, Lower and Middle Guadalupian Facies, Stratigraphy, and Reservoir Geometries, San Andres/Grayburg Formations, Guadalupe Mountains, New Mexico and Texas. *Society of Economic Paleontologists and Mineralogists, Permian Basin Section, Publication*, 86-25:49-63, plates 1-5.
- 1986b. An Important Occurrence of Early Guadalupian (Roadian) Fusulinids from the Cutoff Formation, Western Guadalupe Mountains, Texas. In G.E. Moore and G.L. Wilde, editors, Lower and Middle Guadalupian Facies, Stratigraphy, and Reservoir Geometries, San Andres/Grayburg Formations, Guadalupe Mountains, New Mexico and Texas. *Society of Economic Paleontologists and Mineralogists, Permian Basin Section, Publication*, 86-25:65-68, plate 1.
1988. Fusulinids of the Roadian Stage. In S.T. Reid, R.O. Bass, and P. Welch, editors, Guadalupe Mountains Revisited, Texas and New Mexico. *West Texas Geological Society, Publication*, 88-84:143-147, plates 1, 2 [no text].
1990. Practical Fusulinid Zonation: The Species Concept, with Permian Basin Emphasis. *West Texas Geological Society, Bulletin* 29(7):5-34.
2000. Formal Middle Permian (Guadalupian) Series: A Fusulinacean Perspective. In B.R. Wardlaw, R.E. Grant, and D.M. Rohr, editors, The Guadalupian Symposium. *Smithsonian Contributions to the Earth Sciences*, 32:89-100, 3 figures.
- Wilde, G.L., and R.G. Todd
1968. Guadalupian Biostratigraphic Relationships and Sedimentation in the Apache Mountain Region, West Texas. In B.A. Silver, editor, Guadalupian Facies, Apache Mountains Area, West Texas. *Society of Economic Paleontologists and Mineralogists, Permian Basin Section, Publication*, 68-11:10-31.
- Wilkerson, C.E., Jr., S.M. Ritter, L.L. Lambert, and G.L. Wilde
1991. Stratigraphy and Biostratigraphy of the Lower and Middle San Andres Formation in Last Chance Canyon, Guadalupe Mountains, New Mexico. In S. Meader-Roberts, M.D. Candelaria, and G.E. Moore, editors, Sequence Stratigraphy, Facies, and Reservoir Geometries of the San Andres, Grayburg, and Queen Formations, Guadalupe Mountains, New Mexico and Texas. *Society of Economic Paleontologists and Mineralogists, Permian Basin Section, Publication*, 91-32:99-110.
- Wood, J.W.
1968. Geology of the Apache Mountains, Trans-Pecos Texas. *Bureau of Economic Geology, University of Texas, Austin, Geologic Quadrangle Map*, 33: 32 pages.
- Yang, Zhendong, and Thomas E. Yancey
2000. Fusulinid Biostratigraphy and Paleontology of the Middle Permian (Guadalupian) Strata of the Glass Mountains and Del Norte Mountains, West Texas. In B.R. Wardlaw, R.E. Grant, and D.M. Rohr, editors, The Guadalupian Symposium. *Smithsonian Contributions to the Earth Sciences*, 32:185-259, 7 figures, 17 plates, 36 tables.
- Youngquist, W., R.W. Hawley, and A.K. Miller
1951. Phosphoria Conodonts from Southeastern Idaho. *Journal of Paleontology*, 25(3):356-364, plate 54.

Plates 8-1-8-4

PLATE 8-1

Exposures in the Guadalupe Pass area of the Guadalupe Mountains (type Guadalupian), showing Shumard's (1860) lithostratigraphic units: 1 = black limestone, 2 = yellow sandstone, 3 = dark limestone, and 4 = white limestone. Note depositional dip.



PLATE 8-2

Index ammonoids from the Roadian Stage, West Texas.

FIGURES 1–3.—*Demarezites* n. sp.: apertural, lateral, and ventral views, $\times 1$, hypotype, SUI 32402. Pipeline Shale Member type section, Brushy Canyon Formation, Loc. 1. (Reduced to 84% of original for publication.)

FIGURES 4–6.—*Waagenoceras* n. sp.: ventral view, $\times 1$, at whorl diameter of 58 mm (estimated), and lateral and ventral views, $\times 1.5$, at whorl diameter of 35 mm (estimated), hypotype, SUI 32407. Note that ontogenetic changes occur rapidly in cyclolobins, and distinction between minor sutural differences and phyletic modification requires detailed analysis. Study of additional specimens will be required to confidently resolve whether the forms illustrated in Figures 1–6 actually represent separate genera. Pipeline Shale Member type section, Brushy Canyon Formation, Loc. 1. (Reduced to 84% of original for publication.)

FIGURES 7, 8.—*Perrinites vidriensis* Böse, 1919: apertural and lateral views, $\times 1.5$, hypotype, SUI 5976. Road Canyon Formation, AMNH Loc. 503. (Reduced to 84% of original for publication.)

FIGURES 9, 10.—*Glassoceras normani* (Miller and Furnish, 1957): lateral and apertural views, $\times 1.25$, holotype, AMNH 28022. Road Canyon Formation, AMNH Loc. 503. (Reduced to 84% of original for publication.)

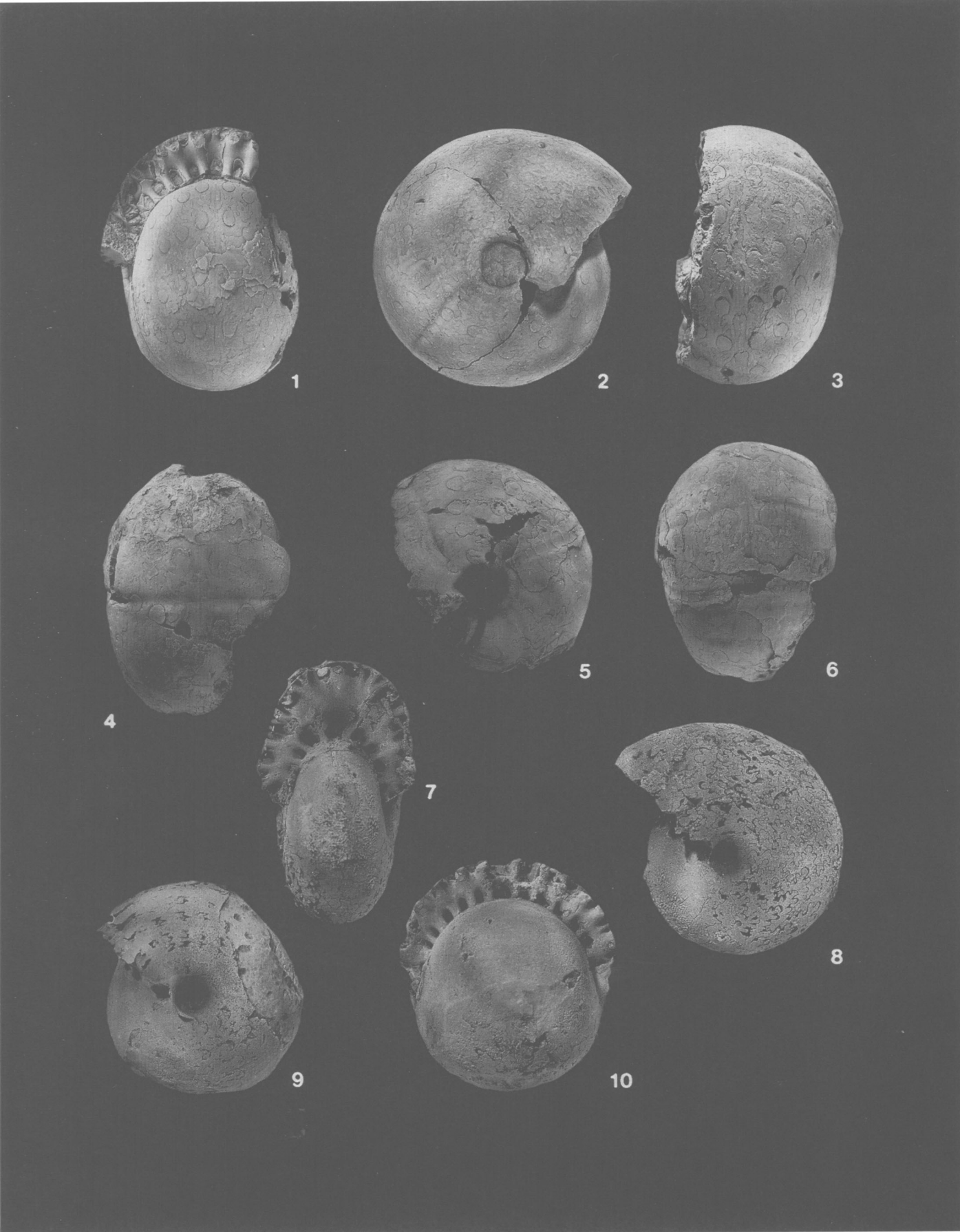


PLATE 8-3**Ammonoids of the Roadian Stage, West Texas.**

FIGURES 1, 2.—*Texoceras texanum* (Girty, 1908): 1, lateral view, $\times 2$, well-preserved conch showing shell and mature modification, hypotype, SUI 64702, Williams Ranch Member, Cutoff Formation, Loc. 2; 2, apertural view, $\times 2$, phragmacone without shell, hypotype, SUI 64703, Williams Ranch Member, Cutoff Formation, Loc. 4. (Reduced to 84% of original for publication.)

FIGURES 3, 4, 9.—*Peritrochia* n. sp.: ventral, lateral, and apertural views, $\times 2.5$, SUI 64700, Road Canyon Formation, USNM Loc. 732z. (Reduced to 84% of original for publication.)

FIGURE 5.—*Peritrochia erebus* Girty, 1908: lateral view, $\times 2.3$, well-preserved conch showing shell and mature modification, hypotype, SUI 64701, Williams Ranch Member, Cutoff Formation, Loc. 2. (Reduced to 84% of original for publication.)

FIGURES 6–8.—*Paracelmites elegans* Girty, 1908: 6, 7, lateral and ventral views, $\times 2$, well-preserved phragmacone, hypotype, SUI 31925A, Williams Ranch Member, Cutoff Formation, Loc. 4; 8, lateral view, $\times 2$, conch with well-preserved shell, hypotype, SUI 64705, Williams Ranch Member, Cutoff Formation, Loc. 2. (Reduced to 84% of original for publication.)

FIGURES 10–12.—*Stenolobulites stenolobulus* Mikesh, Glenister, and Furnish, 1988: lateral, apertural, and ventral views, $\times 2$, hypotype, SUI 52583, Williams Ranch Member, Cutoff Formation, Loc. 4. (Reduced to 84% of original for publication.)

FIGURES 13, 16, 17.—*Epithalassoceras* (?) n. sp.: apertural, ventral, and lateral views, $\times 2$, SUI 64704, Pipeline Shale Member type section, Brushy Canyon Formation, Loc. 1. (Reduced to 84% of original for publication.)

FIGURES 14, 15.—*Eumedlicottia burckhardti* (Böse, 1919): lateral and apertural views, $\times 1.3$, hypotype, SUI 64699, Pipeline Shale Member type section, Brushy Canyon Formation, Loc. 1. (Reduced to 84% of original for publication.)

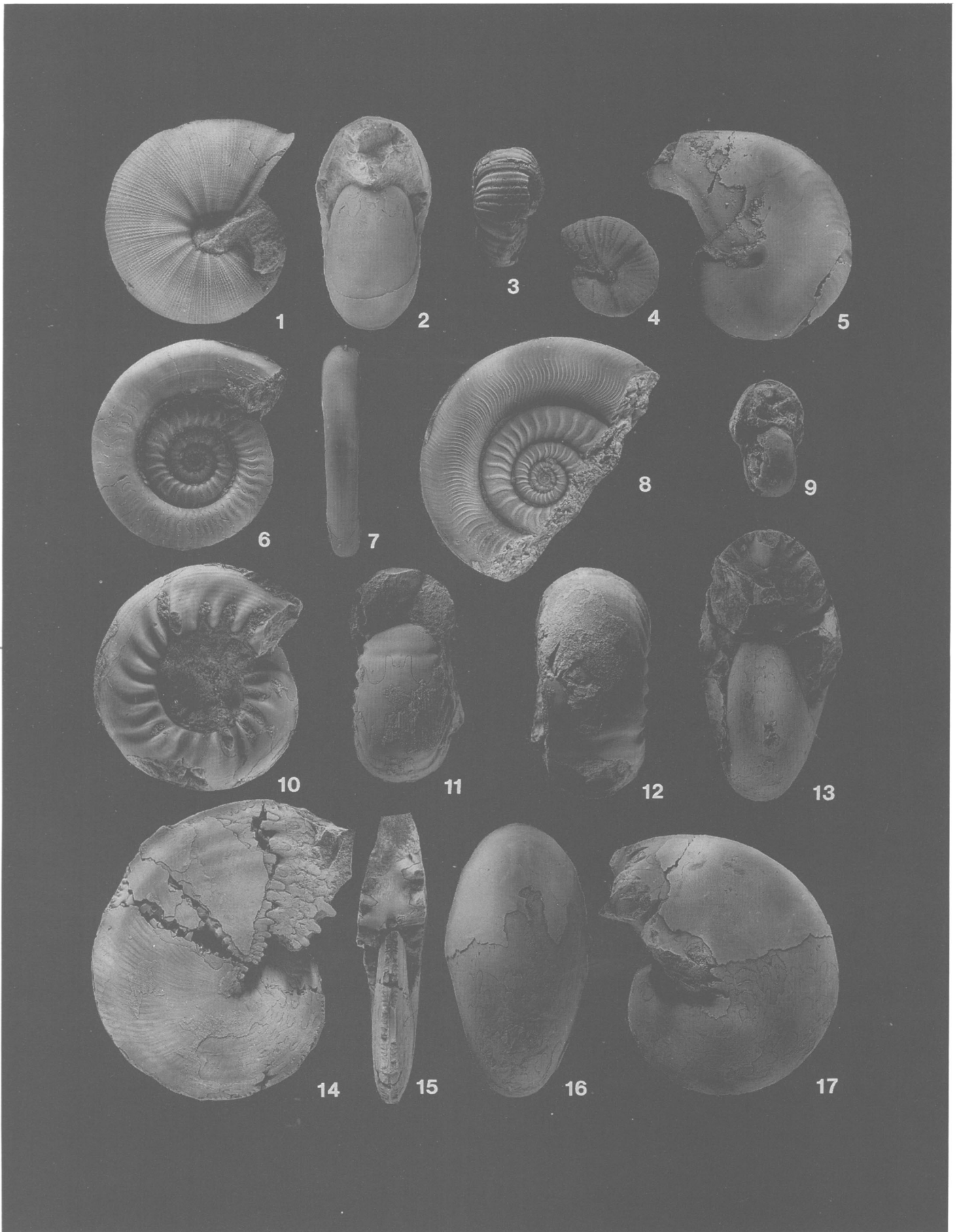


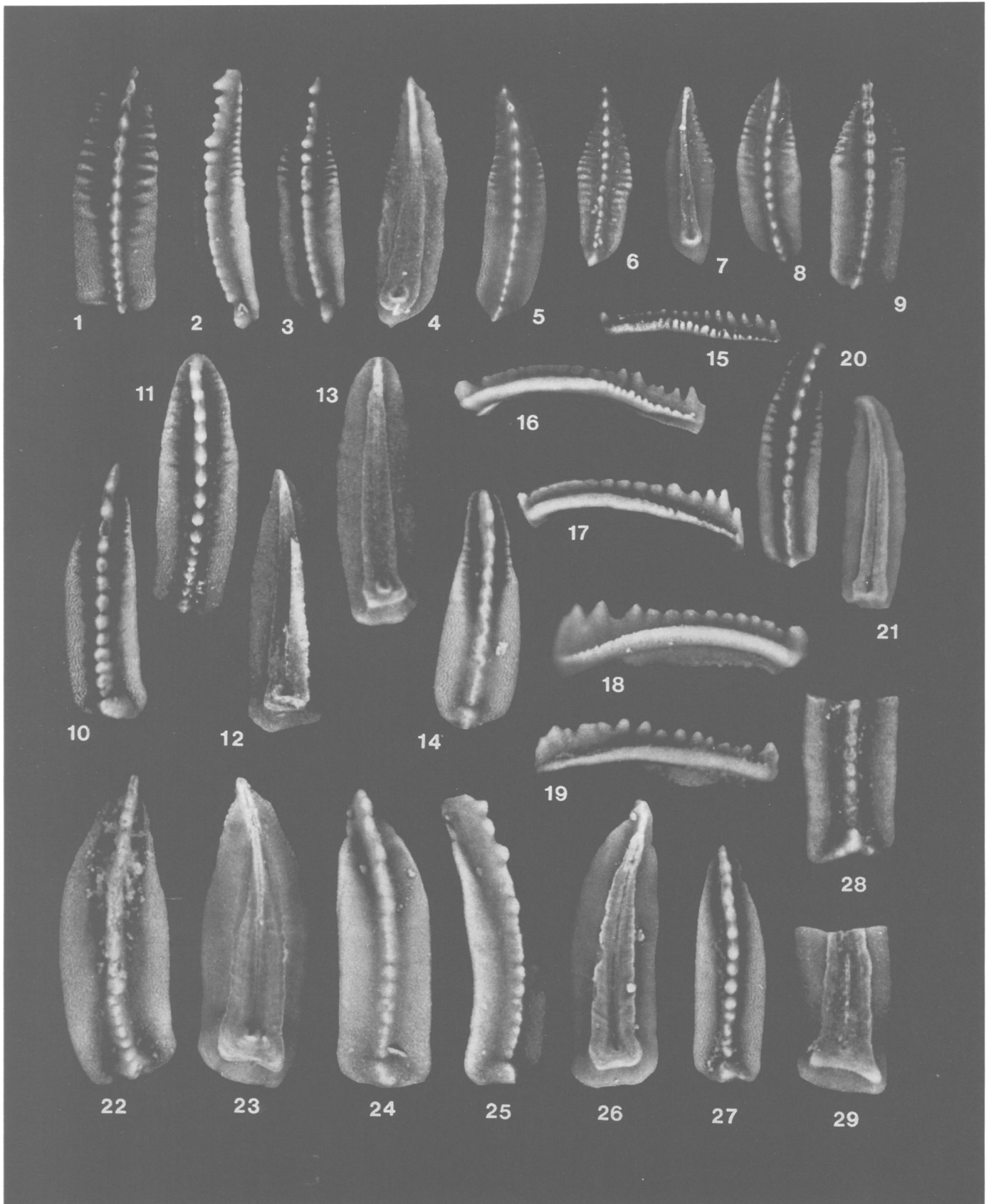
PLATE 8-4

Conodonts from the basal Guadalupian and the Roadian–Wordian boundary strata, West Texas. (All figures are of Pa elements at ×50 magnification.)

FIGURES 1–9, 15, 16.—*Mesogondolella nankingensis* (Ching, 1960): 1, upper view, quadrate form, hypotype, SUI 64521; 2–4, 16, upper oblique, upper, lower, and right lateral views, specimen with atypically large rounded cusp, hypotype, SUI 64522; 5, upper view, hypotype, SUI 64523; 6, 7, 15, upper, lower, and right lateral views, subadult with abundant serrations, hypotype, SUI 64524; 8, upper view, subadult of earliest *M. nankingensis* s.s., exhibiting several characters of the transitional form, hypotype, SUI 64525; 9, upper view, quadrate form less serrated than Figure 1, hypotype, SUI 64526. 1–5, 9, 16, Pipeline Shale Member type section, Brushy Canyon Formation, Loc. 1 (type stratum of *M. nankingensis*); 6, 7, 15, Williams Ranch Member, Cutoff Formation, Loc. 3; 8, Road Canyon Formation type section, Loc. 7. (Reduced to 84% of original for publication.)

FIGURES 10–14, 17, 18, 20, 21.—Forms transitional between *M. idahoensis* and *M. nankingensis*: 10, 12, 18, upper, lower, and left lateral views, transitional form with primarily *M. idahoensis*-like characters, hypotype, SUI 64527; 11, 13, upper and lower views, form with approximately equal mix of ancestral and descendant characters, hypotype, SUI 64528; 14, upper view, specimen with incipient serrations but otherwise more reminiscent of *M. idahoensis*, hypotype, SUI 64529; 17, 20, 21, right lateral, upper, and lower views, transitional form dominated by many *M. nankingensis*-like characters, hypotype, SUI 64530. 10–13, 18, El Centro Member, Cutoff Formation, Loc. 5; 14, 17, 20, 21, El Centro Member, Cutoff Formation, Loc. 6. (Reduced to 84% of original for publication.)

FIGURES 19, 22–29.—*Mesogondolella idahoensis* (Youngquist, Hawley, and Miller, 1951): 19, 27, left lateral and upper views, note posterior termination of adcarinal furrows, hypotype, SUI 64531; 22, 23, upper and lower views, very large specimen with characteristic lower view, hypotype, SUI 64532; 24–26, upper, upper oblique, and lower views, very large specimen with characteristic carina, hypotype, SUI 64533; 28, 29, upper and lower views, note triangular cusp complex, hypotype, SUI 64534. 19, 27–29, Leonardian lectostratotype, Loc. 8; 22–26, Victorio Peak Limestone, Loc. 9. (Reduced to 84% of original for publication.)



9. Fusulinid Biostratigraphy and Paleontology of the Middle Permian (Guadalupian) Strata of the Glass Mountains and Del Norte Mountains, West Texas

Zhendong Yang and Thomas E. Yancey

ABSTRACT

A study of new collections of fusulinids from the Guadalupian Series in the Glass Mountains and Del Norte Mountains, West Texas, documents the presence of 44 species (in 10 genera) of fusulinids in the middle Permian strata. One species of *Rauserella* Dunbar, 1944, three species of *Reichelina* Erk, 1942, and six species of *Parafusulina* Dunbar and Skinner, 1931, are described as new. The Guadalupian fusulinid-bearing sequence of strata in the Glass Mountains and Del Norte Mountains area contains abundant fusulinid faunas, with especially diverse fusulinid faunas present in the Road Canyon Formation and the Altuda Formation, primarily in sediments of shelf margin and slope-to-basin depositional environments. The *Mesogondolella nankingensis* (conodont) first appearance datum lies between the *Parafusulina boesei* first appearance datum and the *Parafusulina rothi* first appearance datum, within the Road Canyon Formation.

Nine fusulinid zones are recognized. Of these zones, the *Parafusulina durhami* Zone is placed in the Leonardian Stage, the *Parafusulina boesei* Zone spans the boundary of the Leonardian and Guadalupian (as defined by the *Mesogondolella nankingensis* first appearance datum), and the *Parafusulina rothi* Zone, *Parafusulina trumpyi* Zone (Roadian Stage), *Parafusulina sellardsi* Zone, *Parafusulina antimonioensis* Zone (Wordian Stage), *Polydiexodina shumardi* Zone, *Reichelina lamarensis* Zone, and *Lantschichites splendens* Zone (Capitanian Stage) are placed in the Guadalupian Series.

Introduction

During the Permian, the geographic position of continents (spanning a wide range of paleolatitudes) and the occurrence of pronounced climatic gradients combined to produce much paleobiogeographic isolation and the associated appearance of many endemic taxa. With many biotic provinces present during most of the Permian, biotas are not easily correlated from one region to another. The result has been lower accuracy for interregional correlation and slow progress toward establishing standard global chronostratigraphic units for the Permian. No single region has a complete sequence of fossiliferous Permian strata, so the proposed global stratotype of the Permian is based on three series-level subdivisions located in different biogeographic provinces. Organisms with pelagic and nekto-benthic life habits (conodonts and ammonoids) are being used to develop interregional correlations, whereas benthic fusulinids are being used for detailed zonation on a regional level.

The middle Permian is best known and documented from strata in the western part of North America, along the margins of the Delaware basin, which is exposed in the Glass Mountains of western Texas and the Guadalupe Mountains of southeastern New Mexico. Guadalupian strata in the Glass and Guadalupe Mountains contain richly fossiliferous marine deposits from reef, shelf, slope, and basin environments. Strata in the Guadalupe Mountains are accepted as the standard for the Guadalupian Series of North America (Adams et al., 1939). This interval is proposed as the basis of the global stratotype for the Middle Permian (Glenister et al., 1992), based on the type section of the Guadalupian located at the south end of the Guadalupe Mountains.

This study was undertaken to improve the documentation of middle Permian fusulinid zones and to provide data on the ranges of fusulinid species that could be compared directly with the ranges of conodonts and ammonoids. Wolfcampian and

Zhendong Yang, Amoco Production Company, 501 West Lake Park Blvd., P.O. Box 3092, Houston, Texas 77253-3092. Thomas E. Yancey, Department of Geology, Texas A&M University, College Station, Texas 77843-3115.

(Figure 9-1), of which the lower one (the *Parafusulina sullivanensis-boesei-wildei* Zone) was divided into three subzones (*Parafusulina lineata* Subzone at the base, *Parafusulina ironensis* Subzone in the middle, and *Parafusulina sellardsi* Subzone at the top). This was the most detailed study available on middle Permian fusulinids in the Glass Mountains until the present study. Wilde (in Cooper and Grant, 1977:3309–3318) identified 229 fusulinid samples collected in the Glass and Del Norte mountains by Cooper and Grant, 90 of which are from the middle Permian (Road Canyon Formation, Word Formation, and Capitan Limestone). Although only a list of species and short comments were provided, the work added valuable information on fusulinid occurrences in the Glass Mountains.

With the continuing documentation of Permian biotas in the Glass Mountains, controversy arose over the placement of the Leonardian–Guadalupian boundary. The series boundary had been set at the top of the “Leonard Formation” by Adams et al. (1939), a horizon that corresponds to the base of the Word Formation (at the base of the Road Canyon Formation of current usage), but the Road Canyon Formation contains ammonoids and brachiopods of Leonardian aspect along with fusulinids of Guadalupian aspect. Ross and Ross (1985) and Ross (1986) accepted a Leonardian age for the Road Canyon Formation (which includes the *Parafusulina boesei* Zone), but in a later publication (Ross and Ross, 1987) they put the Roadian Stage (regarded as essentially equivalent with the limits of the Road Canyon Formation) in an intermediate position between the Leonardian and Guadalupian. In contrast, Wilde (1975, 1986a,b, 1990) consistently held that fusulinids from the Road Canyon Formation mark the beginning of the Guadalupian. In 1990 he designated Roadian, Brushyan, Cherryan, and Capitanian stages for the Guadalupian with the *Parafusulina boesei-Skinnerina* Zone for the Roadian Stage, *Parafusulina rothi-maleyi* Zone for the Brushyan Stage, and *Parafusulina lineata-deliciasensis* Zone as the basal zone of his Cherryan Stage (Figure 9-1). Yang and Yancey (1990) proposed that the *Parafusulina rothi* Zone be used as the earliest fusulinid zone of the Guadalupian. The base of this zone occurs a short distance above the base of the Road Canyon Formation, indicating that the boundary horizon between the Leonardian and the Guadalupian is located within the Road Canyon Formation.

The biggest difference between the fusulinid zonations for the lower and middle parts of the Guadalupian, as proposed by Ross (1963b) and Wilde (1975, 1990), is the placement of a zone defined on *Parafusulina lineata* Dunbar and Skinner, 1937. In both proposals, *P. lineata* is shown confined to a single zone, but Ross (1963b) placed this zone in the lowest part of the Guadalupian, whereas Wilde (1990) placed this zone in the middle part of the Guadalupian. Material collected for this study shows that *P. lineata* is an uncommon species with

a longer range than either worker indicated, accounting for the confusion about its zonal status. The species ranges through the lower and middle portions of the Guadalupian, through three fusulinid zones (*Parafusulina rothi* Zone, *Parafusulina trumpyi* Zone, and *Parafusulina sellardsi* Zone).

Middle Permian Stratigraphy of the Glass and Del Norte Mountains

Strata of middle Permian age in the Glass and Del Norte mountains include most of the Road Canyon Formation, the Word Formation, the Vidrio Formation, the Capitan Limestone, the Altuda Formation, and the Gilliam Limestone. Recent study (Rohr et al., 1991; Haneef, 1993) of the Capitanian formations has greatly clarified the stratigraphic relations of these units, which are similar in many ways to the Guadalupian strata in the Guadalupe Mountains. The present study follows the stratigraphic framework of Rohr et al. (1991), except that the Vidrio Formation (at least the upper part) belongs in the Capitanian.

The fusulinid genus *Polydiexodina* occurs in the Vidrio Formation in both the eastern and western parts of the study area, providing evidence that it is of Capitanian age based on fusulinids. As *Polydiexodina* is a diagnostic indicator of the Capitanian, its first appearance separates the Wordian below from the Capitanian above. Therefore, the Vidrio Formation includes reef or shelf margin deposits of lower Capitanian age, and the Capitan Limestone includes reef deposits of upper Capitanian age. The Gilliam Limestone includes coeval deposits from the inner shelf, and the Altuda Formation includes coeval deposits from the slope and basin settings. The position of the shelf margin shifted during this time, so formational units intertongue.

MEASURED SECTIONS

Fusulinid samples were collected from 10 stratigraphic sections in the middle Permian of the Glass and Del Norte mountains (Figures 9-2, 9-3). The sections cover a stratigraphic interval extending upward from the top of the Cathedral Mountain Formation to the top of the Capitan Limestone and Altuda Formation, and they include reef, shelf, shelf margin, and basin depositional settings. Many samples come from sections that cover the lowest and highest intervals of the Guadalupian Series (see Yang, 1992, which contains detailed descriptions of stratigraphic sections). A comparison of the environmental settings of the Glass and Del Norte mountains with the Guadalupe Mountains areas suggests that the same fusulinid fauna should occur in both areas, and the sampling strategies were set to test this hypothesis as well as to complete the fusulinid biostratigraphy in this classic area of Permian studies. The youngest Guadalupian fusulinid fauna (previously described by Skinner and Wilde, 1954, 1955, in the Guadalupe

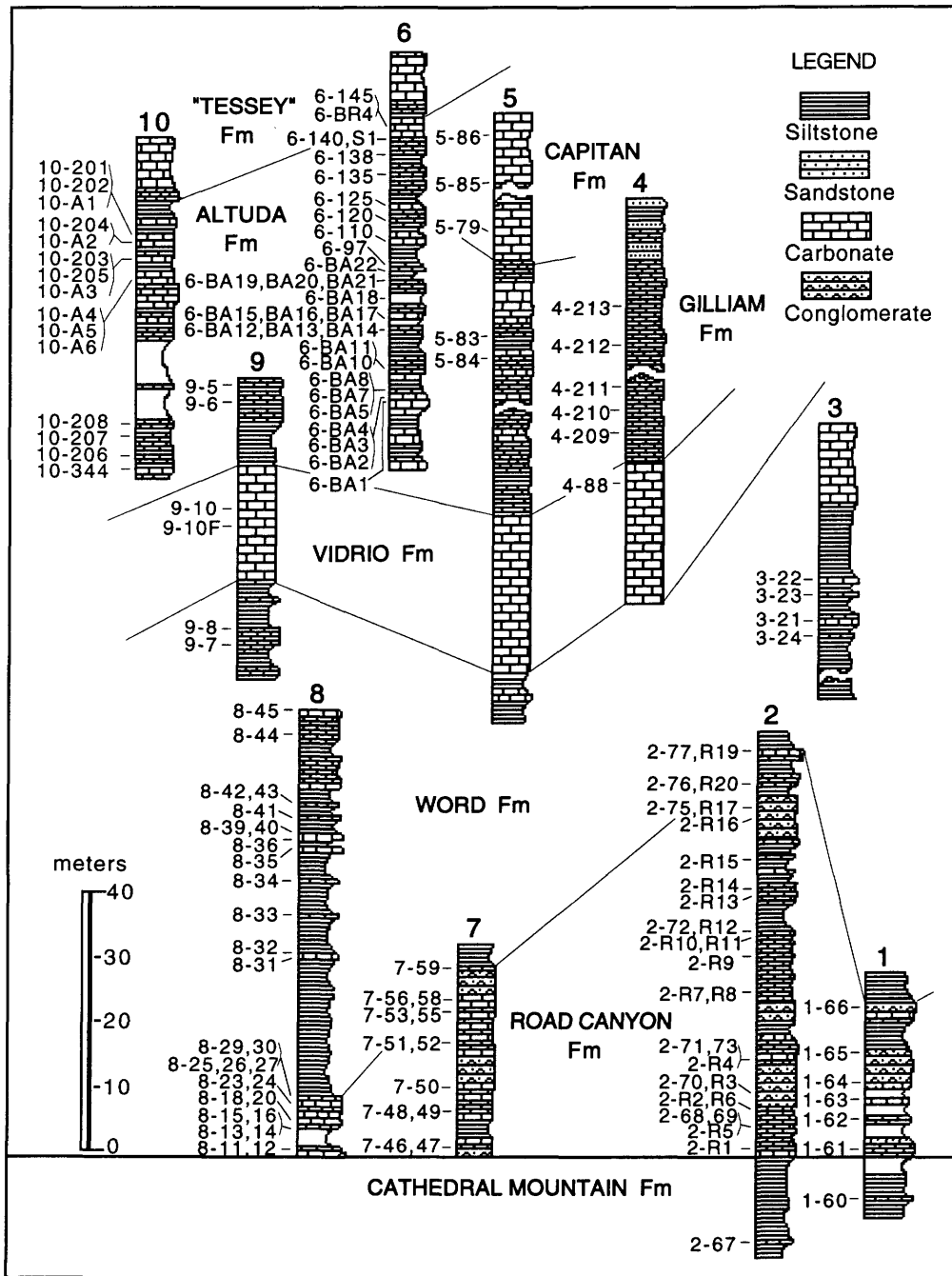


FIGURE 9-2.—Measured sections and stratigraphic positions of samples.

Mountains area, but unknown in the Glass and Del Norte mountains) was sampled in two stratigraphic sections.

Fossil preservation is best in intervals of interbedded carbonate and noncarbonate sediments deposited in deep-water environments located in the lowest and highest parts of the Guadalupian section, whereas preservation is poor in the thick, dolomitized carbonates of the Vidrio Formation and Capitan Limestone and the shoal-water facies of the Word Formation where rocks are commonly recrystallized and dolomitized.

FUSULINID SPECIES AND FUSULINID ZONES

A total of 44 fusulinid species (in 10 genera) is documented in samples collected from the Glass and Del Norte mountains, of which 10 species are new. The ranges of fusulinid species collected from the stratigraphic sections are shown in Figure 9-4, and all species are illustrated in Plates 1-17. The illustrations presented in the plates provide the documentation of the fusulinid species used to establish the zonation. It is

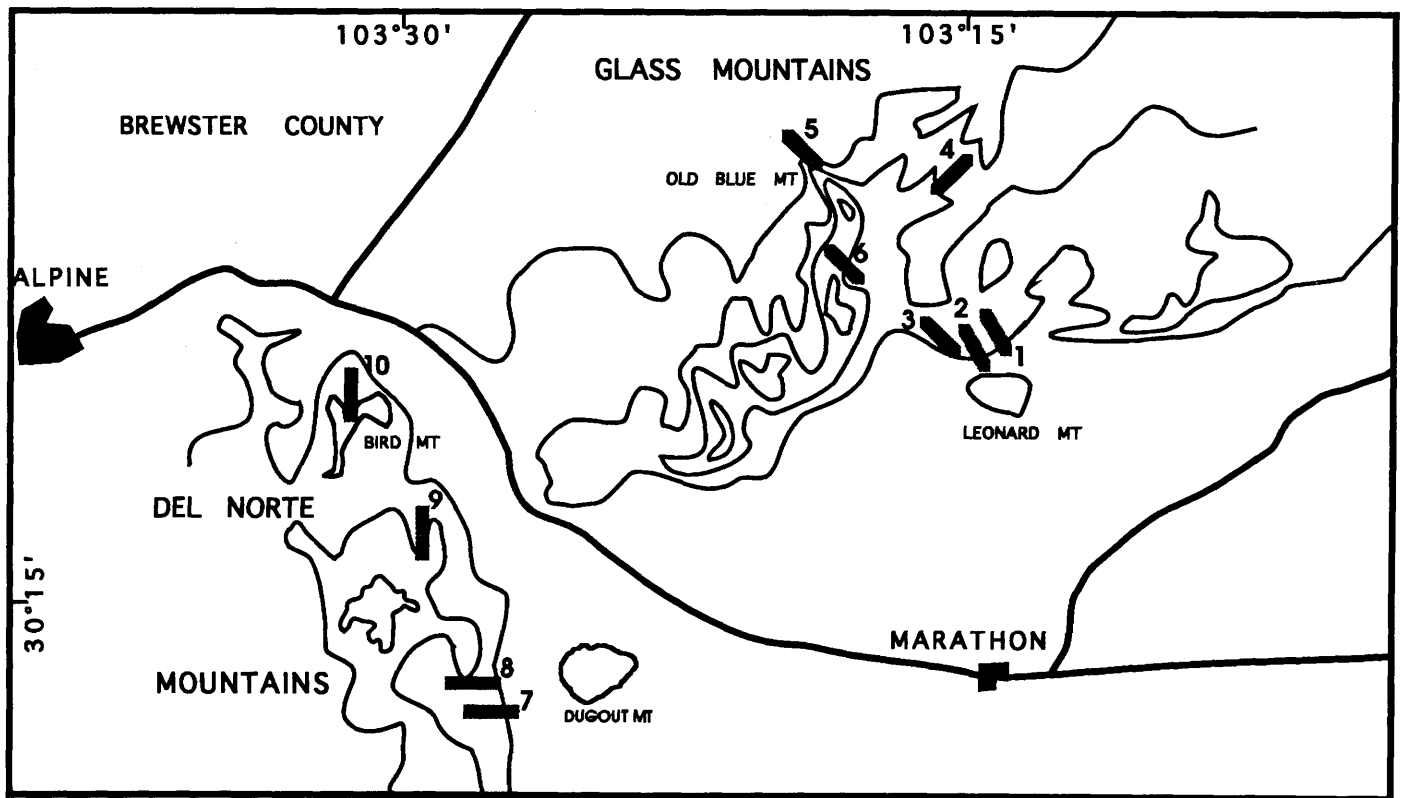


FIGURE 9-3.—Sketch map of the Glass and Del Norte mountains showing the locations of the measured sections.

noteworthy that some species of *Parafusulina* (*P. biturbinata* Kling, 1960, *P. guatemalaensis* Dunbar, 1939, *P. trumpyi* Thompson and Miller, 1949, and *P. durhami* Thompson and Miller, 1949) previously reported from Latin America (Guatemala, Colombia) have been identified in samples from the Glass and Del Norte mountains area. This suggests a close relationship of Permian deposits presently located in central America and northern South America with the Delaware basin, which was positioned along the southern margin of North America during the Permian. The genus *Yangchienia*, previously reported only in the Tethyan realm, is also identified in these samples.

Based on the stratigraphic ranges of fusulinid species, nine fusulinid zones have been recognized in the sampled interval (Figures 9-4, 9-5). The *Parafusulina durhami* Zone is placed in the Leonardian Stage; the *Parafusulina boesei* Zone is placed partly in the Leonardian stage and partly in the Roadian Stage (straddling the *Mesogondolella nankingensis* first appearance datum, which defines the stage boundary); the *Parafusulina rothi* Zone and *Parafusulina trumpyi* Zone are placed in the Roadian Stage; the *Parafusulina sellardsi* Zone and *Parafusulina antimonioensis* Zone are placed in the Wordian Stage; and the *Polydiexodina shumardi* Zone, *Reichelina lamarensis* Zone, and *Lantschichites splendens* Zone are placed in the Capitanian Stage. The lower boundary corresponds with the

first appearance datum of the species for which the zone is named, and the upper boundary corresponds with the base of the overlying zone, which is defined on the first appearance datum of the zone-naming species. The highest zone in the sequence is defined on the total range of the defining species of that zone. Zones used previously are of several different types, some of which were provisional or not formally defined. These include assemblage zones, range zones, concurrent range zones, and even acme zones. The different manner in which zones were defined and the failure to acknowledge these differences has caused confusion when comparing zonations. Discrepancies between previously proposed zonations have been resolved with additional documentation of fusulinid species.

Parafusulina durhami Zone

The base of this zone corresponds with the first appearance datum of *Parafusulina durhami*, and the upper boundary corresponds with the first appearance datum of *P. boesei* Dunbar and Skinner, 1937. The zone was first defined by Ross (1962). Other fusulinid species occurring in this zone include *Parafusulina* cf. *P. biturbinata*. This zone occurs in the upper part of the Cathedral Mountain Formation, which consists mostly of fine-grained siliciclastic sediments containing a few fusulinid-bearing limestone interbeds.

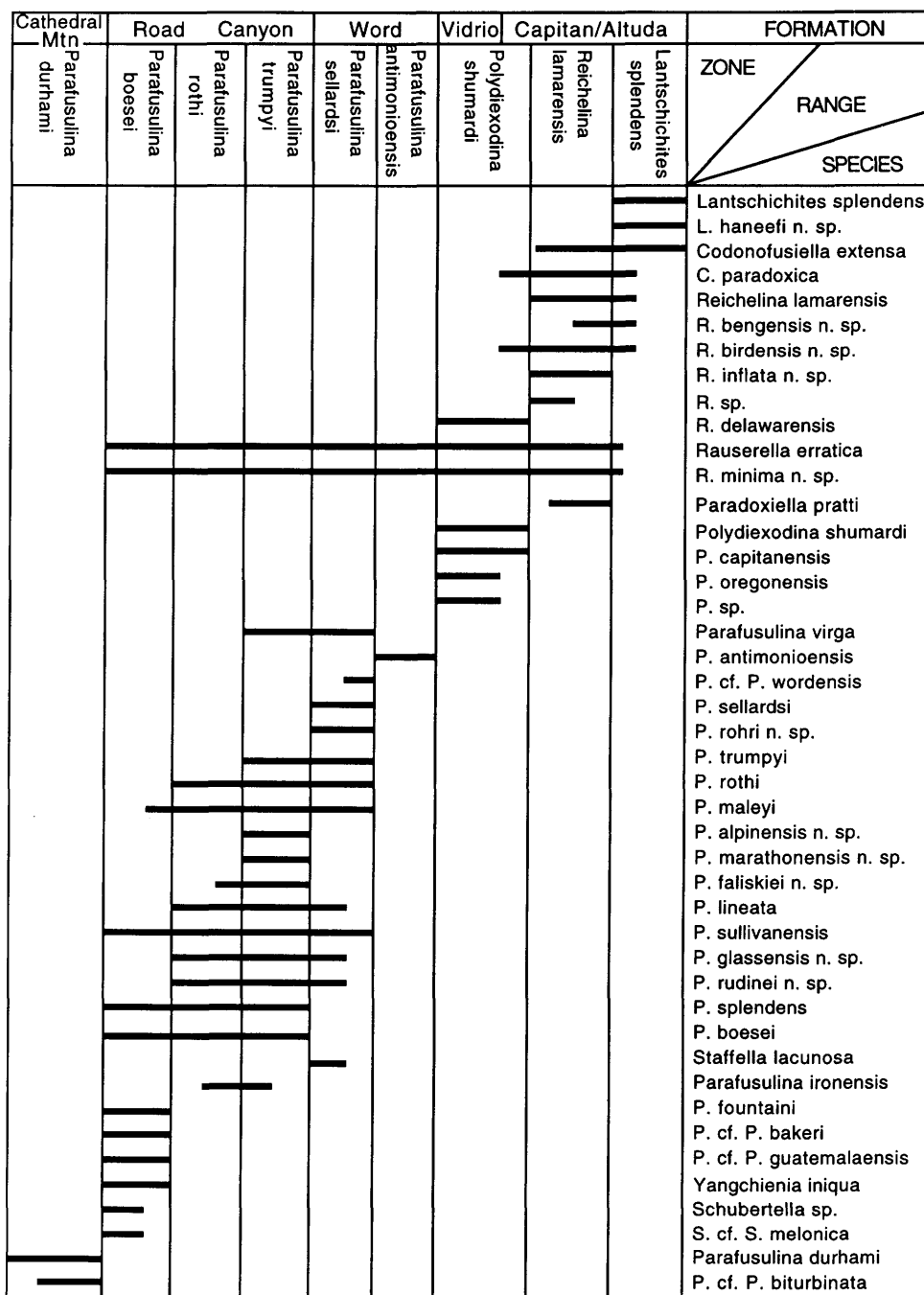


FIGURE 9-4.—Stratigraphic ranges of fusulinid species.

Parafusulina boesei Zone

The base of this zone corresponds with the first appearance datum of *Parafusulina boesei* Dunbar and Skinner, 1937, and the upper boundary corresponds with the first appearance datum of *P. rothi* Dunbar and Skinner, 1936. Other fusulinid species occurring in this zone include *P. cf. P. bakeri* Dunbar and Skinner, 1937, *P. fountaini* Dunbar and Skinner, 1937, *P. cf. P. guatemalaensis*, *P. maleyi* Dunbar and Skinner, 1937, *P.*

splendens Dunbar and Skinner, 1937, *P. sullivanensis* Ross, 1963, *Yangchienia iniqua* Lee, 1934, *Schubertella* cf. *S. melonica* Dunbar and Skinner, 1937, *S. sp.*, *Rauserella erratica* Dunbar, 1944, and *R. minima*, new species. This zone occurs in the lower part of the Road Canyon Formation, in grainstones and conglomeratic debris flow deposits. The *Mesogondolella nankingensis* first appearance datum occurs within this zone, showing that it spans the Leonardian–Guadalupian boundary.

			FUSULINID ZONE	FORMATION
PERMIAN	Upper	Ochoan	(No fusulinids discovered)	"Tessey"
		Capitanian	Lantschichites splendens	
	Reichelina lamarensis			
	Polydiexodina shumardi			
	Middle	Wordian	Parafusulina antimonioensis	Word
			Parafusulina sellardsi	
		Roadian	Parafusulina trumpyi	Road Canyon
			Parafusulina rothi	
	Lower	Leonardian	Parafusulina boesei	Cathedral Mtn
			Parafusulina durhami	

FIGURE 9-5.—Fusulinid zonation proposed in this study.

Parafusulina rothi Zone

The base of this zone corresponds with the first appearance datum of *Parafusulina rothi*, and the upper boundary corresponds with the first appearance datum of *Parafusulina trumpyi*. Other fusulinid species occurring in this zone include *Parafusulina boesei*, *P. faliskiei*, new species, *P. ironensis* Ross, 1963, *P. lineata*, *P. maleyi* Dunbar and Skinner, 1937, *P. splendens*, *P. sullivanensis*, *P. glassensis*, new species, *P. rudinei*, new species, *Rauserella erratica*, and *R. minima*, new species. The fusulinid *P. ironensis*, used by Ross (1963b:22) to define the *P. ironensis* Subzone, is confined to the *P. rothi* Zone and the *P. trumpyi* Zone in the sample set studied. However, it is rare compared with other species, and it is less useful as a zonal species than *P. rothi*. This zone occurs in the middle part of the Road Canyon Formation.

Parafusulina trumpyi Zone

The base of this zone corresponds with the first appearance datum of *Parafusulina trumpyi*, and the upper boundary corresponds with the first appearance datum of *Parafusulina sellardsi* Dunbar and Skinner, 1937. Other fusulinid species occurring in this zone include *Parafusulina boesei*, *P. lineata*,

P. maleyi, *P. rothi*, *P. sullivanensis*, *P. glassensis*, new species, *P. rudinei*, new species, *P. alpinensis*, new species, *P. virga* Thompson and Wheeler, 1946, *P. marathonensis*, new species, *P. splendens*, *P. faliskiei*, new species, *P. ironensis*, *Rauserella erratica*, and *R. minima*, new species. This zone occurs at the top of Road Canyon Formation at the type and nearby sections (Cooper and Grant, 1966) in the Glass Mountains and at the top of the Road Canyon Formation of nearby sections.

Parafusulina sellardsi Zone

The base of this zone corresponds with the first appearance datum of *Parafusulina sellardsi*, and the upper boundary corresponds with the first appearance datum of *Parafusulina antimonioensis* Dunbar, 1953. Other fusulinid species occurring in this zone include *Parafusulina lineata*, *P. rothi*, *P. maleyi*, *P. rudinei*, new species, *P. sullivanensis*, *P. trumpyi*, *P. virga*, *P. cf. P. wordensis* Dunbar and Skinner, 1931, *P. rohri*, new species, *P. glassensis*, new species, *Rauserella erratica*, *R. minima*, new species, and *Staffella lacunosa* Dunbar and Skinner, 1937. This zone occurs in the lower part of the Word Formation, in the Willis Ranch Member (i.e., King's No. 3 limestone member).

Parafusulina antimonioensis Zone

The base of this zone corresponds with the first appearance datum of *Parafusulina antimonioensis*, and the upper boundary corresponds with the first appearance datum of *Polydiexodina shumardi* Dunbar and Skinner, 1931. *Parafusulina antimonioensis*, which has a very large and elongate test, has an axis that is commonly arched or sharply bent at the middle, making exact orientation necessary for accurate comparison of the axial section of this and related species. Slightly oblique orientation may cause considerable foreshortening of the poles. The *P. antimonioensis* Zone occurs in the upper part of the Word Formation, which is commonly dolomitized.

Polydiexodina shumardi Zone

The base of this zone corresponds with the first appearance datum of *Polydiexodina shumardi*, and the upper boundary corresponds with the first appearance datum of *Reichelina lamarensis* Skinner and Wilde, 1955. Other fusulinid species occurring in this zone include *Polydiexodina capitaneensis* Dunbar and Skinner, 1931, *P. oregonensis* Bostwick and Nestell, 1965, *P. sp.*, *Rauserella erratica*, *R. minima*, new species, *Reichelina delawarensis* (Dunbar and Skinner, 1937), *R. birdensis*, new species, and *Codonofusiella paradoxa* Dunbar and Skinner, 1937. Strata of this zone in the Glass and Del Norte mountains, as well as in the Guadalupe Mountains, contain a great abundance of *Polydiexodina*, reflecting the proliferation of this genus in shallow marine environments. *Polydiexodina* occurs in the Vidrio Formation, Gilliam Limestone, the lower part of the Altuda Formation, and the lower part of the Capitan Limestone. This is the lowest fusulinid zone of the Capitanian Stage.

Reichelina lamarensis Zone

The base of this zone corresponds with the first appearance datum of *Reichelina lamarensis* Skinner and Wilde, 1955, and the upper boundary corresponds with the first appearance datum of *Lantschichites splendens* (Skinner and Wilde, 1954). Other fusulinid species occurring in this zone include *Codonofusiella extensa* Skinner and Wilde, 1955, *C. paradoxa*, *Reichelina bengensis*, new species, *R. haneefi*, new species, *R. birdensis*, new species, *R. sp.*, *Rauserella erratica*, *R. minima*, new species, and *Paradoxiella pratti* Skinner and Wilde, 1955. This zone occurs in the middle part of the Altuda Formation in the Glass Mountains and the upper part of the Altuda Formation in the Del Norte Mountains, which consists of sediments deposited in deep-water slope and basin environments. The *Reichelina lamarensis* Zone contains tiny fusulinids that tend to have an irregular last whorl or become uncoiled in the adult growth stage.

Lantschichites splendens Zone

This is the only zone in the present fusulinid zonation based on the full range of a species. The base of this zone corresponds

with the first appearance datum of *Lantschichites splendens*, and the upper boundary of this zone corresponds with its last appearance. Associated fusulinid species include *Lantschichites sp.*, *Codonofusiella extensa*, *C. paradoxa*, *Reichelina lamarensis*, *R. bengensis*, new species, *R. birdensis*, new species, *Rauserella erratica*, and *R. minima*, new species. The lower part of this zone is characterized by a high diversity of species from different genera; however, the upper part of this zone is dominated by species of *Lantschichites* in the absence of *Reichelina*. The *Lantschichites splendens* Zone contains small, diaphanotheca-walled fusulinids that tend to have an irregular last whorl or become uncoiled in the adult growth stage.

LOWER BOUNDARY OF THE GUADALUPIAN SERIES

When the Guadalupian Series was formally defined by Adams et al. (1939), the lower boundary was placed at the contact of the Brushy Canyon Formation with the underlying Bone Spring Formation (which included the Cutoff Shale). Of two zones recognized in the Guadalupian, the lower was defined as containing the ammonoid *Waagenoceras* and evolutionarily advanced species of the fusulinid genus *Parafusulina*. The criterion for determining the lower boundary was the first appearance datum of *Waagenoceras*; however, with the development of detailed zonations based exclusively on fusulinids or ammonoids, a long-standing disagreement arose over the proper placement of this boundary. This disagreement came from trying to position the Leonardian–Guadalupian boundary on a horizon that best separates a “Leonardian” biota (corresponding to the *Perrinites* Zone) from a “Guadalupian” biota (containing the *Waagenoceras* Zone). In the Glass Mountains this boundary was first drawn at the base of King’s (1931) first limestone member (now named the Road Canyon Formation) of the Word Formation (Adams et al., 1939).

Ross (1962, 1963b) adhered to this placement of the series boundary, but Cooper and Grant (1966) suggested that the Road Canyon Formation should be included in the Leonardian Series because of the presence of the ammonoid *Perrinites* and because the brachiopods present in the formation are more similar to those of the underlying Leonardian than to the Guadalupian. Furnish (1966, 1973) proposed the Roadian Stage between the Leonardian Stage (a part of the Leonardian Series) and the Wordian Stage, based on a stratigraphically distinct assemblage of ammonoids in these strata, and he advocated placement of the Roadian Stage in the Leonardian Series. However, Wilde and Todd (1968) and Wilde (1986a,b) correlated the Road Canyon Formation of the Glass Mountains with the Cutoff Formation and with the lower and middle parts of the San Andres Formation in the Guadalupe Mountains, suggesting that they are best placed in the Guadalupian Series. This interval contains the *Parafusulina boesei* Zone, which has usually been assigned (Ross, 1963b; Wilde, 1975, 1990) to the lowest part of the Guadalupian Series in fusulinid zonations. Following the erection of the Roadian Stage, the opinion that

the Roadian Stage forms the top of the Leonardian (Series) gained some acceptance (e.g., Cys, 1981; Ross, 1986).

Because of this debate, different criteria have been used in establishing the base of the Guadalupian Series in the Glass Mountains area, resulting in five different horizons being proposed as the base of the Guadalupian. The first proposed horizon is at the base of the Road Canyon Formation, which is coincident with the boundary between the Leonard Formation (of Udden, 1917) and the Word Formation that was selected by Adams et al. (1939) as the top of the Leonardian Series. (The type section of the Road Canyon Formation, which is the basal portion of the Word Formation of Udden, 1917, and King, 1931, directly overlies the type section of the Leonard Formation of Udden, 1917, along the sides of Leonard Mountain. An exact placement for this boundary can be determined on the basis of lithologic change.) The second proposed horizon is at the base of the *Parafusulina boesei-Skinnerina* Zone of Wilde (1990). This horizon lies at or near the base of the Road Canyon Formation. The third horizon is coincident with the boundary between the *Neostreptognathodus sulcopicatus* Zone and the *Mesogondolella nankingensis* Zone. This horizon lies within the lower part of the Road Canyon Formation. The fourth horizon is at the base of the *Parafusulina rothi* Zone. This horizon lies within the lower part of the Road Canyon Formation, a short distance above the *Mesogondolella nankingensis* first appearance datum. The fifth proposed horizon is coincident with the mutual boundary between the *Perrinites* Zone and the *Waagenoceras* Zone, which is similar to the definition of Adams et al. (1939) that Furnish (1973) described as being the horizon marking the concurrent extinction of *Perrinites* and appearance of *Waagenoceras*. However, both Newell et al. (1953) and Furnish (1973) used the first appearance datum of *Waagenoceras* to place the boundary. This horizon lies roughly at the base of the China Tank Member of the Word Formation in the Glass Mountains.

The debate over placement of the Leonardian-Guadalupian boundary was reduced with the acceptance among participants of the March, 1991, Guadalupian Symposium to use the *Mesogondolella nankingensis* first appearance datum as the base of the Roadian Stage (and Guadalupian Series). In a stratigraphic study of conodonts in the Road Canyon Formation, Wardlaw and Grant (1987) found that the *Mesogondolella nankingensis* first appearance datum (which defines the *Mesogondolella idahoensis*-*M. nankingensis* zonal boundary) lies in the lower part of the formation. They suggested that this datum provides an excellent marker for the boundary between the Leonardian and Guadalupian.

In the Glass and Del Norte mountains area the *Mesogondolella nankingensis* first appearance datum occurs within the *Parafusulina boesei* Zone, which spans the Leonardian-Guadalupian boundary (Yang and Yancey, 1990). The position of the *Mesogondolella nankingensis* first appearance datum relative to the *Parafusulina boesei* and *Parafusulina rothi* first appearance datums has been determined within two stratigraphic

sections of the Road Canyon Formation (Figure 9-6). The position of the *Mesogondolella nankingensis* first appearance datum in the Road Canyon Formation type section (section 2) is based on determinations by Lance Lambert (pers. comm., 1991), and the position of the *Mesogondolella nankingensis* first appearance datum in section 7 is based on determinations by Bruce Wardlaw (pers. comm., 1991). The position of fusulinid first occurrence data are compiled from samples collected for this study.

The *Parafusulina rothi* first appearance datum is a good fusulinid indicator of (but does not define) the base of the Guadalupian. This horizon coincides with an evolutionary change in the genus *Parafusulina*, in which species having a more advanced stage of evolutionary development appear. Evolutionary development is indicated by several features in the species of *Parafusulina*, including test size, intensity and regularity of septal fluting, and especially by the degree of development of the cuniculi. Cuniculi are not fully developed in any Leonardian species of *Parafusulina*. In primitive species, such as *Parafusulina spissisepta* Ross, 1960, *P. allisonensis* Ross, 1960, *P. brookensis* Ross, 1960, *P. deltoides* Ross, 1960, *P. vidrioensis* Ross, 1960, and others, cuniculi appear first in the outer whorls and are limited to the middle part of the test. These openings are so low and narrow that they can only be observed in tangential slices cut very close to the floor of a whorl. With further evolutionary development, cuniculi appear earlier and earlier in ontogeny and spread progressively toward the poles, and the septal flutings that form cuniculi become wider and higher. Species of *Parafusulina* with moderately developed cuniculi, such as *Parafusulina durhami*, *P. biturbinata*, *P. fountaini*, *P. boesei*, and *P. splendens*, are common in the upper part of the Leonardian and range up into the basal part of the Guadalupian. In advanced species of *Parafusulina*, such as *P. rothi*, *P. trumpyi*, *P. sellardsi*, *P. wordensis*, and *P. antimonioensis*, although development of cuniculi varies from species to species, cuniculi may occupy a large portion of a septal fold and up to one-half the height of the septum. Species with this grade of development appear in the *Parafusulina rothi* Zone and are present in Guadalupian strata. *Parafusulina rothi*, with its large size, intensive and regular fluting, and well-developed cuniculi, is a good marker for the beginning of the advanced evolutionary stage of *Parafusulina* and the base of the Guadalupian.

UPPER BOUNDARY OF THE GUADALUPIAN SERIES

The upper limit of the Guadalupian Series was originally defined on the basis of lithologic change from fossiliferous marine strata of the Delaware Group to evaporitic strata of the overlying section (Adams et al., 1939). This corresponds with a geologically sudden change from normal marine environments to hypersaline environments throughout the Delaware basin and occurs within an interval represented by continuous sedimentation in the deeper parts of the basin (King, 1948). The

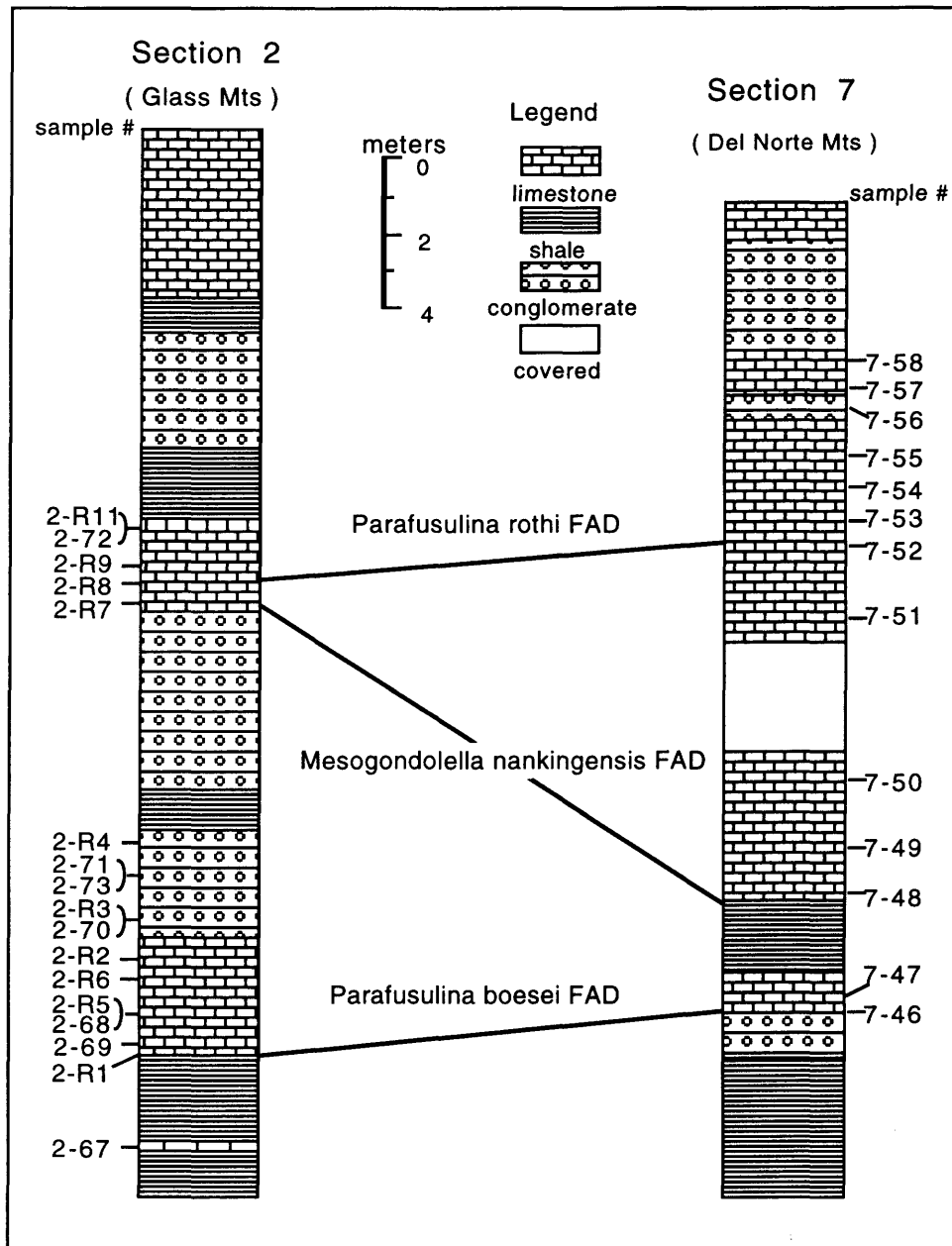


FIGURE 9-6.—Relative positions of first appearance datum (FAD) levels of *Parafusulina boesei*, *P. rothi*, and *Mesogondolella nankingensis* in the Road Canyon Formation in the Glass and Del Norte mountains.

stratotype section for the Guadalupian Series at the south end of the Guadalupe Mountains is incomplete at the top, so it was supplemented with a subsurface section located near Carlsbad, New Mexico. This designation by Adams et al. (1939) places the boundary stratotype in a subsurface section, but the interval is exposed in surface outcrops in the vicinity of the reef escarpment near the New Mexico–Texas state line.

Dunbar and Skinner (1937) established the *Polydiexodina* Zone as the highest fusulinid zone in the Delaware Mountain Group and Capitan Limestone, and Adams et al. (1939)

reported that the fusulinid *Polydiexodina* and the ammonoid *Timorites* co-occur in the youngest zone of the Guadalupian Series. On the basis of new records of fusulinids in the Lamar Limestone Member of the Bell Canyon Formation (Skinner and Wilde, 1954, 1955), Wilde (1975) designated a *Yabeina-Paradoxiella* Zone as the highest zone of the Guadalupian, which he (Wilde, 1990) later renamed as the *Paraboultonia splendens* Zone. This zone occurs in the Lamar Member and post-Lamar interval of the Delaware Mountain Group and is part of the Capitanian Stage of the Guadalupian Series. Furnish

(1973) suggested that the ammonoid and fusulinid assemblages in the Lamar Limestone Member be placed in an overlying Amarassian Stage rather than the Capitanian Stage, but this suggestion was not followed by subsequent workers because the Capitanian had been established for the stratigraphic interval extending to the top of the Bell Canyon Formation.

Strata of the Ochoan Series lack normal marine fossils, so the upper boundary of the Guadalupian Series is indistinct in a biostratigraphic sense and useless for accurate chronostratigraphic correlation.

Work on fusulinids from Guadalupian strata in the Glass and Del Norte mountains provides data that can help solve problems associated with the upper boundary of the Guadalupian Series. A major change in fusulinid assemblages takes place in the upper part of the Altuda Formation, in which large-size fusulinids having a keriotheca in their test walls disappear and are replaced upward with assemblages dominated by tiny fusulinids having a diaphanotheca in their test walls. A similar changeover in fusulinid faunas occurs in Permian strata in other parts of the Delaware basin (at the top of the Lamar Limestone Member of the Bell Canyon Formation) and other parts of the world, suggesting that the lowest portion of the Late Permian may be present in the highest parts of the Guadalupian interval (of Adams et al., 1939). Two fusulinid zones, the *Reichelina lamarensis* Zone and the *Lantschichites splendens* Zone, occur above the highest occurrences of keriotheca-walled fusulinids in the Altuda Formation. Several genera of small fusulinids with numerous species occur in these zones, providing the potential for additional zones to be defined.

Correlation of Fusulinid Zones with South China

Although fusulinid faunas are quite different in the tropical regions of North America and Tethys during the Permian, similar evolutionary trends and the co-occurrence of some species allow for the correlation of fusulinid zones between the two regions. A chart showing the suggested correlation of middle Permian fusulinid zones between the Delaware basin region of North America and the South China region of the Tethyan province is shown in Figure 9-7.

The *Mesogondolella nankingensis* first appearance datum provides a standard for correlating the base of the middle Permian in the two areas. Clark and Wang (1988) showed that the *Mesogondolella nankingensis* first appearance datum occurs in the middle part of the Qixia (previously transliterated as Chihsia) Formation in South China. Despite the difference in fusulinid faunas between North America and the Tethyan province, three fusulinid species (*Parafusulina boesei*, *P. splendens*, *Yangchienia iniqua*) present in the lower part of the Road Canyon Formation also occur in the *Maklaya-Shengella* Zone in the middle of the Qixia Stage of South China (*Parafusulina boesei*, Sheng, 1963:72; *P. splendens*, Sheng, 1963:71; Yang, 1985:309; *Yangchienia iniqua*, Sheng,

1963:38; Yang, 1985:310; Xiao et al., 1986:38; Zhang et al., 1988:271). Therefore, the *Parafusulina boesei* Zone of this study may be correlated with the *Maklaya-Shengella* Zone. The *Parafusulina boesei* first appearance datum appears to be contemporaneous in the two regions.

Parafusulina rothi has been reported from a few localities in China (Zhang, 1957; Yang, 1985), where it occurs in the *Neoschwagerina simplex* Zone, immediately above the *Cancelina liuzhiensis* Zone. The *Neoschwagerina simplex* Zone appears to correlate with the *Parafusulina rothi* and *P. trumpyi* zones.

Fusulinids of the middle and late Guadalupian are more difficult to correlate with those in South China. *Leella* Dunbar and Skinner, 1937, which occurs in middle and upper Guadalupian strata of the Delaware basin (Dunbar and Skinner, 1937; Wilde and Todd, 1968), occurs in the *Afghanella schencki-Neoschwagerina craticulifera* Zone (Xiao et al., 1986) in South China. This suggests a correlation of the middle Guadalupian with the lower part of the Maokouan. The evolutionary development of polydiexodinids also provides a basis for correlating the *Parafusulina sellardsi* and *P. antimonioensis* zones with the *Afghanella schencki-Neoschwagerina craticulifera* Zone and the *Polydiexodina shumardi* Zone with the *Yabeina gubleri* Zone. Primitive species of polydiexodinids (such as *Polydiexodina afghanensis* Thompson, 1946, *P. craticula* Da, 1983, and *P. regularis* Da, 1986) referable to *Eopolydiexodina* Wilde, which lack a well-defined median tunnel and bear irregularly distributed supplementary tunnels, occur in strata of *Afghanella schencki-Neoschwagerina craticulifera* Zone in the Maokou Formation of Gansu, the Yiesangang Formation and Qipan Formation of Xinjiang, and the Bayinhe Formation of Qinghai. These are less evolutionarily advanced than species of *Polydiexodina* (*P. capitanensis*, *P. shumardi*, etc.) that occur in the *Polydiexodina shumardi* Zone of North America.

The highest two zones of the Guadalupian (the *Reichelina lamarensis* Zone and the *Lantschichites splendens* Zone) can be correlated with the highest zone of the Maokouan in South China, which also contains assemblages of small, diaphanotheca-walled, last-whorl-uncoiled fusulinids. Within the Tethyan realm there is a trend of disappearance of large, keriotheca-walled fusulinids and subsequent replacement with assemblages containing tiny, diaphanotheca-walled ones similar to those seen in the Delaware basin. *Lantschichites splendens*, *L. minima* (Chen, 1956), and species of *Reichelina* occur in the *Neomisellina multivoluta* Zone, and *Codonofusiella paradoxa* occurs in the underlying *Yabeina gubleri* Zone in South China (Sheng, 1963; Yang, 1985; Xiao et al., 1986), suggesting a correlation with the *Lantschichites splendens*, *Reichelina lamarensis*, and *Polydiexodina shumardi* zones in the Glass and Del Norte mountains.

Yabeina texana Skinner and Wilde, 1955, does not provide direct evidence for correlation to the Tethyan province. Although it has been described as a primitive species of the

	NORTH AMERICA			SOUTH CHINA			
	This study			Yang (1985)	Xiao et al. (1986)	Sheng et al. (1982)	
	PERMIAN	Upper	Ochoan	(No fusulinids found)			Codonofusiella Wujia-pingian
Middle		Guadalupian	Capitanian	Lantschichites splendens	Neomisellina multivoluta	Yabeina - Neomisellina (Polydiexodina - Neomisellina)	Maokouan
				Reichelina lamarensis			
				Polydiexodina shumardi			
		Wordian	Parafusulina antimonioensis	Neoschwagerina Range Zone	Afghanella schencki - Neoschwagerina craticulifera	Neoschwagerina (Chusenella conicocylindrica)	
			Parafusulina sellardsi				
			Parafusulina trumpyi				
		Roadian	Parafusulina rothi	Neoschwagerina simplex	Cancellina liuzhiensis	Parafusulina - Cancellina	
			Parafusulina boesei				
			Parafusulina durhami				
Lower	Leonardian	Misellina Range Zone	Maklaya - Shengella	Qixian (Chihhsian)			
		Misellina claudiae	Misellina claudiae				

FIGURE 9-7.—Correlation of fusulinid zones between North America and South China.

genus (implying a correlation with the lower part of the *Yabeina gubleri* Zone), it is probably an aberrant form adapted to unusual environmental conditions. Similar malformation of neoschwagerinids occurs in the top of the Maokou Formation in South China (Yang, 1985). Similarly, stratigraphically high occurrences of species of *Polydiexodina* (*P. chekiangensis* Sheng, 1962; *P. tunghuensis* Sheng, 1962, and *P. altilis* Lin, 1982) from the *Neomisellina-Polydiexodina-Codonofusiella* Zone of Zhang (1984) (equivalent to the *Neomisellina multivoluta* Zone) of southeast China are quite different from other species of polydiexodinids and cannot be correlated with the range zone of *Polydiexodina* in North America. These

species of *Polydiexodina* reported in the southeastern part of China have a poorly developed median tunnel and sporadic supplementary tunnels, and, unlike earlier species of polydiexodinids, they are very small in size (for the genus), with few volutions, a short axial length, and a small proloculus.

Systematic Descriptions

For specimen measurements and description of fusulinid species, this study adopts the measurement methodology and terminology employed by Dunbar and Skinner (1937), Thompson (1948), and Kling (1960). All specimens studied and

illustrated were collected from the Glass Mountains and Del Norte mountains of West Texas. All figures on the plates are unretouched photographs. All type specimens, illustrated specimens, and study materials are housed in the Department of Paleobiology, National Museum of Natural History, Smithsonian Institution, Washington, D.C.

Family OZAWAINELLIDAE Thompson and Foster, 1937

***Rauserella* Dunbar, 1944**

TYPE SPECIES.—*Rauserella erratica* Dunbar, 1944.

***Rauserella erratica* Dunbar, 1944**

PLATE 9-1: FIGURES 1-7

Rauserella erratica Dunbar, 1944:37-38, pl. 9: figs. 1-8.—Ross, 1964:315, pl. 50: figs. 1, 2.

TYPES.—*Hypotypes*: USNM 482975-482981; from the Road Canyon Formation and Altuda Formation of the Glass and Del Norte mountains, Texas.

MATERIAL STUDIED.—Samples from the Road Canyon Formation, Word Formation, Vidrio Formation, and Altuda Formation in the Glass and Del Norte mountains, Texas: 2-68, 2-R6, 2-77; 6-BA3, 6-BA13; 7-49; 8-19, 8-28, 8-41, 8-45; 9-6, 9-10; 10-202, 10-206.

AGE AND DISTRIBUTION.—*Parafusulina boesei* Zone to *Lantschichites splendens* Zone of the Guadalupian Series, Glass and Del Norte mountains; Apache Mountains and Guadalupe Mountains of West Texas (Dunbar, 1944); Las

TABLE 9-1.—Measurements of *Rauserella erratica* Dunbar.

	Volution	USNM 482975	USNM 482976	USNM 482977	USNM 482978
Radius vector (mm)	0	0.03	0.03	0.03	0.035
	1	0.085	0.08	-	0.07
	2	0.13	0.14	-	0.12
	3	0.25	0.24	-	0.22
	4	-	-	(0.22)	-
Half length (mm)	5	-	-	(0.38)	-
	1	0.065	0.05	0.04	0.05
	2	0.12	0.08	0.08	0.09
	3	0.22	0.15	0.15	0.14
	4	-	0.65	-	-
Form ratio	5	-	1.35	-	-
	1	0.76	0.63	-	0.71
	2	0.81	0.57	-	0.75
Wall thickness (mm)	3	0.88	0.63	-	0.64
	1	0.012	0.010	0.010	0.010
	2	0.018	0.015	0.015	0.020
	3	0.020	0.020	0.020	0.022
Tunnel angle (°)	4	0.035	0.030	-	0.030
	1	-	12	-	16
	2	-	18	-	22

Delicias area of Coahuila, Mexico (Dunbar, 1944). Lower part of Maokou Formation in Datieguan, Guizhou Province, China (Yang, 1985), and the upper part of Qixia Formation in Dalianshan, Jiangsu Province, China (Zhang et al., 1988).

REMARKS.—*Rauserella* is characterized by having an abrupt change in the orientation of the axis of coiling during growth, which occurs after forming nautiliform, symmetrically coiled inner volutions. This juvenile nautiliform shell usually has three to four volutions. *Rauserella erratica* is larger than other species associated with it. The specimens studied resemble the type specimens of *Rauserella erratica* Dunbar in all respects. Measurement data of specimens are given in Table 9-1.

***Rauserella minima*, new species**

PLATE 9-1: FIGURES 8-16

TYPES.—*Holotype*: USNM 482987; *Paratypes*: USNM 482982-482986, 482988-482990; from the Road Canyon Formation and Altuda Formation of the Glass and Del Norte mountains, Texas.

MATERIAL STUDIED.—Samples from the Road Canyon Formation and the Altuda Formation in the Glass and Del Norte mountains, Texas: 1-62; 2-68, 2-R5, 2-R6; 6-BA3, 6-BA10, 6-BA11; 8-18, 8-24; 10-202.

DIAGNOSIS.—Test minute, irregularly ellipsoidal; 3 to 3½ volutions; inner two volutions planispiral and discoidal; outer volutions expanding abruptly and aberrant in form, with axis of coiling askew at high angle or right angle to axis of inner volutions; chomata small, weak, and present only in inner volutions.

AGE AND DISTRIBUTION.—*Parafusulina boesei* Zone to *Lantschichites splendens* Zone of the Guadalupian Series, Glass and Del Norte mountains, Texas.

DESCRIPTION.—Minute size; irregularly ellipsoidal form; 3 to 3½ volutions; attaining a maximum length of 1.12 mm and maximum diameter of 0.58 mm; first two volutions planispiral and discoidal in shape, with narrowly rounded periphery and short axis of coiling, forming a nautiliform juvenile; outer volutions irregularly coiled and expanded, abruptly elongated, with axis of coiling askew at large angle (even at right angle) to axis of inner volutions; proloculus small and spherical, 0.04 to 0.07 mm in outside diameter; spirotheca thin, consisting of tectum and diaphanotheca; spirotheca about 0.01 mm in inner volutions and about 2.0 mm in outer ones; septa planar in inner volutions, but irregularly arched without obvious fluting in outer volutions; chomata small and weakly developed, present only in inner volutions; tunnel narrow and not well marked; tunnel angle averaging 15° in first volution. Measurement data of specimens given in Table 9-2.

REMARKS.—This species differs from *Rauserella erratica* Dunbar, 1944, in having a smaller and shorter test, a thinner spirotheca, and only two volutions in the inner nautiloid juvenile portion compared to three to four volutions. It is somewhat similar to *Rauserella fujimotoi* Kobayashi, 1956, but

TABLE 9-2.—Measurements of *Rauserella minima*, new species.

	Volution	USNM 482983	USNM 482984	USNM 482982	USNM 482987	USNM 482985
Radius vector (mm)	0	0.020	0.030	0.025	0.035	0.035
	1	0.050	0.050	0.050	0.060	0.060
	2	0.110	0.130	0.090	0.130	0.120
Half length (mm)	1	0.030	0.040	0.040	0.040	0.050
	2	0.060	0.060	0.055	0.060	0.070
Form ratio	1	0.60	0.66	0.80	0.66	0.83
	2	0.55	0.46	0.61	0.46	0.58
Wall thickness (mm)	1	0.010	0.018	0.010	0.010	0.010
	2	0.012	0.015	0.015	0.010	0.012
	3	0.020	0.025	0.025	0.020	0.015
Tunnel angle (°)	1	13	14	—	15	11
	2	—	—	—	16	18

differs in having a smaller size, fewer volutions, and less angular periphery on the inner volutions. Some specimens reported as *Rauserella* sp. from the Road Canyon Formation and Willis Ranch Member of the Word Formation in the Glass Mountains (Wilde in Cooper and Grant, 1977) and from the San Andres Formation in the northern Guadalupe Mountains (Wilde, 1986a) might be conspecific with the new species.

ETYMOLOGY.—The species name is derived from the Latin word *minimus*, meaning small; an important feature of this species compared with other species of the genus.

Reichelina Erk, 1942

TYPE SPECIES.—*Reichelina cribroseptata* Erk, 1942.

Reichelina bengensis, new species

PLATE 9-2: FIGURES 17-20

TYPES.—*Holotype*: USNM 482992; *Paratypes*: USNM 482991, 482993-482994; from the Altuda Formation of the Glass and Del Norte mountains, Texas.

MATERIAL STUDIED.—Samples from the middle part of the Altuda Formation at Benge Ranch in the Glass Mountains and the upper part of the Altuda Formation near Bird Mountain in the Del Norte Mountains, Texas: 6-BA8, 6-BA10; 10-202, 10-205.

DIAGNOSIS.—Test minute, lenticular; axis of coiling extremely short; umbilical areas slightly depressed; periphery subangular; spirotheca very thin, consisting of tectum and diaphanotheca; septa unfluted; proloculus very small.

AGE AND DISTRIBUTION.—*Reichelina lamarensis* Zone to *Lantschichites splendens* Zone of the Guadalupian Series, Glass and Del Norte mountains, Texas.

DESCRIPTION.—Minute size; lenticular form; 5 volutions, with the last one-half volution uncoiled; coiled part ~0.20 mm long and 0.58 mm in diameter, resulting in a form ratio of 0.35;

TABLE 9-3.—Measurements of *Reichelina bengensis*, new species.

	Volution	USNM 482992	USNM 482993	USNM 482991
Radius vector (mm)	0	0.012	0.011	0.014
	1	0.030	0.035	0.035
	2	0.070	0.060	0.060
	3	0.120	0.110	0.100
Half length (mm)	4	0.180	0.180	0.150
	1	0.020	0.025	0.024
	2	0.040	0.040	0.040
	3	0.060	0.060	0.060
Form ratio	4	0.080	0.085	0.080
	1	0.67	0.63	0.68
	2	0.57	0.66	0.66
	3	0.50	0.54	0.60
Tunnel angle (°)	4	0.44	0.47	0.53
	1	0.010	0.010	0.010
	2	0.012	0.015	0.012
	3	0.015	0.015	0.015
Wall thickness (mm)	4	0.010	0.020	0.015
	5	—	0.010	0.010
	1	—	—	—
	2	12	8	10
Tunnel angle (°)	3	14	11	12
	4	—	10	15

axis of coiling extremely short with gently depressed umbilical areas; first two volutions subdiscoidal, with relatively rounded periphery; subsequent volutions lenticular, with angular periphery; proloculus very small, averaging 0.028 mm in outside diameter, and spherical in shape; spirotheca of tectum and diaphanotheca, about 0.010 to 0.018 mm thick; septa thin and closely spaced, almost planar but broadly sinuous in the uncoiled part; chomata low and broad, extending laterally to the poles; tunnel low and narrow; tunnel angle averaging 11°, 13°, and 10° in the second to the fourth volutions, respectively. Measurement data of specimens given in Table 9-3.

REMARKS.—This species differs from *Reichelina lamarensis* Skinner and Wilde, 1955, in being much smaller, having a more sharply lenticular shape, a smaller proloculus, and a much shorter axis of coiling. The specimens studied mostly resemble the type specimens of *Reichelina changhsingensis* Sheng, 1963, but differ in having a smaller size, a shorter axis of coiling, more volutions, lower chamber height in corresponding volutions, and more rounded periphery of the inner volutions.

ETYMOLOGY.—The species is named for the Benge Ranch, on the northwest side of the Glass Mountains, Texas, where the type specimens were collected.

Reichelina birdensis, new species

PLATE 9-2: FIGURES 21-27

TYPES.—*Holotype*: USNM 482998; *Paratypes*: USNM

482995–482997, 482999–483001; from the Altuda Formation of the Glass and Del Norte mountains, Texas.

MATERIAL STUDIED.—Samples from the upper part of the Altuda Formation near Bird Mountain in the Del Norte Mountains and from the middle part of the Altuda Formation at Bengé Ranch in the Glass Mountains, Texas: 6-BA5, 6-BA10, 6-BA11; 10-202, 10-205, 10-208.

DIAGNOSIS.—Test minute; first volution subdiscoidal; later volutions lenticular; uncoiled last one-half volution is rather large; spirotheca consists of two layers; septa unfluted; small and broad chomata border a low tunnel; proloculus very small.

AGE AND DISTRIBUTION.—*Polydiexodina shumardi* Zone to *Lantschichites splendens* Zone of the Guadalupian Series, Glass and Del Norte mountains, Texas.

DESCRIPTION.—Minute size; lenticular form; 4½ to 5 volutions; attaining length of 0.26–0.30 mm and diameter of 0.70–0.90 mm; first volution subdiscoidal, with a narrowly rounded periphery; second to fourth volutions lenticular, with angular periphery; last one-half volution uncoiled; proloculus small, 0.03 to 0.04 mm in outside diameter; spirotheca thin, consisting of tectum and diaphanotheca, the thickest part about 0.02 mm; septa planar; chomata low and narrow; tunnel low and narrow, with tunnel angle about 10° and 20° in the first and fourth volutions, respectively. Measurement data of specimens given in Table 9-4.

REMARKS.—This species is very similar to *Reichelina media*

TABLE 9-4.—Measurements of *Reichelina birdensis*, new species.

	Volution	USNM 482998	USNM 482999	USNM 483000	USNM 482996
Radius vector (mm)	0	0.015	0.015	0.020	0.020
	1	0.05	0.04	0.04	0.04
	2	0.08	0.07	0.08	0.06
	3	0.13	0.12	0.12	0.11
	4	0.24	0.22	0.22	0.20
Half length (mm)	5	0.47	0.40	-	0.41
	1	0.03	0.02	0.03	0.03
	2	0.05	0.04	0.05	0.05
	3	0.07	0.07	0.08	0.09
	4	0.10	0.12	0.11	0.12
Form ratio	5	0.14	0.15	0.14	0.16
	1	0.60	0.63	0.75	0.75
	2	0.63	0.57	0.64	0.83
	3	0.54	0.58	0.66	0.82
	4	0.42	0.55	0.50	0.60
Wall thickness (mm)	5	0.30	0.38	-	0.39
	1	0.010	-	-	0.012
	2	0.014	-	-	0.018
	3	0.018	-	-	0.020
	4	0.015	0.020	-	0.015
Tunnel angle (°)	5	0.010	0.010	0.015	-
	1	-	-	-	12
	2	-	10	10	18
	3	10	12	22	19
	4	13	18	-	-

Miklukho-Maklay, 1954, but *R. media* is more slender in shape, is slightly smaller, and has a higher form ratio in corresponding volutions. It differs from *Reichelina lamarensis* Skinner and Wilde in having a smaller size, more slender shape, and fewer volutions. It can be easily distinguished from *Reichelina bengensis*, new species, in having a larger size, a longer axis of coiling, and a higher form ratio.

ETYMOLOGY.—The species is named for Bird Mountain, a large hill in the northern Del Norte Mountains, Texas, where the holotype specimen was collected.

***Reichelina delawarensis* (Dunbar and Skinner, 1937),
new combination**

PLATE 9-4: FIGURES 15, 16; PLATE 9-9: FIGURES 1–3

Ozawainella delawarensis Dunbar and Skinner, 1937:602, pl. 46: figs. 21–26.

TYPES.—*Hypotypes*: USNM 483002, 483003, 483132–483134; from the Altuda Formation of the Del Norte Mountains, Texas.

MATERIAL STUDIED.—Samples from the Altuda Formation and the upper part of the Vidrio Formation in the Del Norte Mountains, Texas: 9-5, 9-6, 9-10; 10-204, 10-206, 10-208, 10-344.

AGE AND DISTRIBUTION.—*Polydiexodina shumardi* Zone of the Guadalupian Series, Del Norte Mountains, Texas; Guadalupe Mountains, Texas (Dunbar and Skinner, 1937).

REMARKS.—The specimens studied resemble the type specimens of *Ozawainella delawarensis* Dunbar and Skinner, 1937, in major respects. An assignment to the genus *Reichelina* is warranted by the sharply expanded or uncoiled character of the last one-half volution and by the presence of well-preserved wall structure with distinct layers. Skinner and Wilde (1955:930) were correct in stating that the species is not a member of the genus *Ozawainella*. *Reichelina delawarensis* is characterized by a larger test, a smaller uncoiled part, and thicker spirotheca than other species of *Reichelina*. Measurement data of specimens are given in Table 9-5.

***Reichelina haneefi*, new species**

PLATE 9-4: FIGURES 9–13

TYPES.—*Holotype*: USNM 483005; *Paratypes*: USNM 483004, 483006–483008; from the Altuda Formation of the Glass Mountains, Texas.

MATERIAL STUDIED.—Samples from the middle part of the Altuda Formation at Bengé Ranch in the Glass Mountains, Texas: 6-BA2, 6-BA3, 6-BA10, 6-BA11.

DIAGNOSIS.—Test minute; lenticular, with highly inflated polar regions; last one-half volution uncoiled; spirotheca thick for genus, consisting of tectum and diaphanotheca; septa unfluted; chomata low, broad, and extending to the poles; proloculus small, with a spherical form.

TABLE 9-5.—Measurements of *Reichelina delawarensis* (Dunbar and Skinner).

	Volution	USNM 483134	USNM 483133	USNM 483002
Radius vector (mm)	0	0.03	0.04	0.035
	1	0.09	-	0.08
	2	0.18	-	0.15
	3	0.30	-	0.27
	4	0.50	-	-
Half length (mm)	1	0.06	0.06	0.06
	2	0.12	0.11	0.10
	3	0.20	0.21	0.17
	4	0.34	0.32	0.28
	5	0.50	0.42	-
Form ratio	1	0.67	-	0.75
	2	0.67	-	0.67
	3	0.67	-	0.63
	4	0.68	-	-
Wall thickness (mm)	1	0.02	-	0.02
	2	0.03	0.02	0.02
	3	0.04	-	0.03
	4	0.05	-	-
	5	0.03	-	-
Tunnel angle (°)	1	18	-	-
	2	20	-	24
	3	35	-	38

AGE AND DISTRIBUTION.—*Reichelina lamarensis* Zone of the Guadalupian Series, Glass Mountains, Texas.

DESCRIPTION.—Minute size; thickly lenticular form; 5 volutions in maturity; attaining a length of 0.5 to 0.6 mm and diameter of 1.0 to 1.6 mm; axis of coiling short and straight; first volution subdiscoidal, with narrowly rounded periphery; remaining volutions lenticular, with bluntly angular periphery; polar regions distinctly inflated, resulting in an extraordinarily great length and high form ratio for the genus; proloculus small and spherical, 0.3 to 0.4 mm in outside diameter; spirotheca consisting of tectum and diaphanotheca; thickness averaging 0.010, 0.018, 0.029, 0.030, and 0.018 mm in first to fifth volutions, respectively; septa unfluted, counting 10, 14, 15, 17, and 28 in first to fifth volutions, respectively; chomata low, broad, and extending to the poles, looking like a thick outer tectorium; tunnel low and slit-shaped; tunnel angle averaging 9°, 11°, 16°, and 22° in the first to fourth volutions, respectively. Measurement data of specimens given in Table 9-6.

REMARKS.—This species is similar in several features to *Reichelina turgida* Sheng, 1963; however, the longer axis of coiling, higher form ratio, and more inflated polar regions distinguish it from the latter species. It is also similar to *Reichelina lamarensis* Skinner and Wilde but differs in having fewer volutions, larger size, higher form ratio, inflated poles, and broader and heavier chomata. *Reichelina delawarensis* (Dunbar and Skinner) has a larger test, lower form ratio, and less inflated poles than *R. haneefi*. *Reichelina haneefi* is

TABLE 9-6.—Measurements of *Reichelina haneefi*, new species.

	Volution	USNM 483005	USNM 483007	USNM 483008	USNM 483004
Radius vector (mm)	0	0.015	0.018	0.020	0.016
	1	0.06	0.05	0.05	0.06
	2	0.11	0.10	0.09	0.11
	3	0.18	0.17	0.15	0.20
	4	0.29	0.26	0.25	0.33
Half length (mm)	5	0.50	0.52	0.42	0.80
	1	0.04	0.035	0.03	-
	2	0.08	0.07	0.07	-
	3	0.14	0.11	0.13	-
	4	0.21	0.18	0.22	-
Form ratio	5	0.28	0.23	-	-
	1	0.66	0.70	0.60	-
	2	0.73	0.70	0.78	-
	3	0.78	0.65	0.86	-
	4	0.72	0.69	0.88	-
Wall thickness (mm)	5	0.60	0.49	-	-
	1	0.010	0.010	0.010	0.010
	2	0.020	0.015	0.020	0.015
	3	0.030	0.028	0.030	0.020
	4	0.030	0.030	0.030	0.030
Tunnel angle (°)	5	0.020	0.015	0.020	-
	1	-	8	10	-
	2	10	9	13	-
	3	12	14	20	-
	4	17	19	30	-

characterized by its inflated polar regions and thereby is easily distinguished from other species of the genus.

ETYMOLOGY.—The species is named for Mohamed Haneef, a graduate student at Sul Ross State University, who helped with the field work of this study.

Reichelina lamarensis Skinner and Wilde, 1955

PLATE 9-2: FIGURES 1-16

Reichelina lamarensis Skinner and Wilde, 1955:929-930, pl. 89: figs. 1-9.

TYPES.—*Hypotypes*: USNM 483009-483024; from the Altuda Formation of the Glass and Del Norte mountains, Texas.

MATERIAL STUDIED.—Samples from the Altuda Formation at Benge Ranch in the Glass Mountains and near Bird Mountain in the Del Norte Mountains, Texas. Localities: 6-BA1, 6-BA2, 6-BA3, 6-BA4, 6-BA7, 6-BA8, 6-BA10, 6-BA11, 6-BA12, 6-BA17; 10-202, 10-204, 10-205.

AGE AND DISTRIBUTION.—*Reichelina lamarensis* Zone of *Lantschichites splendens* Zone of the Guadalupian Series, Glass and Del Norte mountains, Texas; Guadalupe Mountains, Texas (Skinner and Wilde, 1955).

REMARKS.—The specimens studied resemble the type specimens of *Reichelina lamarensis* Skinner and Wilde in all respects. Measurement data of specimens are given in Table 9-7.

TABLE 9-7.—Measurements of *Reichelina lamarensis* Skinner and Wilde.

	Volution	USNM 483016	USNM 483013	USNM 483014	USNM 483011	USNM 483010
Radius vector (mm)	0	0.020	0.023	0.025	0.030	0.021
	1	0.05	0.05	0.06	0.05	0.04
	2	0.09	0.08	0.09	0.10	0.07
	3	0.15	0.15	0.15	0.16	0.11
	4	0.23	0.24	0.28	0.23	0.20
	5	0.51	0.54	0.60	0.70	0.30
Half length (mm)	6	-	-	-	-	0.78
	1	0.03	0.03	0.03	0.03	0.03
	2	0.05	0.05	0.05	0.05	0.05
	3	0.08	0.08	0.08	0.09	0.08
	4	0.13	0.13	0.14	0.15	0.14
	5	0.19	0.21	0.22	0.21	0.20
Form ratio	6	-	-	-	-	0.26
	1	0.60	0.60	0.50	0.60	0.75
	2	0.56	0.63	0.56	0.50	0.71
	3	0.53	0.53	0.53	0.56	0.73
	4	0.56	0.54	0.50	0.65	0.70
	5	0.37	0.33	0.37	0.30	0.67
Wall thickness (mm)	6	-	-	-	-	0.33
	1	0.008	0.007	0.008	0.010	0.008
	2	0.010	0.010	0.010	0.010	0.010
	3	0.012	0.010	0.010	0.015	0.010
	4	0.015	0.015	0.010	0.015	0.015
	5	0.015	-	0.015	0.020	0.020
Tunnel angle (°)	6	-	-	-	-	0.020
	1	-	-	14	15	-
	2	16	15	16	16	16
	3	22	17	17	24	18
4	-	-	24	-	22	

***Reichelina* sp.**

PLATE 9-4: FIGURE 14

MATERIAL STUDIED.—Sample from the middle part of the Altuda Formation at Benge Ranch in the Glass Mountains, Texas: 6-BA3; specimen: USNM 483025.

AGE AND DISTRIBUTION.—*Reichelina lamarensis* Zone of the Guadalupian Series, Glass Mountains, Texas.

DESCRIPTION.—Minute size; slender and lenticular form; 3½ volutions, attaining a length of 0.27 mm and a diameter of 0.71 mm; form ratio of about 0.38; first volution subdiscoidal, with narrowly rounded periphery; outer volutions lenticular, with sharply angular periphery; proloculus small, about 0.08 mm in outside diameter; spirotheca very thin, consisting of tectum and diaphanotheca; thickest part of spirotheca about 0.015 mm; septa planar; chomata low, occurring only in the inner two volutions, and extending to polar areas; tunnel low and narrow; tunnel angle 10° and 20° in the first and second volutions, respectively. Measurement data of the specimen given in Table 9-8.

REMARKS.—This is a distinct species, but there is inadequate material to justify naming a new species. It is similar to

TABLE 9-8.—Measurements of *Reichelina* sp.

	Volution	USNM 483025
Radius vector (mm)	0	0.04
	1	0.08
	2	0.15
	3	0.25
Half length (mm)	4	0.43
	1	0.04
	2	0.07
	3	0.10
Form ratio	4	0.14
	1	0.67
	2	1.50
	3	1.43
Wall thickness (mm)	4	1.45
	5	1.40
	1	0.010
Tunnel angle (°)	2	0.010
	3	0.010
	4	0.015
	1	12
	2	16

Reichelina birdensis, new species, but it is more slender in shape, has a lower form ratio, and has sharper angular periphery in corresponding volutions. It differs from *Reichelina bengensis*, new species, in being larger but having fewer volutions. It can be easily distinguished from *Reichelina lamarensis* in that the latter has a much larger size, a longer axis of coiling, and a higher form ratio.

Family STAFFELLIDAE Miklukho-Maklay, 1949

***Staffella* Ozawa, 1925**

TYPE SPECIES.—*Fusulina sphaerica* Abich, 1859.

***Staffella lacunosa* Dunbar and Skinner, 1937**

PLATE 9-1: FIGURE 17

Staffella lacunosa Dunbar and Skinner, 1937:598-599, pl. 52: figs. 9-13.

TYPES.—*Hypotype*: USNM 483026; from the Word Formation of the Del Norte Mountains, Texas.

MATERIAL STUDIED.—Sample from the lower part of the Word Formation in the Del Norte Mountains, Texas: 8-32.

AGE AND DISTRIBUTION.—Leonardian (Dunbar and Skinner, 1937) and Guadalupian Series, Glass and Del Norte mountains, Texas. Found only in the *Parafusulina sellardsi* Zone of the Guadalupian Series in this study.

REMARKS.—The illustrated specimen is an immature individual, but it resembles the type specimens of *Staffella lacunosa* Dunbar and Skinner in all respects. Measurement data of the specimen are given in Table 9-9.

TABLE 9-9.—Measurements of *Staffella lacunosa* Dunbar and Skinner.

	Volution	USNM 483026
Radius vector (mm)	0	0.06
	1	0.06
	2	0.11
	3	0.20
	4	0.30
	5	0.43
Half length (mm)	6	0.64
	1	0.04
	2	0.08
	3	0.15
	4	0.24
	5	0.35
Form ratio	6	0.51
	1	0.67
	2	0.73
	3	0.75
	4	0.80
	5	0.81
Wall thickness (mm)	6	0.78
	1	0.02
	2	0.03
	3	0.03
	4	0.04
	5	0.04
Tunnel angle (°)	6	0.03
	1	12
	2	17
	3	19
	4	34
	5	51

Family FUSULINIDAE von Möller, 1878

Subfamily SCHUBERTELLINAE Skinner, 1931

Codonofusiella Dunbar and Skinner, 1937

TYPE SPECIES.—*Codonofusiella paradoxica* Dunbar and Skinner, 1937.

Codonofusiella extensa Skinner and Wilde, 1955

PLATE 9-3: FIGURE 10

Codonofusiella extensa Skinner and Wilde, 1955:930, pl. 89: fig. 10, pl. 90: figs. 1-5, pl. 91: figs. 1-6.

TYPES.—*Hypotypes*: USNM 483027; from the Altuda Formation of the Glass Mountains, Texas.

MATERIAL STUDIED.—Samples from the upper part of the Altuda Formation at Bengé Ranch in the Glass Mountains and near Bird Mountain in the Del Norte Mountains, Texas: 6-S2, 6-110, 6-120; 10-204.

AGE AND DISTRIBUTION.—*Reichelina lamarensis* Zone to *Lantschichites splendens* Zone of the Guadalupian Series,

Glass and Del Norte mountains, Texas; Guadalupe Mountains, Texas (Skinner and Wilde, 1955).

REMARKS.—The specimens studied resemble the type specimens of *Codonofusiella extensa* Skinner and Wilde in all respects.

Codonofusiella paradoxica Dunbar and Skinner, 1937

PLATE 9-3: FIGURES 7-9

Codonofusiella paradoxica Dunbar and Skinner, 1937:607-609, pl. 45: figs. 1-9.—Sheng, 1963:47, pl. 6: figs. 21-24.

TYPES.—*Hypotypes*: USNM 483029-483031; from the Altuda Formation of the Glass and Del Norte mountains, Texas.

MATERIAL STUDIED.—Samples from the Altuda Formation at Bengé Ranch in the Glass Mountains and near Bird Mountain in the Del Norte Mountains, Texas: 6-110; 10-202, 10-208.

AGE AND DISTRIBUTION.—*Polydiexodina shumardi* Zone to *Lantschichites splendens* Zone of the Guadalupian Series, Glass and Del Norte mountains, Texas; Guadalupe Mountains, Texas (Dunbar and Skinner, 1937; Skinner and Wilde, 1955); Chinati Mountains, Texas (Skinner, 1940). Wujiaping Limestone near Zisongzhen of Wangmo, Guizhou Province, China (Sheng, 1963).

REMARKS.—The specimens studied resemble the type specimens of *Codonofusiella paradoxica* Dunbar and Skinner in all respects.

Lantschichites Toumanskaya, 1953

TYPE SPECIES.—*Codonofusiella (Lantschichites) maslennikovi* Toumanskaya, 1953.

Lantschichites splendens (Skinner and Wilde, 1954)

PLATE 9-3: FIGURES 1-6, 11

Paraboultonia splendens Skinner and Wilde, 1954:441, pl. 44: figs. 1-7, pl. 45: figs. 1-4.

Lantschichites splendens (Skinner and Wilde)—Sheng, 1963:42, pl. 12: figs. 16-22.

TYPES.—*Hypotypes*: USNM 483028, 483032-483037; from the Altuda Formation of the Glass and Del Norte mountains, Texas.

MATERIAL STUDIED.—Samples from the upper part of the Altuda Formation at Bengé Ranch in the Glass Mountains and near Bird Mountain in the Del Norte Mountains, Texas: 6-BA12, 6-BA13, 6-BA14, 6-BA15, 6-BA16, 6-BA17, 6-BA18, 6-BA19, 6-BA20, 6-BA21, 6-BA22, 6-110, 6-120, 6-125, 6-135, 6-138, 6-140, 6-S1, 6-S2, 6-BR4, 6-145; 10-204.

AGE AND DISTRIBUTION.—*Lantschichites splendens* Zone of the Guadalupian Series, Glass and Del Norte mountains, Texas; Apache Mountains and Guadalupe Mountains, Texas (Skinner

and Wilde, 1954). Upper part of the Maokou Limestone in Yishan, Guangxi Province, China (Sheng, 1963).

REMARKS.—*Lantschichites splendens* is characterized by its small size and slender, cylindrical test with bluntly rounded poles. It is the largest species in this genus and has the most volutions at maturity; however, the expansion of its last one-half volution is commonly not as great as that of other species. The specimens studied resemble the type specimens of *Paraboultonia splendens* Skinner and Wilde in all respects. Measurement data of specimens are given in Table 9-10.

The genus *Lantschichites* was originally established as a subgenus of *Codonofusiella* by Toumanskaya (1953) and later was raised to full genus level (Sheng, 1963). It differs from *Codonofusiella* in having a larger test size, a cylindrical form, more numerous volutions, and more intensely fluted septa. However, the wall structure and coiling features of the inner and outer volutions are quite similar in the two genera. Regarding the relationship between *Lantschichites* and *Paraboultonia*, the authors agree with Sheng (1963) and Xiao et al. (1986) that *Paraboultonia* Skinner and Wilde is a junior synonym of *Lantschichites* Toumanskaya. This conclusion is based on the observation that characters of the type specimens of both *Lantschichites maslennikovi* Toumanskaya and *Paraboultonia splendens* Skinner and Wilde are essentially the

same, including rapid expansion or uncoiling of the last one-half volution. Because thin sections cut through different positions of the uncoiled part may show different dimension of expansion, it is difficult to define limits of scope between "expansion" and "uncoiling" for species of these nominal genera.

Lantschichites splendens is an important zonal species of the latest Guadalupian, and it commonly occurs in deeper water deposits. Discovery of it in the Glass Mountains area extends its range from the northwestern shelf of the Delaware basin, where it occurs in the Lamar Limestone Member of the Bell Canyon Formation (Skinner and Wilde, 1954), to the southern shelf of the basin.

Lantschichites sp.

PLATE 9-4: FIGURES 1-8

MATERIAL STUDIED.—Samples from the Altuda Formation at Benge Ranch in the Glass Mountains and near Bird Mountain in the Del Norte Mountains, Texas: 6-120, 6-145, 6-BA12, 6-BA14, 6-BA15, 6-BA18, 6-BA20, 6-BA22, 6-BR4, 6-S2, 10-204; specimens: USNM 483038-483045.

DIAGNOSIS.—Small size; ellipsoidal to shortly cylindrical form; 4½ to 5 volutions; inner two volutions discoidal and coiled askew to the outer volutions, with weak chomata present; last one-half volution expanding rapidly and greatly; cuculi well developed.

AGE AND DISTRIBUTION.—*Lantschichites splendens* Zone of the Guadalupian Series, Glass Mountains, Texas.

DESCRIPTION.—Test small; ellipsoidal to short cylindrical form; 4½ to 5 volutions in maturity; first two volutions endothyroidal and coiled askew or at right angle to outer volutions; third and fourth volutions thickly fusiform to fusiform in shape, with bluntly pointed poles; last one-half volution abruptly expanded or uncoiled, resulting in elliptical to rectangular shape on axial section; proloculus very small, 0.05 to 0.06 mm in outside diameter; spirotheca very thin, consisting of tectum and diaphanotheca; spirotheca thickness averaging 0.010, 0.010, 0.015, 0.022, and 0.021 mm in the first to fifth volutions, respectively; septa intensely and regularly fluted throughout length of test; cuculi well developed in outer volutions; chomata very weak and only present in the endothyroidal inner volutions; tunnel low, narrow, and indistinct; thin axial fillings sometimes present in the inner four volutions. Measurement data of specimens given in Table 9-11.

REMARKS.—This species differs from *Lantschichites splendens* (Skinner and Wilde) in having a smaller and shorter test, less numerous volutions, and a larger uncoiled portion of the test. An elliptical to rectangular shape is characteristic of this species on a properly cut axial section, thus readily distinguishing these two species from each other. It closely resembles *Lantschichites minima* (Chen, 1956), but the latter has a more slender coiled part of the test, more sharply pointed poles, and a larger uncoiled portion.

TABLE 9-10.—Measurements of *Lantschichites splendens* (Skinner and Wilde).

	Volution	USNM 483032	USNM 483035	USNM 483034	USNM 483033
Radius vector (mm)	0	0.026	0.025	0.022	0.030
	1	0.05	0.06	0.05	0.05
	2	0.07	0.09	0.08	0.08
	3	0.12	0.15	0.11	0.10
	4	0.20	0.27	0.18	0.19
	5	0.31	0.44	0.26	0.32
Half length (mm)	6	0.65	—	0.55	—
	1	0.03	0.06	0.05	0.04
	2	0.08	0.12	0.07	0.06
	3	0.25	0.31	0.24	0.34
	4	0.62	0.80	0.55	0.89
	5	1.31	1.71	1.16	1.40
Form ratio	6	1.95	—	1.84	—
	1	0.60	1.00	1.00	0.80
	2	1.14	1.33	0.88	0.75
	3	2.08	2.07	2.18	3.40
	4	3.10	2.96	3.05	4.68
	5	4.23	3.89	4.46	4.38
Wall thickness (mm)	6	3.00	—	3.35	—
	1	0.01	0.01	0.008	0.01
	2	0.01	0.15	0.008	0.01
	3	0.015	0.15	0.01	0.015
	4	0.02	0.20	0.015	0.025
	5	0.025	0.25	0.02	0.02
Tunnel angle (°)	6	0.025	—	0.02	—
	1	—	—	—	—
	2	18	15	17	—

TABLE 9-11.—Measurements of *Lantschichites* sp.

	Volution	USNM 483041	USNM 483040	USNM 483038	USNM 483039
Radius vector (mm)	0	0.030	0.025	0.024	0.025
	1	0.06	0.05	0.07	0.04
	2	0.08	0.08	0.10	0.07
	3	0.11	0.10	0.15	0.11
	4	0.20	0.19	0.24	0.19
Half length (mm)	5	0.34	0.32	0.58	0.31
	1	0.03	0.04	0.06	0.07
	2	0.05	0.06	0.16	0.24
	3	0.23	0.34	0.43	0.45
	4	0.63	0.89	1.05	0.82
Form ratio	5	1.06	1.40	1.48	1.60
	1	0.50	0.80	0.86	-
	2	0.63	0.75	1.60	3.43
	3	2.09	3.40	2.87	4.09
	4	3.15	4.68	4.38	4.31
Wall thickness (mm)	5	3.12	4.37	2.55	5.16
	1	0.01	0.01	0.01	0.01
	2	0.01	0.01	0.01	0.01
	3	0.015	0.015	0.015	0.016
	4	0.02	0.025	0.02	0.02
Tunnel angle (°)	5	0.025	0.02	0.02	0.024
	1	-	-	-	-
	2	20	-	-	-

This species is being formally named in a companion paper in this volume. (See Wilde and Rudine, this volume.)

Paradoxiella Skinner and Wilde, 1955

TYPE SPECIES.—*Paradoxiella pratti* Skinner and Wilde, 1955.

Paradoxiella pratti Skinner and Wilde, 1955

PLATE 9-3: FIGURES 12-15

Paradoxiella pratti Skinner and Wilde, 1955:935, pl. 91: figs. 7-9, pl. 92: figs. 1-10, pl. 93: fig. 1.

TYPES.—*Hypotypes*: USNM 483046-483049; from the Altuda Formation of the Del Norte Mountains, Texas.

MATERIAL STUDIED.—Sample from the upper part of the Altuda Formation near Bird Mountain in the Del Norte Mountains, Texas: 10-204.

AGE AND DISTRIBUTION.—*Reichelina lamarensis* Zone of the Guadalupian Series, Del Norte Mountains, Texas; Guadalupe Mountains, Texas (Skinner and Wilde, 1955).

REMARKS.—The specimens illustrated herein are fragmentary, showing either the inner coiled portion or the uncoiled flare of the test. The shape and distribution pattern of the septal folds are exactly the same as those of the type specimens of *Paradoxiella pratti* Skinner and Wilde.

Schubertella Staff and Wedekind, 1910

TYPE SPECIES.—*Schubertella transitoria* Staff and Wedekind, 1910.

Schubertella cf. *S. melonica* Dunbar and Skinner, 1937

PLATE 9-1: FIGURE 18

Schubertella melonica Dunbar and Skinner, 1937:611-613, pl. 57: figs. 10-14.

MATERIAL STUDIED.—Sample from the lower part of the Road Canyon Formation in the Glass Mountains, Texas: 2-68; specimen: USNM 483050.

AGE AND DISTRIBUTION.—Found only in the Leonardian Series portion of the *Parafusulina boesei* Zone, Glass Mountains, Texas, in this study.

REMARKS.—Although the proloculus and the first juvenile volution are not visible, the specimens studied resemble the type specimens of *Schubertella melonica* Dunbar and Skinner in major respects. *Schubertella melonica* is characterized by a shorter and thicker test and a lower form ratio than the similar species, *Schubertella kingi* Dunbar and Skinner, 1937.

Schubertella sp.

PLATE 9-1: FIGURE 19

MATERIAL STUDIED.—Sample from the lower part of the Road Canyon Formation in the Glass Mountains, Texas: 2-R2; specimen: USNM 483051.

AGE AND DISTRIBUTION.—Leonardian Series portion of the *Parafusulina boesei* Zone, Glass Mountains, Texas.

DESCRIPTION.—Minute size; fusiform test; vaulted in the median part and bluntly pointed at poles; 5 volutions, attaining a length of 0.68 mm and a diameter of 0.34 mm; first volution short and coiled at a large angle to outer volutions; form ratio 0.56, 1.60, 1.63, 1.67, and 2.00 in first to fifth volutions, respectively; proloculus small, 0.06 mm in outside diameter; spirotheca very thin, consisting of tectum and diaphanotheca, about 0.010 to 0.020 mm thick; septa planar; chomata small and low, extending laterally to the polar regions; tunnel distinct, narrow, and high; tunnel angle 24° in third volution. Measurement data of the specimen given in Table 9-12.

REMARKS.—This specimen differs from *Schubertella melonica* Dunbar and Skinner and *Schubertella pseudogiraudi* Sheng, 1963, in having a smaller, more tightly coiled test and more expanded chomata. *Schubertella compacta* Sheng, 1963, is also tightly coiled, but it has a smaller test, thinner spirotheca, and smaller chomata than the studied specimen.

Family FUSULINIDAE von Möller, 1878

Subfamily FUSULININAE von Möller, 1878

Yangchienia Lee, 1934

TYPE SPECIES.—*Yangchienia iniqua* Lee, 1934.

TABLE 9-12.—Measurements of *Schubertella* sp.

	Volution	USNM 483051
Radius vector (mm)	0	0.03
	1	0.045
	2	0.05
	3	0.08
	4	0.12
Half length (mm)	5	0.17
	1	0.025
	2	0.08
	3	0.13
	4	0.20
Form ratio	5	0.34
	1	0.56
	2	1.60
	3	1.63
	4	1.67
Wall thickness (mm)	5	2.00
	1	—
	2	—
Tunnel angle (°)	3	0.02
	1	—
	2	18
	3	24

***Yangchienia iniqua* Lee, 1934**

PLATE 9-6: FIGURES 7, 8

Yangchienia iniqua Lee, 1934:14, pl. 1: figs. 1, 1a.—Sheng, 1963:38, pl. 4: figs. 30–35.—Xiao et al., 1986:79, pl. 2: figs. 3, 4.—Zhang et al., 1988:276, pl. 5: fig. 9.

TYPES.—*Hypotypes*: USNM 483052, 483053; from the Road Canyon Formation of the Glass Mountains, Texas.

MATERIAL STUDIED.—Samples from the lower part of the Road Canyon Formation in the Glass Mountains, Texas: 2-68, 2-R6.

AGE AND DISTRIBUTION.—Leonardian Series portion of the *Parafusulina boesei* Zone, Glass Mountains, Texas. Upper portion of the Qixian Stage at the top of the Qixia Formation, Ningzhen Mountains, southern Jiangsu Province, China (Lee, 1934), the lower part of the Maokou Formation in Guangxi Province (Sheng, 1963) and Guizhou Province, China (Yang, 1985), and the Qixia Formation in the Qixia Mountains, Nanjing, Jiangsu Province, China (Zhang et al., 1988).

REMARKS.—*Yangchienia iniqua* is characterized by its very small size, fusiform test, few volutions, planar septa, axis of coiling of inner volutions perpendicular to that of the outer volutions, and massive chomata extending to the polar extremities. The specimens studied are juveniles, but they resemble the type specimens of *Yangchienia iniqua* in all respects. This species differs from *Yangchienia compressa* (Ozawa, 1927) in having a shorter but more inflated test and a lower form ratio. Compared with *Yangchienia minuta* Xiao et al. (1986), it has a slightly larger and more inflated test, more

TABLE 9-13.—Measurements of *Yangchienia iniqua* Lee.

	Volution	USNM 483053
Radius vector (mm)	0	0.05
	1	0.06
	2	0.08
	3	0.14
	4	0.20
Half length (mm)	5	0.28
	1	0.04
	2	0.12
	3	0.20
	4	0.29
Form ratio	5	0.39
	1	0.67
	2	1.50
	3	1.43
	4	1.45
Wall thickness (mm)	5	1.40
	1	—
	2	—
Tunnel angle (°)	3	—
	1	—
	2	0.03
	3	21
	4	23
	4	25

volutions in maturity, and more extended chomata. Some species of *Neofusulinella* Deprat look similar to species of *Yangchienia* in size, form, and presence of massive chomata; however, *Neofusulinella* does not change coiling direction during ontogeny, and it has polar extremities with slightly fluted septa but with no chomata deposits. Measurement data of one specimen are given in Table 9-13.

Yangchienia is a common and important genus of Permian fusulinid fauna in the Tethyan realm. This is the first time it has been reported in North America.

Family FUSULINIDAE von Möller, 1878**Subfamily SCHWAGERININAE Dunbar and Henbest, 1930*****Parafusulina* Dunbar and Skinner, 1931**

TYPE SPECIES.—*Parafusulina wordensis* Dunbar and Skinner, 1931.

***Parafusulina alpinensis*, new species**

PLATE 9-10: FIGURES 6, 7

TYPES.—*Holotype*: USNM 483054; *Paratype*: USNM 483055; from the Road Canyon Formation of the Del Norte Mountains, Texas.

MATERIAL STUDIED.—Samples from the upper part of the Road Canyon Formation in the Del Norte Mountains, Texas: 7-53; 8-24.

DIAGNOSIS.—Ellipsoidal outline; low, narrow, and crowded septal folds; very thin spirotheca; distinctive secondary deposits distributed throughout length along axis, narrow near proloculus but gradually wider and heavier toward poles.

AGE AND DISTRIBUTION.—*Parafusulina trumpyi* Zone of the Guadalupian Series, Del Norte Mountains, Texas.

DESCRIPTION.—Large size; ellipsoidal form; $6\frac{1}{2}$ to $7\frac{1}{2}$ volutions; attaining a length of about 10 mm and a diameter of about 3 mm; chamber height and length increase gradually, resulting in average form ratio changing from 2.25 in first volution to 3.85 in sixth volution; proloculus ranging between 0.28 to 0.36 mm in outside diameter, subspherical or slightly depressed on one side; spirotheca very thin, consisting of

tectum and keriotheca, thickness averaging 0.020, 0.020, 0.030, 0.035, 0.040, 0.050, and 0.050 mm from first to seventh volutions, respectively; septa intensely and regularly fluted; septal folds low, narrow, and crowded; cuniculi well developed; chomata lacking; secondary deposits occur along axis throughout length of test, narrow near proloculus but gradually wider and heavier toward poles; tunnel narrow and not well marked; tunnel angle averaging 30° and 45° in first and fifth volutions, respectively. Measurement data of specimens given in Table 9-14.

REMARKS.—This species differs from other species of the genus *Parafusulina* in having an ellipsoidal test, extraordinarily thin spirotheca, and a unique pattern of secondary deposits that extend along the entire axis and become gradually wider and heavier toward the poles.

ETYMOLOGY.—The species is named for the town of Alpine, Texas, located west of the Glass and Del Norte mountains.

TABLE 9-14.—Measurements of *Parafusulina alpinensis*, new species.

	Volution	USNM 483054	USNM 483055
Radius vector (mm)	0	0.18	0.14
	1	0.24	0.24
	2	0.32	0.36
	3	0.46	0.48
	4	0.60	0.67
	5	0.80	0.86
	6	1.04	1.08
	7	1.30	1.32
Half length (mm)	8	1.52	-
	1	0.58	0.50
	2	1.06	0.92
	3	1.58	1.40
	4	2.32	2.08
	5	3.08	2.84
	6	3.92	3.68
Form ratio	7	5.00	-
	1	2.42	2.08
	2	3.31	2.56
	3	3.43	2.92
	4	3.86	3.10
	5	3.85	3.30
	6	3.77	3.41
Wall thickness (mm)	7	3.85	-
	1	0.02	0.02
	2	0.02	0.02
	3	0.03	0.03
	4	0.04	0.03
	5	0.04	0.04
	6	0.04	0.06
	7	0.05	-
Tunnel angle (°)	8	0.04	-
	1	30	-
	2	36	-
	3	-	35
	4	-	38
	5	43	48

Parafusulina antimonioensis Dunbar, 1953

PLATE 9-15: FIGURES 1-4

Parafusulina antimonioensis Dunbar, 1953:15, pl. 2: figs. 1-8, pl. 3: figs. 1-3.—Ross, 1963b:28, pl. 5: figs. 2, 3.

TYPES.—*Hypotypes*: USNM 483056-483059; from the Word Formation of the Del Norte Mountains, Texas.

MATERIAL STUDIED.—Samples from the upper part of the Word Formation in the Del Norte Mountains, Texas: 9-7, 9-8.

AGE AND DISTRIBUTION.—*Parafusulina antimonioensis* Zone of the Guadalupian Series, Glass and Del Norte mountains, Texas; Sonora, Mexico.

REMARKS.—The specimens studied resemble the type specimens of *Parafusulina antimonioensis* in these major features: a very large and elongate, subcylindrical test, large proloculus, highly developed cuniculi, and secondary deposits heavily filling the septal folds in the polar extremities along the axis. Because this species has an exceptionally long, slender, and irregular test, it is very difficult to obtain thin sections cut through the entire length of the test. Even a slightly oblique axial section distorts the apparent length of the test, such that the specimens obtained look shorter than the type specimens. Measurement data of specimens are given in Table 9-15.

Parafusulina cf. *P. bakeri* Dunbar and Skinner, 1937

PLATE 9-6: FIGURE 6

Parafusulina bakeri Dunbar and Skinner, 1937:677-679, pl. 71: figs. 1-10.

MATERIAL STUDIED.—Sample from the lower part of the Road Canyon Formation in the Glass Mountains, Texas: 2-68; specimen: USNM 483060.

AGE AND DISTRIBUTION.—Leonardian Series, Glass Mountains, Texas. Found only in the Leonardian portion of the *Parafusulina boesei* Zone.

TABLE 9-15.—Measurements of *Parafusulina antimonioensis* Dunbar.

	Volution	USNM 483058	USNM 483057	USNM 483059	USNM 483056
Radius vector (mm)	0	0.24	0.28	0.30	0.38
	1	0.30	0.32	0.36	0.44
	2	0.44	0.40	0.52	0.56
	3	0.52	0.56	0.66	0.70
	4	0.64	0.72	0.78	0.88
	5	0.76	0.84	0.93	1.04
	6	0.96	1.04	1.12	1.22
	7	1.16	1.28	1.35	1.52
Half length (mm)	8	1.36	1.52	-	-
	1	0.48	0.68	0.48	0.78
	2	1.52	1.20	1.34	1.44
	3	2.28	2.04	2.00	2.24
	4	3.60	3.40	3.16	3.48
	5	4.84	4.28	4.20	4.72
	6	6.68	5.44	5.24	6.08
	7	8.32	7.00	7.00	8.40
Form ratio	8	10.00	8.20	-	-
	1	1.60	2.13	1.33	1.77
	2	3.45	3.00	2.58	2.57
	3	4.38	3.64	3.03	3.20
	4	5.63	4.72	4.05	3.59
	5	6.37	5.10	4.52	4.54
	6	6.96	5.23	4.68	4.98
	7	7.17	5.78	5.20	5.53
Wall thickness (mm)	8	7.35	5.39	-	-
	1	0.03	0.03	0.03	0.03
	2	0.03	0.04	0.03	0.03
	3	0.03	0.04	0.04	0.04
	4	0.04	0.04	0.04	0.05
	5	0.04	0.05	0.05	0.05
	6	0.05	0.05	0.06	0.06
	7	0.06	0.06	-	0.06
Tunnel angle (°)	8	0.06	0.07	-	-
	1	-	-	-	24
	2	30	25	-	28
	3	-	33	28	28
	4	32	36	-	46
	5	-	40	-	35
6	-	36	-	-	

***Parafusulina cf. P. biturbinata* Kling, 1960**

PLATE 9-5: FIGURES 3-5

Parafusulina biturbinata Kling, 1960:653, pl. 81: figs. 4, 5, 7-9.

MATERIAL STUDIED.—Sample from the upper part of the Cathedral Mountain Formation in the Glass Mountains, Texas: 1-60; specimens: USNM 483061-483063.

AGE AND DISTRIBUTION.—*Parafusulina durhami* Zone of the Leonardian Series, Glass Mountains, Texas; Guatemala (Kling, 1960).

REMARKS.—*Parafusulina biturbinata* is characterized by having a small, fusiform test with convex slopes and sharply pointed poles, large proloculus, and narrow axial fillings. The

specimens studied resemble the type specimens of *P. biturbinata* in major respects, but they differ slightly from them in having less pointed poles and lighter secondary deposits.

***Parafusulina boesei* Dunbar and Skinner, 1937**

PLATE 9-13: FIGURES 1-5

Parafusulina boesei Dunbar and Skinner, 1937:679, pl. 73: figs. 1-9.—Ross, 1963b:26, pl. 3: figs. 1-10.—Sheng, 1963:72, pl. 20: figs. 6, 7, pl. 21: fig. 1. *Parafusulina boesei* var. *attenuata* Dunbar and Skinner, 1937:680, pl. 74: figs. 5-13.

TYPES.—*Hypotypes*: USNM 483064-483068; from the Road Canyon Formation of the Glass and Del Norte mountains, Texas.

MATERIAL STUDIED.—Samples from the Road Canyon Formation in the Glass and Del Norte mountains, Texas: 2-68, 2-70, 2-73, 2-R1; 7-56, 7-58; 8-13, 8-20, 8-24, 8-29.

AGE AND DISTRIBUTION.—*Parafusulina boesei* Zone to *Parafusulina trumpyi* Zone of the Leonardian and Guadalupian series, Glass and Del Norte mountains, Texas; Guadalupe Mountains, Texas (Wilde, 1986a); Chinati Mountains, Texas (Skinner, 1940). Lower part of the Maokou Formation, China (Sheng, 1963; Yang 1985).

REMARKS.—*Parafusulina boesei* is a species of moderate size and is characterized by a variable fusiform shape, lower and less closely crowded septal folds, and light secondary deposits. Ross (1963b) considered this species to have wider morphological limits than those suggested by Dunbar and Skinner (1937), who erected the variety name *attenuata* for more elongate forms. Ross held that *P. boesei* is most comparable to late Leonardian species, such as *Parafusulina durhami* and *P. leonardensis* Ross, 1962. The present study agrees with Ross and adopts the same practice in dealing with the scope of this species. Measurement data of specimens are given in Table 9-16.

This species was collected only from the Road Canyon Formation during this study (in three sections), but it has been reported from a stratigraphic interval ranging from the Road Canyon Formation through the Willis Ranch Member of the Word Formation in the Glass Mountains (Dunbar and Skinner, 1937; Ross 1963b; Wilde in Cooper and Grant, 1977).

***Parafusulina durhami* Thompson and Miller, 1949**

PLATE 9-5: FIGURES 1, 2

Parafusulina durhami Thompson and Miller, 1949:15, pl. 3: figs. 3-7, pl. 5: figs. 9, 11, 12.—Ross, 1962:15, pl. 6: figs. 1-7.

TYPES.—*Hypotypes*: USNM 483069, 483070; from the Cathedral Mountain Formation of the Glass Mountains, Texas.

MATERIAL STUDIED.—Samples from the upper part of the Cathedral Mountain Formation in the Glass Mountains, Texas: 1-60; 2-67.

TABLE 9-16.—Measurements of *Parafusulina boesei* Dunbar and Skinner.

	Volution	USNM 483064	USNM 483065	USNM 483067	USNM 483066	USNM 483068
Radius vector (mm)	0	0.20	0.19	0.24	0.20	0.20
	1	0.27	0.26	0.36	0.28	0.28
	2	0.39	0.38	0.52	0.44	0.40
	3	0.54	0.50	0.72	0.64	0.64
	4	0.78	0.69	0.96	0.88	0.76
	5	1.05	0.94	1.24	1.12	1.06
	6	1.31	1.20	1.56	1.36	1.34
Half length (mm)	7	1.74	1.48	-	-	-
	1	0.84	0.77	0.72	0.64	0.68
	2	1.27	1.23	1.20	1.12	1.08
	3	2.16	1.85	1.96	1.72	1.72
	4	3.23	2.70	2.95	2.56	2.36
	5	4.24	3.62	4.36	3.40	3.20
	6	5.47	4.73	5.44	4.42	4.44
Form ratio	7	6.01	5.90	-	-	-
	1	3.11	2.96	2.00	2.29	2.43
	2	3.26	3.24	2.31	2.55	2.70
	3	4.00	3.70	2.72	2.69	2.89
	4	4.14	3.91	3.08	2.91	3.11
	5	4.04	3.85	3.52	3.04	3.02
	6	4.18	3.94	3.49	3.25	3.31
Wall thickness (mm)	7	3.45	3.98	-	-	-
	1	0.03	0.03	0.03	0.03	0.03
	2	0.04	0.04	0.04	0.03	0.03
	3	0.04	0.05	0.04	0.04	0.04
	4	0.06	0.06	0.06	0.05	0.06
	5	0.07	0.08	0.07	0.05	0.07
	6	0.08	0.09	0.07	0.07	0.08
Tunnel angle (°)	7	0.10	-	-	-	-
	1	-	-	30	29	-
	2	-	-	31	30	-
	3	-	-	37	44	41
	4	-	-	46	48	46
5	-	-	42	-	-	

TABLE 9-17.—Measurements of *Parafusulina durhami* Thompson and Miller.

	Volution	USNM 483070	USNM 483069
Radius vector (mm)	0	0.15	0.16
	1	0.20	0.32
	2	0.28	0.44
	3	0.40	0.60
	4	0.56	0.78
	5	0.76	1.00
	6	1.04	1.28
Half length (mm)	7	1.32	-
	1	0.44	0.64
	2	0.86	1.12
	3	1.30	1.68
	4	2.08	2.48
	5	3.24	3.64
	6	4.82	4.80
Form ratio	7	4.16	-
	1	2.20	2.00
	2	3.07	2.55
	3	3.25	2.80
	4	3.71	3.18
	5	4.26	3.64
	6	4.63	3.75
Wall thickness (mm)	7	4.67	-
	1	0.03	0.03
	2	0.03	0.03
	3	0.04	0.04
	4	0.05	0.04
	5	0.07	0.06
Tunnel angle (°)	6	0.07	0.08
	1	33	25
	2	42	36
	3	48	-
	4	54	-
	5	50	45
6	47	-	

AGE AND DISTRIBUTION.—*Parafusulina durhami* Zone of the Leonardian Series, Glass Mountains, Texas; Colombia (Thompson and Miller, 1949).

REMARKS.—Measurement data of specimens are given in Table 9-17.

Parafusulina faliskiei, new species

PLATE 9-11: FIGURES 5-7

TYPES.—*Holotype*: USNM 483072; *Paratypes*: USNM 483071, 483073; from the Road Canyon Formation of the Glass Mountains, Texas.

MATERIAL STUDIED.—Samples from the lower and middle parts of the Road Canyon Formation in the Glass Mountains, Texas: 1-63; 2-68, 2-73, 2-R14.

DIAGNOSIS.—Test large; elongated ellipsoidal, with bluntly rounded poles; septal fluting very strong and regular; septal

folds commonly low, with rounded crests; tunnel path irregular; tunnel angle rather high.

AGE AND DISTRIBUTION.—*Parafusulina rothi* Zone to *Parafusulina trumpyi* Zone of the Guadalupian Series, Glass Mountains, Texas.

DESCRIPTION.—Large size; elongate ellipsoidal to shortly subcylindrical form; 7½ volutions in maturity; commonly attaining a length of 10.0 to 13.0 mm and a diameter of 3.3 to 3.7 mm; lateral slopes of volutions nearly parallel and ending in bluntly rounded poles; form ratio increasing gradually from first to sixth volutions, but decreasing in last 1½ volutions, giving a final form ratio about 3.0; proloculus of medium size, averaging 0.28 to 0.34 mm in outside diameter; spirotheca consisting of tectum and keriotheca; spirotheca thickness averaging 0.023, 0.030, 0.040, 0.056, 0.070, 0.080, and 0.083 mm in first to seventh volutions, respectively; septa intensely and regularly fluted; cuniculi well developed; septal folds commonly low, in small, slim arches with rounded crests;

chomata completely lacking; secondary deposits very light; tunnel path irregularly present; tunnel angle averaging 35° and 56° in first and fourth volutions, respectively. Measurement data of specimens given in Table 9-18.

REMARKS.—This species is characterized by its elongate ellipsoidal shape, bluntly rounded poles, and low, slim septal folds with rounded crests. It may be distinguished from *Parafusulina wildei* Ross, 1963, in having a less slender shape, more bluntly rounded poles, and lower form ratio, as well as lower and less crowded septal folds and less developed secondary deposits. The present species is somewhat similar in shape to *Parafusulina elliptica* Sheng, 1963, but differs in having a larger and much longer test, different fluting style, and much more developed secondary deposits.

ETYMOLOGY.—This species is named for Ray Faliskie, a

graduate student at Sul Ross State University, who helped with the field work of this study.

***Parafusulina fountaini* Dunbar and Skinner, 1937**

PLATE 9-10: FIGURES 1, 2

Parafusulina fountaini Dunbar and Skinner, 1937:675-677, pl. 70: figs. 1-10.

TYPES.—*Hypotypes*: USNM 483074, 483075; from the Road Canyon Formation of the Glass Mountains, Texas.

MATERIAL STUDIED.—Samples from the lower part of the Road Canyon Formation in the Glass Mountains, Texas: 2-70, 2-R3.

AGE AND DISTRIBUTION.—Leonardian Series portion of the *Parafusulina boesei* Zone, Glass Mountains, Texas; Guadalupe Mountains, Texas (Dunbar and Skinner, 1937).

REMARKS.—The specimens studied resemble the type specimens of *Parafusulina fountaini* Dunbar and Skinner in all respects. Measurement data of specimens are given in Table 9-19.

TABLE 9-18.—Measurements of *Parafusulina faliskiei*, new species.

	Volution	USNM 483071	USNM 483072	USNM 483073
Radius vector (mm)	0	0.16	0.23	0.17
	1	0.24	0.28	0.26
	2	0.36	0.38	0.38
	3	0.48	0.57	0.50
	4	0.64	0.79	0.68
	5	0.84	1.04	0.90
	6	1.08	1.42	1.16
	7	1.36	1.72	1.52
8	1.64	-	1.88	
Half length (mm)	1	0.50	0.78	0.65
	2	0.80	1.32	1.04
	3	1.38	2.00	1.68
	4	2.12	2.76	2.42
	5	2.88	3.60	3.46
	6	3.64	4.85	5.00
	7	4.36	6.20	5.84
	8	4.92	-	-
Form ratio	1	2.08	1.73	2.50
	2	2.22	3.47	2.74
	3	2.88	3.51	3.36
	4	3.31	3.49	3.56
	5	3.43	3.46	3.85
	6	3.37	3.42	4.31
	7	3.21	3.60	3.61
	8	3.00	-	-
Wall thickness (mm)	1	0.02	0.03	0.03
	2	0.02	0.04	0.04
	3	0.03	0.05	0.05
	4	0.04	0.06	0.07
	5	0.04	0.06	0.08
	6	0.06	0.06	0.09
	7	0.08	0.05	0.07
	8	0.06	-	-
Tunnel angle (°)	1	31	-	38
	2	38	45	46
	3	43	44	60
	4	56	40	62
	5	46	47	-

TABLE 9-19.—Measurements of *Parafusulina fountaini* Dunbar and Skinner.

	Volution	USNM 483074	USNM 483075
Radius vector (mm)	0	0.20	0.23
	1	0.25	0.30
	2	0.38	0.42
	3	0.55	0.56
	4	0.76	0.78
	5	1.04	1.02
	6	1.40	1.32
7	1.82	1.64	
Half length (mm)	1	0.88	0.68
	2	1.42	1.20
	3	2.00	1.76
	4	2.68	2.36
	5	3.92	4.00
	6	5.48	5.20
	7	8.00	6.96
Form ratio	1	3.52	2.27
	2	3.74	2.86
	3	3.64	3.14
	4	3.50	3.03
	5	3.77	3.92
	6	3.91	3.94
	7	4.40	4.24
Wall thickness (mm)	1	0.03	0.03
	2	0.04	0.04
	3	0.05	0.04
	4	0.06	0.06
	5	0.10	0.08
	6	0.10	0.09
	7	0.09	0.07
Tunnel angle (°)	1	29	26
	2	35	41
	3	44	32
	4	46	48
	5	43	56
	6	22	-

Parafusulina glassensis, new species

PLATE 9-8: FIGURES 1-3

Parafusulina rothi Dunbar and Skinner, 1937:684, pl. 76: fig. 10 [in part, not figs. 1-9].

TYPES.—*Holotype*: USNM 483076; *Paratypes*: USNM 483077, 483078; from the Road Canyon Formation of the Glass Mountains, Texas.

MATERIAL STUDIED.—Samples from the middle and upper part of the Road Canyon Formation and Willis Ranch Member of the Word Formation in the Glass and Del Norte mountains, Texas: 1-62; 2-72, 2-R8, 2-R10; 8-39.

DIAGNOSIS.—Very large size; almost cylindrical form, with bluntly rounded poles; septa numerous and strongly fluted; septal folds high, narrow, closely spaced, and very regular; tunnel low and not well defined; secondary deposits light.

AGE AND DISTRIBUTION.—*Parafusulina rothi* Zone to *Parafusulina sellardsi* Zone of the Guadalupian Series, Glass and Del Norte mountains, Texas; Guadalupe Mountains, Texas (Dunbar and Skinner, 1937).

DESCRIPTION.—Very large size; subcylindrical to almost cylindrical form; 8 to 9 volutions, attaining a length of 18 to 21 mm and a diameter of 3.5 to 4.2 mm; axis of coiling irregular, but slightly curved; slopes of volutions nearly parallel, tapering slightly near the bluntly rounded ends; chamber height increasing very slowly as length increases rapidly, resulting in a nearly cylindrical test; form ratio averaging from 2.4 in first volution to 4.20 and 5.00 in fifth and eighth volutions, respectively; proloculus ranging between 0.36 to 0.44 mm in outside diameter, and spherical or subspherical in shape; spirotheca consisting of tectum and keriotheca; spirotheca thickness averaging 0.030, 0.035, 0.045, 0.060, 0.075, 0.090, 0.093, 0.100, and 0.080 mm from first to ninth volutions, respectively; septa numerous and intensely fluted; septal folds narrow, regular, and closely spaced; cuculi very well developed; chomata completely lacking; secondary deposits scarcely or very slightly developed, filling septal loops in the inner volutions; tunnel low and not well defined; tunnel angle may reach 55° to 60° in outer volutions. Measurement data of specimens given in Table 9-20.

REMARKS.—This species differs from *Parafusulina wordensis* Dunbar and Skinner in having a smaller test and less developed cuculi. It differs from *Parafusulina trumpyi* Thompson and Miller in having an almost cylindrical test, more numerous and regular septal folds, and a low and not well-defined tunnel. *Parafusulina antimonioensis* Dunbar and *Parafusulina deliciosensis* Dunbar and Skinner, 1936, somewhat resemble the present species, but they differ in having a much larger proloculus and denser secondary deposits. The present species also differs from *Parafusulina rohri*, new species, in having a slender test and lighter secondary deposits.

TABLE 9-20.—Measurements of *Parafusulina glassensis*, new species.

	Volution	USNM 483078	USNM 483076	USNM 483077
Radius vector (mm)	0	0.18	0.18	0.22
	1	0.21	0.24	0.28
	2	0.31	0.32	0.40
	3	0.43	0.48	0.56
	4	0.58	0.64	0.72
	5	0.78	0.85	0.94
	6	1.04	1.12	1.24
	7	1.27	1.46	1.52
	8	1.51	1.84	—
Half length (mm)	9	1.75	—	—
	1	0.58	0.60	0.64
	2	1.01	1.10	1.00
	3	1.54	1.92	1.68
	4	2.28	2.40	2.72
	5	3.39	4.00	3.80
	6	4.66	5.12	5.84
	7	6.52	6.72	7.12
	8	8.22	8.12	—
Form ratio	9	8.90	—	—
	1	2.76	2.50	2.29
	2	3.26	3.44	2.50
	3	3.58	4.00	3.00
	4	3.93	4.38	3.78
	5	4.35	4.70	4.04
	6	4.48	4.57	4.71
	7	5.13	4.60	4.68
	8	5.44	4.41	—
Wall thickness (mm)	9	5.29	—	—
	1	0.03	0.03	0.04
	2	0.03	0.03	0.04
	3	0.04	0.05	0.05
	4	0.05	0.07	0.06
	5	0.08	0.07	0.07
	6	0.10	0.08	0.08
	7	0.10	0.10	0.06
	8	0.10	0.10	—
Tunnel angle (°)	9	0.08	—	—
	1	31	28	28
	2	26	34	44
	3	28	46	54
	4	32	40	60
5	34	45	—	

Furthermore, the large, almost cylindrical test, more numerous, narrower, and more regular septal folds, and denser secondary deposits may distinguish this species from *Parafusulina rothi* Dunbar and Skinner. The exceptionally large individual referred with some uncertainty to *Parafusulina rothi* by Dunbar and Skinner (1937), and illustrated by them (pl. 76: fig. 10), resembles *P. glassensis* in all respects, and thus is considered to be conspecific.

ETYMOLOGY.—This species is named for the Glass Mountains, located in West Texas.

***Parafusulina cf. P. guatemalaensis* Dunbar, 1939**

PLATE 9-5: FIGURES 6, 7

Parafusulina guatemalaensis Dunbar, 1939:347, pl. 36: figs. 1-10.

MATERIAL STUDIED.—Samples from the lower part of the Road Canyon Formation in the Glass Mountains, Texas: 2-R5, 2-R6; specimens: USNM 483079, 483080.

AGE AND DISTRIBUTION.—Leonardian Series portion of the *Parafusulina boesei* Zone, Glass Mountains, Texas; Guatemala (Dunbar, 1939).

REMARKS.—The specimens studied resemble the type specimens of *Parafusulina guatemalaensis* Dunbar in most respects, but they differ in having a smaller test and slightly lower form ratio, probably because the thin sections obtained are slightly oblique.

***Parafusulina ironensis* Ross, 1963**

PLATE 9-7: FIGURES 5-7

Parafusulina ironensis Ross, 1963b:25, pl. 4: figs. 13-15.

TYPES.—*Hypotypes*: USNM 483081-483083; from the Road Canyon Formation of the Glass and Del Norte mountains, Texas.

MATERIAL STUDIED.—Samples from the middle part of the Road Canyon Formation in the Glass and Del Norte mountains, Texas: 1-62, 1-63; 7-55.

AGE AND DISTRIBUTION.—*Parafusulina rothi* Zone to *Parafusulina trumpyi* Zone of the Guadalupian Series, Glass Mountains, Texas.

REMARKS.—The specimens studied resemble the type specimens of *Parafusulina ironensis* Ross in all respects. Measurement data of specimens are given in Table 9-21.

***Parafusulina lineata* Dunbar and Skinner, 1937**

PLATE 9-12: FIGURES 2-5

Parafusulina lineata Dunbar and Skinner, 1937:681-682, pl. 74: figs. 1-4.—Ross, 1963b:29, pl. 3: figs. 12, 13.

TYPES.—*Hypotypes*: USNM 483084-483087; from the Road Canyon Formation and the Word Formation of the Glass and Del Norte mountains, Texas.

MATERIAL STUDIED.—Samples from the Road Canyon Formation and lower part of the Word Formation in the Glass and Del Norte mountains, Texas: 2-R12, 2-R16; 8-38.

AGE AND DISTRIBUTION.—*Parafusulina rothi* Zone to *Parafusulina sellardsi* Zone of the Guadalupian Series, Glass and Del Norte mountains, Texas; Guadalupe Mountains, Texas (Dunbar and Skinner, 1937; Wilde, 1990).

REMARKS.—*Parafusulina lineata* is characterized by its small size, extremely slender, subcylindrical form, compact

TABLE 9-21.—Measurements of *Parafusulina ironensis* Ross.

	Volution	USNM 483082	USNM 483083
Radius vector (mm)	0	0.09	0.12
	1	0.15	0.18
	2	0.22	0.25
	3	0.32	0.34
	4	0.45	0.48
	5	0.60	0.67
	6	0.84	0.90
	7	1.12	1.21
Half length (mm)	8	1.40	1.52
	1	0.33	0.36
	2	0.66	0.68
	3	1.08	1.04
	4	1.52	1.56
	5	2.76	2.64
	6	4.08	3.60
	7	5.56	4.92
Form ratio	8	6.16	5.90
	1	2.20	2.00
	2	3.00	2.72
	3	3.38	3.05
	4	3.38	3.25
	5	4.60	3.94
	6	4.85	4.00
	7	4.96	4.07
Wall thickness (mm)	8	4.46	3.88
	1	0.020	0.020
	2	0.030	0.020
	3	0.030	0.030
	4	0.040	0.040
	5	0.040	0.060
	6	0.060	0.070
	7	0.070	0.080
Tunnel angle (°)	8	0.080	0.080
	1	28	25
	2	29	28
	3	30	26
	4	35	42
	5	48	49
6	44	-	

coiling, and poorly developed axial filling. The specimens studied resemble the type specimens of *Parafusulina lineata* in nearly all respects. It resembles *Monodiexodina linearis* (Dunbar and Skinner, 1937), in test size, wall thickness, and external form, but *M. linearis* differs greatly in having low, irregular, and loose septal folds, a poorly defined tunnel, and very heavily developed axial filling. Measurement data of specimens are given in Table 9-22.

Parafusulina lineata is an uncommon species in the Delaware basin and has a relatively long stratigraphic range. Ross (1963b) and Wilde (1990) both recognized a zone defined on *P. lineata*, which Ross placed in the lower part of the

TABLE 9-22.—Measurements of *Parafusulina lineata* Dunbar and Skinner.

	Volution	USNM 483085	USNM 483087	USNM 483086
Radius vector (mm)	0	0.15	0.14	0.14
	1	0.18	0.18	0.22
	2	0.24	0.28	0.32
	3	0.32	0.44	0.44
	4	0.44	0.60	0.62
	5	0.56	0.84	0.82
	6	0.76	1.04	1.04
Half length (mm)	7	1.01	—	—
	1	0.36	0.54	0.44
	2	0.70	1.20	1.10
	3	1.24	1.96	1.68
	4	1.84	3.04	2.48
	5	2.80	4.52	3.96
	6	3.60	6.24	5.20
Form ratio	7	4.20	—	—
	1	2.00	3.00	2.00
	2	2.92	4.28	3.44
	3	3.88	4.45	3.82
	4	4.18	5.06	4.00
	5	5.00	5.38	4.83
	6	4.74	6.00	5.00
Wall thickness (mm)	7	4.16	—	—
	1	0.02	0.03	0.03
	2	0.02	0.04	0.03
	3	0.02	0.04	0.04
	4	0.03	0.05	0.06
	5	0.03	0.07	0.06
	6	0.05	0.08	0.05
Tunnel angle (°)	7	0.07	—	—
	1	24	38	20
	2	—	36	47
	3	—	56	41
	4	—	57	45
5	40	—	—	

Guadalupian, whereas Wilde placed it in the middle part of the Guadalupian. Material collected for this study shows that *P. lineata* has a longer range than either worker indicated, accounting for the confusion about its zonal status. The species also has been reported from the China Tank Member of the Word Formation in the Glass Mountains (Wilde in Cooper and Grant, 1977) and the Grayburg Formation in the northern Guadalupe Mountains (Wilde, 1986a). Wilde (1990) pointed out that there were some unfortunate errors in locality numbering in Dunbar and Skinner (1937), contending that the type specimens of *P. lineata* came from locality 171, in the Cherry Canyon Formation in Trew Canyon, southern Delaware Mountains, not from locality 157 as published.

***Parafusulina maleyi* Dunbar and Skinner, 1937**

PLATE 9-13: FIGURES 7, 8

Parafusulina maleyi Dunbar and Skinner, 1937:686–687, pl. 77: figs. 1–12.

TYPES.—*Hypotypes*: USNM 483088, 483089; from the Word Formation of the Glass and Del Norte mountains, Texas.

MATERIAL STUDIED.—Samples from the Road Canyon Formation and the lower part of the Word Formation in the Glass and Del Norte mountains, Texas: 1-64; 2-R12; 3-24; 7-53; 8-14, 8-18, 8-24, 8-27, 8-39.

AGE AND DISTRIBUTION.—*Parafusulina boesei* Zone to *Parafusulina sellardsi* Zone of the Guadalupian Series, Glass and Del Norte mountains, Texas.

REMARKS.—*Parafusulina maleyi* is characterized by a large, elongate, fusiform test, a slowly increasing diameter, and scarcely or very lightly developed secondary deposits. Ross (1963b) included *Parafusulina maleyi* and *P. maleyi* var. *referta* Dunbar and Skinner, 1937, in *Parafusulina deliciasensis* Dunbar and Skinner, 1936. On the basis of the rather prominent axial filling from pole to pole and the narrow and more closely crowded septal folds, *P. deliciasensis* (which includes *P. maleyi* var. *referta*) and *P. maleyi* are considered to be separate species in this study. The specimens studied closely resemble the type specimens of *Parafusulina maleyi*. The only difference is that some specimens having light secondary deposits are included in this species. Measurement data of specimens are given in Table 9-23.

***Parafusulina marathonsensis*, new species**

PLATE 9-8: FIGURES 4, 5; PLATE 9-10: FIGURE 8

TYPES.—*Holotype*: USNM 483091; *Paratypes*: USNM 483090, 483092; from the Road Canyon Formation and the Word Formation of the Glass and Del Norte mountains, Texas.

MATERIAL STUDIED.—Samples from the upper part of the Road Canyon Formation and the lower part of the Word Formation in the Glass and Del Norte mountains, Texas: 3-23; 8-26.

DIAGNOSIS.—Test large; elongate fusiform shape; slightly curved axis of coiling and bluntly pointed poles; septal fluting very strong and regular; septal folds commonly low and very narrow; cuniculi highly developed; on axial section, foramina are numerous, subcircular in shape, and present on the septal folds of all volutions except those filled with secondary deposits; secondary deposits usually occupy the inner 2 to 3 volutions.

AGE AND DISTRIBUTION.—*Parafusulina trumpyi* Zone of the Guadalupian Series, Glass and Del Norte mountains, Texas.

DESCRIPTION.—Large size; elongate, fusiform test; 8 to 8½ volutions, attaining a length of 18.0 mm and a diameter of 3.6 mm, giving a form ratio of about 5; axis of coiling slightly curved; lateral slopes of volutions taper to bluntly pointed poles; proloculus ranging between 0.24 and 0.32 mm in outside diameter; spirotheca consisting of tectum and keriotheca; spirotheca thickness averaging 0.027, 0.030, 0.037, 0.043, 0.050, 0.067, 0.083, and 0.070 mm in first to eighth volutions, respectively; septa intensely and regularly fluted; septal folds

TABLE 9-23.—Measurements of *Parafusulina maleyi* Dunbar and Skinner.

	Volution	USNM 483089	USNM 483088
Radius vector (mm)	0	0.20	0.20
	1	0.28	0.25
	2	0.45	0.34
	3	0.60	0.41
	4	0.78	0.52
	5	1.00	0.72
	6	1.28	0.98
	7	1.50	1.20
	8	-	1.52
Half length (mm)	1	0.68	0.48
	2	1.20	0.80
	3	2.04	1.08
	4	3.20	1.68
	5	4.36	2.64
	6	5.72	4.20
	7	6.88	5.96
	8	-	7.40
Form ratio	1	2.43	1.92
	2	2.67	2.35
	3	3.40	2.63
	4	4.10	3.23
	5	4.36	3.67
	6	4.47	4.29
	7	4.59	4.97
	8	-	4.87
Wall thickness (mm)	1	0.02	0.02
	2	0.03	0.03
	3	0.04	0.03
	4	0.05	0.03
	5	0.05	0.04
	6	0.07	0.06
	7	0.08	0.07
	8	-	0.08
Tunnel angle (°)	1	21	-
	2	35	-
	3	49	-
	4	-	-
	5	-	-
	6	-	52

TABLE 9-24.—Measurements of *Parafusulina marathonensis*, new species.

	Volution	USNM 483090	USNM 483092	USNM 483091
Radius vector (mm)	0	0.14	0.16	-
	1	0.20	0.19	0.26
	2	0.26	0.25	0.32
	3	0.35	0.36	0.44
	4	0.45	0.50	0.56
	5	0.66	0.72	0.78
	6	0.94	0.96	1.04
	7	1.28	1.24	1.28
	8	1.68	-	1.64
	9	1.96?	-	2.00
Half length (mm)	1	0.40	0.44	0.72
	2	0.76	0.86	1.04
	3	1.08	1.32	1.40
	4	1.60	1.82	1.96
	5	2.60	2.70	2.84
	6	3.88	3.86	3.88
	7	6.72	6.08	5.76
	8	8.64	-	7.44
	9	-	-	9.28
Form ratio	1	2.00	2.31	2.76
	2	2.92	3.44	3.25
	3	3.08	3.66	3.18
	4	3.33	3.64	3.50
	5	3.94	3.75	3.64
	6	4.13	4.02	3.73
	7	5.25	4.90	4.50
	8	5.14	-	4.53
	9	-	-	4.64
Wall thickness (mm)	1	0.03	0.03	0.03
	2	0.03	0.03	0.04
	3	0.04	0.04	0.04
	4	0.04	0.05	0.05
	5	0.05	0.05	0.07
	6	0.07	0.07	0.08
	7	0.09	0.09	0.09
	8	0.10	0.06	0.10
	9	0.06	-	0.08
Tunnel angle (°)	1	-	24	-
	2	-	40	-
	3	36	54	-
	4	52	-	-
	5	44	-	-

commonly low and very narrow; cuniculi highly developed; on axial section, basal foramina numerous, subspherical in shape, and present in volutions without axial filling; chomata completely lacking; secondary deposits fill the inner 2 to 3 volutions; tunnel singular and well marked; tunnel angle averaging 24° and 48° in first and fifth volutions, respectively. Measurement data of specimens given in Table 9-24.

REMARKS.—This species is characterized by its shape and highly developed foramina, which distinguishes it from most species of the genus. It is somewhat similar to *Parafusulina glassensis*, new species, but differs in that it is smaller, elongate in form, has a smaller proloculus, narrower septal folds, and more developed foramina.

ETYMOLOGY.—This species is named for Marathon, a small town located about 10 miles south of the Glass Mountains and 35 miles southeast of Alpine, Texas. Many geologists and students of the Permian have stayed in Marathon while doing field work in the Glass Mountains area.

***Parafusulina rohri*, new species**

PLATE 9-14: FIGURES 1-3

TYPES.—*Holotype*: USNM 483093; *Paratypes*: USNM

483094, 483095; from the Word Formation of the Glass Mountains, Texas.

MATERIAL STUDIED.—Samples from the Willis Ranch Member of the Word Formation in the Glass Mountains, Texas: 3-21, 3-23, 3-24.

DIAGNOSIS.—Very large and subcylindrical; rather small proloculus; septal folds closely spaced, narrow, high, and regular; tunnel narrow; secondary deposits dense along axis.

AGE AND DISTRIBUTION.—*Parafusulina sellardsi* Zone of the Guadalupian Series, Glass Mountains, Texas.

DESCRIPTION.—Very large size; subcylindrical form; 9 to 10 volutions; attaining a length of 20 to 22 mm and a diameter of 3.5 to 5.0 mm; lateral slopes of volutions end in bluntly rounded poles; chamber height increasing very slowly as length increases rapidly, resulting in average form ratio changing from 2.28 in first volution to 5 or 6 at maturity; proloculus ranging between 0.30 to 0.40 mm in outside diameter and commonly subspherical; spirotheca consisting of tectum and keriotheca; spirotheca thickness averaging 0.030 to 0.040 mm in inner two volutions, but 0.10 to 0.11 mm in outer volutions; septa intensely and regularly fluted; septal folds narrow, high, and closely spaced; cuniculi very well developed; chomata completely lacking; dense secondary deposits largely fill the chambers of most inner volutions; tunnel narrow and well marked; tunnel angle averaging 16° and 43° in first and sixth volutions, respectively. Measurement data of specimens given in Table 9-25.

REMARKS.—This species is most similar to *Parafusulina trumpyi* Thompson and Miller, but it differs in having a larger test, more highly folded septa, and denser secondary deposits. It differs from *Parafusulina sellardsi* Dunbar and Skinner in having a rather small proloculus, higher form ratio of inner volutions, and heavier secondary deposits. Compared with *Parafusulina deliciosensis* Dunbar and Skinner, the present species has more volutions, smaller proloculus, thicker spirotheca, and lower form ratio.

ETYMOLOGY.—This species is named for David Rohr, professor of geology at Sul Ross State University, Alpine, Texas, in appreciation for his great help in field work and discussions of stratigraphy.

***Parafusulina rothi* Dunbar and Skinner, 1936**

PLATE 9-7: FIGURES 1-4

Parafusulina rothi Dunbar and Skinner, 1936:181-183, pl. 2: figs. 1-8.—Dunbar and Skinner, 1937:684-686, pl. 76: figs. 1-9 [in part, not fig. 10].

TYPES.—*Hypotypes*: USNM 483096-483099; from the Road Canyon Formation of the Glass Mountains, Texas.

MATERIAL STUDIED.—Samples from the Road Canyon Formation and the lower part of the Word Formation in the Glass and Del Norte mountains, Texas: 1-62, 1-63; 2-R8, 2-76, 2-R11, 2-R19; 7-49, 7-52; 8-14, 8-20, 8-23, 8-29, 8-42.

TABLE 9-25.—Measurements of *Parafusulina rothi*, new species.

	Volution	USNM 483094	USNM 483093	USNM 483095
Radius vector (mm)	0	0.14	0.18	0.20
	1	0.20	0.26	0.34
	2	0.25	0.41	0.46
	3	0.33	0.60	0.68
	4	0.42	0.80	0.88
	5	0.52	1.10	1.12
	6	0.65	1.24	1.40
	7	0.83	1.46	1.72
	8	1.05	1.78	2.08
	9	1.39	2.12	2.50
Half length (mm)	10	1.73	-	-
	1	0.56	0.44	0.64
	2	0.96	0.96	0.96
	3	1.38	1.56	1.60
	4	1.96	2.28	2.40
	5	2.68	2.82	3.68
	6	3.86	3.90	5.20
	7	5.28	5.88	6.80
	8	6.82	7.92	8.32
	9	8.44	9.64	11.72
Form ratio	10	9.76	-	-
	1	2.80	1.70	1.88
	2	3.84	2.34	2.09
	3	4.18	2.60	2.35
	4	4.66	2.85	2.73
	5	4.12	2.56	3.28
	6	5.94	3.15	3.71
	7	6.36	4.03	3.95
	8	6.50	4.45	4.00
	9	6.07	4.55	4.70
Wall thickness (mm)	10	5.64	-	-
	1	0.02	0.03	0.03
	2	0.03	0.03	0.03
	3	0.03	0.03	0.04
	4	0.04	0.05	0.05
	5	0.05	0.07	0.06
	6	0.05	0.08	0.08
	7	0.07	0.09	0.10
	8	0.07	0.11	0.10
	9	0.08	0.11	0.09
Tunnel angle (°)	10	0.10	-	-
	1	16	-	-
	2	35	-	-
	3	25	-	-
	4	36	-	31
	5	48	-	37
	6	43	-	-
	7	58	-	-
8	54	-	-	

AGE AND DISTRIBUTION.—*Parafusulina rothi* Zone and *Parafusulina sellardsi* Zone of the Guadalupian Series, Glass and Del Norte mountains, Texas; Guadalupe Mountains, Texas (Dunbar and Skinner, 1937). Upper Qixia Formation and lower Maokou Formation, China (Zhang, 1957; Yang, 1985).

REMARKS.—The specimens studied resemble the type specimens of *Parafusulina rothi* in all respects; however, the specimen illustrated in pl. 76: fig. 10 by Dunbar and Skinner (1937) has an elongate test, more intensive and regular fluting, and more extensive and heavier secondary deposits in the septal folds than the other specimens, and it is not included in *Parafusulina rothi* in this report. That specimen is included within the range of *Parafusulina glassensis*, new species. Measurement data of specimens are given in Table 9-26.

Ross (1963b) included this species within his concept of *Parafusulina deliciosensis*, which he reported as having a stratigraphic range from the upper part of the Road Canyon Formation to the top of the Appel Ranch Member of the Word Formation. It also has been reported (Wilde in Cooper and Grant, 1977) from the China Tank Member of the Word Formation in the Glass Mountains, Texas.

TABLE 9-26.—Measurements of *Parafusulina rothi* Dunbar and Skinner.

	Volution	USNM 483096	USNM 483098	USNM 483099
Radius vector (mm)	0	0.18	0.23	0.22
	1	0.24	0.31	0.28
	2	0.38	0.44	0.40
	3	0.56	0.64	0.58
	4	0.88	0.92	0.82
	5	1.32	1.26	1.08
	6	1.68	1.56	1.40
Half length (mm)	7	2.12	2.04	-
	1	0.42	0.68	0.64
	2	0.86	1.2	0.98
	3	1.60	2.24	1.56
	4	2.36	3.32	2.86
	5	3.28	4.80	4.04
	6	5.84	6.24	5.60
Form ratio	7	7.28	7.36	-
	1	1.75	2.19	2.28
	2	2.20	2.72	2.45
	3	2.85	3.50	2.68
	4	2.68	3.61	3.48
	5	2.48	3.80	3.74
	6	3.48	4.00	4.00
Wall thickness (mm)	7	3.43	3.61	-
	1	0.04	0.03	0.03
	2	0.04	0.04	0.04
	3	0.05	0.06	0.04
	4	0.07	0.08	0.06
	5	0.10	0.09	0.08
	6	0.11	0.11	0.10
Tunnel angle (°)	7	0.10	0.08	-
	1	-	38	27
	2	-	51	30
	3	-	60	-
	4	52	66	-
	5	40	71	24
6	56	-	-	

***Parafusulina rudinei*, new species**

PLATE 9-10: FIGURES 3-5

TYPES.—*Holotype*: USNM 483100; *Paratypes*: USNM 483101, 483102; from the Road Canyon Formation of the Glass and Del Norte mountains, Texas.

MATERIAL STUDIED.—Samples from the upper part of the Road Canyon Formation in the Glass and Del Norte mountains, Texas: 1-64, 1-66; 7-59; 8-28.

DIAGNOSIS.—Stout, fusiform test; very large proloculus; thin spirotheca; septal folds low and not very crowded; secondary deposits commonly filling septal loops along the outsides of the tunnel in the inner 2 to 3 volutions.

AGE AND DISTRIBUTION.—*Parafusulina rothi* Zone to *Parafusulina sellardsi* Zone of the Guadalupian Series, Glass and Del Norte mountains, Texas.

DESCRIPTION.—Large size; stubby, fusiform test; 6 to 7 volutions; attaining a length of 9 to 11 mm and a diameter of 3.2 to 3.4 mm; convex lateral slopes of volutions end in bluntly pointed poles; chamber height and length increasing slowly and gradually, resulting in average form ratio changing from about 2.0 in first volution to about 3.0 or 3.5 at maturity; proloculus very large, averaging 0.60 mm in outside diameter and usually subspherical in shape; spirotheca quite thin, consisting of tectum and keriotheca; spirotheca thickness averaging 0.030, 0.035, 0.044, 0.052, 0.063, and 0.065 mm from first to sixth volutions, respectively; septa intensely fluted; septal folds fine, low, and not crowded; cuculi well developed; chomata lacking; secondary deposits irregularly distributed along outsides of tunnel in first 2 to 3 volutions; tunnel broad but not well defined; tunnel angle averaging 34° and 67° in first and sixth volutions, respectively. Measurement data of specimens given in Table 9-27.

REMARKS.—This species somewhat resembles *Parafusulina boesei* Dunbar and Skinner and *Parafusulina biturbinata* Kling, but it differs in having a stouter test, a larger proloculus, less regular folds, and thinner spirotheca.

ETYMOLOGY.—This species is named for Shannon F. Rudine, a graduate student at Sul Ross State University, who helped with the field work of this study.

***Parafusulina sellardsi* Dunbar and Skinner, 1937**

PLATE 9-12: FIGURES 1, 6; PLATE 9-13: FIGURE 6

Parafusulina sellardsi Dunbar and Skinner, 1937:688-689, pl. 78: figs. 1-11.—Dunbar, 1944:44, pl. 11: fig. 2, pl. 14: figs. 1-4.—Ross, 1963b:26, pl. 4: fig. 8, pl. 5: figs. 9-12, 16.

TYPES.—*Hypotypes*: USNM 483103-483105; from the Word Formation of the Glass Mountains, Texas.

MATERIAL STUDIED.—Samples from the lower part of the Word Formation in the Glass and Del Norte mountains, Texas: 3-21, 3-22, 3-23, 3-24; 8-39, 8-45.

TABLE 9-27.—Measurements of *Parafusulina rudinei*, new species.

	Volution	USNM 483100	USNM 483102	USNM 483101
Radius vector (mm)	0	0.22	0.28	0.30
	1	0.38	0.45	0.40
	2	0.52	0.64	0.52
	3	0.68	0.80	0.68
	4	0.89	1.02	0.88
	5	1.16	1.28	1.12
	6	1.44	1.60	1.40
Half length (mm)	7	1.70	—	1.68
	1	0.74	0.96	0.98
	2	1.08	1.61	1.45
	3	1.44	2.40	1.92
	4	1.84	3.28	2.52
	5	2.40	4.56	3.36
	6	3.28	—	4.68
Form ratio	7	4.20	—	5.52
	1	1.95	2.13	2.45
	2	2.08	2.52	2.79
	3	2.12	3.00	2.82
	4	2.07	3.22	2.86
	5	2.07	3.56	3.00
	6	2.28	—	3.34
Wall thickness (mm)	7	2.47	—	3.29
	1	0.03	0.03	0.03
	2	0.03	0.03	0.04
	3	0.03	0.04	0.05
	4	0.05	0.05	0.06
	5	0.05	0.06	0.07
Tunnel angle (°)	6	0.06	0.05	0.08
	1	—	30	34
	2	28	45	41
	3	36	46	50
	4	—	32	42
	5	—	—	62
6	—	—	67	

AGE AND DISTRIBUTION.—*Parafusulina sellardsi* Zone of the Guadalupian Series, Glass and Del Norte mountains, Texas; Guadalupe Mountains, Texas (Dunbar and Skinner, 1937); Chinati Mountains, Texas (Skinner, 1940).

REMARKS.—The specimens studied resemble the type specimens of *Parafusulina sellardsi* in all respects. Some specimens have a test that is larger than any reported specimens of this species. Measurement data of specimens are given in Table 9-28.

Parafusulina splendens Dunbar and Skinner, 1937

PLATE 9-6: FIGURES 1-5

Parafusulina splendens Dunbar and Skinner, 1937:682-684, pl. 75: figs. 1-11, pl. 73: fig. 10.—Sheng, 1963:71, pl. 17: figs. 1-6, pl. 21: figs. 6-8.—Ross, 1963b:29, pl. 4: figs. 14, 16, 17, pl. 5: fig. 1.—Xiao et al., 1986:108, pl. 14: figs. 1, 4, 6.

TABLE 9-28.—Measurements of *Parafusulina sellardsi* Dunbar and Skinner.

	Volution	USNM 483103	USNM 483104	USNM 483105
Radius vector (mm)	0	0.39	0.25	0.36
	1	0.54	0.38	0.43
	2	0.72	0.48	0.56
	3	0.96	0.60	0.70
	4	1.20	0.78	0.92
	5	1.54	1.00	1.16
	6	1.92	1.32	1.44
	7	2.34	1.68	1.84
	8	2.83	2.04	—
Half length (mm)	9	—	2.52	—
	1	1.08	0.78	0.88
	2	1.52	1.52	1.46
	3	3.08	2.36	2.24
	4	4.20	3.08	3.36
	5	6.00	4.00	5.30
	6	7.90	5.64	7.00
	7	9.62	7.16	7.60
	8	11.40	8.87	—
Form ratio	9	—	11.04	—
	1	2.00	2.05	2.05
	2	2.11	3.17	2.61
	3	3.21	3.93	3.20
	4	3.50	3.95	3.65
	5	3.90	4.00	4.57
	6	4.11	4.27	4.86
	7	4.11	4.26	4.13
	8	4.03	4.35	—
Wall thickness (mm)	9	—	4.38	—
	1	0.03	0.04	0.04
	2	0.04	0.04	0.05
	3	0.06	0.05	0.06
	4	0.06	0.06	0.07
	5	0.10	0.07	0.08
	6	0.12	0.08	0.10
	7	0.09	0.09	0.12
	8	0.10	0.10	—
Tunnel angle (°)	9	—	0.11	—
	1	28	24	—
	2	—	27	—
	3	32	38	40
	4	47	41	41
	5	48	52	50
6	58	—	—	

TYPES.—*Hypotypes*: USNM 483106-483110; from the Road Canyon Formation of the Glass Mountains, Texas.

MATERIAL STUDIED.—Samples from the Road Canyon Formation in the Glass and Del Norte mountains, Texas: 1-63; 2-R3, 2-R16, 2-77; 7-52; 8-13, 8-15.

AGE AND DISTRIBUTION.—Leonardian Series portion of the *Parafusulina boesei* Zone to *Parafusulina trumpyi* Zone of the Guadalupian Series, Glass and Del Norte mountains, Texas; Guadalupe Mountains, Texas (Wilde, 1986a). Upper part of the Qixia Formation and the lower part of the Maokou Formation, China (Sheng, 1963; Yang, 1985; Xiao et al., 1986).

TABLE 9-29.—Measurements of *Parafusulina splendens* Dunbar and Skinner.

	Volution	USNM 483106	USNM 483110	USNM 483108	USNM 483109	USNM 483107
Radius vector (mm)	0	0.24	0.24	0.14	0.26	0.23
	1	0.26	0.32	0.36	0.34	0.36
	2	0.40	0.44	0.52	0.46	0.51
	3	0.58	0.58	0.72	0.64	0.74
	4	0.80	0.79	0.96	0.88	1.04
	5	1.08	1.06	1.24	1.12	1.32
	6	1.34	1.34	1.60	1.36	1.68
	7	1.68	1.65	-	-	2.12
Half length (mm)	8	2.00	-	-	-	-
	1	0.54	0.44	0.64	0.52	0.90
	2	0.88	1.02	1.04	1.00	1.44
	3	1.26	1.68	1.84	1.46	2.02
	4	1.84	2.24	2.76	2.20	3.04
	5	2.60	3.26	4.20	3.36	4.60
	6	3.72	4.42	5.42	4.68	6.20
	7	5.14	6.40	-	-	7.48
Form ratio	8	6.86	7.04	-	-	-
	1	2.08	1.38	1.78	1.53	2.50
	2	2.20	2.31	2.00	2.17	2.82
	3	2.17	2.90	2.56	2.28	2.73
	4	2.30	2.84	2.88	2.50	2.92
	5	2.41	3.08	3.39	3.00	3.48
	6	2.78	3.30	3.39	3.44	3.69
	7	3.06	3.88	-	-	3.53
Wall thickness (mm)	8	3.43	-	-	-	-
	1	0.02	0.03	0.03	0.03	0.03
	2	0.03	0.03	0.03	0.04	0.03
	3	0.04	0.04	0.04	0.06	0.04
	4	0.06	0.05	0.06	0.07	0.06
	5	0.07	0.06	0.07	0.08	0.07
	6	0.08	0.08	0.08	-	0.08
	7	0.08	0.06	-	-	0.07
Tunnel angle (°)	8	0.06	-	-	-	-
	1	28	30	-	26	25
	2	32	38	36	30	37
	3	32	37	36	35	34
	4	27	46	45	40	33
	5	31	38	-	42	42
6	34	-	-	-	-	

REMARKS.—The specimens studied resemble the type specimens of *Parafusulina splendens* Dunbar and Skinner in all respects. Measurement data of specimens are given in Table 9-29.

This species is widely distributed in the Delaware basin and is also widely distributed in South China.

***Parafusulina sullivanensis* Ross, 1963**

PLATE 9-11: FIGURES 1-4

Parafusulina sullivanensis Ross, 1963b:23, pl. 4: figs. 9, 12, pl. 5: figs. 13-15, 17-22.

TYPES.—*Hypotypes*: USNM 483111-483114; from the Road Canyon Formation and the Word Formation of the Del Norte Mountains, Texas.

TABLE 9-30.—Measurements of *Parafusulina sullivanensis* Ross.

	Volution	USNM 483112	USNM 483111	USNM 483113	USNM 483114
Radius vector (mm)	0	0.18	0.21	0.17	0.20
	1	0.26	0.32	0.25	0.25
	2	0.40	0.44	0.36	0.36
	3	0.56	0.61	0.52	0.49
	4	0.74	0.78	0.74	0.68
	5	0.99	1.01	0.92	0.92
	6	1.26	-	1.24	1.20
	7	1.44	-	1.52	1.56
Half length (mm)	8	-	-	1.90	-
	1	0.60	0.80	0.68	0.60
	2	1.08	1.32	1.08	1.04
	3	1.68	2.24	1.80	1.72
	4	2.60	3.28	2.60	2.64
	5	3.92	4.52	3.55	3.92
	6	5.52	-	4.84	5.56
	7	-	-	5.78	-
Form ratio	1	2.31	2.50	2.72	2.40
	2	2.70	3.00	3.00	2.89
	3	3.00	3.67	3.46	3.51
	4	3.51	4.21	3.51	3.88
	5	3.95	4.48	3.86	4.26
	6	4.38	-	3.90	4.63
	7	-	-	3.80	-
Wall thickness (mm)	1	0.03	0.03	0.03	0.03
	2	0.04	0.04	0.03	0.04
	3	0.04	0.04	0.05	0.04
	4	0.04	0.06	0.05	0.06
	5	0.06	0.06	0.06	0.06
	6	0.07	-	0.08	0.07
	7	0.06	-	0.06	0.08
	8	-	-	0.05	-
Tunnel angle (°)	1	29	-	24	24
	2	50	30	35	35
	3	43	-	41	44
	4	37	-	40	41
	5	37	-	47	-

MATERIAL STUDIED.—Samples from the Road Canyon Formation and the lower part of the Word Formation in the Glass and Del Norte mountains, Texas: 1-62; 2-R11, 2-R16; 7-53; 8-15, 8-24, 8-32, 8-38.

AGE AND DISTRIBUTION.—*Parafusulina boesei* Zone to *Parafusulina sellardsi* Zone of the Guadalupian Series, Glass and Del Norte mountains, Texas.

REMARKS.—The specimens studied resemble the type specimens of *Parafusulina sullivanensis* in all respects. Measurement data of specimens are given in Table 9-30.

***Parafusulina trumpyi* Thompson and Miller, 1949**

PLATE 9-9: FIGURES 4-7

Parafusulina trumpyi Thompson and Miller, 1949:18-21, pl. 4: figs. 1-3, pl. 5: figs. 7, 8, 10.

TYPES.—*Hypotypes*: USNM 483115–483118; from the Road Canyon Formation of the Glass and Del Norte mountains, Texas.

MATERIAL STUDIED.—Samples from the Road Canyon Formation and the lower part of the Word Formation in the Glass and Del Norte mountains, Texas: 1-66; 2-R19, 2-R20; 3-21; 7-53; 8-25.

AGE AND DISTRIBUTION.—*Parafusulina trumpyi* Zone to *Parafusulina sellardsi* Zone of the Guadalupian Series, Glass and Del Norte mountains, Texas; Colombia (Thompson and Miller, 1949).

TABLE 9-31.—Measurements of *Parafusulina trumpyi* Thompson and Miller.

	Volution	USNM 483116	USNM 483117	USNM 483115	USNM 483118
Radius vector (mm)	0	0.16	0.22	0.16	0.15
	1	0.26	0.24	0.23	0.24
	2	0.38	0.34	0.35	0.42
	3	0.54	0.46	0.50	0.60
	4	0.76	0.68	0.72	0.78
	5	0.96	0.92	0.96	1.04
	6	1.28	1.22	1.24	1.36
	7	1.60	1.56	1.50	1.76
	8	1.97	1.96	1.80	2.16
9	2.26	2.24	—	2.48	
Half length (mm)	1	0.64	0.72	0.50	0.64
	2	0.98	1.04	0.78	1.00
	3	1.42	1.68	1.20	1.40
	4	2.04	2.52	1.96	2.00
	5	2.92	3.92	2.92	2.88
	6	4.20	6.12	4.24	4.00
	7	5.96	7.76	5.68	4.84
	8	7.64	9.12	6.92	7.04
	9	9.40	9.72	—	9.04
Form ratio	1	2.46	3.00	2.17	2.67
	2	2.58	3.06	2.51	2.38
	3	2.63	3.65	2.40	2.33
	4	2.68	3.70	2.72	3.69
	5	3.04	4.08	3.04	2.77
	6	3.28	5.01	3.42	2.94
	7	3.03	4.97	3.79	3.56
	8	3.88	4.65	3.84	3.26
	9	4.16	4.34	—	3.65
Wall thickness (mm)	1	0.02	0.03	0.02	0.03
	2	0.03	0.04	0.03	0.03
	3	0.04	0.04	0.03	0.04
	4	0.04	0.06	0.05	0.04
	5	0.05	0.07	0.05	0.07
	6	0.06	0.08	0.06	0.09
	7	0.08	0.09	0.06	0.10
	8	0.09	0.09	0.07	0.08
	9	0.07	0.08	—	0.07
Tunnel angle (°)	1	28	28	32	27
	2	37	28	36	31
	3	31	32	42	30
	4	40	39	40	34
	5	50	40	42	40
	6	59	32	49	45
	7	—	—	62	52

REMARKS.—The specimens studied resemble the type specimens of *Parafusulina trumpyi* Thompson and Miller in all respects. Thompson and Miller (1949) assigned an age of Leonardian or early Guadalupian for this species in Colombia. This is the first time it has been reported in North America. Measurement data of specimens are given in Table 9-31.

Parafusulina virga Thompson and Wheeler, 1946

PLATE 9-15: FIGURES 5, 6

Parafusulina virga Thompson and Wheeler, 1946:32, pl. 9: figs. 1–7 [in part, not pl. 6: figs. 1–3].

TYPES.—*Hypotypes*: USNM 483119, 483120; from the Word Formation of the Del Norte Mountains, Texas.

MATERIAL STUDIED.—Samples from the upper part of the Road Canyon Formation and the lower part of the Word Formation in the Glass and Del Norte mountains, Texas: 2-75, 2-77; 8-45.

AGE AND DISTRIBUTION.—*Parafusulina trumpyi* Zone to *Parafusulina sellardsi* Zone of the Guadalupian Series, Glass and Del Norte mountains, Texas; Klamath Mountains, California (Thompson and Wheeler, 1946).

REMARKS.—*Parafusulina virga* is characterized by a large, elongate-fusiform to subcylindrical test with very low lateral slopes and broadly rounded poles, thick spirotheca, broad tunnel, and light discontinuous axial fillings through the length of the test. The specimens studied differ from the type specimens of *Parafusulina virga* (pl. 9: figs. 1–7) only in having a slightly lower form ratio and thicker spirotheca in outer volutions. When *Parafusulina virga* was named by Thompson and Wheeler in 1946, no holotype was designated. Among all specimens illustrated as syntypes, only pl. 6: fig. 1 and pl. 9: fig. 3 are axial sections; however, they are so different in shape, form ratio, size of proloculus, and shape and arrangement of septal folds that they probably belong to different species. The specimen shown in pl. 6: fig. 1 has a slender test, low and loosely spaced septal folds, and virtually no axial fillings, thus resembling *Parafusulina nosonensis* Thompson and Wheeler, 1946. The specimen illustrated in pl. 9: fig. 3 bears the characteristics of *Parafusulina virga* as described by the authors, and thereby it is herein designated as the lectotype of this species. This is the first time this species has been reported in the Glass and Del Norte mountains area. Measurement data of specimens are given in Table 9-32.

Parafusulina cf. *P. wordensis* Dunbar and Skinner, 1931

Parafusulina wordensis Dunbar and Skinner, 1931:261, pl. 2: figs. 1–4; 1937:690–691, pl. 72: figs. 1–8.

MATERIAL STUDIED.—Sample from the upper part of the Word Formation in the Del Norte Mountains, Texas: 8-45.

AGE AND DISTRIBUTION.—*Parafusulina sellardsi* Zone of the Guadalupian Series, Glass and Del Norte mountains, Texas.

TABLE 9-32.—Measurements of *Parafusulina virga* Thompson and Wheeler.

	Volution	USNM 483119	USNM 483120
Radius vector (mm)	0	0.30	0.26
	1	0.33	0.36
	2	0.44	0.46
	3	0.60	0.64
	4	0.82	0.85
	5	1.05	1.14
	6	1.42	1.51
	7	1.80	1.84
Half length (mm)	8	2.28	-
	1	0.74	0.80
	2	1.24	1.40
	3	1.92	2.08
	4	2.96	3.12
	5	4.52	5.40
	6	5.96	7.40
	7	7.16	9.00
Form ratio	8	8.00	-
	1	2.24	2.22
	2	2.82	3.04
	3	3.20	3.25
	4	3.61	3.67
	5	4.30	4.74
	6	4.20	4.90
	7	3.98	4.89
Wall thickness (mm)	8	3.51	-
	1	0.03	0.03
	2	0.04	0.03
	3	0.04	0.04
	4	0.06	0.06
	5	0.07	0.08
	6	0.10	0.09
	7	0.11	0.11
Tunnel angle (°)	8	0.10	-
	1	-	21
	2	25	36
	3	38	46
	4	49	48
	5	58	55
6	65	65	

REMARKS.—*Parafusulina wordensis* is characterized by an exceptionally large, subcylindrical test, very numerous septa, highly developed cuniculi and basal foramina, very thick spirotheca, and a well-marked tunnel. Size and shape will normally distinguish this species from any other species of the genus *Parafusulina*. The major features of the specimens studied resemble those of the type specimens of *Parafusulina wordensis* Dunbar and Skinner, although no good axial sections were observed. The sample material available is too heavily dolomitized to produce reasonable illustrations of the species.

Polydiexodina Dunbar and Skinner, 1931

TYPE SPECIES.—*Polydiexodina capitanensis* Dunbar and Skinner, 1931.

Polydiexodina capitanensis Dunbar and Skinner, 1931

PLATE 9-17: FIGURES 1, 2

Polydiexodina capitanensis Dunbar and Skinner, 1931:264, pl. 3: figs. 7-11; 1937:693-695, pl. 80: figs. 2, 4-11.

TYPES.—*Hypotypes*: USNM 483121, 483122; from the Gilliam Limestone of the Glass Mountains, Texas.

MATERIAL STUDIED.—Samples from the upper part of the Vidrio Formation, the Gilliam Limestone, the lower part of the Capitan Limestone, and the lower part of the Altuda Formation in the Glass and Del Norte mountains, Texas: 4-88, 4-210, 4-211, 4-212, 4-213; 5-79, 5-85; 9-6, 9-10F; 10-206, 10-208, 10-344. Most samples are heavily dolomitized.

AGE AND DISTRIBUTION.—*Polydiexodina shumardi* Zone of the Guadalupian Series, Glass and Del Norte mountains, Texas; Guadalupe Mountains, Texas (Dunbar and Skinner, 1937); Las Delicias area of Coahuila, Mexico (Dunbar, 1944).

REMARKS.—The specimens studied resemble the type specimens of *Polydiexodina capitanensis* Dunbar and Skinner in all respects. Measurement data of specimens are given in Table 9-33.

Polydiexodina oregonensis Bostwick and Nestell, 1965

PLATE 9-17: FIGURES 3, 4

Polydiexodina oregonensis Bostwick and Nestell, 1965:612, pl. 74: figs. 1-10.

TYPES.—*Hypotypes*: USNM 483123, 483124; from the Vidrio Formation and the Altuda Formation of the Del Norte Mountains, Texas.

MATERIAL STUDIED.—Samples from the upper part of the Vidrio Formation and the lower part of the Altuda Formation in the Del Norte Mountains, Texas: 9-10, 9-10F; 10-206, 10-344.

AGE AND DISTRIBUTION.—*Polydiexodina shumardi* Zone of the Guadalupian Series, Del Norte Mountains, Texas; Oregon (Bostwick and Nestell, 1965).

REMARKS.—*Polydiexodina oregonensis* is characterized by a very elongate and slender test, relatively low septal folds, broad median tunnel, and rather weak supplementary tunnels. Bostwick and Nestell (1965) considered this species to be an early form of the lineage. On the basis of rather close similarities of this species to *Polydiexodina shumardi*, its moderately developed characters for the genus, and its occurrence in the lowest level of all collections of this study that yield *Polydiexodina*, the authors suggest that *P. oregonensis* may be the immediate ancestor of *P. shumardi*. The specimens studied resemble the type specimens of *P. oregonensis* in all respects except they are not well oriented;

TABLE 9-33.—Measurements of *Polydiexodina capitanensis* Dunbar and Skinner.

	Volution	USNM 483121	USNM 483122
Radius vector (mm)	0	0.30	0.26
	1	0.44	0.32
	2	0.52	0.40
	3	0.64	0.52
	4	0.78	0.64
	5	0.94	0.79
	6	1.10	0.96
	7	1.27	1.20
	8	1.44	1.42
	9	1.66	1.60
	10	1.90	1.84
	11	2.14	-
	12	2.40	-
13	2.68	-	
Half length (mm)	1	0.84	0.72
	2	1.44	1.58
	3	2.28	2.52
	4	3.04	3.80
	5	4.32	5.60
	6	5.76	6.80
	7	7.04	8.60
	8	8.08	10.40
	9	9.48	11.48
	10	11.24	12.60
	11	13.12	-
	12	14.60	-
	13	15.76	-
Form ratio	1	1.91	2.25
	2	2.77	3.95
	3	3.56	4.85
	4	3.90	5.94
	5	4.60	7.08
	6	5.24	7.08
	7	5.54	7.20
	8	5.61	7.32
	9	5.71	7.18
	10	5.92	6.85
	11	6.13	-
	12	6.08	-
	13	5.88	-
Wall thickness (mm)	1	0.03	0.03
	2	0.04	0.03
	3	0.04	0.04
	4	0.04	0.04
	5	0.05	0.05
	6	0.05	0.06
	7	0.06	0.06
	8	0.07	0.07
	9	0.06	0.07
	10	0.07	-
	11	0.07	-
	12	0.06	-

therefore, they appear somewhat shorter than their actual lengths. Measurement data of one specimen are given in Table 9-34.

TABLE 9-34.—Measurements of *Polydiexodina oregonensis* Bostwick and Nestell.

	Volution	USNM 483124
Radius vector (mm)	0	0.16
	1	0.32
	2	0.44
	3	0.54
	4	0.64
	5	0.78
	6	0.94
Half length (mm)	1	0.60
	2	1.12
	3	1.80
	4	3.08
	5	4.40
	6	6.92
	7	9.60
Form ratio	1	1.88
	2	2.55
	3	3.33
	4	4.81
	5	5.64
	6	7.36
Wall thickness (mm)	1	0.03
	2	0.04
	3	0.04
	4	0.04
	5	0.05
	6	0.05
	7	0.06

Polydiexodina shumardi Dunbar and Skinner, 1931

PLATE 9-16: FIGURES 1-4

Polydiexodina shumardi Dunbar and Skinner, 1931:267, pl. 3: figs. 1-6; 1937:695-697, pl. 81: figs. 3-10.

TYPES.—*Hypotypes*: USNM 483125-483128; from the Altuda Formation of the Del Norte Mountains, Texas.

MATERIAL STUDIED.—Samples from the upper part of the Vidrio Formation, the Gilliam Limestone, the lower part of the Capitan Limestone, and the lower part of the Altuda Formation in the Glass and Del Norte mountains, Texas: 4-88, 4-210, 4-212, 4-213; 5-79, 5-86; 9-5, 9-6, 9-10, 9-10F; 10-206, 10-207, 10-208, 10-344.

AGE AND DISTRIBUTION.—*Polydiexodina shumardi* Zone of the Guadalupian Series, Glass and Del Norte mountains, Texas; Guadalupe Mountains, Texas (Dunbar and Skinner, 1937).

REMARKS.—The specimens studied resemble the type specimens of *Polydiexodina shumardi* Dunbar and Skinner in all respects. Measurement data of specimens are given in Table 9-35.

TABLE 9-35.—Measurements of *Polydiexodina shumardi* Dunbar and Skinner.

	Volution	USNM 483128	USNM 483127	USNM 483126	USNM 483125
Radius vector (mm)	0	0.24	0.25	0.23	0.17
	1	0.28	0.31	0.28	0.24
	2	0.40	0.43	0.42	0.32
	3	0.53	0.59	0.54	0.40
	4	0.67	0.66	0.68	0.52
	5	0.82	0.81	0.86	0.68
	6	1.09	0.97	1.02	0.80
	7	1.35	1.16	1.25	0.92
	8	1.58	1.35	1.46	1.08
	9	-	1.64	1.24	-
	10	-	-	1.40	-
Half length (mm)	1	0.88	1.04	0.84	0.72
	2	1.37	1.81	1.42	1.24
	3	2.15	2.78	2.00	1.64
	4	3.28	4.00	2.77	2.18
	5	4.92	5.04	3.59	2.96
	6	7.10	6.02	5.89	4.45
	7	-	7.58	8.58	5.78
	8	-	9.45	10.10	6.83
	9	-	-	-	8.90
	10	-	-	-	10.84
Form ratio	1	3.14	3.35	3.00	3.00
	2	3.43	4.21	3.38	3.88
	3	4.06	4.71	3.70	4.10
	4	4.90	6.06	4.07	4.19
	5	6.00	6.22	4.17	4.35
	6	6.51	6.21	5.77	5.56
	7	-	6.53	6.87	6.28
	8	-	7.00	6.91	6.42
Wall thickness (mm)	1	0.03	0.03	0.03	0.03
	2	0.03	0.03	0.03	0.03
	3	0.04	0.04	0.04	0.03
	4	0.05	0.04	0.04	0.03
	5	0.05	0.05	0.05	0.04
	6	0.06	0.05	0.05	0.04
	7	0.06	0.05	0.05	0.05
	8	0.05	0.06	0.06	0.06
	9	-	0.05	0.06	-
	10	-	-	0.04	-

Polydiexodina sp.

PLATE 9-17: FIGURES 5-7

MATERIAL STUDIED.—Samples from the upper part of the Vidrio Formation and the lower part of the Altuda Formation in the Del Norte Mountains, Texas: 9-10, 9-10F; 10-208; specimens: USNM 483129-483131.

AGE AND DISTRIBUTION.—*Polydiexodina shumardi* Zone of the Guadalupian Series, Del Norte Mountains, Texas.

DESCRIPTION.—Large size; elongate, fusiform test; 6½ volutions; attaining a length of 14.2 mm and a diameter of 3.2 mm; axis of coiling commonly curved, so that measurements of length probably inaccurate; lateral slopes of volutions taper to broadly rounded poles; average form ratio increasing from 2.20

TABLE 9-36.—Measurements of *Polydiexodina* sp.

	Volution	USNM 483131	USNM 483129	USNM 483130
Radius vector (mm)	0	0.36	0.20	0.40
	1	0.44	0.44	0.42
	2	0.60	0.56	0.56
	3	0.72	0.68	0.70
	4	0.92	0.80	0.88
	5	1.12	0.94	1.04
	6	1.36	1.12	-
Half length (mm)	7	1.60	1.26	-
	1	0.98	0.92	0.96
	2	1.60	1.56	1.58
	3	2.48	2.56	2.28
	4	3.64	-	3.48
	5	4.76	-	4.72
	6	5.28	-	-
Form ratio	7	7.10	-	-
	1	2.23	2.09	2.28
	2	2.67	2.79	2.82
	3	3.44	3.76	3.26
	4	3.96	-	3.95
	5	4.25	-	4.54
	6	3.88	-	-
Wall thickness (mm)	7	4.44	-	-
	1	0.03	0.03	0.03
	2	0.04	0.03	0.03
	3	0.04	0.04	0.03
	4	0.05	0.04	0.04
	5	0.05	0.05	0.04
Tunnel angle (°)	6	0.06	0.05	-
	1	21	20	28
	2	25	32	42
	3	40	-	-
	4	22	-	-

in first volution to 4.44 in sixth volution; proloculus very large, 0.40 to 0.80 mm in outside diameter, and subspherical or irregular in shape; spirotheca very thin and consisting of tectum and keriotheca; spirotheca thickness averaging 0.030, 0.033, 0.036, 0.043, 0.047, and 0.055 mm from first to sixth volutions, respectively; septa intensely and regularly fluted; cuniculi highly developed; chomata completely lacking; secondary deposits fill extremities along axis; median tunnel relatively well marked; tunnel angle averaging 23° and 40° in first and third volutions, respectively; supplementary tunnels occurring in outer volutions. Measurement data of specimens given in Table 9-36.

REMARKS.—The specimens studied resemble the type specimen of *Polydiexodina praecursor* Lloyd, 1963, in having a small size for the genus, a short coiling axis, few volutions, and a large and irregular proloculus, but they differ from that species in bearing a well-marked median tunnel and better developed supplementary tunnels. Evolutionarily, the present specimens seem more primitive than *Polydiexodina capitaneensis* and *P. shumardi*, which are characterized by the presence of

a well-defined median tunnel and supplementary tunnels, but more advanced than *Polydixodina praecursor* and *P. afghanensis* Thompson, which lack a well-defined median tunnel

and have sporadic supplementary tunnels. More specimens with better orientation of thin sections are needed before a new species name can be given.

Literature Cited

- Abich, H.
1859. Vergleichende Grundzüge der Geologie des Kaukasus wie der armenischen und nordpersischen Gebirge. *Mémoires de l'Académie Impériale des Sciences de St. Pétersbourg, Classe Sciences, Mathématiques, Physiques et Naturelles*, series 6, 7:359–534, plates 1–8.
- Adams, J.E., M.F. Cheney, R.K. DeFord, R.I. Dickey, C.O. Dunbar, J.M. Hills, R.E. King, E.R. Lloyd, A.K. Miller, and C.E. Needham
1939. Standard Permian Section of North America. *Bulletin of the American Association of Petroleum Geologists*, 23(11):1673–1681.
- Bostwick, D.A., and M.K. Nestell
1965. A New Species of *Polydixodina* from Central Oregon. *Journal of Paleontology*, 39(4):611–614, plate 74.
- Chen, S.
1956. Fusulinidae of South China, Part 2. *Palaeontologica Sinica*, new series B, 6:17–71, plates 1–14. [In Chinese.]
- Clark, D.L., and Wang Cheng-Yuan
1988. Permian Neogondolellids from South China: Significance for Evolution of the *serrata* and *carinata* Groups in North America. *Journal of Paleontology*, 62(1):132–138.
- Cooper, G.A., and R.E. Grant
1964. New Permian Stratigraphic Units in Glass Mountains, West Texas. *Bulletin of the American Association of Petroleum Geologists*, 48(9):1581–1588.
1966. Permian Rock Units in the Glass Mountains, West Texas. *United States Geological Survey Bulletin*, 1244-E:E1–E9, plates 1, 2.
1972. Permian Brachiopods of West Texas, I. *Smithsonian Contributions to Paleobiology*, 14:1–231, plates 1–23.
1977. Permian Brachiopods of West Texas, VI. *Smithsonian Contributions to Paleobiology*, 32:3161–3370.
- Cys, J.M.
1981. Preliminary Report on Proposed Leonardian Lectostratotype Section, Glass Mountains, West Texas. In *Marathon–Marfa Region of West Texas Symposium and Guidebook. Society of Economic Paleontologists and Mineralogists, Permian Basin Section, Publication*, 81-10:183–203.
- Da, Y.T.
1983. Order Fusulinida. In *Xinjiang Bureau of Geology and Nanjing Institute of Geology and Paleontology*, editors, *Paleontological Atlas of Northwestern China, Xinjiang Fascicle*, 2:107–109, plates 29, 30. Beijing: Geological Publishing House. [In Chinese.]
- Dunbar, C.O.
1939. Permian Fusulines from Central America. *Journal of Paleontology*, 13(3):344–348, plates 35, 36.
1944. Permian and Pennsylvanian (?) Fusulines. In R.E. King, C.O. Dunbar, P.E. Cloud, Jr., and A.K. Miller, *Geology and Paleontology of the Permian Area Northwest of Las Delicias, Southwestern Coahuila, Mexico. Geological Society of America, Special Paper*, 52:35–48, plates 9–16.
1953. A Giant Permian Fusuline from Sonora. In G.A. Cooper, C.O. Dunbar, H. Duncan, A.K. Miller, and J.B. Knight, *Permian Fauna at El Antimonio, Western Sonora, Mexico. Smithsonian Miscellaneous Collections*, 119(2):14–19, plates 2, 3.
- Dunbar, C.O., and L.G. Henbest
1930. The Fusulinid Genera *Fusulina*, *Fusulinnella* and *Wedekindella*. *American Journal of Science*, series 5, 20:357–364, text-fig. 1.
- Dunbar, C.O., and J.W. Skinner
1931. New Fusulinids from the Permian of West Texas. *American Journal of Science*, 22:252–268, plates 1–3.
1936. Systematic Descriptions. In C.O. Dunbar, J.W. Skinner, and R.E. King, editors, *Dimorphism in Permian Fusulines. University of Texas Bulletin*, 3501:179–185, plates 1–3.
1937. Permian Fusulinidae of Texas: The Geology of Texas, Part 2. *University of Texas Bulletin*, 3701:519–825, plates 42–81.
- Erk, A.S.
1942 (“1941”). Sur la présence du genre *Codonofusiella* Dunbar et Skinner dans le Permien de Bursa (Turquie). *Eclogae Geologicae Helveticae*, 34:243–253, plates 12–14. [Date on title page is 1941; actually published in 1942.]
- Furnish, W.M.
1966. Ammonoids of the Upper Permian *Cyclolobus*-Zone. *Neues Jahrbuch für Geologie und Paläontologie, Abhandlungen*, 125: 265–296, plates 23–26.
1973. Permian Stage Names. In A. Logan and L.V. Hills, editors, *The Permian and Triassic Systems and Their Mutual Boundary. Canadian Society of Petroleum Geologists, Memoir*, 2:522–548.
- Glenister, B.F., D.W. Boyd, W.M. Furnish, R.E. Grant, M.T. Harris, H. Kozur, L.L. Lambert, W.W. Nassichuk, N.D. Newell, L.C. Pray, C. Spinosa, B.R. Wardlaw, G.L. Wilde, and T.E. Yancey
1992. The Guadalupian: Proposed International Standard for a Middle Permian Series. *International Geology Review*, 34(9):857–888.
- Haneef, Mohammad
1993. Lithofacies and Depositional Environments of Altuda, Capitan, and Tessey Formations (Permian), Glass Mountains, West Texas. 208 pages. Unpublished master's thesis, Sul Ross State University, Alpine, Texas.
- King, P.B.
1931 (“1930”). The Geology of the Glass Mountains, Texas, Part I: Descriptive Geology. *University of Texas Bulletin*, 3038: 167 pages, 15 plates. [Date on title page is 1930; actually published in 1931.]
1948. Geology of the Southern Guadalupe Mountains, Texas. *United States Geological Survey Professional Paper*, 215: 183 pages, 23 plates.
- Kling, S.A.
1960. Permian Fusulinids from Guatemala. *Journal of Paleontology*, 34(4):637–655, plates 78–82.
- Kobayashi, M.
1956. On Some New Species of *Rauserella* from Mt. Ibuki, Shiga Prefecture, Central Japan. *Transaction and Proceedings of the Paleontological Society of Japan*, new series, 23:226, plate 32.
- Lee, J.S.
1934 (“1933”). Taxonomic Criteria of Fusulinidae with Notes on Seven New Permian Genera. *Academia Sinica, Memoirs of the Geological Institute*, 14:1–32, plates 1–5, figures 1–9. [Date on title page is 1933; actually published in 1934.]

- Lin, G.W.
1982. Order Fusulinida. In Nanjing Institute of Geology and Mineral Resources, editors, *Paleontological Atlas of Eastern China, Later Paleozoic Fascicle*, 2:91-92, plates 25, 26. Beijing: Geological Publishing House. [In Chinese.]
- Lloyd, A.J.
1963. Fusulinids from the Zinnar Formation (Lower Permian) of Northern Iraq. *Journal of Paleontology*, 37(4):889-899, plates 116-120.
- Miklukho-Maklay, A.D.
1949. *Verkhnepaleozoyskie fusulinidy Sredney Azii, Fregana, Darvaz i Pamir* [Upper Paleozoic Fusulinids of Central Asia—Ferghana, Darvaz and Pamir]. Pages 1-111, 14 plates. Leningrad: Leningradskiy Gosudarstvennyy Universitet. [In Russian.]
- Miklukho-Maklay, K.V.
1954. *Foraminifery verkhnepermiskikh otlozheniy Severnogo Kavkaza* [Foraminifera of the Upper Permian Deposits of the Northern Caucasus]. 162 pages, 19 plates. Moscow: Trudy, Vsesoyuznogo Nauchno-Issledovatel'skogo Geologicheskogo Instituta (VSEGEI). [In Russian.]
- Möller, V. von
1878. Die spiral-gewundenen Foraminiferen des Russischen Kohlenkalks. *Mémoires de l'Académie Impériale des Sciences de St. Pétersbourg, Classe Sciences, Mathématiques, Physiques et Naturelles, series 7*, 25(9): 147 pages, 15 plates, 6 figures.
- Newell, N.D., J.K. Rigby, A.G. Fischer, A.J. Whiteman, J.E. Hickox, and J.S. Bradley
1953. *The Permian Reef Complex of the Guadalupe Mountains Region, Texas and New Mexico: A Study in Paleogeology*. 236 pages. San Francisco: W.H. Freeman and Company.
- Ozawa, Y.
1925. On the Classification of Fusulinidae. *Journal of the College of Sciences, Imperial University of Tokyo*, 45(4): 26 pages, 4 plates.
1927. Stratigraphical Studies of the Fusulina Limestone of Akasaka, Province of Mino. *Journal of the College of Sciences, Imperial University of Tokyo, Section 2 (Geology)*, 2(3):121-164, plates 34-46.
- Rohr, D.M., B.R. Wardlaw, S.H. Rudine, A.J. Hall, R.E. Grant, and M. Haneef
1991. Guidebook to the Guadalupian Symposium. In B.R. Wardlaw, R.E. Grant, and D.M. Rohr, editors, *Proceedings of the Guadalupian Symposium, March 13-15, 1991, Sul Ross State University, Alpine, Texas*, pages 18-111.
- Ross, C.A.
1959. The Wolfcamp Series (Permian) and New Species of Fusulinids, Glass Mountains, Texas. *Journal of the Washington Academy of Sciences*, 49(9):299-316, plates 1-4.
1960. Fusulinids from the Hess Member of the Leonard Series (Permian), Glass Mountains, Texas. *Contributions from the Cushman Foundation for Foraminiferal Research*, 11(4):117-133, plates 17-21.
1962. Fusulinids from the Leonard Formation (Permian), West Glass Mountains, Texas. *Contributions from the Cushman Foundation for Foraminiferal Research*, 13(1):1-21, plates 1-6.
1963a. Standard Wolfcampian Series (Permian), Glass Mountains, Texas. *Geological Society of America, Memoir*, 88: 205 pages, 29 plates.
1963b. Fusulinids from the Word Formation (Permian), Glass Mountains, Texas. *Contributions from the Cushman Foundation for Foraminiferal Research*, 14(1):17-31, plates 3-5.
1964. Two Significant Fusulinid Genera from the Word Formation (Permian), Texas. *Journal of Paleontology*, 38(2):311-315, plate 50.
1986. Paleozoic Evolution of Southern Margin of Permian Basin. *Bulletin of the Geological Society of America*, 97(5):536-554.
- Ross, C.A., and J.P. Ross
1985. Late Paleozoic Depositional Sequences are Synchronous and Worldwide. *Geology*, 13(3):194-197.
1987. Late Paleozoic Sea Levels and Depositional Sequences. In C.A. Ross and D. Haman, editors, *Timing and Depositional History of Eustatic Sequences: Constraints on Seismic Stratigraphy. Cushman Foundation for Foraminiferal Research, Special Publication*, 24:137-150.
- Sheng, J.Z.
1962. On the Occurrence of Polydiexodina Fauna from Tunglu, Western Chekiang. *Acta Palaeontologica Sinica*, 3(3):316-321, plates 1, 2. [In Chinese and English.]
1963. Permian Fusulinids of Kwangsi, Kueichow and Szechuan. *Palaeontologica Sinica, new series B*(10): 247 pages, 35 plates. [In Chinese and English.]
- Skinner, J.W.
1931. Primitive Fusulinids of the Mid-Continent Region. *Journal of Paleontology*, 5:253-259, plate 30.
1940. Upper Paleozoic Section of Chinati Mountains, Presidio County, Texas. *Bulletin of the American Association of Petroleum Geologists*, 24(1):180-188.
- Skinner, J.W., and G.L. Wilde
1954. The Fusulinid Subfamily Boultoniinae. *Journal of Paleontology*, 28(4):434-444, plates 42-45.
1955. New Fusulinids from the Permian of West Texas. *Journal of Paleontology*, 29(6):927-940, plates 89-95.
- Staff, H. von, and R. Wedekind
1910. Der Oberkarbon Foraminiferensapropelit Spitzbergens. *Bulletin of the Geological Institute of the University of Upsala*, 10:81-123, plates 2-4.
- Thompson, M.L.
1946. Permian Fusulinids from Afghanistan. *Journal of Paleontology*, 20(2):140-157, plates 23-26.
1948. Studies of American Fusulinids. *University of Kansas Paleontological Contributions, Protozoa, Article 1*: 184 pages, 38 plates.
- Thompson, M.L., and C.L. Foster
1937. Middle Permian Fusulinids from Szechuan, China. *Journal of Paleontology*, 11:126-144, plates 23-25.
- Thompson, M.L., and A.K. Miller
1949. Permian Fusulinids and Cephalopods from the Vicinity of the Maracaibo Basin in Northern South America. *Journal of Paleontology*, 23(1):1-24, plates 1-8.
- Thompson, M.L., and H.E. Wheeler
1946. Permian Fusulinids of Northern California. In M.L. Thompson, H.E. Wheeler, and J.C. Hazzard, *Permian Fusulinids of California. Geological Society of America, Memoir*, 17:21-36, plates 1-9.
- Toumanskaya, O.G.
1953. *O verkhnepermiskikh fusulinidakh yuzhno-Ussuriyskogo Kraya* [Concerning Upper Permian Fusulinids in the South Ussuri Territory]. Pages 1-56, plates 1-15. Moscow: Trudy, Vsesoyuznogo Nauchno-Issledovatel'skogo Geologicheskogo Instituta (VSEGEI). [In Russian.]
- Udden, J.A.
1917. Notes on the Geology of the Glass Mountains. *University of Texas Bulletin*, 1753: 59 pages.
- Wardlaw, B.R., and R.E. Grant
1987. Conodont Biostratigraphy of the Cathedral Mountain and Road Canyon Formations, Glass Mountains, West Texas. In D. Cromwell and L.J. Mazzullo, editors, *The Leonardian Facies in W. Texas and S.E. New Mexico and Guidebook to the Glass Mountains, West Texas. Society of Economic Paleontologists and Mineralogists, Permian Basin Section, Publication*, 87-27:63-66.
- Wilde, G.L.
1975. Fusulinid-Defined Permian Stages. In J.M. Cys and D.F. Toomey, editors, *Permian Exploration, Boundaries, and Stratigraphy. Society of Economic Paleontologists and Mineralogists, West Texas Geological Society and Permian Basin Section, Publication*, 75-65:67-83.

- 1986a. Stratigraphic Relationship of the San Andres and Cutoff Formations, Northern Guadalupe Mountains, New Mexico and Texas. In G.E. Moore and G.L. Wilde, editors, Lower and Middle Guadalupian Facies, Stratigraphy, and Reservoir Geometries, San Andres/Grayburg Formations, Guadalupe Mountains, New Mexico and Texas. *Society of Economic Paleontologists and Mineralogists, Permian Basin Section, Publication*, 86-25:49-63, plates 1-5.
- 1986b. An Important Occurrence of Early Guadalupian (Roadian) Fusulinids from the Cutoff Formation, Western Guadalupe Mountains, Texas. In G.E. Moore and G.L. Wilde, editors, Lower and Middle Guadalupian Facies, Stratigraphy, and Reservoir Geometries, San Andres/Grayburg Formations, Guadalupe Mountains, New Mexico and Texas. *Society of Economic Paleontologists and Mineralogists, Permian Basin Section, Publication*, 86-25:65-68, plate 1.
1990. Practical Fusulinid Zonation: The Species Concept; with Permian Basin Emphasis. *West Texas Geological Society, Bulletin*, 29(7):5-34.
- Wilde, G.L., and R.G. Todd
1968. Guadalupian Biostratigraphic Relationships and Sedimentation in the Apache Mountain Region, West Texas. In B.A. Silver, editor, Guadalupian Facies, Apache Mountains Area, West Texas. *Society of Economic Paleontologists and Mineralogists, Permian Basin Section, Publication*, 68-11:10-31.
- Xiao, W.M., H.D. Wang, L.X. Zhang, and W.L. Dong
1986. *Early Permian Stratigraphy and Faunas in Southern Guizhou*. 364 pages, 40 plates. Guiyang, China: The People's Publishing House of Guizhou. [In Chinese.]
- Yang, Z.D.
1985. Restudy of Fusulinids from the "Maokou Limestone" (Permian) at Datieguan, Langdai, Guizhou. *Acta Micropaleontologica Sinica*, 2(4):307-335. [In Chinese and English.]
1992. Fusulinid Paleontology and Biostratigraphy of the Middle Permian (Guadalupian) Strata of the Glass Mountains and Del Norte Mountains, West Texas. 223 pages. Unpublished doctoral dissertation, Texas A&M University, College Station, Texas.
- Yang, Z.D., and T.E. Yancey
1990. Middle Permian Fusulinids in the Glass Mountains and the Del Norte Mountains, West Texas. [Abstract.] *Geological Society of America, Abstracts with Programs*, 22(1):36.
- Zhang, L.X.
1957. On the Occurrence of *Parafusulina rothi* in the Permian-Carboniferous Rocks of Xilinguole, Inner Mongolia. *Acta Palaeontologica Sinica*, 5(3):452-455. [In Chinese.]
- Zhang, L.X., L. Rui, J.P. Zhou, Z.T. Liao, C.Y. Wang, K.L. Wang, J.M. Zhao, Y.J. Wang, and F.S. Xia
1988. The Permian Biostratigraphy of Jiangsu Region. In *Sinian-Triassic Biostratigraphy of the Lower Yangtze Peneplatform in Jiangsu Region*. Pages 263-313. Beijing: Science Press. [In Chinese.]
- Zhang, Z.Q.
1984. The Permian System in South China. *Newsletters on Stratigraphy*, 13:156-174. [In Chinese.]

Plates 9-1-9-17

PLATE 9-1

FIGURES 1-7.—*Rausserella erratica* Dunbar: 1, axial section, $\times 25$, hypotype, USNM 482975, Road Canyon Formation, sample 8-28; 2, axial section, $\times 25$, hypotype, USNM 482976, Road Canyon Formation, sample 2-68; 3, tangential section, $\times 25$, hypotype, USNM 482977, Road Canyon Formation, sample 2-R6; 4, broken axial section, $\times 40$, hypotype, USNM 482978, Altuda Formation, sample 6-BA13; 5, axial section, $\times 40$, hypotype, USNM 482979, Road Canyon Formation, sample 2-R6; 6, tangential section near proloculus, $\times 40$, hypotype, USNM 482980, Road Canyon Formation, sample 2-68; 7, tangential section near proloculus, $\times 40$, hypotype, USNM 482981, Road Canyon Formation, sample 2-R6.

FIGURES 8-16.—*Rausserella minima*, new species: 8, oblique section, $\times 25$, paratype, USNM 482982, Road Canyon Formation, sample 2-68; 9, axial section, $\times 40$, paratype, USNM 482983, Altuda Formation, sample 6-BA11; 10, axial section, $\times 25$, paratype, USNM 482984, Road Canyon Formation, sample 2-R5; 11, oblique section, $\times 25$, paratype, USNM 482985, Road Canyon Formation, sample 2-R6; 12, axial section, $\times 25$, paratype, USNM 482986, Road Canyon Formation, sample 2-68; 13, axial section, $\times 40$, holotype, USNM 482987, Road Canyon Formation, sample 2-R6; 14, partial axial section, $\times 40$, paratype, USNM 482988, Road Canyon Formation, sample 6-BA3; 15, partial axial section showing inner volutions, $\times 60$, paratype, USNM 482989, Road Canyon Formation, sample 2-68; 16, axial section showing inner volutions, $\times 60$, paratype, USNM 482990, Road Canyon Formation, sample 2-68.

FIGURE 17.—*Staffella lacunosa* Dunbar and Skinner: 17, axial section, $\times 30$, hypotype, USNM 483026, Word Formation, sample 8-32.

FIGURE 18.—*Schubertella* cf. *S. melonica* Dunbar and Skinner: 18, tangential section near proloculus, $\times 40$, hypotype, USNM 483050, Road Canyon Formation, sample 2-68.

FIGURE 19.—*Schubertella* sp.: 19, slightly oblique axial section near proloculus, $\times 40$, USNM 483051, Road Canyon Formation, sample 2-R2.

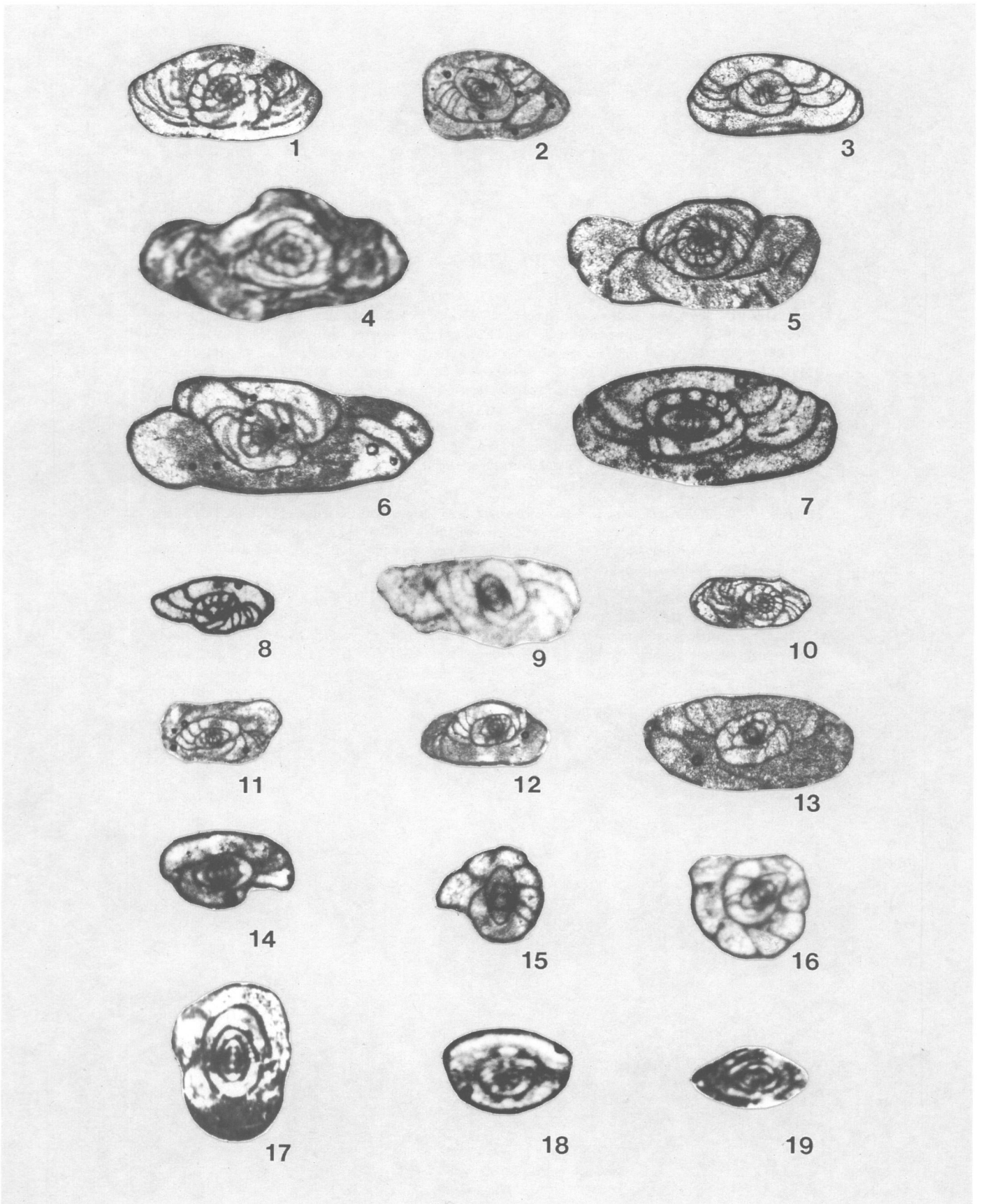


PLATE 9-2

FIGURES 1–16.—*Reichelina lamarensis* Skinner and Wilde: 1–5, axial sections, ×40, hypotypes, USNM 483009–483013, Altuda Formation, sample 10-204; 6, tangential section near proloculus, ×40, hypotype, USNM 483014, Altuda Formation, sample 10-204; 7, 8, axial sections, ×40, hypotypes, USNM 483015, 483016, Altuda Formation, sample 10-205; 9, axial section, ×40, hypotype, USNM 483017, Altuda Formation, sample 10-205; 10, axial section, ×40, hypotype, USNM 483018, Altuda Formation, sample 6-BA10; 11, axial section, ×40, hypotype, USNM 483019, Altuda Formation, sample 6-BA11; 12, oblique section through proloculus, ×40, hypotype, USNM 483020, Altuda Formation, sample 10-205; 13, axial section, ×40, hypotype, USNM 483021, Altuda Formation, sample 6-BA11; 14, 15, parallel sections near proloculus, ×40, hypotypes, USNM 483022, 483023, Altuda Formation, sample 6-BA3; 16, sagittal section, ×40, hypotype, USNM 483024, Altuda Formation, sample 10-204.

FIGURES 17–20.—*Reichelina bengensis*, new species: 17, axial section, ×40, paratype, USNM 482991, Altuda Formation, sample 6-BA8; 18, axial section, ×40, holotype, USNM 482992, Altuda Formation, sample 10-202; 19, axial section, ×40, paratype, USNM 482993, Altuda Formation, sample 6-BA10; 20, sagittal section, ×40, paratype, USNM 482994, Altuda Formation, sample 10-202.

FIGURES 21–27.—*Reichelina birdensis*, new species: 21, axial section, ×40, paratype, USNM 482995, Altuda Formation, sample 10-205; 22, axial section, ×40, paratype, USNM 482996, Altuda Formation, sample 6-BA10; 23, slightly oblique parallel section near proloculus, ×40, paratype, USNM 482997, Altuda Formation, sample 10-202; 24, axial section, ×40, holotype, USNM 482998, Altuda Formation, sample 10-205; 25, sagittal section, ×40, paratype, USNM 482999, Altuda Formation, sample 6-BA10; 26, axial section, ×40, paratype, USNM 483000, Altuda Formation, sample 10-202; 27, sagittal section, ×40, paratype, USNM 483001, Altuda Formation, sample 6-BA5.

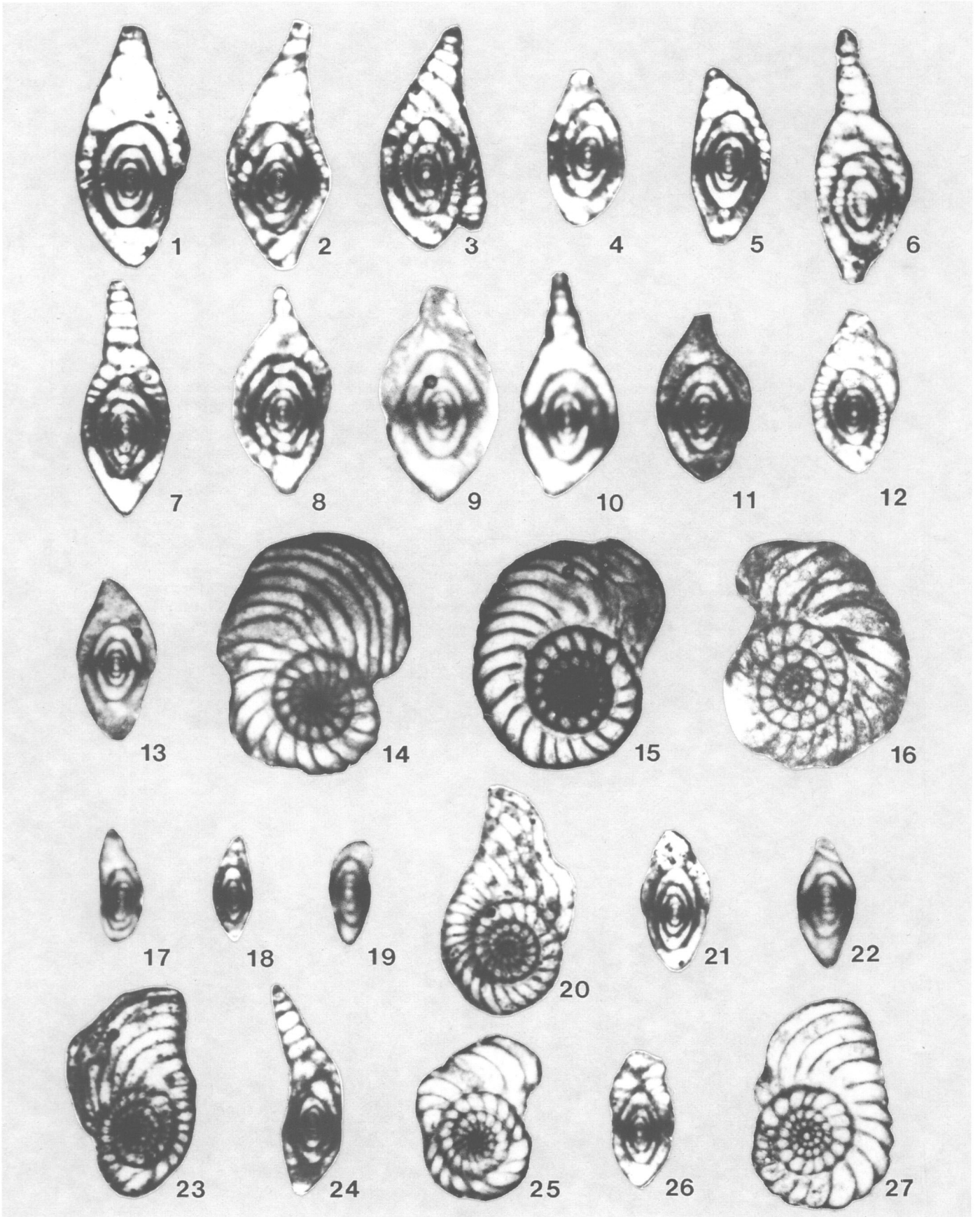


PLATE 9-3

FIGURES 1-6, 11.—*Lantschichites splendens* (Skinner and Wilde): 1, axial section, $\times 30$, hypotype, USNM 483032, Altuda Formation, sample 6-110; 2, axial section, $\times 30$, hypotype, USNM 483033, Altuda Formation, sample 6-S2; 3, slightly oblique axial section, $\times 30$, hypotype, USNM 483034, Altuda Formation, sample 6-BR4; 4, axial section, $\times 30$, hypotype, USNM 483035, Altuda Formation, sample 6-S2; 5, parallel section near proloculus, $\times 30$, hypotype, USNM 483036, Altuda Formation, sample 10-204; 6, sagittal section, $\times 30$, hypotype, USNM 483037, Altuda Formation, sample 10-204; 11, parallel section, $\times 50$, hypotype, USNM 483028, Altuda Formation, sample 6-BR4.

FIGURES 7-9.—*Codonofusiella paradoxica* Dunbar and Skinner: 7, axial section, $\times 30$, hypotype, USNM 483029, Altuda Formation, sample 6-110; 8, parallel section near proloculus, $\times 40$, hypotype, USNM 483030, Altuda Formation, sample 10-202; 9, tangential section near proloculus, $\times 30$, hypotype, USNM 483031, Altuda Formation, sample 10-208.

FIGURE 10.—*Codonofusiella extensa* Skinner and Wilde: 10, axial section, $\times 30$, hypotype, USNM 483027, Altuda Formation, sample 6-120.

FIGURES 12-15.—*Paradoxiella pratti* Skinner and Wilde: 12, fragment of uncoiled final whorl, $\times 60$, hypotype, USNM 483046, Altuda Formation, sample 10-204; 13, partial sagittal section, $\times 40$, hypotype, USNM 483047, Altuda Formation, sample 10-204; 14, partial tangential section, $\times 40$, hypotype, USNM 483048, Altuda Formation, sample 10-204; 15, tangential section, $\times 40$, hypotype, USNM 483049, Altuda Formation, sample 10-204.

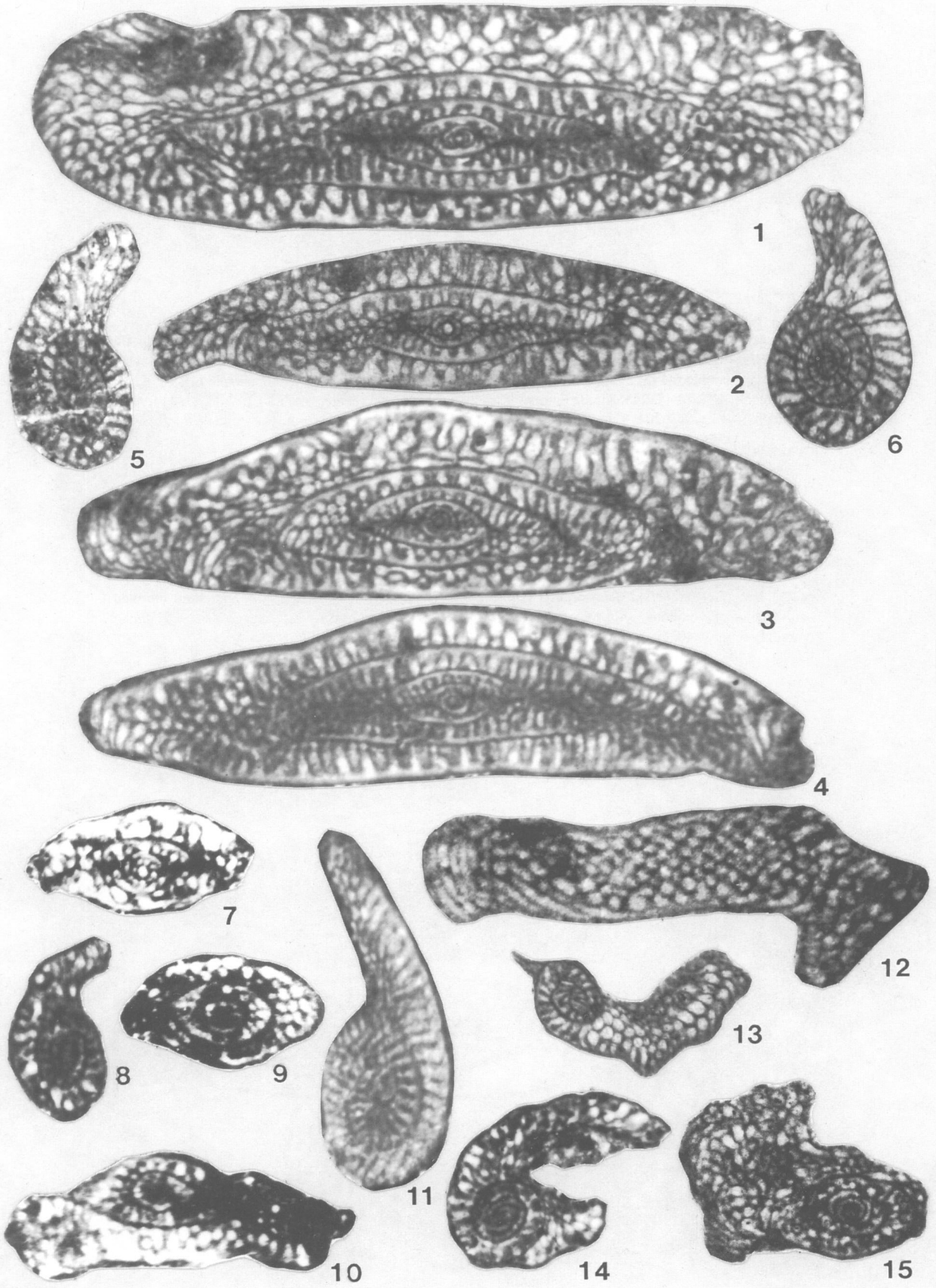


PLATE 9-4

FIGURES 1-8.—*Lantschichites* sp.: 1, axial section, $\times 30$, USNM 483038, Altuda Formation, sample 10-204; 2, axial section, $\times 30$, USNM 483039, Altuda Formation, sample 6-BR4; 3, axial section, $\times 30$, USNM 483040, Altuda Formation, sample 6-145; 4, tangential section near proloculus, $\times 30$, USNM 483041, Altuda Formation, sample 6-145; 5, axial section, $\times 30$, USNM 483042, Altuda Formation, sample 6-BR4; 6, axial section, $\times 30$, USNM 483043, Altuda Formation, sample 6-120; 7, parallel section, $\times 30$, USNM 483044, Altuda Formation, sample 10-204; 8, parallel section, $\times 30$, USNM 483045, Altuda Formation, sample 10-204.

FIGURES 9-13.—*Reichelina haneefi*, new species: 9, sagittal section, $\times 50$, paratype, USNM 483004, Altuda Formation, sample 6-BA3; 10, axial section, $\times 50$, holotype, USNM 483005, Altuda Formation, sample 6-BA2; 11, axial section, $\times 50$, paratype, USNM 483006, Altuda Formation, sample 6-BA10; 12, tangential section near proloculus, $\times 50$, paratype, USNM 483007, Altuda Formation, sample 6-BA10; 13, axial section, $\times 50$, paratype, USNM 483008, Altuda Formation, sample 6-BA11.

FIGURE 14.—*Reichelina* sp.: 14, axial section, $\times 45$, USNM 483025, Altuda Formation, sample 6-BA3.

FIGURES 15, 16.—*Reichelina delawarensis* (Dunbar and Skinner): 15, axial section of immature individual showing inner volutions, $\times 40$, hypotype, USNM 483002, Altuda Formation, sample 10-206; 16, oblique parallel section, $\times 40$, hypotype, USNM 483003, Altuda Formation, sample 9-6.

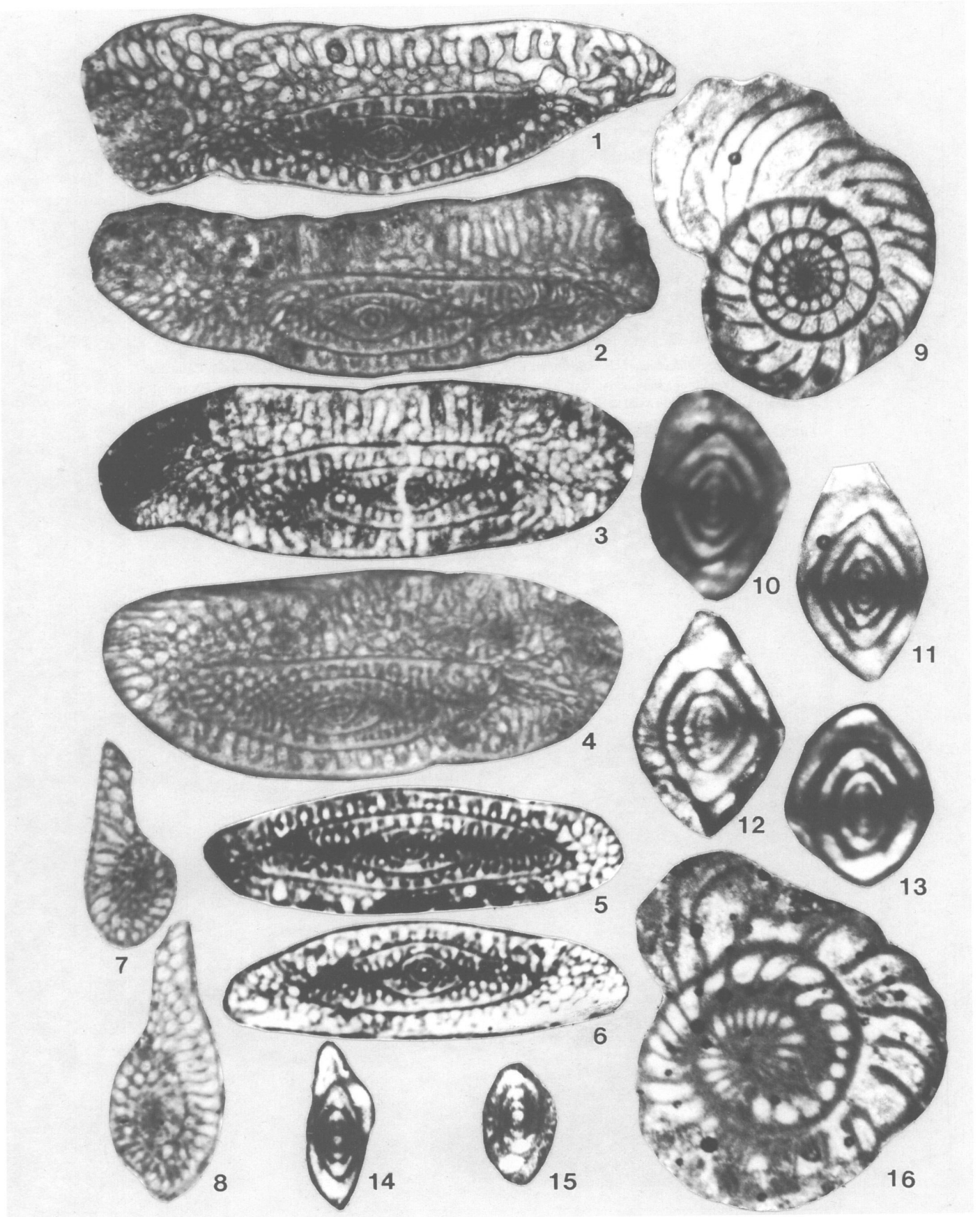


PLATE 9-5

FIGURES 1, 2.—*Parafusulina durhami* Thompson and Miller: 1, 2, axial sections, ×10, hypotypes, USNM 483069, 483070, Cathedral Mountain Formation, sample 1-60.

FIGURES 3-5.—*Parafusulina* cf. *P. biturbinata* Kling: 3, oblique axial section, ×10, USNM 483061, Cathedral Mountain Formation, sample 1-60; 4, axial section, ×10, USNM 483062, Cathedral Mountain Formation, sample 1-60; 5, oblique axial section, ×10, USNM 483063, Cathedral Mountain Formation, sample 1-60.

FIGURES 6, 7.—*Parafusulina* cf. *P. guatemalaensis* Dunbar: 6, slightly oblique axial section, ×10, USNM 483079, Road Canyon Formation, sample 2-R6; 7, axial section, ×10, USNM 483080, Road Canyon Formation, sample 2-R5.

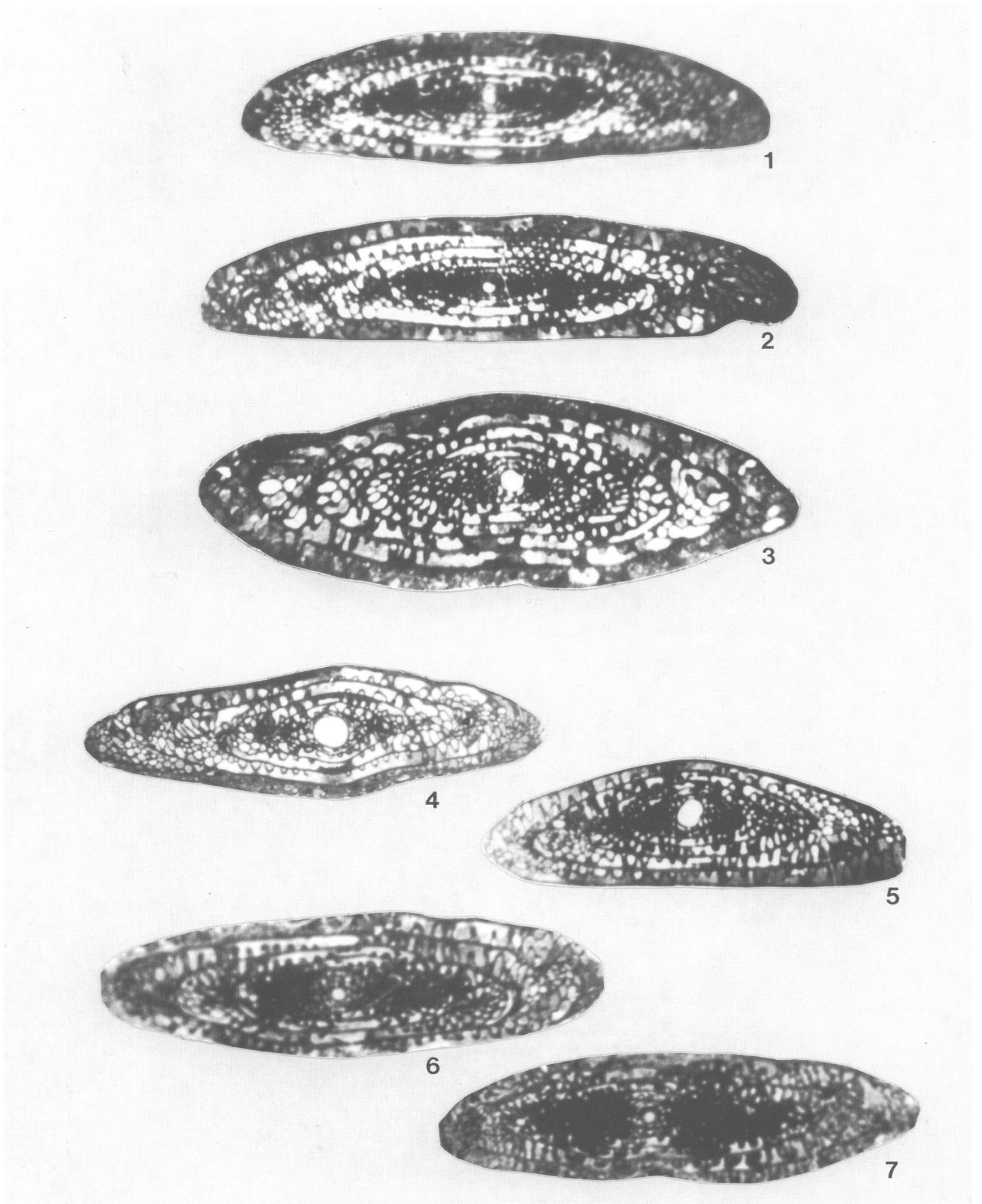


PLATE 9-6

FIGURES 1-5.—*Parafusulina splendens* Dunbar and Skinner: 1-3, axial sections, $\times 10$, hypotypes, USNM 483106-483108, Road Canyon Formation, sample 2-R3; 4, axial section, $\times 10$, hypotype, USNM 483109, Road Canyon Formation, sample 2-R16; 5, axial section partially obscured by dolomitization, $\times 10$, hypotype, USNM 483110, Road Canyon Formation, sample 2-R3.

FIGURE 6.—*Parafusulina* cf. *P. bakeri* Dunbar and Skinner: 6, axial section, $\times 10$, USNM 483060, Road Canyon Formation, sample 2-68.

FIGURES 7, 8.—*Yangchienia iniqua* Lee: 7, tangential section showing massive chomata, $\times 40$, hypotype, USNM 483052, Road Canyon Formation, sample 2-68; 8, axial section, $\times 40$, hypotype, USNM 483053, Road Canyon Formation, sample 2-68.

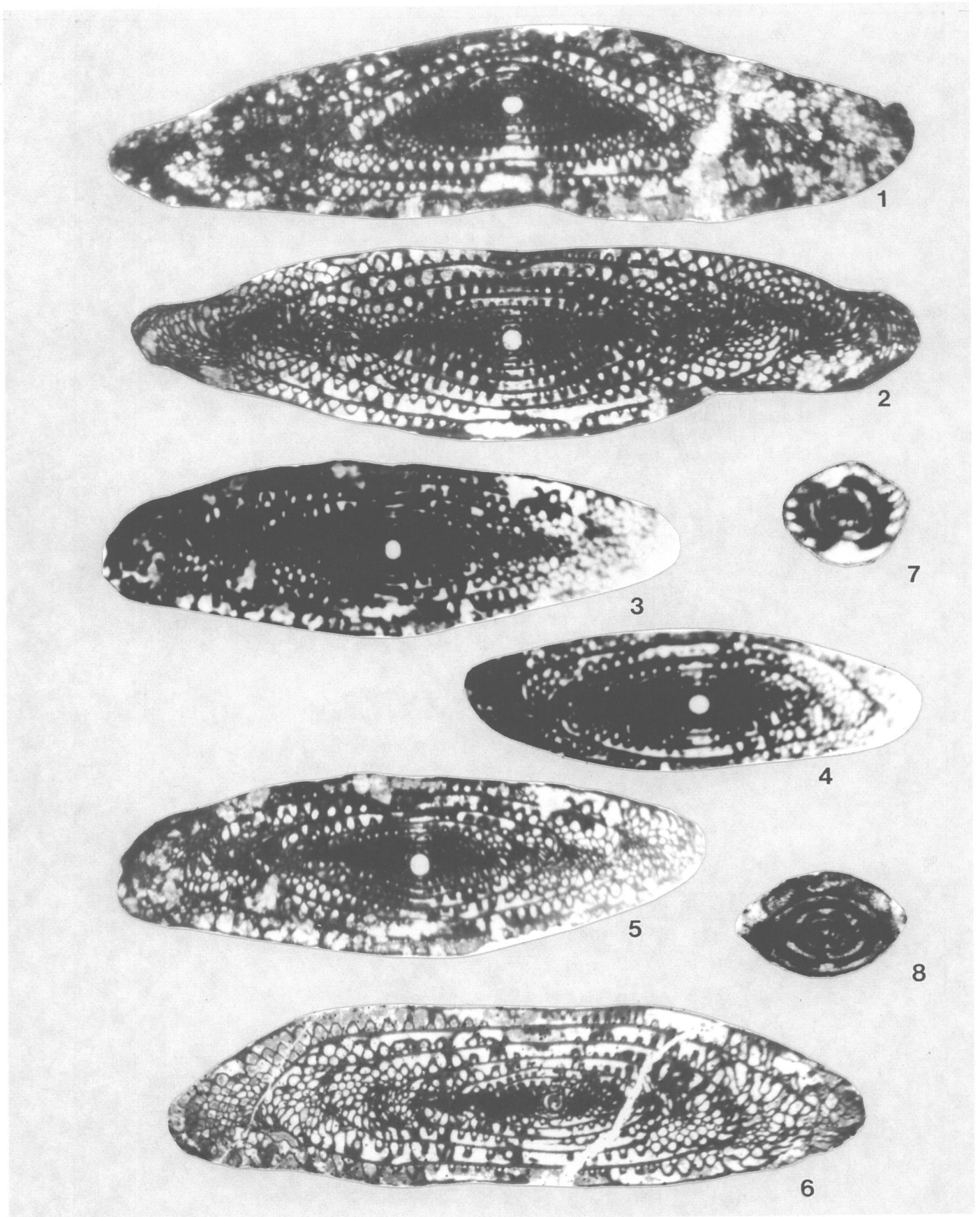


PLATE 9-7

FIGURES 1-4.—*Parafusulina rothi* Dunbar and Skinner: 1, 2, axial sections, $\times 10$, hypotypes, USNM 483096, 483097, Road Canyon Formation, sample 2-76; 3, slightly oblique axial section, $\times 10$, hypotype, USNM 483098, Road Canyon Formation, sample 2-R11; 4, axial section of immature individual, $\times 10$, hypotype, USNM 483099, Road Canyon Formation, sample 2-76.

FIGURES 5-7.—*Parafusulina ironensis* Ross: 5, partial axial section of immature individual, $\times 10$, hypotype, USNM 483081, Road Canyon Formation, sample 7-55; 6, axial section, $\times 10$, hypotype, USNM 483082, Road Canyon Formation, sample 1-62; 7, slightly oblique axial section, $\times 10$, hypotype, USNM 483083, Road Canyon Formation, sample 1-63.

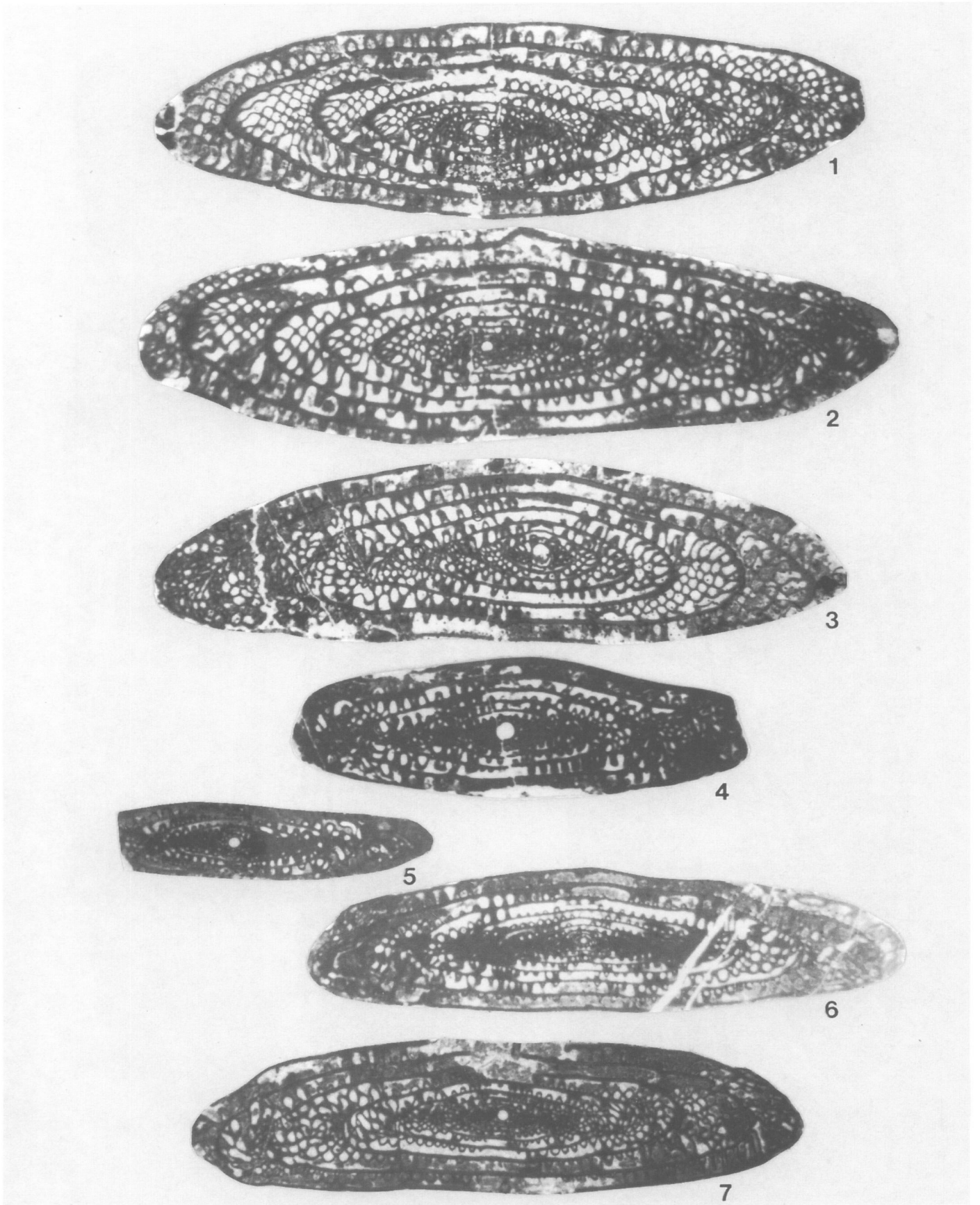


PLATE 9-8

FIGURES 1-3.—*Parafusulina glassensis*, new species: 1, axial section, $\times 10$, holotype, USNM 483076, Road Canyon Formation, sample 2-72; 2, axial section, $\times 10$, paratype, USNM 483077, Road Canyon Formation, sample 2-R10; 3, partial axial section, $\times 10$, paratype, USNM 483078, Road Canyon Formation, sample 2-R8.

FIGURES 4, 5.—*Parafusulina marathonensis*, new species: 4, slightly oblique axial section, $\times 10$, paratype, USNM 483090, Road Canyon Formation, sample 8-26; 5, axial section, $\times 10$, holotype, USNM 483091, Word Formation, sample 3-23.

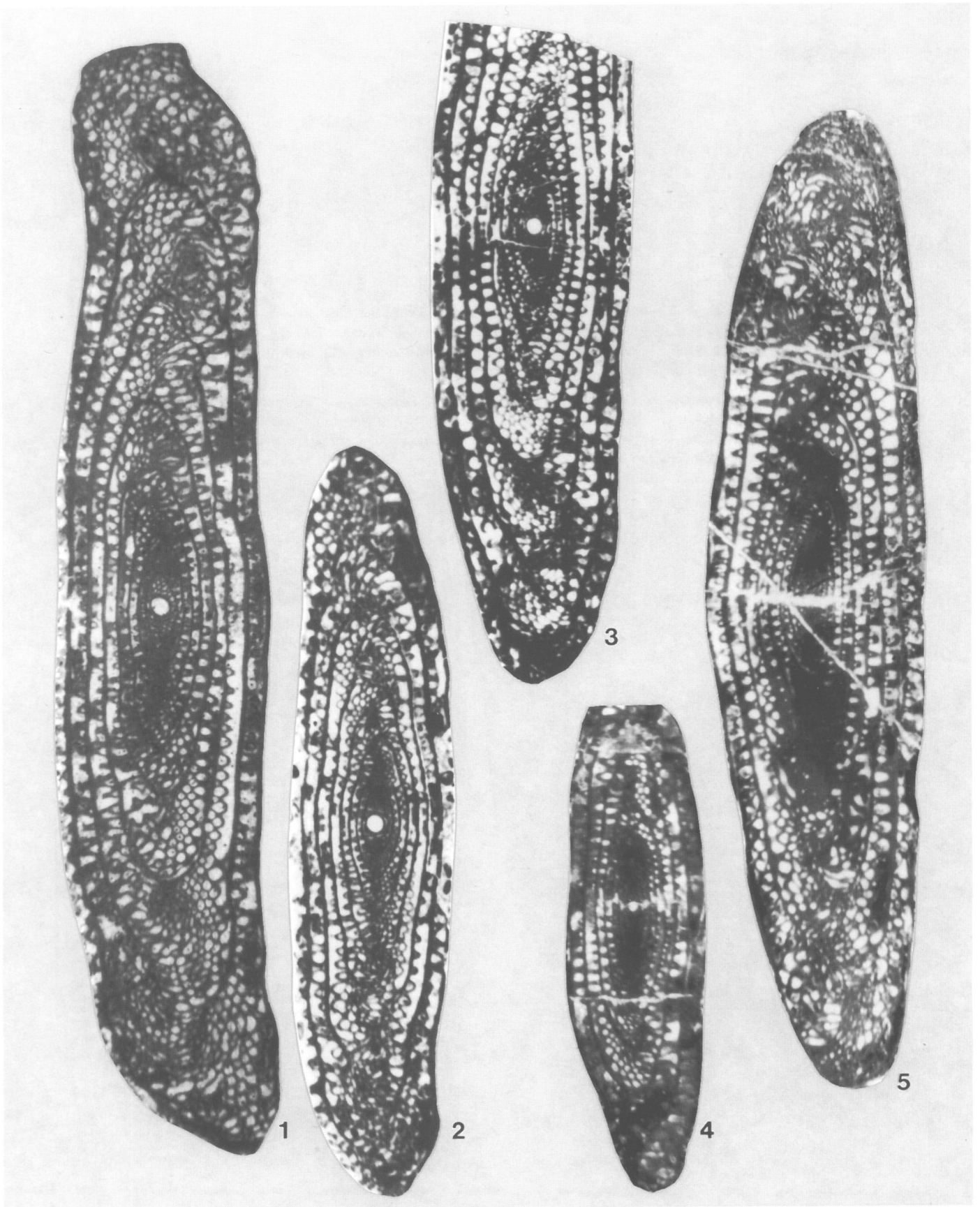


PLATE 9-9

FIGURES 1-3.—*Reichelina delawarensis* (Dunbar and Skinner): 1, tangential section, $\times 40$, hypotype, USNM 483132, Altuda Formation, sample 9-6; 2, partial, slightly oblique axial section, $\times 40$, hypotype, USNM 483133, Altuda Formation, sample 9-6; 3, slightly oblique axial section, $\times 40$, hypotype, USNM 483134, Altuda Formation, sample 9-6.

FIGURES 4-7.—*Parafusulina trumpyi* Thompson and Miller: 4, axial section of immature individual, $\times 10$, hypotype, USNM 483115, Road Canyon Formation, sample 7-53; 5, partial axial section, $\times 10$, hypotype, USNM 483116, Road Canyon Formation, sample 2-R19; 6, slightly oblique axial section, $\times 10$, hypotype, USNM 483117, Road Canyon Formation, sample 2-R20; 7, axial section, $\times 10$, hypotype, USNM 483118, Road Canyon Formation, sample 1-66.

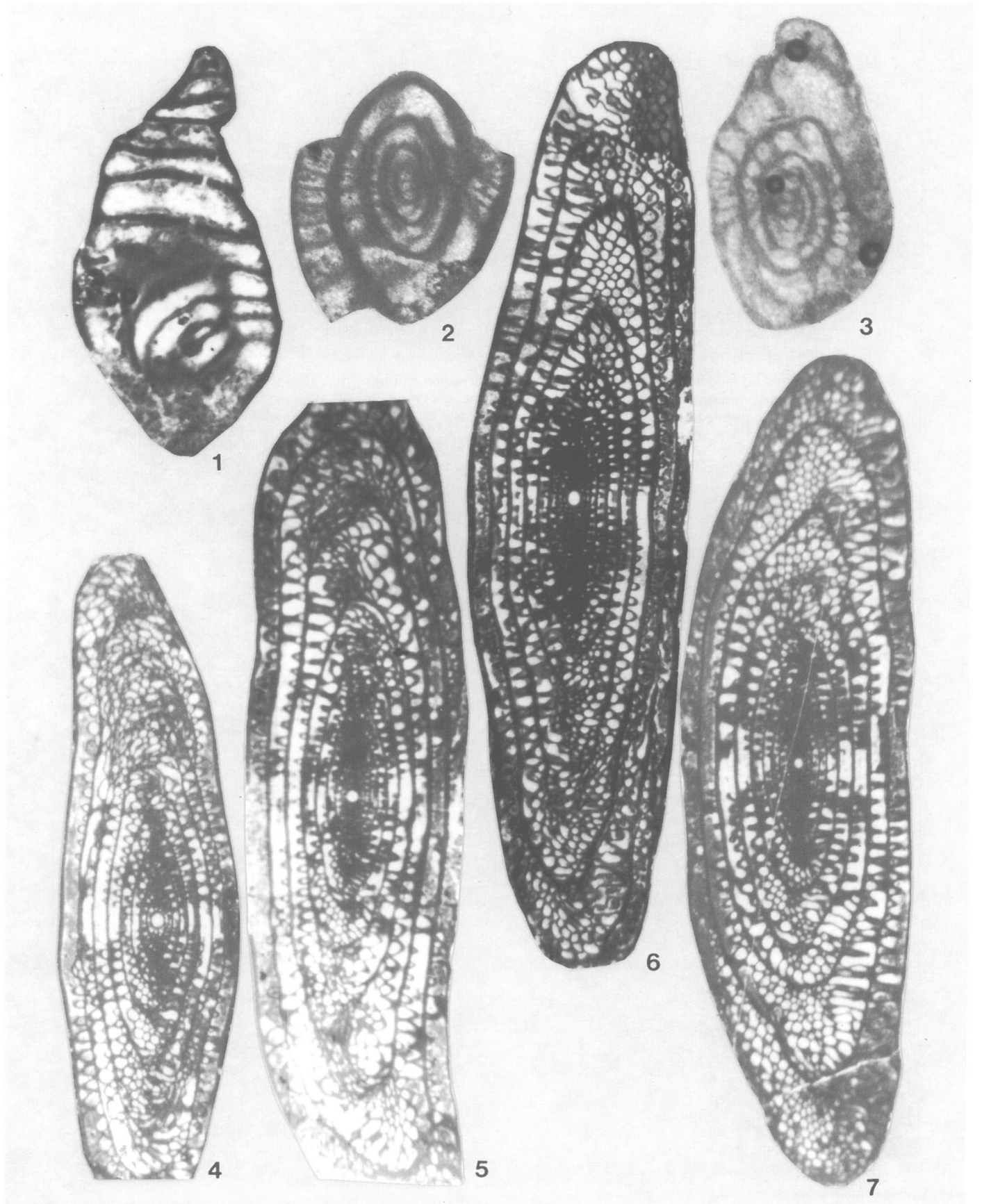


PLATE 9-10

FIGURES 1, 2.—*Parafusulina fountaini* Dunbar and Skinner: 1, axial section, $\times 10$, hypotype, USNM 483074, Road Canyon Formation, sample 2-70; 2, axial section, $\times 10$, hypotype, USNM 483075, Road Canyon Formation, sample 2-R3.

FIGURES 3-5.—*Parafusulina rudinei*, new species: 3, axial section, $\times 10$, holotype, USNM 483100, Road Canyon Formation, sample 7-59; 4, axial section, $\times 10$, paratype, USNM 483101, Road Canyon Formation, sample 1-66; 5, slightly oblique axial section, $\times 10$, paratype, USNM 483102, Road Canyon Formation, sample 8-28.

FIGURES 6, 7.—*Parafusulina alpinensis*, new species: 6, axial section, $\times 10$, holotype, USNM 483054, Road Canyon Formation, sample 8-24; 7, axial section, $\times 10$, paratype, USNM 483055, Road Canyon Formation, sample 8-24.

FIGURE 8.—*Parafusulina marathonensis*, new species: 8, axial section, $\times 10$, paratype, USNM 483092, Road Canyon Formation, sample 8-26.

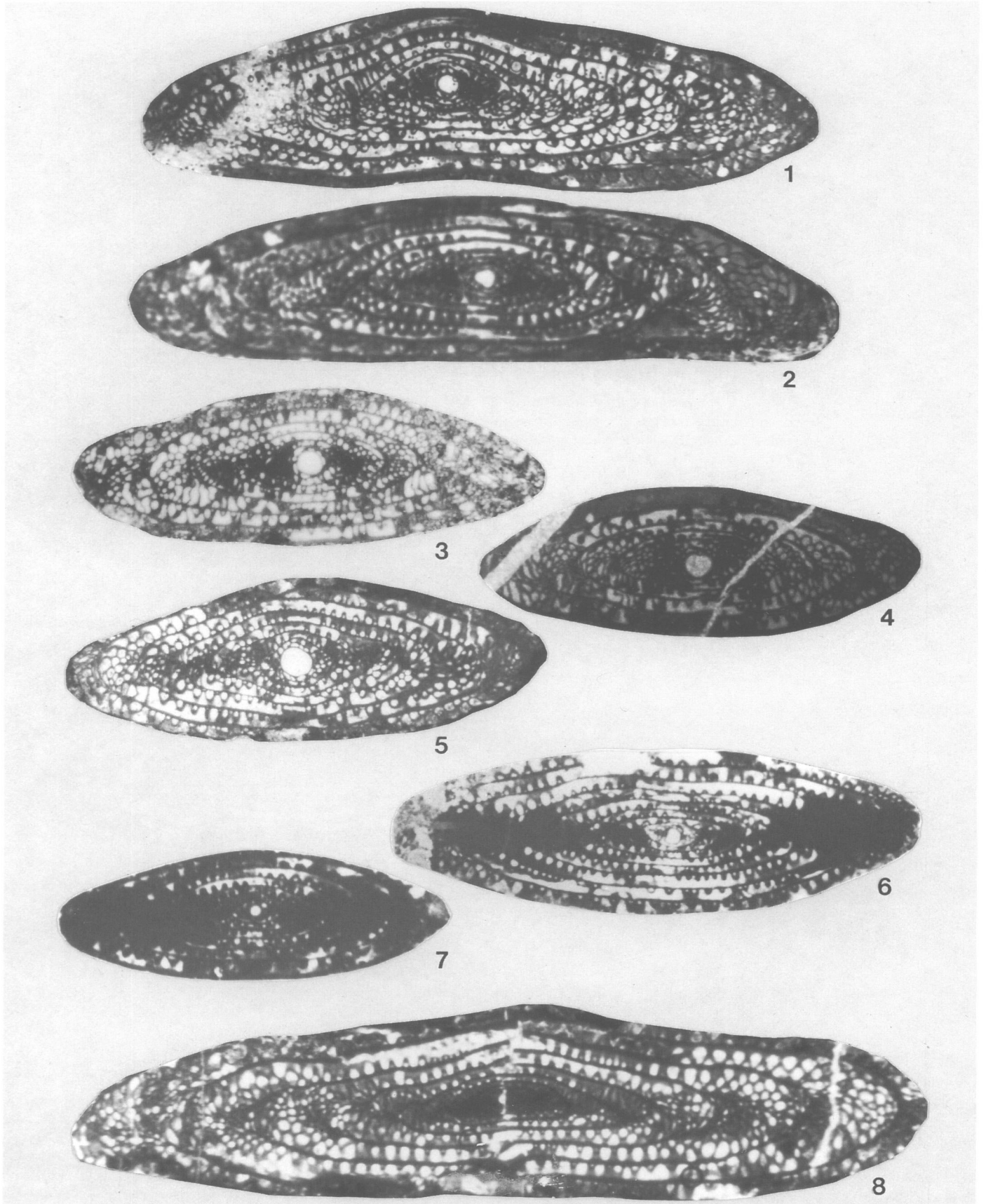


PLATE 9-11

FIGURES 1-4.—*Parafusulina sullivanensis* Ross: 1, slightly oblique axial section, ×10, hypotype, USNM 483111, Road Canyon Formation, sample 7-53; 2, axial section, ×10, hypotype, USNM 483112, Word Formation, sample 8-38; 3, 4, axial sections of individuals with partial dolomitization of interior, ×10, hypotypes, USNM 483113, 483114, Road Canyon Formation, sample 8-15.

FIGURES 5-7.—*Parafusulina faliskiei*, new species: 5, axial section, ×10, paratype, USNM 483071, Road Canyon Formation, sample 2-68; 6, axial section, ×10, holotype, USNM 483072, Road Canyon Formation, sample 2-73; 7, slightly oblique axial section, ×10, paratype, USNM 483073, Road Canyon Formation, sample 2-R14.

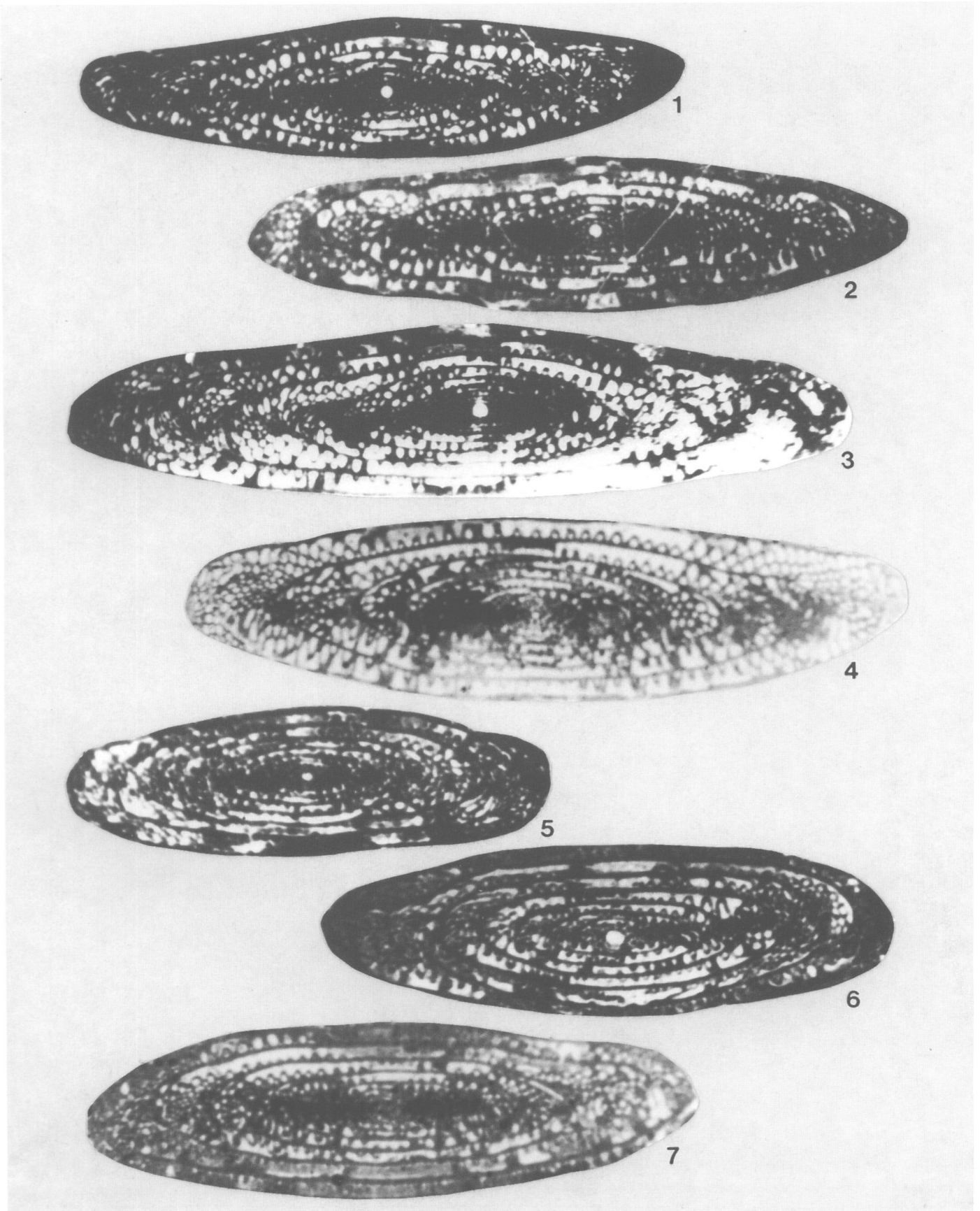


PLATE 9-12

FIGURES 1, 6.—*Parafusulina sellardsi* Dunbar and Skinner: 1, axial section, $\times 10$, hypotype, USNM 483103, Word Formation, sample 3-21; 6, slightly oblique axial section, $\times 10$, hypotype, USNM 483104, Word Formation, sample 3-21.

FIGURES 2-5.—*Parafusulina lineata* Dunbar and Skinner: 2, tangential section near proloculus, $\times 10$, hypotype, USNM 483084, Road Canyon Formation, sample 2-R16; 3, slightly oblique axial section, $\times 10$, hypotype, USNM 483085, Road Canyon Formation, sample 2-R12; 4, axial section, $\times 10$, hypotype, USNM 483086, Word Formation, sample 8-38; 5, axial section, $\times 10$, hypotype, USNM 483087, Road Canyon Formation, sample 2-R16.

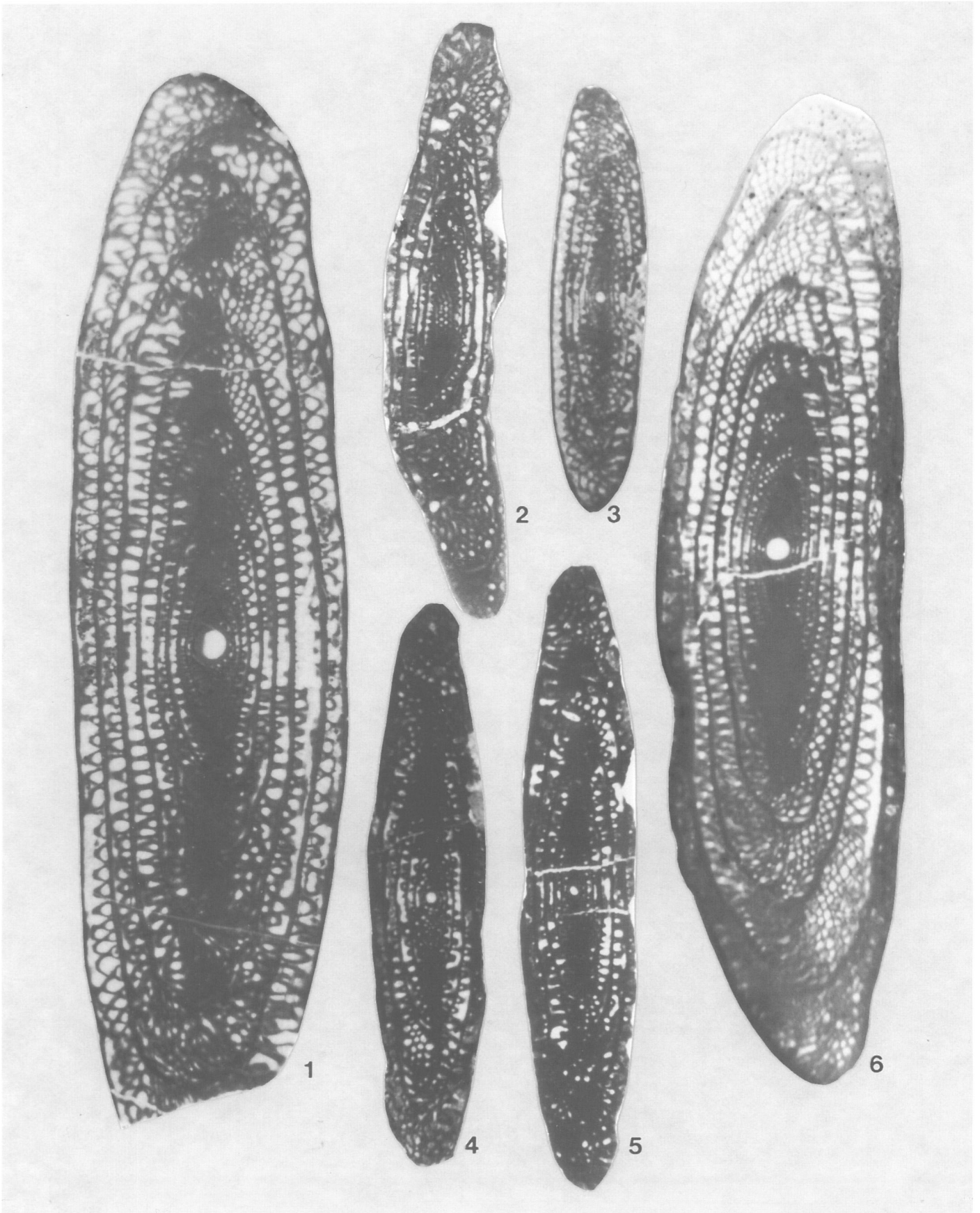


PLATE 9-13

FIGURES 1-5.—*Parafusulina boesei* Dunbar and Skinner: 1, axial section, $\times 10$, hypotype, USNM 483064, Road Canyon Formation, sample 2-R1; 2, axial section, $\times 10$, hypotype, USNM 483065, Road Canyon Formation, sample 2-68; 3, slightly oblique axial section, $\times 10$, hypotype, USNM 483066, Road Canyon Formation, sample 8-13; 4, slightly oblique axial section, $\times 10$, hypotype, USNM 483067, Road Canyon Formation, sample 7-58; 5, slightly oblique axial section, $\times 10$, hypotype, USNM 483068, Road Canyon Formation, sample 8-24.

FIGURE 6.—*Parafusulina sellardsi* Dunbar and Skinner: 6, axial section of individual with partial dolomitization of interior, $\times 10$, hypotype, USNM 483105, Word Formation, sample 3-22.

FIGURES 7, 8.—*Parafusulina maleyi* Dunbar and Skinner: 7, axial section, $\times 10$, hypotype, USNM 483088, Word Formation, sample 3-24; 8, axial section, $\times 10$, hypotype, USNM 483089, Word Formation, sample 8-39.

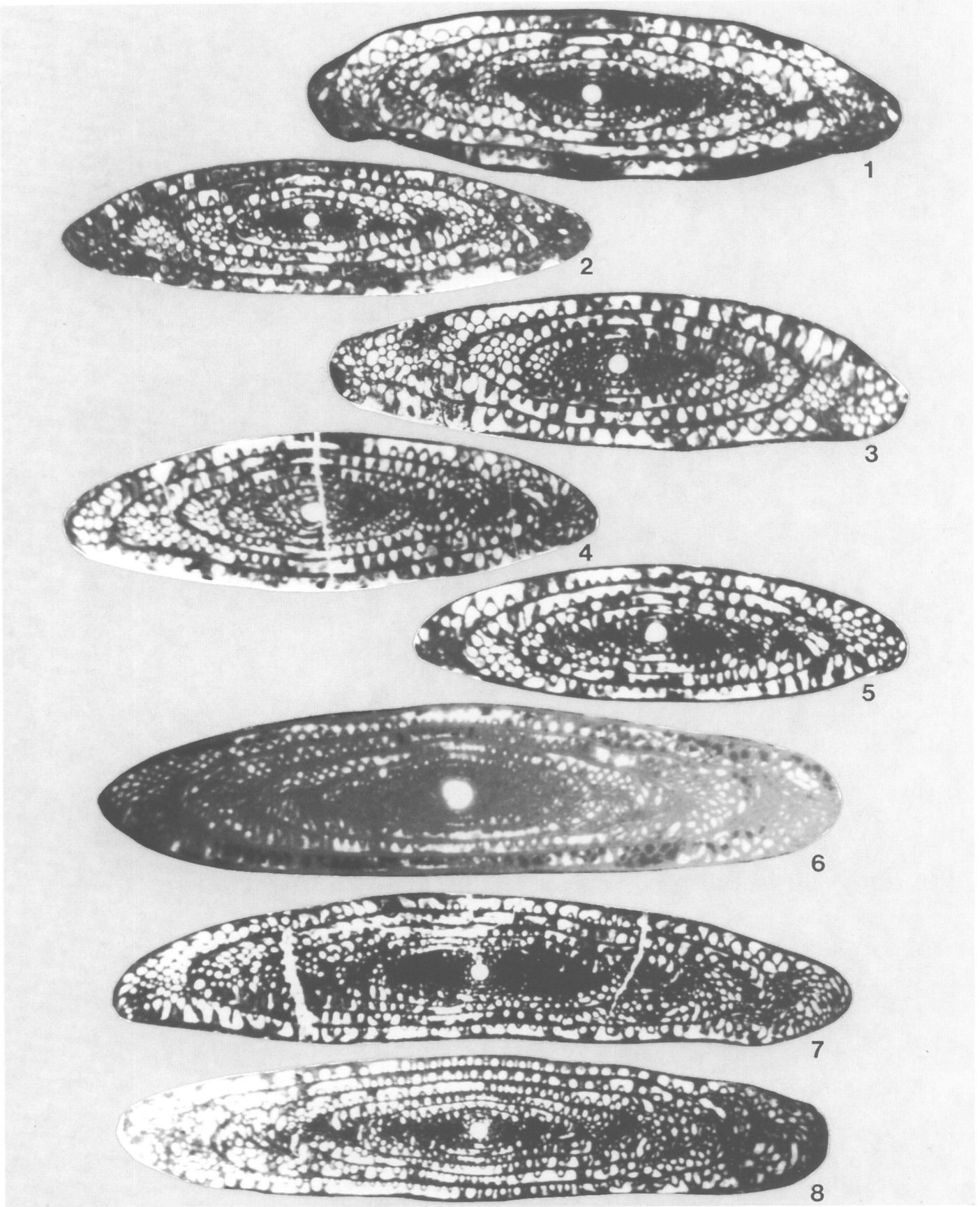


PLATE 9-14

FIGURES 1-3.—*Parafusulina rohri*, new species: 1, axial section, ×10, holotype, USNM 483093, Word Formation, sample 3-24; 2, axial section, ×10, paratype, USNM 483094, Word Formation, sample 3-23; 3, axial section, ×10, paratype, USNM 483095, Word Formation, sample 3-24.

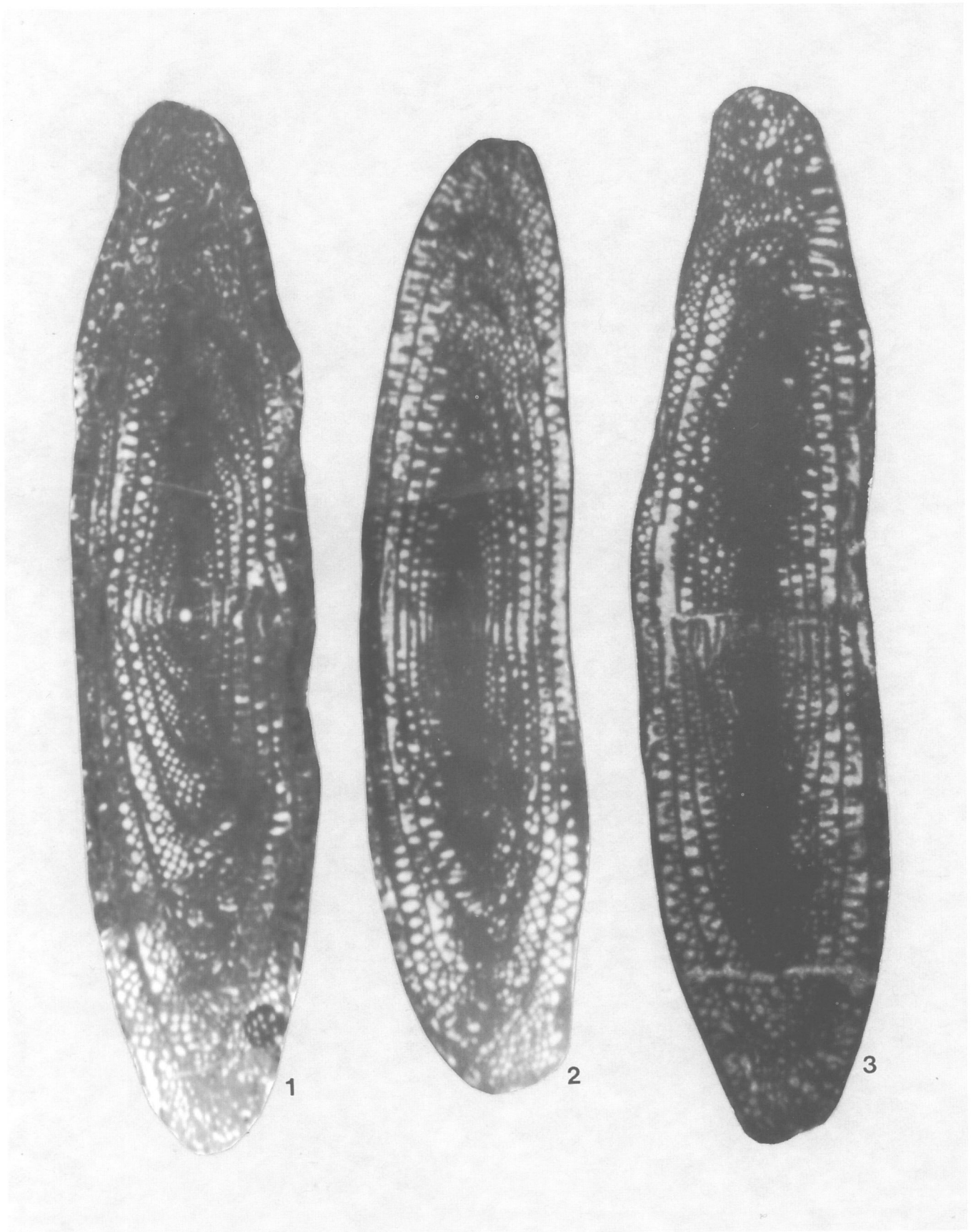


PLATE 9-15

FIGURES 1-4.—*Parafusulina antimonioensis* Dunbar: 1, 2, axial sections, ×10, hypotypes, USNM 483056, 483057, Word Formation, sample 9-8; 3, axial section, ×10, hypotype, USNM 483058, Word Formation, sample 9-7; 4, partial axial section, ×10, hypotype, USNM 483059, Word Formation, sample 9-8.

FIGURES 5, 6.—*Parafusulina virga* Thompson and Wheeler: 5, slightly oblique axial section, ×10, hypotype, USNM 483119, Word Formation, sample 8-45; 6, axial section, ×10, hypotype, USNM 483120, Word Formation, sample 8-45.

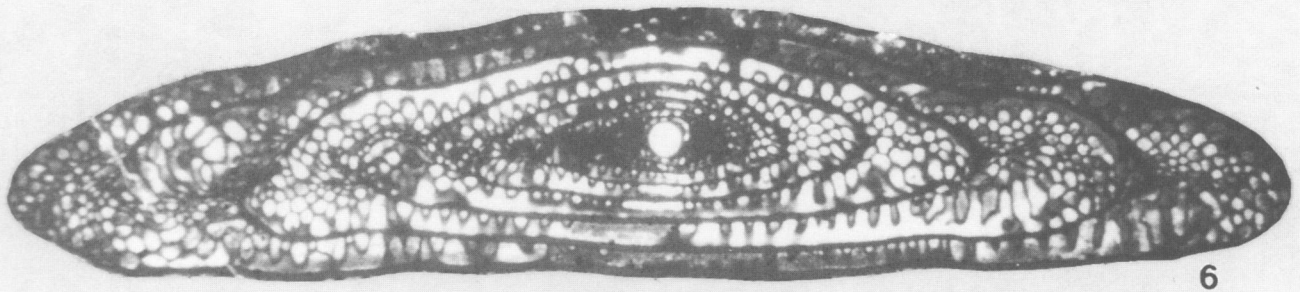
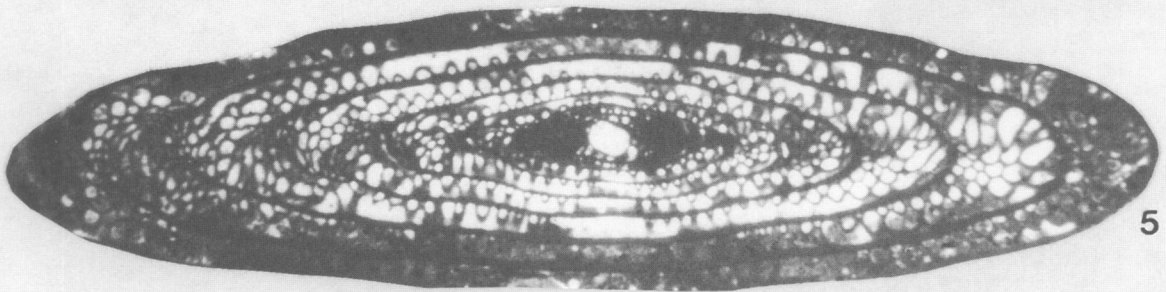
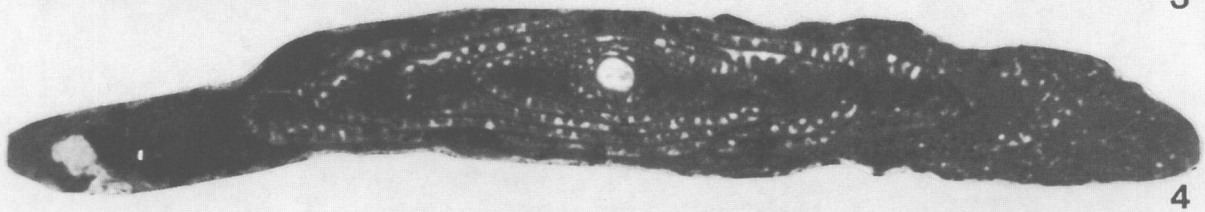
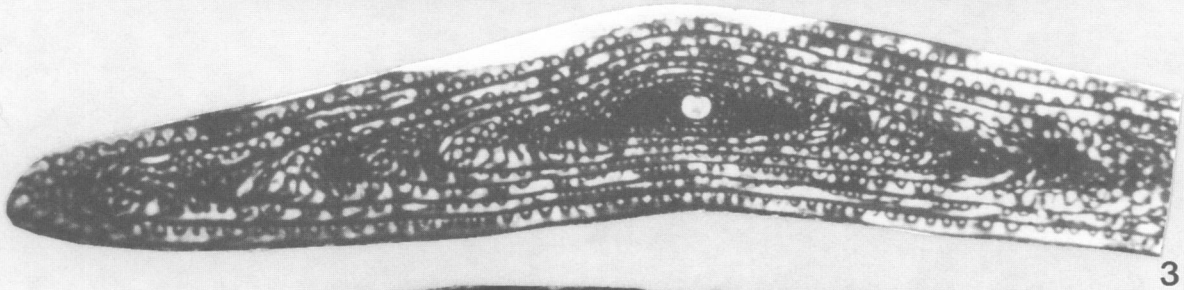
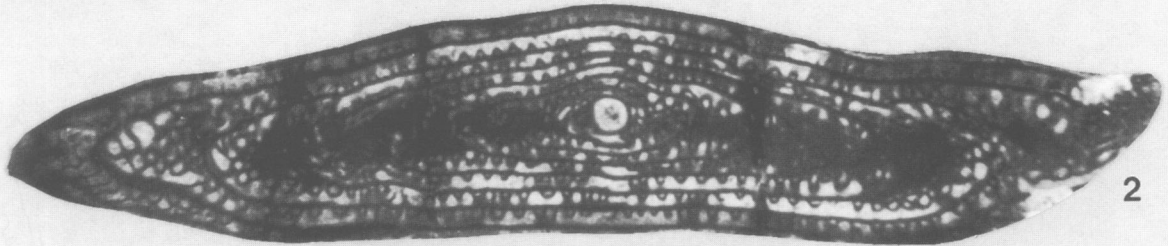
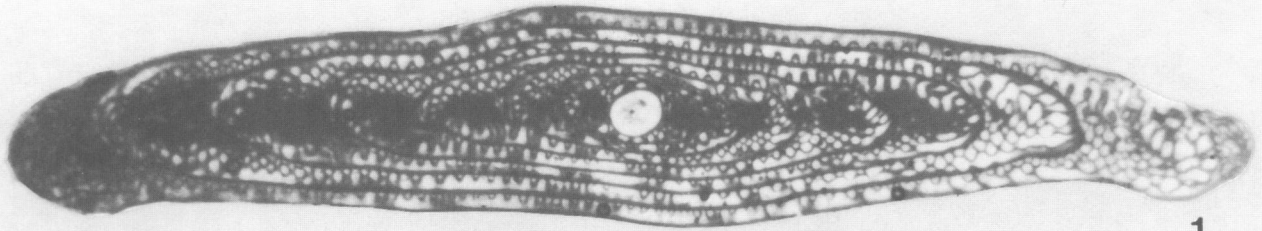


PLATE 9-16

FIGURES 1-4.—*Polydiexodina shumardi* Dunbar and Skinner: 1, 2, axial sections, $\times 10$, hypotypes, USNM 483125, 483126, Altuda Formation, sample 9-6; 3, oblique axial section, $\times 10$, hypotype, USNM 483127, Altuda Formation, sample 9-6; 4, axial section, $\times 10$, hypotype, USNM 483128, Altuda Formation, sample 10-206.

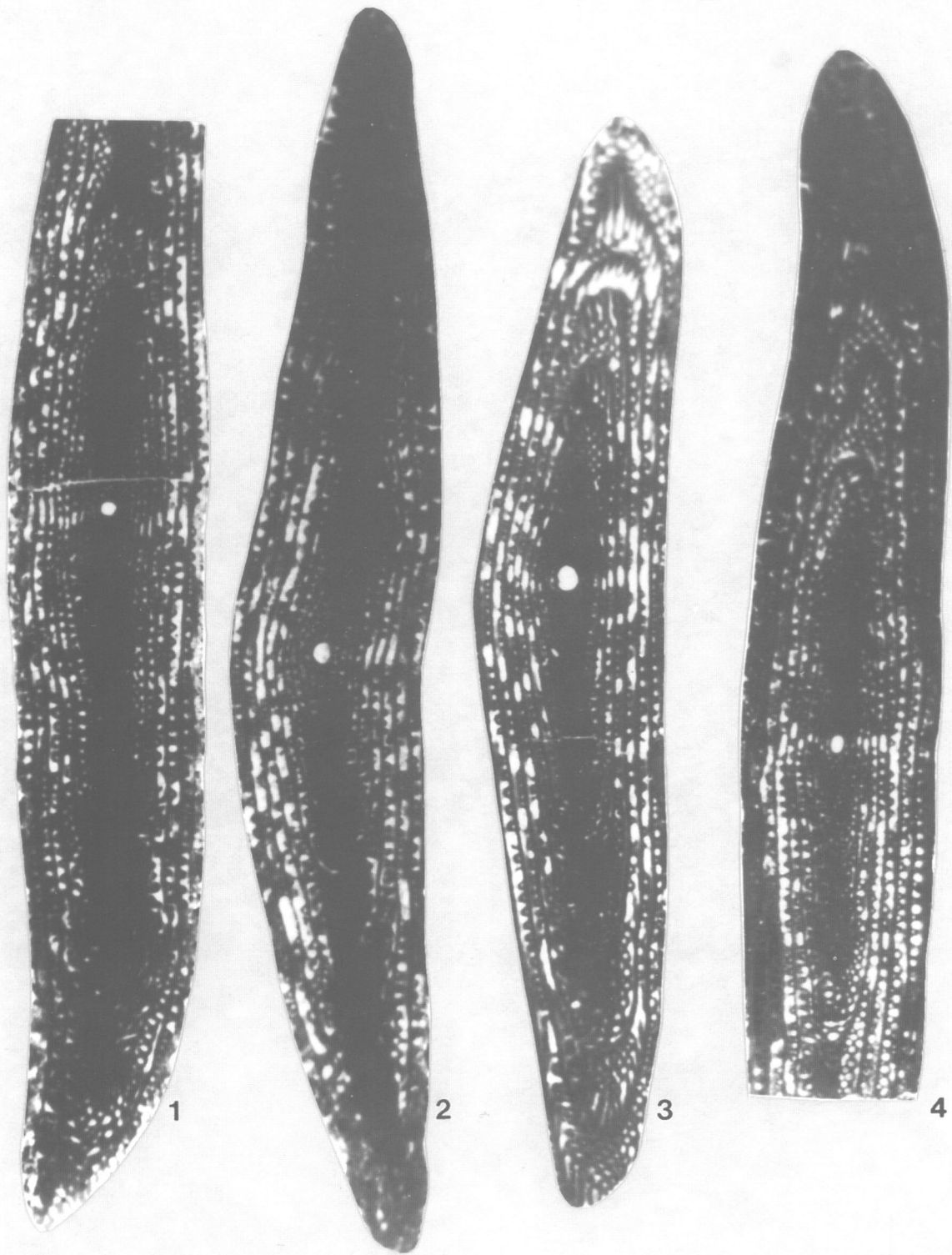
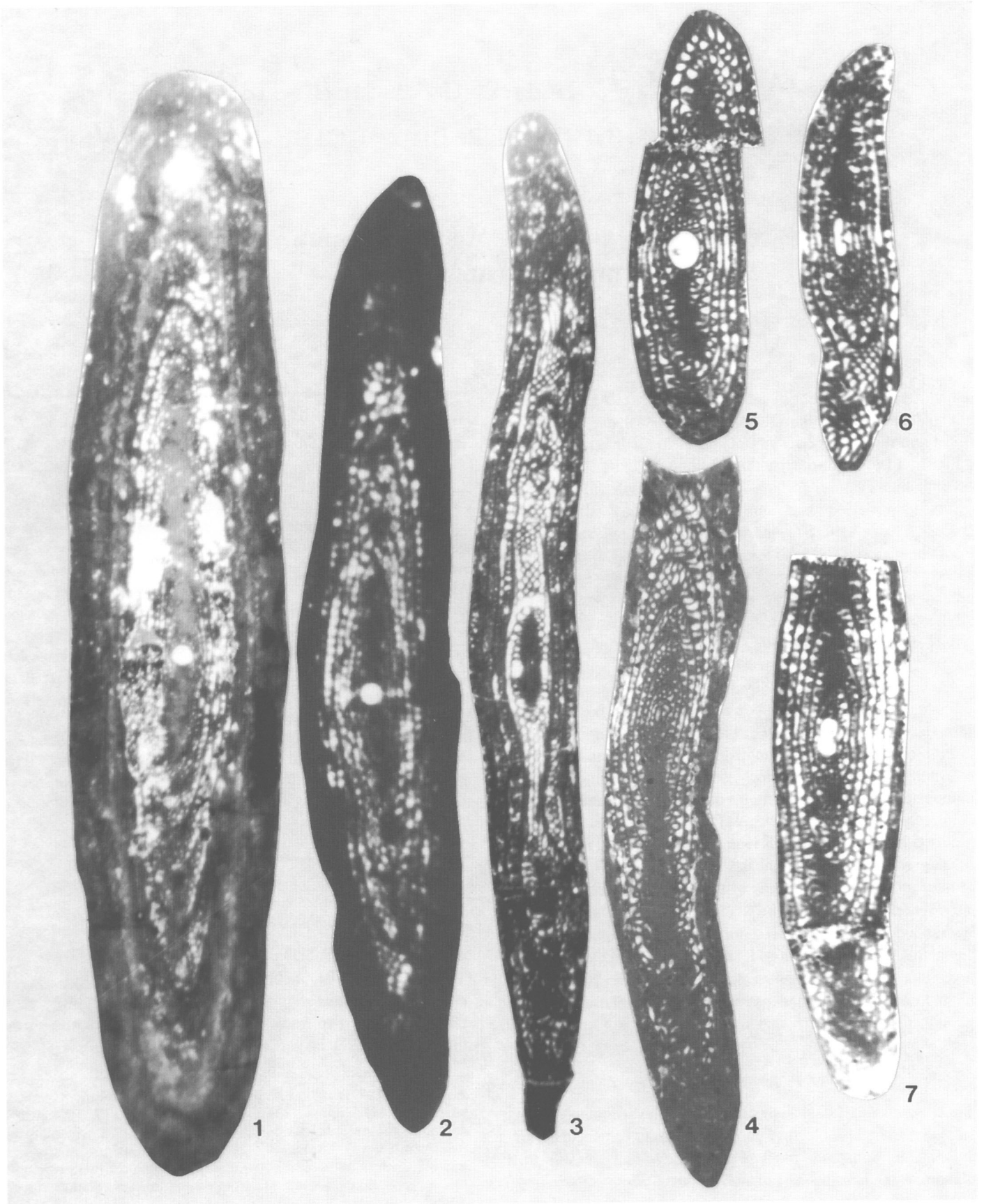


PLATE 9-17

FIGURES 1, 2.—*Polydiexodina capitanensis* Dunbar and Skinner: 1, axial section of individual with heavily dolomitized outer volutions, $\times 8$, hypotype, USNM 483121, Gilliam Limestone, sample 4-212; 2, axial section, $\times 8$, hypotype, USNM 483122, Gilliam Limestone, sample 4-213.

FIGURES 3, 4.—*Polydiexodina oregonensis* Bostwick and Nestell: 3, tangential section showing cuniculi and supplemental tunnels, $\times 8$, hypotype, USNM 483123, Altuda Formation, sample 10-206; 4, slightly oblique tangential section near proloculus, $\times 10$, hypotype, USNM 483124, Vidrio Formation, sample 9-10.

FIGURES 5-7.—*Polydiexodina* sp.: 5, axial section of immature individual, $\times 10$, USNM 483129, Vidrio Formation, sample 9-10F; 6, oblique axial section, $\times 10$, USNM 483130, Vidrio Formation, sample 9-10; 7, partial axial section, $\times 10$, USNM 483131, Vidrio Formation, sample 9-10F.



10. Carbonate Deposition of the Permian Word Formation, Glass Mountains, West Texas

*James D. Rathjen, Bruce R. Wardlaw, David M. Rohr,
and Richard E. Grant*

ABSTRACT

The carbonates of the Word Formation are restricted to the Word, undifferentiated, China Tank, Willis Ranch, and Appel Ranch members, and to the thin lens between the Willis Ranch and Appel Ranch members. The sediments of the Word can be divided into five mappable lithofacies in the central Glass Mountains: mudstone, peloidal packstone, skeletal wackestone/packstone, fusulinid-crinoid grainstone/bioturbated wackestone, and recrystallized limestone/dolostone. The mudstone lithofacies grades into sandstone and siltstone to the west.

The Word Formation represents deposition in a shallow shoal to backbay environment. Dolostones, recrystallized grainstones and wackestones, and fusulinid-crinoid packstones/grainstones mixed with bioturbated wackestones represent transitional deposition between the shoal and backbay. Peloidal packstones, mudstones, sandstones, and siltstones represent backbay deposition.

Introduction

The Word Formation was named by Udden, Baker, and Böse (1916) and was expanded by Udden (1917). King (1931) redescribed the formation, establishing a western shale facies, an eastern carbonate facies, and a zone of transition (transitional facies) between Hess Canyon and Gilliland Canyon.

James D. Rathjen, 214 W. Texas, Midland, Texas 79701. Bruce R. Wardlaw, U.S. Geological Survey, 926A National Center, Reston, Virginia 20192. David M. Rohr, Geology Department, Sul Ross State University, Alpine, Texas 79832. Richard E. Grant (deceased), Department of Paleobiology, National Museum of Natural History, Smithsonian Institution, Washington, D.C. 20560-0121.

King (1931) designated numbered limestone members in the transitional facies. Cooper and Grant (1964) named the numbered members of King (1931). Cooper and Grant (1966) removed the Road Canyon Member from the Word Formation and raised the Road Canyon to formation rank. The brachiopod faunas of the Road Canyon Formation supported this revision as they indicated strong Leonardian affinities to Cooper and Grant (1966). Grant and Wardlaw (1984), Wardlaw and Grant (1990), and Wardlaw, Ross, and Grant (this volume) strongly suggest that the Road Canyon Formation belongs in the Wordian than in the Leonardian. The proper placement of the Road Canyon is dealt with by Lambert, Lehrman, and Harris (this volume). The Vidrio Limestone Member at the top of the Word Formation is unconformably bounded and highly recrystallized and dolomitized and is not dealt with here.

The regional stratigraphy of the Word Formation in the Glass Mountains and the Del Norte Mountains is described in Rohr et al. (this volume). In that paper, Rohr et al. raised the Vidrio to formation rank, thereby removing it from the Word Formation. The members of the Word (as revised) consist of the China Tank, the Willis Ranch, the Appel Ranch, and the lens between the Willis Ranch and Appel Ranch members. The eastern carbonate facies is generally referred to as the Word, undifferentiated (King, 1931). The transitional facies of the Word Formation crops out along Hess Canyon in the central part of the Glass Mountains (Figure 10-1). The limestone members of the Word in the transitional facies and their gradation into the eastern carbonate facies is described in detail in this study.

General Stratigraphy

The generally perceived stratigraphic relationships of the Word Formation (Figure 10-2) do show the general facies of King (1931). The Word changes from sandstone and "shale" (western) to "shale" and carbonate (transitional) to carbonate

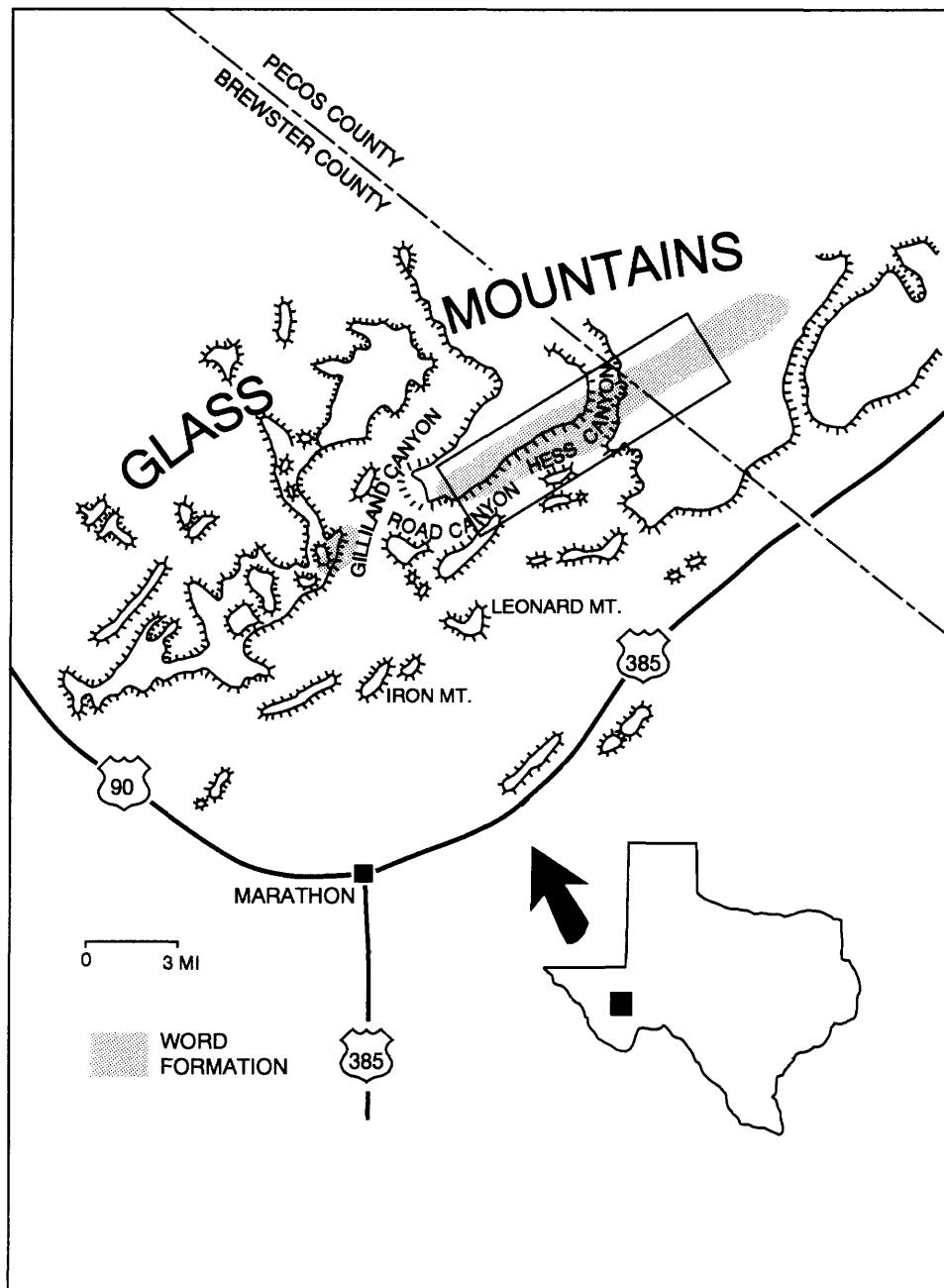


FIGURE 10-1.—Location of the Word Formation in the Glass Mountains, showing map area of Figure 10-3.

(eastern). The Word in the study area (Figure 10-1) is largely made up of mudstones (“shales”) and carbonates. Figure 10-3 shows the distribution of Word “shales,” Word undifferentiated, and the Word members along with the location of the sections used for facies analysis in the study area. The stratigraphic relationships of mudstones and carbonates of the Word are shown in Figure 10-4. This figure is plotted as a true distance diagram, with the distance measured from the easternmost section, 12PW. Conodont biostratigraphy (Ward-

law, this volume) provides a sharp datum at the top of the Willis Ranch Member. Here, faunas dominated by *Mesogondolella nankingensis* below are replaced by faunas dominated by *Mesogondolella aserrata* above.

WORD “SHALES” (MUDSTONES)

The “shales” (King, 1931) of the Word Formation are rarely fissile and are better described as mudstones and some

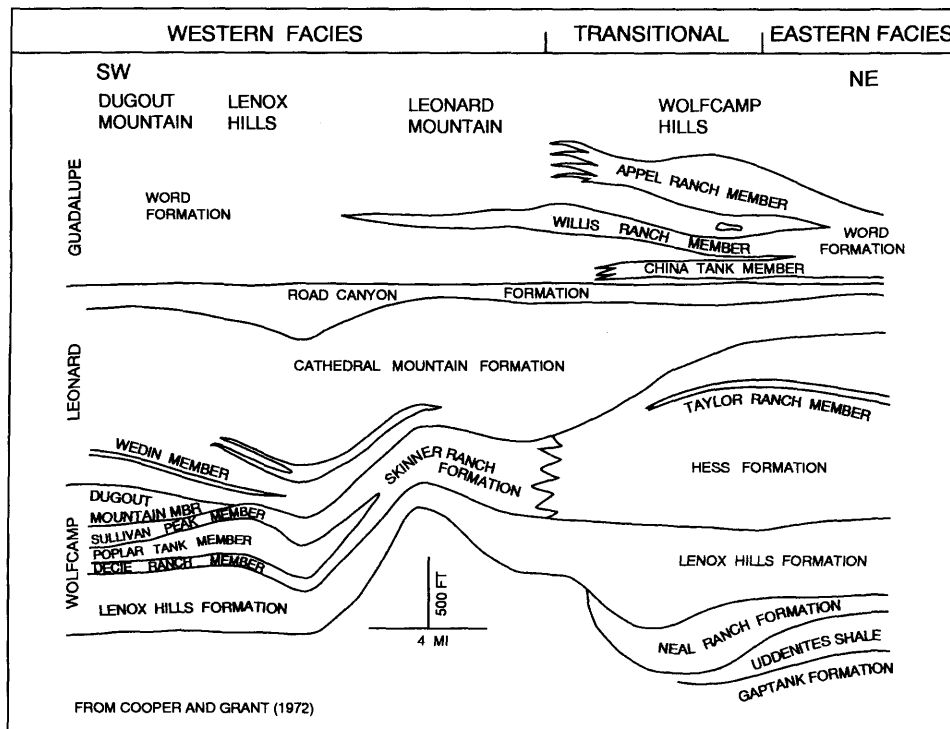


FIGURE 10-2.—General relationship of the Word Formation to the regional Permian stratigraphy defining eastern, transitional, and western facies of the formation. (From Cooper and Grant, 1972.)

claystones. The mudstones of the Word Formation are characteristically yellow and form thin platy beds averaging 10 cm (4 in.) in thickness and occur in scattered blocky and platy outcrops (Figure 10-5). The rocks weather to red or pink hues that form unusual geometric patterns. The mudstones are largely siliceous and contain silicified calcispheres, radiolarians?, and sponge spicules in a dull, earthy, clay matrix. The rocks display scattered traces and burrows and sparse brachiopods and fusulinids. Thin limestone stringers and laterally discontinuous limestone channels are common to the mudstones within the transitional facies.

CHINA TANK MEMBER

The China Tank Member has the most limited extent of the Word Formation members. The China Tank is a thin- to medium-bedded, gray skeletal packstone and wackestone with thin, interbedded yellow mudstone. Packstone generally forms thicker, more prominent ledges and is more common in the lower and middle parts of the unit than wackestone. In addition, packstone is more common to the unit in the northeast and becomes less abundant to the southwest. Limestones contain abundant silicified brachiopods, crinoids, fusulinids, and bryozoans. Most fossils are broken, abraded, and poorly sorted. Complete fossils are rare but more common in the wackestones. In many places, fossils are concentrated into thin fossiliferous

chert layers with no appreciable lime-mud matrix. In general, limestones are roughly parallel-bedded, laterally continuous, poorly sorted, and lack any large-scale sedimentary structures or depositional relief suggesting level bottom conditions at the time of deposition. Thicknesses remain relatively constant and contacts between strata are distinct.

WILLIS RANCH MEMBER

Over most of the study area the Willis Ranch Member is clearly divisible into two carbonate units that are divided by a persistent mudstone (Figure 10-4). The limestones are generally medium-bedded, and the upper part of the units are massive in places. Southwestern sections of the Willis Ranch are dominated by peloidal packstone, which is easily recognized by its concentrations of silicified peloids. Central and eastern sections contain many more fossils and typically consist of alternating packstone and wackestone with dolostone comprising the uppermost parts of these sections. The Willis Ranch is sandy in all parts, but the sand increases in abundance to the southwest. The sand grains are primarily subangular to angular and relatively fine grained. Sections remain relatively uniform in thickness, averaging 38 m (125 ft). Like the China Tank Member, large-scale sedimentary structures and depositional relief are minimal, and contacts between beds are sharp.

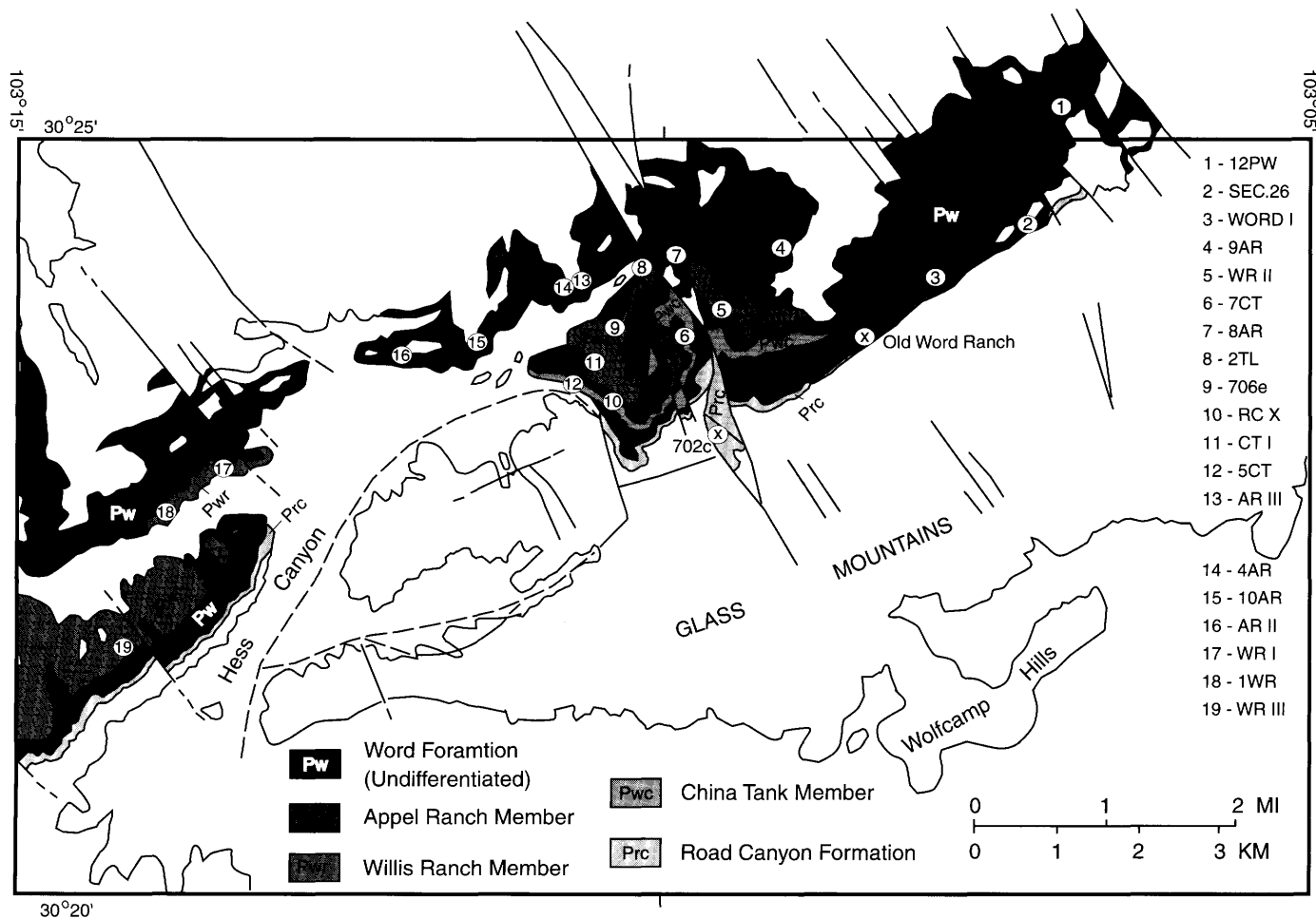


FIGURE 10-3.—Geology of the Word Formation in the Hess Canyon and the Glass Mountains, with the locations of the measured sections. Word Formation (undifferentiated) is largely represented by mudstone in the west and dolostone in the northeast.

APPEL RANCH MEMBER

The Appel Ranch Member is also clearly divisible into two carbonate units, which are divided by a persistent mudstone/claystone unit. The Appel Ranch is composed of limestone and mudstone that is thinly bedded to the southwest but increases in thickness and fossil abundance toward the central and eastern sections. Fusulinid/crinoid packstones and grainstones and bioturbated wackestones and lime mudstones occur in the Appel Ranch, in addition to the skeletal packstones and wackestones typical of the lower part of the Word. In the southwestern sections, the Appel Ranch is composed of peloidal packstones (containing fusulinids and crinoids), skeletal wackestones, and thin interbedded mudstones and claystones. These mudstones and claystones are darker than the typical mudstones found in the lower part of the Word. The darker color of the mudstones is probably due to a much higher clay content. Current-orientated fusulinids and brachiopod spines are not uncommon in the mudstones.

Section 9AR (the easternmost section) consists of medium-bedded, highly pitted, gray dolostone at its base that contains chert nodules and very few silicified fossils. The dolostone is vuggy and silty in parts with some biomoldic (leached fossil) porosity. Above the dolostones are thinner, medium beds of skeletal packstone with current-aligned fusulinids in many places. Fusulinid grainstone near the top of the section contains small black and brown carbonate pebbles, which are possibly authogenic sediments (Flügel, 1982). The top of the section terminates where the strata become massive and largely unfossiliferous, which is presumably at the base of the Vidrio Foramtion.

THIN LENS BETWEEN THE WILLIS RANCH AND APPEL RANCH MEMBERS

This lens has a very limited lateral extent along the southern extension of Hess Canyon to the junction of the west-trending and north-trending Hess canyons. The lens is clean (lacking a

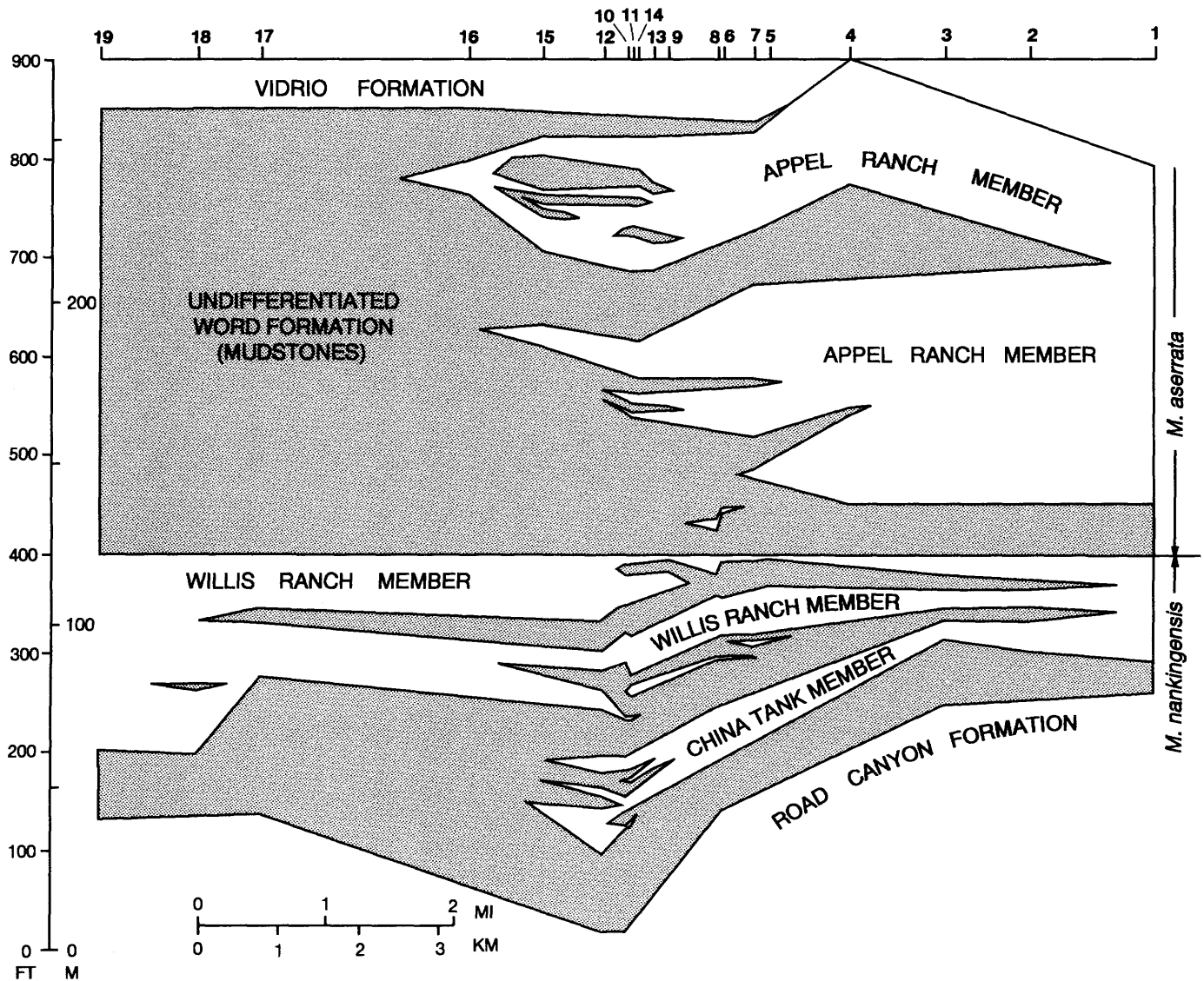


FIGURE 10-4.—Stratigraphy of the Word Formation in the study area of Hess Canyon and the Glass Mountains. Each section is compiled into the cross section by true distance from the easternmost section, 12PW. (Numbers across the top refer back to sections in Figure 10-3.)

significant terrigenous clastic component), and allochems consist primarily of peloids and skeletal debris. Fusulinids, brachiopods, and crinoids are common near the top at USNM Loc. 706b. Small ammonoids and rare trilobites also are present. Matrix at this locality is primarily lime-mud with a trace of sparry calcite in places. Chert nodules are common and are similar to the lower part of the Word, consisting of concentrated masses of fusulinids and brachiopods or other silicified fossils in small layers or pockets.

WORD FORMATION, UNDIFFERENTIATED

In the northeast of the study area, the three carbonate members were not differentiated by King (1931) or Cooper and

Grant (1964, 1966) as the sections consist of medium-to-massive, gray crystalline dolostone. Differentiation between different members is difficult because of the similarity of the strata. Only a few fossils are recognizable, primarily crinoids and fusulinids. The outcrops generally are highly pitted and vuggy on fresh surfaces. The eastern facies are laterally continuous and lack major sedimentary structures. This forms a regular monotonous sequence of dolostones. The members are only differentiable when the major siltstone/mudstone breaks are present.

Carbonate Microfacies of the Word Formation

Five major microfacies are recognized from thin sections,

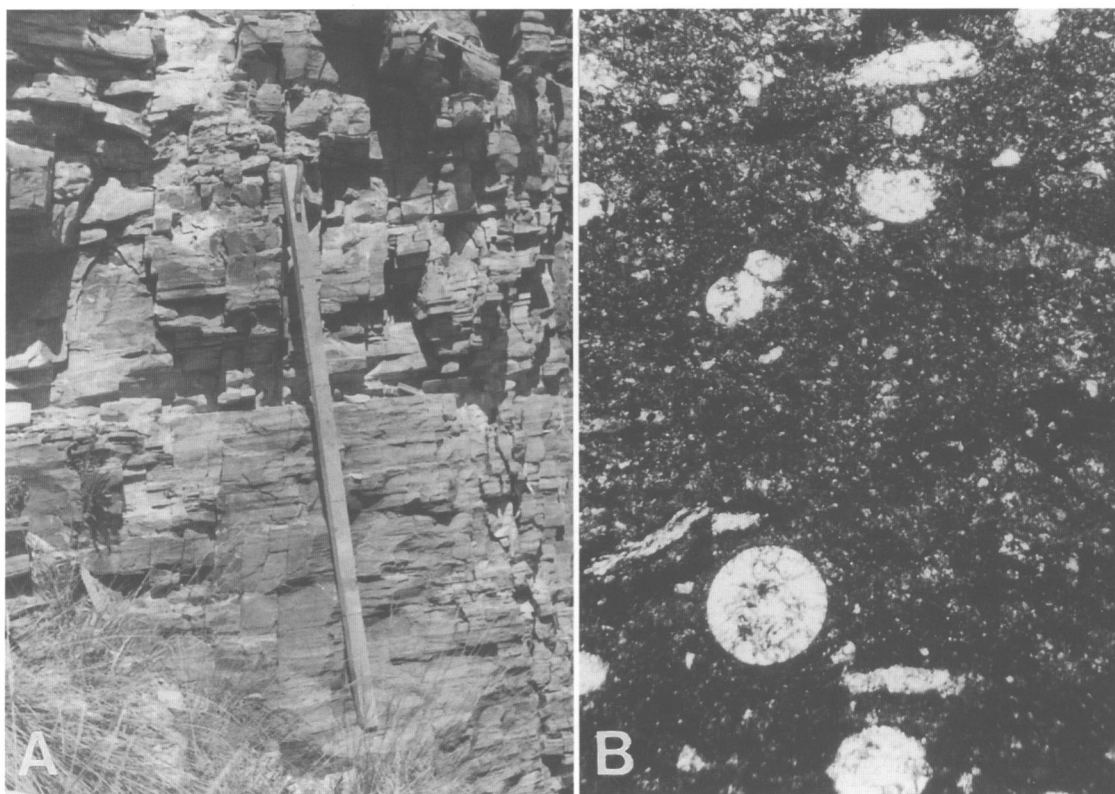


FIGURE 10-5.—Word Formation siltstones and mudstones. A, typical outcrop of yellow, platy-bedded mudstone (just below base of section 7CT; Jacob's staff is 1.5 m long). B, photomicrograph of mudstone to siltstone. Note calcispheres and clotted distribution of clays (section 7CT, 12.2 m; long axis of photomicrograph represents 0.5 mm).

polished slabs, etched samples, and field observations. These are peloidal packstone, skeletal wackestone/packstone, bioturbated wackestone/lime mudstone, fusulinid-crinoid packstone/grainstone, and recrystallized limestone/dolostone. One major microfacies, skeletal wackestone/packstone, is divided into skeletal and whole fossil subfacies.

PELOIDAL PACKSTONE

This microfacies is common in the southwest portion of the study area and is very common to the Willis Ranch Member (Figures 10-6, 10-7). Texturally, this microfacies contains peloids and a few fossil fragments in a lime-mud matrix. Sparry calcite is rare and primarily occurs in intrabiotic cavities and along secondary fractures. Detrital quartz sand is mixed throughout the matrix and in places is a major rock constituent. Dolomite is rare in this microfacies. Matrix material appears homogeneous and consists of a mixture of micrite and microspar. Crystals are uniform in size and shape, generally ranging from less than 4 microns (micrite) and up to 20 microns (microspar). The micrite probably represents lithification of the original lime-mud (orthomicrites of Wolf, 1965), whereas the

microspars are commonly recrystallized micrites (Folk, 1965). A tight, interlocking network is formed by the crystal boundaries, with the boundaries appearing darker than the crystals. This probably results from a high percentage of clays or other inorganic substances concentrated around the perimeters of individual crystals (Folk, 1959). It is very difficult to distinguish between the micrite and microspar because of the small crystal sizes. Micrite, however, generally appears much darker than the microspar (due to the individual crystals stacked on each other), whereas microspar forms lighter, equant subhedral calcite crystals. Skeletal grains are rare in this microfacies, although isolated seams or pockets of richly fossiliferous beds do occur.

Typically, fossils occur scattered throughout the fine-crystalline matrix. Skeletal grains consist of disarticulated, fragmented, and abraded remains of brachiopods and brachiopod spines, bryozoans, fusulinids, and crinoids. Fossil grains are angular and poorly sorted, ranging in size from a few millimeters to several centimeters. Fossil morphologies suggest contrasting depositional environments with delicate branching bryozoans, thick shelled brachiopods, and fusulinids commonly found in the same rock. Because of these differing morphologies and their fragmentary nature, many of the fossils

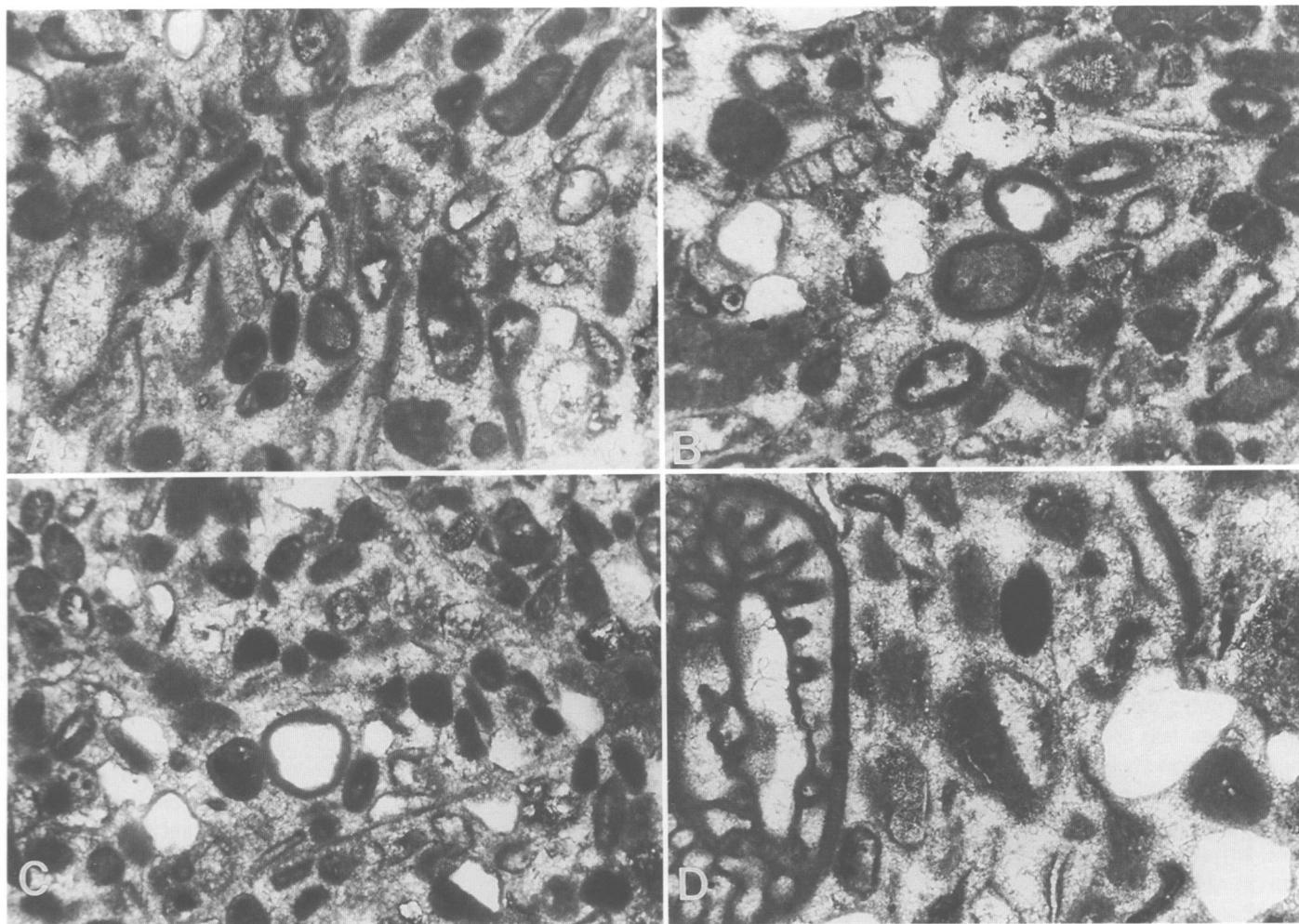


FIGURE 10-6.—Photomicrographs of peloidal packstone microfacies from the Willis Ranch Member (bottom of each photomicrograph represents 0.5 mm). A, fecal pellets appear as well-rounded, dark, structureless grains. Elongate grains are micritized skeletal debris (section 1WR, 11.4 m). B, algal-coated quartz grains (light colored). Note micritized and algal-coated skeletal grains, matrix consists of fine crystalline microspar (section 1WR, 36.3 m). C, characteristic sandy nature of the Willis Ranch Member. Many sand grains are algal encrusted. Fecal pellets and micritized skeletal grains are scattered throughout matrix (section 1WR, 53.4 m). D, various skeletal grains are shown. The grain at the center is partially micritized, other grains have micrite envelopes. The matrix is fine crystalline microspar, and some spar is in intrabiotic cavities (section 1WR, 53.4 m).

probably represent faunal mixing of nearby skeletal microfacies.

Brachiopods, bryozoans, and crinoids are commonly silicified, but fusulinids are very rarely silicified. Silicification of original fossil parts to length-slow chalcedony is the most common type of replacement. Many different stages of silicification can be seen in thin sections and hand samples; these stages range from only partial replacement along the exteriors of fossils (thin coatings) to complete silicification of the entire skeleton. Generally, thinly coated fossils have much more detail preserved, whereas totally silicified fossils are coarsely replaced and noticeably lacking in detail. In some places the fossils are so coarsely silicified that identification of

the fossil type is virtually impossible. Skeletal debris commonly have micrite envelopes or algal encrustations. Peloids are the common type of framework grain in this microfacies and are of two types: fecal pellets and algal peloids. Fecal pellets are spherical, sand-sized particles that average between 0.1–0.2 mm in diameter (Figure 10-7). Most commonly, these particles are well-rounded and appear dark with no internal structure discernible. The dark color of the pellets commonly results from a combination of high organic content and the extremely fine-crystalline nature of the pellets. Peloids in this group are characterized by good “sorting.” No sedimentary features, such as bedding or laminations, can be recognized, probably due to thorough homogenization of the sediments by

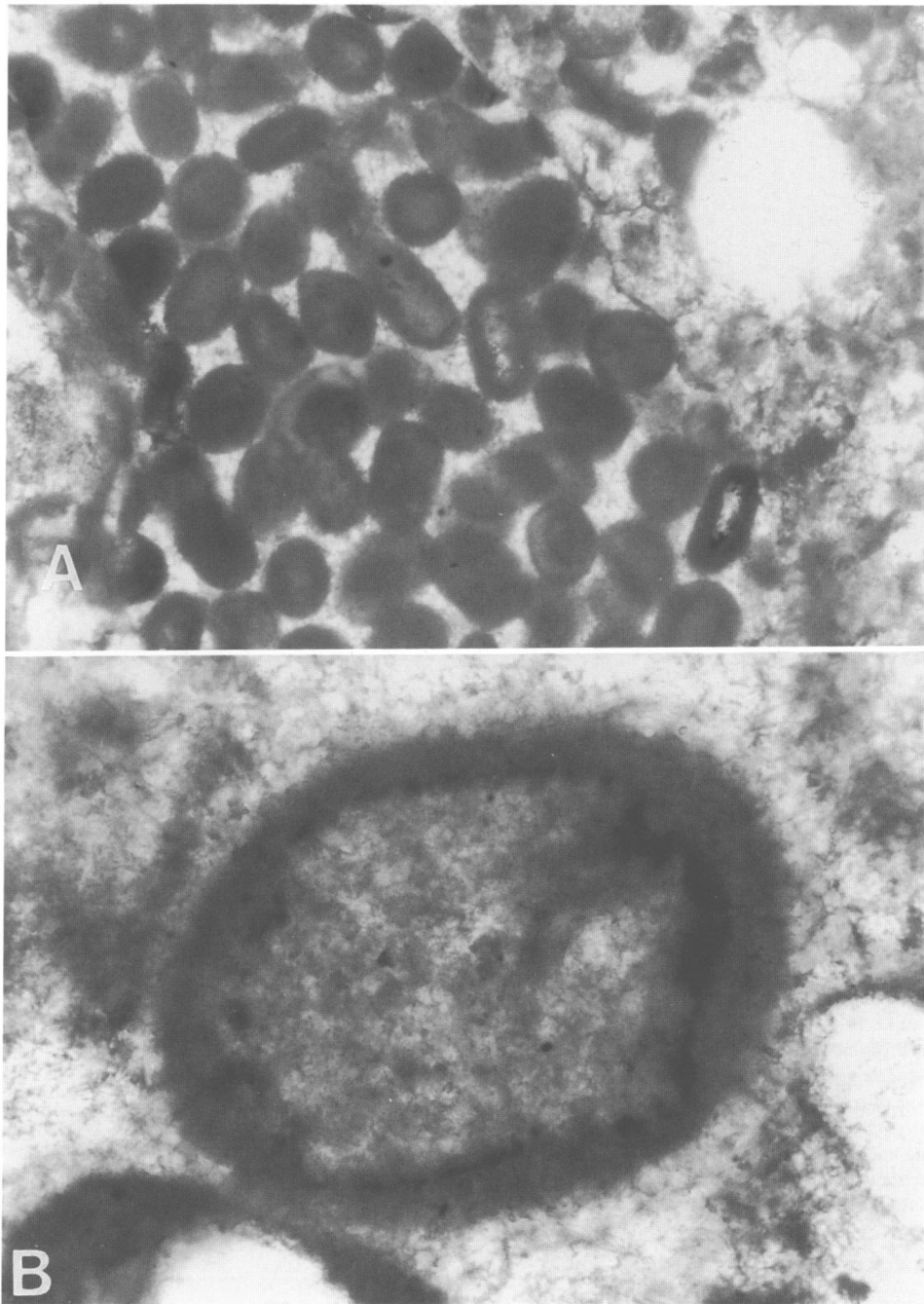


FIGURE 10-7.—Photomicrographs of pellets from the Willis Ranch Member. A, intraclast of pelleted sediment. Note lighter color of matrix in the intraclast, truncated pellets along the margin of the grain, and elongate shape. Pellets are probably fecal because of their uniform size and “good sorting” (section 1WR, 2.9 m; bottom of photomicrograph represents 0.5 mm). B, close-up of pellet from matrix. The grain has no internal structure, is composed of micrite and terrigenous mud, and is in a fine crystalline matrix (section 1WR, 25.9 m; bottom of photomicrograph represents 0.05 mm).

the organisms responsible for the pellets. Common producers of fecal pellets are brachiopods, amphineura, gastropods, worms, ostracodes, echinoderms, and tunicates (Flügel, 1982:133). Fecal pellets are also produced by other deposit

feeders and herbivorous animals as well as plankton feeders, such as copopods and fishes.

In Recent carbonate sediments, fecal pellets are probably the most common type of allochem. They dominate subtidal and

shallow intertidal environments and occur preferentially in low energy zones. In these shallow water, low energy environments, rapid cementation is possible because these areas are commonly supersaturated with calcium carbonate (Bathurst, 1971). This seems to be the general case in the peloidal microfacies, with early, rapid cementation followed by very little subsequent diagenetic alteration. With rapid cementation, pore throats become sealed-off and do not permit later fluids to pass through the sediments, which might diagenetically alter the sediments.

The second group of peloids is formed by the interaction of algae with various particles. Types included in this group are algal-coated grains and micritized grains. Almost all of the bioclasts and other allochems are coated by some type of micrite envelope. These coatings range from thin superficial films around the margins of the allochems to thick crusts of micrite that obscure the original particle. Coated grains with skeletal debris as nuclei probably form as a result of boring micro-organisms, most likely endolithic algae. Nuclei for these micrite-coated grains most commonly are brachiopod, bryozoan, fusulinid, and coral fragments. Micritized echinoderm fragments are rare but do occur sporadically. Micritized coatings appear much darker than the surrounding matrix, probably as a result of the "stacking effect" of the micrite plus some organic and terrigenous material mixed in with the sediments.

These micrite envelopes form by micro-organisms that attack and bore into the surfaces of the skeletal debris creating tiny holes, which are subsequently filled with micrite (bacterially produced?) after the death of the organism. Other sources of micrite possibly include the very fine carbonate needles produced after the death and decomposition of certain types of algae that fill in the small voids. If the process of boring and infilling (micritization) continues over a prolonged period of time, micrite replacement of the entire grain is possible. Micritization can be seen in various stages of maturity in this microfacies. Many particles are enclosed by thin micrite envelopes, whereas other grains have been thoroughly micritized and are classified as peloids because the grains are totally unrecognizable.

Quartz sand grains are common in this microfacies. Sand primarily occurs disseminated throughout the matrix, but small sand stringers and thin layers are common in the field and in hand samples. Sand grains are typically subangular to subrounded, well sorted, and fine (0.1–0.2 mm) in size. Like many of the carbonate allochems, sand grains form the "nuclei" of many coated grains. Many dark algal-coated grains commonly have a quartz "nucleus" still visible in the center.

Intraclasts occur in this microfacies, although they are rare. Intraclasts are very similar to the surrounding matrix, consisting of pelleted or peloidal sediments. Identification of these lithoclasts is based on truncated peloids along the margins and the flat, well-rounded nature of the clasts. These lithoclasts probably represent small rip-ups or the products of biologic

activity. The limited number of the intraclasts indicates that these formed in sporadic, rare events.

SKELETAL WACKESTONE/PACKSTONE

Skeletal wackestone/packstone represents the most common microfacies type in the transition facies of the Word Formation (Figure 10-8). This microfacies is truly "transitional" in a strict sense because it represents the transition between normal open marine conditions and a semirestricted lagoonal environment. This microfacies represents most of the China Tank Member, the central part of the Willis Ranch Member, and some parts of the Appel Ranch Member. The microfacies is divided into two subfacies, skeletal and whole fossil.

SKELETAL SUBFACIES.—These rocks consist of very coarse grains of broken or whole brachiopods, crinoids, fusulinids, and bryozoans. This subfacies also contains abundant peloids and minor amounts of silt-sized quartz grains. Most samples are at least partially washed and moderate-to-well sorted but contain varying amounts of lime-mud and terrigenous mud mixed throughout the matrix. Some coarse sparry calcite-cemented sediments are common in places, and dolomite is a locally abundant accessory in many intervals.

Matrix types are highly variable, even in a single thin section or polished slab. Portions may contain areas that are largely spar-cemented, whereas other adjacent areas are rich in lime or terrigenous mud, probably resulting from incomplete winnowing of the sediments. Micrite and microspar are common in the wackestones, whereas sparry calcite occurs only in the well-sorted, fossil-rich, packstones. Sparry calcite also occurs as void-filling cement in many intrabiotic cavities, sheltered voids, and along secondary fractures.

Peloids (fecal and algal) are a common framework grain. Peloids occur in both wackestones and packstones, though they are more common in the wackestones. In the wackestones, most of the peloids are probably fecal pellets produced by some type of detritus feeder. Many peloids in the packstones are algal-coated grains or micritized grains that were probably formed by some type of boring or encrusting algae. Fecal pellets are also common in the packstones. Most fecal pellets are much smaller than the algal-coated grains and are typically better sorted. Algal-coated grains include brachiopod fragments, fusulinids, and bryozoan fragments. Crinoid columnals scattered throughout the matrix have either a thick algal coating or thin micrite envelopes.

Fossils are very common in this subfacies. The most common fossil types include brachiopods, fusulinids, crinoids, and rarely ammonoids and straight nautiloids. Packstones generally contain large amounts of skeletal debris and relatively few complete fossils, whereas the wackestones consist largely of whole fossils that are relatively complete, mixed in with lesser amounts of skeletal debris. Most of the complete fossils are robust forms of brachiopods and bryozoans, which were adapted to higher energy environments,

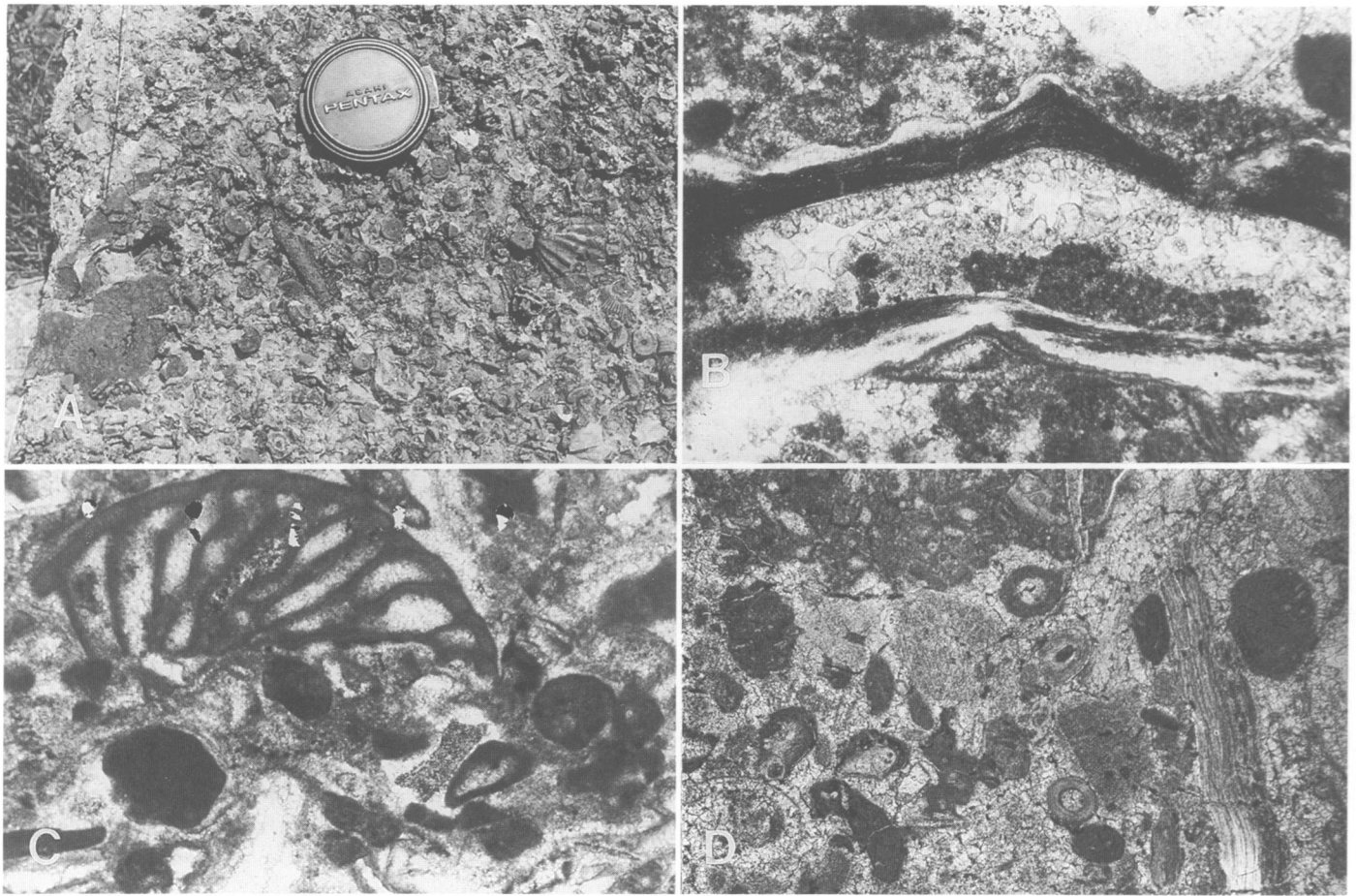


FIGURE 10-8.—Skeletal wackestone/packstone microfacies. A, photograph of the skeletal packstone from the lower part of the Appel Ranch Member (section 8AR, 60.4 m; lens cover is 55 mm wide). B, thin section from the Willis Ranch Member showing the cross section of a brachiopod shell that contains internal sediments and perched sediments, which appear dark and consist of pelleted material. The brachiopod is also filled with micrite and sparry calcite (section RC X, 29.3 m). C, thin section of skeletal packstone showing broken and abraded grains. Many grains are micritized or have algal coatings. Intrabiotic cavities are filled with clear microspar (section 5CT, 25 m). D, thin section of skeletal and intraclastic packstone. Many clasts and grains have dark micritic algal encrustations or coatings (section 7CT, 8.5 m). (Bottoms of photomicrographs represent 0.5 mm).

including lytonnid brachiopods and encrusting bryozoans. Crinoids are rarely found as more than three articulated columnals. Most of these fossils are randomly oriented but locally are current orientated. The fossils and skeletal debris are commonly well sorted and angular to subangular depending on the size of the particles.

Geopetal structures common in this subsfacies include sheltered voids, partially-filled brachiopods or ammonoids, and perched sediments. Many brachiopods and ammonoids are filled with internal sediment that most commonly consists of pelleted material. The upper portion of the voids are filled with coarse crystalline calcite or silica. Sheltered voids (which commonly form underneath brachiopod valves) contain areas of coarse crystalline calcite and little matrix of skeletal debris, whereas the “roof” or “umbrella” has large amounts of pelleted or skeletal material perched on the upper portion of the valve.

Sheltered voids with perched sediments indicate that sedimentation occurred fairly rapidly and possibly periodically. The contacts between the internal sediment and void-filling cement in oriented samples indicate that the surfaces have not been significantly tilted since the time of deposition. Intrabiotic cavities of brachiopods, fusulinids, bryozoans, and corals contain multiple layers of cements.

Brachiopod shells are commonly replaced by length-slow, fibrous chalcidony. Other fossils, such as corals and bryozoans, are also commonly silicified. Fusulinids are silicified in isolated beds, but generally their tests remain as calcite.

Generally, silicified and calcite fossils contain a thin inner micritic rim along the interior of the shells. These micritic rims grade into an outer, thinly bladed, terminated calcite rim along the interiors of the intrabiotic cavities. The remaining portions of the interiors of the cavities are filled with clear, coarse,

blocky, sparry calcite or, less frequently, with quartz or megaquartz (Figure 10-9). These types of interior cements indicate that the sediments have been subjected to some subaerial exposure. Terminated calcite crystals will only begin to crystallize in open void spaces. Subaerial exposure was also

probably "short" in duration because if the sediments were exposed for a prolonged period of time, the calcite crystals would have continued to grow until they interfered with each other and formed interlocking, compromise boundaries. Also, if these sediments were exposed for any extended period of

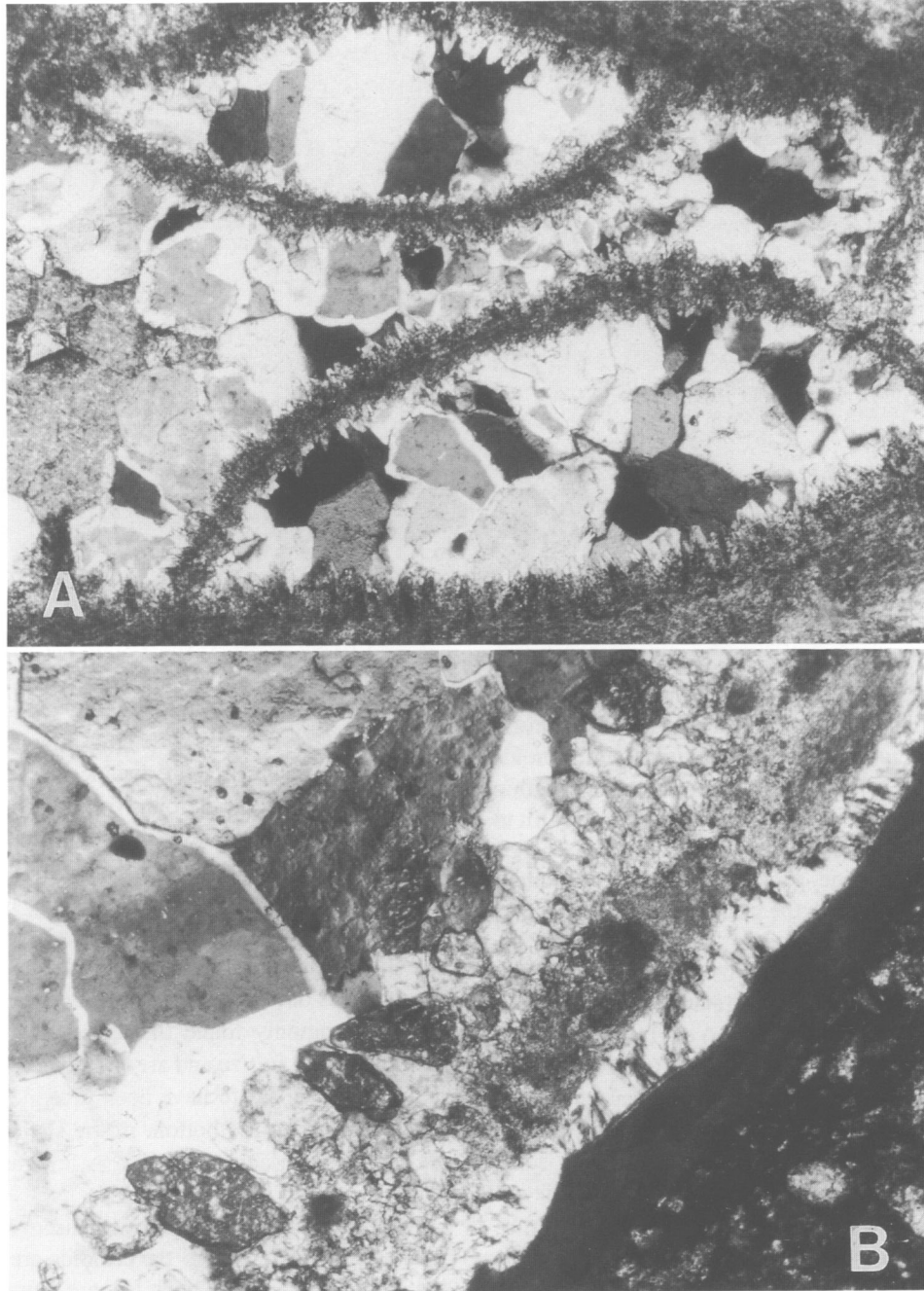


FIGURE 10-9.—Photomicrographs of preserved cements. A, fusulinid intrabiotic cavity is lined by calcite needles and filled with blocky calcite and quartz from the Willis Ranch Member (section 1WR, 70.4 m; bottom of photomicrograph represents 0.5 mm). B, brachiopod shell at lower right is replaced by length-slow chalcedony and calcite needles line the inside of the cavity, which is filled with megaquartz from the China Tank Member (section 5CT, 73.2 m; bottom of photomicrograph represents 0.05 mm).

time, more and better porosity and different types of cements would be expected to be found. Megaquartz occurs as a replacement of carbonates in shallow marine to intertidal environments (Flores et al., 1977:1619), which further supports an environment of deposition in which short-lived exposure can occur.

Most of the fossils in this subfacies probably represent death assemblages (thanatocoenoses) that were piled up into low lying areas or depressions by storms or bottom currents (shell heaps). The majority of these fossils were probably disarticulated, broken, and abraded before they were buried. A few fossils, however, are articulated and well preserved and likely lived in the area attached to the dead, disarticulated brachiopods.

Skeletal wackestones and packstones are intimately related, and micrograding is a common feature in polished slabs. Commonly, a poorly fossiliferous wackestone makes up the lower portion of these units and grades upward into a more fossiliferous packstone. The poorly fossiliferous wackestone contains peloids, the majority of which are probably fecal in origin. Algal-coated grains do occur in this portion, but they are not very common. Fossils are also not common in the wackestone, but they are generally complete specimens.

The packstone contains many more fossils than the underlying wackestone. Generally the packstone matrix consists of lime-mud and peloids, although many areas are sparry calcite cemented. Many of these fossils represent skeletal debris. Commonly this packstone grades into a thin chert layer that consists entirely of silicified fossils. The chert layer probably represents a high energy grainstone phase that has been subsequently silicified. Fossils in these thin chert layers most commonly are brachiopods, but fusulinids and crinoids are also common. These chert layers are overlain by thin mudstone layers or dirty wackestones that represent a return to low energy, semirestricted conditions.

The sequence of wackestone–packstone–chert is the pattern found in this subfacies, although the grainstone (skeletal chert) or thin shale unit is not always present. In this subfacies, the wackestone grading into a more fossiliferous packstone probably represents a change from relatively low energy (wackestone) to higher energy (packstone) environments.

Many portions of the higher energy phase (packstones and grainstones) are slightly dolomitic. Dolomite occurs in many intrabiotic cavities and portions of the matrix. Areas that are dolomitic commonly are slightly vuggy and have some biomoldic (leached fossils) and intercrystalline porosity developed. These dolomite units represent areas that were intermittently subaerially exposed, thus slightly dolomitizing the sediments and leaching out some of the fossils at the same time. Subaerial exposure was probably only brief and sporadic, limiting the amount of dolomitization and leaching.

WHOLE FOSSIL SUBFACIES.—This subfacies is identified by a large percentage of whole fossils and the presence of organically stabilized buildups. This subfacies is located generally to the northeast of the skeletal subfacies. Texturally,

this subfacies consists of whole fossils in a lime-mud matrix. Major fossils include brachiopods, crinoids, bryozoans, and small ammonoids. Skeletal debris is common in this subfacies. Matrix material is most commonly a very fine to fine crystalline mixture of micrite and microspar. Microspar generally forms a tight, interlocking hypidiotopic fabric with no visible pore space. Most crystals are uniform in size and shape. The matrix contains little terrigenous material.

Peloids are a common framework grain in this subfacies. Included in this group of peloids are fecal pellets and algal-coated grains. Fecal pellets represent approximately 60 percent of the nonfossil allochems and are well sorted and uniform in size and shape. Algal-coated grains generally consist of partially micritized skeletal debris. Although not very abundant, this skeletal debris varies in size and shape, with coatings ranging from thin micrite envelopes to thick algal crusts.

Peloids and algal-coated grains appear much darker than the enclosing cement. This is probably due to the fine crystalline nature of the micrite that makes up the peloids and possibly to some organic matter incorporated into the grains. Because of the fine crystalline nature of these sediments, identification of the different cements was difficult. It appears that only one generation of cement is present between the peloids. Much of this cement probably represents very early diagenetic recrystallization of the original lime-mud to microspar shortly after the sediments were deposited. This recrystallization effectively sealed off the pores so the sediments were subjected to little subsequent diagenetic alteration.

Fossils are the most important key in defining this subfacies. Many of the fossils are whole and show little evidence of being transported any appreciable distance. Brachiopods are the most common type of fossil found in the China Tank and Willis Ranch members in the lower part of this subfacies. Other fossils commonly found in association with the brachiopods are bryozoans and ammonoids. Bryozoans include both delicate branching forms as well as massive encrusting types. Bryozoans occur inbetween richthofenids or other brachiopods. Ammonoids occur primarily in seams or clusters, but individuals are commonly found throughout the matrix. Ammonoids are fairly small in size and are complete specimens. Most of the ammonoids appear to have been juvenile forms that probably died and sank to the bottom of the shallow sea floor or were washed in from adjacent areas. A few rare straight nautiloids also were found in this subfacies.

A nearly complete crinoid was discovered in this subfacies by Karen Quick. Most of the crinoids are more complete than the adjoining skeletal subfacies, are commonly silicified, and occur in groups of several (5–10) columnals.

Fossils commonly contain abundant internal sediment consisting of pelleted material and little skeletal debris. Pellets probably are fecal in origin and are well sorted and not graded. Other intrabiotic cavities are either partially or totally filled with blocky sparry calcite.

Stropoli et al. (1991) computer modeled the brachiopod assemblages of the Word Formation and identified organically stabilized shell buildups and shell heaps that correspond exactly with the whole fossil and skeletal subfacies, respectively.

FUSULINID-CRINOID PACKSTONE/GRAINSTONE

Fusulinid-crinoid packstone and grainstone have varying matrix types depending on the outcrop locality (Figures 10-10-10-12). The southwest sections (10AR and 4AR)

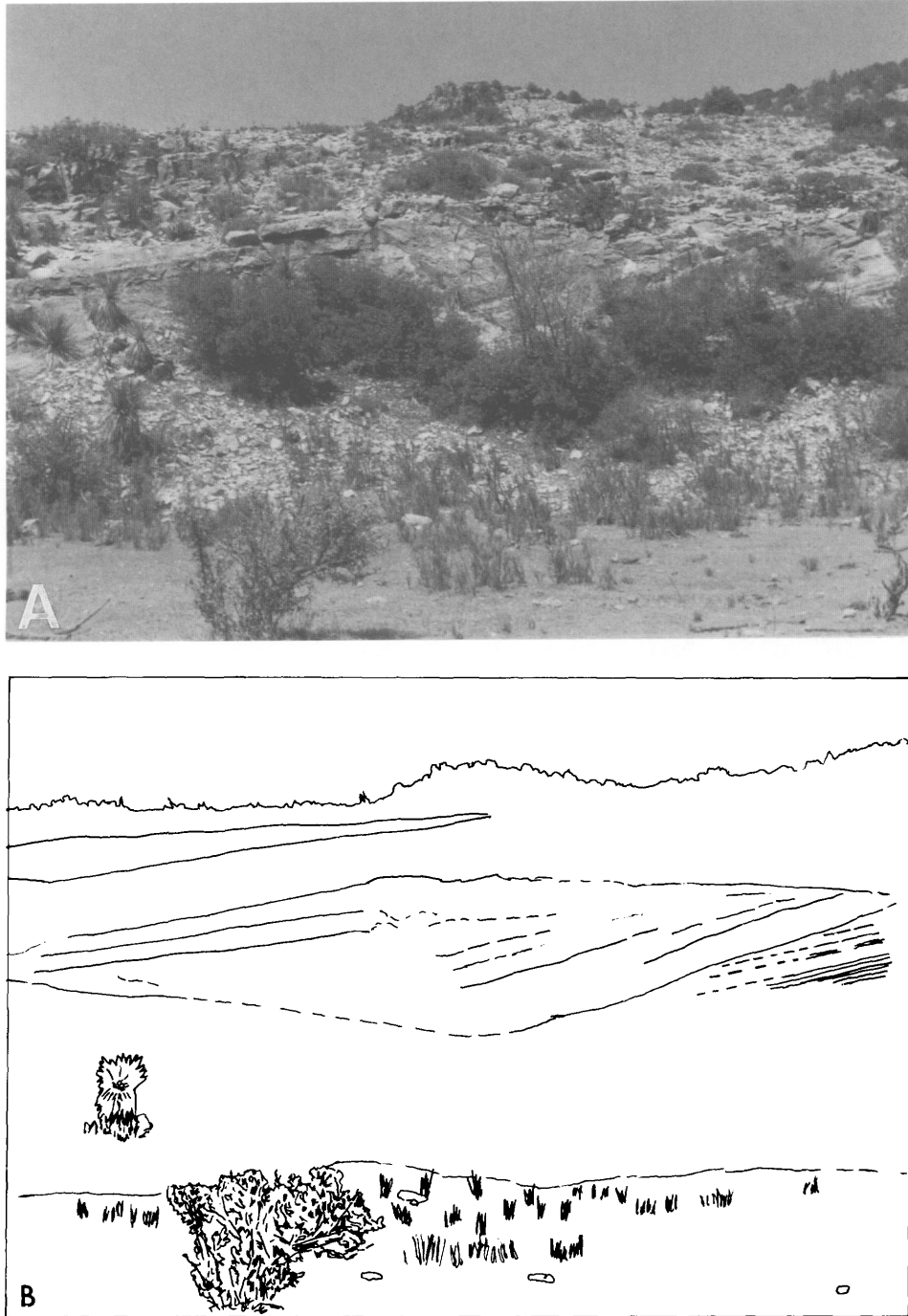


FIGURE 10-10.—Massively bedded channels of fusulinid-crinoid packstone cutting through thinly bedded bioturbated wackestones in the Appel Ranch Member. A, photograph of outcrop. B, sketch of outcrop. (Top of outcrop is 61 m (200 ft.) in section 8AR.)

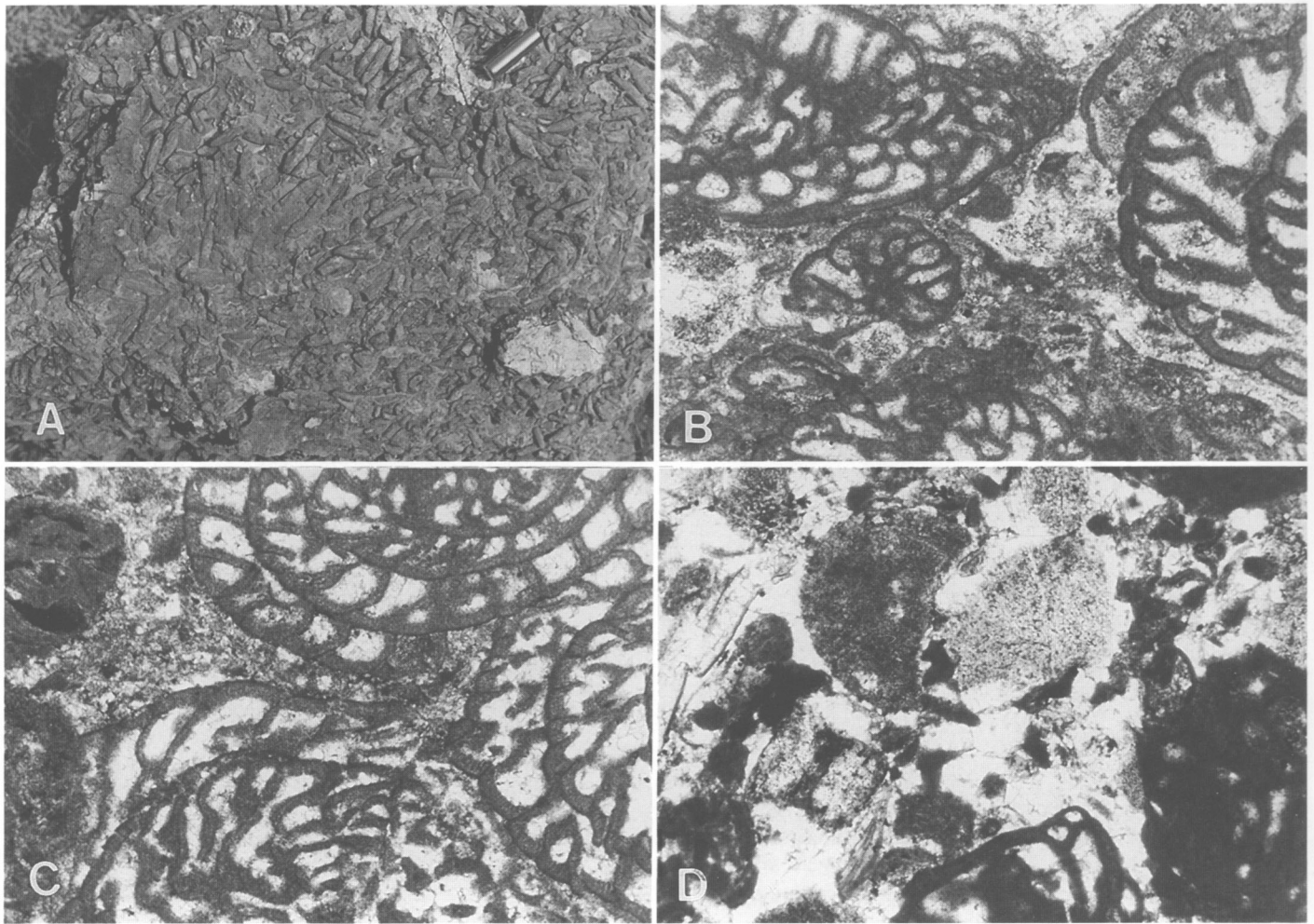


FIGURE 10-11.—Fusulinid-crinoid packstone/grainstone microfacies from the Appel Ranch Member. A, photograph of packed bedding plane (section 8AR, 36.3 m; pen cap is 2 cm long). B, photomicrograph of fusulinid grainstone showing intrabiotic cavities filled with sparry calcite and microspar (section 9AR, 116.6 m). C, photomicrograph of fusulinid packstone. Many fusulinids are micritized along the margins of their tests (section 8AR, 83.8 m). D, photomicrograph of crinoid-fusulinid packstone showing broken up fusulinids and crinoids. Matrix consists of sparry calcite. Scattered peloids are mixed in the matrix (section 8AR, 54.9 m). (Bottoms of photomicrographs represent 0.5 mm.)

generally consist of fine-crystalline micrites and microsars, and the central and northeast sections (8AR and 9AR) are sparry calcite dominated. Sparry calcite is rare in the southwest section, occurring only as void-filling cement. Dominant carbonate allochems are fusulinids and crinoids with lesser numbers of brachiopods and bryozoans. Detrital quartz sand and terrigenous muds (clays) are common in the southwest sections, whereas the central and eastern sections typically are much cleaner and lack appreciable terrigenous clastic material. Dolomite is rare in the southwest sections but becomes an important constituent in the central area and dominates part of the eastern sections. Matrix material is uniform and homogeneous at each outcrop, although it varies between different outcrops. Southwest sections contain matrix of micrite,

microspar, sand grains, and clay-sized material. The matrix is considered to be “dirty” in these sections, with a large percentage of detrital quartz sand and clay-sized particles. The mixture of lime-mud and terrigenous mud gives the slabs and thin sections a brownish color.

The central and northeastern sections contain sparry calcite. Microspar and micrite do occur in these sections, although they represent a smaller percentage. Clastic material is also present in the central locality, but it is widely scattered throughout the matrix. In many thin sections and slabs micrite and sparry calcite are found together, which suggests incomplete winnowing of the sediments. Intrabiotic cavities are calcite filled.

Fossils fall into two different assemblages: mixed assemblages and group dominated assemblages (fusulinids and

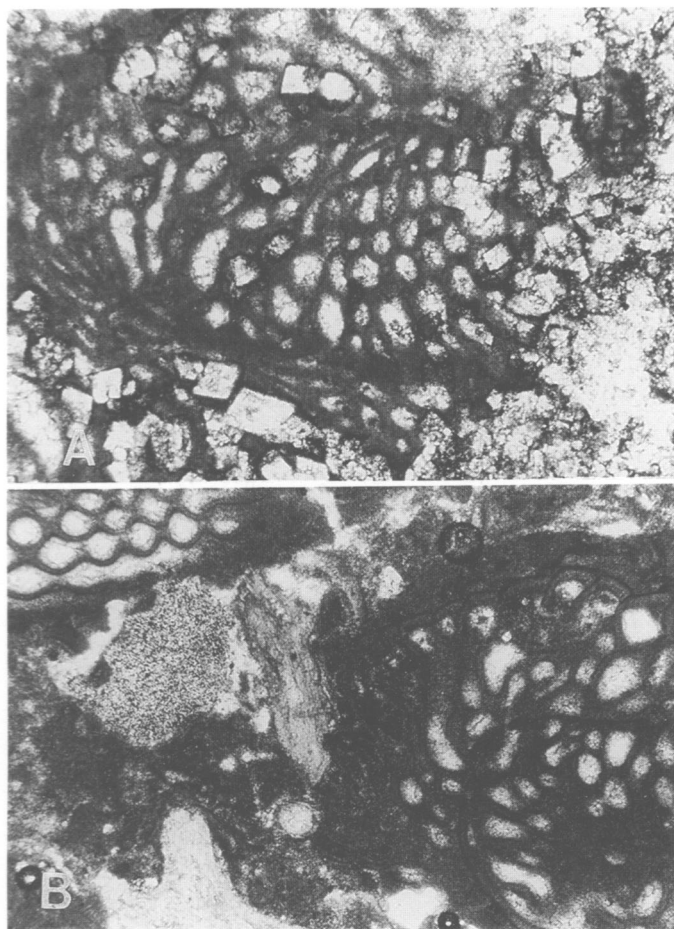


FIGURE 10-12.—Photomicrographs of the fusulinid–crinoid packstone/grainstone microfacies from the Appel Ranch Member. A, fusulinid packstone showing replacement dolomite in matrix and intrabiotic cavities (section 9AR, 127.1 m). B, fusulinid–crinoid packstone showing a fusulinid on the right containing ropey micrite encrustations that are interpreted as the remains of blue-green algae (section 8AR, 38.1 m). (Bottoms of photomicrographs represent 0.5 mm.)

crinoids). The southwest sections contain fusulinids and crinoids mixed with brachiopods, brachiopod spines, and bryozoans. These fossils are poorly sorted and are typically broken, fragmented, and abraded. Fossils are scattered throughout a micrite and terrigenous mud matrix with little or no grading evident. Fusulinids are preferentially aligned, although the directions are somewhat variable.

Fossils in the central and northeastern sections are dominated by fusulinids (*Parafusulina*). Spectacular numbers of *Parafusulina* typically are tightly packed into the rocks (Figure 10-11A). Most fusulinids are complete, although many are broken, crushed, or distorted due to compaction. Brachiopods and bryozoans are rarely seen in the grainstones and occur only as scattered fossil fragments. Cement most commonly is clear sparry calcite, with the intrabiotic cavities also filled with sparite. Crinoid columnals are found mixed in with the

fusulinids, but other thin sections and slabs commonly have the reverse situation, with crinoids being the dominant allochem and fusulinids as the accessory. Crinoids are more abundant in the northeast section (9AR), probably reflecting more stenohaline conditions. Fusulinids still remain a very important contributor to the sediments at this locality.

Silicified fossils occur throughout the different sections. Brachiopods and bryozoans are the most commonly silicified fossils, but fusulinids and crinoids are also replaced. In the northeast section (9AR), only scattered brachiopods are silicified and fusulinids are not altered. Replacement by length-slow chalcedony is the most common type of silicification. Replacement is good, with many skeletal details faithfully mimicked.

Peloids (fecal and algal-coated grains) are important framework contributors in the central and northeast sections, and especially in the southwest sections. These peloids are very similar to those described from the peloid packstone microfacies common to the China Tank and Willis Ranch members. Most commonly, fusulinids and crinoids are coated by micrite envelopes and thick algal encrustations. Areas between fusulinids contain ropey micrite rinds or calcareous tubes, which possibly are blue-green algal remains. Peloids appear to be coated with layered micritic films, which probably are also blue-green algal remains. These films might form in semi-agitated water, similar to that in which modern ooids or oncoids form, with micrite added on to the exteriors of the grains layer by layer.

Intraclasts occur in the southwest and central portions of the Appel Ranch but are absent in the sections in the northeast. Lithoclasts primarily consist of pellet and peloidal material with few fossil inclusions. Lithoclasts are flat, rounded, and relatively small (several millimeters to a few centimeters) and probably represent small rip-ups or the results of biologic activity because these lithoclasts are very similar to the surrounding sediments. Peloids and fossil fragments are truncated along the margins. Small, brown, round terrigenous intraclasts are also common in the southwest portion of the Appel Ranch.

Dolostone is primarily limited to the central and northeast sections of the Appel Ranch (8AR and 9AR) where it occurs in both the fusulinid–crinoid packstone/grainstone as well as the bioturbated wackestone microfacies. Dolomite in the fusulinid-rich beds occurs mostly as replacement dolomite in isolated intrabiotic cavities and scattered throughout the matrix. The replacement dolomite is composed of coarse crystals (0.2–1.0 mm), most of which are euhedral, and is primarily limited to the fusulinid–crinoid packstone/grainstone microfacies. In contrast, penecontemporaneous dolomite is made up of finer crystals (<0.25 mm) and commonly forms a hypidiopic fabric. Pervasive dolomitization of the wackestones and packstones has destroyed most of the original textures, but some relict textures and allochems are still recognizable as “ghosts.”

BIOTURBATED WACKESTONE/LIME MUDSTONE

Interbedded with the fusulinid–crinoid packstone and grainstone is sparsely fossiliferous, bioturbated, and burrowed wackestone and lime mudstone (Figure 10-13). This microfacies typically contains few fossils and is uniquely recognized by the large number of chertified burrows. This microfacies occurs throughout the Appel Ranch Member, but it is best developed in the central portions of the field area (sections 8AR and AR III).

A variety of different matrix types occurs in this microfacies. Some are very argillaceous and can be considered to be marls, whereas others are considered to be clean lime mudstones. Still others have been dolomitized and lack any original texture. These dolostones are most commonly finely crystalline and probably represent diagenetic dolostones that formed during or shortly after deposition. Except for being bioturbated, this microfacies lacks any other primary sedimentary structure.

Rare articulated brachiopods occur in this microfacies and show little evidence of being transported. Brachiopods are concentrated along the margins of the burrows and occur very rarely inside the burrows. These fossils probably were pushed aside by the burrowing infauna.

In the sediments that have not been dolomitized, pellets and peloids are the most common allochems. Most of these pellets probably represent fecal pellets because of their uniform sizes and shapes. The large number of burrows also supports a fecal origin for these pellets, which are products of mud ingestors. Micritized grains are rare, although some algal-coated grains are present.

Burrows are randomly oriented and typically form “spaghetti noodle” patterns in vertical and horizontal directions. These probably represent fodinichnal, or randomly oriented, feeding burrows. The burrows are a much darker brown than the surrounding sediments because they contain a much higher content of terrigenous and organic matter. The high organic content and the fact that the burrows were probably more porous than the surrounding sediments helps explain why only the burrows were chertified and not the surrounding sediments.

RECRYSTALLIZED LIMESTONE/DOLOSTONE

Dolostone makes up the majority of the rocks in the eastern facies of the Word Formation of King (1931). This microfacies is identified by the presence of 20 percent or more of the mineral dolomite in the rock. The primary texture has been largely destroyed, and the dolomite consists mainly of replacement dolomite in which relict textures, such as fossils, peloids, and crude bedding, are preserved (Figures 10-14, 10-15). Other dolomite probably represents penecontemporaneous dolomite as identified by small crystal size and no relict features.

Texturally, this microfacies consists of two different sizes of dolomite crystals. Most replacement dolomite is composed of

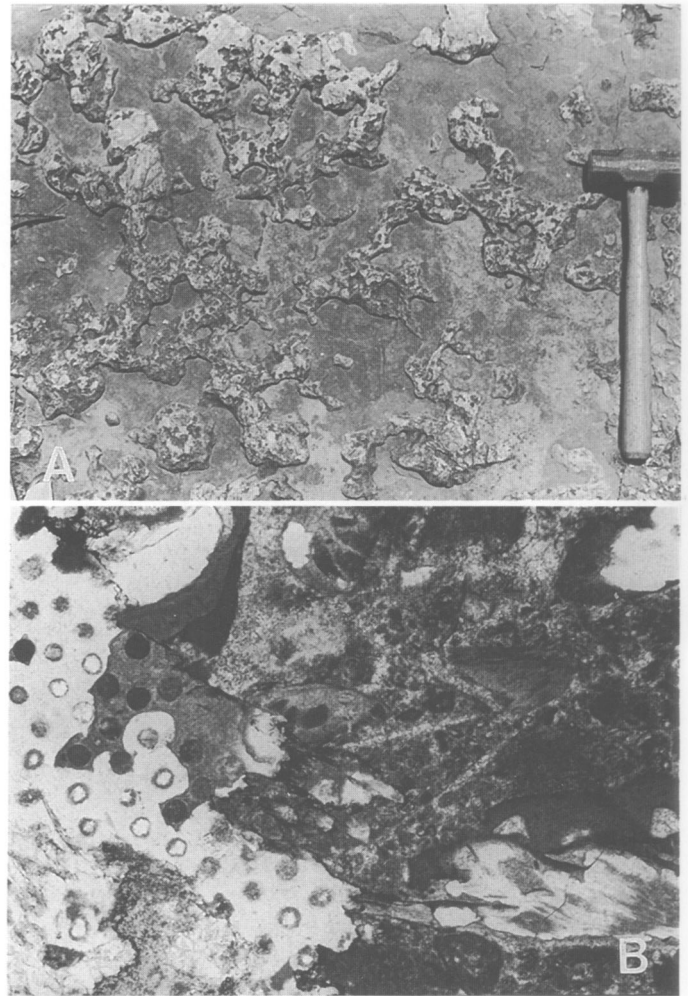


FIGURE 10-13.—Bioturbated wackestone/lime mudstone microfacies. A, photograph of chertified burrows in the Appel Ranch Member (section 8AR, 2.1 m; hammer is 0.46 m long). B, photomicrograph of skeletal wackestone from the Appel Ranch Member (section 8AR, 2.1 m; bottom of photomicrograph represents 0.5 mm).

coarse (0.25–1.0 mm) crystals that typically form a tight, interlocking, xenotopic fabric. In contrast, the penecontemporaneous dolomite is made up of finer crystalline (generally less than 0.25 mm) dolomite. Many of these dolomite crystals are euhedral and, in part, form a sucrosic texture. Most of the fine crystalline dolomite is restricted between framework grains and is considered to be recrystallized matrix material.

Fossils in this microfacies generally consist of fusulinids and crinoids. Fusulinids are fairly common, and most are unbroken and are rarely dolomitized. Disarticulated crinoid columnals are dark in thin sections and remain relatively unaffected by dolomitization. Many of the crinoids have been epitaxially cemented by coarse crystalline calcite, which occurs as optically continuous overgrowths along the margins of crinoid columnals. Some of this calcite can be considered to be

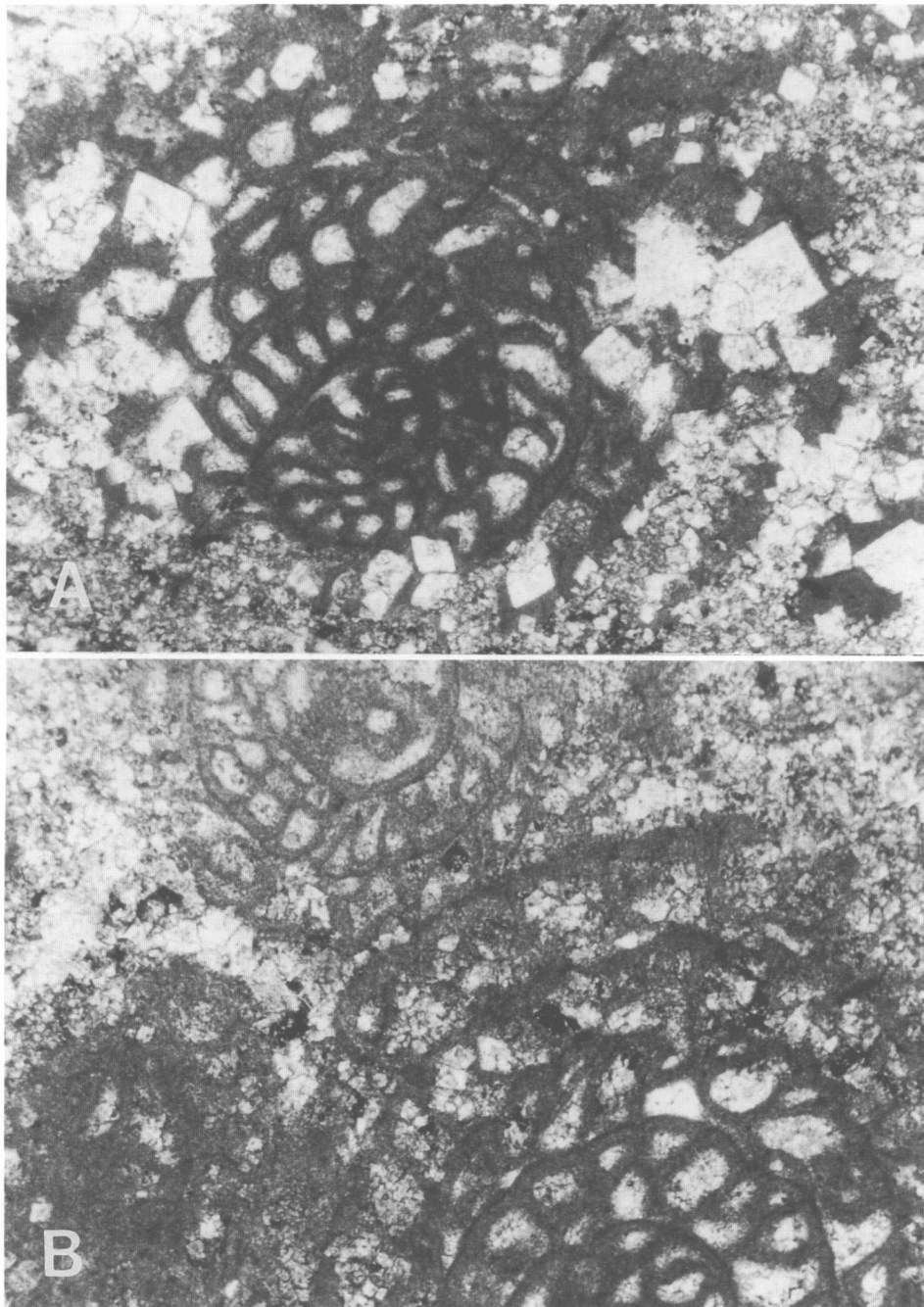


FIGURE 10-14.—Photomicrographs of the recrystallized limestone/dolomite microfacies from the undifferentiated Word Formation (eastern facies). A, coarse crystalline dolomite destroying a fusulinid (section 12PW, 30.8 m). B, various stages of the recrystallization of fusulinids from a “ghost” at the lower left to a fairly well-preserved large fusulinid with coarse crystalline dolomite in the intrabiotic cavities at the lower right (section 12PW, 30.8 m). (Bottoms of photomicrographs represent 0.5 mm.)

poikilotopic, enclosing several grains. This cement probably was deposited during the leaching and dolomitization of the sediments, or it could have occurred during a void-filling late stage of diagenesis. Brachiopods, bryozoans, and other fossils that have been silicified are recognizable, but these are rare.

Pervasive dolomitization and recrystallization of this microfacies has destroyed most of the original texture; however, some relict features of the original limestone are commonly preserved as “ghosts,” including peloids (fecal and algal), crinoids, fusulinids, and bryozoans. Another relict feature

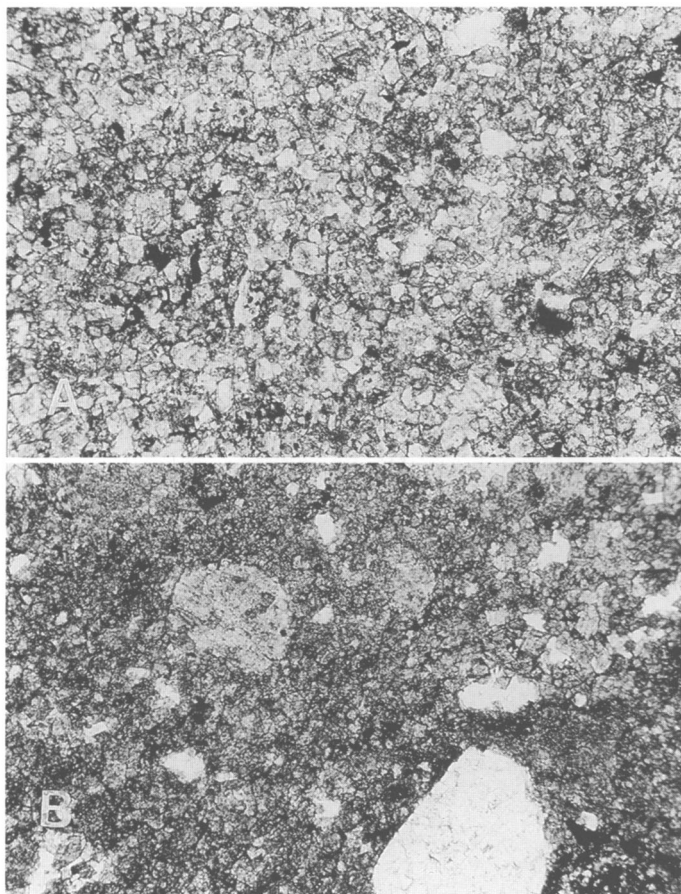


FIGURE 10-15.—Photomicrographs of the recrystallized limestone/dolostone microfacies from the undifferentiated Word Formation (eastern facies). A, complete dolomitization has left no recognizable skeletal grains (section 12PW, 55.3 m). B, recognizable crinoid debris. Note the pore at center right, which probably represents a fossil that has been leached out (section 12PW, 78.7 m). (Bottoms of photomicrographs represent 0.5 mm.)

commonly found in this microfacies are leached fossils. The most common leached fossils are brachiopods and less commonly crinoids and fusulinids. Other areas of the sediment contain irregular vugs whose specific origin is unknown. These vugs are irregular in size and shape and possibly are the result of the dissolution of sulfates or are enlarged fossil molds.

Lithofacies

The carbonate microfacies and Word mudstones define five mappable lithofacies: (1) mudstone, (2) peloidal packstone, (3) skeletal wackestone/packstone, (4) fusulinid–crinoid grainstone/bioturbated wackestone, and (5) recrystallized limestone/dolostone. The distribution of these lithofacies is shown in Figure 10-16. All lithofacies intergrade and are identified by the dominant rock type. Beds of an identifiable facies thicker than 1 m are identified as that lithofacies.

1. *Mudstone*: The mudstone lithofacies consists of mud-

stone, claystone, and fine sandstone with scattered thin beds of peloidal packstone and scattered lenses that represent channel deposits of skeletal to conglomeratic wackestone and peloidal packstone. Carbonates thicker than 1 m were classified in the appropriate carbonate lithofacies. Thin beds and interbeds of mudstone are common to all the carbonate lithofacies.

2. *Peloidal Packstone*: The peloidal packstone lithofacies consists of peloidal packstone, skeletal peloidal packstone, and thin beds of mudstone, fine sandstone, and skeletal wackestone/packstone.

3. *Skeletal Wackestone/Packstone*: The skeletal wackestone/packstone lithofacies consists of two intimately related subfacies, skeletal and whole fossil. Even though the whole fossil subfacies is restricted to the eastern part of the distribution of this lithofacies (Figure 10-16), persistent interbeds of the skeletal subfacies makes it impossible to separate it as a mappable lithofacies. Thin interbeds of mudstone, peloidal packstone, bioturbated wackestone, and fusulinid–crinoid packstone are common.

4. *Fusulinid–Crinoid Packstone/Bioturbated Wackestone*: The fusulinid–crinoid packstone/bioturbated wackestone lithofacies consists of two intimately related carbonate microfacies. Typically, fusulinid–crinoid packstone and grainstone form channel deposits that cut the bioturbated wackestone. Thin beds of mudstone and skeletal wackestone and packstone are common. This lithofacies grades laterally into the recrystallized limestone/dolostone lithofacies.

5. *Recrystallized Limestone/Dolostone*: This lithofacies consists of the carbonate microfacies of the same name. Most of the rock appears to be recrystallized and dolomitized fusulinid–crinoid packstone and grainstone and bioturbated wackestone.

Depositional Environments

The various microfacies types and their mutual relationship in space, as well as their sedimentary structures and paleontology, define the depositional environments of the Word Formation more precisely than has been previously reported. In general, the lower portion of the Word (China Tank and Willis Ranch members) represents a shallow-water lagoonal or back-reef environment, whereas the upper portion of the Word (Appel Ranch Member) represents higher energy shoals or tidal flat deposits.

The peloidal packstone microfacies in the lower part of the Word is interpreted to have been formed in a shallow-water lagoonal environment with varying degrees of water circulation and energy levels, especially toward the northeast. A lagoonal environment is identified by the abundance of pelleted sediments, which comprise nearly all the sand-size grains in the southwestern part of the Willis Ranch. Here the Willis Ranch is very argillaceous and sandy, indicating that this area was relatively close to a clastic source area. Quartz sand grains are angular to subangular, suggesting that they have not been

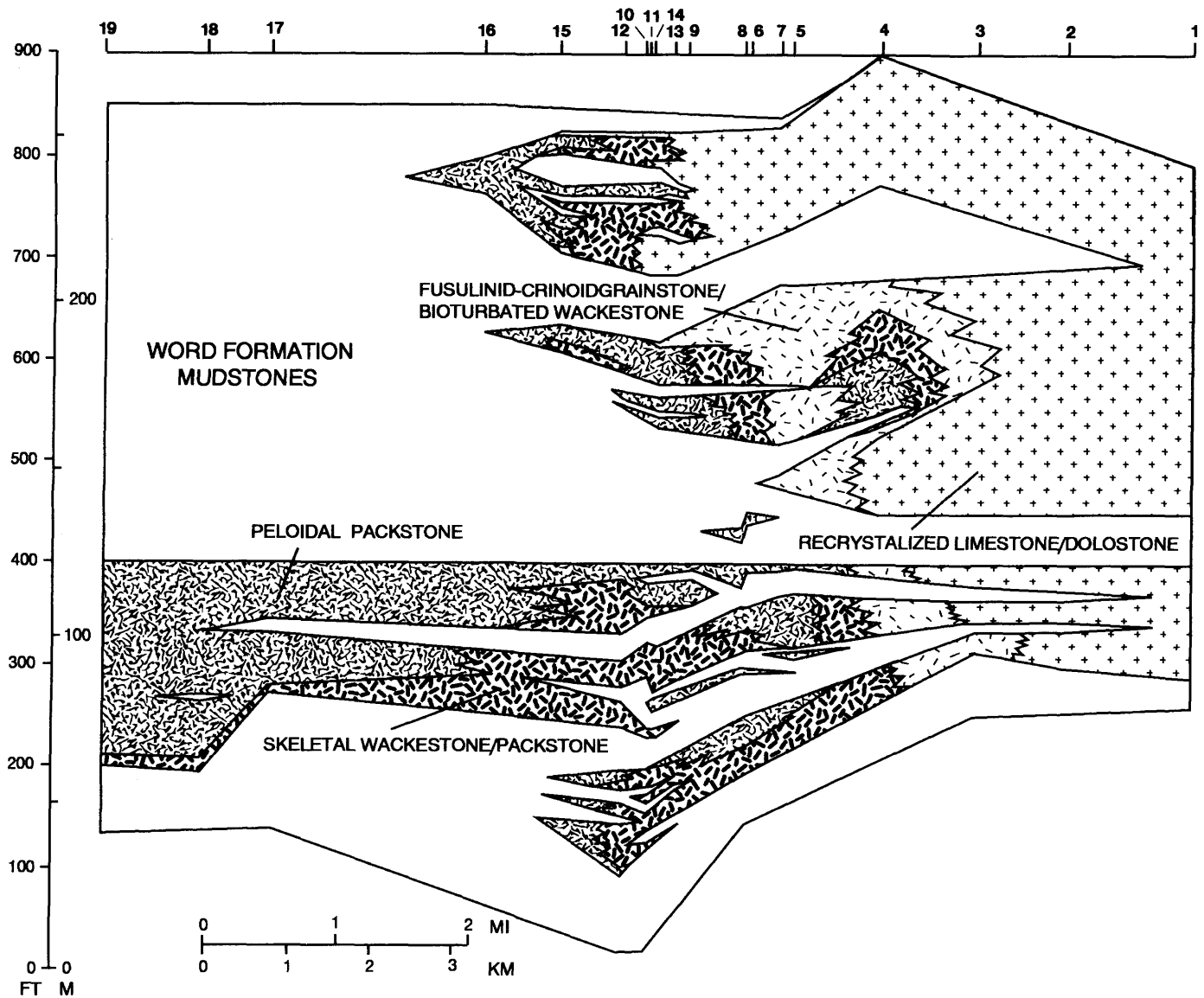


FIGURE 10-16.—Facies analysis of the Word Formation displayed as a true distance cross section (as in Figure 10-4; numbers across the top refer back to sections in Figure 10-3).

transported any appreciable distance. This was a low-energy environment as indicated by the fine textures of the mudstones, siltstones, and lime mudstones deposited here. This type of environment was an ideal habitat for infaunal deposit feeders, such as worms, gastropods, or other mud ingestors. Conversely, this environment was not suitable for filter feeding organisms, such as brachiopods or crinoids, whose respiratory and feeding organs do not function well in a muddy, turbid environment. Thus, only a relatively few broken and transported fossils are found in this microfacies. Primary sedimentary structures, such as laminations or small-scale bedding, are also lacking probably as a result of bioturbation. The peloidal packstones have not been winnowed, which also contributes to

the lack of small-scale sedimentary structures. The finely crystalline nature (micrite and clay-sized particles) and the absence of any sparry calcite within this microfacies again suggest deposition in a quiet, low energy environment. This was a shallow water environment as indicated by the abundance of algal-coated grains and small intraclasts. The conodont *Hindeodus*, which is indicative of near-shore conodont biofacies, is common to this microfacies. This environment was probably semirestricted, with little epifauna as indicated by the scarcity of fossils. Most of the fossils that are found in this microfacies represent allochthonous debris. Tidal currents and periodic storms, or other high energy events brought in fossil debris from a nearby, more normal marine

environment. This microfacies is interpreted to represent a low energy, shallow water lagoon between a normal marine environment but still near a positive land area from which the detrital quartz sand was derived. This microfacies is similar to the "Restricted Marine Shelf Lagoons (Facies Belts 7 and 8)" of Wilson (1975:68), which are characterized as being bioturbated pelleted lime-mud wackestones that occasionally grade into higher energy fabrics. The fauna is somewhat reduced and represents deposition in quiet, restricted bays and ponds.

The peloidal packstone microfacies grades into a much more fossiliferous skeletal wackestone/packstone subfacies of the wackestone/packstone microfacies that also represents a shallow-water lagoonal or back-reef environment. This part of the lagoon was further from land, and much cleaner carbonates were deposited. The subfacies represents more normal marine conditions as indicated by the greater abundance of stenohaline organisms (crinoids and other echinoderms). Most commonly, low energy conditions existed, which allowed the lime-mud to settle out without affecting the brachiopods or other filter feeding organisms. The abundance of fecal pellets suggests mud-ingesting infaunal organisms thrived in this environment.

This low energy environment persisted during most of the time of deposition; however, sporadic higher energy conditions occurred probably as the result of storms or unusually strong tides. These higher energy events are recognized by heaps of shells. Shell heaps appear to be represented by two types: moderately large heaps, which were colonized by hard substrate-loving organisms exemplified by some of the productid brachiopod localities of Cooper and Grant (1972), and packed thin beds and seams that are commonly chertified. Many outcrops show a relationship of alternating high and low energy deposits. Sparsely fossiliferous and pellet-rich sediments represent the low energy deposits, which are commonly overlain by a mixture of more abundant fossils with pelleted sediments that reflect a change to higher energy conditions. Commonly this unit is capped by thin fossiliferous cherts containing nothing but tightly packed fossils with little or no matrix material. This represents the highest energy phase with all of the lime-mud being winnowed out of the sediments. These high energy chert layers are relatively thin and sporadic, indicating they were possibly storm events and not normal for this microfacies.

The skeletal wackestone/packstone subfacies was deposited in very shallow water as indicated by the abundance of algal-coated grains. Many of these encrustations are interpreted to be the product of blue-green algae, which thrives only in very shallow water. The conodont faunas also support a shallow water environment of deposition. This subfacies corresponds to the "Open Platform (Facies Belt 7)" of Wilson (1975), which is a shallow water environment with moderate circulation just below the wave base and with common bioturbation of the sediments.

The skeletal wackestone/packstone subfacies is intimately associated with the whole-fossil wackestone/packstone subfacies. This whole-fossil subfacies is identified by abundant

whole, or relatively complete fossils, many of which are interpreted to be in life position. Skeletal debris does occur in this subfacies, but it is not as abundant as in the adjacent, skeletal subfacies. The carbonates in this subfacies are very clean of terrigenous material compared to those to the southwest, indicating that they were deposited further from the clastic source area. Carbonates in this subfacies were also deposited in a low energy environment as indicated by the high percentage of lime-mud and fine crystalline carbonates. Many of the brachiopods contain internal sediment, which generally is a mixture of pellets and lime-mud. Very little sparry calcite was found in this subfacies, suggesting that this area was not subjected to high energy conditions. This subfacies corresponds to the "Open Platform or Shelf (Facies Belt 7)" of Wilson (1975), which forms in quiet water below the wave base and generally preserves some infauna and epifauna.

The fusulinid-crinoid packstone/grainstone microfacies is commonly interbedded with the sparsely fossiliferous, bioturbated wackestone/lime mudstone microfacies. Packstone and grainstone contain abundant current-aligned fossils and are commonly spar-cemented indicating high energy conditions. Most of the lime-mud has been winnowed out of these sediments. Of course, the lime-mud is abundant in the adjacent bioturbated wackestone/lime mudstone. A shallow-water environment is recognized by the abundance of algal-coated and encrusted grains. The abundance of stenohaline organisms, such as crinoids, also indicates normal marine conditions. The large sedimentary feature (Figure 10-10), which is interpreted to be a tidal channel, consists of fusulinid-crinoid packstone that cuts into the underlying bioturbated wackestone. The channel is slightly dolomitic, probably due to its original high permeability and porosity and to its subsequent flushing with meteoric waters. This dolomitization suggests near-surface conditions. The intimately intermixed high and low energy depositional environments and the abundant shallow-water indicators of these two microfacies represent tidal mud flats cut by tidal channels.

The most common type of organisms present in the bioturbated wackestone/lime mudstone microfacies were burrowing organisms and other mud ingestors. Burrows within this microfacies became chertified because of their originally high organic content and high permeability. Little skeletal material was washed into this microfacies, and the majority of that present represents allochthonous debris.

The upper portion of the Word Formation (Appel Ranch Member) represents high energy platform sands in the central part and grades into adjacent lower energy tidal or lagoon environments. The high energy environment is represented by fusulinid-crinoid grainstone. Fusulinids are current-oriented in a roughly north-south direction. Further southwest, the samples become more shaly and sandy, and the fusulinids have more varied orientations but still indicate north-south current directions. The lower velocity orientation (Futterer, 1978) was used because the samples contain abundant mud, indicating a lower energy environment than in other portions of the Appel

Ranch. The Appel Ranch represents the fusulinid–crinoid packstone/bioturbated wackestone lithofacies and is similar to the “Open Platform Sands (Facies Belt 6)” of Wilson (1975).

The eastern facies still remains somewhat of an enigma. Dolomitization and recrystallization has destroyed most of the fabric and texture, which makes identification of the depositional environment difficult. The few recognizable crinoids and fusulinids in this microfacies indicate that this was a normal marine environment. This was a very shallow water environment that was probably subaerially exposed at times, thereby dolomitizing the sediments and causing the vuggy nature of the sediments. Because of the abundance of crinoids and fusulinids in places and the general lack of fossils in others, this microfacies is thought to have been very similar to the fusulinid–crinoid packstone/grainstone microfacies interbedded with the bioturbated wackestone/lime mudstone microfa-

cies, but it was shallower and commonly exposed. This microfacies is similar to Wilson’s “Organic Reef or Platform Sands (Facies Belts 5 and 6).” These microfacies are described as being massive limestones and dolomites, which may be vuggy due to periodic subaerial exposure (Wilson, 1975).

The sediments of the Word Formation suggest very shallow deposition in the area studied, probably along a shoal developed on the seaward rim or geantiform of a foreland basin (Rohr et al., this volume; Wardlaw, this volume) and deposition into the foreland basin. The eastern facies represents a shoal facies, and the remaining facies represent shallow foreland basin facies. The distribution of facies and flow directions appear to be directly opposite of those hypothesized by Harris et al. (this volume) for the underlying Road Canyon Formation. It appears that by Word time most of the foreland basin was filled in yielding backbay depositional settings.

Appendix 10-1: Measured Sections

Locations of the sections measured for this study are shown in Figure 10-3, and the sections are graphically displayed in Figures 10-17–10-22. (The latitude and longitude is for the base of the section.)

Section	Figure	Measured by	Location
WR III	Figure 10-17	Wardlaw and Grant	30°21.42'N, 103°14.06'W
1WR	Figure 10-17	Rathjen	30°22.48'N, 103°13.79'W
WR I	Figure 10-17	Wardlaw and Grant	30°22.80'N, 103°13.41'W
5CT	Figure 10-18	Rathjen	30°23.35'N, 103°10.70'W
RC X	Figure 10-18	Wardlaw, Grant, Rohr, and Rathjen	30°23.23'N, 103°10.43'W
CT I	Figure 10-18	Wardlaw and Grant	30°23.53'N, 103°10.58'W
706e	Figure 10-18	Wardlaw and Grant	30°23.75'N, 103°10.45'W
7CT	CT II, Figure 10-19	Wardlaw, Grant, and Rathjen	30°23.74'N, 103°09.81'W
WR II	Figure 10-19	Wardlaw and Grant	30°23.92'N, 103°09.53'W
WORD I	Figure 10-19	Wardlaw and Grant	30°24.05'N, 103°07.85'W
Above 7CT	CT II, Figure 10-20	Wardlaw, Grant, and Rathjen	30°23.74'N, 103°09.81'W
2TL	Figure 10-20	Wardlaw and Rohr	30°24.16'N, 103°10.18'W
AR II	Figure 10-21	Wardlaw and Grant	30°23.56'N, 103°12.08'W
10AR	Figure 10-21	Rathjen	30°23.51'N, 103°11.42'W
4AR	Figure 10-21	Rathjen	30°23.97'N, 103°10.80'W
AR III	Figure 10-21	Wardlaw and Grant	30°24.01'N, 103°10.67'W
8AR	AR I, Figure 10-22	Rathjen, Wardlaw, and Grant	30°24.27'N, 103°09.84'W
9AR	Figure 10-22	Rathjen	30°24.43'N, 103°09.33'W
12PW	Figure 10-22	Rathjen	30°25.35'N, 103°06.98'W

APPENDIX 10-1.—Continued.

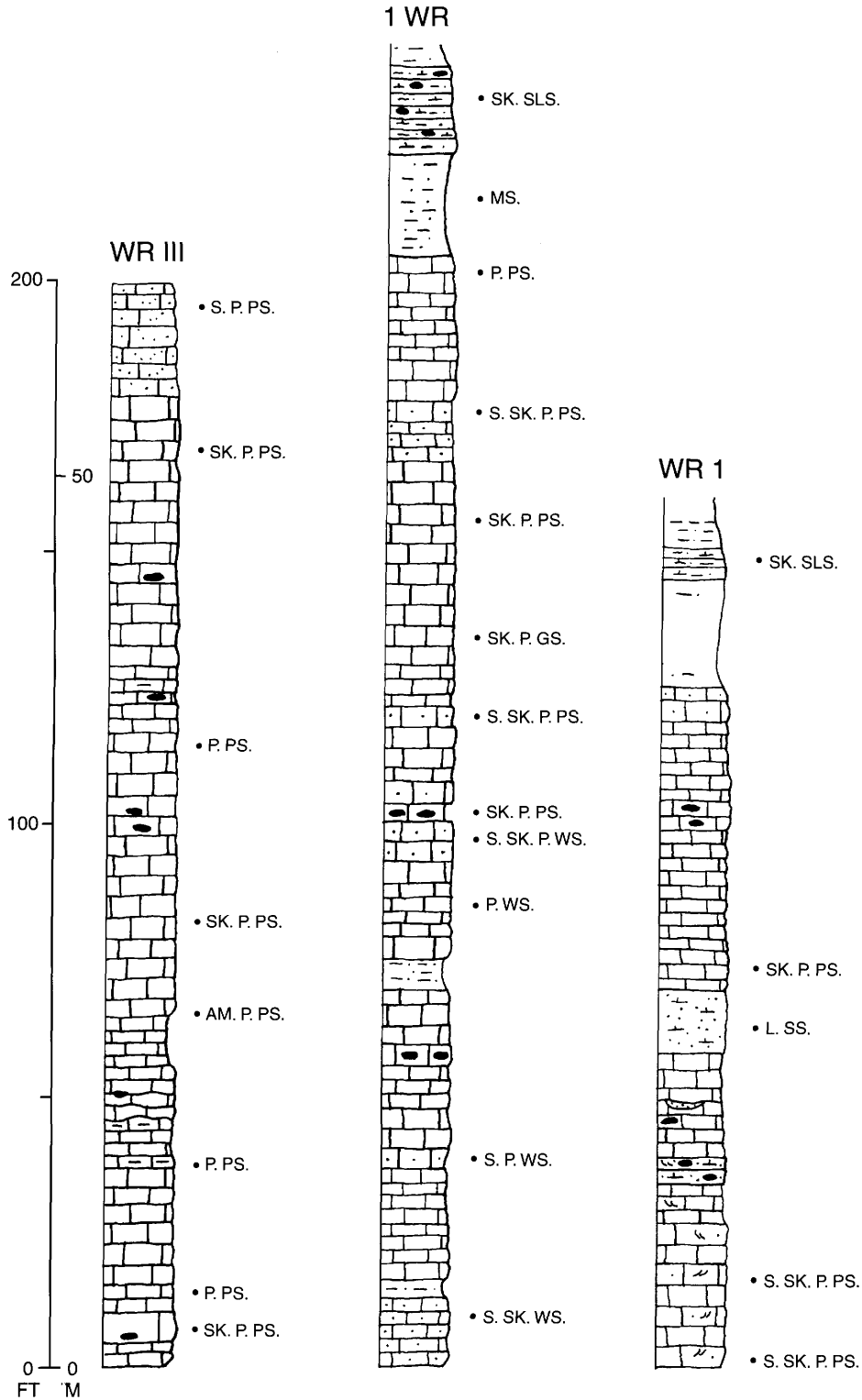


FIGURE 10-17.—Measured sections of the Willis Ranch Member from the western part of the study area showing the petrographic sample location and identification. (Petrographic abbreviations: AM, ammonoid; GS, grainstone; L, limy; MS, mudstone; P, peloidal; PS, packstone; S, sandy; SK, skeletal; SLS, siltstone; SS, sandstone; WS, wackestone.)

APPENDIX 10-1.—Continued.

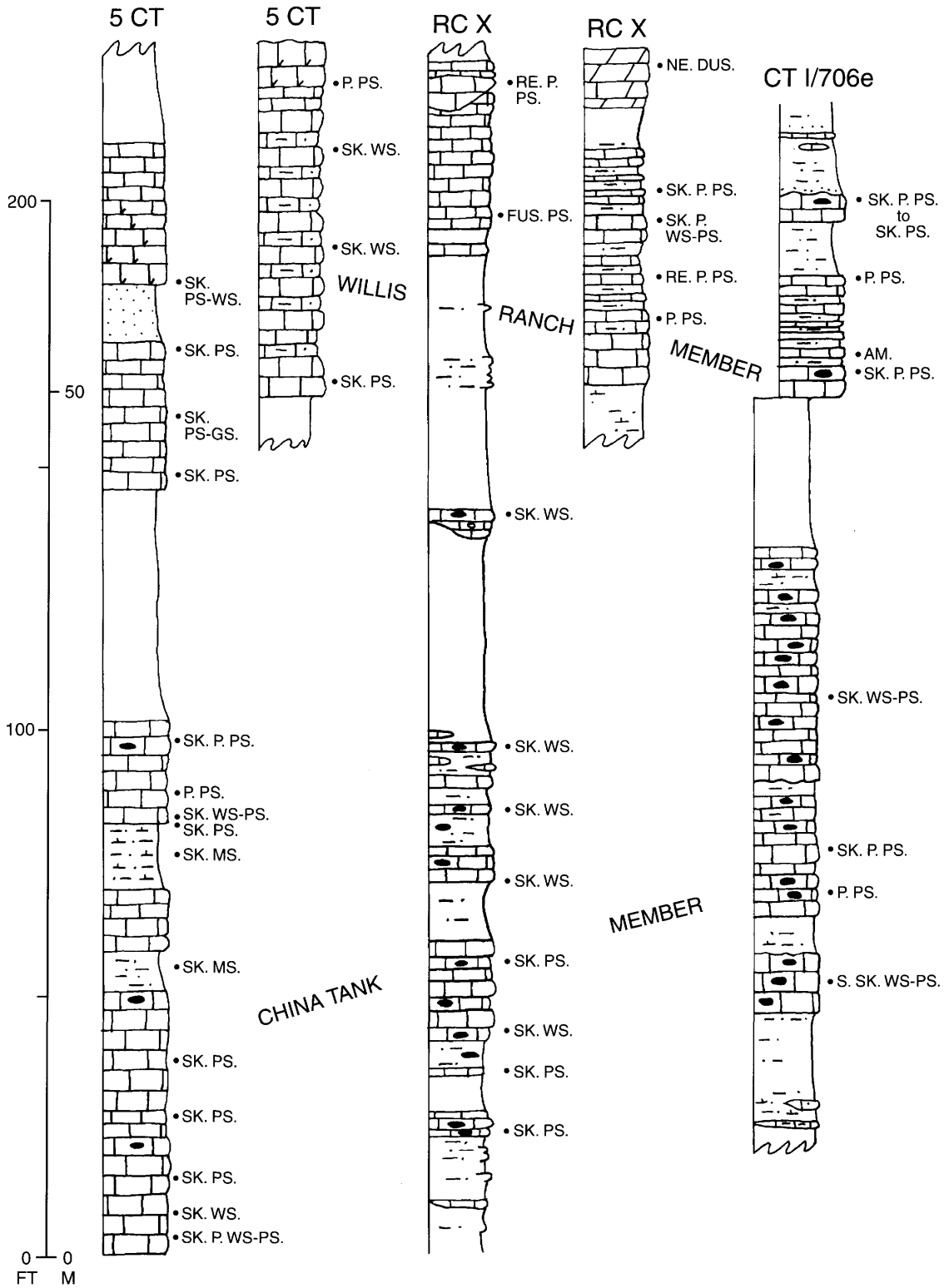


FIGURE 10-18.—Measured sections of the China Tank and Willis Ranch members from the central part of the study area. (Petrographic abbreviations: AM, ammonoid; DS, dolostone; FUS, fusulinid; GS, grainstone; MS, mudstone; NE, neomorphic; P, peloidal; PS, packstone; RE, recrystallized; SI, silty; SK, skeletal; WS, wackestone.)

APPENDIX 10-1.—Continued.

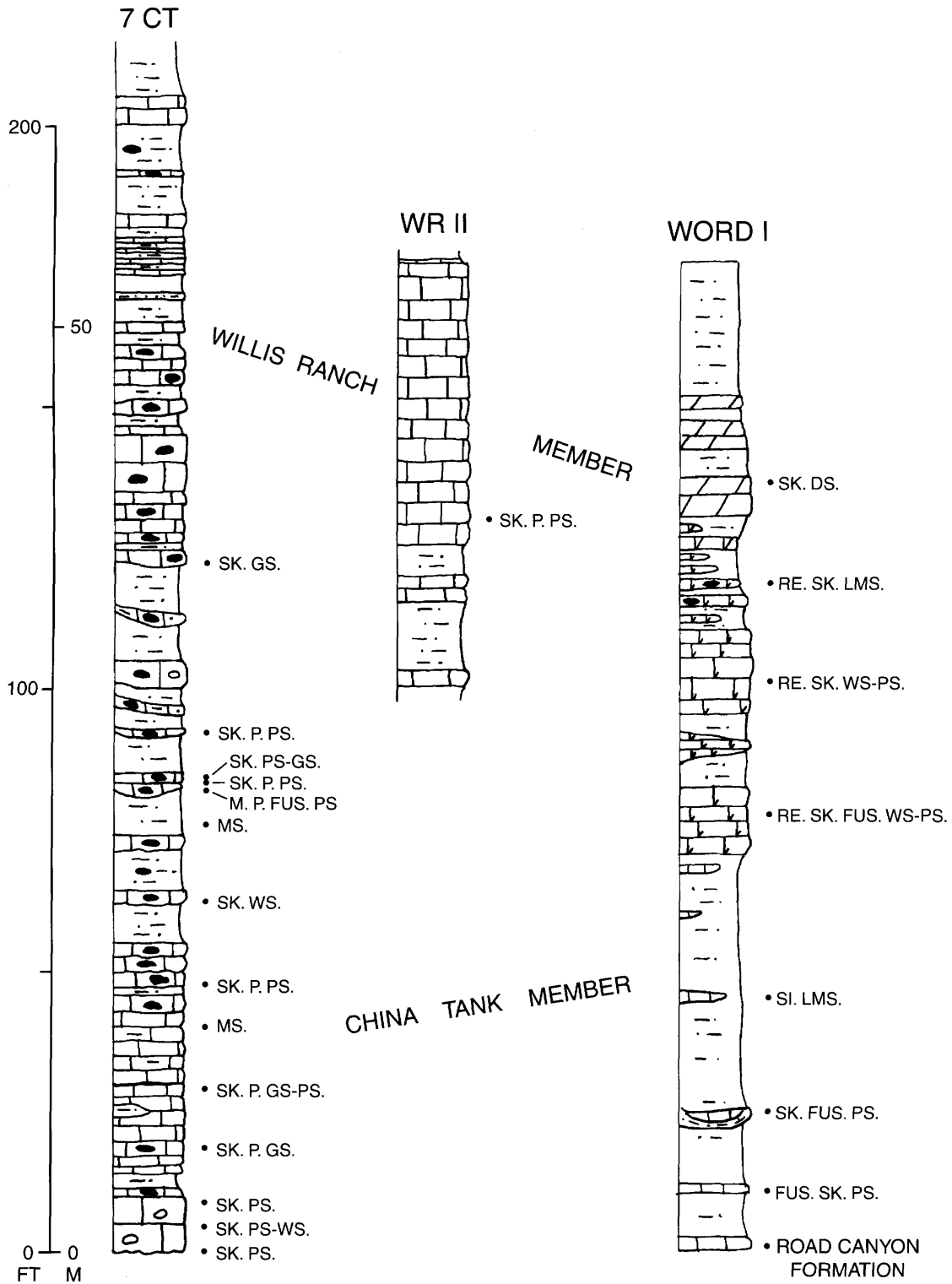


FIGURE 10-19.—Measured sections of the China Tank and Willis Ranch members from the eastern part of the study area. (Petrographic abbreviations: FUS, fusulinid; GS, grainstone; LMS, lime mudstone; M, muddy; MS, mudstone; P, peloidal; PS, packstone; RE, recrystallized; SK, skeletal; WS, wackestone.)

APPENDIX 10-1.—Continued.

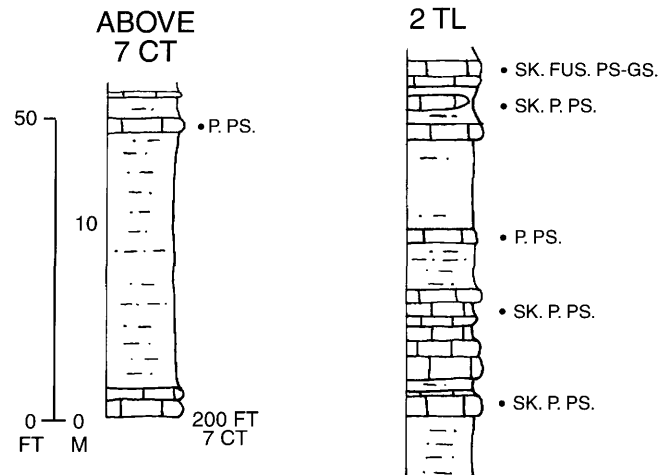


FIGURE 10-20.—Measured section of the lens between the Willis Ranch Member and the Appel Ranch Member. (Petrographic abbreviations: FUS, fusulinid; GS, grainstone; P, peloidal; PS, packstone; SK, skeletal.)

APPENDIX 10-1.—Continued.

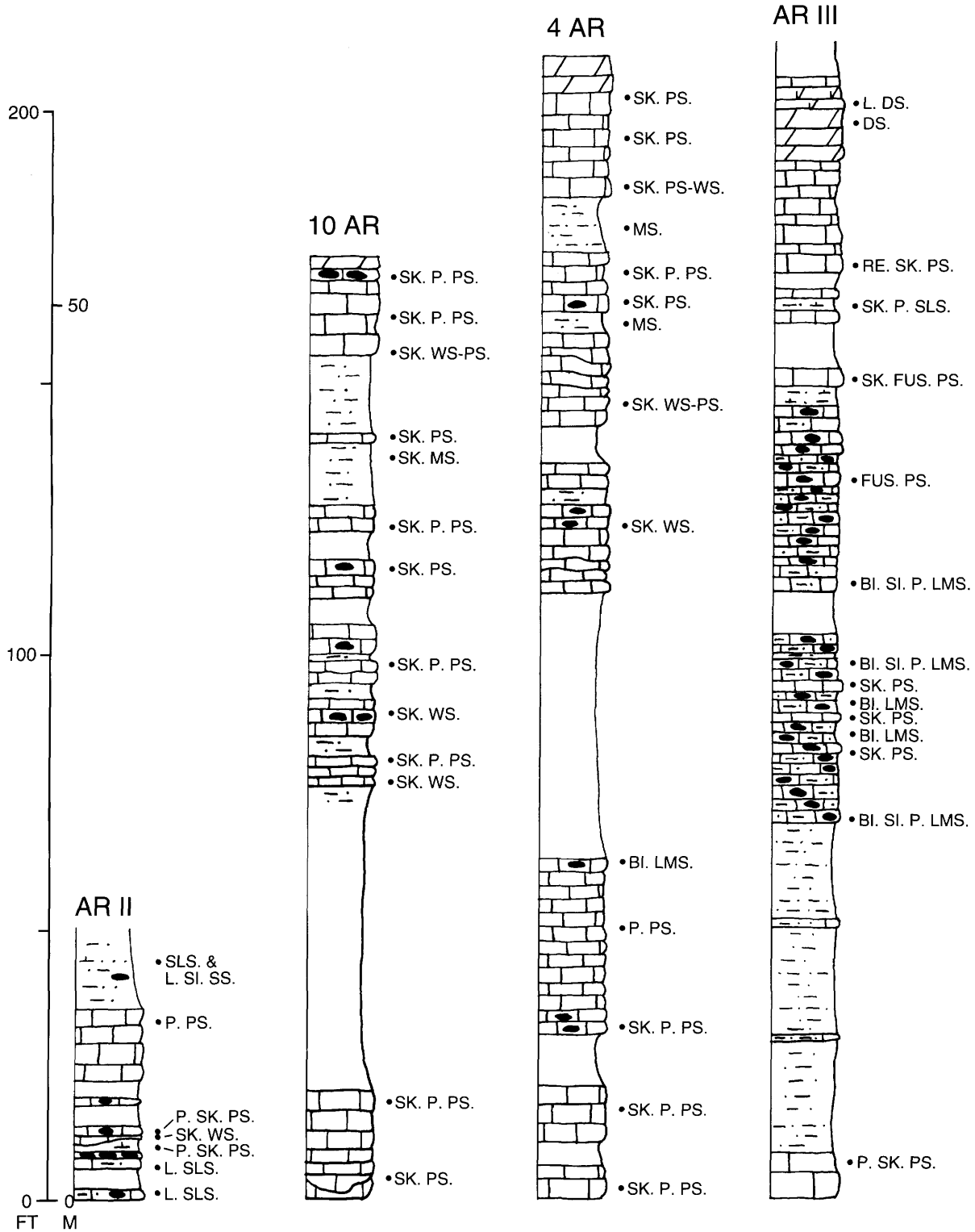


FIGURE 10-21.—Measured sections of the Appel Ranch Member in the central part of the study area. (Petrographic abbreviations: BI, bioturbated; DS, dolostone; FUS, fusulinid; L, limy; LMS, lime mudstone; MS, mudstone; P, peloidal; PS, packstone; RE, recrystallized; SI, silty; SK, skeletal; SLS, siltstone; SS, sandstone; WS, wackestone.)

APPENDIX 10-1.—Continued.

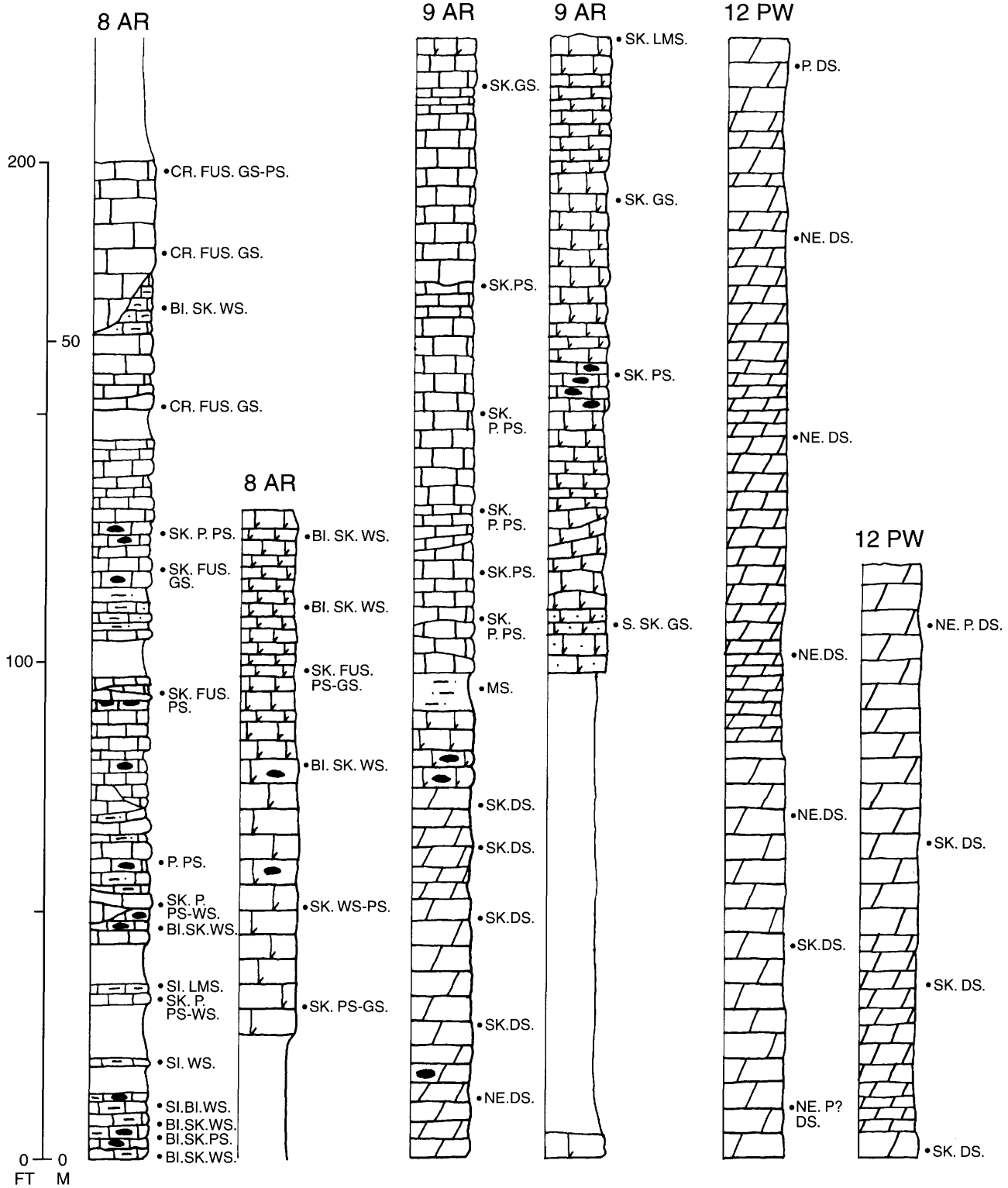


FIGURE 10-22.—Measured sections of the Appel Ranch Member from the eastern part of the study area. (Petrographic abbreviations: BI, bioturbated; CR, crinoid; DS, dolostone; FUS, fusulinid; GS, grainstone; LMS, lime mudstone; MS, mudstone; NE, neomorphic; P, peloidal; PS, packstone; S, sandy; SI, silty; SK, skeletal; WS, wackestone.)

Literature Cited

- Bathurst, R.G.C.
1971. *Carbonate Sediments and Their Diagenesis (Developments in Sedimentology, 12)*. 658 pages. Amsterdam: Elsevier Publishing Company.
- Cooper, G.A., and R.E. Grant
1964. New Permian Stratigraphic Units in Glass Mountains, West Texas. *Bulletin of the American Association of Petroleum Geologists*, 48(9):1581–1588.
1966. Permian Rock Units in the Glass Mountains, West Texas. *United States Geological Survey Bulletin*, 1244-E:E1–E9, plates 1, 2.
1972. Permian Brachiopods of West Texas, I. *Smithsonian Contributions to Paleobiology*, 14:1–231, plates 1–23.
- Flores, R.M., T.L. McMillan, and G.E. Watters
1977. Lithofacies and Sedimentation of Lower Permian Carbonate of the Leonard Mountain Area, Glass Mountains, Western Texas. *Journal of Sedimentary Petrology*, 47(4):1610–1622.
- Flügel, E.
1982. *Microfacies Analysis of Limestones*. 633 pages. Berlin: Springer-Verlag.
- Folk, R.L.
1959. Practical Petrographic Classification of Limestone. *Bulletin of the American Association of Petroleum Geologists*, 43(1):1–38.
1965. Some Aspects of Recrystallization in Ancient Limestones. In L.C. Pray and R.C. Murray, editors, Dolomitization and Limestone Diagenesis: A Symposium. *Society of Economic Paleontologist and Mineralogists, Special Publication*, 13:14–48.
- Futterer, Elke
1978. Hydrodynamic Behaviour of Biogenic Particles. In A. Seilacher and F. Westphal, editors, *Paleoecology; Constructions, Sedimentology, Diagenesis and Association of Fossils. Neus Jahrbuch für Geologie und Paläontologie, Abhandlungen*, 157:37–42.
- Grant, R.E., and B.R. Wardlaw
1984. Redefinition of Leonardian–Guadalupian Boundary in Regional Stratotype for the Permian of North America. *27th International Geological Congress, Moscow, USSR, Abstracts*, 1:58.
- Harris, M.T., D.J. Lehrmann, and L.L. Lambert
2000. Comparison of the Depositional Environments and Physical Stratigraphy of the Cutoff Formation (Guadalupe Mountains) and the Road Canyon Formation (Glass Mountains): Lowermost Guadalupian (Permian) of West Texas. In B.R. Wardlaw, R.E. Grant, and the D.M. Rohr, editors, *The Guadalupian Symposium. Smithsonian Contributions to the Earth Sciences*, 32:127–152, 25 figures.
- King, P.B.
1931 (“1930”). The Geology of the Glass Mountains, Texas, Part I: Descriptive Geology. *University of Texas Bulletin*, 3038: 167 pages, 15 plates. [Date on title page is 1930; actually published in 1931.]
- Lambert, L.L., D.J. Lehrman, and M.T. Harris
2000. Correlation of the Road Canyon and Cutoff Formations, West Texas, and Its Relevance to Establishing an International Middle Permian (Guadalupian) Series. In B.R. Wardlaw, R.E. Grant, and D.M. Rohr, editors, *The Guadalupian Symposium. Smithsonian Contributions to the Earth Sciences*, 32:153–183, 11 figures, 4 plates, 3 tables.
- Rohr, D.M., B.R. Wardlaw, S.F. Rudine, M. Haneef, A.J. Hall, and R.E. Grant
2000. Guidebook to the Guadalupian Symposium. In B.R. Wardlaw, R.E. Grant, and D.M. Rohr, editors, *The Guadalupian Symposium. Smithsonian Contributions to the Earth Sciences*, 32:5–36, 31 figures.
- Stropoli, C.K., R.E. Grant, and B.R. Wardlaw
1991. Wordian (Permian) Brachiopod Assemblages, Western USA. In D.I. MacKinnon, D.E. Lee, and J.D. Campbell, editors, *Brachiopods through Time. Proceedings of the Second International Brachiopod Congress, University of Otago, Dunedin, New Zealand, 5–9 February 1990*, pages 227–232. Rotterdam: A.A. Balkema.
- Udden, J.A.
1917. Notes on the Geology of the Glass Mountains. *University of Texas Bulletin*, 1753: 59 pages.
- Udden, J.A., C.L. Baker, and E. Böse
1916. Review of the Geology of Texas. *University of Texas Bulletin*, 44: 164 pages.
- Wardlaw, B.R.
2000. Guadalupian Conodont Biostratigraphy of the Glass and Del Norte Mountains. In B.R. Wardlaw, R.E. Grant, and D.M. Rohr, editors, *The Guadalupian Symposium. Smithsonian Contributions to the Earth Sciences*, 32:37–87, 3 figures, 12 plates, 1 table.
- Wardlaw, B.R., and R.E. Grant
1990. Conodont Biostratigraphy of the Permian Road Canyon Formation, Glass Mountains, Texas. *United States Geological Survey Bulletin*, 1895-A:A1–A18, plates 1–4.
- Wardlaw, B.R., C.A. Ross, and R.E. Grant
2000. Cyclic Deposition of the Permian Road Canyon Formation, Glass Mountains, West Texas. In B.R. Wardlaw, R.E. Grant, and D.M. Rohr, editors, *The Guadalupian Symposium. Smithsonian Contributions to the Earth Sciences*, 32:121–126, 3 figures.
- Wilson, J.L.
1975. *Carbonate Facies in Geologic History*. 471 pages. Berlin: Springer-Verlag.
- Wolf, K.H.
1965. Petrogenesis and Paleoenvironment of Devonian Algal Limestones of New South Wales. *Sedimentology*, 4:113–178.

11. Geology and Depositional Environments of the Guadalupian Rocks of the Northern Del Norte Mountains, West Texas

*Shannon F. Rudine, Bruce R. Wardlaw, David M. Rohr,
and Richard E. Grant*

ABSTRACT

The Guadalupian rocks of the northern Del Norte Mountains were deposited in a foreland basin between land of the Marathon orogen and a carbonate shoal established on the geanticline separating the foreland basin from the Delaware basin. Deposition was alternately influenced by coarse clastic input from the orogen and carbonate input from the shoal, which interrupted shallow basinal siltstone deposition. Relatively deeper-water deposition is characterized by carbonate input from the shoal, and relatively shallow-water deposition is characterized by sandstone input from the orogen. Deposition was in five general transgressive-regressive packages that include (1) the Road Canyon Formation and the first siltstone member and first sandstone member of the Word Formation, (2) the second siltstone member, Appel Ranch Member, and limy sandy siltstone member of the Word Formation, (3) the Vidrio Formation, (4) the lower and part of the middle members of the Altuda Formation, and (5) part of the middle and upper members of the Altuda Formation.

Introduction

The northern Del Norte Mountains have received little attention since King mapped (1931) and interpreted (1937) the

Shannon F. Rudine, Geology Department, Sul Ross State University, Alpine, Texas 79832. Bruce R. Wardlaw, U.S. Geological Survey, 926A National Center, Reston, Virginia 20192. David M. Rohr, Geology Department, Sul Ross State University, Alpine, Texas 79832. Richard E. Grant (deceased), Department of Paleobiology, National Museum of Natural History, Smithsonian Institution, Washington, D.C. 20560-0121.

section, other than the intensive fossil collecting of Cooper and Grant (1972) and others. Wardlaw et al. (1990) initiated an interpretative study and revised the map of the northern part of the northern Del Norte Mountains (Figure 11-1). The current study maps a more southern part of the northern Del Norte Mountains and attempts to build upon the work of Wardlaw et al. (1990) and to refine and improve it. The area between the two mapped areas has been visited by the authors, but general access has commonly been denied, so our work in this area is based solely on one measured section (section 6). The bulk of the mapping was carried out by Rudine in 1985–1987. Wardlaw and Grant, commonly accompanied by the other authors, measured and described sections throughout the northern Del Norte Mountains from 1983 to 1990. Rudine has, subsequently to 1987, measured additional sections throughout the area.

General Stratigraphy

The stratigraphy of the northern Del Norte Mountains is complex because many units are laterally discontinuous. Much of this problem was clarified with the identification of King's (1931) lower massive member of the Capitan Limestone to be the Vidrio Formation (Rudine et al., 1987; Rohr et al., this volume) and the collapse breccias King (1931) assigned to the upper massive member of the Capitan to be the Tessey Formation (Haneef et al., 1990; Rohr et al., this volume). Still, the Word Formation displays a great deal of lateral variation, which is the focus of this paper.

The general relationships of the Road Canyon, Word, Vidrio, Altuda, and Tessey formations are those of unconformably bounded units containing lateral facies changing from shoal and basin in the north to shallow foreland basin and shore to the south (Figure 11-2). Detailed relations of the upper part of the

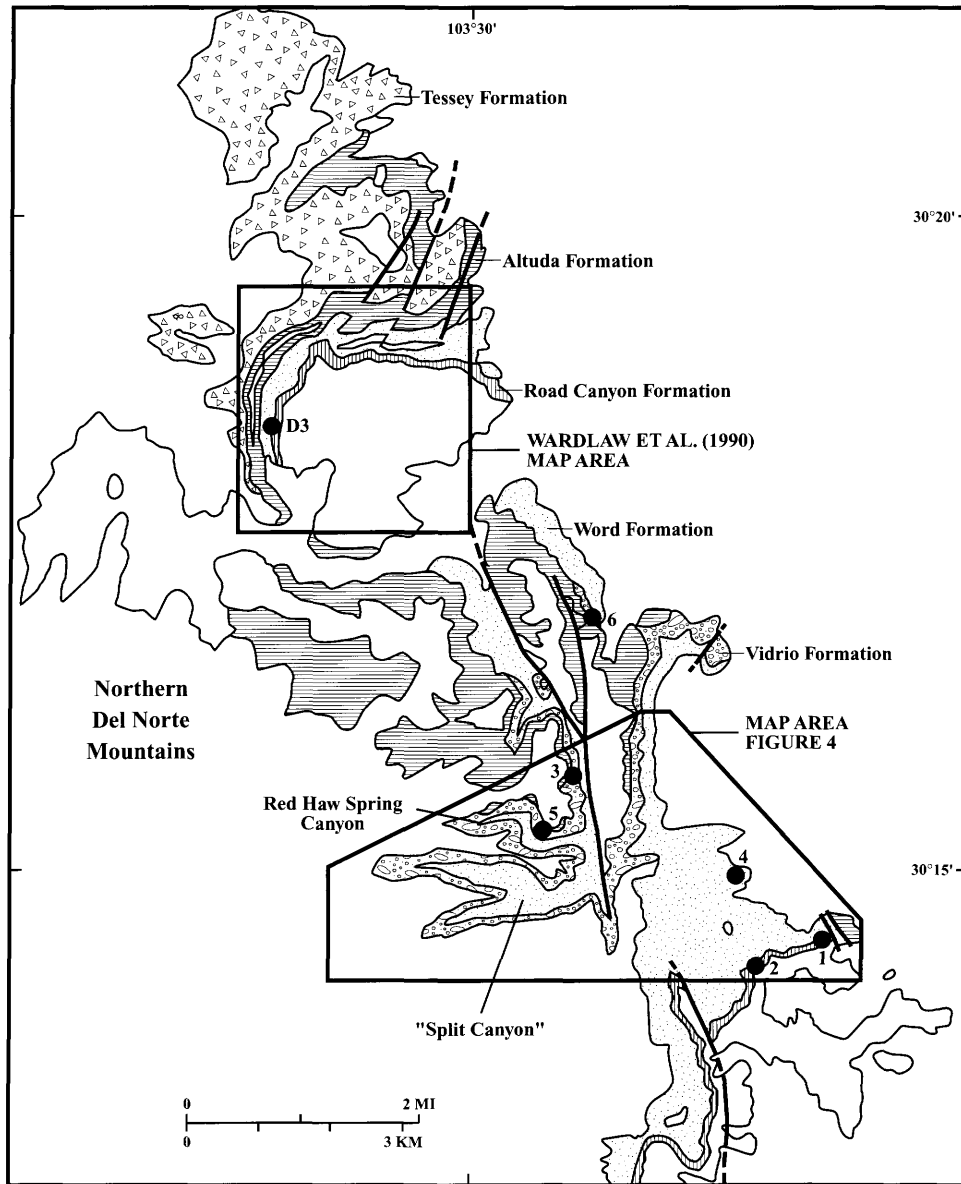


FIGURE 11-1.—General geologic map of the northern Del Norte Mountains showing section locations, the study area (enlarged in Figure 11-4), and the area mapped by Wardlaw et al. (1990) (square).

Cathedral Mountain Formation (uppermost Leonardian), the Road Canyon Formation, the many members of the Word Formation, the Vidrio Formation, the members of the Altuda Formation (see Wardlaw and Rudine, this volume), and the Tessey Formation are displayed in Figure 11-3. The Capitan Limestone, so pervasive in the northern part of the Glass Mountains, is completely missing from the Del Norte Mountains. The Capitan may not have been deposited in the Del Norte region, suggesting a platform did not develop but that ramp deposition persisted through the late Guadalupian as represented by the Altuda Formation. The three lower members of the Altuda are certainly deposited over most of the area

(Figure 11-3; sections 3, 6, D3), suggesting persistent ramp deposition, as opposed to the Glass Mountains, where only the first member of the Altuda is widespread as a ramp deposit before the development of the Capitan platform (Haneef et al., 1990). If the Capitan was deposited at all, it was much more limited than in the Glass Mountains, and it has been completely removed by pre-Tessey or pre-Cretaceous erosion.

Stratigraphic Units

The Road Canyon Formation, the members of the Word Formation, the Vidrio Formation, and the Altuda Formation in the study area (Figure 11-4) are described in detail below.

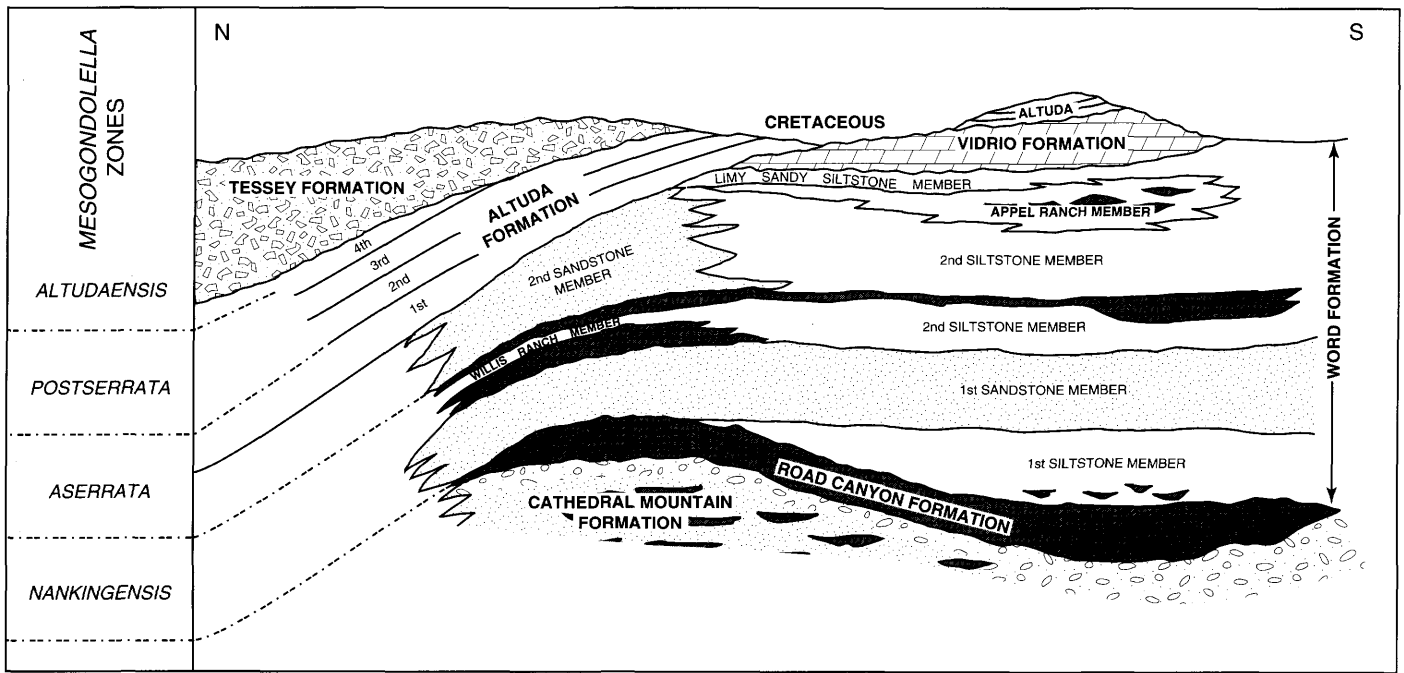


FIGURE 11-2.—Stratigraphic relationships on a general south to north trend through the northern Del Norte Mountains for the upper part of the Cathedral Mountain Formation (Leonardian), Guadalupian units, and the Tessey Formation (Ochoan), and also showing the conodont zonation of *Mesogondolella* species.

ROAD CANYON FORMATION

The Road Canyon Formation consists of interbedded limestones and siltstones forming moderately steep slopes, broken in part by small ledges of limestone. Grayish orange siltstones form slightly recessive slopes. Siltstones are commonly thin- to very thin-bedded, platy, or flaggy, and appear similar to basal Word siltstones. Limestones are medium- to thick-bedded with minor thin beds. Limestone beds frequently exhibit marked lateral thickness variations; all are laterally discontinuous. The uppermost limestone bed appears to have the largest lateral extent.

Skeletal packstones in channel bedforms characterize most of the formation. Carbonates range from muddy, poorly sorted wackestones to well-sorted grainstones. Minor beds of limy siltstones and silty lime mudstones are rare. Scattered, subrounded grains of quartz silt and fine sand are present in many thin sections. Well-rounded, chert pebble channel lags are present at the base of several limestone lenses.

Carbonates commonly consist of silty, peloid, lithoclastic, skeletal wackestones and packstones (Figure 11-5). Lenses of winnowed, skeletal grainstone are locally developed in channels. Microspar cements prevail over coarser interparticle blocky calcite. Dolomite and ankerite rarely replace the spar cements. Spar cements and skeletal fabrics are sporadically replaced by chalcedony. Sedimentary structures include graded bedding, cross-bedding, planar and stromatolitic laminations, load deformation structures, and channel lag deposits.

Carbonate allochem percentages vary substantially from bed to bed. Peloid allochem distribution is erratic. Peloids appear to be of fecal origin based on their uniform size and degree of sorting. Intraclasts of lime mudstone are commonly angular, ranging in size from fine sand- to pebble-sized clasts. Finely divided planar laminations are present in many pebble-sized clasts.

Skeletal elements are dominant constituents in all of the Road Canyon carbonates. Skeletal grains are generally partially micritized or recrystallized. Silicification is sporadic and commonly incomplete. Fusulinids, ostracodes, sponge spicules, and dasycladacean algae are common in the channels. Other elements include uniserial and biserial foraminifers, brachiopod valves and spines, echinoderm plates, bryozoans, codiacean and solenoporacean algae, and rare cephalopods, gastropods, trilobites, and plant material. Calcispheres and cortoids are minor accessories. Kerogen-filled skeletal chambers and finely comminuted plant debris occur in thin sections from the top of the Road Canyon.

The Cathedral Mountain–Road Canyon contact is generally covered, but it appears gradational based on observed field relations. The Road Canyon–Word contact appears to be conformable throughout the study area. The contact is difficult to map in areas where limestone channels are not abundant. In areas where limestones of the Road Canyon are overlain by lower Word limestone channels, the two can be separated on the basis of lateral extent and faunal content. Generally, the highest Road Canyon limestone has a greater lateral extent than

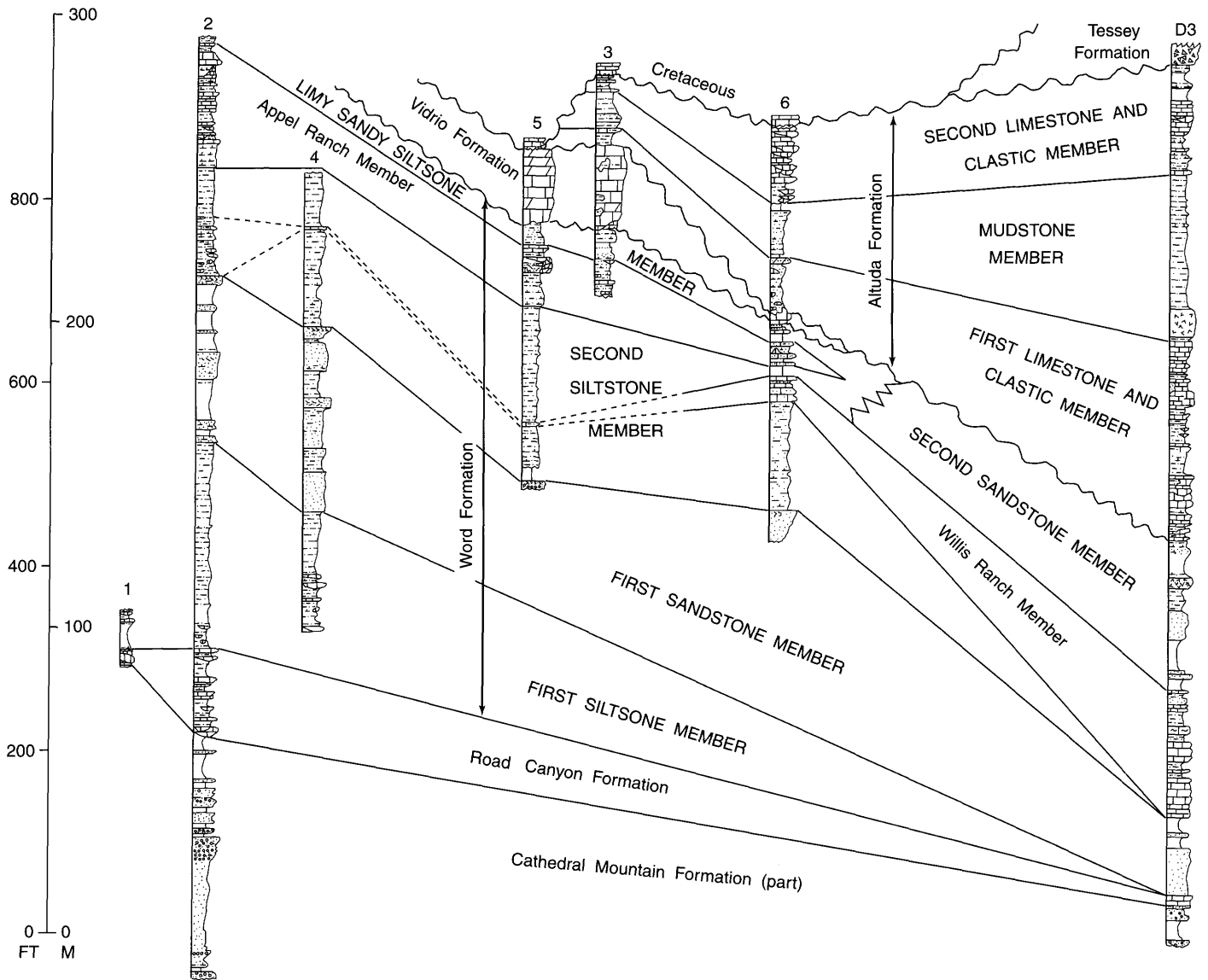


FIGURE 11-3.—Columnar sections showing the stratigraphic units. (The location of the sections is shown in Figure 11-1.)

the overlying Word limestones, which rarely exceed 91 m (300 ft) in lateral extent. The lytonnid brachiopod *Coscinophora* distinguishes beds of the Road Canyon Formation.

The Road Canyon Formation in the northern Del Norte Mountains is characterized by marked variation in thickness, ranging from 1 m (3.3 ft.) of limestone to 32.6 m (107 ft.) of interbedded limestone and siltstone in the south. In the north, the unit varies from 6.1 m (20 ft.) of limestone to 61 m (200 ft.) of interbedded limestone, sandstone, and siltstone.

WORD FORMATION

Eight Word lithostratigraphic units were delimited in the

northern Del Norte Mountains. A southern succession (Figure 11-3) consists of, in ascending order, the first siltstone member, the first sandstone member, the second siltstone member, the Appel Ranch Member, and the limy, sandy siltstone member. A northern succession consists of, in ascending order, the first sandstone member, the Willis Ranch Member, and the second sandstone member. Wardlaw et al. (1990) described the northern succession in detail; the southern succession is described in detail herein (Figure 11-3).

FIRST SILTSTONE MEMBER.—The first siltstone member is largely characterized by siltstone, but it also contains common limestone lenses and channels near its base. Fresh and weathered surfaces of the siltstone are consistently grayish

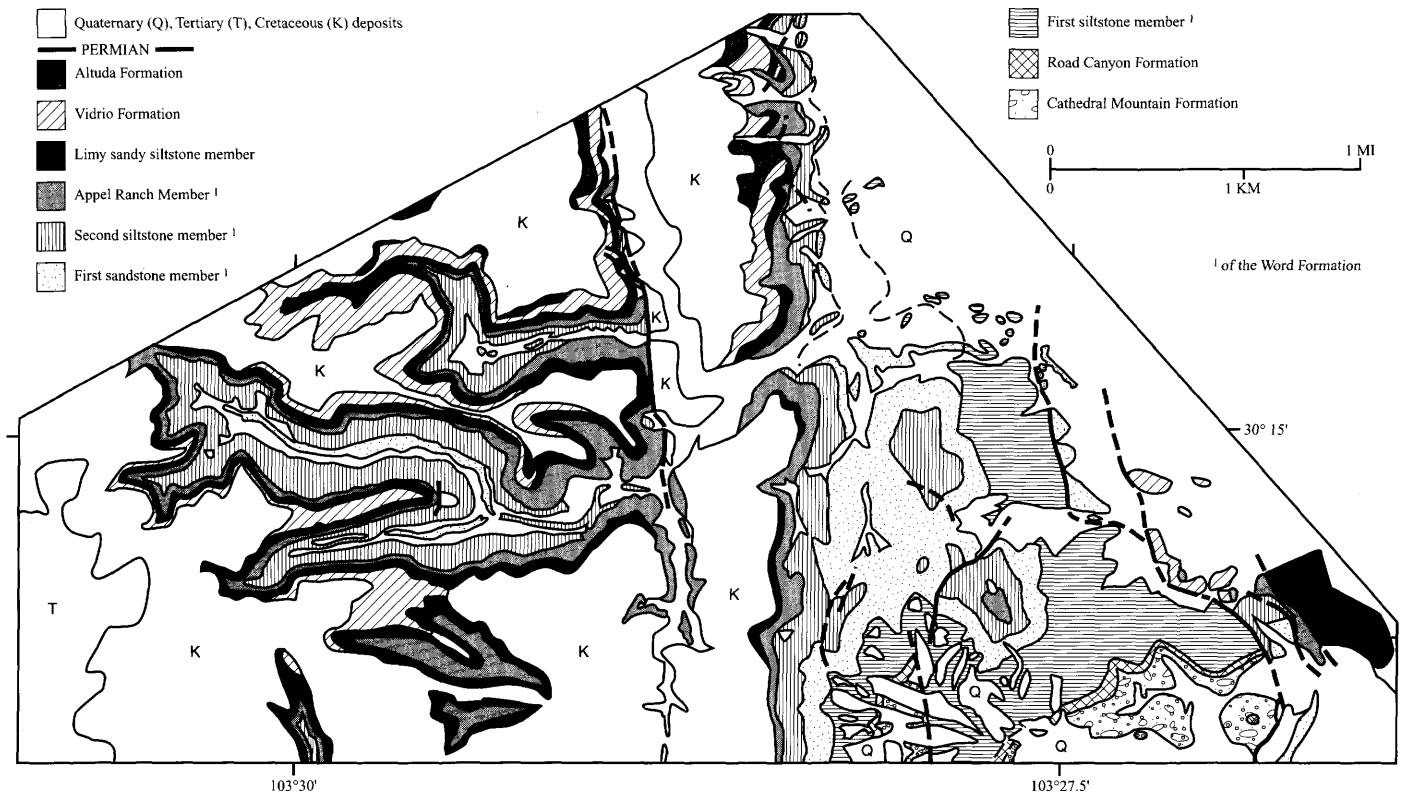


FIGURE 11-4.—Geologic map of the area shown in Figure 11-1 of the southern part of the northern Del Norte Mountains. The topographic base is from the SW part of Altuda, SE part of Bird Mountain, NW part of Dugout Mountain, and NE part of Mount Ord 7.5 min. quadrangles.

orange. Fresh surfaces of the limestone in the lower portion of the member vary from yellowish gray and brown, to brownish gray; weathered surfaces are commonly of a lighter color than that of the fresh surface. Fresh surfaces of the limy siltstone lenses are of a moderate yellowish gray color; weathered surfaces are pale yellowish gray.

Gentle, rounded hills are formed by the siltstones and limestones of this unit. Excellent exposures of strata are provided by the arroyos that cut deeply into the siltstones. The siltstones occur as platy, thin beds, generally less than 1 cm thick (Figure 11-6).

The limestones display a wide variety of bedding styles. Peloid packstone/grainstone lenses are commonly dispersed in thin, featureless beds, generally less than 15.3 cm (6 in.) thick (Figure 11-6A). Channel bedforms of wackestones, packstones, and grainstones are massive and medium- to thick-bedded, with beds ranging from 0.3 m (1 ft.) to 2.4 m (8 ft.) thick, but generally less than 0.9 m (3 ft.) thick (Figure 11-6B). Lenses of limy siltstone are similar to those of the peloid packstone/grainstone, except that they are commonly thicker, not exceeding 0.9 m (3 ft.) in thickness.

The siltstones are composed of fine, angular grains of quartz silt and fine sand (Figure 11-6C). Other constituents include

skeletal grains and ferroan opaque minerals. Planar and wavy laminations are subordinate to massive, possibly bioturbated, beds. Trough cross-bedded, sandy siltstones were observed in one locality above a limestone channel sequence. Thin sections reveal a fine ferroan-stained chert cement with vague, distorted, planar laminations. Chalcedony replacements of skeletal grains are present. Calcareous cements are present in many thin sections.

Thin-bedded, peloid packstones and grainstones are characterized by well-sorted coarse silt and fine sand-sized carbonate grains. Skeletal grains commonly constitute the largest sedimentary particles. Coarse sand-sized carbonate lithoclasts are not common. Peloids appear as featureless, ovoid- to angular-shaped grains of coarse silt-sized micrite, and many appear to be a product of sediment-ingesting organisms, based on their shape, size, and structureless interior. Rare angular peloids may represent finely comminuted lime-mud lithoclasts derived from a nearby source. Micritization of skeletal debris by boring algae and sponges would produce similar featureless silt-sized micrite clasts.

Channel-form wackestones and packstones represent the most common type of carbonate developed in the first siltstone member. Carbonate allochems are moderately sorted and

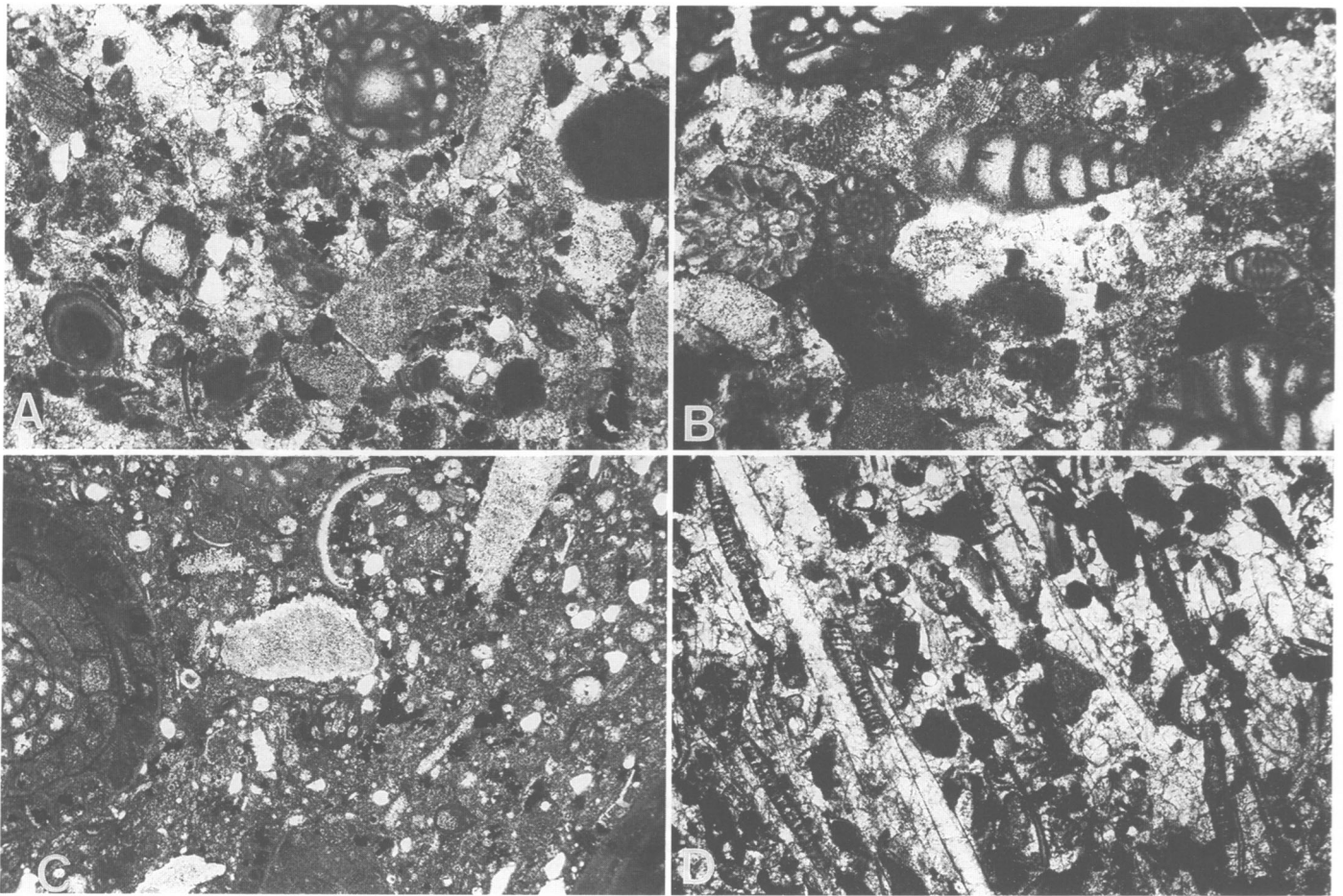


FIGURE 11-5.—Photomicrographs of the Road Canyon Formation. A, silty, skeletal, lithoclastic packstone (sample 2-302). B, lithoclastic, skeletal packstone to grainstone (sample 313A). C, silty, skeletal wackestone (sample 2-300). D, silty, pelletal, skeletal packstone with *Epimastopora* and sponge spicules (sample 2-302). Scale of the long axis in the photomicrographs equals 2.9 cm. (Further information on thin-section locations can be found in Rudine (1988); generally the measured section number is followed by the footage in the section.)

coarser grained in comparison with peloid packstones/grainstones. Allochem constituents exhibit large bed-by-bed variations. Most grains are sand sized; however, some beds contain a significant percentage of granule- to pebble-sized clasts. Peloids and quartz sand are commonly subordinate to carbonate lithoclasts and skeletal debris. Numerous small pebbles of chert, novaculite, and sandstone occur in coarse channel lags. These “exotic” grains were probably derived from nearby pre-Permian formations of the uplifted rocks of the Marathon basin.

Fusulinids are the dominant allochem in many of the lower carbonate channels. In many channels, they occur almost to the exclusion of all other allochems. The highest channels in the sequence contain fewer fusulinids and are marked by a more diverse, normal marine fauna. Allochems in thin section are cemented by varying amounts of microspar and blocky spar. Chert replacement of skeletal grains and cements is common. Dolomite rhombs and cements are not common. Sedimentary

structures include graded bedding, cross-bedding, cut-and-fill, and current aligned skeletal tests; imbricated clasts are rare.

Sporadic lenses of argillaceous lime mudstone and limy, skeletal siltstone occur, respectively, below and above the main carbonate channel sequence in the lower part of the member. Lime mudstones contain minor amounts of clay, quartz, silt, and sand-sized particles of lime-mud, and are interbedded with many thin beds of shale and siltstone. Load-deformed bases are common where lime mudstones overlie shale interbeds. In many areas, bedding planes are covered by numerous ammonoid shells.

Scattered lenses of limy, skeletal siltstone occur above the channel sequence. Beds are locally replete with sponge spicules and brachiopod spines. Large concretions of sandy, limy siltstone, several feet across, are found in close association with the limy, skeletal siltstone. Pebble- to cobble-sized concretions are present near the top of the member in section 4.

Fossils in the first siltstone member are largely confined to

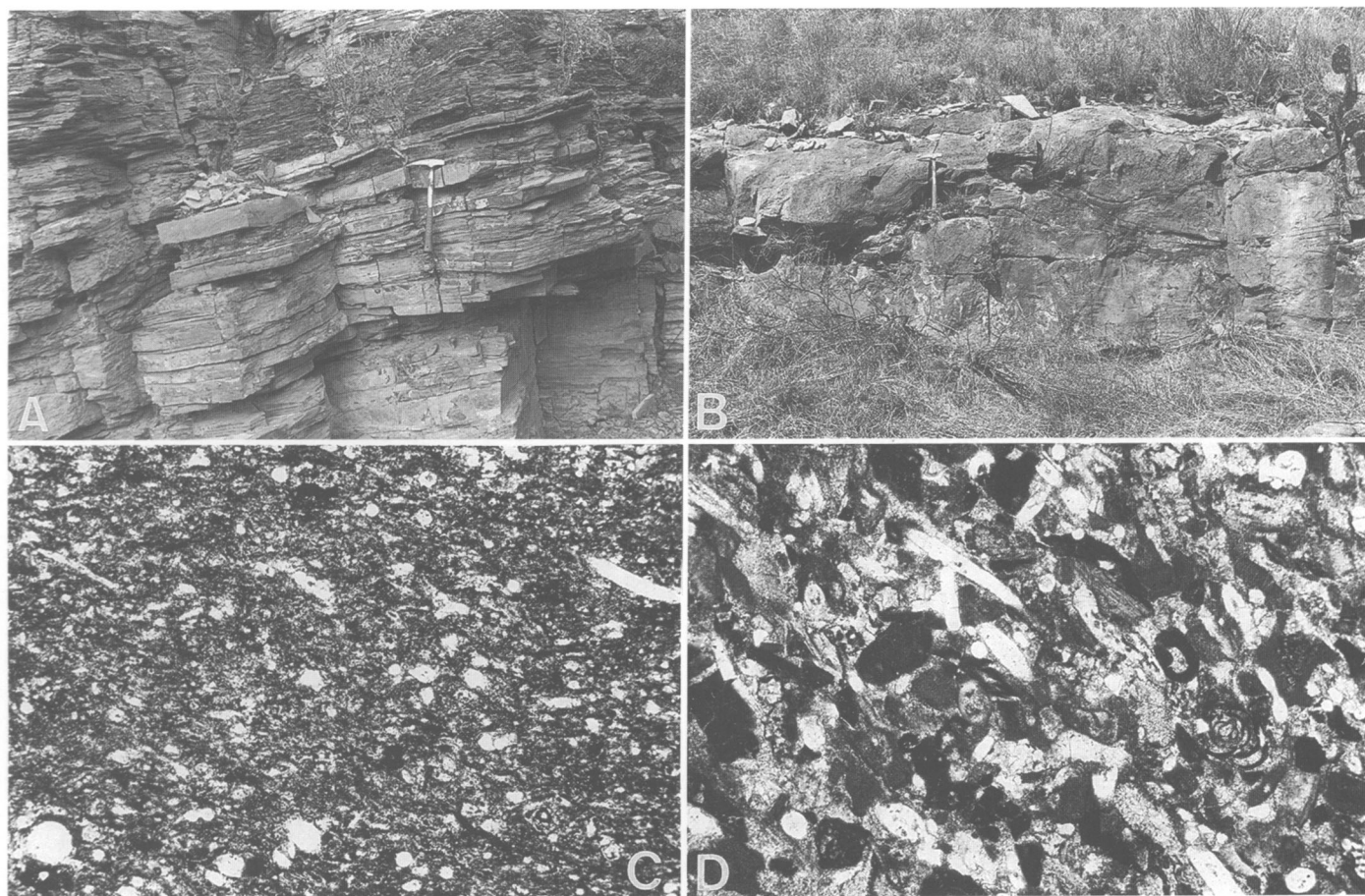


FIGURE 11-6.—The first siltstone member of the Word Formation. A, view of thin beds of peloidal packstone (below hammer) separated by thin-bedded siltstones, located south of section 4. These are interpreted as overbank deposits. B, view of a limestone channel, south of section 4. Note sandy cross-beds to the left of hammer and multiple reactivation surfaces to the right of hammer. (Hammer is 39.5 cm long.) C, photomicrograph of siltstone containing calcispheres and sponge spicules (sample 4-85). D, photomicrograph of peloidal skeletal packstone (sample 299B). Scale of the long axis in the photomicrographs equals 2.9 cm.

the carbonate beds. No fossils were observed in the shale interbeds. Horizontal burrows are present in many of the siltstone beds. Featureless siltstones may represent beds that were extensively burrowed by infaunal organisms. Marine megafossils (other than sporadic beds of spicule-rich siltstone) are absent.

Ammonoids are rare but occur abundantly on some bedding planes of lime mudstones. The rich ammonoid fauna described by Furnish and Glenister (in Cooper and Grant, 1977, USNM Loc. 732z) occurs in a channel carbonate equivalent to the top of section 1 (Figures 11-1, 11-3) a few hundred meters around the hill to the northeast. Fusulinids dominate the fauna in most of the channel bedforms. Brachiopods are present in moderate numbers and diversity, but most are broken and unidentifiable. Whole specimens are generally not silicified. Cryptostome bryozoans, such as *Fenestella*, and ramose forms are also present in small numbers. Crinoid columns and ostracodes are frequent accessories in the channel deposits. Chambered

calcareous sponges, trilobites, corals, and echinoid tests are rare.

Algal remains were observed in many carbonate thin sections. Packstones and grainstones contain sporadic occurrences of dasycladacean and solenoporacean algae (*Mizzia* and *Epimastopora*; *Solenpora* and *Parachaetetes*?, respectively). Algal? filaments of undetermined origin are also present.

The upper contact of the first siltstone member with the overlying first sandstone member is poorly exposed and is probably gradational in nature. The uppermost beds of the first siltstone are more sandy in comparison with beds below. The lowest beds of the overlying first sandstone member consist of fine- to medium-grained, moderately sorted, quartz sands with flakes of muscovite. Sands of the first sandstone member are rusty, reddish orange. The contact is generally marked by a small increase in slope.

FIRST SANDSTONE MEMBER.—The first sandstone member divides the first siltstone member from the second siltstone

member and also helps to define structural features in the study area (Figure 11-4). The sandstones of this unit form smooth, nondescript slopes, somewhat steeper in comparison with those of the siltstone units above and below. Two prominent ledges are present in the upper part of the member near sections 2 and 4. The highest ledge was traced out by King (1931:132) on his geologic map.

Medium- to thick-bedded sandstones are common with subordinate very thin- to thin-bedded intervals. Sandstones are sublitharenites (Dott, 1964). The sandstones in the lower two-thirds of the member are poorly sorted, very fine- to medium-grained, with dominantly angular grains of quartz sand. Quartz and strained quartz compose the sand-sized grains. Accessory grains of chert prevail over sand-sized grains of siltstone, shale, and spicular chert. Grain boundaries are sharp. Many grains display the effects of corrosion by surrounding calcite and dolomite cements. Identification of cement(s) proved difficult due to pervasive ferroan staining. Point contact dissolution features are present in some thin sections; sutured contacts are rare. Flakes of muscovite are common at the base of the member.

Sandstones in the upper one-third of the member exhibit a greater textural maturity in comparison with those below. Sandstones in the upper portion are well-sorted, medium-grained, subround to subangular quartz sands. Quartz sands significantly outnumber the other detrital grains common in the beds below. The detrital constituents are bound together by multiple cements. The cement texture is dominated by an equigranular, medium silt-sized, ankeritic cement bounded by minor amounts of nonferroan calcite microspar. Siliceous syntaxial cements and overgrowths are present. Quartz grains commonly occur as sutured aggregate (polycrystalline) grains. Sutures are straight or slightly crenulate. Stylolites were not observed. Strained quartz grains are common. No feldspar grains were observed.

Minor beds of coarse siltstone occur at irregular intervals. The siltstone beds are commonly covered and form recessive benches between beds of sandstone.

Sedimentary structures include uncommon low-angle cross-stratification, trough cross-bedding, and normally graded beds. Thin conglomeratic intervals are present at a few locations. Clasts in the conglomeratic interval are composed of flattened pebbles of siltstone and silicified wood (Figure 11-7A). Abundant *Skolithos*-type burrows are found in the upper 1.25 m (4 ft.) of the member (Figure 11-7B). Limy siltstone concretions, 1.3 cm (0.5–1.5 in.) in diameter, are locally abundant.

Fossils are rare in the first sandstone member. Silicified wood fragments were found in the conglomeratic interval at the base of section 5. Abraded fragments of crinoids, brachiopod spines and valves, bryozoans, and cephalopods are rare. One reworked concretion bed contained abundant, poorly preserved crinoids, bryozoans, brachiopods, fusulinids, trilobites, and possible algae.

The upper contact with the overlying second siltstone member is marked by an abrupt decrease in grain size, bed thickness, and weathering resistance. The highest bed in the first sandstone member is commonly thick-bedded and heavily bioturbated. Burrows are common to (if not diagnostic of) the top surface of the first sandstone member, apparently indicating a preserved surface (nondepositional or erosional). In contrast, the beds of the overlying second siltstone are very thin-bedded and lack abundant burrows. Concretions are rare in the second siltstone, whereas they are fairly abundant in the siltier intervals in the first sandstone member.

This unit is found in the northern part of the northern Del Norte Mountains (Wardlaw et al., 1990) where it is similar. There it is composed largely of angular quartz grains with some chert, sparse mica, and sedimentary rock fragments. Bioturbation is not apparent, but discontinuous pebble beds and low-angle cross-bedding is common in the upper part of the unit. The member is reported to be very thick south of the study area (King, 1937), reaching a thickness in excess of 152 m (500 ft.). The upper beds of the member can be traced along discontinuous outcrops from the study area to Bird Mountain; however, thickness variations cannot be determined because of insufficient exposure.

SECOND SILTSTONE MEMBER.—The siltstones and fine sandstones that make up the majority of this unit form smooth, featureless slopes (Figure 11-8); benches and ledges are rarely developed. The majority of exposures are covered with a thin veneer of talus or regolith. Bedding habits are varied in the study area, but very thin beds are commonly found at the base of the unit (Figure 11-9A). As a whole, the member is thin-bedded with subordinate medium beds. The unit is largely represented by a medium to coarse siltstone. Beds of fine sandy siltstone, silty fine sandstone, and minor beds of sandy and silty lime mudstone are locally present. Sedimentary structures include flaser bedding, planar laminated beds, wavy laminations, and abundant horizontal burrows. Structureless beds may represent rapid deposition and/or extensive bioturbation.

The siltstones are immature, poorly sorted, and fine- to coarse-grained. The majority of the quartz silt grains are angular. Ferroan-stained siliceous and/or ankeritic cements are common. Calcareous cements, frequently noted in the field, appear to be rare in thin section. Ferroan masking of the cements could explain this apparent discrepancy. Skeletal elements are frequently replaced with chalcedony.

Limestones are commonly represented by thin lenses of silty, skeletal lime mudstones and frequently lack any well-defined sedimentary structures. Wackestones are rare. Graded bedding and burrow infilling are present in a few beds, and stringers of off-white and reddish orange chert are present. Fossils are generally rare; however, sponge spicules and ammonoids are present in many beds, and brachiopods, bryozoans, crinoids, ostracodes, and fusulinids are rare accessories. Abundant algal remains, peloids, and a mixed normal marine fauna were observed in thin section. One collected bed from section 2

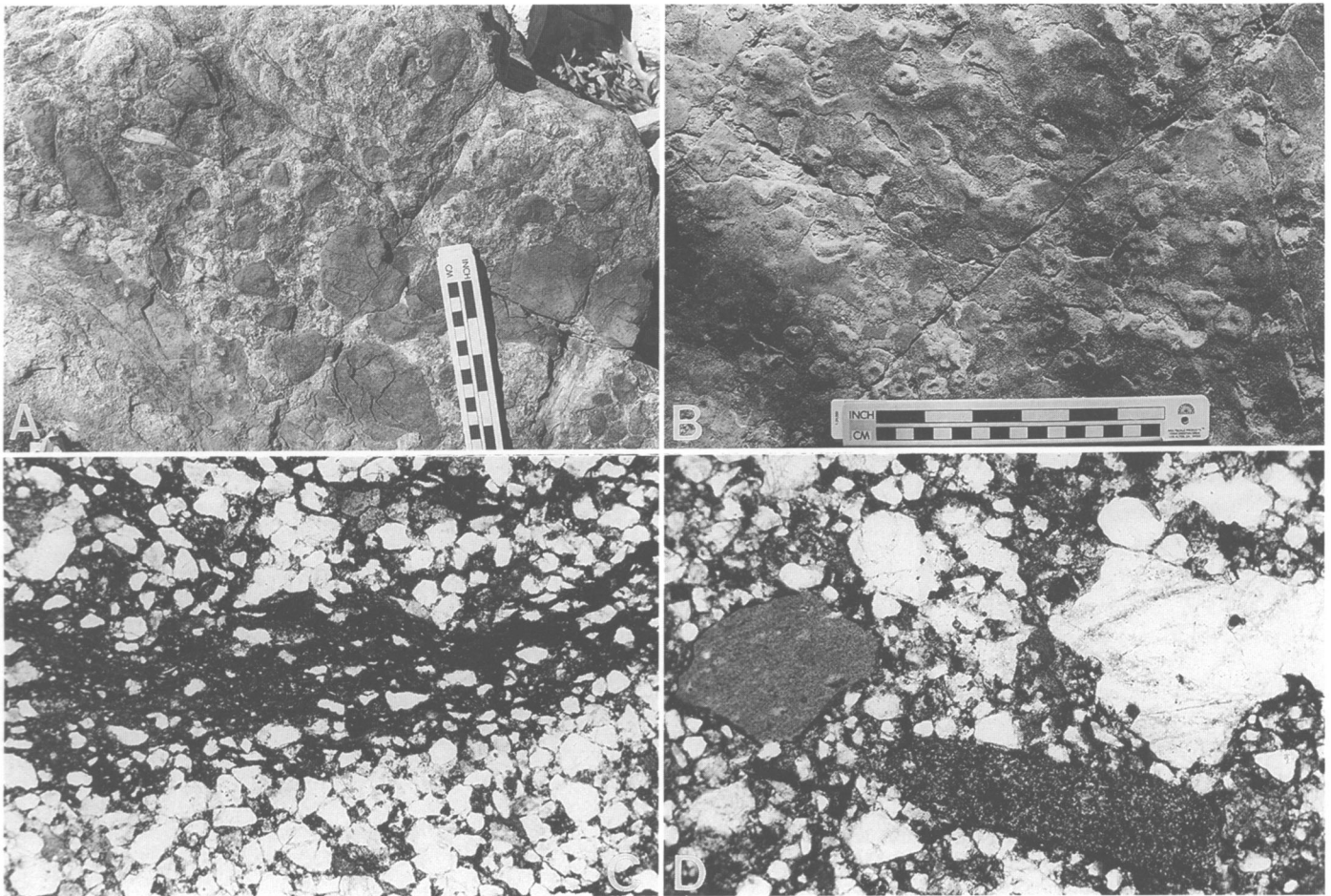


FIGURE 11-7.—The first sandstone member of the Word Formation. A, view of conglomeratic sandstone with clasts of siltstone and silicified wood, Red Haw Spring Canyon. B, view of *Skolithos*-type burrows at the top of unit. C, photomicrograph of argillaceous sandstone (sample 4-380). D, photomicrograph of lithoclastic sandstone (sample 4-290). Scale of the long axis in the photomicrographs equals 2.9 cm.

contained an abundant silicified ammonoid fauna. The limestone beds appear to represent the lateral extension (although not mappable) of the Willis Ranch Member of the Word Formation (Figure 11-3) from the northern part of the northern Del Norte Mountains described by Wardlaw et al. (1990).

The contact of the second siltstone member with the Appel Ranch Member is gradational. Beds belonging to the overlying Appel Ranch consist largely of silty, skeletal lime mudstones and wackestones. In the western half of the study area (Figure 11-4), the boundary is consistently difficult to discern due to a significant increase of silt in the lower carbonates of the Appel Ranch. In Red Haw Spring Canyon, approximately 23 m (75 ft.) of Appel Ranch limestones grade laterally, over a distance of 0.8 km (0.5 mi.), into very limy siltstones. In this gradational interval, thin-bedded siltstones were assigned to the second siltstone member, and medium-bedded, limy siltstones and silty lime mudstones were assigned to the overlying Appel Ranch Member. The second siltstone member becomes more

sandy in its northern extent (Figures 11-1, 11-3; section 6), apparently grading laterally into the second sandstone member described by Wardlaw et al. (1990) in the northern part of the northern Del Norte Mountains.

APPEL RANCH MEMBER.—Carbonates and clastics of the Appel Ranch Member form a variety of slope types in the study area (Figures 11-8, 11-10). Carbonates in the lower one-third of the unit form moderately inclined slopes of greater declivity than in adjacent beds. Middle beds form nondescript convex slopes, broken in part by random, mound-shaped carbonate masses. The upper one-third of the Appel Ranch forms slopes similar in appearance to the middle beds except they lack the abundant carbonate masses.

The Appel Ranch carbonates are medium-bedded with subordinate thick beds (excluding carbonate masses). Thin-bedded intervals are abundant in the upper one-third of the member. Interbeds of siltstone and sandstone are thin- to medium-bedded. Clastics are either featureless or finely



FIGURE 11-8.—View of the Word and Vidrio formations in the central portion of "Split Canyon." The top of the second siltstone member of the Word forms the smooth slope at the extreme lower right corner of the photograph. The first resistant bench above the slope marks the base of the Appel Ranch Member. Note that the lighter colored layer above this bench contains a large channel (left and slightly below center). Uniform, even beds of limestone at the top of the Appel Ranch Member and the recrystallized peloidal wackestone bench (poorly defined in this photograph) form the interval below the nonbedded carbonates of the Vidrio Formation (upper part of the photograph). Cretaceous limestones form the top of the hill above the Vidrio Formation.

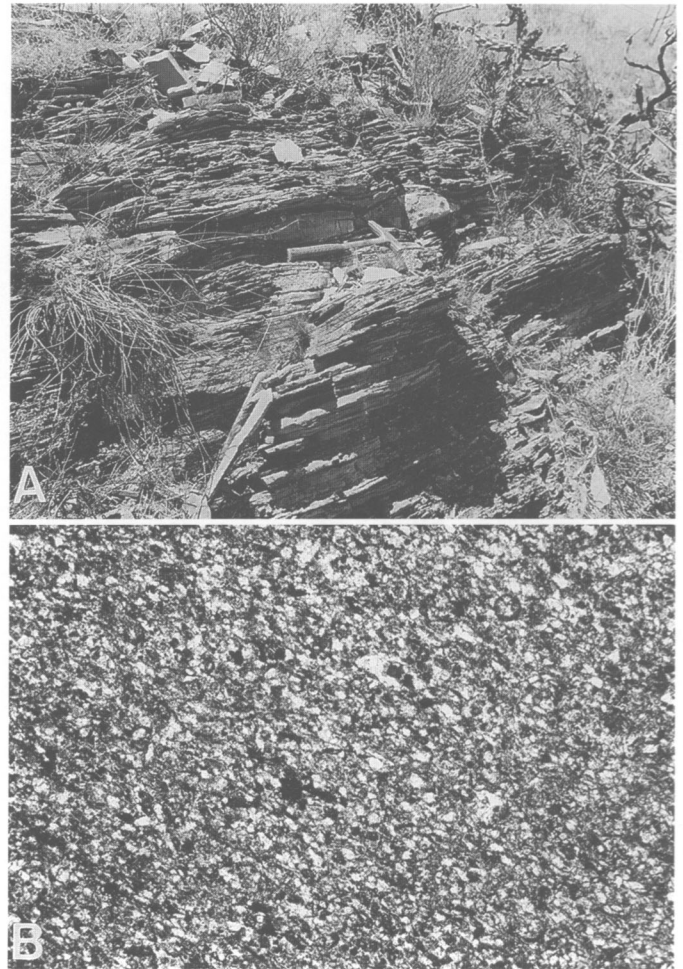


FIGURE 11-9.—The second siltstone member of the Word Formation. A, view of the characteristic bedding habit; hammer point points to an irregular lens of poorly graded, lithoclastic and dolomitic wackestone. (Hammer is 39.5 cm long.) B, photomicrograph of siltstone (sample 4-394). Scale of the long axis in the photomicrographs equals 2.9 cm.



FIGURE 11-10 (left).—View of two carbonate masses in the Appel Ranch Member. The carbonate masses form resistant, nonbedded bodies of limestone that occur at the same stratigraphic horizon (in the middle of the Appel Ranch Member). Typical Appel Ranch limestones are seen above and below the masses. Cretaceous limestones cap the hill above the masses. Tertiary volcanics form the hill seen in the upper left corner of the photograph (Mount Ord).

laminated. Wavy laminations are present in the lower one-third of the Appel Ranch carbonates, whereas planar, wispy, and cross-laminations are locally abundant in higher carbonate beds. Carbonate masses are uniformly massive and thick-bedded. Thick beds also occur in channel bedforms (Figure 11-8).

Appel Ranch lithologies consist primarily of silty, lithoclastic, skeletal lime mudstones and wackestones. Packstones, grainstones, and dolostones are not common, constituting just 15 percent of the Appel Ranch carbonates. The lime mudstones and wackestones are sparsely sandy and pelletal. Peloidal limestones are very common in the upper one-third of the member. Siltstone and sandstone interbeds contain variable amounts of skeletal and carbonate lithoclastic debris. Gradational sequences of siltstone, limy siltstone, and silty lime mudstone or wackestone are common in the interbedded intervals.

Sedimentary structures include low angle cross-stratification, normal- and reverse-graded bedding, current-aligned fossils, clastic dikes, penecontemporaneous and post-lithification load deformation structures, penecontemporaneous slumping, and trace fossils. Channel bedforms are common in the middle and upper portions of the Appel Ranch. Channels were not observed in the lower part of the member. The majority of the channels are small, rarely exceeding 6 m (20 ft.) in width. Depth-to-width ratios are estimated to range from 1:4 to 1:10 or greater. The greatest channel widths and depths are 15–20 m (50–70 ft.) and 6 m (20 ft.), respectively.

The carbonates of the Appel Ranch Member are described as lower, middle, upper, and carbonate masses. The lower Appel Ranch carbonates are characterized by sparsely sandy and dolomitic, peloid, lithoclastic, skeletal, silty lime mudstones and wackestones. Recrystallization and dolomitization are generally uncommon; however, some dolomitization is fabric selective, replacing micrite particles. Ferroan microspar cements are common. Ostracodes, crinoids, and sponge spicules are abundant, but algal traces are absent.

The middle Appel Ranch carbonates are characterized by sparsely sandy and pelletal, dolomitic, lithoclastic, skeletal, silty lime mudstones. Wackestones, packstones, and grainstones are uncommon. Recrystallization is slight, with rare matrix inversion. Dolomitization is slight to moderate and is matrix selective. The majority of samples (86 percent) contain some dolomite. Ankerite is present in 45 percent of the samples, and nonferroan dolomite is present in 60 percent of the samples. Microspar and coarse calcite cements are dominantly ferroan. Calcite void-fills may exhibit up to 20 subtle generations of cement. Faunal constituents consist of crinoids and fusulinids and minor bryozoans, sponge spicules, ostracodes, and algal traces. Prelithification, sediment stabilization features are present.

The upper Appel Ranch carbonates are characterized by sparsely sandy, pelletal, and lithoclastic, dolomitic, skeletal, silty, peloid lime mudstones and wackestones. Packstones are

rare. Samples are generally slightly recrystallized, but the recrystallization varies from minor to extensive. Dolomite is present in 75 percent of the samples. Microspar cements prevail over coarser calcite. One-half of the calcitic cements are ferroan. Calcite and dolomite void-fills commonly display several dozen generations of cement. Moldic porosity is common. Ostracodes, crinoids, bryozoans, foraminifers, calcispheres, sponges, and sponge spicules are common.

The middle beds of the Appel Ranch are frequently interrupted by massive mound-shaped carbonate accumulations, referred to herein as "masses." These structures are limited to the upper half of the Appel Ranch Member. Sixty-four mound-shaped masses were observed (Figure 11-11), with the majority occurring in the middle portion of the member. Low altitude aerial reconnaissance suggests several such occurrences also may be present in the southwestern Glass Mountains, due east of Altuda siding. The masses range in size from inconspicuous structures 61 cm high and 93 cm long (2 × 3 ft.) to immense structures 12.2–15.2 m high (40–50 ft.) and 76.2 m (250 ft.) in length. The large mass at the top of section 2 was originally interpreted by King (1931:132, section 7, bed 1) as an isolated remnant of the lower massive member of the Capitan Limestone (= Vidrio Formation).

The masses commonly form resistant mounds of massive, nonbedded carbonate that stand in sharp contrast with the adjacent bedding. Weathered surfaces frequently mask internal textures, but occasional "windows" reveal much of the hidden features. The mass sequences are characterized by recurrent vertical and lateral facies successions. These facies are subdivided into underlying, mass, mass flank, and overlying beds.

The underlying lithologies vary considerably from mass to mass. Underlying beds include siltstones, fine sandstones, lime mudstones, and wackestones. All underlying lithologies appear to contain skeletal debris and/or lime-mud lithoclasts. The contact relationships are frequently poorly exposed. Partially winnowed lags were observed below a few of the masses; however, it is uncertain whether all masses overlie such deposits. Underlying bedforms are generally undulatory and lack definable sedimentary structures. The examined carbonates are characterized by sparsely sandy and lithoclastic, silty, skeletal, peloid lime mudstones, and they are rarely dolomitic. Bryozoans, crinoids, and algal structures are present. Sparry patches are not present.

The composition of the carbonate mass facies varies from mass to mass. These mass facies include massive skeletal lime mudstones and skeletal and/or lithoclastic wackestones. Intramass facies can be subdivided into basal, middle mass or mass core, and upper mass regimes. Intramass facies are gradational and may be difficult to define in each mass. Flank facies are marked by variations in thickness, lateral extent, and overall texture. Flank beds exhibit both symmetric and asymmetric development. Mass and mass flank facies may be

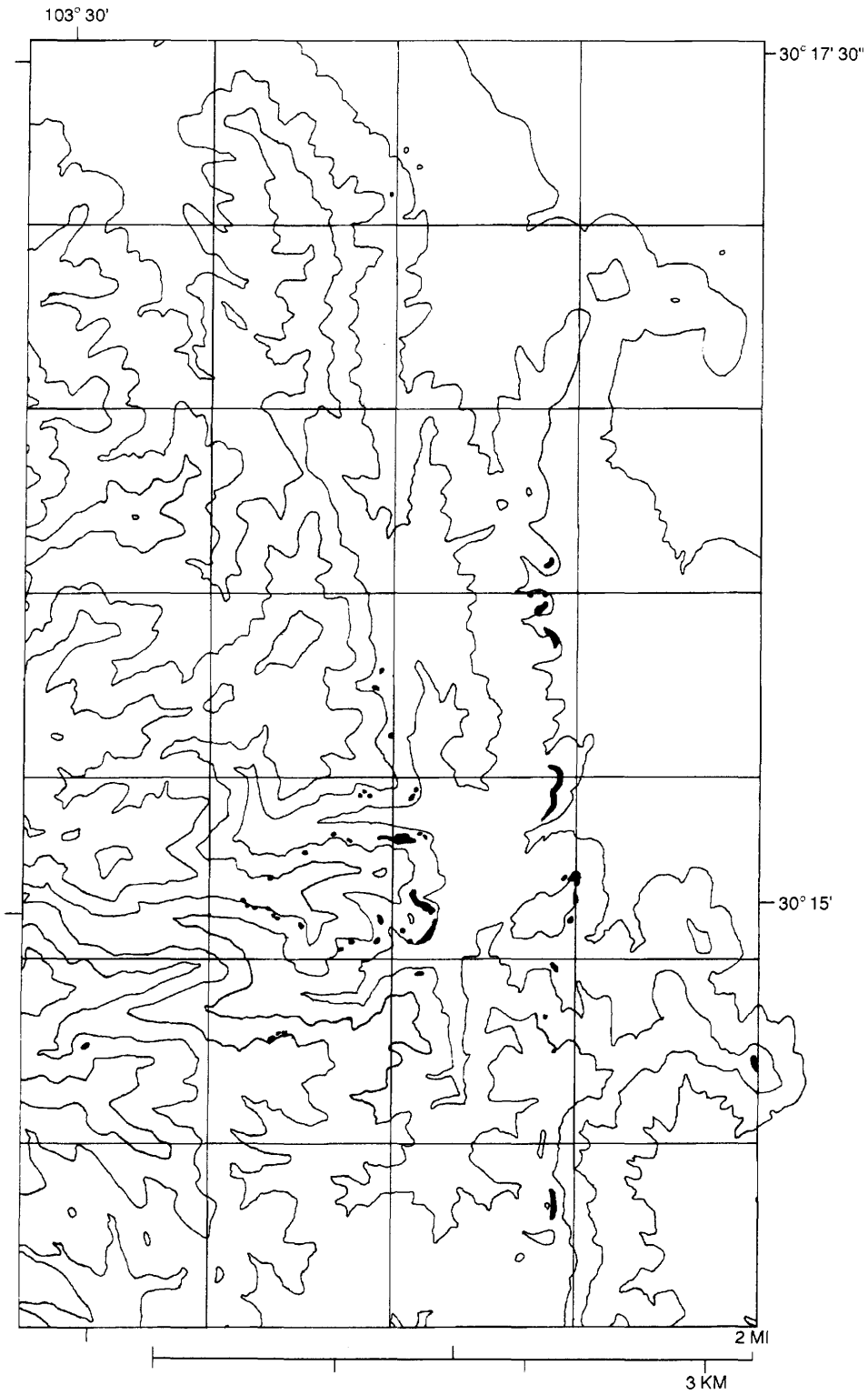


FIGURE 11-11.—Map showing the distribution of carbonate masses in the Appel Ranch Member. The masses are designated by the solid black areas.

overlain by draping beds that thin proximal to the mass. Some masses do not have discernable draping beds.

The transition from underlying bed to basal mass is abrupt and apparently rarely gradational. The underlying beds–basal mass contacts are generally undulatory with a thin lithoclast-rich underlying horizon. Underlying lithoclasts are ordinarily composed of angular, granule- to cobble-sized clasts of lime mudstone. Underlying and lateral beds rarely interfinger with the basal portion of the mass. Basal mass beds consist of growth assemblages of crinoids, bryozoans, and/or sponges. Basal mass beds also may contain recrystallized, angular lime-mud lithoclasts cemented in a darker lime mudstone. Similar lithoclast-rich deposits occur in the flank breccia beds; however, the flank breccia deposits are cemented in a markedly siltier lime-mud matrix. Clastic dikes are occasionally injected into the basal and middle portions of the mass, indicating moderate lithoclastic loading of the underlying strata. The clastic dikes are composed of lithic-rich, silty lime mudstone with common flow-line features.

The basal mass carbonates consist of a partially dolomitized, moderate to heavily recrystallized, sparsely silty and pelletal, lithoclastic, peloid, skeletal wackestone. Microspar cements outnumber pseudospar and blocky spar cements. Peripheral enlargement of microspar cement indicates an inversion of fine-grained cements to coarser pseudospar. Dolomite and ankerite occur at random in 60 percent of the samples examined. One dedolomitized sample was noted. Ostracodes and sponge spicules are background accessories to crinoids, bryozoans, and algal structures. Sediment stabilization structures, such as algal overgrowths and encrustations of sediment, are present in 25 percent of the thin sections.

The mass core sediments are similar to the basal facies sediments; they primarily differ in the degree of substrate modification. Prolific crinoid and bryozoan bafflestones and framestones are developed in many of the smaller masses (Figure 11-12). Calcareous sponges are found commonly in association with the crinoids and bryozoans. In many cases, sponges appear to be the primary sediment contributor because of the abundance of spicules in thin section. The mass core facies appear to vary depending on the size and orientation of the structure. Masses with widths greater than 12 m (40 ft.) commonly lack abundant skeletal remains in the central portions of the structure. In larger masses, skeletal accumulations tend to concentrate along the outer margins of the mass core.

The mass core sediments differ from the basal sediments in that they possess sheltered voids and early marine cements (Figure 11-13). The mass core sediments consist of dolomitic and moderately recrystallized, lithoclastic, skeletal, peloid wackestone. Peloid packstones and grainstones are rare. Cements vary from microspar to blocky spar. Primary sheltered void spaces are commonly lined with a fibrous, early marine cement. Sheltered voids are filled with spar-cemented peloidal

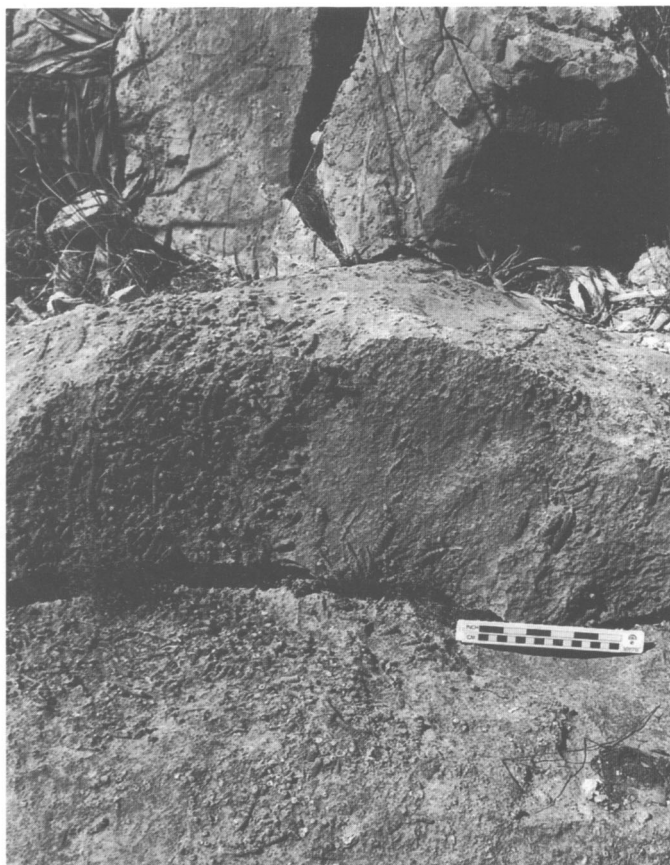


FIGURE 11-12.—View of abundant well-preserved crinoids in a carbonate mass.

sediments, blocky calcite, or a combination of the two. Algal-stabilized sediments and numerous *Tubiphytes* occur in thin sections containing early marine cements (Figure 11-14). The occurrence of these structures suggests initial cementation in shallow marine waters.

Voids formed during exposure to a freshwater phreatic environment are found in mass core sediments. Evidence suggests that these voids formed via selective solution and replacement of several precursor grain types and textures. Thin section and field observations support the interpretation that many voids represent extensively recrystallized molds after sponges. Other voids appear to have formed as a result of dissolution of recrystallized peloid lime mudstones, particularly in areas where fractures and coarser inverted microspar cements are present. Fracturing events are difficult to date in thin section. Cathodoluminescence analysis of mass carbonates revealed several generations of fracture fillings and secondary mineralization. The voids are generally lined with zone-free ankerite surrounded by multiple zones of dolomite and nonluminescent dolomite and ferroan calcite. Dolomite growth is terminated by a thin, highly luminescent, nonferroan calcite. Blocky calcite void fillings consist of alternating luminescent

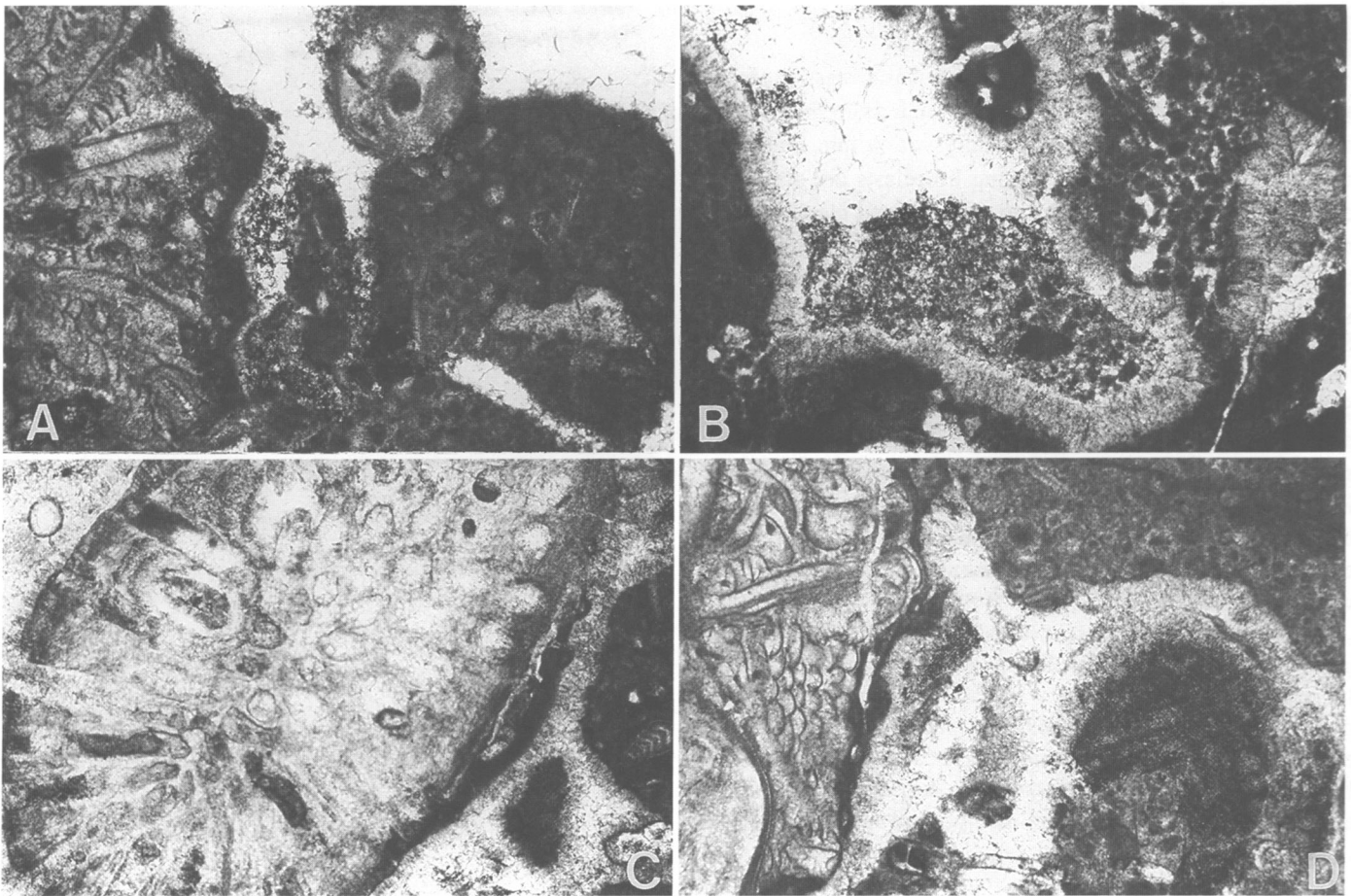


FIGURE 11-13.—Photomicrographs of the Appel Ranch Member carbonate mass from sample 147M. A, skeletal, peloid packstone. B, void lined with recrystallized fibrous cement, partially filled with sediment and spar. C, skeletal and lithoclast grains in recrystallized fibrous cement. D, skeletal, peloid wackestone showing recrystallized fibrous cement. Scale of the long axis in the photomicrographs equals 2.9 cm.

marine (?) calcite and nonluminescent, ferroan, freshwater phreatic calcite. A majority of void fillings exhibit crystal coarsening toward the void center. Loucks (1977) believed such a trend to be distinctive of freshwater phreatic cementation. Individual calcite crystals may contain several dozen zoned cement generations. Peloid lime mudstones may be partially or completely replaced with rhombs of ankerite rimmed with dolomite. Dolomitic replacements possibly represent transitions between marine phreatic and freshwater phreatic diagenetic environments.

The sediments of the upper mass facies are lithologically similar to the mass core sediments, only they differ slightly in the degree of dolomitization and character of the highest horizon. The upper mass sediments exhibit greater variations in dolomite content than the facies below. Extensively dolomitized zones were observed in many thin sections. The observation of syntaxial overgrowths on echinoderm fragments further strengthens the arguments for freshwater phreatic cementation (Loucks, 1977).

The character of the upper mass horizon varies from structure to structure. Many masses possess a crinoidal limestone cap replete with current-aligned, disarticulated crinoid columnals. Crinoid accumulations are absent from a majority of masses. The abundance of algae and the lack of coarse skeletal debris in thin sections of the mass sediments may suggest either a restricted water chemistry or perhaps algal stabilization, if present, inhibited the attachment of other marine fauna.

The mass flank facies demonstrate a wide developmental range. Flank beds consist of moderately to poorly sorted mass-derived breccias admixed with skeletal debris. Flank sediments vary from granule-sized particles of lime mudstone to boulders of lithified mass material, several 10s of cm (1–3 ft.) across (Figure 11-15B). Flank breccia development may be symmetric, asymmetric, or absent. Breccia beds extend from the mass core for a few meters (10s of ft.) to 30 m (100 ft.) or more. Moderately sorted flank breccias are cemented in blocky calcite and silty micrite matrix. Poorly sorted flank breccias

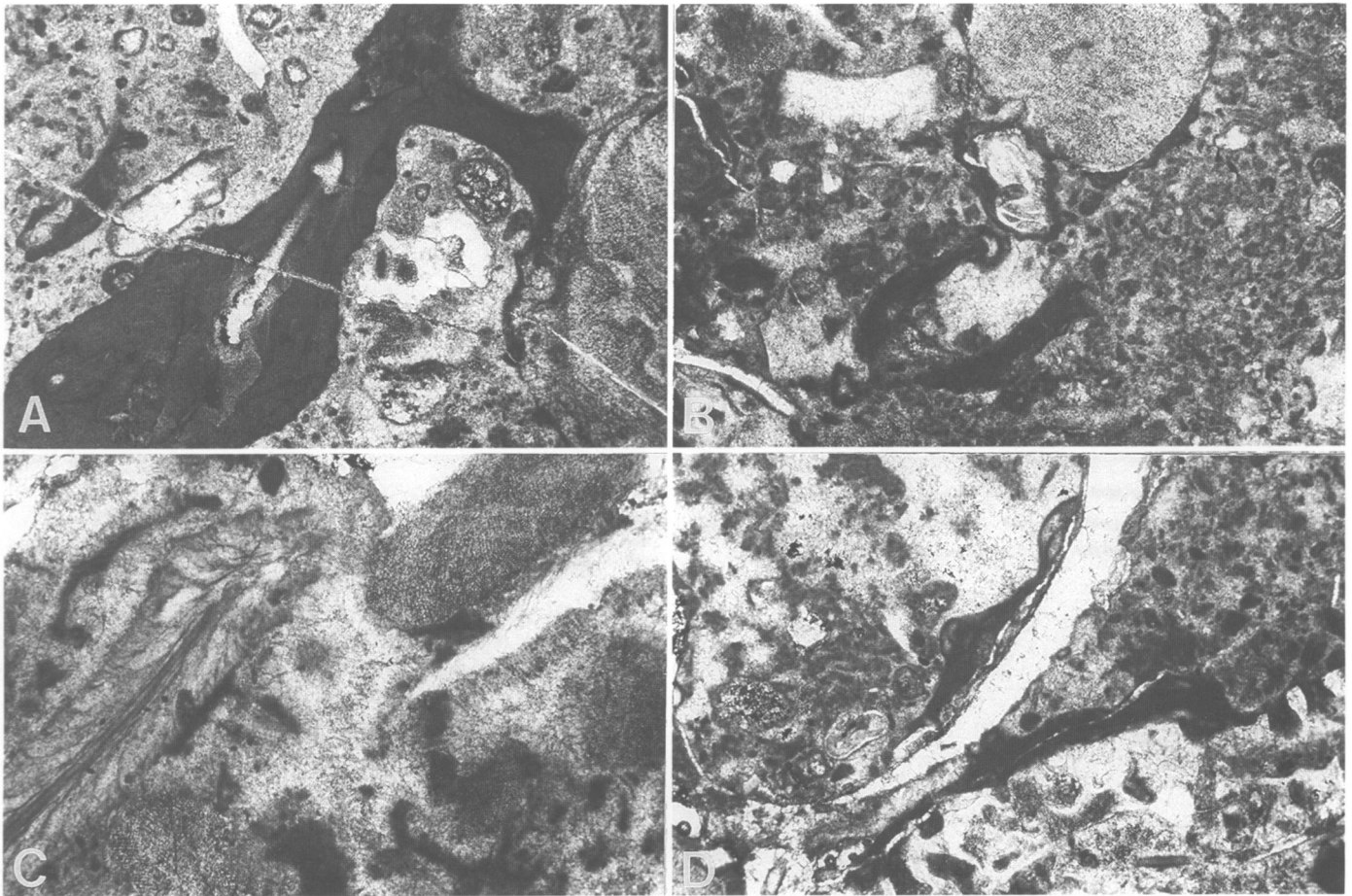


FIGURE 11-14.—Photomicrographs of the Appel Ranch Member carbonate mass from sample 253. A, *Tubiphytes* in peloid wackestone. B, skeletal, peloid packstone containing *Tubiphytes*. C, skeletal fragments in isopachous cement. D, partially recrystallized skeletal, peloid wackestone containing recrystallized mollusk shell and *Tubiphytes* with isopachous cement above. Scale of the long axis in the photomicrographs equals 2.9 cm.

commonly consist of chaotic boulder- to pebble-sized clasts floating in a massive, thick-bedded silty lime mudstone matrix. Distal portions of these beds grade laterally into the typical medium-bedded, slightly lithoclastic silty lime mudstones of the Appel Ranch. Flank breccias “lime up” proximal to the mass, grading laterally into massive carbonates. No apparent relationship exists between the extent of the flank breccias and the size of the mass.

The masses that display well-developed flank facies generally display an overlying facies. The overlying facies are characterized by a sequence of graded beds that drape over the mass and mass flank facies (Figure 11-15A). These drape beds thin proximal to the mass and thicken distally off mass where they may interfinger with upper portions of the flank facies. The lower drape beds consist of skeletal packstones and grainstones that grade upward into skeletal wackestones and lime mudstones. The highest drape beds consist of cross-laminated, silty lime mudstones with well-defined silty

laminations. The highest drape beds can be traced for great distances away from the mass, thus indicating an even post-mass topography. Drape-bed development appears to be limited to the highest mass horizon. Vertically stacked masses were observed at several locations. In each case, the mass(es) positioned below the uppermost structure(s) lacked a definable overlying facies. Beds of the overlying facies grade upward into medium- and thin-bedded Appel Ranch siltstones and carbonates.

The contact between the Appel Ranch Member and the overlying limy sandy siltstone member is gradational in the majority of exposures; however, at many locations, carbonates of the Vidrio Formation directly overlie carbonates and siltstone of the Appel Ranch. This suggests the presence of an unconformity beneath the Vidrio that cut out the limy, sandy siltstone member. North of the study area, in section 6, the upper Appel Ranch consists of interbedded, sandy, channel carbonates and sandstones that, in turn, are overlain by recrystallized carbonates of the Vidrio Formation. The more

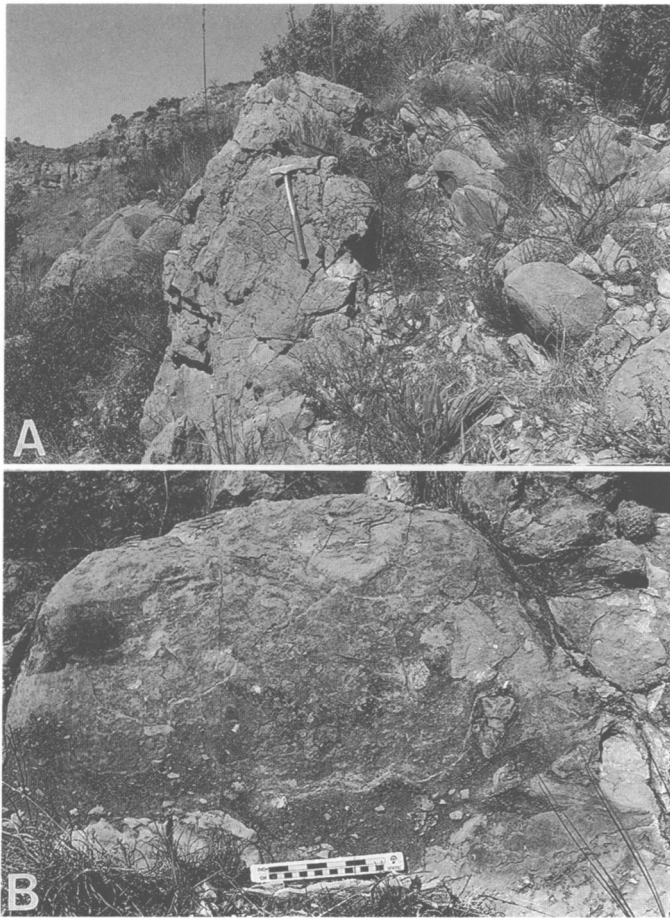


FIGURE 11-15.—Views of the Appel Ranch Member carbonate masses. A, carbonate mass and draping bed; hammer rests on mass. Note the steeply inclined, thin-bedded limestones above and to the right of the hammer. B, flanking bed of a mass. Note the angular character of the mass-derived breccia clasts. The clasts range from pebble to boulder size and “float” in a featureless silty lime-mudstone matrix.

sandy interval in the upper portion of the Appel Ranch may represent a condensed limy, sandy siltstone interval separating the two units.

Western exposures of the upper Appel Ranch are characterized by rapid vertical and lateral lithologic changes, and they contain a variety of carbonate lithologies interbedded with limy siltstones. Silty, skeletal, and lithoclastic wackestones common to the eastern part of the study area are replaced westward by extensively recrystallized, partially dolomitized, skeletal wackestones. Dissolution voids filled with coarse, milky calcite spar and cherty patches dominate the surface texture. Recrystallized sparry and cherty wackestones commonly occur as massive channel-fill deposits, some of which produce load deformation structures in the underlying limy siltstone. Another common lithology found in the western outcrops consists of thin-bedded, recrystallized, cherty, peloid, and silty mudstones. Bedforms common in the eastern outcrops also are found in the

western area. Channel intervals appear to occur with higher frequency in the western area. Along the south wall of Red Haw Spring Canyon, silty carbonates of the Appel Ranch are successively replaced up section, in a westward direction, by limy siltstones. Carbonate mass numbers drop off substantially in the western portions of the canyon.

LIMY, SANDY SILTSTONE MEMBER.—In the western half of the study area, carbonates of the Appel Ranch Member and the Vidrio Formation are separated by a thin wedge of clastics and dolomitic carbonates. This unit is best exposed in the south-facing slopes of Red Haw Spring Canyon, due east of section 5. Exposures in the low, east-facing foothills are not as easily defined as are those in the deep western canyons. The unit apparently pinches out to the north of the study area. Cretaceous limestones unconformably overlie the unit to the south of hill 6129 (Figure 11-4).

Interbedded limy, sandy siltstones and skeletal, peloid wackestones characterize the unit. Most of the unit is thin-bedded, but minor medium beds may be locally abundant. The lower beds of the unit form a prominent bench of dolomitized, skeletal, peloid wackestones with subordinate sand and silt-rich beds. Channel bedforms are common in the wackestone/siltstone interbeds. Planar laminations and cross-bedding are present in channel bedforms. Chert-rimmed, spar-filled voids, resembling dissolution gypsum rosettes, are frequently present in the peloid wackestone bench. Calcareous fenestrae, reminiscent of “bird’s eye” fabrics, were noted at several locations.

Limy, sandy siltstones constitute the remainder of the unit above the peloid wackestone bench. The siltstones are noticeably coarser-grained in comparison with those in the members below. Coarse siltstones contain a moderate amount of fine to medium-sized quartz sand. Quartz grains are angular. Calcareous and dolomitic cements are commonly present. Thin sections of the peloid wackestones are texturally and compositionally uniform. Wackestones possess minor amounts of angular quartz silt and/or sand. Anhedral and subhedral microdolospars prevail over calcitic microspar cement. Allochems consist of abundant micritized skeletal grains and peloids. Lithoclasts are present in a few beds, but very few were observed in thin section (Figure 11-16). Recrystallized (dolomitized?) skeletal grains are present in many thin sections. The majority of the carbonates consist of very well-sorted, skeletal (foraminiferal-algal), peloid wackestone. Peloid lime mudstones and packstones are present, but they occur less commonly.

Skeletal elements appear to represent a restricted marine environment. Few marine megafossils were observed in the field. The brachiopod *Hustedia* and fusulinid molds were noted in exposures near hill 6129 (Figure 11-4), and skeletal-bearing intraclasts were noted southeast of section 5. Of the fossils observed in thin section, all appeared to be juvenile forms. Foraminifers and algal remains are common constituents in many thin sections. Many foraminifers resemble poorly

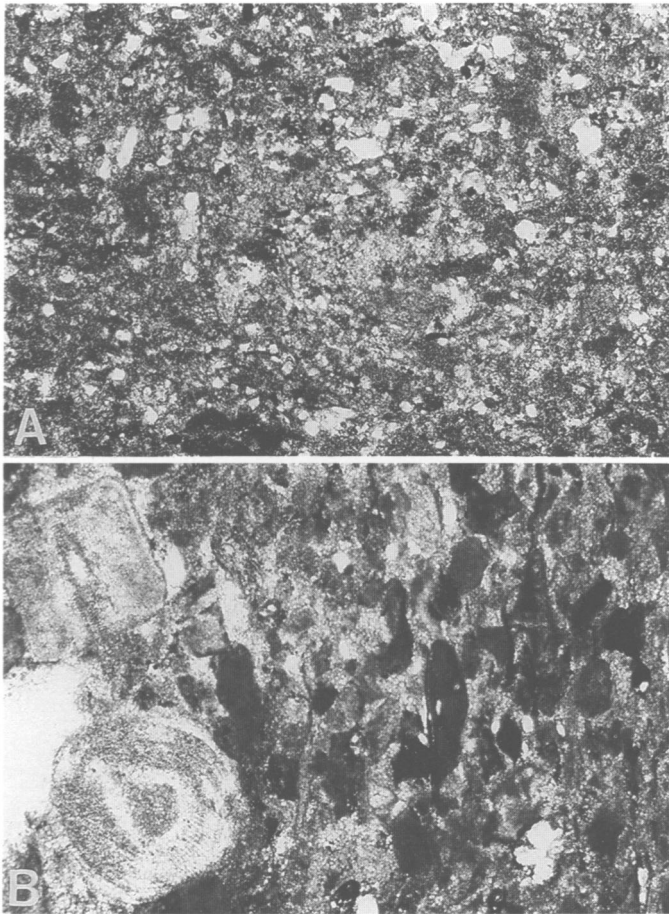


FIGURE 11-16.—Photomicrographs of carbonates from the limy sandy siltstone member of the Word Formation. A, sandy, silty lime mudstone (sample 5-299). B, slightly silty, skeletal, lithoclastic wackestone (sample 3-6). Scale of the long axis in the photomicrographs equals 2.9 cm.

oriented specimens of the fusulinacean *Rauserella*?. Algal remains consist of the partially recrystallized dasycladaceans, *Macroporella*? and *Epimastopora*?. Other elements include heavily recrystallized and/or micritized echinoderm plates, ostracodes, fusulinids, and brachiopod spines.

Peloids constitute the dominant allochem in all of the carbonates sampled. Peloids are composed of fine sand-sized grains of structureless micrite. All are well sorted and most are well rounded. Shapes vary from ovoid particles to elongate, subangular grains. Ovoid particles possibly represent fecal grains, whereas larger, elongate grains may represent organically decomposed skeletal fragments.

Siltstones and wackestones of the limy, sandy siltstone member apparently conformably overlie the carbonates of the Appel Ranch Member. Dolomitic peloid wackestones are more common in the majority of the western exposures. Siltstone distribution is erratic, apparently reflecting a response to the paleotopography and to the overlying unconformity below the Vidrio Formation, which commonly cuts out the member.

VIDRIO FORMATION

Carbonates of the Vidrio Formation typically form fairly steep convex cliffs along the east-west trending canyons. Generally, the Vidrio exhibits little topographic expression in areas where slope gradients are low and/or uniform. The majority of the Vidrio consists of massive recrystallized and dolomitized carbonates, nearly devoid of bedding. Thin to medium-thick beds may be locally present near the upper and lower boundaries.

Unaltered and moderately recrystallized carbonates consist of silty and nonsilty, lithoclastic, skeletal mudstones, wackestones, and packstones (Figure 11-17). Mudstones and wackestones are commonly peloid-rich. Peloid packstones are present in section 3 and section 5. Sedimentary structures are rare. Wispy, planar laminations resembling algal laminites are present in two thin sections. Scattered grains of coarse quartz silt and very fine sand are present in many thin sections. Quartz grains are angular to subround. Authigenic quartz grains are rare. Ferroan stains and opaque minerals sporadically occur along fractures and in the groundmass. Silt-rich beds are present at the base and the top of the formation. Siltstone lithoclasts and void/cavern fillings are locally present in the middle and upper portions of the formation. Siltstone fillings are interpreted to represent vadose/karst silt infillings. Corroded, angular to subround pebbles and cobbles of carbonate are commonly found in larger karstic zones, near the upper boundary of the formation (Figure 11-18).

Thin section and cathodoluminescence studies document a complex history of post-depositional diagenetic events that include extensive recrystallization and dolomitization. Commonly, peloids have been completely replaced with ankerite or dolomite. Microspar cements have been replaced with micro-



FIGURE 11-17.—View of corroded limestone pebbles and cobbles floating in a silty lime mudstone matrix, which represent karst sink infill, in the Vidrio Formation near section 6.

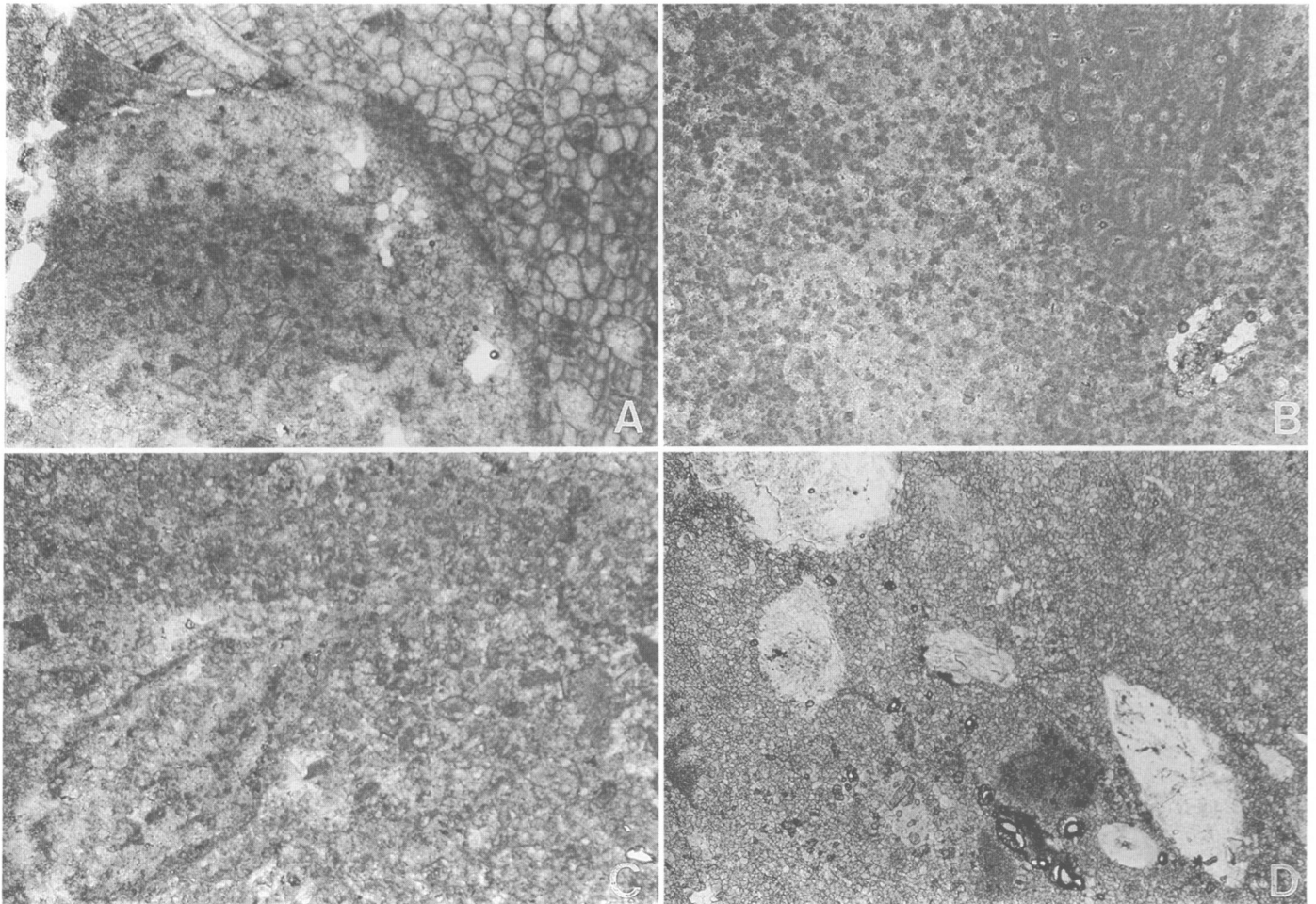


FIGURE 11-18.—Photomicrographs of the Vidrio and Altuda formations. A, recrystallized bryozoan in a peloid wackestone (sample PLMDUGOUT, recrystallized Altuda for comparison with Vidrio lithologies). B, recrystallized fusulinid in a peloid packstone (sample 3-9). C, recrystallized and dolomitized skeletal, peloid wackestone? (sample 5-405). D, recrystallized and dolomitized skeletal lime mudstone (sample 179). Scale of the long axis in the photomicrographs equals 2.9 cm.

dolospars. Fractures and voids are common, and fractures are commonly coated with dolomite linings. Skeletal grains are recrystallized and show internal dolomite growth. Rarely, depositional textures and skeletal grains are completely obliterated. Calcite infilling of voids and fractures, which show dozens of generations or zones, has been observed. Dolomite and/or ankerite growth is rarely observed in the calcite void fill. Dedolomitization is rare. Chalcedony replacement of calcite void filling also has been observed. Micritic, nonskeletal, fine sand-sized allochems are preferentially dolomitized over other allochems. Thin sections reveal that peloids are commonly replaced first, followed by micritic lithoclasts, lime mudstones, calcitic cement, and skeletal components.

Local variations in lithology, permeability, and diagenetic susceptibility appear to be primary constraints influencing the degree of alteration. Shallow-burial meteoric diagenesis is probably responsible for most of the recrystallization seen in

the Vidrio Formation, a large part of which may be attributable to subaerial exposure.

Skeletal constituents varied in abundance from sample to sample. Normal marine forms, such as crinoids, ostracodes, dasycladacean algae, bryozoans, sponges and sponge spicules, fusulinids, and brachiopods, are present. Bryozoans are present in virtually every sample. Allochems are commonly micritized or recrystallized.

Fossils in the Vidrio Formation are generally poorly preserved. A small number of silicified brachiopods and fairly well-preserved fusulinids are present in a fault block, 701 m (2300 ft.) northeast of hill 4893 (Cooper and Grant, 1972:162, 1977:3270-3271, 3316), originally mapped by King (1931) as the lower massive member of the Capitan (= Vidrio) and identified as Capitan by Cooper and Grant. The fauna clearly belongs to the Altuda, and it has been mapped as a dolomitized fault sliver of the Altuda Formation.

The contact relationship of the Vidrio Formation with the underlying and overlying units appears to vary over the extent of its exposure. Basal conglomerates and lags are very rare. The lower depositional surface is generally level; however, in the north-facing slopes of Red Haw Spring Canyon, the Vidrio appears to be deposited on a highly irregular surface. Estimates indicate that in this area there is 18 m (60 ft.) of depositional relief developed on the pre-Vidrio surface. The origin of this relief cannot be completely ascertained due to poor exposures. Outcrop symmetry is suggestive of a massive channel fill, but channel features are not clearly developed. A similar type of contact is present in the immediate vicinity of section 5, but the relief involved appears to be less than 3 m (10 ft.). This relief appears to be primary, suggesting that a channel surface may be locally developed. No such relief was noted in the remaining exposures. Field observations of the Vidrio along sections 3, 5, and 6 note the presence of locally abundant siltstone-rich layers and void fillings. These features are highly suggestive of meteoric diagenetic processes. Karstic surfaces and void fills are well developed in section 6. There, irregular voids and sinks are filled with angular, corroded pebbles and boulders of carbonate encased in a siltstone fill (Figure 11-18). The presence of abundant karst features in the vicinity of section 6 suggests a period of subaerial exposure prior to deposition of the Altuda Formation. The wide variation in preserved thickness (0–41 m; 0–133 ft.) in the Del Norte Mountains is believed to reflect extensive pre-Altuda erosion. In the vicinity of section 6, pre-Altuda erosion has removed more than one-half of the Vidrio, leaving a large erosional remnant of the member nearly isolated by surrounding clastics of the Altuda. An estimated erosional relief of 12 m (40 ft.) is developed in the area on top of the Vidrio.

ALTUDA FORMATION

Clastics and carbonates of the Altuda Formation crop out in limited exposures in northern and central portions of the study area. The unit commonly forms uniform, intermediate slopes, occasionally broken by small benches. Thin and medium beds are common in all Altuda lithologies.

Altuda carbonates consist of moderately to extensively recrystallized, peloid, skeletal, lithoclastic, dolomitic lime mudstones and wackestones with beds of slightly recrystallized peloid, skeletal, lithoclastic packstones. Carbonates are generally silty. Sedimentary structures include channel bedforms, planar and wavy laminations, and slightly cross-stratified laminations. Stromatolitic laminations were noted in several thin sections of the lime mudstones.

The majority of the lime mudstones and wackestones have undergone extensive dolomitization. Dolomitized carbonates are characterized by a roughly uniform, subhedral to euhedral, medium to coarse silt-sized ankerite and subordinate dolomite. Ankerite rhombs frequently possess thin isopachous rims of dolomite. Nonferroan calcitic cements commonly consist of

microspar and pseudospar with blocky cement limited to just dissolution voids. Many voids have been replaced by secondary chert cements. Skeletal content and diversity are markedly low in the lime mudstone/wackestone lithologies and are represented by only minor occurrences of crinoids and trilobites. Possible silicified fecal pellets are present in section 6.

Slightly recrystallized packstone occurs at irregular intervals in the Altuda. Cement characteristics are similar to those of the lime mudstones and wackestones with the exception of minor micrite cement in one thin section. Dolomitized carbonates are rare in thin section. Skeletal elements are very abundant, consisting of bryozoans, brachiopods, crinoids, ostracodes, foraminifers, dasycladacean algae, trilobites, fusulinids, and sponge spicules (Figure 11-19).

The vast majority of the Altuda Formation consists of limy, peloid siltstone and limy, sandy siltstone. Combined, these two lithologies form beds that are visually similar to the peloid wackestone bench-former of the Word limy, sandy siltstone

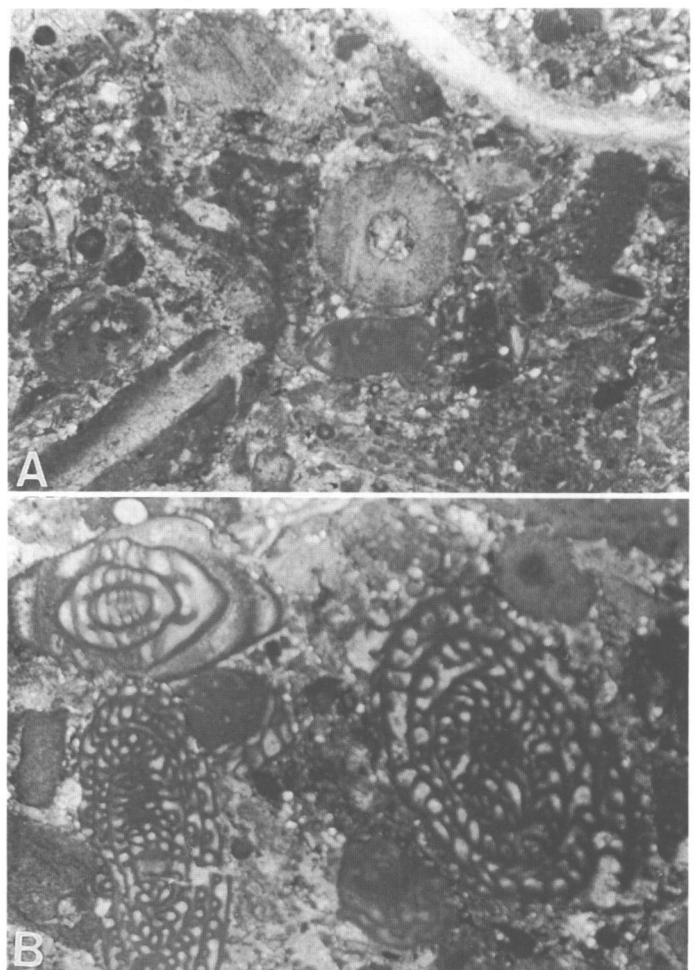


FIGURE 11-19.—Photomicrographs of skeletal carbonate in the Altuda Formation. A, skeletal packstone (sample 3-261). B, fusulinid, skeletal packstone (sample 3-261). Scale of the long axis in the photomicrographs equals 2.9 cm.

unit. Sedimentary structures include planar and ripple laminations, low-angle cross-stratification, and horizontal burrows. Peloid siltstone beds frequently contain small chert rosettes, possibly after gypsum. Lithoclasts of siltstone and limestone occur in sections 3 and 6, respectively.

The siltstones are composed of angular grains of medium- to coarse-grained quartz silt that is cemented in a wispy laminated, ferroan-stained calcitic microspar. Cross-laminations and minor medium silt-sized rhombs of dolomite are present in thin section. Peloids are medium- to coarse-silt size and consist of occluded, moderately sorted, ovoid- to rod-shaped grains of micrite. No internal structures were visible in thin section. Skeletal grains are represented by rare, poorly preserved sponge spicules. Skeletal debris appears to be relatively rare overall.

The Altuda Formation is unconformably overlain by Cretaceous sandstones and limestones in the study area. Pre-Cretaceous erosion has removed much of the Altuda. The three informal units of the Altuda recognized by Wardlaw et al. (1990) in the northern Del Norte Mountains can be generally recognized in the northern part of the study area. In comparison to the study area, it appears that all three units have thinned, indicating that the Altuda thins to the south in addition to being progressively more cut out to the south by the overlying Cretaceous deposits.

Depositional Environments

A foreland basin developed along the southern "shelf" of the Delaware basin in front of and in response to the Marathon orogen (Marathon Fold Belt, Rohr et al., this volume). Early Permian (middle Wolfcampian) orogenic deformation and uplift of the Dugout and Marathon allochthons resulted in the widespread development of thick conglomerate deposits of the Lenox Hills Formation in the Glass Mountains area (Ross, 1986). Coarse clastics of the Lenox Hills are overlain by conglomeratic delta front, sandy fore-delta, marine carbonates, and fine clastics of the Skinner Ranch and Cathedral Mountain formations (Ross, 1986). Wolfcampian and lower Leonardian lithologies in the Del Norte–Dugout Mountain–Lenox Hills area are dominated by a transgressive fining upward sequence of nonmarine, marginal marine, and marine deposits (Cooper and Grant, 1972; Ross, 1986). Regional tectonic stability following the mid-Wolfcampian orogeny is reflected by the decreased abundance of coarse-grained clastics in middle and late Leonardian time (King, 1937; Cooper and Grant, 1972; Ross, 1986).

In the study area, the Cathedral Mountain Formation consists of conglomerates, sandstones, sandy conglomerates, argillaceous skeletal limestones, and siltstones interpreted to be deposited in lower delta plain, distributary channel, and marginal delta plain/tidal flat settings (Rudine, 1988). Wardlaw et al. (1990) interpreted the Cathedral Mountain Formation north of the study area as deposited in a marine, distal fan delta

lobe plain, interlobe plain, and prodelta, implying more distal deposition on the same delta system prograding out from the Marathon fold belt into the foreland basin. Guadalupian deposition begins over this setting in the Del Norte Mountains.

Sediments of the Road Canyon and lowest Word formations are characterized by repetitious beds of thin, flaggy siltstones separated by laterally discontinuous lenses and sheets of limestone. The overall morphology, internal sedimentary structure, and allochem character indicate deposition in a channel complex in a shallow basinal setting. The siltstones offer few clues as to their depositional origin due to the scarcity of biogenic and primary sedimentary structures. Homogenized siltstones are believed to represent intensive burrowing of sediments by infaunal organisms, as burrow traces are locally abundant in some of the siltstones.

Carbonates are separable into two depositional categories based on thickness, sedimentary structures, grain size, sorting, and composition. Medium- to thick-bedded, peloidal, lithoclastic, skeletal wackestones, packstones, and coarse grainstones are interpreted to represent channel deposits, whereas thin-bedded, well-sorted, peloidal packstones and grainstones represent channel overbank deposits. Cross-bedding, lithoclast lags, and current-oriented skeletal elements are common. Fusulinids are the dominant skeletal channel constituent in the sequence. Channels contain reworked shallow marine faunas with common dasycladacean and solenoporacean algal remains. Stromatolitic lime mudstones and plant remains were found capping some of the channel sequences. Thin channel overbank deposits consist of well-sorted peloidal packstones and grainstones and contain abundant fecal derived peloids, dasycladacean algae, and algal-coated grains. Coarse-grained skeletal and lithoclast allochems are rare constituents compared to the channel deposits.

The Road Canyon deposits in the study area appear to be distal to the rare massive conglomerates found in the Road Canyon Formation of the Glass Mountains and the more continuous limestones, both in the northern Del Norte Mountains (north of the study area) and the Glass Mountains, which implies an opposite direction of flow (south vs. north) to that hypothesized by Harris et al. (this volume) and deposition into the foreland basin.

The upper half of the basal siltstone member of the Word is interpreted to represent a transitional environment from the foreland basin deposits below, devoid of channel influence, and the sandstones above. Concretions in the upper half of the unit may represent early paleosol development (Miall, 1982).

The massive character, the presence of minor cross-bedding, and abundant burrowing in the first sandstone member of the Word Formation indicate a lower shoreface setting (McCubbin, 1982). Muscovite placers in the lowest portions of section 4 are reminiscent of the beach shoreface placers described by Galloway (1976). Siltstone interbeds in the first sandstone member contain numerous penecontemporaneous concretions, some of which are reworked with marine skeletal material in

planar laminated and poorly graded conglomeratic beds. Conglomeratic beds are relatively rare, but when present they contain reworked pebbles of siltstone, marine fossils, and silicified wood. The highest bed in the first sandstone member is uniquely identifiable in the study area due to the presence of a 1.2 m (4 ft.) horizon of heavily burrowed (*Skolithos*-type) sands.

The second siltstone member represents a transitional depositional environment, juxtaposed between the strand line and shallow basinal settings. Deposition is believed to be similar to that of the upper part of the first siltstone member.

The carbonate masses of the Appel Ranch Member appear to represent shallow-water mud mound deposition, formed by a baffle of crinoids, bryozoans, and sponges. Repeated or prolonged exposure is suggested by the recrystallization, dolomitization, and cement history. Whether the masses were deposited in situ is problematic. The lack of enveloping breccia, the consistency of mass core and flank lithic successions, bed loading, and drape beds implies that if these masses did move, their movement was slight, and they all appear to be right side up implying they slid into place if they did not develop where they now reside.

The upper member of the Word Formation suggests regression. The initial sediments consists of skeletal, peloidal wackestones that are overlain by siltstones.

Skeletal, peloidal lime mudstones, wackestones, and packstones of the Vidrio Formation represent carbonate shelf deposition. Marine fossils are scattered throughout the unit, but extensive recrystallization and dolomitization obscure most of the primary features. Subaerial exposure and karst formation are abundantly evidenced.

Siltstones of the Altuda Formation possess ripple, planar, and cross-laminations and are dolomitic in part. Peloidal siltstones frequently contain small chert rosettes, possibly representing replacement after gypsum. Altuda carbonates are extensively recrystallized and dolomitized in the lower and middle part of the Altuda. Sedimentary structures are identical to those of the siltstones. Stromatolitic laminations were noted in several carbonate thin sections. Skeletal content and diversity are markedly low in mudstone/wackestone lithologies, suggesting a restricted and/or stressed environment. The highest Altuda carbonates in the study area are slightly recrystallized and contain a rich, normal marine fauna. Abundant channel bedforms and thin, even beds suggest a return of channel complexes in a shallow basinal setting. Wardlaw et al. (1990) suggested a deepening upwards/shallowing upwards sequence to explain the three general members of the Altuda, with the mudstone representing the deepest deposition; however, it appears that the carbonate and clastic members (equivalent to their units 14 and 15 and 17 and 18) represent transgressive-regressive (T-R) packages unto themselves, and the mudstone represents instead shallowest deposition (see Wardlaw and Rudine, this volume). The mudstone of the middle member laterally changes to siltstone to the south.

Summary

The Guadalupian rocks of the northern Del Norte Mountains confirm deposition within a foreland basin (Rohr et al., this volume) between land of the Marathon orogen and a carbonate shoal established on the geanticline fringing the Delaware basin. Deposition was alternately influenced by coarse clastic input from the south-southeast and carbonate input from the north-northwest, which interrupted the shallow basinal siltstone deposition that pervades the section.

The Road Canyon Formation and the first siltstone member of the Word Formation represent a shallow basinal setting of bioturbated siltstones with scattered channel and channel overbank carbonate deposits derived from the shallow carbonate shoal to the north and northwest.

The first sandstone member of the Word Formation indicates lower shoreface deposition.

The second siltstone member of the Word Formation reflects a change back to a shallow basinal setting.

The Appel Ranch Member represents a return to carbonate channel deposition derived from the north-northwest and contains carbonate masses, which represent shallow-water mud mounds that were frequently exposed, and which probably slid into the area from a very local source. The limy, sandy siltstone member of the Word suggests regression and a return to a shallow basinal setting. The Vidrio Formation represents unconformably bounded carbonate shelf deposition that was extensively recrystallized, dolomitized, and karstified by frequent subaerial exposure. The Altuda Formation indicates shallow deposition in its lower part and a return to carbonate channels in a basinal siltstone setting in its upper part.

Relatively deep-water deposition appears to be characterized by carbonate channels and masses and influence from the carbonate shoal. Relatively shallow-water deposition appears to be characterized by sandstone deposition or unconformities and influence from the Marathon orogen.

Deposition was in five general transgressive-regressive (T-R) packages that are eustatically driven. The first is represented in the Road Canyon Formation and first siltstone and first sandstone members of the Word Formation, with maximum transgression at the top of the Road Canyon Formation. The second general T-R package includes the second siltstone member, the Appel Ranch Member, and the limy, sandy siltstone member of the Word, with maximum transgression in the Appel Ranch Member.

Work by Wardlaw et al. (this volume), Rathjen et al. (this volume), and Rohr et al. (this volume) shows that these T-R packages can be further divided for the Road Canyon and Word formations. The finer differentiation of T-R packages, which is easily discernable near the carbonate shoal, is masked by the clastic input from the Marathon orogen, preserving only the major eustatic signals.

The third general T-R package is wholly contained within the unconformity bounded Vidrio Formation.

The fourth general T-R package includes the lower member

and part of the second member of the Altuda Formation, but it is very small. Maximum transgression is represented in the upper part of the lower member, whereas maximum regression is represented in the middle of the second member.

The fifth general T-R package includes the upper part of the second member and the third member of the Altuda. Maximum transgression is evidenced in the lower part of the third member.

Literature Cited

- Cooper, G.A., and R.E. Grant
 1972. Permian Brachiopods of West Texas, I. *Smithsonian Contributions to Paleobiology* 14:1-231, plates 1-23.
 1977. Permian Brachiopods of West Texas, VI. *Smithsonian Contributions to Paleobiology*, 32:3161-3370.
- Dott, R.H.
 1964. Wacke, Graywacke, and Matrix—What Approach to Immature Sandstone Classification? *Journal of Sedimentary Petrology*, 34(3):625-632.
- Galloway, W.E.
 1976. Sediments and Stratigraphic Framework of the Copper River Fan-Delta, Alaska. *Journal of Sedimentary Petrology*, 46(3):726-737.
- Haneef, Mohammad, S.F. Rudine, and B.R. Wardlaw
 1990. Shelf to Basin Transition in the Capitanian (Permian) Deposition in the Glass Mountains, West Texas. [Abstract.] *Geological Society of America, Abstracts with Programs*, 22:A46.
- Harris, M.T., D.J. Lehrmann, and L.L. Lambert
 2000. Comparison of the Depositional Environments and Physical Stratigraphy of the Cutoff Formation (Guadalupe Mountains) and the Road Canyon Formation (Glass Mountains): Lowermost Guadalupian (Permian) of West Texas. In B.R. Wardlaw, R.E. Grant, and D.M. Rohr, editors, The Guadalupian Symposium. *Smithsonian Contributions to the Earth Sciences*, 32:127-152, 25 figures.
- King, P.B.
 1931 ("1930"). The Geology of the Glass Mountains, Texas, Part I: Descriptive Geology. *University of Texas Bulletin*, 3038: 167 pages, 15 plates. [Date on title page is 1930; actually published in 1931.]
 1937. Geology of the Marathon Region, Texas. *United States Geological Survey Professional Paper*, 187: 148 pages, 24 plates.
- Loucks, R.G.
 1977. Porosity Development and Distribution in Shoal-Water Carbonate Complexes: Subsurface Pearsall Formation (Lower Cretaceous), South Texas. *University of Texas, Bureau of Economic Geology, Report of Investigations*, 89:97-126.
- McCubbin, D.G.
 1982. Barrier-Island and Strand-Plain Facies. In P.A. Scholle and D. Spearing, editors, Sandstone Depositional Environments. *American Association of Petroleum Geologists, Memoir*, 31:247-280.
- Miall, A.D.
 1982. Analysis of Fluvial Depositional Systems. *American Association of Petroleum Geologists, Education Course Notes Series*, 20: 73 pages.
- Rathjen, J.D., B.R. Wardlaw, D.M. Rohr, and R.E. Grant
 2000. Carbonate Deposition of the Permian Word Formation, Glass Mountains, West Texas. In B.R. Wardlaw, R.E. Grant, and D.M. Rohr, editors, The Guadalupian Symposium. *Smithsonian Contributions to the Earth Sciences*, 32:261-289, 22 figures.
- Rohr, D.M., B.R. Wardlaw, S.F. Rudine, M. Haneef, A.J. Hall, and R.E. Grant
 2000. Guidebook to the Guadalupian Symposium. In B.R. Wardlaw, R.E. Grant, and D.M. Rohr, editors, The Guadalupian Symposium. *Smithsonian Contributions to the Earth Sciences*, 32:5-36, 31 figures.
- Ross, C.A.
 1986. Paleozoic Evolution of Southern Margin of Permian Basin. *Bulletin of the Geological Society of America*, 97(5):536-554.
- Rudine, S.F.
 1988. Geology and Depositional Environments of the Permian Rocks, Northern Del Norte Mountains, Brewster County, Texas. 186 pages. Unpublished master's thesis, Sul Ross State University, Alpine, Texas.
- Rudine, S.F., B.R. Wardlaw, D.M. Rohr, R.A. Davis, and R.E. Grant
 1987. Depositional Setting of Late Leonardian-Wordian (Permian) Rocks, Southern Margin, Permian Basin: Basin or Lagoon? [Abstract.] *Geological Society of America, Abstracts with Programs*, 19(7):826.
- Wardlaw, B.R., R.A. Davis, D.M. Rohr, and R.E. Grant
 1990. Leonardian-Wordian (Permian) Deposition in the Northern Del Norte Mountains, West Texas. *United States Geological Survey Bulletin*, 1881-A:A1-A14.
- Wardlaw, B.R., C.A. Ross, and R.E. Grant
 2000. Cyclic Deposition of the Permian Road Canyon Formation, Glass Mountains, West Texas. In B.R. Wardlaw, R.E. Grant, and D.M. Rohr, editors, The Guadalupian Symposium. *Smithsonian Contributions to the Earth Sciences*, 32:121-126, 3 figures.
- Wardlaw, B.R., and S.F. Rudine
 2000. The Altuda Formation of the Glass and Del Norte Mountains. In B.R. Wardlaw, R.E. Grant, and D.M. Rohr, editors, The Guadalupian Symposium. *Smithsonian Contributions to the Earth Sciences*, 32:313-318, 4 figures.

12. The Altuda Formation of the Glass and Del Norte Mountains

*Bruce R. Wardlaw and
Shannon F. Rudine*

ABSTRACT

The Altuda Formation was deposited in a variety of environments from shelf to basin settings. The formation is divided into five informal units, which are increasingly limited in their areal distribution. The first unit is widespread and deposited in shelf, slope, and basin settings, whereas the last unit is only common to basinal settings.

Introduction

The Altuda Formation is a unit that is commonly misinterpreted to have been deposited in a single depositional setting; however, evidence is presented herein to demonstrate that it was deposited in several settings from shelf to basin. It contains the youngest conodont and fusulinid faunas found in the Glass and Del Norte mountains (see Wardlaw, this volume; Wilde and Rudine, this volume).

The shelf-to-basin stratigraphy of the Altuda was examined along two south-to-north transects; one in the Del Norte Mountains (sections 1-6, Figure 12-1), and one through the central Glass Mountains (along Old Blue Mountain) to a control well in the plains to the north of the mountain range (sections 7-12, Figure 12-1). Sections 1 and 2 were originally described by Rudine (1988) and appear in Rudine et al. (this volume). Sections 3 and 4 were originally described by Davis (1984). Davis lost the description of the upper part of section 4

(the Altuda Formation!), and it was redescribed by Rudine and is reported herein (Figure 12-2). The conodont data for both sections 3 and 4 was preliminarily reported by Wardlaw et al. (1990). The conodonts recovered from any of the sections used for this study are reported in Wardlaw (this volume). Section 5 is reported herein (Figure 12-2). Section 6 is reported by Rohr et al. (this volume). Sections 7-10 were originally reported by Faliskie (1989). Those descriptions are not very detailed, and section 7, originally measured by Wardlaw, is reported herein (Figure 12-2). Section 11 is reported by Rohr et al. (this volume). The control well to the north of the Glass Mountains (section 12) was originally described by Bloom (1988) as Kalinga Corporation's Margaret #1 and is reinterpreted herein (Figure 12-2).

Stratigraphy

The clastic and carbonate sediments of the Altuda Formation unconformably overlie the Vidrio Formation shoreward along the first transect (Figure 12-3). They overlie sands of the Word Formation (second sandstone member, Wardlaw et al., 1990) further from shore. The Altuda is unconformably overlain by Cretaceous limestone in the southern two sections and by the Tessey Formation in the northern four sections. King (1931) originally mapped the collapse breccias (Tessey Formation), which overlie the Altuda, as the massive member of the Capitan Limestone. In the second transect (Figure 12-4), the Altuda also unconformably overlies the Vidrio Formation in the south and the Word Formation in the north. Differentiating the siltstones and sandstones of the Word Formation and the siltstones and limestones of the Altuda Formation along the second transect can be difficult. In the well (section 12, Figure 12-2), a silty dolostone divides the two formations. This dolostone is thought to be a weathering profile on top of the Word Formation developed by the exposure surface, which represents the

Bruce R. Wardlaw, U.S. Geological Survey, 926A National Center, Reston, Virginia 20192. Shannon F. Rudine, Geology Department, Sul Ross State University, Alpine, Texas 79832.

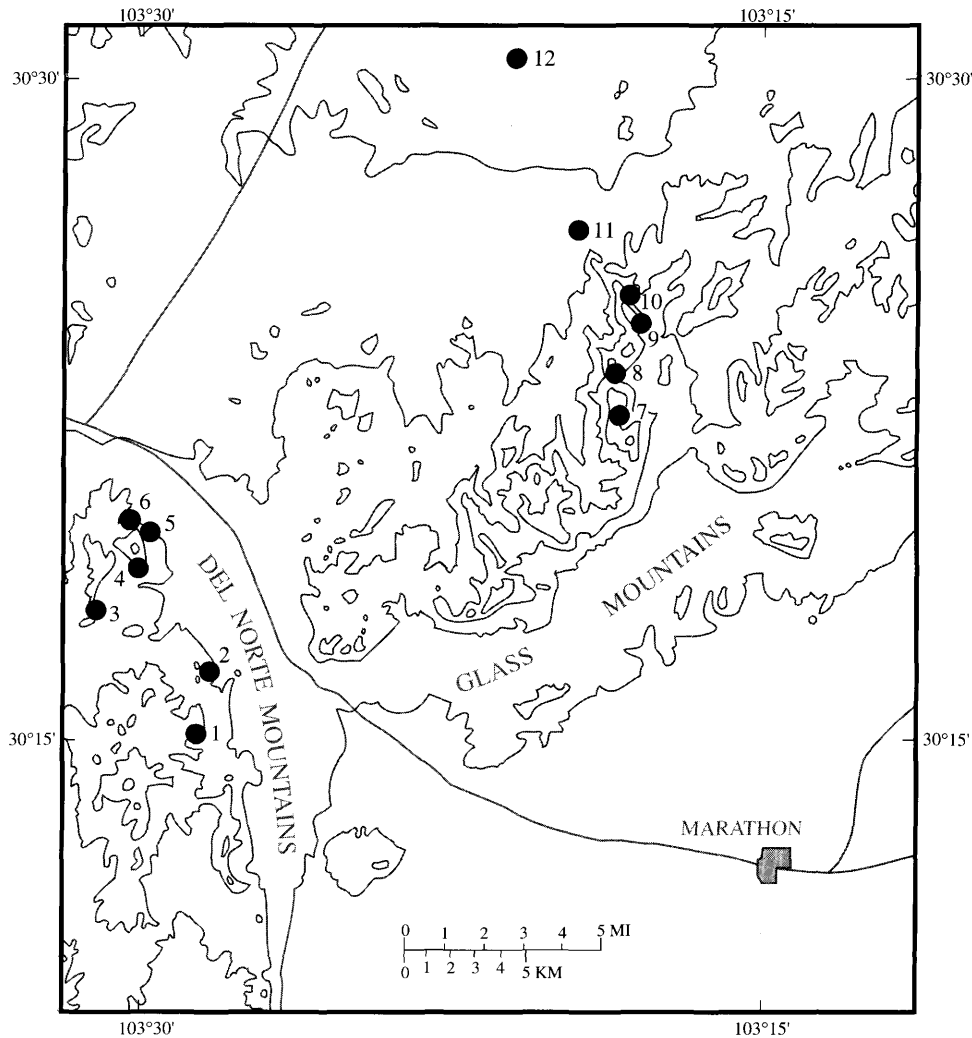


FIGURE 12-1.—Map of the Glass Mountains and Del Norte Mountains in West Texas showing the locations of sections.

unconformity that separates it from the Altuda. The upper part of the Altuda Formation clearly interfingers with the Capitan Limestone along the second transect. The Capitan was missing from the first transect and may not have been deposited in the Del Norte Mountains.

The Altuda Formation can be divided into five informal units based on the presence or absence of carbonates, which alternate in the units in the sections. Generally, all units have a clastic component.

UNIT 1.—The first limestone member. This unit in the Del Norte Mountains is represented by interbedded carbonate, mudstone, and siltstone that changes from mudstone to siltstone upwards. This unit in the Glass Mountains is represented by silty, sandy carbonates. Carbonates in both areas are generally lime mudstones to skeletal wackestones.

UNIT 2.—The first clastic member. This unit in the Del Norte Mountains is represented by mudstone. A few sparse carbonate

channels are present. In the Glass Mountains it is represented by interbedded siltstone and carbonate.

UNIT 3.—The second limestone member. This unit in the Del Norte Mountains is represented by interbedded carbonate, mudstone, and siltstone. Mudstone is the common clastic sediment in the north, and it is replaced by siltstone to the south. The carbonate is generally lime mudstone. In the Glass Mountains the unit is represented by sandy carbonates, commonly wackestones.

UNIT 4.—The second clastic member. This unit in the Del Norte Mountains is represented by siltstone. Carbonates are very rare. In the Glass Mountains it is represented by siltstone and sandstone. Here too, carbonates are rare.

UNIT 5.—The third limestone member. This unit is represented by interbedded carbonate and siltstone in both mountain ranges. The carbonates are lime mudstone to skeletal wackestone, rarely packstone.

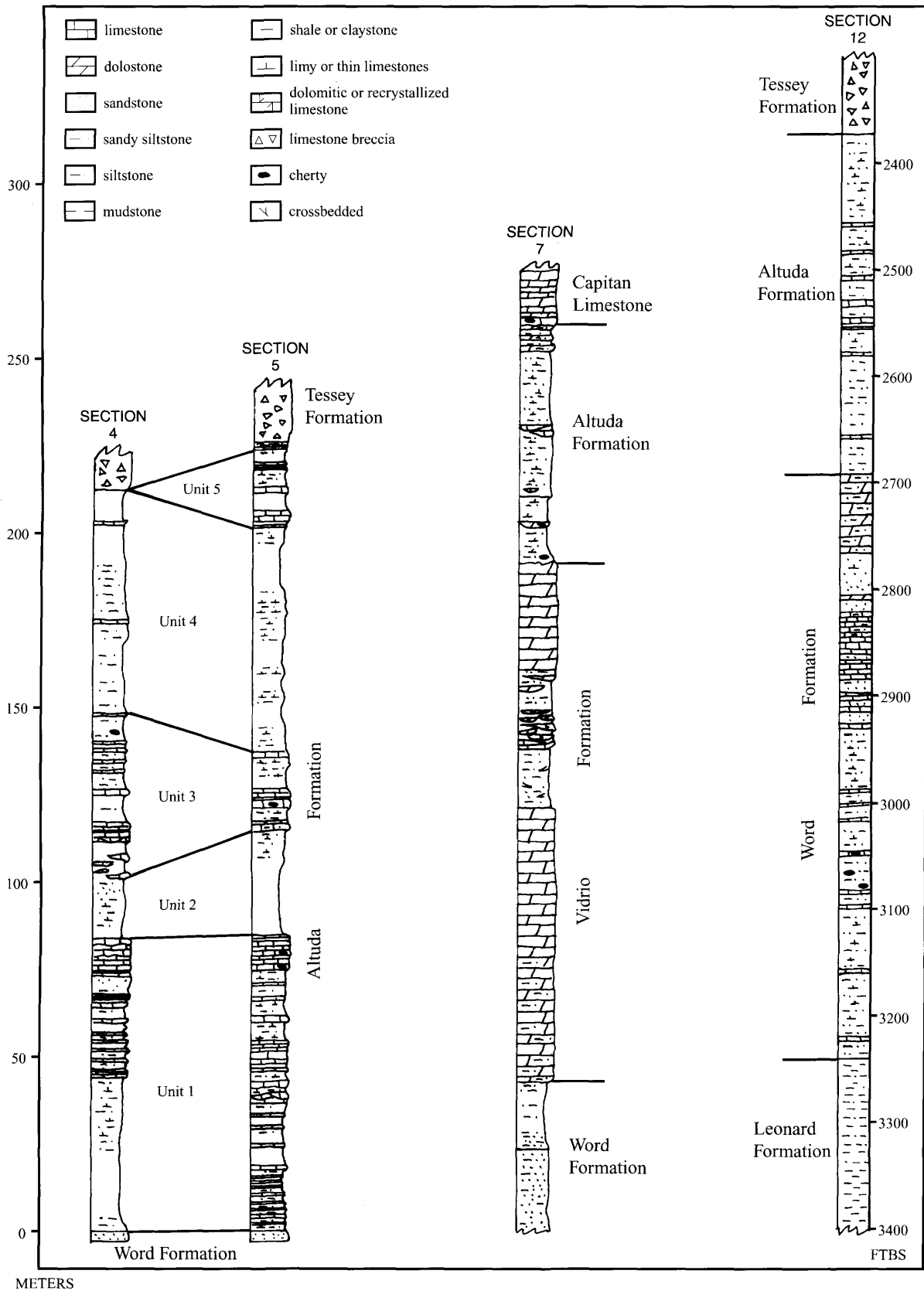


FIGURE 12-2.—Columnar sections showing stratigraphic units; locations of the sections are shown in Figure 12-1.

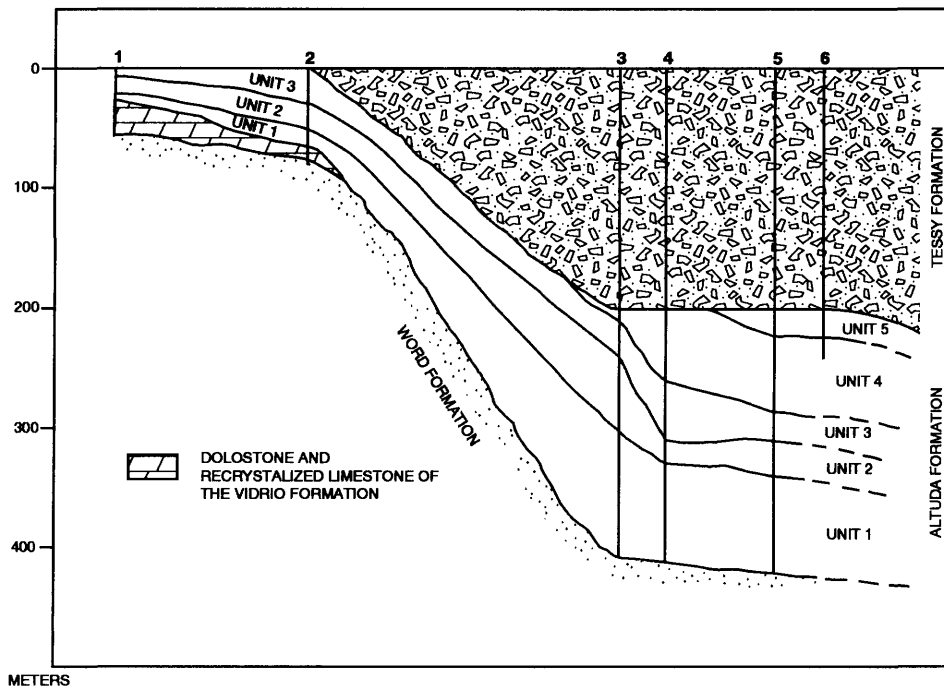


FIGURE 12-3.—Fence diagram of the units comprising the Altuda Formation and the formations immediately overlying and underlying the Permian units on transect 1 (sections 1–6) in the Del Norte Mountains. Sections shown are in proportionally true distance from section 1. The base of the Cretaceous was used as an arbitrary datum because it reflects the depositional nature of the transect in this diagram.

Interpretation

Haneef et al. (1990) first pointed out that the Altuda Formation is not everywhere a seaward equivalent of the Capitan Limestone. They noted that it also underlies the Capitan, and this underlying part represents ramp deposition that developed during a major regression, which destroyed the carbonate platform of the Vidrio Formation. The ramp existed before the development of the carbonate platform of the Capitan Limestone.

The units of the Altuda Formation appear to represent depositional response to general large scale sea-level fluctuations, with carbonate-rich units representing transgression (sea-level rise) and clastic-rich units representing regression (sea-level fall). Prior to Altuda deposition, a major regression resulted in the exposure and destruction of the Vidrio carbonate platform. This regression is also recorded in the unconformity

between the Cherry Canyon and Bell Canyon formations in the Guadalupe Mountains.

The Capitan carbonate platform developed during deposition of unit 2 of the Altuda Formation (during regression) in the Glass Mountains and managed to maintain itself through ensuing sea-level rises in the Guadalupian. In the Del Norte Mountains, carbonate platform development may not have occurred. The first three units of the Altuda Formation carry all the way to the south, supposedly well up on the shelf. Erosion prior to Tessey deposition and/or Cretaceous deposition has removed any evidence of whether carbonate platform deposition existed during the deposition of units 4 and 5 of the Altuda Formation in this area. The lack of widespread carbonate platform development suggests that tectonic driven subsidence may still have been an important factor in deposition in the southern foreland basin in the late Guadalupian (see Rudine et al., this volume, for a discussion of tectonic effects in the Leonardian and early Guadalupian).

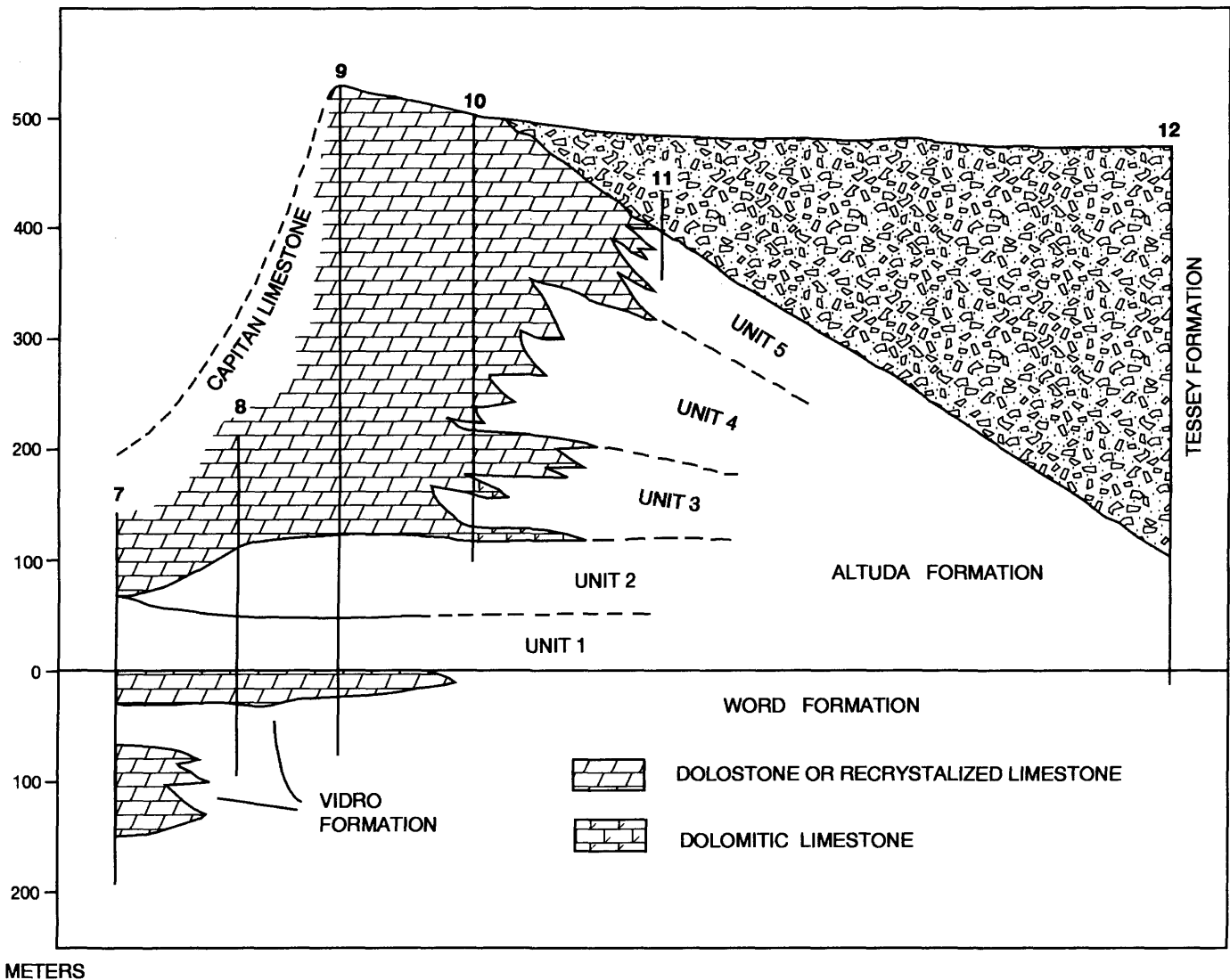


FIGURE 12-4.—Fence diagram of the units comprising the Altuda Formation and the formations immediately overlying and underlying the Permian units on transect 2 (sections 7–12) in the central Glass Mountains. Sections shown are in proportionally true distance from section 7. The base of the Altuda Formation was used as an arbitrary datum because it reflects the depositional nature of the transect in this diagram.

Literature Cited

Bloom, M.A.
 1988. A Subsurface Geologic Study of Northern Brewster County, Texas. 157 pages. Unpublished master's thesis, Sul Ross State University, Alpine, Texas.

Davis, R.A.
 1984. Depositional Environments of the Western Cathedral Mountain, Road Canyon, Word and Capitan Formations (Permian), Glass Mountains Area, West Texas. 104 pages. Unpublished master's thesis, Sul Ross State University, Alpine, Texas.

Faliskie, R.A.
 1989. Depositional Environments of the Vidrio Member of the Word, Altuda, and Capitan Formations (Upper Permian) in the Northwestern Glass Mountains, West Texas. 87 pages. Unpublished master's thesis, Sul Ross State University, Alpine, Texas.

Haneef, Mohammad, S.F. Rudine, and B.R. Wardlaw
 1990. Shelf to Basin Transition in the Capitanian (Permian) Deposition in the Glass Mountains, West Texas. [Abstract.] *Geological Society of America, Abstracts with Programs*, 22(7):A46.

King, P.B.

1931 ("1930"). The Geology of the Glass Mountains, Texas, Part I: Descriptive Geology. *University of Texas Bulletin*, 3038: 167 pages, 15 plates. [Date on title page is 1930; actually published in 1931.]

Rohr, D.M., B.R. Wardlaw, S.F. Rudine, M. Haneef, J.A. Hall, and R.E. Grant

2000. Guidebook to the Guadalupian Symposium. In B.R. Wardlaw, R.E. Grant, and D.M. Rohr, editors, The Guadalupian Symposium. *Smithsonian Contributions to the Earth Sciences*, 32:5–36, 31 figures.

Rudine, S.F.

1988. Geology and Depositional Environments of the Permian Rocks, Northern Del Norte Mountains, Brewster County, Texas. 186 pages. Unpublished master's thesis, Sul Ross State University, Alpine, Texas.

Rudine, S.F., B.R. Wardlaw, D.M. Rohr, and R.E. Grant

2000. Geology and Depositional Environments of the Guadalupian Rocks of the Northern Del Norte Mountains, West Texas. In B.R. Wardlaw,

R.E. Grant, and D.M. Rohr, editors, The Guadalupian Symposium. *Smithsonian Contributions to the Earth Sciences*, 32:291–312, 19 figures.

Wardlaw, B.R.

2000. Guadalupian Conodont Biostratigraphy of the Glass and Del Norte Mountains. In B.R. Wardlaw, R.E. Grant, and D.M. Rohr, editors, The Guadalupian Symposium. *Smithsonian Contributions to the Earth Sciences*, 32:37–87, 3 figures, 12 plates 1 table.

Wardlaw, B.R., R.A. Davis, D.M. Rohr, and R.E. Grant

1990. Leonardian–Wordian (Permian) Deposition in the Northern Del Norte Mountains, West Texas. *United States Geological Survey Bulletin*, 1881-A:A1–A14.

Wilde, G.A., and S.F. Rudine

2000. Late Guadalupian Biostratigraphy and Fusulinid Faunas, Altuda Formation, Brewster County, Texas. In B.R. Wardlaw, R.E. Grant, and D.M. Rohr, editors, The Guadalupian Symposium. *Smithsonian Contributions to the Earth Sciences*, 32:343–371, 3 figures, 9 plates.

13. A Deep Water Turbidity Origin for the Altuda Formation (Capitanian, Permian), Northwestern Glass Mountains, Texas

*Mohammad Haneef, David M. Rohr,
and Bruce R. Wardlaw*

ABSTRACT

The Altuda Formation (Capitanian) in the northwestern Glass Mountains is comprised of thin, evenly bedded limestones, dolostones, mixed clastic-carbonates, and silt/sandstones interbedded with basinward dipping wedge-shaped clinoforms of the Capitan Limestone. The formation is characterized by graded bedding, planar laminations, flame structures, contorted/convolute bedding, horizontal branching burrows, and shelf-derived normal marine fauna. A detailed study of the Altuda Formation north of Old Blue Mountain, Glass Mountains, reveals that the formation in this area was deposited by turbidity currents in slope to basinal settings.

Introduction

The Altuda Formation is early to late Capitanian (late Guadalupian) in age and is correlated with the Bell Canyon Formation of the Delaware basin. Conodont biostratigraphic studies of the Altuda Formation in the Del Norte Mountains (Rudine et al., 1987; Wardlaw, 1987, this volume) report *Mesogondolella aserrata* from the lower part, correlating it with the Hegler Limestone Member of the Bell Canyon Formation.

Wilde and Rudine (this volume) identified three fusulinid subzones (herein regarded as zones) in the Altuda Formation in

the Glass and Del Norte mountains. From top to bottom they are the *Paraboultonia-Lantscichites* Zone, the *Richelina lamarensis* Zone, and the *Paradoxiella* Zone. Rocks below those containing *Paradoxiella* were not investigated by Wilde and Rudine (this volume), but they are suspected to contain the *Yabiena texana* Zone as this zone is found below the investigated zones in the Guadalupe Mountains. They reported a biostratigraphic correlation with the upper part of the Bell Canyon Formation (Lamar Limestone Member and post-Lamar siltstones) and the Tansill Formation (shelf) of the Guadalupe Mountains.

The Altuda Formation exhibits lateral and vertical variations in facies relationships over the entire extent of the outcrop (King, 1931). The lateral variation in facies is marked by time equivalent lithostratigraphic units represented by, from west to east, the Altuda Formation, the Capitan Limestone, and the Gilliam Limestone. At Old Blue Mountain, the Altuda Formation laterally merges into the Capitan Limestone, exhibiting interfingering of both facies.

The present study offers an environmental analysis of the Altuda Formation north of Old Blue Mountain, Glass Mountains, Texas (Figure 13-1).

Stratigraphy

The Altuda Formation lies unconformably on the Vidrio Formation. Rudine et al. (1988) reported a major unconformity between the two units based on the erosional (karstic) upper surface of the Vidrio and on the change in fusulinid fauna from *Parafusulina* to *Polydiexodina*. Faliskie (1989) noted undulatory, erosional contacts marked by discordance in dip between the two units. In the study area, the base of the Altuda Formation is not exposed. All lithologies belong to the Altuda's upper unit, the third limestone member (Unit 5 as

Mohammad Haneef and David M. Rohr, Geology Department, Sul Ross State University, Alpine, Texas 79832. Bruce R. Wardlaw, U.S. Geological Survey, 926A National Center, Reston, Virginia 20192.

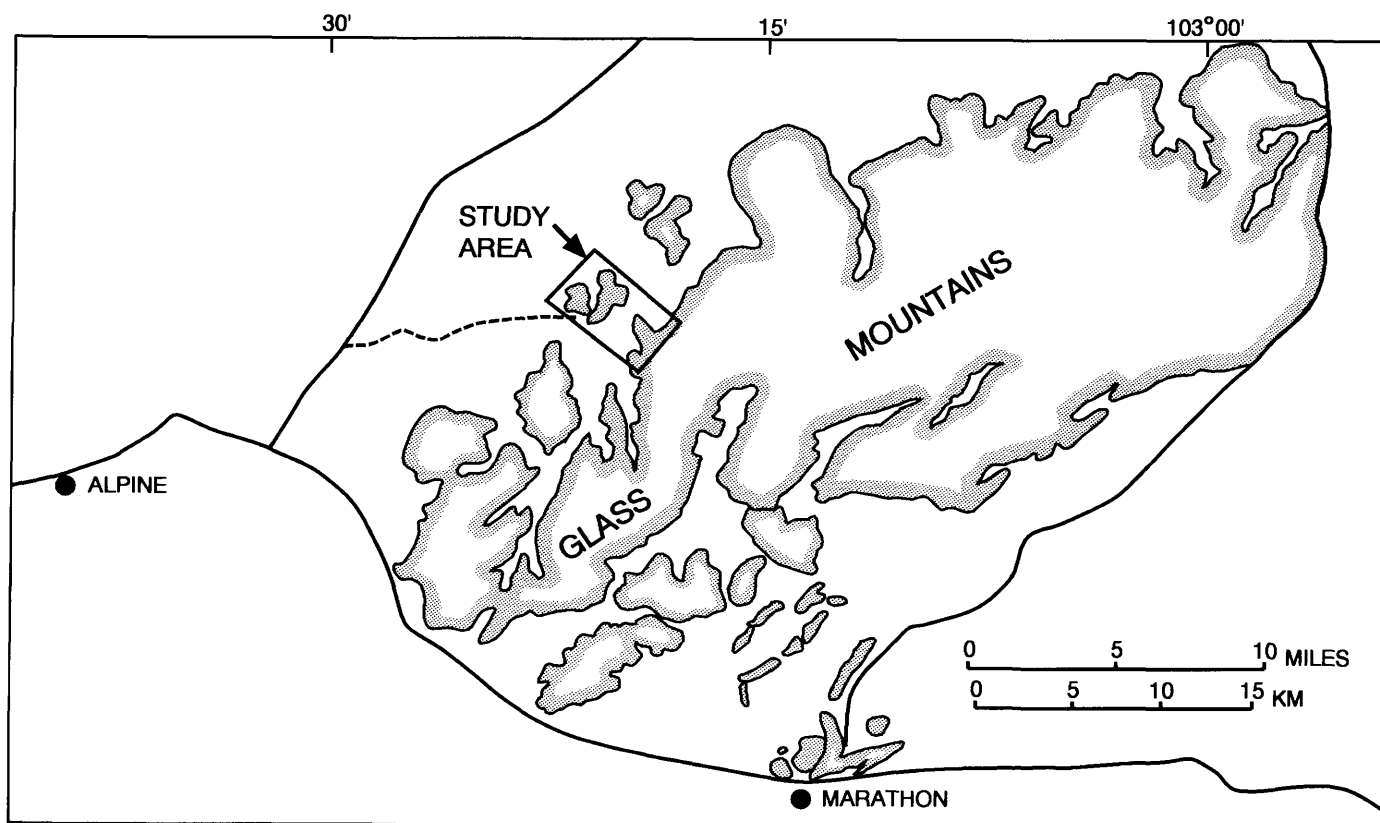


FIGURE 13-1.—Map of the Glass Mountains region with the study area indicated.

identified by Wardlaw and Rudine (this volume)). The lateral relationships with the foreset beds of the Capitan Limestone are transitional and are marked by the interfingering of both formations. The Altuda Formation has an unconformable upper contact with the overlying upper part of the Capitan in sections BR 5, BR 6, and BR 8. In sections BR 1, BR 3, BR 4, and BR 7, the Altuda Formation shows an unconformable upper contact with the Tessey Formation of Ochoan (post-Guadalupian) age.

Exposures of the Altuda Formation in the western and southwestern part of the Glass Mountains can be traced continuously for about 7.2 km in a northwest-southeast direction and for about 14.5 km in a northeast-southwest direction from Old Blue Mountain. The thickness of the formation varies from 15.2 m (King's (1931) section number 8, 6.6 km NNW of Altuda Mountain) to 254.2 m in the vicinity of Sullivan Peak (King's (1931) section number 12). Rudine (1988) reported the thickness of the Altuda Formation at Bird Mountain to be 168 m, and Faliskie (1989) measured its thickness as being 128.6 m at 4 km south of Gilliland Peak.

In the study area, the thickness of the Altuda Formation varies from 35.7 m in section BR 7 to 90.1 m in section BR 6 (Figure 13-2).

Lithofacies

The Altuda Formation is composed of carbonates, clastics, and mixed clastic-carbonate units interbedded with Capitan Limestone foreset beds.

Sedimentary structures vary and include planar laminations, cross-stratification, graded bedding, slump deformation, flame structures, dish structures, vertical and horizontal burrows, wavy to channelized bedforms, and spar- and chert-replaced anhydrite rosettes. The rocks of the Altuda Formation are broadly subdivided into three major lithofacies: sandstone/siltstone lithofacies, silty, spiculitic dolomud-wackestone lithofacies, and mixed skeletal wackestone/packstone lithofacies.

SANDSTONE/SILTSTONE LITHOFACIES

Laminated to bioturbated, poorly sorted, fine sandstone and siltstone occur in thin- to medium-sized (2–30 cm), planar, wavy, and convolute beds in the Altuda Formation. Weathered surfaces are colored light yellow, brownish yellow, and brown. The sandstone is dominated by fine, angular to subangular, monocrystalline quartz (> 80%) with subordinate amounts of polycrystalline quartz, muscovite, and biotite, which is cemented by calcite or finely crystalline dolomite (Figure 13-3A).

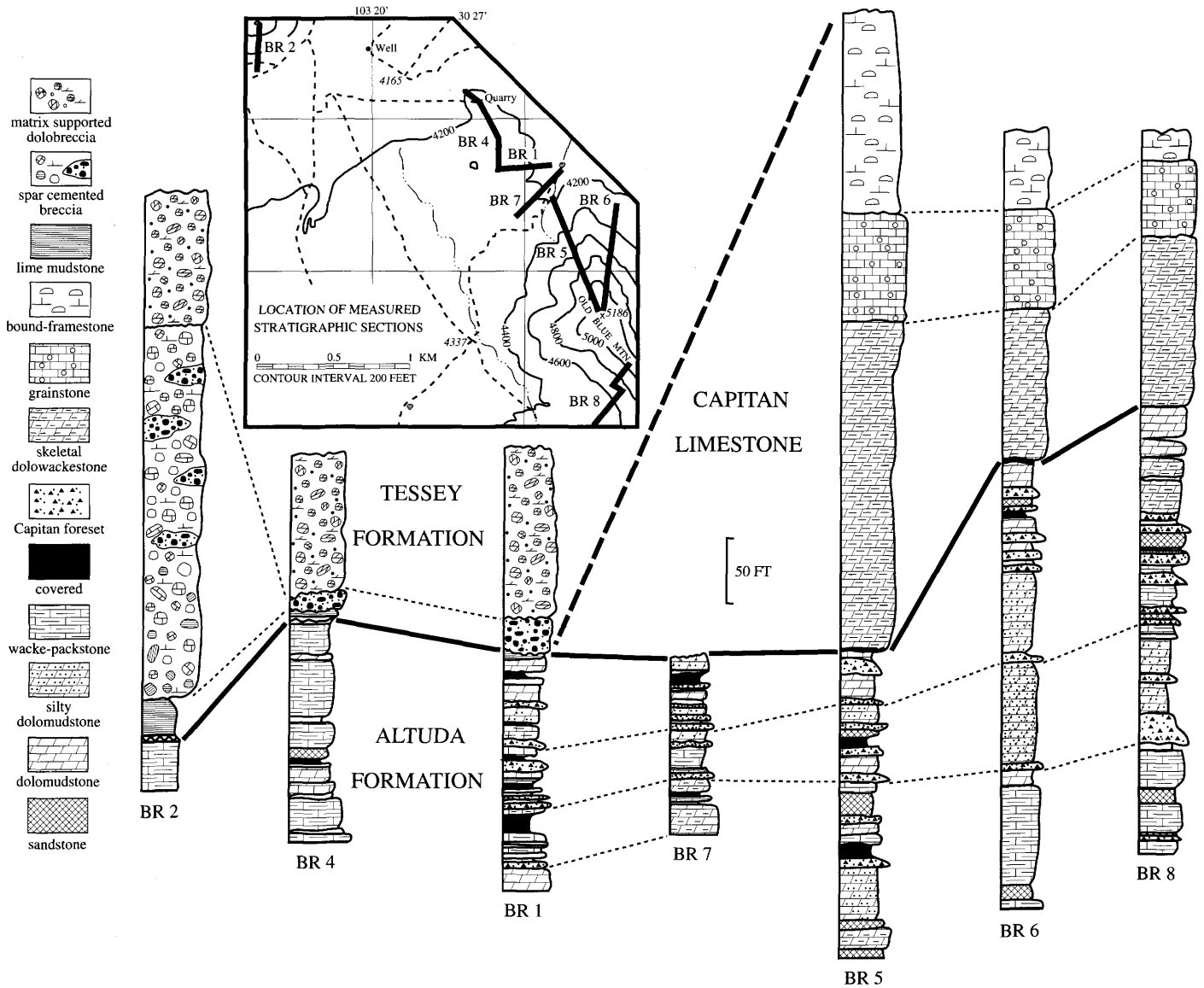


FIGURE 13-2.—Stratigraphic correlation of the lithofacies in Old Blue Mountain, Glass Mountains, Texas.

In the siltstone, the abundance of micaceous minerals varies from 5 percent to 25 percent, whereas angular monocrystalline quartz makes up 30 percent to 60 percent of the rock (Figure 13-3B). Anhydral pyrite is common in brownish sandstone and siltstone. Sandstone is volumetrically minor compared to siltstone, which constitutes approximately 75 percent of the lithofacies. The sandstone/siltstone lithofacies represents approximately 10 percent of the total measured sections. The lithofacies is repeated six times vertically and occurs laterally in all sections except BR 2; however, this section represents only the top 10 m of the Altuda Formation and lacks siliciclastics. This lithofacies lacks lateral continuity in all the stratigraphic sections. The thickness of the lithofacies varies from 3–20 m.

The sandstone/siltstone lithofacies is characterized by planar bedforms wherever it has lower and upper contacts with the skeletal packstone lithofacies, and it shows wavy to undulatory contacts with foreset beds of the Capitan Limestone. Most beds display millimeter-scale planar lamination and are accentuated by iron oxide and chert layers that parallel the bedding. The laminations are caused by minor variations in grain size and/or biotic content. Fossils are generally rare or absent. Skeletal fragments are siliceous sponge spicules that comprise less than 5 percent of the rocks. Many small tube-shaped branching burrows (Figure 13-3C), probably representing grazing traces, and rare, small (1–3 cm long) vertical tube burrows (Figure 13-3D) are present on the bedding surfaces of some homogeneous beds, indicating organic activity. The homogeneous beds

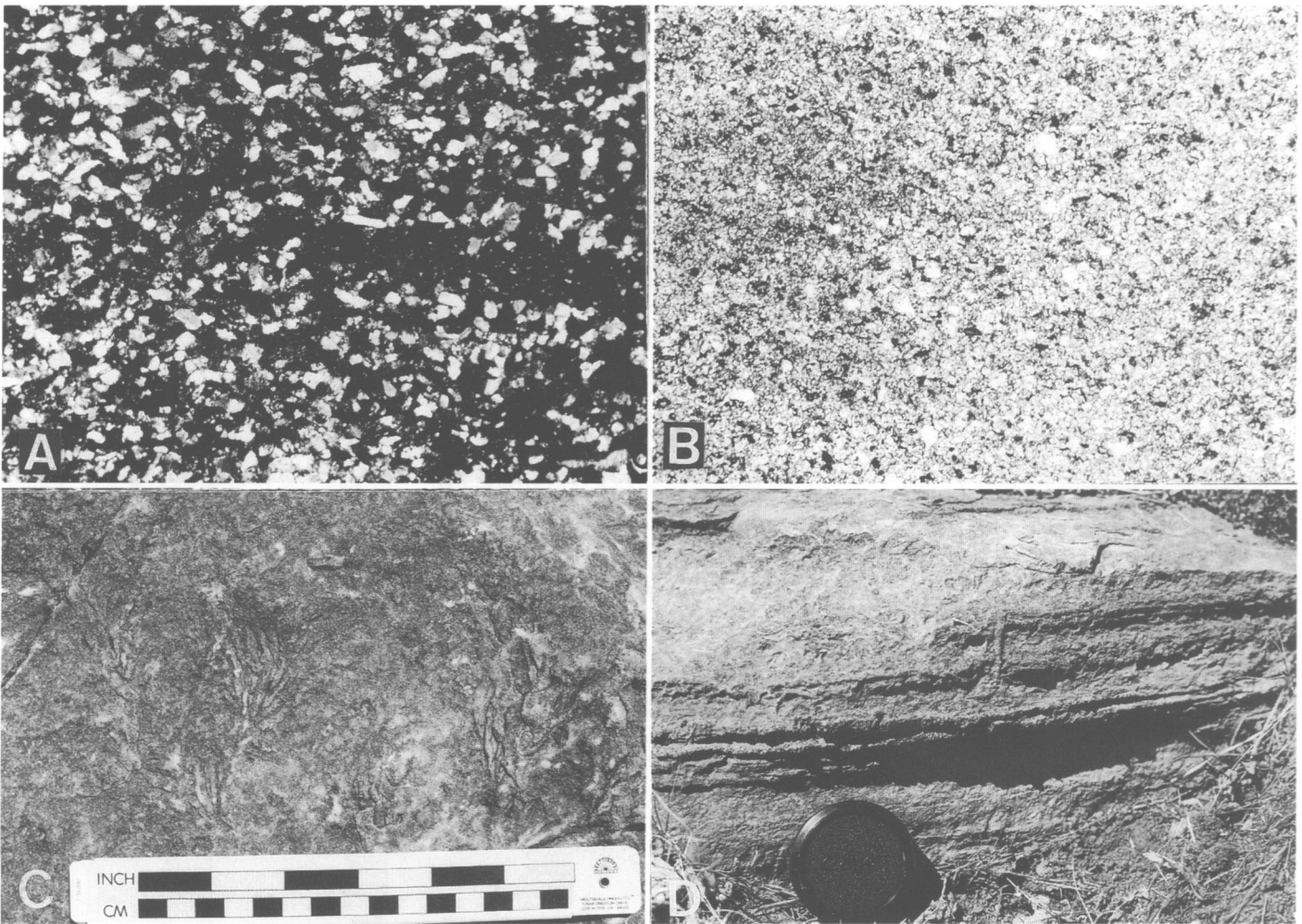


FIGURE 13-3.—A, photomicrograph of poorly sorted, fine-grained sandstone of the Altuda Formation. Note size variations and angularity of the grains. Dark areas in the photo are lime-mud. Long axis of the photo equals 2 mm. B, photomicrograph of Altuda Formation siltstone. Long axis of the photo equals 1 mm. C, bedding plane view of small, tube-shaped branching burrows in sandstone beds of sandstone/siltstone lithofacies of the Altuda Formation. D, vertical escape burrow in laminated, quartzose sandstone beds of the Altuda Formation. Camera lens cap is 5.5 cm in diameter.

are probably caused by fairly uniform grain size as well as by organic activity. The recessive nature of the sandstone/siltstone outcrops and the differential weathering of these beds also makes the recognition of burrows difficult.

This lithofacies contains small-scale graded bedding, dish structures, ball and pillow structures, cross-laminations, and convolute laminations (Figure 13-4A,B). Ball and pillow structures or pull-apart structures are restricted to medium-bedded sandstone. Figure 13-4C shows these structures associated with laminated siltstone interbedded with sandstone. The pillows are parallel to the bedding and display uniform thickness with rounded and tapering ends, and they are coated with thin (1–2 cm), brownish chert layers. The length of the pillows varies from 15–20 cm, whereas the width is uniformly 2–5 cm. Pillows assume spheroidal, nodular shapes downslope

within the same beds. Dish structures in some beds, which are barely visible on the surface, are 1–3 cm long, arc-shaped, and concave and have faint, dark lines that are irregularly stacked on top of each other. Convolute or contorted bedding and slump features (Bouma interval Tc) are typically associated with this lithofacies and are common to both lithologies. The axes of the slump folds are perpendicular to the dip directions of the beds. Small-scale cross-laminations are present in some beds.

SILTY, SPICULITIC DOLOMUD-WACKESTONE LITHOFACIES

This lithofacies constitutes about 35 percent of the Altuda Formation. The thickness of the beds varies from 10–40 cm. Vertical repetition of this lithofacies occurs in various

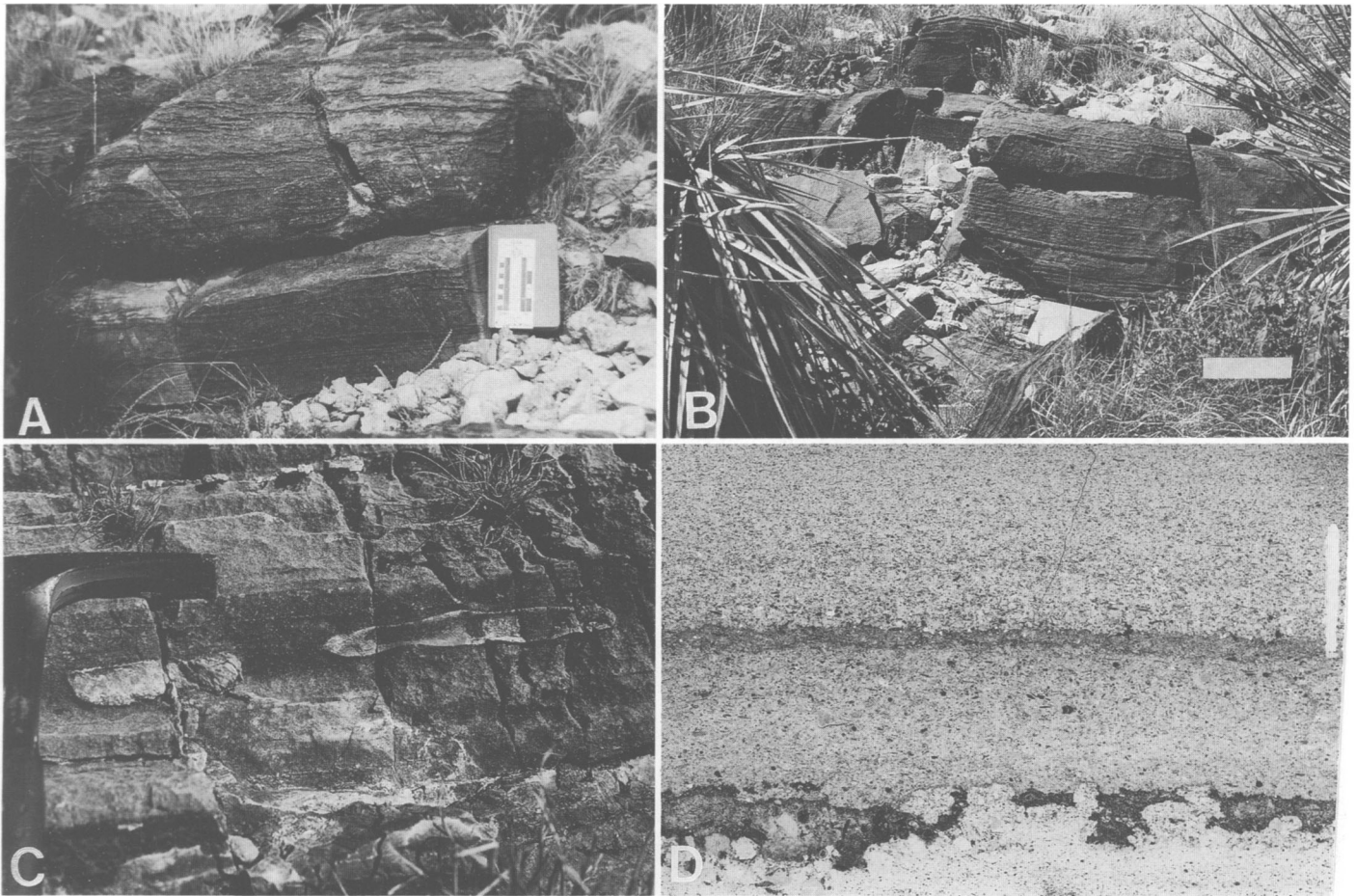


FIGURE 13-4.—A, sandstone/siltstone lithofacies of the Altuda Formation displaying planar laminations, wavy ripple laminations, and cross-laminations marked by chert layers. B, laminated, internally graded, sandstone beds of the Altuda Formation. Note chert accentuated penecontemporaneous slump deformation in the uppermost bed. Bar scale is 28 cm. C, ball and pillow structures in the Altuda Formation. D, thin section reversal print showing thin, alternating layers of bioclastic packstone and silty, spiculitic mud-wackestone. Note irregular chert stringers marking the contacts of the layers. Bar scale is 1 mm.

noncorrelatable intervals in the majority of the sections. The lithofacies shows planar contacts with the superjacent beds and is characterized by millimeter-scale internal laminations.

The siliciclastic content of the lithofacies varies from 10 percent to 30 percent and is represented predominantly by poorly sorted, angular to subrounded, monocrystalline and polycrystalline quartz and by chert fragments. Feldspar and mica constitute less than 5 percent of the siliciclastics in the rocks. The most abundant skeletal elements are calcareous and siliceous sponge spicules, generally monaxons. In 75 percent of the thin sections studied from this lithofacies, sponge spicules and quartz sand and silt, either laminated or unlaminated, mark the top of the graded bed. Other skeletal debris include worn, abraded, and partially to completely recrystallized or dolomitized grains of brachiopods, bryozoans, *Tubiphytes*, echinoderms, pelecypods, small foraminifers (uniserial and biserial), and ostracodes in varying proportions. In laminated beds, intrastratification of alternating thin (mm to few cm thick)

layers of skeletal wackestone, packstone, and silty dolomudstone is common (Figures 13-4D, 13-5). The irregular scoured contact of these layers is evident in thin section. It appears that each layer or set of layers was deposited from successive turbidity currents. The sequence is marked by numerous small scale (mm to cm) cyclic repetitions within a single bed, and these repetitions consistently occur in a majority of the beds. A complete Bouma sequence is not present in this lithofacies; however, Bouma intervals Ta, Tab, and Te commonly occur (Figure 13-6A).

Dolomitization varies from moderate to complete replacement and obliteration of depositional textures. The dolomite occurs from fine anhedral to subhedral crystals to a xenotopic mosaic including fabric selective to fabric destroying types of dolomitization. Chert occurs as micro-quartz, polycrystalline grains, nodules, thin wavy layers, and as partial to complete skeletal replacement.

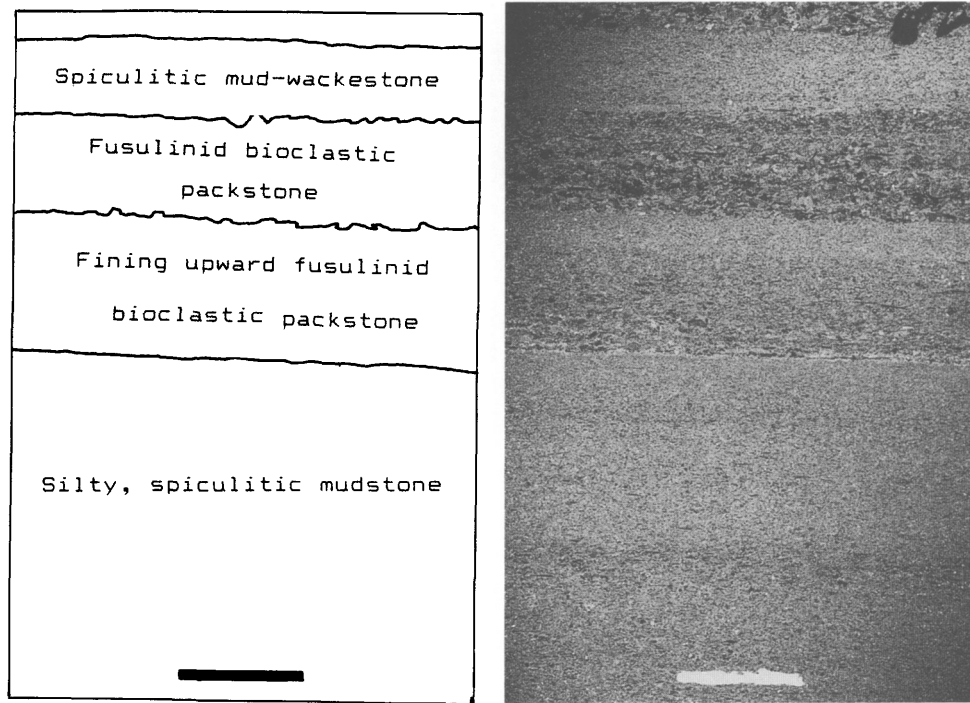


FIGURE 13-5.—Thin section reversal print and line drawing of intrastratified, silty mudstone and bioclastic packstone. Note the irregular, scoured contacts of the layers and the internal grading within each layer. The Bouma intervals shown are (bottom to top) Te, Tac, and Tab. Bar scale is 1 mm.

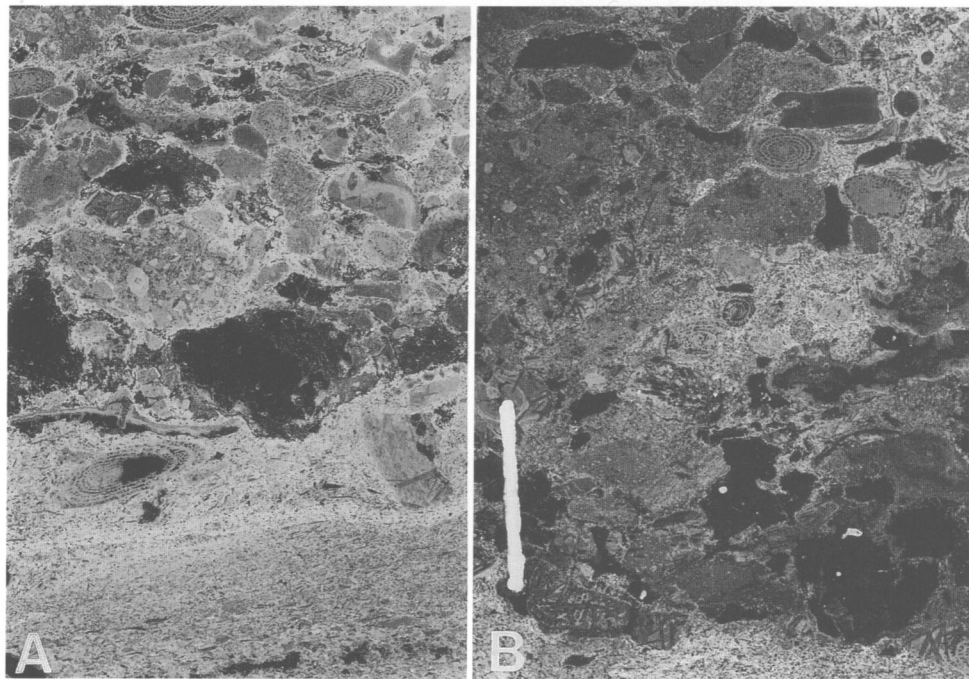


FIGURE 13-6.—A, thin section reversal print of silty, spiculitic dolomudstone grading upwards into mixed bioclastic, intraclastic packstone. The allochthonous nature of the allochems is evident from the worn and abraded condition of the clasts of a diverse fauna. Bar scale is 1 cm. B, thin section reversal print of laminated, graded, bioclastic packstone. Note silty spiculitic dolowackestone at the base (Te) grading upwards into cherty, microstylolitic, mixed bioclastic, intraclastic packstone (Ta). The allochems include *Tubiphytes*, *Archaeolithoporella*, fusulinid, intraclast, and sponge. Note the irregular, wavy contact between Bouma intervals Te and Ta and also the normal graded bedding. The bar scale is 0.8 cm.

The typical feature of these rocks is the presence of small circular to semicircular spar calcite-filled cavities. These cavities range from microscopic size to more than 4 cm in diameter (Figure 13-7A,B). Most cavities are lined by an iron oxide coating and are filled with uniform, large calcite crystals. Length-slow chalcedony representing partial to complete replacement is present in some cavities. These cavities are frequently associated with a completely dolomitized fabric in dolomudstone lithologies, but they are also present in rocks that show dolo-wackestone textures. These features are interpreted as relic evaporite fabrics that formed after the dissolution of anhydrite rosettes. The presence of length-slow chalcedony, the circular shape, and the lack of evidence suggesting the replacement of allochems favor this interpretation. The timing of the formation of these features is not known.

MIXED SKELETAL WACKESTONE/PACKSTONE LITHOFACIES

This lithofacies is characterized by thin to medium thick (4–20 cm) planar beds (Figure 13-7C). The thickness of this lithofacies ranges from 2–20 m. The lithofacies is present in all sections, although there is a general increase in thickness towards the basin in sections BR 3 and BR 4 (Figure 13-2). On weathered surfaces the rocks are light gray to olive gray. The skeletal elements are diverse and include brachiopods, bryozoans (fenestrate and ramose), foraminifers, *Tubiphytes*, *Archaeolithoporella*, echinoderms, pelecypods, ostracodes, ammonoids, trilobites, and calcareous and siliceous sponge spicules (Figures 13-6B, 13-7D, 13-8). Small foraminifers and fusulinids include *Richelina*, *Codonofusiella*, and *Rauserella*. Other allochems are represented by partly to completely

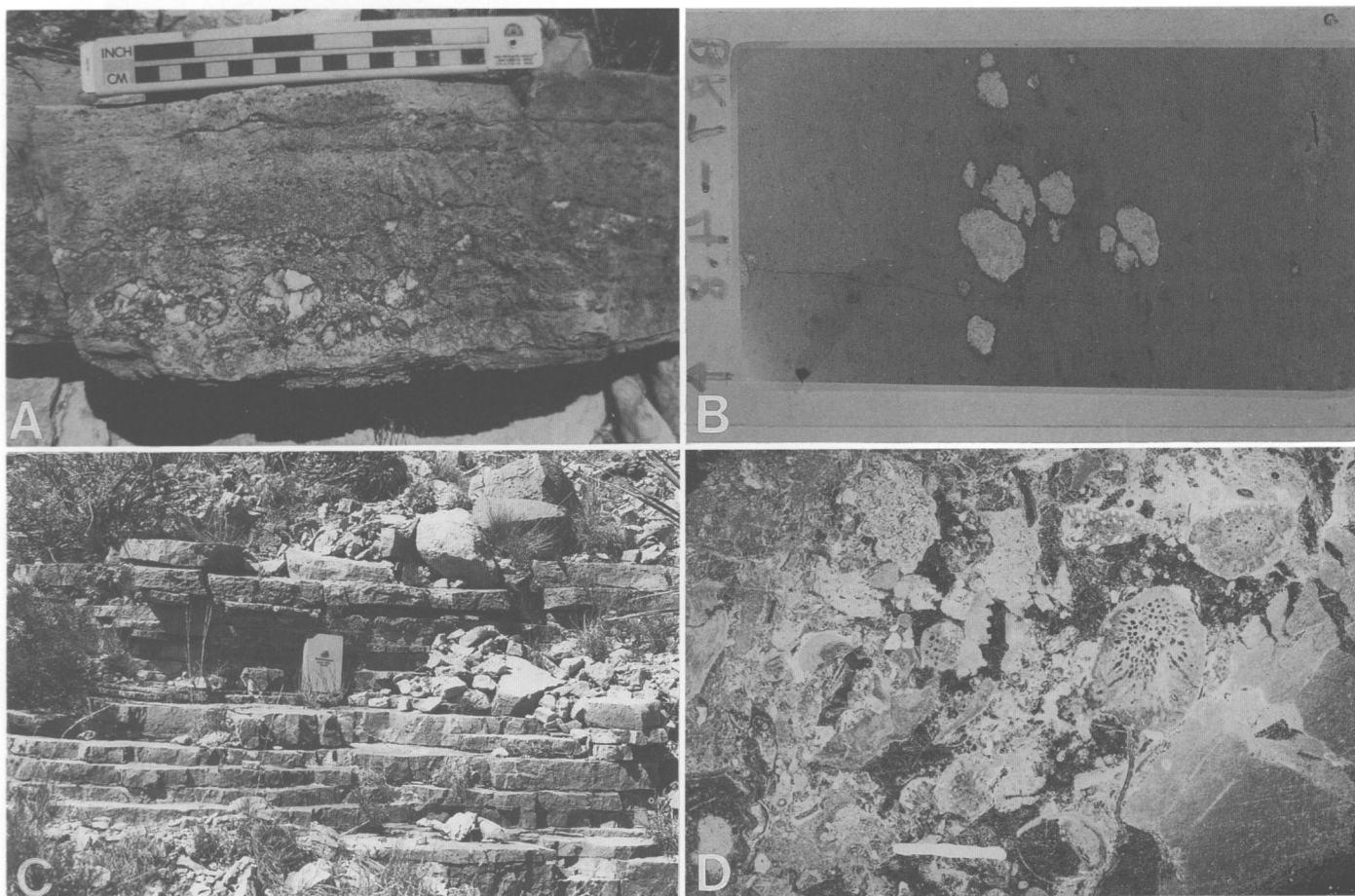


FIGURE 13-7.—A, small, circular to semicircular coarse spar-filled cavities interpreted as replaced anhydrite rosettes within the silty dolomud-wackestone lithofacies of the Altuda Formation. The rocks show vague laminations and lack fossils. B, thin section reversal print of replaced anhydrite rosettes. The rosettes are replaced by coarse sparry calcite with a thin coating of brownish chert. The width of the photo is 2.3 cm. C, laminated, planar-bedded, mixed bioclastic packstone of the Altuda Formation. The thickness of the beds varies from 2–15 cm. Notebook is 28 cm in length. D, thin section reversal print of mixed bioclastic packstone–floatstone. Note the large, worn and abraded skeletal grains of bryozoans, echinoderms, and brachiopods. Also visible is a fractured echinoderm in the lower right corner of the photograph. Bar scale is 1 cm.

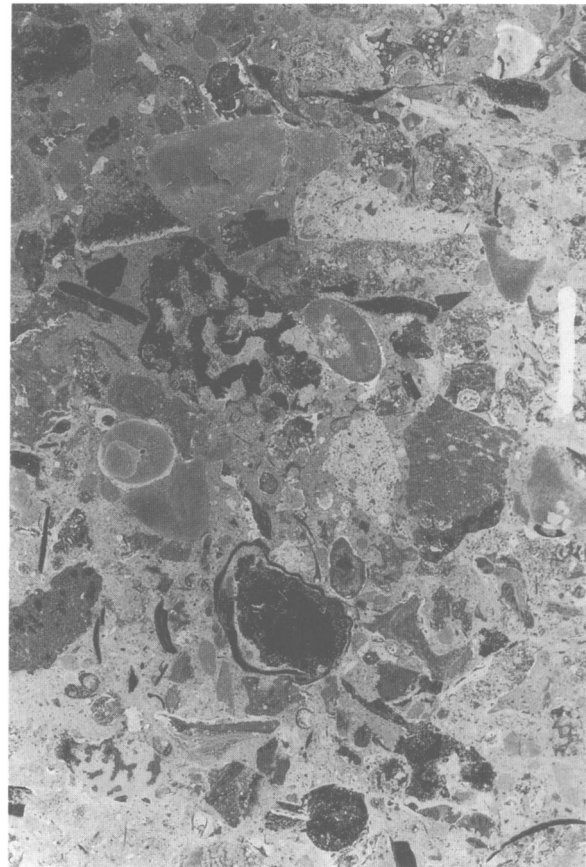
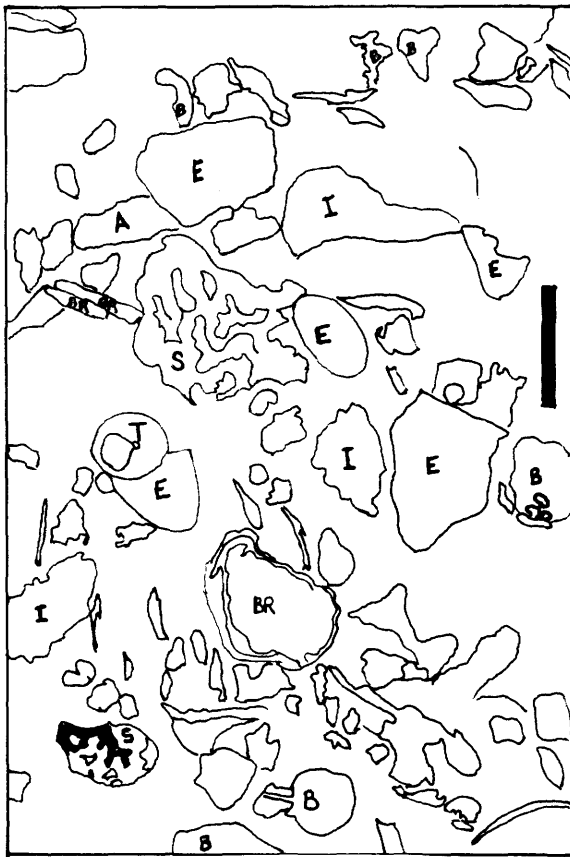


FIGURE 13-8.—Thin section reversal print of intraclastic, mixed bioclastic packstone–floatstone. The line drawing shows the whole shell of a brachiopod (BR), echinoderm fragments (E), sponge (S), bryozoans (B), *Tubiphytes* (T), *Archaeolithoporella* (A), and intraclast (I). Note micrite envelopes on the skeletal grains. Bar scale is 0.5 cm.

micritized skeletal elements and pellets. Intraclasts vary from a few millimeters to 3 cm and contain various combinations of allochems. They are common and most occur in the basal part of the graded beds. Skeletal elements typically show micrite rinds and are worn and abraded. The matrix of these rocks is predominantly lime-mud. Chert composed of microquartz, megaquartz, and cryptocrystalline quartz occurs as nodules, lenses, and layers. Silicification of skeletal elements is common to this lithofacies. Sparry calcite replacement and dolomitization of the allochems and matrix is present throughout the lithofacies.

The rocks are characterized by micrograding and intrastratification of alternating wackestone, packstone, and spiculitic mudstone layers. The sequence may be repeated 3 to 4 times in a single, thin bed (4 cm). The thickness of the intrastratified layers vary from a few millimeters to a few centimeters. The basal layer always shows a scoured, irregular contact. The rocks show Tab, Tabc, and Tad Bouma sequences. No complete Bouma sequence was observed.

Interpretations

The Altuda Formation has been studied in both the Del Norte Mountains and the northwestern Glass Mountains. In the Del Norte Mountains, it is interpreted as a marine tidal flat deposit marked by shallow subtidal to supratidal facies (Rudine, 1988; Wardlaw et al., 1990). In the northwestern Glass Mountains, south of the study area, Faliskie (1989) recognized three lithofacies and concluded that the Altuda Formation represents deposition in a transitional setting from lagoon on the middle shelf to foreslope of the platform.

In the Bengé Ranch area (Old Blue Mountain) of the Glass Mountains, the Altuda Formation exhibits transitional lateral facies relationships with shelf-edge reef facies of the Capitan Limestone. The Altuda is interpreted as successive turbidity current deposits in slope to basinal settings basinward of the Capitan shelf-edge because of its interfingering stratigraphic relationship with the Capitan Limestone and its depositional fabrics and sedimentary structures, which include planar

laminations, macro- and micro-grading, diverse allochthonous fauna, syndimentary deformation, and Bouma intervals. Except for the planar laminations, these features are not common where the Altuda has been interpreted to be a shallow-water deposit (see Wardlaw et al., 1990).

PLANAR LAMINATIONS

The rocks typically display fine millimeter-scale, planar laminations in all the lithofacies. Laminations occur in fine-grained siltstones, sandstones, and skeletal wackestone-packstone lithologies (Figures 13-9A,B, 13-10A, 13-11A,B). Laminae range from 1–4 cm in coarser rocks with abundant allochems, but they are only in the millimeter range in siltstone and dolomudstone. Fine-grained rocks contain size-graded couplets of siliciclastic/carbonate layers (Figure 13-10B). Some layers have a mixture of quartz silt and calcareous sponge spicules or parallel-bedding alignment of spicules (Figure 13-12A). Burrows are common to sandstones. Where the sandstone beds display surface tracks and trails, the underlying units are generally bioturbated and homogenized. Commonly, burrowing within the sandstone beds is not deep enough to affect the underlying layers. These layers contain undisturbed laminations that suggest partly stagnant, poorly oxygenated bottom conditions that lacked indigenous benthic fauna on the slope and basinal environments. Fluid escape structures (dish structures) also destroyed the depositional fabric, but they are

rare. Laminated intervals in the Altuda Formation represent Td and Te Bouma intervals and are interpreted as fall-out from turbidity currents.

MACRO- AND MICRO-GRADING

Graded bedding is the most common sedimentary structure in the Altuda Formation, amounting to about 70 percent of the formation. Graded beds or layers vary in thickness from a few millimeters to about 4 cm. The beds display normal grading, with coarse skeletal, lithoclastic, and intraclastic grains at the base of the bed, or layer, that grades upwards into finer grains. In the uppermost interval of the graded bed, fine silt is commonly mixed with calcareous and siliceous sponge spicules. The basal contact of the graded bed with the underlying layers is marked by a scoured, irregular, wavy surface truncating the sedimentary structures. In macro-graded beds the scoured contact is easily visible. In micro-graded layers where contacts are sharp, small-scale scoured contacts are present on a microscopic scale (Figure 13-13A,B). Most units have thin chert layers, silicified skeletal fragments, or thin dolomitized and silicified layers marking the boundary between beds.

The ratios of skeletal elements, lithoclasts, and intraclasts varies among lithofacies. Some dolomitic rocks have their textural details completely obliterated, so graded intervals cannot be ascertained. Where skeletal elements are selectively

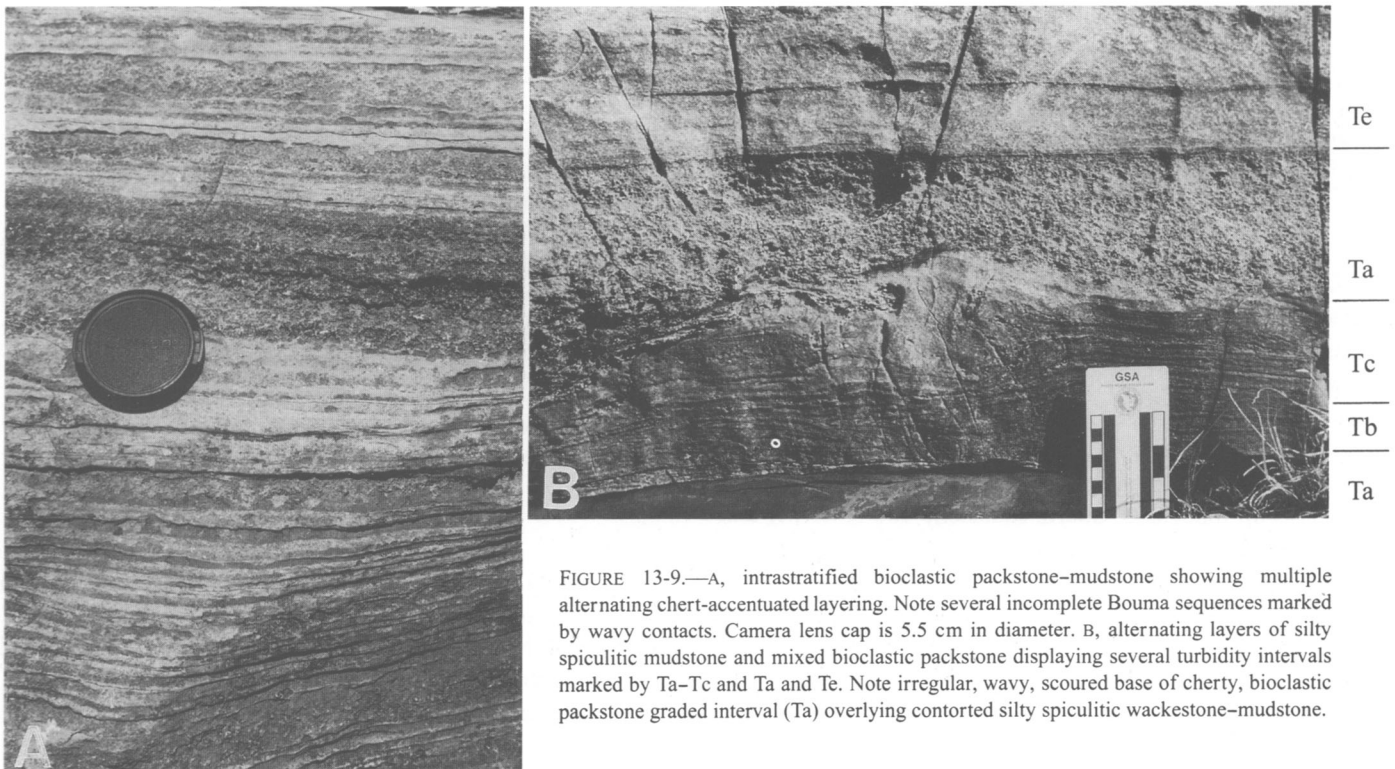


FIGURE 13-9.—A, intrastratified bioclastic packstone-mudstone showing multiple alternating chert-accentuated layering. Note several incomplete Bouma sequences marked by wavy contacts. Camera lens cap is 5.5 cm in diameter. B, alternating layers of silty spiculitic mudstone and mixed bioclastic packstone displaying several turbidity intervals marked by Ta–Tc and Ta and Te. Note irregular, wavy, scoured base of cherty, bioclastic packstone graded interval (Ta) overlying contorted silty spiculitic wackestone-mudstone.

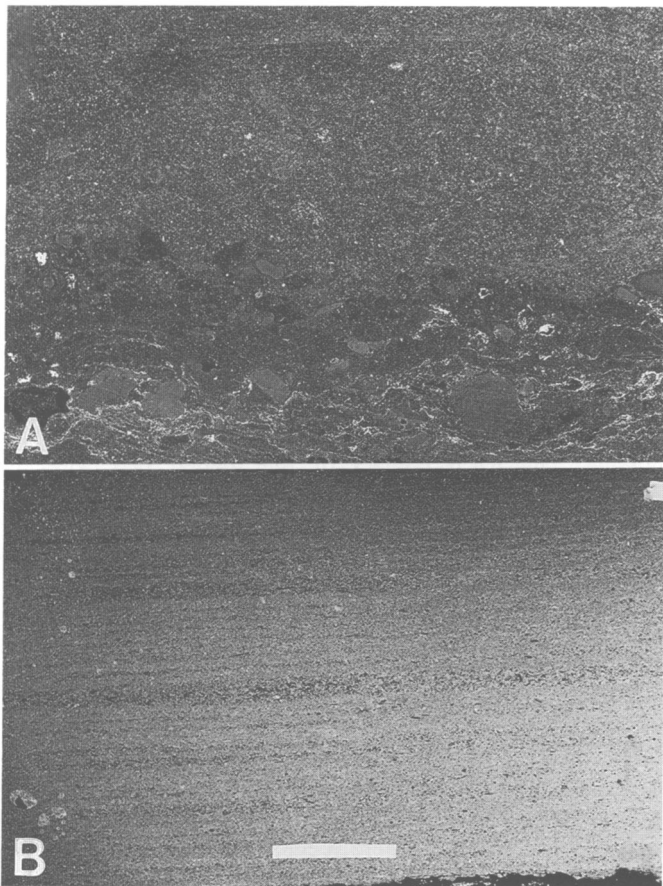


FIGURE 13-10.—A, thin section reversal print of cherty, bioclastic packstone grading upwards into silty, fine dolomudstone. Note the irregular, scoured contact between Bouma Ta and Te. The long axis of the photograph is 3.5 cm. B, thin section reversal print of spiculitic mudstone-wackestone (dark layers) alternating with silty dolomudstone. The dominant allochems in wackestone layers are siliceous sponge spicules (monaxons), calcispheres, and possibly radiolarians. Note planar lamination caused by the alignment of the spicules.

silicified, grading is visible even in a dolomudstone matrix. Coarse lags in the graded beds are represented by grains of skeletal elements, intraclasts, and lithoclasts. Skeletal elements include brachiopods, bryozoans, echinoderms, *Tubiphytes*, *Archaeolithoporella*, fusulinids, ostracodes, pelecypods, and sponges and sponge spicules. Intraclasts contain peloidal, skeletal wackestone to packstone textures. Lithoclasts include angular rip-up mudclasts, quartz sandstone and siltstone, and chert fragments.

DIVERSE ALLOCHTHONOUS FAUNA

The Altuda Formation is characterized by a wide diversity of imported biogenic components, which indicates the skeletal

elements were transported from various environments. The mixed skeletal elements include fusulinids, *Tubiphytes*, *Archaeolithoporella*, echinoderms, brachiopods, bryozoans, trilobites, sponges and sponge spicules, ostracodes, pelecypods, corals, and ammonoids (Figures 13-12B,C, 13-13B-D). A shallow-water origin of the skeletal elements is indicated by the fusulinids and alga mixed with peloidal grains, the micrite rinds on most skeletal elements, and the boring of skeletal grains. The allochthonous origin of the allochems is evident from the worn, abraded, fractured, and disarticulated nature of the skeletal grains.

Lime-mud formed the matrix of the carbonate dominated lithofacies. This lime-mud is believed to have originated by the disintegration of organisms and by biochemically induced precipitation in shallow waters (<30 m deep). As pointed out by Wilson (1969), mud can be washed down into deeper waters just as easily as it is carried landwards into the tidal flats. The lime-mud in the Altuda Formation likewise was transported from the shallow-water shelf areas to slope and basinal environments.

SYNSEDIMENTARY DEFORMATION

Synsedimentary depositional features of the Altuda Formation include slump structures, flame structures, and convolute laminations or bedding. These features are typically associated with slope and basinal environments. The slump and convolute structures occur predominantly in the sandstone/siltstone lithofacies, but they are also present in other facies (Figure 13-12D). Flame structures are associated with intrastratified carbonate/clastic rocks, as they developed under fluidized flow where stringers of water-saturated sediments were injected into overlying layers under loading pressure.

BOUMA INTERVALS.—The Altuda Formation characteristically displays Bouma turbidity intervals in carbonates and terrigenous clastic lithologies. As pointed out by Thomson and Thomasson (1969:74), a complete Bouma sequence is rare in carbonate rocks; rather, various types of partial or incomplete sequences are the rule. The Bouma intervals recognized in the Altuda lithofacies include, Tab, Tabc, and Tde. Among these intervals, Tab and Tde are the most common type of turbidity intervals, as they are present in 70 percent of the lithofacies. The thickness of a single Bouma interval in the Altuda Formation varies from 2–20 cm.

Acknowledgements

This study is based on one of the author's (Mohammad Haneef) masters thesis research at Sul Ross State University. Funding for this study was provided by an AAPG Grant-in-Aid to Mohammad Haneef and an American Chemical Society, Petroleum Research Fund (Grant # 22216-ACS) to David Rohr.

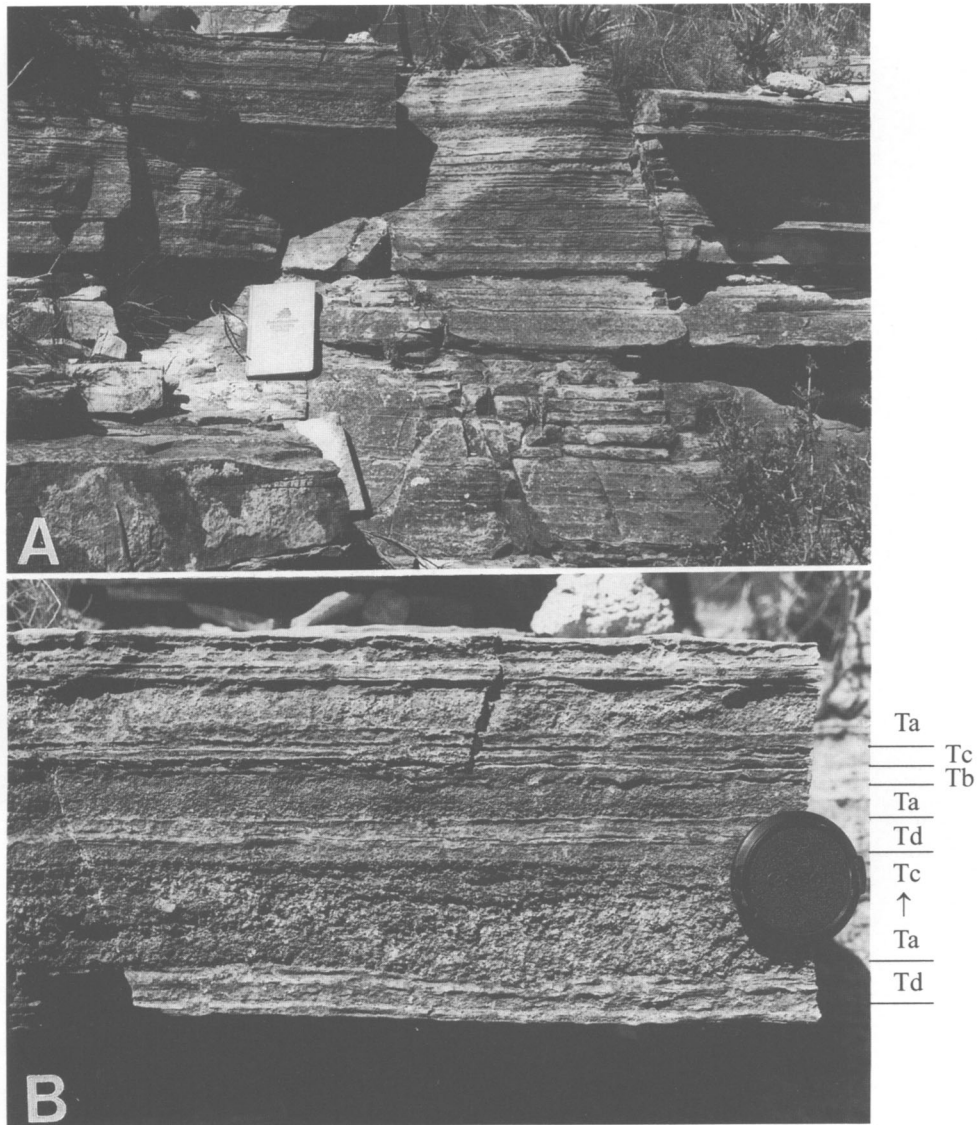


FIGURE 13-11.—A, planar laminated, thin, evenly bedded, internally graded, intrastratified, bioclastic packstone-mudstone turbidites of the Altuda Formation. Field notebook is 28 cm in length. B, close-up of the uppermost bed in A. Note bed displays alternating multiple layers of bioclastic packstone and laminated siliciclastic, spiculitic mudstone-wackestone. The bioclastic packstone layers have an irregular scoured contact with the underlying layers and are composed of shelf and shelf-edge derived, allochthonous, diverse fauna. The beds display multiple turbidity intervals labelled Tac, Td, and Tabc. The camera lens cap is 5.5 cm in diameter.

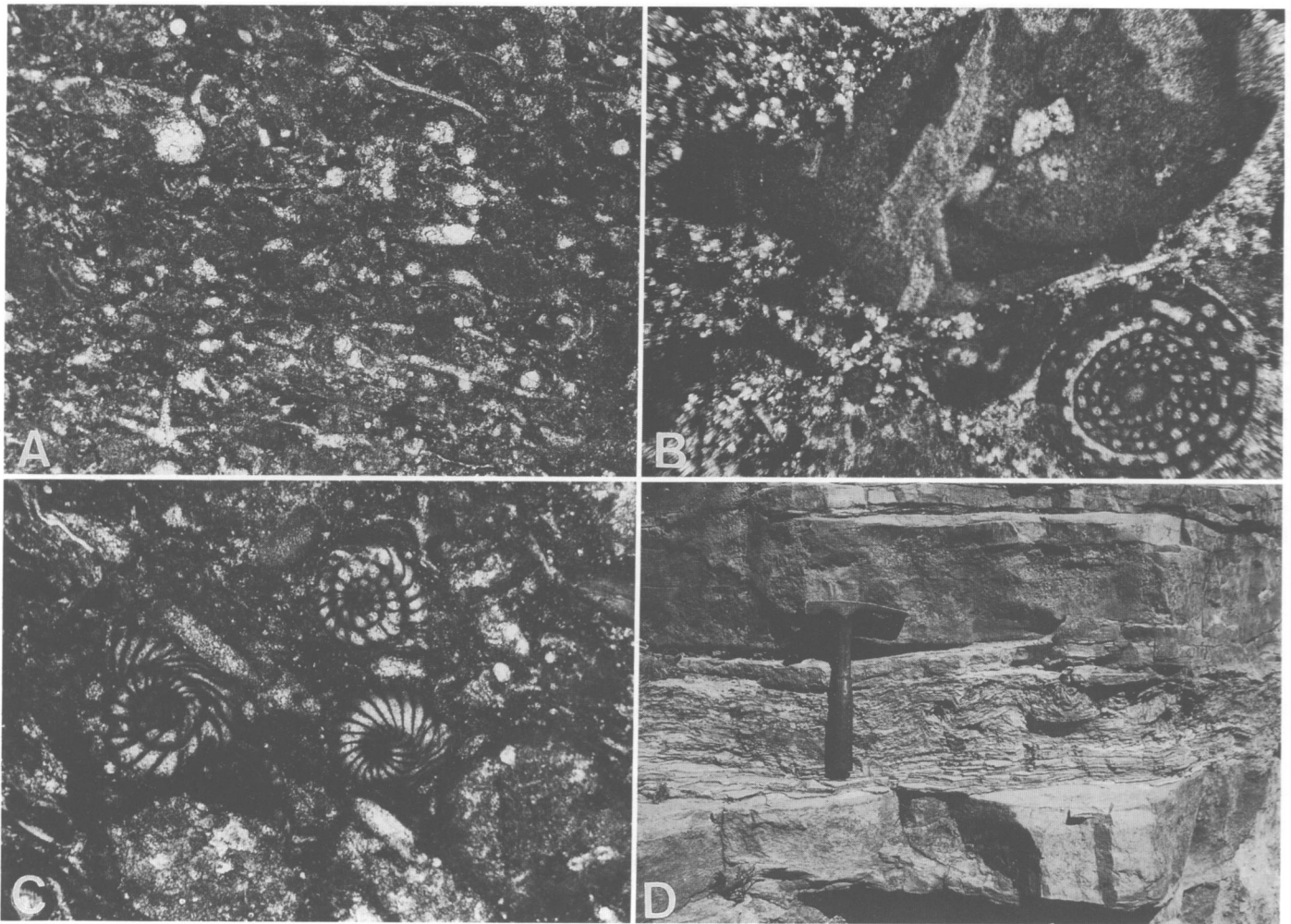


FIGURE 13-12.—A, photomicrograph of silty, spiculitic mudstone-wackestone. Note the calcareous sponge spicules (monaxons and triaxons) and calcispheres in a silty dolomudstone matrix. Width of the photo equals 1 mm. B, photomicrograph of silty bioclastic packstone showing *Tubiphytes*, fusulinids, and peloids in a lime mudstone matrix. Field of view is 2 mm. C, photomicrograph showing fusulinids (*Richelina*) in the bioclastic packstone lithofacies. These fusulinids are common throughout the Altuda Formation. Field of view is 2 mm. D, contorted bedding (Bouma Tc) in thinly bedded sandstone/siltstone lithofacies of the Altuda Formation. Note truncation of the top of the contorted bed.

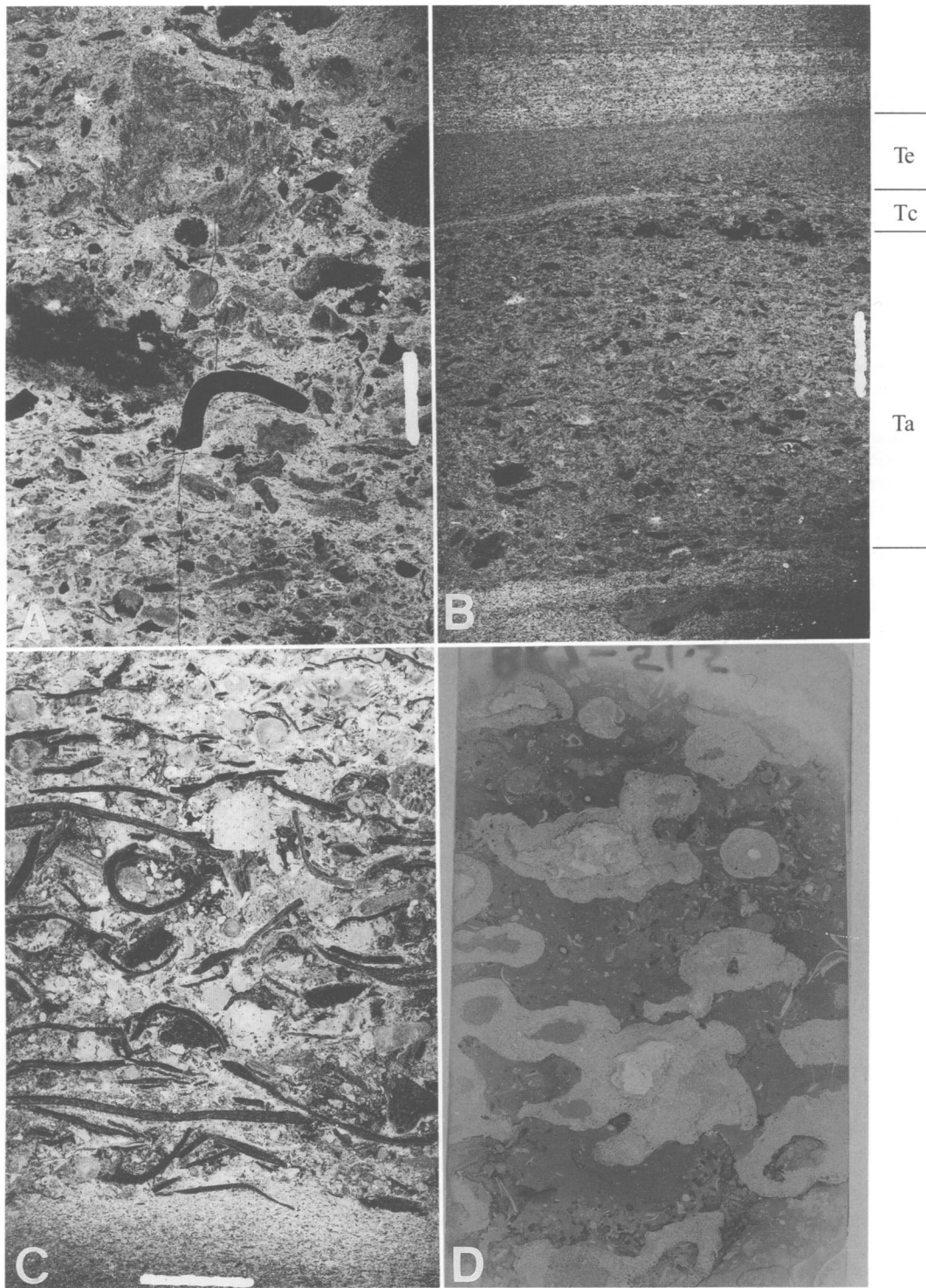


FIGURE 13-13.—A, thin section reversal print of cherty, intraclastic, bioclastic packstone. The dark allochem in the center is a mollusk shell fragment. Bar scale is 1 cm. B, thin section reversal print of bioclastic wackestone—packstone grading upwards into finely laminated spiculitic wackestone. Bouma intervals present are a graded layer with a scoured base (Ta), Tc, and Te. Bar scale is 0.5 cm. C, thin section reversal print of a mixed bioclastic packstone. Note the parallel alignment of brachiopods. Bar scale is 1 mm. D, thin section reversal print of reworked allochthonous skeletal grains of calcareous sponges in the graded bed of mixed bioclastic packstone. The rock is composed of the skeletal debris of brachiopods, bryozoans, echinoderms, small foraminifers, and sponge spicules. The bed grades upwards into finely laminated, silty spiculitic mudstone. Field of view is 2.3 cm.

Literature Cited

- Faliskie, R.A.
 1989. Depositional Environments of the Vidrio Member of the Word, Altuda, and Capitan Formations (Upper Permian) in the Northwestern Glass Mountains, West Texas. 100 pages. Unpublished master's thesis, Sul Ross State University, Alpine, Texas.
- King, P.B.
 1931 ("1930"). The Geology of the Glass Mountains, Texas, Part I: Descriptive Geology. *University of Texas Bulletin*, 3038: 167 pages, 15 plates. [Date on title page is 1930; actually published in 1931.]
- Rudine, S.F.
 1988. Geology and Depositional Environments of the Permian Rocks, Northern Del Norte Mountains, Brewster County, Texas. 186 pages. Unpublished master's thesis, Sul Ross State University, Alpine, Texas.
- Rudine, S.F., B.R. Wardlaw, D.M. Rohr, R.A. Davis, and R.E. Grant
 1987. Depositional Setting of the Late Leonardian–Wordian (Permian) Rocks, Southern Margin, Permian Basin: Basin or Lagoon? [Abstract.] *Geological Society of America, Abstracts with Programs*, 19(7):826.
- Rudine, S.F., R.A. Faliskie, D.M. Rohr, and B.R. Wardlaw
 1988. Major Unconformity Defines Wordian–Capitan Boundary (Upper Permian) in Glass and Del Norte Mountains, Texas. [Abstract.] *Geological Society of America, Abstracts with Programs*, 20: A122–A123.
- Thomson, A.F., and M.R. Thomasson
 1969. Shallow to Deep Water Facies Development in the Dimple Limestone (Lower Pennsylvanian), Marathon Region, Texas. In G.M. Friedman, editor, *Depositional Environments in Carbonate Rocks*. *Society of Economic Paleontologists and Mineralogists, Special Publication*, 14:57–78.
- Wardlaw, B.R.
 1987. Leonardian–Wordian (Permian) Conodont Biostratigraphy of the Del Norte and Glass Mountains, West Texas. [Abstract.] *Geological Society of America, South Central Section, Abstracts with Program*, 19(7):180.
 2000. Guadalupian Conodont Biostratigraphy of the Glass and Del Norte Mountains. In B.R. Wardlaw, R.E. Grant, and D.M. Rohr, editors, *The Guadalupian Symposium. Smithsonian Contributions to the Earth Sciences*, 32:37–87, 3 figures, 12 plates, 1 table.
- Wardlaw, B.R., R.A. Davis, D.M. Rohr, and R.E. Grant
 1990. Leonardian–Wordian (Permian) Deposition in the Northern Del Norte Mountains, West Texas. *United States Geological Survey Bulletin*, 1881-A:A1–A14.
- Wardlaw, B.R., and S.F. Rudine
 2000. The Altuda Formation of the Glass and Del Norte Mountains. In B.R. Wardlaw, R.E. Grant, and D.M. Rohr, editors, *The Guadalupian Symposium. Smithsonian Contributions to the Earth Sciences*, 32:313–318, 4 figures.
- Wilde, G.L., and S.F. Rudine
 2000. Late Guadalupian Biostratigraphy and Fusulinid Faunas, Altuda Formation, Brewster County, Texas. In B.R. Wardlaw, R.E. Grant, and D.M. Rohr, editors, *The Guadalupian Symposium. Smithsonian Contributions to the Earth Sciences*, 32:343–371, 3 figures, 9 plates.
- Wilson, J.L.
 1969. Microfacies and Sedimentary Structures in "Deeper Water" Lime Mudstones. In G.M. Friedman, editor, *Depositional Environments in Carbonate Rocks: A Symposium. Society of Economic Paleontologists and Mineralogists, Special Publication*, 14:4–19, plates 1, 2.

14. Anatomy and Origin of Capitan Limestone Foreset Beds in the Glass Mountains, West Texas

Mohammad Haneef

ABSTRACT

Foreset beds found in the Capitan Limestone in the Glass Mountains are clinoforms of basinward dipping, massive, partially to completely dolomitized beds that interfinger with the slope and basinal facies of the time-equivalent Altuda Formation. The foreset beds represent deposition of reef and backreef derived, allochthonous sediments shed off of the Capitan shelf-edge in shelf-to-basin slope transition. On the basis of lithology, texture, and bedforms various subaqueous gravity flow processes are recognized, including debris flow, grain flow, and submarine slide and slump blocks. High energy conditions along with sea-level fluctuations on the Capitan shelf-edge produced carbonate debris that moved under the influence of gravity and was deposited on the foreslope as multiple debris sheets.

Introduction

The Capitanian stratigraphic sequence in the Glass Mountains is represented by the Gilliam Limestone, the Capitan Limestone, and the Altuda Formation in a shelf-to-basin transition (Haneef et al., 1991). The Capitan Limestone crops out in a narrow, laterally discontinuous carbonate belt along the rim of the Delaware basin (Pray, 1989). Along the entire extent of exposure, only the Guadalupe Mountains, at the northwestern shelf of the Delaware basin, have been the focus of extensive sedimentological studies in the past six decades. In the Glass Mountains, the Capitan Limestone fringes the southern shelf of the Delaware basin and has largely been ignored. Most of the previous work in the Glass Mountains dealt with stratigraphic and biostratigraphic relationships.

Mohammad Haneef, Geology Department, Sul Ross State University, Alpine, Texas 79832.

Emerging from the Capitan Limestone (late Guadalupian) are clinoforms of steeply dipping, massive beds that extend downslope and interfinger with the gently inclined Altuda beds (Figure 14-1). King (1931) noticed this peculiar feature along the east face of Old Blue Mountain, which he referred to as upper massive (Capitan) foreset beds. The purpose of the present study is to document the nature and origin of these beds on Old Blue Mountain in the Glass Mountains (Figure 14-2).

Field Relations

The Capitan foreset beds are light to dark gray to olive in color on weathered surfaces and white to cream in color on fresh surfaces. In outcrop, the majority of the beds are fractured and jointed and are marked by honeycombed weathering and wavy, nonsutured to sutured microstylolites with brownish iron residue seams. Most of the fractures are irregular and are filled with coarse spary calcite. The beds are hard, resistant, and massive with obscure bedding. They contain irregular vuggy porosity, coarse spar-filled cavities, brownish chert layers/lenses or isolated pods, and partially to completely recrystallized internal fabric, and they are sparsely bioclastic. Lithoclasts and intraclasts of various shapes, sizes, and compositions are present in the majority of the foresets but are difficult to recognize on weathered surfaces because of the chaotic internal structure and dolomitized fabric. The foresets typically weather to large irregular to semicircular blocks that litter the lower slopes around the mountain.

The foreset beds typically form resistant ledges and can be differentiated from the recessive, slope-forming, bedded Altuda Formation in which they occur. The foreset beds display a variety of bedforms, including irregular (hummocky), wavy, channelized, and planar bedding surfaces (Figure 14-3A-C). The thickness range of the foreset beds is from a few centimeters to more than eight meters. The beds display pinch and swell bedforms and generally exhibit a decrease in

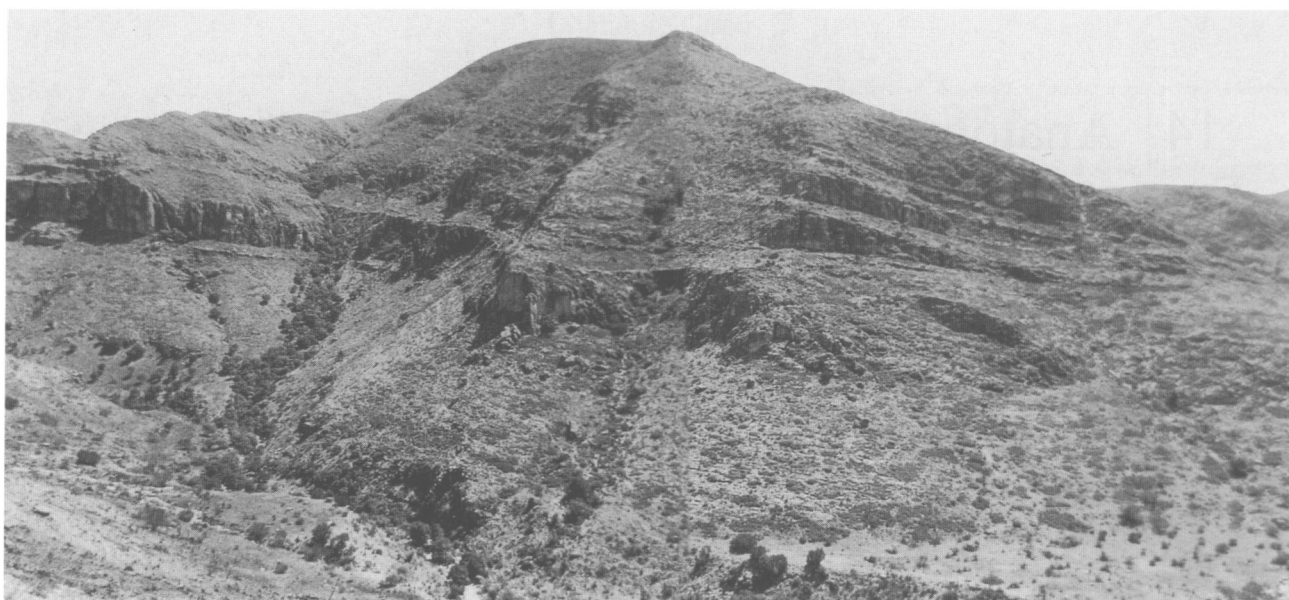


FIGURE 14-1.—Panoramic view of the east face of Old Blue Mountain on the Parker Ranch. The Capitan Limestone is represented by massive, resistant beds at the top. The recessive weathering profile is the Altuda Formation. Note the eastward-dipping, thick, massive, wedge-shaped foreset beds interfingering with the Altuda Formation.

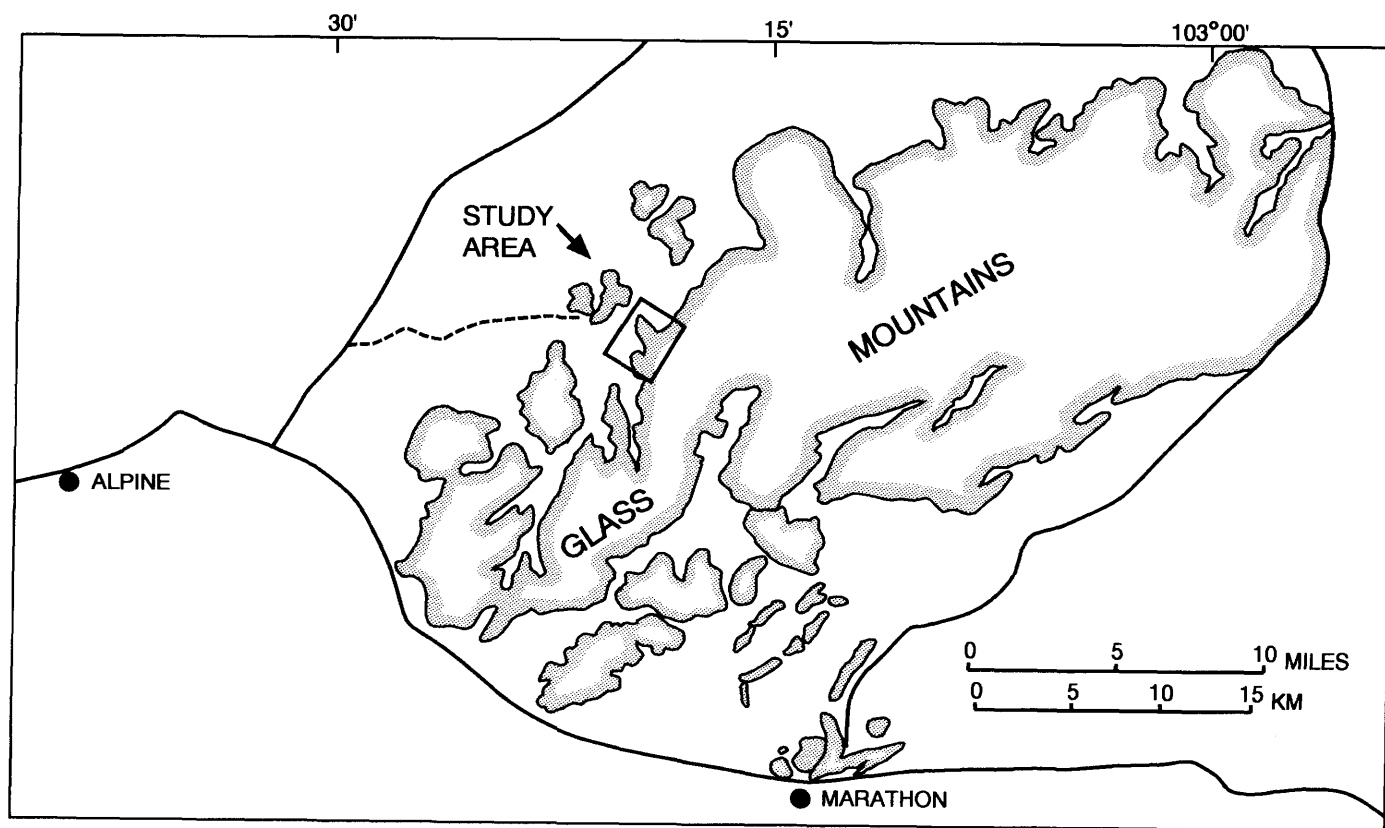


FIGURE 14-2.—Map of the Glass Mountains region with the study area indicated.

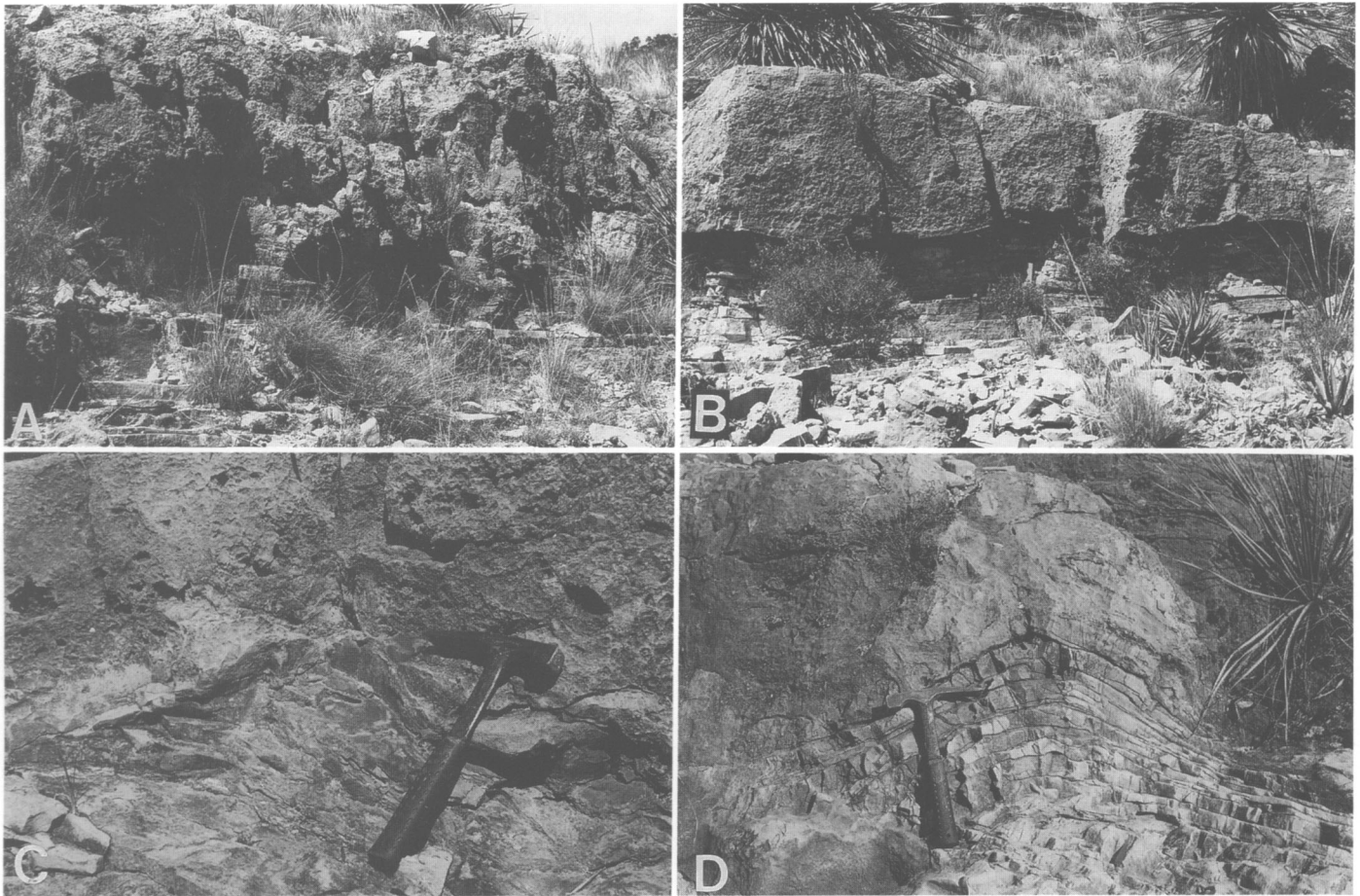


FIGURE 14-3.—A, view of a jointed and complexly fractured massive foreset bed with an undulatory base and top. The massive bed is vuggy, lithoclastic, sparsely bioclastic, dolo-floatstone. It is characterized by large (centimeter size), irregular coarse spar-filled cavities/fractures and brownish chert nodules. The planar beds beneath the foreset are silty spiculitic dolomudstone of the Altuda Formation. Field notebook is 18 centimeters in length. B, view of vuggy, recrystallized skeletal dolomudstone/wackestone beds of the Capitan foreset. The lower contact of the foreset bed is wavy (hummocky) with the thin-bedded Altuda Formation. Note truncation of beds near the hammer (length 28.5 cm). The foresets exhibit a downslope decrease in thickness and die out within a short distance. C, view of the irregular base of a Capitan foreset beds. The foreset bed displays pinch and swell bedforms. Note the abrupt truncation of the underlying thin, graded beds of the Altuda Formation. D, view of the symmetrical folding in thin-bedded Altuda that is formed by the drag created by the overriding debris flow bed of the Capitan foreset. Also visible are recumbent folds outlined by brownish cherty layers within the massive, matrix-supported foreset bed.

thickness along dip and die out within a few kilometers down dip. The massive beds also display variation in depositional dip from a low angle (8° – 10°) in the upper reaches of the outcrop where they seem to emerge, to as steep as 25° in the lower slopes of the outcrop at the termination of the beds. The beds below the foreset beds are characterized by planar, abruptly truncated, drag-folded contact relationships (Figure 14-3D). At places, these beds are marked by the squeezing upwards (injection) of Altuda beds into the massive foreset beds (Figure 14-4) and by ball and pillow structures (Figure 14-5A,B).

Lithological Characteristics

In the study area more than 10 foreset beds occur within the Altuda Formation, although only five of these foresets are mappable and can be traced laterally. Detailed field observations, petrographic examinations of polished slabs, and thin sections of the foreset beds reveal a wide spectrum of lithologies, textures, and fabric variations with genetic implications. The variation in sedimentary parameters has a bearing on the mode and mechanism of transportation, paleotopography, and source, which can be explained in terms of the sedimentary



FIGURE 14-4.—View of a sedimentary dike formed by the squeezing up (injection) of thin-bedded Altuda sandstone beds into the Capitan debris foreset. The foreset is interpreted as a grain flow deposit.

processes and then related to environments of deposition. The following lithological and fabric types are recognized in the foreset beds.

MATRIX SUPPORTED DOLO-BRECCIA.—The matrix as well as the clast lithology of these beds is predominantly dolomudstone (Figure 14-5C). The clasts range in size from a few millimeters to more than three centimeters. The shape of the clasts varies from irregular sharp edged to subangular. The

clasts are composed of fine dolomudstone with rare siltstone, sandstone, chert, and micritized bioclasts. Angular, fine, quartz silt occurs scattered in the dolomudstone matrix. In some cases, localized disruption and brecciation of the original bedding can be inferred on the basis of the similarity of clast lithology and parallel orientation. The rocks display irregular fractures and solution vugs filled with clear, coarse cavity-filling sparry calcite. Microstylolitic seams mark the boundaries of the grains. The clast to matrix ratio of these beds is generally 3 : 1.

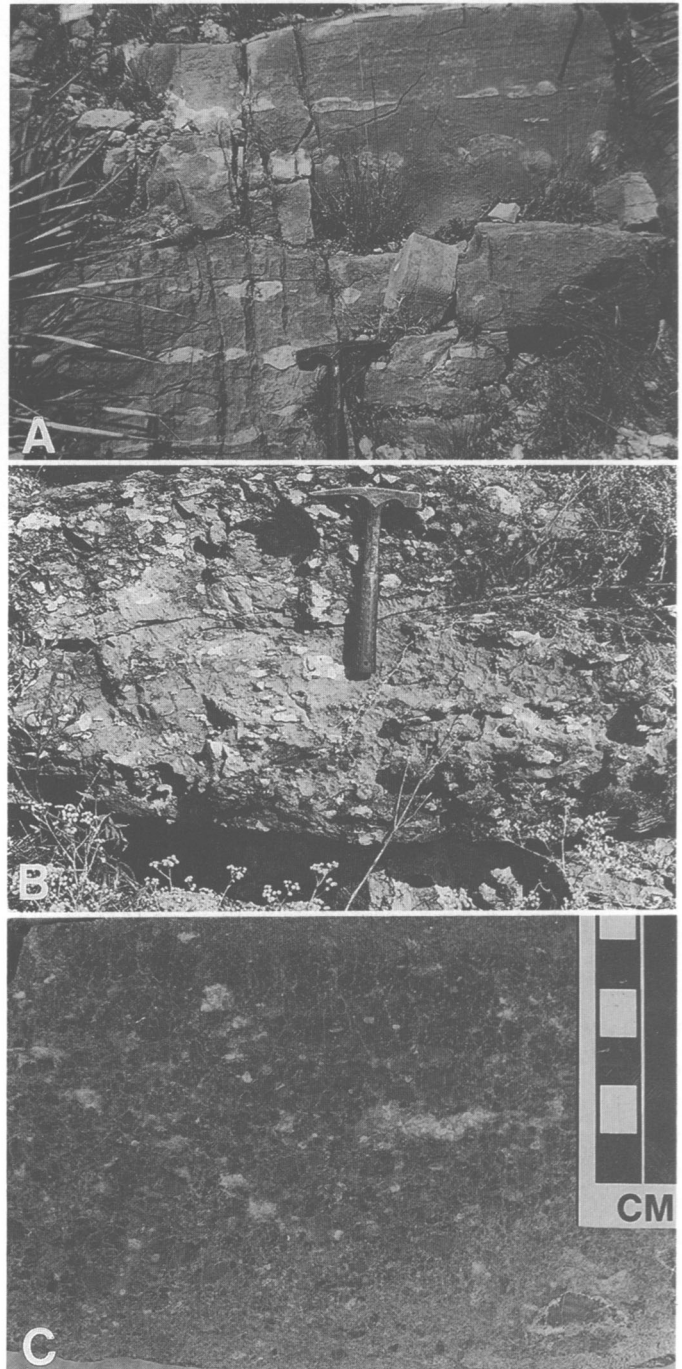


FIGURE 14-5 (right).—A, view of ball and pillow structures within matrix-supported, sandy debris flow beds of the Capitan foreset. The parallel alignment of the subrounded sandstone clasts indicates a pull-apart structure as the result of the compaction of a modified gravity flow. B, view of the same foreset bed about 100 meters down slope exhibiting nodular fabric. The clasts are subrounded to rounded and include chert-coated sandstone clasts, large silicified sponges, and chert nodules. The foreset bed does not show any appreciable decrease in thickness. Apparently the gravity flow began as a matrix-supported debris flow and changed into a grain flow down slope. C, polished slab of a 1 m thick foreset bed. Note the monomict clast lithology represented by the resedimented clasts of dolomudstone and dolowackestone. Note the poorly sorted, subangular to subrounded clasts with rare echinoderm fragments. The foreset displays grain flow to debris flow fabric, which indicates multiple episodic deposition of material derived from the shelf and shelf-edge.

CLAST-SUPPORTED, LITHOCLASTIC, BIOCLASTIC FLOATSTONE.—This lithology is represented by angular to sub-rounded clasts exhibiting a mixture of rectangular, tabular, elongate, and irregular shapes. The clast lithologies include dolomudstone, intraclasts and lithoclasts of siltstone, silty spiculitic dolomudstone, and detrital chert fragments (Figure 14-6). The matrix of these beds is dolomudstone with quartz silt, fine sand, and micritized skeletal debris. The bioclasts are represented by brachiopods, bryozoans, echinoderms, *Archaeolithoporella* sp., *Tubiphytes*, dasycladacean algae, and sponge spicules. The rocks display a variety of internal structures varying from chaotic to faint normal to reverse grading. The upper and lower contacts with the Altuda beds vary from planar, irregular, wavy, and undulatory to channelized (Figures 14-7A,B, 14-8A). The truncation of, and the injection into, the underlying Altuda sandstone and siltstone beds is visible in some beds.

LITHOCLASTIC, INTRACLASTIC, BIOCLASTIC RUDSTONE.—The foresets characterized by rudstone texture are dominantly clast-supported with a clast to matrix ratio of 6 : 1. The matrix is lime-mud with varying admixtures of quartz silt, fine sand, skeletal debris, and chert fragments. Irregular microstylolite swarms are abundant and exhibit compacted fabric (fitted lens response of Wanless, 1979). The clasts are marked by irregular interpenetrating stylolitic grain boundaries. Dolomite rhombs and brownish iron oxide residue occur along the stylolitic boundaries. The irregular, nonparallel orientation of the stylolites indicate compacted grain fabric. These beds are characterized by large clast sizes, generally in the centimeter range. The lithology is dominated by broken and whole shells of brachiopods and bivalves. Other bioclasts include sponges, echinoderms, encrusting algae, *Tubiphytes*, *Archaeolithoporella* sp., sponge spicules, solitary corals, and foramanifers. Chert occurs as replaced bioclasts, cavity fill, and nodules. The intraclasts are subround to round in shape and contain bivalves and peloids in a lime mudstone-dolomudstone matrix. The lithoclasts (rip-up, noncarbonate clasts) constitute 10 percent to 15 percent of the rudstone fabric and are represented by laminated siltstone, spiculitic siltstone, and nonfossiliferous sandstone clasts (Figure 14-8B,C). A preferred orientation of the clasts is not evident. The beds are characterized by chaotic to crude normal to reverse graded bedding.

RECRYSTALLIZED, DOLOMUDSTONE/WACKESTONE.—The recrystallized dolomudstone/wackestone lithology represents

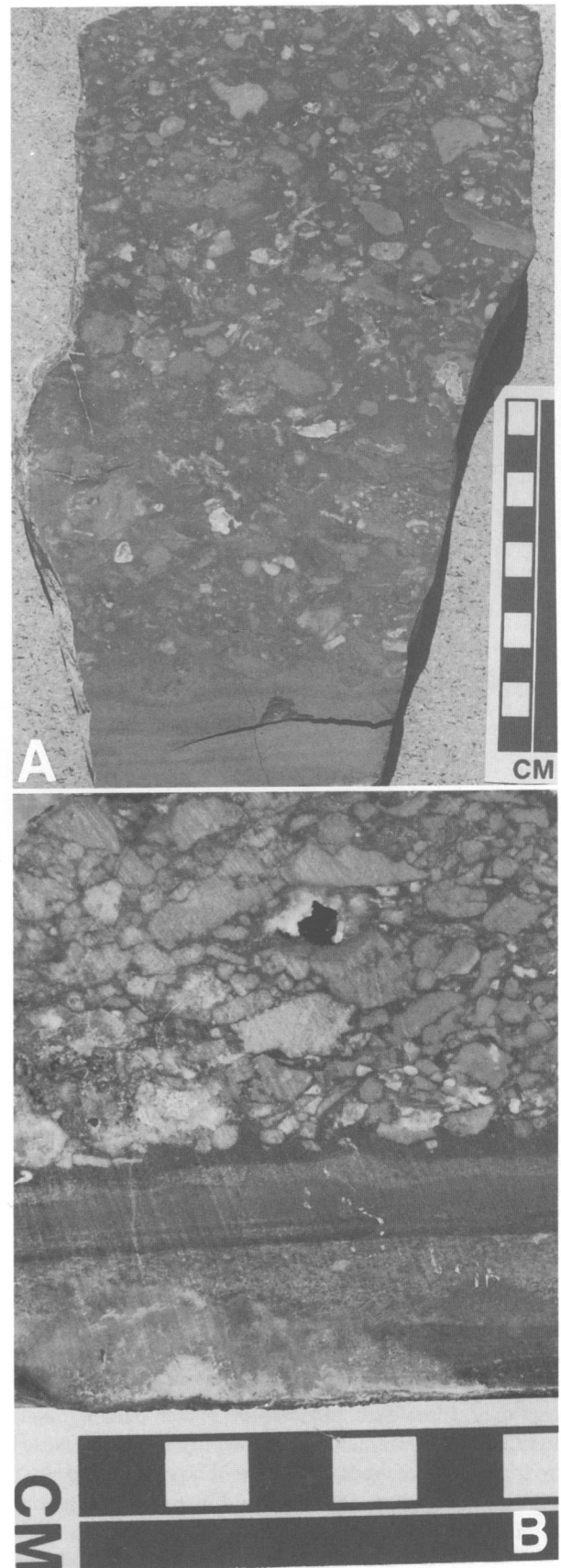


FIGURE 14-6 (right).—A,B, polished slabs of the Capitan foreset displaying clast-supported fabric interpreted as a grain flow deposit. The grain flow bed has an irregular (scoured) contact with the laminated spiculitic mudstone-wackestone beds of the Altuda slope facies. The clasts are represented by intraclasts, lithoclasts of siltstone and sandstone, and bioclasts of echinoderms, solitary corals, fenestrate bryozoans, dasycladacean algae, *Tubiphytes*, *Archaeolithoporella* sp., and disarticulated bivalves. The foreset bed is poorly sorted and exhibits clast-size variation from a few millimeters to more than four centimeters. Note the reverse grading and slight alignment of the clasts.

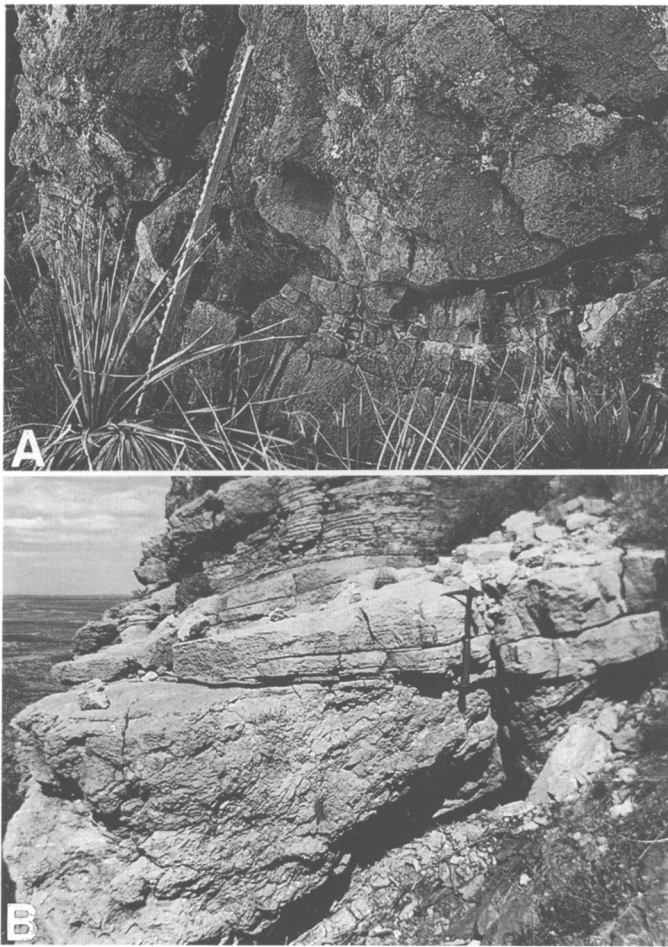


FIGURE 14-7.—A, cross-sectional view of massive Capitan debris flow foreset. The foreset bed is more than 2 m thick and has an irregular channelized base truncating the Altuda beds below. The debris flow forms a channel 4 m wide and 2 m deep. The beds below display truncation and compactional deformation. The debris flow is characterized by jointed and brecciated lithoclastic, vuggy, recrystallized, sparsely skeletal, cherty dolomitic floatstone texture. The lithoclasts include vaguely skeletal, dolowackestone and laminated to nonlaminated dolomudstone. The rock possesses irregular, coarse, calcite-filled cavities and fractures. The stadia rod scale is 1 m long. B, view of Capitan debris flow bed displaying lithoclastic, bioclastic, dolomitic floatstone-rudstone fabric. The lower contact of the foreset is channelized into thin-bedded dolomudstone of the Altuda Formation. The debris flow bed shows a slight alignment of clasts parallel to the flow direction. The upper contact of the debris flow with Altuda silty, spiculitic, laminated dolomudstone beds is planar. Hammer length is 28.5 centimeters.

the majority of the foreset beds. The thinner foreset beds are composed exclusively of this lithology. These beds are 30 cm to less than 1 m thick and display planar bedding surfaces. Spar-filled vugs and fractures are the only similarity these beds show with the other types of foresets. The rocks are extensively dolomitized, and there is complete obliteration of the depositional fabric. Rarely, some silicified echinoderms, sponges, solitary corals, brachiopods, and bryozoans are visible on the

outcrop surface. The beds are massive internally. The lower and upper contacts of these foresets with the Altuda Formation are planar. Some of the foresets have broad wavy (hummocky), nonchannelized bedforms. The foresets of this lithology appear to extend farther into the basin, and the decrease in thickness is more gradual than those of the other lithologies. Chert accentuated slump structures and recumbent folding are commonly associated (although not restricted) with this lithology. The trend of all the deformational features found in the foreset beds indicate basinward movement. The beds beneath the foresets mimic the bedforms of the foresets and exhibit load and drag deformation without any evidence of truncation.

CARBONATE SLIDE BLOCK.—Interbedded with the thin-bedded sandstone and siltstone of the Altuda Formation on the south side of Old Blue Mountain is a large carbonate block composed of sponge, bioclastic wackestone/packstone. The block is about 10 m long, 0.5–5 m thick, and has a lenticular shape with an updip tapering end. On weathered surfaces the block is olive gray in color, and on fresh surfaces it is pink. The block is internally massive and lacks any discernable bedding. Included bioclasts consist of calcareous sponges, fenestrate bryozoans, brachiopods, dasycladacean algae, echinoderms, and bivalves. The rock contains abundant spar-filled irregular cavities. The basal part of the block is composed of a mixture of clasts of sandstone, siltstone, and skeletal fragments. The lower contact of the block with the underlying Altuda Formation is undulatory, and the upper contact is covered with alluvium. The geopetal fabric indicates that the block is right-side up without any rotation.

DETACHED BRECCIA BLOCK.—An isolated large semicircular block of lithoclastic breccia overlies thin- to medium-bedded dolomudstone beds of the Altuda Formation (Figure 14-8D). The block contains boulder- to pebble-sized, angular to subangular clasts of dolomudstone, silty dolomudstone, and fine sandstone. The block displays a chaotic internal structure with crudely inclined bedding and slump features in the center. The top of the block is irregular with outward-projecting clasts. The block contains coarse spar-filled irregular cavities and fractures.

Interpretations

King (1931:79) described these foreset beds as reef-derived material poured over the slope. He also observed similar features on the slopes of the Guadalupe Mountains and regarded them as part of the Capitan foreereef facies. Newell (1957) believed the foresets are composed of reef-derived material but did not agree with the notion that they represent part of the reef itself. The detailed study of these rocks reveal that they are composed of shelf, backshelf, and shelf-edge derived allochthonous material. Garber et al. (1989), in their study of the Capitan foreslope facies in the Guadalupe

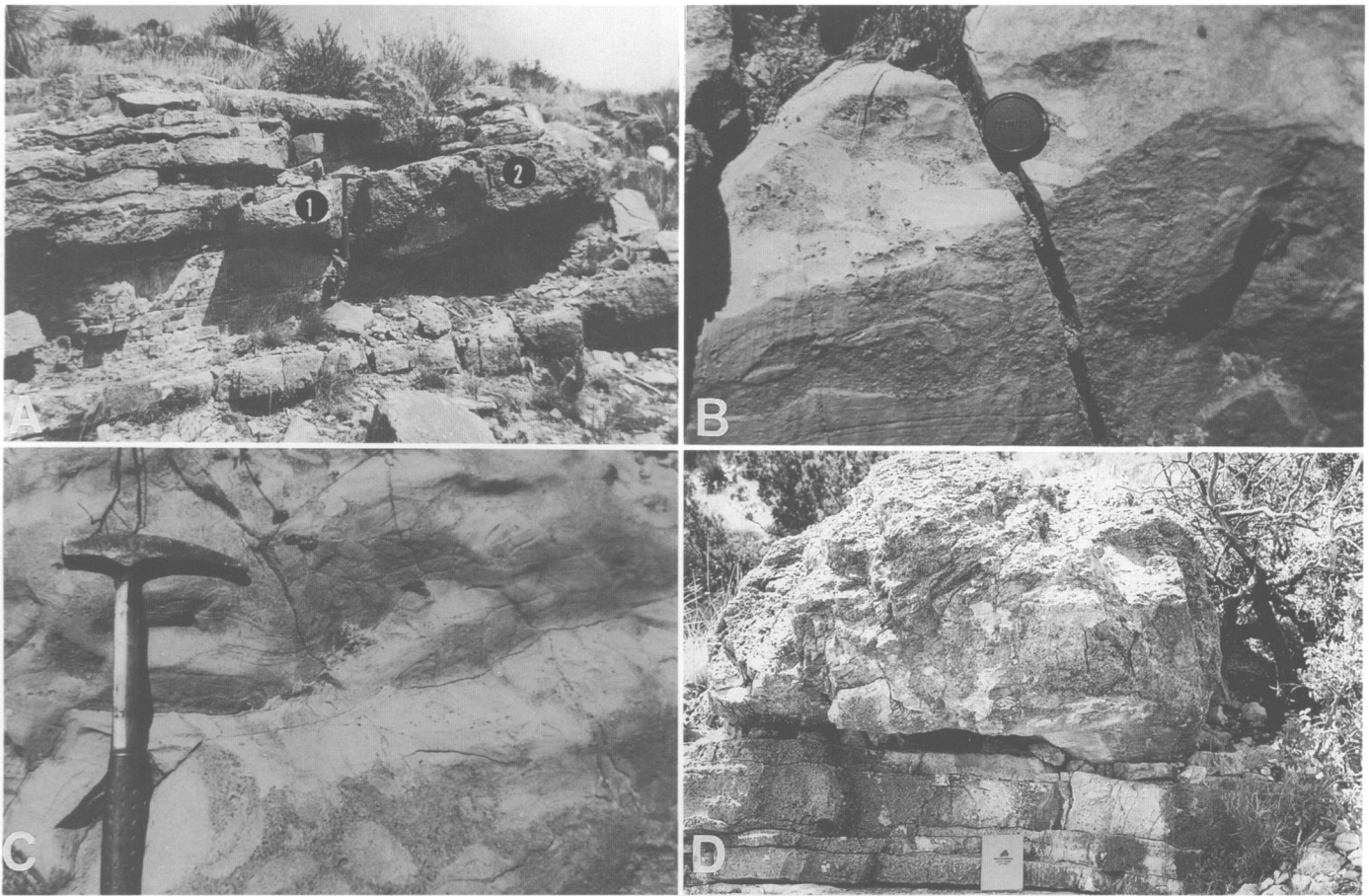


FIGURE 14-8.—A, view of channelized bedforms displayed by the Capitan foreset beds. The rocks are massive, cherty, lithoclastic, recrystallized bioclastic floatstone. Note the multiple shifting shallow channels labelled 1 and 2 within the bed. The Altuda beds below the debris flow are truncated along the channel floor. B, debris flow bed from the upper part of the Capitan foreset is 1.5 m thick at this locality. Pinch and swell bedforms are shown throughout this foresets extent. The foreset is characterized by a basal zone of shearing followed upwards by clast-supported, poorly sorted, randomly oriented, outward projecting, subangular to rounded clasts of fine quartzose sandstone and laminated siltstone clasts. The clast size in this foreset is exceptionally large as compared to other foresets in the study area. The similarity of the clasts to the Altuda sandstone beds of the slope facies suggests that these clasts are probably rip-up clasts of the underlying bed being incorporated into the debris flow. The lack of sandstone clasts within the basal part of the foreset indicates dispersive pressure and buoyancy effects within the debris flow. Camera lens cap is 5.5 centimeters in diameter. C, close-up view of the same area. Hammer is 28.5 centimeters in length. D, view of rotated slump block of Capitan foreset within thin- to medium-bedded Altuda dolomudstone. The block displays slump deformation outlined by the inclined disrupted bedding in the middle of the photograph. The basal part of the block contains boulder-sized angular clasts of dolomudstone and silty dolomudstone. Note brecciated internal fabric and spar-filled fractures and cavities. Field notebook is 19 cm in length.

Mountains, concluded that similar clinoforms are shelf-derived allochthonous carbonate debris deposited on the Capitan foreslope. Carbonate breccia deposited around the seaward margin of carbonate shelves and buildups is known from many places in the geologic record (Hopkins, 1977).

The Capitan foreset beds in the Glass Mountains display features diagnostic of subaqueous gravity-flow deposits. The presence of poor sorting, grading, variation in sizes and compositions of clasts, lack of distinct internal structure, slump

folding, truncation of underlying beds, wavy, channelized and planar bedforms, slide and slump blocks, and basinward inclined, laterally thinning wedges favor this interpretation. This interpretation also best fits the overall shelf-to-basin transition for the Guadalupian sequence in the Glass Mountains (Haneef et al., 1991; Rohr et al., this volume). The variations in texture, fabric, and bedforms within the Capitan foresets represent a variety of transport and depositional mechanisms. The following gravity flow types are recognized in the study area.

DEBRIS FLOW DEPOSITS.—The foreset beds characterized by the matrix-supported dolobreccia and the recrystallized dolomudstone-wackestone lithology types are interpreted as debris flow deposits. The matrix support, angular clasts, and hummocky to planar bedforms indicate coherent, nonturbulent movements of the mass on a gently sloping surface. Dott (1963), Carter (1975), Middleton and Hampton (1976), Lowe (1976, 1979), and Nardin et al. (1979) classified debris-flow deposits according to rheological behavior, grain matrix ratio, angle of slope, shear stress, viscosity, and yield strength, as these are the main factors that influence the nature and lateral extent of the gravity flow deposits. According to these workers, the matrix in a debris flow serves several purposes, including lubrication of clasts, buoyant support for denser clasts, and elevated pore pressure to overcome frictional resistance to flow. The presence of slump/recumbent folding, restricted only to some foresets beds, indicates a lack of intragranular support, steeper slopes, and a rapid rate of deposition of these foresets (Figure 14-9A,B). The drag and distortion produced in the underlying beds by overriding debris flow tongues illustrates the cohesive nature of these flows.

GRAIN FLOW DEPOSITS.—Foreset beds dominated by clast-supported floatstone and rudstone fabrics are interpreted as grain flow deposits. The clasts in these beds were derived from the shelf and shelf-edge environments (Figures 14-9C, 14-10). Some of the clasts are similar to the Altuda slope facies and probably represent rip-up clasts incorporated during flow. The high grain to matrix ratio and the reverse grading indicate that grain interaction in these beds was the main transporting mechanism, which resulted in an upward movement of the larger clasts.

SUBMARINE SLIDE AND SLUMP BLOCKS.—The large carbonate block and detached brecciated block are believed to be submarine slide and rockfall deposits derived from the shelf-edge and slope environments. The carbonate slide block exhibits lithological characteristics similar to the massive facies of the Capitan reef. The block appears to have been detached by waves and currents on the seaward side of the reef, whereupon it slid downslope under the influence of gravity without any significant rotation. The block displays lithology similar to the Capitan foreset beds.

The isolated breccia block in Figure 14-8D exhibits brecciated and deformed internal structure. The rotation of the block is evident from the tilted geopetal fabric. It probably represents a detached segment of a debris flow tongue during a subsequent flow.

Conclusions

The Capitan foreset beds in the Glass Mountains were formed by a subaqueous gravity flow processes. Figure 14-11 shows the proposed depositional setting of the Capitan foreset

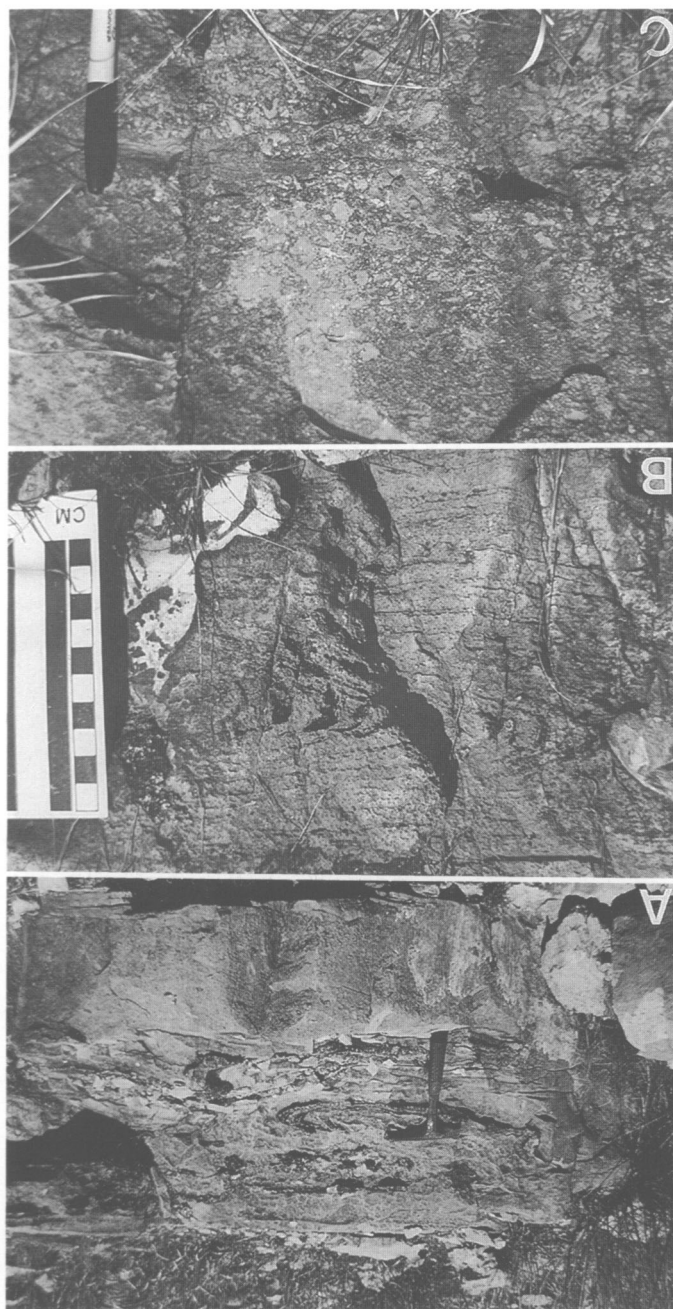


FIGURE 14-9.—A, view of penecontemporaneous slump deformation and contortion accentuated by dark brown cherty layers within Capitan foreset beds formed as a consequence of downslope en masse movement of matrix-supported debris flow. B, view of penecontemporaneous slump deformation and contortion of one of the Capitan foreset beds exhibiting clast-supported texture. C, close up of weathered surface of one of the Capitan foreset beds exhibiting clast-supported texture. The stylolitic compacted fabric and predominantly sandy, cherty matrix clearly displays the internal fabric not visible in most of the Capitan foreset beds. The clasts are angular to subrounded and represent a mixture of lithologies, shapes, and sizes. The foreset is interpreted as a grain flow deposit. The pen length is 10 centimeters.



FIGURE 14-10.—View of a clast-supported Capitan foreset grain flow deposit. The foreset is 1.2 m thick and has a flat top and bottom with the superjacent Altuda silty dolomudstone beds. The lower contact contains a brownish iron-oxide coated thin chert layer. The foreset lacks any grading and is composed of poorly sorted dolomudstone breccia.

beds. The high energy conditions on the seaward side of the reef along with fluctuations in sea level produced carbonate debris on the shelf-edge. The material thus formed moved downslope under the influence of gravity and was deposited on the foreslope. A lack of deep submarine channels and associated features suggest that the sediment movement was predominantly in the form of widespread debris sheets with only a few shallow and rare deep channels.

Acknowledgements

This paper stems from the author's masters thesis research at Sul Ross State University. The research for this study was funded by an AAPG Grant-in-Aid and a teaching assistantship by the Department of Geology to Mohammad Haneef, and an American Chemical Society Research Grant # 1641-24595 to David Rohr.

Literature Cited

- Carter, R.M.
1975. A Discussion and Classification of Subaqueous Mass Transport with Particular Application to Grain-flow, Slurry-flow and Fluxoturbidites. *Earth Science Reviews*, 11:145-177.
- Dott, R.J., Jr.
1963. Dynamics of Subaqueous Gravity Depositional Processes. *Bulletin of the American Association of Petroleum Geologists*, 47(1):104-128.
- Garber, R.A., G.A. Grover, and P.M. Harris
1989. Geology of the Capitan Shelf Margin-Subsurface Data from the Northern Delaware Basin. In P.M. Harris, and G.A. Grover, editors, Subsurface and Outcrop Examination of the Capitan Shelf Margin, Northern Delaware Basin. *Society of Economic Paleontologists and Mineralogists, Core Workshop*, 13:3-269.
- Haneef, Mohammad, S.F. Rudine, and B.R. Wardlaw
1991. Shelf to Basin Transition in the Capitanian (Permian) Deposition in the Glass Mountains, West Texas. [Abstract.] *Geological Society of America, Abstracts with Programs*, 22:A46.
- Hopkins, J.C.
1977. Production of Foreslope Breccia by Differential Submarine Cementation and Downslope Displacement of Carbonate Sands, Miette and Ancient Wall Buildups, Devonian, Canada. In H.E. Cook and P. Enos, editors, Deep-Water Carbonate Environments. *Society of Economic Paleontologists and Mineralogists, Special Publication*, 25:155-170.
- King, P.B.
1931 ("1930"). The Geology of the Glass Mountains, Texas, Part I: Descriptive Geology. *University of Texas Bulletin*, 3038: 167 pages, 15 plates. [Date on title page is 1930; actually published in 1931.]
- Lowe, D.R.
1976. Grain Flow and Grain Flow Deposits. *Journal of Sedimentary Petrology*, 46(11):188-199.
1979. Sediment Gravity Flows, Their Classification and Some Problems of Application to Natural Flows and Deposits. In L.J. Doyle and O.H. Pilkey, editors, Geology of Continental Slopes. *Society of Economic Paleontologists and Mineralogists, Special Publication*, 27:75-82.
- Middleton, G.V., and M.A. Hampton
1976. Subaqueous Sediment Transport and Deposition by Gravity Flows. In D.J. Stanley and D.J.P. Swift, editors, *Marine Sediment Transport and Environmental Management*, pages 197-218. New York: John Wiley.
- Nardin, T.R., F.J. Hein, D.S. Gorsline, and D. Edwards
1979. A Review of Mass Movement Processes, Sediment and Acoustic Characteristics, and Contrasts in Slope and Base-of-Slope Systems Versus Canyon-Fan-Basin Floor Systems. In L.J. Doyle and O.H. Pilkey, editors, Geology of Continental Slopes. *Society of Economic Paleontologists and Mineralogists, Special Publication*, 27:61-73.
- Newell, N.D.
1957. Paleogeology of Permian Reefs in the Guadalupe Mountains Area. In H.S. Ladd, editor, *Treatise on Marine Ecology and Paleogeology, Volume 2: Paleogeology*. *Geological Society of America, Memoir*, 67:407-436.
- Pray, L.C.
1989. Lateral Variability of the Capitan Reef Complex, West Texas and New Mexico. In P.M. Harris and G.A. Grover, editors, Subsurface and Outcrop Examination of the Capitan Shelf Margin, Northern Delaware Basin. *Society of Economic Paleontologists and Mineralogists, Core Workshop*, 13:273-278.
- Rohr, D.M., B.R. Wardlaw, S.F. Rudine, M. Haneef, J.A. Hall, and R.E. Grant
2000. Guidebook to the Guadalupian Symposium. In B.R. Wardlaw, R.E.

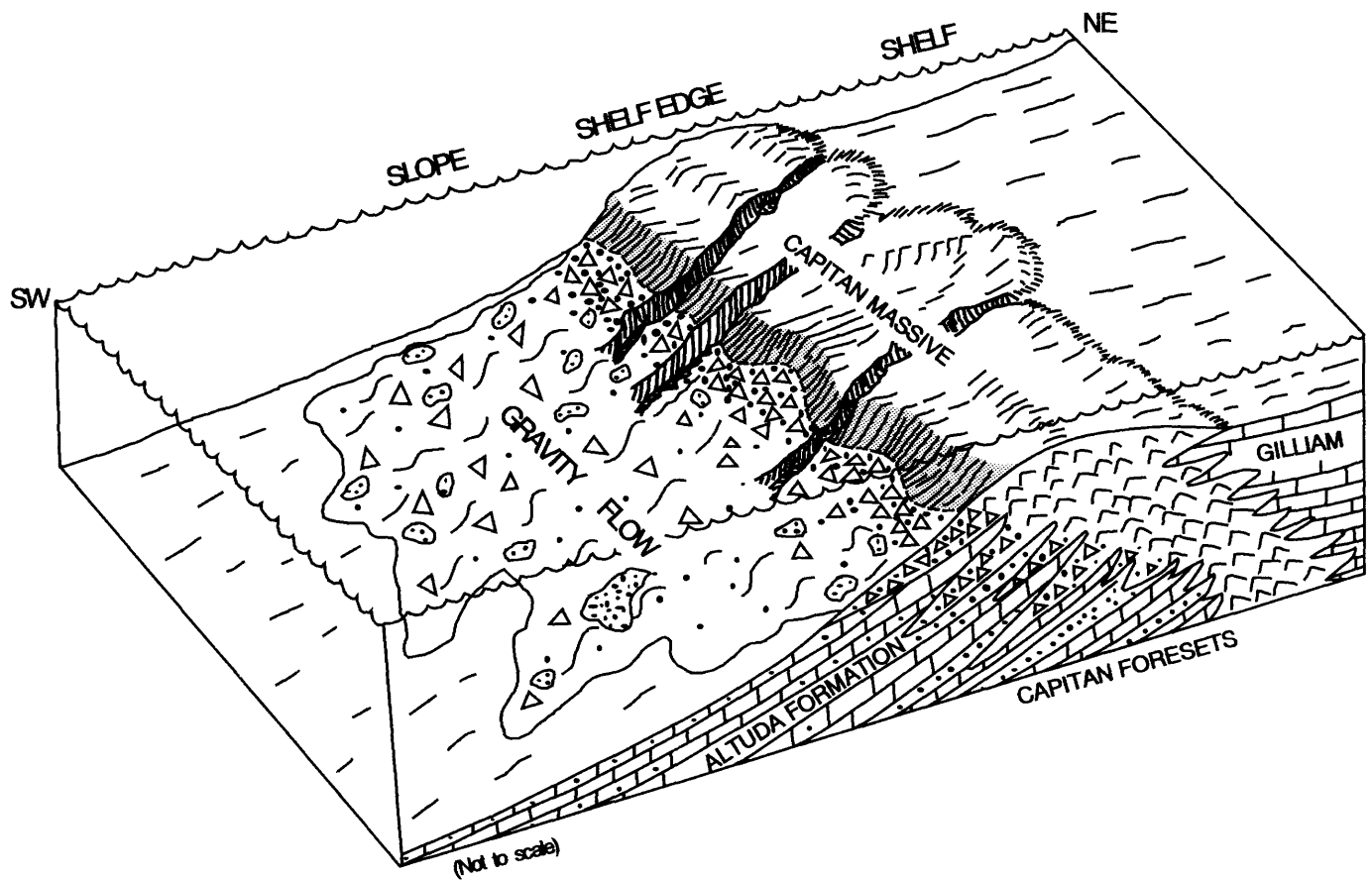


FIGURE 14-11.—Block diagram showing the proposed depositional setting of Capitan foreset beds in the Glass Mountains.

Grant, and D.M. Rohr, editors, The Guadalupian Symposium. *Smithsonian Contributions to the Earth Sciences*, 32:5-36, 31 figures.

Wanless, H.R.
1979. Limestone Response to Stress: Pressure Solution and Dolomitization. *Journal of Sedimentary Petrology*, 49(12):437-462.

15. Late Guadalupian Biostratigraphy and Fusulinid Faunas, Altuda Formation, Brewster County, Texas

Garner L. Wilde and Shannon F. Rudine

ABSTRACT

Occurrences of late Guadalupian (Zone PG-6, Wilde, 1990) fusulinid faunas in the Altuda Formation of the western Glass Mountains, Texas, confirm a biostratigraphic correlation with the upper Bell Canyon Formation (Lamar Limestone Member and post-Lamar siltstones) and the Tansill Formation of the Guadalupe Mountains.

Codonofusiella (Lantschichites) altudaensis, new species, *Paraboultonia splendens* Skinner and Wilde, *Reichelina lamarensis* Skinner and Wilde, and *Rauserella bengeensis*, new species, all occur in the upper part of the Altuda Formation and above the zone of *Polydiexodina* (Zone PG-5, Wilde, 1990). The Altuda beds are overlain unconformably by strata referred to the Tessey Formation (originally King's upper massive member, Capitan Limestone).

At least three important fusulinid subzones (in the sense of Wilde, 1990, but referred to herein as zones) have been identified in the Altuda, and another is suspected. *Paraboultonia* and *Lantschichites* mark a zone in the upper part of the Altuda covering a maximum thickness of about 20 m (65 ft.); *Reichelina lamarensis* marks the next older zone covering a maximum of approximately 12 m (40 feet); *Paradoxiella* marks a zone below this of unknown thickness. Although not identified as yet from collections, a lower zone of *Yabeina texana* should be expected below *Paradoxiella* because of its presence in this identical zonal configuration in the Guadalupe Mountains.

Paraboultonia and *Lantschichites* are both recognized on the basis of their coiling habit, and *Lantschichites* is returned to *Codonofusiella* as a subgenus.

Lateral thickness changes of strata in each of the fusulinid zones and the nature of the sediments therein are suggestive of a northeastward transgression accompanied by a gradual steepening of the shelf margin and a southwestward deepening in the Del Norte Mountains area.

Introduction

During the course of detailed mapping and stratigraphic studies in the western Glass and northern Del Norte mountains, one of the authors (Rudine) discovered a tiny fusulinid fauna in the Altuda Formation. A cursory examination suggested that the fauna might be similar, if not identical, to that described by Skinner and Wilde (1954, 1955) from the late Guadalupian Lamar Limestone Member, upper Bell Canyon Formation, southern Delaware and Guadalupe mountains. Rudine contacted the senior author for verification and possible collaboration. The present paper is the result of that collaboration.

Locality Data

Closely spaced samples were collected from four measured sections (Figure 15-1), three of which are located in the Bird (Altuda) Mountain area of the northern Del Norte Mountains, and a fourth is at the northwest point of Old Blue Mountain in the western Glass Mountains. Each section covers portions of the Altuda and Tessey formations. The four measured sections are identified as follows.

Section 1 was measured and collected by Rudine as MS77-2 (the second section on the 77 Ranch). The section begins at the 4880 foot contour, located 4000 feet (1219 m) N48E of the summit of Bird Mountain, U.S.G.S. 7.5 minute Bird Mountain Quadrangle. It begins at the top of the second unnamed sandstone member of the Word Formation (Wardlaw et al., 1990), proceeds in a westerly direction toward the northwestern corner of Bird Mountain, and ends in the lower portion of the Tessey Formation at the 5320 foot contour.

Section 2 was measured by Bruce Wardlaw and collected by Rudine as MS-W90. The section is located approximately 1 km west of Section 1, on the west side of a small spur. There is a mine location on the opposite, or east, side of the spur. The section begins at the 5080 foot contour, proceeds upwards (due south) to the 5280 foot contour, U.S.G.S. 7.5 Bird Mountain Quadrangle, and ends in the lower Tessey Formation.

Garner L. Wilde, GLW International, Midland, Texas 79705. Shannon F. Rudine, Geology Department, Sul Ross State University, Alpine, Texas 79832.

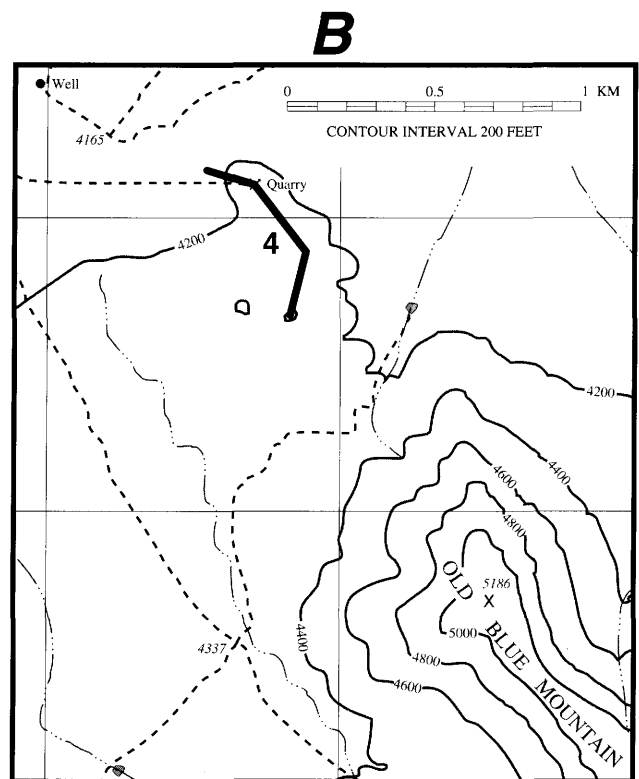
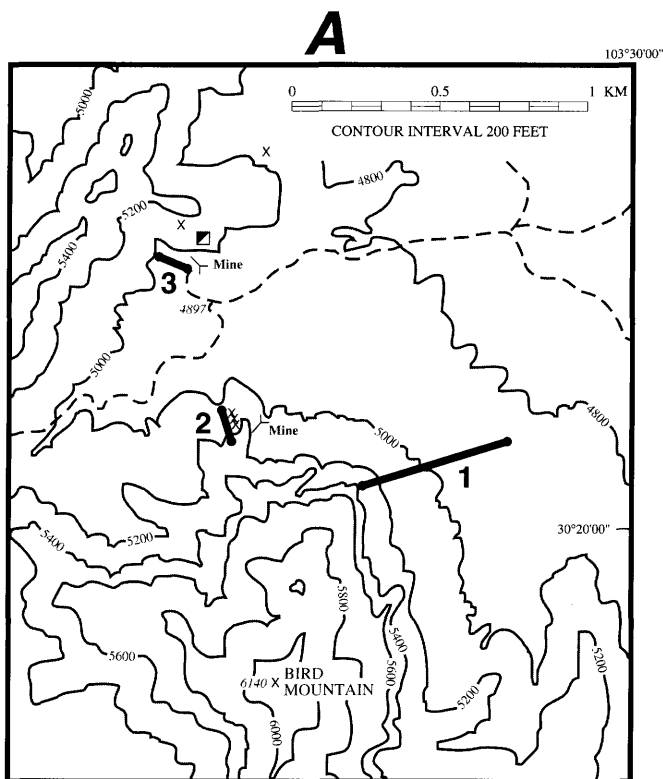
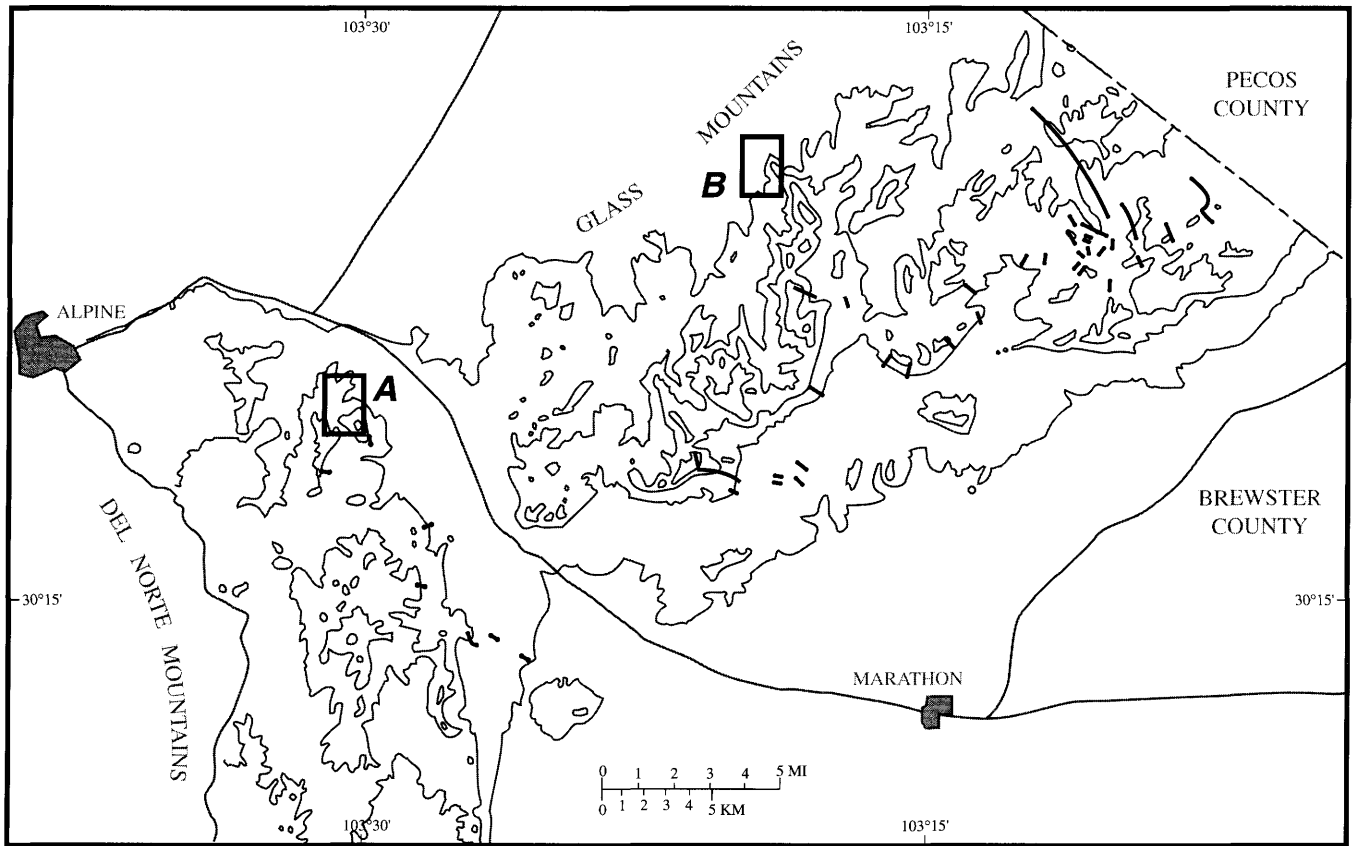


FIGURE 15-1.—Location of the four measured sections in the Glass and Del Norte mountains.

Section 3 was measured by Rudine as MS-BM5, about 0.5 km from Section 2, northwestward across a canyon. It is located about 4600 feet (1402 m) NNW of the summit of Bird Mountain, beginning at the 4920 foot contour line at the point where the "8" in road elevation marker 4897 contacts the 4920 contour, and proceeds NW along the projecting spur where it stops at the 5000 foot contour, U.S.G.S. 7.5 minute Bird Mountain Quadrangle. The area in which the above three sections were measured is referred to in this paper as the Bird Mine area, named for mining activity associated with Tertiary intrusives.

Section 4 was measured by Rudine as MS-B1, on the Bengé Ranch, beginning just below a stone quarry approximately 5700 feet (1737 m) NW of the 5186 foot elevation marker on Old Blue Mountain, western Glass Mountains, U.S.G.S. 7.5 minute Quadrangle. It begins a short distance north of the stone quarry road and below the 4200 foot contour, proceeds SE up a prominent spur to the 4400 foot contour, and ends in the lower portion of the Tessey Formation.

In the systematic paleontology portion, locations of collections within the individual measured sections can be identified as feet above the base (ex. Coll. BM5-34, is 34 feet above the base of Section 3).

Zonation and Stratigraphic Analysis

The correlation of fusulinid occurrences, shown in Figure 15-2, allows for the stratigraphic analysis of these rock sequences with an eye to better understanding the sedimentology. This paper, however, is not intended to be definitive in that regard. Our main concern is to demonstrate the presence and sequential accuracy of a late Guadalupian fusulinid zonation already recognized farther to the north in the southern Delaware and Guadalupe mountains.

The stratigraphic relationships in the area of study are already reasonably well known, thanks to the early excellent work of P.B. King (1931), R.E. King (1931), and later workers (Figure 15-3).

Rohr et al. (1991) and Rudine's continuing studies in the area, show that the rocks, which overly the Altuda Formation and were originally assigned to the upper massive member of the Capitan Limestone by P.B. King (1931), actually belong to the Tessey Formation. The Tessey in this area is composed of a complex sequence of laminated, stromatolitic, and evaporitic limestones at the base, followed by a sequence of collapse breccias that are dolomitic. These breccias resemble what have been called "Castiles" within the Castile Formation. The two formations are probably coeval, at least in part.

This paper, however, is concerned with only the upper Altuda Formation. The middle and late Guadalupian boundary is identifiable at the base of the lower Altuda in the Bird Mountain area. This separation is based upon occurrences of the fusulinid genera *Parafusulina*, of the middle Guadalupian Word Formation, and *Polydiexodina*, of the late Guadalupian

Altuda Formation. The study, however, considers only those rocks of the Altuda Formation that are younger than the highest occurrence of *Polydiexodina*. This is illustrated at the base of Figure 15-2 to show the stratigraphic relationships of the younger faunas to the older.

These relationships are important to note because in the Guadalupe Mountains, *Polydiexodina* occurs no higher than the McCombs Limestone Member of the Bell Canyon Formation (Newell et al., 1953). We believe that this same level is identifiable in the northern Del Norte and western Glass Mountains.

In the section on systematic paleontology the various levels in the upper Altuda Formation have been determined from which fusulinid faunas have been identified. Those occurrences are the basis for the zonation summarized in Figure 15-2. At the top of the Altuda is the zone of *Paraboultonia-Lantschichites*, underlain by the zone of *Reichelina lamarensis*. Based upon a single, but well-documented float collection, the zone of *Paradoxiella* appears to underlie the *Reichelina* zone. A lower zone of *Yabeina texana* might be expected, but specimens of this species have not been found.

Skinner and Wilde (1954, 1955), Wilde (1955, 1990), and Tyrrell (1964, 1969) have demonstrated the presence of just such a zonation in the Guadalupe Mountains in the Lamar-post Lamar beds of the Bell Canyon Formation and its shelf equivalent, the Tansill Formation. Interestingly, a decade after the first recognition of these faunal zones, Tyrrell (1964), who made a detailed stratigraphic analysis of core drill material taken from the Dark Canyon area, a number of miles north of the type localities of the above noted species of Skinner and Wilde, found an identical sequence of faunas. From time to time these kinds of data have been attacked as being erroneous by those whose agenda seem not to have been based upon an understanding of lateral facies and faunal succession. Only recently, for example, Achauer (1990), in reviewing an important publication of the Society of Economic Paleontologists and Mineralogists, comments, "the efforts of the book's authors should stimulate additional work on the Capitan ... this reviewer is convinced that the widely accepted correlation of the Lamar Limestone to the Tansill [sic] Formation across the Capitan shelf is questionable" (Achauer, 1990:1665). Perhaps the present data describing a similar sequence of fossils from coeval rocks located at a greater distance will help to convince skeptics of the reality of these correlations.

What are some of the sedimentological implications that can be drawn from the fusulinid zonation shown in Figure 15-2? First, one needs to understand that all of these sections are located near the edge of the Hovey channel, which provided the only known connection between the Delaware basin and the open ocean during late Guadalupian time. The Bengé Ranch area (MS-4) probably laid farthest shelfward during late Altuda deposition; however, even there, the facies probably represents toe of slope deposition. In Section 4 the zone of *Paraboul-*

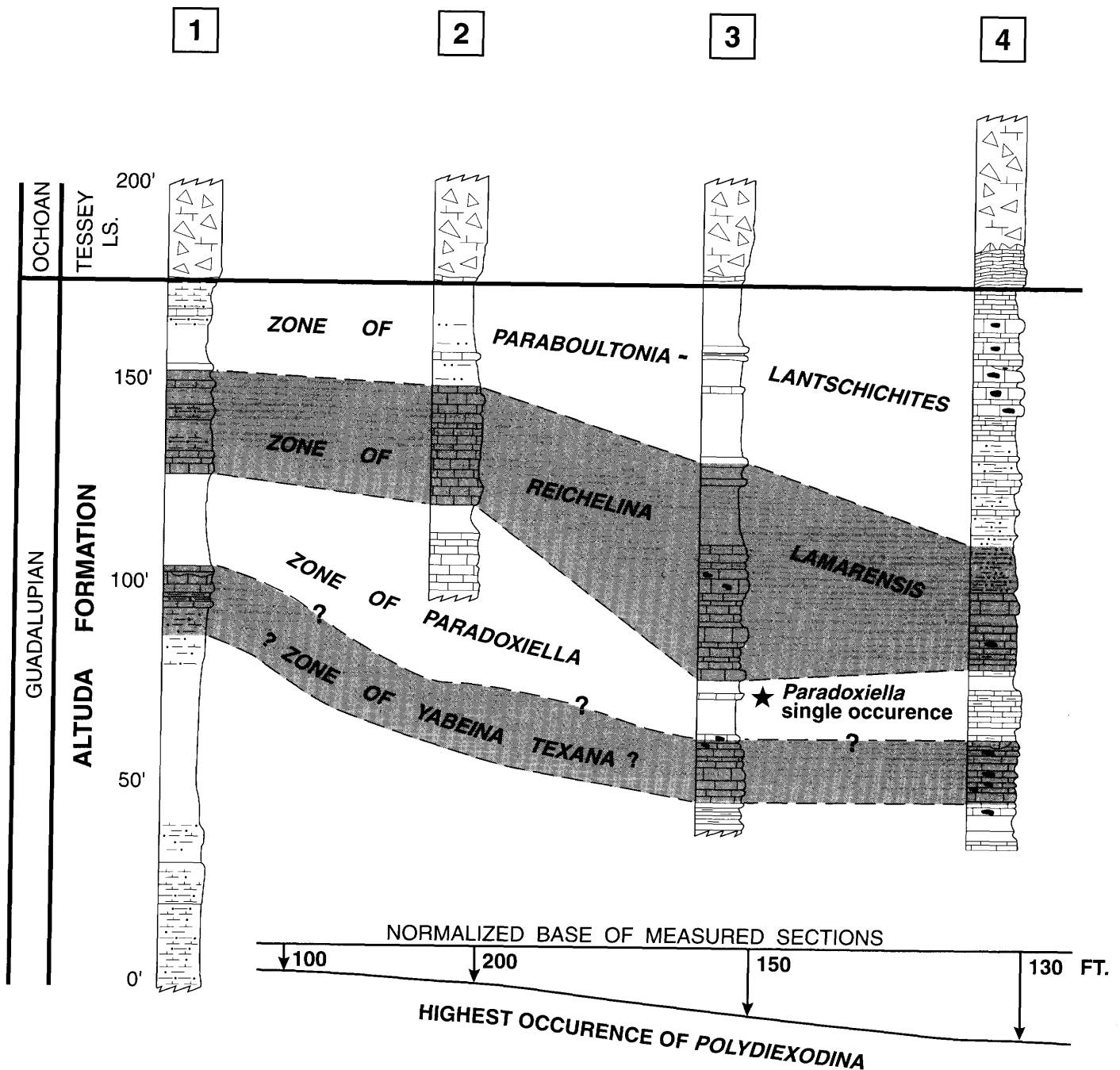


FIGURE 15-2.—Correlation of the fusulinid zones in the Altuda Formation.

tonia-Lantschichites is thickest and contains a rich, silicified megafauna, especially brachiopods and ammonoids.

At Section 3 the underlying zone of *Reichelina lamarensis* is at its thickest development. There, too, an abundant, silicified megafauna occurs. Not enough zonal definition is known from Section 2, but it is suggested that the zone of *Paradoxiella* should exhibit its thickest development there, based upon the type of rocks and megafaunal content.

Comparison of the location map (Figure 15-1) with Figure

2-2 (Rohr et al., this volume) suggests the shelf edge was prograding northward through the area during deposition of the Altuda. There is a vague hint, however, that a gradual steepening of slope was occurring through time, beginning in the Bird Mine area and progressing northeastward toward the Benge Ranch area. Further illumination of the depositional history of this portion of the Altuda Formation can only be obtained from a detailed study of the sequence stratigraphy of this interesting unit.

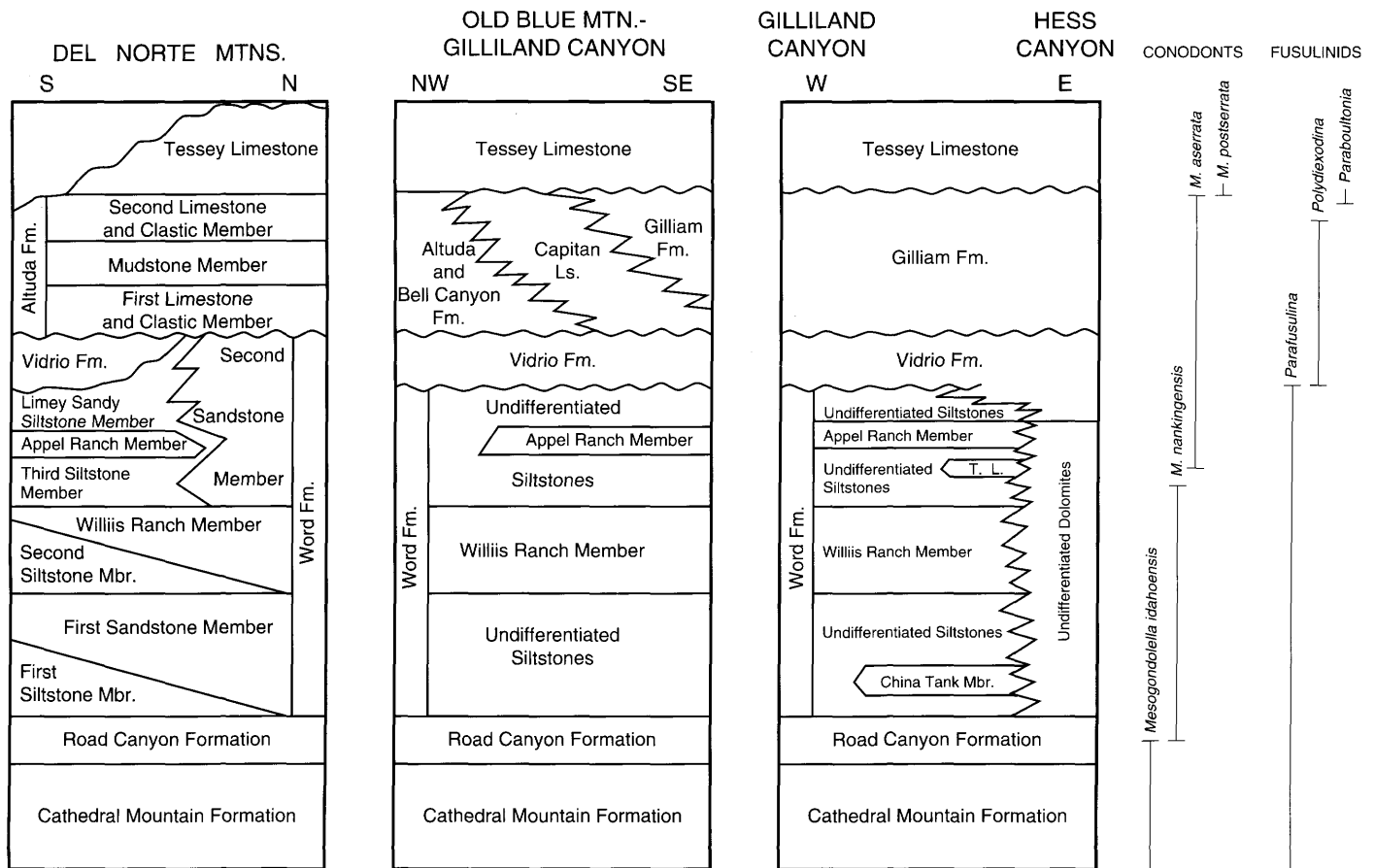


FIGURE 15-3.—Stratigraphic relationships in the northern Del Norte and Glass mountains. (Modified after Cooper and Grant (1972), Davis (1984), Rudine (1988), Wardlaw et al. (1990), and Wilde (1990).)

Systematic Paleontology

Family OZAWAINELLIDAE Thompson and Foster, 1937

***Reichelina* Erk, 1942**

***Reichelina lamarensis* Skinner and Wilde, 1955**

PLATE 15-2: FIGURES 1-5, PLATE 15-3: FIGURES 1-11, PLATE 15-4: FIGURES 1-9, PLATE 15-5: FIGURES 1-3

Reichelina lamarensis Skinner and Wilde, 1955:927-940, pl. 89: figs. 1-9.

Inner whorls with sharply rounded or bluntly angular periphery; ultimate whorl periphery usually sharply angular in adult specimens. Mature individuals with 4B-5B whorls; axial length 0.36-0.52 mm, average 0.41 mm in nine specimens. Specimen width 0.76-1.13 mm, average 0.43 mm. Final 1/3-1/2 volution greatly expanded in height in fully mature specimens, with corresponding increase in septa length. Rarely specimens appear uncoiled, but condition of such specimens too poor for accurate determination.

Spirotheca very thin, consisting of a tectum and diaphanotheca. Septa unfluted but strongly convex anteriorly. Some

specimens with tunnel rising from floor in last few septa coincident with marked inflation of final volution. Septal pores common, usually appearing as dark spots due to plugging by secondary material. In 11 specimens: first whorl with 7-12 septa, average 9; second whorl with 11-16 septa, average 14; third whorl with 12-18 septa, average 16; fourth whorl with 16-22 septa, average 19. In three specimens: fifth whorl with 22-25 septa, average 24.

Proloculus minute, spherical, with outside diameter varying from 33-56 microns, average 45 microns for 15 specimens. Tunnel low, narrow, averaging 18° in fourth whorl. Chomata low, broad, extending laterally to poles and joining across tunnel floor.

DISCUSSION.—The material described herein appears to fall well within the limits of specific variation for the species. The studied specimens are slightly larger in most whorls and have a slightly smaller form ratio. Correspondingly, the specimens have a slightly greater number of septa per whorl. Skinner and Wilde's types are from the Lamar Limestone Member of the Bell Canyon Formation, Guadalupe Mountains, which corresponds very well stratigraphically with the studied material.

OCCURRENCE.—*Reichelina lamarensis* Skinner and Wilde occurs, often in profusion, in each of the four measured sections discussed herein. In Section 1, however, the zone is poorly represented by a single collection, Coll. 77-2-718. In Section 2, the species is represented in two collections. In Coll. W90-48, the species is not common; however, in Coll. W90-50+2, it is abundant. In Section 3, it is seen in abundance in Colls. BM5-34, 91, 95, 103, 109, and 114. It also occurs in Coll. 343 (float). At Section 4, it was found in Colls. B1-48, 52, 59.5, 60.25, 76, 77.5, 77.6, and 83. Thus, there is a slight overlap of the zone of *Reichelina lamarensis* with the higher zone of *Paraboultonia-Lantschichites* in sections 2, 3, and 4.

***Rauserella* Dunbar, 1944**

***Rauserella bengeensis*, new species**

PLATE 15-1: FIGURES 1-9, PLATE 15-2: FIGURES 6-10

Shell extremely minute and highly irregular in shape. Mature specimens with 4-5 volutions; first 2-3 volutions commonly coiled askew or even at right angles to later axis of coiling. Direction of axis of coiling commonly shifting, so appearance varying greatly among mature specimens. Shell length 0.54-0.81 mm, average 0.68 mm; shell width 0.34-0.43 mm, average 0.37 mm. Form ratio for five specimens 1.42-2.4, average 1.85. Spirotheca very thin, composed of a tectum and diaphanotheca. Septa unfluted throughout, but commonly convex anteriorly, particularly in later whorls. In five specimens: first whorl with 6 septa; second whorl with 10-13 septa, average 11; third whorl with 11-13 septa, average 12. In one specimen: fourth whorl with 8 septa; fifth whorl with 6 septa. Septal pores relatively common throughout.

Proloculus very small, with outside diameter 22-56 microns, average 33 microns for five specimens. Tunnel narrow in juvenarium, becoming wider in adult whorls, but practically impossible to measure with accuracy because of changes in coiling and absence of prominent chomata bordering tunnel in outer whorls.

DISCUSSION.—*Rauserella bengeensis*, new species, is perhaps the smallest member of the genus yet known; thus, it bears little resemblance to previously described forms of the genus. Somewhat similar forms have been seen from rocks as old as late Leonardian, but no significant size increase occurred before the late Guadalupian. That such a tiny species as *R. bengeensis* is seen in these late Guadalupian beds may indicate the presence of two lineages of *Rauserella*, an early minute and less differentiated group, and a later, small but fully differentiated group.

OCCURRENCE.—*Rauserella bengeensis*, new species, occurs in all four of the measured sections of this paper. It occurs in a single sample from Section 1, Coll. 77-2-718. In Section 2, it occurs in Coll. W90-48, but like *Reichelina*, it is only poorly represented in terms of numbers, although the preservation is

excellent. In Section 3, it occurs in Coll. 343 (float) and in Colls. BM5-34, 95, and 114. In Section 4, it occurs in Colls. B1-40, 46, and 59.5. It thus occurs throughout the zone of *Reichelina lamarensis* and the lower portion of the overlying zone of *Paraboultonia-Lantschichites*, but never in great numbers.

Subfamily BOULTONIINAE Skinner and Wilde, 1954

***Paraboultonia* Skinner and Wilde, 1954**

***Paraboultonia splendens* Skinner and Wilde, 1954**

PLATE 15-8: FIGURES 1-11, PLATE 15-9: FIGURES 1-16

Paraboultonia splendens Skinner and Wilde, 1954:441, pl. 44: figs. 1-7, pl. 45: figs. 1-4.

Shell minute, slender cylindrical, with bluntly rounded poles, particularly in outer volution. Adult specimens with 4B to 5B whorls; first whorl discoidal and coiled askew to succeeding whorls. Shell length 2.14-3.86 mm, average 2.84 mm. Shell width 0.57-1.02 mm, average 0.75 mm. Form ratio for 10 specimens 3.2-4.6, average 3.83. Last $\frac{1}{4}$ volution in ultimate whorl rather abruptly expanded; expansion commonly occurring at any point following beginning of fifth volution, but can begin earlier in fourth.

Spirotheca and septa very thin, consisting of a tectum and diaphanotheca. Septa intensely fluted from pole to pole; folds high and regular throughout shell, except in expanded portion of final volution. Cuniculi present, at least in outermost volution; septal pores abundant and easily identified because of plugging with dark, secondary material (a common characteristic of the Boultoniinae). In 10 specimens: juvenarium with 8 or 9 septa; second whorl with 9-15 septa, average 11; third whorl with 13-20 septa, average 17; fourth whorl with 20-29 septa, average 24. One specimen: fifth whorl with 32 septa.

Proloculus spherical, with outside diameters 35-86 microns, average 55 microns in 10 specimens. Tunnel low, narrow, and quite erratic throughout, but not commonly observed in outer whorls.

DISCUSSION.—*Paraboultonia splendens* Skinner and Wilde remains the only described species of this genus. The genus has been confused with *Codonofusiella (Lantschichites)* Touman-skaya, 1953, and indeed, the two are difficult to separate in some axial sections. In *Paraboultonia*, however, only the ultimate whorl expands, and all septa continue to touch the floor of the penultimate volution (Plate 15-9: Figures 1, 2, 10-12, 14, 15). In *C. (Lantschichites)*, on the other hand, the final whorl not only greatly expands, but it lifts off of the penultimate volution, uncoiling, and the septa in the uncoiled portion implant themselves against the previous septal face, as in typical *Codonofusiella* (Plate 15-6: Figure 13; Plate 15-7: Figures 1-4, 7, 9).

The studied specimens differ only slightly from Skinner and Wilde's types from the southern Delaware Mountains. Indeed,

the form ratios differ by less than 0.20, and average proloculus diameters differ by less than 10 microns. This is extremely close for such an unusual species as they are separated by the Hovey channel and a distance of about 90 miles (145 km).

OCCURRENCE.—*Paraboultonia splendens* Skinner and Wilde occurs, commonly in abundance, in Sections 2, 3, and 4. In Section 2, it occurs with *Lantschichites altudaensis*, new species, and *Reichelina lamarensis* Skinner and Wilde in Coll. W90-50+2. In Section 3, it occurs in Colls. BM-109 and 114. In Section 4, it occurs in Colls. B1-77.5, 77.6, 83, 83.1, 85.5, 87.5, 92.7, 96, 97, 97.5, 100, 108.5, 108.7, 110, 114, 115.1, 116.5, 121.5, 128, 135, 136, and 138.

Codonofusiella Dunbar and Skinner, 1937

Subgenus *Lantschichites* Toumanskaya, 1953

***Codonofusiella (Lantschichites) altudaensis*, new species**

PLATE 15-5: FIGURES 4-7, PLATE 15-6: FIGURES 1-13,
PLATE 15-7: FIGURES 1-7, 9

Shell minute, bluntly cylindrical, with bluntly rounded poles except in penultimate whorl, which varies from bluntly rounded to bluntly pointed. Mature specimens with 4-5 volutions; first volution commonly discoidal and coiled askew to succeeding volutions, in such instances proloculus quite small. Specimens with normally coiled initial whorl, proloculus quite large. Adult specimen shell length 1.91-3.26 mm, average 3.00 mm; shell width 0.56-0.94 mm, average 0.81 mm. Form ratio 2.6-4.9, average 3.2 in 7 specimens.

Final-whorl expansion similar to *Paraboultonia*, but expansion developing into uncoiling, commonly of great extent, with concomitant axial extension, much as in *Codonofusiella extensa* Skinner and Wilde, 1937. In some specimens, coiled portion rectangular-shaped with extremely blunt polar areas, followed by a greatly expanded, uncoiled portion, resulting in strange appearance.

Spirotheca and septa very thin, consisting of a tectum and diaphanotheca. Septa intensely fluted from pole to pole; folds high and regular throughout coiled portion, becoming highly irregular as expansion begins. High septal folds squared off at top, as in *Paraboultonia*, but folds more extreme. In *Paraboultonia splendens* such folds with more secondary material associated with them than in *C. (L.) altudaensis*. Cuniculi not detected, but their presence still possible.

Septal count for juvenarium undeterminable. For five specimens: second whorl with 9-16 septa, average 11; third whorl with 14-21 septa, average 17; fourth whorl with 19 to more than 26 septa, average 23. In two specimens: fifth whorl with average of 34 septa.

Proloculus spherical, outside diameters 57-86 microns, average 78 microns. Tunnel low, narrow, and more easily discernible than in *Paraboultonia splendens*.

DISCUSSION.—*Codonofusiella (Lantschichites) altudaensis*,

new species, is closely similar to the type of the subgenus, *L. maslennikov* Toumanskaya (1953), particularly in the large size of the proloculus compared to the shell size, and in the cylindrically quadrate shape of the coiled test. The new species is much larger than the type in both length and width. One of Toumanskaya's specimens of nearly 5 whorls, measures only 0.05 mm in length and 0.45 mm in width (pl. X: fig. 2), yet the proloculus is 50 microns in outside diameter. On the same plate (fig. 3) she illustrates *C. (L.) weberi* (Schubert), which also has 5 complete whorls and measures only 1.18 mm in length and 0.50 mm in width, yet the proloculus is also 50 microns in outside diameter, which is quite large for the overall size of the specimen.

Sosnina (1968) described three new species of *Lantschichites*: *L. exilis*, *L. elegans*, and *L. tenuitheca*. *Lantschichites elegans* is elongate cylindrically, as is *Paraboultonia splendens* Skinner and Wilde; however, Sosnina illustrated a sagittal section of the species that shows appreciable uncoiling, as do the other two species, which are also more quadrate-shaped, as in the types.

Sheng (1963) identified two species as *Lantschichites* from the south China province of Kwangsi. One of the species, *Lantschichites minimus* (Chen), was described originally as *Gallowainella minima*; however, Sheng's specimens demonstrate extremes of uncoiling in a number of specimens, which supports its placement in *Lantschichites*. In the same paper, Sheng identified other specimens as *Lantschichites splendens* (Skinner and Wilde). These forms do not uncoil, but they do inflate in the final whorl. The specimens may or may not belong to *P. splendens*, as they appear to be more slender than the types. Regardless, there is a consistency with the types in the absence of an uncoiled portion.

Wang, Sheng, and Zhang (1981) described some fusulinid faunas collected on an expedition to the Qinghai-Xizang Plateau Region in which they report *Lantschichites kalamulunica*, new species, *L. xizangicus*, new species, and *L. minimus* (Chen). Based on their description and illustrations, *L. kalamulunica* is obviously a *Codonofusiella* and is similar to *C. extensa* Skinner and Wilde. Wang et al. (1981) did not illustrate sagittal sections of *L. xizangicus*, but it could be a *Paraboultonia*. Sagittal illustrations were included for *L. minimus*, and they show that the species is correctly placed in the genus.

To be fair, there is no sound basis for concluding that the sagittal sections shown on Plate 15-7: Figures 5, 6 actually belong to this new species. No flare is present, and the septal counts and proloculus measurements are not different from some of *Paraboultonia splendens*. Both species occur in the collections from which these specimens came. It is suspected that without the prominent uncoiled flare one might have some difficulty in making a separation based on sagittal sections. Finding well-oriented sagittal sections that show the flaring portion is difficult at best.

The reasons for placing *Lantschichites* once again as a subgenus of *Codonofusiella* are twofold. First, the only

difference between the two is the length of the coiled portion, which is hardly a generic difference. Furthermore, by going back to Toumanskaya's original designation, the differences between *Lantschichites* and *Paraboultonia* can be amplified, not merely to preserve the generic name of the latter, but to demonstrate what so many workers seem to have overlooked, namely the former uncoils, but the latter does not (Wilde, 1975:80). This characteristic is certainly generic, as is the overall difference in shape.

OCCURRENCE.—*Codonofusiella (Lantschichites) altudaensis*, new species, is present in three of the measured sections of this paper. It is found in great profusion in Coll. W90-50+2 of Section 2, in Coll. BM5-109 of Section 3, in Colls. B1-83, 87.5, and 136 in Section 4, and in Coll. BR4-113. In all but the last cited collection, the new species occurs with *Paraboultonia splendens* Skinner and Wilde and with *Reichelina lamarensis* Skinner and Wilde.

***Paradoxiella* Skinner and Wilde, 1955**

***Paradoxiella pratti*? Skinner and Wilde, 1955**

PLATE 15-7: FIGURE 8

A single specimen of an undoubted *Paradoxiella* was recovered, and it is suspected to belong to *P. pratti*; however, it is only a parallel section, so it is difficult to unquestionably assign it to *P. pratti*. By straightening the specimen for maximum dimension of the annular flare, a size of 1.44 mm was obtained; however, because the specimen is not sectioned near the center of the shell, this would be a minimum width. Maximum width of the entire flare in the types for *P. pratti* was 2.88 mm. The measured width of the coiled portion of the shell is 0.46 mm, compared to 0.34 mm for the type specimens.

Again, comparisons are practically meaningless because of the location of the cuts of the section.

Regardless of the difficulty of comparisons, the discovery of *Paradoxiella* beneath the zone of *Reichelina lamarensis* is important. Further search will almost certainly produce better material.

OCCURRENCE.—The single specimen occurred in a float sample picked up by Rudine in Section 3. The sample (Coll. 343) is shown on the cross section (Figure 15-2) by a symbol. Rudine believes this to be very close to the in situ occurrence of *Paradoxiella*.

Acknowledgments

The authors are grateful to a number of persons for their generous hospitality and assistance in various aspects of this study. Mr. and Mrs. Mac Benge, owners of the Benge Ranch, Mr. and Mrs. Kyle Seales, owners of the 77 Ranch, and Mr. Tommie Woodward, owner of the Bird Mine, generously allowed access to properties for mapping, section-measuring, and collecting. Bruce Wardlaw, U.S. Geological Survey, measured Section 2 and shared generously considerable stratigraphic data. Merlynd Nestell, University of Texas, Arlington, translated important Russian papers. David Rohr and the Geology Department of Sul Ross State University kindly made facilities available for thin-section preparation. Finally, the authors thank Bruce Wardlaw, David Rohr, Richard Grant, and Merlynd Nestell for critically reading the manuscript and making useful suggestions.

All of the illustrated specimens included in this study are deposited in the Department of Paleobiology, National Museum of Natural History, Smithsonian Institution, Washington, D.C.

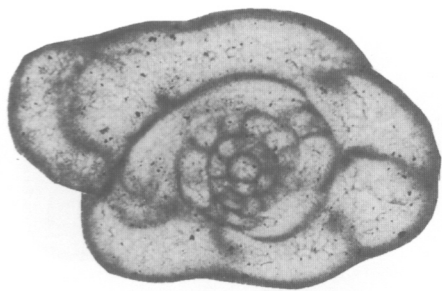
Literature Cited

- Achauer, C.W.
1990. Subsurface and Outcrop Examination of the Capitan Shelf Margin, Northern Delaware Basin. *Bulletin of the American Association of Petroleum Geologists*, 74(10):1665.
- Cooper, G.A., and R.E. Grant
1972. Permian Brachiopods of West Texas, I. *Smithsonian Contributions to Paleobiology*, 14:1-231, plates 1-23.
- Davis, R.A.
1984. Depositional Environments of the Western Cathedral Mountain, Road Canyon, Word and Capitan Formations (Permian), Glass Mountain Area. 104 pages. Unpublished master's thesis, Sul Ross State University, Alpine, Texas.
- Dunbar, C.O.
1944. Permian and Pennsylvanian (?) Fusulines. In R.E. King, C.O. Dunbar, P.E. Cloud, Jr., and A.K. Miller, Geology and Paleontology of the Permian Area Northwest of Las Delicias, Southwestern Coahuila, Mexico. *Geological Society of America, Special Paper*, 52:35-45, plates 9-16.
- Dunbar, C.O., and J.W. Skinner
1937. Permian Fusulinidae of Texas: The Geology of Texas, Part 2. *University of Texas Bulletin*, 3701:519-825, plates 42-81.
- Erk, A.S.
1942 ("1941"). Sur la présence du genre *Codonofusiella* dans le Permien de Bursa (Turquie). *Eclogae Geologicae Helveticae*, 34:234-253, plates 12-14. [Date on title page is 1941; actually published in 1942.]
- King, P.B.
1931 ("1930"). The Geology of the Glass Mountains, Texas, Part I: Descriptive Geology. *University of Texas Bulletin*, 3038: 167 pages, 15 plates. [Date on title page is 1930; actually published in 1931.]
- King, R.E.
1931 ("1930"). The Geology of the Glass Mountains, Texas, Part II: Faunal Summary and Correlation of the Permian Formations with Description of Brachiopoda. *University of Texas Bulletin*, 3042: 245 pages, 44 plates. [Date on title page is 1930; actually published in 1931.]
- Newell, N.D., J.K. Rigby, A.G. Fischer, A.J. Whiteman, J.E. Hickox, and J.S. Bradley
1953. *The Permian Reef Complex of the Guadalupe Mountains Region, Texas and New Mexico: A Study in Paleocology*. 236 pages. San Francisco: W.H. Freeman and Company.
- Rohr, D.M., B.R. Wardlaw, S.F. Rudine, A.J. Hall, R.E. Grant, and M. Haneef
1991. Guidebook to the Guadalupian Symposium. In B.R. Wardlaw, R.E. Grant, and D.M. Rohr, editors, *Proceedings of the Guadalupian Symposium, March 13-15, 1991, Sul Ross State University, Alpine, Texas*, pages 18-111.
- Rudine, S.F.
1988. Geology and Depositional Environments of the Permian Rocks, Northern Del Norte Mountains, Brewster County, Texas. 186 pages. Unpublished master's thesis, Sul Ross State University, Alpine, Texas.
- Sheng, J.C.
1963. Permian Fusulinids of Kwangsi, Kueichow, and Szechuan. *Palaeontologia Sinica*, 149, new series B(10): 247 pages, 35 plates. [In Chinese and English.]
- Skinner, J.W., and G.L. Wilde
1954. The Fusulinid Subfamily Boultoniinae. *Journal of Paleontology*, 28(4):434-444, plates 42-45.
1955. New Fusulinids from the Permian of West Texas. *Journal of Paleontology*, 29(6):927-944, plates 89-95.
- Sosnina, M.L.
1968. New Species of Fossil Plants and Invertebrates of the USSR. *Ministry of Geology of the USSR, Nedra Press*, 2(1):124-128, 31 plates. [In Russian.]
- Toumanskaya, O.G.
1953. *O verkhnepermiskilch fuzulinidakh yuzhno-Ussuriyskogo Kraya*. [Concerning Upper Permian Fusulinids in the Southern Ussuri Territory.] Pages 19-21, plates 10-12. Moscow: Trudy, Vsesoyuznogo Nauchno-Issledovatel'skogo Geologicheskogo Instituta (VSEGEI). [In Russian.]
- Tyrrell, W.W., Jr.
1964. Paleontology and Stratigraphy of Near-Reef Tansill-Lamar Strata, Guadalupe Mountains, Texas and New Mexico. In Geology of the Capitan Reef Complex of the Guadalupe Mountains, Culberson County, New Mexico. *Roswell Geological Society Guidebook*, pages 66-82.
1969. Criteria Useful in Interpreting Environments of Unlike but Time-Equivalent Carbonate Units (Tansill-Capitan-Lamar), Capitan Reef Complex, West Texas and New Mexico. In G.M. Friedman, editor, *Depositional Environments in Carbonate Rocks: A Symposium. Society of Economic Paleontologists and Mineralogists, Special Publication*, 14:80-97.
- Wang, Y., J.C. Sheng, and L. Zhang
1981. Fusulinids from Xizang, China. In *The Comprehensive Scientific Expedition of the Qinghai-Xizang Plateau*. 80 pages, 21 plates. Palaeontology of Xizang, Science Press, Book III.
- Wardlaw, B.R., R.A. Davis, D.M. Rohr, and R.E. Grant
1990. Leonardian-Wordian (Permian) Deposition in the Northern Del Norte Mountains, West Texas. *United States Geological Survey Bulletin*, 1881-A:A1-A14.
- Wilde, G.L.
1955. Permian Fusulinids of the Guadalupe Mountains. In Permian Field Conference, October 1955. *Society of Economic Paleontologists and Mineralogists, Permian Basin Section, Publication*, 55-1:59-62.
1975. Fusulinid-Defined Permian Stages. In J.M. Cys and D.F. Toomey, editors, *Permian Exploration, Boundaries, and Stratigraphy. Society of Economic Paleontologists and Mineralogists, West Texas Geological Society and Permian Basin Section, Publication*, 75-65:67-83.
1990. Practical Fusulinid Zonation: The Species Concept; with Permian Basin Emphasis. *West Texas Geological Society, Bulletin*, 29(7): 5-34.

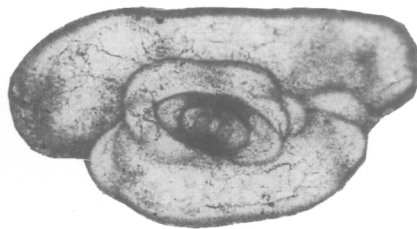
Plates 15-1-15-9

PLATE 15-1

FIGURES 1-9.—*Rausserella bengeensis*, new species: 1, axial section, $\times 90$, paratype, USNM 462297, Coll. W90-48, Section 2, Bird Mine area; 2, axial section, $\times 90$, paratype, USNM 462298, Coll. W90-48, Section 2, Bird Mine area; 3, tangential section, $\times 90$, paratype, USNM 462299, Coll. W90-48, Section 2, Bird Mine area; 4, 5, axial sections, $\times 90$ and $\times 180$, respectively, holotype, USNM 462300, Coll. B1-59, Section 4, Benge Ranch; 6, tangential section, $\times 180$, paratype, USNM 462301, Coll. 343, Section 3, Bird Mine area; 7, axial section, $\times 180$, paratype, USNM 462302, Coll. 77-2-718, Section 1, Bird Mine area; 8, sagittal section, $\times 180$, paratype, USNM 462303, Coll. 77-2-718, Section 1, Bird Mine area; 9, sagittal section, $\times 180$, paratype, USNM 462304, Coll. 77-2-718, Section 1, Bird Mine area. (Reduced to 94% of original for publication.)



1



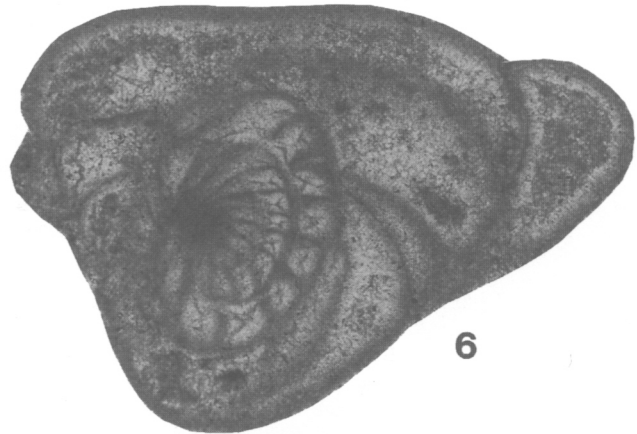
2



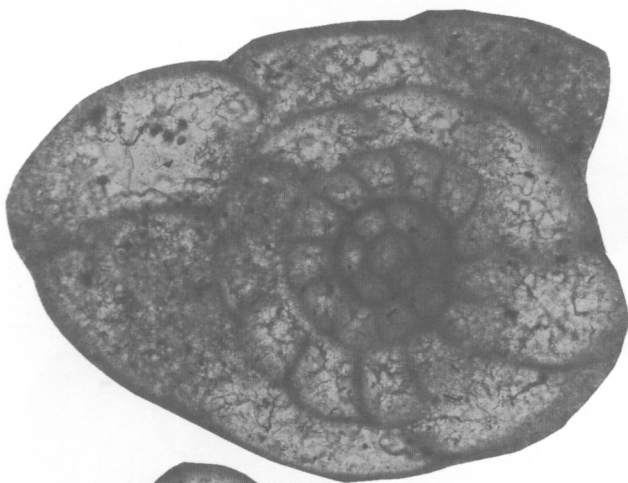
3



4



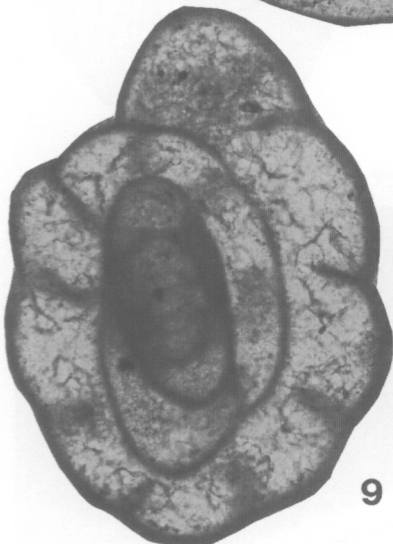
6



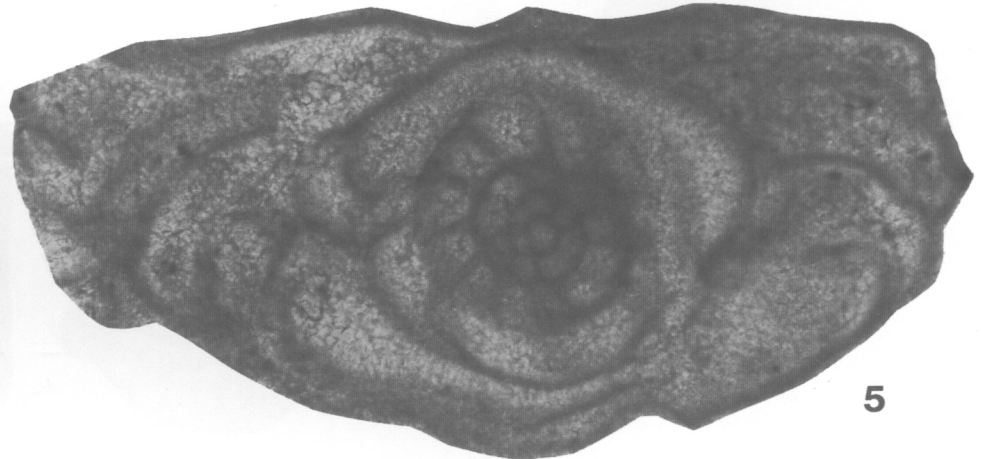
8



7



9



5

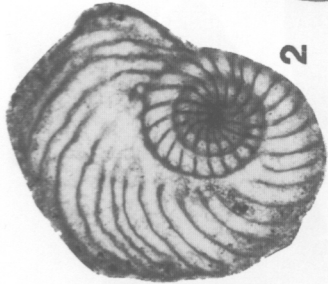
PLATE 15-2

FIGURES 1-5.—*Reichelina lamarensis* Skinner and Wilde: 1, two tangential sections with a nearby calcisphere or radiolarian?, $\times 35$, USNM 462305, Coll. W90-50+2, Section 3, Bird Mine area; 2, sagittal section, $\times 35$, USNM 462306, Coll. W90-50+2, Section 3, Bird Mine area; 3, sagittal section, $\times 35$, USNM 462307, Coll. W90-50+2, Section 3, Bird Mine area; 4, sagittal section, $\times 90$, USNM 462308, Coll. W90-50+2, Section 3, Bird Mine area; 5, sagittal section, $\times 90$, USNM 462309, Coll. BM5-114, Section 3, Bird Mine area. (Reduced to 93% of original for publication.)

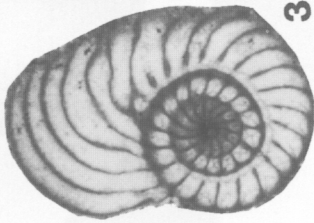
FIGURES 6-10.—*Rauserella bengeensis*, new species: 6, parallel section, $\times 35$, hypotype, USNM 462310, Coll. BM5-34, Section 3, Bird Mine area; 7, tangential section, $\times 35$, hypotype, USNM 462311, Coll. BM5-95, Section 3, Bird Mine area; 8, tangential section, $\times 35$, hypotype, USNM 462312, Coll. BM5-114, Section 3, Bird Mine area; 9, tangential section, $\times 90$, hypotype, USNM 462313, Coll. BM5-114, Section 3, Bird Mine area; 10, tangential section, $\times 90$, hypotype, USNM 462314, Coll. BM5-114, Section 3, Bird Mine area. (Reduced to 93% of original for publication.)



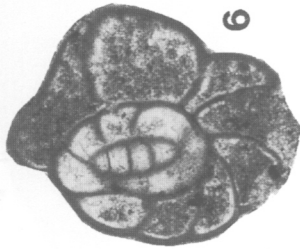
1



2



3



6



7



8



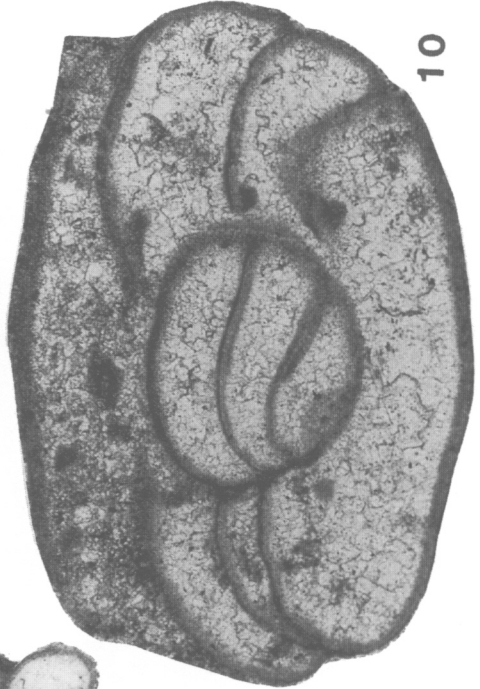
4



5



9



10

PLATE 15-3

FIGURES 1-11.—*Reichelina lamarensis* Skinner and Wilde: 1-5, axial and near-axial sections, $\times 90$, USNM 462315-462319, Coll. BM5-34, Section 3, Bird Mine area; 6-8, 10, axial and near-axial sections, $\times 90$, 8 is a portion of same specimen as 7, $\times 180$, USNM 462320, 462321, 462323, Coll. BM5-95, Section 3, Bird Mine area; 9, near-axial section, USNM 462322, Coll. BM5-34, Section 3, Bird Mine area; 11, near-axial section, USNM 462324, Coll. BM5-103, Section 3, Bird Mine area. (Reduced to 94% of original for publication.)

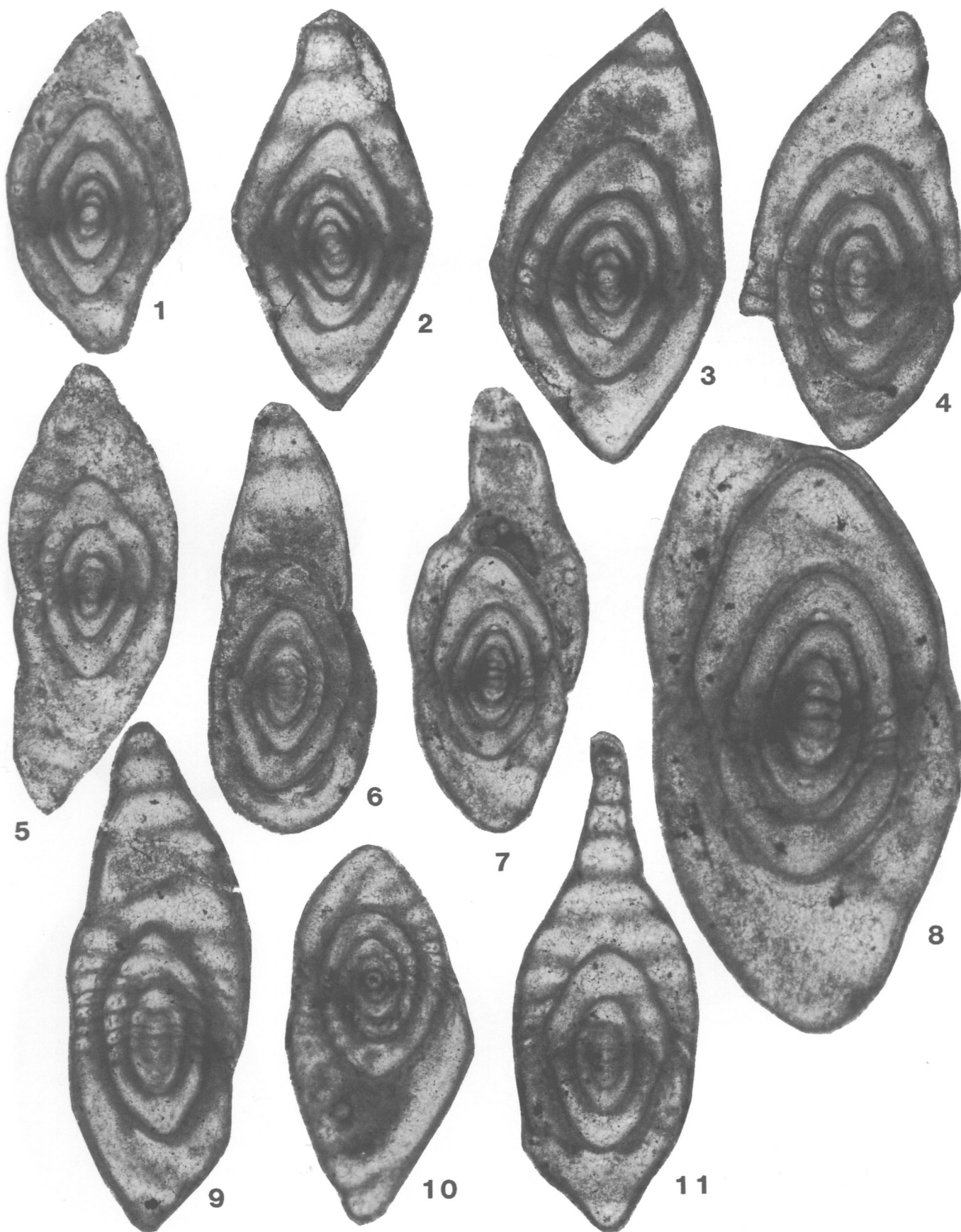


PLATE 15-4

FIGURES 1-9.—*Reichelina lamarensis* Skinner and Wilde: 1-5, sagittal sections, ×90, USNM 462325-462329, Coll. BM5-109, Section 3, Bird Mine area; 6, sagittal section, ×90, USNM 462330, Coll. BM5-114, Section 3, Bird Mine area; 7-9, sagittal sections, ×90, USNM 462331-462333, Coll. BM5-109, Section 3, Bird Mine area. (Reduced to 94% of original for publication.)

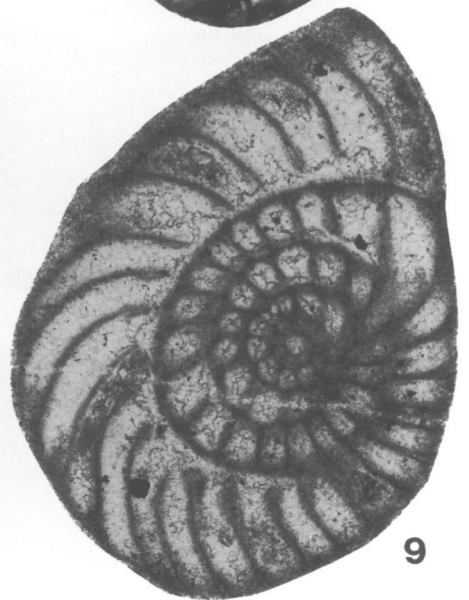
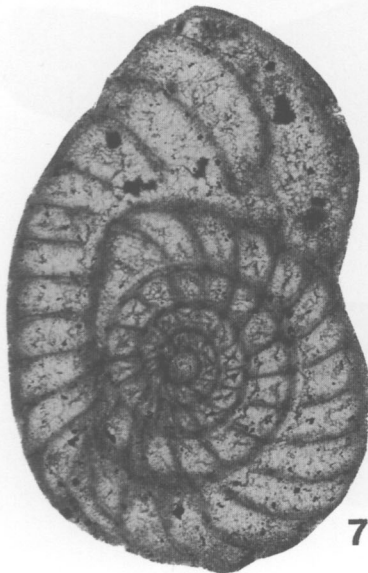
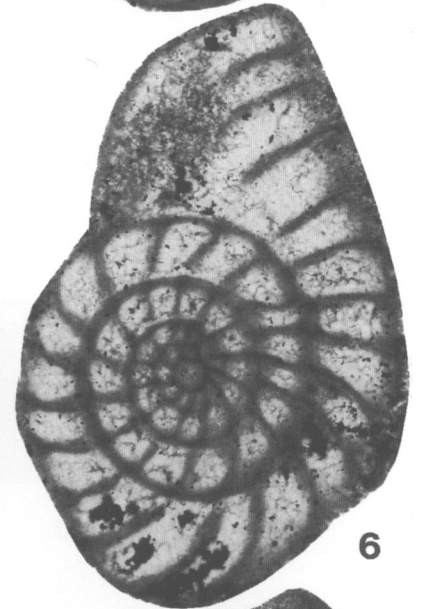
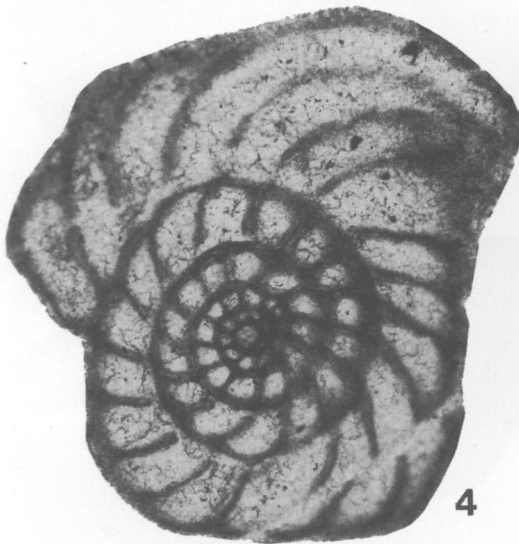
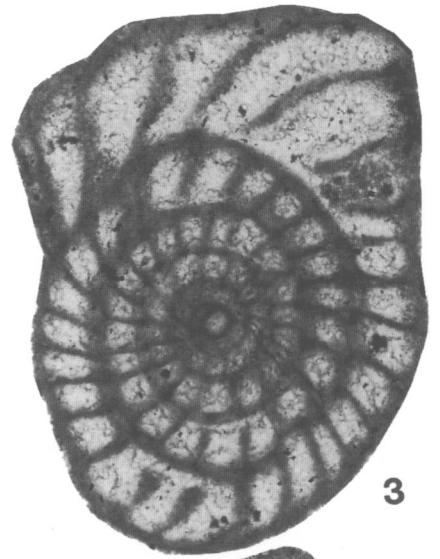
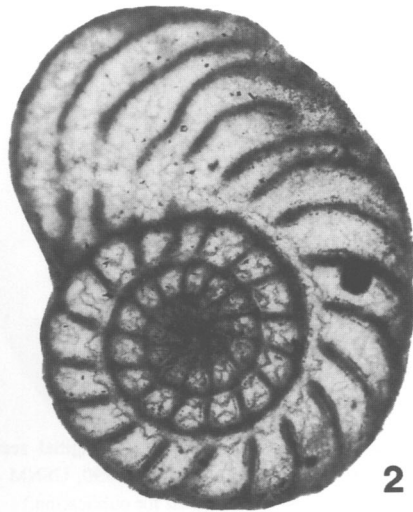
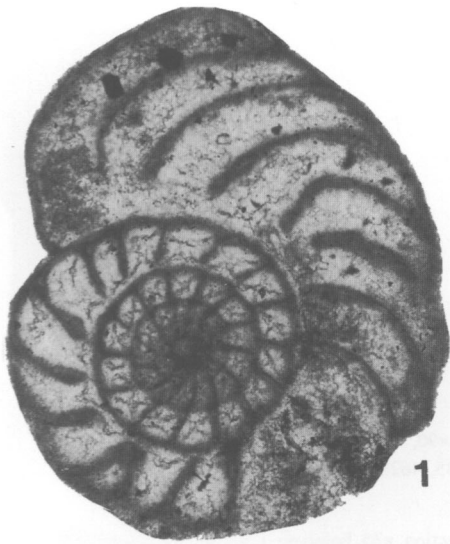


PLATE 15-5

FIGURES 1-3.—*Reichelina lamarensis* Skinner and Wilde: 1, sagittal section, $\times 90$, USNM 462334, Coll. BM5-95, Section 3, Bird Mine area; 2, 3, sagittal sections, $\times 90$, USNM 462335, 462336, Coll. BM5-109, Section 3, Bird Mine area. (Reduced to 94% of original for publication.)

FIGURES 4-7.—*Codonofusiella (Lantschichites) altudaensis*, new species: 4, axial section, $\times 35$, holotype, USNM 462337, Coll. W90-50+2, Section 2, Bird Mine area; 5-7, axial sections, $\times 35$, paratypes, USNM 462338-462340, Coll. W90-50+2, Section 2, Bird Mine area. (Reduced to 94% of original for publication.)

FIGURES 8-10.—*Codonofusiella (Lantschichites) altudaensis*?: 8, tangential section, $\times 35$, USNM 462341, Coll. W90-50+2, Section 2, Bird Mine area; 9, tangential section, $\times 35$, USNM 462342, Coll. BM5-109, Section 3, Bird Mine area; 10, tangential section, $\times 35$, USNM 462343, Coll. BR4-113, Section 4, Bengé Ranch. (Reduced to 94% of original for publication.)

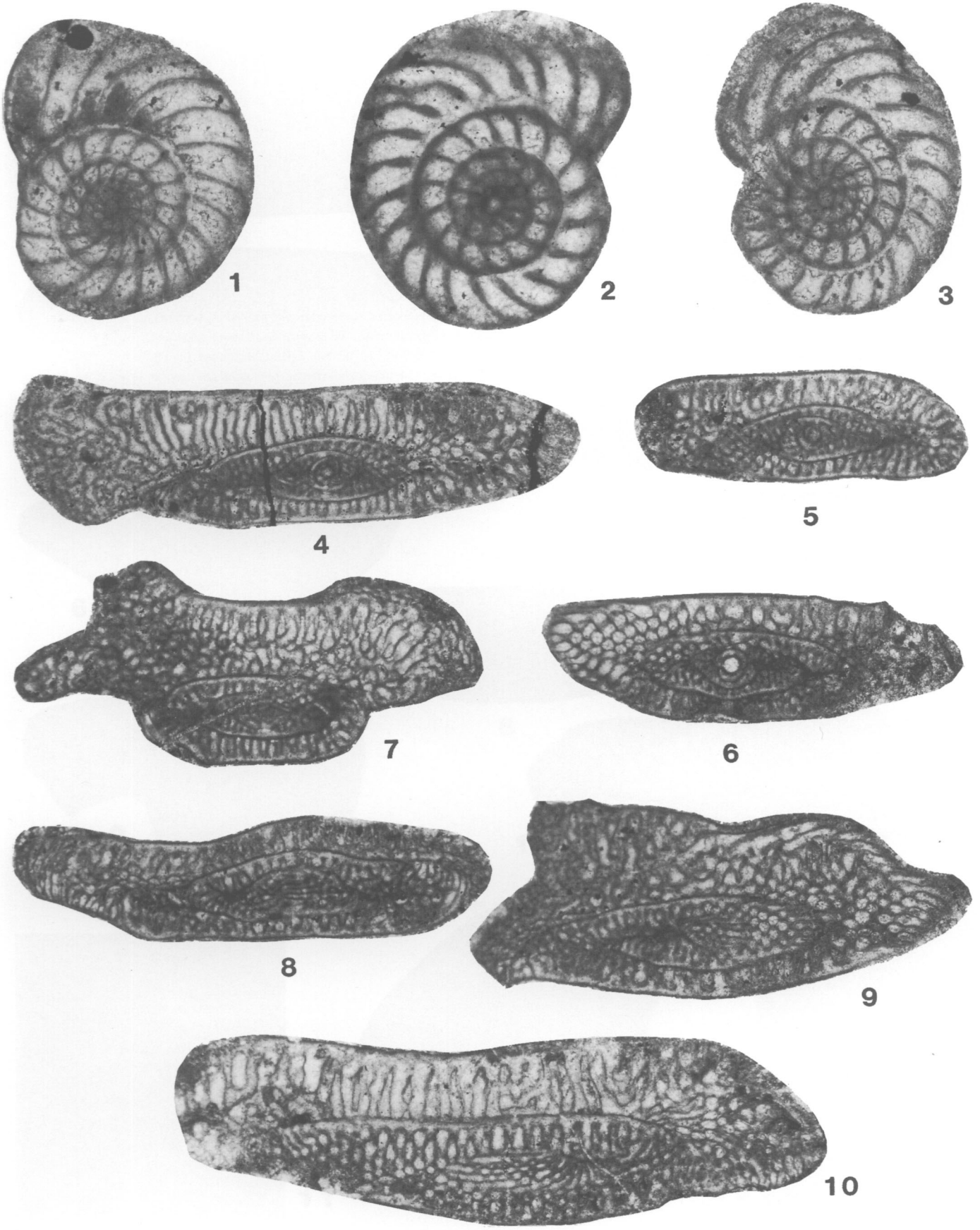


PLATE 15-6

FIGURES 1-13.—*Codonofusiella (Lantschichites) altudaensis*, new species: 1-5, axial and near-axial sections, $\times 35$, paratypes, USNM 462344-462348, Coll. W90-50+2, section 2, Bird Mine area; 6-10, tangential and oblique sections, $\times 35$, paratypes, USNM 462349-462353, Coll. W90-50+2, section 2, Bird Mine area; 11, 12, sagittal sections, $\times 35$ and $\times 90$, respectively, paratype, USNM 462354, oblique section of *Reichelina lamarensis* Skinner and Wilde seen in matrix, Coll. W90-50+2, section 2, Bird Mine area; 13, near-sagittal section showing flare, $\times 35$, paratype, USNM 462355, same specimen as Plate 15-7: Figure 9, Coll. W90-50+2, section 2, Bird Mine area. (Reduced to 94% of original for publication.)

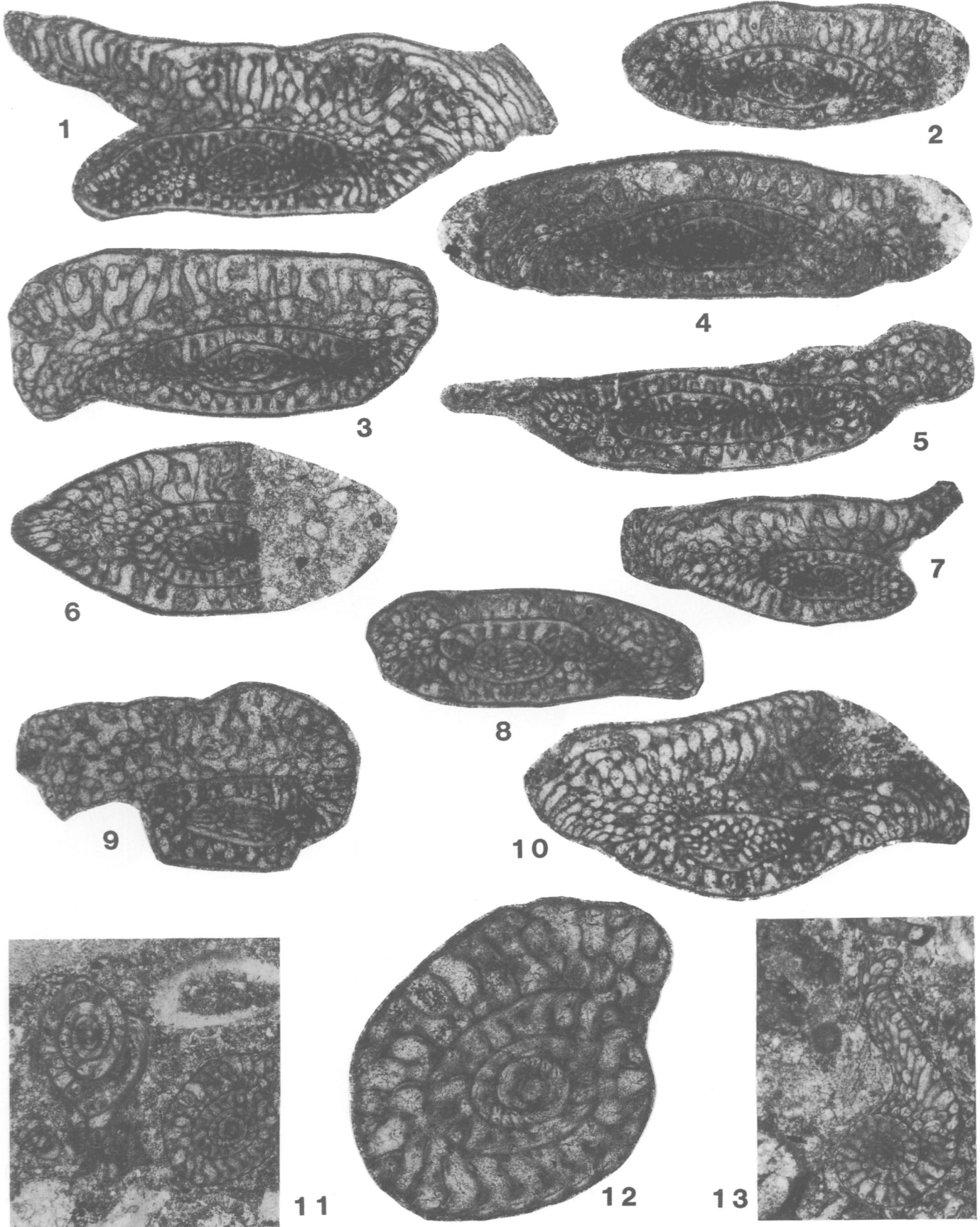
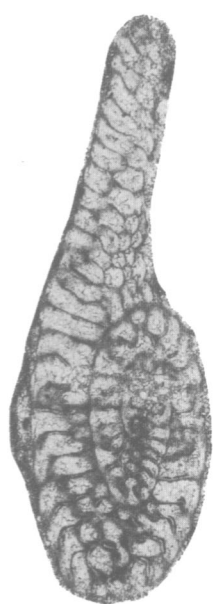


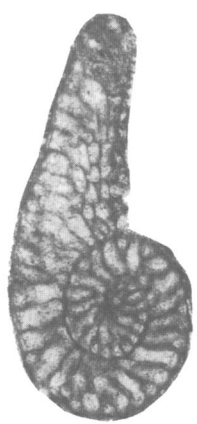
PLATE 15-7

FIGURES 1-7, 9.—*Codonofusiella (Lantschichites) altudaensis*, new species: 1, parallel section, $\times 35$, paratype, USNM 462356, Coll. B1-136, Section 4, Benge Ranch; 2, parallel section, $\times 35$, paratype, USNM 462357, Coll. B1-87.5, Section 4, Benge Ranch; 3, parallel section, $\times 35$, paratype, USNM 462358, Coll. B1-83, Section 4, Benge Ranch; 4, near-sagittal section, $\times 35$, paratype, USNM 462359, Coll. B1-136, Section 4, Benge Ranch; 5, sagittal section without flare, $\times 90$, paratype, USNM 462360, Coll. B1-83, Section 4, Benge Ranch; 6, sagittal section without flare, $\times 90$, paratype, USNM 462361, Coll. B1-87.5, Section 4, Benge Ranch; 7, parallel section, $\times 90$, paratype, USNM 462362, Coll. W90-50+2, Section 2, Bird Mine area; 9, near-sagittal section showing flare, $\times 90$, paratype, USNM 462364, same specimen as Plate 15-6: Figure 13, Coll. W90-50+2, Section 2, Bird Mine area. (Reduced to 94% of original for publication.)

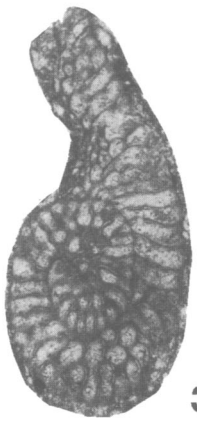
FIGURE 8.—*Paradoxiella pratti*? Skinner and Wilde: parallel section, $\times 90$, USNM 462363, Coll. 343, Section 3, Bird Mine area. This is the only specimen of *Paradoxiella* thus far recovered in any of the four sections, and it was in a float sample. The characteristic "tail," however, makes the generic identification undeniable. (Reduced to 94% of original for publication.)



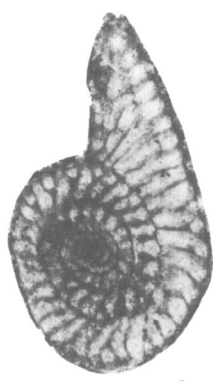
1



2



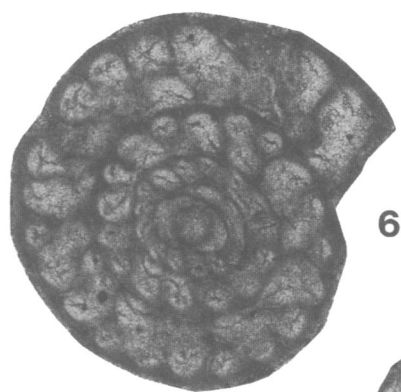
3



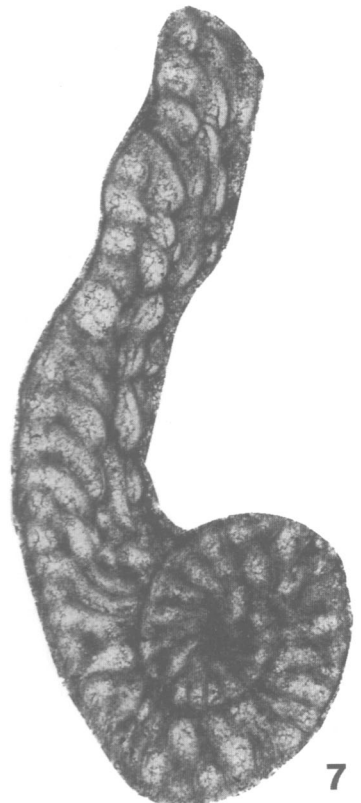
4



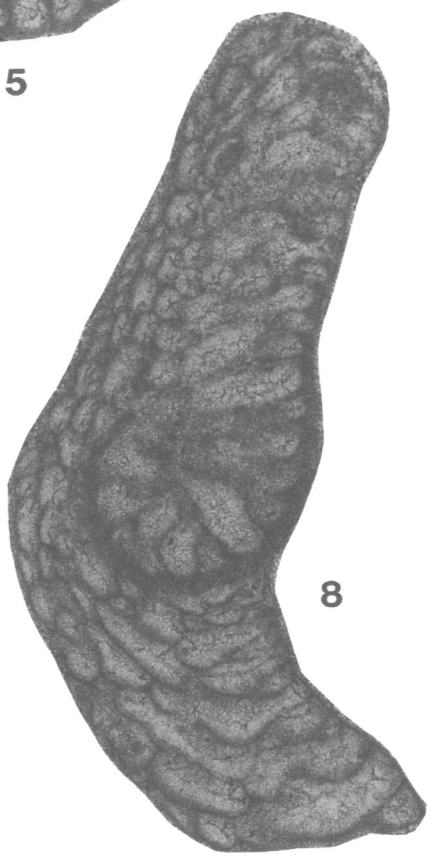
5



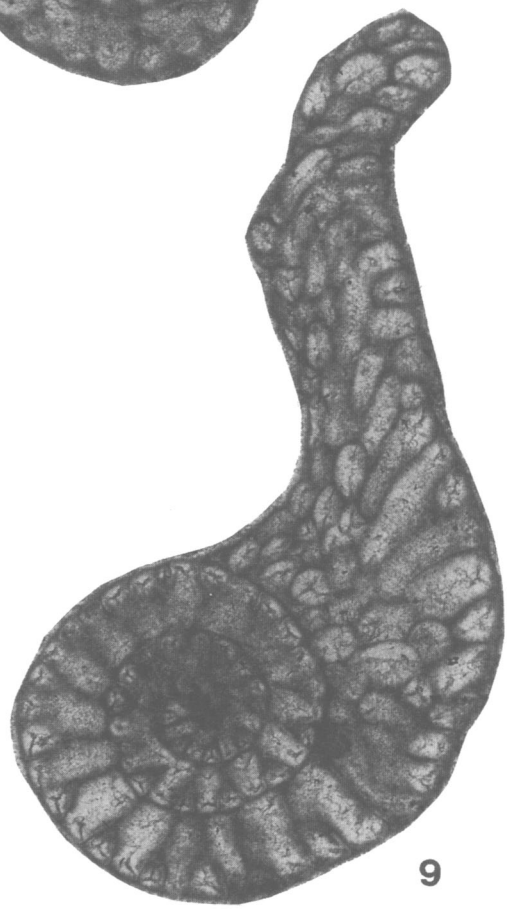
6



7



8



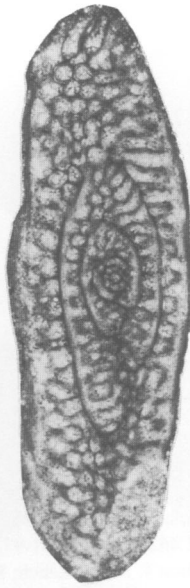
9

PLATE 15-8

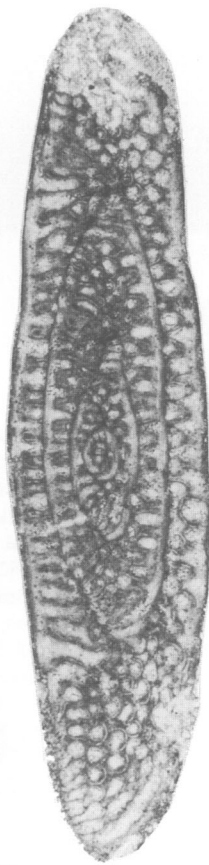
FIGURES 1-11.—*Paraboultonia splendens* Skinner and Wilde: 1-11, axial sections, ×35, USNM 462365-462375, Coll. BR4-113, Section 4, Bengé Ranch. Pseudomorphic gypsum blades obliterate portions of some specimens. (Reduced to 94% of original for publication.)



2



5



8



11



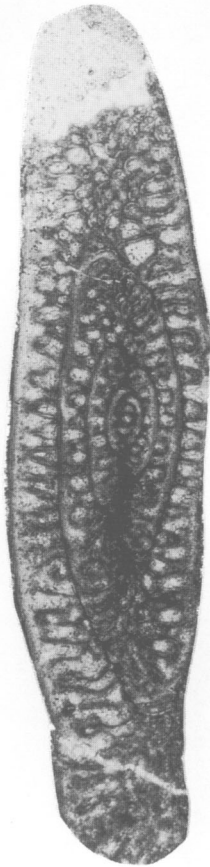
1



3



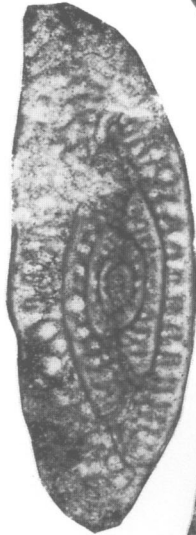
6



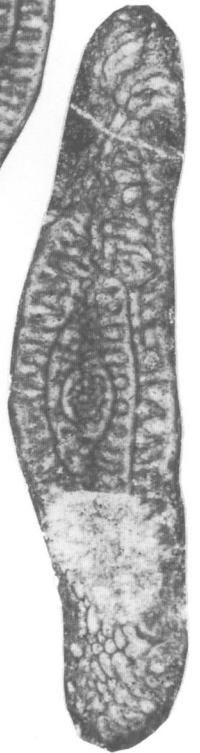
4



7



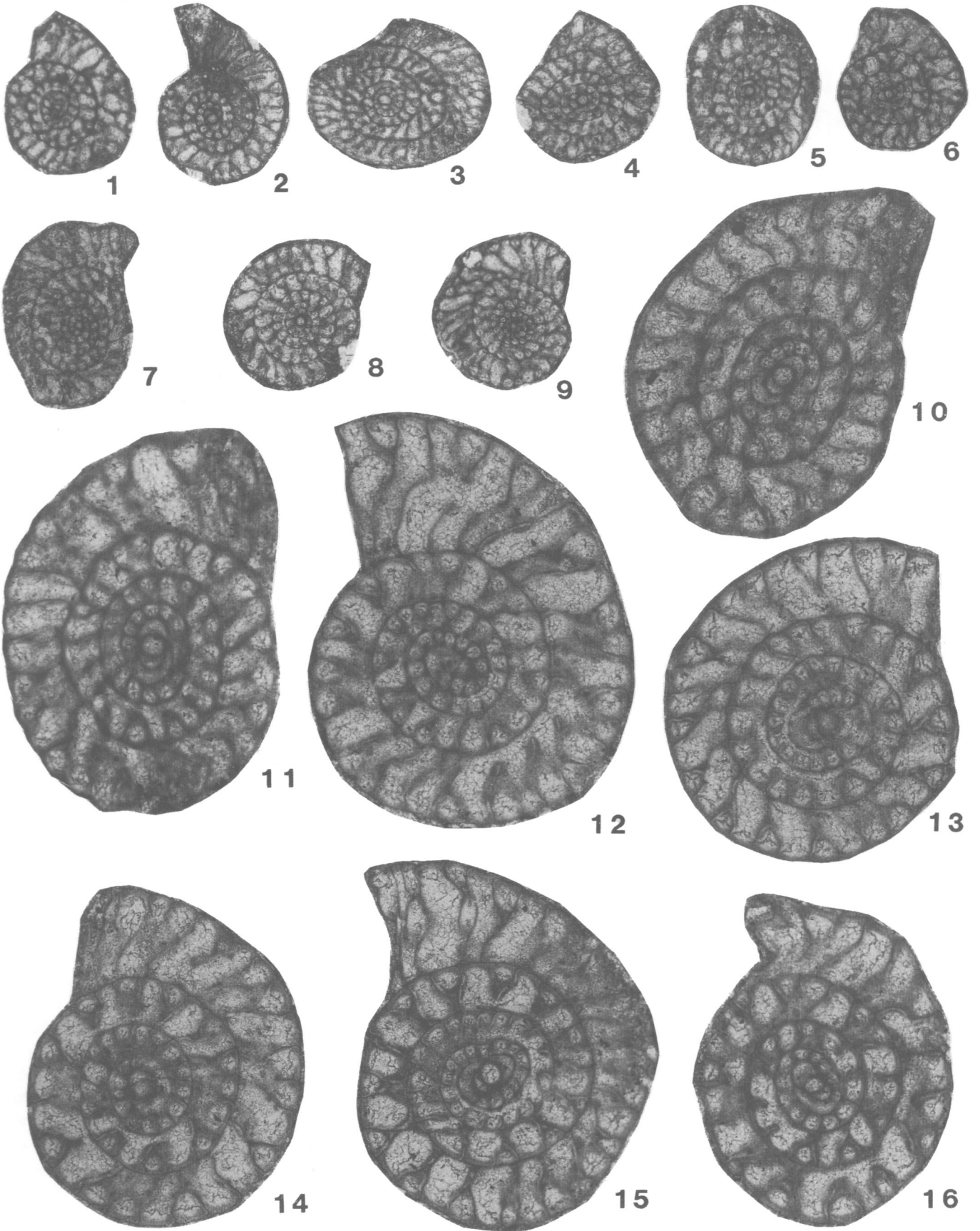
9



10

PLATE 15-9

FIGURES 1-16.—*Paraboultonia splendens* Skinner and Wilde: 1, sagittal section, ×35, USNM 462376, Coll. B1-87.5, Section 4, Bengue Ranch; 2, sagittal section, ×35, USNM 462377, Coll. B1-87.5, Section 4, Bengue Ranch; 3, sagittal section, ×35, USNM 462378, Coll. B1-87.5, Section 4, Bengue Ranch; 4, sagittal section, ×35, USNM 462379, Coll. B1-87.5, Section 4, Bengue Ranch; 5, sagittal section, ×35, USNM 462380, Coll. B1-87.5, Section 4, Bengue Ranch; 6, sagittal section, ×35, USNM 462381, Coll. B1-97.5, Section 4, Bengue Ranch; 7, sagittal section, ×35, USNM 462382, Coll. B1-87.5, Section 4, Bengue Ranch; 8, sagittal section, ×35, USNM 462383, Coll. B1-87, Section 4, Bengue Ranch; 9, sagittal section, ×35, USNM 462384, Coll. B1-97, Section 4, Bengue Ranch; 10, sagittal section, ×90, USNM 462385, Coll. B1-87.5, Section 4, Bengue Ranch; 11, sagittal section, ×90, USNM 462386, Coll. B1-97, Section 4, Bengue Ranch; 12, sagittal section, ×90, USNM 462387, Coll. B1-97, Section 4, Bengue Ranch; 13, sagittal section, ×90, USNM 462388, Coll. B1-83, Section 4, Bengue Ranch; 14, sagittal section, ×90, USNM 462389, Coll. B1-97, Section 4, Bengue Ranch; 15, sagittal section, ×90, USNM 462390, Coll. B1-97, Section 4, Bengue Ranch; 16, sagittal section, ×90, USNM 462391, Coll. B1-97, Section 4, Bengue Ranch. (Reduced to 94% of original for publication.)



16. Lithofacies and Depositional History of the Tessey Formation, Frenchman Hills, West Texas

Mohammad Haneef and Bruce R. Wardlaw

ABSTRACT

The Tessey Formation in the Frenchman Hills, northwestern Glass Mountains, represents deposition in a basinal setting. The formation consists of at least two shallowing-upward sequences of carbonate and evaporite deposition marked by two episodes of subaerial exposure, meteoric water dissolution, and collapse brecciation.

Introduction

The Tessey Formation is generally poorly understood. Udden (1917) first proposed the name Tessey Formation for an unstratified dolomitic rock located 3.2 km north of Gilliam (Gilliand) Canyon. It appears, however, that Udden (1917) included some fossiliferous Gilliam Limestone in the description of the unit because he referred to abundant fusulinids, which are absent from the Tessey as currently defined. King (1931) corrected most of the relationships of the Tessey as he described the unit as a poorly bedded dolomite and dolomitic limestone about 304.8 m (1000 ft.) thick that extends from Gilliam Canyon in the Glass Mountains to the hills southwest of Sierra Madera. About 6.4 km north of Sanderson Cabin, King found *Permophorous* concentrated in one bed. An arroyo 12 km S 75° W of the summit of Sierra Madera contains a coarsely brecciated mass of dolomite, sandstone, and gypsum that passes laterally into undisturbed Tessey strata. The coarse breccia represents a slump into a leached out, underground gypsum bed (King, 1931). King (1931) mapped the massive limestone breccia as the upper massive member of the Capitan

Mohammad Haneef, Geology Department, Sul Ross State University, Alpine, Texas 79832. Bruce R. Wardlaw, U.S. Geological Survey, 926A National Center, Reston, Virginia 20192.

Limestone in the Frenchman Hills and Bird (Altuda) Mountain, but they are better placed into the Tessey Formation. The purpose of this paper is to describe the Tessey exposed in the Frenchman Hills and to clarify its depositional history.

The Tessey Formation unconformably overlies the Gilliam Limestone (upper Guadalupian) in the eastern part of the Glass Mountains and the Altuda Formation in Old Blue Mountain and the Frenchman Hills. The upper boundary of the formation is an erosional unconformity with the Bisset Conglomerate (Cretaceous; Wilcox, 1986). The Tessey Formation lacks any recognizable fossils that can be used for assigning a relative age. It is regarded as laterally correlatable with the Ochoan Castile and Salado formations of the Delaware basin (Ross, 1986).

Subsurface well-log studies by Bloom (1988) show that the Tessey Formation was penetrated by wells drilled in the Hovey channel 8 km northwest of the Glass Mountains, near the Frenchman Hills. The Tessey Formation there consists of sparsely fossiliferous limestones, gray and brown in color, with anhydrite nodules and inclusions interbedded with red to brown calcareous, silty to sandy shales and dolomites of microcrystalline to finely crystalline texture. The limestone is reported to contain charophytes, ostracodes, and rare bryozoans, echinoderms, sponge spicules, foraminifers, calcispheres, peloids, intraclasts, and detrital quartz (Bloom, 1988). The anhydrite inclusions are composed of bladed to fine-grained "chicken wire" fabric. Locally brecciated peloidal wackestone-packstone was encountered for 4 m in the core from the Gunnel's Kim #1 drillhole. The thickness in the subsurface is reported as 700 m (Bloom, 1988).

Stratigraphy

The study area consists of three isolated erosional remnants of the Tessey Formation in the Frenchman Hills, northwestern Glass Mountains, approximately 1 km northwest of Old Blue Mountain (Figures 16-1, 16-2). The stratigraphic thickness of the Tessey Formation measured on the south side of hill 4544

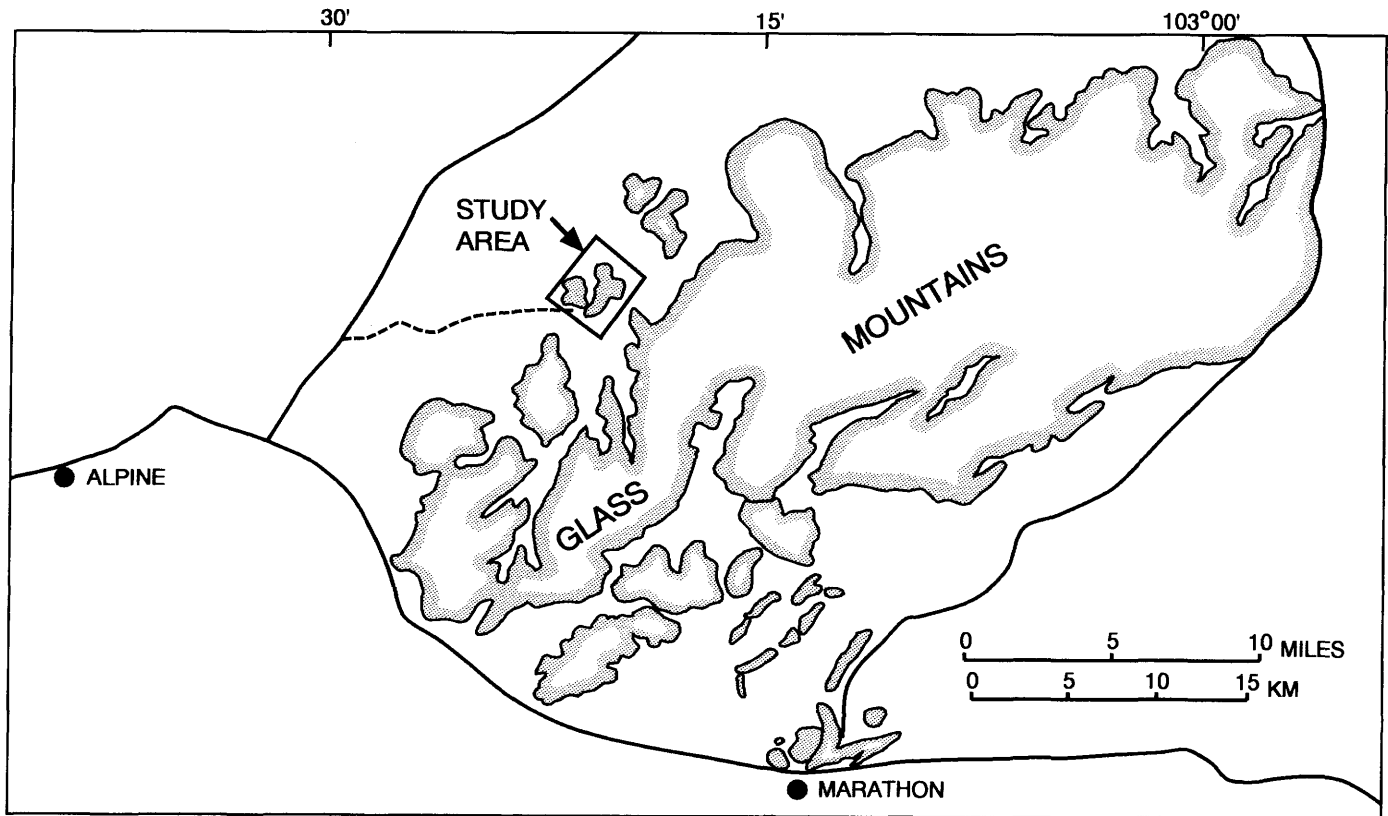


FIGURE 16-1.—Map of the Glass Mountains region with the study area indicated.

is 121.9 m (Figure 16-3). There the lower contact of the Tessey Formation is covered but appears to be conformable or paraconformable with basal facies of the Altuda Formation. Three lithically distinct units are recognized in this area (Figure 16-4A).

The basal unit defined informally as Tessey unit 1 (Tu1) is composed of fine (mm scale), evenly laminated lime mudstone with thin alternating laminae of calcitized anhydrite/gypsum with typical laminated to nodular to “chicken wire” fabric. The unit is 0.5–1.5 m thick and is present in the Frenchman Hills outcrop as well as in Old Blue Mountain. The unit is locally folded and intensely fractured with coarse, clear-calcite fracture infilling.

The middle unit (Tu2) is characterized by massive, slope forming, clast supported, spar-cemented, limestone breccia (Figure 16-4B). The unit is 45–83 m thick across the extent of the outcrop. No intact bedding was found in the entire area of the outcrop. The clasts are composed dominantly of light gray, gray, yellowish brown, to brown lime mudstone, sandstone, and siltstone and display a variety of shapes and sizes. The size of the clasts varies from a few millimeters to more than one-half meter. Clasts generally are angular with rare sub-rounded and rounded shapes. Clasts shapes are tabular, rectangular, blocky, and irregular. At the base and in a few

restricted horizons up-section, papery laminated lime mudstone in rectangular clast shapes predominate. Composition of the clasts varies from lime mudstone/dolomudstone, light gray, dark gray, and olive in color, to yellowish brown to brown, laminated siltstone and fine sandstone. Chert and dolomite clasts of various shapes and sizes are less abundant. The clasts are predominantly cemented by clear coarse sparry calcite. Matrix-supported breccias composed of dolomite clasts and matrix occur locally within the section. This unit contains conglomerate lenses or patches that are 1–2 m in lateral extent and about 0.5 m thick with round clasts of lime mudstone, sandstone, siltstone, quartz, and chert. The matrix of the conglomerates varies from lime-mud to fine silt and sand. The conglomerates are rarely cemented by sparry calcite. Unlike the Frenchman Hills outcrop, conglomerates are 4–7 m thick in Old Blue Mountain. The olive color lime mudstone clasts become the dominant lithology in the middle and upper part of the unit. The rocks show no bedding and weather into large circular blocks 4–5 m in diameter. Irregular, nonsutured stylolites with brownish residue occur throughout the unit. Clasts generally lack skeletal fragments.

The uppermost unit (Tu3) is characterized by matrix-supported carbonate breccia. The matrix and the clasts are composed of dolomudstone. The clasts are angular, irregular to

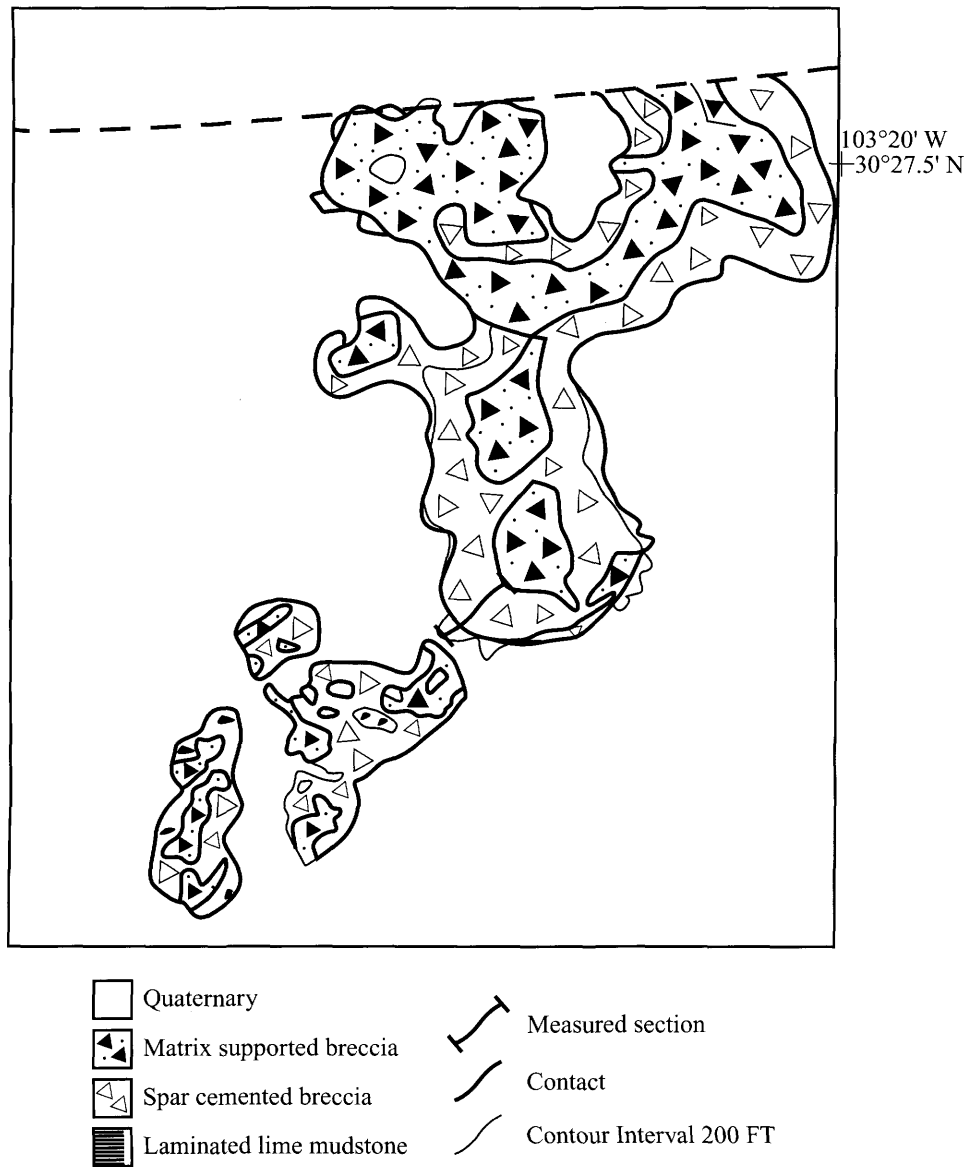


FIGURE 16-2.—Geologic map of the Frenchman Hills area of the Glass Mountains.

blocky in shape. Most clasts display lamination with fenestral fabric. Planar to wavy algal lamination containing bird's eye features, is typical. The unit is marked by hard, resistant, cliff-forming, massive beds. The contact of this unit with the lower spar-cemented breccia is irregular and mostly covered by its own debris. Northern outcrops have a matrix of pinkish siltstone.

Lithofacies

Based on lithic characteristics, two depositional facies comprising three lithostratigraphic units are recognized in the Frenchman Hills. These include the laminated lime mudstone/

calcitized anhydrite lithofacies and the matrix-supported dolomudstone lithofacies.

LAMINATED LIME MUDSTONE/CALCITIZED ANHYDRITE LITHOFACIES.—This lithofacies comprises the stratigraphic units Tu1 and Tu2 of the Tessey Formation. The lithofacies is characterized by the following features.

Papery Lamination: The basal beds of the Tessey Formation are composed of thin (mm scale), even, planar, non-algal laminations, locally folded and brecciated (Figure 16-4C,D). These basal beds are present throughout the study area. The lithofacies grades upwards into brecciated and folded beds and contains alternating clear calcite laminae. The calcite laminae exhibit nodular mosaic, enterolithic folding, and chicken wire

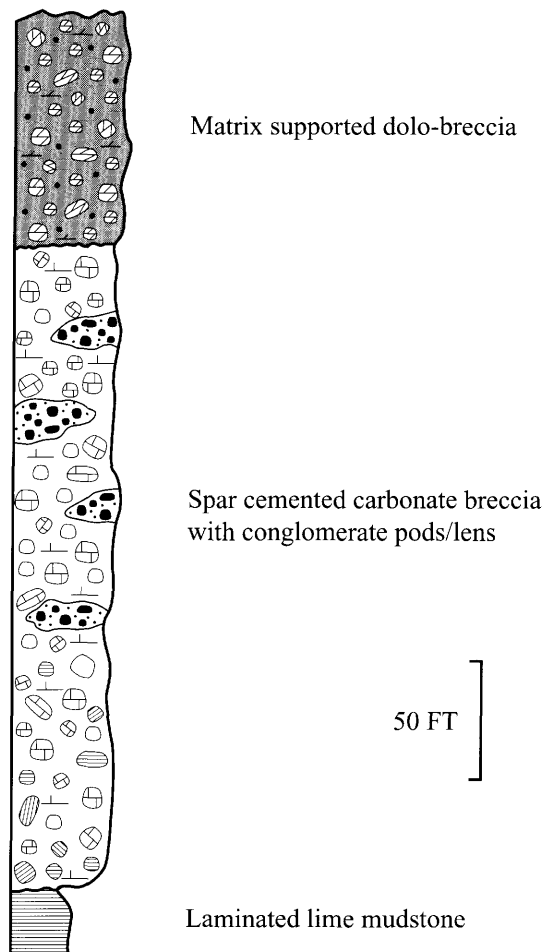


FIGURE 16-3.—Stratigraphic section in the Frenchman Hills. Location of the section is shown in Figure 16-2.

fabric similar to modern anhydrite (Figure 16-5A,B). The beds are devoid of any skeletal material.

Spar-Cemented Breccia: Stratigraphic unit 2 (Tu2) of the Tessey Formation is characterized by carbonate breccia with angular to subangular clasts with sharp edges. The breccia composition is dominated by laminated lime mudstone clasts with a subordinate amount of sandstone, laminated siltstone, and rare chert fragments. The distinct feature of these breccias is the presence of coarse calcite as both a cement and as fracture fill (Figure 16-5C,D). The cements include equant and circumgranular equant spar.

Polymictic Conglomerate: Interbedded with the breccias are isolated pods and lenses of conglomerate. The conglomerate is composed of rounded clasts of laminated to nonlaminated lime mudstone, fossiliferous mudstone, dolomudstone, silty dolomudstone, siltstone, and chert (Figure 16-6A). The matrix is composed of angular to subangular quartz silt and sand, micritized grains, and varying amounts of lime-mud and

dolomite-mud. Coarse spar coating of the grains or cavity fill is present.

Scalloped Surfaces: The contact of the spar-cemented breccia with the underlying laminated lime mudstone and overlying matrix-supported breccia is highly irregular, producing scalloped surfaces.

MATRIX-SUPPORTED DOLOMUDSTONE LITHOFACIES.—This lithofacies comprises stratigraphic unit Tu3 and is distinguished by its clast lithology and dolomite fabric. Exposures have irregular contacts and draping beds.

Clast Lithology: The lithofacies is dominated by rectangular to tabular dolomudstone clasts exhibiting planar to wavy, algal lamination and fenestral fabric (Figures 16-6B, 16-7A,B). Laminations are thin, planar to wavy and display alternating layers of light dolomudstone and dark organic-rich algal layers. Other clasts include nonlaminated dolomudstone, peloidal dolowackestone, and silty dolomudstones. The matrix is predominantly dolomudstone with minor quartz silt and sand.

Dolomite Fabric: The breccia is characterized by fine, euhedral, equigranular dolomudstone, both as clasts and matrix. The dolomite is interpreted to be penecontemporaneous in origin. Algal laminated dolomudstone clasts and matrix support this interpretation.

Interpretation

The laminated lime mudstone/calcitized anhydrite lithofacies is interpreted herein as a solution collapse breccia formed as a result of karstification of a shallowing-upwards evaporitic basinal facies (Figure 16-8). The presence of evaporite fabric, pyrite, and an unfossiliferous lime mudstone lithology indicates that the lithofacies was deposited in hypersaline, reducing (anaerobic?) environments. This interpretation is further supported by the presence of thick interbeds of anhydrite and gypsum in the Tessey Formation of the subsurface (King, 1931; Bloom, 1988) and the overall restricted hypersaline basinal conditions in the Permian basin at the onset of Ochoan time (King, 1931; Ross, 1986). The sediments were deposited in deep water, not in a subaerial environment, as evidenced by the absence of algal stromatolites and desiccation structures that normally are associated with subaerial or peritidal conditions. The deeper water origin is supported by the presence of parallel laminations and by alternating lime mudstone/calcite (originally calcium sulphate) couplets. Studies in the Castile Formation of Texas and New Mexico by Anderson and Kirkland (1966) and Anderson et al. (1972), and studies of similar couplets in western Canada by Davis and Ludlam (1973) and Wardlaw and Reinson (1971) favor this interpretation. Kendall (1984) ascribed the presence of planar laminations to stagnant, permanently stratified bodies of water.

The third phase (Figure 16-8) of laminated lime mudstone/calcitized anhydrite facies development is marked by subaerial exposure, meteoric dissolution of evaporites, and the subse-

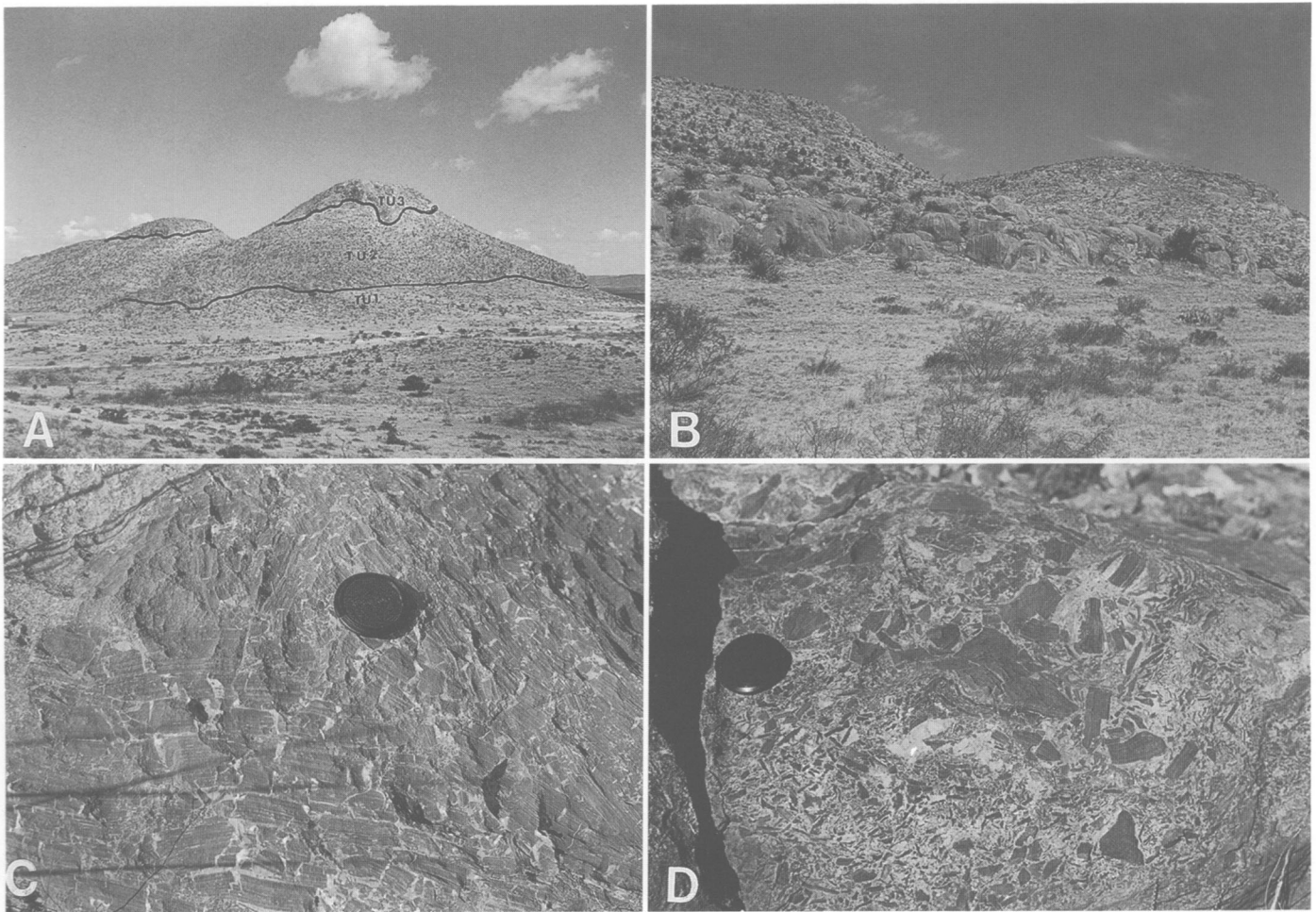


FIGURE 16-4.—A, outcrop of Tessey Formation at Frenchman Hills in the Benge Ranch area showing various stratigraphic units. Tu1, laminated lime mudstone; Tu2, spar-cemented breccia; and Tu3, matrix-supported breccia. Note the irregular contact between the units. B, spar-cemented limestone breccia weathering in large circular blocks at the base of the Frenchman Hills outcrop. C, view of locally folded laminated lime mudstone unit (Tu1). D, view of intensely brecciated spar-cemented breccia (Tu2). The size of the clasts varies from a few millimeters to more than 20 centimeters. Note spar infilling of fractures. (Camera lens cap is 5.5 cm in diameter.)

quent collapse brecciation of the suprastructure. It is presumed that extensive dissolution of evaporites and carbonates was achieved by the development of a subterranean erosional landscape associated with karst. The lack of intact bedding and karst related geomorphic features, such as dolines, rundkarren, and kamenitzas, which are regarded as paleokarst indicators, is attributed to complete dissolution and subsequent brecciation. The presence of extensive intraformational brecciation, nonferroan, nonluminescent, coarse blocky calcite, and speleothems attest to this interpretation. The subaerial exposure might have been achieved by the filling of the basin and/or a drop in sea level. Scalloped surfaces at the top of the lithofacies represents an erosional unconformity.

The matrix-supported dolomudstone lithofacies is interpreted as a collapse breccia of a shallowing-upwards sequence

of intertidal/supratidal (sabkha) dolostones. Initial deposition of the matrix-supported dolomudstone lithofacies marks the return (or near return) of marine waters following the exposure that created the lower breccia. The common algal lamination and the fenestral fabric of the clasts and matrix indicate deposition on a frequently exposed tidal flat. The collapse brecciation of the intertidal/supratidal sequence did not take place at the same time as the brecciation of the lower lithofacies. This is evident from the presence of two discrete lithofacies. One collapse brecciation would have resulted in the vertical mixing of lithologies. A second collapse brecciation of the original intertidal/supratidal sequence probably resulted from a further drop in sea level. The area was subaerially exposed, resulting in fresh water dissolution and the formation of collapse breccia (Figure 16-8).

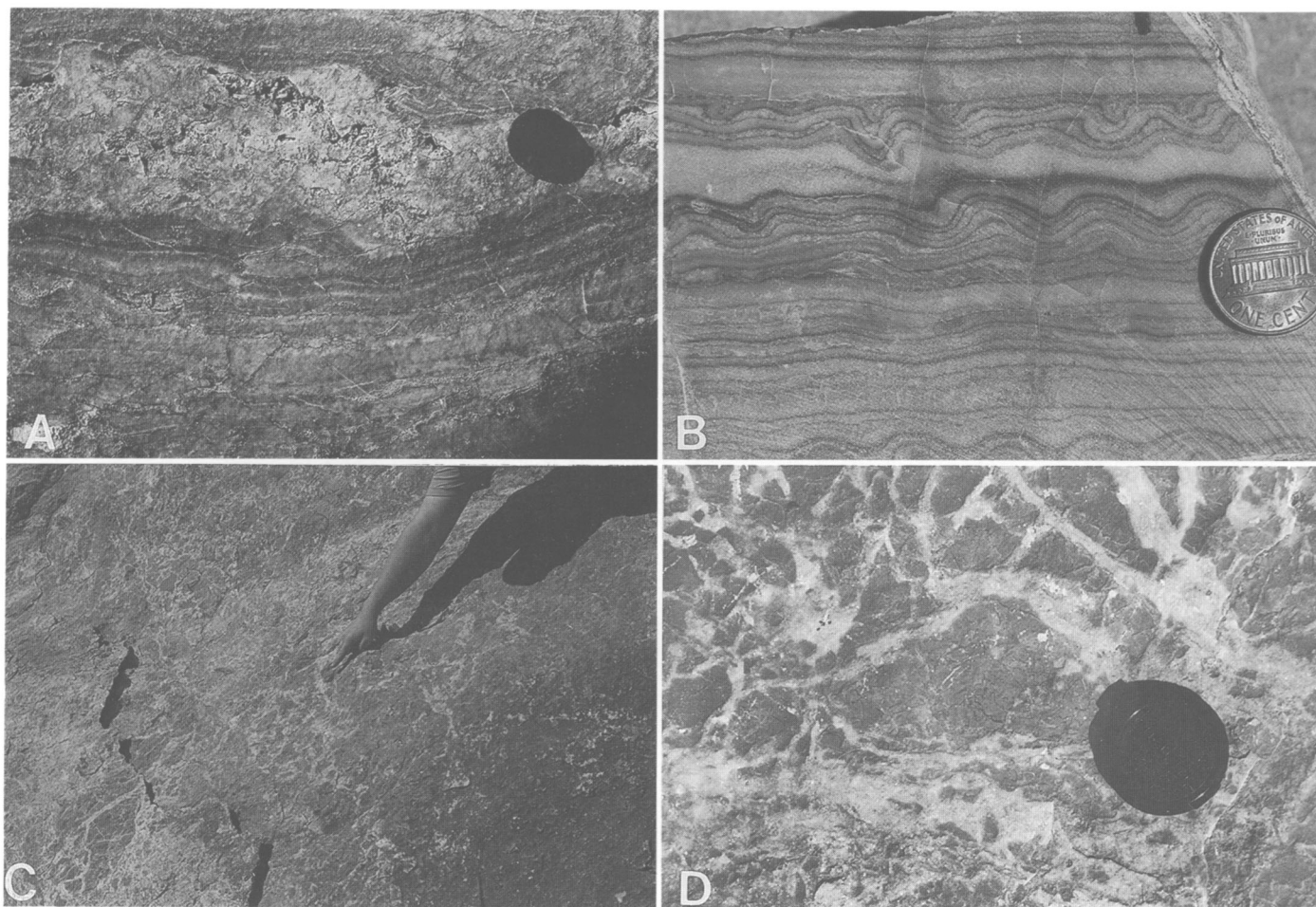


FIGURE 16-5.—A, view of laminated to relic anhydrite nodular mosaic fabric in the laminated lime mudstone/calcitized anhydrite lithofacies. (Camera lens cap is 5.5 cm in diameter.) B, photograph of polished slab showing enterolithic folding in the laminated lime mudstone/calcitized anhydrite lithofacies. C, view of outcrop surface of spar-cemented breccia of Tu2. D, close-up of area shown in C. (Camera lens cap is 5.5 cm in diameter.)

Literature Cited

- Anderson, R.Y., and D.W. Kirkland
1966. Intrabasin Varve Correlation. *Bulletin of the Geological Society of America*, 77(3):241–256, plates 1–5.
- Anderson, R.Y., W.E. Dean, Jr., D.W. Kirkland, and H.I. Snider
1972. Permian Castile Varved Evaporite Sequence, West Texas and New Mexico. *Bulletin of the Geological Society of America*, 83(1):59–86.
- Bloom, M.A.
1988. A Subsurface Geologic Study of Northern Brewster County, Texas. 150 pages. Unpublished master's thesis, Sul Ross State University, Alpine, Texas.
- Davis, G.R., and S.D. Ludlam
1973. Origin of Laminated and Graded Sediments, Middle Devonian of Western Canada. *Bulletin of the Geological Society of America*, 84(11):3527–3546.
- Kendall, A.C.
1984. Evaporites. In R.G. Walker, editor, *Facies Models*. Geoscience Canada Reprint Series # 1, 2nd edition, pages 259–296.
- King, P.B.
1931 (“1930”). The Geology of the Glass Mountains, Texas, Part I: Descriptive Geology. *University of Texas Bulletin*, 3038: 167 pages, 15 plates. [Date on title page is 1930; actually published in 1931.]
- Ross, C.A.
1986. Paleozoic Evolution of Southern Margin of Permian Basin. *Bulletin of the Geological Society of America*, 97(5):536–554.
- Udden, J.A.
1917. Notes on the Geology of the Glass Mountains. *University of Texas Bulletin*, 1753: 59 pages.
- Wardlaw, N.C., and G.E. Reinson
1971. Carbonate and Evaporite Deposition and Diagenesis, Middle Devonian Winnipegosis and Prairie Evaporite Formations of South-Central Saskatchewan. *Bulletin of the American Association of Petroleum Geologists*, 55(10):1759–1786.
- Wilcox, R.E.
1986. Evidence for an Early Cretaceous Age for the Bissett Formation, Western Glass Mountains, Brewster and Pecos Counties, West Texas: Implications for Regional Stratigraphy, Paleogeography, and Tectonics. 250 pages. Unpublished master's thesis, Sul Ross State University, Alpine, Texas.

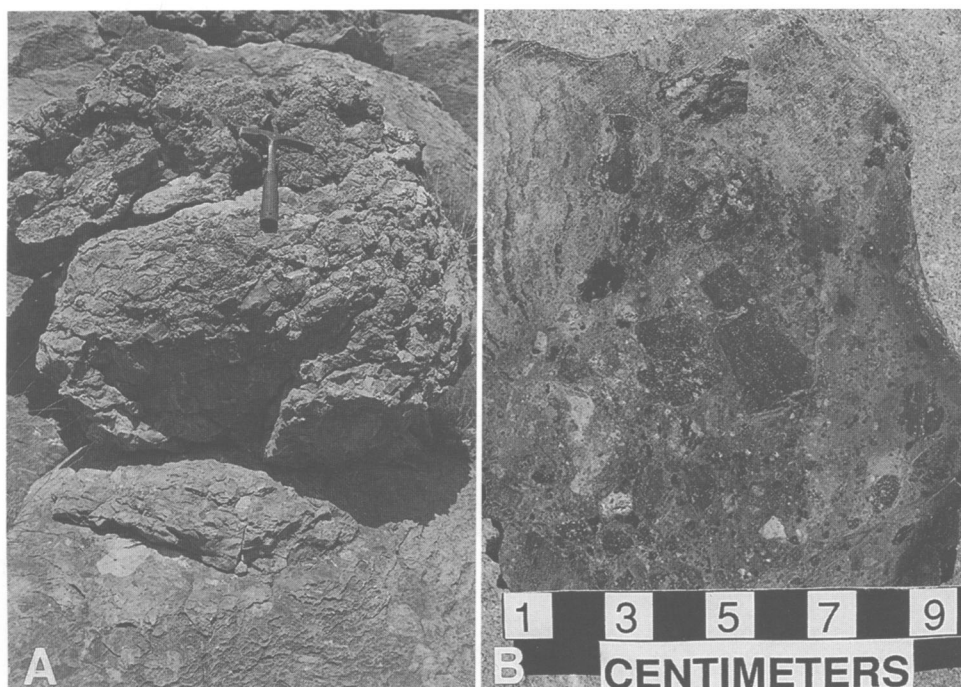


FIGURE 16-6.—A, view of polymictic conglomerate in Tu2. Note the size variation and roundness of the clasts. Clast lithologies consist of lime mudstone, dolomudstone, silty dolomudstone, and siltstone. B, close-up of matrix-supported dolomudstone breccia. Note the algal-laminated dolomudstone clasts. (Hammer is 28 cm in length.)

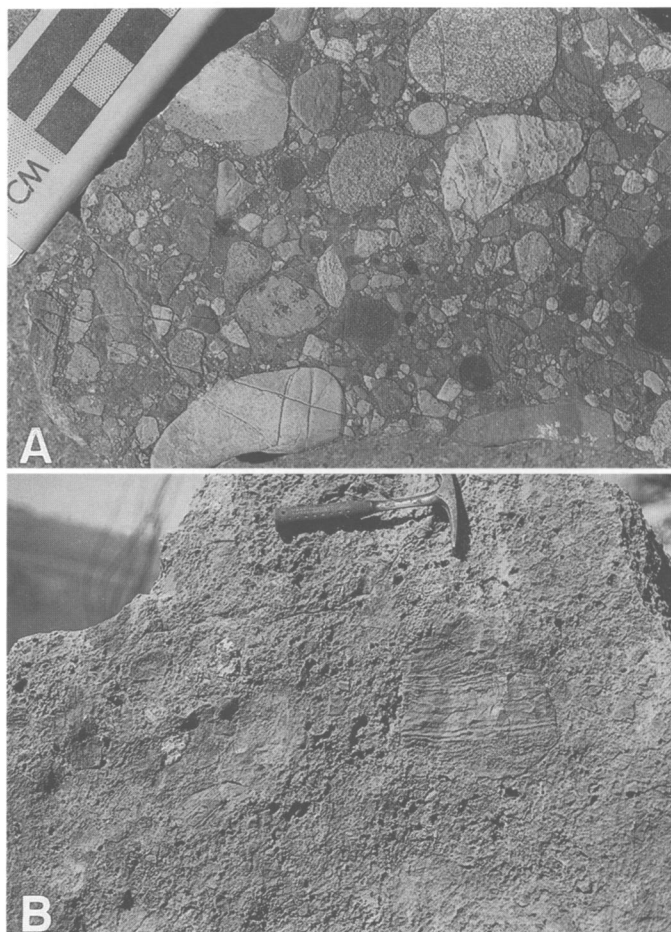


FIGURE 16-7 (right).—A, view of weathering surface of matrix-supported dolomudstone breccia (Tu3). B, polished slab of matrix-supported dolomudstone breccia showing brecciated fabric.

17. Conodont Biostratigraphy of the Permian Beds at Las Delicias, Coahuila, Mexico

*Bruce R. Wardlaw, Shannon F. Rudine,
and Merlynd K. Nestell*

ABSTRACT

Conodont faunas from the basinal deposits of the Permian near Las Delicias, Mexico, are dominated by shallow-water species of *Hindeodus*. Three long-ranging *Hindeodus* zones, similar to those recognized in shallow-water deposits in much of the world, are *H. excavatus*, *H. wordensis*, and *H. julfensis*. The conodonts indicate an age range for the Permian deposits from Sakmarian to Dzhulfian. The conodonts and brachiopods are closely related to those from the Permian basin of West Texas.

Introduction

The Permian rocks near Las Delicias, Coahuila, Mexico, are of great interest because they have yielded excellent ammonoid collections of much of the Permian, including some of the youngest Permian preserved in North America. However, the geology of the area is far from clear, and the Permian rocks are remote and difficult to access. The area has been visited by many parties of geologists that included King et al. (1944), Newell (1957), Spinosa et al. (1970), Wardlaw et al. (1979), and McKee et al. (1988).

General Geology

The Permian rocks of Las Delicias are exposed in an arcuate pattern below the steep cliffs and high mountains of Cretaceous

limestone to the west (Figure 17-1). One narrow pass through the high mountains exposes lower beds of the Permian sequence. The structure of the Permian rocks is dominated by a major syncline (as mapped by King et al., 1944; and Wardlaw et al., 1979). This syncline is disrupted by normal faults that trend to the northeast and locally fold the beds (Figure 17-2). McKee et al. (1988) interpreted the geology much differently, as they reported a major syncline disrupted by northwest-trending faults and also confused the basal conglomerate as part of their volcanic chaotic lithosome on the eastern flank of the syncline (the southwestern tip of the outcrop, Figure 17-1). This later interpretation is highly implausible because fossils collected by King et al. (1944), Wardlaw et al. (1979), and even McKee et al. (1988) clearly indicate Early Permian in the southern portion of the outcrop belt. The beds in question yielded the oldest fauna from the basal unit of the Permian succession (Las Sardinias beds) (see Gordon and Wardlaw, written comm., in McKee et al., 1988:39).

The sequence is very difficult to map as it is covered by a thick pediment that supports a lush cover of *Lechiguia* plants. Exposures are generally along the arroyos that cut through the pediment and in resistant beds that stand as hills above the pediment. The geology is such that there is tremendous lateral variability. The several ammonoid shales of King et al. (1944) and modified by Spinosa et al. (1970; i.e., *Perrinites*, *Waagenoceras*, *Timorites*, *Kingoceras*, and *Eoaxoceras*) can be traced from arroyo to arroyo with reliability. Two major resistant units that form a string of hills throughout the area are critical to mapping the geology. The first unit is composed of two prominent limestone block-bearing megabreccias in close stratigraphic succession (referred to by Wardlaw et al., 1979, as the La Difunta limestone beds). These beds can be traced throughout the area (Figure 17-2) and can be easily followed. It was the consistency of these beds that unraveled the geology for Wardlaw et al. (1979), but it also led them astray in their interpretation as they could not imagine a megabreccia that

Bruce R. Wardlaw, U.S. Geological Survey, 926A National Center, Reston, Virginia 20192. Shannon F. Rudine, Geology Department, Sul Ross State University, Alpine, Texas 79832. Merlynd K. Nestell, Geology Department, University of Texas, Arlington, Texas 76019.

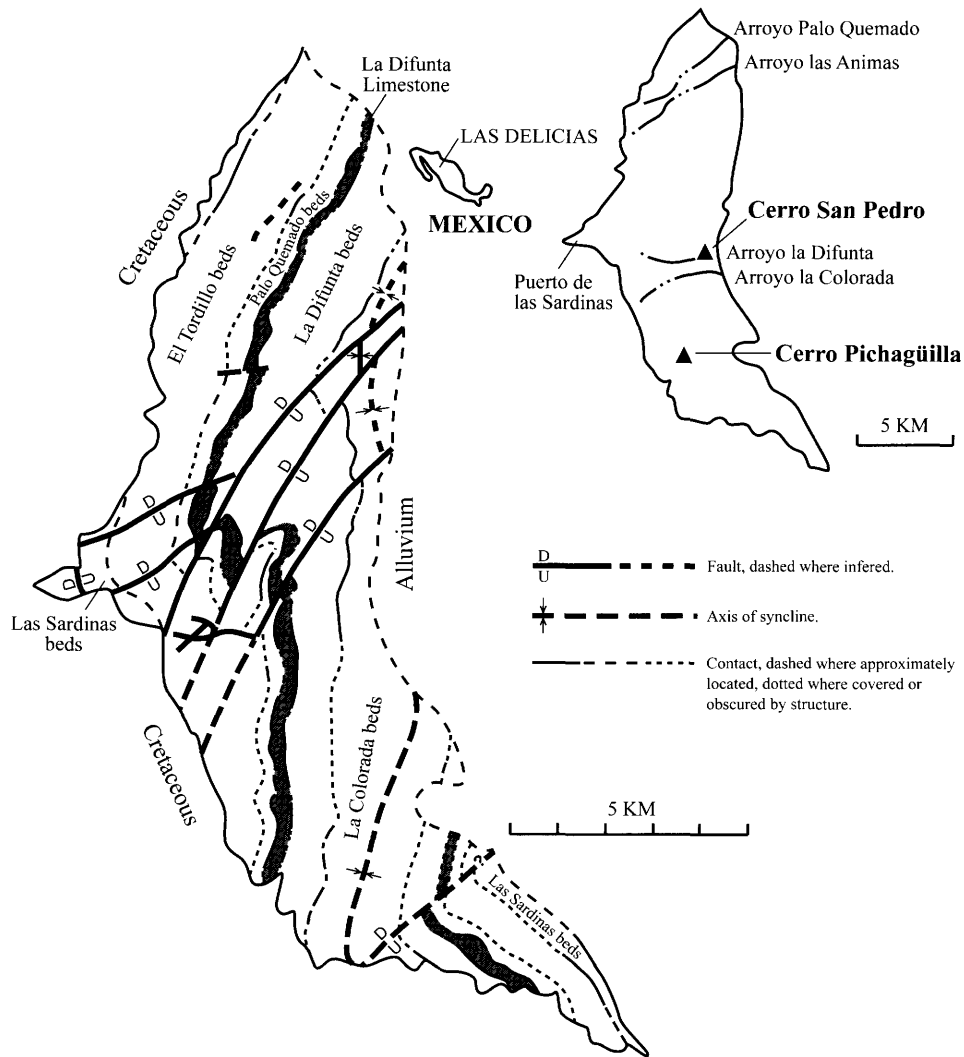


FIGURE 17-1.—Location and geologic map of the Permian beds at Las Delicias, Coahuila, Mexico.

cropped out the entire length of the mapped area (over 21 km). The second unit is a volcanic megabreccia (volcanic chaotic lithosome of McKee et al., 1988). This unit also can be traced throughout most of the area in the upper part of the section. It occurs just above the *Timorites* shale.

General Stratigraphy

The general informal units proposed by Wardlaw et al. (1979) are still the most useful division of the sequence at Las Delicias. The units are, in ascending order, as follows: (1) the Las Sardinas beds, (2) the El Tordillo beds, (3) the Palo Quemado beds, (4) the La Difunta beds, and (5) the La Colorada beds. The Las Sardinas beds are composed of a basal conglomerate and the overlying *Perrinites* shale. The El Tordillo beds are a thick sequence dominated by graywackes

between the underlying *Perrinites* shale and the overlying *Waagenoceras* shale. The Palo Quemado beds are composed of the *Waagenoceras* shale and overlying graywackes, shales, and tuffaceous sands. The La Difunta beds start with the marker unit, the limestone megabreccia, which is largely overlain by graywackes. In the upper part of the La Difunta beds is a laterally inconsistent limestone megabreccia lying just beneath the *Timorites* shale, which makes up the top of the unit. The La Colorada beds are marked at their base by the volcanic megabreccia and overlain by graywackes, conglomerates, and the *Kingoceras* and *Eoaraxoceras* shales (Figure 17-3).

LAS SARDINAS BEDS.—The lower part of the Las Sardinas beds are composed of conglomeratic shales and graywackes (Figure 17-4A,B). Most clasts are cobble- to boulder-sized, igneous rock, graywacke, and limestone. The matrix is sandy shale to coarse graywacke; the shale has slaty cleavage. The

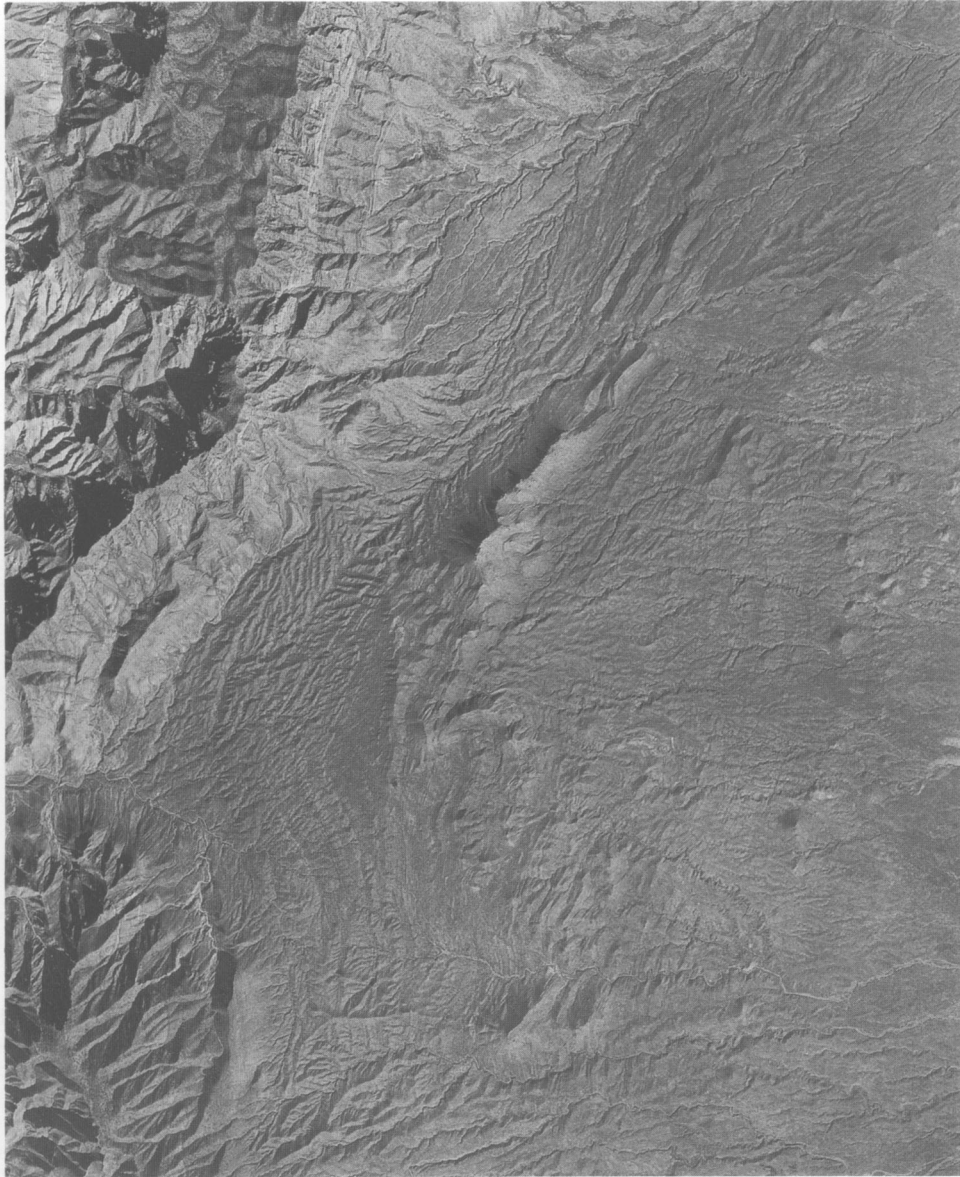


FIGURE 17-2.—Aerial photograph of the Permian beds at Las Delicias and surrounding Cretaceous highlands clearly showing major structural faults and folds of the beds.

limestone clasts are mostly crinoidal packstone to grainstone with scattered skeletal packstone and wackestone containing bryozoans, fusulinids, and brachiopods in addition to crinoids. The ammonoid *Perrinites* was found within the conglomeratic beds in matrix. The remainder of the fauna recovered from these beds was reported by Wardlaw et al. (1979) and indicates a Permian, probably Artinskian to Leonardian age (conodont stages of Wardlaw, 1994). The base of the conglomeratic beds was not observed.

The upper part of the Las Sardinias beds is composed of the *Perrinites* shale. This is a thick black shale with common lime mudstone concretions in its upper and lower parts, which are

separated by a dark sandy shale. The limestone concretions yield an abundant ammonoid fauna, but mollusks other than ammonoids are rare. Plant leaves and brachiopods are also common. One large petrified gymnosperm log also was found in the shale. Conodonts are common to the concretions. The base of the *Perrinites* shale is undulatory.

EL TORDILLO BEDS.—The El Tordillo beds consist of a thick section of graywackes, thin impure shales and siltstones, and thin dirty skeletal limestones (mudstones to wackestones) with the skeletal elements barely recognizable. One S element to *Hindeodus* sp. was recovered from one of the thin limestones. Near the top of the El Tordillo beds are graywackes interbedded

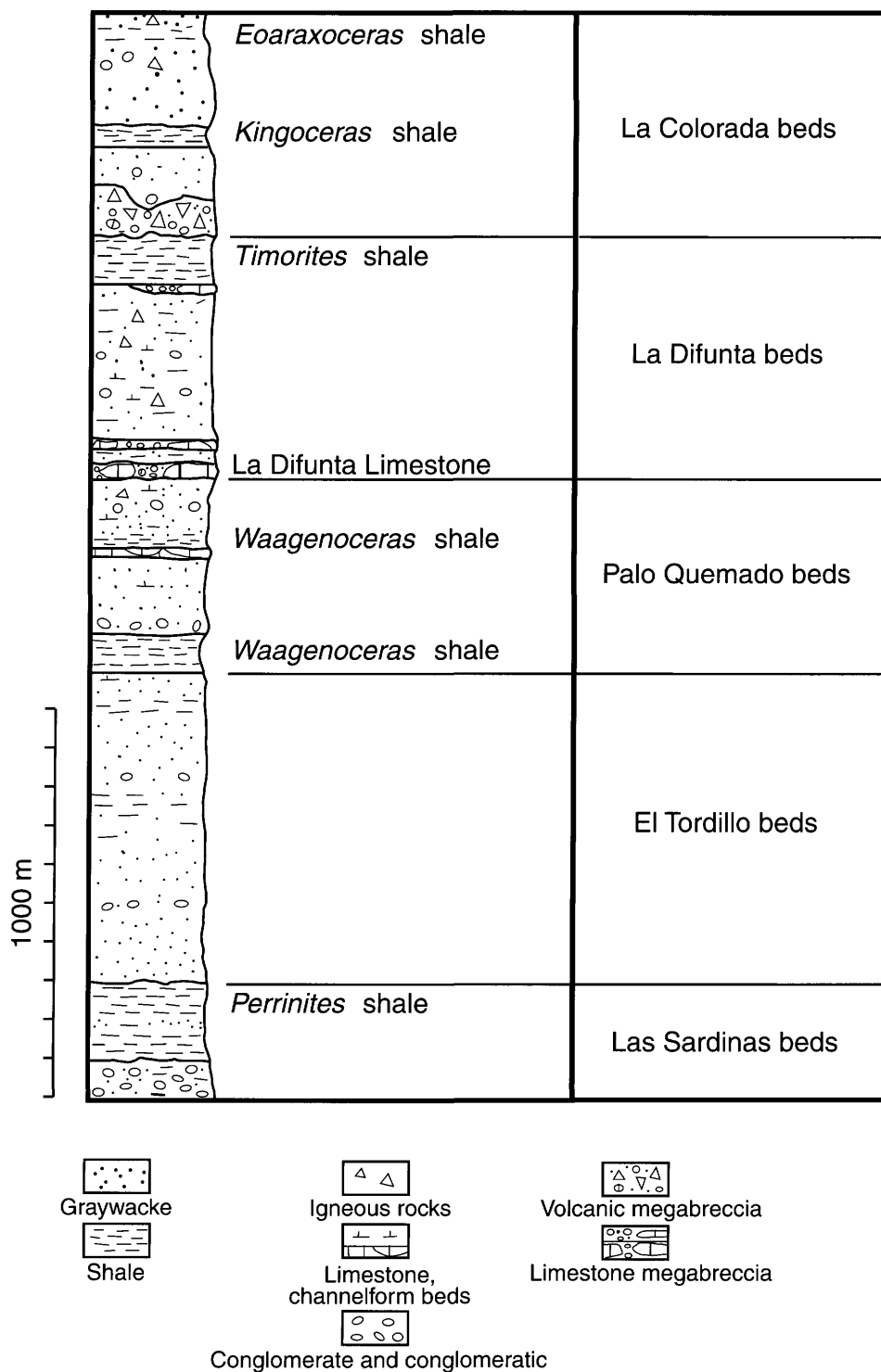


FIGURE 17-3.—Columnar section of the Permian rocks at Las Delicias.

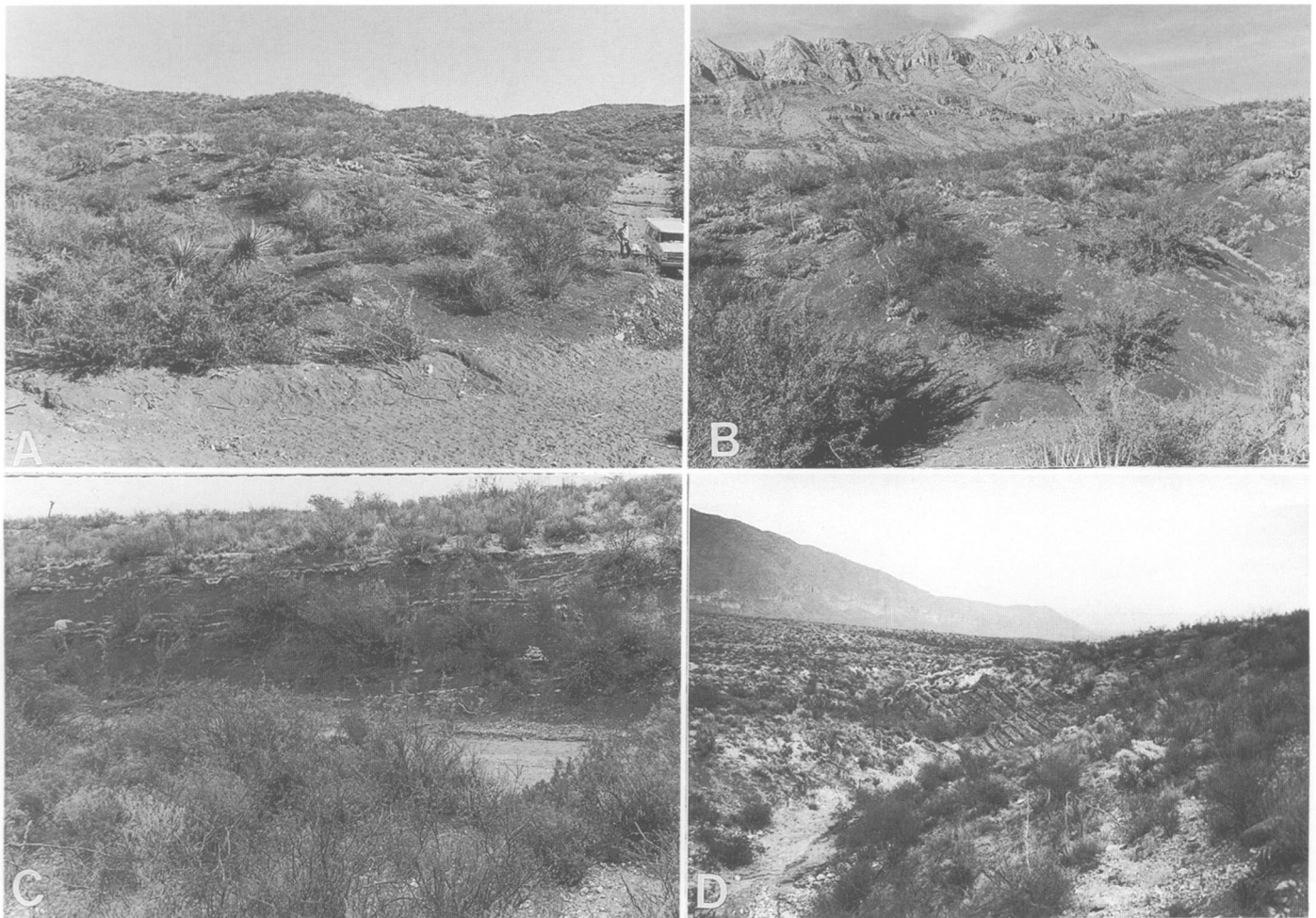


FIGURE 17-4.—Photographs of Las Sardinias, El Tordillo, and Palo Quemado beds. A,B, *Perrinites* shale in Puerto de las Sardinias. C, *Waagenoceras* shale along Arroyo las Animas. D, interbedded graywackes and radiolarian cherts in the El Tordillo beds near El Tordillo.

with thin radiolarian-rich shales (Figure 17-4D). Rip-ups of the shales are common in the graywackes. Some of the graywacke beds show a cross-bedded conglomeratic top. The radiolarians appear to be too badly preserved to be useful. The base of the El Tordillo beds is undulatory.

PALO QUEMADO BEDS.—The Palo Quemado beds show the greatest diversity of lithic units, which are dominated by graywackes, but contain many varied channeliform and turbiditic mixed units (Figures 17-4C, 17-5A,C,D, 17-6A-D, 17-8B, 17-10A). Channeliform beds include tuffaceous sandstone, sandy limestone, limey conglomeratic sandstone, and limey and silty mudstone. The channeliform beds commonly display cross-bedding and pinching and swelling of beds, especially in the upper part of the unit. Many of the graywackes are locally conglomeratic with mixed lithoclasts, including sandstone, skeletal limestone, and chert. The skeletal limestone lenses are generally sandy and commonly contain abundant

broken and abraded skeletal debris. One igneous sill was identified in close proximity to a large tuffaceous sandstone channel in the Arroyo las Animas. The tuffaceous sandstone channel displays scour and load features and abundant soft sediment deformation. Also close to the tuffaceous sandstone is a megabreccia with vague boundaries laterally merging with a conglomeratic graywacke. The megabreccia is composed of tuffaceous conglomerate clasts in tuffaceous conglomerate, graywacke clasts, sandy mudstone clasts, and conglomeratic fusulinid limestone clasts with a graywacke matrix. An ammonoid was floating in the matrix as a clast (Figure 17-9C,D). Two black shales, referred to as the *Waagenoceras* shale (Spinosa et al., 1970), occur within the unit; one marks the base of the unit, and the other marks the middle. The lower *Waagenoceras* shale has a sharp contact with the underlying El Tordillo beds. Limestone nodules within the lower *Waagenoceras* shale are scarce in the lower part and contain a sparse

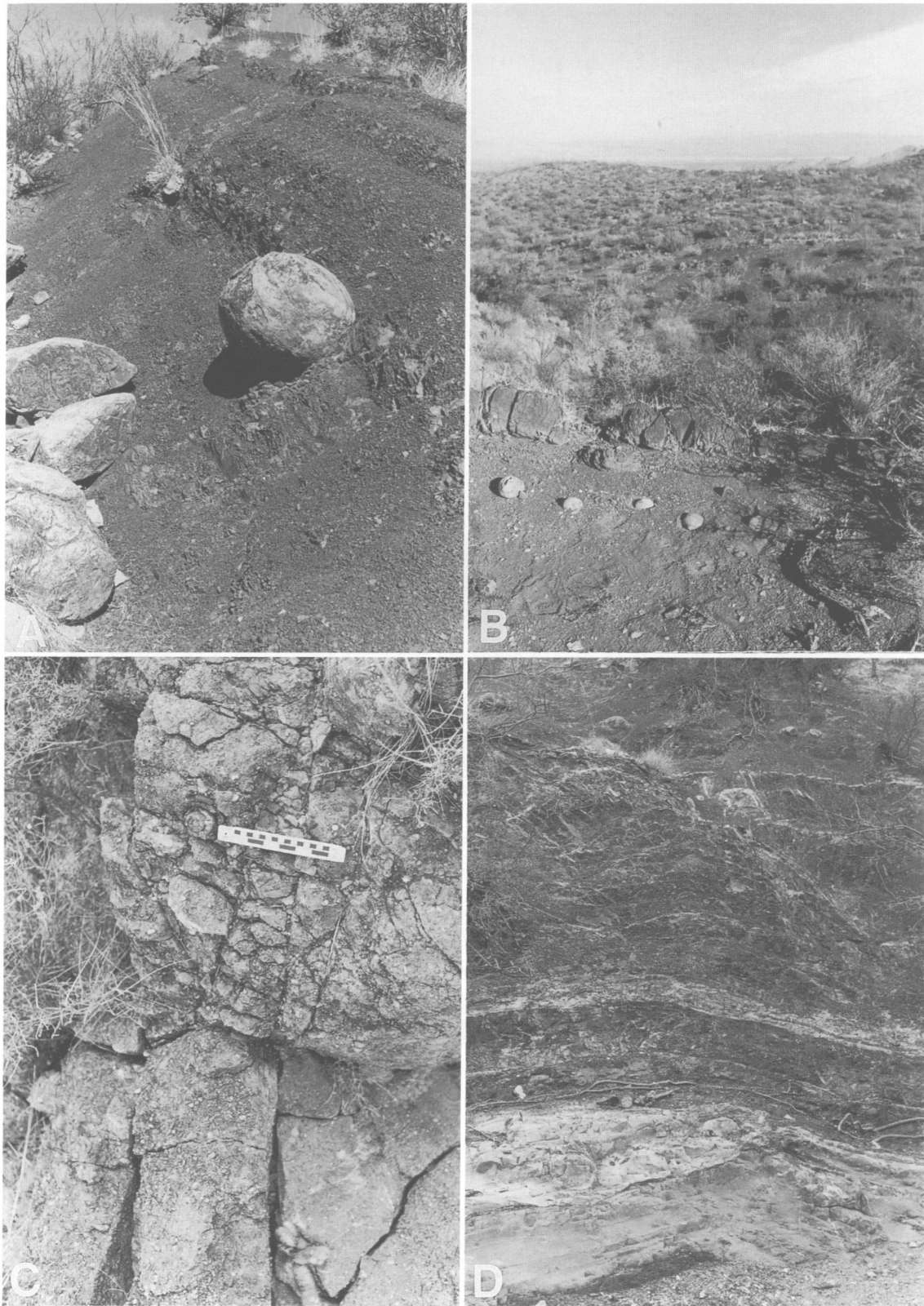


FIGURE 17-5.—Photographs of ammonoid occurrences. A, large concretion in *Waagenoceras* shale in Arroyo las Animas. B, concretion bed in *Timorites* shale between Arroyo la Difunta and Arroyo la Colorada. C, *Waagenoceras* in skeletal conglomerate of Palo Quemado beds along Arroyo las Animas. D, *Waagenoceras* shale in Arroyo las Animas.

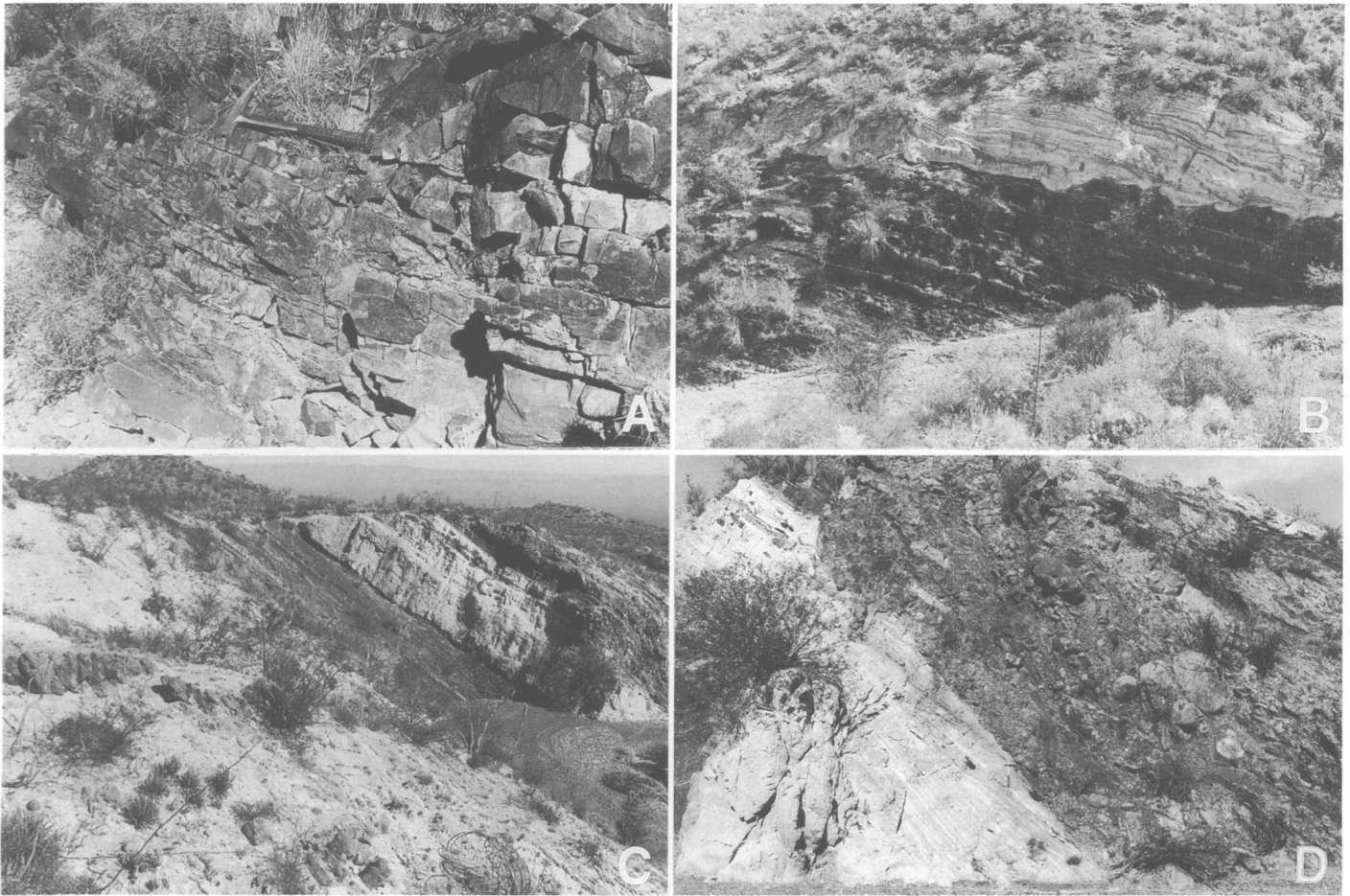


FIGURE 17-6.—Photographs of Palo Quemado beds. A, cross-bedded sandstone channel. B, large irregular body of tuffaceous sandstone. C, D, tuffaceous sandstone overlain by chaotic conglomerate, from a distance and close-up (hammer as scale).

fauna of brachiopods, echinoids, ammonoids, clams, fish debris, and conodonts. Nodules become more abundant, silty, and larger in the upper part of the lower *Waagenoceras* shale and contain poorly preserved bryozoans, ammonoids, and conodonts. The upper *Waagenoceras* shale is a thinner bed than the lower shale and becomes alternating graywacke and sandy mudstone in its upper part. It contains nodules with conodonts and ammonoids. The brachiopods, ammonoids, and fusulinids recovered from this unit are listed in Wardlaw et al. (1979).

LA DIFUNTA BEDS.—The La Difunta beds are characterized by two limestone megabreccias at its base, which crop out for the entire length of the outcrop area, and are referred to as the La Difunta limestone (Figures 17-5B, 17-7A, 17-8A,C,D, 17-10B-D). These limestone megabreccias generally consist of a skeletal limestone conglomerate composed of granule- to cobble-sized clasts dominated by crinoidal packstone in a graywacke matrix throughout its extent. Locally, large blocks of the limestone megabreccia form resistant hills. The limestone blocks vary from a few meters to nearly a kilometer in width and a few to nearly 100 meters in height. The

composition of the limestone blocks is of three types: (1) recrystallized limestone or dolostone with poorly preserved primary features appearing very much like the Capitan Limestone in West Texas; (2) sponge framestone, boundstone, and floatstone; and (3) bryozoan-brachiopod (*Sestropoma*) framestone, bafflestone, and packstone. The limestone blocks are always associated with the skeletal limestone conglomerate. The conglomerate is generally below and to the sides of the blocks and rarely occurs above the blocks. To complicate the issue, the area of Permian exposure is an exhumed pediment with many large exotic limestone blocks across the surface. Typically, these exotic blocks are recrystallized limestone from the nearby Cretaceous cliffs, but rarely, Permian limestone blocks are also encountered. These exotic blocks are always floating in the alluvium and not in the skeletal limestone conglomerate. The bases of the limestone megabreccias are very undulatory.

The middle part of the La Difunta beds is similar to the Palo Quemado beds, in that they are dominated by graywacke, but they are less variable with fewer channels and more volcano-

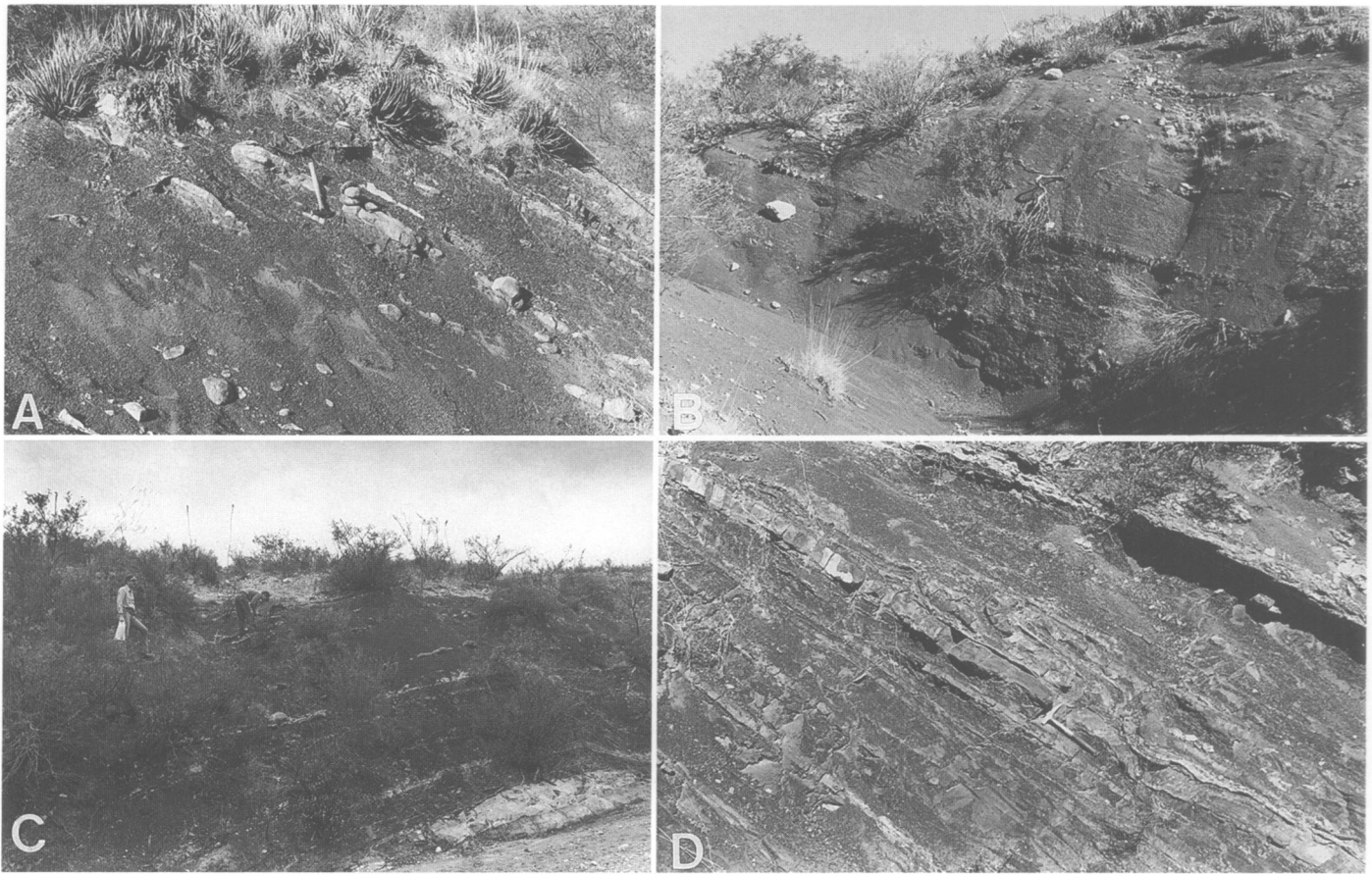


FIGURE 17-7.—Photographs of ammonoid-bearing shales. A, *Timorites* shale between Arroyo la Difunta and Arroyo la Colorada. B, *Kingoceras* shale along Arroyo la Colorada. C, *Eoaraxoceras* shale along Arroyo la Colorada. D, *Kingoceras* shale along Arroyo la Colorada; note S-fold in beds showing soft-sediment deformation.

clastic clasts in the graywacke. The upper part of the La Difunta beds consists of a local limestone megabreccia and the *Timorites* shale. The limestone megabreccia is typified by the limestone block at Cerro Pichaguilla, which is composed of a bryozoan-brachiopod-crinoid packstone to framestone. The *Timorites* shale is a thick black shale traceable throughout the area. It has a sharp contact with the underlying limestone megabreccia or graywacke. Limestone concretions are spread throughout the unit but commonly occur in three zones, namely, near the base, middle, and top. The lower concretion zone is a narrow zone, only about 3 m thick, immediately below a sandy skeletal limestone to limy skeletal graywacke that is conglomeratic in places. The middle zone is also narrow. In one section it is about 1 m thick and contains small, generally cobble-sized concretions. The upper zone is about 8 m thick and is located approximately 6 m below the top of the unit. Ammonoids are very common to all three zones, and conodonts are common to the lower and upper concretion zones. The brachiopods, ammonoids, and fusulinids recovered from this unit are listed in Wardlaw et al. (1979).

LA COLORADA BEDS.—The La Colorada beds consist of a lower unit that contains a thick volcanic megabreccia at its base and the *Kingoceras* shale at its top, and an upper unit of graywacke with the *Eoaraxoceras* shale very near its top (Figures 17-7B–D). The thick volcanoclastic megabreccia at the base of the La Colorada beds (the chaotic volcanic lithosome of McKee et al., 1988) contains many large volcanic blocks, which are several meters to tens of meters in width and height, that occur in a conglomeratic matrix of volcanoclastic graywacke. Common within the volcanoclastic graywacke are limestone cobbles to boulders that are fusulinid (*Polydixodina*) packstones to grainstones. These are particularly common on the north side of Cerro San Pedro. The large volcanic blocks consist of andesite, dacite, welded tuff, and laharc breccia (McKee et al., 1988). Like in the La Difunta limestone megabreccia in the unit below, these large blocks, here of igneous rock, form hills because they are more erosionally resistant than the surrounding conglomeratic matrix. The basal contact of the volcanic megabreccia with the *Timorites* shale is very irregular. After a short intervening graywacke interval, the

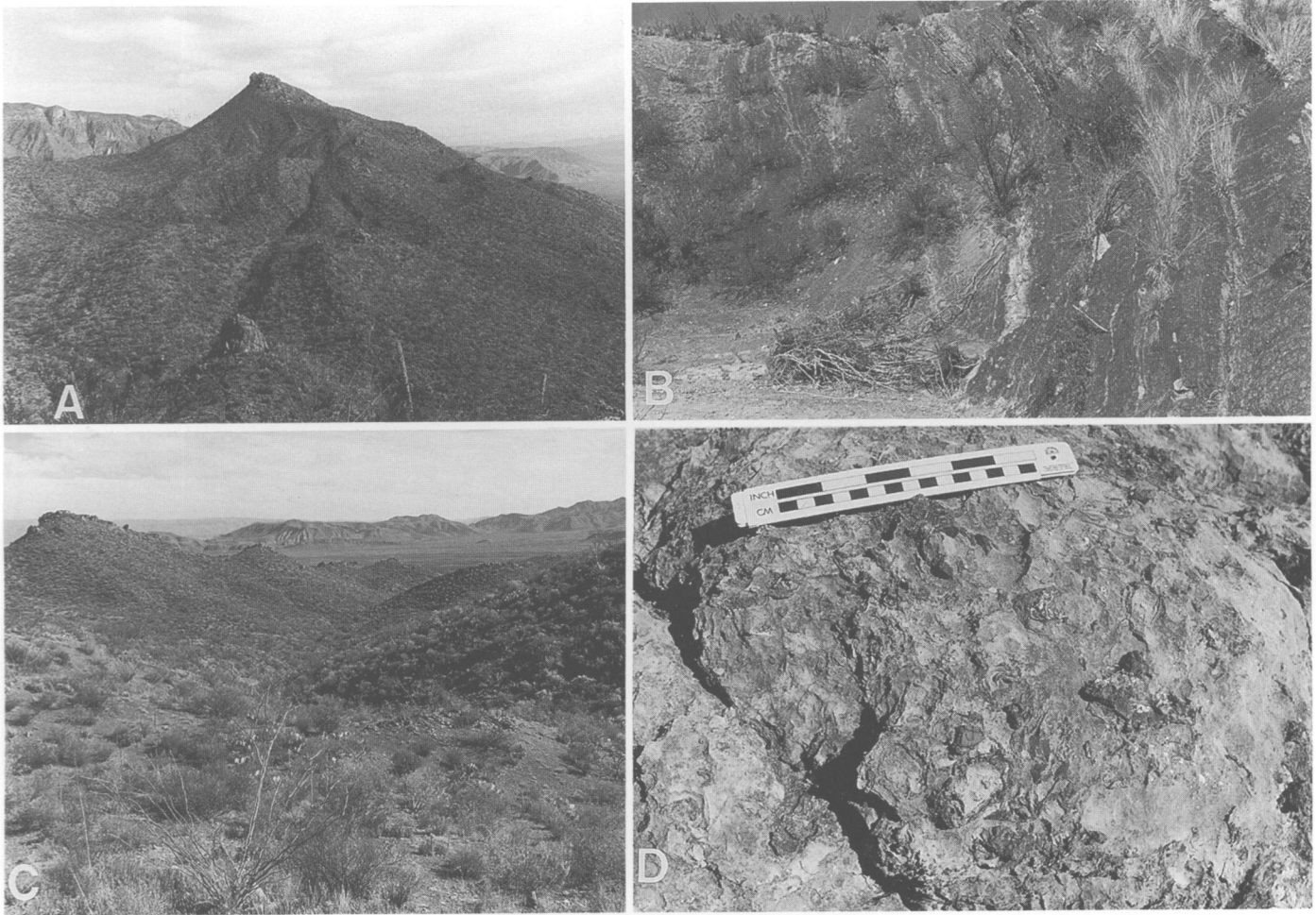


FIGURE 17-8.—Photographs of Palo Quemado beds and La Difunta megabreccias. A, large reefoid limestone blocks floating in skeletal conglomerate-making limestone knobs and peaks. Cerro Prieto del Norte is in the distance. B, interbedded graywacke and shale of Palo Quemado beds in Arroyo las Animas. C, large reefoid limestone blocks in skeletal conglomerate. D, close-up of knob in left corner in C showing *Sestropoma* limestone.

Kingoceras shale occurs above the volcanoclastic megabreccia. The *Kingoceras* shale is a black shale with several thin to medium beds of skeletal conglomeratic graywacke, which pinch and swell and commonly show low angle cross-bedding. Limestone nodules are common in the lower 12 m and are mostly composed of lime mudstone with a sparse fauna of ammonoids, brachiopods, and some radiolarians. The contact with the underlying graywackes is fairly sharp.

The upper unit of the La Colorada beds begins with a relatively thick graywacke, which is locally conglomeratic, and contains abundant volcanic debris in places. The *Eoaraxoceras* shale is a poorly developed dirty shale located very near the top of the section and has an indistinct basal contact. Silty, argillaceous graywacke in thin beds is common within the thin shale unit. Limestone nodules and thin limestone lenses, which are both generally silty, are not common and contain a sparse fauna of ammonoids and brachiopods. A graywacke containing

sparse ammonoids immediately overlies the *Eoaraxoceras* shale and is folded into a small anticline. This graywacke represents the highest bed exposed in the sequence. The brachiopods, ammonoids, and fusulinids recovered from this unit are listed in Wardlaw et al. (1979).

Conodont Biostratigraphy

Conodonts, together with mollusks and leaves, are common to the concretions in the black shales of the sequence, but they are uncommon in the megabreccias, volcanoclastic graywackes, and limestone turbidites, all of which represent rapid deposition.

Hindeodus excavatus (Behnken) is common in the *Perrinites* and *Waagenoceras* shales. *Hindeodus wordensis*, new species, (see Wardlaw, this volume) is common to the La Difunta limestone and the *Timorites* shale. *Hindeodus julfensis* Sweet is

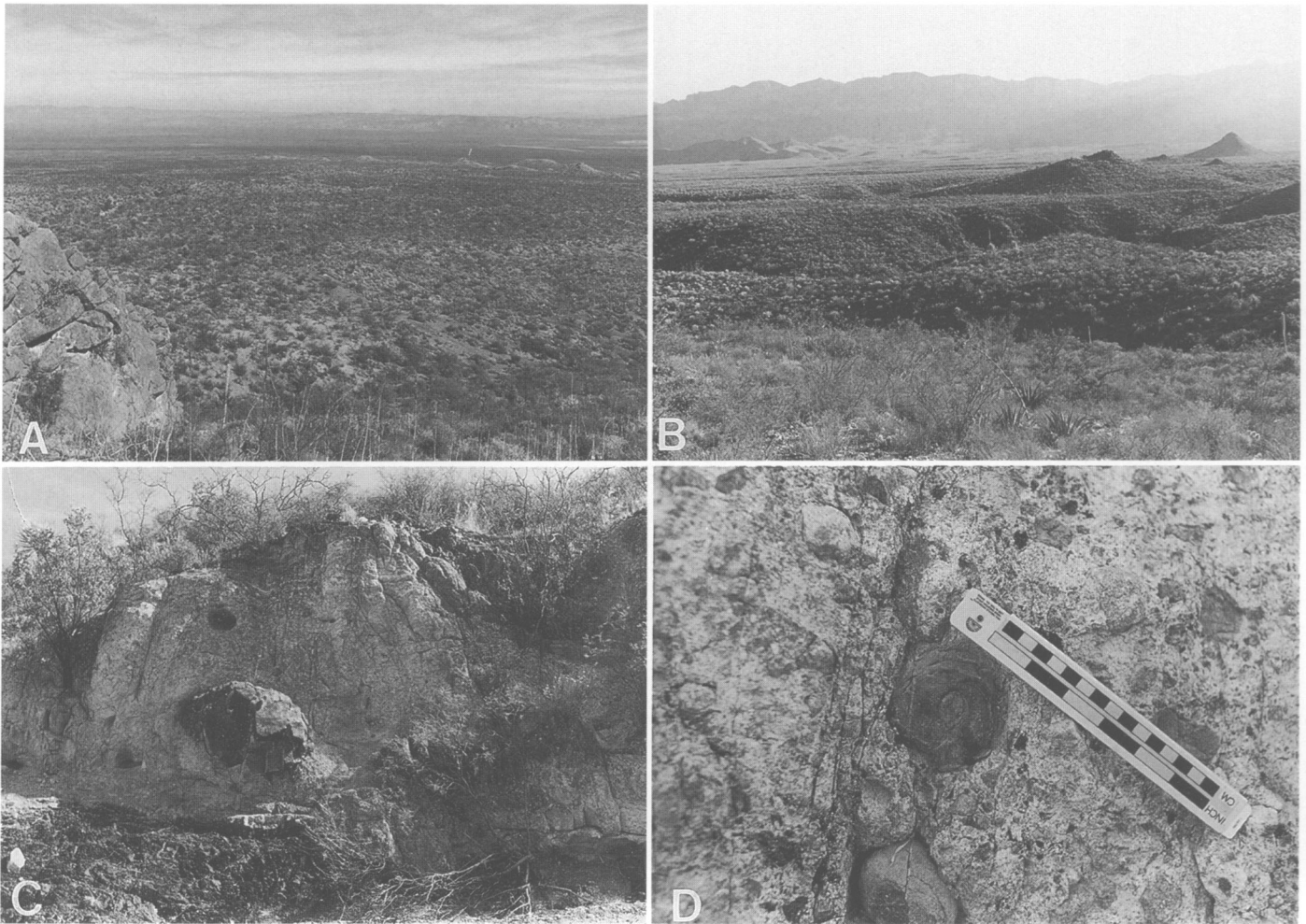


FIGURE 17-9.—A, view of the upper part of the Permian sequence from the limestone knob east of Cerro Prieto del Norte looking across the northern outcrop belt to the chaotic volcanic megabreccia that forms the hills in the distance. B, view of the upper part of the sequence from top of the hill of chaotic volcanic megabreccia on the south side of Arroyo la Colorada. C, view of the conglomeratic tuffaceous sandstone in channel. D, closeup of ammonoid in the conglomeratic tuffaceous sandstone (*Waagenoceras*).

common to the volcanic megabreccia containing *Polydiexodina* cobbles immediately above the *Timorites* shale. Other important conodonts include *Mesogondolella nankingensis* (Ching) from the *Waagenoceras* shale, *Mesogondolella aserrata* (Clark and Behnken) and *Sweetina triticum* Wardlaw and Collinson from the La Difunta limestone, and *Sweetognathus expansus* (Perlmutter) from the conglomerate beds at the base of the section. Conodonts were not recovered from the *Kingoceras* and *Eoaraxoceras* shales.

The rocks at Las Delicias can be divided into three conodont zones based on the nearshore genus *Hindeodus*. In ascending order they are *Hindeodus excavatus*, *Hindeodus wordensis*, and *Hindeodus julfensis*. These zones are similar to those recognized by Wardlaw (1988) for the shallow-water Permian sequence in the Salt Range, Pakistan. Although the conodonts are dominantly washed in, there appears to be little stratigra-

phic reworking or mixing of faunas, suggesting that the conodonts represent contemporaneous to penecontemporaneous deposition of forms transported in from nearby shelves and slopes on or about volcanic edifices.

The *Hindeodus* zones are long-ranging. The base of the *Hindeodus excavatus* Zone is not well constrained, but it is at least as old as Sakmarian. It ranges through the Roadian. The presence of *Sweetognathus expansus* in the basal conglomerate of the Las Sardinas beds suggests a Sakmarian age for the base. The Sakmarian is generally missing from the Permian rocks of West Texas, indicating a local hiatus and a relative low stand of sea level, which could possibly correlate to conglomerate shedding into the basin at Las Delicias. The *Hindeodus wordensis* zone is Wordian–Capitanian. The *Hindeodus julfensis* zone is post-Guadalupian and Wuchiapingian (it appears that a part of the upper Maokouan in China is

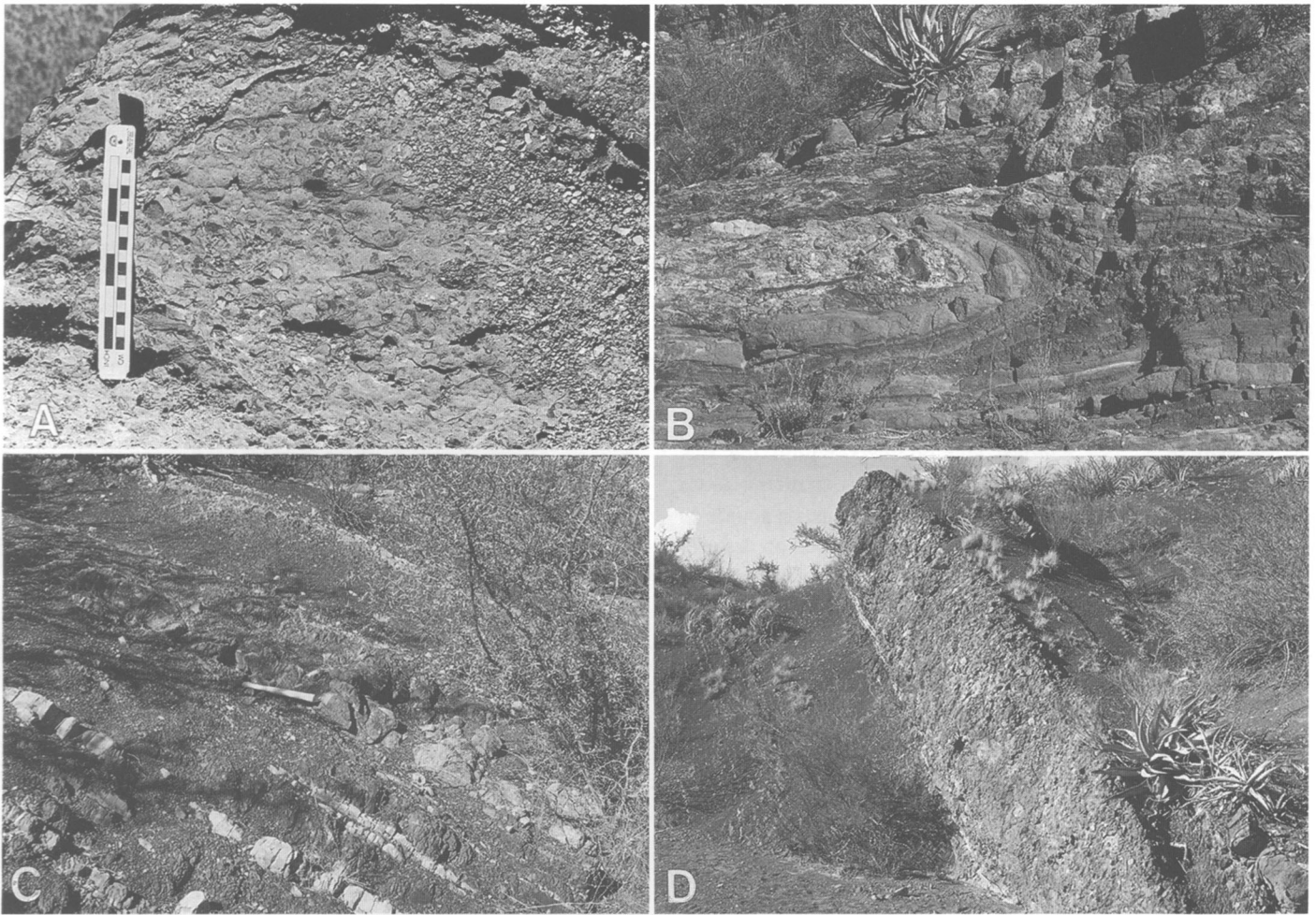


FIGURE 17-10.—A, close-up of the skeletal conglomerate at the top of the Palo Quemado beds. B, view of the folded beds within the La Difunta limestone near spring in Arroyo la Difunta. C, view of interbedded shales and graywackes and turbiditic limestone in the La Difunta beds along Arroyo la Difunta. D, coarse conglomeratic sand below the *Timorites* shale in the La Difunta beds along Arroyo la Difunta.

post-Guadalupian and, of course, pre-Wuchiapingian). In the lower *Waagenoceras* shale the ranges of *Hindeodus excavatus* and *Mesogondolella nankingensis* overlap, which is also the case in the Road Canyon Formation, and thus indicates that this part of the Palo Quemado beds is Roadian. The upper *Waagenoceras* shale is probably Wordian. The La Difunta limestone megabreccia also appears to be Wordian and may be equivalent to the Manzanita Limestone Member of the Cherry Canyon Formation in the Delaware basin, as both were deposited during a major low stand of the sea, hence the major carbonate-block shedding in the Las Delicias area. The remainder of the La Difunta beds, including the *Timorites* shale, is Capitanian. The *Timorites* shale is roughly equivalent to the Lamar Limestone Member of the Bell Canyon Formation where *Timorites* also occurs. The volcanic megabreccia at the base of the La Colorada beds is post-Guadalupian and contains *Hindeodus julfensis*, just like the uppermost beds of the Altuda

Formation in the Del Norte Mountains, Texas (Kozur, 1992). The breccia shedding, which caused the volcanic megabreccia, probably is also related to a major low stand of sea level, and it appears to be the same low stand that caused the end of Guadalupian deposition in West Texas. The *Kingoceras* and *Eoanaxoceras* shales are post-Guadalupian, possibly Wuchiapingian (Dzhulfian), but no conodonts were recovered to refine the correlations.

Paleogeographic Affinities of the Faunas

The presence of shallow-water conodonts and common leaves in the black shales indicates a very close source from which these biotic elements were washed in. The conodonts from the black shales and the brachiopods from the massive limestones blocks within the megabreccias indicate very close affinities to faunas of West Texas. The coralliform brachiopod

Sestropoma is common to, and only known from, Guadalupian faunas of West Texas and Las Delicias (Cooper and Grant, 1975). The overall brachiopod fauna as reported in King et al. (1944) and Wardlaw et al. (1979) is very close to that found in West Texas. *Mesogondolella aserrata* with common *Sweetina* are restricted to the West Texas and China warm-water endemic provinces (Wardlaw, 1994). The fauna indicates a close proximity to West Texas, suggesting that the Las Delicias basin developed along a volcanic arc in the sea or seaway that led to the Permian basin of West Texas and New Mexico and the Pedregosa basin of Arizona, New Mexico, and northern Mexico. As noted by King et al. (1944) and Wardlaw et al. (1979), the conglomerate at the base of the section (Las Sardinas beds) thins from west to east, as do most of the units in the sequence. The cobbles and boulders within the Las Sardinas conglomerate appear to become smaller (more cobbles than boulders) in the east. This all suggests a source to the west, which would indicate the basin developed on the east side of a volcanic arc. McKee et al. (1988) suggested that "the arc lay to the south or southeast of the Las Delicias area,

judging from the facies relations and macroscopic structures that form the principal basis for our interpretation of paleoslope" (McKee et al., 1988:39).

Conclusions

The conodonts recovered from the Permian beds at Las Delicias can be divided into three zones: *Hindeodus excavatus*, *H. wordensis*, and *H. julfensis*. The conodonts, along with the previously reported ammonoids and fusulinids, indicate that deposition was Sakmarian through Wuchiapingian (basal Dzhulfian).

The Las Delicias basin developed as a deep basin along the east side of a volcanic arc of size significant enough to develop occasionally widespread carbonate platforms. Black shale was deposited in the basin during times of quiescence (high-water stands?). Megabreccia and conglomerate were deposited during low stands of sea level. Graywacke was deposited during most other times. Faunas indicate that the volcanic arc was in close proximity to and related to the Permian and Pedregosa basins to the north.

Literature Cited

- Cooper, G.A., and R.E. Grant
1975. Permian Brachiopods of West Texas, III. *Smithsonian Contributions to Paleobiology*, 19:795–1921, plates 192–502.
- King, R.E., C.O. Dunbar, P.E. Cloud, and A.K. Miller
1944. Geology and Paleontology of the Permian Area Northwest of Las Delicias, Southwestern Coahuila, Mexico. *Geological Society of America, Special Paper*, 52: 172 pages, 45 plates.
- Kozur, Heinz
1992. Dzhulfian and Early Changxingian (Late Permian) Tethyan Conodonts from the Glass Mountains, West Texas. *Neues Jahrbuch für Geologie und Paläontologie, Abhandlungen*, 187(1):99–114, figures 1–21.
- McKee, J.W., N.W. Jones, and T.H. Anderson
1988. Las Delicias Basin: A Record of Late Paleozoic Arc Volcanism in Northeastern Mexico. *Geology*, 16:37–40.
- Newell, N.D.
1957. Supposed Permian Tillites in Northern Mexico are Submarine Slide Deposits. *Bulletin of the Geological Society of America*, 68(11):1569–1576, plates 1, 2.
- Spinosa, C., W.M. Furnish, and B.F. Glenister
1970. Araxoceratidae, Upper Permian Ammonoids from the Western Hemisphere. *Journal of Paleontology*, 44(4):730–736, plate 109.
- Wardlaw, B.R.
1988. Permian Conodonts from the Salt Range, Pakistan. [Abstract.] *Geological Society of America, Abstracts with Programs*, 20:393–394.
1995. Permian Conodonts. In P.A. Scholle, T.M. Peryt, and D.S. Ulmer-Scholle, editors, *The Permian of Northern Pangea, 1: Paleogeography, Paleoclimates, Stratigraphy*, pages 186–195. Heidelberg: Springer-Verlag Publishers.
- Wardlaw, B.R., W.M. Furnish, and M.K. Nestell
1979. Geology and Paleontology of the Permian Beds near Las Delicias, Coahuila, Mexico. *Bulletin of the Geological Society of America*, 90(1):111–116.

Plate 17-1

PLATE 17-1

Conodonts from Las Delicias, Mexico.

FIGURES 1–6.—*Hindeodus julfensis* Sweet: 1, lateral view, Pa element, $\times 81.5$, USNM 482792; 2, lateral view, Pa element, $\times 79.4$, USNM 482793; 3, lateral view, Pa element, $\times 79.4$, USNM 482794; 4, lateral view, Pa element, $\times 79.4$, USNM 482795; 5, lateral view, Pa element, $\times 79.4$, USNM 482796; 6, lateral view, Pa element, $\times 79.4$, USNM 482797. All specimens from USGS 31655-PC (W88-16M), *Polydixodina* cobbles in igneous dominated megabreccia above the *Timorites* shale, lower La Colorada beds. (Reduced to 90% of original for publication.)

FIGURE 7.—*Hindeodus wordensis* Wardlaw (new species, this volume): lateral view, Pa element, $\times 79.1$, USNM 482798. From USGS 31652-PC (W88-5M), from concretions near the base of the *Timorites* shale, upper La Difunta beds. (Reduced to 90% of original for publication.)

FIGURES 8–16.—*Hindeodus wordensis* Wardlaw (new species, this volume): 8, posterior view, Sa element, $\times 79.5$, USNM 482799; 9, posterior view, Sb element, $\times 79.4$, USNM 482800; 10, inner view, Pb element, $\times 80.8$, USNM 482801; 11, posterior view, M element, $\times 79.4$, USNM 482802; 12, inner view, Sc element, $\times 79.4$, USNM 482803; 13, lateral view, Pa element, $\times 80.8$, USNM 482804; 14, lateral view, Pa element, $\times 80.8$, USNM 482805; 15, lateral view, Pa element, $\times 80.8$, USNM 482806; 16, inner view, Sc element, $\times 79.4$, USNM 482807. All specimens from USGS 31654-PC (W88-14M), from the mollusk limestone within the La Difunta limestone, lower La Difunta beds. (Reduced to 90% of original for publication.)

FIGURES 17–19.—*Mesogondolella aserrata* (Clark and Behnken): 17, upper view, Pa element, $\times 79.1$, USNM 482808; 18, upper view, Pa element, $\times 79.4$, USNM 482809; 19, upper view, Pa element, $\times 79.4$, USNM 482810. All specimens from USGS 31654-PC (W88-14M). (Reduced to 90% of original for publication.)

FIGURE 20.—*Sweetina triticum* Wardlaw and Collinson: lateral view, Pa element, $\times 79.1$, USNM 482811. From USGS 31654-PC (W88-14M). (Reduced to 90% of original for publication.)

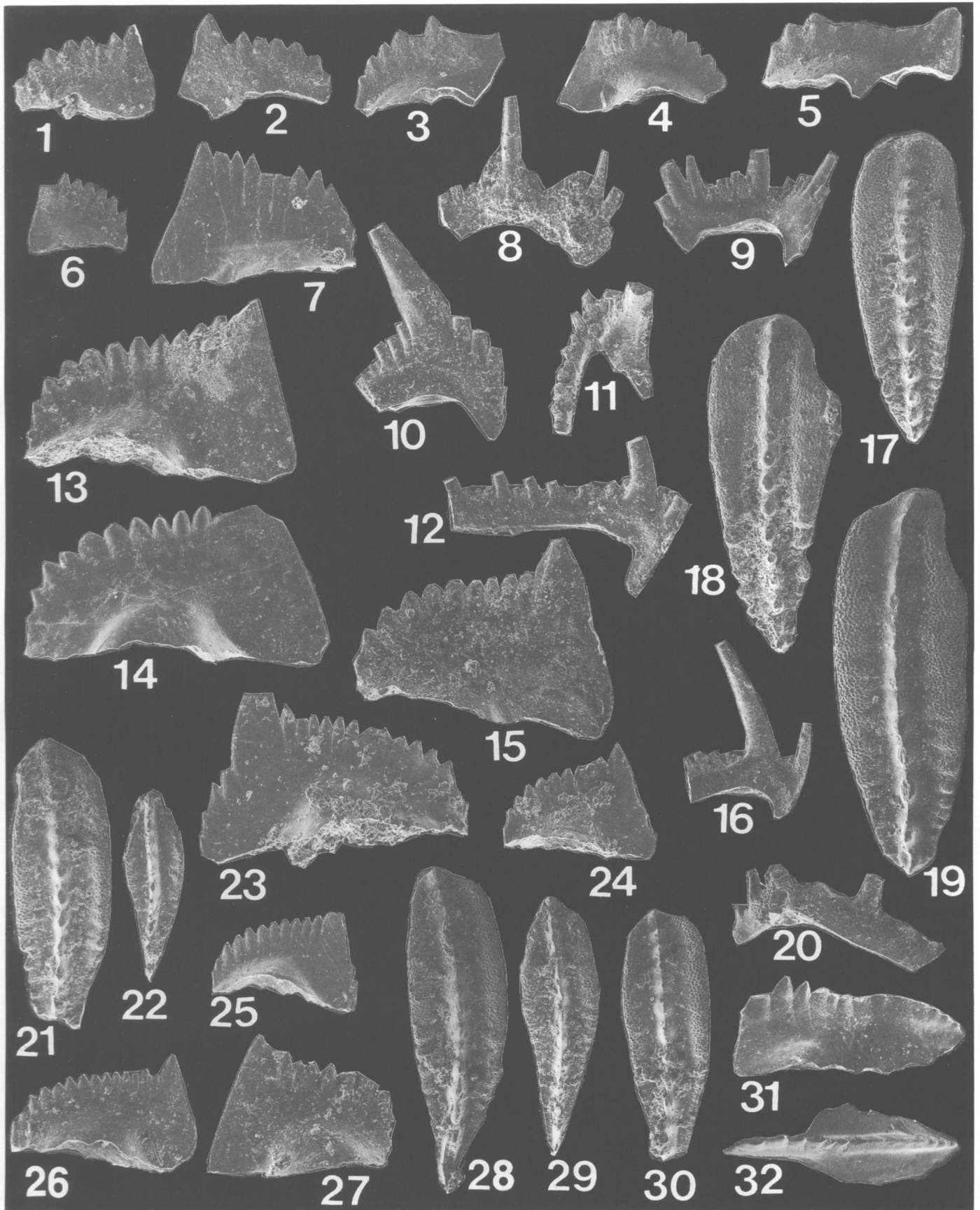
FIGURES 21, 22.—*Mesogondolella nankingensis* (Ching): 21, upper view, Pa element, $\times 79.4$, USNM 482812; 22, upper view, Pa element, $\times 79.4$, USNM 482813. Both specimens from USGS 31649-PC (W88-2M), from large limestone nodules near the top of the lower *Waagenoceras* shale, lower Palo Quemado beds. (Reduced to 90% of original for publication.)

FIGURES 23–25.—*Hindeodus excavatus* (Behnken): 23, lateral view, Pa element, $\times 79.1$, USNM 482814; 24, lateral view, Pa element, $\times 79.4$, USNM 482815; 25, lateral view, Pa element, $\times 79.4$, USNM 482816. All specimens from USGS 31650-PC (W88-3M), from limestone nodules near the top of the lower *Waagenoceras* shale, lower Palo Quemado beds. (Reduced to 90% of original for publication.)

FIGURES 26, 27.—*Hindeodus excavatus* (Behnken): 26, lateral view, Pa element, $\times 79.4$, USNM 482817; 27, lateral view, Pa element, $\times 80.8$, USNM 482818. Both specimens from USGS 31651-PC (W88-4M), from a bed of marble-sized concretions near the bottom of the lower *Waagenoceras* shale, lower Palo Quemado beds. (Reduced to 90% of original for publication.)

FIGURES 28–30.—*Mesogondolella nankingensis* (Ching): 28, upper view, Pa element, $\times 79.4$, USNM 482819; 29, upper view, Pa element, $\times 79.4$, USNM 482920; 30, upper view, Pa element, $\times 76.3$, USNM 482821. All specimens from USGS 31648-PC (W88-1M), from scattered limestone nodules at the base of the lower *Waagenoceras* shale, lower Palo Quemado beds. (Reduced to 90% of original for publication.)

FIGURES 31, 32.—*Sweetognathus expansus* (Perlmutter): lateral view, $\times 80.0$, upper view, $\times 79.4$, Pa element, USNM 482822. From USGS 31653-PC (W88-13M), from a large ammonoid-bearing cobble from the conglomerate beds, lower Las Sardinas beds. (Reduced to 90% of original for publication.)



18. Ancestral Araxoceratinae (Upper Permian Ammonoidea) from Mexico and Iran

Claude Spinosa and Brian F. Glenister

ABSTRACT

Araxoceratinae are ceratitoid ammonoids that characterize the restricted marine facies of the Upper Permian Dzhulfian Stage. Representatives of the ancestral genera *Kingoceras* and *Eoaxoceras* are abundant in the post-Guadalupian upper La Colorada beds of Coahuila, Mexico. Both genera from the *Araxoceras* beds of Abadeh, central Iran, which can be correlated in turn with the type Dzhulfian of the Araxes River valley, are described. Agreement on the precise definition of the Dzhulfian is yet to be achieved, but it is concluded that the Dzhulfian Stage can be defined to succeed the Guadalupian without major overlap or omission. *Eoaxoceras robustum* is proposed as a new species from central Iran.

Introduction

Araxoceratinae are otoceratid ammonoids (Ceratitida) that are a distinctive element of Upper Permian (Dzhulfian) faunas. They originated from the ancestral ceratitids, the xenodiscid subfamily Paraceltitinae, are found across the middle Permian (Guadalupian)–Upper Permian (Dzhulfian) boundary, and serve significantly in the correlation of that datum. The phylogenetic relationships of these groups were outlined by Spinosa et al. (1975) and are reproduced in a somewhat modified form herein (Figure 18-1). The nominate genus of Otoceratidae is generally considered to be Lower Triassic (Griesbachian) and is believed to constitute the youngest

representative of the family (e.g., Tozer, 1988); however, both the definition of the Erathem boundary and the correlation of adjacent strata are still open to question (Sweet, 1992), casting the strictly Triassic age in doubt.

Among the earliest araxoceratins are *Eoaxoceras* Spinosa et al. (1970) and, questionably, *Kingoceras* Miller (1944). Both genera have been reported from the upper portion of the stratigraphic section in Arroyo La Colorada (Coahuila, Mexico) and from Kuh-e-Hambast, Abadeh, central Iran (Spinosa et al., 1975). Four Iranian specimens of *Eoaxoceras* were subsequently described (Bando, 1979) and were referred to the Mexican species *E. ruzhencevi* Spinosa et al. (1970). The purpose of the present study is to describe additional collections of Abadeh *Eoaxoceras* and *Kingoceras* and to reevaluate the taxonomic assignments and biostratigraphic implications of these ancestral otoceratids.

Correlation of the Guadalupian–Dzhulfian Boundary in North America and Transcaucasia

The youngest Permian outcrops at Las Delicias (Coahuila, Mexico) occur in Arroyo La Colorada, where the top 375 m of the section have been designated the “upper La Colorada beds” (Wardlaw et al., 1979). Neither fusulinaceans nor conodonts are known from this interval, and only ammonoids have any biostratigraphically useful representation. Ammonoids are abundant (Spinosa et al., 1970; Wardlaw et al., 1979) and are represented by at least eight species (Figure 18-2): *Kingoceras kingi* Miller, *Timorites* sp., *Stacheoceras toumanskyae* Miller and Furnish, *Xenodiscus wanneri* Spinosa, Furnish, and Glenister, *Neocrimites* sp., *Difuntites hidius* (Ruzhencev), *Nodosageceras nodosum* (Wanner), and *Eoaxoceras ruzhencevi* Spinosa, Furnish, and Glenister. *Eoaxoceras* is particularly noteworthy as the probable ancestor of the Araxoceratinae, the otoceratid subfamily that characterizes the restricted-

Claude Spinosa, Department of Geosciences, Boise State University, Boise, Idaho 83725. Brian F. Glenister, Department of Geology, The University of Iowa, Iowa City, Iowa 52242.

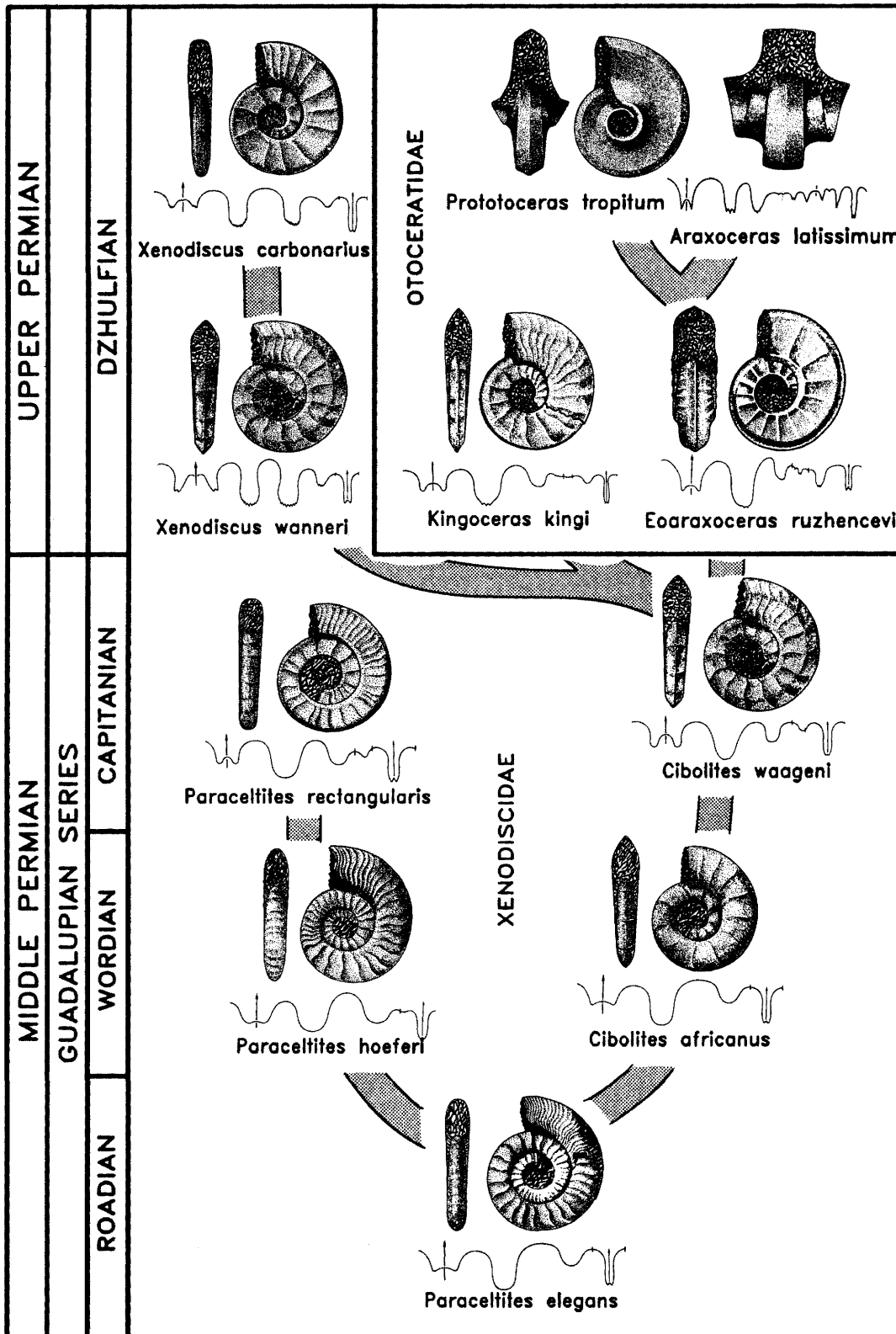


FIGURE 18-1 (left).—The early evolution of the ceratitoid ammonoid families Xenodiscidae and Otoceratidae. The otoceratid subfamily Araxoceratinae can be interpreted to have been derived from a Guadalupian paraceltitid ancestor, such as *Cibolites*; it underwent spectacular diversification at the base of the Dzhulfian to characterize that stage.

circulation facies of the Dzhulfian (Zhou et al., 1989). Associations of *Eoaxoceras*, *Kingoceras*, *Xenodiscus*, and *Timorites* also occur in the bottom one-half of the *Araxoceras* beds (Taraz, 1971) at Abadeh in central Iran (Figure 18-3), which in turn can be correlated bed-for-bed with the Guadalupian/type-Dzhulfian transition sequence of the Araxes River valley of Transcaucasia.

Agreement on the precise definition of the base of the Dzhulfian is yet to be achieved (e.g., Kotlyar et al., 1989); however, pending such agreement, the common consensus of recognizing the base of the Dzhulfian in the type section at Dorasham 2, Nakhichevan, Azerbaijan (Ruzhencev and Sarycheva, 1965) is adopted as the base of the *Araxoceras*-*Oldhamina* beds, which is the equivalent of the *Araxoceras* beds of Abadeh (Taraz, 1971). This base corresponds to the

initial diversification of the Araxoceratinae. The upper La Colorado beds in Coahuila thus correlate with the basal type Dzhulfian.

The upper La Colorado beds occur in objective stratigraphic superposition with the lower La Colorado beds. The uppermost 15 m of the latter (Bed 57 of Newell, 1957; Figure 18-2) can be demonstrated by reference to both fusulinaceans and ammonoids (Wilde, 1990; Wardlaw et al., 1979) as the approximate equivalent of the Bell Canyon Formation, which is the uppermost type Guadalupian. It follows that the Dzhulfian can be defined to succeed the Guadalupian without major overlap or omission.

Systematic Paleontology

The origin and affinities of the Otocerataceae were reviewed by Spinosa et al. (1975), Zhao et al. (1978), Shevyrev and Yermakova (1979) amongst others, and most recently by Zhakharov (1988). Despite fundamental disagreements in interpretation, it seems clear that the Otocerataceae evolved

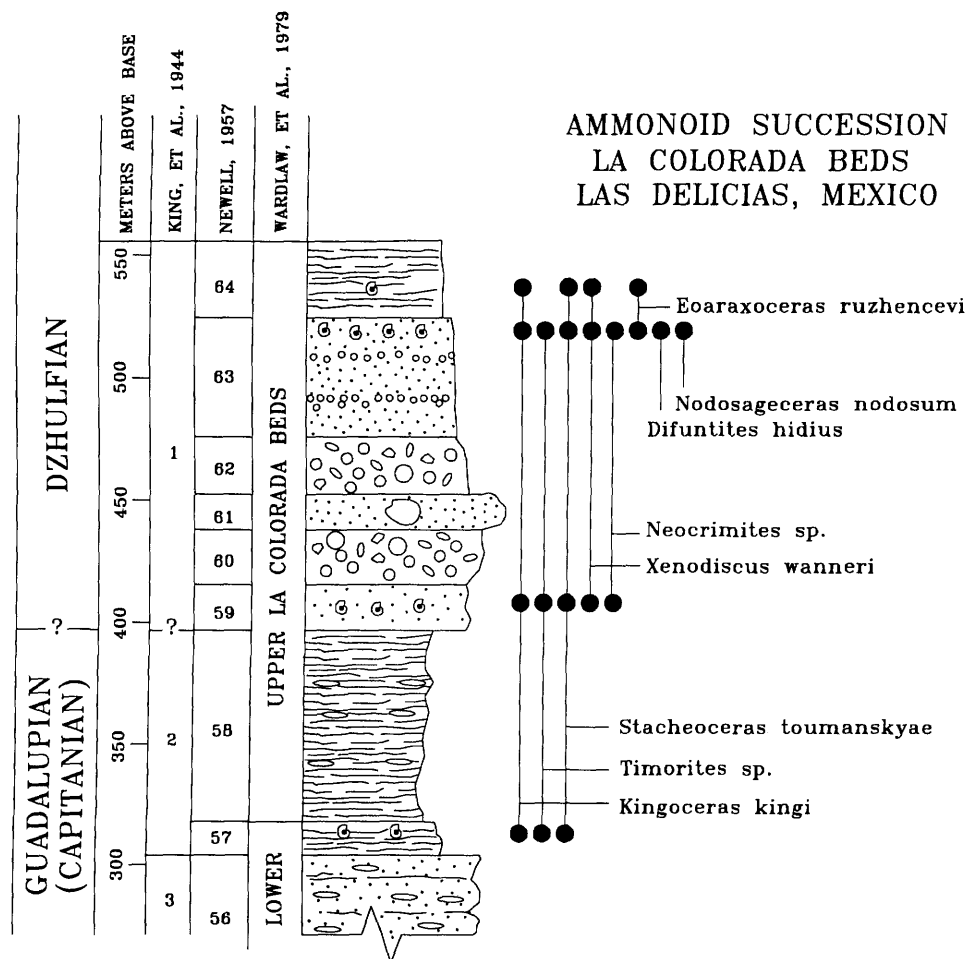


FIGURE 18-2.—The ammonoid succession in the uppermost part of the Permian section, Las Delicias area, Coahuila, Mexico. Occurrences are related to sections published by King et al. (see Miller, 1944) and Newell (1957).

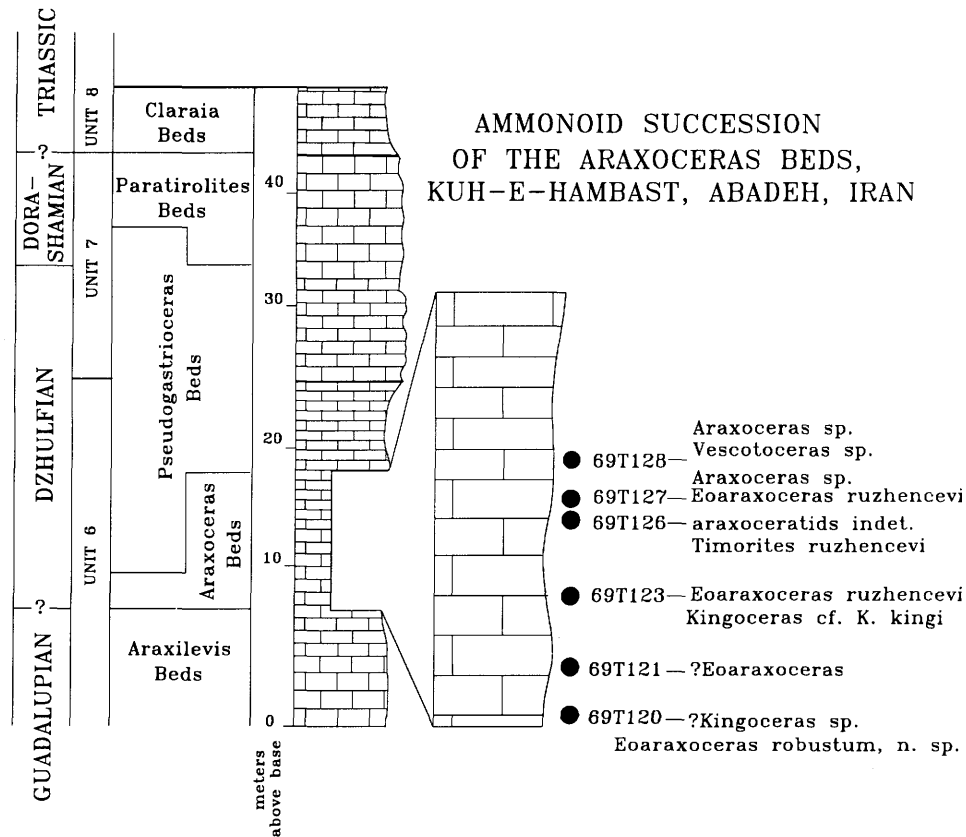


FIGURE 18-3.—The ammonoid succession in the *Araxoceras* beds of Kuh-e-Hambast, Abadeh area, central Iran. Stratigraphic control is courtesy of Hooshang Taraz; the section is modified after Taraz (1971).

from the Paracelitinae. Two of the genera involved in this transition are the subject of the present study. *Eoaraxoceras* is an unquestionable otoceratid and is considered to belong in the Araxoceratinae. The assignment of *Kingoceras* is less certain (Spinosa et al., 1975), and it can be referred with almost equal propriety to either the Paracelitinae or the Otoceratidae. In the present study it is continued to be regarded as having been derived from the paracelitid genus *Cibolites* Plummer and Scott (1937), but it is best considered an araxoceratin.

Superfamily OTOCERATACEAE Hyatt, 1900

Family OTOCERATIDAE Hyatt, 1900

Subfamily ARAXOCERATINAE Ruzhencev, 1959

Eoaraxoceras Spinosa, Furnish, and Glenister, 1970

TYPE SPECIES.—*Eoaraxoceras ruzhencevi* Spinosa, Furnish, and Glenister, 1970:732-734, pl. 109: figs. 1-9, text-figs. 1, 2A, 3; original designation.

DIAGNOSIS.—Ancestral araxoceratins with strongly evolute conch (U/D ranges from 0.2 to 0.45 at D 25-35 mm), broadly

acuminate venter, and pronounced umbilical flange. Sutures of mature and submature specimens comprise ten lobes; lobes serrate, except dorsal and ventral elements bifid.

DISTRIBUTION.—The type species of *Eoaraxoceras* is abundant in the lower Dzhulfian upper La Colorada beds of Mexico (Spinosa et al., 1970). The genus also occurs in the lower Dzhulfian *Araxoceras* beds of Abadeh, central Iran (Spinosa et al., 1975; Bando, 1979; Taraz et al., 1981), from whence it was identified and described. A new species (*E. robustum*) also occurs in the *Araxoceras* beds of Abadeh, where it is a rare element. These two species represent the oldest araxoceratins in the succession. Closely related forms are abundant in strata of comparable age in the Longtan Formation (Wujiapingian = Dzhulfian) of South China (e.g., Zhao et al., 1978), but a detailed assessment of these occurrences is beyond the scope of the present study.

Eoaraxoceras ruzhencevi Spinosa, Furnish, and Glenister, 1970

FIGURE 18-4A-M

Kingoceras kingi Miller in King et al., 1944:125-126, pl. 42: figs. 8, 9 [in part, not pl. 42: figs. 6, 7, text-fig. 29E].

Eoaraxoceras ruzhencevi Spinosa, Furnish, and Glenister, 1970:732-735, pl. 109: figs. 1-9, text-figs 1, 2A, 3. [Not *E. ruzhencevi* [sic], Bando, 1979:116, pl. 2: fig. 6a,b, text-fig. 6C (= ?*Araxoceras* sp.); pl. 2: fig. 3a,b (= *E. robustum*, new species).]

DESCRIPTION.—*Holotype*: SUI 32895 (Figure 18-4A-C); *Paratypes*: SUI 31948, 31949 (Figure 18-4G), 31951, 31952, 32890 (Figure 18-4D-F). Approximately 400 additional topotypes of *Eoaraxoceras ruzhencevi* from the lower Dzhulfian La Colorada beds of Mexico are available for study. Most were analyzed when the species was erected, and new collections from Mexico add nothing significant to an understanding of the taxon; however, additional material from the *Araxoceras* beds of central Iran (Figure 18-3) can now be compared directly with the topotypes. Included are one well-preserved hypotype (GSI 69 T 123, Figure 18-4H-J) and two unillustrated specimens from the same horizon, as well as one hypotype (GSI 69 T 127, Figure 18-4K-M) and two poorly preserved representatives (GSI 69 T 121) provisionally referred to *E. ruzhencevi*. The assignment of Iranian specimens (GSI Ab-72158, Bando, 1979, pl. 2: fig. 6a,b; 72174, Bando, 1979, pl. 2: fig. 3a,b, text-fig. 6B; 72224; 72302, Bando, 1979, text-fig. 6C) previously referred to *E. ruzhencevi* by Bando (1979) is rejected, based on published information.

Known representatives of *Eoaraxoceras ruzhencevi* are small, with the maximum observed conch diameter being approximately 35 mm. The holotype demonstrates subparallel but slightly concave flanks that converge from the prominent ventrolateral shoulders to form a tectiform venter (Figure 18-4A,B). Flanged dorsolateral regions form a conspicuously raised umbilical shoulder that possesses a series of faint nodes extending a short distance across the dorsolateral flanks. Nodes are more pronounced in conchs less than 20 mm in diameter (e.g., Miller, 1944, pl. 42: figs. 8, 9).

Figure 18-4C-G portrays the sutural ontogeny of the primary types. Larger representatives display a pair of rounded nonserrate ventral prongs and a narrowly bifid dorsal lobe; four intervening lobes can be observed to be serrate in well-preserved specimens. In addition to the 10 major lobes, as many as six incipient elements are sporadically observable on the umbilical and internal saddles (e.g., Figure 18-4G).

COMPARISONS.—The previous analysis of conch form and sutures of the abundant Mexican representatives of *Eoaraxoceras ruzhencevi* suggests high intraspecific variation. Relatively rare representatives now known from central Iran seem to fall within this range; therefore, they do not warrant a separate designation. The relationship to the new Iranian species, *E. robustum*, is considered under the heading for that species.

OCCURRENCE.—Detailed occurrence data for the Mexican representatives were presented previously (Spinosa et al., 1970). In summary, they are apparently confined to the uppermost 60 m of the youngest Permian known from the site, which is near the top of the upper La Colorada beds, Las Delicias, Coahuila. Most were derived from the upper 2 m of

Bed 63 of Newell (1957), but the best preserved specimens were from calcareous nodules in the uppermost unit, Bed 64 of Newell. Iranian representatives were from Kuh-e-Hambast, Abadeh area, central Iran, 2.8 m (69 T 123) and 5.3 m (69 T 127) above the base of the *Araxoceras* beds of Taraz (1971).

REPOSITORY.—Topotype YPM 16282 is repositated at the Peabody Museum, Yale University. Holotype SUI 32895, paratypes SUI 31948, 31949, 31951, 31952, and 32890 are in the University of Iowa, and hypotypes GSI 69 T 123, 69 T 127, and 69 T 121 are in the collections of the Geological Survey of Iran, Tehran.

Eoaraxoceras robustum, new species

FIGURE 18-5A-D

Eoaraxoceras ruzhencevi Spinosa, Furnish, and Glenister, 1970.—Bando, 1979:116, pl. 2, fig. 3a,b, text-fig. 6B [in part, published as *Eoaraxoceras ruzhencevi* (sic)].

DIAGNOSIS.—A species of *Eoaraxoceras* characterized by a relatively broad conch (W/D approaching 0.5 in larger specimens) and narrow umbilicus (U/D near 0.25).

DESCRIPTION.—The species is based upon the holotype (GSI 69 T 120), from the base of the *Araxoceras* beds (Taraz, 1971) at Abadeh, central Iran; however, an additional specimen (GSI Ab-72174) from the same locality is compared with question. The holotype is a well-preserved specimen of 33 mm diameter that retains one-half volution of body chamber but does not display the contours of the aperture. The umbilical ratio U/D ranges from 0.36 at 16 mm diameter to 0.22 at 33 mm, and the width ratio W/D decreases from 0.66 to 0.47 over this same size interval. Figure 18-5A,C reveals change in the ventral transverse profile in the ultimate one-half volution, from rounded at 20 mm to strongly tectiform at diameters greater than 30 mm. In this same interval, the ventrolateral shoulders become better defined, partially due to flattening and eventual slight concavity of the dorsolateral flanks. Low nodes that are discernible on the outer umbilical wall become faint as they extend onto the umbilical shoulder.

The external suture (Figure 18-5D) exhibits rounded, nonserrate ventral prongs separated by a median ventral saddle slightly higher than one-third the depth of the entire lobe. The first "lateral" lobe, located on the ventrolateral shoulder, is symmetrical, narrow, and approximately one-third deeper than the adjacent lobes. It is serrate and is constricted slightly two-thirds the distance from the base. The second "lateral" is asymmetrical, comparable in depth to the ventral lobe, and displays a flat base with numerous small but conspicuous crenulations. A small, narrow, simple lobe is positioned on the umbilical shoulder, and two similar elements are located on the umbilical wall. The internal suture is unknown.

COMPARISONS.—The conch of the type for *Eoaraxoceras robustum* is much broader in all growth stages than that of *E.*

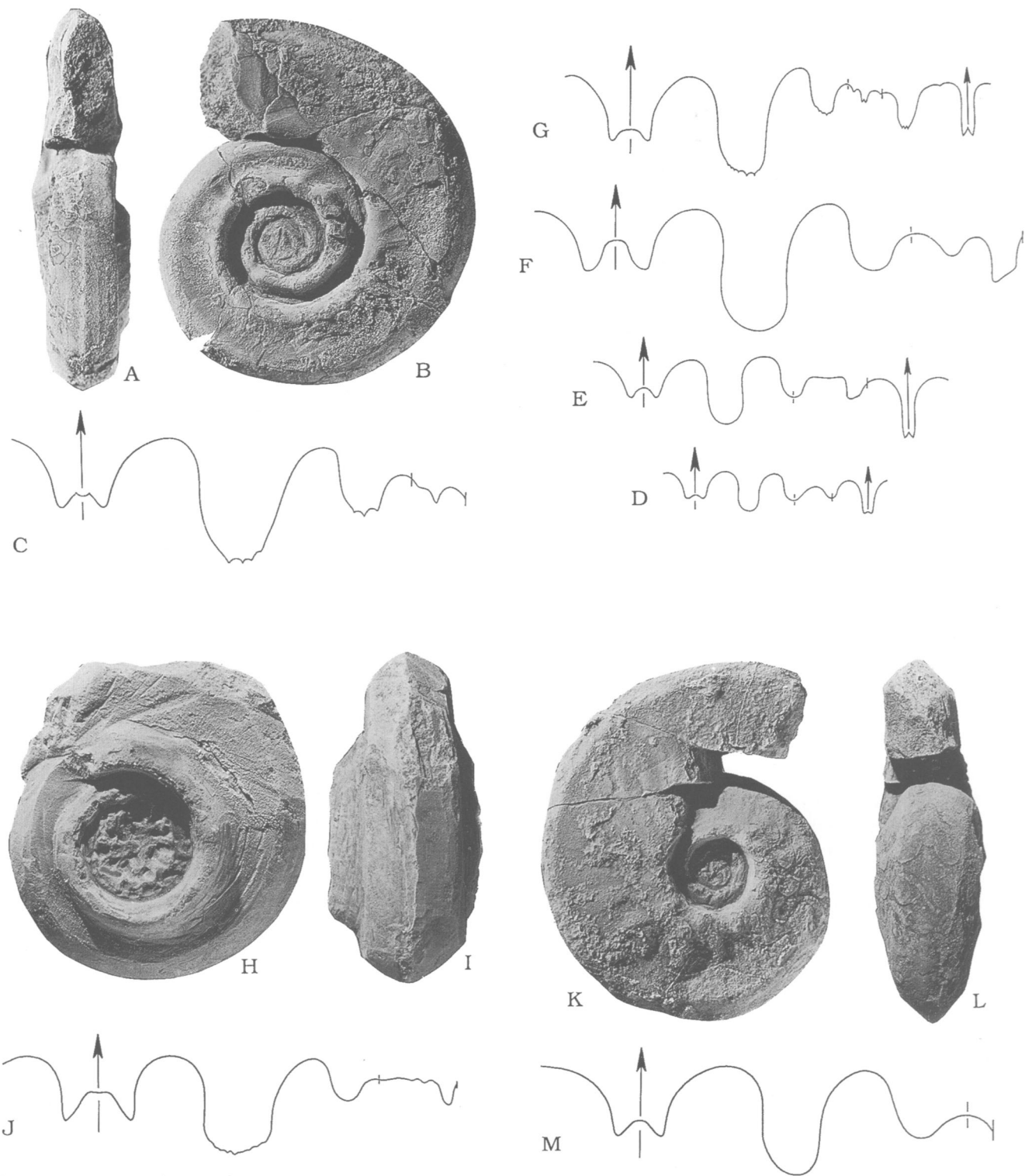


FIGURE 18-4.—*Eoaraxoceras ruzhencevi* Spinosa, Furnish, and Glenister, 1970, from the upper La Colorada beds, Las Delicias, Mexico (A–G), and the *Araxoceras* beds, Kuh-e-Hambast, Abadeh area, central Iran (H–M). A–C, holotype, SUI 32895: A, B, $\times 2.1$; C, diagrammatic representation of the external suture, diameter 23 mm. D–G, inferred sutural ontogeny: D–F, paratype, SUI 32890, diameters 4.6 mm, 7.1 mm, and 11.7 mm, respectively (sutures D and E are complete, F is external only); G, paratype, SUI 31949, complete suture, diameter 20.8 mm. H–J, hypotype, GSI 69 T 123: H, I, $\times 3.5$; J, external suture, diameter 14.4 mm. K–M, hypotype, GSI 69 T 127: K, L, $\times 2.8$; M, external suture, diameter 15 mm. (Reduced to 64% of original for publication.)

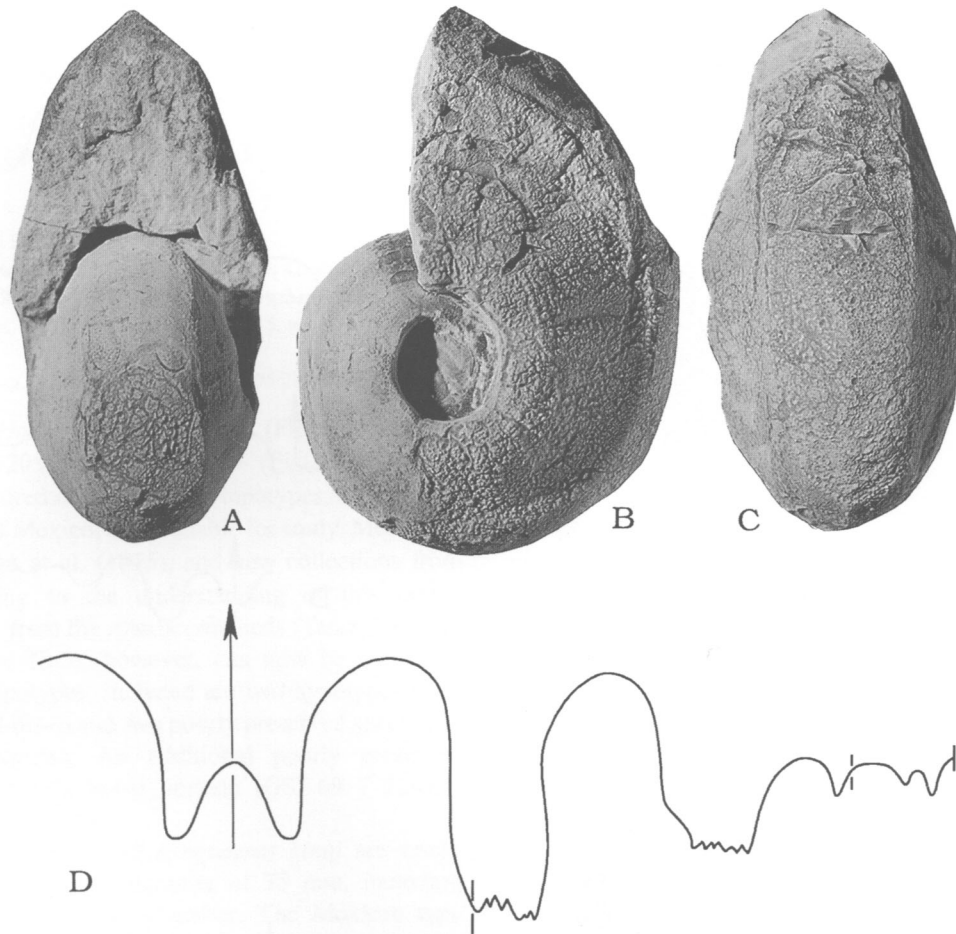


FIGURE 18-5.—*Eoanaxoceras robustum*, new species, *Araxoceras* beds, Kuh-e-Hambast, Abadeh area, central Iran. Holotype, GSI 69 T 120; A–C, $\times 2.2$; D, diagrammatic representation of the external suture, diameter is approximately 17 mm. (Reduced to 73% of original for publication.)

ruzhencevi, and the umbilicus is significantly narrower. The sutures of the two species are similar, with most elements of *E. robustum* falling within the limits of variation documented for *E. ruzhencevi*; however, the first “lateral” lobe of *E. robustum* is proportionally narrower, with distinctive adoral constriction.

Specimen GSI Ab-72174, described by Bando (1979) as *Eoanaxoceras ruzhencevi* (*E. ruzhencevi* [sic]) and questionably referred herein to *E. robustum*, closely resembles the type species in conch form. However, the illustrated suture (Bando, 1979, text-fig. 6B), if accurately portrayed, may permit discrimination based primarily on the divergent form of the first “lateral” lobe.

OCCURRENCE.—The holotype is from Kuh-e-Hambast, Abadeh area, central Iran, within the basal 1 m of the *Araxoceras* beds of Taraz (1971). It represents the lowest araxoceratin occurrence recorded by Taraz (1971, fig. 3). The questionable second specimen is from the “lower part of Unit 6...” at the same locality (Bando, 1979:116), presumably from a level closely comparable to that of the holotype.

REPOSITORY.—Holotype GSI 69 T 120 and the questionably referred specimen (GSI Ab-72174) are in the collections of the Geological Survey of Iran, Tehran.

Kingoceras Miller, 1944

TYPE SPECIES.—*Kingoceras kingi* Miller, 1944:125–126, pl. 42: figs. 6, 7, text fig. 29E [in part, not pl. 42: figs. 8, 9, text-fig. 29E (= *Eoanaxoceras ruzhencevi* Spinosa, Furnish, and Glenister, 1970)].

DIAGNOSIS.—Transitional between Paraceltitinae and Araxoceratinae, and characterized by a thinly lenticular conch form and sutures with only eight fully isolated lobes.

DISTRIBUTION.—The type species of *Kingoceras* is abundant throughout the lower Dzhulfian upper La Colorada beds of Mexico and the uppermost unit (Bed 57 of Newell, 1957) of the subjacent lower La Colorada beds (Spinosa et al., 1975). This lower occurrence is assigned to the upper Guadalupian Capitanian Stage (Figures 18-1, 18-2). Congeneric occurrences

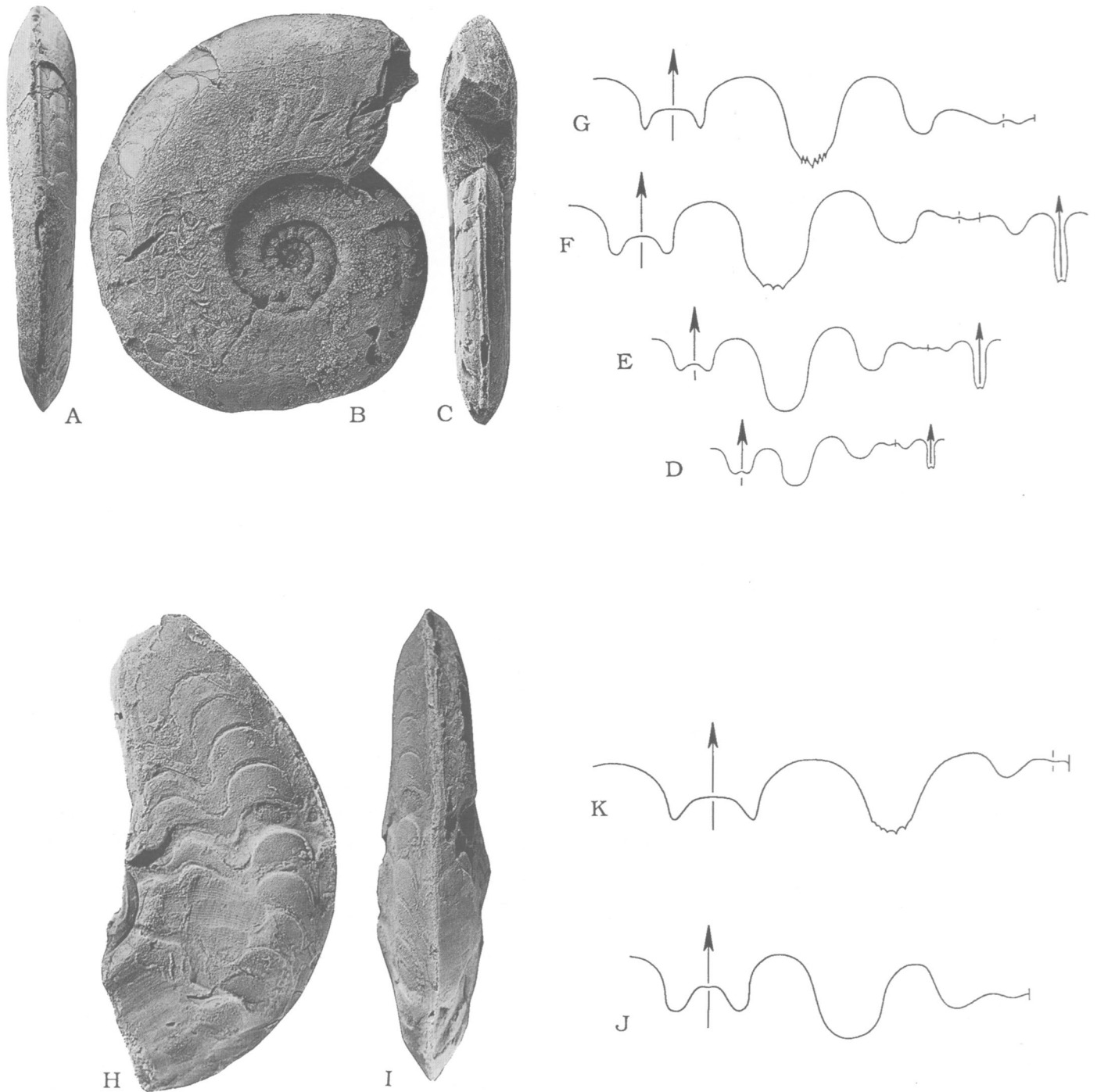


FIGURE 18-6.—*Kingoceras kingi* Miller, 1944, La Colorada beds, Las Delicias, Mexico (A–G), and *Araxoceras* beds, Kuh-e-Hambast, Abadeh area, central Iran (H–K). A–C, holotype, YPM 16281, $\times 2.0$; D–G, diagrammatic representation of the sutures; D,E, complete sutures, hypotype, SUI 12055, diameters 5 mm and 10 mm; F, complete suture, hypotype, SUI 12056, diameter 20 mm; G, external suture, hypotype, SUI 12052, diameter 23 mm. H,I,K, hypotype, GSI 69 T 123: H,I, $\times 3.6$. K, diagrammatic representation of the external suture, diameter is approximately 21 mm. J, hypotype, GSI 69 T 123, diagrammatic representation of the external suture, diameter is approximately 10 mm. (Reduced to 67% of original for publication.)

have been reported as a rare element in the lower Dzhulfian *Araxoceras* beds of Abadeh, central Iran (Spinosa et al., 1975) and are described herein (Figures 18-3, 18-6H-K).

Kingoceras kingi Miller, 1944

FIGURE 18-6A-K

Cibolites? sp. Miller and Furnish, 1940:73.

Kingoceras kingi Miller in King et al., 1944:125-126, pl. 42: figs. 6, 7, text-fig. 29E [in part, not pl. 42: figs. 8, 9 (= *Eoaxoceras ruzhencevi*)].—Spinosa, Furnish, and Glenister, 1975:280-281, pl. 5: figs. 4, 5, text-figs. 2, 15A, 16, tables 2, 3.

Kingoceras n. sp., Spinosa, Furnish, and Glenister, 1975:281, table 3.

DESCRIPTION.—*Holotype*: YPM 16281 (Figure 18-6A-C); *Hypotypes*: SUI 12052, 12055, 12056 (Figure 18-6D-G), 31946. Several hundred additional SUI topotypes, all from the La Colorada beds of Mexico, are available for study. Most were analyzed by Spinosa et al. (1975), and new collections from Mexico add nothing to the understanding of this taxon. Additional material from the *Araxoceras* beds (Taraz, 1971) of central Iran (Figure 18-3), however, can now be compared directly with the topotypes. Included are two hypotypes (GSI 69 T 123, Figure 18-6H-J) and two poorly preserved specimens from the same horizon. An additional poorly preserved specimen from a slightly lower horizon (GSI 69 T 120) is tentatively assigned to *K. kingi*.

All known representatives of *Kingoceras kingi* are small, with the largest achieving a diameter of 35 mm, including one-half volution of the body chamber. The Mexican type material displays a narrowly discoidal, moderately evolute conch. The width ratio W/D decreases from 0.3 to 0.15, and the umbilical ratio U_{\min}/D increases from 0.2 to 0.35 as the diameter increases from 10-35 mm. Coarse transverse ribs are present up to the 10 mm conch diameter, but they are progressively replaced in larger whorls by relatively inconspicuous plications. Growth striations form a low salient across the midflanks and on the venter.

The sutural ontogeny of Mexican *Kingoceras kingi* is represented by Figure 18-6D-G. The first "lateral" lobe is twice as deep as any other external sutural element; serration of this lobe appears in whorls as small as 12 mm diameter, and is present almost invariably at diameters greater than 25 mm. The primary internal element (*I*) is located externally, adjacent to the lateral lobe; it is approximately one-half as deep as the lateral and is commonly serrate at maturity. Characteristically, a variable number of tertiary internal elements ($I^2, I^3 \dots$) is present on either side of the umbilical seam. The number and depth of these tertiary lobes increase with growth from a single element at approximately 5 mm diameter to four or more at maturity. There exists, however, no consistent correlation between conch size and the number or depth of tertiary internal

elements, as some small conchs possess numerous tertiary lobes whereas some larger forms have significantly fewer. The secondary internal element I^1 is located internally, adjacent to the dorsal lobe; it is approximately one-half as deep as element *I*, and it usually remains unserrated.

The occurrence of *Kingoceras* in the Dzhulfian of Iran is significant in supporting the correlation with the *Eoaxoceras* beds of Mexico. Four of the Iranian specimens (GSI 69 T 123) are moderately well preserved, and they exhibit sutures (Figure 18-6J,K) that fall within the range of *K. kingi* (Figure 18-6D-G). The Iranian conchs, however, appear to be broader (W/D 0.25 at 35 mm diameter) than Mexican specimens of similar size (compare Figure 18-6H,I with 18-6A,C). The confirmation of this relationship with better-preserved material would warrant erection of a new species. One additional Iranian specimen (GSI 69 T 120), from slightly below those figured herein, is referable to *Kingoceras* with reservation, but it is too poorly preserved for specific assignment.

OCCURRENCE.—Detailed occurrence data for the Mexican representatives of *Kingoceras kingi* were presented previously (Spinosa et al., 1975). In summary, they range (Figure 18-2) from the top of the lower La Colorada beds (Bed 57 of Newell, 1957), Las Delicias, Coahuila, to association with *Eoaxoceras ruzhencevi* in the uppermost unit of the superjacent upper La Colorada beds (Bed 64 of Newell, 1957). This range is interpreted as upper Guadalupian (Capitanian) to lower Dzhulfian. The better-preserved Iranian representatives (GSI 69 T 123) are from Kuh-e-Hambast, Abadeh area, central Iran, 2.8 m above the base of the *Araxoceras* beds of Taraz (1971). The questionably assigned specimen (GSI 69 T 120) is from the same section but is within the basal 1 m of the *Araxoceras* beds.

REPOSITORIES.—The holotype, YPM 16281, is repositated at the Peabody Museum, Yale University. Mexican hypotypes (SUI 12051, 12052, 12055, 12056, 31946) and several hundred topotypes are in the University of Iowa. Described Iranian specimens (GSI 69 T 123, 69 T 120) are in the collections of the Geological Survey of Iran, Tehran.

Acknowledgments

The authors thank their colleagues W.M. Furnish (University of Iowa), Zhou Zuren (Nanjing Institute of Geology and Palaeontology), and W.W. Nassichuk (Geological Survey of Canada) for stimulating discussions. Hooshang Taraz (Nicholls State University) and personnel of the Geological Survey of Iran provided access to ammonoids from Iran, and Dora Gallegos and Tamra A. Schiappa (both Boise State University) contributed invaluable technical assistance. Financial support came from the Idaho State Board of Education (S 92-127), the National Science Foundation (INT-8822531 and EAR-9004907), and the National Geographic Society (3948-88).

Literature Cited

- Bando, Y.
1979. Upper Permian and Lower Triassic Ammonoids from Abadeh, Central Iran. *Memoires of the Faculty of Education, Kagawa University*, Part 2, 29:103–182, plates 1–11.
- Hyatt, A.
1900. [Tetrabranchiate] Cephalopoda. In K.A. von Zittel, translated and edited by C.R. Eastman, *Text-Book of Palaeontology*, volume 1, part 2:502–592. London.
- Kotlyar, G.V., Y.D. Zakharov, G.S. Kropatcheva, G.P. Pronina, I.O. Chedijia, and V.I. Burago
1989. Evolution of the Latest Permian Biota, Midian Regional Stage in the USSR. *Leningrad Nauka*, 185 pages. [In Russian.]
- Miller, A.K.
1944. Permian Cephalopods. In R.E. King, C.O. Dunbar, P.E. Cloud, Jr., and A.K. Miller, *Geology and Paleontology of the Permian Area Northwest of Las Delicias, Southwestern Coahuila, Mexico*. *Geological Society of America, Special Paper*, 52:71–127, plates 20–45.
- Miller, A.K., and W.M. Furnish
1940. Permian Ammonoids of the Guadalupe Mountain Region and Adjacent Areas. *Geological Society of America, Special Paper*, 26: 242 pages, 44 plates.
- Newell, N.D.
1957. Supposed Permian Tillites in Northern Mexico are Submarine Slide Deposits. *Bulletin of the Geological Society of America*, 68(11):1569–1576, plates 1, 2.
- Plummer, F.B., and G. Scott
1937. Upper Paleozoic Ammonites in Texas. In *The Geology of Texas*, Volume III, Part 1. *University of Texas Bulletin*, 3701:1–516, 41 plates.
- Ruzhencev, V.E.
1959. Classification of the Superfamily Otocerataceae. *Paleontologicheskii Zhurnal*, 1959(2):56–67. [In Russian.]
- Ruzhencev, V.E., and T.G. Sarycheva, editors
1965. Evolution and Change of Marine Organisms at the Boundary between the Paleozoic and Mesozoic. *Trudy, Paleontologicheskogo Instituta, Akademiya Nauk SSSR*, 108: 431 pages, 58 plates. [In Russian.]
- Shevyrev, A.A., and S.P. Yermakova
1979. On the Systematics of Ceratitoids. *Paleontologicheskii Zhurnal*, 1979(1):52–58. [In Russian.]
- Spinosa, C., W.M. Furnish, and B.F. Glenister
1970. Araxoceratidae, Upper Permian Ammonoids, from the Western Hemisphere. *Journal of Paleontology*, 44(4):730–736, plate 109.
1975. The Xenodiscidae, Permian Ceratitoid Ammonoids. *Journal of Paleontology*, 49(2):239–283, plates 1–8.
- Sweet, W.C.
1992. A Conodont-Based High-Resolution Biostratigraphy for the Permo–Triassic Boundary Interval. In W.C. Sweet, Yang Zunyi, J.M. Dickins, and Yin Hongfu, editors, *Permo–Triassic Events in the Eastern Tethys*, pages 120–133. Cambridge: Cambridge University Press.
- Taraz, H.
1971. Uppermost Permian and Permo–Triassic Transition Beds in Central Iran. *Bulletin of the American Association of Petroleum Geologists*, 55(8):1280–1294.
- Taraz, H., F. Golshani, K. Nakazawa, D. Shimizo, Y. Bando, K. Ishii, M. Murata, Y. Okimura, S. Sakagami, K. Nakamura, and T. Tokuoka
1981. The Permian and the Lower Triassic Systems in Abadeh Region, Central Iran. *Memoirs of the Faculty of Science, Kyoto University, Series of Geology & Mineralogy*, 47(2):61–133, plates 1–6.
- Tozer, E.T.
1988. Towards a Definition of the Permian–Triassic Boundary. *Episodes*, 11:251–155.
- Wardlaw, B.R., W.M. Furnish, and M.K. Nestell
1979. Geology and Paleontology of the Permian Beds near Las Delicias, Coahuila, Mexico. *Bulletin of the Geological Society of America*, 90(1):111–116.
- Wilde, G.L.
1990. Practical Fusulinid Zonation: The Species Concept; with Permian Basin Emphasis. *West Texas Geological Society, Bulletin*, 29(7):5–34.
- Zakharov, Y.D.
1988. Parallelism and Ontogenetic Acceleration in Ammonoid Evolution. In J. Wiedmann and J. Kullmann, editors, *Second International Cephalopod Symposium: Cephalopods Past and Present: O.H. Schindewolf Symposium, Tübingen, 1985*, pages 191–206. Stuttgart: Schweizerbart'sche Verlagsbuchhandlung.
- Zhao, J., X. Liang, and Z. Zheng
1978. Late Permian Cephalopods of South China. *Palaeontologia Sinica*, Whole Number 154, new series B, 12: 194 pages, 34 plates. [In Chinese, with English summary.]
- Zhou, Z., B.F. Glenister, and W.M. Furnish
1989. Two-fold or Three-fold: Concerning Geological Time Scale of Permian Period. *Acta Palaeontologica Sinica*, 28(3):269–282. [In Chinese, with English summary.]

19. Depositional Controls on Selective Silicification of Permian Fossils, Southwestern United States

Douglas H. Erwin and David L. Kidder

ABSTRACT

Differential silicification imposes an important taphonomic control on fossil biotas that must be considered before paleoecologic analysis, but the nature of that control has received little attention. Permian rocks in the southwestern United States contain a diversity of biogenic and abiogenic silica from a variety of sources, and many different types of replacement appear to be involved. Analysis of the taphonomic effects of silicification requires understanding the sources of silica, the timing and differential patterns of replacement, the mechanisms, and the controls at single localities.

The controls on silicification include differences between open and less open marine settings; more complete silicification and greater fidelity of preservation occur in more open marine environments, probably because of greater silica availability. A second factor involves a taxonomic bias with better preservation in echinoids, articulate brachiopods, and scaphopods than in various gastropods, with bivalves, bryozoans, and corals most poorly preserved. A third factor is imposed by a silicification bias against large-sized fossils; echinoid spines and some infaunal or semi-infaunal organisms are the exception, and their silicification may have been enhanced by immediate postmortem isolation. The patterns are expected to differ between localities, and different elements at a single locality may have been subject to different episodes of silicification. Considerable work remains to determine the relative significance of these and other potential controls on silicification.

Introduction

Silicified faunas are ubiquitous throughout the fossil record. Their fidelity of preservation and the relative ease of laboratory

preparation via acid dissolution makes them important for many paleontologic studies. The bulk of the recovered Permian fossil record in the southwestern United States is silicified, yet despite the importance of these deposits for systematic, paleoecological, and evolutionary studies their taphonomic history has been poorly studied (see Carson, 1991, for a recent review). This is particularly striking since Newell et al. (1953; see also Cooper and Grant, 1972) first noted the existence of taxonomic selectivity, or differential silicification, within the Guadalupe Mountains.

Differential silicification may have several taphonomic consequences that influence the amount of information paleontologists can recover from the sedimentary record. Taxonomic selectivity may destroy particular components of the fauna. For example, acid residues dominated by articulate brachiopods and echinoids may reflect the original composition of the durably skeltonized biota, or they may reflect incomplete or nonreplacement of a more diverse biota resulting in the loss of certain faunal elements (e.g., molluscs) during reworking or laboratory processing. Without taphonomic analysis, it is impossible to distinguish between these two alternatives. Other potential taphonomic biases include differences in the extent of replacement in different depositional environments and size-selectivity. Each of these biases limits the amount of information that can be retrieved from different settings, and they limit our ability to compare faunas from different localities. Although the diagenetic history of silicified material is of interest in its own right, the taphonomic aspects of silicified deposits become particularly important when different components of an assemblage respond to the same event in different ways, biasing our record of the original fauna.

Differentially replaced faunas have played an important role in reconstructing the paleoecology and paleoenvironments of the Permian basin, and they are important for detailing the extinction history of the marine biota during the end-Permian mass extinction. For example, much of the Changxingian fauna (latest Permian) in South China is silicified (R.L. Batten, pers. comm., 1986). The last record of many genera of gastropods,

Douglas H. Erwin, Department of Paleobiology, National Museum of Natural History, Smithsonian Institution, Washington, D.C. 20560-0121. David L. Kidder, Department of Geological Sciences, Ohio University, Athens, Ohio 45701.

brachiopods, and other marine invertebrates occurs in the Guadalupian of the southwestern United States. In both cases, evaluating the extinction record depends upon an understanding of the silicification process.

This is the first detailed taphonomic and diagenetic analysis of differential silicification, and it emphasizes the Wolfcampian–Leonardian Colina Limestone in southeastern Arizona and the equivalent Hueco Formation in New Mexico (Figures 19-1, 19-2). We chose these units in part because there appears to have been less silica in the system than in units in the Permian basin of West Texas and greater overall taxonomic diversity, although the absolute number of specimens is far lower. The reduced amount of silica makes it easier to

determine the relative significance of different controls on silicification. Our results shed light on paleoecological studies of Guadalupian deposits in the Glass Mountains and elsewhere. Previous studies of silicification in fossils include Carson (1991), Hatfield (1975), Holdaway and Clayton (1982), Jacka (1974), Leljdahl (1986), Maliva and Siever (1988b), Meyers (1977), Schmitt and Boyd (1981), and Wilson (1966). Only Boyd and Newell (1972) and Newton et al. (1987) considered the taphonomic effects of silicification. In this preliminary report the possible controls on differential silicification of fossil material and their taphonomic implications are discussed. Future work will consider in more detail the diagenetic patterns of silicification and taphonomic history.

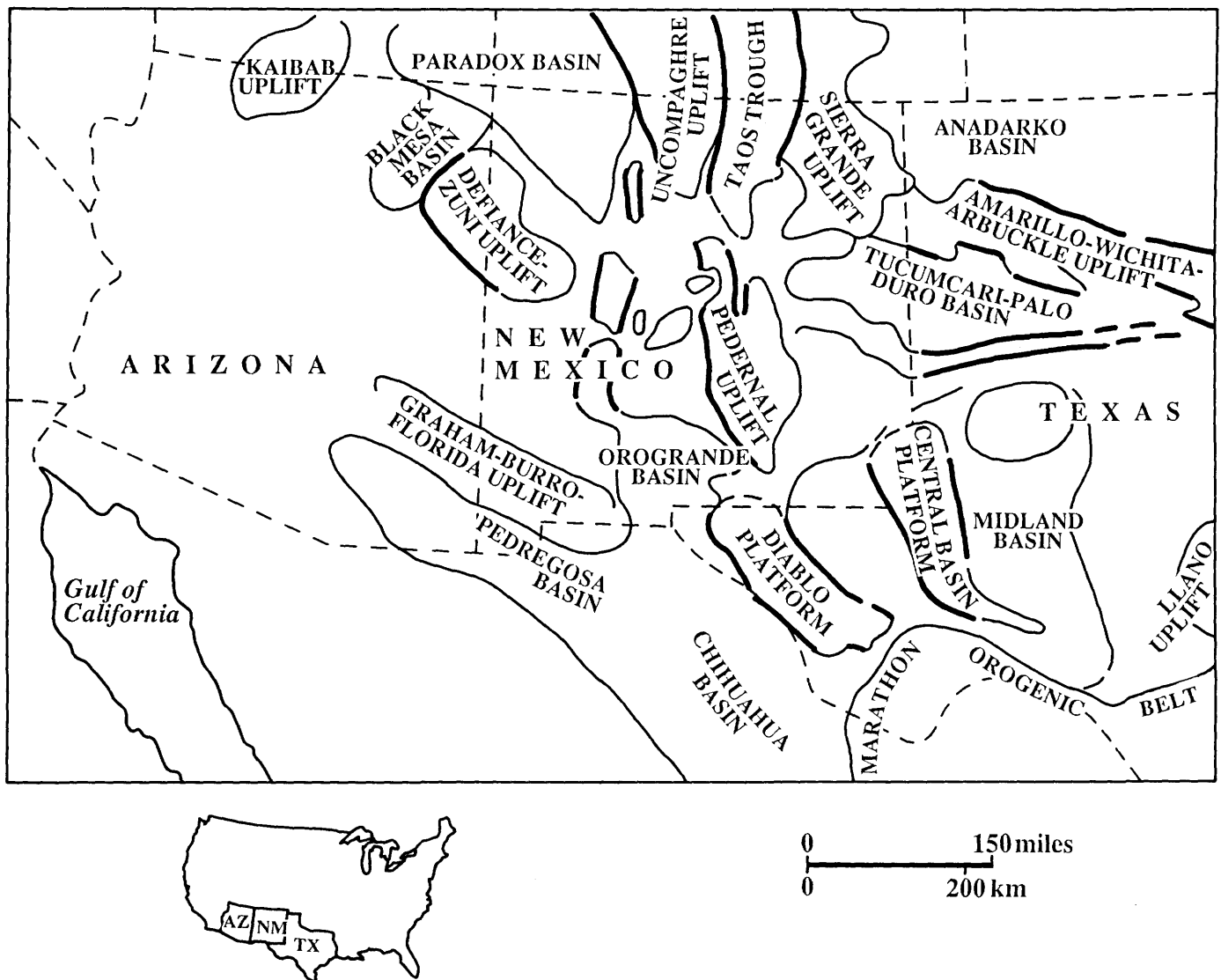


FIGURE 19-1.—Regional map showing the relationships among Permian basins and uplifts in the southwestern United States (from various sources).

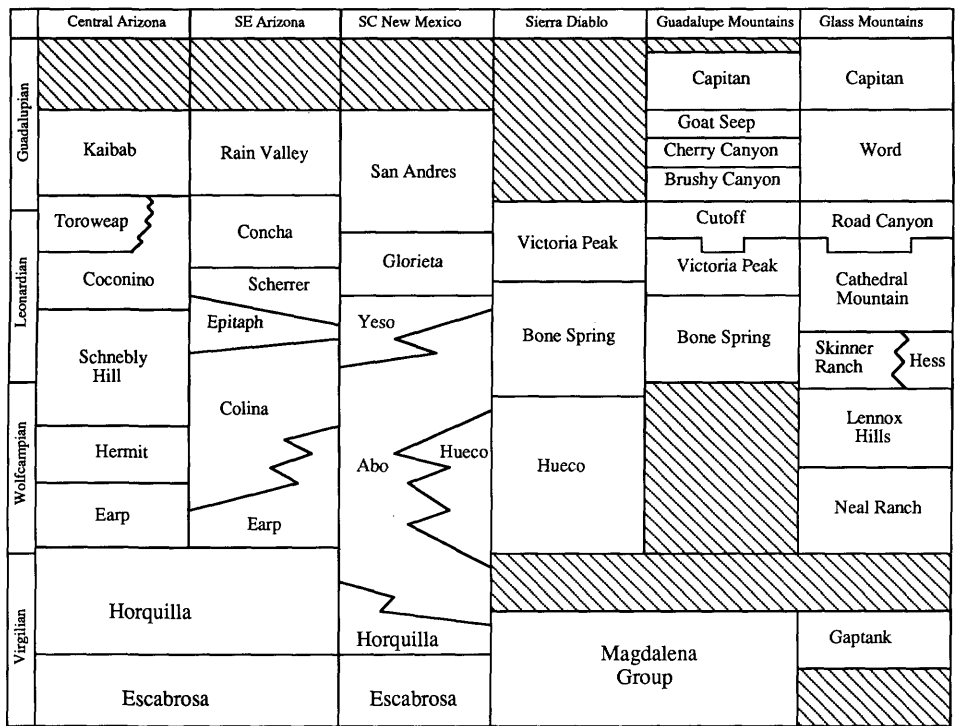


FIGURE 19-2.—Generalized Permian stratigraphy of the southwestern United States. Correlations between the Hueco, Colina, and Earp are controversial. Most sections are cut by numerous unconformities (e.g., Blakey (1990)), which are not shown here.

The Process of Silicification

Important aspects of the replacement of original skeletal material by silica include the sources of silica, the timing of the replacement process(es), the mechanism of replacement, and the controls that produce taphonomic variability. Silica in replaced fossils may involve Beekite disks, siliceous coatings or rinds on the surface, complete replacement with cryptocrystalline quartz, and void-filling silica (Cooper and Grant, 1972; Schmitt and Boyd, 1981). The Colina Limestone is characterized by a wide variety of silica types (Lyons, 1987, 1989; Kidder and Erwin, unpublished data) in addition to its well-silicified faunas. The varieties of silica include replaced vertical and horizontal burrows, dispersed siliceous blebs and nodules, a very fine-grained, box-work silica structure, and crack-filling silicification. The diversity of silica phases raises the possibility that several episodes of silica genesis may have occurred, although further field, petrographic, and isotopic work is needed to resolve the relative timing of these events.

Potential biogenic and abiogenic silica sources include the siliceous tests or skeletons of sponges and radiolarians, together with abundant Tertiary volcanics and clay diagenesis.

Data

The faunas of the Colina Limestone and Hueco Formation

(Figure 19-3) are dominated by gastropods and echinoid fragments with lesser amounts of brachiopods, bivalves, scaphopods, and corals (Table 19-1). Gastropod diversity is far higher than in the Permian basin, but the diversity of brachiopods is an order of magnitude less (Erwin, 1989). Field data, slab and thin-section analysis, and the study of acid-

TABLE 19-1.—Faunal list for the upper portion of the section at Warren, Arizona.

- various corals, mostly tabulates
- echinoid spines
- fenestellid bryozoans
- Composita*
- occasional large productid brahiopods
- small nuculid bivalves
- cephalopod fragments
- scaphopods (?*Plagioglypta*)
- gastropods:
 - bellerophonts
 - Omphalotrochus*
 - various pleurotomarids, including *Apachella*
 - Naticopsis*
 - Glyptospira*
 - Anomphalus*
 - Stegocoelia*
 - ?*Soleniscus*
 - various caenogastropods

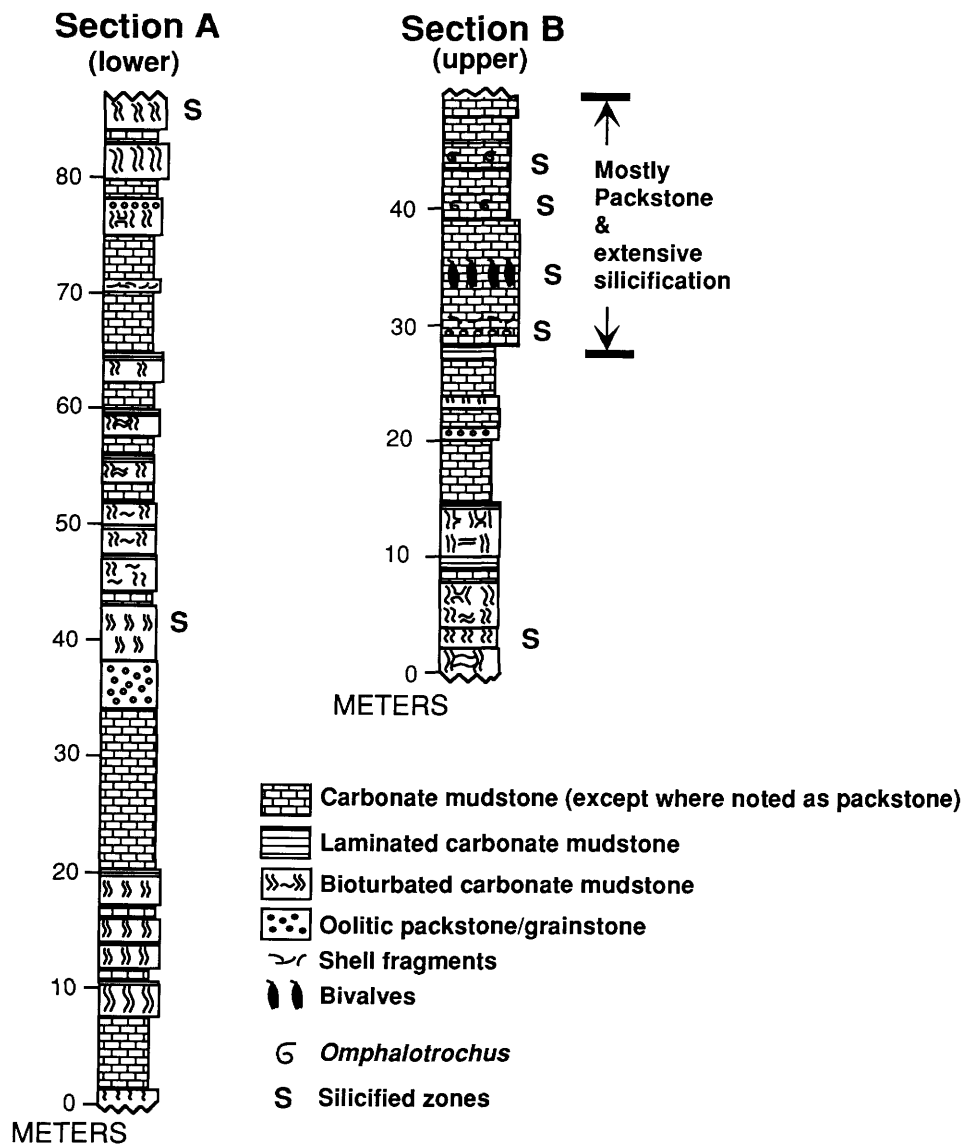


FIGURE 19-3.—Measured sections of upper Colina Limestone at Warren, Arizona. Sections A and B are separated by a fault of unknown displacement.

digested bulk samples have revealed considerable information relating environmental factors to the degree of silicification. We have noted correlations between silicification and taxonomic affinity, size of organism, depositional environment, and fossil mode of life.

The taxonomic bias in silicification is presented as a series of hierarchies for localities in the Hueco Formation (Florida Mountains, New Mexico; Wolfcampian), and the Colina Limestone (Tombstone Hills and Warren, Arizona; Wolfcampian-?Leonardian) (Tables 19-2, 19-3). Considerable variation is obvious, but a general pattern emerges: echinoid spines, brachiopods, and scaphopods are generally the best preserved fossils, followed by bellerophontid and trochid gastropods,

then caenogastropods, and finally *Omphalotrochus*, *Straparolus* (sensu lato), and pleurotomarid gastropods. The best preserved specimens are the most completely silicified; the silica is finely crystalline quartz.

Fossil fragments are the bulk of the silicified material recovered from most localities in the Colina Limestone and the Hueco Formation. This fragmentation has a variety of causes, including predepositional mechanical destruction and weathering, bioerosion, and chemical dissolution. Postdepositional alteration may stem from destruction by bioturbation, incomplete silicification, fracturing during structural deformation of the units, and breakage during the etching process as specimens collapse.

TABLE 19-2.—Silicification hierarchies for selected localities (from best (most complete, finest-scale silicification) to worst).

Warren, Arizona
approx. 70 m in section A
<i>Composita</i> , echinoid spines
caenogastropods
other gastropods, unidentified large brachiopod
bellerophonitid gastropods, nuculid bivalves
fenestellid bryozoa
approx. 30 m in section B
<i>Composita</i> , echinoid spines
<i>Glyptospira</i> , bellerophonitids, <i>Anomphalous</i>
caenogastropods, unidentified large brachiopod
bivalves
[no bryozoans observed]
approx. 42–45 m in section B
all gastropods, scaphopods
bivalves
brachiopods, corals
Gym Limestone [= Hueco], Florida Mountains, New Mexico
brachiopods (several), echinoid spines, scaphopods
caenogastropods, <i>Glyptospira</i> , bellerophonitids
<i>Omphalotrochus</i> , pleurotomarids
bivalves, corals

Estimates of the relative significance of each of these factors for one sample collected from the 45 m level at the Warren, Arizona locality (Figure 19-3) revealed that approximately one-third of the insoluble residue is identifiable. Some 90 percent of identifiable specimens are gastropods, with only minor contributions from (in descending order) echinoid spines, brachiopods, scaphopods, and bivalves. Within the silicified gastropod fraction, about 10 percent to 15 percent of the specimens show considerable evidence of pre-depositional weathering or breakage; however, the bulk of the specimens show no signs of any mechanical degradation. This suggests that the assemblage consists of a mixture of shells, most of which were either alive or fairly recently dead when buried, and a minor component of material that had either been lying on the seafloor or was transported in from a higher energy setting prior to burial. There is no apparent difference in the quality of silicification between the two components.

Not surprisingly, the importance of predepositional weathering and transport varies widely between localities. A bed 2 m

below that described above (Figure 19-3) has a much higher percentage of abraded specimens, indicating a higher energy environment. An even more highly abraded sample collected from near the top of Colina Ridge in the Tombstone Hills consists solely of well-worn silicified fragments of large (6+ cm original shell length) bellerophonitids.

Virtually all specimens with a maximum dimension greater than 3–4 cm show signs of postdepositional fracturing. Inspection of the residue suggests that such fracturing probably accounts for a far higher percentage of the fragmentary remains than does weathering. Evidently smaller specimens are less subject to fracturing. Estimating the relative significance of the remaining factors was not possible.

The incomplete replacement also imparts a clear size bias to the silicified material recovered: smaller fossils are more completely preserved than are larger fossils. Exceptions to this generalization include echinoid spines, the brachiopod *Composita*, and the large gastropod *Omphalotrochus*. At the sample from the 45 m level at Warren, discussed above, the only identifiable fossils with a maximum dimension greater than 3 cm are high-spined gastropods, bellerophonitids, echinoid spines, *Omphalotrochus*, *Straparollus*, and some fragmentary brachiopods. More than 80 percent of the specimens recovered are less than 2 cm maximum dimension. This locality is somewhat surprising in that brachiopods appear to have been incompletely silicified and, thus, are more poorly represented in the residues than they are in the initial deposit. Although bivalves are relatively few, the small nuculid bivalves are much better preserved than some larger, non-nuculid taxa; however, smaller organisms always outnumber larger organisms and, thus, should comprise a larger portion of the fossilized remains.

The degree of silicification varies systematically within the Pedragosa region (Figure 19-4). When combined with stratigraphic and sedimentologic data, this suggests that the depositional environment influences the degree of silicification. The coarseness of silicification among specimens of *Glyptospira*, a widespread trochid gastropod (Erwin, 1988), varies within the basin. The best preservation occurs at the top of the section at Warren, Arizona (Figure 19-3; Table 19-4); fidelity decreases toward the Tombstone Hills and Scherrer Ridge. A similar pattern occurs in bellerophonitid and pleurotomarid gastropods.

Lyons (1989) interpreted the Colina Limestone as a lagoonal deposit that was restricted by ooid shoals in southeasternmost Arizona. The Warren locality is within the lagoonal boundaries, and Colina localities to the west and north, such as the Tombstone Hills, Scherrer Ridge, and the Whetstone Mountains, were shoreward of Warren (Figure 19-4). Faunal diversity in the Colina (Table 19-1) indicates that there must have been significant interchange between lagoonal water and marine water. If ooid shoals inhibited circulation, their main function was to shelter the lagoon from high energy conditions, and they did not completely cut off marine water. Samples collected at the Warren section suggest that more open marine conditions correlate with improved fidelity of silicification.

TABLE 19-3.—A generalized hierarchy of silicification.

Best
brachiopods echinoid spines scaphopods
various gastropods
<i>Glyptospira</i> bellerophonitids
<i>Omphalotrochus</i> straparolids pleurotomarids
Worst

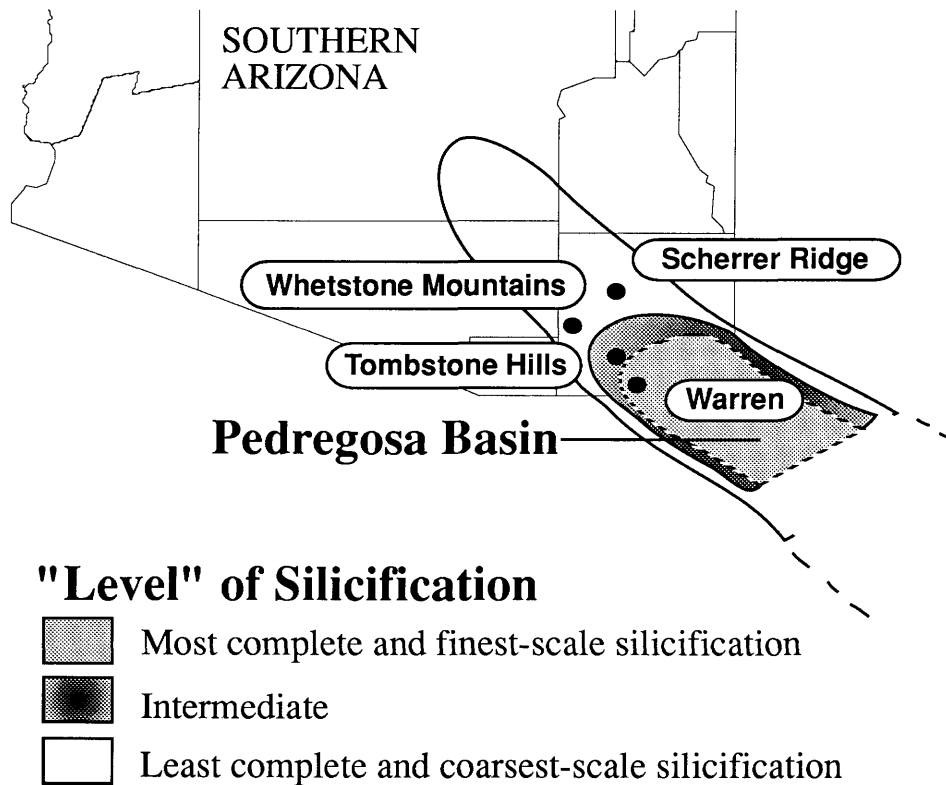


FIGURE 19-4.—Map of southeastern Arizona showing the general position of the Pedregosa basin and localities of Colina Limestone investigated in this study. The basin has been contoured to show the rough variation in completeness and general nature of silicification. Shells with the most complete and finest-scale silica replacement are the best preserved.

The lower 33.5 m of section B at Warren are barren (Figure 19-3). Silicified infaunal bivalves appear at the 33.5 m level of the Warren section; the lower part of the section lacks macrofossils, but considerable bioturbation is apparent. Faunal diversity and preservational fidelity increases up section, with abundant echinoid spines and the brachiopod *Composita*, well-preserved caenogastropods and nuculid bivalves, occasional remains of pleurotomarids and bellerophontids, and fragments of fenestellid bryozoans and cephalopods. Scaphopods and corals appear near the top of the section. Although our evidence is fragmentary, it suggests a similar pattern occurs in the sections at Tombstone Hills. In general, both regional and single-section comparisons suggest that the fidelity of preservation increases as one approaches more open marine conditions.

TABLE 19-4.—The silicification hierarchy for *Glyptospira*.

Best
Upper part of section at Warren locality
Gym Limestone (Florida Mountains, New Mexico)
Middle part of section at Warren locality
Tombstone Hills sections
Worst

The only well-silicified bivalves at this locality were infaunal, and they are always found in life position. Other larger bivalves fragment during etching and are generally not identifiable. Commonly the other silicified gastropods, echinoid spines, and bryozoans occur in beds that are interpreted as storm beds (although some may be highly bioturbated). Furthermore, many beds appear to be shell lags with silicified fossils surrounded by unsilicified shell debris. This bias toward replacement of buried taxa may partially explain the exceptions to the bias against large-sized fossils. For example, the upper silicified beds in Figure 19-3 are assemblages of mixed silicified fossils and unsilicified shell hash. It is unclear why the shell hash is generally resistant to silicification. *Omphalotrochus* is a large, suspension-feeding gastropod, which lived with its apex buried in the sediment (Erwin and Kidder, unpublished data), and is generally well-silicified. Similarly, when scaphopods are present they are well preserved.

Discussion

The factors that control fossil silicification fall into two different classes: (1) environmental controls, including the depositional environment, extent of transport and reworking of

fossils, rapidity of burial, and chemistry of depositional and diagenetic pore waters; and (2) biologic controls, including original shell mineralogy, skeletal microstructure, and the organic content of shells. Newell et al. (1953) and Dapples (1967) identified and summarized patterns of taxonomic influence on silicification (presumably controlled by some of the factors discussed above), in which fidelity of preservation varied with taxonomic affinity. The hierarchical pattern varied with locality, but little consideration has been given to what produced these patterns.

General progress in isolating the effects of these controls has been limited, but some advances have been made. Fluctuating pH gradients can enhance precipitation of silica in certain settings (e.g., alkaline lakes (Eugster, 1967)). The influence of pH on silicification has led to the belief that pH fluctuations are important in silicification of fossils in normal marine settings; however, the dramatic fluctuations on a microscopic scale needed for fine silicification may be possible, but are difficult to test. More recent work (e.g., Holdaway and Clayton, 1982) suggests that organic matter can be effective in lowering the kinetic threshold that would otherwise prevent silicification. Maliva and Siever (1988a,b) recently revived the concept of force of crystallization as an important factor in silicification and presented several specific textural criteria for recognizing that mechanism. A combination of organics complexing with silica and calcite dissolution driven by the force of crystallization might silicify fossils more easily than would drastic fluctuations in pH.

More specific advances related to the influence of original shell mineralogy on silicification come from Permian fossil assemblages in the Park City Formation of Wyoming (Boyd and Newell, 1972; Schmitt and Boyd, 1981) and from the author's current studies in the southwestern United States. Original mineralogy strongly influenced the patterns of silicification in the bivalves of the Park City Formation. Much of the silicification occurred preferentially in originally aragonitic fossils; the aragonite dissolved, and the resulting voids were filled with quartz (Schmitt and Boyd, 1981). Conversely, our Permian localities reveal silicification patterns that seem to have little to do with original mineralogy. Petrographic and microprobe analysis indicates that silicification occurred by simultaneous dissolution and replacement by cryptocrystalline quartz. The spongy texture of some fossils and the fine-scale alternation between calcite and silica indicate that dissolution and replacement is frequently incomplete or on a very small scale. There is little indication of the void-filling quartz described by Schmitt and Boyd (1981).

Evaluation of the relative significance of the environmental and biologic controls in different settings is extremely complex. It must be emphasized that these factors are not mutually exclusive but often may act in concert. The evidence presented below is limited to only Wolfcampian-Guadalupean localities from the southwestern United States; other factors may be of greater importance in other regions. The process of silicification can be divided into the following phases.

ENVIRONMENTAL CONTROLS.—The depositional environment imposes general controls through sediment composition and the quantity of sediment and through the nature and type of silica, detritus, and/or organic material originally present (for example, substantial organic material that was originally present as algae). Individual deposits are affected by the rapidity of burial and transport and/or by the extent of mechanical, chemical, and biologic reworking of sediments and fossils.

Davies et al. (1989) pointed out that the preservation of shell material requires rapid burial to a point below the layer in which taphonomic processes are common, in part because rates of shell loss by dissolution greatly exceed those from biological or mechanical degradation both at the sea floor and within the upper layer of sediment. Many of the assemblages in the limestones of the Hueco Formation and Colina Limestone appear to be event beds of probable storm origin, and in some cases the concentrated deposits seem to be more readily, and perhaps more completely, replaced than dispersed fossils. The apparent increased silicification in these concentrations might also be due to rapid burial, rather than simply concentration of the fossils, or to greater original porosity in the event bed. If storms quickly killed and buried organisms, a greater amount of organic matter in the shells may have been preserved and facilitated later silicification. It seems unlikely that the concentrations of shell beds in the Colina Limestone and Hueco Formation could have arisen other than by rapid burial associated with storm deposits. The preferential silicification of the basinal facies of the Capitan Reef complex (e.g., Newell et al., 1953) suggests that rapid burial of those fossils may have enhanced their silicification (although radiolarians, the abundant silica source, also must have been a major factor in those beds). The observation by Read (1985) that lagoonal deposits and turbidites in carbonate settings are commonly silicified suggests that rapid burial may be a significant factor in those settings. Rapid burial, however, appears not to have been involved in preservation of a silicified gastropod assemblage from the Plympton Formation (Permian, Nevada) (Yochelson, 1973). In this case the bellerophonid and neritid gastropods and the scaphopod *Plagiogypta* are highly worn, and the deposit was apparently formed as a high energy beach deposit.

Environmental controls on later diagenesis include destruction of replaced fossils by leaching either the carbonate or the siliceous phases (via the introduction of new pore waters, for example) and the introduction of later silica phases. Many of the localities in Cochise County, Arizona, with a rich silicified fauna, are within one mile of volcanic necks; the Warren locality is immediately adjacent to one of the largest copper ore bodies in the country. These Tertiary events generated substantial changes in pore waters, but there has been virtually no attention given to what effect these events might have had on silicified fossils.

The final phase in the history of silicified fossil deposits involves weathering on the outcrop and laboratory etching during preparation. Newton et al. (1987) noted that silicified

Triassic faunas from Oregon generally contain many incompletely preserved fossils, which fall apart during the etching process. Although the effects of incomplete replacement can be partially ameliorated by coating such fossils with an insoluble compound during etching, some degradation still occurs. The controls on silicification that operate only during this phase have not yet been identified.

BIOLOGIC CONTROLS.—The careful analysis of shell microstructure, the amount of organic material in the shell matrix, and the size of the organisms are essential for understanding patterns of silicification. These elements each influence the amount of surface area available for the replacement reaction and the mobility of silica. It would be expected that the rate of silicification and the fidelity of preservation should increase with surface area; however, brachiopods and bryozoans have very similar mineralogies (Williams, 1990), but brachiopods are far more readily preserved. In addition, bivalves have broadly similar mineralogy, but the small, infaunal nuculid bivalves are among the best preserved elements in the fauna whereas other bivalves are generally only weakly silicified. These examples indicate that in the Permian of the southwestern United States original mineralogy does not seem to have been an important factor.

The striking size bias in etched residues in New Mexico and Arizona may be due to differential silicification, which suggests that silica was limiting. There is less evidence of size bias in samples from the Glass Mountains, perhaps because more silica was available in the Permian basin than on adjacent carbonate shelf regions.

HIERARCHY OF HYPOTHESES.—Clearly there are multiple controls on silica replacement of fossils within Permian rocks in the southwestern United States. Present evidence suggests the controls over silicification may be arranged hierarchically. The primary control may have been between open and restricted marine settings with increased silicification in more open marine situations. This is supported by the lack of size bias in the Permian basin and by stratigraphic and geographic silicification gradients from southeastern Arizona to West Texas. These gradients require further testing, as they span several basins. A secondary level of control was provided by taxonomic selectivity. The factors behind the taxonomic selectivity have not yet been identified, but it is suggested that differing degrees of organic material in the shells and/or shell microstructure may be involved. A tertiary level of control was provided by bias in favor of smaller shells. In part, this bias may reflect the limiting nature of silica in some of these systems, which also may be reflected by the difference between open and restricted marine settings. Rapid burial of certain taxa in storm deposits seems to have enhanced their degree of silicification, but it is not certain where to place this potential control within this possible hierarchy.

The pattern of differential silica replacement is an important taphonomic control on paleoecological studies, although its significance has not been generally appreciated. Differential

silicification can bias samples in several ways. First, the pattern of taxonomic selectivity means that comparisons of entire assemblages between localities may be biased by the completeness of silicification. A fauna of apparently high diversity may simply represent more complete silicification. Second, particular depositional environments and settings (e.g., rapid burial along slopes) appears to enhance silicification, so fossils found in, or transported to, these areas will be well represented in collections. Third, the preferential silicification of infaunal and semi-infaunal elements may increase their representation in collections relative to the epifauna. Fourth, there is at least circumstantial evidence that in areas where silica is limiting, larger specimens may be incompletely silicified, thus imposing a size-bias on the assemblage. Because of the exquisite preservation of silicified faunas, these difficulties hardly suggest that paleontologists should ignore the paleoecologic and paleoenvironmental potential of these assemblages, but they do indicate that, as with all fossil assemblages, careful taphonomic analysis is an essential prerequisite to paleoecologic studies.

Conclusions

1. Original shell mineralogy is not an important control on silicification in the Permian of southeastern Arizona, although there may be some exceptions to this generalization.

2. Specific environmental and biologic influences control most of the silicification in the Permian of southeastern Arizona. Environmental controls include open versus less open marine settings, which could reflect the amount of locally available silica. Rapid burial is also a significant control. Biologic controls include taxonomic affinity and size.

3. The specific environmental and biologic influences outlined above may be arranged into one or more hierarchies that control silicification. If further work validates these hierarchies of control in the Permian of the southwestern United States, the approach may apply to many other settings.

Future Directions

This preliminary research has identified a number of questions for future work in the complex problem of fossil silicification. Although it was not possible to rule out original shell mineralogy as influencing silicification in these deposits, many other avenues of research remain, including the relationship between organic material and silicification; characterization of which depositional environments are more likely to have silicified deposits; petrographic relations between microstructure and silicification patterns; and application of stable isotopes to chart pore water history and to identify the origin of different silica phases. Clearly, integrated paleontologic, sedimentologic, and diagenetic studies may be able to further isolate controls on silicification to the point of providing some predictive value.

Acknowledgements

Douglas H. Erwin acknowledges support from the National Museum of Natural History and prior support of this work from the Petroleum Research Fund administered by the American

Chemical Society and National Science Foundation Grant BSR 87-22510. David L. Kidder acknowledges support from the Ohio University Research Council. We appreciate reviews of the manuscript from Richard Grant, Donald Boyd, David Rohr, Bruce Wardlaw, and Ellis Yochelson.

Literature Cited

- Blakey, R.C.
1990. Stratigraphy and Geologic History of Pennsylvanian and Permian Rocks, Mogollon Rim Region, Central Arizona and Vicinity. *Bulletin of the Geological Society of America*, 102(9):1189-1217.
- Boyd, D.W., and N.D. Newell
1972. Taphonomy and Diagenesis of a Permian Fossil Assemblage from Wyoming. *Journal of Paleontology*, 46(1):1-14, plates 1-4.
- Carson, G.A.
1991. Silicification of Fossils. In P.A. Allison and D.E.G. Briggs, editors, *Taphonomy: Releasing the Data Locked in the Fossil Record*, pages 455-499. New York: Plenum Press.
- Cooper, G.A., and R.E. Grant
1972. Permian Brachiopods of West Texas, I. *Smithsonian Contributions to Paleobiology*, 14:1-231, plates 1-23.
1974. Permian Brachiopods of West Texas, II. *Smithsonian Contributions to Paleobiology*, 15:233-793, plates 24-191.
1975. Permian Brachiopods of West Texas, III. *Smithsonian Contributions to Paleobiology*, 19:795-1921, plates 192-502.
1976a. Permian Brachiopods of West Texas, IV. *Smithsonian Contributions to Paleobiology*, 21:1923-2607, plates 503-662.
1976b. Permian Brachiopods of West Texas, V. *Smithsonian Contributions to Paleobiology*, 24:2609-3159, plates 663-780.
1977. Permian Brachiopods of West Texas, VI. *Smithsonian Contributions to Paleobiology*, 32:3161-3370.
- Dapples, E.C.
1967. Silica as an Agent in Diagenesis. In G. Larsen and G.V. Chilingar, editors, *Diagenesis in Sediments*, pages 323-342. New York: Elsevier Publishing Company.
- Davies, D.J., E.N. Pwll, and R.J. Stanton, Jr.
1989. Relative Rates of Shell Dissolution and Net Sediment Accumulation, a Commentary: Can Shell Beds Form by Gradual Accumulation of Biogenic Debris on the Sea Floor? *Lethaia*, 22(2):207-212.
- Erwin, D.H.
1988. The Genus *Glyptospira* (Gastropoda: Trochacea) from the Permian of the Southwestern United States. *Journal of Paleontology*, 62(6):868-879.
1989. Regional Paleogeology of Permian Gastropod Genera, Southwestern United States, and the End-Permian Mass Extinction. *Palaios*, 4(5):424-438.
- Eugster, H.D.
1967. Hydrous Sodium Silicates from Lake Magadi, Kenya: Precursors of Bedded Chert. *Science*, 157(3793):1177-1180.
- Hatfield, C.B.
1975. Replacement of Fossils by Length-Slow Chalcedony and Associated Dolomitization: By Alonzo D. Jacka, Jour. Sed. Petrology, V. 44, p. 421-427. *Journal of Sedimentary Petrology*, 45(4):951-952.
- Holdaway, H.K., and C.J. Clayton
1982. Preservation of Shell Microstructure in Silicified Brachiopods from the Upper Cretaceous Wilmington Sands of Devon. *Geological Magazine*, 119(4):371-382.
- Jacka, A.D.
1974. Dolomitization of Fossils by Length-Slow Chalcedony and Associated Dolomitization. *Journal of Sedimentary Petrology*, 44(2):421-427.
- Leljedahl, L.
1986. Endolithid Micro-Organisms and Silicification of a Bivalve Fauna from the Silurian of Gotland. *Lethaia*, 19(3):267-278.
- Lyons, T.W.
1987. Replacement Silicification in the Colina Limestone (Lower Permian) of Southeastern Arizona. [Abstract.] *Geological Society of America, Abstracts with Programs*, 19(7):753.
1989. Stratigraphy and Depositional Environment of the Colina Limestone (Lower Permian), Southeastern Arizona. 260 pages. Unpublished master's thesis, University of Arizona, Tucson, Arizona.
- Maliva, R.G., and R. Siever
1988a. Diagenetic Replacement Controlled by Force of Crystallization. *Geology*, 16(8):688-691.
1988b. Mechanisms and Controls of Silicification of Fossils in Limestones. *Journal of Geology*, 96(4):387-398.
- Meyers, W.J.
1977. Chertification in the Mississippian Lake Valley Formation, Sacramento Mountains, New Mexico. *Sedimentology*, 24(1):75-104.
- Newell, N.D., J.K. Rigby, A.G. Fischer, A.J. Whiteman, J.E. Hickox, and J.S. Bradley
1953. *The Permian Reef Complex of the Guadalupe Mountains Region, Texas and New Mexico: A Study in Paleogeology*. 236 pages. San Francisco: W.H. Freeman and Company.
- Newton, C.R., M.T. Whalen, J.B. Thompson, N. Prins, and D. Delalla
1987. Systematics and Paleogeology of Norian (Late Triassic) Bivalves from a Tropical Island Arc: Wallowa Terrane, Oregon. *Paleontological Society, Memoir*, 22: 83 pages.
- Read, J.F.
1985. Carbonate Platform Facies Models. *Bulletin of the American Association of Petroleum Geologists*, 69(1):1-21.
- Schmitt, J.G., and D.W. Boyd
1981. Patterns of Silicification in Permian Pelecypods and Brachiopods from Wyoming. *Journal of Sedimentary Petrology*, 51(4):1297-1308.
- Williams, A.
1990. Biomineralization in the Lophoporates. In J.G. Carter, editor, *Skeletal Biomineralization: Patterns, Processes and Evolutionary Trends, I*, pages 67-82. New York: Van Nostrand Reinhold.
- Wilson, R.C.L.
1966. Silica Diagenesis in Upper Jurassic Limestones of Southern England. *Journal of Sedimentary Petrology*, 36(4):1036-1049.
- Yochelson, E.L., and G.R. Fraser
1973. Interpretation of Depositional Environment in the Plympton Formation (Permian), Southern Pequop Mountains, Nevada, from Physical Stratigraphy and a Faunule. *Journal of Research of the United States Geological Survey*, 1(1):19-32.